

TMS 2006

135th Annual Meeting & Exhibition

■ *Linking science and technology for global solutions*

Meeting Information

*March 12-16, 2006
Henry B. Gonzalez Convention Center
San Antonio, Texas, USA*

Technical Program Follows Meeting Information



Dear Colleague,

After months of hard work from dedicated professionals such as yourself, it gives me great pleasure to welcome you to the 135th TMS Annual Meeting & Exhibition. You have shown your dedication to your profession by taking the time and effort to travel to San Antonio, and TMS is dedicated to providing you with a valuable experience while you are here, so you may *learn* from your colleagues, *network* to forge new working relationships, and, in the process, *advance* your career. That is what TMS 2006 is all about.



It begins with the varied technical program offered this year, which is organized into three main areas: light metals; structure, extraction, processing and properties; and emerging materials. These areas have been built with in-depth symposia that mirror the technical needs of today's materials science and engineering professionals. We have brought seven of the world's leading aluminum company executives together to discuss common issues faced in fabrication, with "The Aluminum Fabrication Industry: Global Challenges and Opportunities," on Monday, March 13, from 8:30 a.m. to noon. Meanwhile, the definitive forum for new technological developments in the process metallurgy community takes place here with the Extraction & Processing Division Congress addressing advances in furnace integrity as well as separation technology for aqueous processing. Keeping on the cutting-edge of materials technology, TMS 2006 is also examining subjects such as nanomaterials and biological materials.

Learning and networking at TMS 2006 also takes place outside of the 240 technical sessions through events such as honorary lectures, awards presentations, and the exhibition. The Hume-Rothery Award Lecture, "Entropies of Formation and Mixing in Alloys," on Monday, March 13, at 2 p.m. reveals how entropy plays a major role in determining the relative stability of phases in a system at high temperatures. Aside from Alan Oates receiving the Hume-Rothery Award, 27 of our other esteemed colleagues will be recognized at the annual awards banquet on Tuesday evening. Valuing tradition as well as nurturing new ideas, TMS 2006 presents new and intriguing events on the exhibit floor, including a furnace systems technology workshop, and a materials library exhibit from King's College, London. I strongly encourage you to spend time at the exhibition to benefit from the knowledge, products and services that will assist you in your work.

I hope you make time to enjoy the beautiful city of San Antonio as well. Should you need any assistance navigating through TMS 2006 or the city of San Antonio, please stop by the information booth outside exhibit hall "C" on level "1" of the Henry B. Gonzalez Convention Center.

As always, your opinions about the TMS Annual Meeting & Exhibition are extremely important to us in order to improve your experience. Please complete the electronic survey at the computers located near the escalators and the TMS Publications Sales area on Tuesday or Wednesday. It will only take a few minutes to complete the touch-screen questionnaire. I look forward to your responses.

Have an exceptional experience at TMS 2006!

Sincerely,

A handwritten signature in dark ink that reads "Tresa M. Pollock".

Tresa M. Pollock
2005 TMS President

Review These Policies and Procedures to Help You Navigate TMS 2006!

Location

- The Marriott Rivercenter Hotel is the headquarters hotel for TMS 2006 Annual Meeting & Exhibition. All events, including registration, technical sessions and the exhibition take place at the Henry B. Gonzalez Convention Center.
- Badges are required for admission to all technical sessions, the exhibition and social functions.
- Technical sessions begin on Monday, March 13, and end on Thursday, March 16.

Authors' Coffee

Attention speakers, session chairs and organizers!

Your attendance at Authors' Coffee is required on the day of your session in order to coordinate last minute changes and to receive instructions before the presentations begin. Authors' coffee is held each morning, 7:30 to 8:30, at the Henry B. Gonzalez Convention Center, Third Floor, Ballroom C1.

Publications Sales

Print and CD-ROM editions of individual symposia from this meeting are available at the TMS Publications Sales area outside the entrance to Hall C of the Henry B. Gonzalez Convention Center. Select from more than 145 proceedings volumes, textbooks, monographs and CD-ROMS covering varied areas in minerals, metals and materials, many at reduced prices. The TMS Publications Sales area is open during the following hours: Sunday, 11 a.m. to 6 p.m.; Monday, 7 a.m. to 6 p.m.; Tuesday/Wednesday, 7 a.m. to 5 p.m.; Thursday, 7 to 10 a.m. (See page 14 for details on symposia included on the Light Metals; Structure, Extraction, Processing and Properties; and Emerging Materials CD-ROMs.)

Cyber Center

Visit the Cyber Center outside exhibit hall "C" on level "1" to check your e-mail and send messages from a computer terminal at no charge.

Employment Referral Board

Looking for a job? Need to fill a position? An employment referral board is located at the TMS Member Services booth. Attendees may leave their resumes, and employees may post job openings at no charge.

Guest Hospitality at the Marriott

A special guest hospitality area is hosted each day from 7 to 9:30 a.m. at the Marriott Rivercenter Hotel in conference room 15. TMS sponsors a continental breakfast for the convenience of spouses and others accompanying meeting attendees. The Guest Hospitality Room is an ideal place to meet, socialize and gather before tour departures. All tours depart from the Marriott Rivercenter Hotel, Commerce Street door. (To learn about the tours available, see page 25.)

The conference guest badge is intended for spouses and accompanying persons of registered attendees and for identification purposes only. It does not permit access to technical presentations.

Audio/Video Recording Policy

TMS reserves the right to all audio and video reproductions of presentations at TMS sponsored meetings. Recording of sessions (audio, video, still photography, etc.) intended for personal use, distribution, publication or copyright without the express written consent of TMS and the individual authors is strictly prohibited.

Refund Policy

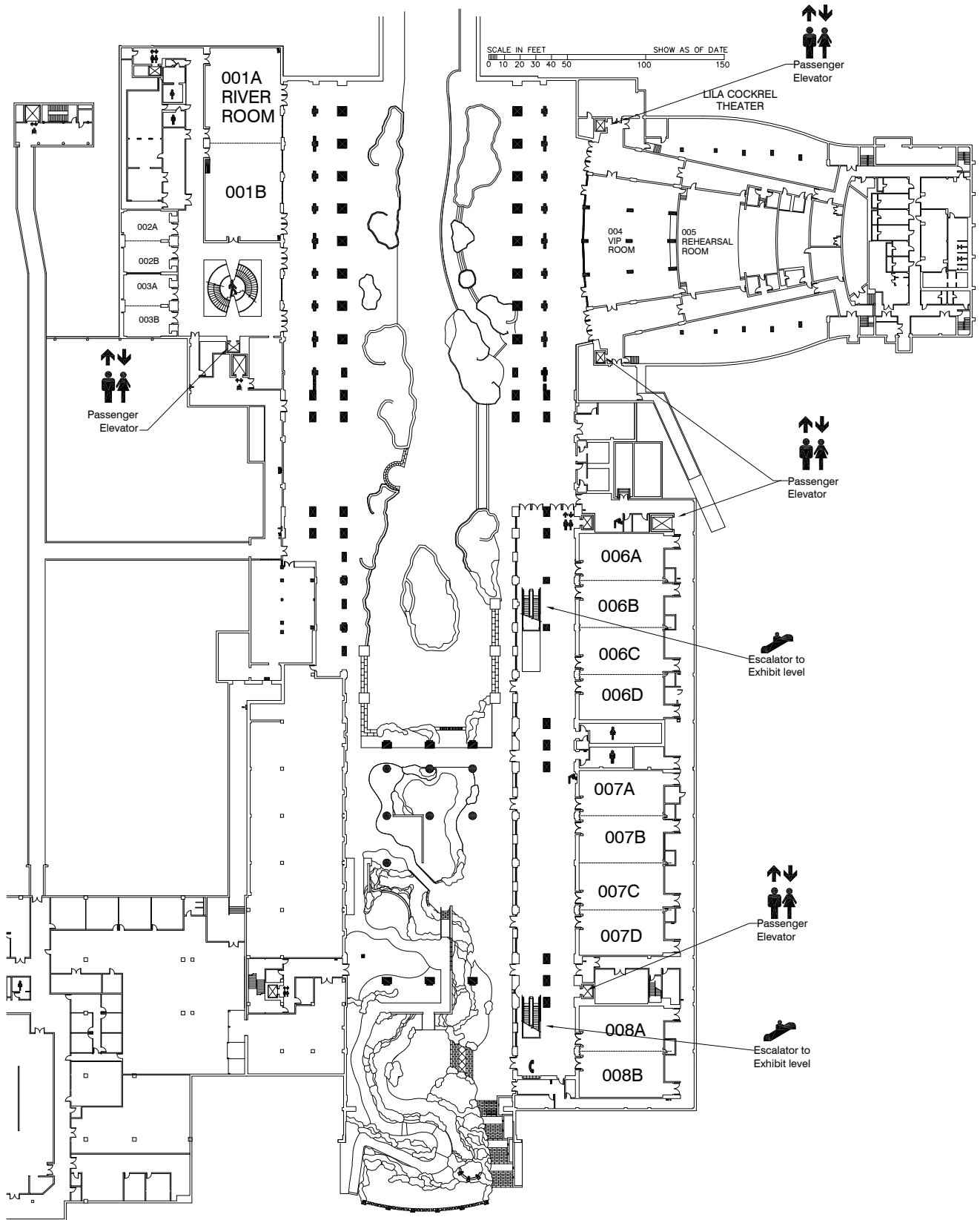
The deadline for refunds was February 13, 2006. No refunds are issued at this meeting. All fees and tickets are nonrefundable after the deadline.

Americans With Disabilities Act

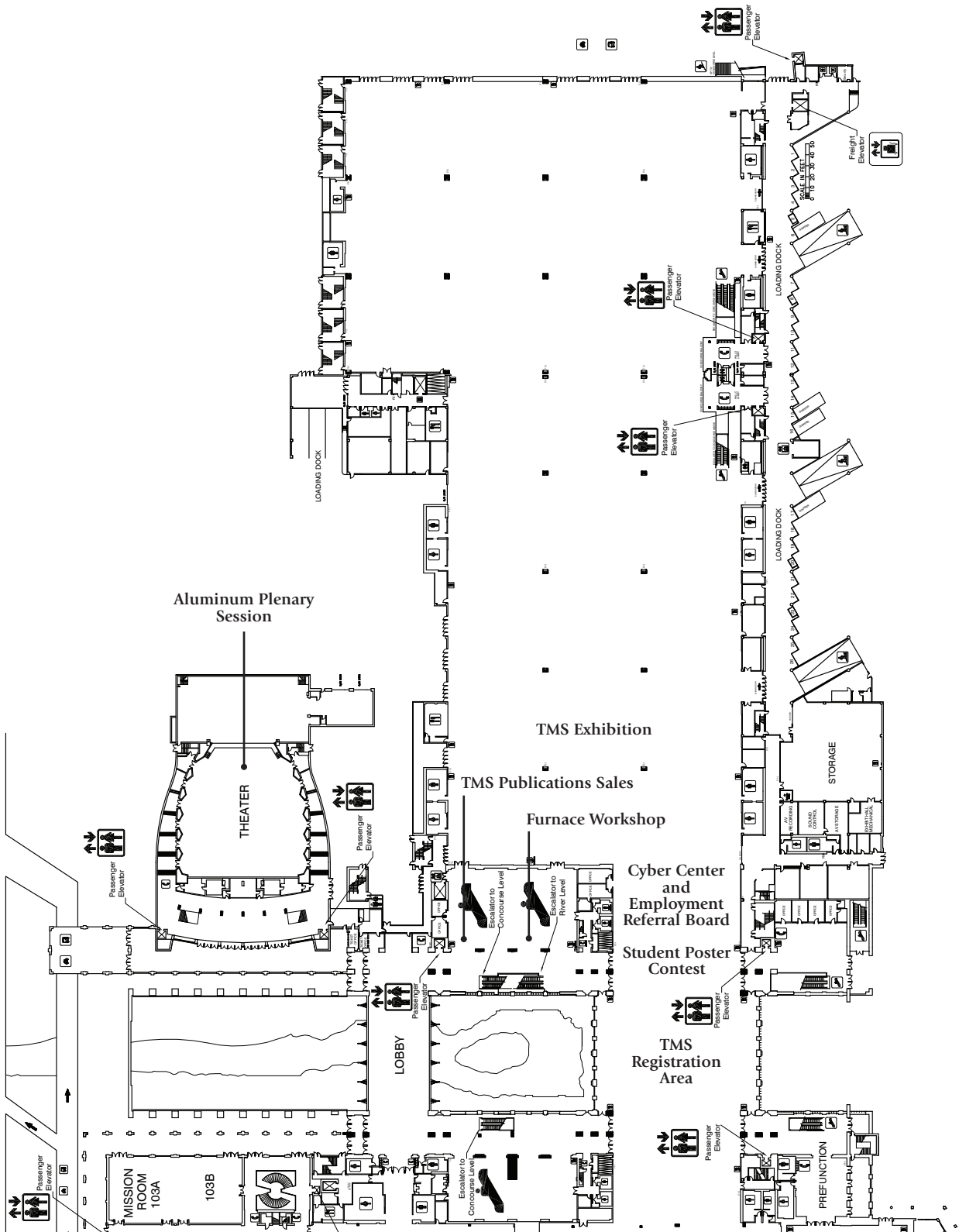


TMS strongly supports the federal Americans with Disabilities Act (ADA) which prohibits discrimination against, and promotes public accessibility for, those with disabilities. In support of, and in compliance with, ADA, we ask those requiring specific equipment or services to notify an individual at the meeting registration desk.

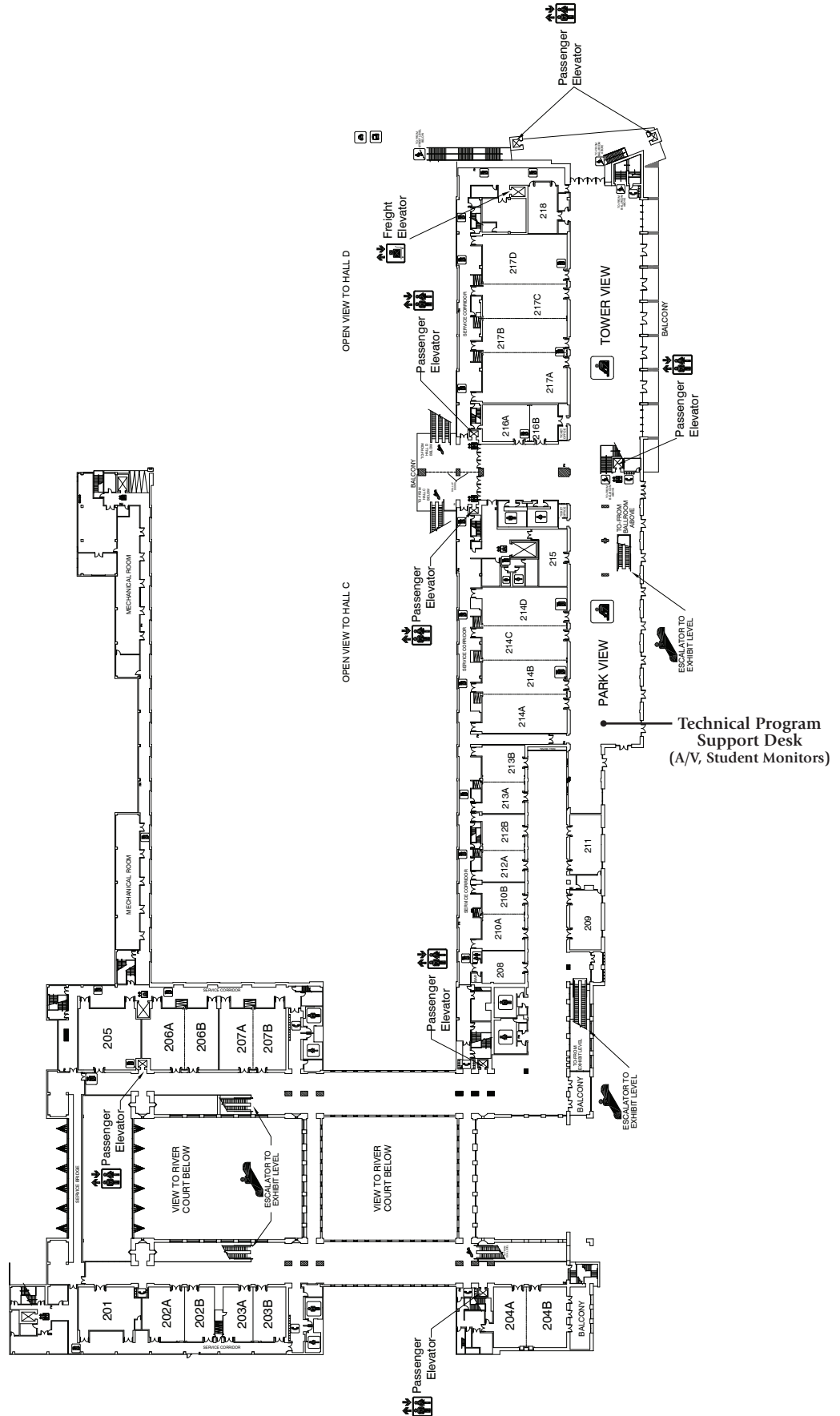
HENRY B. GONZALEZ CONVENTION CENTER, River Level



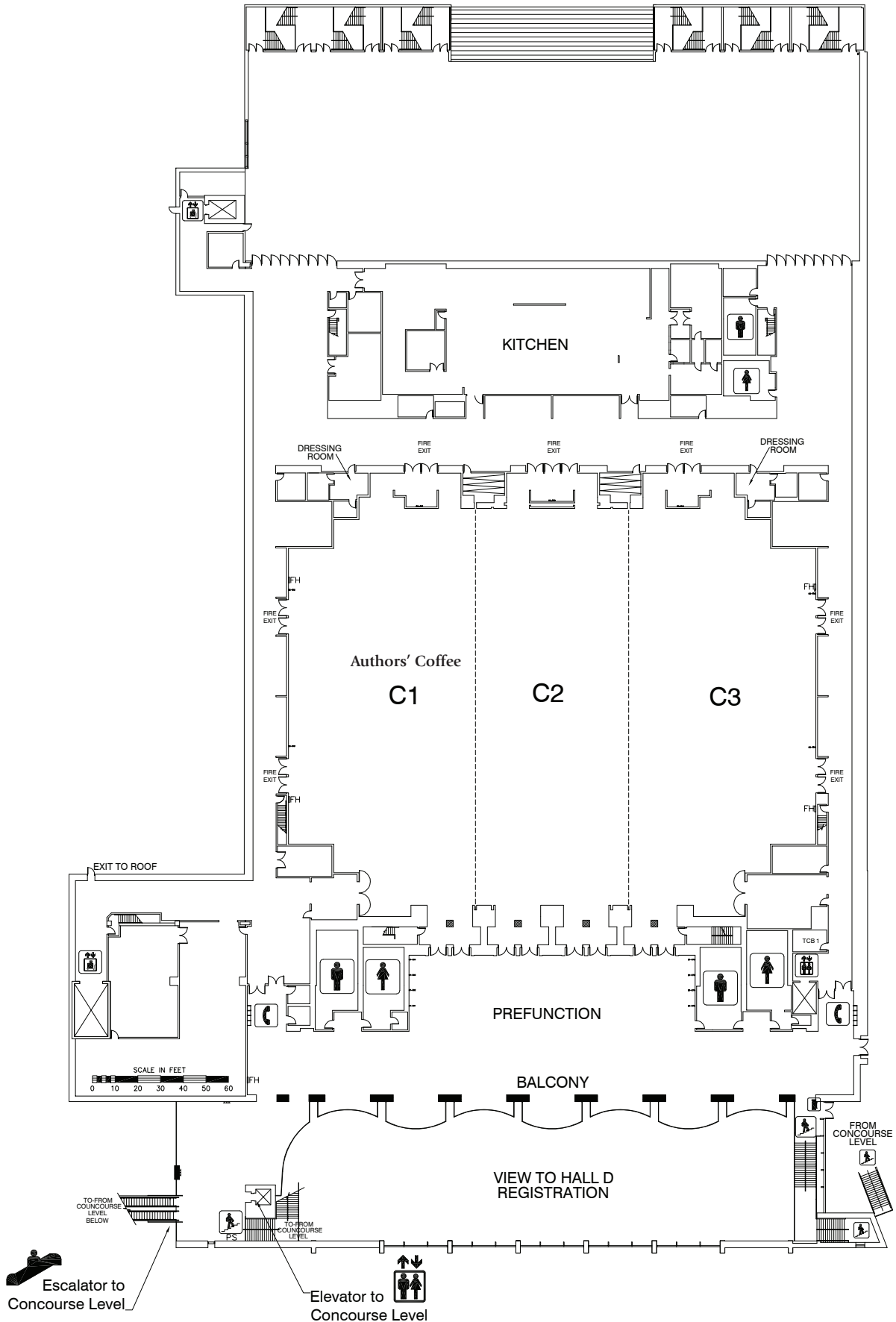
HENRY B. GONZALEZ CONVENTION CENTER, Street Level



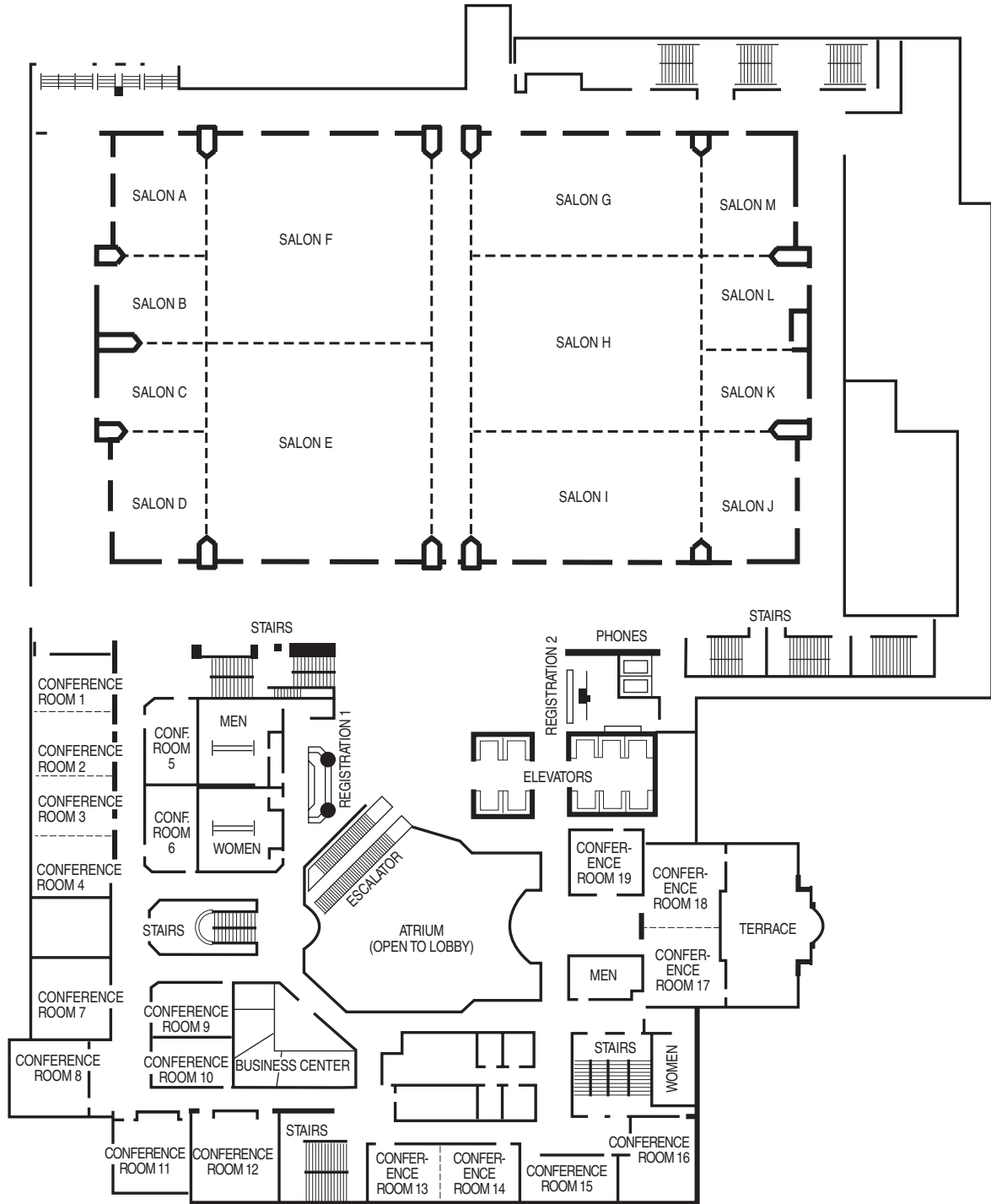
HENRY B. GONZALEZ CONVENTION CENTER, Concourse Level



HENRY B. GONZALEZ CONVENTION CENTER, *Ballroom C*



SAN ANTONIO MARRIOTT RIVERCENTER HOTEL, *Third Floor*



Calendar of Events

Key: C = Henry B. Gonzalez Convention Center / M = San Antonio Marriott Rivercenter Hotel

Sunday, March 12

REGISTRATION	11 a.m. to 6 p.m.....	C.....	Bridge Hall, Level 1
TMS MEMBERSHIP AREA	11 a.m. to 6 p.m.....	C.....	Outside Exhibit Hall C, Level 1
TMS PUBLICATIONS SALES	11 a.m. to 6 p.m.....	C.....	Outside Exhibit Hall C, Level 1

SOCIAL FUNCTIONS

Student Attendee Orientation	2 to 3 p.m.....	M.....	Salon C
Student Career Forum.....	3:30 to 5 p.m.....	M.....	Salon C
Student Career Tips Session.....	5 to 6 p.m.....	M.....	Salon C
Young Leaders Reception for New Members	5 to 6 p.m.....	M.....	Salon K
President's Reception (<i>by invitation</i>).....	6 to 7:30 p.m.....	C.....	The Grotto, Riverwalk Level
Purdue University Reception.....	6 to 7:30 p.m.....	M.....	Salon B
University of Virginia Alumni Reception.....	6 to 8 p.m.....	M.....	Salon G
Student Networking Mixer	8 to 10:30 p.m.....	M.....	Salon H

LEAD-FREE TECHNOLOGY WORKSHOP

.....	8 a.m. to 6 p.m.....	M.....	Salon G
-------	----------------------	--------	---------

COMMITTEE MEETINGS

PMP-III Organizing Committee.....	8 to 9:30 a.m.....	M.....	Conference Room 11
Professional Registration Leadership Committee.....	8:30 a.m. to 5 p.m.....	M.....	Conference Room 13
Accreditation Committee	8:30 to 10:30 a.m.....	M.....	Conference Room 14
TMS Board of Directors Meeting	9:30 to 11 a.m.....	M.....	Conference Room 8
Pyrometallurgy Committee	10 to 11 a.m.....	M.....	Conference Room 15
TMS/ABET Assessment Training.....	10:30 a.m. to 5 p.m.....	M.....	Conference Room 9
Recycling Committee.....	11 a.m. to noon.....	M.....	Conference Room 2
Global Innovations Committee.....	11 a.m. to 12:45 p.m.....	M.....	Salon D
Student Affairs Committee.....	11 a.m. to 12:45 p.m.....	M.....	Conference Room 1
Waste Treatment & Minimization Committee	noon to 1 p.m.....	M.....	Conference Room 16
Young Leaders Business Meeting	12:30 to 2 p.m.....	M.....	Conference Room 10
Information Session/Committee Orientation.....	1 to 3 p.m.....	M.....	Conference Rooms 17 and 18
Nominating Committee.....	2 to 3 p.m.....	M.....	Conference Room 4
Thin Films & Interfaces Committee.....	2 to 3 p.m.....	M.....	Salon M
Process Fundamentals Committee	3 to 4 p.m.....	M.....	Conference Room 15
Aluminum Committee	3 to 5 p.m.....	M.....	Salon E
Program Committee	3 to 5 p.m.....	M.....	Conference Room 3
Public & Governmental Affairs Committee	3 to 5 p.m.....	M.....	Conference Room 11
SMD Strategic Planning Committee.....	3 to 5 p.m.....	M.....	Salon L
Professional Registration Leadership Committee.....	3:30 to 5 p.m.....	M.....	Conference Room 13
Copper, Nickel, Cobalt Committee.....	4 to 5 p.m.....	M.....	Conference Room 5
Lead, Zinc Committee	4 to 5 p.m.....	M.....	Conference Room 8
Nanomechanical Material Behavior Committee	4 to 6 p.m.....	M.....	Conference Room 7
Publications Coordinating Committee	4 to 6 p.m.....	M.....	Conference Room 12
Magnesium Committee.....	4:30 to 6 p.m.....	M.....	Conference Room 1
Aqueous Processing Committee	5 to 6 p.m.....	M.....	Salon M
Light Metals Division Council.....	5 to 6:30 p.m.....	M.....	Conference Rooms 17 and 18
Precious Metals Committee.....	6 to 7 p.m.....	M.....	Conference Room 4
Mechanical Behavior of Materials Committee	6:30 to 8 p.m.....	M.....	Conference Room 16
Materials Characterization Committee	7 to 8 p.m.....	M.....	Conference Room 2
Computational Materials Science & Engineering Committee.....	7:30 to 8:30 p.m.....	M.....	Conference Room 10
Alloy Phases Committee	7:30 to 9 p.m.....	M.....	Conference Room 8
Phase Transformations Committee.....	7:30 to 9:30 p.m.....	M.....	Conference Room 5
MSCTS Council Meeting.....	9:00 to 10:30 p.m.....	M.....	Conference Room 3

Calendar of Events

Key: C = Henry B. Gonzalez Convention Center / M = San Antonio Marriott Rivercenter Hotel

Monday, March 13

REGISTRATION	7 a.m. to 6 p.m.....	C.....	Bridge Hall, Level 1
TMS MEMBERSHIP AREA	7 a.m. to 6 p.m.....	C.....	Outside Exhibit Hall C, Level 1
TMS PUBLICATIONS SALES	7 a.m. to 6 p.m.....	C.....	Outside Exhibit Hall C, Level 1
GUEST HOSPITALITY	7 to 9:30 a.m.....	M.....	Conference Room 15
AUTHORS' COFFEE	7:30 to 8:30 a.m.....	C.....	Ballroom C1, Level 3
2006 EXHIBITION			
Exhibit Hours	noon to 6:30 p.m.....	C.....	Exhibit Hall C, Level 1
Hosted Grand Opening Reception	5 to 6:30 p.m.....	C.....	Exhibit Hall C, Level 1
FURNACE SYSTEMS TECHNOLOGY WORKSHOP	2 to 5 p.m.....	C.....	East Registration Area
TECHNICAL DIVISION-SPONSORED			
STUDENT POSTER CONTEST & RECEPTION	5 to 6:30 p.m.....	C.....	Outside Exhibit Hall C, Level 1
HUME-ROTHERY AWARD LECTURE			
“Entropies of Formation and Mixing in Alloys”	2 p.m.....	C.....	Room 202A, Level 2
YOUNG LEADERS TUTORIAL LUNCHEON LECTURE			
“Negotiating Life in Academia – a Young Faculty Member’s Perspective”.....	noon to 1:30 p.m.....	M.....	Conference Rooms 13 and 14
INSTITUTE OF METALS/MEHL LECTURE			
“The Promise and Perils of Extreme Grain Refinement to Produce Superior Structural Materials”	12:30 to 1:30 p.m.....	C.....	Room 8B
SOCIAL FUNCTIONS			
Women in Science Breakfast Presentation	7 to 8 a.m.....	C.....	Room 217A
Aluminum Association Luncheon (by invitation)	noon to 1:30 p.m.....	M.....	Salon B
TMS Fellows Reception.....	5:30 to 7 p.m.....	M.....	Conference Room 4
David Brandon Honorary Dinner	6:30 to 9:30 p.m.....	M.....	Salon D
Mysore Dayananda Honorary Dinner	6:30 to 9:30 p.m.....	M.....	Salon C
William Gerberich Honorary Dinner.....	6:30 to 9:30 p.m.....	M.....	Salon J
John Hunt Honorary Dinner.....	6:30 to 9:30 p.m.....	M.....	Salon B
Arthur McEvily Honorary Dinner.....	6:30 to 9:30 p.m.....	M.....	Salon A
Amiya Mukherjee Honorary Dinner	6:30 to 9:30 p.m.....	M.....	Salon M
Pradeep Rohatgi Honorary Dinner	6:30 to 9:30 p.m.....	M.....	Salon L
Monroe Wechsler Honorary Dinner	6:30 to 9:30 p.m.....	M.....	Salon K
Colorado School of Mines Alumni Reception	7 to 8 p.m.....	M.....	Conference Room 13
COMMITTEE MEETINGS			
Education Committee	7 to 8 a.m.....	M.....	Conference Room 9
<i>Metallurgical & Materials Trans.</i> “A” Board of Review	7 to 8 a.m.....	M.....	Salon M
Chemistry & Physics of Materials Committee.....	7:30 to 8:30 a.m.....	M.....	Conference Room 8
Past Presidents’ Breakfast.....	8 to 9:30 a.m.....	M.....	President’s Suite
Membership Development Committee	noon to 1:30 p.m.....	M.....	Conference Room 9
Electronic, Magnetic & Photonic Materials Division Council.....	noon to 2 p.m.....	M.....	Conference Rooms 17 and 18
Extraction & Processing Division Council.....	noon to 2 p.m.....	M.....	Conference Room 16
Seven Springs Int’l. Symposium on Superalloys: Program Committee.....	noon to 2 p.m.....	M.....	Conference Room 5
Solidification Committee	12:30 to 1:30 p.m.....	M.....	Conference Room 8
Process Modeling Analysis & Control Committee	12:30 to 2 p.m.....	M.....	Conference Room 6
Copper 2007 Organizing Committee	5 to 7 p.m.....	M.....	Conference Room 9
Seven Springs Int’l. Symposium on Superalloys: Organizing Committee	5 to 7 p.m.....	M.....	Conference Room 5
Advanced Characterization, Testing & Simulation Committee	5:30 to 6:30 p.m.....	M.....	Conference Room 6
Surface Engineering Committee.....	5:30 to 6:30 p.m.....	M.....	Conference Room 2
Nuclear Materials Committee	5:30 to 7 p.m.....	M.....	Conference Room 10
Composite Materials Committee	5:45 to 7:15 p.m.....	M.....	Conference Room 7
Biomaterials Committee	6 to 7 p.m.....	M.....	Conference Room 11
REWAS 2008 Organizing Committee.....	8 to 9:30 p.m.....	M.....	Conference Room 12

Tuesday, March 14

REGISTRATION	7 a.m. to 5 p.m.....	C.....	Bridge Hall, Level 1
TMS MEMBERSHIP AREA	7 a.m. to 5 p.m.....	C.....	Outside Exhibit Hall C, Level 1
TMS PUBLICATIONS SALES	7 a.m. to 5 p.m.....	C.....	Outside Exhibit Hall C, Level 1
GUEST HOSPITALITY	7 to 9:30 a.m.....	M.....	Conference Room 15

AUTHORS' COFFEE	7:30 to 8:30 a.m.....	C.....	Ballroom C1, Level 3
2006 EXHIBITION HOURS	9:30 a.m. to 5:30 p.m.....	C.....	Exhibit Hall C, Level 1
FURNACE SYSTEMS TECHNOLOGY WORKSHOP	8:30 a.m. to 5 p.m.....	C.....	East Registration Area
MATERIALS LIBRARY LECTURE	12:30 to 1:30 p.m.....	C.....	East Registration Area
TMS & AIME ANNUAL AWARDS BANQUET			
Reception.....	6 to 7 p.m.....	M.....	Salons H and I
Dinner and Awards.....	7 to 9:30 p.m.....	M.....	Salons H and I
EXTRACTION & PROCESSING DIVISION LECTURES			
Luncheon Lecture: "China's Growing Importance in the Metals Field With an Emphasis on Alloying Additions for the Aluminum Industry".....	noon to 1:45 p.m.....	C.....	Ballroom C3, Level 3
Distinguished Lecture: "Extractive Metallurgy Principles Applied to the Synthesis of Value-Added Materials, Waste Minimization and Recycling".....	1:45 to 2:30 p.m.....	C.....	Ballroom C2, Level 3
ACTA MATERIALIA INC. BOARD OF GOVERNORS			
LUNCHEON AND DINNER (<i>by invitation</i>).....	11:30 a.m. to 9:30 p.m.....	M.....	Conference Room 14
COMMITTEE MEETINGS			
Electronic Packaging & Interconnection Materials Committee.....	7 to 8 a.m.....	M.....	Conference Room 10
<i>Metallurgical & Materials Trans. "B" Board of Review</i>	7 to 8 a.m.....	M.....	Conference Room 14
Materials Processing & Manufacturing Division Council.....	7 to 9 a.m.....	M.....	Conference Rooms 17 and 18
Nanomaterials Committee.....	7:30 to 8:30 a.m.....	M.....	Conference Room 7
Fellows Award Committee.....	7:30 to 9 a.m.....	M.....	Salon G
Hume-Rothery/Acta Met Award Committee.....	7:30 to 9 a.m.....	M.....	Salon G
IOM/Mehl Award Committee.....	7:30 to 9 a.m.....	M.....	Salon G
Acta Materialia Inc. Board of Governors Meeting.....	8 a.m. to 6 p.m.....	M.....	Conference Room 13
Honors & Professional Recognition Committee.....	9 to 10 a.m.....	M.....	Salon G
TMS Executive Committee.....	10 a.m. to 1 p.m.....	M.....	Presidential Suite
Structural Materials Division Council.....	noon to 2 p.m.....	M.....	Conference Rooms 17 and 18
Powder Materials Committee.....	12:15 to 1:45 p.m.....	M.....	Conference Room 10
Aluminum Association Molten Metal Review Session.....	2 to 5 p.m.....	M.....	Salon B
Reactive Metals Committee.....	5 to 6 p.m.....	M.....	Conference Room 10
TDB Meeting.....	5 to 6 p.m.....	M.....	Conference Room 8
Refractory Metals & Materials Committee.....	5:30 to 6:30 p.m.....	M.....	Conference Room 12
Shaping & Forming Committee.....	5:30 to 6:30 p.m.....	M.....	Conference Room 4
Titanium Committee.....	6 to 7 p.m.....	M.....	Conference Room 16
High Temperature Alloys Committee.....	6:30 to 8 p.m.....	M.....	Conference Room 7

Wednesday, March 15

REGISTRATION	7 a.m. to 5 p.m.....	C.....	Bridge Hall, Level 1
TMS MEMBERSHIP AREA	7 a.m. to 5 p.m.....	C.....	Outside Exhibit Hall C, Level 1
TMS PUBLICATIONS SALES	7 a.m. to 5 p.m.....	C.....	Outside Exhibit Hall C, Level 1
GUEST HOSPITALITY	7 to 9:30 a.m.....	M.....	Conference Room 15
AUTHORS' COFFEE	7:30 to 8:30 a.m.....	C.....	Ballroom C1, Level 3
2006 EXHIBITION			
Exhibit Hours.....	9:30 a.m. to 3 p.m.....	C.....	Exhibit Hall C, Level 1
Complimentary Afternoon Snack.....	12:15 to 2 p.m.....	C.....	Exhibit Hall C, Level 1
FURNACE SYSTEMS TECHNOLOGY WORKSHOP	8:30 a.m. to noon.....	C.....	East Registration Area
LIGHT METALS DIVISION LUNCHEON LECTURE			
"Design Drives Consumption: The Revolution in Metal Packaging Design".....	noon to 2 p.m.....	C.....	Ballroom C3, Level 3
COMMITTEE MEETINGS			
TMS Board of Directors Meeting.....	7 a.m. to noon.....	M.....	Conference Rooms 17 and 18
Smelter Survey Committee.....	12:30 to 2 p.m.....	M.....	Conference Room 12

Thursday, March 16

REGISTRATION	7 to 10 a.m.....	C.....	Bridge Hall, Level 1
TMS MEMBERSHIP AREA	7 to 10 a.m.....	C.....	Outside Exhibit Hall C, Level 1
TMS PUBLICATIONS SALES	7 to 10 a.m.....	C.....	Outside Exhibit Hall C, Level 1
AUTHORS' COFFEE	7:30 to 8:30 a.m.....	C.....	Ballroom C1, Level 3
COMMITTEE MEETINGS			
Light Metals Subject Chairs Breakfast.....	7 to 8:30 a.m.....	M.....	Conference Room 1
Light Metals Executive Committee.....	8:30 to 10:30 a.m.....	M.....	Conference Room 1

You are invited...

Help chart the technological course for future TMS annual meetings, as well as the materials science and engineering profession, by participating in a TMS technical committee. While attending TMS 2006 Annual Meeting & Exhibition, you are invited to attend the technical committee meeting that best serves your area of interest.

Technical Committee Schedule

Sunday, March 12

Pyrometallurgy Committee	10 to 11 a.m.	M	Conference Room 15
Recycling Committee	11 a.m. to noon	M	Conference Room 2
Waste Treatment & Minimization Committee	noon to 1 p.m.	M	Conference Room 16
Thin Films & Interfaces Committee	2 to 3 p.m.	M	Salon M
Process Fundamentals Committee	3 to 4 p.m.	M	Conference Room 15
Aluminum Committee	3 to 5 p.m.	M	Salon E
Copper, Nickel, Cobalt Committee	4 to 5 p.m.	M	Conference Room 5
Lead, Zinc Committee	4 to 5 p.m.	M	Conference Room 8
Nanomechanical Material Behavior Committee	4 to 6 p.m.	M	Conference Room 7
Magnesium Committee	4:30 to 6 p.m.	M	Conference Room 1
Aqueous Processing Committee	5 to 6 p.m.	M	Salon M
Precious Metals Committee	6 to 7 p.m.	M	Conference Room 4
Mechanical Behavior of Materials Committee	6:30 to 8 p.m.	M	Conference Room 16
Materials Characterization Committee	7 to 8 p.m.	M	Conference Room 2
Computational Materials Science & Engineering Committee	7:30 to 8:30 p.m.	M	Conference Room 10
Alloy Phases Committee	7:30 to 9 p.m.	M	Conference Room 8
Phase Transformations Committee	7:30 to 9:30 p.m.	M	Conference Room 5

Monday, March 13

Chemistry & Physics of Materials Committee	7:30 to 8:30 a.m.	M	Conference Room 8
Solidification Committee	12:30 to 1:30 p.m.	M	Conference Room 8
Process Modeling Analysis & Control Committee	12:30 to 2 p.m.	M	Conference Room 6
Advanced Characterization, Testing & Simulation Committee	5:30 to 6:30 p.m.	M	Conference Room 6
Surface Engineering Committee	5:30 to 6:30 p.m.	M	Conference Room 2
Nuclear Materials Committee	5:30 to 7 p.m.	M	Conference Room 10
Composite Materials Committee	5:45 to 7:15 p.m.	M	Conference Room 7
Biomaterials Committee	6 to 7 p.m.	M	Conference Room 11

Tuesday, March 14

Electronic Packaging & Interconnection Materials Committee	7 to 8 a.m.	M	Conference Room 10
Nanomaterials Committee	7:30 to 8:30 a.m.	M	Conference Room 7
Powder Materials Committee	12:15 to 1:45 p.m.	M	Conference Room 10
Reactive Metals Committee	5 to 6 p.m.	M	Conference Room 10
Refractory Metals & Materials Committee	5:30 to 6:35 p.m.	M	Conference Room 12
Shaping & Forming Committee	5:30 to 6:30 p.m.	M	Conference Room 4
Titanium Committee	6 to 7 p.m.	M	Conference Room 16
High Temperature Alloys Committee	6:30 to 8 p.m.	M	Conference Rooms 7

Make Time in Your Schedule for These Programming Features

“The Aluminum Fabrication Industry: Global Challenges and Opportunities”

Monday, March 13, 8:30 a.m. to noon

Dieter Braun, *President, Automotive Sector, Hydro Aluminium Deutschland GmbH, Germany*

“The Importance of the Automotive Industry for the Future Application of Aluminum Components”

Patrick Franc, *President, ARCO Aluminum Inc., USA*

“What are the Challenges and Opportunities for the Rolled Can Sheet Industry?”

Steven Demetriou, *Chairman of the Board & CEO, Aleris International Inc., USA*

“Innovations in Recycling, Continuous Casting and Rolling of Aluminum Products”

Helmut Wieser, *Group President, Alcoa Inc., USA*

“Driving Demand and Cost in a Global Market”

Kevin Greenawalt, *President, Novelis North America, Novelis Corporation, USA*

“Innovative and Sustainable Products for the Aluminum Industry”

Thomas A. Brackmann, *President, Nichols Aluminum, USA*

“The Impact of Alloy Specifications on Aluminum Fabrication and Products - A Future View”

Ding Haiyan, *Board Chairman, Southwest Aluminum (Group) Company Limited; President Assistant, Chinalco, China*

“Developing Aluminum Fabrication in Chinalco: Challenge and Opportunity”

Subodh Das, *President & CEO, Secat Inc., USA*

Moderator



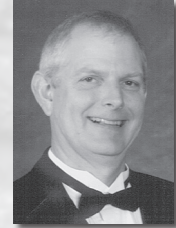
Dieter Braun



Kevin Greenawalt



Patrick Franc



Thomas A. Brackmann



Steven Demetriou



Ding Haiyan



Helmut Wieser



Subodh Das

Rolling, continuous casting and extrusion present many challenges in today's worldwide aluminum fabrication industry. Turning those challenges into opportunities is the subject of this plenary session. Eight corporate leaders from around the world continue the discussion begun at last year's standing-room-only plenary session, “The Role of Technology in the Global Primary Aluminum Industry Today and in the Future,” heading downstream from the cast house to the fabricated product in the 2006 session.

“Cast House Operations”

Monday, March 13

Learn from aluminum cast house professionals about the day-to-day technology issues associated with cast house operation, efficiency and quality improvement, including:

- Crack reduction measures
- Energy control
- Scrap rate and scrap flow control
- Alloying and grain refiner practice
- Melt cleanliness
- Cost reduction projects
- Cast quality control (in- and off-line)
- Efficiency improvement projects

“A Century of Nickel Alloy Discovery and Innovation”

Monday, March 13

The year 2006 is the 100th anniversary of the development of Monel metal. To mark this anniversary, this symposium uncovers the history of the development of alloys over the last 100 years:

- Evolution of Wrought Age Hardenable Superalloys
- Evolution of Solid Solution Nickel-Base Alloys for Corrosion Applications
- A Century of Discoveries, Inventors and New Nickel Alloys
- Evolution of Cast Nickel-Base Superalloys
- A Century of Monel Metal 1906-2006

This session concludes with a panel discussion about current material problems and future material requirements in several industries, and a question-and-answer session.

Purchase TMS 2006 Proceedings

Collected Proceedings on CD-ROM

To provide added value for attendees, CD-ROMs containing multiple symposia on a topical area are available on-site at TMS 2006 Annual Meeting & Exhibition.

- I. Light Metals
- II. Structure, Extraction, Processing and Properties
- III. Emerging Materials

The CD-ROMs include:

- Multiple symposia proceedings in the topical area
- Links to additional resource information
- Table of contents

Each symposium is presented as an individual publication on the CD-ROM, with its own table of contents, standard publication reference numbers, and copyright information.

All three CD-ROMs are available for purchase but only on-site during the annual meeting at the TMS Publications Sales area. The cost per CD-ROM is \$150 with a student price of \$75.

I. Light Metals CD-ROM

Papers Contained on CD:

Advances in Furnace Integrity
Alumina and Bauxite
Aluminum Reduction Technology
Carbon Technology
Cast House Operations
Cast Shop Technology
Furnace Systems Technology Workshop: Emerging Technologies and Energy Efficiency
General Abstracts (EPD)
Granulation of Molten Materials
Magnesium Technology 2006
Recycling-Aluminum Session
Sampling, Sensors, and Control for High Temperature Metallurgical Processes
Simulation of Aluminum Shape Casting: From Alloy Design to Mechanical Properties
The James Morris Honorary Symposium on Aluminum Wrought Products for Automotive, Packaging, and Other Applications
Titanium Alloys for High Temperature Applications: A Symposium Dedicated to the Memory of Dr. Martin Blackburn

Hyperlinks Included on CD to Journals Publishing These Papers:

Solidification Modeling and Microstructure Formation: A Symposium in Honor of Professor John Hunt

Additional Features on CD:

General Abstracts (LMD, MPMD, SMD)
Technical Division Student Poster Contest
The Aluminum Fabrication Industry: Global Challenges and Opportunities

II. Structure, Extraction, Processing and Properties CD-ROM

Papers Contained on CD:

Advances in Furnace Integrity
Characterization of Minerals, Metals, and Materials
General Abstracts (EPD)
Granulation of Molten Materials
Materials Processing Fundamentals
Recycling-General and Electronics Sessions
Sampling, Sensors, and Control for High Temperature Metallurgical Processes
Separation Technology for Aqueous Processing
Simulation of Aluminum Shape Casting: From Alloy Design to Mechanical Properties
Surfaces and Interfaces in Nanostructured Materials II
The James Morris Honorary Symposium on Aluminum Wrought Products for Automotive, Packaging, and Other Applications
The Rohatgi Honorary Symposium on Solidification Processing of Metal Matrix Composites
Titanium Alloys for High Temperature Applications: A Symposium Dedicated to the Memory of Dr. Martin Blackburn

Hyperlinks Included on CD to Journals Publishing These Papers:

- 3-Dimensional Materials Science*
- Computational Thermodynamics and Phase Transformations*
- Deformation and Fracture from Nano to Macro: A Symposium Honoring W.W. Gerberich's 70th Birthday*
- Effects of Water Vapor on High-Temperature Oxidation and Mechanical Behavior of Metallic and Ceramic Materials*
- Fatigue and Fracture of Traditional and Advanced Materials: A Symposium in Honor of Art McEvily's 80th Birthday*
- Hume-Rothery Symposium: Multi-Component Alloy Thermodynamics*
- Materials Design Approaches and Experiences II*
- Multi-Component/Multi-Phase Diffusion Symposium in Honor of Mysore A. Dayananda*
- Phase Stability, Phase Transformation and Reactive Phase Formation in Electronic Materials V*
- Phase Transformations in Magnetic Materials*
- Processing and Mechanical Response of Engineering Materials*
- Solidification Modeling and Microstructure Formation: A Symposium in Honor of Professor John Hunt*
- The Brandon Symposium: Advanced Materials and Characterization*
- Wechsler Symposium on Radiation Effects, Deformation and Phase Transformations in Metals and Ceramics*

Additional Features on CD:

- A Century of Nickel Alloy Discovery and Innovation*
- General Abstracts (EMPMD, MPMD, SMD)*
- Technical Division Student Poster Contest*
- The Aluminum Fabrication Industry: Global Challenges and Opportunities*

III. Emerging Materials CD-ROM

Papers Contained on CD:

- 7th Global Innovations Symposium: Trends in Materials R&D for Sensor Manufacturing Technologies*
- Advanced Materials for Energy Conversion III: A Symposium in Honor of Drs. Gary Sandrock, Louis Schlapbach, and Seijirau Suda*
- Bulk Metallic Glasses*
- Materials in Clean Power Systems: Applications, Corrosion, and Protection*
- Polymer Nanocomposites*
- Recycling-Electronics Session*
- Surfaces and Interfaces in Nanostructured Materials II*
- Ultrafine Grained Materials - 4th International Symposium*

Hyperlinks Included on CD to Journals Publishing These Papers:

- 2006 Nanomaterials: Materials and Processing for Functional Applications*
- Biological Materials Science*
- Lead-Free Solder Implementation: Reliability, Alloy Development, New Technology*
- Space Reactor Fuels and Materials*

Additional Features on CD:

- General Abstracts (EMPMD, MPMD, SMD)*
- Technical Division Student Poster Contest*
- The Aluminum Fabrication Industry: Global Challenges and Opportunities*

Printed Proceedings

For those interested in purchasing printed copies of individual symposia, arrangements can be made during and after the annual meeting. Visit the TMS Publications Sales area on-site or, to order after the meeting, e-mail publications@tms.org.

Printed Proceedings Available for Purchase: Take advantage of special at-meeting prices with free shipping and handling!

<i>Advanced Materials for Energy Conversion III (softcover)</i>	\$119
<i>EPD Congress 2006 (CD-ROM)</i>	\$154
<i>Light Metals 2006 (hardcover and CD-ROM set)</i>	\$149
<i>Magnesium Technology 2006 (hardcover and CD-ROM set)</i>	\$154
<i>Simulation of Aluminum Shape Casting Processing: From Alloy Design to Mechanical Processing (softcover)</i>	\$124
<i>Solidification Processing of Metal Matrix Composites (softcover)</i>	\$124
<i>Ultrafine Grained Materials IV (softcover)</i>	\$94

Plus, find hundreds of related proceedings, textbooks and journals available for purchase in the Publications Sales area, and enjoy free shipping and handling for any orders placed during TMS 2006. Look for more than 20 titles on sale at the on-site clearance price of only \$20 each!*

After the meeting, the TMS Document Center is always open at <http://doc.tms.org> for all of your publications needs.

*Clearance books cannot be shipped by TMS.

Honor Your Colleagues by Attending These Special Events

Honorary Dinners

Monday, March 13, San Antonio Marriott Rivercenter Hotel

Dinner tickets must be purchased at the meeting registration desk; no tickets are sold at the door.



Professor John Hunt Honorary Dinner

In conjunction with the symposium "Solidification Modeling and Microstructure Formation: A Symposium in Honor of Professor John Hunt"

Location: Salon B

Tickets: \$65 per person



Professor Mysore A. Dayananda Honorary Dinner

In conjunction with the symposium "Multi-Component/Multi-Phase Diffusion Symposium in Honor of Mysore A. Dayananda"

Location: Salon C

Tickets: \$55 per person



Professor Monroe Wechsler Honorary Dinner

In conjunction with the symposium "Wechsler Symposium on Radiation Effects, Deformation and Phase Transformations in Metals and Ceramics"

Location: Salon K

Tickets: \$65 per person



Professor David Brandon Honorary Dinner

In conjunction with the symposium "The Brandon Symposium: Advanced Materials and Characterization"

Location: Salon D

Tickets: \$65 per person



Professor Pradeep Rohatgi Honorary Dinner

In conjunction with the symposium "The Rohatgi Honorary Symposium on Solidification Processing of Metal Matrix Composites"

Location: Salon L

Tickets: \$65 per person



Professor William Gerberich Honorary Dinner

In conjunction with the symposium "Deformation and Fracture from Nano to Macro: A Symposium Honoring W.W. Gerberich's 70th Birthday"

Location: Salon J

Tickets: \$65 per person

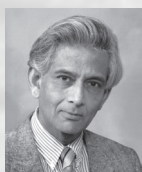


Professor Arthur McEvily Honorary Dinner

In conjunction with the symposium "Fatigue and Fracture of Traditional and Advanced Materials: A Symposium in Honor of Art McEvily's 80th Birthday"

Location: Salon A

Tickets: \$65 per person



Professor Amiya Mukherjee Honorary Dinner

In conjunction with the symposium "Processing and Mechanical Response of Engineering Materials"

Location: Salon M

Tickets: \$65 per person

Institute of Metals/Mehl Lecture

“The Promise and Perils of Extreme Grain Refinement to Produce Superior Structural Materials”

Monday, March 13, 12:30 to 1:30 p.m., Henry B. Gonzalez Convention Center

by **Julia R. Weertman**, *Department of Materials Science and Engineering, Northwestern University*

About the Topic

The ability to produce metals with very small grain sizes has led to materials with both the positive aspect of high strength and a number of negative attributes, especially brittle behavior. Attendees of this lecture are updated on the recent developments in the study of the mechanical properties of nanocrystalline metals and alloys, including attempts to make them into useful materials. Julia Weertman's research is sponsored by the Department of Energy Grant DE-FG02-02ER.



Julia R. Weertman

About the Speaker

Julia R. Weertman is the Walter P. Murphy Professor Emerita in Service at Northwestern University. At Northwestern for nearly 20 years, she holds three patents and has authored more than 150 technical publications. Weertman has received many professional honors, and is a member of the NRC National Materials Advisory Board.

Hume-Rothery Award Lecture

“Entropies of Formation and Mixing in Alloys”

Monday, March 13

*Henry B. Gonzalez Convention Center
Room 202A, Level 2*

by **W. Alan Oates**, *University of Salford, UK*



W. Alan Oates

About the Topic

Attendees learn about:

- Examples in which entropy plays a major role in determining the relative stability of phases in a system at high temperatures
- Methods used for estimating the magnitude of the contributions to formation/mixing entropies
- Models of value in the calculation of formation/mixing entropies for real multi-component alloys and of value in the calculation of phase diagrams for multi-component, multi-phase systems
- The value of the cluster/site approximation for describing the configurational contributions in multi-component, multi-phase systems, and recent developments in its application
- Methods suitable for the estimation of the magnitude of other contributions to formation/mixing entropies

About the Speaker

W. Alan Oates is the Honorary Visiting Professor at the Institute for Materials at the University of Salford in the United Kingdom. A Fellow at the Institute of Metals, Mining and Materials in London since 1978, he earned his doctorate from The University of Newcastle in Australia. Oates' interests recently are in developing a higher order approximation which is suitable for multi-component alloys and in the thermodynamic modeling of intermetallic compounds.

Extraction & Processing Division Luncheon Lecture

“China’s Growing Importance in the Metals Field With an Emphasis on Alloying Additions for the Aluminum Industry”

*Tuesday, March 14, Noon to 1:45 p.m.
Henry B. Gonzalez Convention Center
Ballroom C3, Level 3*

Luncheon tickets may be purchased at the meeting registration desk.

by **Albert Hayoun**

President of Standard Resources Corporation



Albert Hayoun

About the Topic

This presentation relates the history leading to China's ascendance to the important position it now holds in the metals market and traces its recent history as a supplier and consumer of alloying additions, such as silicon metal and magnesium metal, in the aluminum industry.

About the Speaker

Albert Hayoun is president of Standard Resources Corporation, a marketing firm specializing in metals, minerals and alloys. He assisted in establishing the company in 1994 and has helped develop relations with a number of mining and metallurgical companies in China. Hayoun has also established agencies, companies and subsidiaries in several countries including China, Mexico and Venezuela. His work over the past 33 years has involved importing and exporting castings, forgings, pig iron, ferro alloys, metals, minerals and alloys. He began his career in the metallurgical field in 1973 after receiving a bachelor's degree from Brooklyn College.

Honor Your Colleagues by Attending These Special Events

**Extraction & Processing Division
Distinguished Lecture**

“Extractive Metallurgy Principles Applied to the Synthesis of Value-Added Materials, Waste Minimization and Recycling”

*Tuesday, March 14, 1:45 to 2:30 p.m.
Henry B. Gonzalez Convention Center
Ballroom C2, Level 3*

Luncheon tickets may be purchased at the meeting registration desk.

by **Patrick R. Taylor**, *Colorado School of Mines*

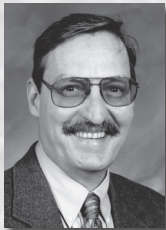
About the Topic

Attendees benefit from Patrick Taylor’s overview of extractive metallurgy techniques and principles, which are essential tools when addressing technology for the synthesis of value-added materials, waste minimization and recycling. Various laboratory scale experiments are described, illustrating applications of pyrometallurgy, hydrometallurgy and electrometallurgy to these resource recovery opportunities.

- Thermal plasma synthesis of ultra-fine ceramic powders from minerals
- Reactive thermal plasma spraying of specialty coatings
- Closed-top cyclone treatment of radioactive wastes
- High-temperature oxide electro-reduction and metal recovery from residues through leaching

About the Speaker

Patrick R. Taylor is the George S. Ansell Chair Distinguished Professor of Chemical Metallurgy, and director of the Kroll Institute for Extractive Metallurgy, at the Colorado School of Mines. His research expertise includes mineral processing, extractive metallurgy, chemical processing of materials, thermal plasma processing, recycle and waste minimization. He holds seven patents and has published more than 135 papers. Taylor is a registered Professional Engineer with a doctorate in metallurgical engineering. He has been an active member of TMS for more than 30 years and is currently a member of the Process Fundamentals Committee.



Patrick R. Taylor

Light Metals Division Luncheon Lecture

“Design Drives Consumption: The Revolution in Metal Packaging Design”

*Wednesday, March 15
Noon to 2 p.m.
Henry B. Gonzalez Convention Center
Ballroom C3, Level 3*

Luncheon tickets may be purchased at the meeting registration desk.

by **Edward B. Martin**, *CCL Container*

About the Topic

Attendees learn about:

- New innovative designs driving consumer products companies to utilize better metal packaging
- How and why rigid aluminum bottle packaging has displaced glass and plastic packaging in segments of the beverage industry and other markets
- A market that has traditionally utilized metal packaging but now is using new designs and shapes to drive industry growth

The common thread weaving through this presentation is that the world is evolving, and the end-use consumer will pay more for relevant value.

About the Speaker

Edward B. Martin is the vice president of sales and marketing for CCL Container. He has helped to diversify the company’s business mix over the past seven years while continuing to grow its core aluminum aerosol container business. Martin has worked in the packaging industry for more than 20 years with experience in manufacturing management and planning in addition to sales and marketing. Prior to joining CCL Container, he was the national accounts manager for Tenneco Packaging Paperboard Pkg. Division.

Martin serves on the board of directors of both the Consumer Specialty Products Association (CSPA) and the National Aerosol Association (NAA). He is also a member of the Rochester Institute of Technology’s (RIT) School of Packaging Science Industry Advisory Board. Martin holds a master’s degree in international business from the University of Connecticut.



Edward B. Martin

135th TMS & AIME Dinner and Awards Presentation

With Installation of 2006 TMS President

**Tuesday, March 14, San Antonio Marriott Rivercenter Hotel • 6 p.m. Cash Bar; 7 p.m. Dinner
Tickets are \$65 and may be purchased at the meeting registration desk.**

This annual, time-honored event includes recognition of the 2006 society and technical division award recipients followed by an address from 2005 TMS President Tresa M. Pollock. She also introduces the new president, Brajendra Mishra.

Brajendra Mishra is professor and associate director at the Colorado School of Mines Kroll Institute for Extractive Metallurgy. A TMS member for 18 years, Mishra is an accomplished educator and researcher in the areas of extraction and processing of materials, thin films processing, and corrosion engineering. Mishra received his doctorate from the University of Minnesota, Minneapolis in 1986.

He has held leadership positions on TMS committees in both the Light Metals Division and the Extraction & Processing Division (EPD). In addition, he has served as treasurer and chair of EPD and as a member of the Publications Coordinating Committee. Mishra played a key role in enhancing the TMS international membership through dialogues with the executives of the Indian Institute of Metals. He joined TMS as a student in 1982 and has remained an active member.



Brajendra Mishra
2006 TMS President



Tresa M. Pollock
2005 TMS President

AIME AWARDS

AIME HONORARY MEMBER • **Merton C. Flemings**, *Massachusetts Institute of Technology*

AIME MINERAL ECONOMICS AWARD • **Chris Twigge-Molecey**, *Hatch*

AIME ROBERT EARLL MCCONNELL AWARD • **Don J. Glenister**, *Alcoa Inc.*

SOCIETY AWARDS

TMS FELLOW CLASS OF 2006

Diran Apelian, *Worcester Polytechnic Institute*

Clyde L. Briant, *Brown University*

Doris Kuhlmann-Wilsdorf, *University of Virginia*

APPLICATION TO PRACTICE

Vinod Kumar Sikka, *Oak Ridge National Laboratory*

JOHN BARDEEN AWARD

Isamu Akasaki, *Meijo University*

BRUCE CHALMERS AWARD

Diran Apelian, *Worcester Polytechnic Institute*

EDUCATOR AWARD

John P. Hager, *Colorado School of Mines*

ROBERT LANSING HARDY AWARD

Mark C. Hersam, *Northwestern University*

WILLIAM HUME-ROTHERY AWARD

William Alan Oates, *University of Salford*

INSTITUTE OF METALS/
ROBERT FRANKLIN MEHL AWARD

Julia R. Weertman, *Northwestern University*

LEADERSHIP AWARD

Toni Grobstein Marechaux
Strategic Analysis Inc.

CHAMPION H. MATHEWSON AWARD

K.S. Ravi Chandran, *University of Utah*

TMS FOUNDATION SHRI RAM ARORA AWARD

Krishau Biswas, *Indian Institute of Science*

TECHNICAL DIVISION AWARDS

EXTRACTION & PROCESSING DISTINGUISHED LECTURER

Patrick R. Taylor, *Colorado School of Mines*

EXTRACTION & PROCESSING SCIENCE AWARD

Gamini Senanayake, *Murdoch University*

EXTRACTION & PROCESSING TECHNOLOGY AWARD

Michelle G. Lee, *MSE Technology Applications Inc.*

Jay McCloskey, *MSE Technology Applications Inc.*

Jennifer Saran, *Kennecott Copper*

Larry G. Twidwell, *University of Montana*

LIGHT METALS DISTINGUISHED SERVICE AWARD

John Hryn, *Argonne National Laboratory*

Howard J. Kaplan, *US Magnesium*

LIGHT METALS TECHNOLOGY AWARD

Jan Van Linden, *Recycling Technology Services*

LIGHT METALS AWARD

Gary P. Tarcy, *Alcoa Inc.*

Knut Torklep, *Elkem Aluminium*

STRUCTURAL MATERIALS
DISTINGUISHED SERVICE AWARD

Russell H. Jones, *Pacific Northwest National Laboratory*

STRUCTURAL MATERIALS DISTINGUISHED SCIENTIST/
ENGINEER AWARD

Edgar A. Starke Jr., *University of Virginia*

Events With an Academic Focus

**Young Leaders Tutorial
Luncheon Lecture**

**“Negotiating Life in Academia –
a Young Faculty Member’s Perspective”**

*Monday, March 13, Noon to 1:30 p.m.
San Antonio Marriott Rivercenter Hotel
Conference Rooms 13 and 14*

by **Nik Chawla**, Associate Professor of Chemical and
Materials Engineering, Arizona State University

About the Topic

Life in academia can be an enjoyable rollercoaster ride, filled with exhilarating experiences. This talk focuses on some of the important issues facing young faculty members, and post-doctorate and graduate students seeking faculty positions.

Learn how to:

- Assemble an effective application package
- Build a diverse and satisfying research portfolio
- Develop effective teaching skills
- Balance teaching, research, and service activities

Plus, get tips for navigating life in academia based on successes, challenges, and lessons learned firsthand by the presenter.

About the Speaker

Nik Chawla is associate professor in the department of Chemical and Materials Engineering at Arizona State University. He serves as director of ASU’s interdisciplinary Mechanical Behavior of Materials Facility. Professor Chawla received his doctorate from the University of Michigan in 1997. His research interests encompass the mechanical behavior of advanced materials at bulk and small length scales, including Pb-free solders, metal matrix composites, ceramic fibers, multilayered materials at nanoscale, biocompatible coatings, powder metallurgy alloys, and 3-D microstructure-based finite element modeling. He has authored or co-authored close to 90 publications in these areas, and is the author of Metal Matrix Composites. The recipient of the 2004 Bradley Stoughton Award for Young Teachers, Professor Chawla is chair of the TMS Composite Materials Committee and serves on the Editorial Board of Review for *Metallurgical & Materials Transactions*.

**Alumni Receptions at the Marriott
Rivercenter Hotel**

Alumni of the following universities and colleges are invited to renew old acquaintances and make new ones at the following receptions:

Purdue University
*Sunday, March 12, 6 to 7:30 p.m.
Salon G*

University of Virginia
*Sunday, March 12, 6 to 8 p.m.
Salon B*

Colorado School of Mines
*Monday, March 13, 7 to 8 p.m.
Conference Room 13*



**Your opinions about
your experience at
TMS 2006 matter!**

**Stop by the computers near the
escalators and the TMS Publications
Sales area on level “1” on Tuesday
or Wednesday to take a quick,
touch-screen questionnaire. Your
responses will help in shaping
future annual meetings.**

Make sure we hear from you!

Student Events

Orientation

Sunday, March 12, 2 to 3 p.m., Marriott Rivercenter Hotel

Make sure you're in the right place at the right time—attend student orientation and get your questions answered about TMS and the different activities taking place during the week. It's your first chance to meet other students with similar interests.



Career Forum

Sunday, March 12, 3:30 to 5 p.m., Marriott Rivercenter Hotel

Determining an appropriate career path is an important decision for any student. This career forum addresses the many pertinent issues that students in the minerals, metals, and materials field face today. Key industry figures provide personal insight into preparation strategies and tips for developing and fostering a rewarding career. Come prepared with questions for the speakers.



Career Tips

Sunday, March 12, 5 to 6 p.m., Marriott Rivercenter Hotel

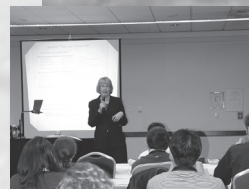
Find out what human resources representatives are looking for when reviewing resumes and interviewing candidates. This session gives you the tips you need to get your resume noticed, get your foot in the door and land that perfect job.



Networking Mixer

Sunday, March 12, 8 to 10:30 p.m., Marriott Rivercenter Hotel, Salon H

Open the door to endless career possibilities at this networking mixer sponsored by the TMS Student Affairs Committee. Make connections with faculty, government, and industry officials in this relaxing, casual and fun atmosphere as they share experiences of professional growth. Beer,* soft drinks, snacks and music are provided.



*In accordance with Texas state law, alcoholic beverages are served only to attendees who are 21 years of age or older; proper photo I.D. with birth date must be presented upon entry.

Technical Division Student Poster Contest

Monday, March 13, 5 to 6:30 p.m., Henry B. Gonzalez Convention Center, Outside Exhibit Hall C

Don't miss the poster contest showing, which will result in \$7,500 in prize money awarded by TMS technical divisions!



Technical Sessions, Lectures, Exhibit

Monday, March 13 through Thursday, March 16, Henry B. Gonzalez Convention Center

Material Advantage students may attend at no charge.



Collected Proceedings on CD-ROM

Students may purchase CD-ROMs of TMS 2006 collected proceedings at a reduced rate of \$75 each. Visit the Publications Sales area. (See page 14 for full details on CD contents.)

Travel Reimbursement for Material Advantage Chapters

Each active Material Advantage chapter is eligible to receive \$500 per calendar year in travel reimbursement related to attendance at TMS conferences. Each chapter should select a representative to complete and mail the TMS Travel Reimbursement Program form with original travel receipts by March 31, 2006, to: Chris McKelvey, Member Services & Student Affairs Coordinator, TMS, 184 Thorn Hill Road, Warrendale, PA 15086-7514. The form may be downloaded as a portable document format file at <http://www.tms.org/Students/StuChptrTravelRmbrsmntForm.pdf>.



Meeting Information

*Look for These New Presentations in the Exhibit Area***Technical Division Student Poster Contest****Monday, March 13****5 to 6:30 p.m.****Outside Exhibit Hall C, Level I****Poster # / Abstract Title**

1. Three-Dimensional (3D) Microstructure Visualization of Sn-Rich Pb-Free Solder Alloys
2. Correlation of Mechanical and Microstructural Properties with Magnetic Properties for FeCo/Ru Multilayers
3. Dissolution of Copper from Substrate Surfaces into Lead-Free Solder Joints
4. Functionalized Singlewall Carbon Nanotubes for Toxic Gas and Relative Humidity Detection
5. Electromigration Induced High Reactive Diffusion Path in Sn-In/Cu Joints
6. Study of Electrical Resistivity and Hardness of Cu-Nb Cold Roll Bonded Multi-Layered Materials
7. Imaging Charge Carrier Transport in Single Intrinsic Semiconductor Nanowires: Carrier Mobility and Lifetime
8. A Review of Conducting Polymers
9. Aluminum Electrorefining and Electrowinning in Ionic Liquid Electrolytes
10. Characterization of Intercalation and Melt-Related Phenomena of [001] Single-Crystal W Ballistic Penetrators Interacting with Steel Targets
11. Electrochemical Studies of the Influence of Ore Mineralogy on the Bioleaching of Complex Sulphide Ores
12. Numerical Modeling of Deformation Phenomena in Magnesium Alloys
13. Modeling Methods for Managing Raw Material Compositional Uncertainty in Alloy Production
14. TiN Coating for Metallic Bipolar Plates of Direct Methanol Fuel Cell (DMFC)
15. Nanostructure of High-Temperature Precipitation-Strengthened Al-Sc Alloys with Ternary Additions (Ti, Gd or Yb)
16. Metallurgical and Acoustical Characterization of an Aluminum Alloy (6061) Caribbean Pan
17. Characterization of Aluminum Boron Copper Composites for Aerospace Applications
18. The Effect of Manganese Oxide and Iron Oxide Mold Flux Phase of Slag Disc Chemistry in Continuous Casting
19. A Research Study on the Production of Advanced High Strength Steels (ULSAB-VAC), Applied in Auto Structural Parts for the Optimization of Auto Fuel Performance
20. High-Temperature Tensiometry
21. Energy Savings in Forging and Heat Treatment of an Aluminum Alloy Subjected to Severe Plastic Deformation
22. A Study of Gas Atomized Powder and Melt Spun Ribbon for Improved MRE_{Fe₂B}
23. Interfacial Phenomena in Carbon Nanotube Reinforced Aluminum Composite Structure Fabricated by Plasma Spray Forming
24. Effect of Carrier Gas on Microstructure, Corrosion and Mechanical Properties of Cold Sprayed 1100 Aluminum Coatings
25. Solidification Microstructures with Solidification Rates and Thermal Gradients in Single Crystal Superalloys, CMSX-4 and CMSX-10
26. Solidification Microstructure and Phase Transformation Temperature Analysis in the Ni-base Superalloy 738LC
27. Study on the Load-Deflection Characteristics of Diaphragm Springs
28. Improving the High Temperature Wear Characteristics of Industrial Tools, Dies and Processing Equipment Using Functionally Graded Refractory Metals
29. Thermal Stability of Refractory Alloys Deposited on H13 by Laser Powder Deposition
30. Evaluation of Optical and Electronic Properties in Nanocrystalline Cerium Oxide Using Uv – Vis Spectroscopy
31. Teaching Modules Development at Rensselaer Polytechnic Institute
32. Preparation of LAST Thermoelectric Powders by Planetary Ball Milling
33. Determination of the Optimum Temperature and Strain for Open-Die Forgings of Ti-6Al-4V ELI at Beta-Phase Temperatures
34. Microstructure Effects on Tin Whisker Growth
35. Evaluation of Nanocrystalline Powder Assisted Spot Welding of Aluminum
36. The Feasibility of High Grade X100 Steels in Northern Gas Pipelines
37. The Effects of Hf Addition on the Glass-Forming Ability and Mechanical Properties of Cu-Based Bulk-Metallic Glasses
38. Corrosion-Fatigue Study of Hastelloy® C-2000®: Structural Materials Division, Graduate Student Submission
39. Severe Plastic Deformation Induced Fe-W Alloy Composite Formation by Mechanical Mixing of Fe and W
40. Kinetics of Secondary γ' in Ni-base PM Superalloys
41. The Physical Properties of Nylon-66/Ferrite Nano Hybrids
42. Effects of Silver Nanoparticle on Rheological and Other Physical Properties of Syndiotactic Polypropylene
43. Physical Properties ZnO Nanoparticle-Filled Polyacrylonitrile
44. Adiabatic Shear Bands Associated with Plug Formation and Penetration in Ti-6Al-4V Targets: Formation, Structure and Performance
45. Effects of Zinc Oxide Nanoparticle on Physical Properties of Polystyrene
46. The Rheological and Thermal Properties of PVA/DEG Nanocomposite
47. Rheological and Other Physical Properties of PVA/PG Solution
48. Crystallization and Amorphization Behavior of Al90Sm10 Alloy Solidified Far from Equilibrium
49. Nanocrystalline Metal Indentation: Novel Insights from Atomic Contact Simulation
50. The Design of a Biomimetic Self-Healing Alloy Composite
51. Elastic-Plastic Shock Wave Profiles in Oriented Single Crystals of Cyclotrimethylene Trinitramine (RDX); LA-UR-05-9437
52. Gas Barrier Properties of Polymer Nanocomposite
53. Effect of Layered Double Hydroxide (LDH) on Flame Retardant Properties in Polyvinyl Chloride
54. Heat Treatment of the Thermal Spray Objects
55. Investigation of the Effect of Filler Metal on the Microstructure and Microhardness of Inconel 600
56. 3D Microscopy via Serial Sectioning of Shocked Tantalum

Materials Library Lecture & Exhibit

Tuesday, March 14, 12:30 to 1:30 p.m.
Exhibit Hall, Booth #501

by Mark A. Miodownik
King's College London



"We are becoming more and more theoretical; we are losing touch with the more sensual side of what we do," so says Mark Miodownik, the curator of the Materials Library at King's College London, but the university lecturer is trying to change that.

Join us as we bring materials science to life through Dr. Miodownik's materials library exhibit and his presentation about the development and uses of materials libraries. More than 300 new materials, including aerogel, magnetic liquid and artificial skin, will be within reach at this interactive, tactile, aesthetic display!

About the Speaker

Mark A. Miodownik is a materials scientist and NESTA Fellow at King's College London, as well as the curator of the Materials Library there. He works in the department of Mechanical Engineering in the school of Physical Sciences and Engineering. In 2005 Miodownik organized and chaired a seminar series at the Tate Modern Museum in London on the influence of new materials on the arts. He is engaged in several collaborative art/science projects including a NESTA project to build a new materials library for artists and designers, and organizes "EngineeringArt," a network dedicated to the art and science of materials. Miodownik has published 37 research papers and writes a regular column on the arts and science of materials for the journal *Materials Today*. He earned his doctorate in turbine jet engine alloys from Oxford University in 1996.

TMS Thanks our Corporate Sponsors for Their Generosity!



GE
Water & Process Technologies

Sponsor of Badge Lanyards



Sponsor of Program Bags



the language of science

Sponsor of the Cyber Center



**Sponsor of Information Booth, Event
Signs and Banners**

Lawrence Livermore National Laboratory
Sponsor of Biological Materials Science Symposium

FEI Company • JEOL • Carl Zeiss SMT
Sponsor of The Brandon Symposium: Advanced Materials and Characterization

Air Force Office of Scientific Research
Sponsor of the Ultrafine Grained Materials - 4th International Symposium

Information About San Antonio

Restaurants Within Walking Distance of the Henry B. Gonzalez Convention Center

For more information, stop by the restaurant reservation desk outside Hall C, Lobby Level, near the exhibition.

Across the Street

1. Ibiza (Hilton)
2. Cantina del Rio (Hilton)
3. Cactus Flower (Marriott Riverwalk)
4. Little Rhein Steakhouse
5. Guadalajara Grill

Within 1/2 Block

1. Rivercenter Food Court
2. Luciano's
3. Steers & Beers
4. Fig Tree
5. Tower of the Americas
6. Garden Cafe (Marriott Rivercenter)
7. Chili's
8. Hooters
9. Tony Roma's/A Place for Ribs

Within 1 Block

1. Morton's of Chicago
2. JW Marriott Steakhouse
3. Denny's
4. La Villita Cantina Cafe
5. Sage (Fairmount Hotel)
6. McDonald's
7. Casa Rio

Within 1-1/2 Blocks

1. Fuddrucker's
2. G/M Steak House
3. Pizza Hut
4. Lone Star Cafe
5. Republic of Texas
6. Schilo's Delicatessen
7. Anaqua Room (Plaza San Antonio)

Within 2 Blocks

1. Boudro's
2. Caliza Grille (Westin Riverwalk)
3. Rio Rio
4. Landry's Seafood
5. Acenar
6. Zuni Grill
7. Chaps (Hyatt Regency)
8. Mad Dog Saloon
9. Michelino's
10. The Original Mexican Restaurant
11. The Landmark (Crockett Hotel)
12. Ernie's (Crockett Hotel)
13. Colonial Room & Garden (Menger Hotel)

Within 2-1/2 Blocks

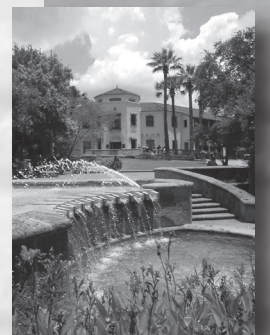
1. Hunan River Garden
2. Pieca d'Italia
3. Paloma
4. Rendez-Vous Cafe
5. Starbuck's

Within 3 Blocks

1. Biga on the Banks
2. Sushi Zushi
3. La Foccacia
4. Oro (Emily Morgan Hotel)
5. Paesano's
6. County Line BBQ
7. Hard Rock Café

Within 4 Blocks

1. Johnny Rockets
2. Rita's on the River
3. Rosario's
4. Dick's Last Resort
5. Ruth's Chris Steakhouse
6. Aldaco's
7. Pesca on the River
8. Las Canarias (La Mansion)



Tours

“Celebrating San Antonio!”

Monday, March 13
8:30 a.m. to 12:30 p.m.
\$39 per person



Stop #1 King William Historic District

The King William Historic District recalls a more gracious era. Prosperous German merchants who made their fortunes in San Antonio in the late 1800s built these grand homes. They are showcased along tree-lined avenues, with ornately carved wood, delicately scrolled ironwork and beautiful landscaping.

Just at the end of King William Street is the Guenther House, built by the German immigrant who operated the first flourmill on the San Antonio River. This house is still part of the Pioneer Flour Mill and run by the Guenther family. A tour of the house reveals wonderful memorabilia from the Pioneer Mill.

A visit to King William is not complete without a tour of the Steves Homestead. Edward Steves built this home in 1876. It is now a museum owned and operated by the San Antonio Conservation Society. The house has been meticulously restored to the period of the early 1900s.

Stop #2 San Fernando Cathedral

At the center of San Antonio, the San Fernando Cathedral was founded in 1731 by a group of 15 families who came from the Canary Islands at the invitation of King Phillip V of Spain. Over 5,000 people participate at weekend Masses, and symphonies, concerts, and television specials are held in the cathedral regularly. Hundreds of people of all denominations enter the church daily to pray, visit or light a candle.

Stop #3 El Mercado (Mexican Market)

The last stop on the tour is the border-style El Mercado, or Mexican Market. Serving as a hub of commerce years ago, Market Square, as it has become known, has retained much of its charm of the past with its quaint shops, which offer local crafts, art, clothing and food.

Caverns and Cabernet!

Wednesday, March 15 • 8:30 a.m. to 12:30 p.m. • \$55 per person

Over 30 million years ago, what is known now as the picturesque Texas Hill Country was a volcanic bed of activity and violent earthquakes. Today, rich farmland lies to the east and rugged ranch land to the west.

One amazing feat of nature is the Natural Bridge Caverns, named for the 60-foot natural limestone arch that spans the entrance. Trails through these caverns cover more than one mile, and the temperature is 70 degrees year round. Tourists are amazed by the natural formations; the constant sound of dripping water is a reminder the cave is still alive and growing. Following the tour, each guest has the opportunity to pan for gold!

Next, it's time to enjoy the fruits of ancient Texas at Dry Comal Creek Vineyards, nestled in a small protected valley. Proprietor Franklin Houser's passion for the grape has resulted in a quality winery. From the picking to the bottling, every step is completed by hand. Tasting four unique wines with Mr. Houser is a special treat as he explains the history and character of each wine.

Tours depart from the San Antonio Marriott Rivercenter Hotel, Commerce Street door.

To sign up for any of these tours, stop by the meeting registration desk.

Spanish Mission Trail

Tuesday, March 14
8:30 a.m. to 12:30 p.m.
\$39.50 per person



Site #1 The Alamo

The most well-known, Mission San Antonio de Valero, or the Alamo, was established in 1718 and played a pivotal role in Texas history. The shrine displays exhibits from the battle, and guests can explore the beautifully landscaped grounds.

Site #2 Mission San Jose

The largest and most restored of the Missions is Mission San Jose. Known as the “Queen of the Missions,” it was established in 1720 and is the showpiece of the San Antonio Missions National Historical Park. Visitors tour the Indians’ quarters, located within the walls, as well as the Spanish soldiers’ quarters. The famous “Rose Window,” intricately carved, is said to be dedicated to its creator’s lost love.

Site #3 Espada Dam

The next stop is the Espada Dam, an engineering marvel. Built curving the wrong way, the dam has withstood floods for more than 200 years.

Site #4 Mission Concepcion

Established in 1731, Mission Concepcion, the oldest unrestored Mission church in Texas, marks the final stop on the trail. Construction of the building, graced with twin towers, beautiful cupola and rare frescoes decorating the side rooms, spanned more than 20 years.

As an everlasting memory of the beautiful Missions, every guest receives a complimentary book of the Spanish Mission Trail.



An Added Benefit for Nonmembers

Attendees registered in the Nonmember Author and Nonmember categories receive a one-year, complimentary associate membership to TMS for 2006!

As an associate member, you will have access to the technical information and professional network you need to advance your work:

- Free print and electronic subscription to *JOM*, a monthly technical journal covering varied subjects important to the minerals, metals and materials world
- Access to TMS E-Library, with online databases, engineering reference books and analytical tools, powered by Knovel
- Free subscription to *TMS Letters*, the online technical journal providing updates to cutting-edge research in a concise format.
- Discounts on additional TMS publications, including archival technical journals and proceedings
- Reduced registration fees for TMS meetings
- Access to the online TMS membership directory, and more!

Your membership card and new member packet will be on their way to your mailbox following the annual meeting, but you may begin taking advantage of your membership once your annual meeting registration fee is received and processed.

For additional information about activating your membership, contact TMS Member Services at (800) 759-4TMS or (724) 776-9000, ext. 259.

TMS

Your Professional Partner for Career Advancement

The Minerals, Metals & Materials Society (TMS) is the professional organization encompassing the entire range of materials in science and engineering, from minerals processing and primary metals production to basic research and the advanced applications of materials. The Society's broad technical focus covers light metals; electronic, magnetic and photonic materials; extraction and processing; structural materials; and materials processing and manufacturing.

Our Members

Included among TMS professional and student members are metallurgical and materials engineers, scientists, researchers, educators and administrators who work in industry, government and academia. They hail from more than 70 countries on six continents.

Our Mission

The mission of TMS is to promote the global science and engineering professions concerned with minerals, metals and materials. The Society works to accomplish its mission by providing technical learning and networking opportunities through interdisciplinary and specialty meetings; short courses; publications, including five journals and proceedings; and its Web site.

To learn more, visit www.tms.org.

TMS
184 Thorn Hill Road
Warrendale, PA 15086-7514 USA
Telephone: (724) 776-9000 / (800) 759-4TMS
Fax: (724) 776-3770
E-mail: tmsgeneral@tms.org

The People Behind TMS and the 2006 Annual Meeting & Exhibition

2005-2006 TMS Board of Directors

Executive Committee

PRESIDENT

Tresa M. Pollock
University of Michigan

VICE PRESIDENT

Brajendra Mishra
Colorado School of Mines

PAST PRESIDENT

Gregory J. Hildeman
Alcoa

INCOMING VICE PRESIDENT

Robert Shull
NIST

FINANCIAL PLANNING OFFICER

John Parsey
ATMI

INCOMING FINANCIAL PLANNING OFFICER

Garry Warren
University of Alabama

Functional Area Directors

PROFESSIONAL DEVELOPMENT

Anthony Pengidore
Veolia Water Systems

MEMBERSHIP DEVELOPMENT

Wolfgang Schneider
Hydro Aluminium Deutschland GmbH

INCOMING MEMBERSHIP DEVELOPMENT DIRECTOR

W. Jud Ready
GTRI-EOEML

PROGRAMMING

Richard N. Wright
Idaho National Engineering Laboratory

INCOMING PROGRAMMING DIRECTOR

James Foley
Los Alamos National Laboratory

INFORMATION TECHNOLOGY

Marc DeGraef
Carnegie Mellon University

PUBLIC & GOVERNMENTAL AFFAIRS

Iver Anderson
Iowa State University, Ames Laboratory

PUBLICATIONS

Rusty Gray
Los Alamos National Laboratory

STUDENT AFFAIRS

Walter W. Milligan
Michigan Technological University

Technical Division Directors

ELECTRONIC, MAGNETIC &
PHOTONIC MATERIALS DIVISION

Patrice Turchi
Lawrence Livermore National Laboratory

EXTRACTION & PROCESSING DIVISION

Robert Stephens
Teck Cominco Metals Ltd.

LIGHT METALS DIVISION

Ray Peterson
Aleris International

MATERIALS PROCESSING & MANUFACTURING
DIVISION

John Smugeresky
Sandia National Laboratory

STRUCTURAL MATERIALS DIVISION

Elizabeth Holm
Sandia National Laboratory

The People Behind TMS and the 2006 Annual Meeting & Exhibition

TMS 2006 Annual Meeting Technical Program Committee

DIRECTOR AND CHAIRPERSON

Richard N. Wright

Idaho National Laboratory

PAST CHAIRPERSON

Dan J. Thoma

Los Alamos National Laboratory

VICE CHAIRPERSON

James C. Foley

Los Alamos National Laboratory

AIST REPRESENTATIVE

E. Buddy Damm

The Timken Company

TMS EXTRACTION & PROCESSING
DIVISION REPRESENTATIVE

Boyd R. Davis

Queens University

TMS EXTRACTION & PROCESSING
DIVISION REPRESENTATIVE

Michael L. Free

University of Utah

TMS ELECTRONIC, MAGNETIC & PHOTONIC
MATERIALS DIVISION REPRESENTATIVE

Long Qing Chen

Pennsylvania State University

TMS ELECTRONIC, MAGNETIC & PHOTONIC
MATERIALS DIVISION REPRESENTATIVE

Sung K. Kang

IBM Corporation

TMS LIGHT METALS DIVISION REPRESENTATIVE

Jim McNeil

Novelis Inc.

TMS LIGHT METALS DIVISION REPRESENTATIVE

Neale R. Neelameggham

US Magnesium LLC

TMS MATERIALS, PROCESSING & MANUFACTURING
DIVISION REPRESENTATIVE

Thomas R. Bieler

Michigan State University

TMS MATERIALS, PROCESSING & MANUFACTURING
DIVISION REPRESENTATIVE

Fernand D. Marquis

South Dakota School of Mines & Technology

TMS MATERIALS, PROCESSING & MANUFACTURING
DIVISION REPRESENTATIVE

Ralph E. Napolitano Jr.

Iowa State University

ASM-MSCTS REPRESENTATIVE

Ramana G. Reddy

University of Alabama

TMS STRUCTURAL MATERIALS
DIVISION REPRESENTATIVE

Ellen K. Cerreta

Los Alamos National Laboratory

TMS STRUCTURAL MATERIALS
DIVISION REPRESENTATIVE

Dennis M. Dimiduk

U.S. Air Force

TMS STRUCTURAL MATERIALS
DIVISION REPRESENTATIVE

Rollie E. Dutton

U.S. Air Force

TMS STAFF LIAISON

Christina Raabe

TMS 2006

135th Annual Meeting & Exhibition

■ *Linking science and technology for global solutions*

Technical Program

*March 12-16, 2006
Henry B. Gonzalez Convention Center
San Antonio, Texas, USA*



TECHNICAL PROGRAM GRID

	MONDAY		TUESDAY		WEDNESDAY		THURSDAY
	AM	PM	AM	PM	AM	PM	AM
201		Titanium Alloys for High Temperature Applications - A Symposium Dedicated to the Memory of Dr. Martin Blackburn: Titanium Alloys for High Temperature Applications - In Memory of Dr. Martin Blackburn - and Applications of High Temperature Titanium Alloys	Titanium Alloys for High Temperature Applications - A Symposium Dedicated to the Memory of Dr. Martin Blackburn: Processing of High Temperature Titanium Alloys	Titanium Alloys for High Temperature Applications - A Symposium Dedicated to the Memory of Dr. Martin Blackburn: Microstructure and Properties of High Temperature Titanium Alloys	Titanium Alloys for High Temperature Applications - A Symposium Dedicated to the Memory of Dr. Martin Blackburn: Titanium Alloys for High Temperature Oxidation Resistance - and - Titanium Based Intermetallic Alloys for High Temperature Applications - Alpha 2 and Orthorhombic	Titanium Alloys for High Temperature Applications - A Symposium Dedicated to the Memory of Dr. Martin Blackburn: Titanium Based Intermetallic Alloys for High Temperature Applications - Gamma	
202A		Hume Rothery Symposium: Multi-Component Alloy Thermodynamics: Alloy Physics	Hume Rothery Symposium: Multi-Component Alloy Thermodynamics: Alloy Thermodynamics I: Experiment and Modeling	Hume Rothery Symposium: Multi-Component Alloy Thermodynamics: Alloy Thermodynamics II: Experiment and Modeling	Hume Rothery Symposium: Multi-Component Alloy Thermodynamics: Alloy Design and Properties	Hume Rothery Symposium: Multi-Component Alloy Thermodynamics: Kinetics and Microstructural Modeling	
202B	Separation Technology for Aqueous Processing: Session I	General Abstracts: Extraction and Processing Division: Hydrometallurgy	Materials Design Approaches and Experiences II: Superalloys	Materials Design Approaches and Experiences II: Light Alloys	Materials Design Approaches and Experiences II: Steels and Titanium Alloys	Materials Design Approaches and Experiences II: New Tools	
203A	Materials Processing Fundamentals: Process Modeling	Materials Processing Fundamentals: Solidification and Deformation Processing	General Abstracts: Extraction and Processing Division: Copper and Nickel Hydrometallurgy	Materials Processing Fundamentals: Smelting and Refining	Materials Processing Fundamentals: Powders and Composites		
203B	Multicomponent Multiphase Diffusion Symposium in Honor of Mysore A. Dayananda: Phenomenology	Multicomponent Multiphase Diffusion Symposium in Honor of Mysore A. Dayananda: Modeling and Simulation	Multicomponent Multiphase Diffusion Symposium in Honor of Mysore A. Dayananda: Metals and Alloys	Multicomponent Multiphase Diffusion Symposium in Honor of Mysore A. Dayananda: Intermetallics and Ceramics	Multicomponent Multiphase Diffusion Symposium in Honor of Mysore A. Dayananda: Industrial Applications	Multicomponent Multiphase Diffusion Symposium in Honor of Mysore A. Dayananda: Surfaces and Interfaces	
204A		7th Global Innovations Symposium: Trends in Materials R&D for Sensor Manufacturing Technologies: Session I	7th Global Innovations Symposium: Trends in Materials R&D for Sensor Manufacturing Technologies: Session II	7th Global Innovations Symposium: Trends in Materials R&D for Sensor Manufacturing Technologies: Session III			
205	3-Dimensional Materials Science: Microstructure Representation	3-Dimensional Materials Science: 3-D Representation and Computation	3-Dimensional Materials Science: X-Ray Methods	3-Dimensional Materials Science: X-Ray Methods II/ Quantitative Characterization	3-Dimensional Materials Science: 3-D Atom Probe	3-Dimensional Materials Science: Serial Sectioning	Characterization of Minerals, Metals and Materials: Advances in Methodologies
206A	Characterization of Minerals, Metals and Materials: Extraction & Processing Applications	Characterization of Minerals, Metals and Materials: Ceramic and Refractories	Characterization of Minerals, Metals and Materials: Structural Engineering Mats I	Characterization of Minerals, Metals and Materials: Structural Engineering Mats II	Characterization of Minerals, Metals and Materials: Structural Engineering Mats III	Characterization of Minerals, Metals and Materials: Composites and Other Materials	Characterization of Minerals, Metals and Materials: Mineralogical Studies
206B	The Brandon Symposium: Advanced Materials and Characterization: Grain Boundary Theory and Experiments	The Brandon Symposium: Advanced Materials and Characterization: Interfaces - Theory and Experiments	The Brandon Symposium: Advanced Materials and Characterization: Atom Probe	The Brandon Symposium: Advanced Materials and Characterization: Interfaces	The Brandon Symposium: Advanced Materials and Characterization: Small Length-Scales and Microstructures	The Brandon Symposium: Advanced Materials and Characterization: Microstructure and Properties	
207A	General Abstracts: Extraction and Processing Division: Lead and Other Metals	General Abstracts: Extraction and Processing Division: Copper/Nickel	The James Morris Honorary Symposium on Aluminum Wrought Products for Automotive, Packaging, and Other Applications: Fundamental Studies	The James Morris Honorary Symposium on Aluminum Wrought Products for Automotive, Packaging, and Other Applications: Automotive Alloys	The James Morris Honorary Symposium on Aluminum Wrought Products for Automotive, Packaging, and Other Applications: Continuous Casting and Related Technologies	The James Morris Honorary Symposium on Aluminum Wrought Products for Automotive, Packaging, and Other Applications: Processing Related Studies	

TECHNICAL PROGRAM GRID

MONDAY		TUESDAY		WEDNESDAY		THURSDAY	
AM	PM	AM	PM	AM	PM	AM	
The Rohatgi Honorary Symposium on Solidification Prog of Metal Matrix Composites: Overview of Developments in Cast MMCs	The Rohatgi Honorary Symposium on Solidification Processing of Metal Matrix Composites: Processing and Microstructure of MMCs - I	The Rohatgi Honorary Symposium on Solidification Processing of Metal Matrix Composites: Processing and Microstructure of MMCs - II	The Rohatgi Honorary Symposium on Solidification Processing of Metal Matrix Composites: Properties of MMCs	The Rohatgi Honorary Symposium on Solidification Processing of Metal Matrix Composites: Modeling and Nanocomposites	The Rohatgi Honorary Symposium on Solidification Processing of Metal Matrix Composites: Advanced Applications of MMCs		207B
Wechsler Symposium on Radiation Effects, Deformation and Phase Transformations in Metals and Ceramics: Irradiation Effects	Wechsler Symposium on Radiation Effects, Deformation and Phase Transformations in Metals and Ceramics: Irradiation Microstructure/Microchemistry	Wechsler Symposium on Radiation Effects, Deformation and Phase Transformations in Metals and Ceramics: Dislocations/Obstacles/Channeling	Wechsler Symposium on Radiation Effects, Deformation and Phase Transformations in Metals and Ceramics: Irradiation Pressure Vessel	Wechsler Symposium on Radiation Effects, Deformation & Phase Transformations in Metals and Ceramics: Irradiation Facilities and Techniques	Wechsler Symposium on Radiation Effects, Deformation and Phase Transformations in Metals and Ceramics: Shape Memory Alloys		208
	A Century of Nickel Alloy Discovery and Innovation: Session I	Surfaces and Interfaces in Nanostructured Materials II: Nano-Structured Metals and Oxides	Surfaces and Interfaces in Nanostructured Materials II: Liquid Phase and Biological Interactions	Surfaces and Interfaces in Nanostructured Materials II: Nanoscale Powders, Tubes and Composites	Surfaces and Interfaces in Nanostructured Materials II: Coatings, Films, Multi-Layers and Arrays		209
Computational Thermodynamics and Phase Transformations: Atomic Modeling Based Alloy Thermodynamics I	Computational Thermodynamics and Phase Transformations: Atomic Modeling Based Alloy Thermodynamics II	Computational Thermodynamics and Phase Transformations: Atomic Modeling of Solid-Liquid Structures	Computational Thermodynamics and Phase Transformations: Alloy Models and Thin Films	Computational Thermodynamics and Phase Transformations: Phase Field Models I	Computational Thermodynamics and Phase Transformations: Phase Field Models II	Computational Thermodynamics and Phase Transformations: Thermodynamic Models	210A
Point Defects in Materials: New Techniques	Point Defects in Materials: Mechanical and Boundary Properties	Point Defects in Materials: Bulk Metal Diffusion	Point Defects in Materials: Other Diffusion	Point Defects in Materials: Thermodynamics	Computational Thermodynamics and Phase Transformations: Atomic Kinetics Processes – Jt. Sess w/ Point Defects in Matls		210B
General Abstracts: Electronic, Magnetic, and Photonic Materials Division: Session I	General Abstracts: Electronic, Magnetic, and Photonic Materials Division: Session II	General Abstracts: Materials Processing and Manufacturing Division: Novel Processing Methods	General Abstracts: Materials Processing and Manufacturing Division: Surface Modification and Properties	General Abstracts: Materials Processing and Manufacturing Division: Powder Processing			211
Biological Materials Science: Implant Biomaterials	Biological Materials Science: Computational Biomaterials/The Biomaterials-Tissue Interface	Biological Materials Science: Biological Materials	Biological Materials Science: Biological Materials Science	Biological Materials Science: Bioinspired Materials	Biological Materials Science: Functional Biomaterials and Devices		212A
Materials in Clean Power Systems: Applications, Corrosion, and Protection: Hydrogen Transport and Separation	Materials in Clean Power Systems: Applications, Corrosion, and Protection: Hydrogen Separation, Delivery, and Materials Issues in Clean Power Plants	Materials in Clean Power Systems: Applications, Corrosion, and Protection: Corrosion in Clean Coal Power Plants and Fuel Cells	Materials in Clean Power Systems: Applications, Corrosion, and Protection: Interconnection and Sealing in Fuel Cells I	Materials in Clean Power Systems: Applications, Corrosion, and Protection: Interconnection and Sealing in Fuel Cells II	Materials in Clean Power Systems: Applications, Corrosion, and Protection: Interconnection and Sealing in Fuel Cells III		212B
Effects of Water Vapor on High-Temperature Oxidation and Mechanical Behavior of Metallic and Ceramic Materials: Behavior of Alloys: Chromia-Formers and Low Alloy Additions	Effects of Water Vapor on High-Temperature Oxidation and Mechanical Behavior of Metallic and Ceramic Materials: Coatings and Ceramics	Phase Transformations in Magnetic Materials: Magnetic Nanocrystals and Nanoparticles	Phase Transformations in Magnetic Materials: Magnetic Shape Memory Alloys	Phase Transformations in Magnetic Materials: Magnetic Shape Memory Alloys and Information Storage	Phase Transformations in Magnetic Materials: Information Storage	Phase Transformations in Magnetic Materials: Processing and Characterization	213A
Space Reactor Fuels and Materials: Refractory Alloy Properties and Welding	Space Reactor Fuels and Materials: Environmental Effects and Fuels	Phase Stability, Phase Transformation and Reactive Phase Formation in Electronic Materials V: New Process for Cu Interconnects and Semiconductor Materials	Phase Stability, Phase Transformation and Reactive Phase Formation in Electronic Materials V: 3D, Fine Pitch and High Temperature/Low Temperature Interconnects in Electronics Packages	Phase Stability, Phase Transformation and Reactive Phase Formation in Electronic Materials V: Electromigration in Leaded and Lead-Free Solder Joints	Phase Stability, Phase Transformation and Reactive Phase Formation in Electronic Materials V: Phase Simulation and Interface Reactions in Solder Joints	Phase Stability, Phase Transformation and Reactive Phase Formation in Electronic Materials V: Damage Structures: Ni Plating, Tin Whiskers and Thermal Cycling	213B

TECHNICAL PROGRAM GRID

	MONDAY		TUESDAY		WEDNESDAY		THURSDAY
	AM	PM	AM	PM	AM	PM	AM
214A	Lead Free Solder Implementation: Reliability, Alloy Development, and New Technology: Mechanical Behavior I: Thermal Fatigue, Shock, and Reliability	Lead Free Solder Implementation: Reliability, Alloy Development, and New Technology: Mechanical Behavior II: Creep	Lead Free Solder Implementation: Reliability, Alloy Development, and New Technology: Interfacial Reactions and Role of Intermetallics	Lead Free Solder Implementation: Reliability, Alloy Development, and New Technology: Microstructure Evolution	Lead Free Solder Implementation: Reliability, Alloy Development, and New Technology: Electromigration	Lead Free Solder Implementation: Reliability, Alloy Development, and New Technology: Electromigration and Reliability	Advanced Materials for Energy Conversion III: A Symposium in Honor of Drs Gary Sandrock, Louis Schlapback, and Seijirau Suda: Carbon, Borohydrides and Other Materials
214B	Advanced Materials for Energy Conversion III: A Symposium in Honor of Drs Gary Sandrock, Louis Schlapback, and Seijirau Suda: Plenary Session	Advanced Materials for Energy Conversion III: A Symposium in Honor of Drs Gary Sandrock, Louis Schlapback, and Seijirau Suda: FreedomCAR and Fuel Partnership-Metal Hydrides I	Advanced Materials for Energy Conversion III: A Symposium in Honor of Drs Gary Sandrock, Louis Schlapback, and Seijirau Suda: Complex Hydrides I	Advanced Materials for Energy Conversion III: A Symposium in Honor of Drs Gary Sandrock, Louis Schlapback, and Seijirau Suda: Metal Hydrides II	Advanced Materials for Energy Conversion III: A Symposium in Honor of Drs Gary Sandrock, Louis Schlapback, and Seijirau Suda: Complex Hydrides II	Advanced Materials for Energy Conversion III: A Symposium in Honor of Drs Gary Sandrock, Louis Schlapback, and Seijirau Suda: Magnets, Superconductors, Thermoelectrics and Energy Materials I	Advanced Materials for Energy Conversion III: A Symposium in Honor of Drs Gary Sandrock, Louis Schlapback, and Seijirau Suda: Metal, Alloys and Energy Materials
214C	2006 Nanomaterials: Materials and Processing for Functional Applications: Functional Applications of Nanoscale Materials	2006 Nanomaterials: Materials and Processing for Functional Applications: Nanostructure Manufacturing, Characterization and Functionalization	2006 Nanomaterials: Materials and Processing for Functional Applications: Nanoscale Electronics	2006 Nanomaterials: Materials and Processing for Functional Applications: Nanoscale Magnetics	2006 Nanomaterials: Materials and Processing for Functional Applications: Nanomaterial Formation and Manufacture	2006 Nanomaterials: Materials and Processing for Functional Applications: Carbon Nanostructures	
214D	Deformation and Fracture from Nano to Macro: A Symposium Honoring W. W. Gerberich's 70th Birthday: Fracture, Fatigue, Wear, and Adhesion	Deformation and Fracture from Nano to Macro: A Symposium Honoring W. W. Gerberich's 70th Birthday: Materials Properties: Testing and Techniques	Deformation and Fracture from Nano to Macro: A Symposium Honoring W. W. Gerberich's 70th Birthday: Nanoscale Materials	Deformation and Fracture from Nano to Macro: A Symposium Honoring W. W. Gerberich's 70th Birthday: Length Scales	Deformation and Fracture from Nano to Macro: A Symposium Honoring W. W. Gerberich's 70th Birthday: Macroscopic Mechanical Behavior	Deformation and Fracture from Nano to Macro: A Symposium Honoring W. W. Gerberich's 70th Birthday: Simulations of Mechanical Behavior	Deformation and Fracture from Nano to Macro: A Symposium Honoring W. W. Gerberich's 70th Birthday: Environmental and Material Alloying Effects
215			Fatigue and Fracture of Traditional and Advanced Materials: A Symposium in Honor of Art McEvily's 80th Birthday: Fatigue and Fracture IV	Fatigue and Fracture of Traditional and Advanced Materials: A Symposium in Honor of Art McEvily's 80th Birthday: Fatigue and Fracture VI	Fatigue and Fracture of Traditional and Advanced Materials: A Symposium in Honor of Art McEvily's 80th Birthday: Fatigue and Fracture VIII	Fatigue and Fracture of Traditional and Advanced Materials: A Symposium in Honor of Art McEvily's 80th Birthday: Fatigue and Fracture X	
216	Fatigue and Fracture of Traditional and Advanced Materials: A Symposium in Honor of Art McEvily's 80th Birthday: Fatigue and Fracture I	Fatigue and Fracture of Traditional and Advanced Materials: A Symposium in Honor of Art McEvily's 80th Birthday: Fatigue and Fracture II	Fatigue and Fracture of Traditional and Advanced Materials: A Symposium in Honor of Art McEvily's 80th Birthday: Fatigue and Fracture III	Fatigue and Fracture of Traditional and Advanced Materials: A Symposium in Honor of Art McEvily's 80th Birthday: Fatigue and Fracture V	Fatigue and Fracture of Traditional and Advanced Materials: A Symposium in Honor of Art McEvily's 80th Birthday: Fatigue and Fracture VII	Fatigue and Fracture of Traditional and Advanced Materials: A Symposium in Honor of Art McEvily's 80th Birthday: Fatigue and Fracture IX	Fatigue and Fracture of Traditional and Advanced Materials: A Symposium in Honor of Art McEvily's 80th Birthday: Fatigue and Fracture XI
217A			Polymer Nanocomposites: Session I	Polymer Nanocomposites: Session II			
217B	Bulk Metallic Glasses: Elastic, Plastic Behavior, and Computation	Bulk Metallic Glasses: Mechanical Behaviors	Bulk Metallic Glasses: Atomic Study and Processing	Bulk Metallic Glasses: Processing and Characterization	Bulk Metallic Glasses: Physical Properties	Bulk Metallic Glasses: Processing and Mechanical Behaviors	Bulk Metallic Glasses: Characterization and Mechanical Behaviors
217C	Amiya Mukherjee Symp. on Processing and Mechanical Response of Engineering Materials: NanoBehavior of Materials	Amiya Mukherjee Symp. on Processing and Mechanical Response of Engineering Materials: NanoProcessing for NanoGrain Materials	Amiya Mukherjee Symp. on Processing and Mechanical Response of Engineering Materials: Mechanical Behavior of Materials	Amiya Mukherjee Symp. on Proc & Mechl Response of Engrg Mats: Processing of Materials - and - Poster Session	Amiya Mukherjee Symp. on Proc & Mechl Response of Engrg Mats: Steady State Deformation of Materials - Part I	Amiya Mukherjee Symp. on Processing and Mechanical Response of Engineering Materials: Steady State Deformation of Materials - Part II	Amiya Mukherjee Symp. on Processing and Mechanical Response of Engineering Materials: Modeling of Material Behavior
217D	Ultrafine Grained Materials - Fourth International Symp: Fundamentals of Ultrafine Grained Materials	Ultrafine Grained Materials - Fourth International Symposium: Processing and Microstructures I	Ultrafine Grained Materials - Fourth International Symposium: Processing and Microstructures II	Ultrafine Grained Materials - Fourth International Symp: Microstructures and Properties - and - Poster Session	Ultrafine Grained Materials - Fourth International Symposium: Mechanical Properties	Ultrafine Grained Materials - Fourth International Symposium: High Temperature and Physical Properties	

TECHNICAL PROGRAM GRID

MONDAY		TUESDAY		WEDNESDAY		THURSDAY	
AM	PM	AM	PM	AM	PM	AM	
		General Abstracts: Structural Materials Division: Advances in Steel	General Abstracts: Structural Materials Division: Processing and Properties of Light Metals	General Abstracts: Structural Materials Division: Microstructure and Properties of Materials I		General Abstracts: Structural Materials Division: Microstructure and Properties of Materials II	218
Magnesium Technology 2006: Primary Production, Recycling and Environmental Issues	Magnesium Technology 2006: Casting and Solidification I	Magnesium Technology 2006: Casting and Solidification II	Magnesium Technology 2006: Wrought Alloys and Forming Processes I	Magnesium Technology 2006: Wrought Alloys and Forming Processes II	Magnesium Technology 2006: Wrought Alloys and Forming Processes III	Magnesium Technology 2006: Welding and Joining	6A
Magnesium Technology 2006: Corrosion and Coatings	Magnesium Technology 2006: Automotive and Other Applications	Magnesium Technology 2006: Microstructure and Properties I	Magnesium Technology 2006: Microstructure and Properties II	Magnesium Technology 2006: Thermodynamics and Fundamental Research	Magnesium Technology 2006: Alloy Development I	Magnesium Technology 2006: Alloy Development II	6B
Solidification Modelling and Microstructure Formation: A Symp in Honor of Prof. John Hunt: Dendritic Growth I	Solidification Modelling and Microstructure Formation: A Symp in Honor of Prof. John Hunt: Dendritic Growth II	Solidification Modelling and Microstructure Formation: A Symp in Honor of Prof. John Hunt: Columnar to Equiaxed Transition	Solidification Modelling and Microstructure Formation: A Symposium in Honor of Prof. John Hunt: Eutectic Growth	Solidification Modelling and Microstructure Formation: A Symposium in Honor of Prof. John Hunt: Solidification Defects	Solidification Modelling and Microstructure Formation: A Symposium in Honor of Prof. John Hunt: Solidification Processing and Thermophysical Properties		6C
		Simulation of Aluminum Shape Casting Processing: From Alloy Design to Mechanical Properties: Alloy Design and Treatment	Simulation of Aluminum Shape Casting Processing: From Alloy Design to Mechanical Properties: Through Process Modeling	Simulation of Aluminum Shape Casting Processing: From Alloy Design to Mechanical Properties: Casting Defect Simulation & Validation	Simulation of Aluminum Shape Casting Processing: From Alloy Design to Mechanical Properties: Heat Treatment Modeling	Simulation of Aluminum Shape Casting Processing: From Alloy Design to Mechanical Properties: Prediction of Mechanical Properties	6D
Aluminum Reduction Technology: Environmental Elements	Aluminum Reduction Technology: Cell Development and Operations - Part I	Alumina and Bauxite: Jt. Session of Alumina and Bauxite & Aluminum Reduction Technology	Aluminum Reduction Technology: Cell Development and Operations - Part II	Aluminum Reduction Technology: Pot Control and Modeling	Aluminum Reduction Technology: Cell Development Part III and Emerging Technologies	Aluminum Reduction Technology: Fundamentals, Emerging Technologies and Inert Anodes - Part II	7A
Aluminum Reduction Technology: Inert Anodes - Part I	Alumina and Bauxite: Solids/Liquid Separation	Granulation of Molten Materials: Session II	Alumina and Bauxite: Bauxite and Bauxite Characterization	Alumina and Bauxite: Bayer Digestion Technology	Alumina and Bauxite: Plant Design, Operation and Maintenance	Alumina and Bauxite: Precipitation Fundamentals	7B
Granulation of Molten Materials: Session I	Cast Shop Technology: Furnace Operation and Refractory Materials	Cast Shop Technology: Melt Treatment, Quality and Product Properties	Cast Shop Technology: Shape Casting and Foundry Alloys	Cast Shop Technology: Casting, Solidification and Cast Defects	Cast Shop Technology: Cast Processes and Chain Analysis		7C
	Cast House Operations: Session I	Advances in Furnace Integrity: Advances in Furnace Integrity and Pyrometallurgical Processes		General Abstracts: Light Metals Division: Session I	General Abstracts: Light Metals Division: Session II	General Abstracts: Light Metals Division: Session III	7D
	Carbon Technology: Anode Raw Materials	Carbon Technology: Greenmill/Rodding	Carbon Technology: Anode Baking	Carbon Technology: Cathode Properties/ Refractory Materials	Carbon Technology: Cathode Preheating/ Wettable Cathodes		8A
		Sampling, Sensors & Control for High Temperature Metallurgical Processes: Session I	Recycling - General Sessions: Electronics Recycling	Recycling - General Sessions: Aluminum Recycling	Recycling - General Sessions: General Recycling		8B
					Furnace Systems Technology Workshop: Emerging Technologies and Energy Efficiency: Energy Efficiency and Emerging Technologies in Secondary Aluminum Melting		Exhibit Floor
The Aluminum Fabrication Industry: Global Challenges and Opportunities: Aluminum Plenary Session							Theatre

Session Listing		ROOM	DAY	PAGE
SESSION TITLE				
2006 Nanomaterials: Materials and Processing for Functional Applications: Functional Applications of Nanoscale Materials	214C		Mon-AM	15
2006 Nanomaterials: Materials and Processing for Functional Applications: Nanostructure Manufacturing, Characterization and Functionalization	214C		Mon-PM	53
2006 Nanomaterials: Materials and Processing for Functional Applications: Nanoscale Electronics	214C		Tues-AM	96
2006 Nanomaterials: Materials and Processing for Functional Applications: Nanoscale Magnetics	214C		Tues-PM	145
2006 Nanomaterials: Materials and Processing for Functional Applications: Nanomaterial Formation and Manufacture	214C		Wed-AM	203
2006 Nanomaterials: Materials and Processing for Functional Applications: Carbon Nanostructures	214C		Wed-PM	251
3-Dimensional Materials Science: Microstructure Representation	205		Mon-AM	16
3-Dimensional Materials Science: 3-D Representation and Computation	205		Mon-PM	55
3-Dimensional Materials Science: X-Ray Methods	205		Tues-AM	97
3-Dimensional Materials Science: X-Ray Methods II/Quantitative Characterization	205		Tues-PM	147
3-Dimensional Materials Science: 3-D Atom Probe	205		Wed-AM	204
3-Dimensional Materials Science: Serial Sectioning	205		Wed-PM	252
7th Global Innovations Symposium: Trends in Materials R&D for Sensor Manufacturing Technologies: Session I:	204A		Mon-PM	56
7th Global Innovations Symposium: Trends in Materials R&D for Sensor Manufacturing Technologies: Session II	204A		Tues-AM	99
7th Global Innovations Symposium: Trends in Materials R&D for Sensor Manufacturing Technologies: Session III	204A		Tues-PM	148
A Century of Nickel Alloy Discovery and Innovation: Session I	209		Mon-PM	57
Advanced Materials for Energy Conversion III: A Symposium in Honor of Drs. Gary Sandrock, Louis Schlapbach, and Sejjirau Suda: Plenary Session	214B		Mon-AM	17
Advanced Materials for Energy Conversion III: A Symposium in Honor of Drs. Gary Sandrock, Louis Schlapbach, and Sejjirau Suda: FreedomCAR and Fuel Partnership-Metal Hydrides I	214B		Mon-PM	58
Advanced Materials for Energy Conversion III: A Symposium in Honor of Drs. Gary Sandrock, Louis Schlapbach, and Sejjirau Suda: Complex Hydrides I	214B		Tues-AM	99
Advanced Materials for Energy Conversion III: A Symposium in Honor of Drs. Gary Sandrock, Louis Schlapbach, and Sejjirau Suda: Metal Hydrides II	214B		Tues-PM	149
Advanced Materials for Energy Conversion III: A Symposium in Honor of Drs. Gary Sandrock, Louis Schlapbach, and Sejjirau Suda: Complex Hydrides II	214B		Wed-AM	205
Advanced Materials for Energy Conversion III: A Symposium in Honor of Drs. Gary Sandrock, Louis Schlapbach, and Sejjirau Suda: Magnets, Superconductors, Thermoelectrics and Energy Materials I	214B		Wed-PM	254
Advanced Materials for Energy Conversion III: A Symposium in Honor of Drs. Gary Sandrock, Louis Schlapbach, and Sejjirau Suda: Carbon, Borohydrides and Other Materials	214A		Thurs-AM	294
Advanced Materials for Energy Conversion III: A Symposium in Honor of Drs. Gary Sandrock, Louis Schlapbach, and Sejjirau Suda: Metal, Alloys and Energy Materials	214B		Thurs-AM	296
Advances in Furnance Integrity: Advances in Furnance Integrity and Pyrometallurgical Processes	7D		Tues-AM	101
Alumina and Bauxite: Solids/Liquid Separation	7B		Mon-PM	59
Alumina and Bauxite: Joint Session of Alumina and Bauxite & Aluminum Reduction Technology	7A		Tues-AM	102
Alumina and Bauxite: Bauxite and Bauxite Characterization	7B		Tues-PM	150

SESSION TITLE	ROOM	DAY	PAGE
Alumina and Bauxite: Bayer Digestion Technology	7B	Wed-AM	207
Alumina and Bauxite: Plant Design, Operation and Maintenance	7B	Wed-PM	255
Alumina and Bauxite: Precipitation Fundamentals	7B	Thurs-AM	297
Aluminum Reduction Technology: Environmental Elements	7A	Mon-AM	18
Aluminum Reduction Technology: Inert Anodes - Part I	7B	Mon-AM	20
Aluminum Reduction Technology: Cell Development and Operations - Part I	7A	Mon-PM	60
Aluminum Reduction Technology: Joint Session of Alumina and Bauxite & Aluminum Reduction Technology	7A	Tues-AM	102
Aluminum Reduction Technology: Cell Development and Operations - Part II	7A	Tues-PM	151
Aluminum Reduction Technology: Pot Control and Modeling	7A	Wed-AM	208
Aluminum Reduction Technology: Cell Development Part III and Emerging Technologies	7A	Wed-PM	256
Aluminum Reduction Technology: Fundamentals, Emerging Technologies and Inert Anodes - Part II	7A	Thurs-AM	298
Amiya Mukherjee Symposium on Processing and Mechanical Response of Engineering Materials: NanoBehavior of Materials	217C	Mon-AM	21
Amiya Mukherjee Symposium on Processing and Mechanical Response of Engineering Materials: NanoProcessing for NanoGrain Materials	217C	Mon-PM	61
Amiya Mukherjee Symposium on Processing and Mechanical Response of Engineering Materials: Mechanical Behavior of Materials	217C	Tues-AM	103
Amiya Mukherjee Symposium on Processing and Mechanical Response of Engineering Materials: Processing of Materials	217C	Tues-PM	152
Amiya Mukherjee Symposium on Processing and Mechanical Response of Engineering Materials: Poster Session: Processing and Mechanical Response of Engineering Materials	217C	Tues-PM	154
Amiya Mukherjee Symposium on Processing and Mechanical Response of Engineering Materials: Steady State Deformation of Materials - Part I	217C	Wed-AM	209
Amiya Mukherjee Symposium on Processing and Mechanical Response of Engineering Materials: Steady State Deformation of Materials - Part II	217C	Wed-PM	257
Amiya Mukherjee Symposium on Processing and Mechanical Response of Engineering Materials: Modeling of Material Behavior	217C	Thurs-AM	299
Biological Materials Science: Implant Biomaterials	212A	Mon-AM	23
Biological Materials Science: Computational Biomaterials/The Biomaterials-Tissue Interface	212A	Mon-PM	63
Biological Materials Science: Biological Materials	212A	Tues-AM	105
Biological Materials Science: Biological Materials Science	212A	Tues-PM	156
Biological Materials Science: Bioinspired Materials	212A	Wed-AM	211
Biological Materials Science: Functional Biomaterials and Devices	212A	Wed-PM	259
Bulk Metallic Glasses: Elastic, Plastic Behavior, and Computation	217B	Mon-AM	24
Bulk Metallic Glasses: Mechanical Behaviors	217B	Mon-PM	64
Bulk Metallic Glasses: Atomic Study and Processing	217B	Tues-AM	106
Bulk Metallic Glasses: Processing and Characterization	217B	Tues-PM	157
Bulk Metallic Glasses: Physical Properties	217B	Wed-AM	212
Bulk Metallic Glasses: Processing and Mechanical Behaviors	217B	Wed-PM	260
Bulk Metallic Glasses: Characterization and Mechanical Behaviors	217B	Thurs-AM	301

TMS2006 Annual Meeting & Exhibition

SESSION TITLE	ROOM	DAY	PAGE
Carbon Technology: Anode Raw Materials	8A	Mon-PM	66
Carbon Technology: Greenmill/Rodding	8A	Tues-AM	108
Carbon Technology: Anode Baking	8A	Tues-PM	159
Carbon Technology: Cathode Properties/Refractory Materials	8A	Wed-AM	213
Carbon Technology: Cathode Preheating/Wettable Cathodes	8A	Wed-PM	261
Cast House Operations: Session I	7D	Mon-PM	66
Cast Shop Technology: The Aluminum Fabrication Industry: Global Challenges and Opportunitites: Aluminum Plenary Session	Theatre	Mon-AM	26
Cast Shop Technology: Furnace Operation and Refractory Materials	7C	Mon-PM	67
Cast Shop Technology: Melt Treatment, Quality and Product Properties	7C	Tues-AM	109
Cast Shop Technology: Shape Casting and Foundry Alloys	7C	Tues-PM	159
Cast Shop Technology: Casting, Solidification and Cast Defects	7C	Wed-AM	214
Cast Shop Technology: Cast Processes and Chain Analysis	7C	Wed-PM	262
Characterization of Minerals, Metals and Materials: Extraction and Processing Applications	206A	Mon-AM	26
Characterization of Minerals, Metals and Materials: Ceramic and Refractories	206A	Mon-PM	68
Characterization of Minerals, Metals and Materials: Structural Engineering Materials I	206A	Tues-AM	110
Characterization of Minerals, Metals and Materials: Structural Engineering Materials II	206A	Tues-PM	160
Characterization of Minerals, Metals and Materials: Structural Engineering Materials III	206A	Wed-AM	215
Characterization of Minerals, Metals and Materials: Composite and Other Materials	206A	Wed-PM	263
Characterization of Minerals, Metals and Materials: Advances in Methodologies	205	Thurs-AM	302
Characterization of Minerals, Metals and Materials: Mineralogical Studies	206A	Thurs-AM	304
Computational Thermodynamics and Phase Transformations: Atomic Modeling Based Alloy Thermodynamics I	210A	Mon-AM	27
Computational Thermodynamics and Phase Transformations: Atomic Modeling Based Alloy Thermodynamics II	210A	Mon-PM	69
Computational Thermodynamics and Phase Transformations: Atomic Modeling of Solid-Liquid Structures	210A	Tues-AM	111
Computational Thermodynamics and Phase Transformations: Alloy Models and Thin Films	210A	Tues-PM	162
Computational Thermodynamics and Phase Transformations: Phase Field Models I	210A	Wed-AM	216
Computational Thermodynamics and Phase Transformations: Atomic Kinetics Processes - Joint Session with Point Defects in Materials	210B	Wed-PM	264
Computational Thermodynamics and Phase Transformations: Phase Field Models II	210A	Wed-PM	266
Computational Thermodynamics and Phase Transformations: Thermodynamic Models	210A	Thurs-AM	305
Deformation and Fracture from Nano to Macro: A Symposium Honoring W. W. Gerberich's 70th Birthday: Fracture, Fatigue, Wear, and Adhesion	214D	Mon-AM	28
Deformation and Fracture from Nano to Macro: A Symposium Honoring W. W. Gerberich's 70th Birthday: Materials Properties: Testing and Techniques	214D	Mon-PM	70
Deformation and Fracture from Nano to Macro: A Symposium Honoring W. W. Gerberich's 70th Birthday: Nanoscale Materials	214D	Tues-AM	112
Deformation and Fracture from Nano to Macro: A Symposium Honoring W. W. Gerberich's 70th Birthday: Length Scales	214D	Tues-PM	163

SESSION TITLE	ROOM	DAY	PAGE
Deformation and Fracture from Nano to Macro: A Symposium Honoring W. W. Gerberich's 70th Birthday: Macroscopic Mechanical Behavior	214D	Wed-AM	218
Deformation and Fracture from Nano to Macro: A Symposium Honoring W. W. Gerberich's 70th Birthday: Simulations of Mechanical Behavior	214D	Wed-PM	267
Deformation and Fracture from Nano to Macro: A Symposium Honoring W. W. Gerberich's 70th Birthday: Environmental and Material Alloying Effects	214D	Thurs-AM	306
Effects of Water Vapor on High-Temperature Oxidation and Mechanical Behavior of Metallic and Ceramic Materials: Behavior of Alloys: Chromia-Formers and Low Alloy Additions	213A	Mon-AM	30
Effects of Water Vapor on High-Temperature Oxidation and Mechanical Behavior of Metallic and Ceramic Materials: Coatings and Ceramics	213A	Mon-PM	72
Fatigue and Fracture of Traditional and Advanced Materials: A Symposium in Honor of Art McEvily's 80th Birthday: Fatigue and Fracture I	216	Mon-AM	31
Fatigue and Fracture of Traditional and Advanced Materials: A Symposium in Honor of Art McEvily's 80th Birthday: Fatigue and Fracture II	216	Mon-PM	73
Fatigue and Fracture of Traditional and Advanced Materials: A Symposium in Honor of Art McEvily's 80th Birthday: Fatigue and Fracture III	216	Tues-AM	114
Fatigue and Fracture of Traditional and Advanced Materials: A Symposium in Honor of Art McEvily's 80th Birthday: Fatigue and Fracture IV	215	Tues-AM	115
Fatigue and Fracture of Traditional and Advanced Materials: A Symposium in Honor of Art McEvily's 80th Birthday: Fatigue and Fracture V	216	Tues-PM	164
Fatigue and Fracture of Traditional and Advanced Materials: A Symposium in Honor of Art McEvily's 80th Birthday: Fatigue and Fracture VI	215	Tues-PM	165
Fatigue and Fracture of Traditional and Advanced Materials: A Symposium in Honor of Art McEvily's 80th Birthday: Fatigue and Fracture VII	216	Wed-AM	219
Fatigue and Fracture of Traditional and Advanced Materials: A Symposium in Honor of Art McEvily's 80th Birthday: Fatigue and Fracture VIII	215	Wed-AM	221
Fatigue and Fracture of Traditional and Advanced Materials: A Symposium in Honor of Art McEvily's 80th Birthday: Fatigue and Fracture IX	216	Wed-PM	269
Fatigue and Fracture of Traditional and Advanced Materials: A Symposium in Honor of Art McEvily's 80th Birthday: Fatigue and Fracture X	215	Wed-PM	270
Fatigue and Fracture of Traditional and Advanced Materials: A Symposium in Honor of Art McEvily's 80th Birthday: Fatigue and Fracture XI	216	Thurs-AM	308
Furnace Systems Technology Workshop: Emerging Technologies and Energy Efficiency: Energy Efficiency and Emerging Technologies in Secondary Aluminum Melting	Exhibit Floor	Wed-PM	271
General Abstracts: Electronic, Magnetic, and Photonic Materials Division: Session I	211	Mon-AM	32
General Abstracts: Electronic, Magnetic, and Photonic Materials Division: Session II	211	Mon-PM	74
General Abstracts: Extraction and Processing Division: Lead and Other Metals	207A	Mon-AM	34
General Abstracts: Extraction and Processing Division: Copper/Nickel	207A	Mon-PM	75
General Abstracts: Extraction and Processing Division: Hydrometallurgy	202B	Mon-PM	76
General Abstracts: Extraction and Processing Division: Copper and Nickel Hydrometallurgy	203A	Tues-AM	116
General Abstracts: Light Metals Division: Session I	7D	Wed-AM	222
General Abstracts: Light Metals Division: Session II	7D	Wed-PM	272
General Abstracts: Light Metals Division: Session III	7D	Thurs-AM	309
General Abstracts: Materials Processing and Manufacturing Division: Novel Processing Methods	211	Tues-AM	117
General Abstracts: Materials Processing and Manufacturing Division: Surface Modification and Properties	211	Tues-PM	166

TMS2006 Annual Meeting & Exhibition

SESSION TITLE	ROOM	DAY	PAGE
General Abstracts: Materials Processing and Manufacturing Division: Powder Processing	211	Wed-AM	222
General Abstracts: Structural Materials Division: Advances in Steel	218	Tues-AM	118
General Abstracts: Structural Materials Division: Processing and Properties of Light Metals	218	Tues-PM	168
General Abstracts: Structural Materials Division: Microstructure and Properties of Materials I	218	Wed-AM	223
General Abstracts: Structural Materials Division: Microstructure and Properties of Materials II	218	Thurs-AM	310
Granulation of Molten Materials: Session I	7C	Mon-AM	34
Granulation of Molten Materials: Session II	7B	Tues-AM	119
Hume Rothery Symposium: Multi-Component Alloy Thermodynamics: Alloy Physics	202A	Mon-PM	77
Hume Rothery Symposium: Multi-Component Alloy Thermodynamics: Alloy Thermodynamics I: Experiment and Modeling	202A	Tues-AM	120
Hume Rothery Symposium: Multi-Component Alloy Thermodynamics: Alloy Thermodynamics II: Experiment and Modeling	202A	Tues-PM	169
Hume Rothery Symposium: Multi-Component Alloy Thermodynamics: Alloy Design and Properties	202A	Wed-AM	225
Hume Rothery Symposium: Multi-Component Alloy Thermodynamics: Kinetics and Microstructural Modeling	202A	Wed-PM	272
Lead Free Solder Implementation: Reliability, Alloy Development and New Technology: Mechanical Behavior I: Thermal Fatigue, Shock, and Reliability	214A	Mon-AM	35
Lead Free Solder Implementation: Reliability, Alloy Development and New Technology: Mechanical Behavior II: Creep	214A	Mon-PM	78
Lead Free Solder Implementation: Reliability, Alloy Development and New Technology: Interfacial Reactions and Role of Intermetallics	214A	Tues-AM	121
Lead Free Solder Implementation: Reliability, Alloy Development and New Technology: Microstructure Evolution	214A	Tues-PM	170
Lead Free Solder Implementation: Reliability, Alloy Development and New Technology: Electromigration	214A	Wed-AM	226
Lead Free Solder Implementation: Reliability, Alloy Development and New Technology: Electromigration and Reliability	214A	Wed-PM	273
Magnesium Technology 2006: Corrosion and Coatings	6B	Mon-AM	37
Magnesium Technology 2006: Primary Production, Recycling and Environmental Issues	6A	Mon-AM	38
Magnesium Technology 2006: Automotive and Other Applications	6B	Mon-PM	80
Magnesium Technology 2006: Casting and Solidification I	6A	Mon-PM	81
Magnesium Technology 2006: Casting and Solidification II	6A	Tues-AM	122
Magnesium Technology 2006: Microstructure and Properties I	6B	Tues-AM	124
Magnesium Technology 2006: Microstructure and Properties II	6B	Tues-PM	171
Magnesium Technology 2006: Wrought Alloys and Forming Processes I	6A	Tues-PM	172
Magnesium Technology 2006: Thermodynamics and Fundamental Research	6B	Wed-AM	227
Magnesium Technology 2006: Wrought Alloys and Forming Processes II	6A	Wed-AM	229
Magnesium Technology 2006: Alloy Development I	6B	Wed-PM	274
Magnesium Technology 2006: Wrought Alloys and Forming Processes III	6A	Wed-PM	276
Magnesium Technology 2006: Alloy Development II	6B	Thurs-AM	311
Magnesium Technology 2006: Welding and Joining	6A	Thurs-AM	312

SESSION TITLE	ROOM	DAY	PAGE
Materials Design Approaches and Experiences II: Superalloys	202B	Tues-AM	125
Materials Design Approaches and Experiences II: Light Alloys	202B	Tues-PM	174
Materials Design Approaches and Experiences II: Steels and Titanium Alloys	202B	Wed-AM	230
Materials Design Approaches and Experiences II: New Tools	202B	Wed-PM	277
Materials in Clean Power Systems: Applications, Corrosion, and Protection: Hydrogen Transport and Separation	212B	Mon-AM	39
Materials in Clean Power Systems: Applications, Corrosion, and Protection: Hydrogen Separation, Delivery, and Materials Issues in Clean Power Plants	212B	Mon-PM	82
Materials in Clean Power Systems: Applications, Corrosion, and Protection: Corrosion in Clean Coal Power Plants and Fuel Cells	212B	Tues-AM	126
Materials in Clean Power Systems: Applications, Corrosion, and Protection: Interconnection and Sealing in Fuel Cells I	212B	Tues-PM	175
Materials in Clean Power Systems: Applications, Corrosion, and Protection: Interconnection and Sealing in Fuel Cells II	212B	Wed-AM	231
Materials in Clean Power Systems: Applications, Corrosion, and Protection: Interconnection and Sealing in Fuel Cells III	212B	Wed-PM	278
Materials Processing Fundamentals: Process Modeling	203A	Mon-AM	40
Materials Processing Fundamentals: Solidification and Deformation Processing	203A	Mon-PM	83
Materials Processing Fundamentals: Smelting and Refining	203A	Tues-PM	176
Materials Processing Fundamentals: Powders and Composites	203A	Wed-AM	232
Multicomponent-Multiphase Diffusion Symposium in Honor of Mysore A. Dayananda: Phenomenology	203B	Mon-AM	41
Multicomponent-Multiphase Diffusion Symposium in Honor of Mysore A. Dayananda: Modeling and Simulation	203B	Mon-PM	84
Multicomponent-Multiphase Diffusion Symposium in Honor of Mysore A. Dayananda: Metals and Alloys	203B	Tues-AM	127
Multicomponent-Multiphase Diffusion Symposium in Honor of Mysore A. Dayananda: Intermetallics and Ceramics	203B	Tues-PM	177
Multicomponent-Multiphase Diffusion Symposium in Honor of Mysore A. Dayananda: Industrial Applications	203B	Wed-AM	233
Multicomponent-Multiphase Diffusion Symposium in Honor of Mysore A. Dayananda: Surfaces and Interfaces	203B	Wed-PM	279
Phase Stability and Phase Transformation and Reactive Phase Formation in Electronic Materials V: New Process for Cu Interconnects and Semiconductor Materials	213B	Tues-AM	128
Phase Stability and Phase Transformation and Reactive Phase Formation in Electronic Materials V: 3D, Fine Pitch and High Temperature/Low Temperature Interconnects in Electronics Packages	213B	Tues-PM	178
Phase Stability and Phase Transformation and Reactive Phase Formation in Electronic Materials V: Electromigration in Leaded and Lead-Free Solder Joints	213B	Wed-AM	234
Phase Stability and Phase Transformation and Reactive Phase Formation in Electronic Materials V: Phase Simulation and Interface Reactions in Solder Joints	213B	Wed-PM	280
Phase Stability and Phase Transformation and Reactive Phase Formation in Electronic Materials V: Damage Structures: Ni Plating, Tin Whiskers and Thermal Cycling	213B	Thurs-AM	313
Phase Transformations in Magnetic Materials: Magnetic Nanocrystals and Nanoparticles	213A	Tues-AM	129
Phase Transformations in Magnetic Materials: Magnetic Shape Memory Alloys	213A	Tues-PM	180

SESSION TITLE	ROOM	DAY	PAGE
Phase Transformations in Magnetic Materials: Magnetic Shape Memory Alloys and Information Storage	213A	Wed-AM	236
Phase Transformations in Magnetic Materials: Information Storage	213A	Wed-PM	281
Phase Transformations in Magnetic Materials: Processing and Characterization	213A	Thurs-AM	315
Point Defects in Materials: New Techniques	210B	Mon-AM	42
Point Defects in Materials: Mechanical and Boundary Properties	210B	Mon-PM	86
Point Defects in Materials: Bulk Metal Diffusion	210B	Tues-AM	130
Point Defects in Materials: Other Diffusion	210B	Tues-PM	181
Point Defects in Materials: Thermodynamics	210B	Wed-AM	237
Point Defects in Materials: Joint Session with Computational Thermodynamics and Phase Transformations: Atomic Kinetics Processes	210B	Wed-PM	264
Polymer Nanocomposites: Session I	217A	Tues-AM	131
Polymer Nanocomposites: Session II	217A	Tues-PM	182
Recycling-General Sessions: Electronics Recycling	8B	Tues-PM	183
Recycling-General Sessions: Aluminum Recycling	8B	Wed-AM	238
Recycling-General Sessions: General Recycling	8B	Wed-PM	282
Sampling, Sensors and Control for High Temperature Metallurgical Processes: Session I	8B	Tues-AM	132
Separation Technology for Aqueous Processing: Session I	202B	Mon-AM	43
Simulation of Aluminum Shape Casting Processing: From Alloy Design to Mechanical Properties: Alloy Design and Treatment	6D	Tues-AM	134
Simulation of Aluminum Shape Casting Processing: From Alloy Design to Mechanical Properties: Through Process Modeling	6D	Tues-PM	184
Simulation of Aluminum Shape Casting Processing: From Alloy Design to Mechanical Properties: Casting Defect Simulation and Validation	6D	Wed-AM	239
Simulation of Aluminum Shape Casting Processing: From Alloy Design to Mechanical Properties: Heat Treatment Modeling	6D	Wed-PM	283
Simulation of Aluminum Shape Casting Processing: From Alloy Design to Mechanical Properties: Prediction of Mechanical Properties	6D	Thurs-AM	316
Solidification Modelling and Microstructure Formation: A Symposium in Honor of Prof. John Hunt: Dendritic Growth I	6C	Mon-AM	44
Solidification Modelling and Microstructure Formation: A Symposium in Honor of Prof. John Hunt: Dendritic Growth II	6C	Mon-PM	87
Solidification Modelling and Microstructure Formation: A Symposium in Honor of Prof. John Hunt: Columnar to Equiaxed Transition	6C	Tues-AM	135
Solidification Modelling and Microstructure Formation: A Symposium in Honor of Prof. John Hunt: Eutectic Growth	6C	Tues-PM	185
Solidification Modelling and Microstructure Formation: A Symposium in Honor of Prof. John Hunt: Solidification Defects	6C	Wed-AM	240
Solidification Modelling and Microstructure Formation: A Symposium in Honor of Prof. John Hunt: Solidification Processing and Thermophysical Properties	6C	Wed-PM	284
Space Reactor Fuels and Materials: Refractory Alloy Properties and Welding	213B	Mon-AM	46
Space Reactor Fuels and Materials: Environmental Effects and Fuels	213B	Mon-PM	88

SESSION TITLE	ROOM	DAY	PAGE
Surfaces and Interfaces in Nanostructured Materials II: Nano-Structured Metals and Oxides	209	Tues-AM	136
Surfaces and Interfaces in Nanostructured Materials II: Liquid Phase and Biological Interactions	209	Tues-PM	187
Surfaces and Interfaces in Nanostructured Materials II: Nanoscale Powders, Tubes and Composites	209	Wed-AM	241
Surfaces and Interfaces in Nanostructured Materials II: Coatings, Films, Multi-Layers and Arrays	209	Wed-PM	286
The Aluminum Fabrication Industry: Global Challenges and Opportunites: Aluminum Plenary Session	Theatre	Mon-AM	47
The Brandon Symposium: Advanced Materials and Characterization: Grain Boundary Theory and Experiments	206B	Mon-AM	48
The Brandon Symposium: Advanced Materials and Characterization: Interfaces - Theory and Experiments	206B	Mon-PM	89
The Brandon Symposium: Advanced Materials and Characterization: Atom Probe	206B	Tues-AM	137
The Brandon Symposium: Advanced Materials and Characterization: Interfaces	206B	Tues-PM	188
The Brandon Symposium: Advanced Materials and Characterization: Small Length-Scales and Microstructures	206B	Wed-AM	242
The Brandon Symposium: Advanced Materials and Characterization: Microstructure and Properties	206B	Wed-PM	287
The James Morris Honorary Symposium on Aluminum Wrought Products for Automotive, Packaging, and Other Applications: Fundamental Studies	207A	Tues-AM	138
The James Morris Honorary Symposium on Aluminum Wrought Products for Automotive, Packaging, and Other Applications: Automotive Alloys	207A	Tues-PM	189
The James Morris Honorary Symposium on Aluminum Wrought Products for Automotive, Packaging, and Other Applications: Continuous Casting and Related Technologies	207A	Wed-AM	244
The James Morris Honorary Symposium on Aluminum Wrought Products for Automotive, Packaging, and Other Applications: Processing Related Studies	207A	Wed-PM	288
The Rohatgi Honorary Symposium on Solidification Processing of Metal Matrix Composites: Overview of Developments in Cast MMCs	207B	Mon-AM	49
The Rohatgi Honorary Symposium on Solidification Processing of Metal Matrix Composites: Processing and Microstructure of MMCs - I	207B	Mon-PM	90
The Rohatgi Honorary Symposium on Solidification Processing of Metal Matrix Composites: Processing and Microstructure of MMCs - II	207B	Tues-AM	140
The Rohatgi Honorary Symposium on Solidification Processing of Metal Matrix Composites: Properties of MMCs	207B	Tues-PM	190
The Rohatgi Honorary Symposium on Solidification Processing of Metal Matrix Composites: Modeling and Nanocomposites	207B	Wed-AM	245
The Rohatgi Honorary Symposium on Solidification Processing of Metal Matrix Composites: Advanced Applications of MMCs	207B	Wed-PM	289
Titanium Alloys for High Temperature Applications - A Symposium Dedicated to the Memory of Dr. Martin Blackburn: Titanium Alloys for High Temperature Applications - In Memory of Dr. Martin Blackburn	201	Mon-PM	92
Titanium Alloys for High Temperature Applications - A Symposium Dedicated to the Memory of Dr. Martin Blackburn: Applications of High Temperature Titanium Alloys	201	Mon-PM	92
Titanium Alloys for High Temperature Applications - A Symposium Dedicated to the Memory of Dr. Martin Blackburn: Processing of High Temperature Titanium Alloys	201	Tues-AM	141
Titanium Alloys for High Temperature Applications - A Symposium Dedicated to the Memory of Dr. Martin Blackburn: Microstructure and Properties of High Temperature Titanium Alloys	201	Tues-PM	191
Titanium Alloys for High Temperature Applications - A Symposium Dedicated to the Memory of Dr. Martin Blackburn: Titanium Alloys for High Temperature Oxidation Resistance	201	Wed-AM	246

SESSION TITLE	ROOM	DAY	PAGE
Titanium Alloys for High Temperature Applications - A Symposium Dedicated to the Memory of Dr. Martin Blackburn: Titanium Based Intermetallic Alloys for High Temperature Applications - Alpha 2 and Orthorhombic	201	Wed-AM	247
Titanium Alloys for High Temperature Applications - A Symposium Dedicated to the Memory of Dr. Martin Blackburn: Titanium Based Intermetallic Alloys for High Temperature Applications - Gamma	201	Wed-PM	290
Ultrafine Grained Materials - Fourth International Symposium: Fundamentals of Ultrafine Grained Materials	217D	Mon-AM	50
Ultrafine Grained Materials - Fourth International Symposium: Processing and Microstructures I	217D	Mon-PM	92
Ultrafine Grained Materials - Fourth International Symposium: Processing and Microstructures II	217D	Tues-AM	142
Ultrafine Grained Materials - Fourth International Symposium: Microstructures and Properties	217D	Tues-PM	192
Ultrafine Grained Materials - Fourth International Symposium: Poster Session	217D	Tues-PM	194
Ultrafine Grained Materials - Fourth International Symposium: Mechanical Properties	217D	Wed-AM	248
Ultrafine Grained Materials - Fourth International Symposium: High Temperature and Physical Properties	217D	Wed-PM	291
Wechsler Symposium on Radiation Effects, Deformation and Phase Transformations in Metals and Ceramics: Irradiations Effects	208	Mon-AM	52
Wechsler Symposium on Radiation Effects, Deformation and Phase Transformations in Metals and Ceramics: Irradiation Microstructure/Microchemistry	208	Mon-PM	94
Wechsler Symposium on Radiation Effects, Deformation and Phase Transformations in Metals and Ceramics: Dislocations/Obstacles/Channeling	208	Tues-AM	144
Wechsler Symposium on Radiation Effects, Deformation and Phase Transformations in Metals and Ceramics: Irradiation Pressure Vessel	208	Tues-PM	201
Wechsler Symposium on Radiation Effects, Deformation and Phase Transformations in Metals and Ceramics: Irradiation Facilities and Techniques	208	Wed-AM	250
Wechsler Symposium on Radiation Effects, Deformation and Phase Transformations in Metals and Ceramics: Shape Memory Alloys	208	Wed-PM	292

TECHNICAL PROGRAM

Henry B. Gonzalez Convention Center; San Antonio, Texas USA; March 12-16, 2006

MONDAY

MONDAY AM

2006 Nanomaterials: Materials and Processing for Functional Applications: Functional Applications of Nanoscale Materials

Sponsored by: The Minerals, Metals and Materials Society, TMS Electronic, Magnetic, and Photonic Materials Division, TMS: Nanomaterials Committee

Program Organizers: W. Jud Ready, GTRI-EOEML; Seung Hyuk Kang, Agere Systems

Monday AM
March 13, 2006

Room: 214C
Location: Henry B. Gonzalez Convention Ctr.

Session Chairs: W. Jud Ready, GTRI-EOEML; Seung Hyuk Kang, Agere Systems

8:30 AM Introductory Comments

8:35 AM Invited

Oxide Nanobelts for Electromechanical Coupled Nanodevices: *Zhong Lin Wang*¹; ¹Georgia Institute of Technology

Piezoelectricity is an important phenomenon that characterizes the electromechanically coupled response of a material, and it has widely been used in science and technology. At nano-scale, most of the studies have been carried out for exploring the semiconducting properties of quantum dots, nanowires as well as nanotubes, but the nano-scale piezoelectric property remains an unexplored field until recently. In our laboratory, we have synthesized a series of novel nanostructures of ZnO, a material that is semiconducting and piezoelectric. The piezoelectric coefficient of a piezoelectric nanobelt has been found to be almost tripled compared to the value of the bulk, clearly indicating the exciting applications of piezoelectric ZnO nanobelts for nano-scale electromechanical coupled sensors, transducers, switches and resonators. This talk will focus on our recent progress in investigating the growth, formation process, kinetics and potential applications of piezoelectric nanobelts, nanorings and nanohelices.

9:00 AM Invited

Multifunctional Complex Oxide Heterostructures: *Ramamoorthy Ramesh*¹; ¹University of California

Complex perovskite oxides exhibit a rich spectrum of functional responses, including magnetism, ferroelectricity, highly correlated electron behavior, superconductivity, etc. There exists a small set of materials which exhibit multiple order parameters; these are known as multiferroics. We are studying the role of thin film growth, heteroepitaxy and processing on the basic properties as well as magnitude of the coupling between the order parameters. A very exciting new development has been the discovery of the formation of spontaneously assembled nanostructures consisting of a ferromagnetic phase embedded in a ferroelectric matrix that exhibit very strong coupling between the two order parameters through 3-dimensional heteroepitaxy. This work is supported by the ONR under a MURI program.

9:25 AM Break

9:40 AM Invited

Control of Nanomaterials Geometry for Advanced Technical Applications: *Sungho Jin*¹; ¹University of California, San Diego

The building block of nanotechnology is the nanomaterials. The fascination and great technical promises associated with nanoscale materials are based on the significant changes in their fundamental physical and chemical properties. For eventual engineering applications of nanomaterials, an ability to control not only their intrinsic structures and properties but also their basic geometry in terms of diameter, length, alignment, periodicity and spacing is essential. Synthesis of complex or ad-

vanced shapes and nanocomposites deviating from a simplistic circular or linear geometry is also useful for some applications. In this talk, some unique examples of controlling the geometry of nanomaterials such as carbon nanotubes, Ti-oxide nanotubes, magnetic nanoparticles, nanoislands, and other nanostructures will be described, and the implications of such geometry controls for potential electronic, chemical, mechanical and bio applications will be discussed.

10:05 AM Invited

The Performance of Carbon Nanotube Electron Sources: *Kenneth Teo*¹; N. de Jonge²; E. Minoux³; L. Gangloff¹; L. Hudanski³; O. Groening⁴; M. Allioux²; J. T. Oostveen²; D. Dieumegard³; F. Peauger³; P. Legagneux³; W. I. Milne¹; ¹University of Cambridge; ²Philips Research Laboratories; ³Thales Research and Technology; ⁴Federal Laboratories for Materials Testing and Research

Multiwalled carbon nanotubes/fibers (CN) are pursued here as field emission electron sources because of their whisker-like shape, high aspect ratio, high conductivity, thermal stability and resistance to electromigration. Here, the key performance parameters for individual CN emitters and CN emitters which are arrayed are investigated, and the factors which affect these parameters studied. For individual CN emitters, results which show remarkably stable, low noise, and bright electron emission have been obtained. The emitter current fluctuation observed over 1 hr was merely 0.5% and the emitter noise can be fitted to 1/f behavior over a bandwidth of 0.1 – 25 Hz, above which, random shot noise was observed to dominate over the emitter noise. The noise percentage was determined to be 0.08% +/- 0.06% (ie. signal to noise ratio of 761-5000) various CNT emitters operated at several current levels. The single CNT emitter was also brighter than tungsten cold emitters or Schottky.

10:30 AM Invited

Growth of Y-Junction Single-Wall Carbon Nanotube and Its Application: *Wonbong Choi*¹; ¹Florida International University

The Y-junction single-wall carbon nanotubes (SWNTs) have attracted much attention due to their potential to be used as future nano electronics, where the third terminal is used for controlling the switching, power gain, or other transiting purposes. We synthesized Y-junction SWNTs using controlled catalysts by chemical vapor deposition. Transmission electron microscopy confirmed the formation of Y-junction SWNTs with diameters of 2 – 5 nm. Radial breathing mode peaks of Raman show that our sample has both metallic and semiconducting, indicating the possible formation of Y-branching with different electrical properties. The electrical transport properties across Y-SWNTs show rectifying behavior and exhibit ambipolar at room temperature. Gating operation shows the sub-threshold swing of 0.7~ 1V/decade and Ion/off ratio of 10⁴~10⁵ with off-state leakage current ~10⁻¹³A. Surface modified Y-junction SWNT indicates its potential application as sensor. The further enzyme catalyst modification is employed to sense specific biological analytsts through electrochemical technique.

10:55 AM Break

11:10 AM Invited

Novel Electrical Phenomena in Carbon Nanotube Y-Junctions: *Prabhakar Bandaru*¹; Chiara Daraio¹; Sungho Jin¹; Apparao Rao²; ¹University of California, San Diego; ²Clemson University

Novel nano-engineered Carbon Nanotube (CNT) morphologies such as Y- and T-junctions have been predicted to have new functionalities and herald a new generation of nano-electronic components. These non-linear CNT forms have a natural asymmetry at the junction due to the presence of non-hexagonal defects, required for energy minimization. The carrier delocalization and the inevitable presence of catalyst particles, introduced during synthesis, at the bends induce a net charge and scattering which can be exploited for electronics. I will discuss the structure-electrical prop-

erty correlations in one particular form- the Y-junction. I will show evidence for novel electrical behavior, such as an abrupt modulation of the current from an on- to an off- state, presumably mediated by defects or the topology of the junction. The mutual interaction of the electron currents in the three branches of the Y-junction is shown to be the basis for a potentially new logic device.

11:35 AM Invited

Fabrication and Performance of Novel Carbon Nanotube-Based Biofuel Cell and Biosensor: Yubing Wang¹; Zafar Iqbal¹; ¹New Jersey Institute of Technology

We have grown thin films of vertically aligned single wall carbon nanotubes (SWNTs) on doped silicon wafers using a chemical vapor deposition (CVD) process with ethanol as carbon source and densely deposited bimetallic cobalt/molybdenum as catalyst. Glucose oxidase (GOx) and bilirubin oxidase (BOD) enzymes dissolved in a buffer were reacted with the nanotube tips by our recently developed rapid microwave process¹ and also by electrochemical reaction. A non-compartmentalized glucose/air biofuel cell with SWNT/GOx as anode and SWNT/BOD as cathode in an electrolyte comprised of 100 mM β -D-glucose in pH 7 phosphate buffer, was assembled. The performance characteristics of the biofuel cell and that of a glucose biosensor consisting of a SWNT/GOx sensing electrode and a platinum electrode in a similar electrolyte, will be discussed. ¹Y. Wang, Z. Iqbal and S. Mitra, J. Amer. Chem. Soc. – to be published.

12:00 PM Invited

Long Carbon Nanotubes and Nanotube Cotton by Chemical Vapour Deposition: Yuntian T. Zhu¹; Lianxi Zheng¹; Michael J. O'Connell¹; Steve K. Doorn¹; ¹Los Alamos National Laboratory

In this talk we report the synthesis of long carbon nanotubes and carbon nanotube cotton by catalytic chemical-vapour-deposition. Both were grown on Si substrates. SEM images following a single nanotube revealed its length as 40 μ m, which is a world record. Atomic force microscopy and Raman spectrum were performed, indicating that carbon nanotubes are single walled with diameter range of 1nm~2.25nm. The evolution of surface morphology according to growth conditions was also studied using scanning electronic microscopy. Growth and termination mechanism will be discussed. The carbon nanotube cotton is made of puffy, tangled long multi-wall nanotubes, resembling cotton and individual cotton fibers. The nanotube cotton can be easily spun into nanotube fibers. These long nanotubes and nanotube cotton may have functional applications such as nano electric wires and scaffolding for neuronal growth.

3-Dimensional Materials Science: Microstructure Representation

Sponsored by: The Minerals, Metals and Materials Society, TMS Structural Materials Division, TMS: Advanced Characterization, Testing, and Simulation Committee

Program Organizers: Jeff P. Simmons, U.S. Air Force; Michael D. Uchic, Air Force Research Laboratory; Dorte Juul Jensen, Riso National Laboratory; David N. Seidman, Northwestern University; Anthony D. Rollett, Carnegie Mellon University

Monday AM Room: 205
March 13, 2006 Location: Henry B. Gonzalez Convention Ctr.

Session Chairs: P. W. Voorhees, Northwestern University; Craig S. Hartley, El Arroyo Enterprises LLC

8:30 AM Introductory Comments**8:35 AM Invited**

Three-Dimensional Microstructural Residual-Stress Response Isosurfaces: Edwin R. Fuller¹; Thomas Wanner²; David M. Saylor³; ¹National Institute of Standards and Technology; ²George Mason University; ³Food and Drug Administration

When a polycrystalline material with crystalline thermal expansion anisotropy is cooled (or heated), residual stresses develop within the microstructure. These stresses develop into a network structure with a length

scale that encompasses many grains. The size of the network structure depends strongly upon the intergranular misorientation distribution function, but is also influenced by the grain orientation distribution function. This phenomenon, while readily apparent in two-dimensional, microstructure-based finite-element simulations, is not so clear in similar three-dimensional simulations. To elucidate the microstructure-induced response, response isosurfaces are generated by defining surfaces at a specific threshold level of residual-stress response. The resulting distribution of residual stresses throughout the microstructure is considered as a geometric object itself: a microstructure response isosurface. Computational homology invariants (e.g., Betti numbers) are used to characterize and quantify these residual-stress response isosurfaces.

9:00 AM

The Three-Dimensional Microstructure of Materials: D. Kammer¹; J. Wilson¹; P. W. Voorhees¹; S. A. Barnett¹; R. Mendoza¹; ¹Northwestern University

Recent advances in computational and experimental techniques now allows for the routine visualization of the three-dimensional microstructure of materials. This opens new routes to explore the relationship between materials processing and structure. Examples of three-dimensional reconstructions of microstructure in systems ranging from solid oxide fuel cells to dendritic solid-liquid mixtures will be given. Using this three-dimensional information it is possible to quantify the morphology of complex microstructures using measurements of the interfacial shape distribution, the probability of finding a patch of interface with a given pair of principle curvatures, the spatial anisotropy of the microstructure via measurements of the normals to the interfaces, and the genus of the microstructure. We will also discuss the measurement of the triple junction line length in solid oxide fuel cells, a crucial input to understanding the electrochemical performance of these cells.

9:20 AM

Characterizing 3D Microstructure Using the Minkowski Functionals: James Steele¹; ¹Steele Works

3D microstructural patterns can be globally quantified by the set of valuations (parameters) known as the Minkowski Functionals. These patterns represent 3D spatial arrangements of thermodynamic phases as embedded within E³. The four parameters, which constitute the Minkowski Functionals are; volume, V(X), surface area, S(X), integral mean curvature, M(X), and integral Gaussian curvature, K(X), for a 3D object X. These four parameters form a complete set of global descriptors for 3D microstructure when estimated as volume densities. This is a result of the famous characterization theorem of Hadwiger (1957), which shows that the four parameters, {V_v, S_v, M_v, K_v} form a complete set of global descriptors among those that are kinematically invariant. Stereological methods for estimating volume densities of the Minkowski Functionals will be described. Examples of measurements of the Minkowski Functionals for characterizing dendrites, porosity in sandstone, and bi-continuous "sponge-like" copolymers will be discussed.

9:40 AM

Correlations in Three-Dimensional Evolving Microstructures: Ke-Gang Wang¹; Martin Glicksman¹; ¹Rensselaer Polytechnic Institute

We will discuss our recent modeling efforts to study quantitatively the evolution of spatial and temporal correlations in aging phase mixtures. Large-scale simulations will be shown of three-dimensional microstructures evolving via diffusion-mediated multiparticle diffusion. Spatial correlations developed in such microstructures are revealed via simulation, along with associated stochastic phenomena that occur during aging. Measured pair distribution functions will be shown. Mean inter-particle spacing is characterized in our study as a function of aging time through the distribution of spacings between pairs of phase domains, and through the distribution of nearest-neighbor distances. Characterizing local features developed in a two-phase microstructure employing statistical measures permits demonstrating their influence on the properties of the material. Finally, theoretical and computational results from this study will be compared with experimental observations on two-phase alloys.

10:00 AM

Percolation Theory for Two-Phase Materials with Nonrandom Topologies: Megan E. Frary¹; Christopher A. Schuh¹; ¹Massachusetts Insti-

tute of Technology

Percolation theory is commonly used to develop microstructure-property relationships for two-phase materials. Although many composite microstructures have engineered spatial correlations among the constituent phases, percolation-based models often assume random arrangement of the phases. Using 3-D microstructure simulations, we systematically study topologically-varied two-phase microstructures with different states of ordering or segregation. We find that the topological state of the microstructure strongly affects percolation behavior and that the percolation threshold changes by as much as ± 0.20 when local correlations are introduced. In order to quantify these effects, we propose that all microstructures be mapped into a "correlation-space", upon which percolation behavior is easily superimposed. In this way the correlation-dependence of properties such as the percolation threshold, connectivity length and mean cluster size of the microstructure can be easily predicted.

10:20 AM Break

10:40 AM

Reconstructing 3D Microstructures: A Comparison between Simulated Annealing and Evolutionary Algorithm Methods: David Basanta¹; Elizabeth A. Holm²; Peter Bentley³; *Mark Miodownik*¹; ¹King's College London; ²Sandia National Laboratories; ³University College London

We have investigated two computational methods to reconstruct 3D microstructures from 2D inputs. The first method is a simulated annealing approach based on voxel swapping pioneered by Torquato et al.¹ and the second method is a genetic algorithm approach based on developmental evolutionary algorithm MicroConstructor¹. We take a range of morphologically different 2D input microstructures and use both methods to reconstruct 3D microstructures which have the same stereological parameters. We find that each method performs better than the other on different types of input structure, but that in general the genetic algorithm outperforms the simulated annealing as the system size increases. ¹Yeong, C.L.Y. and Torquato, S. Reconstructing random media. II. Three-dimensional media from two-dimensional cuts. *Physical Review E*, 58:224-233 (1998). ²Basanta D., Miodownik M.A., Holm E.A., and Bentley P.J. Evolving 3D Microstructures from 2D Micrographs using a Genetic Algorithm. *Met Trans A*, 36A:1643-1652. (2005).

11:00 AM

A Simulated Annealing Monte Carlo Approach to the Reconstruction of Two-Phase Microstructures: *Marc J. DeGraef*¹; Jeremiah P. MacSleynne¹; ¹Carnegie Mellon University

The microstructural description of Ni-base superalloys requires the use of two-point correlation functions and lineal path functions. After these functions have been obtained from experimental observations, such as focused ion beam serial sectioning, they may be used to generate new microstructures that are similar to the input microstructures in the statistical sense. In other words, anisotropic 1- and 2-point correlation functions and other higher order characterizations are similar to data compression schemes, where the original digital microstructures are distilled to a few quantities. These few quantities or characterizations, whenever necessary, can be "decompressed" back to an ensemble of digital microstructure images (with some unavoidable loss of detail). We will illustrate this reconstruction by means of a simulated annealing Monte Carlo approach. We will discuss the use of 2-point correlation functions along specific directions relative to the microstructure, as well as the use of the full 3D 2-point correlation function.

11:20 AM

Simulation Models to Generate Realistic Microstructures of Discontinuously Reinforced Aluminum Alloy (DRA) Composites Using Real Particle Morphologies: *Harpreet Singh*¹; Arun Gokhale¹; ¹Georgia Institute of Technology

Computer models have been used to simulate microstructures of DRA composites. This novel technique can generate realistic microstructures by combining the use of real particle morphologies/shapes with non-uniform (clustered) spatial arrangement as observed in the real microstructures. Both short-range and long range order of real microstructures has been captured in the simulations by generating sufficiently large microstructural windows containing over ten thousand particles at high resolution. Simulated microstructures were then statistically compared to

the real ones using two-point correlation functions and were shown to match closely up to 500 micron length.

11:40 AM

Automated Microstructural Feature Representation Using Principal Component Analysis and Classification Techniques: *Jeff P. Simmons*¹; Dennis M. Dimiduk¹; Marc J. DeGraef²; ¹U.S. Air Force; ²Carnegie Mellon University

Fusing computer and experimental techniques, along with a proliferation of simulation techniques, creates opportunities for generating massive collections of statistically significant microstructural data. Taking full advantage of these opportunities requires accelerating the data analysis rate and developing an ability to use the data for solving multiple problems. The human resources available for analysis will likely decrease for the foreseeable future, requiring the development of optimal representations of data to be automated to keep pace with its generation. Utilizing this information will require that representations be standardized without discarding information simply because it does not appear to be relevant to the issues that motivated its generation. Towards these ends, a framework for representing particle and particle neighborhood information in microstructures has been developed that automates sample selection, representation, and classification into typical/rare event classes. It is expected that these basic stochastic building blocks will enable development of automated representations of microstructures.

12:00 PM

An Information-Theoretic Approach for Obtaining Property PDFs from Macro-Specifications of Microstructural Variability: *Nicholas Zabarav*¹; Veera Sundararaghavan¹; Sethuraman Sankaran¹; ¹Cornell University

Probability distribution functions (PDFs) providing a complete representation of property variability in polycrystalline materials are difficult to obtain. Reconstruction of probability distribution of material properties on the basis of limited morphological information is an inverse problem of practical significance since many macroscopic properties depend strongly on geometrical variability of the micro-constituents. We characterize the unknown probabilities of the microstructural parameters making use of the macro-information given in the form of average values (such as average grain sizes) and using the concepts of maximum information entropy (MAXENT) and stochastic geometry. The PDFs are used to generate consistent samples of microstructures whose properties are assessed using a multi-scale framework based on a newly developed fully implicit Lagrangian large strain homogenization framework.

Advanced Materials for Energy Conversion III: A Symposium in Honor of Drs. Gary Sandrock, Louis Schlapbach, and Seijirau Suda: Plenary Session

Sponsored by: The Minerals, Metals and Materials Society, TMS Light Metals Division, TMS: Reactive Metals Committee

Program Organizers: Dhanesh Chandra, University of Nevada; John J. Petrovic, Petrovic and Associates; Renato G. Bautista, University of Nevada; M. Ashraf Imam, Naval Research Laboratory

Monday AM
March 13, 2006

Room: 214B
Location: Henry B. Gonzalez Convention Ctr.

Session Chairs: Sunita Satyapal, U.S. Department of Energy; Scott Jorgensen, General Motors; Farshad Bavarian, Chevron Texaco Technology Ventures LLC

8:30 AM Introduction to the Symposium by Chandra, Petrovic, Bautista and Imam

8:45 AM Presentation of Plaques and Comments by Gary Sandrock

8:55 AM Presentation of Plaques and Comments by Luis Schlapbach

9:05 AM Presentation of Plaques and Comments by Seijirau Suda

9:15 AM Plenary

The Challenge of Vehicular Hydrogen Storage: Grace Ordaz¹; John J. Petrovic²; Carole Read¹; *Sunita Satyapal*¹; George Thomas³; ¹U.S. Department of Energy; ²Los Alamos National Laboratory; ³Sandia National Laboratories

Hydrogen is a potential energy carrier for vehicular applications. However, hydrogen-powered vehicles require a driving range of greater than 300 miles in order to meet customer needs and effectively compete with other technologies. For the overall vehicular fleet, this dictates that a range of 5-13 kg of hydrogen be stored on-board, within stringent weight, volume, and system cost constraints. Vehicular hydrogen storage thus constitutes a major scientific and technological challenge. To meet this challenge, the DOE's National Hydrogen Storage Project has been initiated which focuses on materials-based technologies. Centers of Excellence in metal hydrides, chemical hydrides, and carbon-based materials have been established, as well as independent university and industry projects in the areas of new concepts/materials, hydrogen storage testing, and storage system analysis. Recent technical progress in each of these areas will be presented as well as collaborative hydrogen storage activities under the International Partnership for the Hydrogen Economy (IPHE).

9:40 AM Plenary

Gary Sandrock and Metal Hydrides: *James J. Reilly*¹; ¹Brookhaven National Laboratory

Certainly it would be impossible to give an historical perspective of metal hydride energy storage compounds and their current status without recording the contributions of Gary Sandrock. Gary received his Ph.D. in metallurgy from Case Western Reserve University in 1971 and was employed by INCO in the same year. In 1974 turned his research interests towards rechargeable AB and AB₅ metal hydrides. This lecture will take us from that point to the present time. It will be noted that Gary was involved in almost every novel aspect of the field over a thirty year period; low temperature, low capacity intermetallic compounds for H storage; Ni/MH batteries and the high capacity alanates and alanes of current interest. In addition he currently serves as the U.S. Operating Agent (Task 12) to the IEA.

10:05 AM Break**10:20 AM Plenary**

Sodium Borohydride as the Hydrogen and Protide Source: *Seijia (Seiji) Suda*¹; Zhou-Peng Li¹; Yang-Ming Sun¹; Bing-Hong Liu¹; Nobuto Morigasaki¹; Singo Hara¹; ¹Materials and Energy Research Institute Tokyo, Ltd.

Sodium borohydride (SBH: NaBH₄) can be regarded as one of the most practical H-storage material today. It contains 10.6mass% of hydrogen, which is available under ambient conditions as the safe source of gaseous hydrogen (H₂) by catalytic hydrolysis for PEMFC and protide (H-) by applying directly as the aqueous solution for DBFC (Direct Borohydride Fuel Cell). As SBH is used as the form of aqueous solution in either application, the practical H-capacity is considerably reduced to 3 to 6wt% because of the solubility limits and the formation of crystalline materials. The SBH solution forms condensed sodium metaborate (SMB: NaBO₂·4H₂O) solution as "spent fuel" and it may cause several technical issues. Current SBH production process is definitely unaffordable in the future H-storage applications and SMB must be recyclable and regenerative to produce SBH from the waste-treatment of "B" H-containing materials and cost-reduction viewpoints.

10:45 AM Plenary

Important Events in the Recent Past and Near Future of Hydrogen Storage for Mobile Applications: *Scott Jorgensen*¹; ¹General Motors

Hydrogen storage research has a long history, with a recent surge of new materials and new concepts. Important progress has occurred in the area of solid phase materials for storage, tank materials and engineering, and new types of materials. More importantly, an understanding of these materials is beginning to allow prediction of hydrides with improved properties. The performance of these new hydrogen storage systems begins to approach that of physical containment methods. The next step is to directly target performance that will permit commercialization.

11:10 AM Keynote

Activated MgH₂ Powders: Principles of D-Metal Activation Process, Mass Production at Factory Scale, Design and Numerical Simulation of a Tutorial Tank: *Daniel Fruchart*¹; Jean Charbonnier¹; Patricia de Rango¹; Michel Jehan²; Philippe Marty³; Salvatore Miraglia¹; Sophie Rivoirard¹; Nataliya Skryabina⁴; ¹Centre National de la Recherche Scientifique; ²MCP Technologies; ³LEGI-GRETH; ⁴Perm State University

The main principles of activation process with d-metal additions to magnesium powder for fast absorption and desorption kinetics have been evaluated from X-ray diffractometry, in-situ neutron diffraction experiments, as well as from kinetics and PCT measurements. More than 6 wt% reversible hydrogen mass can be stored reversibly and the reaction kinetic was found quite fast even at rather low temperature. Production of such activated powders at a pilot scale in a factory has been made effective by using a two step route with a dedicated autoclave for the production of a primary hydride and then the delivery of kg batches of ball-milled MgH₂ using metal catalysts. Furthermore, we have developed a small size but well equipped with many sensors MgH₂ tank to monitor the gas, heat and cooling flows for time optimized charge/discharge. This experimental operations are analyzed parallel using a specific 2D code for numerical simulation.

11:35 AM Invited

Novel and Safe Sodium Borohydride Based Fuel: *Menachem Givon*¹; Jonathan Goldstein¹; ¹HyoGen Ltd

Sodium borohydride is a good hydrogen carrier for chemical hydride based vehicle systems (the hydrogen content of this material alone is above 10wt%), and borohydrides may well become an important part of a future "Hydrogen Economy". However, sodium borohydride aqueous solutions in use today for hydrogen generation are corrosive and not fully stable, especially at high ambients. In addition, the by-product of hydrogen generation, sodium metaborate, has poor solubility in water and tends to solidify and block pipes, pumps and valves. As a result, systems based on aqueous borohydride only achieve about 4wt% hydrogen storage fraction. A new approach is described, based on encapsulated solid borohydride in a non-aqueous carrier fluid, in which the sodium metaborate by-product is processed, pelletized and stored onboard prior to refueling as a pumpable slurry. This approach leads to practical hydrogen storage fractions of over 7wt% on a systems basis.

Aluminum Reduction Technology: Environmental Elements

Sponsored by: The Minerals, Metals and Materials Society, TMS Light Metals Division, TMS: Aluminum Committee

Program Organizers: Stephen Joseph Lindsay, Alcoa Inc; Tor Bjarne Pedersen, Elkem Aluminium ANS; Travis J. Galloway, Century Aluminum Company

Monday AM
March 13, 2006

Room: 7A
Location: Henry B. Gonzalez Convention Ctr.

Session Chair: Paul G. Campbell, Alcoa Inc

8:30 AM

Soderberg Technology – A Challenge or an Opportunity: *Viktor Mann*¹; ¹RUSAL

One of the key objectives shared by aluminum producers worldwide is to reduce the environmental impact of aluminum production. RUSAL, jointly with some of the world's leading aluminum producers using the Soderberg technology, is undertaking a research program to reduce the environmental impact through modernizing Soderberg cells, installing additional scrubbers, as well as seeking ways to improve technological processes. RUSAL's Engineering and Technology Center is leading the company's effort to reduce volatile hydrocarbon emission levels (bringing them in line with the OsPar Convention recommendations), lower anode mix consumption factor per 1 tone of aluminum by 5-8%, and raise current density to the unparalleled figure of 0.82-0.85 A/sq. cm. (190-210

kA). The new Soderberg or the so-called “colloid anode” technology, is being developed through an upgrade approach that allows introduction of new technology with reasonable investment, making it highly competitive economically and viable environmentally.

9:00 AM

Methods for Calculating PFC Emissions from Primary Aluminium Production: *Jerry Marks*¹; ¹International Aluminium Institute

Accurate calculation of PFC emissions are of increasing importance for primary aluminium producers because of the adoption of the Kyoto Protocol by a number of countries and because a number of other companies have entered into formal agreements with their national governments to reduce greenhouse gas (GHG) emissions. The methods for calculating PFC emissions rates per tonne of aluminum produced have not been updated since 2000. The Intergovernmental Panel on Climate Change (IPCC) is in the process of developing revised Good Practice Guidelines that will result in a number of changes in current methodology. This paper describes the background for these changes, the proposed new equations and the impact of these changes on emissions of PFCs.

9:30 AM

Root Causes of Variability Impacting Short Term In-Plant PFC Measurements: *Neal R. Dando*¹; *Weizong Xu*¹; *Lise Sylvain*¹; ¹Alcoa Inc

The perfluorocarbon gases tetrafluoromethane (CF₄) and hexafluoroethane (C₂F₆) are known greenhouse gases that are emitted from aluminum smelters during transient conditions known as anode effects. Alcoa has voluntarily monitored PFC emissions from aluminum for over 10 years under a voluntary agreement known as the Voluntary Aluminum Industrial Partnership with the US Environmental Protection Agency. The purpose of these relatively short duration (2-3 day) PFC studies was to generate technology-specific “slope” terms that could be used to calculate future PFC emissions from aluminum smelters. In the present effort, PFC emissions were monitored for one-month durations at both pre-bake and Soderberg smelters in order to collect data on significant populations of anode effects of varying duration and kill strategy. The purpose of this study was to identify and characterize the process-based root causes of variability observed in short term studies of PFC emissions.

10:00 AM Break

10:15 AM

Reduction of HF Emissions from the TRIMET Aluminum Smelter Optimizing Dry Scrubber Operations and Its Impact on Process Operations: *Martin Iffert*¹; *Markus Kuenkel*¹; *Maria Skyllas-Kazacos*²; *Barry Welch*²; ¹Trimet Aluminium AG; ²University of New South Wales

Aluminum smelters worldwide are challenged by increasing ecological and economical pressure. Higher line amperages gain production output but increase the HF load on dry scrubbers. Another important factor today is the tight alumina market, hence it is necessary to accommodate dry scrubber and potline operations to different alumina sources and qualities regarding their HF generation and scrubbing efficiency as well as its impact on bath chemistry. The TRIMET smelter optimised dry scrubber operations by the use of a laser based HF measuring system in each of the 20 filter modules. Based on the HF level in the outlet of each filter the alumina flow to each filter is pulse-duration modulated, thus tightly control the HF emission level in the outlet gas. This paper describes the application of the new measuring and control principle and its impact on HF scrubbing efficiency and bath chemistry.

10:40 AM

Impact of Pot Cover Integrity on HF Emission and Evolution: *Neal R. Dando*¹; *Robert Tang*¹; ¹Alcoa Inc

Aluminum electrolysis pots evolve gaseous fluoride (HF) owing to hydrolysis of the molten salt bath. The fluoride that enters the fume treatment system is considered evolution, while that which does not enter or escapes the fume treatment system is considered emission. A range of smelter-owned factors such as pot chemistry, operating practice, pot tending practice and ore feeding affect the dynamics of HF evolution from smelting cells. Issues such as hooding efficiency, hooding flow rates and crust cover integrity are primary factors impacting HF emissions from the pots. Real-time HF evolution and emission monitoring was performed on individual operating smelting pots to generate quantitative measurements

of evolved fluoride as a function of crust cover condition. The purpose of this effort was to gain a better understanding of the relationship between fluoride evolution and emission as impacted by pot tending practices.

11:05 AM

Correlation of Fluoride Evolution with on Line Gas Duct Temperature: *Nilton Freixo Nagem*¹; *Eliezer S. Batista*¹; *Ari F. Silva*¹; *Valerio Gomes*¹; *Haroldo Ferreira*¹; *Raimundo R. S. Mendes*¹; ¹Consórcio de Alumínio do Maranhão - ALUMAR

A global strategy to reduce all emissions sources is in action. Continuous improvement and sustainable development are the driving forces to seek new ways to reduce and control fluoride emissions. The fluoride generation is mainly produced by smelting activity; it forms by the reaction of a source of hydrogen (moisture, H ion) and molten or volatilized cryolitic bath. Literature shows the impact of operation activities on fugitive fluoride emission. This work shows an on line duct temperature measurements of the pot gas and correlate with fluoride emissions (using an open pass tunable diode laser). The conclusion demonstrates the correlations with the operations activities, process parameters with fluoride emission. Finally, this paper shows that the pot duct temperature can be an important process parameter to control and minimize the fugitive fluoride. This system is able to monitor pot conditions and operational activities based on temperature variation of the pot gas.

11:30 AM

New Design of Cover for Anode Trays: *Jean-Pierre Gagne*¹; *Robin Boulianne*¹; *Jean-François Magnan*¹; *Marc-André Thibault*¹; *Gilles Dufour*²; *Claude Gauthier*²; ¹STAS; ²Alcoa

During the production of aluminium in smelters, the anodes used in electrolysis cells have to be replaced frequently. Anode butts are usually disposed on anode trays for transportation and cooling, a practice where Hydrogen Fluoride (HF) is emitted in large quantities. In 2001, special lids developed by Alcoa Deschambault to fit on the anodes trays close and open according to the anode movements, with the result of significant reductions of HF emissions. However, they are expensive to maintain and require short life consumable parts. In January 2004, STAS and Alcoa decided to develop a more efficient design of lid, with lower maintenance costs and no need of consumable material (like red silicone cushions). This paper presents a summary of the work performed to obtain the new design as well as a summary of the test results.

11:55 AM

Running Results of the SPL Detoxifying Pilot Plant in CHALCO: *Wangxing Li*¹; *Xiping Chen*¹; ¹Chalco

A new process to detoxify SPL had been developed in Chalco in December 2003, and the first SPL detoxifying pilot plant of China had been established in Chalco by the end of 2004. During the past five months of 2005, the pilot plant has been put into running. Till the end of May 2005, 104 tons SPL have been detoxified, and 119 tons innocuous SPL solid residue have been received for processing. The average soluble F— and CN—in the solid residue are respectively 39.7mg/l and 0.053mg/l, which are lower than China national permitted discharge standard 50.0mg/l and 1.0mg/l, the final product is benign. Now the pilot plant is working well, and experiments on how to make use of the benign SPL solid residue are processing.

12:20 PM End

Aluminum Reduction Technology: Inert Anodes - Part I

Sponsored by: The Minerals, Metals and Materials Society, TMS Light Metals Division, TMS: Aluminum Committee

Program Organizers: Stephen Joseph Lindsay, Alcoa Inc; Tor Bjarne Pedersen, Elkem Aluminium ANS; Travis J. Galloway, Century Aluminum Company

Monday AM Room: 7B
March 13, 2006 Location: Henry B. Gonzalez Convention Ctr.

Session Chair: Geoffrey Paul Bearne, Comalco Ltd

8:30 AM

Anodic Overvoltage on Metallic Inert Anodes in Low-Melting Bath: Jomar Thonstad¹; Adolf Kiszka²; Jan Hives³; ¹Norwegian University of Science and Technology; ²University of Wroclaw; ³Slovak Technical University

For inert anodes the standard emf is about one volt higher than for carbon anodes, and it is then important that the anodic overvoltage is as low as possible in order to save energy. An overview of existing literature will be given. In the experimental work inert anodes made of a Cu-Ni-Fe alloy, with the composition 40 Cu-30 Ni-30 Fe (wt%), were tested in a low-melting electrolyte at 750°C with the composition 55 mol% NaF and 45 mol% AlF₃, containing about 10 wt% excess alumina (weighed-in 13 wt%). Anodic overvoltage data were derived from impedance measurements. In unstirred melts it was observed that the Tafel lines bent upwards at quite low current densities, indicating diffusion limitations. In stirred melts straight Tafel lines were obtained, the overvoltage at 1 A/cm² being of the order of 0.4 V. The diffusion coefficient of the electroactive species (dissolved alumina) was 2.23.10⁻⁵ cm²/s.

8:55 AM

Gas Evolution on Graphite and Oxygen-Evolving Anodes during Aluminium Electrolysis: Torstein Utigard¹; Laurent Cassayre²; Gabriel Plascencia³; Tanai Marin⁴; Sharon Fang¹; ¹University of Toronto; ²Institute of Transuranium Elements; ³CIITEC – IPN; ⁴University of Chile

Anode gas evolution, growth and flow behaviour during aluminium electrolysis have been investigated using various experimental techniques, including water modelling, X-ray visualization and direct observation. Video recordings of oxygen-evolving anodes (SnO₂, Cu, Cu-Ni, Cu-Al) and carbon anodes were performed in laboratory electrolysis cells of various scales. The water model also investigated the effects of slotted anodes on the gas escape from beneath large anodes. Beneath large horizontal anodes individual bubbles form and are then subsequently swept away by large sweeping bubbles flowing rapidly beneath the bottom surface. The gas behaviour on oxygen evolving anodes was very different from that with carbon with the formation of very small bubbles that released very quickly from the anode due to improved wetting of the anode by the electrolyte.

9:20 AM

The Oxygen-Evolving Metallic Anode for Aluminum Reduction Cells: Thinh Nguyen¹; Vittorio De Nora¹; Rene Von Kaenel¹; ¹MOLTECH SA

The new nickel-doped cobalt oxide coating greatly improves the performance of the oxygen-evolving metal anode. The active coating is obtained by the oxidation of the Co-Ni alloy coating electroplated onto the surface of the anode. The dense and stable structure of the active coating constitutes a physical barrier against gaseous AlF₃ and O₂. Corrosion of the alloy substrate by fluoridation is suppressed, and its stationary oxidation rate under anodic polarization is very low. The experimental oxygen potential on the Co(Ni)O-coated metal anode has been measured. Analyses of the chemical environment and the temperature above the melt-line induced the development of a stem with a steel core protected by a copper oxide envelope. The structural stability of the stem under attack by HF at high temperature has been proved by testing under industrial conditions. The metallic anode-stem system has been tested successfully in cells at currents up to 30 kA.

9:45 AM

Modeling of a 30 kA Metallic Anode Test Cell: Jacques Antille¹; Laurent Klinger¹; Thinh Nguyen²; Vittorio De Nora²; ¹KAN-NAK SA; ²MOLTECH SA

A 30 kA oxygen-evolving metallic anode test cell is modeled mathematically to predict the energy consumption and thermal balance under given operating conditions. The model is then used to find the optimal anode-to-cathode distance and the critical anode current densities for an improved design. The model predictions are validated by measurements on the 30 kA test cell.

10:10 AM Break

10:20 AM

Technical and Economical Evaluation of the Oxygen Evolving Metallic Anode in Aluminum Reduction Cells: Rene Von Kaenel¹; Vittorio De Nora¹; Thinh Nguyen¹; ¹MOLTECH SA

A cell with metallic anodes could have a higher energy consumption than the conventional cell because the oxygen-evolving reaction has a higher thermodynamic potential than those at the conventional anode, while being less exothermal. As in conventional cells, good thermal balance is essential to ensure protection of the cell structure with a side ledge. To ensure thermal balance and minimise energy consumption, cells with metallic anodes must operate at a high current level, by maximising the anode current density and the active surface area. In commercial cells, two practical factors limiting the current density are the anode to cathode distance and the anode current density. An economic evaluation of the metallic anode is presented, for retrofitting a conventional cell and for a new design in a non-horizontal configuration. Production cost savings and further developments direction are discussed. A significant competitive advantage is achieved by using metallic anodes.

10:45 AM

Electrochemical Behavior of Metals and Binary Alloys in Cryolite-Alumina Melts: G. A. Tsirlina¹; E. V. Antipov¹; A. Yu. Filatov¹; V. V. Ivanov²; S. M. Kazakov¹; P. M. Mazin¹; V. M. Mazin¹; V. I. Shtanov¹; Yu. A. Velikodny¹; D. A. Simakov²; S. Yu. Vassiliev¹; ¹Moscow State University; ²Engineering and Technological Centre, Ltd.

Electrochemistry of Ni, Fe, and Cu metals as well as of their binary alloys (including alloys with Al) is reported. To determine the characteristic potential regions of certain redox processes in cryolite-alumina melts, cyclic voltammetry, chronopotentiometry, and preparative potentiostatic electrolysis of Fe(III) and Cu(II) oxides dissolved in the melt are applied. The nature of electrolysis products and thin oxide films formed under open circuit and in the course of anodic polarisation is clarified by means of X-ray diffractometry and EDX analysis. Finally, some general trends of selective dissolution and oxidation for binary systems are formulated in the context of predicting the role of each component in the multicomponent alloys tested as the future inert anodes.

11:10 AM

Electrical Conductivity of Low Melting Cryolite Melts: Olga Tkatcheva¹; Alexander Redkin¹; Yurii Zaikov¹; Vladimir Khokhlov¹; Alexei Apisarov¹; Vasylii Kryukovsky²; Anton Frolov³; ¹Institute of High Temperature Electrochemistry; ²Russian Aluminum Company RUSAL; ³Engineering-Technological Center Ltd, RUSAL

The modern industrial aluminum electrolysis is carried out at high temperature that leads to great energy consumption and fast corrosion of the construction materials. This situation can be improved by using low melting electrolytes such as KF-AlF₃ (CR=1,3) with melting temperature below 600°C. The most important in this case is the value of electrical conductivity because it decreases with temperature very fast. The electrical conductivity of molten system KF-AlF₃ (CR=1,3) has been measured in 680-770°C temperature range in capillary cell by impedance method. The electrical conductivity temperature dependence in molten systems KF-AlF₃-Al₂O₃ (CR=1,3), KF-AlF₃-LiF (CR=1,3), KF-AlF₃-Al₂O₃-LiF (CR=1,3) have been measured in Egear type cell. The Al₂O₃ concentration was varied from 0 to 4,8 wt.% and the LiF concentration was changed from 0 to 10 wt.%. The results obtained show the possibility of usage of this electrolyte for industrial electrolyses.

11:35 AM

Study on the Nickel Ferrate Spinel Inert Anode for Aluminum Electrolysis: *Yihan Liu*¹; Guangchun Yao¹; Hongjie Luo¹; Xiaoming Zhang¹; ¹Northeastern University

In the late decades, a series of new technologies such as inert anode, wettable cathode and lower temperature electrolysis for primary aluminum production had been studied, for saving energy, debasing cost and erasing environment pollution. The thesis studied the preparation and the properties of cermet inert anode based on NiFe₂O₄ spinel. We choose the Ni₂O₃ and Fe₂O₃ as primary ingredients to synthesize spinel by means of powder metallurgy. We studied the preparation technology and the characteristics of the cermet material at first, then we tried to add small amount of superaddition for improve its performance such as conductivity and corrosion resistance. The results showed that the foreign additive containing different chemical valence ion from Ni²⁺ and Fe³⁺ could significantly refine characteristics of the cermet inert anode, and the inert anode based on NiFe₂O₄ spinel could be improved by the means of adding TiO₂ and MnO₂ to the ceramic phase.

12:00 PM

Aluminum Electrolysis Tests with Inert Anodes in KF-AlF₃-Based Electrolytes: *Jian-Hong Yang*¹; John N. Hryn¹; Gregory K. Krumdick¹; ¹Argonne National Laboratory

A low-temperature KF-AlF₃-based electrolyte was used to perform aluminum electrolysis tests in a cell fitted with aluminum bronze metal anodes and wetted cathodes. Several 100A-100h tests were performed to investigate the effect of NaF concentration in the bath, current density, and temperature on cell operation. Results indicate that larger 1000A tests are warranted.

12:25 PM End

Amiya Mukherjee Symposium on Processing and Mechanical Response of Engineering Materials: NanoBehavior of Materials

Sponsored by: The Minerals, Metals and Materials Society, TMS Materials Processing and Manufacturing Division, TMS Structural Materials Division, TMS/ASM: Mechanical Behavior of Materials Committee, TMS: Shaping and Forming Committee

Program Organizers: Judy Schneider, Mississippi State University; Rajiv S. Mishra, University of Missouri; Yuntian T. Zhu, Los Alamos National Laboratory; Khaled B. Morsi, San Diego State University; Viola L. Acoff, University of Alabama; Eric M. Taleff, University of Texas; Thomas R. Bieler, Michigan State University

Monday AM
March 13, 2006

Room: 217C
Location: Henry B. Gonzalez Convention Ctr.

Session Chairs: Rajiv S. Mishra, University of Missouri; Ruslan Z. Valiev, UFA State Aviation Technical University

8:30 AM Invited

Superplasticity in Nanostructured Materials: New Challenges: *Ruslan Z. Valiev*¹; Rinat Islamgaliev¹; ¹UFA State Aviation Technical University

Prof. A. K. Mukherjee laboratory's discoveries in 1999-2002 have revealed that nanostructured metals and alloys can demonstrate extraordinary superplasticity at low temperatures and/or high strain rates. This work presents the new results on superplasticity in several nanostructured Al and Ti alloys focusing on microstructure evolution and strain hardening, as well as the challenges of their application. Grain refinement in these alloys was accomplished using severe plastic deformation techniques, and subsequent superplastic deformation allowed not only to produce their efficient forming, but also increase significantly mechanical properties of the produced articles retaining the ultrafine-grained structure. For instance, using superplastic forming of nanostructured titanium we could process long-sized rods with extraordinary mechanical properties, e.g. yield stress over 1000 MPa and fatigue strength over 500 MPa. The obtained results demonstrate the possibilities of principally new applications of superplastic forming using nanostructured materials.

8:50 AM

Plasticity at Really Diminished Length Scales: *Alla V. Sergueeva*¹; Nathan A. Mara¹; Amiya K. Mukherjee¹; ¹University of California

In recent years, the plastic behavior of technologically attractive nanocrystalline materials has become more prominent in the mainstream scientific community. In this work a review on the current understanding of the effects of microstructural characteristics on mechanical behavior of nanocrystalline materials produced by different methods including severe plastic deformation is presented. The microstructural information with the mechanical data obtained from these nanoscale materials was analyzed in the context of plasticity at really diminished length scales. An experimental data arising from testing at different conditions clearly demonstrate that some microstructural features other than just grain size (grain boundary structure, grain size distribution, etc.) can also be responsible for the exhibited material behavior. Special emphasis is given to the difficulty of intragranular dislocation generation inside the matrix in truly nanoscale structure and its effect on accommodation processes in grain boundary mediated plastic behavior. This investigation is supported by NSF grant (NSF-DMR-0240144).

9:10 AM Invited

Mechanical Behavior of Nanocrystalline Metals: *K. Linga Murty*¹; Ramesh K. Guduru¹; Khaled M. Youssef¹; Ronald O. Scattergood¹; Carl C. Koch¹; ¹North Carolina State University

Recent efforts have been very fruitful in producing artifact-free materials with nanosize grains less than 50nm. These nanograined metals exhibit very high strengths with reasonably good ductility. While there have been large amount of studies on hardness and strength characteristics, studies on strain-rate sensitivity are very limited. We describe here some of our recent work in characterizing SRS as well as activation volumes of nanograined metals using micro-tensile specimens. These tests have been carried out under iso-strain-rate conditions at ambient and we are in the process of evaluating these parameters using strain-rate jump tests during tensile loading. This work is supported in parts by the National Science Foundation grant #DMR-0201474 and by the Department of Energy grant #DE-FG02-02ER46003.

9:30 AM Invited

Influence of Specimen Size, Grain Size and Stacking-Fault Energy on the Mechanical Properties of Ultra-Fine Grained and Nanocrystalline Cu/Cu-Zn Alloys: *Yonghao Zhao*¹; Xiaozhou Liao²; Yuntian Zhu¹; Cheng Xu³; Zenji Horita³; Terence G. Langdon³; ¹Los Alamos National Laboratory; ²University of Chicago; ³University of Southern California

Much attention is currently devoted to the ductility achieved in nanocrystalline and ultrafine-grained materials. This report shows that several factors affect the ductility of tensile specimens including specimen size, grain size and the stacking-fault energy. Ultrafine-grained and nanocrystalline Cu/Cu-Zn alloys were prepared using different severe plastic deformation (SPD) techniques including equal-channel angular pressing (ECAP), high-pressure torsion (HPT), cold rolling and their combinations. It is shown in tensile testing that the ductility is reduced with decreasing specimen thickness and increased with decreasing specimen gauge length. With decreasing stacking-fault energy, the strain hardening of the samples increases thereby enhancing the tensile toughness. Evident strain hardening was observed in a nanocrystalline Cu-Zn alloy with a grain size smaller than 10 nm but there was no evident strain hardening in an ultrafine-grained Cu-Zn alloy. This paper discusses the origins of these effects.

9:50 AM Invited

Analysis of the Deformation Mechanisms in Bulk Ultrafine Grained Metallic Materials: *Igor V. Aleksandrov*¹; Roza Chembarisova¹; Vil Sitdikov¹; ¹Ufa State Aviation Technical University

Numerous experimental investigations of the recent years demonstrate activation of specific mechanisms in the process of deformation of bulk ultrafine grained metallic materials processed by severe plastic deformation (SPD). In this report the results of analysis of microstructure evolution and deformation behavior on the example of pure copper subjected to high pressure torsion and equal-channel angular pressing are presented. The analysis was carried out with the help of computer simulation within the modified Estrin-Toth dislocation model. Upgrading of the model consisted in attempts to take into account specific features of SPD. The ob-

tained results of modeling are compared with the results of experimental investigations.

10:10 AM

Increase of Strength in Ni Due to Change of Methods of Severe Plastic Deformation: *Nikolay Krastilnikov*¹; Georg Raab²; Witold Lojkowski³; Zbigniew Pakielat⁴; ¹Ulyanovsk State University; ²Ufa State Aviation Technical University; ³Polish Academy of Sciences; ⁴Warsaw University of Technology

In present work the influence of combinations of severe plastic deformation (SPD) methods on achievement of high strength of nickel is investigated. It is shown, that the change of scheme of SPD results in formation of a new type of structure in Ni, effective refinement of grains and an increase of structure uniformity, that enables to increase considerably the strength of metal. So the consecutive using of equal channel angular pressing, rolling and high-pressure torsion has allowed to generate homogeneous structure of Ni with grain size 120 nm. The samples obtained were characterized by record strength 1270 MPa. The analysis of deformation behavior of ultrafine grained Ni samples has shown, that the change of deformation mechanism of UFG metal is connected with activation of grain boundaries sliding already at room temperature.

10:30 AM Break

10:40 AM Invited

Verification of Constitutive Equation for Ultrafine Grain Ti-6Al-4V Alloy Based on Dislocation Mechanics: *Amit K. Ghosh*¹; Peter Comley¹; ¹University of Michigan

Precise simulation of superplastic forming process requires a precise description of constitutive equation at elevated forming temperature and over a wide range of strain rates. Tensile test to determine superplastic properties suffer from the problem that with increasing strain rate the distribution of strain within the specimen does not remain uniform, thereby making the values of measured stress and strain unreliable with increasing strain. Recent efforts to standardize the superplastic tensile test have revealed that strain hardening and softening rates increase with increasing strain rate, however, the measured stress-strain curves are not free from the uncertainties due to neck growth. Considering the hardening and softening effects, a dislocation mechanics based form of constitutive equation has been developed that permits one to distinguish between true material response and that due to necking effects. Verification of constitutive equation against experiments will be shown.

11:00 AM

Nanocrystalline Fe(Al,Si) Alloys: Hardening by Annealing: *T. D. Shen*¹; John G. Swadener¹; Jian Y. Huang²; Ricardo B. Schwarz¹; ¹Los Alamos National Laboratory; ²Boston College

We have used mechanical alloying (MA) to prepare single-phase nanocrystalline Fe₂Al₂Si₆ alloys with an average crystallite size of approximately 10 nm. The nanostructure is thermally stable to at least 450°C. The structural and mechanical properties were studied as a function of isochronal annealing treatments. After annealing at 450°C for 1 hour, the grain size remained almost constant, the dislocation density decreased by a factor of ten, and the hardness increased by ~20%. The increase in hardness is contrary to what one should expect from the changes in grain size and dislocation density. The data suggests that this abnormal behavior is caused by a strong increase in the solute-dislocation interaction (aging). Different models for the superposition of the dislocation and solute contributions to the strength of nanocrystalline alloys will be discussed.

11:20 AM Invited

Analysis of Strain Distribution in Equal Channel Angular Extrusion by Finite Element Method Simulation and Experimental Validation: Brett A. Pond¹; *Shankar M. Sastry*¹; ¹Washington University

Equal channel angular extrusion (ECAE) has been shown to produce ultra-fine grains in materials. Previous studies on ECAE consider only two-dimensional analysis on primarily low-temperature ECAE processing. The current study focuses on three-dimensional strain distribution in cylindrical samples resulting from ECAE processing at T > 0.4T_m. The effects of die geometry, sample size, friction coefficient, stress-strain behavior, and backpressure on strain distribution by ECAE are studied. The strain distributions is analyzed by a three-dimensional finite element com-

puter program DEFORM 3D, as well as experimental measurements and validation.

11:40 AM Invited

Structure Formation, Phase Transformations and Properties in Cr-Ni Austenitic Steel after ECA Pressing and Heating: *Sergey Dobatkin*¹; Olga Rybal'chenko¹; Georgy Raab²; ¹A.A.Baikov Institute of Metallurgy and Materials Science; ²Ufa State Aviation Technical University

It is shown that cold ECA pressing of 0.07%C - 17.3%Cr - 9.2%Ni - 0.7%Ti austenitic steel leads to formation of submicrocrystalline structure: generally oriented subgrains with separated grains (100-250 nm in size). The steel samples of 20 mm in diameter and 80 mm in length were subjected to ECAP at room temperature for 4 passes. The angle between the channels was 120°. ECAP promotes the martensitic transformation which becomes more active only at N = 4, leading to the formation of 45% martensite. During heating the fraction of high angle boundaries as well as volume of austenite is increased and structure become more equiaxed. Submicrocrystalline structure with grain size 150-250 nm and 80% of austenite was obtained at heating to 550° C. Such structure exhibits a substantial strain hardening to YS = 1090 MPa relative to the initial state (YS = 320 MPa) and EL = 12%.

12:00 PM

Influence of Sputter-Deposition Rate on Microstructures and Mechanical Properties of 330 Stainless Steel Thin Films with Nanoscale Growth Twins: *Xinghang Zhang*¹; Amit Misra²; Richard G. Hoagland²; ¹Texas A&M University; ²Los Alamos National Laboratory

We have recently synthesized single-phase 330 stainless steel (330 SS) thin films with a high density of growth twins, oriented parallel to the film surface and separated, on average, by a few nanometers. Sputter-deposited 330 SS films have the same face-centered-cubic structure as their bulk counterpart. However, the strength of as-deposited 330 SS films, derived from nanoindentation hardness measurement, is about an order of magnitude higher than that of bulk 330 SS. In twinned structures with average twin spacing of a few nanometers, plasticity may be controlled by the motion of single rather than pile-ups of dislocations. By varying sputter-deposition rate, we have changed the average twin spacing in 330 SS films. A decrease in hardness is observed in 330 SS films with enlarged twin spacing. The formation mechanism of twin nuclei is explained using an analytical model, which shows the nucleation of growth twins is influenced by sputter-deposition rate.

12:20 PM

Mechanical Behavior of Nano-Laminate Cu Foils Synthesized by Multilayer Technology: *Andrea M. Hodge*¹; Yinmin Morris Wang¹; Troy W. Barbee Jr.¹; ¹Lawrence Livermore National Laboratory

Atomic level deposition of layers by magnetron sputtering enables the fabrication of free-standing nano-laminate foils. In this talk, we report results on high purity (99.999%), fully dense, free-standing Cu/Cu nanolaminates composed of sixty-eight thousand (68,000) 2.5 nanometer-thick Cu layers for a total sample thickness of ~170 microns. Extensive plan view and cross-section transmission electron microscopy (TEM) demonstrate the nanostructured nature of the Cu/Cu multilayers, a very low apparent dislocation density and medium density growth twins. Tensile tests were performed in air and in liquid nitrogen using 6.0 mm gauge length dogbone-shaped samples. All samples studied exhibited a yield point, subsequent localized deformation within the initial shear band, and no evidence of work hardening. Overall the Cu/Cu nano-laminates had high yield strength (> 550 MPa) fracturing by near knife edge ductile necking within the first shear band formed.

Biological Materials Science: Implant Biomaterials

Sponsored by: The Minerals, Metals and Materials Society, ASM International, TMS Structural Materials Division, TMS: Biomaterials Committee, TMS/ASM: Mechanical Behavior of Materials Committee
Program Organizers: Andrea M. Hodge, Lawrence Livermore National Laboratory; Chwee Teck Lim, National University of Singapore; Richard Alan LeSar, Los Alamos National Laboratory; Marc Andre Meyers, University of California, San Diego

Monday AM Room: 212A
March 13, 2006 Location: Henry B. Gonzalez Convention Ctr.

Session Chairs: C. T. Lim, National University of Singapore; Jikou Zhou, Lawrence Livermore National Laboratory

8:30 AM

Mini-Implant for Orthodontic Anchorage: *Carlos Nelson Elias*¹; Liliene Siqueira Morais¹; Glaucio Serra Gumarães¹; ¹Instituto Militar de Engenharia

In an orthodontic treatment, one way of having teeth movement done with minimal undesired movement is by having a large anchorage group of teeth. Another way of obtaining anchorage is by using an extraoral arch, which needs great co-operation by the patient. The third orthodontic anchorage process is by using an osseointegrated titanium implants. In this case the implant can be surgically removed after the orthodontic treatment. Nowadays, an orthodontics mini-implants has been used to anchor different movements such as the intrusion of anterior and posterior teeth, mesio-distal teeth, space closure, upright of posterior teeth, extrusion of impacted teeth, orthopedic traction and expansion of maxillary suture. The purpose of this work was to analyze the bone reactions of immediately loaded mini-implants of titanium alloy (grade 5) by histological, histomorphometrical and mechanical parameters. The present study used eighteen New Zealand White rabbits. The mechanical properties of mini-implant has been determined.

8:50 AM

Substrate Creep Effects on the Fatigue Behavior of a Dental Restoration Structure: *Jikou Zhou*¹; Min Huang²; Wole O. Soboyejo²; ¹Lawrence Livermore National Laboratory; ²Princeton University

This paper investigates the effects of substrate creep on the fatigue behavior of a multilayer dental restoration model structure. Two sets of specimens with different subsurface crack sizes were prepared. Each set of specimens was tested with increasing load levels until the top glass failed monotonically. The results showed that at high load levels (higher than 60 N), slow crack growth is the major fatigue mechanisms; while fatigue life is significantly degraded by the substrate creep under low cyclic load levels (less than 60 N), in which longer testing duration involved. A previously established substrate creep model was then modified, and was successfully fitted to the experimental data.

9:10 AM

Mechanical Properties and Biocompatibility of Laser-Deposited Orthopaedic Alloys: *Soumya Nag*¹; *Rajarshi Banerjee*²; Hamish L. Fraser¹; ¹Ohio State University; ²University of North Texas

Due to the rapidly increasing number of surgical procedures involving prosthesis implantation, there is an urgent need for improved biomaterials and processing technologies for orthopaedic implants such as hip implants. By employing novel near-net shape processing technologies, such as laser engineered net shaping (LENSTM), it is possible to rapidly manufacture custom-designed implants. From the materials perspective, orthopaedic alloys for implant applications typically require a combination of appropriate mechanical and osseo-integration properties. Since the beta phase in Ti alloys exhibits a favorable balance of properties, there is a thrust towards the development lower modulus beta-Ti alloys. The present paper will discuss the microstructure and mechanical properties of beta Ti alloys deposited using LENSTM for orthopaedic applications. In addition, the biocompatibility of these materials will also be assessed via in vitro studies and the results discussed in this presentation.

9:30 AM

A Novel Combinatorial Approach to the Development of Metallic Biomaterials for Orthopaedic Implants: *Soumya Nag*¹; Rajarshi Banerjee²; Hamish L. Fraser¹; ¹Ohio State University; ²University of North Texas

Metallic biomaterials for orthopaedic implant applications typically require a combination of appropriate mechanical properties with excellent biocompatibility including osseo-integration properties. In recent years there has been a thrust towards the development lower modulus beta-Ti alloys for implant applications. While a number of biocompatible beta-Ti alloys have been reported in recent literature, there is still a large scope for improvement in terms of alloy design via optimization of alloy composition and thermo-mechanical treatments. A novel combinatorial approach has been developed for understanding composition-microstructure-property relationships in these alloys. This approach is based on the use of directed laser deposition to rapidly process compositionally graded alloys, administer appropriate heat-treatments, characterize and quantify their microstructures, assess their mechanical properties, and finally develop composition-microstructure-property relationships. This combinatorial approach will be employed for studying the binary, Ti-Ta, and Ti-Nb, as well as the ternary Ti-Nb-Ta, and quaternary Ti-Nb-Zr-Ta systems, which are promising for implant applications.

9:50 AM

Biocorrosion Behaviour of Magnesium Alloys as Degradable Metallic Biomaterials: *Hao Wang*¹; Mingxing Zhang¹; Zhiming Shi¹; Ke Yang²; ¹University of Queensland; ²Chinese Academy of Sciences

Drawbacks associated with permanent metallic implants lead to the search for degradable metallic biomaterials. Magnesium alloys have been highly considered as Mg is essential to bodies and has a high biocorrosion potential. In this study, corrosion behaviour of pure magnesium and magnesium alloy AZ31 in both static and dynamic physiological conditions (Hank's solution) has been systematically investigated. It was found that both materials degraded fast at beginning, then stabilised at a rate of 0.5mm/year. The mechanical properties of the materials also decreased with immersion time. The electrochemical tests indicated that the AZ31 had a lower anodic polarisation current and high polarisation resistance in the first 100h, indicating a more stable protection film was formed. For static applications (hard issue replacements), the hydrogen release might be an issue, while for dynamic applications (stents), constant pH resulted in a high degradation rate. Surface coating has been developed to achieve a controllable biodegradation.

10:10 AM Break

10:30 AM

Compare Corrosion Resistance and Wear Resistance of Boronized Ti-6Al-4V with Stainless Steel Used as Medical Implants: *Roumiana Petrova*¹; Boris Goldenberg¹; Naruemon Suwattanont¹; ¹New Jersey Institute of Technology

The use of titanium and its alloy has increased over the past years as medical implants, but wear resistance and corrosion resistance have limited its use in hip and other joints replacements. The present study describes investigation of boron coating on stainless steel compared with alloy Ti-6Al-4V. The coatings were produced by a thermo-chemical treatment with an original technology powder mixture at a temperature range of 850-1050°C. Metallographic examination, x-ray diffraction, and microhardness testing were used to determine the characteristics of the diffusion layer. The potentiodynamic polarization measurements were used to investigate the corrosion resistance. It was shown that the boronizing process created a boride layers with a thickness of 10-15 µm depending on substrates, temperatures, and time, with microhardness of about 4-6 times greater than that of the substrate. The corrosion and wear resistance of the boronized coating was determined to be better than that of the substrate.

10:50 AM

Evaluation of Attachment, Differentiation, and Growth of MC3T3-E1 Osteoblasts on Ti-Al-Nb Alloys: *Jeffrey P. Quast*¹; Melissa J. Baumann¹; Carl J. Boehlert¹; ¹Michigan State University

To date, the most common material choice for load bearing implants is titanium-aluminum-vanadium (Ti-Al-V) alloys. However, the substitution

of V for niobium(Nb) has produced an alloy with mechanical properties that more closely match bone. In this study, growth and differentiation of MC3T3-E1 osteoblasts on two alloys, Ti-15Al-33Nb(at%) and Ti-21Al-29Nb(at%), were compared to that on Ti-6Al-4V(wt%). Osteoblasts(OBs) were plated onto 2cm x 2cm square samples at a concentration of 11,320 cells/cm², and grown at 37°C in a humidified atmosphere of 95% air and 5% CO₂. OBs were fed with alpha-MEM supplemented with 10% fetal bovine serum. Cell attachment was measured after 2 and 4 days using a hemocytometer. Scanning electron microscopy and optical microscopy were also employed to compare cell attachment behavior. Preliminary data has shown little variance in attachment and differentiation among the three different alloys. The implications of these results on the future of implant design will be discussed.

11:10 AM

Grindability of Ti-Alloys for Dental Applications: *Kwai S. Chan*¹; Marie Koike²; Masafumi Kikuchi³; Osamu Okuno³; Toru Okabe²; ¹Southwest Research Institute; ²Baylor College of Dentistry; ³Tohoku University

The grindability of Ti-based alloys for dental applications was analyzed by considering the fracture behavior of individual alloys in response to the stress field of a grinding wheel. The stress field was computed by treating the grinding wheel as a cylindrical disk with a flat region acting on a flat substrate. The initiation and propagation of microcracks in the substrate was examined on the basis of the contact stress field and a set of fracture criteria. Grindability was computed as a function of grinding speed for Ti-based alloys containing an alpha, alpha + beta, or beta microstructure with or without intermetallic precipitates. The theoretical results are compared against experimental data to elucidate the role of microstructure in grindability. The comparison revealed that alloying addition that leads to the formation of brittle intermetallics enhances grindability by reducing fracture toughness, tensile ductility, and the resistance to crack initiation and propagation.

11:30 AM

A Degradation Study of Poly (DL-Lactide) Bone Plate and Screw for Fracture Fixation: *Carlos Nelson Elias*¹; Ana Maria Bolognese²; Aleandre Ribeiro²; ¹Instituto Militar de Engenharia; ²Universidade Federal do Rio de Janeiro

Some polymer are used for the controlled delivery of protein and peptide drugs, for the manufacture of medical devices and wound dressings as well as for fabricating scaffolds in tissue engineering. In the present study bone plates and screws for fixation of mandibular and zygomatic fractures of PDLA (poly-DL-lactic acid) from Purac (Biochem Gorinchem, The Netherlands) were made. These materials are useful for a bone fixation, cartilage repair, and drug delivery. The kinetics of the polymerizations were followed by DSC, and the mechanical behavior was monitored as a function of temperature to obtain the T_g. Plates were subjected to hydrolytic degradation in an aqueous phosphate buffer solution at a pH 7 and 37°C. Degradation as function of time was studied via tensile testing and scanning electron microscopy observation after 10, 20, 30 and 40 days aqueous solution immersion. Complete degradation had not occurred by the end of the study.

11:50 AM

Cell Formation Enhancement on Ultrafine Grained Orthopedic Ti and Ti Alloy Surfaces: Chang Yao¹; Thomas Webster¹; Henry J. Rack²; ¹Purdue University; ²Clemson University

Previous investigations have shown that ultra-fine grain sizes formulated by severe plastic deformation have the potential for materially enhancing the mechanical performance of titanium alloys. These achievements are of particular interest to the orthopedic community since these alloys, i.e., c.p. Ti (grade 2 and grade 4) and Ti-6Al-4V, constitute the vast majority of titanium alloys currently used for biomedical devices. However, little is known about their ability to support new bone growth. This presentation will examine the cellular response of these systems as determined through in-vivo and in-vitro investigations. These biological studies provided evidence of greater osteoblast (bone-forming cell) functions on UFG compared to currently-used Ti and Ti6Al4V. For example, osteoblast cell adhesions were up to 40-60 % greater when surface features were decreased from conventional (micron) to biologically-inspired re-

gimes for c.p. Ti. In summary, UFG c.p. Ti and Ti6Al4V provide substantial promise for enhancing the performance of orthopedic devices.

12:10 PM

Prototyping the Dental Materials Data Warehouse for Materials Selection: *Yong Li*¹; ¹IMS

In this project, the effectiveness of the new data management technique of data warehousing was critically evaluated for integrating dental materials data, in order to facilitate the informational services including data retrieval and materials selection for dental materials. A scaled-down version of the dental materials data warehouse was successfully constructed and an English Query application, which allows the end users to formulate their queries in natural English language, was developed on top of the data warehouse. The current application supports five types of queries from basic practice of data access and retrieval to more advanced information analytical service of materials selection. The results demonstrate that the data warehousing technique is of a great potential in storing, processing and managing dental materials data, and will have a significant impact on research, education and operation in the dental materials community.

Bulk Metallic Glasses: Elastic, Plastic Behavior, and Computation

Sponsored by: The Minerals, Metals and Materials Society, TMS Structural Materials Division, TMS/ASM: Mechanical Behavior of Materials Committee

Program Organizers: Peter K. Liaw, University of Tennessee; Raymond A. Buchanan, University of Tennessee

Monday AM
March 13, 2006

Room: 217B
Location: Henry B. Gonzalez Convention Ctr.

Session Chairs: Peter K. Liaw, University of Tennessee; William L. Johnson, California Institute of Technology

8:30 AM Keynote

Plastic Yielding, Flow, and Configurational Entropy in Metallic Glasses: *William L. Johnson*¹; ¹California Institute of Technology

Metallic glasses are "atomic" solids in which the potential energy depends mainly on atomic density and centro-symmetric pair potentials. The bonding is weakly directional. Deformation is dominated by the stress driven cooperative shear motion of large atomic clusters (called shear transformation zones or STZ's) between intrinsic glass configurations. A model for the yielding and plastic flow is presented based on a description of "average" properties STZ's. The fundamental properties of STZ's are related to the configurational entropy and elastic properties (G,B, and Poisson's ratio) of the glass and liquid. The model predicts that all metallic glasses share certain universal characteristics while the material specific properties are primarily attributable to variations in the Poisson Ratio among metallic glasses. Topics will include plastic yielding and flow in the glass, liquid viscosity and liquid fragility. The discussion will include extensive comparison of the model with experimental observations.

9:00 AM Invited

Statistics of Shear Band Activation in Metallic Glasses: *Christopher A. Schuh*¹; Corinne E. Packard¹; ¹Massachusetts Institute of Technology

The in-situ study of shear localization in metallic glasses is difficult using conventional mechanical tests, because shear bands form very quickly and their preferred formation sites are not known a priori. Using instrumented nanoindentation, shear bands can be induced in specified locations, under a well-defined stress state. In this presentation our latest work using this technique will be outlined, focusing upon the statistics of shear band activation in bulk glass forming alloys. Significant scatter is found in the stress state at yield, and analysis techniques are presented to assess whether the scatter arises due to variations in the glass structure or due to thermal activation effects.

9:25 AM Invited

Strain-Rate Dependence of Shear-Band Behavior and Serrated Flow in a Metallic Glass: *Michael Atzmon*¹; *Wenhui Jiang*²; ¹University of Michigan; ²University of Tennessee

Nanoindentation of a metallic glass leads to the formation of shear bands, the density of which increases with displacement rate. At low displacement rates, pronounced serrations, i.e., displacement bursts, are observed in the load-displacement curves. In an effort to improve the understanding of shear band behavior, we have conducted nanoindentation studies of amorphous Al86.8Ni3.7Y9.5 at varying rates. The initial amount and distribution of free volume were varied by cold rolling and/or annealing. Not only the density of shear bands, but their shape is dependent on the strain rate. The results are examined using both an accepted microscopic model and continuum analysis. The microscopic model alone cannot account for the observed trends, but combination of the microscopic model and 3-D continuum mechanics explains several observed trends. The results suggests that a high shear-band propagation velocity is required for serrations to be observed.

9:50 AM

Rate-Dependent Shear Banding in a Zr-Based Bulk Metallic Glass: *W. H. Jiang*¹; *G. J. Fan*¹; *H. Choo*¹; *P. K. Liaw*¹; ¹University of Tennessee

Metallic glasses exhibit the inhomogeneous plastic deformation at low temperatures and high strain rates. The inhomogeneous deformation concentrates on highly-localized, narrow, shear bands. Shear banding affects substantially the plastic-flow behavior. It has been demonstrated that the shear-band formation is dependent on strain rates during indentation¹. However, we are not aware of any research addressing this rate-dependence in uniaxially loading. Using geometrically-constrained samples, we investigated the shear-band formation at various strain rates in uniaxial compression. The results will be compared with the numerical calculations using the free volume model². The present work is supported by the National Science Foundation International Materials Institute (IMI) program, under DMR-0231320, with Dr. C. Huber as the program director. ¹W. H. Jiang and M. Atzmon, *J. Mater. Res.*, 2003, 18, 755. ²P. S. Steif, F. Spaepen, and J.W. Hutchinson, *Acta Metall.* 1982, 30, 477.

10:10 AM

Strain Rate Effects on the Mechanisms of Deformation and Nanocrystallization in Bulk Metallic Glasses: *Anantharamkrishnan Puthucode*¹; *Rajarshi Banerjee*¹; *Suman Vadlakonda*¹; *Michael Kaufman*¹; ¹University of North Texas

Nanoindentation loading curves frequently display pop-ins at low loading rates but not at higher loading rates. These “pop-ins” reportedly correspond to the activation of shear bands, which are readily resolved at the lower rates. Several reasons for their loss at higher loading rates have been speculated including instrumental resolution, homogenization of shear bands and, more recently, strain-induced free volume effects. In this study, a series of indents were made on a Zr-based BMG composition at different strain rates (displacement-controlled) and, indeed, the pop-ins blur with increasing strain-rate. In order to understand this strain-rate dependence and the possibility of nanocrystallization accompanying the localized deformation, TEM samples were cut from the indented regions using a focused ion beam and examined by analytical high resolution TEM methods. Similar studies were performed on an Al-based BMG in order to determine whether the results are alloy specific or more general to this class of materials.

10:30 AM Break

10:40 AM Invited

Temperature Dependence of the Elastic Constants of Metallic Glasses and Single Crystals: *Ricardo B. Schwarz*¹; *D. J. Safarik*¹; ¹Los Alamos National Laboratory

The low-temperature elastic properties of metallic glasses show various anomalies not found in crystalline alloys. We have measured the elastic constants of the glass and single crystal Pd₄₀Cu₄₀P₂₀ over the range 4 < T < 300 K. The glass shear modulus is 15-60% lower than that the lowest shear modulus in the crystal (the tetragonal symmetry Pd₄₀Cu₄₀P₂₀ crystal has 4 independent shear moduli). For 4 < T < 15 K, the shear modulus of the Pd₄₀Cu₄₀P₂₀ crystal decreased as T⁴, which is the normal trend for crystals, attributed to the anharmonicity of the lattice vibrations. Over the

same temperature range, the shear modulus of the Pd₄₀Cu₄₀P₂₀ glass decreases linearly with temperature. We describe the linear temperature dependence of the glass shear modulus in terms of anelastic relaxations involving groups of atoms. We discuss the origin of these relaxations in terms of atomistic models for the glassy structure in metals.

11:05 AM

Elastic Properties of Ca-Based and Zr-Based Bulk Metallic Glasses Studied by Resonant Ultrasound Spectroscopy: *Zhiying Zhang*¹; *Raphaël P. Hermann*¹; *Veerle Keppens*¹; *Mark L. Morrison*¹; *Guojiang Fan*¹; *Peter K. Liaw*¹; *Oleg N. Senkov*²; *Daniel B. Miracle*³; *Yoshihiko Yokoyama*⁴; ¹University of Tennessee; ²UES Inc.; ³Air Force Research Laboratory; ⁴Tohoku University

Resonant ultrasound spectroscopy (RUS) yields the elastic constants for millimeter-sized samples simultaneously and nondestructively. In this work, the elastic properties of the Ca-based bulk metallic glasses (BMGs), Ca65Mg15Zn20, Ca50Mg20Zn30 and Ca55Mg18Zn11Cu16, were investigated by RUS as a function of temperature between 2 and 400 K, which is close to and above the glass-transition temperature of these alloys. In addition, the elastic properties of the Zr-based BMGs, Zr50Cu40Al10, Zr50Cu30Ni10Al10 and Zr52.5Cu17.9Ni14.6Al10Ti5, were studied as a function of temperature between 2 and 400 K. Results show that both the Young's modulus and the shear modulus decrease with increasing temperature. On the other hand, Poisson's ratio increases with increasing temperature. The influence of the composition on the fragility, the glass-forming ability and mechanical properties of BMGs will be discussed. The present work is supported by NSF DMR-0206625 and NSF IMI DMR-0231320, with Dr. C. H. Huber as the program director.

11:25 AM Invited

Calculated and Measured Elastic Constants of Zr50Cu(40-x)Al10Pdx Metallic Glasses: *Don M. Nicholson*¹; *V. Keppens*²; *Z. Zhang*²; *R. Hermann*²; *Y. Yokoyama*³; *Gongyao Wang*²; *P. K. Liaw*²; *Akihisa Inoue*³; ¹Oak Ridge National Laboratory; ²University of Tennessee; ³Tohoku University

Recent studies correlate the elastic constants with the mechanical behavior of bulk metallic glasses (BMGs). In particular, BMGs with higher toughnesses exhibit greater Poisson's ratios. It has been found that the addition of the 3 atomic percent of Pd in the Zr-Cu-Al BMGs significantly improves the fatigue strength, relative to other Zr-based BMGs. Moreover, the improved fatigue resistance was found to be related to the high ratio of the shear modulus to bulk modulus, and, thus, the high Poisson's ratio in the Zr-Cu-Al-Pd BMG. To understand the role of Pd, we measured and calculated elastic constants of Zr50Cu(40-x)Al10Pdx. The calculations employ the ab initio molecular dynamics of liquids instantaneously quenched to a glass. The distribution of the free volume and elastic constants are predicted for the glass structures. The elastic constants are also measured, using the Resonant Ultrasound Spectroscopy.

11:50 AM Invited

Applications of Metallic Glasses: Thin Films and Nanostructured Parts: *Jinn P. Chul*¹; *Chun Ling Chiang*¹; *Hadi Wijaya*¹; *Chih Wei Wu*¹; ¹National Taiwan Ocean University

Considerable progresses in the processing of bulk metallic glasses (BMG) have been attained recently. In this presentation, the potential applications of metallic glasses in the fields of thin films and nanostructured parts are given. First, the annealing-induced extensive amorphization in glass-forming thin films in the supercooled liquid (SCL) region is reviewed. Controllable extensive amorphization is useful to regulate specific film properties such as electrical and magnetic properties. Materials structured on the nanometer scale give rise to many interesting new properties and phenomena, which lead to a wide variety of linear and nonlinear device applications. In the second part of the presentation, properties of nanostructured BMG prepared by superplastic-forming in SCL region in air are presented. Characterization results based on transmission and scanning electron microscopes, atomic force microscopy and optical properties performed on nanostructured BMG are discussed. This work was supported by the National Science Council of Taiwan (NSC 93-2216-E-019-007, 94-2218-E-110-009).

12:15 PM

Molecular Dynamics Simulations for the Effect of Hydrogen on the Mechanical Behavior of an Amorphous Metal: *Pil-Ryung Cha*¹; Yu-Chan Kim²; Ki-Bae Kim²; Hyun-Kwang Seok²; ¹Kookmin University; ²Korean Institute of Science and Technology

Using molecular dynamics simulations, with a realistic many-body embedded-atom potential, and a novel method to characterize local order, we study the structural stabilities of amorphous nickel systems with different amount of hydrogen and the effect of hydrogen on the structural change of the system during loading. We find the nonlinear increase of atomic volume of amorphous Ni with increasing hydrogen concentration while crystalline Ni shows linear increase. We also find crystallization of amorphous Ni at room temperature above a critical hydrogen concentration (the crystallization temperature (Tx) of pure amorphous Ni is between 500 and 600 K) and the decrease of its Tx with increasing hydrogen concentration. We call the above enhanced crystallization of amorphous nickel hydrogen-induced crystallization (HIC) and discuss its microscopic mechanism.

Cast Shop Technology: The Aluminum Fabrication Industry: Global Challenges and Opportunities: Aluminum Plenary Session

Sponsored by: The Minerals, Metals and Materials Society, Aluminum Association, TMS Light Metals Division, TMS: Aluminum Committee
Program Organizers: Subodh K. Das, Secat Inc; Michael Hal Skillingberg, Aluminum Association; Ray D. Peterson, Aleris International; Rene Kieft, Corus Group; Travis J. Galloway, Century Aluminum Company

Monday AM Room: Theater
March 13, 2006 Location: Henry B. Gonzalez Convention Ctr.

Session Chair: Subodh K. Das, Secat Inc

See The Aluminum Fabrication Industry: Global Challenges and Opportunities Symposium on page 47 for presentations.

Characterization of Minerals, Metals and Materials: Extraction and Processing Applications

Sponsored by: The Minerals, Metals and Materials Society, TMS Extraction and Processing Division, TMS: Materials Characterization Committee
Program Organizers: Jiann-Yang James Hwang, Michigan Technological University; Arun M. Gokhale, Georgia Institute of Technology; Tzong T. Chen, Natural Resources Canada

Monday AM Room: 206A
March 13, 2006 Location: Henry B. Gonzalez Convention Ctr.

Session Chairs: Yoshiaki Umetsu, Tohoku University; John E. Dutrizac, CANMET-MMSL

8:30 AM

Characterization of the Cr(III) Analogues of Jarosite-Type Compounds: *John E. Dutrizac*¹; Tzong T. Chen¹; ¹CANMET- Mining and Mineral Science Laboratories

A new class of compounds, the Cr(III) analogues of jarosite-type compounds (MCr₃(SO₄)₂(OH)₆, where M is H₃O, Na, K, Rb, Tl, Ag, NH₄ or Pb²⁺), was synthesized at 230°C using either Cr(SO₄)_{1.5} or CrCl₃ media. X-ray diffraction analysis confirmed that the new compounds were well crystallized and had the structure characteristic of both natural and synthetic jarosites. The morphology of the precipitates was characterized by scanning electron microscopy (SEM) of both loose powers and polished cross sections of the various precipitates. Typically, the precipitates consist of tiny cauliflower-like agglomerates; discrete crystals are rare

despite the high synthesis temperatures employed. Electron microprobe analyses confirmed the bulk chemical assays of the various precipitates and demonstrated the homogeneity of the compounds. Overall, the characterization results suggest that the Cr(III) analogues of jarosite-type compounds formed by the in situ crystallization of an initially formed amorphous chromium oxyhydroxide gel.

8:55 AM Invited

Iron Removal from Titanium Ore by Electrochemical Method: *Obana Isao*¹; Toru H. Okabe¹; ¹University of Tokyo

With the objective of establishing a new titanium production process, a novel process for the selective removal of iron from titanium ore by an electrochemical method was investigated. The thermodynamic analyses of the chlorination reactions in a Ti-Fe-O-Cl system were carried out prior to the fundamental experimental work, and the possibility of the chlorination reactions was investigated. In the experiment, low-grade titanium ore in a carbon crucible was immersed in molten calcium chloride and polarized anodically at 1100 K under an argon atmosphere in order to remove iron from the ore. At this stage, 80 mass% of iron in the low-grade titanium ore was successfully removed. This result shows that iron in the titanium ore was chlorinated and removed by the electrochemical method.

9:20 AM Invited

Some Reactions of MgO in the MgO-Based Binder Materials for Slurried Soils in the Aqueous Media under a Flow of CO₂: Tomohito Kameda¹; Jun Ishikawa¹; Tetsuo Shirota¹; *Yoshiaki Umetsu*¹; ¹Tohoku University

The MgO-based binder materials applicable to slurried soils and, sometimes, to contaminated wet soils have been paid attention to because of the moderate nature of MgO in exposure to natural environment. For investigation of the behaviors of MgO during soil-binding process, reactions of MgO in suspension in water have been determined in the presence of CO₂ at different partial pressures and temperatures by X-ray diffraction and morphology observation of the solid phase and monitoring of the solution pH. Under CO₂ stream in the aqueous phase, MgO was found to be easily leached and then needle-shaped crystals of MgCO₃·3H₂O with hexagonal cross section were precipitated at a higher CO₂ partial pressure at temperatures lower than about 50°C. At lower CO₂ partial pressure or high temperatures, MgCO₃·3H₂O was precipitated first and then converted into very thin, flaky crystals of basic magnesium carbonate.

9:45 AM Invited

The Effect of the Mineralogy of the Platinum Group Metals on Their Recovery and Leachability: *Cesar Joe Ferron*¹; Chris C. Hamilton¹; O. Valeyev¹; ¹SGS Lakefield Research Limited

The mineralogy of the platinum group minerals is fairly complex, and it is therefore not surprising that the different minerals have variable response to metallurgical processes, in particular, flotation and leaching. The PLATSOL™ process was developed to extract simultaneously, base metals, gold and platinum group metals from various materials. Extensive research has indicated that most PGM's were amenable to the PLATSOL™ process, with the notable exception of cooperate PtS. Further work showed that a thermal pretreatment at 500-700°C transformed the structure of the cooperate and similar refractory minerals (Pt,Pd)S into Pt metal and Pt-Pd alloys that responded very well to the PLATSOL™ process. Examples are presented of the mineralogy of PGM concentrates as produced, in the residue from the PLATSOL™ leach and after thermal pretreatment.

10:10 AM Break

10:20 AM

Materials Characterization of Electrocoagulation By-Products Using Al-Fe Combination Electrode System: *Jewel A. Gomes*¹; Praveen Daida¹; George Irwin¹; Hylton McWhinney²; Tony Grady²; Hector Moreno¹; Eric Peterson³; Jose R. Parga⁴; David L. Cocke¹; ¹Lamar University; ²Prairie View A&M University; ³Highland Community College; ⁴Institute Technology of Saltillo

Electrocoagulation (EC) has been performed with Al-Fe electrode system with changing polarity for the removal of arsenic from water. The removal process has been studied using ICP-AES and Anodic Stripping Voltammetry with a wide range of arsenic concentration (1-1000 ppm) at various pH (4-10) and residence times (1-60 min). Electrochemically gen-

erated by-products have been analyzed using XRD, FTIR, XPS, SEM/EDS and Mössbauer Spectroscopy. Results revealed expected crystalline iron oxides (magnetite (Fe₃O₄), lepidocrocite (FeO(OH)), iron oxide (FeO)) and aluminum oxides (bayerite (Al(OH)₃), diaspore (AlO(OH)), mansfieldite (AlAsO₄·2(H₂O)), as well as some interactions among the phases. The amorphous or ultra-fine particular phase was also found in the floc. The substitution of Fe³⁺ ions by Al³⁺ ions in the solid surface has been observed, indicating an alternative removal mechanism of arsenic in these metal hydroxides and oxyhydroxides by providing larger surface area for arsenic adsorption via retarding the crystalline formation of iron oxides.

10:45 AM

Microtexture and X-Ray Nanotomography of a Silver-Bearing Siliceous Ore: *Tzong T. Chen*¹; Alexander Sasov²; John E. Dutrizac¹; Peter D. Kondos³; Glenn Poirier¹; ¹CANMET- Mining and Mineral Sciences Laboratories; ²SkyScan; ³Barrick Gold Corporation

Drill core samples containing 16-127 ppm Ag were analyzed by SEM and X-ray nanotomography to determine the occurrences of the Ag and the microtexture of the siliceous matrix. The core samples consist essentially of porous masses of quartz and amorphous silica that contain abundant pores which have sizes ranging from less than 1 micrometer to several millimetres. The pores seem to have only limited connections to one another. The fine pore sizes, together with the limited pore connections, greatly reduce the permeability of the core samples. Silver occurs mainly as less than 1 micrometer-sized particles of silver sulphide and, in subordinate amounts, as silver-copper sulphide, silver chloride, silver iodide, native silver and silver selenide. These minerals commonly occur embedded in the quartz matrix adjacent to the micrometer-sized pores. Intergrowths of silver sulphide with pyrite, silver chloride, or mercury chloride are common.

11:10 AM

Applied Mineralogical Studies on Colombian (Bagre, Antioquia) Black Sands: *Clara María Lamus Molina*¹; Marco Antonio Márquez Godoy¹; José Carlos Gaspar²; ¹Universidad Nacional de Colombia; ²Universidade de Brasília

The following minerals found in the residual black sands from gold mining in El Bagre, Antioquia (Colombia) were identified as having major economic interest: ilmenite (FeTiO₃), with an average of 49% of TiO₂, frequently altered presenting crowns, lamellae of rutile and alteration textures; titanomagnetite with up to 25% of TiO₂; magnetite (Fe₃O₄) in individual grains or associated with others minerals as hematite and ferromagnesian silicates; rutile (TiO₂) with considerable quantities of Nb₂O₅ (0.1-3.7% weight); zircon (ZrSiO₄) with 66% weight of ZrO₂, and monazite with an average of 63.43% weight of REE, this frequently associated to xenotime and thorite forming textures as little drops. Analysis in EPMA and SEM/EDS showed percentages of minor elements and traces, thereby clearly establishing the applications of these minerals in diverse industries. Furthermore, a detailed granulometric study of the different minerals and textural relationships among them also allowed for establishing the basis for possible processing and exploitation.

Computational Thermodynamics and Phase Transformations: Atomic Modeling Based Alloy Thermodynamics I

Sponsored by: The Minerals, Metals and Materials Society, TMS Electronic, Magnetic, and Photonic Materials Division, TMS Materials Processing and Manufacturing Division, TMS Structural Materials Division, TMS: Chemistry and Physics of Materials Committee, TMS/ASM: Computational Materials Science and Engineering Committee
Program Organizers: Dane Morgan, University of Wisconsin; Corbett Battaile, Sandia National Laboratories

Monday AM
March 13, 2006

Room: 210A
Location: Henry B. Gonzalez Convention Ctr.

Session Chairs: John Rodgers, Innovative Materials Technologies, Inc; Gerbrand Ceder, Massachusetts Institute of Technology

8:30 AM Invited

Ab Initio Thermodynamic Modeling of Multicomponent Alloys: *Axel Van De Walle*¹; Mark D. Asta¹; Gautam Ghosh¹; ¹Northwestern University

The construction of multicomponent thermodynamic databases is often limited by the amount experimental data available and the costs associated with collecting such data. Ab initio calculations of solid state alloy thermodynamics provide a quick and cost effective way to gather large amounts of thermodynamic data suitable for the construction of multicomponent thermodynamic databases. The algorithms and computational tools included in the Alloy Theoretic Automated Toolkit that enable this approach will be discussed. Special attention will be devoted to the determination of free energies via thermodynamic integration coupled with Monte Carlo simulations using new algorithms specifically designed to deal with the high-dimensionality of composition space in multicomponent alloys. Algorithms based on stochastic sampling are ideally suited for this task and offer the additional advantage of being naturally parallelizable. Examples of application to the Fe-Ni-Co-Cr system will be presented.

9:00 AM Invited

First-Principles Thermodynamic Properties of the Stable Binary B2 Phases in the Al-Ni-Ru-Ir-Pd System: *Raymundo Arroyave*¹; Sara N. Prins¹; Zi-Kui Liu¹; ¹Pennsylvania State University

The B2 phases in the Al-Ni-Ru-Ir-Pd system are important for high temperature applications, especially as bond coat materials in turbine blades. To study the phase stability of these phases it is first necessary to obtain a sound thermodynamic description of the system, based on the CALPHAD method, for example. The parameters of the CALPHAD models are usually obtained through fitting of experimental data. Unfortunately, thermodynamic information on the B2 phases in this system is scarce. In this paper, we use first-principles methods to calculate the contributions of vibrational and electronic degrees of freedom to the total free energies of the stable B2 phases in this quinary system. The harmonic and quasi-harmonic approximations are used to determine the vibrational behavior of the structures, while the thermal electronic effects are taken into account through the integration of the electronic DOS.

9:30 AM

Structure, Energetics and Mechanical Stability of Fe-Cu BCC Alloy from First-Principle Calculations: *Zhe Liu*¹; Axel van de Walle¹; Gautam Ghosh¹; Mark Asta¹; ¹Northwestern University

Atomic volumes, magnetic moments, mixing energies and elastic properties of bcc Fe_{1-x}Cu_x solid solutions are studied by ab-initio calculations based on the cluster expansion framework. A generalization of the cluster expansion technique is developed to compute the elastic constant tensor for disordered solid solutions. Calculated mixing energies, atomic volumes and magnetic moments are found to be in good agreement with available measurements for metastable alloys prepared through non-equilibrium processing techniques. While the predicted bulk modulus and C₄₄ in the solid solution are positive for all concentrations, C'₂=(C₁₁-C₁₂)/2 is predicted to be positive only for Cu concentrations less than 50 at%.

These results indicate that the mechanical instability of bcc Cu persists over a wide range of compositions. Implications of the present results are discussed in relation to the observed metastability of bcc Fe-Cu alloys, and the strengthening mechanism of nanoscale bcc precipitates in a bcc-Fe matrix.

9:50 AM

First Principles Study of Surface Ordering and Segregation in Pt-Rh Binary Alloys: *Koretaka Yuge*¹; *Atsuto Seko*¹; *Akihide Kuwabara*¹; *Humiyasu Oba*¹; *Isao Tanaka*¹; ¹Kyoto University

The cluster expansion technique in conjunction with the first principles calculation have been applied in the Monte Carlo simulation to derive the equilibrium configuration of (111) surface in Pt-Rh alloys. Calculated surface composition profiles far above the bulk order-disorder transition temperature show the enrichment of Pt at top layer and Pt depleted at sublayer, which is in consistent with experimental observation in literature. At low temperatures, a completely different temperature-dependence of layer composition profile is found between Pt₂₅Rh₇₅ and Pt₅₀Rh₅₀. While Pt composition of Pt₂₅Rh₇₅ sublayer shows positive temperature-dependence, that of Pt₅₀Rh₅₀ has a local minimum at 200 K. The former is attributed to the relatively strong Rh segregation to sublayer, which induces the disruption of ordering. For the latter, sublayer-confined phase transition from ($\sqrt{3} \times \sqrt{3}$)R30° order to disorder phase occurs due to the competition between segregation and ordering effects.

10:10 AM Break

10:30 AM Invited

Phase Relationships in Selected Functional Ceramics from First Principles: *Isao Tanaka*¹; *Atsuto Seko*¹; *Koretaka Yuge*¹; *Fumiyasu Oba*¹; *Akihide Kuwabara*¹; ¹Kyoto University

In the present authors' group, phase equilibria, transitions and structure of solid solutions for a number of pseudo-binary oxides have been systematically investigated both by theory and experiments. Theoretical works have been made by first principles calculations combined with cluster expansion and cluster variation method or Monte Carlo method. Contribution of phonons has been explicitly computed using first principles lattice dynamic method within the quasi-harmonic approximations. Experimental works by x-ray absorption near edge structures technique have been made in parallel to these theoretical works. Effects of external pressure on the phase equilibria have also been investigated both by theory and experiments.

11:00 AM

First Principles Study on Pressure-Induced Phase Transition in ZnO and ZnO-MgO System: *Atsuto Seko*¹; *Fumiyasu Oba*¹; *Akihide Kuwabara*¹; *Isao Tanaka*¹; ¹Kyoto University

The pressure-induced phase transition from wurtzite to rocksalt in ZnO was investigated using first principles lattice dynamics calculations within the quasi-harmonic approximation. Structural and thermodynamical properties at finite temperatures were well reproduced for both phases. The transition pressure shows negative temperature dependence in consistent with previous experimental observations. This can be attributed to a greater increase in vibrational entropy of the rocksalt phase with temperature. The effect of alloying with MgO on the phase transition was also examined in conjunction with the cluster expansion and cluster variation method. The transition pressure decreases with an increase of MgO content. This behavior is due to the energetical preference of the rocksalt phase to the wurtzite phase in MgO and the increase in configurational entropy.

11:20 AM

Predicted Metastable Phase Boundaries in Al-Mg-Si from First-Principles: *Hui Zhang*¹; *Chinnappan Ravi*²; *Chris Wolverton*²; *Long-Qing Chen*¹; *Zi-Kui Liu*¹; ¹Pennsylvania State University; ²Ford Motor Company

The Al-Mg-Si system forms important alloys, in part due to their age hardening characteristics. For Al-rich alloys in this system, the metastable precipitate β'' is often the most effective hardening precipitate. Knowledge about the solvus of metastable phases is critical for understanding the physical and mechanical properties of these alloys. However, due to the complexity of the precipitation sequence, the metastable phase solvus boundaries are very difficult to determine experimentally. In present work,

we have obtained the formation enthalpies and vibrational entropies of the stable β (Mg₂Si) phase and the metastable β' (Mg₂Si) and β'' (Mg₅Si₆) phases through first-principles total energy and frozen phonon calculations. We have then used these first-principles thermodynamic values as input to a computational thermodynamics, or CALPHAD, approach to predict the solvus boundaries of β , β' , and β'' for Al-rich compositions different Mg/Si ratios. In all cases, the results are compared with existing experimental results.

11:40 AM

Linear Response Theory versus Frozen Phonon Method: Ab Initio Thermodynamic Calculation: *Yi Wang*¹; ¹Pennsylvania State University

Comparing calculations for the thermodynamic properties have been done between the linear response theory and the frozen phonon method using Al, Cu, Mg, Si, Mo, Ta, and q'-Al₂Cu as the prototype. We have examined the linear thermal expansion coefficient, heat capacity, and entropy as the functions of temperature up to about melting point. We found that the results produced by the two methods are comparable.

12:00 PM

Thermodynamic Effects of Resonance Modes in Al-Ag: *Max Guy Kresch*¹; *Tabitha L. Swan-Wood*¹; *Oliver Delaire*¹; *Brent T. Fultz*¹; ¹California Institute of Technology

There is an unusually strong temperature dependence of the solubility of Ag in Al. Resonance modes, where heavy atoms undergo damped, low frequency vibrations, are known to exist in this system. To investigate the thermodynamic effects of these modes, we measured phonon densities of states (DoS) of Al-7 at. % Ag at 20°C (RT) and 520°C, and of elemental Al at RT. A Mannheim model showed that the resonant peak should have a large impact on the thermodynamics of the alloy. The low frequency Ag vibrations were observed in our Born von Karman fit of the Al-7 at. % Ag DoS at RT, and the calculated frequencies compared favorably with experimental findings. By fitting the remaining DoS, we are able to further characterize the effects of the resonance mode on the phase stability of Al-Ag.

Deformation and Fracture from Nano to Macro: A Symposium Honoring W. W. Gerberich's 70th Birthday: Fracture, Fatigue, Wear, and Adhesion

Sponsored by: The Minerals, Metals and Materials Society, TMS Materials Processing and Manufacturing Division, TMS Structural Materials Division, TMS/ASM: Mechanical Behavior of Materials Committee, TMS: Nanomechanical Materials Behavior Committee
Program Organizers: David F. Bahr, Washington State University; James Lucas, Michigan State University; Neville R. Moody, Sandia National Laboratories

Monday AM
March 13, 2006

Room: 214D
Location: Henry B. Gonzalez Convention Ctr.

Session Chairs: David F. Bahr, Washington State University; John M. Jungk, Sandia National Laboratories

8:30 AM Invited

Adhesion and Mechanical Behavior of Thin-Film Structures for Emerging Technologies: *Reinhold H. Dauskardt*¹; ¹Stanford University

The mechanical behavior of materials when confined to small length scales together with their fracture and fatigue behavior effects the mechanical integrity of a wide range of thin-film device structures. Two unique challenges for emerging technologies involve the introduction of new nanostructured materials and the effect of device architecture including length-scales and aspect ratios. Materials and interfaces are nearly always optimized for other desired properties (e.g. dielectric properties, diffusion resistance, reduced carrier scattering) and the resulting effects on thermo-mechanical performance can be significant. We will present results from experiments and multiscale simulations showing the effects of interface parameters and thin-film deformation on mechanisms of debonding. Accelerated crack growth in complex chemical environments is also dis-

cussed. Implications for device reliability, integration of new materials, and life prediction are discussed.

8:50 AM

Wear-Induced Nanoscale Surface Reconstruction Patterns: *Alex A. Volinsky*¹; Bartek Such²; Marek Szymanski²; ¹University of South Florida; ²Jagiellonian University

The formation of surface patterns has been previously observed when scanning the surface of single crystals with an AFM tip in ultra-high vacuum. These patterns are formed of the periodic surface ripples aligned perpendicular to the scanning direction. The same experiments, but conducted in air, did not yield the same result, with a wear hole forming in the scan area. We were able to reproduce similar ripple formations by using a scanning nanoindenter in air. A KBr (001) freshly-cleaved surface was repeatedly scanned with the first ripples forming after the first several scans. We believe that there is a similarity between the nanowear-induced ripples, sand dunes and ocean-floor ripples. This paper will describe the experimental details of nanowear-induced patterns, and will try to explain the origin of surface nanostructuring and ripple formation.

9:05 AM Invited

Interfacial and Near-Interfacial Fatigue-Crack Growth: *Jamie J. Kruzic*¹; Rowland M. Cannon²; *Robert O. Ritchie*²; ¹Oregon State University; ²University of California

In this presentation, we describe the factors that affect the growth of cracks at, or near, bimaterial interfaces (primarily ceramic-metal) in micron-scale layered (sandwich) structures. For Al₂O₃/metal interfaces, cyclic fatigue-crack growth was found to occur primarily at the interface, while cracks deviated into the polycrystalline alumina for highly constrained samples at high cyclic driving forces or during overload fracture. In the presence of moisture, accelerated cracking was observed in many glass/metal and alumina/metal systems, but Al₂O₃/Al appeared to be relatively immune. Indeed, under static loading in a moist environment, interfacial crack growth was never observed at measurable rates; however, for highly constrained samples cracks did deviate off the interface and grow into the alumina, causing premature fracture. Such results are discussed in terms of the role of plastic constraint (assessed by varying the metal-layer thickness), crack path, loading mode, modulus mismatch, crack size, and the role of the environment.

9:25 AM

Properties of Wear Tested Single Crystal Nickel at the Nanoscale: *Neville Moody*¹; Megan Cordill²; John Jungk¹; Soumari Prasad¹; William Gerberich²; ¹Sandia National Laboratories; ²University of Minnesota

Strength, friction, and wear are dominant factors in the performance and reliability of nickel based LIGA devices. However, the effects of frictional contacts and wear are not well-defined. To address these effects on a fundamental level, we have begun a program using nanoscratch and nanoindentation to study wear on <001> oriented single crystal nickel. Nanoscratch techniques were used to generate wear patterns as a function of load and number of cycles. Nanoindentation was then used to measure properties in each wear pattern. The results showed a strong increase in hardness with increasing applied load but no effect of cyclic deformation, in contrast to the strong cyclic response of polycrystalline nickel. In this presentation, we will show how flow stress and plasticity evolve under sliding contacts and how these differences lead to different responses contacts in single and polycrystalline nickel. This work supported by Sandia National Laboratories under USDOE contract DE-AC04-94AL85000.

9:40 AM

Fracture Mechanics Approach to Analyzing Collapse of Micro-Contact Printing Stamps: *K. Jimmy Hsia*¹; John Rogers¹; Yonggang Huang¹; Weixin Zhou¹; ¹University of Illinois

Collapse of elastomeric elements used for pattern transfer in soft lithography is studied through experimental measurements and theoretical modeling. The objective is to identify the driving force for such collapse. Two potential driving forces, the self-weight of the stamp and the interfacial adhesion, are investigated. An idealized configuration of periodic rectangular grooves and flat punches is considered. Experimental observations demonstrate that groove collapse occurs regardless whether the gravitational force promotes or suppresses such collapse, indicating that self-weight is not the driving force. On the other hand, model predictions based

on the postulation that interfacial adhesion is the driving force exhibit excellent agreement with the experimentally measured collapse behavior. The interfacial adhesion energy is also evaluated by matching an adhesion parameter in the model with the experimental data.

9:55 AM

Durability of FeCo Thin Films on Ti-6Al-4V: *Kwai S. Chan*¹; Stephen J. Hudak¹; Bruce R. Lanning¹; Casey E. Smith¹; Andrew L. Veit¹; Glenn Light¹; ¹Southwest Research Institute

The durability of FeCo thin films bonded on Ti-6Al-4V was studied as a function of layer thickness at ambient temperature. Interface toughness of the thin films was characterized by indentation and analyzed using an interface fracture model. The critical stresses for interface decohesion and the fatigue life response of Ti-6Al-4V with and without FeCo thin films were evaluated by three-point bend fatigue. The results indicated that the critical stress for interface debonding increased with decreasing layer thickness according to a critical energy release rate criterion. The FeCo thin films did not alter the fatigue life of the Ti-6Al-4V substrate. The presence of microcracks in the thin films did not affect the functionality of the sensor to detect strain via the inverse magneto-elastic effect. The overall durability of the films was in the range needed for practical application of the film as an imbedded sensor.

10:10 AM

Development of Adhesion Layer Dynamics for Metal Interfaces: *Marian S. Kennedy*¹; Richard P. Vance¹; David P. Adams²; Neville R. Moody²; David F. Bahr¹; ¹Washington State University; ²Sandia National Laboratories

The exact mechanism that influences the adhesion of metallic-ceramic interfaces has not been clearly identified and is generally ascribed to the mixture of several mechanisms including chemical bonding, texture, strain transfer, and plasticity. In addition, transitions between each of these mechanisms may occur during the aging process, when interlayer diffusion occurs. This study examines the combined influence of plasticity and chemical bonding with respect to the interlayer thickness and the effects of aging. The effect of film thickness was studied varying the thickness of the Ti from 0 to 17nm in a Pt/Ti/SiO₂ system. Annealing heat treatments were applied to Au/SiO₂ systems with a barrier layer of W to study aging kinetics. With the addition of interlayers, the toughness of the Pt/SiO₂ system increased from 0.7N/m and Au/SiO₂ from 0.16N/m. Work was supported by Sandia National Laboratories under contract DE-AC04-94AL85000.

10:25 AM Break

10:45 AM

Fracture at the Nanoscale: An In-Situ Study: *Julia Deneen*¹; William M. Mook¹; Andrew M. Minor²; William W. Gerberich¹; *C. Barry Carter*¹; ¹University of Minnesota; ²Ernest Orlando Lawrence Berkeley National Laboratory

The transmission electron microscope (TEM) is an essential characterization tool when working to bridge the gap between nanoscale and bulk mechanical behavior. Unlike traditional instrumented indentation testing methods, the TEM can discern defects, surface layers and crystal orientation at the appropriate scale. Plus, with the relatively recent development of an in-situ indentation sample holder, it is now possible not only to see a nanostructure, but also to probe it mechanically while simultaneously viewing the event in the TEM. This makes the TEM an ideal tool for investigating the deformation and failure mechanisms of individual nanoparticles. Using an in-situ indentation holder, this study investigates the mechanical response of silicon nanospheres by compressing the particles between a sapphire substrate and a diamond tip. With this approach it is possible to observe directly the dynamic processes associated with nanoscale mechanical behavior. This study presents direct evidence of plasticity-induced cleavage fracture in silicon nanoparticles.

11:05 AM

High-Cycle Fatigue in Freestanding Thin Film Metal Structures: *Maarten P. de Boer*¹; Alex D. Corwin¹; Paul G. Kotula¹; Michael J. Shaw¹; ¹Sandia National Laboratories

The elastic, plastic and interfacial properties of freestanding metal thin films are of interest in microsystems applications such as radio-frequency

devices, microrelays and optical reflectors. In this work, we have developed a new methodology to measure strength and fatigue of thin films. The test structure is an Al/0.5% Cu freestanding fixed-fixed beam of 0.5 micrometer thickness with a stress concentrating notch. We focus here on high-cycle fatigue, which is crucial in MEMS applications. Due to residual stress alone, notched structures experience plasticity. When stretched further by actuation, they unexpectedly exhibit elastic behavior until a significantly higher stress level is attained. TEM images indicate a very high dislocation density in the notched region, which is likely responsible for this strain hardening effect. When notched structures are subjected to 10 million fatigue cycles, plasticity effects are observed at much lower applied stresses. TEM then indicates striation patterns. Acknowledgment: Sandia is a multiprogram laboratory operated by Sandia Corporation, a Lockheed Martin Company, for the United States Department of Energy's National Nuclear Security Administration under Contract DE-AC04-94AL85000.

11:20 AM

Fatigue Behavior of Freestanding Al Thin Films: *Nicholas Barbosa III¹*; Paul A. El-Deiry²; Robert R. Keller¹; Walter L. Brown²; Richard P. Vinci²; ¹National Institute of Standards and Technology; ²Lehigh University

A test system has been developed that is capable of imposing constant total strain fatigue conditions on freestanding thin film structures 600 μm long, 100 μm wide, and 1 μm thick. Using this system, pure Al thin films have been tested under tension-tension conditions at 100 Hz with strain amplitudes from 0.08 % to 0.34 %. The Al films were found to follow a Coffin-Manson relationship with a fatigue ductility coefficient and fatigue ductility exponent of 0.022 and -0.278, respectively. Fracture morphology was similar in nature to bulk tension-tension fatigue. Slip offsets were present in the near fracture region. The behavior of the 1 μm Al freestanding films was very similar to the fatigue properties of bulk materials when the significantly smaller grain size of the films was considered. These results will be compared to work currently underway to understand the fatigue of films on substrates through an electrically-driven method.

11:35 AM

Slip Band Formation in Single Crystal Aluminum Studied by Photoelectron Emission: *Mingdong Cai¹*; Lyle E. Levine²; Mark R. Stoudt²; J. Thomas Dickinson¹; ¹Washington State University; ²National Institute of Standards and Technology

We employ photoelectron emission to monitor slip band formation in single crystal aluminum (99.995%) during uniaxial tensile deformation. Deformation of single crystal aluminum with four orientations (with tensile axes near [001], [-213], [1-1-1] and [3-32], respectively) was conducted in vacuum compatible tensile stage at an initial strain rate of $1 \times 10^{-3} \text{ s}^{-1}$. We show that the photoemission intensities are sensitive to changes in surface morphology accompanying deformation, including slip line and band formation. Time-resolved photoemission measurements show step-like increases in intensity consistent with the heterogeneous nucleation and growth of slip bands during tensile deformation. *In-situ* measurements of photoemission and stress versus strain for the four crystals are consistent with percolation models of dislocation motion through a pre-existing cell structure. Characterization of slip bands on the deformed surfaces was performed by optical and atomic force microscopy.

Effects of Water Vapor on High-Temperature Oxidation and Mechanical Behavior of Metallic and Ceramic Materials: Behavior of Alloys: Chromia-Formers and Low Alloy Additions

Sponsored by: The Minerals, Metals and Materials Society, ASM International, TMS Structural Materials Division, TMS/ASM: Corrosion and Environmental Effects Committee

Program Organizers: Bruce A. Pint, Oak Ridge National Laboratory; Peter Tortorelli, Oak Ridge National Laboratory; Karren More, Oak Ridge National Laboratory; Elizabeth Opila, NASA Glenn Research Center

Monday AM
March 13, 2006

Room: 213A
Location: Henry B. Gonzalez Convention Ctr.

Session Chairs: Peter F. Tortorelli, Oak Ridge National Laboratory; Bruce A. Pint, Oak Ridge National Laboratory

8:30 AM

Thermochemistry of the CrO₂(OH)₂ Gas Species: *Elizabeth Opila¹*; Nathan Jacobson¹; Dereck Johnson¹; Jami Olminsky²; Dwight Myers³; Mark Allendorf⁴; Ida Beck Nielsen⁴; ¹NASA Glenn Research Center; ²QSS Group Inc; ³East Central University; ⁴Sandia National Laboratories

Chromia is known to volatilize in the presence of high temperature oxygen and water vapor to form CrO₂(OH)₂(g). This reaction is detrimental to chromia forming alloys in high temperature water vapor-containing environments and has been studied previously. However, there are major differences in the available thermodynamic data for the CrO₂(OH)₂(g) species. In this study, thermodynamic data for CrO₂(OH)₂(g) have been determined experimentally using the transpiration technique. In addition, thermodynamic data for this species have been calculated using high level ab initio electronic structure calculations. The experimentally determined temperature dependence as well as the oxygen and water vapor partial pressure dependence for the formation of this species are reported in comparison to the calculated data and other data available in the literature.

8:55 AM

Oxihydroxydes Analysis by TG-Mass and Thermodynamic Studies Formed on Coated and Uncoated Ferritic Steels for Supercritical Steam Turbines: *Francisco J. Perez-Trujillo¹*; Saul Cataneda¹; ¹Universidad Complutense de Madrid

The new supercritical steam turbines will operate at temperatures over 650°C and 300 Bar of pressure. Under those conditions the ferritic steels used upto now with chromium contents below 12% must be modified to be creep resistant. On the other hand at 650°C, the ferritic steels are not oxidation resistant, and thus the coatings are a good alternative to extend the use of those materials. In order to analyse the behavior of the coated and coated materials a TG-Mass spectrometer with a steam loop was used and designed to perform experiments to simulate those conditions. Moreover, simulations by Thermocalc are also done to simulate the oxihydroxydes formation and the solid phase formed under this conditions. Results of the coated and uncoated materials will be shown in order to analyse the coating elements reaction with the steam.

9:20 AM

Oxidation of Alloys Targeted for Advanced Steam Turbines: *Gordon R. Holcomb¹*; Bernard S. Covino¹; Sophie Bullard¹; Malgorzata Ziomek-Moroz¹; David E. Alman¹; ¹Albany Research Center

Ultra supercritical (USC) power plants offer the promise of higher efficiencies and lower emissions. Current goals of the U.S. Department of Energy's Advanced Power Systems Initiatives include coal generation at 60% efficiency, which would require steam temperatures of up to 760°C. This research examines the steamside oxidation of alloys for use in USC systems, with emphasis placed on applications in high- and intermediate-pressure turbines.

9:45 AM

Effect of Exhaust Gas Environment and Stress on the Mechanical Properties of Fe- and Ni-Based Alloys for Heat Exchangers: *Sebastien Dreypondt¹; Bruce Pint¹; Edgar Lara-Curzio¹; Rosa Trejo¹; ¹Oak Ridge National Laboratory*

Candidate foil (100 micrometers thickness) materials for the next generation of microturbine recuperators are being evaluated in a modified 60 kw microturbine with exhaust temperatures up to 840C. Test ports allow materials to be exposed simultaneously to the exhaust gas and an internal pressure applying a hoop stress. Cyclic exposures are performed by a pneumatic equipment designed to move similarly stressed specimens in and out of the exhaust stream. The alloy microstructure was analyzed after testing in the microturbine and miniature tensile specimens were designed to determine the evolution of tensile properties at room and high temperature as a function of the exposure duration. To establish the influence of stress and environment, other foil specimens were also tested after annealing at different temperatures, durations, and in various atmospheres such as inert gas or humid air.

10:10 AM Break

10:25 AM

Effect of Water Vapour on the Oxide Scale Growth of Chromia Forming Alloys in Low- and High-pO₂ Environments: *Joanna Zurek¹; Michael Haensel¹; Emmanuel Essuman¹; Leszek Niewolak¹; Lorenz Singheiser¹; Willem J. Quadackers¹; ¹Research Centre Julich*

The oxidation behaviour of chromia forming model alloys containing minor alloying additions of Mn and/or Ti has been studied. The test gas compositions were Ar-O₂- and Ar-H₂-based gas mixtures containing various amounts of water vapour. The oxidation rates were studied during isothermal exposures by thermogravimetry. Additionally, the scale growth processes were investigated in single- and two-stage oxidation tests using ¹⁸O and H₂¹⁸O-Tracer. The surface scale composition and morphology were analysed by light optical microscopy, scanning electron microscopy and x-ray diffraction in combination with sputtered neutrals mass spectroscopy. Main emphasis of the investigations was put on elucidating the effect of gas composition on the morphology, growth rate and adherence of the oxide scales for the various types of chromia forming alloys.

10:50 AM

Influence of Ce on the Oxidation Behavior of Fe-(9-12)Cr Steels in Moist and Dry Air: *David E. Alman¹; W. Keith Collins¹; Omer N. Dogan¹; Jeffrey A. Hawk¹; Paul D. Jablonski¹; ¹U.S. Department of Energy*

The influence of a Ce surface treatment on oxidation behavior of a commercial (P91) and experimental steels containing 9 to 12 weight percent Cr was examined at 650C in dry and moist air. The oxidation behavior of all the alloys without the Ce modification was significantly degraded by the presence of moisture in the air (e.g., the weight gain of P91 increased by two orders of magnitude in moist air). The Ce treatment improved the oxidation resistance of the experimental steels in both moist and dry air. For instance, in moist air the Ce surface infusion treatment reduced the weight gain of a Fe-9Cr-3Co-3Cu-1Ni-0.7Mo-0.5Ti alloy by three orders of magnitude, and for comparison, was two orders of magnitude lower than P91. The Ce surface treatment did not improve the resistance of P91. The results are discussed in terms of oxide scale formation and the synergistic effects of constituent alloying elements.

11:15 AM

The Influence of Water Vapor on the Internal Oxidation of Chromium and Aluminum in Nickel Base Alloys: *Frederick S. Pettit¹; Nathan Ward¹; Gerald H. Meier¹; ¹University of Pittsburgh*

Exposure of superalloys, such as Rene'-N5, as well as nickel-chromium-aluminum alloys to oxidizing conditions at temperatures from 900° to 1100°C, indicates that internal oxidation of chromium and aluminum becomes more pronounced when water vapor is present. This paper will present results on the oxidation of Ni-1(wt%)Cr and Ni-1(wt%)Al at 1000°C in air containing 10% water vapor, and in an argon-hydrogen gas mixture containing 10% water vapor. The results will be used to account for the effects of water vapor on the internal oxidation of elements in alloys.

11:40 AM

In Situ Surface Characterization of C-Mn-Si Steel during Continuous Annealing: *Tom Van De Putte¹; Zinedine Zermout²; B. C. De Cooman¹; ¹University of Ghent; ²Arcelor Group*

High strength multi phase CMnSi steel is increasingly being used in passenger cars. Si and Mn alloying levels are typically in the range of 1-2% in mass. While Si improves the mechanical properties, it deteriorates the galvanizability of steel considerably. Residual water vapor in the reducing gas atmosphere during the intercritical annealing in a continuous hot dip galvanizing line, results in the selective oxidation of Si and Mn at the steel surface. The dew point of the furnace atmosphere is of great importance for the amount and type of surface oxidation. High dew points lead to internal oxidation and better galvanizability while low dew point values lead to the formation of external oxide films, which are the major cause of the poor galvanising. The annealing temperature also affects the surface oxidation by its influence on the ferrite and austenite phase fractions and the solubility's and diffusivities of Si, Mn and O.

Fatigue and Fracture of Traditional and Advanced Materials: A Symposium in Honor of Art McEvily's 80th Birthday: Fatigue and Fracture I

Sponsored by: The Minerals, Metals and Materials Society, TMS Structural Materials Division, TMS/ASM: Mechanical Behavior of Materials Committee

Program Organizers: Leon L. Shaw, University of Connecticut; James M. Larsen, U.S. Air Force; Peter K. Liaw, University of Tennessee; Masahiro Endo, Fukuoka University

Monday AM
March 13, 2006

Room: 216
Location: Henry B. Gonzalez Convention Ctr.

Session Chairs: Leon L. Shaw, University of Connecticut; Robert O. Ritchie, University of California

8:30 AM Introductory Comments

8:40 AM Invited

Monotonic and Cyclic Crack-Growth Resistance in Ultrahigh-Temperature Mo-Si-B Alloys: *Jamie J. Kruzic¹; Joachim H. Schneibel²; Robert O. Ritchie³; ¹Oregon State University; ²Oak Ridge National Laboratory; ³University of California*

In this presentation, the fracture toughness and fatigue-crack growth resistance of a new class of Mo-Si-B based alloys are examined from ambient to elevated (1300°C) temperatures. These alloys, which have been targeted for ultrahigh-temperature turbine engine applications, consist of an α -Mo matrix containing Mo₃Si, and Mo₅SiB₂ (T2) intermetallic phases. However, to achieve adequate resistance to oxidation, creep, fracture and fatigue, some degree of microstructural optimization is required. The role of microstructural variables including volume fraction of α -Mo, its ductility, and the morphology and coarseness of the microstructure are considered in terms of how each variable affects the observed toughening mechanisms. Primary micro-mechanisms associated with the enhancement of monotonic and cyclic crack growth have been identified as crack trapping, crack bridging, and microcrack toughening.

9:05 AM Invited

Inelastic Deformation and Its Related Life under Cyclic/Creep Loadings in Si₃N₄-Monolithic and Si₃N₄/SiCw-Composite Ceramics at Elevated Temperatures: *K. Hatanaka¹; Y. Ishiga²; R. Kawazoe²; M. Hasui²; J. Ohgi²; H. Ogawa¹; ¹Ube National College of Technology; ²Yamaguchi University*

The push-pull low cycle fatigue and creep tests were performed in the monolithic- Si₃N₄ and the composite- Si₃N₄/SiCw materials at 1,300°C. Cyclic stress-strain response and creep strain were measured with newly developed extensometer. The inelastic strain, which is greatly dependent upon stress rate, was detected in both the materials. It was found that inelastic strain was easier to generate under tensile than compressive loading; the width of the hysteresis loop is larger on tensile stress side than on compressive stress side. Such a characteristic cyclic stress-strain response

is much more enhanced in the composite than in the monolithic-Si₃N₄. The low cycle fatigue life plotted against inelastic strain range is much longer in the former than in the latter. Moreover, the greater creep resistance is attained in the former than in the latter at the lower stress level, while converse is the case at the higher stress level.

9:30 AM Invited

Prediction of the Behavior of Small Fatigue Cracks: Masahiro Endo¹; Arthur J. McEvily²; ¹Fukuoka University; ²University of Connecticut

A modified linear-elastic fracture mechanics approach has been proposed and developed by Art McEvily and co-workers, by which the fatigue crack growth rates of both small cracks and large cracks can quantitatively be evaluated. This paper reviews the recent results of applications of this approach to the following fatigue problems involving the prediction of the behavior of small fatigue cracks: (1) in an examination of the use of Miner's rule in fatigue life estimation under variable amplitude loading, (2) in the prediction of the fatigue strength of components that contain initially small defects or cracks, and (3) in the prediction of the fatigue life and strength of defect-containing components subjected to multi-axial stress.

9:55 AM Break

10:10 AM Invited

Combined High Cycle/Low Cycle Fatigue Crack Growth and the Influence of LCF Overloads: James Byrne¹; Rodney Hall¹; Jian Ding¹; ¹University of Portsmouth

The fatigue crack growth (FCG) behaviour of forged Ti-6Al-4V aero-engine disk material under the conjoint action of low cycle fatigue (LCF) and high cycle fatigue (HCF) cycles, representing a very simplified flight spectrum, has been studied at room temperature and 350C. Systematic increases in LCF overload, applied prior to the commencement of the HCF cycles, reduce the contribution of the HCF cycles to crack growth rate and increase the stress intensity range, ΔK_{onset} , at which the HCF cycles commence to contribute to crack growth rate. The FCG prediction codes FASTRAN and AFGROW are used for both temperatures and compared with experimental results. Reasonable, conservative predictions of pure HCF and combined HCF/LCF crack growth rates and of the onset for HCF activity, ΔK_{onset} , are obtained for room temperature. However, for 350C, much less accurate predictions are obtained and an alternative twoparameter (ΔK and K_{max}) approach is suggested.

10:35 AM Invited

Dislocation Crack Tip Shielding and the Paris Exponent: Johannes Weertman¹; ¹Northwestern University

Fatigue crack growth by the crack tip blunting and sharpening model of Laird and Smith (Phil. Mag v.7 (1962) p. 847) and Neumann (Acta Metall v. 22 (1974) p.1155 and p. 167) leads to the second power Paris equation ($da/dN = (\Delta K/G)^2$ where the symbols have their usual meaning) if no appreciable dislocation crack tip shielding occurs. See Weertman Mechanics of Fatigue, AMD v. 47 (1981) p. 11 and High Cycle Fatigue of Structural Materials, TMS (1997) p.41 for a proof. In the latter publication it was suggested, but not shown quantitatively, that dislocation crack tip shielding could lead to higher exponent values in the Paris equation and lower fatigue crack growth rates. In this talk/paper I give a semi-quantitative account how dislocation crack tip shielding causes a reduction in the fatigue crack growth rate and an increase in the Paris exponent.

11:00 AM Invited

Probes of Localized Fatigue Crack Tip Damage from Plasticity-Environment Interaction: Richard P. Gangloff¹; Yun Jo Ro¹; Vipul Gupta¹; Sean R. Agnew¹; ¹University of Virginia

Alloy development and nanomechanical models of fatigue crack propagation rate require quantitative and high resolution probes of crack tip damage. This paper reviews methods applied to precipitation hardened aluminum. Synchrotron micro-Laue X-ray diffraction tomographically determines crack wake plastic strain accumulation vs local microstructure, microtexture, environment, and ΔK . Combined electron backscattered diffraction and stereology establish the crystallography of faceted regions of a complex fatigue crack surface, as a function of environment and slip morphology. The method orients a several-square micron area with 3-5° uncertainty. Transmission electron microscopy measures crack crystallog-

raphy, dislocation distribution, and composition of crack surface films from environmental reaction. Environmental scanning electron microscopy quantifies crack tip opening shape and surface-strain distribution, and could image crack tip damage in real time. Each method is challenged by the highly localized and graded characteristics of the crack tip process zone, particularly for low growth rates, and the complex microstructures of technological alloys.

11:25 AM Invited

Fatigue and Cyclic Plastic Deformation of Nanostructured and Amorphous Metals and Alloys: Simon Bellemare¹; Timothy Hanlon²; Ming Dao¹; Subra Suresh¹; ¹Massachusetts Institute of Technology; ²General Electric Company

Nanocrystalline metals and bulk metallic glasses are compared for their resistance to cyclic loading. Grains of less than 100 nm increase the total fatigue life but they impair the crack growth resistance. These results are discussed in the light of elasto-plastic properties and fracture path. It is suggested that a surface layer of nanocrystalline grains on conventional alloys could help prevent crack initiation without reducing fracture resistance. In addition to conventional fatigue testing, indenters are used to generate single and repeated scratches while monitoring the friction force and the pile-up. This approach enables the generation of large plastic strain in materials with low tensile ductility. Relationships between the scratch response and material properties have been evaluated via finite element analysis and validated experimentally. Finally, maintaining the material hardness while varying alloying and grain size enable us to isolate microstructural effects on the monotonic and cyclic plastic flow properties.

General Abstracts: Electronic, Magnetic, and Photonic Materials Division: Session I

Sponsored by: The Minerals, Metals and Materials Society, TMS Electronic, Magnetic, and Photonic Materials Division, TMS: Alloy Phases Committee, TMS: Biomaterials Committee, TMS: Chemistry and Physics of Materials Committee, TMS: Electronic Materials Committee, TMS: Electronic Packaging and Interconnection Materials Committee, TMS: Nanomaterials Committee, TMS: Superconducting and Magnetic Materials Committee, TMS: Thin Films and Interfaces Committee

Program Organizers: Sung K. Kang, IBM Corporation; Long Qing Chen, Pennsylvania State University

Monday AM
March 13, 2006

Room: 211
Location: Henry B. Gonzalez Convention Ctr.

Session Chair: Long Qing Chen, Pennsylvania State University

8:30 AM Introductory Comments

8:35 AM

A Detailed Comparative Study of Ferroelectric Lanthanide Doped Bismuth Titanate Films Prepared by Chemical Solution Deposition and Pulsed-Laser-Ablation: Ashish Garg¹; X. Hu²; Z. H. Barber²; ¹Indian Institute of Technology; ²University of Cambridge

Thin films of ferroelectric Bi-layered Lanthanide doped bismuth titanate have been an active area of investigation due to their potential applications in non-volatile ferroelectric random access memories (FRAM) and ferroelectric field effect transistor (FET) devices. In this paper, we present the results of lanthanide-doped (Sm and Nd-doped) bismuth titanate ferroelectric (BLnT) thin films deposited on platinumized Si substrates by chemical solution deposition and pulsed laser ablation. To investigate the influence of type process on the film properties, the films were grown by pulsed laser deposition (PLD) and chemical solution deposition (CSD) followed by detailed structural and ferroelectric characterization. The structural characterization was done using X-ray diffraction (XRD), Raman spectroscopy and atomic force microscopy (AFM). Detailed ferroelectric measurements were performed to study hysteresis behavior (P-E loops), dielectric constant, leakage behavior (J-V plots), and polarization fatigue. The films deposited by both processes were polycrystalline but the film morphology was dependent on the type of process. Pulsed-laser-ablated

Sm-doped Bi₄Ti₃O₁₂ films on Pt/Si substrates show a remanent polarization (2Pr) as high as ~45°C/cm². In case of chemical-solution-derived Nd- and Sm-doped Bi₄Ti₃O₁₂ films grown on Pt/Si substrates, the crystallinity and ferroelectric properties were strongly dependent upon the annealing temperature. All films demonstrate fatigue-free behavior up to 10⁹ read/write switching cycles. Conduction mechanism of the films is found to exhibit a dependence on the type of deposition process.

9:00 AM

A Method for Producing Photonic Crystals with Controlled Defects: *Harris L. Marcus*¹; Ramazon Asmatulu¹; Sejong Kim¹; Robin M. Bright¹; Fotios Papadimitrakopoulos¹; ¹University of Connecticut

This paper describes an approach to make 2D photonic crystals with controlled defects. The approach uses a dielectrophoresis cell to create the ordered polystyrene particles to create a photonic crystal. The polystyrene particles are bound to the substrate with hybridized DNA. A pulsed laser introduces defects into the crystal to create a desired defect structure. The full nature of the processing will be described. Examples of the controlled defects in the crystals will be presented. The 2D photonic crystals when fully developed have a wide range of applications in a variety of optical networks.

9:25 AM

Effect of Grain Orientation on Tantalum Erosion Rate during Magnetron Sputtering: *Zhiguo Zhang*¹; *Ling Kho*¹; *Charles E. Wickersham, Jr.*¹; ¹Cabot Corporation

The differential sputter erosion rates of tantalum grains during argon ion magnetron sputtering are reported. It is well known that there is a crystallographic dependence of sputtering rate and that grains with different crystallographic orientations relative to the bombarding ion direction will sputter at different rates. This differential sputtering when coupled with the strong crystallographic texture of metallic sputtering targets is a significant factor in determining the film thickness uniformity and deposition rate for a given sputtering target. This paper provides measurements of the sputter erosion rates for grains. Electron Backscatter Diffraction (EBSD) is used to determine each grain orientation relative to the impinging argon ion. An inverse pole figure showing contour map of the variation in sputter erosion rate with grain orientation is provided. These results are also compared to the orientation effect expected from ion channeling.

9:50 AM

Electro-Deoxidation of Mixtures of Niobium Pentoxide, Titanium and Tin Oxides to Form NbTi and Nb₃Sn Superconductors: *Derek J. Fray*¹; *Yong Yan*¹; ¹University of Cambridge

NbTi and Nb₃Sn superconductors were synthesised directly from the oxides by electro-deoxidation where an intimate mixture of the sintered oxides was placed in a eutectic mixture of calcium chloride and sodium chloride. The oxide mixture was made the cathode and the overall cathodic reaction was the ionisation of the oxygen to form ions that dissolved in the salt and diffused to the anode where they were discharged. The cathode formed NbTi alloys and the Nb₃Sn superconducting intermetallic compound which were confirmed by X-ray diffraction and their superconducting transitions.

10:15 AM Break

10:45 AM

Preparation and Electrochemical Characteristics of Sialon Bonded SiC: *Shulan Wang*¹; *Ying Yang*¹; *Laan Fan*¹; ¹Northeastern University

Sialon bonded SiC was prepared by the conventional solid reaction at 1600°C and N₂ atmosphere from Si₃N₄, Al₂O₃, AlN and SiC, and its A.C. impedance spectra were measured at the temperature range from 298K to 873K. There were two semicircles in the AC impedance spectra corresponding to the responses of SiC grain and grain boundary. By simulating the AC impedance spectra with equivalent circuits, conductivities of the grain and grain boundary as well as the energy intervals of SiC were obtained. The conductivity of SiC grain is much bigger than that its grain boundary, indicating Sialon mainly in the grain boundary region of the materials and bonded SiC together.

11:10 AM

Processing Novel Nanostructures by Ion Beam Mixing: *Sufian Abedrabbo*¹; *Dia-Eddin Arafah*¹; *Ravi Ravindra*²; ¹University of Jordan; ²New Jersey Institute of Technology

Special nanostructures are processed utilizing the technique of Ion Beam Mixing (IBM). One example is GeO₂ nano-dimensional films that are formed by annealing following the IBM. Other examples include fabrication of silicon on oxides and nitrides (SOI). Characterization processes include investigations of the structural variations noted due to Argon beam irradiation to various fluences by Rutherford Backscattering (RBS), shallow defects and deep trapping level states by Thermo luminescence (TL), X-ray Diffraction (XRD) are performed.

11:35 AM

Electro-Catalyzed Metallorganic Chemical Vapor Deposition of Copper Films: *Yu-Lin Kuo*¹; *Chiapyeong Lee*¹; *Kou-Liang Liu*¹; *Yee-Wen Yen*¹; ¹National Taiwan University of Science and Technology

This study investigated a novel technique of metallorganic chemical vapor deposition (MOCVD) of copper thin films on TaN/Si substrates using (hfac)Cu(COD) as precursor. Owing to the lower nucleation density of Cu(I) complex used in the traditional Cu-MOCVD process, we proposed a new idea of electro-catalyzed Cu-MOCVD process by supplying direct current to TaN/Si substrates. Our results revealed that supplying direct current to TaN/Si substrates not only helps to reduce the Cu incubation time but also significantly enhances Cu nucleus density and reduces Cu nucleus size. In the traditional Cu-MOCVD process without supplying direct current, activation energy (E_a) values of mass-transfer limited and surface-reaction limited regions were 1.28 Kcal/mol and 19.33 Kcal/mol, respectively. Introducing direct current to the Cu-MOCVD process apparently reduced the activation energy of surface-reaction limited region to 7.90 Kcal/mole. The proposed electro-catalysis Cu-MOCVD process was found to succeed in forming smooth and continuous thin copper films.

12:00 PM

A Computational Model to Simulate the SIMOX Process: *Sergio D. Felicelli*¹; *Supapan Seraphin*²; *David Robert Poirier*²; ¹Mississippi State University; ²University of Arizona

A finite element model was developed to simulate the production of silicon-on-insulator substrates through the technique known as SIMOX (Separation by Implantation of Oxygen). The simulation initiates from an as-implanted distribution of SiO₂ precipitates and calculates the time evolution during constant temperature annealing of the number, size, and shape of precipitates. Under proper process conditions, the redistribution of precipitates can lead to the desired formation of a buried oxide layer under a surface-silicon layer. During the evolution, the precipitates grow, dissolve, merge, or split, and can adopt arbitrary shapes under the dynamic interaction of the oxygen concentration diffusion and capillary forces. The simulations show that the model reproduces several phenomena observed during the SIMOX process, like Ostwald ripening and the formation of silicon islands. Results compare qualitatively well with actual TEM images of annealed SIMOX layers.

General Abstracts: Extraction and Processing Division: Lead and Other Metals

Sponsored by: The Minerals, Metals and Materials Society, TMS Extraction and Processing Division, TMS: Aqueous Processing Committee, TMS: Copper and Nickel and Cobalt Committee, TMS: Lead and Zinc Committee, TMS: Precious Metals Committee, TMS: Process Fundamentals Committee, TMS: Process Modeling Analysis and Control Committee, TMS: Pyrometallurgy Committee, TMS: Recycling Committee, TMS: Waste Treatment and Minimization Committee, TMS: Materials Characterization Committee

Program Organizers: Thomas P. Battle, DuPont Company; Michael L. Free, University of Utah; Boyd R. Davis, Kingston Process Metallurgy

Monday AM Room: 207A
March 13, 2006 Location: Henry B. Gonzalez Convention Ctr.

Session Chair: Boyd R. Davis, Kingston Process Metallurgy

8:30 AM

Improving Metallurgical Operations through the Application of Systems Thinking Principles: *K. Narayana Swamy*¹; ¹Doe Run Company

The traditional approach to improving the operating efficiency of a metallurgical plant has been to study individual unit operations and focus on improving the poor-performing unit operations. The complex nature of most metallurgical plants call for a holistic approach that will consider the whole rather than just focus on the individual units of a plant. This holistic approach is part of the systems thinking principles. Numerous case studies highlight the importance of the need to apply systems thinking principles in improving the effectiveness of metallurgical operations. Improving the efficiency of one unit operation without considering its effect on the performance of other unit operations has in many cases lead to lower overall operational efficiency. Modelling and simulation are key to the application of the systems thinking principles. Standard flowsheet models are very useful in scenario analyses though they have to be supplemented with other models for useful predictions.

8:55 AM

Cathodic Refining of Metals in Molten Salts: *Derek J. Fray*¹; George Z. Chen²; ¹University of Cambridge; ²University of Nottingham

The removal of non-metallic impurities, including oxygen, sulphur and selenium, from molten metals was achieved by making the molten metal the cathode in a bath of molten calcium chloride. On the application of a cathodic potential to the metal, the non-metallic impurities ionised and dissolved in the salt and were subsequently discharged at the anode. The form of the ionisation reaction was $O + 2e = O^{2-}$. In order to increase the mass transfer of the impurities a novel recessed electrode was used. The results demonstrated the usefulness of this approach in terms of space, time and yield of product and offering considerable advantages over a simple electrorefining cell.

9:20 AM

Application of Transformational Roasting to the Treatment of Metallurgical Wastes: *Preston C. Holloway*¹; Thomas H. Etsell¹; ¹University of Alberta

Transformational roasting involves the heating of a material to high temperatures along with specific additives to induce mineralogical changes in the starting material. By controlling the chemical composition, roasting atmosphere, temperature and time of reaction, the mineral transformations induced during roasting can be engineered to control the distribution of valuable, or harmful, metals and to produce new mineral assemblages that are more amenable to conventional methods of metals recovery or to environmentally safe disposal. To date, commercial application of this type of process has been limited to the recovery of Cr, Li, V and Zr, but current research is looking to expand the application of these techniques to the recovery of a wider range of metals. An introduction to these techniques is presented along with preliminary results from their application to metals recovery from metallurgical wastes, such as zinc ferrite residues and electric arc furnace dust.

9:45 AM Break

10:05 AM

Reaction Mechanism of the Alumino-Thermic Reduction of Metal Oxide and Its Application to Hot Metal Pretreatment: *Mamoru Kuwabara*¹; Jian Yang¹; Takashi Asano¹; Masamichi Sano¹; ¹Nagoya University

Reaction mechanism of the alumino-thermic reduction of metal oxide in a compact pellet is investigated using a high temperature microscope coupled with SEM observation and EDX analyses. Nano-sized alumina film covering each aluminum powder even at room temperature is further thickened during heating the compact. No alumino-thermic reduction is found to take place until a limiting temperature around 1150°C. When the pellet is heated above the temperature, a great many cracks are formed on the alumina film due to thermal shock, and liquid aluminum coming out through the cracks penetrates into the surrounding metal oxide powder phase to react with. Thus, the initial stage of the reaction mechanism is not governed by a chemical reaction characterized by Arrhenius equation. Typical applications of this alumino-thermic reduction of metal oxides to the ironmaking processes are exemplified to give better insights into improvement of desulphurization operation and low temperature slag formation.

10:30 AM

Thermodynamic Modeling of Copper Drossing Process in Lead Refining: *Pengfu Tan*¹; Pierre Vix¹; ¹Xstrata Copper

Lead blast-furnace bullion cooled to near its freezing point in an operation known as copper drossing or hot drossing usually contains 0.02-0.06% copper. The removal of this copper is usually carried out in a batch operation known as sulphur drossing. Sulphur is stirred into the bullion at temperatures near its freezing point, and the dross of copper and lead sulphides that floats to the surface is skimmed off manually. A thermodynamic model has been developed to simulate the copper drossing. The phase diagram of Pb-Cu-S system has been calculated, and the effects of the process parameters, such as temperature, copper content, and sulphur content, on the drossing process have been simulated and discussed.

10:55 AM

Thermodynamic Modeling of Kivcet Lead Process: *Pengfu Tan*¹; Pierre Vix¹; ¹Xstrata Copper

A thermodynamic model has been developed to predict the distribution behavior of Pb, Zn, Fe, S, O, As, and heat balance in Kivcet direct lead smelting furnace. The compositions of lead bullion, matte, slag and gaseous phases, and heat balance are calculated. The model predictions were compared with the known industrial data from Portovesme Company, and an excellent agreement was obtained. The effects of oxygen, coke, smelting temperature, and temperature of coke checker on the heat balance and furnace control have been discussed. In this paper, the applications of this model have been presented.

Granulation of Molten Materials: Session I

Sponsored by: The Minerals, Metals and Materials Society, TMS Extraction and Processing Division, TMS: Copper and Nickel and Cobalt Committee, TMS: Lead and Zinc Committee, TMS: Pyrometallurgy Committee

Program Organizers: Cameron L. Harris, HG Engineering Ltd; Hani Henein, University of Alberta

Monday AM Room: 7C
March 13, 2006 Location: Henry B. Gonzalez Convention Ctr.

Session Chair: Phillip Mackey, Falconbridge

8:30 AM Introductory Comments by Phillip Mackey

8:35 AM

Granulation of Molten Materials: *David Norval*¹; ¹Bateman Engineering

Water solidification of mattes, metals, alloys and certain slags with high metal entrainment has customarily not been practiced due to the be-

lief that such processes are too dangerous and unproven in the Pyrometallurgical Industry. Slag granulation on the other hand is extensively applied, although in some cases crudely with disastrous effects as a result of not recognizing the high heat capacities prevalent in slags. This paper will examine the most common air solidification processes and compare such processes with water solidification, mainly slag and matte granulation processes and design criteria for safe and reliable operation. Finally, purpose designed granulation and solidification processes will be discussed taking into account specific applications and the individual signatures of alloys and slags, emphasizing that no slag, matte or alloy responds in similar fashion to a granulation practice.

9:00 AM

Evolution of Granulation Technology: *Bob Greiveldinger*¹; ¹Paul Wurth S.A.

Encouraged by a strongly growing and evolving market for granulated products, Paul Wurth continuously improved its granulation and dewatering technologies to provide customers with state of the art installations. Continuously developed know-how about the granulation process of iron blast furnace slag enabled application to non-ferrous materials such as Ni-Slag, Pb-Slag, Blister Copper, Cu-Matte and even TiO₂-Slag, which rank among the most difficult materials to granulate. This paper identifies how critical objectives in granulation and dewatering technologies applied to different molten materials with respect to various product quality objectives can be addressed. The differences between hot and cold water granulation systems are explained, including the step from cold runner to granulation water tank. Development of a flow and pressure controlled blowing box is the latest step to optimize the granulation process in order to meet the latest standards in terms of quality, power consumption and environmental protection.

9:25 AM

Common Granulation Systems in the Metals Industry: *Art Cooper*¹; ¹Carlingview Technologies Ltd.

Granulation systems are common in the metals industry. The process of granulating slags, mattes and metals is more than a century old, and a number of different systems have been developed to accomplish this task. These systems have followed an evolutionary path, and may be characterized by common elements in terms of molten material handling, granulation methods and post-granulation processing. This paper will summarize the more common systems used in the metals industry, with particular reference to non-ferrous applications.

9:50 AM Break

10:15 AM

Copper Matte Granulation at the Kennecott Utah Copper Smelter: *David B. George*¹; ¹David George-Kennedy²; ²Colin Nexhip¹; ¹Robert Foster²; ¹Rio Tinto Technology Services; ²Kennecott Utah Copper

Kennecott Utah Copper adopted Flash Smelting and Flash Converting in 1995, a process based on granulating high grade copper matte. While nickel mattes and small quantities of copper matte had been commercially granulated for years, no large scale copper matte granulation system had been built. This paper summarizes the history and benefits of copper matte granulation, the Kennecott design basis, the successful operation for over 10 years and potential problems inherent in some matte granulation approaches.

10:40 AM

Granulation of Precious Metal-Bearing Alloys and Slags: *William Kelly O'Connor*¹; ¹Paul C. Turner¹; ¹U.S. Department of Energy

A molten metal granulator was designed and fabricated at the U.S. Dept. of Energy, Albany Research Center, for granulation of precious metal-bearing alloys and slags. The system was designed to safely granulate a metal alloy at a temperature of up to 1,600°C at a rate of roughly 100 lb of alloy per minute. The primary water jet was supplied by a 25-hp, 160 gpm pump which provided approximately 1,200 lb of water per minute through the primary jet. Two 5-hp, 80 gpm auxiliary pumps provided additional wash water to wet the granulation trough through 4 secondary jets, which were placed at either side of the primary jet. The water supply was closed-loop, including a 10,000-gallon supply tank and 6,000-gallon recovery tank. Magnetic separators and particulate filters were included for collec-

tion of the finest fraction of the granulation product, which cleaned the water sufficiently for continuous recycle.

11:05 AM

Multimedia Dispersion and Solidification of Molten Material Flows: *David Arana*¹; ¹Hendrik LeRoux²; ²Art Cooper³; ¹Vidabrazil; ²Read, Swatman & Voigt Ltd.; ³Carlingview Technologies Ltd.

The use of gas-water dispersion of a molten material flow onto a vibrating surface is developed as a process to minimize water pumping requirements, minimize the risks of explosions, and minimize the post solidification dewatering and fines handling equipment requirements. The process uses existing vibration transport technologies and common plant utilities. Plant trials using the smaller footprint and the progressive molten particle cooling time have yielded encouraging results. The results are analyzed and reported.

11:30 AM

Properties and Uses of Granulated Non-Ferrous Slag: *Michael P. Sudbury*¹; ¹Denis J. Kemp²; ¹Michael P. Sudbury Consulting Services Inc; ²Falconbridge Ltd

Non-ferrous slags are granulated and stockpiled as an alternative to pit cooling or transporting molten slag to a dump. The chemical composition of such slag is determined by the pyrometallurgical process in which it is produced, while the size distribution is set by safety concerns or a desire to reduce wear of pumps, pipelines and other equipment. Relatively few operations give consideration to the effect of granulation conditions on other properties of the granulate as the material is typically accumulated on the smelter site. It is becoming recognized that slag has many potential commercial uses and carries much of the energy applied to the smelting operation. This paper outlines the findings of extensive work to identify uses for granulated non-ferrous slag, the importance of preparation conditions on the properties, impediments to more extensive use of granulated slag, the real costs of slag stockpiling and the opportunities for further productive research.

11:55 AM Concluding Comments by Cam Harris

Lead Free Solder Implementation: Reliability, Alloy Development, and New Technology: Mechanical Behavior I: Thermal Fatigue, Shock, and Reliability

Sponsored by: The Minerals, Metals and Materials Society, TMS Electronic, Magnetic, and Photonic Materials Division, TMS; Electronic Packaging and Interconnection Materials Committee
Program Organizers: Nikhilesh Chawla, Arizona State University; Srinivas Chada, Medtronic; Sung K. Kang, IBM Corporation; Kwang-Lung Lin, National Cheng Kung University; James Lucas, Michigan State University; Laura J. Turbini, University of Toronto

Monday AM Room: 214A
March 13, 2006 Location: Henry B. Gonzalez Convention Ctr.

Session Chairs: Srinivas Chada, Medtronic; Nikhilesh Chawla, Arizona State University

8:30 AM Invited

Shock-Resistance of SnAgCu Solders: Effects of Ag and Doping: *Dave Daewoong Suh*¹; ¹Heeman Choe¹; ¹Mitesh Patel¹; ¹Tiffany Byrne¹; ¹Ted Martin¹; ¹Ashay Dani¹; ¹Intel Corporation

Current industry standard near-eutectic SnAgCu (SAC405/305) alloys are significantly worse than eutectic SnPb in terms of their shock performance. In this article, effects of Ag and doping elements on shock-resistance of SnAgCu alloys are presented. Technical strategy for bulk and interface optimization is derived from the understanding of shock damage process. For bulk optimization, elastic compliance is identified as a key property and metallurgical simulation/technique to achieve enhanced bulk compliance is presented. It is shown that by optimizing the content of Ag (which does not participate in interfacial reaction), considerable bulk compliance can be achieved and shock performance is accordingly

improved. Effects of optimum Ag content on other relevant properties and performance is also examined. Interface optimization strategy through doping is presented for representative surface finishes. Representative data on doping element effects on interfacial reaction and resultant interface characteristics are presented. The resultant interface characteristics are correlated with drop/shock performance.

8:55 AM

Thermal Fatigue of Pb-Free Solders: Experiments and Microstructure-Based Simulation: *Rajen S. Sidhu*¹; Nikhilesh Chawla¹; ¹Arizona State University

Pb-free solders encounter several mechanical and thermal loading conditions in service. In particular, thermal fatigue is extremely important. In this presentation, the thermal fatigue behavior of individual solder spheres, reflowed on Cu substrates, will be discussed. Sn-Ag, Sn-Cu, Sn-Ag-Cu and pure Sn solder spheres, 1 mm in diameter, were reflowed onto copper substrates to form lap shear specimens and thermal cycling was conducted. The specimens were cycled through the temperature range between -20°C and 130°C. Microstructure evolution during thermal fatigue damage was characterized. By correlating the microstructure with cycles to failure, the underlying mechanisms for deformation during thermal fatigue of Sn-rich solders was elucidated. To further understand the crack growth behavior within these complex solder microstructures, we have used a two-dimensional finite-element approach to understand the effects of: (a) Ag₃Sn particle size and distribution and (b) Cu₆Sn₅ layer morphology and thickness on shear deformation and damage development during thermal fatigue.

9:15 AM

Fatigue Test for Determining the Cyclic Stress-Strain Response of Solder Joints Connecting Rectangular Components to Circuit Boards: *Raymond A. Fournelle*¹; Paul B. Crosbie²; ¹Marquette University; ²Motorola

A new test for analyzing the low cycle fatigue experienced by solder joints on a circuit board has been developed. This test simulates the strains that a solder joint experiences during thermal cycling by mechanically cycling tensile specimens made of fiberglass circuit board with rectangular copper "components" soldered to them. The mismatch between the elastic moduli of the fiberglass and the copper generates strains in the solder joints when the fiberglass specimen is load cycled. The test involves direct measurements of the load in the fiberglass specimen and the tensile strain in the surface of the rectangular copper component. Using an approximate analytical analysis based on a two dimensional FEA model, these measurements are converted into average stresses and strains in the solder joints. Cyclic stress-strain hysteresis loops obtained for a Sn-Ag-Cu alloy exhibit good agreement with those reported in the literature. The joints also cyclically soften during cycling.

9:35 AM

Mechanistic Reliability Model for Thermo-Mechanically Driven Thin Film Delamination in Microelectronic Packages: *Shubhada Sahasrabudhe*¹; Arun Raman¹; Xuejun Fan¹; Mukul Renavikar¹; Alan Lucero¹; Sandeep Sane¹; ¹Intel Corporation

While performing reliability predictions, typically a generic reliability model is used across different microelectronic package failure mechanisms and the physics of failure is rarely tied to the model. This paper presents a science based reliability model developed for a typical thin film delamination mechanism in microelectronic packages that occurs under thermo-mechanical stress. High temperature exposure causes intermetallic compound growth at metal interfaces, inducing Kirkendall voids eventually leading to thin film delamination. Mechanistic understanding will be offered by linking phenomenological observations to key reliability model parameters. During model validation, the predicted failures matched remarkably within 5% of the experimental results. The paper includes elaborate sequential stress testing, intense failure analysis, detailed finite element simulation and complete statistical analysis.

9:55 AM

Critical Void Size and Location on Lead-Free Solder Joint Reliability: *De-Shin Liu*¹; Bo-Kuan Lin¹; Cho-Liang Chung¹; ¹National Chung Cheng University

Voiding occurred in lead-free solder joint due to improper reflow profile and unfit flux system is one of the major failure modes to reduce the solder reliability. However, small voids can act as stress relievers and also can changing the crack pattern to maintain sufficient life cycles. In order to understand the effects of voids on the lead-free package performance, mini-BGA packages with Sn-3.5Ag-0.5Cu solder are used to undergo the temperature cycling test (TCT) with different IR-reflow peak temperatures to examine the void forming mechanism and compared life cycles. A three dimensional finite element (FE) model of mini-BGA was built and analyzed with relative constitutive equations. Analysis results are shown that the critical void size is about one-eighteenth of solder diameter. Higher stress level can be found as the void location closed to solder bond.

10:15 AM Break

10:30 AM

Material Optimization and Reliability Characterization of Indium Solder Thermal Interface Material for CPU Package Technology: *Carl L. Deppisch*¹; Arun Raman¹; Fay Hua¹; Thomas Fitzgerald¹; Mikel Miller¹; Charles Zhang¹; ¹Intel Corporation

Developing new thermal interface materials (TIM) is a key activity to meet package thermal performance requirements for future generations of microprocessors. Indium solder is capable of demonstrating end of line (EOL) performance to meet current targets due to its inherent high thermal conductivity. However, improving its reliability performance, particularly in temperature cycling, proved to be challenging. This study describes the failure mechanisms and reliability performance of indium solder TIM as a function of integrated heat spreader (IHS) metallization thickness, TIM bond line thickness and die size and the steps taken to improve its temperature cycle performance. Analyses were performed using thermal resistance measurement (TRES), scanning electron microscopy (SEM), scanning acoustic microscopy (SAM) and transmission electron microscopy (TEM) to characterize the solder TIM thermal performance, interfacial microstructure and failure mechanisms.

10:50 AM

Thermal Shock Behavior of Sn-3.5Ag Solder Joints at Various Temperature Extremes and Number of Cycles: Bo Li¹; Fu Guo¹; Andre Lee²; K. N. Subramanian²; ¹Beijing University of Technology; ²Michigan State University

There has been increasing number of microstructural and mechanical studies on the thermomechanical fatigue (TMF) behavior of Sn-3.5Ag solder in the joint configuration. However, the TMF behavior of such solder joint and its effect on the residual mechanical properties have not been reported in a systematic manner. In the current research, thermal shock experiment on eutectic Sn-3.5Ag solder joint are carried out at various number of cycles and temperature extremes. Mechanical properties such as shear stress, peak shear stress are evaluated as a function of different temperature extremes, and number of cycles to gain a better understanding of the parameters contributing to thermomechanical fatigue or thermal shock resistance of Sn-3.5Ag solder joint.

11:10 AM

Probabilistic Microstructure Based Approach for Reliability Analysis of Lead-Free Solders: *Ganapathi Krishnan*¹; Robert G. Tryon¹; Robert J. Matthews¹; ¹Vextec Corporation

Reliability of solder interconnects is of prime concern in the transition from lead to lead free solders. Seventy percent of failures in microelectronic components have been attributed to interconnects, therefore accelerated evaluation of reliability a new lead-free solder alloys is needed to save developmental costs and time. Microstructure based damage models developed by VEXTEC Corporation provide the tools needed to evaluate the performance of solder under operating conditions with limited experimental data. This paper presents the methodology developed to evaluate lead-free solder alloys based on models developed for eutectic Sn/Pb solders. The performance of the solder alloy and a solder joint on a PCB under different board configurations and operating conditions can be evaluated.

11:30 AM

Nucleation and Propagation of Fatigue Damage in Near-Eutectic Sn-Ag-Cu Alloy: *Tia-Marie K. Korhonen*¹; Donald W. Henderson²; Matt Korhonen¹; ¹Cornell University; ²IBM Corporation

During thermomechanical cycling, solder joint fatigue process is characterized by recrystallization of Sn grains. Grain boundary sliding and increased grain boundary damage then results in intergranular crack initiation and propagation along the recrystallized grain boundaries. In this work, fatigue tests were used to study the initial stages of deformation in SnAgCu samples. To separate solder properties from constraints introduced by the substrate, free-standing solder specimens were used. The test samples were cast dog-bone specimens with a cross section of 1mm, which corresponds to typical solder joint diameter in ball grid arrays. The solder was heated to 245 degrees, held for ten minutes, cast and cooled at 1 degree/second. Mechanical cycling was performed isothermally at several temperatures, up to 125C. Typical test conditions were 0.5% strain and 30 minute cycles. Optical microscopy, SEM, and electron back-scatter diffraction were used to study the microstructures of the samples before and after fatigue testing.

11:50 AM

Thermomechanical Response of a Lead-Free Solder Reinforced with Shape Memory Alloy: *Bhaskar S. Majumdar*¹; L. Yang¹; S. Ma²; Indranath Dutta²; ¹New Mexico Tech; ²Naval Postgraduate School

In order to improve thermomechanical fatigue (TMF) life of lead-free solders, we have experimented with a NiTi shape memory alloy as a reinforcing phase. The conceptual framework is that the transformation of martensite into austenite at an elevated temperature would induce a backstress on the solder, through a transformation induced eigenstrain. This would reduce the overall creep strain of the solder. In this presentation, we extend our previous work to include the fabrication of Sn-3Ag solders reinforced with multiple fibers and particulates under transverse shear. Processing of such composites pose substantial challenges and are discussed. TMF tests were conducted on the solders, both with and without reinforcements, and the local displacement measurements are compared with results from Eshelby and finite element analysis. Transition of the methodology to actual ball grid arrays will be discussed. We acknowledge support by the Army Research Office with Dr. David Stepp as the program monitor.

Magnesium Technology 2006: Corrosion and Coatings

Sponsored by: International Magnesium Association, TMS Light Metals Division, TMS: Magnesium Committee

Program Organizers: Alan A. Luo, General Motors Corporation; Neale R. Neelameggham, US Magnesium LLC; Randy S. Beals, DaimlerChrysler Corporation

Monday AM
March 13, 2006

Room: 6B
Location: Henry B. Gonzalez Convention Ctr.

Session Chairs: Eric A. Nyberg, Pacific Northwest National Laboratory; En-Hou Han, Chinese Academy of Sciences

8:30 AM

Conversion Coating Treatment for AZ31 Alloy in a Permanganate-Phosphate Solution: Xichang Shi¹; George Jarjoura²; *Georges J. Kipouros*²; ¹Central South University; ²Dalhousie University

One of the major drawbacks to using magnesium parts in automotive application is its poor corrosion resistance. Various techniques have been used to address this concern. The purpose of this work was to produce a conversion coating on AZ31 alloy. This was accomplished using a bath which contained 20g/L KMnO₄, 60g/L Na₂HPO₄·7H₂O, and 25mL/L HNO₃. The optimum conditions for the coating process were a temperature of 50°C and a time of 30 min. A conversion coating of 10 µm thickness was obtained, which was subsequently sealed in a 10g/L sodium silicate bath at 85°C for 10 min. The morphology of the conversion-coated layer was studied using SEM. The crystal structure and the composition were examined by XRD and EDS. The corrosion behaviour of the conversion coat-

ing with and without sealant was studied using potentiodynamic polarization in a 0.5M NaCl solution. The results show that the corrosion resistance improved.

8:50 AM

Corrosion and Protection of Magnesium Alloy AZ91 by a New Electroless Nickel Plating Technique: *Zhenmin Liu*¹; Wei Gao¹; ¹University of Auckland

A plasma electrolytic oxidation (PEO) pretreatment and electroless nickel (EN) plating were applied to AZ91 alloy to improve its corrosion resistance. By PEO pretreatment the corrosion resistance of the alloy was improved to some extent as verified by salt fog spray and potentiodynamic polarization test. A nickel coating was deposited on the PEO pretreated AZ91 alloy. The presence of the PEO film between the nickel plating and the substrate acted as effective barrier layer between them and hence enhanced the corrosion resistance of the alloy. This new EN plating technique was also compared with a traditional EN processing. It was found the polarization current density decreased by almost two orders of magnitudes under the same experimental condition. Neutral salt spray testing further demonstrated that the corrosion property of the new EN plating on AZ91 was improved significantly. More importantly, the new technique is much more environmentally friendly processing.

9:10 AM

Corrosion Behavior and Microstructure of a Broad Range of Mg-Sn-X Alloys: Tarek Abu Leil¹; *Kamineni P. Rao*²; Norbert Hort¹; Carsten Blawert¹; Karl Ulrich Kainer¹; ¹GKSS Research Centre; ²City University of Hong Kong

To launch a new class of magnesium alloys based on the Mg-Sn system and to achieve a adequate combination of mechanical properties and corrosion behavior Mg-Sn alloys with additional elements like Calcium, Silicon, Strontium and Manganese have been investigated in as-cast condition in regard to their microstructure. The corrosion behavior has been investigated by means of salt spray tests and potentiodynamic measurements, accompanied by creep tests. As the microstructure of Magnesium alloys is significantly influenced by the heat treatment, different heat treated conditions were investigated additionally: I) as-cast, II) solution heating followed by quenching in water (T4), III) solution heated and then cooled inside the furnace "naturally" and IV) solution heated and aged (T6). Scanning Electron Microscopy (SEM) as well as EDX were also used to study and analyse the microstructure.

9:30 AM

Corrosion Behaviors of Polyaniline Electrodeposited on AZ91 Magnesium Alloys in Alkaline Solutions: *Y. F. Jiang*¹; Y. G. Wu¹; C. Q. Zhai²; ¹Hehai University; ²Shanghai Jiaotong University

Polyaniline coatings deposited on AZ91 magnesium alloys with potentiodynamic methods are investigated by auger electron spectroscopy (AES) and scanning electron microscopy (SEM). Low conductivity and many microporous are showed in polyaniline coatings, and its chemical compositions are varied in different positions. The anti-corrosion of AZ91 magnesium alloys improves with polyaniline coatings.

9:50 AM

Electroless Nickel-Phosphorus Plating on AZ31 Magnesium Alloy Pretreated with a Chemical Conversion Coating: Xichang Shi¹; George Jarjoura²; *Georges J. Kipouros*²; ¹Central South University; ²Dalhousie University

To further improve the erosion resistance and hardness of conversion coatings on AZ31 samples an electroless nickel-phosphorus layer was successfully deposited on the chemical conversion pre-treated AZ31 alloy. The electroless bath contained nickel sulphate and sodium hypophosphite as main salts and the samples were activated in a 5g/L AgNO₃ solution prior to plating. The presence of the conversion coating between the nickel-phosphorus coating and the AZ31 substrate acted as a barrier and prevented corrosion of the alloy. The morphology of the nickel-phosphorus layer was studied using SEM. The crystal structure and composition were examined by XRD and EDS and the hardness was measured. The corrosion behaviour of the nickel-phosphorus layer deposited on the conversion coating was studied using potentiodynamic polarization in a 0.5M NaCl solution using a saturated standard calomel electrode as a reference

electrode. Results show that the nickel-phosphorus coatings had a significantly better corrosion resistance than the AZ31.

10:10 AM Break

10:25 AM

Nano-ZrO₂ Improved Electroless Ni-P Composite Coating on AZ91D Magnesium Alloy: *En-Hou Han*¹; Yingwei Song¹; Dayong Shan¹; ¹Chinese Academy of Sciences

Nanometer ZrO₂ was added into the Ni-P coating on AZ91D magnesium alloy. The coating was compact, uniform and pore free, and its average chemical composition was 86.9Ni-7.9P-5.2ZrO₂ (wt%). The open circuit potential measurement, potentiodynamic polarization curves, salt spray and immersion tests were carried out to understand corrosion properties of the coating. In different corrosion electrolytes of 3.5%NaCl, 1.0N NaOH and 1.0N NaSO₄, electrochemical experiments showed that the corrosion resistance of Ni-P-ZrO₂ composite coating was superior to that of the traditional Ni-P coating. The salt spray results showed that the time for first corrosion pit in the nano-composite coating were doubled comparing with Ni-P coating. However, the immersion weight loss rate of the nano-composite coating was higher than that of Ni-P coating. The former is general corrosion and the later is pitting corrosion. The possible mechanisms were discussed.

10:45 AM

Sacrificial Magnesium Film Anode for Cathodic Protection of Die Casting AZ91D Alloy: *Bing Lung Yu*¹; Jun-Yen Uan¹; ¹National Chung Hsing University

The coatings on magnesium alloy usually act as a corrosion barrier to the environment. However, the coating must be crack free for applications otherwise the substrate material under the crack becomes local anode, leading to severe local corrosion. In present study, magnesium film was deposited on AZ91D specimen, acting as a sacrificial anode. The corrosion properties of the Mg-film coated specimen were estimated by electrochemical polarization experiments and constant immersion tests, both in 3.5% NaCl solution. The E_{corr} values of the coated specimens were -1.7~-1.66V (AgCl), which was evidently lower than that of the substrate material (AZ91D diecast specimen). According to the electrochemical analyses, the magnesium film could be used as a distributed sacrificial anode, cathodically protecting the substrate (AZ91D diecast specimen). Immersion tests showed that the uncoated specimen was severely corroded while the Mg film-coated specimen was well protected by the sacrificial anode of the magnesium film.

11:05 AM

Selected Etching Surface Treatment for Improving the Corrosion Resistance of Die Cast AZ91D Thin Plate: *Ching Fei Li*¹; Jun-Yen Uan¹; ¹National Chung Hsing University

HF-H₂SO₄/CaCO₃ surface treatment was explored in present study. This selected etching treatment attempted to remove the most corroding phase in the die skin of AZ91D thin plate, but left the rest of the die skin structure behind. It was found that Al-rich- α phase (eutectic α) was the most corroding phase, which located at interdendritic spacing. The I_{corr} value of the HF-H₂SO₄/CaCO₃ - treated specimens were approximately ~5 μ A/cm², significantly lower than that of the as-diecast AZ91D (~300 μ A/cm²). The purpose of the CaCO₃ application was to decrease the fluoride left on the treated specimen surface. The selected etching treatment also resulted in the opening structures that were distributed all over the sample surface. The opening structure could provide good adhesion between the metallic substrate and the protective paint. The etching treatment explored in present study not only improved corrosion performance but also left no fluoride remained on the surface.

11:25 AM

Corrosion Behaviour of Electroless Nickel Plating on AZ91 Mg Alloy: *Zhenmin Liu*¹; Wei Zhang¹; Alec Asadov¹; Wei Gao¹; ¹University of Auckland

AZ91 Mg alloy was electroless plated with nickel-phosphorous (Ni-P) coating containing 2.3 - 12.6 wt.% P. Salt fog spray testing and anodic polarisation were used to study the effects of P, coating thickness and microstructure on the corrosion behaviour. It was found that micro-cracks exist within the high P containing Ni plating (12.6 wt. % P), causing

galvanic corrosion. Corrosion potential and current density were obtained from polarisation curves measured in an aerated 3.5%NaCl solution. The results indicated that the medium and low P containing Ni coatings remained bright in appearance without pitting, showing good corrosion resistance. X-ray diffraction and SEM were used to study the as-plated specimens, showing that the P content has significant effect on the crystal structure and internal stress of coatings. The effects of the plating solution composition on the phosphorous content in the coatings, the deposition rate and corrosion property were also discussed.

11:45 AM

Corrosion Behavior of Pure Magnesium in Sodium Sulfate Solution: *Yar-Ming Wang*¹; Surender Maddela¹; ¹General Motors Research & Development Center

The corrosion behavior of pure magnesium in sodium sulfate solution was studied to establish a baseline understanding for magnesium alloy corrosion in different pH environments. Electrochemical techniques such as potentiodynamic polarization measurements, electrochemical impedance spectroscopy (EIS) and weight loss methods were compared. SEM examinations were conducted on the corroded surface and the cross-section to characterize the corrosion product and to observe the evolution of corrosion process. A six-element equivalent circuit model was used to describe active and passive corrosion behavior of magnesium in 1N sodium sulfate solution at different pH values. Due to the formation of a stable corrosion film, the corrosion current (i_{corr}) at pH 13 was two orders of magnitude lower than at pH 8. Immersion corrosion tests showed that the weight loss at pH 8 increased linearly with time. However, for pH 12 and 13 solutions, the corrosion stopped once the passive film was formed. The importance of corrosion test duration is also described in this paper.

Magnesium Technology 2006: Primary Production, Recycling and Environmental Issues

Sponsored by: International Magnesium Association, TMS Light Metals Division, TMS: Magnesium Committee

Program Organizers: Alan A. Luo, General Motors Corporation; Neale R. Neelameggham, US Magnesium LLC; Randy S. Beals, DaimlerChrysler Corporation

Monday AM
March 13, 2006

Room: 6A
Location: Henry B. Gonzalez Convention Ctr.

Session Chairs: Neale R. Neelameggham, US Magnesium LLC; Howard I. Kaplan, US Magnesium LLC

8:30 AM Introductory Comments Alan Luo, Symposium Chairman

8:40 AM

Simulation of Atmospheric Environments for Storage and Transport of Magnesium and Its Alloys: Guangling Song¹; Sarath Hapugoda¹; David St. John¹; *Colleen Bettles*¹; ¹CRC for Cast Metals Manufacturing

An environmental simulation system was developed to simulate the natural atmospheric environments that could be experienced by magnesium and its alloy ingots during their storage and transport. Magnesium, AZ91D and AM60 ingots were exposed to cycling temperature and humidity conditions in the environment simulation system and the surface degradation of the specimens was determined by measuring their brightness. It was found that the specimen surfaces exposed to the simulated atmospheric environments became duller and the degradation process was accelerated at a higher temperature or higher relative humidity. The presence of salt fog was quite detrimental to the specimen surfaces. AZ91 and AM60 with aluminium as a major alloying element were more resistant to the surface degradation than commercial purity magnesium. It is concluded that controlling humidity is a practical way of preventing rapid surface degradation of magnesium and its alloys during their storage and transport.

9:05 AM

Literature Review on Magnesium Recycling: Amjad Javid¹; *Elhachmi Essadiqi*¹; Stacy Bell²; Boyd Davis²; ¹Material Technology Laboratories/CANMET; ²Kingston Process Metallurgy Inc.

Over the last decade, magnesium recycling has become more important because of the increasing use of the metal in transportation as a light-weight material for fuel economy. In order for magnesium to continue to grow, all forms of magnesium scrap need to be recycled - for both economic and environmental reasons. Today, only high-grade magnesium scrap is being recycled and more than half of the remaining low-grade magnesium scrap cannot be processed economically due to the inability of current sorting and refining technologies to adequately separate and clean the variety of scrap produced. The presence of impurities in magnesium can lead to embrittlement and poor corrosion resistance. Therefore, with the increased use of magnesium there is a growing need for more effective magnesium sorting and refining systems for recycling of all scrap types. This paper reviews current magnesium sorting and refining technologies and explores new techniques on the near horizon.

9:30 AM

Nb-Doped TiO₂ Inert Anodes for Electrolytic Production of Magnesium Metal: *Asem Mousa*¹; Yong Yan¹; Mark Pownceby¹; Mark Cooksey¹; Ken McDonald¹; Marshal Lanyon¹; ¹CSIRO

The synthesis and performance of polycrystalline niobium-doped titanium dioxide mixtures for use as potential inert anodes in magnesium electro-winning cells were investigated. The anode materials were prepared by solid-state reaction between niobium pentoxide and titanium dioxide. The effects of the Nb:Ti ratio, sintering temperature, oxygen partial pressure and the heating/cooling rates on the chemical (solid solution range) and physical (electrical conductivity, porosity, mechanical stability) properties of the anodes material determined. Subsequent testwork examined the electrochemical behaviour of the anodes in a molten mixed chloride bath operating at 700°C. The impact of key parameters including electrolysis time, current density and bath composition on the physical properties of the anodes were investigated.

9:55 AM Break

10:15 AM

The Physical Chemistry of the Carbothermic Route to Magnesium: *Geoffrey Alan Brooks*¹; Michael Nagle¹; Simon Trang¹; ¹CSIRO Minerals

The carbothermic route to magnesium has significant potential to produce cheap magnesium but critical issues associated with the physical chemistry of various proposed processes and practical engineering dilemmas have prevented this route from being commercialized. This paper will examine the basic chemistry of carbothermic reduction of magnesia to produce magnesium. The thermodynamics of the reduction reaction, the kinetics of the reduction reaction, the kinetics of reversion, the kinetics of condensation and the distribution of impurities between phases will be critically reviewed and their potential impact on industrial processing discussed.

10:40 AM

Study on the Protecting Effect of HFC134 on AZ91D Magnesium Alloy in a Sealed Melting Furnace: Shu-Hong Nie¹; *Shou-Mei Xiong*¹; ¹Tsinghua University

The effects of holding time, temperature, furnace seal quality and stirring on the protection of AZ91D magnesium alloy were investigated in a sealed melting furnace under N₂ atmosphere containing 0.01% vol. HFC134 filled once before the experiments. The morphology, thickness, and composition of the surface film were also studied. The results showed that the highest protecting temperature was 864°. At 790°, the effective protection time for AZ91D melt exceeded 10 hours, and the allowable pressure rising velocity in crucible exceeded 10000Pa/min. With surface stirring at a temperature lower than 800°, the new protective films were formed quickly. With the increase of the holding time and temperature, the carbon content in surface films decreased quickly to zero, and the oxygen content increased. The surface morphology of all protective films was a compacted cellular structure with an evenly distributed thickness of about 1~2 μm, whereas that of unprotective films was a wadding like structure.

11:05 AM

Thermal Decoating of Magnesium – A First Step towards Recycling of Coated Magnesium: *Christina Elizabeth Meskers*¹; Anne Kvithyld²; Markus A. Reuter¹; Thorvald Abel Engh²; ¹Delft University of Technology; ²Norwegian University of Science & Technology

Die-cast magnesium is increasingly used for automotive applications and consumer electronics. For protective and decorative purposes it is coated. When the end-of-life goods are processed considerable amounts of coated magnesium scrap are generated. Currently this scrap is not recycled, leaving a resource unused. To close the magnesium utilization cycle the influence of coatings on the remelting process needs to be determined. As a first step thermal decoating of scrap prior to melting is investigated. Four objects were decoated in a thermobalance coupled to an online mass spectrometer. Decoating took place in argon and air using three heating rates. The mass loss, enthalpy and evolved gases were measured. The remaining residue was characterized. The results indicate the different stages in degradation. The combustion stage is only present using air, removing all organic matter. The residue is a mixture of pigments, fillers and conversion coatings. Decoating kinetics are assessed using iso-conversional models.

11:30 AM

Magnesia Solubility in the LaCl₃-MgCl₂ System: *Jian-Hong Yang*¹; Timothy J. Scarpinato¹; Donald G. Graczyk¹; John N. Hryn¹; ¹Argonne National Laboratory

Magnesia direct electrolysis is appealing to primary magnesium production because of significant cost savings that could result from simplified feed preparation. The key is to find a support electrolyte that has an acceptable solubility of magnesia. The LaCl₃-MgCl₂ system is one of the proposed electrolyte systems, but details of magnesia solubility measurements in this system have not been published. In this work, magnesia solubility in the LaCl₃-MgCl₂ system is presented.

Materials in Clean Power Systems: Applications, Corrosion, and Protection: Hydrogen Transport and Separation

Sponsored by: The Minerals, Metals and Materials Society, TMS Structural Materials Division, TMS/ASM: Corrosion and Environmental Effects Committee

Program Organizers: Zhenguo Gary Yang, Pacific Northwest National Laboratory; K. Scott Weil, Pacific Northwest National Laboratory; Michael P. Brady, Oak Ridge National Laboratory

Monday AM
March 13, 2006

Room: 212B
Location: Henry B. Gonzalez Convention Ctr.

Session Chairs: Petros Sofronis, University of Illinois at Urbana-Champaign; Truls Norby, University of Oslo

8:30 AM Introductory Comments

8:35 AM Keynote

State and Transport of Hydrogen in Oxides: *Truls Norby*¹; ¹University of Oslo

The state and transport of hydrogen in oxides is important in several clean energy technologies; proton conducting electrolytes, mixed proton-electron conducting hydrogen separation membranes, and recently for the functioning of oxides for novel electronics and photovoltaics. In addition to protons, the role of neutral hydrogen (atoms or molecules) is becoming clearer. The role of hydrogen in corrosion processes is well documented, but the detailed understanding suffers from the complexity of the process and the wide span in oxygen activity often encountered. The latter may cause all three oxidation states of hydrogen to take part. The talk attempts to look at hydrogen in oxides in the broad perspective of all the technological and scientific fields mentioned. One easily reaches the conclusion that we are in need of better characterisation and modelling of thermodynamics and transport of the three oxidation states of hydrogen in oxides.

9:20 AM Invited

Design of Inorganic Membranes for the Purification and Production of Hydrogen: *Brian Bischoff*¹; ¹Oak Ridge National Laboratory

The U. S. is committed to a future hydrogen economy but hydrogen is not available as an elemental resource. There are many methods for producing hydrogen including coal gasification and using nuclear energy. Coal gasification offers one of the most versatile and cleanest ways to convert the energy content of coal into hydrogen. Hydrogen can also be produced using thermochemical cycles or high temperature electrolysis and the heat from a nuclear reactor. These processes can be improved by using inorganic membranes to perform separations at high temperatures in the presence of potentially corrosive gases. Inorganic membranes have the potential to remain stable under these conditions while performing the needed separations. Each of these applications has unique materials issues. The materials selection criteria and compatibility testing of membranes employed in these hydrogen related separations along with performance data will be presented.

9:50 AM

Co-Synthesis of Mixed-Conducting Composites for Hydrogen Membranes: *John S. Hardy*¹; Nathan L. Canfield¹; Jarrod V. Crum¹; K. Scott Weil¹; Larry R. Pederson¹; ¹Pacific Northwest National Laboratory

Nanoscale powders comprising the two phases of mixed conducting composites for hydrogen membranes were co-synthesized through use of the glycine-nitrate combustion synthesis technique. Co-synthesis of proton conducting cation-doped barium cerate together with an electronic or oxygen ionic conducting phase results in an intimate mixture of the two phases with particle sizes on the order of 10 nm. The hydrogen permeability of membranes made from co-synthesized precursors will be discussed with emphasis on the effects of efforts to optimize composition, processing, and microstructure.

10:15 AM Break

10:30 AM Invited

Improving the Durability of Metal Membranes for Hydrogen Separation: *Stephen N. Paglieri*¹; Dhanesh Chandra²; Iver E. Anderson³; Robert L. Terpstra³; Ronny C. Snow¹; ¹Los Alamos National Laboratory; ²University of Nevada, Reno; ³Ames Laboratory

A durable, more cost-effective membrane material could be utilized extensively for purifying hydrogen in the chemical industries, and in the processes of generating, storing, and using hydrogen as an energy carrier. Two types of composite membranes were fabricated and tested: thin palladium and palladium alloy films supported on porous materials, and vanadium alloy foils coated with thin films (≤ 200 nm) of palladium and palladium alloys. Membrane strength and resistance to hydrogen embrittlement can be improved through the use of binary and ternary alloys of either vanadium or palladium. Another strategy for improving membrane performance, including mechanical durability and stability of hydrogen flux with time, includes supporting thin palladium alloy films on porous membranes that incorporate a diffusion barrier for metallic interdiffusion. The composite metal membranes were fabricated and characterized with respect to hydrogen permeability, permselectivity, and durability with respect to metallic interdiffusion, thermal cycling, and resistance to hydrogen embrittlement.

11:00 AM Invited

Processing of Ultrafine Alloy Powders for Hydrogen Membrane Substrates: *Iver E. Anderson*¹; Robert L. Terpstra¹; ¹Iowa State University

Controlled powder production by gas atomization can benefit emerging Fossil Energy technologies that utilize metal powders of sizes and types not produced efficiently by industry. Improved understanding and design of gas atomization nozzles has helped increase powder yields in special size classes, including ultra-fine (dia. <10 μm) and mid-range (10-75 μm) powders, with reduced standard deviation. If adopted commercially, such improvements can lower a major technological barrier to new hydrogen membrane concepts or novel alloys for thermal spray coatings. To demonstrate process robustness, He atomization trials that produced ultra-fine Fe-16Al-2Cr (wt.%) powder were performed in an up-scaled system. Results of controlled sintering work to form porous sheets explored use of these ultra-fine spherical powders as substrates for hydrogen membranes. Narrow mid-range powder size distributions of elemental Cu

and Al were nitrogen atomized using novel process parameters, anticipating trials on thermal spray alloys. Support from USDOE-FE (ARM) through Ames Laboratory contract No. W-7405-ENG-82.

11:30 AM Invited

Using First Principles Calculations to Screen Alloys for Hydrogen Purification Membranes: *David Sholl*¹; Preeti Kamakoti¹; Lymarie Semidey-Flecha¹; ¹Carnegie Mellon University

Dense metal membranes can play a crucial role in the purification of H₂ generated from coal gasification. A longstanding challenge has been to identify metal membranes that simultaneously give high membrane fluxes while being resistant to attack by common chemical contaminants in gasification streams. Alloys based on Pd have great potential as membranes with these properties, but experimental screening of multicomponent alloys as membranes is extremely resource intensive. We have developed a suite of methods based on rigorous coarse-graining of first principles quantum chemistry calculations that quantitatively predicts the flux of H₂ through Pd-based alloy membranes (P. Kamakoti et al., Science 307 (2005) 569). The accuracy of these methods has been established by comparisons of theoretical predictions with extensive experimental data for Cu-Pd alloy membranes. We will describe how we are applying our methods to identify ternary alloys with promising performance as hydrogen purification membranes.

Materials Processing Fundamentals: Process Modeling

Sponsored by: The Minerals, Metals and Materials Society, TMS Extraction and Processing Division, TMS: Process Fundamentals Committee, TMS: Process Modeling Analysis and Control Committee
Program Organizers: Princewill N. Anyalebechi, Grand Valley State University; Adam C. Powell, Massachusetts Institute of Technology

Monday AM
March 13, 2006Room: 203A
Location: Henry B. Gonzalez Convention Ctr.*Session Chair:* Adam Powell, Massachusetts Institute of Technology

8:30 AM

Fluid Flow and Transport Phenomena during Steel Refining and Casting Process: *Lifeng Zhang*¹; ¹University of Illinois

The transport of fluid, heat, and particles (bubbles and solid inclusions) in flowing molten steel is investigated in steel refining ladles, the continuous casting tundish, continuous casting mold and strand, and steel ingot casting processes. The two-equation k- ϵ model is used to simulate the turbulence. Multiphase fluid flow is numerically simulated with a Lagrangian-Eulerian approach, an Eulerian-Eulerian approach and the Volume Of Fluid (VOF) method. The simulation can predict inclusion trajectories, inclusion removal fraction, free surface waves and other phenomena, which can be used to optimize these important metallurgical operations.

8:55 AM

Numerical Simulations of Jet Break-Up Phenomena for the High Pressure Die Casting Process: *Valerio Viti*¹; Kazunori Kuwana¹; Adrian S. Sabau²; Mohamed Hassan¹; Kozo Saito¹; ¹University of Kentucky; ²Oak Ridge National Laboratory

In the High Pressure Die Casting (HPDC) process, the molten metal is injected through a thin gate into the die cavity. High pressures and high gate velocities yield jet break-up and even atomization. In order to identify the effects that can negatively affect the final quality of the casting, jet break-up phenomena must be understood. In the present work, numerical simulations of the molten Mg flow through a high aspect-ratio rectangular gate are performed. Results are also presented for water analogue for an open. The numerical simulations used Volume of Fluid VOF-type (Eulerian) methods and Lagrangian methods. A sub-grid scale model was implemented that can be used in conjunction with VOF-type formulations to predict the break-up and atomization flow pattern. The proposed formulation was more efficient than traditional VOF methods since it does

not require the use of high-resolution grids. The numerical results were compared to experimental data for validation.

9:20 AM

Computational Simulation of Phase Change in Laser Cutting Process: *Sundar Marimuthu¹*; Dipak Kumar Bandyopadhyay¹; Shankar Prasath Chaudhuri¹; Pradir Kumar Dey¹; ¹Jadavpur University

Laser cutting process is achieved by a combination of laser heating and the oxidation reaction of iron with oxygen. In this paper a three-dimensional simulation of phase change and heat transfer for a Laser Cutting process has been performed using a commercial computation fluid dynamics code, FLUENT. The melting process is incorporated using enthalpy-porosity technique and the phase change, is incorporated using Volume of Flow method. The governing equation is the transient three dimensional liquid fraction, momentum and energy equations for primary and secondary phase with appropriate boundary conditions. Transient temperature distribution, melting and phase change has been predicted. The developed model successfully estimated the kerf width at the inlet and exit and optimal speed required for defect free cutting. Three-dimensional simulation and visualization of the melting and phase change behavior inside the kerf was possible, thus enabling optimum processing windows to be predicted.

9:45 AM

Mathematical Modeling and Design of Heat Pipe-Cooled Metallurgical Furnace Equipment: *Pietro Navarra¹*; Hujun Zhao¹; Frank Mucciardi¹; Tim Van Rompaey²; ¹McGill University; ²Umicore Research

Cooling of critical furnace equipment to produce freeze lining is of particular interest as many metallurgical processes are intensified while attempting to prolong campaign life. This idea was combined with high-capacity heat pipes in the design of a copper slag launder. The design methodology of the launder and heat pipe cooling system is examined in this paper. With reliable material properties and operating conditions, CFD was used to quantitatively predict the skull thickness and the corresponding heat load applied to the slag launder. The operational limitations of heat pipe technology were considered and an appropriate cooling system was incorporated. Parametric modeling was used to simulate several launder and heat pipe configurations. The generated results were then used to optimize the design of the launder, which was built and tested in August of 2005. The experimental performance of the cooling system is evaluated and compared with the model results.

10:10 AM Break

10:25 AM

Computer Modeling Methodology of the Tecnoired Ironmaking Process: José Carlos D'Abreu¹; *Jose H. Noldin²*; Hélio Marques Kohler³; ¹Catholic University of Rio de Janeiro; ²Tecnoired/PUC-Rio; ³Independent

The Tecnoired process is a new ironmaking technology, developed on a unique approach that combined the interaction of empirical and theoretical knowledge, backed by extensive tests carried out in a dedicated pilot-plant and with close support of universities and research centers. Campaigns in the pilot-plant focused on understand, simulate and operate different reactor sizes, including a full size modular slice of the industrial furnace, which provided real-life conditions to develop the main features of the process such as internal dimensions, flame engineering, raceway pattern, thermal and gaseous profiles, formation, shape and maintenance of the melting zone, besides provide reliable data to feed and calibrate a special mathematical process modeling. This paper presents the methodology applied in this modeling, with special focus on the upper shaft of the furnace (zone of solid state reduction). The first results of this modeling are given and discussed in the end of the paper.

10:50 AM

Study of Non-Wetting Liquid Flow in a Bed of Monosized Particle Packing under the Influence of Lateral Gas Injection: *Vikrant Singh¹*; Govind Saran Gupta¹; ¹Indian Institute of Science

Gas-liquid(non-wetting) contacting in packed bed is a common operation in metallurgical reactors. Research has shown that, unlike wetting flow, non-wetting liquid flows in the form of discrete droplets or rivulets. Thus, modeling of liquid phase as a continuum is in contradiction to ob-

servations. Also, for the non-wetting case, continuum models have failed to describe liquid flow path when the liquid source is a point source. The aim of the current work is to put forward a combined lagrangian-eulerian approach to model liquid and gas flow in the packed bed. Liquid is assumed discrete and modeled using a force balance approach. Gas is assumed to be interpenetrating continua and modeled using k-epsilon model for turbulent flow. Structured packing is assumed and x-ray imaging technique used to visualize liquid flow lines in the bed. Simulation results for liquid flow path and liquid collection at bed bottom are compared with the experiments.

11:15 AM

Design of Supersonic Nozzles for Ultra-Rapid Quenching of Metallic Vapours: *Geoffrey Alan Brooks¹*; Hasan Khan¹; Peter Witt¹; Tim Barton¹; Michael Nagle¹; ¹CSIRO Minerals

CSIRO has been experimenting with supersonic flows as a method of rapidly quenching metallic vapours. Cooling rates above one million degrees per second have been achieved. The supersonic flow conditions are achieved through adiabatic expansion of the gas through a Laval nozzle into a vacuum chamber. This paper will describe the basic physics of the process, outlining the CFD modeling of flow in the nozzle, the effects of different flow conditions on the condensation process and discuss the practical design issues associated with operating supersonic nozzles.

Multicomponent-Multiphase Diffusion Symposium in Honor of Mysore A. Dayananda: Phenomenology

Sponsored by: The Minerals, Metals and Materials Society, ASM Materials Science Critical Technology Sector, ASM-MSCTS: Atomic Transport Committee

Program Organizers: Yong-Ho Sohn, University of Central Florida; Carelyn E. Campbell, National Institute of Standards and Technology; Richard Dean Sisson, Worcester Polytechnic Institute; John E. Morrall, Ohio State University

Monday AM Room: 203B
 March 13, 2006 Location: Henry B. Gonzalez Convention Ctr.

Session Chairs: Alexander H. King, Purdue University; Richard Dean Sisson, Worcester Polytechnic Institute

8:30 AM Introductory Comments: Prof. Dayananda as a Colleague and Advisor

8:50 AM Invited

An Examination of Selected Multicomponent Diffusion Couples: *Mysore A. Dayananda¹*; ¹Purdue University

Selected diffusion couples investigated in Cu-based and Fe-based multicomponent systems are examined for zero-flux plane development, interdiffusion up activity gradients, and unusual diffusion paths. The couples are analyzed for interdiffusion fluxes and interdiffusion coefficients with the aid of "MultiDiFlux©" program. The variations of interdiffusion coefficients over various composition ranges within the diffusion zone are assessed in terms of eigenvalues and eigenvectors determined from interdiffusion coefficient matrices. The internal constraints on the diffusion paths are explored in terms of fluxes of the individual components and their variation with composition. These constraints are discussed with application to selected couples. The research is supported by the National Science Foundation.

9:20 AM

A Transfer Matrix Approach for Analysis of Multicomponent Diffusion Couples: *L. R. Ram-Mohan¹*; Mysore A. Dayananda²; ¹Worcester Polytechnic Institute; ²Purdue University

A transfer matrix approach is presented for the development of solutions to diffusion problems in multicomponent systems. Expressions are derived for a transfer matrix and its integral so that the fluxes of the individual components can be obtained at any coordinate x, given an initial value for the fluxes or the concentration gradients at an initial position x₀. Interdiffusion coefficients are determined as average values over various

regions selected in the diffusion zone by the method of moments developed by Dayananda and Sohn. Expressions for concentrations are also obtained from initial conditions on fluxes or concentration gradients. The method employing the matrix approach is applicable to any number of components and may be considered as a generalization of the solutions of Fujita and Gosting originally developed for ternary diffusion. The method is illustrated with an application to a multicomponent diffusion couple.

9:45 AM

Effect of Diffusivity Variations on Interdiffusion Microstructures: *John E. Morrall*¹; Yunzhi Wang¹; ¹Ohio State University

The mathematical equations that describe diffusion couples are greatly simplified by assuming that the diffusivity is constant. To quote a famous modeler "with (constant) diffusion everything is error functions." The error function predictions are simplified too, for they predict concentration profiles, diffusion paths, and zero-flux planes that are symmetric with respect to the initial diffusion couple interface and they predict well defined rules for interdiffusion that can be generalized for n-component systems. However both the symmetry and the rules are broken when the diffusivity varies with composition. Professor Dayananda has made important contributions to the field of diffusion by documenting what happens when the diffusivity varies through his experimental work on multicomponent, multiphase systems. These contributions will be outlined along with other known consequences of diffusivity variations.

10:10 AM Break**10:30 AM Invited**

Some Aspects of Interface Migration in Ternary Systems: *Gary R. Purdy*¹; ¹McMaster University

In recognition of Professor Dayananda's many contributions to our knowledge of multicomponent-multiphase effects, this contribution will focus on certain aspects of transformation interface migration that can be ascribed specifically to the presence of a third element. Some examples considered include (a) liquid film migration in ternary alloy systems, and (b) the role of substitutional alloying elements in the coarsening of carbides in steels and in the growth of ferrite from austenite.

11:00 AM Invited

Aspects of Diffusional Reactions in Multi-Component, Multi-Phase Systems: *John Agren*¹; ¹Royal Institute of Technology

Most practical applications of diffusion theory, within heat treatment and degradation of materials, are not only multicomponent but do also involve several phases that may form or dissolve as a consequence of diffusion. Phase-field modeling is superior in some aspects and allows a detailed prediction of the evolution of one or a few particles. Nevertheless, it has a number of shortcomings that makes it less applicable to solve many practical problems. Some of these shortcomings may be overcome by "effective" models like the ones developed by Hopfe and Morral and by Engström and Ågren. The latter models have turned out to be surprisingly useful to solve a number of practical problems. In this presentation the methods will be summarized and some applications will be reviewed. Some problems of fundamental character will be discussed and some recent advances will be presented.

11:30 AM Invited

Outside the Box of Phenomenological Diffusion Formalism: *Robert T. DeHoff*¹; ¹University of Florida

Professor Dayananda and I have shared an interest in multicomponent and multiphase diffusion for more than three decades. We have enjoyed many periodic palavers at meetings such as this one through the years. He always has something new and interesting on the front burner. We have learned each other's prejudices on the subject and respect them. He knows that one of my pet prejudices is a dissatisfaction with the traditional phenomenological formalism which is used almost exclusively to describe diffusion behavior in these complex systems, and a desire to devise descriptions in terms of parameters that actually have understandable physical meaning. This presentation reviews a litany of problems associated with the ubiquitous phenomenological theory. None of these complaints is new; they are widely known and widely ignored. It may be argued that the importance and significance of these problems lies perhaps in the eye of the beholder. There is half a century of theoretical inertia that discour-

ages thinking outside the phenomenological box. Also reviewed is a description of diffusion behavior that is outside this box. This jump frequency formalism is couched in terms of parameters with physical meaning, but brings some problems of its own.

12:00 PM Invited

Discontinuities in Kirkendall Velocity in Multiphase Diffusion Couples: *William J. Boettinger*¹; Jonathan E. Guyer¹; Carelyn E. Campbell¹; ¹National Institute of Standards and Technology

In multiphase binary diffusion couples that maintain planar interfaces between phases, experimental evidence and analysis by van Loo et al. have revealed interfacial discontinuities in the Kirkendall velocity. Under the usual assumptions of the diffusion model for the Kirkendall effect, the magnitude of the discontinuity is proportional to the difference of the differences of the intrinsic diffusion coefficients for each phase. Questions arise about the implications of the discontinuity in the context of the deformation and stress state in the diffusion couple. To clarify these points, we examine the moving interface problem using the Cahn-Hilliard equation applied to a solid solution with a miscibility gap. The predicted Kirkendall velocity is continuous but suffers a large change across the diffuse interface. The associated displacement fields and strains are also continuous.

Point Defects in Materials: New Techniques

Sponsored by: The Minerals, Metals and Materials Society, TMS Electronic, Magnetic, and Photonic Materials Division, TMS Structural Materials Division, TMS: Chemistry and Physics of Materials Committee

Program Organizers: Dallas R. Trinkle, U.S. Air Force; Yuri Mishin, George Mason University; David N. Seidman, Northwestern University; David J. Srolovitz, Princeton University

Monday AM
March 13, 2006

Room: 210B
Location: Henry B. Gonzalez Convention Ctr.

Session Chair: Dallas R. Trinkle, U.S. Air Force

8:30 AM Invited

Atom-Scale Studies of Solids Using Hyperfine Interactions: *Gary S. Collins*¹; ¹Washington State University

We have investigated intermetallic compounds over 15 years through measurements of nuclear quadrupole interactions using the method of perturbed angular correlation of gamma rays, with radioactive probe atoms introduced at the ppb level. Three applications will be discussed: (1) Point defects arising due to deviations from stoichiometry and/or thermal activation can be distinguished by characteristic interactions; (2) Sublattices occupied by impurity probes can be identified from the magnitude and symmetry of measured electric field gradients; (3) Jump frequencies of diffusing probe atoms can be determined through relaxation of the nuclear quadrupole interaction. Such studies not only provide insight into atomistic phenomena such as defect agglomeration or switching of solute atoms between sublattices as a function of composition or temperature, but will be shown to yield measurables such as defect concentrations, activation enthalpies for defect formation and migration and for solute transfer between sublattices, and probe-atom jump frequencies.

9:00 AM Invited

Quantum Monte-Carlo Examines Accuracy of Density Functionals for Interstitial Defects in Silicon: *Richard G. Hennig*¹; Kevin Driver¹; William Parker¹; Cyrus J. Umrigar²; John W. Wilkins¹; ¹Ohio State University; ²Cornell University

Silicon displays a variety of interstitial defects. Ion-implanted silicon interstitials nucleate extended {311} planar defects limiting device fabrication and performance. Quantum Monte-Carlo calculations for interstitial silicon defects determine accurate defect formation energies that test the accuracy of current density-functionals. Stable defect structures from accelerated tight-binding molecular dynamics are relaxed with density-functional methods to confirm their stability. More than a dozen new stable interstitial clusters are discovered¹. While density-functional determined

structures are reliable, defect energies are sensitive to the exchange-correlation functional. Quantum Monte Carlo correctly predicts the experimental cohesive energy, lattice constant, and bulk modulus of silicon. For interstitial defects in silicon, quantum Monte Carlo shows that local-density and gradient-corrected functionals underestimate the defect energies by about 1 eV. ¹D.A. Richie et al. *Physical Review Letters* 92, 45501 (2004).

9:30 AM Invited

Defects and Off-Stoichiometry in Alloys and Oxides from First-Principles: *Anton Van der Ven*¹; ¹University of Michigan

First-principles computational schemes have reached a stage where they can be used to predict a wide range of materials properties with reasonable accuracy. Most materials are multi-component and contain dilute concentrations of impurities or defects such as vacancies. Predicting thermodynamic and kinetic properties of these materials from first-principles requires an accurate description of their configurational degrees of freedom as configurational entropy plays an important role at finite temperature. The cluster expansion has proven to be a powerful tool to extrapolate first-principles energies to the energy of any state of disorder within a multicomponent solid. In this talk, I will describe the latest developments in first-principles alloy theory and show how it can be used to predict the thermodynamic properties of vacancies within alloys and oxides.

10:00 AM

Thermochemistry of Point Defects in PuO(2-X): *Petrica Cristea*¹; *Marius Stan*¹; ¹Los Alamos National Laboratory

We developed a thermochemical model to predict the behavior of hypostoichiometric plutonia under different temperatures and partial pressures of oxygen. Based on the observed similarities between CeO(2-x) and PuO(2-x), five types of point defects were considered as major contributors to the thermochemical properties of PuO(2-x): the reduced plutonium ions Pu(3+), two types of oxygen vacancies, and two types of Pu(3+)-oxygen vacancy clusters. A number of example applications, such as the calculation of partial Gibbs free energy of oxygen, nonstoichiometry, defect configuration entropy, and the behavior of chemical potential of defect species at different oxygen deficiencies are presented in order to highlight some of the current capabilities of the approach. Advanced topics such as calculation of self and chemical oxygen diffusivities as a function of nonstoichiometry and temperature are addressed. The results are validated against available experimental data on nonstoichiometry and oxygen diffusivity.

10:20 AM Break

10:35 AM Invited

High Resolution Materials Studies with the Magnetic Resonance Force Microscope: *P. Chris Hammel*¹; *Tim Mewes*¹; *Jongjoo Kim*¹; *Sharat Batra*²; *Denis Pelekhov*¹; *Palash Banerjee*¹; *Kin Chung Fong*¹; *Yuri Obukhov*¹; ¹Ohio State University; ²Seagate Technology

The magnetic resonance force microscope (MRFM) is a novel scanned probe instrument which combines the three-dimensional imaging capabilities of magnetic resonance imaging with the high sensitivity and resolution of atomic force microscopy. It will enable non-destructive, chemical-specific, high-resolution microscopic studies and imaging of subsurface properties of a broad range of materials. Here we present the principles of the MRFM and discuss applications of the MRFM to the detection of NMR, ESR and Ferromagnetic Resonance (FMR). As an example we present studies of investigations of the dynamic magnetic properties of permalloy disc arrays using ultrasensitive low temperature ferromagnetic resonance force microscopy. Local spectroscopy reveals properties of the dot array and local information about individual dots. The ferromagnetic resonance of a dot in the presence of the tip field enables us to clearly resolve individual 50 nm thick dots with a 1.5 micron diameter.

11:05 AM

Compositional Point Defect Evaluation Using Diffusion Experiments: *Ji-Cheng Zhao*¹; *Xuan Zheng*²; *David G. Cahill*²; ¹General Electric Company; ²University of Illinois at Urbana-Champaign

Compositional point defects such as vacancies and anti-sites have a significant effect on the properties of alloys and intermetallic compounds. For instance, the formation of point defects in NiAl results in three orders of magnitude change in its diffusion coefficients. There are two indirect

ways to find the formation of compositional point defects in alloys and intermetallics using diffusion couples/multiples. The first one is to use a novel micro-scale thermal conductivity probe to measure thermal conductivity across a concentration gradient. A sharp change in thermal conductivity in a very narrow range of composition is indicative of compositional point defect formation. Thermal conductivity measurements can also be used to study the site preference/elemental substitution in intermetallic compounds. The second method is to examine the shape of diffusion profiles. Examples will be used to illustrate these methodologies. Both methods are sufficient, but not necessary tests of the compositional point defects.

11:25 AM Invited

Structure and Mobility of Defects Formed in Collision Cascades in Ceramics: *Blas Pedro Uberuaga*¹; ¹Los Alamos National Laboratory

The evolution of radiation damage is a problem spanning many time and length scales. Damage production occurs on the atomic scale via collision cascades that last picoseconds. This damage manifests itself macroscopically as swelling or cracking which can take years to develop. There is a wide range of phenomena inbetween, including defect diffusion, the formation of loops and voids, and the development of more complex microstructure. We apply several simulation techniques to study damage production and evolution in ceramic materials. Using molecular dynamics, we study low-energy cascades in MgO and MgAl₂O₄. We use temperature accelerated dynamics to probe the long-time evolution of the resulting damage. A surprising picture emerges for MgO, with large interstitial clusters being very mobile. Using these results, we have developed a rate theory model describing the formation of dislocation loops in MgO, where we see an impact of the mobile clusters on loop size.

11:55 AM

Kinetic Monte Carlo Studies of Radiation Induced Segregation in Metal Alloys: *Joerg Rottler*¹; *David J. Srolovitz*¹; *Roberto Car*¹; ¹Princeton University

In irradiated metals, the material degradation is largely controlled by point defects that are produced in collisions between the energetic particles and the host atoms. In alloys, point defect fluxes to sinks such as grain boundaries and free surfaces may cause radiation induced segregation. The alloy composition is dynamically changed due to point defect concentration gradients and different couplings between the host atoms and defects. We perform a detailed comparison between kinetic Monte Carlo simulations and the continuum rate-diffusion theory of RIS. In the absence of thermodynamic effects, continuum theory agrees well with kMC provided that correlation effects are accurately taken into account. Standard treatments of alloy thermodynamics on the level of regular solution theory are shown to be inconsistent with the kMC results. We suggest corrections to the continuum theory that provide good agreement with the numerics and also consider specifically the case of FeCr.

Separation Technology for Aqueous Processing: Session I

Sponsored by: The Minerals, Metals and Materials Society, TMS Extraction and Processing Division, TMS: Aqueous Processing Committee, TMS: Copper and Nickel and Cobalt Committee, TMS: Lead and Zinc Committee, TMS: Process Fundamentals Committee
Program Organizer: Robert L. Stephens, Teck Cominco Metals Ltd

Monday AM
March 13, 2006

Room: 202B
Location: Henry B. Gonzalez Convention Ctr.

Session Chair: Courtney A. Young, Montana Tech of the University of Montana

8:30 AM

Bioleaching of Nickel Laterite Ores Using Halotolerant *Aspergillus Foetidus* under Saline Conditions: *Anat Deepatana*¹; *V. Thangavelu*¹; *Jessica Annalishia Tang*¹; *Marjorie Valix*¹; ¹University of Sydney

Biological leaching of low-grade nickel laterite is based on a non-traditional leaching of oxide minerals using heterotrophic micro-organisms.

The organisms solubilise metals by excreting organic acids; these acids then form complexes with heavy metals. High salinity of water supplies and soils in the vicinity of nickel laterite ore bodies is a major abiotic stress to fungi and represents a major challenge in the application of bioleaching process in-situ. Salinity exposes fungi cells to Na⁺ toxicity and osmotic stress. This study examined the salt tolerance development of *Aspergillus foetidus* based on gradual acclimatization of organism, its salt threshold and the salinity effect on its metabolism. The biological leaching of limonite and nontronite minerals with the resulting halotolerant organism under saline conditions was assessed. It was observed that salinity stress affected the organism's growth and energy utilization efficiency. Metal dissolution kinetics and capacity were equivalently influenced by salt stress.

8:55 AM

Ion Exchange Recovery of Nickel and Cobalt from Metal-Organic Complexes Generated in Bioleaching of Low Grade Nickel Laterite Ores: *Anat Deepatana*¹; Marjorie Valix¹; ¹University of Sydney

Bioleaching of nickel laterite ores is based on the use of heterotrophic fungi organisms and their metabolites (organic acids) to dissolve nickel and cobalt from oxide minerals to form metal-organic complexes. Metal recovery from this process using an aminophosphonic acid based chelating resin (Purolite S950) was investigated as a function of metal concentrations, complexing agent including citric, dL-malic and lactic acids. Batch adsorptions were conducted using synthetic leachate solutions of nickel and cobalt with concentrations from 15 to 2000 mg/L prepared in 0.01 and 0.1 M organic acids. Equilibrium adsorption data were fitted into the Langmuir and Freundlich models. Metal elution was conducted using 2 M nitric acid in which up to 90% of the metals were recovered. It was observed that the maximum adsorption capacities of nickel and cobalt were 3.26 and 10.48 mg/g resins respectively achieved in 0.01 M lactic acid.

9:20 AM

Kinetics of Limonite and Nontronite Ore Leaching by Fungi Metabolic Acids: *Anat Deepatana*¹; Jessica Annalishia Tang¹; Marjorie Valix¹; ¹University of Sydney

Bioleaching of nickel laterite ores is the extraction technology based on the use of heterotrophic micro-organisms and their organic acid products to dissolve metals from oxide minerals. This study examined the chemical leaching kinetics of limonite and nontronite ores with pure fungi metabolites including citric, lactic and malic acids. Leaching was undertaken at 30°C, with ore pulp density of 2-10 g/L in acid concentrations 0.2- 3M for a period of 24 days. The chemical leaching data were compared to metal dissolution achieved with bioacids generated by *Aspergillus foetidus* grown in sucrose based substrate. Leaching was investigated as a function of acid type, acid activity, oxygen reduction potential, particle size and pulp density. The application of an ex-situ bioleaching process in extracting nickel and cobalt from laterite ores was assessed.

9:45 AM

Modeling of Electrodifusion in Aqueous Processing: Witold Kucza¹; Marek Danielewski¹; Andrzej Lewenstam¹; ¹AGH University of Science and Technology

The model of electrodiffusion (the ionic flow in various continuous media) based on the Nernst-Planck-Poisson equations (NPP) is presented. The NPP equations and the continuity equation, including the reactive term, are discretized in space and time. The resulting set of equations is solved numerically using the Rosenbrock method in Mathcad 12. The NPP model is used for simulations of transient and steady state concentrations and electric potential profiles. The impedance spectra of electrochemical systems with different boundary conditions are presented, including a permselective case. The method allows for obtaining the direct relationship between transport properties of the bulk solution and the interfaces (ionic diffusivities and heterogeneous rate constants) and the complex impedances of electrochemical systems. The method is applied for modeling of selective precipitation and ion exchange processes.

10:10 AM Break

10:25 AM

Semi-Batch Precipitation of Manganese from an Industrial Zinc Leach Solution Using SO₂/O₂: *Vincent Menard*¹; George P. Demopoulos¹; ¹McGill University

The purpose of the present work was to remove selectively manganese from a neutral leach zinc-rich solution ([Zn] =150 g/L) at 80°C using a gas mixture of sulphur dioxide (SO₂) and oxygen (O₂) as oxidizing agent. In order to determine the optimum conditions for manganese removal, several semi-batch experiments were performed, where the effects of pH, ORP, SO₂/O₂ ratio, mixing intensity, etc. were investigated. Results of these tests showed that SO₂/O₂ was a fast and effective oxidant for removing manganese down to ppm level provided that the appropriate reactor design, agitation and SO₂/O₂ ratio were employed.

10:50 AM

Study of Organic Phase Composition and Solvent Extractive Process for Purifying Nickel Chloride Solution with N235: *Chen Song*¹; Wang Lijun¹; Zhang Li¹; Luo Yuanhui¹; ¹General Research Institute for Non-Ferrous Metals

In the experiments of purifying the solution of chlorine leaching from nickel concentrate with N235, the effects of organic phase composition on purifying efficiency have been studied. From the results obtained, the optimal organic phase composition is found to be 25%+12%isomeric alcohol +63%ulfonic kerosene (V/V) and the saturated content of cobalt in organic phase is 7.95 g·L⁻¹. And then the serial experiment is carried out. The results show that at the given organic phase composition, the purified solution contains ρ(Ni) >200 g·L⁻¹, ρ(Ni)/ ρ(Co) >50000 and the contents of Cu, Fe, Mn, Zn meet the technical criterion of standard nickel electrolyte. The cobalt chloride solution contains ρ(Co) >110 g·L⁻¹, ρ(Co)/ρ(Ni) >50000 and the enrichment of cobalt has been achieved.

Solidification Modelling and Microstructure Formation: A Symposium in Honor of Prof. John Hunt: Dendritic Growth I

Sponsored by: The Minerals, Metals and Materials Society, TMS Materials Processing and Manufacturing Division, TMS: Solidification Committee

Program Organizers: D. Graham McCartney, University of Nottingham; Peter D. Lee, Imperial College; Qingyou Han, Oak Ridge National Laboratory

Monday AM
March 13, 2006

Room: 6C
Location: Henry B. Gonzalez Convention Ctr.

Session Chairs: Graham McCartney, University of Nottingham; Martin Glicksman, Rensselaer Polytechnic Institute

8:30 AM Introductory Comments

8:35 AM Invited

Growth and Stability of Solidification Microstructures: *Rohit Trivedi*¹; ¹Iowa State University

The key aspects of the theoretical models on cellular, dendritic and eutectic growth will be summarized with specific emphasis on the contributions made by John Hunt. These models will be validated through critical experimental studies in metallic and transparent systems. Emphasis will then be placed on the stability of these microstructures in bulk samples, and it will be shown that the stability conditions in 3D growth are significantly different from those in the 2D systems. The differences in these stability conditions will be discussed and the role of the additional degree of freedom in the third dimension will be emphasized.

9:10 AM

Phase-Field Simulations of Rapid Solidification in Binary Alloys: Jun Fan¹; Mikko Haataja²; *Nikolas Provatas*¹; ¹McMaster University; ²Princeton University

The kinetics of rapid solidification is important for alloys developed by powder metallurgy. The resulting powder microstructure and phase

composition controls the properties of the final solidification product. In this work, we carry out a quantitative study of rapid solidification kinetics in binary alloys using a phase-field model simulated with a novel adaptive mesh refinement algorithm in two spatial dimensions. At a high undercooling, we observe a morphological transition from dendritic to non-dendritic structures. Furthermore, growth velocity is shown to undergo a sharp transition at an undercooling that coincides with the transition in dendritic morphology. These results are shown to be in good agreement with experimental measurements. We elucidate the underlying mechanisms of these transitions and demonstrate that they are linked to non-equilibrium solute partitioning as the solute diffusion length becomes comparable to the interface width.

9:35 AM

3-D Numerical Simulation of Dendritic Crystal Growth with Phase-Field Model: *Tao Jing*¹; *Hongzhao Zhao*¹; *Baicheng Liu*¹; ¹Tsinghua University

Three-dimensional simulation of the dendritic growth for aluminum alloy was studied by coupling with thermal noise. Macro-micro coupled method and a capturing liquid method were adopted here. Since 3-D numerical simulation takes too much calculation, thermal noise was only added at the cell interface instead of the whole cell. When the dendrite grows, the capturing liquid method captures the liquid cells into the interface ones and pushes the interface region forward. Three-dimensional simulation of multiple grains for aluminum alloy was also realized. Different optimized growing directions were introduced in multi-grains simulation, which makes the simulation more coincident with the practical case. One parameter of dendritic growth interface was introduced to distinguish the original grains with different optimized growing directions. The simulation result was compared with those obtained experimentally.

10:00 AM Break

10:15 AM Invited

Dendrite Growth Directions in Al-Zn Alloys: *Frédéric Gonzales*¹; *Michel Rappaz*¹; ¹Ecole Polytechnique Fédérale de Lausanne

Recent investigations on aluminum-base alloys have revealed that dendrites can grow along various directions as a result of the low anisotropy of the interfacial energy (less than 1%). In this area, Al-Zn alloys provide a unique system, as the hcp (and much more anisotropic) Zn element can be diluted up to 95wt% in the liquid phase while still producing fcc dendrites during solidification. In specimens which have been directionally solidified or grown in a Bridgman furnace, a gradual transition from <100>- to <110>-dendrites has been observed when the zinc concentration is gradually increased: <100> dendrites form up to about 30wt% of Zn, while <110> dendrites are clearly observed above 75wt%. Such measurements should allow a correlation between the anisotropy of the interfacial energy and the zinc concentration to be made, thus providing useful information for molecular dynamic simulations of the solid-liquid interfacial energy/stiffness.

10:40 AM

Diffuse and Sharp Interface Approaches to Thermosolutal Dendritic Growth: *Juan C. Ramirez*¹; *Pinghua Zhao*²; *Juan C. Heinrich*²; ¹Los Alamos National Laboratory; ²University of New Mexico

We model the equiaxed dendritic solidification of dilute binary alloys into an undercooled melt with a finite element based interface tracking technique (sharp interface approach) as well as a phase-field technique (diffuse interface approach). This type of problem exhibits a complex interplay of species and heat diffusion combined with interface movement. Although equiaxed dendritic growth appears to be well understood in many respects, its direct numerical simulation still represents a major challenge, even in two dimensions. For different values of undercooling, grain orientation and initial melt concentration, we use both diffuse and sharp interface approaches and discuss the features associated with each approach while comparing the results obtained. We observe that relatively minor changes in physical conditions can affect significantly the difficulty of obtaining a solution to the problem, regardless of the approach employed. The organic system succinonitrile-acetone, popular with experimental researchers, is used as the substance in all simulations.

11:05 AM

Study of the Dendritic Growth in Directional Solidification of Bulk Transparent Alloys: *Cédric Weiss*¹; *Nathalie Bergeon*¹; *Nathalie Mangelinck-Noel*¹; *Bernard Billia*¹; ¹L2MP

A directional solidification facility, developed by CNES (French Space Agency) in the frame of the DECLIC project, enables the in situ and real time characterization of the solid-liquid interface on bulk transparent materials. The optical diagnostics of this device provide top and side views of the interface during the solidification of the alloy (succinonitrile based) contained in a long cylindrical glass crucible. Results of columnar dendritic growth studies performed with the laboratory model of this solidification furnace, especially focusing on pattern formation and characterization will be presented here. To extend the range of solidification parameters available and of corresponding microstructure types, a power-down furnace has also been developed in the laboratory for bulk transparent alloys. The very low thermal gradients obtained with this furnace have enabled the very first observations of superdendritic growth and columnar-to-equiaxed transition in this kind of systems.

11:30 AM

A 6-Site Force Field for Succinonitrile and Its Crystal-Melt Interfacial Free Energy Anisotropy: *Xiaobing Feng*¹; *Brian B. Laird*¹; ¹University of Kansas

A 6-site succinonitrile force field has been developed. The model has produced proper proportions of the succinonitrile conformers, which is necessary to avoid the thermal contraction of the plastic crystal phase around melting point. The initial charges are obtained with quantum chemistry calculations, and they are adjusted to improve the melting point while keeping the dipole moment fixed at 5.7 Debye. The melting point of the model has been adjusted using the Gibbs-Duhem integration method. The melting point of the model, determined by using interface method, is in good agreement with experiment. Using the fluctuation spectrum method and the new force field we calculated the crystal-melt interfacial free energies. The preliminary results are: the average free energy is 7.15×10^{-3} (Jm⁻²), and the anisotropy parameter (ϵ_4) is ~0.2%. (For a two-dimensional case, the free energy is expressed as $\gamma(\theta) = \gamma_0 [1 + \epsilon_4 \cos(\theta)]$). The amplitude of the free energy is in agreement with experiment.

11:55 AM Invited

Non-Equilibrium Segregation in Alloys: *Kenneth A. Jackson*¹; ¹University of Arizona

During growth the segregation coefficient increases from the equilibrium value as the growth rate increases. This effect has been well documented experimentally for small concentrations of dopant in rapidly crystallized silicon, and has been studied in detail using Monte Carlo computer simulations. These simulations also predict that the non-equilibrium distribution coefficient is strongly dependent on composition for non-dilute alloys. There is a change in the growth direction of ammonium chloride dendrites from <100> to <111> in ammonium chloride-water solutions. It is suggested that this change in growth direction is due to increased anisotropy in the distribution coefficient with increasing growth rate. A significant increase in distribution coefficient is predicted to be a general phenomenon which occurs at nominal growth rates in non-dilute alloys.

Space Reactor Fuels and Materials: Refractory Alloy Properties and Welding

Sponsored by: The Minerals, Metals and Materials Society, ASM International, TMS Structural Materials Division, TMS/ASM: Nuclear Materials Committee, TMS: Refractory Metals Committee

Program Organizers: David James Senor, Pacific Northwest National Laboratory; Brian D. Wirth, University of California; Robert Hanrahan, Los Alamos National Laboratory; Steven J. Zinkle, Oak Ridge National Laboratory; Mehmet Uz, Lafayette College; Evan K. Ohriner, Oak Ridge National Laboratory; Brian V. Cockeram, Bechtel Bettis Inc

Monday AM Room: 213B
March 13, 2006 Location: Henry B. Gonzalez Convention Ctr.

Session Chairs: David James Senor, Pacific Northwest National Laboratory; Brian V. Cockeram, Bechtel Bettis Inc

8:30 AM

Processing, Microstructure and Properties of Nb – Zr – C Alloys. I. Microstructure Characterization of Tube and Sheet Products: *Mehmet Uz*¹; Robert H. Titran²; ¹Lafayette College; ²NASA Glenn Research Center

We studied the effects of processing and high temperature exposure on microstructures of Nb-1Zr-0.1C tubes and sheets. Tube shells were extruded 8:1 from a vacuum arc-melted ingot at 1900K and 1550 K. Tubes were fabricated from tube shells by cold drawing with in-process anneals. Sheets were fabricated by cold rolling bars that were single-, double- or triple-extruded 4:1 at 1900K. Both tube and sheet samples were double annealed (1h @1755K+2h@1475K) following fabrication. Some sheet samples were also exposed to 1350K and 1450K for up to 34,500h with/without applied load. Microstructure characterization included grain size measurement, chemical analysis, optical and electron microscopy, and analysis of phase-extracted residue of the samples. The results are presented with the emphasis on the effects of processing on the microstructure, and its high temperature stability. This work was performed for USDOE, Nuclear Energy, Reactor Sys. Development and Tech., Washington, D.C. 20545, under Interagency Agreement DE-AI03-86SF16310.

8:55 AM

Processing, Microstructure and Properties of Nb – Zr – C Alloys. II. Tensile, Creep and Microhardness Properties of Sheet Products: *Mehmet Uz*¹; Robert H. Titran²; ¹Lafayette College; ²NASA Glenn Research Center

This paper deals with the effects of thermomechanical processing on microhardness, tensile and creep properties of Nb-1wt.%Zr- 0.1wt.%C sheet. Sheet bars were cold rolled into 1-mm thick sheets following single, double, or triple extrusion operations at 1900K. All specimens were given a two-step heat treatment of 1h at 1755K+2h at 1475K prior to testing. Creep tests were conducted at 1350K and 34.5MPa for up to 34,500h, and at 1450K and 24MPa for up to 12,000h. Tensile properties were determined at both 300K and 1350K. Microhardness measurements were performed on samples at various stages of processing and testing. The results are discussed in correlation with thermomechanical processing and microstructure, and compared to results obtained from testing of Nb - 1 wt.%Zr and Nb - 1 wt.%Zr and 0.06 wt.%C alloys. This work was performed for USDOE, Nuclear Energy, Reactor Sys. Development and Tech., Washington, D.C. 20545, under Interagency Agreement DE-AI03-86SF16310.

9:20 AM

Factors Affecting the Texture and Recrystallization of Annealed Nb-1Zr: *David T. Hoelzer*¹; Scott A. Speakman¹; Edward A. Kenik¹; Steven J. Zinkle¹; ¹Oak Ridge National Laboratory

The purpose of this study was to determine important factors influencing the thermal creep behavior of Nb-1Zr. In this study, a detailed experimentally-based study utilizing advanced characterization techniques including XRD pole mapping, EBSP mapping, and TEM was conducted in order to gain a better understanding of factors that may affect the texture and recrystallization of annealed Nb-1Zr. These factors included the mag-

nitude and directionality of cold-deformation, annealing temperature, and heating rate. It was found that significant changes in texture occurred in Nb-1Zr depending on the deformation level, rolling direction as well as the time and temperature of annealing. The EBSP maps of annealed Nb-1Zr showed that the grains were distributed in groups that shared common texture components and low misorientation boundaries. Details of the texture results of Nb-1Zr will be presented and compared to those obtained from studies of the similar group VB metals V, Nb, and Ta.

9:45 AM

Effect of Texture on Creep Properties of Nb-1%Zr Alloy: *Yan Cui*¹; Tim McGreevy²; David Hoelzer²; Steve Zinkle²; T. G. Nieh¹; ¹University of Tennessee; ²Oak Ridge National Laboratory

The creep properties of Nb-1%Zr alloy was evaluated with special emphasis on the texture effect. Fully crystallized Nb-1%Zr samples with various grain sizes and crystallographic textures were prepared from cold-rolled material. Strain rate change as well as short-term and longer-term creep tests were conducted. Microstructure and texture were characterized using OIM, TEM, and XRD. Deformation mechanism, in particular long-term creep, will be discussed.

10:10 AM Break

10:25 AM

Alloying Development and Microstructure Stability in High-Temperature Mo-Si-B System: *Ridwan Sakidja*¹; John H. Perepezko¹; ¹University of Wisconsin-Madison

Mo-Si-B alloys have been considered as potential high temperature structural materials due to their high melting points (above 2000°C) and excellent high-temperature oxidation resistance attributed to their self-healing characteristics. In the current study, the effect of alloying additions such as Ti and Cr to lower the overall weight density has been examined. The microstructure stability with the alloying additions is due to the stability of the high melting ternary-based T2 borosilicide phase.

10:50 AM

In-Situ Fracture Studies and Modeling of the Toughening Mechanism Present in Wrought LCAC, TZM< and ODS Molybdenum Flat Products: *Brian Vern Cockeram*¹; Kwai S. Chan²; ¹Bechtel-Bettis; ²Southwest Research Institute

Fractographic examinations of tensile and fracture toughness specimens from wrought LCAC unalloyed, ODS, and TZM molybdenum have indicated that these alloys exhibit a ductile laminate toughening mechanism that is characterized as thin sheet toughening. In-situ examinations of fracture toughness specimens using a DISMAP method provide information on the stress-intensity values needed for crack propagation, path of crack propagation, and localized measurements of strain at the crack tip. C-scan measurements confirm that delaminations occur at the crack tip, and the development of the delamination zone with increasing stress-intensity is determined. A micromechanical model is developed to relate the toughness values to the features of the microstructure. Molybdenum alloys with a finer grain size, such as ODS molybdenum, are shown to exhibit higher toughness values at lower temperatures. The improvement in DBTT with respect to microstructural features is understood in terms of the thin sheet toughening mechanism.

11:15 AM

Electron-Beam and Laser Welding Techniques for Refractory Alloys: *Dean M. Paxton*¹; D. J. Senor¹; A. Jones¹; T. A. Delucchi²; ¹Pacific Northwest National Laboratory; ²Cogema Engineering

An established electron-beam and laser welding capability at the Hanford Site recently was incorporated into the Pacific Northwest National Laboratory. In the past, electron-beam and laser welding techniques were developed and qualified for a variety of refractory alloys and other materials of interest for space reactor applications. These techniques were used for a variety of applications related to space reactor materials research including fabrication of pressurized biaxial creep test specimens. Many of these materials were subsequently subjected to irradiation testing in FFTF and EBR-II. The focus of this paper is the historical development and qualification of the electron-beam and laser weld techniques and an assessment of the irradiation performance of the welds using a

variety of characterization methods including metallography and radiography.

11:40 AM

A Study of Resistance Spot Welding of 50Mo-50Re (Wt%) Sheets: *Jianhui Xu*¹; *Tongguang Zhai*¹; *John Farrell*²; *William Umstead*²; *Michael P. Effgen*²; ¹University of Kentucky; ²Semicon Associates

In this study, resistance-spot-welding was employed to pre-join refractory alloy 50Mo-50Re (wt%) sheets (0.002" and 0.005" thick). Different combinations of welding parameters, including weld current, weld time, electrode force, hold time, squeeze time, were used in resistance-spot-welding. The welding quality was evaluated by tensile-shear tests and microstructure examination. It was found that the strength of these welds was enhanced from 100 N to 120 N with increase in hold time from 50 ms to 999 ms, due to a higher cooling rate in the molten nugget. When the pre-weld current was linearly increased from 0 to 900 A in 8 ms, weld strength was further increased to 157 N in 0.005" samples, around 37 N higher than that of the weldment by the normally used faster heating rate. Welding defects, including porosities, columnar grains and grain boundary segregation, were also studied in these samples.

The Aluminum Fabrication Industry: Global Challenges and Opportunities: Aluminum Plenary Session

Sponsored by: The Minerals, Metals and Materials Society, Aluminum Association, TMS Light Metals Division, TMS: Aluminum Committee
Program Organizers: Subodh K. Das, Secat Inc; Michael Hal Skillingberg, Aluminum Association; Ray D. Peterson, Aleris International; Rene Kieft, Corus Group; Travis J. Galloway, Century Aluminum Company

Monday AM Room: Theatre
March 13, 2006 Location: Henry B. Gonzalez Convention Ctr.

Session Chair: Subodh K. Das, Secat Inc

8:30 AM Plenary

The Importance of the Automotive Industry for the Future Application of Aluminium Components: *Dieter Braun*¹; ¹Hydro Aluminium Deutschland GmbH

The need for further weight reduction of cars is a great opportunity for the Aluminium Fabricating Industry to introduce more Aluminium components for a car. Here, intelligent light weight solutions are necessary to compete with other materials. Selected examples will be presented. Additionally, to serve the Automotive Industry in a global market, especially in the fast growing markets in Asia, efficient supplying concepts are necessary. The Hydro Supplying Concept will be presented which serves the global and local demands of the Industry with selected products. Finally, examples for possible future product applications will be given.

8:55 AM Plenary

What are the Challenges and Opportunities for the Rolled Can Sheet Industry?: *Patrick M. Franc*¹; ¹ARCO Aluminum Inc

Arco Aluminum (a subsidiary of BP N. America) has been a significant manufacturer and marketer of Aluminum rolled can sheet primarily to the beverage industry in North America for over the past 20 years. They are a joint venture owner of Logan Aluminum, an 800k ton p.a. rolling mill in Russellville Ky. Arco Aluminum develops its technology with SECAT Inc., a research and development consortium located in Lexington, KY. The current state of the RCS industry offers many challenges and opportunities for Aluminum sheet fabricators. The development of cost – competitive, sustainable solutions for current and future industry challenges as well as innovative new technology needs to begin with a fundamental understanding of value creation and enhancement along the supply chain. The creation of concepts and their development into value enhanced processes that build on these relationships will further support the long term viability of the Aluminum RCS Industry and will be the focus of this talk. The Aluminum industry continues to position itself as a material of choice to the RCS market by continuously addressing these current

and future challenges and opportunities through cohesive industry partnerships and strategies.

9:20 AM Plenary

Innovations in Recycling, Continuous Casting and Rolling of Aluminum Products: *Steve Demetriou*¹; ¹Aleris International, Inc.

Aleris International, Inc. was created with merger of IMCO Recycling, Inc. and Commonwealth Industries, Inc. on December 9, 2004. The merger established Aleris as a vertically integrated “best-in-class” aluminum recycler and sheet manufacturing company. The aluminum recycling technology combined with continuous cast technology provides the lowest cost option in making common aluminum alloy sheet for building and construction, consumer durable, transportation and distribution stocks. The combination of Aleris’ direct chill ingot casting technology, with its broad alloy capabilities, and highly efficient continuous casting technology gives Aleris a competitive advantage in the market place. This talk will illustrate how the innovations in recycling, continuous casting and rolling technologies are providing the value-added products to meet customers demanding and changing needs.

9:45 AM Plenary

Driving Demand and Cost in a Global Market: *Helmut Wieser*¹; ¹Alcoa, Inc.

Alcoa is the world’s leading producer and manager of primary aluminum, fabricated aluminum and alumina facilities, and is active in all major aspects of the industry, serving the aerospace, automotive, packaging, building and construction, commercial transportation and industrial markets, bringing design, engineering, production and other capabilities to its customers. The Company’s Flat Rolled Products group (which includes Mill Products and rigid container sheet) had 2004 third-party revenues of approximately \$6 billion. The Company recently reorganized around 6 global businesses in order to better serve customers globally. The reorganization is designed to allow business such as the Global Mill Products group to this drive out costs as part of a global system, while working with customers to also drive demand. This discussion will illustrate key elements of Alcoa’s Global Mill products business from both an operation and growth perspectives.

10:10 AM Break

10:20 AM Plenary

Innovative and Sustainable Products for the Aluminum Industry: *Kevin R. Greenawald*¹; ¹Novelis Corporation

Formed in January 2005 as an independent company, Novelis is comprised of the majority of the rolled products operations separated from Alcan Inc. Today, Novelis, is the global leader in aluminum rolled products and aluminum can recycling, with 36 operating facilities in 11 countries and more than 13,000 dedicated employees. This talk will describe how Novelis through its technically sophisticated and advanced production capabilities develops innovative and sustainable aluminum sheet and foil products for the automotive, transportation, beverage and food packaging, construction, industrial and printing markets.

10:45 AM Plenary

The Impact of Alloy Specifications on Aluminum Fabrication and Products - A Future View: *Thomas A. Brackmann*¹; ¹Nichols Aluminum

As the US aluminum industry moves from primary to recycle-based raw materials, we need to examine the existing paradigm of product specification based upon the “primary metal tradition” and suggest ways to shift to an “attribute-based needs” specification which is more suited to the recycled aluminum economy. Nichols Aluminum Company, headquartered in Davenport, Iowa, is a leading manufacturer of coated and mill finish aluminum sheet for a wide variety of applications such as building and construction, transportation, machinery and equipment and consumer durable aluminum products, markets which depend sensitively on metal price and can benefit greatly from a change in paradigm. What will it take to move in this direction? This paper will examine ways and suggest strategies to make this market-driven transition.

11:10 AM Plenary**Developing Aluminum Fabrication in Chinalco: Challenge and Opportunity:** *Ding Haiyan*¹; ¹Aluminum Corporation of China

As a backbone state-owned enterprise under the direct leadership of the Central Government, Aluminum Corporation of China (Chinalco) aims to be a first-class enterprise with full vertical integration of its aluminum production assets, ranging from mining, refining, smelting and downstream fabricating. Comparing with its dominant production of alumina and primary aluminum in Chinalco, the downstream fabrication is a little small in terms of scale and capacity. In Mr. Ding's presentation, strategy and related programs on developing aluminum fabrication in Chinalco are proposed from the viewpoint of global challenge and opportunity in aluminum industry.

11:35 AM Panel Discussion**The Brandon Symposium: Advanced Materials and Characterization: Grain Boundary Theory and Experiments**

Sponsored by: The Minerals, Metals and Materials Society, Indian Institute of Metals, TMS Extraction and Processing Division, TMS: Materials Characterization Committee

Program Organizers: Srinivasa Ranganathan, Indian Institute of Science; Wayne D. Kaplan, Technion; Manfred R. Ruhle, Max-Planck Institute; David N. Seidman, Northwestern University; D. Shechtman, Technion; Tadao Watanabe, Tohoku University; Rachman Chaim, Technion

Monday AM
March 13, 2006

Room: 206B
Location: Henry B. Gonzalez Convention Ctr.

Session Chairs: Srinivasa Ranganathan, Indian Institute of Science; Wayne D. Kaplan, Technion-Israel Institute of Technology

8:30 AM Introduction to the Brandon Symposium**8:40 AM Invited****Metrics in the Five-Dimensional Angle Space for Grain Boundaries:**

*John W. Cahn*¹; Jean E. Taylor²; ¹National Institute of Standards and Technology; ²Courant Institute of Mathematical Sciences

Analysis of experimental data on grain boundaries (GBs) can involve putting data into angle "bins." An extreme example is Brandon's classification: if rotation angle and axis are each within $15/(\sqrt{n})$ degrees of a perfect Sigma n coincidence site lattice (CSL), the GBs are in a CSL, and not if otherwise. Other examples are studies of GB distributions in the full 5-D angle space by Saylor, et al. To determine the size of a bin (necessary for gradients), one must find a useful way, respecting symmetry, of determining metrics on the full 5-dimensional space of both misorientation and interface normal. For low-angle GBs, the issue of metric is complicated by the fact that both the rotation axes and the GB normals can stay far apart as the rotation angles approach zero. We address all these issues, and provide a framework for choosing answers.

9:05 AM Invited**Relation between Anisotropies of Grain Boundary Energy and Segregation:** *Paul P. Wynblatt*¹; Dominique Chatain²; Ying Pang¹; ¹Carnegie Mellon University; ²CRMCN-CNRS

Results obtained on fcc alloys, by a recently developed model that allows calculation of the grain boundary (GB) energy and GB segregation as a function of the five parameters of GB orientation, will be presented. The model uses the regular solution approximation (and includes solute strain energy interactions). Some important conclusions may be summarized as follows: (a) Segregation at GB's increases with increasing GB energy; (b) The segregation profile across a GB depends on the crystallographic orientations of the two planes which terminate the crystals on the two sides of the GB. (c) The composition profile for GB's terminated by identical crystallographic planes is symmetric, but is asymmetric when GB's are terminated by different planes. (d) The strength of the segregation on one side of a GB influences the extent of segregation on the other.

Experimental verification of these predictions, obtained from Nb segregation to TiO₂ GB's, will be presented.

9:30 AM Invited**Special Grain Boundaries without a Coincidence Site Lattice:** *Leonid A. Bendersky*¹; John W. Cahn¹; ¹National Institute of Standards and Technology

Special, low energy grain boundaries (GB) are said to occur whenever there is a 3-dimensional coincidence site lattice (CSL) that provides good fits of the atoms along GBs. CSL focuses on lattices, which are points, rather than on the actual atoms. There is little reason for the CSLs to be significant for GBs between crystals with large, or non-cubic, unit cells. We report here about special, large angle GBs between Al-Mn-Fe-Si grains of a cubic phase having irrational orientation relationship. The GB's have many of the other attributes of a special GB, yet there is no CSL. Motifs of the phase continue to pack across these GBs and retain orientational order, while paying little attention to the change in a lattice. These results suggest an enlarged criterion for the existence of special GBs. Variations in compositions result in the formation of quasicrystals and an unusual glass, dubbed q-glass.

9:55 AM Invited**What Does it Mean to be Special?:** *Alexander H. King*¹; Shashank Shekhar¹; ¹Purdue University

In 1966, David Brandon introduced an ad hoc geometrical rule to categorize grain boundaries as either "special" or "general." Forty years later, the Brandon criterion is widely used and is often applied where it was never intended. We examine the assumptions of the Brandon criterion, and other criteria of "specialness." We compare their predictions with experimental data from the literature and show that the choice of a particular criterion, and of particular parameters within any criterion, should depend upon the underlying physics of the property of interest. A grain boundary that is special with respect to diffusion, for example, may not be special with respect to mechanical properties. Studies of the dihedral angles formed between "nearly special" boundaries are used to demonstrate a distinction between special and general properties, in terms of interfacial energy. Acknowledgement: This work is supported by the US Department of Energy, under Contract Number DE-FG01-01ER45940.

10:20 AM Break**10:35 AM Invited****On the Effect of Grain Boundary Junctions on Grain Growth:** *Günter Gottstein*¹; Lasar S. Shvindlerman¹; ¹RWTH Aachen University

Grain growth in polycrystalline materials is traditionally interpreted in terms of curvature driven grain boundary motion. Recent investigations on tricrystals have provided unambiguous evidence that grain boundary triple junctions are defects on their own with specific thermodynamic and kinetic properties. As a consequence they can exert a substantial drag on grain growth kinetics and thus, microstructure and texture evolution. Since the strength of junction drag does not only depend on the ratio of triple junction and grain boundary mobility but is also proportional to the grain size, this effect is expected to be particularly pronounced in ultra fine grained and nanocrystalline materials. At very strong junction drag the grain growth kinetics can be entirely controlled by junction kinetics. This does not only affect the instantaneous grain growth rate but also causes a conspicuous retardation of the grain growth rate during subsequent annealing under conditions where grain boundary kinetics prevail.

11:00 AM Invited**Grain Boundary Character and Dopant Effects of Oxide Ceramics:** *Yuichi Ikuhara*¹; ¹University of Tokyo

Bicrystal-experiments have an advantage to be performed because grain boundary character and the kind of dopants can be controlled, and the fabricated boundaries are easily treated for the subsequent characterization. We have systematically fabricated the bicrystals for Al₂O₃ and ZrO₂ so as to include low angle, CSL and high angle grain boundaries to cover all types of grain boundaries. In addition, several dopants such as Y₂O₃, SiO₂ were doped for the fabricated bicrystals. The atomic structures, chemistry and energy of the grain boundaries in the respective bicrystals were investigated by HREM, HAADF-STEM, EDS, EELS and thermal grooving techniques. It was found that the grain boundary structures and ener-

gies strongly depend on the grain boundary characters and the kinds of dopants. In addition, the most stable grain boundary structures were theoretically calculated by the static lattice and molecular orbital calculations to compare with the experimentally obtained results.

11:25 AM Invited

Grain Boundary Engineering by Magnetic Field Application: *Tadao Watanabe*¹; *Sadahiro Tsurekawa*¹; *Xiang Zhao*²; *Liang Zuo*²; *Claude Esling*³; ¹Tohoku University; ²Northeastern University; ³University of Metz

A new approach to the grain boundary engineering for advanced materials has been recently proceeded by using different processing methods under a magnetic field. The advent of a helium-free superconducting magnet and the orientation imaging microscopy (OIM) has enabled us to develop such new processing methods of the grain boundary engineering for high performance materials. Recent experimental works on nanocrystalline nickel, iron alloys and steels have demonstrated that magnetic annealing, magnetic crystallization from the amorphous state and magnetic phase transformation under a high magnetic field, have a high potential for development of advanced materials and can produce various unique microstructures which can be the origins of high performance and desirable bulk properties, and cannot be produced by presently existing processing methods.

11:50 AM Invited

Magnetically Controlled Grain Boundary Motion and Microstructure Evolution in Non-Ferromagnetic Metals: *Dmitri A. Molodov*¹; ¹RWTH Aachen University

The current research on grain boundary dynamics, texture and grain structure development in high magnetic fields will be reviewed. Grain boundary motion can be affected by a magnetic field, if the anisotropy of the magnetic susceptibility generates a gradient of the magnetic free energy density across the boundary. The application of a magnetic field to locally deformed zinc single crystals results in growth selection, i.e. in a growth of new preferentially oriented grains. It is demonstrated for zinc and titanium sheet that a magnetic driving force superimposed to a capillary driving force can bias the microstructure evolution during grain growth with regard to grain size and crystallographic texture. A theoretical analysis of grain growth kinetics in the presence of an external magnetic field predicts that magnetically affected grain growth will result in a change of the grain orientation distribution in favour of grains with a lower magnetic free energy density.

12:15 PM

Exploring the Structure of Asymmetrical Tilt Grain Boundaries in Gold: *J. Anthony Brown*¹; *Douglas L. Medlin*²; *Yuri Mishin*¹; ¹George Mason University; ²Sandia National Laboratories

Results of atomistic simulation studies of $\langle 110 \rangle 90^\circ$ asymmetrical tilt grain boundaries (GBs) in gold are presented and compared with HRTEM observations of the same boundaries. The structure of interfacial disconnections associated with the $\{111\}/\{112\}$ boundary that accommodate coherency strains at this interface has been investigated in great detail. The stress accommodation at other GBs of the $\langle 110 \rangle 90$ deg series has also been explored through the range of inclination angles between the $\{111\}/\{112\}$ interface and the symmetrical $\{557\}/\{557\}$ GB. The results are interpreted in terms of the formation of facets, disconnections, and the emission of intrinsic stacking faults into the bulk. This study presents a clarification of the role of coherency strains and disconnections in the structure of asymmetrical GBs in metals. The combination of atomistic modeling and experiment leads to a better understanding of asymmetrical GBs and their possible role in mechanical behavior of metals.

The Rohatgi Honorary Symposium on Solidification Processing of Metal Matrix Composites: Overview of Developments in Cast MMCs

Sponsored by: The Minerals, Metals and Materials Society, TMS Materials Processing and Manufacturing Division, TMS Structural Materials Division, TMS/ASM: Composite Materials Committee, TMS: Solidification Committee

Program Organizers: *Nikhil Gupta*, Polytechnic University; *Warren H. Hunt*, Aluminum Consultants Group Inc

Monday AM
March 13, 2006

Room: 207B
Location: Henry B. Gonzalez Convention Ctr.

Session Chairs: *Krishan K. Chawla*, University of Alabama; *Nikhil Gupta*, Polytechnic University

8:30 AM Introductory Comments: A brief introduction to the life and work of Dr. Rohatgi

8:45 AM Invited

Opportunities and Challenges in Cast Metal Matrix Composites: *Pradeep Kumar Rohatgi*¹; *Atef Daoud*²; *Nikhil Gupta*³; *Rajiv Asthana*¹; ¹University of Wisconsin; ²Central Metallurgical Research and Development Institute; ³Polytechnic University

The present work reviews the historical evolution of Cast Metal Matrix Composites (MMCs), which can be produced in foundries. After a brief introduction on the structure, solidification and processing of composites, the possible effects of reinforcements on solidification are discussed, including a reduction in microsegregation of solute and concentration of particles in the interdendritic regions due to particle pushing phenomenon. This is followed by some applications of MMCs, which include automotive and space applications. Cast MMCs that are being currently developed are also discussed; these include Aluminum and Magnesium based MMCs, Lead free Copper-Graphite, and Composite Foams. Future research needs in Cast MMCs are also discussed and a possible scenario of extending the present cast MMC technology to manufacture higher performance and lower cost composites and advanced materials such as functionally gradient materials, nanocomposites, biomedical composites, smart composites, superconducting composites and porous and cellular metals, is presented.

9:10 AM Invited

Cast Aluminum Composite Applications and Barriers to Volume Production: *David J. Weiss*¹; ¹ECK Industries Inc

Many important components for the transportation and industrial markets are produced as castings. The flexibility of the casting process and the many casting techniques available make the use of castings economically viable over a wide range of volumes. Aluminum metal matrix composite castings are used in a number of niche applications in the electronics, commercial braking and metrology markets but have never found a wide market. This paper discusses a number of successful applications and discusses the barriers that currently prevent more extensive use of cast aluminum metal matrix composite castings. Recent technical breakthroughs and suggestions for further work are discussed.

9:35 AM Invited

Hollow Particle Filled Lightweight Composites: *Nikhil Gupta*¹; ¹Polytechnic University

Hollow particle filled advance composite materials have potential for being used in a variety of applications that include aircraft and spacecraft structures, ship and boat structures and buildings. A comparison of mechanical properties of metal, polymer and ceramic matrix hollow particle filled syntactic composites is presented. Fly ash cenospheres and glass microballoons are used as hollow particles in synthesizing syntactic composites. Particle size, volume fraction and wall thickness are some of the common approaches of modifying the properties of syntactic foams. A comparative study of the effectiveness of these approaches in modifying material properties of syntactic foams is carried out. The material micro-

structure, specific strength and energy absorption characteristics of these materials are discussed.

10:00 AM Invited

Synthesis of Stir Cast Aluminum Alloy Matrix Composites-Indian Contributions: *Satyanarayana Gundappa Kestur*¹; Marimuthu Raman Pillai²; Bellembettu Chandrasekhar Pai²; Pradeep Kumar Rohatgi³; ¹Federal University of Parana; ²Regional Research Laboratory, CSIR; ³University of Wisconsin

Cast aluminum matrix composites with discontinuous dispersoids have been most favored new millennium advanced engineering material. Solidification route is the most attractive processing method with India taking the lead. Different casting processes, size and shape of dispersoids, melt treatments and heat treatment are employed to achieve better properties with resulting microstructures to be a function of these parameters. Indian researchers with initiative from Prof. Rohatgi have a major share in the development of the stir cast technique, the most simple and economical solidification route for metal matrix composite. Many challenges are involved in this synthesis. Also, laboratory scale technologies are developed in India with microstructure and properties comparable with those of commercially available MMCs abroad. This paper highlights the scientific contributions made by Indian Scientists in the development of Science and Technology of cast aluminum matrix composite, which include mixing, wettability of dispersoids, melt and surface treatments, and interface reaction.

10:25 AM Break

10:40 AM Invited

In-Situ Processing of Lightweight Alloy Composites: *Ramana G. Reddy*¹; ¹University of Alabama

A new in-situ processing method for production of lightweight alloys matrix with ceramic particles reinforcements is discussed. Successful in-situ formation of Al and Mg alloys with ceramic particles (i.e. SiC, AlN) composites by bubbling reactive gas (i.e. methane, nitrogen, ammonia) into Al and Mg alloy melts was discussed. Effect of processing parameters on the formation of AlN and SiC composites was investigated. The SiC formation rate increased with decrease in the bubble size. The composites contained up to 30 wt% SiC. Kinetic rate equations of in-situ formation of composites were developed. The productions of composites by molten metal technology were discussed.

11:05 AM

Solidification Microstructures of Hybrid Aluminum Matrix Composites: *B. C. Pai*¹; T. P. D. Rajan¹; S. G. K. Pillai¹; R. M. Pillai¹; ¹Regional Research Laboratory, CSIR

Hybrid Metal Matrix Composites (HMMC) are second-generation metallic composites, where more than one type, shape and size of reinforcements are introduced into the matrix alloy. Presence of more reinforcements gives much superior properties due to synergistic effects. HMMC provides enhanced structural, mechanical and tribological properties than conventional alloys and mono composites depending upon the constituent materials. Among the various processing methods available for the fabrication of HMMC, the solidification route is preferred due to its ease of fabrication and cost effectiveness. The most common solidification technique used is the liquid metal stir casting followed by shaping using gravity, investment, pressure, squeeze and centrifugal casting methods. The solidification microstructure of these cast hybrid metal matrix composites plays an important role in determining the physical, mechanical and tribological behaviour of the composites. Hence, an understanding of solidification microstructures in HMMC becomes more vital.

11:30 AM

Developments in Science and Technology of Cast Aluminium Matrix Composites - An Overview: *Satyanarayana Gundappa Kestur*¹; Marimuthu Raman Pillai²; Chandrasekhara Bellembettu Pai²; Pradeep Kumar Rohatgi³; Jeongkyon Kim³; Mahesh Kestursatya⁴; ¹Federal University of Parana; ²Regional Research Laboratory, CSIR; ³University of Wisconsin; ⁴Hewlett Carbon Products

During the last three decades, substantial R&D efforts in the area of metal matrix composites have been directed to understand their processing, structure-properties as well as potentials and limitations invoking the

principles of different areas such as casting/solidification, physical metallurgy, stress analysis, etc. This paper focuses mainly on some market, the quality, the intellectual property rights, cost aspects and the selection criteria for matrix and reinforcements as well as some developments taking place both in theoretical and experimental aspects of processing and structure-property correlation along with the some application aspects of cast aluminum based composites. The gaps existing for greater acceptance and commercialization as well as comparison of all aspects of cast composites in the developed countries and India are brought out in totality to take stock of the developments in science and technology with a view to strive for faster growth of applications of cast Al composites.

11:55 AM

Composite Development Activity at NPL: *Anil Kumar Gupta*¹; Rajiv Sikand¹; Rakesh B. Mathur¹; Tasreem L. Dhami¹; ¹National Physical Laboratory

The National Physical Laboratory has been engaged in undertaking systematic research on the development of wide varieties of composite materials, such as, Metal Matrix Composites, Carbon-Carbon Composites, Carbon fiber reinforced plastic composites. The developmental work includes processing, characterization and their possible applications. The emphasis has been on synthesis and secondary processing of Metal Matrix Composites and high modulus structural components. Different MMC materials have been developed using stir-casting, spray formed and Powder Metallurgy route and have been secondary processed employing hot extrusion and forging using 500 ton vertical hydraulic press. Carbon-Carbon Composites are light weight, high strength, high stiffness, low coefficient of thermal expansion, high thermal conductivity material. In addition to low recession in high temperature environment, it has capability to withstand high temperatures upto 3000C in inert atmosphere. The talk will highlight some of the important aspects related to processing, characterization and possible applications.

Ultrafine Grained Materials - Fourth International Symposium: Fundamentals of Ultrafine Grained Materials

Sponsored by: The Minerals, Metals and Materials Society, TMS Materials Processing and Manufacturing Division, TMS Structural Materials Division, TMS/ASM: Mechanical Behavior of Materials Committee, TMS: Shaping and Forming Committee

Program Organizers: Yuntian T. Zhu, Los Alamos National Laboratory; Terence G. Langdon, University of Southern California; Zenji Horita, Kyushu University; Michael Zehetbauer, University of Vienna; S. L. Semiatin, Air Force Research Laboratory; Terry C. Lowe, Los Alamos National Laboratory

Monday AM
March 13, 2006

Room: 217D
Location: Henry B. Gonzalez Convention Ctr.

Session Chairs: Yuntian T. Zhu, Los Alamos National Laboratory; Dieter Wolf, Argonne National Laboratory; Evan Ma, Johns Hopkins University; Marc A. Meyers, University of California

8:30 AM Introductory Comments

8:35 AM Invited

Dislocation Structures in Cyclically Loaded Ultra Fine-Grain Copper: Kai Zhang¹; Xiaozhou Liao²; *Julia R. Weertman*¹; ¹Northwestern University; ²University of Chicago

Previous experiments have shown that cryogenically-rolled UFG Cu subjected to cyclic loading undergoes significant softening, grain growth, and the development of surface extrusions/intrusions. In the present talk the dislocation structure that develops during cycling is analyzed and related to the changes that evolve in the fatigued material. Research sponsored by US DOE Grant #DE-FG02-02ER46002.

8:55 AM Invited

Dislocation and Grain-Boundary Processes during Deformation and Grain Growth in Nanocrystalline Materials by Molecular Dynamics Simulation: *Dieter Wolf*¹; ¹Argonne National Laboratory

Molecular-dynamics simulations have been used to elucidate the deformation and grain-growth behavior of nanocrystalline fcc metals. These simulations have now become large and sophisticated enough where they begin to provide novel, materials-physics based insights into the intricate interplay between dislocation and grain-boundary processes controlling the thermo-mechanical behavior of these materials. In particular, such simulations now capture, with atomic-level resolution, the entire range of grain sizes in which the experimentally suggested transition from a dislocation-based deformation mechanism to one involving grain-boundary processes takes place as the grain size approaches dimensions of the order of tens of nanometers. By investigating the intricate coupling between grain growth and grain-boundary diffusion creep, these simulations also provide insight into the dislocation and grain-boundary processes that control the high-temperature stability of these materials. Work supported by the U.S. Department of Energy, Basic Energy Sciences-Materials Sciences, under Contract W-31-109-Eng-38.

9:15 AM Invited

An In Situ TEM Study of Dislocation Behavior in Nanocrystalline Copper Alloys with Different Stacking Fault Energies: *Thomas J. Balk*¹; Yong Hao Zhao²; Yuntian T. Zhu²; Zenji Horita³; Terence G. Langdon⁴; ¹University of Kentucky; ²Los Alamos National Laboratory; ³Kyushu University; ⁴University of Southern California

In nanocrystalline materials, both the nucleation and glide of dislocations are subjected to strong constraints. This study aims to uncover details of dislocation nucleation and motion within nanocrystalline materials by in-situ mechanical testing in the transmission electron microscope (TEM). High-pressure torsion and cold rolling were used to produce flat sheets of nanocrystalline copper (70 nm grain size), bronze (25 nm) and brass (13 nm). The resultant grain size was found to scale with the stacking fault energy of each material, and these two factors therefore simultaneously affect dislocation behavior within the ultrafine grains. Each metal/alloy was subjected to uniaxial tension testing in the TEM, during which the deformation microstructure was continuously observed. This talk will discuss the relative roles of dislocation emission versus deformation twinning in these copper-based materials, as well as the evolution of dislocation density, which affects the work hardening and therefore the ductility of each material.

9:35 AM

Deformation Induced Grain Growth and Softening in Electrodeposited Nanocrystalline Ni Film: *Yuntian T. Zhu*¹; Shenggao Hong²; Xiaodong Chris Li²; Xiaozhou Liao³; Ruslan Z. Valiev⁴; Amiya Mukherjee⁵; ¹Los Alamos National Laboratory; ²University of South Carolina; ³University of Chicago; ⁴Ufa State Aviation Technical University; ⁵University of California

This paper reports deformation induced grain growth in electrodeposited nanocrystalline Ni film during high pressure torsion (HPT). Grain growth has been experimentally observed in nanocrystalline and ultrafine-grained Al and Cu under the deformation mode of indentation, but not under any other deformation mode. In this study, nanocrystalline Ni films produced by electro-deposition were subjected to high-pressure torsion (HPT) and grain growth was found subsequently. The HPT deformation also led to lower hardness and lower elastic modulus, which are attributed to the reduction of internal stress and change of texture. High stress and severe plastic deformation are believed required for the grain growth and the final grain size is determined by the deformation parameters.

9:50 AM

Rate-Controlling Deformation Mechanism of Electrodeposited Nanocrystalline Ni: *Yinmin (Morris) Wang*¹; Alex V. Hamza¹; Evan Ma²; ¹Lawrence Livermore National Laboratory; ²Johns Hopkins University

Commercially available electrodeposited nanocrystalline Ni with grain sizes below 100 nm is a wide-used material to investigate the deformation and failure mechanisms of nanostructured materials. More recently attention has been focused on the rate-controlling deformation mechanisms of these materials. Repeated transition tests were applied to extract the activation volume and strain rate sensitivity of nanocrystalline Ni at different deformation temperatures. The magnitudes of these deformation parameters obtained from our experimental data indicates that unlike many models proposed in the literature, the grain boundary diffusion controlled

process such as Coble creep is not a dominant deformation mechanism for the deformation temperature studied. Other possible mechanisms involved in these deformation processes are suggested. This work was performed under the auspices of the U.S. Department of Energy by University of California, Lawrence Livermore National Laboratory under contract of No.W-7405-Eng-48. Y.M. Wang acknowledges the support of Graboske Fellowship at Lawrence Livermore National Laboratory.

10:05 AM

Measurements of Vacancy Type Defects in SPD Deformed Nickel: Gerd Steiner¹; Erhard Schafner¹; Elena Korznikova²; Michael Kerber¹; *Michael Josef Zehetbauer*¹; ¹University of Vienna; ²Ufa State Aviation Technical University

Ni of different purities between 99.9x% and 99.99x% have been deformed by various paths of ECAP and HPT. Results have been compared with investigations by conventional deformation (rolling, compression). In order to conclude the concentration of vacancy type lattice defects, annealing resistometry and calorimetry have been performed and combined with X-ray diffraction Bragg profile analyses. While the first two methods are sensitive to both vacancies and dislocations, the latter determines the dislocation density solely so that the vacancy concentration can be found by proper combination of results¹. Similarly to Cu, the vacancy concentrations measured from SPD are definitely higher than those from conventional plastic deformation. The resulting vacancy concentrations are discussed in terms of their dependencies on the deformation strain, the deformation mode, the hydrostatic pressure and the purity of Ni used. ¹E.Schafner, G.Steiner, E.Korznikova, M.Zehetbauer, TMS 05, Mater.Sci Eng. A, accepted.

10:20 AM

Deformation Twinning Mechanisms in Nanocrystalline Ni: *Xiao-Lei Wu*¹; En (Evan) Ma²; Ke Lu³; ¹Institute of Mechanics, Chinese Academy of Sciences; ²Johns Hopkins University; ³Institute of Metal Research, Chinese Academy of Sciences

Twinning has recently been identified as a contributing plastic deformation mechanism in nanocrystalline (nc) metals. When nc metals are forced to deform to large strains, in the deforming nanostructure there will inevitably be build up of local stress concentrations that are at sufficient levels for deformation twinning to become a competitive response. In the present paper, we studied deformation twinning mechanisms in nc-Ni severely deformed by the surface mechanical attrition treatment and ball milling. Extensive HREM examinations confirmed that twinning does occur upon large plastic deformation in nc Ni. The heterogeneous and homogeneous twinning mechanisms included 1) the nucleation at the grain boundary and growth (lengthening and thickening) into the grain interior via partial dislocation emission, 2) dynamic overlapping of stacking faults on adjacent planes, and 3) the dissociation of an initial segment of the high angled grain boundary and its subsequent migration to producing the twin lamella.

10:35 AM Break

10:50 AM Invited

Simultaneously Achieving High Strength, Strain Hardening, and Large Plasticity in Ultrafine-Grained Bulk Alloys: *Evan Ma*¹; ¹Johns Hopkins University

Bulk ultrafine-grained or nanostructured metals/alloys, prepared via severe plastic deformation for example, usually exhibit a high strength. But sometimes this advantage comes at the expense of plasticity. Even for cases where both high strength and large plastic strains are attained, the material often lacks the strain hardening capability needed to sustain uniform elongation in tensile deformation. For elemental metals, we have discussed a number of ways to improve strain hardening, at previous conferences. Here we discuss one of the strategies for alloys, using a model bulk Ti-based alloy made via chill casting. The origin of the high strength and the dislocation pile-up, the extensive dislocation slip and their interactions responsible for the obvious strain hardening to large strains, the alloy/microstructure design recipe, and the one-step bulk processing protocol, will be discussed. This work was performed in collaboration with the MANS research team (SYNL) and Dr. J. Eckert's group (DTU).

11:10 AM Invited

Possibility to Manage Both Strength and Ductility in Ultrafine Grained Structural Metallic Materials: Nobuhiro Tsuji¹; ¹Osaka University

One of the problems of ultrafine grained metallic materials is limited uniform elongation contrary to high strength. The issue is discussed on the basis of the author's original evidences. The limited uniform elongation is due to early plastic instability caused by limited strain-hardening capability in the ultrafine grained microstructures. One of the ways to manage both high strength and adequate ductility is to increase the strain-hardening rate by any means, such as by dispersing nano precipitates/particles. A successful example is the multiphased nano-structure composed of submicrometer ferrite grains and nano carbides in the low carbon steel fabricated by a special thermomechanical treatment starting from martensite structure. Another possibility has been found recently in some aluminum alloys which showed unexpected increase in elongation as the SPD strain increased. The mechanism is discussed from a viewpoint of strain rate sensitivity of the ultrafine grained materials.

11:30 AM Invited

Mechanisms of Grain-Size Refinement and Plastic Deformation in Ultra-Fine-Grained Metals: Marc A. Meyers¹; ¹University of California, San Diego

The evolution of the microstructure leading from conventional polycrystalline to submicrometer sized grains is described in terms of the break up of the existing grains and grain-boundary rotations at the latter stages, leading to an equiaxed structure. The analogies between the structure generated within adiabatic shear bands and ECAP are drawn, with attention to the Zener parameter. Plastic deformation mechanisms operating in the ultrafine grain size domain are reviewed and compared with nanocrystalline and conventional polycrystalline aggregates. Research Support: DMR 0419222; CMS 0210173(NIRT).

11:50 AM Invited

Mechanical Behavior of Individual Grains in Nanocrystalline Ni during Tensile Deformation: Zhiwei S. Shan¹; Andy Minor²; Jorg M. K. Wiezorek³; David M. Follstaedt⁴; James Knapp⁴; Eric Stach⁵; Oden L. Warren⁶; Scott X. Mao³; ¹University of Pittsburgh and NCEM, LBL; ²NCEM, LBL; ³University of Pittsburgh; ⁴Sandia National Laboratories; ⁵Purdue University; ⁶Hysitron, Inc.

Ever since the concept of nanocrystalline (nc) materials was proposed, it has been thought that the grain boundary (GB) structure of nc materials is different from that of their coarse-grained counterpart and that the unique properties of nc materials result mainly from this difference. However, increasing evidence shows that the GB structure of nc materials is similar to their coarse-grained counterpart. This naturally leads to the following question: do individual nano grains behave differently during deformation from what has been expected? In this work, nano beam electron diffraction has been used to study the behavior of individual grains in nc Ni during deformation. Large variations in the magnitude of grain rotation were found. Moreover, direct measurement of lattice distortions during straining reveals that grain interiors may experience large elastic distortions during tensile deformation. Implications of these experimental findings for the deformation behavior of nc materials are discussed.

12:10 PM Invited

Deformation Analysis of Strain Hardening and Softening Materials during Equal Channel Angular Pressing: Hyoung Seop Kim¹; ¹Chungnam National University

From the viewpoint of grain refinement by severe plastic deformation, the processing temperature generally needs to be as low as possible. However, ECAP at elevated temperatures is inevitable for hard-to-deform materials to prevent fracture during the processing. Material deformation characteristics to be noted at higher temperatures are strain softening (decreasing flow stress with increasing strain) and higher strain rate sensitivity, which were particularly important in the degree of inhomogeneous deformation. Strain hardening response of a workpiece material highly affects plastic flow behaviour during ECAP; a larger corner gap and the inhomogeneous strain distribution. In the present study, deformation behavior of strain hardening and strain softening materials during ECAP is investigated using the finite element method. The predicted deformation

homogeneity is compared to the experimental results of Al alloys at room temperature, Ti alloy at high temperature and plasticine polymer.

Wechsler Symposium on Radiation Effects, Deformation and Phase Transformations in Metals and Ceramics: Irradiation Effects

Sponsored by: The Minerals, Metals and Materials Society, ASM International, TMS Structural Materials Division, ASM Materials Science Critical Technology Sector, TMS Materials Processing and Manufacturing Division, TMS/ASM: Mechanical Behavior of Materials Committee, TMS/ASM: Nuclear Materials Committee, TMS/ASM: Phase Transformations Committee

Program Organizers: Korukonda L. Murty, North Carolina State University; Lou K. Mansur, Oak Ridge National Laboratory; Edward P. Simonen, Pacific Northwest National Laboratory; Ram Bajaj, Bettis Atomic Power Laboratory

Monday AM

Room: 208

March 13, 2006

Location: Henry B. Gonzalez Convention Ctr.

Session Chairs: K. Linga Murty, North Carolina State University; Louis K. Mansur, Oak Ridge National Laboratory

8:30 AM Introductory Comments**8:55 AM Keynote****Then and Now with Radiation Effects, Deformation, and Phase Transformations:** Monroe S. Wechsler¹; ¹North Carolina State University

Research in radiation physics and materials science is, by its very nature, a forward-looking enterprise, but sometimes it may be worthwhile to review past developments and suggest where further work needs to be done. In this short review, we briefly discuss martensite crystallography, the shape memory phenomenon, and some radiation-effects topics, i.e., radiation hardening and embrittlement, impurity-defect interactions, and calculations of the production of displacements, helium, hydrogen and transmutation products in fission neutron and accelerator-driven spallation systems.

9:30 AM Invited**Point Defect Interactions in Fe-Cr Alloys:** Jae-Hyeok Shim¹; Kwan L. Wong²; Brian D. Wirth²; ¹Korea Institute of Science and Technology; ²University of California

Fe-Cr alloys are a leading candidate material for Generation IV and Fusion reactors. Complete understanding of the response of Fe-Cr alloys to irradiation requires knowledge of point defect and point defect cluster interactions with Cr solute atoms and impurities. In this work, we have used two different Finnis-Sinclair type potentials for Fe-Cr alloys. The potentials predict different interactions between Cr and self-interstitial defects. Results of atomistic molecular dynamics and kinetic Monte Carlo simulations to investigate the point defect behavior in Fe-Cr alloys are presented as a function of Cr content and the character of Cr interactions with self-interstitial defects. The modeling results are compared to experiments performed by Maury and co-workers to investigate the isochronal annealing recovery of electron irradiated Fe-Cr. The results provide insight into the effect of Cr atoms on self-interstitial cluster behavior and indicate potential is more accurate for describing point defect - Cr interactions.

9:55 AM**The Effects of Helium and Hydrogen in Irradiated Single Crystal Body-Centered Cubic Iron:** Maria A. Okuniewski¹; Chaitanya S. Deo²; Srivilliputhur G. Srinivasan²; Michael I. Baskes²; Michael R. James²; Stuart A. Maloy²; James F. Stubbins¹; ¹University of Illinois at Urbana-Champaign; ²Los Alamos National Laboratory

Ferritic-martensitic steels are candidate structural materials for Generation IV reactors, fusion systems, and accelerator driven systems (ADS). These steels have been selected due to their resistance to void swelling, irradiation creep, and helium (He) and hydrogen (H) embrittlement at higher temperatures. During fusion or ADS reactor operations the structural materials will be subjected to displacement damage, as well as gen-

eration of He and H via (n, α) and (n,p) transmutation reactions, respectively. A systematic study utilizing both simulation and experimental methods has been carried out to examine the effects that He and H have on irradiated single crystal body-centered cubic iron. Molecular dynamics was used to study the effects of incident ion energies, He and H concentrations and the temperature on the evolution of defects. The modified embedded atom method was used to describe the interatomic interactions. The experimental studies employed positron annihilation spectroscopy and transmission electron microscopy for defect characterization.

10:15 AM

Kinetics of the Migration and Clustering of Helium and Hydrogen during Spallation Reactions in bcc Iron: *Chaitanya S. Deo*¹; Maria A. Okuniewski²; Srinivasan G. Srivilliputhur¹; Michael I. Baskes¹; Stuart Andrew Maloy¹; Michael R. James¹; James Stubbins²; ¹Los Alamos National Laboratory; ²University of Illinois

Spallation refers to nuclear reactions that occur when energetic subatomic particles (such as protons in an accelerator beam) strike or interact with the nucleus of an atom (such as in a target) in which many particles, including many neutrons, are ejected from the nucleus. High levels of transmutation products such as H and He are produced in spallation reactions in structural materials such as bcc ferritic steels. We investigate the defect production energetics, defect mobility, and cluster properties of the Fe-He system using a combination of molecular dynamics and kinetic Monte Carlo (kMC) calculations. The kMC results illustrate the competition of the vacancies and clusters as sinks for the interstitial He in the system and as possible nucleation sites for bubbles. Order kinetics of transmutation gas mechanisms are studied with the kMC method and analyzed using diffusion limited reaction rate theory.

10:35 AM Break

10:55 AM

Kinetics of Coarsening of Helium Bubbles during Implantation and Post-Implantation Annealing: *Stanislav Golubov*¹; Roger Stoller¹; Steve Zinkle¹; ¹Oak Ridge National Laboratory

To understand the effects of He on irradiated metals requires modeling of helium-vacancy clusters evolution. Recently, a new method of solving the two-dimensional master equation describing He-vacancy cluster evolution has been applied to calculate bubble evolution in a stainless steel irradiated with alpha particles near room temperature and annealed in the temperature range of 600-900°C. For the first time, the evolution of the helium bubble size distribution function was precisely calculated in 2D phase space and good agreement with experimental results was obtained. The results indicate that: Brownian motion of bubbles via surface vacancy diffusion provides a reasonable explanation of bubble evolution, most bubbles are near the equilibrium state at T>700°C, lack of vacancies at temperatures lower than about 700°C leads to a decrease in bubble growth, and use of a non-ideal He equation of state influences bubble density and swelling, both are higher than for the ideal gas case.

11:15 AM

Review of Primary Damage Production in Iron: *Roger E. Stoller*¹; ¹Oak Ridge National Laboratory

Results of extensive investigations of primary damage formation in iron using molecular dynamics (MD) displacement cascade simulations in iron will be reviewed. The database of MD cascades includes energies from near the displacement threshold to 200 keV and temperatures from 100 to 900K. The review will focus on the role of cascade energy and temperature in primary damage formation. Damage production is characterized in terms of the total number of point defects produced, the partitioning of the this total into isolated and clustered defects, and the size distributions of the interstitial and vacancy clusters. The database primarily includes cascades produced in perfect material, with the impact of pre-existing damage and free surfaces evaluated for a limited number of conditions. The applicability of the atomistic simulations for evaluating neutron energy spectrum effects in different irradiation conditions (fission, fusion, spallation) will also be discussed.

11:35 AM

The Thermal Annihilation Process of Stacking Fault Tetrahedra: *Yoshitaka Matsukawa*¹; Stanislav I. Golubov¹; Bachu N. Singh²; Steven J. Zinkle¹; ¹Oak Ridge National Laboratory; ²Risø National Laboratory

Thermal stability and annihilation of defect clusters are fundamental issues necessary to understand the kinetics of defect microstructure evolution under irradiation. The stacking fault tetrahedron is a common defect cluster directly produced during neutron irradiation in fcc metals. The objective of the present study is to identify the mechanism of thermal annihilation of SFTs at various sizes by in situ annealing in a transmission electron microscope (TEM). Various sizes of SFTs (<2~50nm) were introduced into gold by quenching from high temperatures. Also, small SFTs (\approx 2nm) were introduced into gold, copper, silver, nickel, and aluminum thin foils (<50nm) by Kiritani's high-speed deformation method. Annihilation temperature strongly depended on SFT size. A medium-sized SFT (10nm) in quenched gold was observed to annihilate at 938K, whereas a large SFT (40nm) disappeared at 1010K. In both cases annihilation occurred instantaneously; neither morphological nor size changes were detected within 33ms timestep resolution.

2006 Nanomaterials: Materials and Processing for Functional Applications: Nanostructure Manufacturing, Characterization and Functionalization

Sponsored by: The Minerals, Metals and Materials Society, TMS Electronic, Magnetic, and Photonic Materials Division, TMS: Nanomaterials Committee
Program Organizers: W. Jud Ready, GTRI-EOEML; Seung Hyuk Kang, Agere Systems

Monday PM Room: 214C
March 13, 2006 Location: Henry B. Gonzalez Convention Ctr.

Session Chairs: Seung Hyuk Kang, Agere Systems; W. Jud Ready, GTRI-EOEML

2:00 PM Introductory Comments

2:05 PM Invited

X-Ray Nano-Diffraction of Individual Zinc Oxide Nano-Rings: *Iuliana Dragomir-Cernatescu*¹; *Robert L. Snyder*¹; *Puxian Gao*¹; *Zhong Lin Wang*¹; *Yanan Xiao*²; *Zhonghou Cai*²; ¹Georgia Institute of Technology; ²Argonne National Laboratory

Nano-structures, whose lateral dimensions fall in the range of 1 to 100 nm, have received growing interests due to their outstanding properties and their potential applications. The development of these new structures into future nano-devices crucially depends on the development of new characterization techniques and theoretical models for a fundamental understanding of the relationship between the structure and properties. X-ray diffraction (XRD) has been successfully applied to microstructural characterization of bulk powder nano-structured materials, where useful information, such as crystallite size distribution, crystallite shapes and lattice defects were evaluated from the X-ray pattern. In the present case XRD analysis was employed for the characterization of individual ZnO nano-rings. Measurements of XRD lines from a single-crystal nano-ring were achieved by using the unique nano-diffraction facility at the APS. This new approach provides detailed information about the nano-structural parameters of individual ZnO nano-rings. The results were compared with those obtained from SEM/TEM.

2:30 PM Invited

Nanomechanical Testing and Nanomechanical Machining of Nanobuilding Blocks: *Xiaodong Li*¹; ¹University of South Carolina

The extremely small dimensions of nanobuilding blocks, such as nanoparticles, nanotubes, nanowires, and nanobelts, impose a tremendous challenge to many existing testing and measuring techniques for experimental studies of their mechanical properties. We have developed a nanomanipulator that can be used inside a scanning electron microscope (SEM) to perform tensile, bending, creep and fatigue tests for nanobuilding

blocks. We have also extended application of traditional nanoindentation approaches to nanobuilding blocks for directly measuring their mechanical properties. Hardness, elastic modulus and fracture toughness of nanoparticles, nanowires and nanobelts were measured using a nanoindenter. Nanoscale deformation behavior and fracture mechanisms were studied by post in-situ imaging of the indents. We have developed novel nanomechanical machining methodologies and tools that are able to perform operations such as indenting, cutting, milling, shaping, forging, polishing to realize functional nanostructures and nanodevices.

2:55 PM Break

3:10 PM Invited

Manufacturing with Micro-Organisms: A New Biological/Synthetic Chemical Paradigm for the Mass Production of Functional 3-D Nanoparticle Structures: *Kenneth H. Sandhage*¹; Sam Shian¹; Michael R. Weatherspoon¹; Shawn M. Allan¹; Ye Cai¹; Chris S. Gaddis¹; Phillip D. Graham¹; Michael Haluska¹; Gul Ahmad¹; Ben Church¹; Robert L. Snyder¹; Mark Hildebrand²; Brian P. Palenik²; Dori Landry²; ¹Georgia Institute of Technology; ²University of California at San Diego

The widespread commercial use of three-dimensional (3-D) nanostructured devices will require fabrication protocols capable of: i) precise 3-D assembly on a fine scale and ii) mass production on a large scale. These often-conflicting requirements can be addressed with a new paradigm that merges biological self-assembly with synthetic chemistry: Bioclastic and Shape-preserving Inorganic Conversion (BaSIC). Nature provides spectacular examples of micro-organisms (diatoms, coccolithophorids, etc.) that assemble intricate bioclastic 3-D structures. Through sustained reproduction of such micro-organisms, enormous numbers of 3-D micro/nanostructures with identical morphologies may be generated. Such massive parallelism and species-specific (genetically-controlled) precision are highly attractive for device manufacturing. However, natural bioclastic chemistries are rather limited. With BaSIC, biogenic assemblies can be converted into non-natural functional chemistries (e.g., TiO₂, ZrO₂, BaTiO₃, Zn₂SiO₄, polymers), while preserving the biogenic morphologies. Future genetic engineering of biomineralizing micro-organisms may be coupled with BaSIC to yield low-cost nanostructured devices with tailored shapes and tailored chemistries.

3:35 PM Invited

Novel Nanostructured Materials by Physical Vapor Deposition and Sol-Gel Techniques: *Ashutosh Tiwari*¹; ¹University of Utah

Nanoscience and Nanotechnology represents one of the hottest frontiers in Physical Sciences and Engineering. Confinement effects due to boundary conditions make "Nanostructured Materials" behave much differently than their bulk counterparts. In this talk, I will present some of my interesting results related to these materials. Major focus will be on following three topics: (i) Nanodots for magnetic data storage (ii) Novel Superlattice Structures for low-field magnetic sensor applications (iii) Nanostructured Epitaxial thin films of Oxide-based Diluted Magnetic Semiconductors.

4:00 PM Break

4:15 PM

Field Deployable Nano-Band Electrode System for Arsenic Analysis: *David L. Cocke*¹; Jewel A. Gomes¹; Sudharshan Varma¹; Bonnie Ardoin¹; Sujith Mididuddi¹; Hector Moreno¹; Eric Peterson²; ¹Lamar University; ²Highland Community College

Arsenic has long been an USEPA priority pollutant and is an important environmental concern because of its toxicity and carcinogenicity even at parts per billion level. It is very important to speciate its different oxidation states of arsenic for better understanding of its chemical behavior, the removal efficiency and removal mechanism. In the present work, a relatively new nano-band electrode system has been optimized for the determination of both As(III) and As(V) in water samples using Anodic Stripping Voltammetric technique. The influence of deposition potential, different supporting electrolytes and plate time on the arsenic stripping peak was investigated. A detection limit of 0.4 ppb has been obtained using USEPA method of detection limit, with plate times of just 10 seconds. The major interference was found to be from copper during measurements.

Finally, the optimized system has been used for arsenic determination in real water samples, e.g. Rio Grande basin.

4:35 PM

Sensing Properties of a Novel Fe-Fe₂O₃/Polyoxocarbosilane Core-Shell Nanocomposite Powder Prepared by Laser Pyrolysis: *Adelina Tomescu*¹; *Rodica Alexandrescu*²; Ion Morjan²; Florian Dumitrache²; Lavinia Albu²; Victor Ciupina³; Zdenek Bastl⁴; Ana Galikova⁵; Josef Pola⁵; ¹National Institute of Materials Physics; ²National Institute for Lasers Plasma and Radiation Physics; ³Ovidius University of Constanta; ⁴J. Heyrovsky Institute of Physical Chemistry; ⁵Czech Academy of Science

Metal oxide materials are widely used for gas sensing. Capable of operating at elevated temperatures and in harsh environments, they are mechanically robust and relatively inexpensive and offer exquisite sensing capabilities, the performance of which is dependent upon the nanoscale morphology. We report here about the synthesis and sensing properties of a thermally stable Fe-based nanocomposites prepared by continuous-wave IR laser-induced and ethylene sensitized co-pyrolysis of gaseous iron pentacarbonyl and hexamethyldisiloxane in argon. The simultaneously occurring formation of iron from iron pentacarbonyl and that of organosilicon polymer from hexamethyldisiloxane yield iron nanoparticles surrounded by organosilicon polymer shell. The particles were characterized by spectral analyses, electron microscopy, thermal gravimetry. They become superficially oxidized in atmosphere. For testing the sensing properties (sensitivity and selectivity) of the Fe/organosilicon based nanocomposites, thick films deposited on alumina substrates were heated at 450 C and the variation of their electrical resistance in presence of CO and CH₄ (in dry and humid air) was measured. Preliminary results indicate a marked selectivity of the new sensor relatively to the tested toxic gases.

4:55 PM Break

5:10 PM

Synthesis and Characterization of Ag Nanorods in AAO Templates through Sol-Gel Method: *Khwaja Moinuddin*¹; *Paul Keierleber*¹; Louisa Hope-Weeks¹; Iris V. Rivero¹; ¹Texas Tech University

The objective of this research is to characterize the efficiency of synthesis techniques for the fabrication of Ag nanorods. Specifically, template-based methods were selected for further investigation based on the quality of its products which is characterized by yields of highly-ordered structure of monodisperse nanorods and nanotubules. Two template-based syntheses (using AAO) have been combined with sol-gel method. The first method involves preparation of a (2M) silver salt (AgNO₃) solution followed by suspension of the commercially available AAO templates (pore size 0.02µm) in the solution. The second method involves preparation of a pre-reduced solution of metal salt - silver nitrate (2M), sodium citrate (2M) and sodium borohydride (2M) followed by suspension of the AAO templates in the solution. Results from these fabrication procedures were evaluated in terms of the characteristics of its products (Ag nanorods' structure and dimensions), production costs, and simplicity of replication procedure.

3-Dimensional Materials Science: 3-D Representation and Computation

Sponsored by: The Minerals, Metals and Materials Society, TMS Structural Materials Division, TMS: Advanced Characterization, Testing, and Simulation Committee

Program Organizers: Jeff P. Simmons, U.S. Air Force; Michael D. Uchic, Air Force Research Laboratory; Dorte Juul Jensen, Riso National Laboratory; David N. Seidman, Northwestern University; Anthony D. Rollett, Carnegie Mellon University

Monday PM Room: 205
March 13, 2006 Location: Henry B. Gonzalez Convention Ctr.

Session Chairs: Jeff P. Simmons, U.S. Air Force; Jaimie S. Tiley, U.S. Air Force

2:00 PM

3D Digital Microstructures with Distributions of Particles: *Anthony D. Rollett¹; Stephen Sintay¹; Abhijit Brahma¹; Joseph Fridy²; David Saylor³; ¹Carnegie Mellon University; ²Alcoa Technical Center; ³FDA*

A method for statistical reconstruction of digital microstructures in three dimensions is described that includes orientation information as well as grain structure. Recent progress is described in developing a method for inserting small particles with variable shape into such structures. The approach is illustrated by an example of application to modeling an aerospace aluminum alloy.

2:20 PM Invited

Databases and Web Services in Support of Computational Materials: *Gerd Heber¹; Anthony R. Ingraffea¹; ¹Cornell Theory Center*

The datasets underlying sophisticated multi-scale and multi-physics models of 3D computational materials have grown dramatically over the last decade in both, size and complexity. The increase in size reveals scalability issues in traditionally file-based application designs, which are inadequate for applications involving (meta-) data-sharing and distributed applications (e.g., Web services, GRID). The higher complexity demands more rigorous data-modeling in form of database-, XML-, and RDF schemas, as well as domain ontologies. The challenge at hand is to create integrated environments providing access to the best available experimental data and powerful simulation and intelligent search capabilities. This is a report on ongoing efforts in the Cornell Fracture Group (CFG) to create Web portal-like environments for computational materials research. These portals offer users access (through a Web browser) to various materials resources and suites of modeling tools developed by the CFG and others.

2:45 PM Invited

Computational Models for Crystal Plasticity Simulations: *Somnath Ghosh¹; ¹Ohio State University*

The recent years have seen a paradigm shift towards the use of crystal plasticity models to understand deformation and damage mechanisms for life prediction. In this approach, the mechanical response of polycrystalline aggregates is deduced from the behavior of constituent crystal grains. A crystal plasticity based FEM model is developed using multiple time scaling for predicting fatigue of metals and alloys in this paper. The multi-time scaling invokes compression and rarefaction of time scales to enable simulation of a large number of cycles. Methods of digital microstructure reconstruction are discussed for image based modeling. The material constitutive parameters are calibrated from experimental results and the model is validated with experiments. Creep and cyclic deformation simulations are conducted for simulating the development of local stresses, strains. Localization phenomenon is studied as a function of the microstructure.

3:10 PM

Finite Element Based Methodology for the Prediction of Mechanical Properties of Al/SiC_p Composites Using Realistic Computer Simulated Microstructures: *Arun Sreeranganathan¹; Harpreet Singh¹; Arun M. Gokhale¹; ¹Georgia Institute of Technology*

Finite element (FE) based simulations of micro-mechanical response are performed on computer simulated microstructures of discontinuously reinforced aluminum matrix composites that incorporates realistic com-

plex particle morphologies/shapes, spatially non-uniform distribution of particles and anisotropic particle orientations. The simulated microstructures contain over ten thousand particles and the FE results are compared with that for real microstructures to validate the simulation model. Virtual microstructures are created by varying numerical parameters in the model and FE simulations are carried out to reflect the effect of microstructure (and therefore, processing conditions) on the mechanical response of the materials.

3:30 PM

3D Image-Based Modeling of the Effect of Microstructure on Mechanical Response: *Andrew B. Geltmacher¹; Alexis C. Lewis¹; ¹Naval Research Laboratory*

It is well known that the true 3D nature of microstructures strongly dictates the mechanical performance of materials. Thus, it is critical to understand the impact of real 3D microstructures in developing accurate predictive models of the performance of advanced materials. This presentation will focus on the mesoscale mechanical response of a super-austenitic stainless steel and a beta titanium alloy. This research uses 3D analysis, scientific visualization, and Finite Element Modeling (FEM) to understand the relationships between mechanical behavior and microstructural features in these materials. 3D analysis of digitally reconstructed microstructures, 3D image-based FEM simulations, and percolation analyses are performed on real 3D microstructures to track evolution of stress, strain, yield, and damage under the influence of various applied stress states, with particular emphasis on determining the types of microstructural features which serve as initiation sites of deformation and failure.

3:50 PM Break

4:10 PM

Three-Dimensional (3D) Microstructure Visualization and Finite Element Modeling of the Mechanical Behavior of Heterogeneous Materials: *Nikhilesh Chawla¹; Rajen S. Sidhu¹; V. V. Ganesh¹; ¹Arizona State University*

The mechanical behavior of materials is inherently controlled by microstructure. In particular, heterogeneous materials, consisting of two or more components or phases, have complex microstructures. This makes modeling of the mechanical behavior a challenge. We have developed a three dimensional (3D) approach to (a) constructing a "virtual microstructure" in 3D by serial sectioning technique, and (b) finite element modeling using the 3D microstructure as a basis. In this talk we will explore the fundamentals of the 3D virtual microstructure modeling methodology. This methodology was used to study the deformation behavior of SiC particle reinforced metal matrix composites. The role of second phase fraction, morphology, and aspect ratio on deformation was quantified and will be discussed. Results from the microstructure based 3D simulations were found to be in good agreement with the experimental observations, indicating the importance and effectiveness of 3D microstructure-based simulations.

4:30 PM

A Formulation Based on Fast Fourier Transforms for the Calculation of the Micromechanical Behavior of Plastically Deformed 3-D Polycrystals: *Ricardo A. Lebensohn¹; ¹Los Alamos National Laboratory*

In this work we present a numerical formulation based on Fast Fourier Transforms to efficiently obtain the micromechanical fields in plastically deformed 3-D polycrystals. This formulation was developed in the last decade by P.Suquet and coworkers as a fast algorithm to compute the elastic and elastoplastic response of composites, using as input a digital image of their microstructures. The model provides an exact solution of the governing equations and has better performance than a Finite Element calculation for the same purpose and resolution. This formulation has been in turn adapted to deal with 3-D polycrystals deforming by dislocation glide (R.Lebensohn, Acta Mater. 49, 2723, 2001). To illustrate its capabilities we will show results for a periodic polycrystal generated by Voronoi tessellation. The constituent grains are strongly anisotropic ice crystals. The results show transgranular deformation bands, stress concentrations near triple junctions and non-basal activity in unfavorably oriented grains.

4:50 PM

Modeling Deformation and Fracture Phenomena in 3 Dimensions:Diana Farkas¹; ¹Virginia Tech

This work analyzes the 3 dimensional aspects of phenomena observed in plastic deformation of polycrystalline metallic materials at the nano scale. The studies are based on molecular dynamics simulations of deformation and fracture response in these materials. We specifically point out the limitations of modeling these phenomena in a quasi 2 dimensional framework. We also discuss techniques for visualization of the results of the 3D simulations, including sectioning and CAVE virtual reality visualization.

5:10 PM

Three-Dimensional Phase-Field Simulations of Equilibrium Morphology of Misfitting Precipitates: *Jingxian Zhang*¹; Weiming Feng¹; Shenyang Hu²; Zi-Kui Liu¹; Long-Qing Chen¹; ¹Pennsylvania State University; ²Los Alamos National Laboratory

Elastic energy arising from a difference of lattice parameter between precipitate and parent phases have a strong influence on the equilibrium morphology of the precipitates. It depends on many parameters, including (i) elastic anisotropy, (ii) elastic inhomogeneity (the difference in the elastic constants of the two phases), and (iii) misfit strain. Recent advances in microelasticity theory and numerical simulations have made it possible to efficiently calculate the elastic energy for systems with rather general elastic anisotropies for the precipitate and matrix, arbitrarily large elastic inhomogeneity, and a general misfit strain. In this presentation, we studied the three-dimensional equilibrium shapes of misfitting precipitates by phase-field simulations. The effects of elastic constants, elastic inhomogeneity and misfit strains are investigated systematically. Relevant examples in real alloy systems will be discussed.

5:30 PM **Invited****Interfacing Finite Element Simulations with Three-Dimensional Characterizations of Polycrystalline Microstructures:** *Paul Dawson*¹; ¹Cornell University

Experimental methods to characterize the microstructural state of polycrystalline samples have progressed rapidly in recent years. Automated serial sectioning combined with diffraction measurements provide digital images of the crystalline microstructure of material samples in three-dimensions. These complement x-ray tomography and bulk diffraction measurements to give both detailed definition of specific samples and statistically-based distributions of microstructural attributes. From a modeling perspective, the availability of spatially-resolved microstructures of actual samples together with measures of the likely variability of these microstructures offers fresh opportunities for investigating the links between microstructural state and mechanical properties, including how the state evolves under thermomechanical processing. In this presentation, we will discuss strategies for building virtual samples using mathematical representations of the material founded on the experimental characterization. Some samples are intended to closely replicate the experimental images, while others are intended for exploring variations that are consistent with the statistics of larger samples. The virtual samples evolve under loading via finite element simulations and the results are used to explore the connections between microstructural state and mechanical performance. This effort will be described in the context of a larger, ONR/DARPA-funded project that encompasses several thrusts to characterize and evolve polycrystalline microstructures in three-dimensions.

7th Global Innovations Symposium: Trends in Materials R&D for Sensor Manufacturing Technologies: Session I

Sponsored by: The Minerals, Metals and Materials Society, TMS Materials Processing and Manufacturing Division, TMS: Global Innovations Committee

Program Organizers: Hamish L. Fraser, Ohio State University; Iver E. Anderson, Iowa State University; John E. Smugeresky, Sandia National Laboratories

Monday PM
March 13, 2006

Room: 204A
Location: Henry B. Gonzalez Convention Ctr.

Session Chair: Hamish L. Fraser, Ohio State University

2:00 PM Introductory Comments by John E. Smugeresky**2:05 PM Invited****Sensing: From Nanometers to Megameters:** *Alton D. Romig*¹; ¹Sandia National Laboratories

The application of advanced scientific, technological and engineering capabilities are essential to help our nation detect, repel, defeat, or mitigate the threat of chemical, biological, radiological, nuclear and explosive (CBRNE) weapons. Nanotechnology is a very promising area that will enable the creation of functional materials, devices, and systems by controlling matter at the atomic and molecular scales. Similarly, microtechnologies have helped produce smaller, smarter, and less costly sensors which feature desirable characteristics including lower power consumption, greater sensitivity, and better specificity than previous macro-level equivalents. Sensing systems based upon the integration of these technologies support a broad range of sensing applications – from the nm to Mm.

2:35 PM Invited**Global Innovations in Sensor Technologies: Materials Issues in Sensors for Automotive Applications:** *Paul C. Killgoar*¹; ¹Ford Motor Company

The number and variety of sensors used in automobiles has dramatically increased over the past several decades, a trend that is expected to continue in the future. Sensors are used in four major areas: active and passive safety systems, powertrain control systems, emissions control and monitoring systems, and climate control systems. Automotive safety technologies have evolved from seat belts and single-stage air bags to individually tailorable occupant protection systems in part because of affordable, sensitive accelerometers and occupant sensors. Increasingly refined interactive vehicle dynamics systems are enabled by body height, yaw, and other sensors. The availability of diverse physical and chemical sensors capable of operating in the harsh automotive environment, together with improvements in engine and catalyst technologies, has enabled far more precise and effective control of engine performance and emissions than in the past. The continuous improvements and new directions in safety, powertrain (gasoline, clean diesel, electric hybrid, hydrogen), emissions, and climate control require new and improved sensors. The principles and limitations of various automotive sensors and some of the evolving needs will be described. A number of new sensors are close to being production-ready, while others are still very much in the research and development stage. In this presentation, particular emphasis will be placed on the materials challenges, because cost and durability requirements severely constrain the possible automotive sensor and materials solutions.

3:05 PM Invited**Materials Which Undergo a First Order Transition as Sensors – Gd⁵(Si^xGe^{1-x})⁴:** *Karl A. Gschneidner*¹; Min Zou¹; H. Tang¹; Vitalij K. Pecharsky¹; ¹Iowa State University

Gd⁵(Si^xGe^{1-x})⁴ undergoes a magnetostructural first order transition between 40 and 275K, depending upon the Si to Ge ratio (high Si – high temperature). When the Gd⁵(Si^xGe^{1-x})⁴ transforms, it spontaneously generates a voltage (SGV). The SGV can be utilized in sensors, which respond not only to changes in temperature, pressure, and/or magnetic field,

but most importantly to the rates of their changes without the need for a complicated analysis of signals. Furthermore, all of this can be done by a single sensor requiring no standby power.

3:35 PM Break

3:50 PM Invited

Nanostructured Materials for Infrared Detection: *Gail J. Brown*¹; ¹Air Force Research Laboratory

Quantum Confinement effects in semiconductor heterostructures has opened up many new approaches to designing infrared sensing materials. These nanostructured heterostructures come in a variety of forms such as quantum wells, quantum wires, quantum dots and superlattices. In addition, carbon nanotubes, colloidal nanoparticles and photonic crystals are attracting some interest for infrared detector applications. An attractive feature of all these materials is the ability to tailor the optical and electrical properties by changing simple parameters like layer thickness, materials composition, and layer combinations. Depending on the materials used, the nanoscale heterostructures can be designed for optical absorption anywhere from the ultraviolet to terahertz portion of the electromagnetic spectrum. This talk is an overview of these various materials and how they may be applied to infrared sensing.

4:20 PM Invited

Development and Application of Gas Sensing Technologies for Combustion Processes: *Prabir K. Dutta*¹; ¹Ohio State University

The Center for Industrial Sensors and Measurements at The Ohio State University is developing microsensors to monitor combustion processes. Our approach in designing highly selective sensors includes optimized sensing principles, novel materials and use of catalysts. For O₂ sensing, potentiometric measurements with internal references and a novel sealing technology is being developed. A potentiometric design with a catalyst filter is the basis for a total NO_x sensor. CO sensing is being done with titania, modified by catalysts to produce selectivity. Hydrocarbon sensing exploits a filter that oxidizes the hydrocarbon to water. The CO₂ sensor is based on a Li-conducting electrolyte. Miniaturized versions of these sensors are being integrated into a sensor array with data analysis by non linear regression techniques. A complete combustion monitoring/optimization system is possible for the first time with the miniaturized sensor arrays and is expected to lead to significant energy savings as well as minimizing emissions.

4:50 PM Invited

Issues Regarding Present and Future Characterization of Nanomaterials for Sensors at the Atomic Scale: *David B. Williams*¹; ¹Lehigh University

In the main, the scale of sensor devices has been decreasing significantly during the development of nanomaterials. The processes that govern these sensors occur generally on the nanometer, or smaller, scale, and so it is important to have techniques for characterization at the atomic scale. This includes morphological information as well as compositional and chemical information obtained from spectral analysis. In this paper, the techniques available presently for such characterization will be described and limitations to resolution outlined. In concert with dramatic and revolutionary advances that have been made in the very recent past regarding aberration-corrected electron microscopy, solutions to present-day limitations will be described. Exciting examples of the application of these new instruments to nanomaterials for sensor applications will be presented. These will include spatial resolution imaging close to 0.06nm and spectral analyses, similar to those obtained by EXAFS, from regions defined by incident beam diameters of ~1nm.

A Century of Nickel Alloy Discovery and Innovation: Session I

Sponsored by: The Minerals, Metals and Materials Society, TMS Structural Materials Division, TMS: High Temperature Alloys Committee

Program Organizers: Lewis Edward Shoemaker, Special Metals Corporation; Gaylord Smith, Special Metals Corporation

Monday PM
March 13, 2006

Room: 209
Location: Henry B. Gonzalez Convention Ctr.

Session Chair: Lewis Edward Shoemaker, Special Metals Corporation

2:00 PM Invited

A Century of Discoveries, Inventors and New Nickel Alloys: *Shailesh Jayanti Patel*¹; ¹Special Metals Corporation

The 20th century was an explosive period for the growth of the nickel industry beginning in 1906 with the development of Monel metal. What followed over the next 100 years is literally hundreds of new alloys uniquely designed for a multitude of industries in scores of applications. Leading the charge was the International Nickel Company with major new alloys in every decade. This impressive track record is briefly reviewed and acknowledgement given to a number of the prolific inventors that pioneered new fields of alloy development. Acknowledgement is equally given to the major metallurgical discoveries made by the metallurgists of the International Nickel Company, including gamma prime hardening of nickel alloys, ductilization of cast iron, the role of nickel in inhibiting stress corrosion cracking, maraging, mechanical alloying and the Pilling/Bedworth ratio of scale adhesion.

2:20 PM Invited

A Century of Monel Metal 1906 - 2006: *Lewis Edward Shoemaker*¹; *Gaylord D. Smith*¹; ¹Special Metals Corporation

Monel can arguably be considered the first nickel-base, corrosion-resistant alloy developed. It is essentially a binary alloy of nickel and copper. Since its ratio of nickel to copper is the same as that found in the ore from which it is derived, it can also be considered a "natural" alloy. Being patented in 1906, Monel is ready to celebrate its 100th birthday. Over its first century it has seen use in many different applications in many different industries ranging from huge naval leviathans to tiny electronic components and from food processing to gasoline production to electric power generation. The alloy and its descendants continue to be widely used today and it seems likely that trend will continue into the next century and beyond.

2:40 PM Invited

The Evolution of Solid Solution Nickel-Base Alloys for Corrosion Applications: *Galen Hodge*¹; ¹Materials Technology Institute

The element nickel has some interesting metallurgical and electrochemical properties that make it an important material in the chemical industry. One of those is its ability to dissolve and hold in solid solution significant amounts of other alloying elements. This ability has made it possible to develop a large number of solid solution single-phase corrosion resistant alloys. Alloys containing iron, chromium, molybdenum and tungsten have, therefore, been developed to support more aggressive applications in the chemical industry. This paper will review the development of several of these alloys, describe their properties and applications.

3:00 PM Invited

The Evolution of Cast Nickel-Base Superalloys: *Tresa M. Pollock*¹; ¹University of Michigan

Investment casting of complex nickel base superalloys has enabled continuous increases in their properties and performance of cast components in a wide range of applications, and particularly in gas turbine engines. Processing advances that permit a high degree of control of cast microstructure will be reviewed. The complementary role of solidification modeling will be discussed. An overview of the evolution of the chemistry of cast alloys will be presented. Finally, recent developments in single crystal growth will be highlighted.

MONDAY PM

3:20 PM Invited

Evolution of Wrought Age-Hardenable Superalloys: *Raymond F. Decker*¹; ¹Thixomat

The discovery of gamma prime hardening early in the 20th century seeded a continuous evolution of remarkable engineering alloys, the Superalloys. This high technology field grows even to this day, some 85 years later. The sequence of development of all the wrought Superalloys will be traced as part of the story of the enlightenment gained on alloy theory and hardening mechanisms. Skillful use of the latest in composition/property theory has been the hallmark of Superalloy developments. Revolutionary processing discoveries have played their role. Finally, these alloys have enjoyed an eager market pull in ever evolving high tech applications.

3:40 PM Break**4:00 PM Panel Discussion**

Future Trends in the Key Markets Served by Nickel Alloys: A brief introduction of the current status and future of materials technology in each industry followed the opportunity for audience comments, questions, and open discussion.

Aerospace Industry

Power Industry

Oil, Gas and Petrochemical Industry

Nickel Alloy Trends in China

Advanced Materials for Energy Conversion III: A Symposium in Honor of Drs. Gary Sandrock, Louis Schlapbach, and Seijirau Suda: FreedomCAR and Fuel Partnership-Metal Hydrides I

Sponsored by: The Minerals, Metals and Materials Society, TMS Light Metals Division, TMS: Reactive Metals Committee

Program Organizers: Dhanesh Chandra, University of Nevada; John J. Petrovic, Petrovic and Associates; Renato G. Bautista, University of Nevada; M. Ashraf Imam, Naval Research Laboratory

Monday PM

Room: 214B

March 13, 2006

Location: Henry B. Gonzalez Convention Ctr.

Session Chairs: Scott Jorgensen, General Motors; Farshad Bavarian, Chevron Texaco Technology Ventures LLC; Sunita Satyapal, U.S. Department of Energy

2:00 PM Plenary

Overview of DOE Metal Hydride Center of Excellence: *James C. Wang*¹; Jay Keller¹; ¹Sandia National Laboratories

In July 2003, The Office of Hydrogen, Fuel Cells and Infrastructure Technologies of the Department of Energy (DOE) Office of Energy Efficiency and Renewable Energy solicited Grand Challenge Proposals to establish three Centers of Excellence in hydrogen storage developments for reversible metal hydrides, non-reversible chemical hydrides and carbon storage materials, respectively. The program mission is to research and develop cost-effective, on-board hydrogen storage systems that enable a minimum range of 300 miles within the weight and volume constraints of the vehicle. Currently, no hydrogen storage technology available can meet the DOE cost and performance targets. In April 2004, Sandia National Laboratories was selected by DOE to lead the Metal Hydride Center of Excellence with partners from 5 other national laboratories. We will present the organization and recent accomplishments of the Metal Hydride Center which is confident to accomplish DOE/FreedomCAR objectives for 2010 in hydrogen storage for vehicular transportation applications.

2:25 PM Plenary

A Thermodynamic Database for Metal-Hydrogen Systems: *Ursula R. Kattner*¹; ¹National Institute of Standards and Technology

The thermodynamic properties of metal-hydrogen systems are key to assessing the suitability of particular systems for hydrogen storage. Thermodynamic modeling using the Calphad method provides a way to incorporate results from experimental investigations and ab-initio calculations into an overall temperature-pressure-composition framework. The calculations provide temperature and pressure of the hydriding reaction as well as heats of reaction and reaction sequences. A comprehensive thermodynamic database with Gibbs energy functions for the phases in metal-hydrogen systems and relevant metal-metal systems has been assembled from published data evaluations and newly generated thermodynamic descriptions. The initial focus in the construction of the database is on ternary and quaternary hydride systems with light elements.

2:50 PM Plenary

Novel Complex Hydrides for Hydrogen Storage: *Ragaiy Zidan*¹; ¹Savannah River National Laboratory

The aim of the overall effort is to produce hydrogen storage materials of high hydrogen capacity higher than 8% by weight, stable with cycling and possessing favorable thermodynamics and kinetics characteristics compatible with on-board hydrogen storage transportation applications. In order to achieve this goal new methods for material synthesis are employed and guided by theoretical modeling, thermodynamic and material structural characterization. A new material synthesis method, molten state process, was developed and tested. This method is used to modify and form new complex hydride compounds with the desired characteristics. Other possible high capacity hydrides are also investigated.

3:10 PM Keynote

An Overview of Analytical Techniques Being Used to Characterize Today's Most Advanced Hydrogen Storage Materials: *Karl J. Gross*¹; ¹Sandia National Laboratories

The wide variety of materials being proposed for hydrogen storage today present a number of different challenges to the researcher from an analytical characterization perspective. These include both evaluating the true performance of the materials for real-world applications as well as understanding the underlying physical mechanisms controlling the materials properties. An overview will be presented on the state of the art analytical methods for characterizing the hydrogen storage properties of materials. Some challenges to measurements on particular types of materials or conditions and in will be discussed.

3:30 PM Invited

Neutron and Synchrotron Studies on Li-Based Nitride and Hydride: *Wen-Ming Chien*¹; Dhanesh Chandra¹; Ashfia Huq²; James W. Richardson, Jr.²; Evan Maxey²; Martin Kunz³; Sirine Fakra³; ¹University of Nevada-Reno; ²Argonne National Laboratory; ³Lawrence Berkeley National Laboratory

Thermal expansions and phase identification of Li₃N and LiAlD₄ samples have been studied by using time-of-flight (TOF) neutron powder diffraction (NPD) and synchrotron diffraction methods. Low temperature neutron powder diffraction studies have been performed for both Li₃N and LiAlD₄ samples from 10 K to 300 K. Neutron and synchrotron studies of Li₃N show that commercial Li₃N is a two phase mixture (β+β). It was shown ~70 wt.% α-Li₃N and ~30 wt.% β-Li₃N for the commercial Li₃N. Crystal structures of both α and β phases of Li₃N are hexagonal, and LiAlD₄ is monoclinic. Volume expansions of Li₃N α+β phases are 0.56% and 1.1%, respectively, and for LiAlD₄ is 0.88% from 10 K to 300 K. Detail lattice and volume expansions will be presented.

3:50 PM Break**4:05 PM Invited**

Theoretical Contributions towards the Development of Storage Media and Related Materials for Hydrogen Processing: *Susanne Marie Opalka*¹; Donald Anton¹; Thomas Vanderspurt¹; ¹United Technologies Research Center

Realization of the hydrogen economy will require new materials with unprecedented performance attributes for hydrogen generation, storage, and delivery. To meet these challenges, recent advances in first-principles methodologies are currently being used to guide and streamline the experimental development of materials, such as hydrogen storage media, fuel processing catalysts, and hydrogen-selective membranes. Implemen-

tation of these methodologies has been focused along two fronts: first, coupling of theoretical methodologies for enhanced physical property prediction, and second, the integration of modeling as an investigative tool alongside experimentation. The atomic-thermodynamic methodologies used to survey broad compositional phase space for hydrogen storage media with enhanced retrievable capacity will be discussed in detail, with special emphasis on the approaches used to create new candidate phase structures for evaluation. Additional examples will be used to highlight the unique role that theoretical methodologies play in elucidating mechanisms, and guiding the experimental optimization of hydrogen storage media.

4:25 PM Invited

Aluminum Hydride (AlH₃) as a Hydrogen Storage Compound: *Jason Greatz¹; James J. Reilly¹; Gary Sandrock²; John Johnson¹; Wei Min Zhou¹; James Wegrzyn¹; ¹Brookhaven National Laboratory; ²Brookhaven National Laboratory/Sandia National Laboratory*

AlH₃ is a covalent hydride known for more than 60 years. It is a very attractive medium for on-board automotive hydrogen storage since it contains 10.1 wt.% hydrogen with a density of 1.48 g/ml. There are 7 non-solvated AlH₃ phases, α , α' , β , γ , δ , ϵ , ζ . The properties of α -AlH₃ obtained from the Dow Chemical company in 1980 has been previously reported. Here we present a description of the thermodynamic and kinetic properties of freshly prepared α , β and γ AlH₃. In all cases the decomposition kinetics are below 100 degrees C and will meet DOE 2010 gravimetric and volumetric vehicular system targets (6 wt% H₂ and 0.045 kg/l). However further research is needed to develop a practical regeneration process for the dehydrogenated material.

4:45 PM Keynote

Risk Assessment of High Capacity Solid State Hydrides: *Donald L. Anton¹; Frank E. Lynch²; Joseph Senecal³; ¹United Technologies; ²Hydrogen Components, Inc.; ³Kidde-Fenwal, Inc.*

A critical consideration in the design of commercial hydrogen storage systems is safe operation. In the search for high hydrogen capacity materials such as alanates, this attribute has been overlooked. Conventional metal hydrides have been documented to be relatively safe, and this has fallaciously led to confidence in all hydrides. While the US Dept. of Transportation has detailed guidelines for the determination of risks associated with the transport of hazardous chemicals, no guideline exist for comparing the relative safety of new hydride materials. This study was instituted to define tests appropriate for determining the risks associated with using complex hydrides and to apply these tests to catalyzed NaAlH₄. Standardized ASTM and UN-DOT tests were identified. These tests and results for 2%TiCl₃ catalyzed NaAlH₄ will be described. The risks in handling and using these materials will be summarized and experiences gained in synthesizing 30 kg of catalyzed NaAlH₄ reviewed.

5:05 PM

First Principles Calculations of Destabilized Alloys for Hydrogen Storage Applications: *Sudhakar V. Alapati¹; Bing Dai²; Karl Johnson²; David S. Sholl¹; ¹Carnegie Mellon University; ²University of Pittsburgh*

A novel approach to hydrogen storage has been proposed recently that utilizes destabilization of metal hydrides with other materials. The hydrides of period 2 and 3 metals have relatively high hydrogen densities but are thermodynamically very stable, releasing hydrogen only at high temperatures. Vajo et al. have shown that the thermodynamics of the reaction can be modified by using additives to form compounds in the dehydrogenated state that are stable with respect to the constituents of the initial reaction. Having a stabilized dehydrogenated state reduces the enthalpy of dehydrogenation and increases the equilibrium partial pressure of the dehydrogenation reaction. We have calculated enthalpies for destabilization reactions from density functional theory. Comparison with experiments show very good agreement for known reactions. We have predicted heats of reactions for a large number of hypothetical reactions and have identified promising candidates. We discuss calculation of dissociation pressures and kinetics.

Alumina and Bauxite: Solids/Liquid Separation

Sponsored by: The Minerals, Metals and Materials Society, TMS Light Metals Division, TMS: Aluminum Committee

Program Organizers: Jean Doucet, Alcan Inc; Dag Olsen, Hydro Aluminium Primary Metals; Travis J. Galloway, Century Aluminum Company

Monday PM
March 13, 2006

Room: 7B
Location: Henry B. Gonzalez Convention Ctr.

Session Chair: Monique Authier, Alcan Inc

2:00 PM Introductory Comments

2:10 PM

Development of New Polyacrylate Flocculants for Red Mud Clarification: *Kevin L. O'Brien¹; Everett C. Phillips¹; ¹Nalco Company*

Conventional polyacrylate flocculants have been widely used to settle red mud in the Bayer process over the past two decades. A new manufacturing process has led to the development of higher molecular weight polyacrylate flocculants that outperform existing polyacrylate flocculants by 20% or more. Commercialization of the new polyacrylate flocculants has allowed plants to reduce overall consumption of flocculant. Lab test results and plant applications of these new flocculants at several refineries are summarized in this paper. Other benefits of these new flocculants such as their impact on mud rheological properties are currently under investigation and will also be discussed.

2:35 PM

Effect of Flocculant Molecular Weight on Rheology: *Donald P. Spitzer¹; Qi Dai¹; ¹Cytec Industries Inc*

Any polymeric flocculant used to settle suspended mud solids in reasonable times increases underflow mud yield stress, making the mud more difficult to flow. Yield stress (at a given solids concentration) always increases with polymer dosage, but depends somewhat on the type of polymer used. Primary emphasis of this paper is on the effects of molecular weight and the finding that, over quite a wide range, rheology does not depend on molecular weight. Thus, for lowest possible yield stress, molecular weight should be as high as possible, since this will give the lowest dosage for the required settling rate.

3:00 PM

A Fractal Model Describing the Aggregation of Various Mineral Materials: *Michel J. Gagnon¹; André Leclerc¹; Guy Simard¹; René Verreault¹; Guy Pélouquin¹; ¹Université du Québec à Chicoutimi*

The agglomeration of the particulate materials is necessary in many mineral processes. Depending upon physical and chemical parameters, the aggregates generated demonstrate specific density-size distributions that reflect the dominant agglomeration process. A fractal and empirical model was initially constructed to describe the red mud flocculation using simple variables such as density, particle sizes and fractal order. The application of the model to other data sets found in the scientific literature demonstrates a wider utilization of the model and was helpful in the development of a criterion that should facilitate the identification of the dominant mechanism by which the aggregation occurs. In this paper, data from different sources, various mineral materials and agglomeration processes is analysed and compared in the light of the proposed model and criterion. The values obtained with the linear fit are discussed in relation with the coagulation or flocculation, the fractal dimension and the resulting fractal structures.

3:25 PM

Study on the Clarification of a Red Mud Slurry during Flocculation: *Mélanie Normandin¹; Michel Gagnon¹; Guy Simard¹; André Leclerc¹; René Verreault¹; Guy Pélouquin²; ¹Université du Québec à Chicoutimi; ²Centre de Recherche et de Développement Arvida*

One of the important steps in the Bayer process is the solid-liquid separation by which the particulate materials are removed from the feed slurry. Obtaining perfect overflow clarity is one of the ultimate goals of the alumina industry. In this study, the parameters that can influence the clarity

of the overflow liquor resulting from the flocculation of the red mud slurry are systematically evaluated. Several laboratory tests are done combining commercial synthetic flocculants and new polymers. By varying the concentration of polymer solutions, the quantity and the sequence of introduction of polymeric materials, extremely low levels of turbidity were found in the overflow liquor. This represents a definite step toward the objective of reaching the absolute decantation by which perfectly clear overflow liquor is obtained right out of the decanters.

3:50 PM Break

4:10 PM

Waste Water Treatment Methods: *Dana Smith*¹; Fred S. Williams²; Scott Moffatt³; ¹Alcoa; ²CMIS Corporation; ³Cytec Industries Inc

Alcoa's Point Comfort, Texas industrial facility is a combination of a bauxite refining plant utilizing the Bayer process and an aluminum fluoride production plant. Due to the location's use of dry stack technology for disposing of the bauxite residue, the pond surface areas for evaporation are minimal compared to the rainfall catchment areas. This results in the periodic need to reduce accumulated volumes of storm water at the Residue Disposal Area (RDA). Described in this paper will be options for treating a combination of waste waters from the RDA. The current water treatment method utilizes ferric sulfate for total organic carbon (TOC) and metallic ion adsorption. The precipitated solids are separated and the treated water neutralized prior to discharge. Experimental work will also be presented for the treatment of Bayer process water alone.

Aluminum Reduction Technology: Cell Development and Operations - Part I

Sponsored by: The Minerals, Metals and Materials Society, TMS Light Metals Division, TMS: Aluminum Committee

Program Organizers: Stephen Joseph Lindsay, Alcoa Inc; Tor Bjarne Pedersen, Elkem Aluminium ANS; Travis J. Galloway, Century Aluminum Company

Monday PM

Room: 7A

March 13, 2006

Location: Henry B. Gonzalez Convention Ctr.

Session Chair: Mark Taylor, University of Auckland

2:00 PM

Alouette Line 2: Starting-Up the Right Way: *Pierre Reny*¹; Joe H. Lombard¹; ¹Aluminerie Alouette Inc

Alouette Aluminum Smelter, located in Sept-Iles, Quebec, Canada successfully started its 330 AP30 pots expansion during the first months of 2005. Evidently, a plethora of challenges faced both the construction and operation teams at all steps of the project. This article focuses on one of the broader challenges that was at the root of many others, namely to maintain and improve the performance of the existing part of the smelter while so much attention is devoted to the project start-up of the new line. This article will describe how innovative project organization, along with well planned operational changes implementation allowed to smoothly start the anode plant, reduction and casthouse expansions while improving productivity of the older part of the smelter. Other critical aspects such as emissions control, safety and work quality during start-up as well as interaction with the project are discussed.

2:25 PM

35 Years of Improvement at Anglesey Aluminium: *Daniel Woodfield*¹; Dewi Roberts¹; Mike Wilson¹; Gerry Forde¹; ¹Anglesey Aluminium Metal

As part of our 35th anniversary year, this paper reviews 35 years of technical improvement at Anglesey Aluminium, focusing on improvements in hot metal production. From a low of 76 000 t in 1973, hot metal production has almost doubled to today's levels of 147, 000 tpa. Amperage has increased from 134 kA to 172 kA and CE% from the mid 80's to 95%. Key aspects of achieving these outcomes in a cost effective manner are discussed, in particular changes to the anode and anode assembly and improvements in feed control.

2:50 PM

Reduction of Amperage at New Zealand Aluminium Smelters: *Daniel Whitfield*¹; Gabe Oldenhof¹; ¹New Zealand Aluminium Smelters Ltd.

During 2004, the amperage of Line 3 at New Zealand Aluminium Smelters Ltd. had to be reduced to allow the line to run on only three out of four rectifiers, to allow maintenance to be performed on each of the four rectifiers. This paper details the reduction of amperage of Line 3 to 175kA (from 184.3kA) and the subsequent ramp up to 185 kA, and reports on various observations during this period. Despite the many changes during this possibly tumultuous period of operation, the line managed to make record current efficiency, power efficiency, and purity. Process knowledge gained from the amperage reduction period was used to develop the application for capital expenditure for a booster rectifier connection, and avoid the need to repeat the exercise in the future.

3:15 PM

180 kA Booster Cells Operation at ALBRAS: *Jose Eduardo M. Blasques*¹; Guilherme Epifano da Mota¹; Handerson Penna Dias¹; Giancarlo De Gregoriis¹; ¹Aluminio Brasileiro ALBRAS S.A.

In recent years, Albras has been increasing line current. The necessary adjustments to the work practices and process variables need to be made on all potlines, which in this case means on 960 cells at the same time. It was a challenging task to adjust the operation to the new amperage. In July 2003 potlines II, III and IV were running at 173 kA and the goal at that time was to reach 180 kA. Preliminary trials were performed on a group of 10 boosted cells in order to investigate possible operational problems. It was decided to increase the amperage in three steps accompanied by continual evaluation of the state of the process. In July 2004 the target of 180 kA was achieved with good operational results. This paper presents the overall results, the parameter adjustments made during the amperage increase and how it was implemented on the other potlines.

3:40 PM

The Next Step to the AP3X-HALE Technology: Higher Amperage, Lower Energy and Economical Performances: *Oliver Martin*¹; Claude Richard¹; ¹Alcan

The Aluminium Pechiney AP35 technology is presently the spearhead of the ALCAN technological offer. To maintain its technological leadership, Alcan has continued to optimise the AP35 and will soon propose to its clients an AP36 at 360kA. At the same time, an intensive technology development program aiming at continuing the amperage increase potential while improving the energy performance is started and should give rise to an AP37 in the next months. This article describes the operational tests allowing to bring the AP35 at a 360 kA level as well as the results to date of the R&D AP37 program (370 kA). The positioning of this technology is compared to, in technical and economical terms, the AP35 cell and shows advantageous benefits resulting in the investment and operation cost reduction program for future projects using ALCAN AP3X-HALE technologies.

4:05 PM

Development of the B32 Cell Technology: *David Billinghurst*¹; Bill Paul¹; Geoff Bearne¹; Ian Coad²; ¹Comalco Research & Technical Support; ²Boyer Smelters Ltd

In 2002 five prototype B32 cells were started at the Boyne Island Smelter (BSL) in Queensland, Australia. The purpose of this trial was to provide a magnetically compensated technology for use in an expansion of BSL Line 1 and 2. This required the development of a highly asymmetric busbar design capable of operating at a bay to bay spacing of 24 m. The cells were designed to operate at 265 kA, but were commissioned at 270 kA and are now running at 280 kA. The technology has achieved design targets and exceeded expectations. It is now considered suitable for expansion opportunities should they exist.

4:30 PM

Analysis of Prebake Anode Assembly of Hall-Heroult Cells to Enhance Life of Conductor Bar: Bir Kapoor¹; S. C. Tandon²; R. N. Prasad²; K. Kamaraj³; ¹Aditya Birla Management Corporation Ltd; ²Hindalco Industries Ltd.; ³Indian Institute of Technology

Significant efforts have been made over the years at Hindalco Smelter Renukoot to improve the efficiency of smelter operation by pushing the

design limit of various components. Enhancing the life of copper bar conductor, which holds the anode assembly, is one such example. These bars are exposed to static load of the anode assembly and severe thermal conditions and due to bath proximity. Failure of these bars was seen due to cracks after few cycles, thus preventing repeated use of these bars. The causes of failure have been analyzed by conducting a combination of thermo-mechanical modeling and micro-structural analysis. A simple finite element model with experimentally measured temperatures as boundary conditions has been used for thermal stress analysis. The creep deformation has been identified as the primary mechanism. The point of onset of creep can be attributed to micro-structural deficiencies and high temperature exposure of the bar.

4:55 PM

Upgrading Outdated Rectifier Control Systems with an AC 800PEC Digital Controller: *Ann K Roberts*¹; Joseph Frisch¹; ¹ABB

Every industrial rectifier system must meet at least four basic requirements. The system must provide continuous, reliable, adequate and safe DC power. The costs of the aging installed base of high-power rectifier systems are mounting with process industries paying dearly with unreliable equipment and extended downtimes for maintenance. These financial losses are dramatic because rectifiers provide the DC current supply to a host of critical process applications. Over years electrical performance of a plant deteriorates. Implementation of conventional maintenance procedures is not practical to improve the availability, safety, productivity and efficiency. Failures in old control components generally cause longer down times since these parts are not available, obsolete or need to be repaired. The following paper presents results of recent upgrades of rectifier control systems by replacing the original installed control systems with a digital controller; leading to increased plant availability, resulting in a significant increase of production.

5:20 PM

Analysis of the Start-Up of Q-350 Prebaked Aluminum Reduction Cell: *Zeng Shuiping*¹; Li Jinhong¹; Lan Tao²; Ding Lei¹; ¹North China University of Technology; ²Qingtongxia Aluminum Plant

Q-350 prebaked alumina reduction cell line is the largest one in china. Some of the cells were started April 2004 at Qingtongxia aluminum plant in west China without industrial experiment beforehand. For the lack of experience, the start-up process has met some problems. This paper introduced the method for preheating and start-up of the cells, showed some typical data which include the computer sampling data and manual measuring one using the Dassie system, which is a comprehensive system integrated many kinds of function, and was designed specially for the aluminum production management. It was found that the metal instability and the volt rising schedule were the main problems, and it was difficult to set the cell voltage to the required value and keep the cell stable at same time. With consideration of the cell design, the paper indicated the defaults of start-up process and some improvements for cell operation.

5:40 PM End

Amiya Mukherjee Symposium on Processing and Mechanical Response of Engineering Materials: NanoProcessing for NanoGrain Materials

Sponsored by: The Minerals, Metals and Materials Society, TMS Materials Processing and Manufacturing Division, TMS Structural Materials Division, TMS/ASM: Mechanical Behavior of Materials Committee, TMS: Shaping and Forming Committee
Program Organizers: Judy Schneider, Mississippi State University; Rajiv S. Mishra, University of Missouri; Yuntian T. Zhu, Los Alamos National Laboratory; Khaled B. Morsi, San Diego State University; Viola L. Acoff, University of Alabama; Eric M. Taleff, University of Texas; Thomas R. Bieler, Michigan State University

Monday PM
March 13, 2006

Room: 217C
Location: Henry B. Gonzalez Convention Ctr.

Session Chairs: Eric M. Taleff, University of Texas; Nathan A. Mara, University of California

2:00 PM Invited

Encounter between an Ancient Steel and Modern Science: *Srinivasa Ranganathan*¹; ¹Indian Institute of Science

Wootz steel as an advanced material dominated several landscapes: the geographic landscape spanning the continents of Asia, Europe and the Americas; the historic landscape stretching over two millennia as maps of nations were redrawn and kingdoms rose and fell; the literary landscape as celebrated in myths and legends, poetry and drama, movies and plays; the linguistic landscape of Sanskrit, Arabic, Urdu, Japanese, Tamil, Telugu and Kannada; the religious landscape of Hinduism, Buddhism, Zoroastrianism, Judaism, Islam and Christianity. The study of this ancient steel inspired European metallurgists to unravel the link among processing, structure, properties and performance. It is amazing that very similar properties can be achieved by an alternate route involving laminates in the Japanese swords. Several metallurgical themes - microalloying, spheroidization, dendrites, microsegregation, superplasticity, composites and nanowires - will be explored to establish wootz steel as an exemplar of the Materials Hypertetrahedron.

2:20 PM Invited

Engineering Structure on a Nanoscale Level to Achieve Targeted Properties in Steels: *Daniel Branagan*¹; ¹NanoSteel Company

Essential aspects of solidification will be presented showing how solid state transformations can be used to refine the microstructural scale in 'steels' to achieve phase sizes in the nanoscale regime. By changing the kinetics of solidification, high undercoolings can be achieved allowing either, complete avoidance of nucleation resulting in a metallic glass which can be subsequently devitrified, or the achievement of an extremely rapid nucleation rates in order to form nanocrystalline scale phases directly during solidification. The achievement of nanoscale microstructures should not be considered the end goal but instead represents an enabling ability to develop vastly improved properties which are not possible on conventional length scales. Three case examples will be presented detailing the challenges and successful approaches that have been used to engineer the nanostructure of steels to achieve high energy density/high intrinsic coercivity, high strength/hardness, and high tensile elongation/low temperature superplasticity.

2:40 PM

Manufacturing of Miniaturized MEMS Parts by ECAP: *Georg Raab*¹; Nikolay Krasilnikov²; Ruslan Valiev¹; Juri Estrin³; ¹Ufa State University of Aviation Technology; ²Ulyanovsk State University; ³Clausthal University of Technology

Miniaturized MEMS parts, with dimensions below 2 mm, are exposed to rather tough service conditions. With their superior properties, materials with ultrafine structure offer themselves for manufacturing such parts. A range of MEMS parts, including cogwheels, axles and casings, are axially symmetrical, and it is possible to produce them by equal channel angular pressing (ECAP), thus combining the forming operation with the development of a desired microstructure. In such a process, the small di-

mensions of the products put serious limitations on the dimension tolerances, tribological conditions, strength of the tooling, etc. Here we report the results of a first feasibility study on manufacturing an axially symmetric part, viz. a cog wheel 2 mm in diameter, from Cu and Ni. Experiments combined with 3D simulations of the ECAP process will be presented along with data on the character of plastic flow, strength and microstructure of the parts manufactured.

3:00 PM

Microstructural Evolution during ECAE Processing of Ti-6Al-4V: Byungin Jung¹; Shankar M. Sastry¹; Rabindra N. Mahapatra²; ¹Washington University; ²U.S. Navy

Microstructural evolution during ECAE processing at 600°C and subsequent annealing at 700-1000°C was studied in Ti-6Al-4V with Widmanstätten $\alpha+\beta$ and equiaxed $\alpha+\beta$ microstructures. In specimens containing Widmanstätten $\alpha+\beta$ microstructure, ECAE processing resulted in break up of beta phase and formation of 200-300 nm sized sub grains in α phase. Upon annealing, spheroidization of fragmented β occurred along with recrystallization in α phase resulting in a fine-grained equiaxed $\alpha+\beta$ microstructure with 2-3 micrometer grains developed. The resulting grain size is determined by the size and spacing of the spheroidized β phase. Specimens with the initial equiaxed $\alpha+\beta$ developed a coarser (> 6 micrometer sized) equiaxed $\alpha+\beta$ microstructure.

3:20 PM Invited

Comparison of Rapid Solidification Results in Improved RE₂(Fe, Co)14B Magnet Alloys Due to Heat Flow and Nucleation Effects (RE=Nd+Y+Dy): Iver E. Anderson¹; Nicholas L. Buelow¹; Wei Tang¹; Yaqiao Wu¹; Peter K. Sokolowski¹; Kevin Dennis¹; Matthew J. Kramer¹; Bill McCallum¹; ¹Iowa State University

New YDy-based RE₂(Fe, Co)14B ribbons and spherical powders for high temperature bonded magnets have been developed by melt spinning (MS) and gas atomization (GA), respectively. Useful magnetic properties from ambient to above 200C were achieved by optimizing compositions and microstructure. Above 125C, (BH)_{max} of optimized alloy ribbon is superior to commercial ribbon. MS wheel speeds of 10-16 m/s produced comparable solidification structures to fine GA (He gas) powders, allowing extensive alloy design with MS. Effects of TiC and Zr additions on promoting glass formation and nucleation of 2-14-1 phase in ribbon and powder microstructures were studied systematically by SEM, TEM, XRD, and DTA. Translation of MS microstructures to GA powders seems to require both additions. Oxidation resistance during fine powder processing and retention of high temperature magnetic properties in polymer-bonded magnets were improved by development of a fluoride surface (15-40nm) layer treatment. Support from DOE-EERE-FCVT through Ames Laboratory contract W-7405-ENG-82.

3:40 PM

Comparison between Shot Peening and Surface Nanocrystallization and Hardening (SNH) Processes: Leon L. Shaw¹; Kun Dai¹; ¹University of Connecticut

The surface nanocrystallization and hardening (SNH) is a relatively new process that has been developed to enhance fatigue and wear resistances. The SNH is similar to widely-used shot peening in the sense that both processes entail repeated impacts of the surface of a workpiece with spheres. The difference between them lies in the sizes of spheres and the impact velocities used. Such a difference results in dramatic changes in kinetic energies and thus thicknesses of the deformation layer and the nanograin surface layer. In this study, finite element modeling is performed to provide quantitative description of these differences. The results show that the kinetic energy in the SNH process is typically 180 times larger than that in shot peening, and the deformation layer in the SNH process is about 10 times thicker than that generated in shot peening. The implication of these differences on fatigue resistance has been examined.

4:00 PM Break**4:10 PM Invited**

Self-Assembly Approach towards Nano-Ordered Structures in High Temperature Ceramics: Julin Wan¹; Patrick Malenfant¹; Seth T. Taylor¹; Sergio M. Loureiro¹; Mohan Manoharan¹; ¹General Electric Global Research Center

In an effort to simulate nanoscale structure with long-range order in natural ceramic structures such as nacre, a new approach called templated synthesis of polymer-derived ceramics was explored to build nano-order in a Si-C-N system. Polymeric precursors that lead to the desired ceramic composition were self-assembled using block copolymers as structure-directing agents. In this presentation, we describe the basic block copolymer physics that governs the formation of self-assembly, and the interactions that enables using this assembly as a template to build nanoscale order in ceramic precursors. Microstructures ranging from classic lamellar to cylindrical to more complicated morphologies are described, and their evolution is shown to vary sensitively with precursor chemistry, loading and heat-treatment history. It will be shown that the ordered nanoscale structure created in the block copolymer/precursor hybrids can be preserved through the pyrolysis process, thereby leading to ordered nanostructures in the final ceramic.

4:30 PM Invited

SPS: A High Strain Rate Low Temperature Forming Tool for Ceramics: Dongtao Jiang¹; Dustin M. Hulbert¹; Joshua D. Kuntz²; Amiya K. Mukherjee¹; ¹University of California; ²Lawrence Livermore National Laboratory

Spark plasma sintering technique is being widely used to produce nanocrystalline materials in virtue of rapid sintering at relatively lower temperatures. In this investigation, it is demonstrated that the technique can also be used to achieve high strain rate superplasticity at low temperature that is impossible by using conventional methods. Fully dense Al₂O₃-ZrO₂-MgAl₂O₄ was superplastically formed into a complex shape in SPS furnace with a strain rate of 10⁻² at a temperature as low as 1150°C. Furthermore, a powder compact can be directly shaped into complex shape by SPS technique, combining sintering and forming into one step. The product is fully dense and free of surface crack. It is argued that the SPS one-step forming is closely related to the superplastic behaviour that might be attributed to the enhanced diffusion under external electric field. Those results indicate that SPS can be a very competitive forming tool for ceramics.

4:50 PM

Development of a Nano-Scale Bioceramic: Tien B. Tran¹; Vladimir Y. Kodash¹; James F. Shackelford¹; Joanna R. Groza¹; ¹University of California

The use of hydroxyapatite (HA), a recognized biocompatible ceramic, is limited to non-load-bearing orthopaedic applications due to its poor fracture toughness. Nanocrystalline HA powders were consolidated via the Field Activated Sintering Technique (FAST) in order to restrain grain growth to the nanoscale regime, thereby enhancing mechanical properties and *in vivo* performance. The method applied pulsed electrical current to powders under a light pressure and produced encouraging results. A density of 97% theoretical was achieved at a relatively low temperature (850°C) in 1 minute under a pressure of 45 MPa. Scanning electron microscopy revealed a final microstructure consisting of nanosized grains. Mechanical properties and *in vitro* characterization of the resulting material will be reported in regards to its potential for load-bearing orthopaedic applications, such as a delivery system for bone morphogenetic proteins (BMP).

5:10 PM Invited

Processing/Microstructure/Property Relationships in Severely Deformed Tantalum: Suveen N. Mathaudhu¹; K. Ted Hartwig¹; ¹Texas A&M University

Bars of as-cast, large grained and highly textured Ta were deformed by multipass equal channel angular extrusion (ECAE) at room temperature to strains of 4.6 through 90° die-angle tooling. Comparisons of the microstructure and mechanical properties after four consecutive extrusions via route C (180° rotation between passes) Bc (90° rotation between passes) and E (2C, 90° rotation then 2C) are made in both the as-worked (submicron-scale grains) and recrystallized (micron-scale grains) conditions. Yield strength decreases from ~950 MPa in the as-worked ($\epsilon = 4.6$) state to ~200 MPa in the recrystallized state, while the ductility (%EL) increases from ~10% to ~50%. Results show that the mechanical behavior of as-worked and recrystallized tantalum follows a typical Hall-Petch relationship. Empirical equations correlating the grain size, microhardness, yield

strength and tensile strength in heavily worked and recrystallized Ta are presented.

5:30 PM Invited

Interface Stability in Copper-Niobium Nanolayered Composites: *Amit Misra*¹; Richard G. Hoagland¹; ¹Los Alamos National Laboratory

Sputter deposited metallic nanolaminates exhibit ultra high hardness when the bilayer periods approach nanometer dimensions. In this presentation, we report on the morphological stability of interfaces in Cu-Nb nanolayered composites. The origins of the unusual thermal stability of the layered structure, at annealing conditions where layer pinch-off and spheroidization is expected but did not occur, is discussed. This research is aimed at exploring the elevated temperature properties of nanolayered composites and has involved collaborations with Prof. Mukherjee's group. In another set of experiments, Cu-Nb multilayers were implanted with Helium ions at room temperature prior to annealing. With decreasing layer thickness in the nanometer range, a suppression of bubble growth and subsequent blistering during annealing of radiated samples was observed. The relation of the interfaces to the evolution of radiation damage will be discussed. This research is funded by DOE, Office of Science, Office of Basic Energy Sciences and LANL LDRD.

5:50 PM

Ultrafine Grain-Sized Zirconium by Dynamic Deformation: *Bimal K. Kad*¹; Marc A. Meyers¹; Joerg-Martin Gebert²; Maria Teresa Perez-Prado³; Michael E. Kassner⁴; ¹University of California, San Diego; ²University of Karlsruhe; ³Centro Nacional de Investigaciones Metalúrgicas; ⁴University of Southern California

Zirconium (gs: 14 μm) was subjected to high plastic shear strain (25-100) at 104 s⁻¹ in hat-shaped specimen/Hopkinson bar. Region of intense plastic deformation (10-25 μm thick) is produced which is analyzed by EBSD and TEM. Microstructure within shear band is characterized by equiaxed grains with size of 200 nm. Temperature, calculated with Zerilli-Armstrong equation, is 930 K for shear strain of 100. EBSD reveals a strong fiber texture. Ultrafine grain structure observed is similar to one obtained in SPD processes (ECAE/ECAP), suggesting that mechanism of grain refinement is same in spite of differences in strain rate and thermal excursion. Mechanism is proposed for breakup of existing equiaxed microstructure into ultra-fine structure: 1. formation of elongated cells and sub-grains; 2. increased misorientation between neighboring grains and breakup of elongated grains into smaller units; 3. rotation of boundaries by grain-boundary rotation and formation of equiaxed structure. Support: NSF DMR 0419222, CMS-0210173.

Biological Materials Science: Computational Biomaterials/The Biomaterials-Tissue Interface

Sponsored by: The Minerals, Metals and Materials Society, ASM International, TMS Structural Materials Division, TMS: Biomaterials Committee, TMS/ASM: Mechanical Behavior of Materials Committee
Program Organizers: Andrea M. Hodge, Lawrence Livermore National Laboratory; Chwee Teck Lim, National University of Singapore; Richard Alan LeSar, Los Alamos National Laboratory; Marc Andre Meyers, University of California, San Diego

Monday PM Room: 212A
March 13, 2006 Location: Henry B. Gonzalez Convention Ctr.

Session Chairs: Richard Alan LeSar, Los Alamos National Laboratory; Sungho Jin, University of California

2:00 PM Invited

Coarse-Grained Model of Biomolecular Structure and Dynamics: *Richard Alan LeSar*¹; Antonio Redondo¹; ¹Los Alamos National Laboratory

Direct modeling and simulation of large-scale biomolecular structures is a computational grand challenge owing to the extremely large numbers of atoms and the short time scales inherent in an atomistic description. We will describe a recently-developed coarse-grained simulation method designed to model the structure and dynamics of proteins and other large biomolecular structures. While being coarse-grained in nature, the method

preserves the essential properties of the individual molecules and their interactions with each other and with solvent molecules. It is a computationally-flexible method that enables us to include complex effects in a simplified, but accurate way. We will show applications of the method to both simple protein structures as well as larger-scale biomolecular structures, e.g., microtubules.

2:30 PM Invited

Molecular-Level Modeling for Erythrocyte Deformation: Ming Dao¹; Ju Li²; *Subra Suresh*¹; ¹Massachusetts Institute of Technology; ²Ohio State University

The mechanical properties of erythrocytes (red blood cells) influence strongly their biological functions and the onset, progression and consequences of a number of human diseases. The hyperelasticity characteristics of erythrocyte subjected to finite-deformation stretching by laser tweezers is studied at the spectrin level by molecular dynamics and conjugate gradient energy minimization methods as well as at the continuum level by finite-element modeling. We have further developed an on-the-fly homogenization scheme for studying the mechanics of living cells that comprise 2D/3D molecular networks as structural bases—Molecular Potential Finite-Element Method (MPFEM). For the spectrin network that provides membrane shear elasticity, we use the worm-like chain (WLC) potential for single spectrin molecular response. MPFEM provides a bridge between whole-cell mechanics and single-molecule response as well as spectrin network structure. Connections among molecular structure, cell mechanical deformation and disease states related to *Plasmodium falciparum* malaria, heredity spherocytosis and Southeast Asian ovalocytosis are discussed.

3:00 PM

Modeling the Influence of Microstructure on Implantable Drug Delivery Devices: *James Aaron Warren*¹; David M. Saylor²; ¹National Institute of Standards and Technology; ²Food and Drug Administration

Experimental work has demonstrated that the microstructure of the polymer-drug mixture that coats a drug-eluting stent and other implantable devices can be extremely complex. From a materials science perspective, it is clear that this structure will influence the dissolution process, yet existing models are unable to quantify the influence of this microstructure, or model the structures formation and its ensuing effects on dissolution. The address these issues we have developed a phase field model of the drug-polymer blend to allow realistic simulations of the fabrication of drug coated implantable devices. In addition to enabling the simulation of the microstructure formed during processing, the model properly accounts for the changing morphology and position of the drug-eluting boundary as the drug dissolves, as well as spinodal decomposition, dewetting, polycrystalline solidification and a host of other phenomena.

3:20 PM

Modeling Cell-Structure Evolution in Biological Multicellular Systems: Jose Munoz¹; Kathy Barrett²; Buzz Baum³; *Mark Miodownik*¹; ¹King's College London; ²University College London; ³Ludwig Institute for Cancer Research

In this work we use the finite element method to study the micromechanics and cell-structure evolution that occurs in biological multicellular systems. The phenomenon is analogous to microstructure evolution in metals, but with the fundamental difference that cells respond both passively and actively to forces. It is the active part that distinguishes the system as biological. These active forces have a big impact on the final structures and are most critical during organism growth when small changes can have a large phenotypic impact, e.g. spina bifida in Humans. We use FEM techniques to model cell mechanics in the presence of both active and passive forces during the early stages of embryo growth of flies (*Drosophila*). A novel master-slave approach is included to model the sliding process of the epithelium along the extracellular matrix. We show in the numerical results that the model can closely reproduce the invagination process and its mechanisms.

3:40 PM

Mechanisms of Cell Spreading on Porous Titanium Surfaces: *Winston O. Soboyejo*¹; ¹Princeton University

This paper presents the mechanisms of cell spreading on porous Ti and Co-Cr surfaces with well controlled pore architectures and RGD surface

chemistries designed to promote increased adhesion. A combination of confocal and scanning electron microscopy is used to study how cells roll, adhere and spread on micron-scale and nano-scale surfaces. The mechanisms by which cells spread across porous gaps are also revealed. In selected cases, the cells spread over nano-particles and over each other until they bridge the gaps between the pores. The subsequent spreading and proliferation of cells then results in a configuration of cells/tissue that appears to be clamped to the porous structure. However, this is the integrated result of several processes that are elucidated by a combination of in-situ microscopy immuno-flourescence techniques, and x-ray computer tomography. The implications of the results are discussed for the design of porous architectures for osseo-integration.

4:00 PM Break

4:20 PM Invited

Enhanced Adhesion and Growth of Cells on Nanostructure Array: Brian Oh¹; *Sungho Jin*¹; ¹University of California

Nanostructures provide a very large surface area and topographical features suitable for cell adhesion and growth. Vertically aligned yet laterally spaced nanoscale TiO₂ nanotubes have been grown on Ti by anodization, and the growth of MC3T3-E1 osteoblast cells and other types of cells on such nanotube array surface has been investigated. The adhesion/propagation of the cells is substantially improved by the topography of the TiO₂ nanotubes with the filopodia of growing cells going into the nanotube pores, producing a locked-in cell structure. The presence of the nanotube structure induced a significant acceleration in the growth rate of osteoblast cells by as much as ~400%. The effect of various biological and materials parameters on cell growth will be described, and the design of desirable nanostructure for maximum cell growth kinetics and cell viability will be discussed.

4:50 PM

Hydroxyapatite Sol-Gel Coating on Titanium Alloys for Biomedical Applications: *Cui'e Wen*¹; Wei Xu²; Wangyu Hu²; Meiheng Li²; ¹Deakin University; ²Hunan University

Hydroxyapatite (HA) coating has many biological benefits such as direct bonding to bone and enhancement of new bone formation around it due to its chemical similarity with hard tissues. In the present study, a simple sol-gel method was developed for hydroxyapatite film deposition on titanium alloys for biomedical applications. Phase formation, surface morphology, and interfacial microstructure were investigated using DSC, XRD and SEM techniques. The hydroxyapatite film was spin-coated on the titanium alloy surface and then heat treated at difference temperatures. Results indicated that the HA phase begins to crystallize after a heat treatment at a relatively low temperature of 600°C; and the crystallinity increases with the increasing of the temperature. The HA film showed a porous structure and a thickness approximating 7 μm after certain heat treatment.

5:10 PM

Laser Textured Biomedical Surfaces for Cell/Surface Integration: *Winston Oluwole Soboyejo*¹; ¹Princeton University

This paper presents the results of experimental studies of cell spreading and adhesion to laser textured Ti-6Al-4V surfaces. The surface textures associated with laser/materials interactions are elucidated via interferometry and scanning electron microscopy. Local changes in surface chemistry are then examined using energy dispersive x-ray spectroscopy before discussing the effects of microgroove geometry and chemistry on cell spreading on Ti-6Al-4V surfaces with/without RGD coatings. The adhesion between the cells and the textured/coated surface is quantified using shear assay and micro-pipette aspiration. The implications of the results are then discussed for the design of orthopedic/dental implants with improved adhesion to bone.

5:30 PM

Nanostructure, Dissolution and Morphology Characteristics of Novel Microcidal Silver Films Deposited by Magnetron Sputtering: *Sudhindra B. Sant*¹; Kashmir S. Gill²; Robert E. Burrell³; ¹Twin Technologies Inc; ²National Research Council of Canada; ³University of Alberta

Novel microcidal silver films for burn dressings have been produced by magnetron sputtering. The nanostructure and dissolution characteris-

tics of these films exhibiting antimicrobial behaviour were studied as a function of the process conditions, namely, gas composition, gas pressure and input power, using transmission electron microscopy (TEM), high-resolution scanning electron microscopy, X-ray photoelectron spectroscopy (XPS) and resistivity. TEM revealed that bioactive films were nanocrystalline with a grain size of the order of 15 nm and the presence of twins. Surface morphology studies before and after dissolution suggested that bioactive films released silver at therapeutic levels in the form of nano-particles or grains. Chemical species identification with XPS showed that the biologically active films were metallic in nature. The importance of oxygen in the sputtering environment, the resultant nanostructure and presence of twins are discussed to explain the unique antimicrobial properties of these silver films.

Bulk Metallic Glasses: Mechanical Behaviors

Sponsored by: The Minerals, Metals and Materials Society, TMS Structural Materials Division, TMS/ASM: Mechanical Behavior of Materials Committee

Program Organizers: Peter K. Liaw, University of Tennessee; Raymond A. Buchanan, University of Tennessee

Monday PM
March 13, 2006

Room: 217B
Location: Henry B. Gonzalez Convention Ctr.

Session Chairs: Raymond A. Buchanan, University of Tennessee; Akiko Inoue, Tohoku University

2:00 PM Keynote

Improved Mechanical Properties of Bulk Glassy Alloys Containing Spherical Pores: *Akihisa Inoue*¹; T. Wada¹; ¹Tohoku University

For future extension of application fields for bulk glassy alloys, it is important to develop a new type of glassy alloy which exhibits simultaneously high strength, low Young's modulus, large elastic elongation, high ductility, high corrosion resistance, low specific weight, high specific surface area and three dimensional bulk form etc. Considering that bulk glassy alloys in non-ferrous metal base systems possess unique characteristics of high strength, low Young's modulus, large elastic elongation, high fracture toughness and high corrosion resistance, the bulk glassy alloys are expected to become an important candidate material after the above-described modifications for alloy component and material surface morphology. One of the ways to develop a new material with the above-described properties is to fabricate ductile bulk glassy alloys containing open or closed pores in a wide range of volume fraction. Little is known about mechanical properties of porous bulk glassy alloys.

2:30 PM Invited

Flow and Fracture Studies on Bulk Metallic Glasses and Composites:

*John J. Lewandowski*¹; ¹Case Western Reserve University

The effects of systematic changes in stress state on the flow and fracture behaviour of a number of different BMGs and composites are being determined. In addition to conducting tension and compression tests with constant levels of confining pressure at different test temperatures, notched specimens are additionally being conducted under similar conditions in order to cover a broader range of stress states. Following a summary of these tests, the effects of changes in alloy chemistry and annealing on the fracture behaviour of a wide range of BMGs will be presented. Correlations of the fracture behaviour with changes in elastic constants will be demonstrated.

2:55 PM Invited

Experimental and Computational Investigation of Structure and Plastic Flow in Bulk Metallic Glasses: Matthew J. Lambert¹; Wolfgang Windl¹; *Katharine M. Flores*¹; ¹Ohio State University

Improving the structural reliability of bulk metallic glass components requires a detailed understanding of the relationship between glass structure and plastic flow behavior. We examine the flow-induced structural changes in a Zr-based bulk metallic glass using a variety of experimental techniques, including positron annihilation spectroscopy. These results indicate a shift in the size distribution of flow defects after inhomoge-

neous flow consistent with the coalescence of free volume into nanovoids. The atomistic structure of several multicomponent glasses was further investigated through molecular dynamics simulations using EAM potentials. We employ a novel annealing technique that allows us to simulate extremely slow quench rates to produce glassy structures. Radial distribution functions of the modeled systems exhibit excellent agreement with experimental data. Comparing the detailed features of the nearest-neighbor order with experimental critical cooling rate data, we establish a set of criteria to predict the effect of changes in composition on glass forming ability.

3:20 PM Invited

Mechanical Properties and Devitrification Behavior of Cu-Zr-Ti-NM (NM-Noble Metals) Bulk Glass-Forming Alloys: *Dmitri Louzguine¹; Akihisa Inoue¹; ¹Tohoku University*

A nanoscale icosahedral phase was recently obtained in a Cu₅₅Zr₃₀Ti₁₀Pd₅ bulk glass-forming alloy. The present work is devoted to an investigation of the formation kinetics, stability and homogeneity area of the nanoscale icosahedral phase formed on heating in the Cu-Zr-Ti-Pd system. Mechanical properties of the studied alloys will be reported. The Cu-Zr-Ti-Pd icosahedral phase is not a Cu-rich part of the compositional homogeneity area of the Zr-Cu-Pd one. Nanoscale icosahedral phase has chemical composition close to that of the alloy composition. The possibility for the Cu-Zr-Ti-Pd icosahedral phase of being a Cu-rich part of the compositional homogeneity area of the Zr-Cu-Pd one is ruled out. Moreover, Ti is found to be important element stabilizing quasicrystalline phase in the Cu-Zr-Ti-Pd alloys. Formation criteria for Cu- and Zr/Hf-based icosahedral phases are discussed based on quasilattice constant to average atomic diameter ratio. Deviation from this criterion leads to destabilization of the icosahedral phase.

3:45 PM Invited

Evolution of Mechanical Properties of Cast Zr-Cu-Al Glassy Alloys by Anneal Treatment: *Yokoyama Yoshihiko¹; Akihisa Inoue¹; Peter K. Liaw²; Raymond A. Buchanan²; ¹Institute of Materials Research; ²University of Tennessee*

The volume of quenched glassy alloy is a variable of cooling rates during amorphization. Hence a change in the volume caused by structural relaxation can be regarded as a degree of amorphousness. The density of ternary eutectic Zr₅₀Cu₄₀Al₁₀ bulk glassy alloys (BGAs) increases linear with annealing temperature below glass transition temperature (T_g). With annealing temperature, tensile strength and Vickers hardness show constant values, whereas the Young's moduli and Charpy impact values become larger and smaller, respectively. Charpy impact values of Zr-Cu-Al BGAs have a linear relationship with relative value of excess free volume. However, off eutectic BGAs in Zr-Cu-Al system exhibit different features changes with structural relaxation. Especially, Zr-enriched compositional BMGs show opposite features change against the eutectic BMG during structural relaxation. As a conclude, we can control the glass structure of cast Zr-Cu-Al BGA using a combination of compositional control and after anneal treatment below T_g.

4:10 PM Break

4:20 PM

Fatigue Behavior of Bulk Metallic Glasses: Role of Free Volume: *Jamie J. Kruczic¹; Maximilien E. Launey¹; Ralf Busch¹; ¹Oregon State University*

Structural differences, such as the amount of free volume, affect the properties of bulk metallic glasses. Thus, a thorough understanding of the relationships between the amorphous structure and the mechanical properties is needed for these materials to achieve widespread use as structural materials. The cyclic fatigue behavior of several zirconium based amorphous alloys were investigated where the composition was held constant while the amount of free volume was varied. Free volume differences were quantified based on enthalpy recovery experiments and were achieved by 1) using different initial processing conditions or 2) by annealing to allow structural relaxation without crystallization. Significant improvements in the measured fatigue lives were found with lower amounts of free volume, even when the materials were in the as cast state. Such differences are considered in terms of how free volume changes affect each of the individual stages of the fatigue life and the associated salient mechanisms.

4:40 PM

The Effect of Frequency on Fatigue Behavior of Bulk Metallic Glass and Composites: *Gongyao Wang¹; P. K. Liaw¹; A. Peker²; Y. Yokoyama³; M. Freels¹; W. H. Peter¹; R. A. Buchanan¹; C. R. Brooks¹; ¹University of Tennessee; ²LiquidMetal Technologies Inc.; ³Advanced Research Center of Metallic Glasses*

LM001 and LM002 are commercial Zr-based bulk-metallic glasses (BMGs). The X-ray diffraction results and optical morphology show that LM001 is a monolithic BMG and LM002 is a BMG composite containing crystalline phases. The high-cycle-fatigue (HCF) experiments were conducted at different frequencies, using an electrohydraulic machine with a R ratio of 0.1 and under tension-tension loading, where $R = \sigma_{\min}/\sigma_{\max}$. σ_{\min} and σ_{\max} are the applied minimum and maximum stresses, respectively. The fatigue-endurance limit (265 MPa) of LM002 was found to be significantly lower than that (630 MPa) of LM001 at a frequency of 10 Hz. Changing the test frequency has no obvious effect on the fatigue behavior of LM001, but it seems that the lifetime of LM002 at the high stress level is lower at a high frequency than that at a low frequency. A mechanistic understanding of the fatigue behavior of the Zr-based BMGs is suggested.

5:00 PM

Effect of Nano Crystallites on the Deformation and Mechanical Behavior of a Nano Crystallite/Amorphous Matrix Composite: An Atomistic Simulation Study: *Young-Min Kim¹; Byeong-Joo Lee¹; ¹Pohang University of Science and Technology*

It is known that mechanical properties of amorphous materials can be further improved by promoting homogeneous precipitation of nano crystallites within the amorphous matrix. Though lots of investigations have been done on the deformation and mechanical behaviors of the nano crystallite/amorphous matrix composite, details of the effect of nano crystallites on those properties are not known yet. In this study, we investigated the effects of embedded pure Cu crystallites on the deformation and mechanical behavior of a nano crystallite/Cu-Zr amorphous matrix composite, by using a molecular dynamics simulation study. We focused on the amount of contribution of the nano crystallites to flow stress and overall deformation during a compression and a tensile test. The role of interfaces between crystallites and matrix on the mechanical behavior and the validity of the rule of mixture which is frequently used to estimate overall physical properties of composite materials will also be discussed.

5:20 PM

High Temperature Deformation Behavior of In-Situ Bulk Metallic Glass Matrix Composites: *Xiaoling Fu¹; Yi Li¹; Christopher Schuh²; ¹National University of Singapore; ²Massachusetts Institute of Technology*

Macroscopic ductility is promoted in bulk metallic glasses by both composite reinforcements (at low temperatures) and by the activation of viscous flow mechanisms (at high temperatures). It is of fundamental interest to understand deformation physics when both of these strategies are employed at the same time. Despite the quickly growing literature around the room-temperature mechanical properties of metallic glass matrix composites (MGMCs), the deformation behavior of MGMCs over a wide range of temperatures and strain rates has yet to be systematically investigated, especially at high temperatures close to T_g. Here the high temperature compressive behavior of both Zr-based and La-based MGMCs with in-situ reinforcements is explored systematically over a series of strain rates. Additionally, the volume fraction of second-phase reinforcements was tailored to explore its effect on both inhomogeneous and homogeneous deformation modes.

5:40 PM

High Temperature Mechanical Behavior of Mg-Based Amorphous Alloys Produced by Low-Pressure Die-Casting: *Bulent Gun¹; Kevin Laws¹; Michael Ferry¹; ¹University of New South Wales*

Using a novel preparation technique, tensile samples of die-cast Mg-Cu-Y amorphous alloys were produced in compliance with ASTM E8-04 for determining elevated-temperature mechanical behaviour. The as-cast microstructures were examined initially by XRD and TEM which confirmed the amorphous nature of the alloys. Prior to mechanical testing, DSC and XRD were carried out to determine the various critical tempera-

tures (glass transition, crystallization and melting temperatures) of each alloy, and to generate reliable static crystallization maps. The flow behaviour of the alloys was investigated at various temperatures in the supercooled liquid region at strain rates ranging from 0.001 to 0.1/s. The mechanical data were used to compute the strain rate sensitivity and other flow characteristics of the alloys. For a given set of testing conditions, samples were deformed to a range of strains and examined using various techniques to highlight the substantial influence of deformation on crystallization behaviour.

Carbon Technology: Anode Raw Materials

Sponsored by: The Minerals, Metals and Materials Society, TMS Light Metals Division, TMS: Aluminum Committee

Program Organizers: Morten Sorlie, Elkem Aluminium ANS; Todd W. Dixon, Conoco Phillips Venco; Travis J. Galloway, Century Aluminum Company

Monday PM Room: 8A
March 13, 2006 Location: Henry B. Gonzalez Convention Ctr.

Session Chair: James B. Metson, University of Auckland

2:00 PM

Viscosity Modification and Control of Pitch: *Melvin D. Kiser*¹; M. B. Sumner¹; B. K. Wilt¹; D. Chris Boyer¹; ¹Marathon Petroleum Company, LLC

The addition of low concentrations of certain oxygenated compounds, particularly esters, to bitumen has been shown to have a profound effect on viscosity. The bitumen in question includes but is not limited to petroleum pitch, coal tar pitch and asphalt cements. A cost effective source of esters has been found to be biodiesel. This paper will provide general information on biodiesel and detail its effect on the viscosity of pitch as a function of concentration. Other topics of discussion are effects on other properties of the bitumen as well as a method of detection and control of ester concentration in the final product.

2:25 PM

Laboratory Anode Comparison of Chinese Modified Pitch and Vacuum Distilled Pitch: John Thomas Baron¹; *Robert H. Wombles*¹; ¹Koppers Industries Inc

The process currently used to produce the large percentage of 100°C to 110°C softening point anode binder pitch in China today is a heat treating process which produces a product called modified pitch. Modified pitch has all the characteristics of a pitch produced by heat treatment including 3% to 10% mesophase content. The presence of mesophase in binder pitch introduces problems with binder pitch and coke mixing and the resultant properties of the baked anode. This paper will present the results of a laboratory anode study comparing the properties of laboratory anodes produced with Chinese modified pitch and Chinese vacuum distilled pitch. The results indicate that the use of vacuum distilled pitch results in significant improvements in anode properties.

2:50 PM

Composition and Intermolecular Reactivity of Binder Pitches and the Influence on Structure of Carbonized Pitch Cokes: *Harald A. Oye*¹; Stian Madshus¹; Trygve Foosnaes¹; Margaret Hyland¹; Jostein Krane¹; ¹Norwegian University of Science and Technology

Hydrogen donor and acceptor abilities for a series of coal-tar and petroleum pitches have been determined as a measure of the intermolecular reactivity. The carbon disulphide soluble part has also been investigated by NMR in order to identify and quantify structures that are considered to either increase or decrease the reactivity. The properties differentiated the pitches studied and were found to correlate with the amount of volatiles released during the critical stages of carbonization. A link was found between the hydrogen transfer properties of the petroleum pitches and the size of optical texture of the resulting cokes. However, for pitches of coal-tar origin the presence and amount of particulate matter (QI) was found to be the most influential factor on the size of the optical texture.

3:15 PM

Vertical Stud Soderberg Emissions Using a Petroleum Pitch Blend:

*Euel R. Cutshall*¹; Linda Maillot¹; ¹Alcoa Inc

At the Alcoa La Coruna Plant in Spain organic emissions and worker exposure levels were determined and compared for individual cells using 100% coal tar pitch and a coal tar/petroleum pitch blend. Advantages and limitations of using the coal tar/petroleum pitch blend are discussed.

3:40 PM Break

3:55 PM

Characterization of Green Anode Materials by Image Analysis: *Stein Rørvik*¹; Arne Petter Ratvik¹; Trygve Foosnaes²; ¹Sintef Materials and Chemistry; ²Norwegian University of Science and Technology

A method to characterize green (unbaked) carbon composite materials has been developed. The method is based on computer-automated microscopy and digital image analysis. A reproducible procedure for sample preparation has been developed, as well as a method for distinguishing the pitch from the coke grains and the pores in the microscope images. The method has been used to examine the distribution of the pitch, pores and coke grains in carbon anode samples. The method has been applied to both laboratory made and industrial materials. Focus has been on anodes for aluminium production, but the method can also be used for cathodes and other composite carbon materials. This paper explains the principles of the method and presents results from analysis of anodes with variations in binder (pitch) content and coke grain size.

4:20 PM

Neural Network in Automatic Process Control System of Coke Calcination: *Vitaly Sinelnikov*¹; ¹RUSAL Engineering and Technological Center

Automatic process control system of coke calcination consists of two levels. Control, data transmission and digital control of the kiln temperature conditions are done with the help of regulators on lower level. Upper level of the kiln automatic process control system consists of two principal sublevels: visualization system of calcination; neural models of forecast and control (changes in regulator setpoints of kiln). Neural network of general regression was chosen as the calcination model. Genetic cone-type algorithm was used for adjustment of network weights. The task of change in regulator setpoints is narrowed down to the task of optimization theory. Necessity in the implementation of control neural network system consists in fact that regulators alone can not provide accuracy response to changing process parameters because their mathematical algorithm is destined for control by target (regulator setpoint) and not by operational change of target depending on the changing process parameters.

Cast House Operations: Session I

Sponsored by: The Minerals, Metals and Materials Society, TMS Light Metals Division

Program Organizers: Rene Kieft, Corus Group; Travis J. Galloway, Century Aluminum Company

Monday PM Room: 7D
March 13, 2006 Location: Henry B. Gonzalez Convention Ctr.

Session Chair: Helmut Suppan, AMAG Rolling GmbH

2:00 PM Introductory Comments

2:10 PM

A Study on the Failure Investigation of Graphite Column Used for Degassing in the Aluminum Caster Plant: *Y. V. Ramana*¹; Rajnish Kumar¹; ¹Hindalco Industries Ltd

A graphite agitator is used for purging chlorine to expel entrapped gases from molten aluminium metal in the Caster Plant process of Hindalco. Uncertainty in life span of the column of the agitator was adversely affecting the production planning activities and operational efficiency. To find out reasons for inconsistency in the life span, a systematic study was conducted on physical, chemical and microstructural parameters using failed samples of life span ranging from a few hours to several days. The predominant reasons observed for failure are porosity and internal voids/

cracks. It was observed that larger pores and increasing porosity is facilitating rapid oxidation of graphite at elevated temperatures hence the early failure. This phenomenon is prevalent particularly at the region of metal-air interface and above of the graphite column where frequent failure was experienced. The column submerged in molten metal is found to be less susceptible for such failures.

2:40 PM

Building the Billet Production Management Process at Alcoa Pocos De Caldas: *Andre Luis Trópia de Abreu*¹; Leonardo Paulino¹; ¹Alcoa Alumínio SA

An issue that comes challenging the actors involved on worldwide aluminum production is how to manufacture a billet that result in a good extrusion performance. The answer to it involves the establishment of measurable quality requirements. On this picture the traditional quality requirements utilized at Alcoa Poços – chemical composition and superficial finishing – can not measure enough the final performance of the process control activities. The change starts with the intensification of the discussion between Alcoa and its customers – Alcoa Extrusion Plants – in order to better understand its needs and creating empathy. The evolution of the discussion creates an appropriate condition to revise the billet quality requirements. On this way, metallographic measures are included to this set to sustain further aluminum billets process developments. The recognition and credibility of the new set of requirements gives objectivity on the supply-customer connection with a regular performance measurement basis.

3:10 PM

Quantifying Factors Affecting Aluminum In-Line Degassing Efficiency: *David W. Busch*¹; ¹Pyrotek Inc

Extensive plant data taken from two significantly different aluminum alloys produced in three different SNIF degassing units was analyzed to help quantify the effects of atmospheric humidity and other operating parameters on dissolved hydrogen removal. Absolute humidity increased by an average of 54% during the summer months in one location while aluminum post-treatment hydrogen level increased on average by 20%. Techniques are discussed which can be employed to increase hydrogen removal efficiency and mitigate the effects of high humidity. Data collected during formal degasser acceptance testing is also presented where sodium and inclusion removal and dross formation is evaluated.

3:40 PM Break

4:00 PM

A Case Study on Failure Analysis of AA 6063 Billets during Extrusion Process: *Y. V. Ramana*¹; Rajnish Kumar¹; Naresh Kumar Singh¹; ¹Hindalco Industries Ltd

Hindalco produces Wagstaff billets of aluminium alloys for downstream processing by different customers. A typical case of frequent failure of AA6063 billets at the customer's end during extrusion process was observed. Failure was due to sagging and breaking of billet after preheating and during extrusion process. To find out the reasons of failure, a systematic comparative study was conducted using as supplied and failed samples. PoDFA analysis and chemistry of the supplied material showed no significant reason for failure. On the other hand, macro and microstructural analysis of the samples revealed interesting observations like rosette formation, grain boundary melting, eutectic and script like structures in the preheated billet samples. These observations indicate that the failure is the result of overheating and liquidation of the metal during preheating process.

4:30 PM

Metal Quality of Secondary Alloys for Al Castings: *Eulogio Velasco*¹; ¹Nemak

High mechanical properties, fatigue, pressure tight and low porosity are requirements of aluminum cylinder heads and blocks related with the quality of liquid metal. With secondary alloys can be possible to reach these characteristics. Several control stages are necessary from raw material (Al scrap) to final stage: liquid metal in the holder furnace. In order to measure the quality of liquid metal, several samples with the PreFil@-Footprinter Unit were taken along the route of melting process. The tracking of the process include melting at reverberatory furnace, fluxing, liquid treatment and degassing. The results showed areas to improve with

operational practices and new degassing equipments and use of fluxes treatment.

Cast Shop Technology: Furnace Operation and Refractory Materials

Sponsored by: The Minerals, Metals and Materials Society, TMS Light Metals Division, TMS: Aluminum Committee

Program Organizers: Rene Kieft, Corus Group; Gerd Ulrich Gruen, Hydro Aluminium AS; Travis J. Galloway, Century Aluminum Company

Monday PM
March 13, 2006

Room: 7C
Location: Henry B. Gonzalez Convention Ctr.

Session Chair: Gerd Ulrich Gruen, Hydro Aluminium AS

2:00 PM

Calcium Aluminate Based Castables for Liquid Aluminium Contact Areas – A Laboratory Evaluation: *Marcel Hogenboom*¹; ¹Corus

Recently calcium hexaluminate (CA6) was introduced as a new synthetic dense refractory aggregate for refractories. Regarding the chemical composition and claimed low wetability by molten aluminium calcium hexaluminate is an interesting aggregate. Refractory materials based on this aggregate can be a solution for application areas suffering from aluminium penetration and corundum growth. Since the introduction of this aggregate several refractory suppliers introduced a castable based on calcium hexaluminate on the market. A selection of those commercially available castables is characterised and tested in the laboratory on relevant properties in respect to potential application areas. In this paper the results of the tests performed are presented and discussed.

2:25 PM

Computational Analysis of the Conversion of Generic Aluminum Holding Furnace from Air-Fired to Oxy-Fired Burners: *Brian Golchert*¹; Ashwini Kumar¹; Hossam Metwally¹; ¹Fluent, Inc.

Many of the gaseous emissions from aluminum furnaces are caused by the use of air as the oxidizer of the fuel. If air were to be replaced by nearly pure oxygen, the volume of greenhouse gas emissions would be drastically reduced. The purpose of this study was to use computational fluid dynamics to model the effect of changing a generic aluminum holding furnace from air-fired to oxy-fuel fired burners. Initially, two cases were created: a base case with air-fired burners and then a case with oxy-fuel burners located in the same position as the air-fired burners with the same natural gas flow rate. The oxy-fuel case produced flue temperatures that were different than the air-fired case so several additional computational cases were created to try and match the air-fired flue temperature. This paper will present the results of this study and will discuss the advantages/disadvantages of converting to oxy-fuel.

2:50 PM

Design Considerations for Charge Preheating Ovens: *Jan Migchielsen*¹; Jan De Groot¹; ¹Thermcon Ovens BV

Driven by valid safety concerns, more and more cast houses install preheating ovens for pre-heating and drying of sows, ingots and scrap before charging into a melting furnace. While preheating of the furnace charge enhances safety and improves fuel consumption at the same time, there are issues that must be addressed to avoid introducing new safety hazards. Special attention must be paid to issues like aluminium dust and combustible contaminants of materials that are charged into a preheating oven as these ovens start their cycle at a temperature well below the auto ignition temperature. Using a preheating oven without the proper technical considerations may therefore lead to exchanging one risk for the other. This paper addresses the design considerations that lead to safe and efficient installations for optimum pre-heating of scrap prior to melting.

3:15 PM Break

3:30 PM

Flame-Object Heat Transfer Using Different Burner Types and Orientations: Geza Walter¹; Laszlo Istvan Kiss¹; Andre Charette¹; Vincent Goutiere²; ¹Université du Québec à Chicoutimi; ²Alcan International

Gas fueled burners are frequently used as heat sources in metallurgy. The heat transfer between the flame and charge in a furnace depends on the type of the burner, its adjustment as well as on its position and orientation relative to the charge. An experimental study was performed in order to clarify the effects of burner and flame types and flame-object geometry on the heat transferred to the charge as well as on the mechanism of the heat transfer. The methodology and the results of flame object interaction in the case when firing is parallel to the horizontal surface of the charge were presented earlier. In the present paper the case of impingement by inclined burners and partial impingement on the corner of a solid charge will be shown. The study is completed with the analysis of the temperature and velocity fields in the gas phase around the objects.

3:55 PM

Melt Down Dross on Magnesium Containing Aluminum Alloys: John A. Clark¹; ¹U.S. Department of Energy

Dross is present on molten baths of aluminum alloy immediately after the remelt of ingots. Semi-quantitatively, prime (unalloyed) aluminum is known to produce very little dross during meltdown, while alloys containing significant additions of magnesium produce much dross. The Albany Research Center (U.S. Department of Energy) developed and operates the Laboratory Scale Reverberatory Furnace (LSRF) which is capable of melting and holding approximately 200 pounds of aluminum. Magnesium containing and prime aluminum alloys have been melted in the LSRF. This paper will generically identify the weight of dross present on aluminum baths of various magnesium contents immediately after meltdown in the LSRF relative to the weight of ingot material charged. Melts in the LSRF have demonstrated dross on prime aluminum ingots of less than 1%. Ingots of aluminum-magnesium alloy have demonstrated 10% dross by weight. Possible correlation between magnesium content and dross formation will be examined.

Characterization of Minerals, Metals and Materials: Ceramic and Refractories

Sponsored by: The Minerals, Metals and Materials Society, TMS Extraction and Processing Division, TMS: Materials Characterization Committee

Program Organizers: Jiann-Yang James Hwang, Michigan Technological University; Arun M. Gokhale, Georgia Institute of Technology; Tzong T. Chen, Natural Resources Canada

Monday PM
March 13, 2006

Room: 206A
Location: Henry B. Gonzalez Convention Ctr.

Session Chairs: Jiann-Yang James Hwang, Michigan Technological University; Sergio Neves Monteiro, State University of the Northern Rio de Janeiro

2:00 PM

Characterization of Ceramic Foam: Sergio Neves Monteiro¹; Carlos Mauricio Fontes Vieira¹; ¹State University of the Northern Fluminense

In the present work, a ceramic foam elaborated with illitic clays was characterized. Properties related to density and compression strength were determined in samples fired at 1300°C, a temperature that permits the clay structure to eliminate and retain gases that will produce the foamy structure. The microstructure of the ceramic foam was studied by X-ray diffraction, scanning electron microscopy and mercury porosimetry. The results showed that the ceramic foam presents a bulk density of 0.38 g/cm³. The microstructure is formed by large open pores, quartz particles and vitreous phase.

2:25 PM

Fibrous Reinforcement in Clay-Bonded Silicon Carbide Refractory Using Andalusite Powder: Bowen Li¹; Jiann-Yang James Hwang¹; Shangzhao Shi¹; ¹Michigan Technological University

Silicon Carbide is an excellent refractory material due to its high melting temperature, excellent thermal conductivity, low thermal expansion, and consequently its good thermal shock resistance. In addition, the high hardness, corrosion resistance and stiffness lead to a wide range of applications where wear and corrosion resistance are primary performance requirements. Commercial silicon carbide refractory is frequently manufactured by bonding silicon carbide particles with clay to provide the green strength and to aid the sintering. However, clay may cause shrinkage, fracture, and thermal shock problems on the products. This study investigate the potential of replacing a portion of clay with the andalusite powder. The results show that micron size andalusite powder can improve not only the strength of refractory but also the sinterability. The mechanisms for the improvements are discussed.

2:50 PM

Characterization of Post-Mortem Refractory Ceramics from Special Al-Metal Alloy and Super-Alloy Melting Furnaces: Musa Karakus¹; William L. Headrick¹; Eric L. Feiner¹; ¹University of Missouri-Rolla

Refractory ceramic linings of special metal and super alloy melting vessels as well as submerged molten-metal handling refractory ceramics are subjected to significant chemical corrosion and mechanical wear/abrasion during melting. The corrosion and wear of refractories results in energy losses and frequent replacement and repair. Study of post-mortem materials provides better understanding of the mechanisms of chemical attack. The chemical attack is identified to be very similar to reactive metal penetration, in which silica component is reduced by liquid aluminum penetration in special Al-alloy melting process. The failure of refractory lining in super alloy melting is identified to be due to thermal spalling, metal penetration and slag attack.

3:15 PM

Characterization of Clayey Ceramic Body Used for Roofing Tile Fabrication: Carlos Mauricio Fontes Vieira¹; Patricia Machado Andrade¹; Enio Vaz Silva¹; Jonas Alexandre¹; Sergio Neves Monteiro¹; ¹State University of the Northern Fluminense

In the present work a ceramic body, elaborated with mixture of clays and sand, used for roofing tiles produced in Campos dos Goytacazes, north of the State of Rio de Janeiro in Brazil, was characterized. Characterization was done by X-ray diffraction, thermo analysis, chemical composition, particle size distribution and plasticity. In addition, technological properties related to water absorption, linear shrinkage and flexural rupture strength were determined in samples fired at 700, 900 and 1100°C. The results showed that the investigated ceramic body has satisfactory plasticity and present a refractory behavior in association with firing due to the predominantly kaolinitic nature of the clays.

3:40 PM Break

3:50 PM

Application of Cathodoluminescence (CL) Microscopy and Spectroscopy to Refractory Raw Minerals and Ceramics: Musa Karakus¹; ¹University of Missouri-Rolla

In this study, a unique characterization technique, cathodoluminescence (CL) microscopy and spectroscopy used in conjunction with reflected light (RL) microscope is described and its applications to wide variety of refractory raw minerals and ceramics are demonstrated. The application of CL microscopy and spectroscopy to refractory ceramics is very comprehensive because almost all thermally processed refractory starting materials and refractory ceramics cathodoluminesce spectacularly, i.e., they display characteristic CL colors when bombarded by electrons. Only phases high in Fe²⁺ will not yield sufficient CL information to allow full application of the method. The CL images and spectra for Al₂O₃, MgO, MgAl₂O₄, ZrO₂, Y₂O₃, AlN, SiAlON, SiC, are obtained. The CL method is proven to be extremely useful for characterizing refractory ceramics.

4:15 PM

Characterization of Steel Slag for Incorporation into Red Ceramics: Sergio Neves Monteiro¹; Stelamaris Chaves Intorne¹; Dylmar Penteado

Dias¹; Elias Lira dos Santos Junior¹; *Carlos Mauricio Fontes Vieira*¹; ¹State University of the Northern Fluminense

This work had as its objective the characterization of a waste, steel slag, generated from integrated steel plant with a view to its recycling into red ceramics fabrication. The characterization was performed in terms of chemical composition by X-ray fluorescence (XRF), particles size distribution, X-ray diffraction (XRD), thermal analysis (DTA/TG) and scanning electron microscopy (SEM). The results indicate that the steel slag presents high amount of Ca, Fe, Mg and Si. The weight loss of the steel slag at temperatures above 800°C is associated with calcium carbonate decomposition. The coarse particle size of the steel slag is inadequate for its direct recycling into red ceramic fabrication. As a possible solution, it suggested that screening or grinding the steel slag to a convenient particle size distribution would allow its successful industrial incorporation into red ceramic products.

4:40 PM

Phase Transformation of Andalusite and Its Impacts on Refractory Brick Reinforcement: *Bowen Li*¹; Jiann-Yang James Hwang¹; Zhiyong Xu¹; ¹Michigan Technological University

Andalusite is an excellent raw material for refractory applications due to its high aluminum oxide content and phase transformation to mullite at high temperature. Traditionally granular andalusite in particle sizes of about 1 to 2 mm was used to produce refractory brick. This study shows that, if powder andalusite in micron particle size is utilized to replace the granular andalusite, reinforcement on the refractory brick can be obtained and the sintering temperature can be reduced. The phase transformation of powder andalusite plays a key role for the difference.

5:05 PM

Characterization of the Ceramic Material for High Pressure Applications: Alan Monteiro Ramalho¹; Guerold Sergevitch Bobrochnitchii¹; *Sergio Neves Monteiro*¹; Ana Lucia Diegues Skury¹; ¹UENF

In the synthesis and sintering process to obtain superhard materials, such as diamond and cubic BN, deformable ceramic capsules are used as gasket to transmit an support the required high pressures and high temperatures. The ceramic material should have special physical and chemical characteristics, such as refractoriness, shear strength and compressibility. In this work Bridgman type anvils, made of hard metal or tool steel, were used to characterize gaskets made of calcite as function of the maximum compressible thickness. Tests were performed with different polymers as binding medium for the calcite powder. Chemical analysis by EDS/SEM and X-ray fluorescence was also performed. The results showed that brazilian calcite can be successfully used in the fabrication of gaskets.

Computational Thermodynamics and Phase Transformations: Atomic Modeling Based Alloy Thermodynamics II

Sponsored by: The Minerals, Metals and Materials Society, TMS Electronic, Magnetic, and Photonic Materials Division, TMS Materials Processing and Manufacturing Division, TMS Structural Materials Division, TMS: Chemistry and Physics of Materials Committee, TMS/ASM: Computational Materials Science and Engineering Committee
Program Organizers: Dane Morgan, University of Wisconsin; Corbett Battaile, Sandia National Laboratories

Monday PM Room: 210A
March 13, 2006 Location: Henry B. Gonzalez Convention Ctr.

Session Chairs: Isao Tanaka, Kyoto University; Axel Van de Walle, Northwestern University

2:00 PM Invited

High-Throughput Measurements as Inputs to Computational Thermodynamics: *Ji-Cheng Zhao*¹; Xuan Zheng²; David G. Cahill²; ¹General Electric Company; ²University of Illinois, Urbana-Champaign

This talk will illustrate the use of diffusion multiples and micro-scale property probes to map phase diagrams, thermal conductivity, and specific heat capacity. The information can be used as inputs to computa-

tional thermodynamics. Phase diagrams are essential input to CALPHAD modeling. The diffusion-multiple approach can map phase diagrams at an efficiency orders-of-magnitude higher than that using individual equilibrated alloys. Micro-scale thermal conductivity measurements on compositional gradients in diffusion couples/multiples can be used to evaluate compositional point defects such as vacancies and anti-sites and to study ordering effects and site preference (elemental substitution) in intermetallic compounds. All the information are important for modeling the thermodynamics, especially for selecting the right sublattice models. Micro-scale specific heat measurements can provide direct inputs to CALPHAD modeling. Examples will be used to illustrate the methodologies.

2:30 PM Invited

Crystallographic Data for Non-Organic Materials: *Vicky Lynn Karen*¹; ¹National Institute of Standards and Technology

Crystallographic data models are used on a daily basis to visualize, explain, and predict the behavior of chemicals and materials. Access to reliable information on crystallographic structure helps researchers concentrate experimental work in directions that optimize the discovery process. In partnership with outside organizations, the National Institute of Standards and Technology (NIST) has extended its crystallographic data program to provide evaluated full structural data for all non-organic materials including inorganics, metals, minerals and ceramics. The Inorganic Crystal Structure Database (ICSD) contains full structural and bibliographic information for more than 80,000 structures; the NIST Structural Database (metals, intermetallics) ~ 60,000 entries. Over recent years, NIST and its partners have been building a modern infrastructure for its databases. This has included a) re-evaluating and re-structuring existing and new database entries; b) developing software tools for the calculation and standardization of derived data items; c) developing modules for the intelligent access of these data; and d) providing access through modern user interfaces and networking capabilities. This presentation will focus on the database content, uses, and software tools to exploit the content of these data. Future directions include plans for interoperability between the non-organic crystal structure data, phase equilibria diagrams, and other NIST materials databases.

3:00 PM Invited

Materials Informatics: Knowledge Acquisition for Materials Design: *John Rodgers*¹; ¹Innovative Materials Technologies, Inc

Combinatorial materials science methods are being used to synthesize, test, characterize and predict promising candidate materials for a number of applications in material science. These methods are producing enormous amounts of experimental, and derived, data that requires storage and analysis. Data mining provides exploration of this multidimensional chemical and property space, at a previously unavailable level of detail, and can rapidly estimate physical properties that are difficult to measure using experimental approaches. Given these vast resources of structure and property data it is possible to extract trends on the structure of materials and their properties and use these results in the materials design stages. These informatics approaches, coupled with ab initio quantum mechanics methodologies, provides many of the tools needed to guide materials selection via combinatorial materials science experiments.

3:30 PM Invited

A Practical Approach to the Prediction of Crystal Structure by Merging Data-Mining Methods with First Principles Quantum Mechanics: *Gerbrand Ceder*¹; Chris Fischer¹; Kevin Tibbetts¹; Dane Morgan²; ¹Massachusetts Institute of Technology; ²University of Wisconsin

The prediction of structure is a key problem in computational materials science. Traditionally, empirical rules have been extracted by observing trends in large amounts of experimental data. On the other hand, computational quantum mechanics is highly accurate in reproducing structural energy differences, but suffers from the difficulty that a global optimization can not really be performed in the physical space of atomic coordinates. As such, ab-initio energy calculations are usually only used to “verify” the relative energy of structures one might have guessed for a given chemical composition. In a departure from previous computational approaches, we combine data-mining to extract information from large amounts of experimental information and a database of over 15,000 first principles computations, with first principles computations to determine

MONDAY PM

energies. We show that this approach is highly efficient in finding the ground states of binary metallic alloys and can be easily generalized to more complex systems.

4:00 PM Break

4:10 PM Invited

Design of New Materials for Hydrogen Storage: *Blanka Magyari-Kope*¹; Vidvuds Ozolins¹; Christopher Wolverton²; ¹University of California, Los Angeles; ²Ford Motor Company

Practical hydrogen storage for mobile applications requires sustainable materials that contain large amounts of hydrogen, have low decomposition temperatures and fast kinetics for absorption and desorption. Theoretical modeling employing quantum mechanics, can help improve the state-of-the-art in hydrogen storage properties by (1) providing insights into the underlying microscopic processes, (2) predicting new materials. One of the most promising classes for reversible hydrogen storage is represented by complex hydrides. In particular the group I, II and III elements Li, Na, Mg, B, Al, N form a large variety of metal-hydrogen complexes. We present systematic first-principles electronic structure calculations for a database of hydrides. Structural stabilities, electronic properties, thermodynamical properties and hydrogen-absorption enthalpies are determined, and structure-property relationships are discussed. These findings are expected to be useful in designing new materials of novel compositions, aimed to improve the hydrogen capacity at rational temperatures and pressures. Research supported by DOE Grant DE-FC36-04GO14013.

4:40 PM

First-Principles Calculations of Lattice Mismatch and Interfacial Energies between β'' -Mg₅Si₆ and α -Al in Al-Si-Mg Ternary Alloys: *Yi Wang*¹; C. Wolverton²; C. Ravi²; Z.-K. Liu¹; L.-Q. Chen¹; ¹Pennsylvania State University; ²Ford Research and Advanced Engineering

The metastable β'' phase is often the most effective hardening precipitate in Al-rich Al-Mg-Si alloys. The amount of strengthening depends critically on the volume fraction, number density as well as the morphology of the precipitates. Two important factors that control the precipitate morphology are the lattice mismatch and the magnitude and anisotropy of interfacial energy between the precipitate and the matrix. In this work, first-principles supercell calculations are employed to calculate the β'' /Al interfacial energies as well as the stress-free lattice parameters of the β'' phase. The three interfacial orientations are chosen based on existing high-resolution TEM observations: [230]Al|[100] β'' , [001]Al|[010] β'' , and [10]Al|[001] β'' . The calculated interfacial energies, strain energies, and lattice mismatches for different interfacial orientations were analyzed and compared. The effect of atomic mixing across the [10]Al|[001] β'' interface is discussed. Finally, the interfacial and strain energies are used to estimate the equilibrium shapes for β'' precipitates.

5:00 PM

Pressure-Induced Spin Transitions in the (Fe_xMn_{1-x})S₂ System: *Kristin Aslaug Persson*¹; Gerbrand Ceder¹; Dane Morgan²; ¹Massachusetts Institute of Technology; ²University of Wisconsin

Pressure-induced spin transitions of the Fe²⁺ and the Mn²⁺ ions in the (Fe_xMn_{1-x})S₂ system are investigated using calculations based on first-principles density-functional theory within the GGA+U formalism. Even though the transition pressures decrease with increasing Fe content, the volume change at the transition remains remarkably constant as long as both Fe and Mn participate. At high Fe content, transition pressures approaching zero are obtained.

5:20 PM

Influence of Many Body Interaction on the Energetics and Dynamics of Metallic Nanoclusters: *Ho-Seok Nam*¹; David J. Srolovitz¹; ¹Princeton University

Metallic nanoclusters exhibit various structural modifications, for example, for fcc metals, cuboctahedra, decahedra, and icosahedra. The energetics and dynamics of nanoclusters was investigated as a function of bonding characteristics by employing a set of embedded atom method (EAM) potentials that can be adjusted to vary the many-body effects. With only pair interaction, icosahedral structure is energetically stable up to sizes N=3000. As the strength of many-body interaction increases, the

crossover size decreases monotonically and icosahedra become metastable even for small clusters (less than 100 atoms). However, our molecular dynamics simulations on freezing of nanoclusters showed that most of clusters of a few hundred atoms were frozen to an icosahedral structure from liquid droplet in spite of its metastability. These results were compared with general trends of transition and noble-metal clusters in the literature.

5:40 PM

Application of the Cluster/Site Approximation to fcc Phases in Ni-Al-Cr System: Weisheng Cao¹; Jun Zhu¹; ¹University of Wisconsin

The Cluster/Site Approximation (CSA) has been used to model the fcc phases (disordered γ with A1 structure and ordered γ' with L1₂ structure) in the Ni-Al-Cr ternary system. The CSA takes into account short-range order (SRO), which is essential to satisfactorily describe the thermodynamics of order/disorder transitions such as occur between the fcc phases in the Ni-Al-Cr system. It possesses computational advantages over the Cluster Variation Method (CVM) while offering comparable accuracy in the calculation of multi-component phase diagrams. This makes the CSA a practical method for calculations on real alloy systems. These points are illustrated in the application of the CSA to fcc phases in the Ni-Al-Cr system. The CSA-calculated phase diagrams, which use fewer model parameters than used in previous descriptions, based on the point approximation, show good agreement with the experimental data. In addition, the fcc metastable phase diagrams show reasonable ordering/disordering behavior and phase relationships.

Deformation and Fracture from Nano to Macro: A Symposium Honoring W. W. Gerberich's 70th Birthday: Materials Properties: Testing and Techniques

Sponsored by: The Minerals, Metals and Materials Society, TMS Materials Processing and Manufacturing Division, TMS Structural Materials Division, TMS/ASM: Mechanical Behavior of Materials Committee, TMS: Nanomechanical Materials Behavior Committee
Program Organizers: David F. Bahr, Washington State University; James Lucas, Michigan State University; Neville R. Moody, Sandia National Laboratories

Monday PM
March 13, 2006

Room: 214D
Location: Henry B. Gonzalez Convention Ctr.

Session Chairs: William D. Nix, Stanford University; Tim Foecke, National Institute of Standards and Technology

2:00 PM Invited

Nanomechanical Contact Studies of PDMS: Donna M. Ebenstein¹; Kathryn J. Wahl¹; ¹Naval Research Laboratory

The Johnson-Kendall-Roberts (JKR) theory of elastic contact is used to evaluate work of adhesion and modulus of elastomeric thin films. We present a comparison of five approaches to analyze quasi-static and dynamic JKR force curve data obtained using instrumented indentation. Indentation experiments were performed on poly(dimethylsiloxane) (PDMS) samples (E < 10 MPa) with a 200 μ m radius glass sphere. Direct curve fitting as well as simplified 2- and 3-point analysis methods were used to compare modulus values determined from load-displacement and stiffness-load data. Simple curve fit methods not requiring determination of the tip-sample contact point ("zero" displacement) provided modulus values closest to those obtained by direct curve fitting. The dynamic stiffness-load data revealed a frequency dependent modulus; simultaneous load-displacement measurements were consistent with the relaxed, or low-frequency, modulus of the PDMS sample. Hence, both the frequency dependent and relaxed modulus can be obtained from a single measurement.

2:20 PM

Nanoindentation Behavior of Ultrathin Polymeric Films: *Kebin Geng*¹; Fuqian Yang¹; Thad Druffel²; Eric A. Grulke¹; ¹University of Kentucky; ²Optical Dynamics Corporation

Measurement of the mechanical properties of ultrathin polymer films is important for the fabrication and design of nanoscale layered materials. Nanoindentation was used to study the viscoelastic deformation of ultrathin polymeric films with thicknesses of 47 nm, 125 nm and 3000 nm. The reduced contact modulus increases with the indentation load and penetration depth due to the effect of substrate, which is quantitatively in agreement with an elastic contact model. The flow of the ultrathin films subjected to constant indentation loads is shear-thinning and can be described by a linear relation between the indentation depth and time with the stress exponent being 1/2. FY is grateful for support from NSF grant DMR-0211706 and support from General Motors Corporation. KG and EG are grateful for support from Optical Dynamic Corporation.

2:35 PM

Electrical Property Measurements of Stressed Dielectric Films Using Nanoindentation: *John M. Jungk¹*; Michael T. Dugger¹; Somuri V. Prasad¹; ¹Sandia National Laboratories

Microsystem-based radio frequency switches allow for lower static power dissipation than existing solid-state switches, but charging and changes in the contacting surfaces can cause a drift in actuation voltage and decrease in reliability of capacitively switched devices. Potential relationships between contact stress and electrical response have yet to be defined. To investigate these behaviors in thin film dielectric systems, PECVD SiON films that are known to store charge have been examined and compared to other dielectric films with varying degrees of conductivity. These comparisons were achieved by coupling a commercial nanoindentation system with a current and voltage source and an electrometer to produce both highly controlled contact stresses and accurate electrical measurements. The electrical behavior of thin film dielectrics as a function of stress, contact hold time and number of contact cycles will be discussed.

2:50 PM

Electrical Methods for Mechanical Testing of Interconnects: *Robert Keller¹*; Nicholas Barbosa III¹; Roy Geiss¹; David Read¹; Andrew Slifka¹; ¹National Institute of Standards and Technology

A new approach to mechanical testing of dimensionally-constrained materials is presented. The testing methods are based on the principle of applying Joule heating to patterned interconnect specimens in a controlled manner, by use of low frequency, high current density a.c. electrical signals. The time scale is such that d.c. electromigration is precluded. Typical testing conditions include 100 Hz sinusoidal signals at a current density of 10 MA/cm². Thermal expansion mismatch between film and substrate then leads to thermal strains, which can be used as the basis for mechanical testing. We will demonstrate thermal fatigue testing on aluminum and copper lines, as well as strength measurements using extrapolations of well-known low-cycle fatigue concepts. The electrical test results are corroborated by microtensile testing. Deformation induced by thermal fatigue results in development of severe topography in non-passivated lines, as well as grain growth and re-orientation. Failure then takes place by open circuit.

3:05 PM

Determining Thin Film Properties by Nanoindentation of Film/Substrate Systems: *Seung Min Jane Han¹*; William D. Nix¹; ¹Stanford University

The Oliver & Pharr method for nanoindentation relies on an accurate determination of the contact area through a calibration process. However, it does not incorporate the effects of indentation shape (pile-up, sink-in) or the effects of elastic modulus mismatch that are typically present in film/substrate systems. Here we report a new methodology for calculating the true hardness of thin films on elastically mismatched substrates using an analytical treatment of the elastic indentation of a film/substrate with a conical indenter given by Yu et al. The method allows us to determine the contact radius and hardness from the measured contact stiffness and known elastic properties, even for indentation depths approaching the thickness of the film. The new method is applied to Al, W, and polymer thin films on various substrates to show that the true hardness of the thin films can be reliably determined using this method.

3:20 PM

Influence of Sample Offset Angle on Nanoindentation Test: *Zhihui Xu¹*; *Xiaodong Li¹*; ¹University of South Carolina

A key factor in measuring mechanical properties using nanoindentation is the accurate determination of real contact area. In nanoindentation analysis, the real contact area is derived from the unloading curve using a formula based on elastic solution of a rigid indenter perpendicularly penetrating a contact surface. In real test, such as indentations on samples with small dimension at micron/nano meter level, indentation is usually performed at a raw sample surface and it often happens that the indenter penetrate into the sample surface with certain offset angle. In this study, finite element simulation has been carried out to investigate the influence of sample offset angle on nanoindentation test. It is found that the increase in real contact area due to the sample offset angle cannot be accounted for with the current analysis technique of nanoindentation. This introduces significant error in the determination of mechanical properties, such as, hardness and elastic modulus.

3:35 PM Break

3:55 PM

Results of the NIST Nanoindentation Round Robin on Thin Film Copper on Silicon: *David Thomas Read¹*; Robert R. Keller¹; ¹National Institute of Standards and Technology

Nanoindentation is used in a variety of fields to measure material strength and stiffness. However, the standardization process for this new measurement method is still in progress. To test the ability of current measurement procedures to provide comparable results, a round robin was conducted. Invitations to participate were sent to over 100 laboratories. Two specimens, a copper film on a silicon substrate and an uncoated substrate, were distributed to 33 laboratories. The choice of measurement procedure was left to the performing organizations. To date 24 sets of results have been received, with more pending. The scatter is larger than expected. As of now, the standard deviation for the hardness of the copper film is 0.7 GPa, and for the substrate it is 1.3 GPa. The results will be examined to see if the scatter can be traced to particular aspects of the measurement procedures.

4:10 PM Invited

Nanoindentation of NiTi Shape Memory Alloys: *Kenneth Gall¹*; Carl Frick²; ¹Georgia Institute of Technology; ²University of Colorado

NiTi shape memory alloys have the ability to regain their shape after to deformation through a reversible thermo-elastic phase transformation. This study investigates the thermoelastic shear-driven martensitic transformation of NiTi at the nano-scale, and illustrates a connection between the martensite phase transformation in a nanometer-sized volume to the local material structure. Testing was performed on specimens machined from hot-rolled, polycrystalline Ti-50.9 at.%Ni. Small-scale mechanical behavior was probed by nanoindentation performed using a Berkovich indenter tip at a constant strain rate of 0.05. Both shape memory and pseudoelastic materials displayed reverse phase transformation upon unloading, specifically the shape memory NiTi showed discrete excursions in the load-depth response during both the loading and unloading. Furthermore, atomic force microscopy measurements subsequent to nanoindentation illustrated increasing deformation recovery upon heating as a function of decreasing indentation depth, for both the shape memory and pseudoelastic NiTi.

4:30 PM

Mechanical Properties of Pb-Free Solder Joints Associated with Intermetallics Growth Investigated Using Nanoindentation and OIM: *James P. Lucas¹*; H. Rhee¹; ¹Michigan State University

Mechanical properties of intermetallic compound (IMC) phases and bulk solder in Pb-free solder joints were assessed using nanoindentation testing (NIT) and orientation imaging (OIM). The elastic modulus and hardness were determined for IMC phases associated with in situ FeSn particle reinforced and mechanically-added Cu particle reinforced composite solder joints. IMC layers that formed around Cu particle reinforcement and at the Cu substrate/solder matrix interface were probed with NIT. Moduli and hardness values obtained by NIT revealed that Cu-rich Cu₃Sn was noticeably higher than those of Cu₆Sn₅. Ag₃Sn platelets that formed during reflow were also examined for eutectic Sn-Ag solder column joints. The indentation modulus of Ag₃Sn platelets was significantly

lower than that of FeSn, SnCuNi, and CuSn IMCs. Indentation creep properties were assessed in localized microstructure regions of as-cast eutectic Sn-Ag solder. The stress exponent, n , associated with secondary creep differed widely and is relatable to microstructure features probed.

4:45 PM

Microbridge Tests on Buckled Thin Film Beams: *Tong-Yi Zhang*¹; ¹Hong Kong University

We report here a microbridge testing method for buckled microbridge thin film beams due to residual compressive stress or/and residual moment in the beams. A theoretical formula based on the elastic beam theory is derived in closed form with the consideration of substrate deformation. Measuring the buckling profile of a microbridge beam without any original residual moment, one can evaluate Young's modulus and residual compressive stress of the beam. If there exists a residual moment in a multi-layer microbridge beam, measuring the buckling profile and the slope of a load-deflection curve under small loads allows one to evaluate simultaneously the tension stiffness, the bending stiffness, the residual moment, and the residual force. Experimental results have verified the proposed microbridge testing method. The work is supported by an RGC grant from the Research Grants Council, HKSAR, China. Mr. B. Huang and Mr. X.S. Wang conducted the experiments.

5:00 PM

In Situ Neutron Measurement of Micromechanical Behavior of Materials under Applied Load at NRSF2: *Ke An*¹; Cam R. Hubbard¹; Hahn Choo²; William W. Bailey¹; ¹Oak Ridge National Laboratory; ²University of Tennessee

A neutron diffraction load frame has been constructed for the Second Generation Neutron Residual Stress mapping Facility (NRSF2) at ORNL's High Flux Isotope Reactor. The load frame is designed to study micromechanical behavior of materials under applied tensile, compressive or cyclic load and to characterize specimens while under load by using the NRSF2 mapping capabilities. Recently, in situ neutron measurements under different load conditions have been done: a) fast neutron measurements of Al 2024 and textured Al 5083 under continuous tensile load. Using the data summed from multiple detectors, we were able to collect neutron as fast as 3s/pattern. b) SiO₂ particles in a compressive loading cell with either continuous or static load. c) SiC particulate reinforced Al2080 alloy composite measured with the SiC and Al hkl's under position control. Details of the load frame design, the performance and those in situ results will be presented.

Effects of Water Vapor on High-Temperature Oxidation and Mechanical Behavior of Metallic and Ceramic Materials: Coatings and Ceramics

Sponsored by: The Minerals, Metals and Materials Society, ASM International, TMS Structural Materials Division, TMS/ASM: Corrosion and Environmental Effects Committee

Program Organizers: Bruce A. Pint, Oak Ridge National Laboratory; Peter Tortorelli, Oak Ridge National Laboratory; Karren More, Oak Ridge National Laboratory; Elizabeth Opila, NASA Glenn Research Center

Monday PM

Room: 213A

March 13, 2006

Location: Henry B. Gonzalez Convention Ctr.

Session Chairs: Karren More, Oak Ridge National Laboratory; Elizabeth J. Opila, NASA Glenn Research Center

2:00 PM

Oxidation Behavior of Iron Aluminide Coatings in Water-Vapor Environment: *Ying Zhang*¹; Bruce A. Pint²; Allen Haynes²; Ian G. Wright²; ¹Tennessee Technological University; ²Oak Ridge National Laboratory

The long-term oxidation behavior of iron aluminide coatings, Fe₃Al or (Fe,Ni)₃Al, produced by a laboratory chemical vapor deposition (CVD) process on commercial ferritic steel Fe-9Cr-1Mo and austenitic stainless steel 304L, was studied in the temperature range of 700-800°C. For both substrates, the as-deposited coatings consisted of a relatively thin (20-25

µm) Al-rich outer layer and a thicker (150-275 µm) inner layer with less Al. The coating specimens were tested in air + 10 vol.% H₂O with 100-h cycle length for over 12,000h at 700°C and over 8,000h at 800°C, and they registered very low mass gains at both temperatures. While the aluminide coatings showed excellent oxidation performance at 700°C, spallation and re-formation of the oxide scale occurred at 800°C. In addition, the effect of N in the substrate alloy on the oxidation behavior of aluminide coatings was investigated via testing coated laboratory alloys with different N contents.

2:25 PM

Cyclic Oxidation and Mechanical Behavior of Slurry Aluminide Coatings for Steam Turbine Components: *Alina Agüero*¹; Raul Muelas¹; Marcos Gutierrez¹; Rijk Van Vulpen²; Steve Osgerby³; L. Brown³; ¹Instituto Nacional de Técnica Aeroespacial; ²KEMA; ³National Physical Laboratory

The excellent steam oxidation resistance of iron aluminide coatings on ferritic steels at 650°C has been demonstrated both by laboratory tests and field exposure. These coatings are formed by the application of an Al slurry followed by diffusion heat treatment at 700°C for 10 hours. The resulting microstructure is mostly composed of Fe₂Al₅ on top of a much thinner FeAl layer. This coating exhibits perpendicular cracks and the results presented in this paper will show that these cracks are caused by a rapid cooling rate after heat treatment. However, these stress relieving cracks do not seem to have an effect in the mechanical properties of the substrate. The results of cyclic oxidation, creep resistance and TMF testing on these coatings will be presented.

2:50 PM

Effect of Water Vapor on Alumina-Forming Alloys and Coatings: *Bruce A. Pint*¹; James Allen Haynes¹; Ian G. Wright¹; ¹Oak Ridge National Laboratory

Turbines fired with hydrogen or syngas from coal gasification will have significantly higher water vapor contents in the hot gas stream than natural-gas fired turbines. Previous work on alumina-forming MCrAl foils showed a consistent 10% reduction in the time to breakaway oxidation at 1100°C with the addition of 10% water vapor. Current work is examining the effect of up to 50% water vapor on the spallation resistance of cast alloys representing the major classes of Ni-base superalloy coatings (NiCrAlYHf, NiPt-40Al and NiPt-22Al+Hf) in cyclic testing at 1100°C. Initial work will be presented on coated superalloys in the same environments.

3:15 PM Break

3:30 PM

Role of Water Vapor in Affecting the Grain-Boundary Strength, Fracture, and Fatigue Properties of Alumina: *Jamie J. Kruzic*¹; Rowland M. Cannon²; Robert O. Ritchie³; ¹Oregon State University; ²Lawrence Berkeley National Laboratory; ³University of California

Although weakened grain boundaries are essential for ceramics to achieve high strength and toughness, further degradation of their strength due to water vapor has been found to be detrimental to both the fracture and fatigue resistance. The role of moisture in affecting the fracture and fatigue-crack growth resistance of a 99.5% pure polycrystalline alumina has been examined in moist and dry environments at ambient temperature. In addition to the expected higher intrinsic toughness, it was found that the R-curves initially rise more steeply in dry environments. Similarly, improved fatigue resistance was found in dry environments and for both this is attributed to changes in the nature of the bridging, with uncracked-ligament bridges playing a larger role in dry atmospheres, while frictional bridges are predominant in moist air. Such behavior is also expected to be relevant at elevated temperatures since the chemical reaction at the crack tip will be further promoted.

3:55 PM

Evaluation of NZP Ceramic Variants for EBC Applications: *Ramachandran Nageswaran*¹; Karren More²; ¹SMAHT Ceramics, Inc.; ²Oak Ridge National Laboratory

Silicon carbide (SiC) and silicon nitride (Si₃N₄) based monolithic or composite turbine engine components require an environmental barrier coating ("EBC") to prevent water vapor attack of the protective silica

layer and associated material recession during high temperature operation. The state-of-the-art EBC, which is based on mullite and BSAS (barium strontium aluminosilicate), provides good environmental protection for the Si-based ceramics for up to several hundred hours at 1250°C. Nevertheless, further enhancement of the EBC performance is critical for reliable operation of advanced turbine engines. A few compositional variants from the [NZP] family of ceramics, such as BZP (Barium Zirconium Phosphosilicate), have attractive properties such as low moisture sensitivity, high thermal cycling stability and low thermal conductivity. Recent high water-vapor pressure rig testing of BZPs at 1200°C up to 1000 hrs., in the Kaiser Rig, yielded promising data. Results from this EBC development effort are presented in this paper.

4:20 PM

Stress-Dependent Molecular Pathways of Silica-Water Reaction: *Ting Zhu¹; Ju Li²; Xi Lin³; Sidney Yip³; ¹Georgia Institute of Technology; ²Ohio State University; ³Massachusetts Institute of Technology*

We study stress-corrosion of silica by water through exploring the stress-dependent molecular pathways of silica-water reaction. An ordered silica nanorod with clearly defined nominal tensile stress is constructed to model a structural unit of the stressed crack tip. Three competing hydrolysis reaction pathways are identified, each involving a distinct initiation step. Water dissociation, molecular chemisorption, and direct siloxane bond rupture dominate at low, intermediate, and high stress levels, respectively. A linear stress dependence in the thermodynamic driving force, not commonly considered in the criterion of brittle fracture initiation, is shown to originate from surface relaxation associated with bond rupture. This effect is particularly important in determining the Griffith condition of crack extension for nano-sized systems when spatial accommodation of foreign molecules is involved in the process of bond breaking.

Fatigue and Fracture of Traditional and Advanced Materials: A Symposium in Honor of Art McEvily's 80th Birthday: Fatigue and Fracture II

Sponsored by: The Minerals, Metals and Materials Society, TMS Structural Materials Division, TMS/ASM: Mechanical Behavior of Materials Committee

Program Organizers: Leon L. Shaw, University of Connecticut; James M. Larsen, U.S. Air Force; Peter K. Liaw, University of Tennessee; Masahiro Endo, Fukuoka University

Monday PM Room: 216
March 13, 2006 Location: Henry B. Gonzalez Convention Ctr.

Session Chairs: Hael Mughrabi, Universität Erlangen-Nuernberg; Paul C. Paris, Washington University in St. Louis

2:00 PM Invited

Damage Mechanisms of Cast Al-Si-Mg-Alloys under Superimposed Thermal-Mechanical- and High-Cycle-Fatigue Loading: *Detlef Loehe¹; Tilmann Beck¹; Jochen Luft¹; Ingo Henne¹; ¹Universität Karlsruhe*

In order to analyze the synergy of damage caused by the low frequency thermal and the high-frequency mechanical loading and to get quantitative fatigue life data of cast aluminium alloys, superimposed thermal-mechanical fatigue (TMF)/high-cycle fatigue (HCF) tests at the cylinder head alloys AlSi7Mg, AlSi5Cu4 and AlSi10Mg were conducted in total strain control. Extensive metallographic and SEM studies of the crack initiation and propagation process were conducted. Under TMF as well as under TMF/HCF loading, cracks are always initiated at the interface between eutectic Si-particles and α -Al matrix. Under pure TMF conditions, the cracks propagate solely along the eutectic regions, whereas with increasing superimposed HCF loading crack propagation along slip bands within the primary α -Al crystals becomes more dominant. Based on the damage parameters developed, a method for lifetime estimation under superimposed TMF/HCF loading on the crack propagation process is developed.

2:25 PM Invited

Parameters and Key Trends Effecting Fatigue Crack Growth - A Tribute to Professor Arthur J. McEvily's Contributions: *Diana A. Lados¹; Paul C. Paris¹; ¹Washington University in St. Louis*

The early 1950s led to high performance aluminum skinned aircraft for which metal fatigue and fatigue crack growth became extremely important considerations. Virtually, no significant range of data on fatigue crack growth existed prior to McEvily's work¹, and controlling parameters were left to be further developed. His pioneering work allowed others to resolve some of the critical issues, and yet a few still remain open even today. This discussion will trace historical milestones in the field, as well as some more recent investigations, with the intention of exposing the major trends. Finally, a new methodology for analyzing fatigue crack growth load-displacement records to determine "effective stress intensity factor ranges", the major mechanical cause of crack growth, will be discussed. ¹A. J. McEvily Jr. and W. Illg; The Rate of Fatigue Crack Propagation in Two Aluminum Alloys, NACA (now NASA), TN 4394, 1958.

2:50 PM Invited

Mechanisms of the Early Fatigue Damage in Crystalline Materials: *Jaroslav Polak¹; ¹Institute of Physics of Materials ASCR*

Cyclic loading of crystalline materials introduces damage, which is difficult to quantify. Recent applications of the transmission electron microscopy, high resolution scanning electron microscopy, atomic force microscopy and electron back scattering to study the early damage in polycrystalline materials will be reviewed and documented. The experimental findings will be used to identify the principal mechanisms leading to fatigue damage. Dislocation rearrangement resulting in cyclic strain localization, the surface relief evolution producing the extrusions and intrusions and ending in crack initiation will be reported and analyzed in reference to recent theories of fatigue crack nucleation. The growth of initiated cracks under constant plastic strain amplitude loading will be reviewed. The growth kinetics and the parameters of the short crack growth law will be compared with the fatigue life curves determined under identical loading conditions. This results in interpretation of the Manson-Coffin law in terms of short crack growth.

3:15 PM Invited

The Use of Modeling and Experiment to Understand "Dwell Fatigue" in Ti Alloys: *James C. Williams¹; Somnath Ghosh¹; Michael J. Mills¹; Stan Rokhlin¹; Vikas Sinha¹; ¹Ohio State University*

There is a fatigue failure mode in high temperature Ti alloys known as Dwell Fatigue. This mode is characterized by a major reduction in fatigue life when the material is subjected to a loading pattern where the load is held at maximum value for a dwell period. Moreover, this failure mode is typified by subsurface crack initiation. Because of its importance, the phenomenology of dwell fatigue is well defined. However, the fundamental reasons for its occurrence are not well understood. This talk will describe the phenomenology of dwell fatigue, followed by results of a multi-year, interdisciplinary study of dwell fatigue in Ti-6Al-2Sn-4Zr-2Mo (+Si). We have used solid mechanics modeling, detailed characterization methods and high resolution acoustic microscopy to study this mode of failure. The current qualitative state of understanding and future directions to develop a quantitative understanding will be described.

3:40 PM Break

3:55 PM Invited

Microstructural Roles in Thermal-Mechanical and Isothermal Low Cycle Fatigues of a Single Crystal Ni-Base Superalloy: *Masakazu Okazaki¹; Motoki Sakaguchi¹; ¹Nagaoka University of Technology*

Behavior of thermal-mechanical fatigue (TMF) failure of CMSX-4 was studied, compared with that of isothermal low-cycle fatigue (ILCF). Strain-controlled TMF and ILCF tests were carried out under various test conditions, where the experimental variables were strain rates, strain ratio, test temperature and the range, and strain/temperature phase angle. It was shown from the experiments that the TMF and LCF failures occurred, associated with some noteworthy characteristics which were rarely seen in the traditional polycrystalline heat-resistant alloys. They could be explained inadequately, on the basis of the macroscopic parameters and the historical failure criteria. A new micromechanics model is proposed to predict the TMF and LCF lives, based on the Eshelby's theory. In the

model the microstructural factors are represented by both the difference of mechanical properties between the gamma matrix and the cuboidal gamma-prime precipitates, and the lattice misfit between them which induces internal stress.

4:20 PM Invited

Cyclic Deformation Behavior of Steels and Light Metal Alloys: *Dietmar Eifler*¹; Frank Walther¹; ¹University of Kaiserslautern

Detailed knowledge about the cyclic deformation behaviour of metallic materials is an indispensable requirement for the comprehensive understanding of fatigue processes and a reliable lifetime prediction of cyclically loaded components. Besides various steels (e.g. SAE 4140, railway wheel steels) aluminium, magnesium and titanium alloys were investigated in stress- and strain-controlled fatigue experiments. In addition to mechanical stress-strain hysteresis measurements, changes of the specimen temperature and the electrical resistance were regarded. The deformation-induced martensite formation of metastable austenite was detected in-situ with a FerriteScope. As advanced measuring technique Giant Magneto Resistance (GMR) sensors were used. The results of all measurements depend on microstructural changes due to plastic deformation processes and therefore show a clear interaction with the actual fatigue state. The measured values were presented in cyclic deformation, Morrow and Manson/Coffin curves for lifetime prediction. S_N-curves were described according to Basquin. The microstructures were characterized by scanning and transmission electron microscopy.

4:45 PM Invited

Effect of Environment on Thermomechanical Fatigue Life: *Hans-Juergen Christ*¹; ¹Institut für Werkstofftechnik, Universität Siegen

Results of various studies on the thermomechanical fatigue (TMF) behaviour of metallic engineering materials performed in the research group of the author are presented showing the effect of laboratory air as compared to high vacuum. In order to illustrate the variety of possible effects, three different materials are considered. An austenitic stainless steel is an example for rather small environmental effects on TMF lifetime. At high maximum temperatures applied in the TMF cycle, creep damage prevails. Hence, in-phase (IP) testing is more detrimental than out-of-phase (OP) loading. Vacuum shifts the crack initiation site from the interior to the surface leading to similar lives in IP and OP. The high-temperature titanium alloy IM1834 suffers from hydrogen embrittlement at moderate temperatures and oxygen uptake at high temperatures. Consequently, the environmental influence on life is pronounced. TiAl-based intermetallic alloys show high environmental susceptibility, which is promoted by the strong ductile-to-brittle transition.

General Abstracts: Electronic, Magnetic, and Photonic Materials Division: Session II

Sponsored by: The Minerals, Metals and Materials Society, TMS Electronic, Magnetic, and Photonic Materials Division, TMS: Alloy Phases Committee, TMS: Biomaterials Committee, TMS: Chemistry and Physics of Materials Committee, TMS: Electronic Materials Committee, TMS: Electronic Packaging and Interconnection Materials Committee, TMS: Nanomaterials Committee, TMS: Superconducting and Magnetic Materials Committee, TMS: Thin Films and Interfaces Committee

Program Organizers: Sung K. Kang, IBM Corporation; Long Qing Chen, Pennsylvania State University

Monday PM Room: 211
March 13, 2006 Location: Henry B. Gonzalez Convention Ctr.

Session Chair: Sung K. Kang, IBM Corporation

2:00 PM Introductory Comments

2:05 PM

Fabrication of Oxide Superconducting Thin Films Using Colloids of Nano-Particles as Precursor: *Vamsee K. Chintamaneni*¹; Jinhua Su¹; Pratik Joshi¹; Sharmila M. Mukhopadhyay¹; Ramchander Revuru²; Troy

Pyles²; Suvankar Sengupta²; ¹Wright State University; ²Metamateria Partners LLC

The most popular non-vacuum method of creating thin film oxide superconductors, YBa₂Cu₃O_{7-x} (YBCO) is the Metal Organic Deposition technique using Tri-fluoroacetate solution (MOD-TFA method). The main draw backs for this process are: (i) long process time, and (ii) porosity in the final film. In this study, an alternative method was used to fabricate lower porosity films at a significantly faster rate. The precursor used is a colloidal suspension of Y-Ba-Cu-O nanoparticles in an organic solvent. Precursor films were deposited on (100) LaAlO₃ by spin coating and heat treated in two stage annealing process to obtain final films. The microstructure, texture, critical temperature (T_c), critical current density (J_c) and chemistry of these films will be compared to YBCO films prepared by other processes (MOD-TFA, as well as well characterized vacuum techniques), and the different mechanisms of film growth discussed.

2:30 PM

Impact of Interface Chemistry on the Occurrence of Anomalous Near-Threshold Debond Growth Rate Behavior in Thin-Film Structures:

*Bree M. Sharratt*¹; Reinhold H. Dauskardt¹; ¹Stanford University

The integrity of thin film structures is often limited by interface adhesion. Polymer/inorganic interfaces are especially vulnerable and understanding the relationship between loading, environment and interface chemistry is crucial. We report the susceptibility of a model bisphenol F/SiN_x interface to subcritical debonding. An anomalous near-threshold region developed where growth rates showed only slight dependence on the applied load but were accelerated with increasing temperature and relative humidity. A new stress-dependent transport model is presented that predicts growth rates in this region. By modifying both the epoxy layer and the interface using adhesion promoting molecules, the effect of interface chemistry was systematically examined. We discuss the effects of blended adhesion promoters on the mechanical properties of the bisphenol F film and relate these to variances in adhesion and subcritical debonding behavior. Finally, with effects on the occurrence of the anomalous near-threshold region highlighted, differences between blended and spun-on specimens are presented.

2:55 PM

Integration of Electroplating and Electropolishing of Cu Damascene Process: *Sue-Hong Liu*¹; Chih Chen¹; Jia-Min Shieh²; Bau-Tong Dai²; Shih-Song Cheng³; Karl Hensen³; ¹National Chiao-Tung University; ²National Nano Device Laboratories; ³BASF Electronic Material Ltd.

An effective technology containing two functions of Cu film depositing and polishing in one-step electrochemical process in one tank has been developed, and it will save many risks and cost at the back end of the interconnect fabrication. A promising method, which can be called Cu dual-mode electroplating, integrates the process of electroplating and electropolishing in one tank by alternating the program of controlled computer and exchanging the electrode during electrochemical process. Furthermore, the novel electrolyte in this study consists of phosphoric acid and other organic additives with appropriate concentration and standard Cu electroplating solutions. The already tested conditions were the pulse-time and cycles, various concentrations of organic additives, phosphoric acid. Finally, a high planar Cu surface and profile, Cu films with high filling capability in small trench width and step-height reduction in various pattern sizes (1-50 μm) were obtained after Cu Dual-Mode plating.

3:20 PM

Photocatalytic Activity and Control of Grain Size in TiO₂ Nanocomposite with Nanometer-Sized Particles by Mechanical Alloying and Heat Treatment: *Dong Hyun Kim*¹; Ha Sung Park¹; Jae Han Jho¹; Sun-Jae Kim²; Kyung Sub Lee¹; ¹Hanyang University; ²Sejong University

Nanocomposite of Ni-doped rutile TiO₂ and NiTiO₃ were synthesized by mechanical alloying and heat treatment. Nanocomposite showed higher photocatalytic activity than that of pure anatase TiO₂ and commercial P-25 for decomposition of benzene. And the absorption threshold of the nanocomposite TiO₂ moved to a longer wavelength. The new absorption was believed to be induced by the trapping band gap between the valence and conduction bands of nanocomposite TiO₂. Formation of NiTiO₃ in Ni doped TiO₂ by heat treatment was found to control the grain growth of

nano size TiO₂ and to enhance the high temperature thermal stability. Nanocomposite TiO₂ powders had a grain size in the range 10-20 nm.

3:45 PM Break

4:15 PM

The Effects of Deformation on the Magnetic Behavior of Stoichiometric Ni₃Al: Q. Zeng¹; Ian Baker¹; ¹Dartmouth College

Strain-induced ferromagnetism (SIF) has been observed in a number of intermetallic compounds containing magnetic moment-bearing elements. This phenomenon has been quantitatively modeled in cold-rolled FeAl, using the local environment theory, based on the idea that the ferromagnetism arises from the local disorder in APB tubes. While compounds such as Fe₂AlMn and Co₃Ti show SIF, the reverse effect has been observed in cold-rolled stoichiometric Ni₃Al single crystals. This presentation describes investigations into the effects of disorder on the magnetic behavior of both cold-rolled, and ball-milled and annealed stoichiometric Ni₃Al via x-ray diffraction, differential scanning calorimetry, and magnetic and thermal-magnetic studies. Research sponsored by NIST grant 60NANB2D0120.

4:40 PM

Magneto-Optic Lens Using Ferrofluids: Jayachandran Nagarajan¹; Namasivayam Murugesan¹; ¹Velammal Engineering College

γ-Fe₂O₃, water based ferrofluid (maghemite) has a good transmittance. At a low magnetic volume fraction it is possible to obtain good magneto-optic effect and transmittance. Without any applied field ferrofluids are isotropic. But when a magnetic field is applied ferrofluids acquire an optical anisotropy. Two cases are possible: *Faraday's rotation of plane polarized light when magnetic field is parallel to the light beam. *Anisotropy is linear in perpendicular configuration. If ferrofluid is placed in a cylinder acting as electromagnet producing lines of flux in direction of light, due to attraction of flux linear, more fluid is attracted near cylinder wall. This pattern acts as a lens and can be varied depending upon the field of electromagnet and produce auto focal lens. With sol-gel doped ferrofluid, higher transmittance is obtained. Uses: *In focusing of laser with wavelet filter. *To develop artificial human eye lens.

5:05 PM

CBED Measurements of Lattice Strain in Strained Silicon – Relaxation, HOLZ Line Splitting and Overall Reliability: David R. Diercks¹; Michael Kaufman¹; ¹University of North Texas

The role of lattice strain is important in next-generation CMOS devices. Convergent beam electron diffraction is potentially well suited for such analyses. By comparing the higher order Laue zone lines in a strained region to those from unstrained material, the nature of the strain can be determined. To date, these measurements are made at large angles relative to the <011> cross-section normal. In this study, to achieve better lateral resolution, zones at smaller tilts such as <056> have been examined using thin Si-15%Ge samples on silicon. It is shown that certain HOLZ lines split near the interface; from this, it is concluded that considerable relaxation occurs during the preparation of TEM specimens resulting in strain behavior not indicative of the bulk strain. The variation in splitting as a function of distance from the interface, sample thickness and specimen geometry is described and related to a physical model of the relaxation.

General Abstracts: Extraction and Processing Division: Copper/Nickel

Sponsored by: The Minerals, Metals and Materials Society, TMS Extraction and Processing Division, TMS: Aqueous Processing Committee, TMS: Copper and Nickel and Cobalt Committee, TMS: Lead and Zinc Committee, TMS: Precious Metals Committee, TMS: Process Fundamentals Committee, TMS: Process Modeling Analysis and Control Committee, TMS: Pyrometallurgy Committee, TMS: Recycling Committee, TMS: Waste Treatment and Minimization Committee, TMS: Materials Characterization Committee
Program Organizers: Thomas P. Battle, DuPont Company; Michael L. Free, University of Utah; Boyd R. Davis, Kingston Process Metallurgy

Monday PM
March 13, 2006

Room: 207A
Location: Henry B. Gonzalez Convention Ctr.

Session Chair: Mark E. Schlesinger, University of Missouri

2:00 PM

Neutralization of Smelter Gases with Limestone in a Countercurrent Multiple Fluidized Bed System: Igor Wilkomirsky¹; F. Parada¹; R. Parra¹; ¹University of Concepcion

A novel process to neutralize SO₂ from concentrated copper smelter off gases is being developed. The process uses a three-stages fluidized beds that allows to react the SO₂ from the ascending gases with a countercurrent flow of fluidized limestone. The overall reaction forms anhydrous sulphate and CO₂, generating a heat surplus of -77.35 kcal/mol of SO₂. The reaction is very fast over 750°C, capturing over 99% of the SO₂ at 800°C. For a gas with 8%SO₂ the off gases contained 0.07% SO₂. The capture is equally efficient for diluted gases (0.5%) and concentrated gases (12%).

2:25 PM

Decomposition Behaviour of Metallic Sulphates and Copper Flash Smelting Flue Dust: Elli Vilhelmiina Nurminen¹; ¹Helsinki University of Technology

Thermodynamics of metallic sulphate decomposition reactions were studied through thermodynamical calculations and thermogravimetric methods including evolved gas analysis. The decomposition temperatures and mechanisms were determined for cupric sulphate, ferric sulphate and also for industrial flue dust from a copper flash smelting process. The aim was to determine the thermodynamic conditions for sulphate decomposition and to estimate whether the reactions are likely to take place in the flash smelting process heat recovery equipment. The information is essential in CFD-modelling of the reactions taking place in the boiler and for optimising the process.

2:50 PM

Intensification and Increase of Smelting Furnace Productivity Through On-Line Optimization and Automation of Pyrometallurgical Processes: Florian Kongoli¹; I. McBow¹; Robert D. Budd¹; S. Llubani¹; ¹FLOGEN Technologies Inc

Process intensification and the increasing the productivity of the smelting furnaces is an important issue for various pyrometallurgical processes. That is closely related to several factors from decreasing the number of smelting problems and accidental shutdowns to the optimization and automation of these processes. In this paper, the authors discuss their recent work in effectively controlling acute industrial furnace problems such as magnetite build-up and accretions, eliminating unnecessary slag foaming, decreasing slag losses etc as well as the intensification, optimization and automation of these processes through a unique process physical modeling that correctly simulate the industrial furnace processes and avoid guessing and uncertainties. The advantages of this new approach have been discussed.

3:15 PM

Dissolution Behavior of Solid Cu₂O in Na₂O-B₂O₃-Based Slags: Weol Dong Cho¹; Jei-Pil Wang¹; ¹University of Utah

The dissolution behavior of copper oxide (Cu₂O) in Na₂O-B₂O₃-based slags has been studied in terms of kinetics and equilibrium solubility in

the temperature range of 900-1100°C. The spherical single phase copper oxide powders were prepared by the oxidation of pure copper powders in a fluidized bed at high temperatures. The oxide particles are added directly into the molten slags and the variation of the particle size with time was determined using optical and electron microscopes to get dissolution rate. The effect of temperature and slag composition on the rate of dissolution and the equilibrium solubility of the solid copper oxide was determined for the slag system. Based on the kinetic data and the properties of the slags, the dissolution mechanism has been discussed.

3:40 PM

Reduction of Nickel Oxide from Liquid Slags with Carbon and Silicon: Antonio Romero-Serrano¹; Patricia Martínez-Nicolas¹; Samuel González-López¹; Miguel Angeles-Hernández¹; ¹National Polytechnic Institute

Nickel and ferronickel are some of the major components in the production of special alloys; however, the energy consumption for their production greatly increases their price. A cheaper option could be to use NiO and a reducing element. This work presents experimental and theoretical analysis to estimate the effect of slag basicity and amount of reducing agents on the NiO reduction from the slag which interacted with molten steel at 1600°C in an EAF. The slag system contained CaO-SiO₂-CaF₂-NiO together with a reducing agent, ferrosilicon or carbon. The NiO content in the slag was 25 mass%. The amounts of the reducing agents were 1 to 4 times the stoichiometric mass to reduce NiO. The CaO/SiO₂ ratio was 1.5 and 2.5. The kinetics of the process was very fast since after 5 min the maximum nickel yield was obtained. The slag basicity had a negligible effect on the NiO reduction.

4:05 PM Break**4:25 PM**

Energy Requirements in Nickeliferous Laterite Treatment: Emmanuel N. Zevgolisi¹; Charalabos Zografidis¹; John Gaitanos²; Ismine Polyxeni Kostika¹; Iliana Halikia¹; ¹National Technical University of Athens; ²General Mining and Metallurgical Company S.A. Larco

Treatment energy for a nickeliferous laterite ore by the rotary kiln - electric furnace process is investigated. From this work it comes that thermal energy is about 65% of the total energy needed and the rest is electrical. Also, 56.2% of thermal energy input in the roasting step (that is, the energy of all combustibles fed into the rotary kilns) is used for preheating, 18% for prereluction and the rest (25.8%) corresponds to energy of remaining carbon in the kiln products (i.e., calcine, dust and coatings). Additionally, 57.1% of total carbon entering the system (Ctot) is used for combustion, 38.6% for reduction and the rest (4.3%) remains unburnt. Exploitation of energy from gases of both furnaces, as well as the higher possible reduction degree, the optimum temperature of the calcine and also elimination of the excess air in the rotary kilns, improve significantly energy balance and economics of the process.

4:50 PM

Control of Foaming Phenomena during Copper Blow in Copper P-S Converter: Pengfu Tan¹; Pierre Vix¹; ¹Xstrata Copper

Xstrata Copper at Mount Isa in Australia has operated copper Isasmelt furnace and 4 P-S converters. The phenomena of foaming occur in above 10% of converter operations. A thermodynamic model of copper P-S converter has been developed to simulate copper blow. The model predicts the chemistry of copper skims during copper blow. The effects of oxygen potential charge of dirty materials, slag carry over, and temperature on the foaming and viscosity of copper skims have been discussed. Some improvements of the industrial operations have been presented.

General Abstracts: Extraction and Processing Division: Hydrometallurgy

Sponsored by: The Minerals, Metals and Materials Society, TMS Extraction and Processing Division, TMS: Aqueous Processing Committee, TMS: Copper and Nickel and Cobalt Committee, TMS: Lead and Zinc Committee, TMS: Precious Metals Committee, TMS: Process Fundamentals Committee, TMS: Process Modeling Analysis and Control Committee, TMS: Pyrometallurgy Committee, TMS: Recycling Committee, TMS: Waste Treatment and Minimization Committee, TMS: Materials Characterization Committee
Program Organizers: Thomas P. Battle, DuPont Company; Michael L. Free, University of Utah; Boyd R. Davis, Kingston Process Metallurgy

Monday PM
March 13, 2006

Room: 202B
Location: Henry B. Gonzalez Convention Ctr.

Session Chair: Michael L. Free, University of Utah

2:00 PM

Effect of Normality, Temperature and Time on the Tungsten Losses in the Residue Separated from Diluted Scheelite-Slurry-in-NaOH after Digestion: Raj Pal Singh¹; ¹Osram Sylvania Inc

Due to high concentration of NaOH in the digested slurry after scheelite digestion, it is diluted to about 4N before filtration to separate sodium tungstate solution from the sludge (residue). However, in practice there may be deviations in the normality of NaOH present in the slurry. There may also be variations in the temperature of the slurry and filtration time. Slight variations in these parameters could cause tungsten losses in the sludge via the back reaction: $\text{Ca}(\text{OH})_2 + \text{Na}_2\text{WO}_4 \rightarrow \text{CaWO}_4 + 2\text{NaOH}$. This paper pertains to the effect of normality, temperature and time on the tungsten losses in the sludge that is separated from "diluted-scheelite-slurry-in-NaOH" via filtration. Results indicated that tungsten losses in the filtered residue (sludge) were quite significant when the slurry temperature was kept at 70°C or higher. The effect of high temperature was less significant at the slurry normality of 3.6 or higher. Combination of low slurry normality (<3.6) and high temperature (>60°C) resulted into large W-losses in the sludge.

2:25 PM

Hydrometallurgical Processing of Mechanically Activated Zircon Concentrate: Ashraf Amer¹; Salah Megahed¹; ¹Alexandria University

Among the minerals of the black sand of Egypt is zircon which is found in an economic value (7.3%). These sands are found along the Mediterranean coast of Nile Delta. The present investigation aimed at studying the effect of mechanical treatment on the extraction of zirconium from Egyptian zircon concentrate, the effect of temperate grinding time, sodium hydroxide concentration and leaching time on the extraction of zirconium as well as the kinetics of the leaching process have been studied. Experimental leaching of zircon concentrate has shown that the zirconium extraction (90%) can be reached after mechanical treatment of the studied zircon concentrate, followed by alkali leaching at 190 C in an autoclave.

2:50 PM

Study on Recovering Iron-Bearing Minerals from a Nickel Metallurgical Residue by Selective Flocculation-Magnetic Separation: Haigang Dong¹; Yufeng Guo¹; Tao Jiang¹; Guanghui Li¹; ¹Central South University

Mineralogy and physico-chemical performance of nickel metallurgical residue and recovery of iron-bearing minerals by flocculation-magnetic separation were studied. The results were as follows: The nickel metallurgical residue is fine mineral and content reaches 85.4%. Iron-bearing minerals are chiefly magnetite and ferruginous vitreum which exist in -0.045mm mainly. Magnetite accounts for 31.7% of total iron which is in existence of monomer. A few magnetite distribute in ferruginous vitreum. Ferruginous vitreum with stronger magnetism and low-iron accounts for 39.9% of total iron, which is a multicomponent amorphous state substance. Addition of iron flocculant increased granularity and magnetic force of fine iron particles and improve iron grade and recovery rate. Iron

grade of 56.08% and recovery rate of 81.72% were obtained by flocculation-magnetic separation under conditions of oleic acid 0.8kg/t, sodium carbonate 2kg/t and magnetic density 2500Gs.

3:15 PM Break

3:30 PM

The Technological Characteristics of Blended Nkalaha and Nsu Clays: *Naubuisi Edennaya Idenyi*¹; *Sampson I. Neife*²; *Stanley O. Agha*¹; ¹Ebonyi State University; ²Enugu State University of Science and Technology

The effects of compositions and firing temperatures on the physico-mechanical properties of blended Nsu fireclay and Nkalaha redbrick clay both in the southeastern states of Imo and Ebonyi in Nigeria have been investigated. The clay samples were compounded according to the following ratios; 10:90, 20:80, 30:70, 40:60, 50:50, 60:40, 70:30, 80:20, and 90:10 in the order Nsu: Nkalaha respectively, and test samples made and fired at 900°C, 1000°C, 1100°C and 1200°C. The properties investigated were the modulus of rupture (green, dry, and fired), apparent porosity, shrinkage (wet, dry, fired and total), apparent density, bulk density, and water absorption. From the results obtained, the blends were found to have a maximum service temperature of 1100°C; with the 30:70 blends presenting the best characteristics. A conclusion is drawn to the effect that the clay blends could be adapted for the production of ceramic earthenware, electrical porcelain pin insulators, in cement making and for lining of metal melting furnaces where temperature requirements are less severe.

3:55 PM

A Clean Method Applying Anion-Exchange Separation and Membrane-Electrolysis to Regenerate Fe-Zn-HCl Spent Pickling Liquors: *Gabor Csicsovszki*¹; *Tamas Kekesi*¹; *Tamas I. Torok*¹; ¹University of Miskolc

We have developed a novel method - at the laboratory scale - comprising an ion-exchange separation and a membrane-electrolysis step for the purpose of zero-waste regeneration of spent HCl pickling liquors originating from hot-dip galvanizing of common steels. It is aimed at the parallel regeneration of HCl and iron. Experiments revealed that iron can be electrodeposited at high current efficiencies by maintaining the following conditions: 0.04-0.08 M HCl, 500-1000 A/m², 20°C and stationary electrolyte in a conventional cell. Zinc in the solution did not disturb the deposition of iron, however it contaminated the product and it poisons the anion-exchange membrane required to tackle acidity during electrolysis. For a preliminary separation, anion-exchange tests were carried out to produce pure iron solutions. Beyond the equilibrium studies, column experiments were carried out showing that low flow rates of the loading solution and the ~1.5 M HCl eluent are essential for separation.

4:20 PM

Comprehensive Utilization of Zinc Leach Residues by Flotation - Reduction Roasting - Magnetic Separation Process: *Tao Jiang*¹; *Yuanbo Zhang*¹; *Zhucheng Huang*¹; *Guanghui Li*¹; *Yongbin Yang*¹; *Yufeng Guo*¹; *Bin Xu*¹; ¹Central South University

Zinc leach residues produced by hydrometallurgical zinc plant contain many valuable elements (zinc, gallium, germanium, silver, etc), while they have not been utilized effectively hitherto. In this paper, a new process of flotation-reduction roasting-magnetic separation to recover them is developed. The results show that, using Na₂S as conditioner, ammonium dibutyl dithiophosphate and SN-9 (assistant collector) as combined collector and terpenic oil as frother, if zinc leach residues with 523 g/t silver are floated at pH = 5.0, over 80% silver is recovered from the residues. When the flotation tailings are subjected to reduction roasting at 1100°C for 2 h, volatilization rates of zinc, lead and indium are over 96%. After roasted products are treated by wet-grinding and magnetic separation, recovery of gallium and germanium can reach 93-95%. The new process brings out no secondary pollution.

Hume Rothery Symposium: Multi-Component Alloy Thermodynamics: Alloy Physics

Sponsored by: The Minerals, Metals and Materials Society, TMS Electronic, Magnetic, and Photonic Materials Division, TMS: Alloy Phases Committee

Program Organizers: Y. Austin Chang, University of Wisconsin; Rainer Schmid-Fetzer, Clausthal University of Technology; Patrice E. A. Turchi, Lawrence Livermore National Laboratory

Monday PM
March 13, 2006

Room: 202A
Location: Henry B. Gonzalez Convention Ctr.

Session Chairs: Y. Austin Chang, University of Wisconsin; Patrice E. A. Turchi, Lawrence Livermore National Laboratory

2:00 PM Introductory Comments

2:05 PM Invited

Entropies of Formation and Mixing in Alloys: *William Alan Oates*¹; ¹University of Salford

Entropy often plays a major role in determining the relative stability of phases in a system at high temperatures. Some examples of where this role is particularly apparent will be presented. Methods which may be used for estimating the magnitude of the contributions to formation/mixing entropies will then be discussed. Special emphasis will be placed on models which can be of value in the calculation of formation/mixing entropies for real multi-component alloys and which are, therefore, of value in the calculation of phase diagrams for multi-component, multi-phase systems. The value of the cluster/site approximation for describing the configurational contributions in such systems will be emphasized and some recent developments in its application will be presented. Some consideration will also be given to methods suitable for the estimation of the magnitude of other contributions to formation/mixing entropies.

2:55 PM Invited

Application of First-Principles Methods in the Modeling of Multi-component Alloys: *Axel Van De Walle*¹; *Gautam Ghosh*¹; *Mark D. Asta*¹; ¹Northwestern University

This talk will review recent applications of first-principles methods in the modeling of multicomponent alloy phase stability. Our overall strategy involves the use of first-principles methods to augment thermodynamic databases with the aim of increasing the predictive capability of more traditional computational-thermodynamic models. In the Al-Ti-Zn system first-principles methods combined with a sublattice cluster-expansion formalism are used to find the optimal concentrations for stabilizing ternary two-phase fcc/L12 microstructures. For Al-Hf-Nb we demonstrate how first-principles calculations of the energies of stable and virtual compounds and solid solutions can facilitate CALPHAD modeling of ternary isothermal sections, with applications to the design of a high-temperature alloy. Finally, we discuss recent additions to the Alloy Theoretic Automated Toolkit (ATAT) which allow first-principles ternary cluster expansions to be formulated for use in deriving ternary ground-state compounds and thermodynamic properties. Applications of this methodology in Ni and Fe based alloys will be shown.

3:25 PM Break

3:45 PM Invited

Atomistic Modeling of Multicomponent Systems with Quantum Approximate Methods: *Guillermo Bozzolo*¹; ¹Ohio Aerospace Institute

The need to accelerate materials design programs based on economical and efficient modeling techniques provides the framework for the introduction of approximations in otherwise rigorous theoretical schemes. Several quantum approximate methods have been introduced through the years, bringing new opportunities for the efficient understanding of complex multicomponent alloys at the atomic level. As a promising example of the role that these methods might have in the development of complex systems, in this work we discuss the BFS method for alloys and its application to a variety of multicomponent systems for a detailed analysis of their defect and phase structure and their properties. Examples include

the study of the phase structure of new Ru-rich Ni-base superalloys, the role of multiple alloying additions in high temperature intermetallic alloys, and interfacial phenomena in nuclear materials, highlighting the benefits that can be obtained from introducing simple modeling techniques to the investigation of complex systems.

4:15 PM Invited

Theoretical Investigation of Phase Equilibria for a Metal-Hydrogen Alloy: *Tetsuo Mohri*¹; ¹Hokkaido University

Theoretical calculation for phase equilibria is attempted for metal-hydrogen alloy system. A particular focus is placed on the formation of superabundant vacancies which has been reported in various metal-hydrogen alloys. The amount of vacancies introduced in the system is nearly 10-20%. The key to understand this anomaly is the binding energy between hydrogen and vacancy. A simple statistical thermodynamics theory which takes this energy into account is successful to grasp the essence of the phenomenon. In the present study, we further consider the wide range of configurational correlation effects by employing Cluster Variation Method. A preliminary study is attempted based on the two dimensional square lattice with Lennard Jones type atomic interactions. The free energy is optimized with respect to volume in addition to cluster probabilities. The results indicate the clear dependences of vacancy concentration on the content of hydrogen.

4:45 PM Invited

When Putting More Physics into CALPHAD Results also into Flavoring Physics with CALPHAD: *Suzana G. Fries*¹; ¹SGF Scientific Consultancy

It is about 10 years ago that a call was done by W. A. Oates on the benefits of a more close cooperation between the different formalisms used by researchers interested in thermodynamic properties of solution materials. This closed interaction is being practised and although, in that time, the major gain was envisaged for the more pragmatic calphaders, nowadays it becomes clear that this pragmatism is not so crude and that theoretical methods can find inside the Calphad results some "realitycourse" where their predictions should lay. The progress done in these last years into the two directional linking (Calphad <->Physics) will be reported.

Lead Free Solder Implementation: Reliability, Alloy Development, and New Technology: Mechanical Behavior II: Creep

Sponsored by: The Minerals, Metals and Materials Society, TMS Electronic, Magnetic, and Photonic Materials Division, TMS: Electronic Packaging and Interconnection Materials Committee
Program Organizers: Nikhilesh Chawla, Arizona State University; Srinivas Chada, Medtronic; Sung K. Kang, IBM Corporation; Kwang-Lung Lin, National Cheng Kung University; James Lucas, Michigan State University; Laura J. Turbini, University of Toronto

Monday PM Room: 214A
March 13, 2006 Location: Henry B. Gonzalez Convention Ctr.

Session Chairs: James Perry Lucas, Michigan State University; Kejun Zeng, Texas Instruments

2:00 PM Invited

Creep and Mechanical Properties of Sn-Based Alloys for Microelectronics Solder Applications Using Impression and Other Test Techniques: G. S. Murthy¹; S. Devaki Rani²; V. V. Subrahmanyam¹; K. Linga Murty³; ¹Andhra University; ²Jawaharlal Nehru Technological University; ³North Carolina State University

A number of Sn-based alloys are selected as possible candidate materials to replace Pb-based alloys for microelectronics interconnects and solder applications. Many binary alloys along with a ternary Sn-57Bi-1.3Zn were examined along with Pb-Sn eutectic (for comparison) with emphasis on impression creep characteristics. In addition, the mechanical properties were determined along with wettability by evaluating the contact angles and substrate contact areas. In addition to the standard creep char-

acteristics such as stress exponent (n) and activation enthalpy (H), the dependence of impression velocity (strain-rate) on impression size (diameter) were determined to assist in the interpretation of the underlying deformation mechanism(s). From these studies, it can be concluded that Sn-3.5Ag, Sn-9Zn and Sn-58Bi alloys are suitable substitutes for high temperature applications (such as for automotive technologies) while Sn-57Bi-1.3Zn alloy can be an effective non-toxic substitute for Pb-Sn eutectic generally considered for normal operating conditions. A summary of ball indentation, lap shear as well as solder bump array (33x33) shear tests will be presented.

2:25 PM Invited

Creep Behavior of Lead Free Solder Interconnects: Creep Testing and Constitutive Modeling: *Indranath Dutta*¹; Chanman Park¹; Deng Pan¹; Susheel Jadhav²; Ravi Mahajan²; ¹U.S. Naval Postgraduate School; ²Intel Corporation

The creep behavior of ball grid array (BGA) or flip-chip (FC) solder joints during thermo-mechanical cycling often limits the reliability of microelectronic packages. In this paper, we present experimental creep results on pure Sn and two different compositions of SnAgCu solders, based on impression creep tests on BGA balls, with emphasis on microstructural effects on creep. Based on the above observations, a microstructurally-adaptive creep model for solder interconnects undergoing in situ strain-enhanced coarsening will be presented. This model accounts for the effects of microstructural aging on the creep response of solder joints, and is capable of adjusting itself as solder joint microstructures evolve during service. Data on experimental determination of the relevant coarsening kinetics parameters for a SnAgCu solder will also be presented. Supported by NSF, SRC, and INTEL Corp.

2:50 PM

Microstructure and Mechanical Behavior of Novel Rare Earth-Containing Pb-Free Solders: *Martha A. Dudek*¹; Rajen S. Sidhu¹; Nikhilesh Chawla¹; M. Renavikar²; ¹Arizona State University; ²Intel Corporation

Currently several Pb-free material systems are available as replacements for traditional Pb-based solders in microelectronic packaging, including near eutectic combinations of Sn-rich alloys. Although these materials have been shown to have superior mechanical properties when compared to the Pb-Sn system, much work remains in developing these materials for electronic packaging. Small additions of rare-earth elements have been shown to improve the mechanical properties of Sn-rich solder. In this work we have investigated the effect of the addition of lanthanum (0.5 wt%) on the shear strength and creep behavior of a Sn-3.9Ag-0.7Cu alloy. Microstructure characterization of as-processed and reflowed samples was conducted in order to determine the influence of LaSn₃ intermetallics on the mechanical properties. The effect of LaSn₃ intermetallics in refining the microstructure of the Sn-Ag-Cu alloy and their role in creep resistance will be discussed.

3:10 PM

Nanoindentation on SnAgCu and SnCu Lead-Free Solder and Analysis: *Luhua Xu*¹; John H. L. Pang¹; ¹Nanyang Technological University

Nano-indentation characterization on SnAgCu and SnCu solder was reported. The solder creep effect on the measured result was analyzed. Nanoindentation test with different maximum loads from 6 to 20mN, time-to-maximum-load from 1 to 100 seconds, hold time from 5 to 400 seconds, were studied. The penetration depth increases vs load and hold time due to creep effect was expressed with an empirical relationship. The pop-in phenomena was observed from load-displacement curve in the first 50-200nm penetration, which is related Sn lattice and boundary sliding. The unloading curve after different holding time were compared at the upper part, the unloading curves begin at higher depths for longer hold periods. It can be clearly seen that the unloading curve shows a bowing towards higher depth if the hold period is too short. An improved method was proposed for measuring Solder's Young's modulus, where the influence of creep can be neglected.

3:30 PM

Effects of Interfacial Intermetallics on Mechanical and Creep Properties on Thin Pb-Free Alloy Solder Joints: *James P. Lucas*¹; ¹Michigan State University

Minimizing electronic packages also demands a concomitant thickness reduction of the solder joint itself that provides both mechanical and electrical connections of components to the substrate. For thin solder joints, the amount of interfacial intermetallic compound (IMC) increases in comparison to the actual solder volume in the joint. With aging isothermal and/or thermo-mechanical aging, the IMC layer may grow to comprise 80-90 percent of the solder joint volume. Nanoindentation testing (NIT) was used to investigate the mechanical properties of interfacial IMCs in ~50 μm-thick solder joints of several Sn-based eutectic and near-eutectic Pb-free solder alloys. Creep studies were performed on as-reflow and aged solder joints to determine the influence of the IMC layer thickness and compositional changes on resultant creep behavior. This investigation reports on the propensity of the IMC layer to affect subsequent mechanical properties in thin Pb-free solder joints.

3:50 PM Break

4:00 PM

Stress Relaxation of Sn3.5Ag Eutectic Alloy: *Fuqian Yang*¹; Lingling Peng¹; Kenji Okazaki¹; ¹University of Kentucky

The localized stress relaxation of a Sn3.5Ag eutectic alloy was studied by using the impression technique in the temperature range of 393-488 K. The impression was made at prescribed indentation load and stopped at a certain depth of the indentation. The stress relaxation at different temperatures was recorded as a function of time. Using the dislocation dynamics, a relation between the punching stress and the relaxation stress rate was established. It was found that the dislocation velocity-stress exponent for the motion of dislocations is in a narrow range of 6.5 – 5.1 but decreases linearly with increasing temperature. The activation energy for the localized stress relaxation of Sn3.5Ag alloy is in the range from 38.1 to 48.4 kJ/mol. This research was supported by NSF through a grant DMR-0211706 monitored by Drs. Guebre Tessema and Bruce A. MacDonald.

4:20 PM

Effects of Specimen Volume of Solder on Creep Deformation: *Sung Bum Kim*¹; Jin Yu¹; ¹Korea Advanced Institute of Science and Technology

Creep characteristics of solders are very important to estimate real life time when the solders are subjected to thermal fatigue environment. However, great inconsistencies exist among creep data in literature due to the differences on specimen volume. As solder volume is smaller, the microstructural change of solders will happen because of higher solidification rate and effects of pad will be greater. In the present work, creep properties of Sn-3.5Ag solder alloy were investigated at 373K. To produce lap shear creep test samples, two FR4 PCBs with Cu pad were reflowed using Sn-3.5Ag alloy balls with various diameters. Moreover, double shear creep test specimen with uniformly shaped solder joints (uniform shear specimen) were also produced using three Cu plates. Experiments show that the minimum strain rate of lap shear specimen using 760μm is lower than that of uniform shear specimen by a factor of 10 due to different failure mechanism.

4:40 PM

Corrosion Resistance of Sn-Ag-Cu Solder Alloys: *Bo Li*¹; Bin Zong¹; Yaowu Shi¹; Yongping Lei¹; Zhidong Xia¹; Fu Guo¹; ¹Beijing University of Technology

The anti-corrosion behavior of Sn-Ag-Cu solder alloys was investigated in the present research. Corrosion resistance tests were conducted in a 5% NaCl solution. The corrosion resistance of Sn-Ag-Cu solder was quantified and compared with Sn-Zn and Sn-Pb solders according to the polarization curve and mass loss of the solder alloys. Morphological features of these alloys were characterized. The mechanism of causing such morphology change due to corrosion was analyzed from the phases formed in the microstructure of Sn-Ag-Cu, Sn-Zn, and Sn-Pb solders, respectively. The effect of rare-earth element addition on the corrosion resistance of Sn-Ag-Cu solder alloy was also investigated.

5:00 PM

Physics Based Reliability Model to Predict Solder Thermal Interface Material Performance in Microelectronic Packages: *Arun Raman*¹; Shubhada Sahasrabudhe¹; Vikram Bala¹; Sankara Subramanian¹; Ashish Gupta¹; Carl Deppisch¹; Sridhar Narasimhan¹; ¹Intel Corporation

Metal-based solder thermal interface material (TIM) is utilized in microelectronic packages for efficient thermal performance. Temperature cycling can affect solder TIM performance. This work focuses on development of a predictive phenomenological reliability model for solder TIM degradation. Metallization of integrated heat spreader (IHS) and backside of Si die facilitates adhesion of solder TIM to both surfaces through the formation of metallurgical bonds. Temperature cycling causes interfacial degradation between intermetallic compounds that are created and bulk solder, leading to thermal performance deterioration. In this study, finite element models based on cohesive elements at the interfaces were developed to predict damage growth through temperature cycling and subsequently to predict thermal performance using thermal finite element models. Validation was performed on experimental builds, using techniques such as acoustic microscopy and electron microscopy. Based on the degradation physics, this reliability model enables solder TIM life prediction eliminating the need for extensive empirical builds.

5:20 PM

Examination of the Microstructure and Failure Mechanisms of Pb Free Solder Joints: *Eric J. Cotts*¹; L. P. Lehman¹; Peter Borgesen²; ¹Binghamton University; ²Universal Instruments Corporation

The microstructure, mechanical properties and reliabilities of ball grid array (BGA), chip scale packaging (CSP), and flip chip components with SnAgCu solder joints were examined as a function of undercooling, and subsequent thermal cycling. Assemblies were removed for cross sectioning and microstructural characterization after different degrees of undercooling (during the initial reflow profile), and later, at various stages of cycling. The microstructures of these different samples were examined by means of optical and scanning electron microscopy. The Sn dendrite arm width was observed to monotonically increase with solder ball diameter. Polarized light microscopy provided delineation of Sn grains, while electron microscopy with EDS provided compositional analysis. The variation in the thermomechanical loads with solder joint location across an area array allowed detailed study of a range of temperature-damage combinations.

5:40 PM

Flip Chip Bonding on Glass and Plastic Substrates Using Sn Bumps and NCAs: *Zhigang Chen*¹; Bae Yong Kim¹; Sang Mok Lee¹; Young-Ho Kim¹; ¹Hanyang University

This study presented the reliability results of NCA applied COG and COP processes. PES was selected as the plastic substrate. Sn bumps were employed especially for its excellent deformation ability, which was capable of compensating for nonuniformity of the bumps height, and being featured as low cost flip chip bonding technique. Thermal cycling tests were carried out between temperatures of 0°C and 100°C. The COG specimens sustained by 1000 cycles without failure and the variation of resistance followed an increasing trend. Comparatively, the average contact resistance of COP specimens descended in the early stage of the cycling test and then leveled off. This beneficial change is owing to the postcuring of NCA during thermal cycling and flexibility of PES, as well as further and sufficient interdiffusion between bumps and pad. This work was supported by Korea Research Foundation Grant(KRF-2004-005-000164).

Magnesium Technology 2006: Automotive and Other Applications

Sponsored by: International Magnesium Association, TMS Light Metals Division, TMS: Magnesium Committee

Program Organizers: Alan A. Luo, General Motors Corporation; Neale R. Neelameggham, US Magnesium LLC; Randy S. Beals, DaimlerChrysler Corporation

Monday PM Room: 6B
March 13, 2006 Location: Henry B. Gonzalez Convention Ctr.

Session Chairs: Randy S. Beals, DaimlerChrysler Corporation; Gerald S. Cole, LightWeightStrategies LLC

2:00 PM

Building a Mg Intensive Engine: A Progress Report on the USAMP Mg Powertrain Cast Components Project: *Joy A. Hines*¹; John E. Allison¹; Robert C. McCune¹; Randy S. Beals²; Lawrence Kopka²; Bob R. Powell³; Larry Ouimet³; William L. Miller³; Peter P. Ried⁴; ¹Ford Motor Company; ²DaimlerChrysler; ³General Motors Corporation; ⁴Ried and Associates, LLC

Over the past five years, USAMP has brought together representatives from Daimler-Chrysler, General Motors, Ford Motor Company and over 40 other participating companies from the Mg casting industry to create and test a low cost Mg alloy engine that would achieve a 15–20% weight savings without compromising performance as compared with an equivalent Al engine. In this program, a 2.5L Ford Duratec engine assembly was modified to create a Mg version. The block, oil pan, front cover, and bed plate were redesigned to take advantage of the properties of both HPDC and sand cast Mg creep resistant alloys. This talk will discuss the alloy selection process and the casting and testing of these new Mg-variant components. This talk will also examine the lessons learned and implications of this pre-competitive technology for future applications.

2:20 PM

AM-HP2: A New Magnesium High Pressure Diecasting Alloy for Automotive Powertrain Applications: *Colleen Bettles*¹; Mark Gibson¹; Gordon Dunlop²; Morris Murray²; ¹CAST Cooperative Research Centre; ²Advanced Magnesium Technologies

AM-HP2 is a new magnesium diecasting alloy that has been specially developed to provide good diecastability and creep resistance at temperatures in the range 150–200°C. This temperature range is important for many automotive powertrain applications. AM-HP2 was developed to have similar properties to the very successful sandcasting alloy AM-SC1 but with modifications to ensure excellent diecastability. The alloy was developed in recognition of high pressure die casting's advantages of higher production rates and lower manufacturing costs compared to sand casting. AM-SC1 is most suitable for production of prototypes and small production runs (as for the V6 engine block of the USCAR MPCC program) while AM-HP2 provides similar properties in the diecast condition. This paper compares the properties of AM-HP2 with other commercially available high temperature creep resistant magnesium alloys.

2:40 PM

Wrought Magnesium Alloys for Structural Applications: *Alan A. Luo*¹; Anil K. Sachdev¹; ¹General Motors Corporation

While high-pressure die casting is the dominant process for current magnesium applications, wrought magnesium alloys are receiving increasing attention from academia and industries. As magnesium is expanding to more critical structural applications in automotive body and chassis systems, there is a great need for developing wrought magnesium products to provide improved mechanical and physical properties and corrosion resistance. This paper summarizes recent wrought magnesium alloy development, grain refinement in billet production, extrusion process optimization, and moderate temperature bending and forming of magnesium tubes. An extensive investigation was carried out to determine the effect of microstructure on the deformation mechanisms of wrought magnesium alloys at a moderate temperature range (100–200°C). The roles of

strain-hardening, twinning and slip in deformation and formability of magnesium alloys will be discussed.

3:00 PM

Fabrication of Carbon Long Fibre Reinforced Magnesium Parts in High Pressure Die Casting: *Gerald Klaus*¹; Christian Oberschelp¹; Martin Fehlbier¹; Andreas Bührig-Polaczek¹; Jens Werner²; Werner Hufenbach²; ¹Aachen University; ²Dresden University

There is an increasing demand for light weight structural parts, which are able to fulfill increased high temperature properties combined with advanced wear resistance. These requirements can be achieved by carbon long fibre reinforced magnesium parts. Within the development of an industrial scale process for fibre infiltration and integration of preinfiltrated metal matrix composites, a suitable high pressure die casting method is under evaluation at the facilities of the Foundry Institute of RWTH Aachen University. The special challenge of high melt velocity and pressure is taken into account and requires innovative solutions, brought forward in this project. A new electric fibre heating system has been implemented in the process to assist infiltration, as well as a new special two step clamping device, which ensures proper fit. As a great advantage of this new method, the fibre preforms are preheated in the closed die under protective atmosphere/vacuum, till casting takes places.

3:40 PM

Machining of Hybrid Reinforced Mg-MMCs Using Abrasive Water Jetting: *Eckhard Aust*¹; Maxim Elsaesser¹; *Norbert Hort*¹; Wolfgang Limberg¹; ¹GKSS Research Centre

Magnesium based Metal Matrix Composites (MMCs) reinforced by a combination of short Al₂O₃-fibres and SiC-particles are promising constructional materials due to the low density and thermal expansion, high creep and wear resistance. Such a material is the hybrid reinforced magnesium alloy AE42, which is produced by the melt infiltration of fibre-particle preforms in the squeeze casting process. Many problems arise by machining these preforms with common machining tools because of the high wear resistance caused by the ceramic reinforcement. Solutions are only expensive tools with cutting edges made of polycrystalline diamonds or CVD-diamond coatings. This work is focussed on the application of abrasive water jet cutting for machining these wear resistant MMCs. Cutting tests were performed at MMC-specimens with thickness of 2 – 25 mm. Experimental results are presented which clearly indicate the high potential and efficiency of the abrasive water jet for machining MMCs.

3:20 PM Break

4:00 PM

The Influence of Mechanical Activation on the Process of Thermal Reduction of SiO₂ by Mg Powder: *Nshan Hovhannes Zulumyan*¹; Agasy Torosyan¹; Anna Rafael Isahakyan¹; Zaruhi Hayk Hovhannisyanyan¹; ¹IGIC NAS RA

Solid state chemical reaction in SiO₂ – Al stoichiometric mixture induced by heat treatment at the temperature 350–400°C has been investigated, depending on the time of mixture's preliminary mechanical processing and activation. It's necessary to note that SiO₂ is an aqua silica gel extracted from serpentinites using a new thermo-chemical method of the serpentinous ultra basic rocks treatment. Different thermal analysis (DTA) and X-ray diffraction (XRD) have shown that the displacement reaction is occurring with forming mainly nanocrystalline magnesium oxide (MgO) and silicon (Si) and partly forsterite (Mg₂SiO₄). Magnesium oxide and forsterite can be easily removed by means of decantation. The quantities of forming products depend on the parameters of mechanical processing. Optimal parameters have been found in order to provide occurring reaction.

4:20 PM Cancelled

Hydrogen Production by Using Ni-Rich AZ91D Recycled Ingot

4:40 PM

Synthesis of Magnesium Diboride Powder by Self-Propagating High-Temperature: *Huimin Lu*¹; Huanqing Han¹; Ruixin Ma¹; Yongheng Wang¹; ¹University of Science and Technology Beijing

Self-propagating high-temperature synthesis (SHS) method was used to fabricate MgB₂ powder from Mg-B system. In this paper, the reaction process of Mg and B was studied by thermodynamic calculation, X-ray

diffract-meter and micro-image analyzer. These results show that the single-phase MgB₂ can be synthesized by self-propagating high-temperature synthesis method. When Mg and B react, Mg firstly melts and then reacts with B to form MgB₂; but if the synthesis temperature is too high, MgB₂ can decompose into MgB₄ and Mg. These synthesized MgB₂ particles appear random geometry and fine crystal grain. At normal pressure, the decomposition temperature of MgB₂ is less than 1320K; but higher gas pressure is beneficial to lifting the decomposition temperature of MgB₂. And at high temperature, there are these phenomena that MgB₂ can also exist or MgB₂ directly decomposes into Mg and amorphous B.

5:00 PM

Surface Cladding of Magnesium Alloy Castings Using Nd:YAG Laser: *Xinjin Cao*¹; *Min Xiao*¹; *Mohammad Jahazi*¹; ¹Institute for Aerospace Research

Magnesium alloys have low hardness, wear and corrosion resistance. With their increased applications in aerospace, aircraft, automotive, electronics and other industries, the surface cladding and repair of magnesium alloy components will become significant. The high heat-input energy associated with conventional arc processes, however, results in large variations in metallurgical structures, large heat affected zone and fusion zone, high shrinkage, high evaporative rates and loss of alloying elements, high residual stresses and distortions. Compared with the arc techniques, high energy-density laser beam has the potential to avoid such shortcomings and thus become an important technique to clad and repair magnesium components. The objective of the present study is to investigate the possibility of laser cladding and repair for ZE41A-T5 sand castings using EZ33A welding wires. This presentation will report on the progress in laser cladding obtained in the Aerospace Manufacturing Technology Center of the NRC Institute for Aerospace Research.

Magnesium Technology 2006: Casting and Solidification I

Sponsored by: International Magnesium Association, TMS Light Metals Division, TMS: Magnesium Committee

Program Organizers: Alan A. Luo, General Motors Corporation; Neale R. Neelameggham, US Magnesium LLC; Randy S. Beals, DaimlerChrysler Corporation

Monday PM Room: 6A
 March 13, 2006 Location: Henry B. Gonzalez Convention Ctr.

Session Chairs: John Hryn, Argonne National Laboratory; Helmut Kaufmann, LKR ARC Leichtmetallkompetenzzentrum

2:00 PM

A Directional Solidification Study of Mg-4Al and AXJ530 Alloys: *Chuan Zhang*¹; *Dong Ma*¹; *Kaisheng Wu*²; *Hongbo Cao*¹; *Guoping Cao*¹; *Sindo Kou*¹; *Y. Austin Chang*¹; ¹University of Wisconsin; ²CompuTherm, LLC

A binary magnesium alloy with 4 wt% Al (Mg-4Al) and a commercial alloy AXJ530 with a base composition of Mg-5Al-3Ca have been investigated using the directional solidification technique. The ability to producing uniform microstructures in directional solidification enables us to correlate the formation of the microstructure and its characteristic length scales (e.g. primary dendrite arm spacing) quantitatively with processing parameters, such as the growth rate (or the solidification front speed that scales with the applied cooling rate). Notably a wide range of cooling rates from 0.02 to 4 K/s are attainable by our DS apparatus, which correspond to the growth rates from 5 to 1000 mm/s at a fixed temperature gradient of 4.0 K/mm. In this presentation, we will report the experimental results obtained as well as the theoretical analysis.

2:20 PM

Experimental Study of Vacuum Die Casting Process of AZ91D Magnesium Alloy: *Bo Hu*¹; *Shou-Mei Xiong*¹; *Masayuki Murakami*²; *Yoshihide Matsumoto*²; *Shingo Ikeda*²; ¹Tsinghua University; ²TOYO Machinery and Metal Company Ltd.

The effect of operation conditions in vacuum die casting process on the porosity and mechanical properties of die cast parts of AZ91 alloy were investigated. Standard tensile test specimens and step-shape test plates were cast on a TOYO BD-650-V4-N cold chamber die casting machine. Five vacuum levels from 5kPa to 80kPa, as well as the non-vacuum condition, were used and five levels of casting pressure from 22.7MPa to 66.7MPa were applied during the experiments. Other operation conditions were kept constant. Pressure measurements at different positions inside the cavity were made during the work cycle. Density, tensile strength and heat treatment results were analyzed. Relationship between mechanical properties of the cast parts and process parameters were discussed and the result show that vacuum application to the die casting process of AZ91D magnesium alloy could not only improve the mechanical properties of castings but also reduce the tonnage requirement of the equipment.

2:40 PM

Hot Cracking Susceptibility of Binary Mg-Al Alloys: *Guoping Cao*¹; *Sindo Kou*¹; *Y. Austin Chang*¹; ¹University of Wisconsin

The susceptibility of binary Mg-Al alloys in permanent mold casting was tested, including Mg-0.25Al, Mg-0.6Al, Mg-1Al, Mg2Al, Mg-4Al and Mg-8Al (all in wt %). A steel mold was used for constrained rod casting, in which rods of various lengths were cast with sudden enlargement at both ends of each rod to prevent it from free contraction during solidification and thus induce hot cracking. The hot cracking susceptibility was evaluated based on the widths and locations of the cracks observed. The curve of crack susceptibility vs. Al content was determined and compared with previous curves based on ring casting in steel molds and constrained rod casting in sand molds. The Scheil model of solidification was used to calculate the curves of temperature vs. fraction solid of the alloys. Possible correlations between the crack susceptibility curve and the curves of temperature vs. fraction solid will be explored.

3:00 PM

Phase Equilibria of Mg-Al-Ca Ternary System at 773 and 673 K: *Akane Suzuki*¹; *Nicholas D. Saddock*¹; *J. Wayne Jones*¹; *Tresa M. Pollock*¹; ¹University of Michigan

Isothermal sections of the Mg-Al-Ca ternary system at 773 and 673 K were determined with consideration of the existence of the ternary (Mg, Al)₂Ca compound with C36 structure. Alloys with compositions Mg-(0~18.8)Al-(1.8~13.4)Ca and Mg-(0~66.7)Al-33.3Ca (at%) were equilibrated and analyzed by EPMA and TEM. The C36 phase exists between C14 (Mg₂Ca) and C15 (Al₂Ca) phases, and its stoichiometry is close to Mg₂Al₄Ca₃. The α-Mg phase equilibrates with C14 and C36 phases at 773 K, but with C14, C15 and β phases at 673 K. This is due to the decomposition of the C36 phase into C14 and C15 phases between these temperatures. Each intermetallic phase has significant solid-solubility in the ternary system. The microstructural stability in the vicinity of the α-Mg grain boundaries will be also discussed in terms of relative change in the eutectic structures containing C14, C36 or β phases during annealing.

3:20 PM

Preliminary Investigation on the Formation and Grain Refinement of Particles in Mg-Al Alloys: *G. Klösch*¹; *B. J. McKay*¹; *Peter Schumacher*²; ¹Austrian Foundry Research Institute; ²University of Leoben

Grain refinement with Zirconium addition is commonly used for non aluminum containing Magnesium alloys. However, Mg-Al alloys with Zirconium addition are assumed to be affected by a poisoning effect leading to the formation of Al₃Zr. The present paper describes the effects on the grain size of Mg-Al alloys by refinement with refractory metals (Zr, Ti) and in-situ formed ZrB₂ particles. Due to the excellent crystallographic orientation compared to Mg and the high thermal stability of ZrB₂ grain refinement is observed when sufficient growth restriction by Ti and Zr is present. This paper gives preliminary results on the formation, nucleation and poisoning mechanism in Mg-Al alloys with Zr addition. Moreover, particles were added to the Mg-Al melt to compare the efficiency of the in-situ formed ZrB₂ particles. Samples were taken according to the TPI test procedure and grain size measured with the intersect method.

3:40 PM

Property Variation in Thin Walled Magnesium Die Cast Components: *Saravanan Subramanian*¹; *Patrick Blanchard*¹; *Nicholas Warrior*²; *James DeVries*¹; ¹Ford Motor Company; ²University of Nottingham

Utilization of magnesium within vehicle design offers substantial opportunity to reduce mass. This has resulted in a wide range of automotive applications. More recently the scope of application has been extended to include components that are considered crash critical. This introduces the problem of how to design effectively using a process that is reported to produce parts that exhibit large local variations in part properties. In order to understand the key factors that contribute to this, a micro-structural examination was performed on a high pressure die cast component to investigate the root cause of property variation. Properties of interest include yield strength, failure strain and bulk density. This paper discusses the influences of microstructure and porosity on mechanical property variation, and identifies key factors that influence final performance. Further discussion also includes proposed methods of reducing property variation using advances in process control.

4:00 PM Break

4:20 PM

Solidification Characteristics and Creep of Permanent Mold Cast Mg-Al-X Ternary Alloys: *Nicholas D. Saddock*¹; Akane Suzuki¹; Jessica R. TerBush¹; Eric C. Heining¹; J. Wayne Jones¹; Tresa M. Pollock¹; ¹University of Michigan

A permanent mold casting technique has been developed to cast tensile creep specimens of Mg – Al – X: (Ca, Sr, Ce, La) ternary alloys. Solidification behavior and microstructure have been analyzed in each of these alloys. Electron microprobe analysis (EPMA) was conducted on as-cast Mg – 4 Al – 4 X alloys (wt.%) to investigate the partitioning of each alloying element to the α grain interior and grain boundary regions. Segregation behavior during solidification and, in particular, the influence of ternary additions on aluminum partitioning was described using a modified Scheil model. Creep behavior of the permanent mold cast alloys was studied and the role of grain boundary microstructure on creep behavior in these alloys will be described.

4:40 PM

Phenomena of Formation of Gas Induced Shrinkage Porosity in Pressure Die-Cast Mg-Alloys: *Soon Gi Lee*¹; Arun M. Gokhale¹; ¹Georgia Institute of Technology

It has been known that the formation of gas and shrinkage porosity has different dependencies on the process conditions, and consequently, the gas and shrinkage pores are usually regarded as independent microstructural attributes. In this contribution, it is shown that in high-pressure die-castings gas pores can lead to the formation of shrinkage porosity under specific conditions. This is because the air/gas in the gas porosity is an efficient heat-insulating medium. Therefore, the presence of gas porosity can retard the heat transfer in the liquid melt as compared to similar regions without gas porosity. Consequently, the local solidification rate is lower in such region, leading to shrinkage porosity formation. The two and three-dimensional (3D) microstructural observations using digital image analysis and numerical simulation for heat transfer support such a hypothesis. Further, the finite element (FE)-based simulations have been performed on the 3D microstructures to reveal the variations of local stress caused by gas induced shrinkage porosity.

5:00 PM

Overview of the Magnesium Casting Industry Technology Roadmap: The Road to 2020: *John N. Hryn*¹; Steve Robison²; David J. Weiss³; Bruce Cox⁴; Katie Jereza⁵; Ross Brindle⁵; ¹Argonne National Laboratory; ²American Foundry Society; ³ECK Industries Inc; ⁴Daimler Chrysler Corporation; ⁵Energetics Incorporated

The American Foundry Society Magnesium Division has led an effort to develop the Magnesium Casting Industry Technology Roadmap. Completed in September 2005, the Roadmap outlines the industry's strategic technology agenda for the next 15 years, focusing on three principal components: (1) improved process technologies that lead to greater productivity and efficiency while delivering consistent, high-quality castings at competitive costs; (2) enhanced information management and sharing to accelerate technological innovation and transfer, and, (3) increased infrastructure development. Experts from across the magnesium casting industry identified R&D needs in each of these areas, indicated the highest priorities, and stratified these needs by time frame. In total, the Roadmap identifies more than 60 R&D needs and offers detailed action plans for

the six highest-priority activities. This paper highlights key concepts presented in the Roadmap.

Materials in Clean Power Systems: Applications, Corrosion, and Protection: Hydrogen Separation, Delivery, and Materials Issues in Clean Power Plants

Sponsored by: The Minerals, Metals and Materials Society, TMS Structural Materials Division, TMS/ASM: Corrosion and Environmental Effects Committee

Program Organizers: Zhenguo Gary Yang, Pacific Northwest National Laboratory; K. Scott Weil, Pacific Northwest National Laboratory; Michael P. Brady, Oak Ridge National Laboratory

Monday PM
March 13, 2006

Room: 212B
Location: Henry B. Gonzalez Convention Ctr.

Session Chairs: Iver E. Anderson, Iowa State University; Ken Natesan, Argonne National Laboratory

2:00 PM Invited

Inorganic Membranes for Energy-Related Gas and Water Purification: *Henk Verweij*¹; ¹Ohio State University

Inorganic membranes consist of a stand-alone or supported material with special transport properties, able to operate at elevated temperatures and pressures. Relevant separations that can be conducted with inorganic membranes are H₂, H₂O and O₂ from other gases, and water purification. Separation of CO₂ from other gases is currently considered. Inorganic membranes are classified according to the presence and size of connected porosity. Dense membranes have 100% selectivity for H₂ and O₂, and acceptable flux at high temperature. Micro-porous membranes have <2 nm pores and combine high selectivity with fairly high fluxes at lower temperatures. Meso-porous membranes have 2-50 nm pores and have a good thermo-chemical stability, moderate selectivity and very high fluxes over a wide temperature range. To make inorganic membranes a viable option the research focus must be directed towards thermochemical stability and operation at relevant conditions, and development of <100 nm defect-free supported membrane structures.

2:30 PM Invited

Materials for Hydrogen Delivery: Embrittlement Problems and Remediation: *Petros Sofronis*¹; I. M. Robertson¹; ¹University of Illinois, Urbana-Champaign

The technology of large scale hydrogen transmission from central production facilities to refueling stations and stationary power sites is at present undeveloped. Among the problems which confront the implementation of this technology is the deleterious effect of hydrogen on structural material properties, in particular at gas pressure of 1000 psi which is the desirable transmission pressure suggested by economic studies for efficient transport. To understand the mechanisms of hydrogen embrittlement our approach integrates mechanical property testing, TEM observations, and finite element modeling. A discussion is presented on how we can develop and verify a lifetime prediction methodology for failure of materials used for pipelines and welds exposed to high-pressure hydrogen. Development of such predictive capability and strategies is of paramount importance to the rapid assessment of using the natural-gas pipeline distribution system for hydrogen transport and of the susceptibility of new alloys tailored for use in the new hydrogen economy.

3:00 PM

Surface Engineering of Sliding Contacts in the Hydrogen Service Environment: *James D. Holbery*¹; Peter Blau²; Laura Riester²; ¹Pacific Northwest National Laboratory; ²Oak Ridge National Laboratory

Sliding metal surface contacts within a 100% Hydrogen environment poses a service challenge due to the hydride formation at the surface causing surface impingement resulting in an increased material-pair friction coefficient. In addition, material integrity at the surface interface will be altered as a function of Hydrogen exposure. In order to begin to understand material behavior in the Hydrogen service environment, we have

constructed a pressure vessel capable of 100% exposure at pressures up to 31 MPa and temperatures as high as 100°C for durations exceeding several hundred hours. In addition, we have developed the ability to measure sliding contact friction utilizing Friction Force Microscopy within a 100% Hydrogen environment, the first such instrument configuration known to the authors at this time. As a result, we have analyzed a series of material surfaces to determine the degradation of surface properties due to Hydrogen exposure. By comparing these results with localized surface modulus properties developed utilizing nanoindentation and other analytical results, we will present data that has enabled us to begin to understand the impact of hydride formation on material sliding contacts that will serve a critical role in transporting, distributing, combusting, and managing Hydrogen.

3:25 PM

Hydrogen-Rich Gas Production from Gasoline in a Short Contact Time Catalytic Reactor: *Ludmilla Bobrova*¹; *Ilya Zolotarsky*¹; *Vladislav Sadykov*¹; *Vladimir Sobyandin*¹; ¹Boreskov Institute of Catalysis

The research concerns the problems emerged from a short contact time adiabatic reactor operation in a pilot plant scale. Hydrogen-rich gas was generated by selective catalytic oxidation of isooctane and gasoline over original monolithic catalysts with the different supports. Thermodynamic analysis was employed with a purpose of determining the operational parameters, maximum hydrogen yield, and adiabatic temperature rise available. Gasoline, which contains 191 types of hydrocarbons, was simulated by a mixture of 28 organic compounds. It was demonstrated, that over the range of operational parameters required for syngas generation, equilibrium synthesis gas was produced over the catalysts employed. However, some drawbacks can make the main catalytic process being complicated. Pre-reforming of fuel with releasing of some chemical energy before the catalytic monolith can occur in reactor. Breakthrough of the feed arises near the reactor wall in a certain case. Feed composition, superficial velocity and reactor design features affect the phenomena mentioned.

3:50 PM Break

4:05 PM Invited

High-Temperature Materials Issues in Syngas/Hydrogen-Fired Turbines: *Ian G. Wright*¹; *Thomas B. Gibbons*²; *Adrian S. Sabau*¹; *Bruce A. Pint*¹; ¹UT-Battelle; ²Consultant

The combination of gasification technology with a gas turbine combined-cycle system can produce electricity from coal in a significantly more environmentally-friendly way, and at higher efficiencies than are possible with the technologies currently deployed. Because coal contains more carbon, and a higher level (and much wider range) of impurities than natural gas, there are challenges to be met to provide a sufficiently clean combustion process to allow the reliable operation of the gas turbine at the high temperatures needed for maximum efficiency. This paper addresses some specific issues associated with the durability of the hot gas path components in the gas turbine resulting from (1) differences in the thermal environment when combusting natural gas, syngas, or hydrogen-enriched syngas; (2) the potential for deposition, erosion, and/or corrosion when firing syngas; and (3) the tendency for increased interdiffusion of any protective metallic coating with the alloy substrate when operating at high temperatures.

4:35 PM Invited

Advanced Alloys for Compact, High-Efficiency, High-Temperature Heat-Exchangers: *Philip J. Maziasz*¹; ¹Oak Ridge National Laboratory

ORNL has for several years focused on the behavior and performance improvements of sheets and foils of various alloys for compact heat-exchangers (recuperators) for advanced microturbines. Performance and reliability of such thin sections are challenged at 650-750°C by fine grain size causing excessive creep, and moisture effects greatly enhancing oxidation attack in exhaust gas environments. Alloys have been identified which can have very good properties for such heat-exchangers, with careful control of microstructure during processing, including alloy 625, HR120 and the new AL20-25+Nb. These alloys, or the mechanistic understanding behind their behavior, are also applicable to the heat-exchanger technology needed for fuel cell or other high-temperature, clean-energy applications. Research at ORNL is sponsored by the U.S. Department of Energy, Assistant Secretary for Energy Efficiency and Renewable Energy,

Office of Power Technologies, Microturbine Materials Program, under contract DE-AC05-00OR22725 with UT-Battelle, LLC.

5:05 PM

Effect of Atmosphere Composition on the High Temperature Oxidation of Chromia Forming Alloys: *Michael Haensel*¹; *Emmanuel Essuman*¹; *Joanna Zurek*¹; *Marek Michalik*¹; *Lorenz Singheiser*¹; *Willem J. Quadackers*¹; ¹Forschungszentrum Juelich

The oxidation behaviour of pure chromium, Ni25Cr and the NiCr ODS alloy MA745 during isothermal exposure in Ar-O₂- and Ar-H₂-based gases containing various amounts of steam was studied at 1000 and 1050°C. The kinetics of scale growth during the isothermal exposure and the scale spalling during subsequent cooling were investigated by thermo gravimetry. The scale growth and morphology and adherence depend on the test gas composition. Scales formed on pure Cr and Ni25Cr in Ar-20%O₂ were thinner, less adherent and showed more substantial porosity than those formed in steam containing gases. Differences in scale growth rates and morphology can be explained by formation of H₂O/H₂ bridges in scale voids. The growth mechanisms of Ni25Cr seems to be different from those for pure Cr. The oxidation rate of MA745 were found to be much smaller than that of Ni25Cr. The ODS alloy exhibited very thin oxide scales in all test environments.

Materials Processing Fundamentals: Solidification and Deformation Processing

Sponsored by: The Minerals, Metals and Materials Society, TMS Extraction and Processing Division, TMS: Process Fundamentals Committee, TMS: Process Modeling Analysis and Control Committee
Program Organizers: *Princewill N. Anyalebechi*, Grand Valley State University; *Adam C. Powell*, Massachusetts Institute of Technology

Monday PM
March 13, 2006

Room: 203A
Location: Henry B. Gonzalez Convention Ctr.

Session Chair: *Prince N. Anyalebechi*, Grand Valley State University

2:00 PM

Comparative Study of the Effects of Solidification Rate on the Cast Microstructures of Aluminum Alloys 6016 and 6009: *Princewill N. Anyalebechi*¹; ¹Grand Valley State University

The effects of solidification rate on the cast microstructures of aluminum alloys 6009 and 6016 have been investigated with directionally cooled laboratory-size ingots at ranges of solidification rate within those observed in commercial-size ingots. In both alloys, the average dendrite cell size and second phase particle size decreased with increase in average solidification rate and with a decrease in average local solidification time. However, at comparable solidification rates, the dendrite cells and second phase particles are finer in the shorter freezing range alloy 6009 than in the longer freezing range alloy 6016. This is provisionally attributed to the earlier formation of second phase intermetallics at higher temperatures during solidification and to the formation of greater amount of the relatively coarse plate-like beta-phase (Al₉Fe₂Si₄) phases in alloy 6016. In general, the types and relative amounts of the second phase particles formed in both alloys are independent of solidification rate.

2:25 PM

The Effects of Internal Convection on the Lifetime of the Metastable Phase in Undercooled Fe-Cr-Ni Alloys: *Alaina B. Hanlon*¹; *D. M. Matson*²; *R. W. Hyers*¹; ¹University of Massachusetts; ²Tufts University

When sufficiently undercooled, Fe-12wt%Cr-16wt%Ni alloys can undergo two-step solidification in which a metastable ferrite phase forms first, followed by the stable austenite phase. Two different levitation techniques show dramatically different lifetimes of the metastable phase. If the lifetime is too short, the sample will have an unfavorable mixed microstructure of fine grains where the sample underwent two-step solidification and dendrites where the melt solidified directly to the stable phase. Prior work has excluded many potential explanations for the difference observed in the metastable phase lifetime. The remaining hypothesis for this difference is dendritic interactions as a result of strong induced con-

vection. If the primary arms of the dendrites deflect enough, secondary arms of adjacent dendrites can collide, triggering early stable phase nucleation. Computational fluid dynamics along with experimental findings show that the difference in induced convection between the different processing methods is the reason for this difference.

2:50 PM

Age Hardening Behavior of AA2618: Hui Lu¹; Puja B. Kadolkar²; Kozo Nakazawa¹; Teiichi Ando¹; Craig Alan Blue²; ¹Northeastern University; ²Oak Ridge National Laboratory

The structural changes in solutionized AA2618 during natural aging and their effects on subsequent artificial aging were investigated by hardness measurements and X-ray diffraction. The changes in lattice parameter and hardness during natural aging indicate that copper-enriched clusters form primarily in the earliest stage, followed by the formation of magnesium-enriched clusters and copper-magnesium co-clusters. Prior natural aging consistently weakened the hardening during subsequent artificial aging at 180, 200 and 230°C but had no effects on artificial aging at 150°C. The decreased age hardening was attributed to the reversion of small clusters or zones that formed during prior natural aging. The lattice parameter exhibited erratic changes during the early stages of artificial aging, reflecting the reversion and the complex sequence of precipitation.

3:15 PM

Metallic Wires Elaboration Directly from Thin Liquid Jets: Ludovic Charpentier¹; Yves Du Terrail-Couvat¹; Yves Delannoy¹; Christian Trassy¹; ¹Electromagnetic Processing of Materials Laboratory

Elaborating metallic wires directly from liquid jets would avoid drawbacks of extrusion (space needed, damaging, cost...) and enable recycling. But liquid jets tend to break, due to capillary instabilities, unless a solid layer (coating or start of solidification) surrounds it. We recently developed a process to elaborate tin wires, cooled by water flow parallel to the jet. Superficial oxidation of tin produces a glass coating around the jet. Studies showed the length of wires increased when increasing speed of tin jets, and that water average speed should be the closest possible to the jet one to have smooth fibers. Producing 1 mm diameter wires is possible. The length of wires is limited by the experimental setup, which does not provide possibilities to coil the wire. Most of other metals do not generate glass-like oxides. The lack of coatings makes it necessary to reduce the capillary instabilities to obtain fibers.

3:40 PM Break**3:55 PM**

Study of the Metallizing of the Continuous Carbon Fiber Surface: Tianjiao Luo¹; Yao Guangchun¹; Wu Linli¹; ¹Northeastern University

Abstract: The electroless copper plating process for continuous carbon fiber using CuSO₄·5H₂O as the main salt and formaldehyde as reducing agent was experimentally studied, including the effects of pH values and concentration of chelating agents, additives and reducing agent on the electroless plating process. The surface morphology and composition of coating were investigated by means of Scanning Electron Microscopy (SEM) and Energy Dispersive X-ray Spectroscopy (EDS), and deposited the coating thickness was measured by way of dissolution. The results indicated that the pretreatment of carbon fiber before plating is so important that it is able to prevent from the "black core" phenomenon. With the process parameters got and optimized experimentally, the carbon fiber plated with copper shows homogeneous coating with favorable mechanical properties due to stable bath, such as the high bonding strength of coating.

4:20 PM

Research on a New Wearable and Electric Material Used in Current Electric Locomotive: Lian Wei Yang¹; Guang Chun Yao¹; ¹Northeastern University

Pantograph slide plate is quite important collecting electricity material of electric locomotive. A new one is developed in view of the existing problems of current pantograph slide plates. The new pantograph slide plate is consisted of copper, carbon fiber, graphite etc. And the influence of pressure and sintering temperature to the performance of pantograph slide plate is studied firstly. Then its performance of friction, abrasion and impact toughness is tested. Performance of the new pantograph slide plate

is contrasted to current pantograph slide plates at last. The results showed the optimal technique of preparing slide plate. Its performance is improved greatly with friction coefficient reduced by 54.5%, abrasion ratio decreased by 41%, impact toughness increased by 9.6 times and conductance increased by 87 times compared with carbon slide plate C26.

4:45 PM

Characterization of Mechanical Properties and Microstructure in Copper Nanopowder Alloyed Al7075 T651 via Friction Stir Process: Dongok Kim¹; Jianhui Wu²; William F. Schmidt²; Ajay P. Malshe²; ¹Korea Automotive Technology Institute; ²University of Arkansas

Regardless of the advantages of Friction Stir Process (FSP), for age-hardened aluminum alloys, the mechanical properties such as hardness in the stir zone were decreased after FSP due to the growth or dissolution of strengthening precipitates. Here, as a new technique, FSP was introduced to alloy copper nanopowders in Al7075 T651. Mechanical properties together with micro and nanostructures were compared with as-FSPed Al7075 T651 using SEM, TEM, and Vickers hardness tests to understand structure-property relationships. It was shown that the Vickers hardness of the stir zone in copper nanopowder alloyed Al7075 T651 was increased by 20% compared to that of the heat affected zone, while the as-FSPed samples did not show a noticeable increase in hardness in the same zone. X-ray mapping showed traces of copper nanopowder after the process, and TEM was used to verify if there is CuAl₂ formed in the copper alloyed sample.

5:10 PM

The Model of Structure Refinement in Metals at Large Deformations and Factors Effecting Grain Sizes: Farid Utyashev¹; Georgy Raab²; ¹Institute for Metals Superplasticity Problems of the Russian Academy of Sciences; ²Ufa State Aviation Technical University

The present work considers the essence of fragmentation: on the level of a simple model as a material response to the curvature accumulated by it at large deformations. It is on this basis that the correlation between curvature and fragment sizes is determined. It is shown that at deformation the area of curvature center inevitably changes. It is revealed that a specific value of variation of center surface area, i.e. ΔAY parameter, is numerically equal to the value of curvature acquired by a material. Minimum sizes of fragments and grains depending on ΔAY have been estimated, and the dependence of this parameter on strain has been established. Besides, the present paper considers the effects exerted by curvature center geometry, material distortion, directions of deformation and thermal warming up in the localization zones on structure refinement when various techniques are applied.

Multicomponent-Multiphase Diffusion Symposium in Honor of Mysore A. Dayananda: Modeling and Simulation

Sponsored by: The Minerals, Metals and Materials Society, ASM Materials Science Critical Technology Sector, ASM-MSCTS: Atomic Transport Committee

Program Organizers: Yong-Ho Sohn, University of Central Florida; Carelyn E. Campbell, National Institute of Standards and Technology; Richard Dean Sisson, Worcester Polytechnic Institute; John E. Morral, Ohio State University

Monday PM
March 13, 2006

Room: 203B
Location: Henry B. Gonzalez Convention Ctr.

Session Chairs: John Agren, Royal Institute of Technology; Irena V. Belova, University of Newcastle

2:00 PM Invited

Phase Field Modeling of Interdiffusion Microstructures: Yunzhi Wang¹; John E. Morral¹; ¹Ohio State University

One of the many outstanding contributions of Professor Dayananda to multicomponent-multiphase diffusion is his systematic experimental characterization of complex interdiffusion microstructures. These observations have posed serious challenges to existing theories and models and offered vast opportunities for new scientific discoveries. With the increasing power

of computers and sophistication of computational models, new understanding of the scientific principles underlying multicomponent diffusion in multiphase systems are anticipated. In this presentation we will review recent applications of the phase field method to studying interdiffusion microstructures and diffusion paths in multicomponent and multiphase systems. In particular, the phenomenon of demixing and the formation of non-linear diffusion paths with “horns” in two-phase/two-phase diffusion couples will be analyzed. Also the influence of the Kirkendall effect on interdiffusion microstructures and diffusion paths will be addressed. Whenever possible, the phase field simulations will be compared with DICTRA simulations and experimental observations.

2:30 PM

Modeling Diffusion in the Multicomponent Ordered L₁₂ and B2 Phases for Ni-Rich Systems: *Carelyn E. Campbell*¹; ¹National Institute of Standards and Technology

Modeling the diffusion in multicomponent ordered phases (L₁₂ and B2) in Ni-base superalloys is essential for diffusion simulations that predict microstructure evolution. The ordered L₁₂ (γ) phase is the primary strengthening precipitate for these alloys and the L₁₂ phase fraction often exceeds 0.5. The ordered B2 phase is the primary component of many of the bond coats used to prevent diffusion between the thermal barrier coating and the superalloy. The ordered diffusion model proposed by Helander and Ågren (1999) is implemented for the L₁₂ and B2 phases in the Ni-based superalloys. A new assessment for the Ni-Al L₁₂ phase is presented. The diffusion mobilities for the B2 Ni-Al phase are re-assessed based on new experimental work by Kim and Chang (2000). The models employed in the assessments are evaluated by comparing measured and calculated composition profiles of various superalloys versus B2-NiAl diffusion couples.

2:55 PM

Modeling of Kinetics of Diffusive Phase Transformation in Binary Systems with Multiple Stoichiometric Phases: *Ernst Kozeschnik*¹; Jiri Svoboda²; Franz D. Fischer³; ¹Graz University of Technology; ²Academy of Sciences of the Czech Republic; ³University of Leoben

Kirkendall experiments were performed on systems forming manifold nearly stoichiometric phases demonstrating, that the originally single Kirkendall plane is split into several planes. Such problem cannot be simply treated as a reactive diffusion problem and must be investigated as a transformation problem with active sources and sinks for vacancies at mobile interfaces between individual phases. The chemically driven strain must also be involved. The thermodynamic extremal principle is used for the treatment of the evolution of the binary system under the assumption that all phases existing in the system are stoichiometric with no sources and sinks for vacancies in the bulk. Furthermore, it is assumed that more than one phase nucleate at the contact plane of the diffusion couple at the start of the experiment. Then it is shown, that just the number of the nucleated phases determines the number of furcations of the Kirkendall plane.

3:20 PM

Phase-Field Simulation of Microstructural Evolution in Ternary Multiphase Diffusion Couples: *Rashmi R. Mohanty*¹; Yong-Ho Sohn¹; ¹University of Central Florida

A ternary phase-field model was devised and applied to examine the evolution of microstructure in multiphase solid-to-solid diffusion couples. Numerical model based on the Cahn-Hilliard and Ginzburg-Landau equations for multicomponent system were employed. The free energy of the system was derived based on the available thermodynamic data from the literature. The chemical mobility was varied as a function of composition from constant atomic mobility for a component as a first approximation. Effect of composition and perturbation on the development of planar and non-planar interfaces in multiphase diffusion couples was studied. Simulation results were compared with the experimental observations reported in literature for selected ternary systems. This work was financially supported by CAREER award from National Science Foundation (DMR-0238356).

3:45 PM Break

4:05 PM Invited

Comparison of Multicomponent Diffusion Programs: *Martin E. Glicksman*¹; Afina Lupulescu¹; Ben Pletcher¹; ¹Rensselaer Polytechnic Institute

Currently three diffusion programs are in use for predicting concentration profiles of multicomponent couples: Profiler[®], MultiDiflux[®], DICTRA[®]. Each is unique in its incorporation of fundamental principles and capabilities, with the common goal of analysis of multicomponent diffusion data. Profiler[®] is useful when the diffusion is linear, and the interdiffusion coefficients or thermodynamic data are known. MultiDiflux[®] is capable of determining interdiffusion coefficients for multicomponent couples. However, accurate experimental penetration data are required to accommodate the interpolation scheme used by the numerical methods. DICTRA[®] is a program that accurately models experimental data from thermodynamic and kinetic coefficients. DICTRA[®] produces both interdiffusion and self-diffusion coefficients. Its use is limited by the accuracy and completeness of the associated data base. Comparison of all 3 software outputs will be presented for Fe-Al-Cr ternary diffusion couples. Experimental data used in our comparison were kindly provided by Professor Gunter Borchardt and Dr. Patrick Dawah.

4:35 PM

Diffusion Phenomena in the Planck-Kleinert Crystal: *Marek Danielewski*¹; ¹AGH University of Science and Technology

The Planck-Kleinert Crystal (PKC) hypothesis is the promising area of Planck scale physics. In such quasi-continuum the energy, momentum and mass transport are diffusion controlled and all fluxes are given by the Nernst-Planck formulae. PKC hypothesis is used here to show the complexity of transport phenomena in cubic crystal. The quasi-stationary collective behavior of particles in the PKC (wave) is equivalent to the body (particle) and such an approach enables the Schrödinger equation to be derived. Transverse wave is equivalent electromagnetic wave. The diffusing interstitial particles create the gravitational type interaction between bodies. Thus, the PKC model implies four different force fields and predicts the vast amount of the “dark matter and dark energy” in the PKC. Apart from its fundamental impact on cosmology and physics, the Planck-Kleinert-Crystal model shows the exciting new possibilities in area of materials science, chemistry and physics of solids.

5:00 PM

MATLAB[®] Implementation of Diffusion Methods: Afina Lupulescu¹; Christopher O'Brien¹; *Martin Eden Glicksman*¹; Wei Yang¹; ¹Rensselaer Polytechnic Institute

We developed a MATLAB[®] code called Inversemethods[®] to determine concentration-dependent diffusivities from binary penetration data. Inversemethods[®] allows comparison between diffusivities calculated by five methods: 1) Boltzmann-Matano (BM); 2) Sauer-Freise/den Broeder (SFB); 3) Fictitious image-sources (error function approximation); 4) Fourier series image-sources, and 5) Linear diffusion couple (Grube-Jedele). Writing this code in MATLAB[®] met the requirement for portability, as MATLAB[®] is multi-platform enabling users to perform analyses on the diffusivity data produced with it. The BM and SFB methods are implemented following Simpson's rule to calculate the integrals, and employ a straightforward finite-difference method to estimate derivatives. The software also implements a Savitzky-Golay filtering algorithm to smooth noisy penetration data by locally fitting a 3rd-order polynomial to 201 concentration-distance data points. A separate GUI has been developed by one of us to obviate the direct use of the MATLAB[®] code itself, and to ease its application for inexperienced users.

Point Defects in Materials: Mechanical and Boundary Properties

Sponsored by: The Minerals, Metals and Materials Society, TMS Electronic, Magnetic, and Photonic Materials Division, TMS Structural Materials Division, TMS: Chemistry and Physics of Materials Committee

Program Organizers: Dallas R. Trinkle, U.S. Air Force; Yuri Mishin, George Mason University; David N. Seidman, Northwestern University; David J. Srolovitz, Princeton University

Monday PM Room: 210B
March 13, 2006 Location: Henry B. Gonzalez Convention Ctr.

Session Chair: Yuri Mishin, George Mason University

2:00 PM Invited

The Influence of Interstitial Oxygen on the Alpha to Omega Phase Transition in Titanium and Zirconium: *Ellen K. Cerreta*¹; George T. Gray¹; Angus C. Lawson¹; Chuck E. Morris¹; Robert S. Hixson¹; Paulo A. Rigg¹; ¹Los Alamos National Laboratory

The pressure for the alpha to omega phase transition was investigated for two grades of titanium and three grades of zirconium. A series of shock experiments were conducted from 5 to 35GPa and revealed that the pressure for the phase transition increases with increasing interstitial oxygen content and is completely suppressed in low purity materials. For the high purity Ti and Zr in this study, the pressure for the phase transition occurred at 10.4 and 7.1GPa, respectively and no reverse transformation was observed upon unloading. Increasing the oxygen content increases the number of octahedral sites occupied; this is postulated to increase the pressure for the phase transition. Neutron diffraction and TEM were utilized to quantify the volume fraction of metastable omega phase and to characterize the microstructures within the shocked and "soft" recovered specimens. Quasi-static reload experiments examined the effect of the shock-induced substructure on post-shock mechanical properties.

2:30 PM

Solid Solution Softening in Mo Alloys: Large-Scale Model with Ab-Initio Parametrization: *Yuri N. Gornostyrev*¹; Nadezhda I. Medvedeva²; Arthur J. Freeman¹; ¹Northwestern University; ²Institute of Solid State Chemistry

The intrinsic mechanism of solid solution softening (SSS) in bcc molybdenum alloys due to transition metal additions is investigated on the basis of *ab-initio* electronic-structure calculations. We demonstrate that additions with an excess of electrons lead to a decrease in the atomic row displacement and generalized stacking fault (GSF) energies, and those with a lack of electrons to its sharp increase. Using the atomic row model, we show that (i) the isotropic core of the screw dislocation in Mo tends to change into a planar core under alloying with softener solutes (Re, Os, Ir, Pt), and (ii) the decrease in GSF energy leads to the enhancement of double kink nucleation and dislocation mobility. Our study explains the experimental dependence of the alloying effect on the atomic number of the addition and provides an understanding of the electronic reasons for SSS in Mo. Supported by the AFOSR (grant No. FA9550-04-1-0013).

2:50 PM

New Quantitative Analysis Explains Softening of Pure Metals by Solutes: *Dallas R. Trinkle*¹; Christopher F. Woodward¹; ¹U.S. Air Force

Solid solution softening observed in bcc transition metals has traditionally been attributed to either extrinsic effects—such as interstitial scavenging—or intrinsic effects—direct solute/dislocation interaction. We investigate intrinsic mechanisms using first principles methods. First, density functional theory calculates directly the interaction energy of Hf, Ta, Re, Os, Ir and Pt solutes with a single straight $\langle 111 \rangle$ screw dislocation in Mo. Next, the interaction energies and changes in resistance to dislocation motion are incorporated into a mesoscopic double-kink model to predict changes in yield stress with temperature and solute concentration. Quantitatively accurate predictions require a model that accounts for clusters of solutes interacting with dislocations. Moreover, using the solute response in bulk as an approximation to the solute response in a disloca-

tion can lead to incorrect predictions. By using solute-dislocation interactions coupled with a realistic mesoscopic model, we reproduce the strength behavior of Mo-Re and Mo-Pt, two systems with dramatically different intrinsic softening.

3:10 PM Invited

Role of Evolving Solute Structures on the Mechanical Behavior of Solid Solutions: *Catalin Picu*¹; ¹Rensselaer Polytechnic Institute

An experimental and combined atomistic, mesoscale and continuum modeling program was developed to investigate the influence of evolving solute structures on the mechanical response of solid solutions. By solute structures we understand clusters located at and away from dislocations, and nanoscale precipitates composed of several solute atoms. We focus on the Al-5%Mg binary alloy, which we take as a model system. The rate sensitivity of this material decreases as the solute concentration increases. The current mechanisms proposed to explain this phenomenon are discussed in light of the new findings. Specifically, we study bulk and pipe diffusion to dislocation cores looking for the size and structure of stable clusters, and the characteristic time of their growth. Several new effects that lead to negative rate sensitivity will be presented and discussed against previously proposed mechanisms.

3:40 PM Break

3:55 PM

The Effect of Oxygen Vacancy on Mechanical Properties of Ceria: *Fereshteh Ebrahimi*¹; Yanli Wang¹; Keith L. Duncan¹; Eric D. Wachsman¹; ¹University of Florida

High concentrations of oxygen vacancies were produced by heat treating ceria at an elevated temperature in various environments with different partial pressures of oxygen, followed by fast cooling to room temperature. The elastic modulus, hardness and fracture toughness were evaluated at room temperature. The results indicate that the intrinsic elastic modulus decreases with increasing the oxygen vacancy concentration, consistent with theoretical predictions. However, hardness and toughness exhibited different relationships with the defect content. Several phenomena, including phase transformation, internal stress gradient, and microcracking, were found as a result of the applied heat treatments. These observations will be discussed and correlated with the variations in mechanical properties as a function of partial pressure of oxygen. The financial support by DOE under contract DE-PS26-02NT41562 for conducting this research is greatly appreciated.

4:15 PM

Study of Defect Structures in B2 Phases via First-Principles Calculations: *Sara N. Prins*¹; Raymundo Arroyave¹; Zi-Kui Liu¹; ¹Pennsylvania State University

The B2 aluminides of Ir, Ni, Pd, Pt, and Ru are studied for their potential application as high temperature structural materials in the bond coats in turbine jet engines. It is well known that the mechanical properties of B2 intermetallic phases are controlled by their defect structures, e.g. the hardness of NiAl is attributed to the presence of vacancies. Thus to optimize the properties of a B2 phase, its defect structures and the effect of alloying additions should be well understood. In the present work, first-principles methods are employed to investigate the defect structure in B2 aluminides as well as the energy of formation of defects through the Wagner-Schottky and Bragg-Williams models.

4:35 PM Invited

Doped Metal Grain Boundaries: *Gerd Duscher*¹; Wolfgang Windl²; Matthew F. Chisholm³; ¹North Carolina State University/Oak Ridge National Laboratory; ²Ohio State University; ³Oak Ridge National Laboratory

The combination of atomic-column resolved Z-contrast imaging, spatially resolved electron energy loss spectroscopy and *ab initio* density functional theory is used to study the atomic structure of doped metal grain boundaries. We will discuss three different materials (Al, Cu, and Ni₃Al), in which the atomic structure of tilt grain boundaries is very similar. We dope these grain boundary with interstitial (Cu in Al and B in Ni₃Al) and substitutional (Bi in Cu) segregants. The changes in the electronic structure are discussed in terms of bond strength. Strained supercells allow the determination of stress concentration on specific atomic sites. We also

will present results of point defect diffusion along Cu doped Al grain boundaries. Our findings suggest a new concept for the determination of grain boundary embrittlement.

5:05 PM Invited

First Principles Calculations of Interfacial Boundaries in Ni-Ni3Al and Al-Al3Sc: *Christopher F. Woodward*¹; Axel van De Walle²; Mark Asta²; ¹U.S. Air Force; ²Northwestern University

Solute and precipitation strengthening are often used to optimize the properties of structural materials used in aerospace applications. A great deal can be learned about these alloys by studying the model binary and ternary systems. Here Ni-Ni3Al and Al-Al3Sc are used as model systems for the Ni-based superalloys and Sc strengthened Al alloys in order to estimate interfacial boundaries (IFB) properties. The thermodynamic properties of these IFB's strongly influence growth and coarsening rates of precipitates and are used in models of precipitation strengthening and microstructural evolution. Cluster expansion methods and lattice gas methods are used to study composition profiles and free energies of IFB's in these materials. In Al-Al3Sc a lattice gas model is used to predict Mg impurity segregation to the Al side of the (100) IFB. This result has recently been verified by atom probe tomography.

Solidification Modelling and Microstructure Formation: A Symposium in Honor of Prof. John Hunt: Dendritic Growth II

Sponsored by: The Minerals, Metals and Materials Society, TMS Materials Processing and Manufacturing Division, TMS: Solidification Committee

Program Organizers: D. Graham McCartney, University of Nottingham; Peter D. Lee, Imperial College; Qingyou Han, Oak Ridge National Laboratory

Monday PM
March 13, 2006

Room: 6C
Location: Henry B. Gonzalez Convention Ctr.

Session Chairs: H. Jones, University of Sheffield; C. Beckermann, University of Iowa

2:00 PM Invited

Dendritic Growth and Melting: *Martin E. Glicksman*¹; Afina Lupulescu¹; Matthew Koss²; ¹Rensselaer Polytechnic Institute; ²College of the Holy Cross

Measurements of video data on melting dendritic fragments in reduced gravity show that the axial ratio of these needle-shaped crystals, C/A , initially rises until the crystal melts to a pole-to-pole length of ~ 5 mm. At that point a sudden fall in the C/A ratio occurs. Analysis and modeling show that the cause of these sudden changes in kinetics and morphology during melting is the shape anisotropy of the fragments. Shape anisotropy leads to steep gradients in the mean curvature of the solid-melt interface, and, acting through the Gibbs-Thomson effect, induce unusual fluxes of heat within the crystallites. When the additional anisotropy of the interfacial free energy is added, a startling result obtains: the Gibbs-Thomson effect becomes non-monotonic! The poles are slightly warmer than the near-polar regions. This non-monotonic boundary condition might provide the physical basis for a dendritic limit cycle and account for the formation of dendritic side branching.

2:25 PM Invited

Formation of Globular Crystals during Semi-Solid Processing: *Weidong Huang*¹; ¹Northwestern Polytechnical University

Both experimental and theoretical researches on the formation mechanism of the globular microstructure formed during semi-solid processing of a binary alloy were carried out, with focus on the strong convection effect induced by the forced melt stirring during the processing. Direct observation of the crystal growth from a transparent model alloy, succinonitrile-5at%water, during semi-solid processing indicates that strong melt convection induced by the forced stirring during semi-solid processing will change the crystal growth morphology from dendritic to spherical shape. This morphology change does not originate from den-

drite arm fragmentation, instead from the increase of the interfacial morphological stability. An interfacial morphological stability analysis of a growing globular crystal indicates that the liquid convection and multi-particle effect will increase the critical radius for stable growth of the crystals.

2:50 PM

Characteristic Evaluation of Semi-Solid Aluminum Alloys Using Electromagnetic Stirring: *Dock-Young Lee*¹; *Ki-Bae Kim*¹; *Jung-Hwa Mun*¹; *Suk-Won Kang*¹; *Seung-Kwon Seol*²; *Jung-Ho Je*²; *Do-Hyang Kim*³; ¹Korea Institute of Science and Technology; ²Pohang University of Science and Technology; ³Yonsei University

Coherent X-rays from synchrotron beam sources are increasingly used in non-conventional techniques. This study presents three dimension microstructural characterization by synchrotron X-ray tomography of Al-15%Cu alloys. Qualitative results concerning the evolution of the shape of the globules and quantitative three dimension image analyses are presented. The microstructure of the solidified specimen was characterized as a size and shape of primary crystal in accordance with the flow density. By using three dimension synchrotron X-ray tomography, three dimension image of primary crystal was pictured and showed that the dendritic primary crystal was truncated due to the electromagnetic stirring during solidification. In this study synchrotron X-ray tomography appears as a very powerful tool for characterizing the microstructure of Al-15%Cu samples during partial solidification. The advantage of Al-15%Cu alloys lies in the possible use of the refraction and absorption mode for the synchrotron X-rays tomography.

3:15 PM

A Solid Fraction Evolution Approach for Modeling of Dendritic Growth in Multicomponent Alloys: *Adrian V. Catalina*¹; *Doru M. Stefanescu*²; *Leo Chuzhoy*¹; *Michael L. Johnson*¹; ¹Caterpillar Inc.; ²Ohio State University

A deterministic model that outputs microstructure images has been developed to simulate microstructure evolution during solidification of single phase multicomponent alloys. The model accounts for nucleation, growth, and coarsening of grains as well as redistribution/segregation of alloying elements during solidification. The model describes the grain growth by means of a strong coupling between the thermal and solutal fields at the solid/liquid interface. This novel coupling procedure allows relaxing the assumption used in previously published models that growth is controlled mainly by solute diffusion, which limits their validity to low cooling rates and growth velocities. Also, the new model can accommodate any number of alloying/impurity elements, including pure metals, in the chemical composition of the melt and account for their effect on the grain growth rate. Computed dendritic microstructures and segregation patterns will be presented for steels of various chemical compositions. Model validation against available literature data will also be discussed.

3:40 PM Break

3:55 PM Invited

Modeling of Single Cell/Dendrite Growth in Directional Solidification: *Shu-Zu Lu*¹; *Shan Liu*²; ¹Michigan Technology University; ²Ames Laboratory

Following the original model of single cell/dendrite growth in directional solidification by Hunt, in which it is assumed that there is no mass transfer cross the boundary walls, computation is carried out in focus on the selection of the tip shape as well as the tip undercooling and the tip radius. The solutions of cell/dendrite shapes are compared with the results of experimental modeling of single cell/dendrite growth in fine capillary tubes of 75 mm and 100 mm in diameter for Succinonitril- Salol system. The effects of the system constants on the single cell/dendrite growth are discussed and it is noticed that surface energy anisotropy has a significant effect on controlling cell/ dendrite shapes.

4:20 PM

Phase-Field Study of the Cellular Bifurcation in Dilute Binary Alloys: *Mathis O. Plapp*¹; *Esteban Meca*²; ¹Ecole Polytechnique, Palaiseau; ²Universitat Politecnica de Catalunya

Phase-field simulations in both two and three dimensions are used to investigate the microstructures which form closely above the threshold of

the Mullins-Sekerka instability in the directional solidification of dilute binary alloys. In particular, the so-called 'node' or 'pox' structures, which consist of regular hexagonal arrays of 'holes' (local depressions of the solidification front), are studied, and their properties are compared to the ones of the well-known hexagonal cell patterns. The results are compared to the predictions of weakly nonlinear amplitude expansions and to experimental data, and the implications of these findings for the selection of the microstructure spacing in extended systems are discussed.

4:45 PM

The Influence of Fluid Flow on the Microstructure of Directionally Solidified AlSi-Base Alloys: *Sonja Steinbach*¹; Lorenz Ratke¹; ¹German Aerospace Center DLR

To obtain a quantitative understanding of the effect of fluid flow on the microstructure of cast alloys a technical Al-Si-Mg alloy (A357) has been directionally solidified with medium temperature gradient under well defined thermal and fluid flow conditions. The solidification was studied in an aerogel-based furnace inducing flat isotherms and allowing the direct optical observation of the solidification process. Three pairs of Helmholtz coils around the sample induce a homogeneous rotating magnetic field (RMF) and hence a well defined flow field. The application of RMFs during directional solidification results in pronounced segregation effects: a change to pure eutectic solidification at the axis of the sample is observed at high magnetic field strengths. Microstructural features like the primary dendrite stem and secondary dendrite arm spacing change in a unique manner with solidification speed and magnetic field induction. In addition the arrangement of intermetallics can be modified with RMF induced fluid flow.

Space Reactor Fuels and Materials: Environmental Effects and Fuels

Sponsored by: The Minerals, Metals and Materials Society, ASM International, TMS Structural Materials Division, TMS/ASM: Nuclear Materials Committee, TMS: Refractory Metals Committee

Program Organizers: David James Senor, Pacific Northwest National Laboratory; Brian D. Wirth, University of California; Robert Hanrahan, Los Alamos National Laboratory; Steven J. Zinkle, Oak Ridge National Laboratory; Mehmet Uz, Lafayette College; Evan K. Ohriner, Oak Ridge National Laboratory; Brian V. Cockeram, Bechtel Bettis Inc

Monday PM

Room: 213B

March 13, 2006

Location: Henry B. Gonzalez Convention Ctr.

Session Chairs: Mehmet Uz, Lafayette College; Steven J. Zinkle, Oak Ridge National Laboratory

2:00 PM

Aging Effects on Microstructural and Mechanical Properties of Select Refractory Alloys for Space Reactor Applications: *Keith John Leonard*¹; Jeremy T. Busby¹; Steven J. Zinkle¹; Rita Baranwal²; T. Angeliu³; Y. Ballout³; ¹Oak Ridge National Laboratory; ²Bechtel Bettis Inc; ³Lockheed Martin Corporation

Refractory alloys based on niobium, tantalum and molybdenum are potential candidate materials for structural applications in proposed space nuclear reactors. Long-term microstructural stability is a requirement of these materials for their use in this type of creep dominated application. Early work on refractory alloys has shown aging embrittlement occurring for some niobium and tantalum-base alloys at temperatures near 40% of their melting temperatures in either the base metal or in weldments. Other work has suggested microstructural instabilities during long-term creep testing leading to decreased creep performance. This paper examines the effect of aging 1,000 hours at 825, 975 and 1125°C on the microstructural and mechanical properties of two niobium (Nb-1Zr and FS-85), tantalum (T-111 and ASTAR811C) and molybdenum (Mo-41Re and Mo-47.5Re) base alloys. Changes in material property are examined through mechanical tensile testing coupled with electrical resistivity changes and microstructural examination through optical and electron microscopy analysis. This work was performed in part by the Oak Ridge National Laboratory for the U.S. Department of Energy (DOE) in support of the National Aero-

nautics and Space Administration (NASA). ORNL is managed for DOE by UT-Battelle, LLC, under contract DE-AC-05-00OR22725. Any opinions expressed in this paper are those of the author(s) and do not necessarily reflect the views of DOE or NASA.

2:25 PM

Radiation-Damage in Molybdenum-Rhenium Alloys for Space Reactor Applications: *Jeremy T. Busby*¹; Keith John Leonard¹; Lance Snead¹; F. W. Wiffen¹; Steven J. Zinkle¹; E. Mader²; R. Nelson³; George A. Newsome³; ¹Oak Ridge National Laboratory; ²Bechtel-Bettis Inc; ³Lockheed Martin

Various Mo-Re alloys are attractive candidates for use as fuel cladding and core structural materials in spacecraft reactor applications. Molybdenum alloys with rhenium contents of 41% to 47.5% (wt%), in particular, have good creep resistance and ductility in both base metal and weldments. However, irradiation-induced changes such as transmutation and radiation-induced segregation could lead to precipitation and, ultimately, radiation-induced embrittlement. This paper presents the characterization of radiation-induced changes in two Mo-Re alloys. Results from Mo-41Re and Mo-47.5Re alloys irradiated to ~ 1 and 2 dpa at 800, 950, and 1100°C in the High Flux Isotope Reactor at Oak Ridge National Laboratory are presented. The impact of irradiation on electrical resistivity and swelling will be assessed. Transmission-electron microscopy analysis will be used to examine radiation-induced segregation of Re, transmutation of Re to Os, and any precipitation resulting from these composition changes. The impact of these irradiation-induced changes on mechanical properties will be discussed. This work was performed in part by the Oak Ridge National Laboratory for the U.S. Department of Energy (DOE) in support of the National Aeronautics and Space Administration (NASA). ORNL is managed for DOE by UT-Battelle, LLC, under contract DE-AC-05-00OR22725. Any opinions expressed in this paper are those of the author(s) and do not necessarily reflect the views of DOE or NASA.

2:50 PM

The Swelling, Microstructure, and Hardening of Wrought LCAC, TZM, and ODS Molybdenum Following Neutron Irradiation: *Brian Vern Cockeram*¹; Rita Baranwal¹; Richard W. Smith¹; Nao Hoshimoto²; Lance L. Snead²; ¹Bechtel-Bettis; ²Oak Ridge National Laboratory

Molybdenum can be susceptible to embrittlement after neutron irradiation at temperatures <800°C. In this work, TEM examinations are used to characterize wrought Low Carbon Arc Cast, ODS, and TZM molybdenum following irradiation in HFIR at 300°C, 600°C, and 870-1100°C. The size and number density of loops and voids are determined. Models for the increase in strength are evaluated by comparing measured tensile strength values from previous work to values that are predicted using the microstructural data. Irradiation of alloys at 300C results in the formation of a high number density of the fine loops and voids (about 1-3 nm). A relatively high number density of small voids (about 5-6 nm) are observed after irradiation at 600°C. A low number density of coarse voids (about 10-20 nm) are observed after irradiation at 870-1100°C. Swelling values obtained from density measurements are consistent with the microstructure data. The evolution of microstructure is discussed.

3:15 PM Break

3:30 PM

Literature Review of W-UO₂ Cermet Thermal and Radiation Performance: *Robert J. Hanrahan*¹; Carol L. Haertling¹; ¹Los Alamos National Laboratory

At minimum, the fuel used in nuclear thermal propulsion reactors must have high-temperature stability and strength and be compatible with hydrogen. The fuel should also retain fissile material and fission products and be stable under thermal cycling. Candidate materials are therefore limited to nuclear materials in the form of or combined with ceramics (oxides, carbides, and nitrides), refractory metals, and graphite. To date, no ideal material has been identified, but ceramic metal composites (cermets) have long been considered as potential fuel materials. Although graphite matrix materials were used in the Rover and NERVA programs, the utility of cermets was studied extensively during the 1960s and early 1970s. The most-investigated fuels were UO₂ in a matrix of tungsten, molybdenum, or alloys thereof. The W-UO₂ system proved to be the most

promising for nuclear thermal propulsion. This presentation will review the thermal stability and irradiation performance of W- UO₂ cermet.

3:55 PM

Mechanical Properties and Microstructure of ZrN Pellets as Surrogates for Nitride Fuels: Effect of Sintering Conditions: Kirk Wheeler¹; Manuel Parra¹; John Dunwoody²; Darrin Byler²; Pedro D. Peralta¹; Ken McClellan²; ¹Arizona State University; ²Los Alamos National Laboratory

In this work, ZrN was studied as a diluent in non-fertile nitride transmutation fuel and as a surrogate to actinide nitrides such as PuN. The microstructure and mechanical properties at room temperature of sintered ZrN pellets were examined to investigate the effects of processing conditions on the structural integrity of fuel pellets. Powder size, mechanical milling, sintering temperature and atmosphere (Ar or N) were varied to form a matrix of conditions. The microstructure of the resulting pellets was examined using optical and electron microscopy and orientation imaging microscopy. Pore size and shape distributions were obtained from the measurements as well as crystallographic texture. Mechanical properties including hardness, fracture toughness and compression strength were measured at room temperature and correlated to microstructure and processing conditions. This, in turn, will lead the optimum processing parameters for manufacturing of actinide nitrides suitable for a variety of applications, including transmutation and space fuels.

4:20 PM

Kinetics of Precipitation of U₄O₉ from Hyper-Stoichiometric UO_{2+x}: Sven Vogel¹; Sheldon White²; Jamie Higgs²; William T. Thompson²; ¹Los Alamos National Laboratory; ²Royal Military College of Canada

For safe and reliable operation of fission reactors in space, the phase diagrams and reaction kinetics of systems used as nuclear fuels, such as U-O, U-N, U-C, are required. Diffraction allows identification of phases and their weight fractions as a function of temperature in situ, with a time resolution of the order of minutes. In this presentation, we will provide results from a neutron diffraction experiment validating the U-O system. Using the neutron diffractometer HIPPO, we investigated the decomposition of UO_{2+x} into UO₂ and U₄O₉ as a function of temperature in situ. From the diffraction data, the participating phases could be identified as UO_{2+x}, UO₂ and U₄O_{8.936} and no stoichiometric U₄O₉ was found. We will also report results on similar experiments in the U-Dy-O system. Results of both experiments were used to improve existing thermodynamic and finite-element models. The presented technique is also applicable to the other systems mentioned above.

The Brandon Symposium: Advanced Materials and Characterization: Interfaces - Theory and Experiments

Sponsored by: The Minerals, Metals and Materials Society, Indian Institute of Metals, TMS Extraction and Processing Division, TMS: Materials Characterization Committee

Program Organizers: Srinivasa Ranganathan, Indian Institute of Science; Wayne D. Kaplan, Technion; Manfred R. Ruhle, Max-Planck Institute; David N. Seidman, Northwestern University; D. Shechtman, Technion; Tadao Watanabe, Tohoku University; Rachman Chaim, Technion

Monday PM Room: 206B
 March 13, 2006 Location: Henry B. Gonzalez Convention Ctr.

Session Chairs: Manfred Ruhle, MPI-Stuttgart; Rachman Chaim, Technion - Israel Institute of Technology

2:00 PM Invited

Exploring the Mechanical Response of Grain Boundaries: J. W. Cahn¹; Y. Mishin²; A. Suzuki²; ¹National Institute of Standards and Technology; ²George Mason University

The response of tilt grain boundaries (GBs) to applied shear stresses was investigated by means of molecular dynamics simulations performed over the entire misorientation range and a wide temperature range. Two fundamentally different types of response are found. At relatively low tem-

peratures the stress induces GB motion accompanied by a coupled shear deformation in the volume traversed by the GB. The observed coupling depends on the tilt angle and is accurately described by a geometric model. The atomic mechanisms of the coupling have been identified and related to the GB crystallography. As the temperature increases, GB sliding events begin to occur until at higher temperatures the mechanical response switches entirely to sliding. The coupling/sliding crossover temperature range depends on the tilt angle. These findings suggest the need for a re-interpretation of many materials phenomena, particularly grain growth, grain rotation, recrystallization, and plastic deformation of nanocrystalline materials.

2:25 PM Invited

Grain Boundary Transitions: Ming Tang¹; W. Craig Carter¹; Rowland Cannon²; ¹Massachusetts Institute of Technology; ²Lawrence Berkeley National Laboratory

A phase field model that incorporates crystallographic orientation and grain boundary disorder has been developed. In fixed stoichiometric materials and binary alloys, we have analyzed the equilibrium properties of grain boundaries as a function of their misorientation using a diffuse interface model that depends on empirical molar free energies and gradient energy coefficients. A graphical construction, similar to that which J. Cahn used to predict surface segregation transitions in his Critical Wetting model (1977), predicts an order-disorder transitions akin to grain boundary melting. We have discovered a similar, but more complicated, thermodynamic construction for alloys which demonstrates the collective behavior or grain boundary disorder and segregation. We catalog the thermodynamic conditions where first and second order boundary transitions are possible and produce a diagrams that, similar to classical phase diagrams, indicate conditions of stability and coexistence of multiple grain boundary complexions.

2:50 PM

On the Features of Dislocation-Obstacle Interactions in Thin Films: Direct Comparison between In Situ Experiments and Large Scale Atomistic Simulations: Yuri Osetsky¹; Yoshitaka Matsukawa¹; Roger Stoller¹; Steven Zinkle¹; ¹Oak Ridge National Laboratory

Large-scale atomistic modelling has demonstrated that the dynamic interactions of dislocations in thin films have a number of remarkable features. A particular example is the interaction between a screw dislocation and a stacking fault tetrahedron (SFT) in Cu which can be directly compared with in situ observations of quenched or irradiated fcc metals. If the specimen is thin, the dislocation velocity is slow and the temperature is high enough, a segment of the original SFT can be transported towards the surface via a double cross-slip mechanism and fast glide of an edge dislocation segment formed during the interaction. The mechanisms observed in the simulations provide an explanation for the results of in situ straining experiments and the differences between bulk and thin film experiments. Research sponsored by the Division of Materials Sciences and Engineering and the Office of Fusion Energy Sciences, U.S. DOE, under contract DE-AC05-00OR22725 with UT-Battelle.

3:05 PM Invited

Atomistic Calculations of Microstructural Evolution in Shocked Nickel: Srinivasan G. Srivilliputhur¹; M. I. Baskes¹; ¹Los Alamos National Laboratory

Shock wave propagation in materials, and the attendant dislocation nucleation and motion, causes phase transformations and complex microstructure development. We present some atomistic calculations of these phenomena in single crystal nickel, a typical fcc metal. Following general observations about shock induced phase transformations at high strain rates and stress may be made: (1) the fcc crystal transforms to a bcc-like crystal behind the shock wave; (2) after a period of time, the bcc structure transforms to domains of a highly faulted fcc structure; (3) the domains grow, forming twin boundaries at their intersections; and (4) the reflected shock wave drives the system to a faulted, polycrystalline fcc material. While these observations appear to be insensitive to the in-plane sample periodicity, the details of fault and twin spacing scales are not. Understanding these microstructural features, and their scaling with system sizes, will help us bridge atomistic calculations with continuum scale experiments.

3:30 PM Invited

Building Carbon Nanotube Architectures for Applications: Pulickel M. Ajayan¹; ¹Rensselaer Polytechnic Institute

The talk will focus on the recent developments in our laboratory on the fabrication of carbon nanotube based architectures tailored for various applications. Various organized architectures of multiwalled and singlewalled carbon nanotubes can be fabricated using relatively simple vapor deposition processes and the work in attaining control on the directed assembly of nanotubes will be highlighted. We have pursued several electrodes novel applications for these structures, for example, as nanostructured electrodes for gas breakdown sensors, horizontal and vertical electrical interconnects, unique filters for separation technologies, thermal management systems, multifunctional brushes, and polymer infiltrated thin film composites. Some of these promising applications of carbon nanotubes and composites will be reviewed from the perspective of what has been accomplished in recent years. Our efforts on the strategies of growth and manipulation of nanotube-based structures and our recent success in controllably fabricating hierarchically branched nanotube structures will be discussed.

3:55 PM Break**4:05 PM Invited**

Stability of Heterophase Boundaries between Different Metals and Sapphire: Manfred R. Ruhle¹; Elena Tchernychova¹; Gunther Richter¹; Sang Ho Oh¹; Christina Scheu¹; ¹Max-Planck Institute

Well defined interfaces between different single crystalline metals (M=Nb, Mo, Al, Ag, Cu) and specific sapphire surfaces (SP) were processed by molecular beam epitaxy (MBE) or high temperature diffusion bonding (HTDB). The structure, composition and bonding of the as-processed interfaces were determined over many length scales to the atomic level by advanced TEM techniques. The bonding across the interface depends on the nature of the SP surface. High density of oxygen ions at the outermost SP layer results in strong bonding across the interface. Post-processing annealing under well defined conditions (temperature), oxygen partial pressure; (pO₂) results in specific reaction products at the interface. These reaction products alter the properties of the interface. Results will be reported for the 5 M/SP systems and discussed on the basis of thermodynamic and kinetic considerations. As expected the interfaces between SP and metals are morphologically stable owing to the specific properties of SP.

4:30 PM Invited

Interfaces between Pb Grains and Cu Surfaces: Dominique Chatain¹; Daniel Galy²; ¹Centre National de La Recherche Scientifique; ²Synergie 4

We report on investigations of the interfaces between liquid or solid Pb and single- or poly-crystalline Cu substrates. EBSD analyses show that Pb grains have a different orientation relationship with Cu depending on whether Pb is deposited by PVD or solidified from droplets. When Pb is solidified from droplets, surprisingly, a cube-on-cube orientation relationship prevails between the Pb crystals and the substrate on each Cu grain surface, whatever its surface orientation, even though the lattice parameter of Pb is 1.37 times larger than that of Cu. SEM and AFM analyses show that during annealing of Pb droplets, ridges build up at the droplet-substrate triple lines, indicating that the interfaces evolve towards equilibrium by diffusion processes. We discuss these features in comparison with experiments and calculations performed on Pb nanocrystals embedded in Al, another fcc solid with a lattice parameter smaller than that of Pb.

4:55 PM Invited

Diffusion Reactions at Metal-Oxide Interfaces: The Effect of an Applied Electric Field: Yeonseop Yu¹; Jeremy Mark¹; Frank Ernst¹; Thomas Wagner²; Gurpreet Singh³; Rishi Raj³; ¹CASE; ²Max-Planck-Institut für Metallforschung; ³University of Colorado

We have studied the effect of an applied electric field on diffusion reactions at Al-MgAl₂O₄ interfaces. Annealing experiments were carried out at 620°C with (i) no applied electric field, (ii) an applied electric field oriented towards the Al epilayer, and (iii) an applied electric field oriented towards the MgAl₂O₄ substrate. The resulting microstructural changes after different annealing times were investigated by advanced,

complementary methods of transmission electron microscopy. Our studies reveal that an electric field oriented towards the MBE-grown Al layer promotes the growth of a Mg-deficient phase — presumably γ -Al₂O₃. A field in the opposite direction, in contrast, does not result in the formation of a reaction phase. A model will be presented to explain these observations, which may be significant for controlling the mechanical properties of related metal-oxide interfaces.

5:20 PM Invited

Bonding and Interface Structures of Metal/SrTiO₃ Systems: Christina Scheu¹; Elena Tchernychova²; Klaus van Benthem²; Gunther Richter²; Thomas Wagner²; Manfred Rühle²; ¹University of Leoben; ²Max-Planck-Institut für Metallforschung

In this study the interface structure of fcc and bcc metals deposited by molecular beam epitaxy on the (100) surface of single-crystalline SrTiO₃ was investigated by high-resolution and analytical transmission electron microscopy. The interfaces are abrupt and, depending on the lattice mismatch, either coherent or semi-coherent interfaces form. Various orientation relationships were observed for the different metal/SrTiO₃ interfaces. In all cases, the interfacial bonding involves metal-oxygen bonds as determined by energy-loss near-edge structure studies. The results indicate that Sr atoms do not participate in the adhesion and that the interfaces are terminated by TiO₂ rather than SrO layers. In contrast, simulations of the high-resolution images indicate a slightly better agreement for SrO terminated models. The formation of the preferred orientation relationships and the interface features will be discussed based on geometrically constructed models and compared to theoretically predicted interface structures! Ochs and Elsässer, Z. Metall. 5 (2002) 406.

The Rohatgi Honorary Symposium on Solidification Processing of Metal Matrix Composites: Processing and Microstructure of MMCs - I

Sponsored by: The Minerals, Metals and Materials Society, TMS Materials Processing and Manufacturing Division, TMS Structural Materials Division, TMS/ASM: Composite Materials Committee, TMS: Solidification Committee

Program Organizers: Nikhil Gupta, Polytechnic University; Warren H. Hunt, Aluminum Consultants Group Inc

Monday PM
March 13, 2006

Room: 207B
Location: Henry B. Gonzalez Convention Ctr.

Session Chairs: David J. Weiss, ECK Industries Inc; Doru M. Stefanescu, University of Alabama

2:00 PM Invited

Particle Interaction with the Solidification Front – A Fundamental, Multidisciplinary Problem: Doru Michael Stefanescu¹; ¹Ohio State University

The interaction of particles with solid-liquid interfaces has been studied since the mid 1960's. While the original interest stemmed from geology applications (frost heaving in soil), researchers soon realized that understanding this phenomenon might yield practical benefits in other fields, including metallurgy and cryobiology. Significant research was focused on applications to metal matrix composites produced by casting or spray forming techniques. In the most common cast metal matrix composites, Al-Si/SiC particles, the particles are distributed at the grain boundaries, decreasing plastic properties. The particle-solid/liquid interface interaction was also found to play an important role in the solidification of ternary eutectics, in the formation of microporosity during solidification, and in the growing of 123 (YBaCu) superconductor crystals from an undercooled liquid. The paper will attempt to summarize the available experimental data for different applications. Then, it will review the main theoretical models discussing their strength and weaknesses in some detail.

2:25 PM Invited

Metal Matrix and Polymer Nanocomposites: *Rahul R. Maharsia*¹;
¹Louisiana State University

Metal matrix composites (MMC) possess excellent thermal and mechanical properties and are widely used in aerospace and automobile applications. In this paper, the current state of research on nanoparticle filled MMCs is presented. Studies related particle packing, pushing and wetting are reviewed and mechanical properties of metal based nanocomposites are discussed. A comparison is made between material characteristics and properties of polymer matrix composites and MMCs modified through various nanoparticles.

2:50 PM Invited

The Technological Aspects of Alfa Composites Synthesis: *Jerzy Sobczak*¹; *Pawel Darlak*¹; *Robert M. Purgert*²; *Natalia Sobczak*¹; *Andrzej L. Wojcieszynski*³; ¹Foundry Research Institute; ²Energy Industries of Ohio; ³Motor Transport Institute

Aluminum alloys containing fly ash (ALFA - Aluminum Fly Ash) composites have been developed in recent years. The use of fly ash as a filler or reinforcement for aluminum matrix composites is very desirable from an environmental standpoint. However, synthesis of ALFA composites by liquid phase routes is difficult due to poor wettability of fly ash by molten Al and Al alloys at industrially important temperatures and its lightweight nature (particularly for hollow spheres). In this work some technological aspects of ALFA composites synthesis have been discussed in order to demonstrate advantages and disadvantages of selected production methods as well as corresponding properties and possible applications of ALFA composites.

3:15 PM

The Influence of the Reinforcement Phase upon the Formation of Casting Defects in Aluminum Matrix - Al-Zr-O-B Particulate Composites: *Richard W. Hamilton*¹; *Yutao Zhao*²; *Peter D. Lee*¹; ¹Imperial College; ²Jiangsu University

The presence of ceramic particles in cast materials at composite levels is well known to act as a reinforcing phase increasing final properties such as tensile and fatigue strength. However, well distributed particulate phases that are stable at melt temperature can also reduce the formation of casting defects such as porosity and segregation. A novel aluminium matrix composite reinforced with in-situ ZrB₂, Al₂O₃ and Al₃Zr particulates was synthesized using a magneto-chemical reaction in molten aluminium to produce a mixture of ZrB₂, Al₂O₃ and Al₃Zr reinforcement particles. The influence of processing parameters on the reinforcement distribution, and the subsequent effect of the reinforcement on the resulting microstructure were investigated using in situ radiography, X-ray microtomography and standard characterisation techniques. The influence of volume fraction particulate on the distribution of porosity and segregation was quantified and reasons for the reduction in casting defects was hypothesised.

3:40 PM Invited

Solidification Rate Effects on Microstructural and Mechanical Properties in Pressure Cast Magnesium Metal Matrix Composites: *Adam Robert Loukus*¹; ¹GS Engineering

Solidification rates play a large role in microstructural evolution in a cast component. Microstructures of cast composites add increased complexity to the solidification process due to the ceramic reinforcements (i.e. inclusions) cast into the component. Current observations suggest that the solidification rates have an impact on the grain size and structure in an MMC material. In the current study a pressure cast composite component is cast solidification rates are varied to study microstructural differences. The component is tensile tested and the grain size beneath the fracture surface is measured using SEM techniques. Effects of grain size, and intermetallic content in the cast component due to the various cooling rates are analyzed using a SEM machine while the macro effects are studied by testing elongation, ultimate strength and elastic modulus.

4:05 PM Break

4:20 PM

Fabrication of Carbon Fiber Reinforced Aluminum – Magnesium Alloy Composite Wires Using Ultrasonic Infiltration Method: *Tadashi*

*Matsunaga*¹; *Kenji Ogata*¹; *Tomei Hatamaya*¹; *Kenji Shinozaki*¹; *Makoto Yoshida*²; ¹Hiroshima University; ²Waseda University

M40J carbon fiber reinforced aluminum – 0, 1.3, 2.4, 4.7, 10 mass % magnesium alloy composite wires were fabricated by using ultrasonic infiltration method. Addition of magnesium into molten aluminum was remarkably improved infiltrability of the molten aluminum alloy into bundle of the carbon fiber regardless of fabricating speed from 0.03 to 0.22 m/s. In order to make clear the mechanism of infiltration of molten metal through the bundle using ultrasonic, the generating cavitations in the molten alloy were measured by means of acoustic emission. The cavitations were generated by addition of magnesium remarkably. As the results, the infiltrability strongly corresponded to the generating acoustic cavitation, which would be caused by addition of magnesium.

4:45 PM

Interaction between Molten Aluminum and Selected Oxides: *Natalia Sobczak*¹; ¹Foundry Research Institute

In situ reactive synthesis of composite materials offers a number of advantages, of which the thermodynamic stability of reinforcing phases is the most important. Oxy-redox reactions between Al and reactive oxides have been successfully applied to synthesize Al-Al₂O₃ type composites having unique C4 structures by liquid phase processing using either vortex casting, reactive metal infiltration of porous ceramic preform or reactive metal penetration of dense ceramics. Whatever the process, the wettability and reactivity between Al and ceramic phase is required. The paper summarizes the experimental results on wettability and reactivity in different couples with simple oxide (Al/SiO₂, Al/ZnO, Al/B₂O₃, Al/TiO₂, Al/ZrO₂, Al/CoO, Al/NiO), binary oxides of SiO₂-Al₂O₃ system and complex oxides of SiO₂-Al₂O₃-Fe₂O₃-TiO₂-CaO-MgO type. The analysis of factors affecting wetting and transformation kinetics in Al/reactive oxide couples has been done to demonstrate the possibility and to determine the conditions for in situ synthesis of composites materials by liquid phase route.

5:10 PM Invited

Processing and Characterization of Fly Ash Particle Reinforced A356 Al Composites: *Mirle Krishnegowda Surappa*¹; *Sudarshan*¹; ¹Indian Institute of Science

A356 Al - fly ash particle composites were fabricated using stir-cast technique. Bulk hardness and matrix microhardness of A356 Al-fly ash composites are higher compared to those of the unreinforced alloy. In the as extruded condition, 0.2% proof stress of the composites is higher compared to that of unreinforced alloy. Additions of fly ash leads to increase in hardness, elastic modulus and 0.2% proof stress. Composites reinforced with 12-volume % fly ash exhibits lower UTS compared to that of unreinforced alloy. The narrow size range fly ash particle reinforced composite shows better mechanical properties compare to wide size range particles. Damping behaviour of unreinforced alloy and their composites have been studied using dynamic mechanical thermal analyzer (DMTA). A356 Al-fly ash MMCs were found to exhibit improved damping capacity when compared to unreinforced alloy both at ambient temperatures and at elevated temperatures.

5:35 PM Invited

Fabrication and Microstructure of Magnesium Alloy- Fly Ash Microballoon Composites: *Atef Awad Doud*¹; *Pradeep Rohatgi*²; ¹CMRDI; ²University of Wisconsin-Madison

The ZC63 alloy- fly ash particles composite was processed by melt stir technique. Optical microscopy was used to reveal the microstructural features and the distribution of the fly ash particles. Compositional spot analyses were performed in and around the particles using an Energy Dispersive X-ray Analysis (EDXA) facility in the SEM. XRD analyses were carried out to identify the phases in the matrix alloy and composite. The density of the composites was determined using Archimedes' method, with ethanol as the suspending medium. Visual inspection of machined surface of the cast composite showed uniform distribution of fly ash microballoons throughout the casting. Casting defects were not noticed on the casting surface. The microstructure demonstrates even distribution of the particles in the Mg alloy matrix and there is no sign of fly ash cluster or residual porosity.

Titanium Alloys for High Temperature Applications - A Symposium Dedicated to the Memory of Dr. Martin Blackburn: Titanium Alloys for High Temperature Applications - In Memory of Dr. Martin Blackburn

Sponsored by: The Minerals, Metals and Materials Society, TMS Structural Materials Division, TMS: Titanium Committee
Program Organizers: Michael W. Peretti, Lyondell Chemical Company; Daniel Eylon, University of Dayton; Ulrike Habel, Munich; Guido C. Keijzers, Del West USA; Michael R. Winstone, DSTL

Monday PM Room: 201
 March 13, 2006 Location: Henry B. Gonzalez Convention Ctr.

Session Chairs: James C. Williams, Ohio State University; Harry A. Lipsitt, Air Force Materials Laboratory, Retired

2:00 PM Introductory Comments

2:10 PM Keynote

Remembering Martin: Technical Contributor, Colleague and Friend: *James C. Williams*¹; Harry A. Lipsitt²; Daniel F. Paulonis³; ¹Ohio State University; ²Air Force Materials Laboratory, Retired; ³Pratt & Whitney

This talk will outline some of the major technical contributions of Martin Blackburn, who truly was a pioneer in defining many aspects of the modern physical metallurgy and behavior of Ti alloys and of other structural alloys. It also will recall some of the wonderful wit and wisdom of this special person in (hopefully) a fun but respectful manner. The talk will comprise several distinct phases of Martin's professional life: The early Boeing years; the Air Force years and the Pratt & Whitney years.

Titanium Alloys for High Temperature Applications - A Symposium Dedicated to the Memory of Dr. Martin Blackburn: Applications of High Temperature Titanium Alloys

Sponsored by: The Minerals, Metals and Materials Society, TMS Structural Materials Division, TMS: Titanium Committee
Program Organizers: Michael W. Peretti, Lyondell Chemical Company; Daniel Eylon, University of Dayton; Ulrike Habel, Munich; Guido C. Keijzers, Del West USA; Michael R. Winstone, DSTL

Monday PM Room: 201
 March 13, 2006 Location: Henry B. Gonzalez Convention Ctr.

Session Chairs: Michael W. Peretti, Lyondell Chemical Company; Michael R. Winstone, DSTL

3:00 PM Introductory Comments Address by Jack Schirra

3:10 PM Keynote

High Temperature Titanium Alloy Usage in Turbine Engines - Applications, Developments and Challenges: *John J. Schirra*¹; Daniel F. Paulonis¹; James O. Hansen¹; Douglas Berczik¹; ¹Pratt & Whitney

Titanium found ready acceptance in the aircraft engine industry with rapid growth in applications since its original implementation as compressor airfoils and fan disks in P&W J57 and JT3 engines. The specific strength capability of titanium was a key enabler to the development and widespread use of gas turbine engines. Titanium usage in commercial engines has plateaued at ~25% of system weight driven primarily by high temperature capability limitations including engineering capability and burn resistance. Due to system level requirements, titanium alloys, particularly burn resistant alloys, continued to find increased usage in military engines where weight requirements can balance the increased cost of these materials. This paper will review the history of titanium alloy usage at P&W, with a focus on advances made during Martin Blackburn's 25 year career in P&W Materials Laboratory, and highlight the application/

development challenges required for continued significance of this material system to the engine community.

4:00 PM Break

4:30 PM Invited

High Temperature Titanium Alloy Applications at GE Aircraft Engines: *Andrew P. Woodfield*¹; ¹GE Transportation

The current usage of high temperature titanium alloys within GE Aircraft Engines will be reviewed, highlighting issues associated with current and potential future alloys. In particular, the importance of understanding lower temperature phenomena such as dwell fatigue are key before introduction of new higher temperature titanium alloys.

5:00 PM Invited

Application of High Temperature Titanium Alloys in Aero-Engines - Limits Due to Bulk and Surface Related Properties: *Dietmar Helm*¹; ¹MTU Aero Engines

This paper describes typical examples of the application of modern high temperature Titanium alloys as Ti 6242 and Timetal 834 in various sections of aero-engines. Specific attention is given to the relevance of optimized microstructures for best balances of required mechanical properties, weight optimization and surface integrity when being operated in air at temperatures exceeding 450°C. The example of Timetal 834, currently representing the alloy with the highest temperature capability being in service for major rotating parts and structural components, will be used to demonstrate the gap of maximum potential service temperature due to good bulk properties and thermodynamically stability and the limitation to lower service temperatures due to surface oxidation. The effects of protective coatings aiming for closing this gap will be discussed with relevance to mechanical properties. Furthermore, results of surface treatments as shot peening at high service temperatures will be presented.

Ultrafine Grained Materials - Fourth International Symposium: Processing and Microstructures I

Sponsored by: The Minerals, Metals and Materials Society, TMS Materials Processing and Manufacturing Division, TMS Structural Materials Division, TMS/ASM: Mechanical Behavior of Materials Committee, TMS: Shaping and Forming Committee
Program Organizers: Yuntian T. Zhu, Los Alamos National Laboratory; Terence G. Langdon, University of Southern California; Zenji Horita, Kyushu University; Michael Zehetbauer, University of Vienna; S. L. Semiatin, Air Force Research Laboratory; Terry C. Lowe, Los Alamos National Laboratory

Monday PM Room: 217D
 March 13, 2006 Location: Henry B. Gonzalez Convention Ctr.

Session Chairs: Carl C. Koch, North Carolina State University; Ibrahim Karaman, Texas A&M University; S. L. Semiatin, Air Force Research Laboratory; Sergey Dobatkin, A.A. Baikov Institute of Metallurgy and Material Science

2:00 PM Invited

Artifact-Free Bulk Nanocrystalline Grain Size (< 100 Nm) Materials: The Processing Challenge: *Carl C. Koch*¹; Khaled M. Youssef¹; Ronald O. Scattergood¹; Korukonda L. Murty¹; ¹North Carolina State University

It has been clear for many years that bulk, artifact-free nanocrystalline materials are required for both meaningful mechanical testing and for potential structural applications. It is desirable to optimize strength by obtaining the smallest practical grain size - less than 50 nm if possible. A major challenge is to produce nanocrystalline materials with a fine grain size in bulk form without processing artifacts such as porosity, incomplete particulate bonding, or deleterious grain boundary impurities. In recent years progress in processing methods has allowed artifact-free metals and alloys to be made in bulk form. These materials can exhibit very high strength along with good ductility. The attractive processing techniques include special electro-deposition methods and certain severe plastic deformation methods. These advances in processing will be described in

this talk along with the results of mechanical tests on artifact-free materials. Future processing needs will be discussed.

2:20 PM Invited

Ductility Enhancement of Ultrafine Grained Commercially Pure 1050 Aluminum Alloy by Cross Accumulative Roll-Bonding (C-ARB): *Yong-Suk Kim*¹; *Suk Ha Kang*¹; *Dong Hyuk Shin*²; ¹Kookmin University; ²Hanyang University

The Cross-ARB (C-ARB) process -changing rolling direction by 90 degrees for each ARB cycle- has been carried out up to nine cycles on a commercially pure 1050 Al alloy to obtain ultra-fine grained microstructure. The C-ARB process was adapted with an expectation of increasing ductility of the severely deformed alloy. Microstructures of the C-ARB processed aluminum alloy were examined as a function of accumulated total strain and direction of the rolling. Mechanical properties including hardness and tensile property of the processed Al alloy were also investigated. Grain sizes of the C-ARB processed alloy were found to vary across thickness of the processed alloy plate. Tensile strength of the processed 1050 Al alloy increased from 100MPa to 160MPa. Tensile elongation varied depending on number of process cycle, tensile axis, and rolling direction, but up to 15% of failure strain was measured from a specimen that experienced six C-ARB cycles.

2:40 PM Invited

High Angle Boundary Formation in Dynamically Recovered Materials during Severe Hot Forging: *Taku Sakai*¹; ¹University of Electro-Communications

The evolution mechanisms of new high-angle boundary as well as ultra-fine grains in large strain were studied using dynamically recovered materials, such as ferritic steels, aluminum and magnesium alloys, by means of multidirectional forging (MDF). The compression tests were carried out using rectangular samples with consequent changing of loading direction in 90° through three of mutually perpendicular axes. The structural changes can be characterized by the evolution of deformation bands, such as kink and microshear bands at moderate strains. MDF accelerates the evolution of many mutually crossing kink and microshear bands developed in various directions. The (sub)grains become more equiaxed and the misorientations between them gradually increase with increase in cumulative strain, finally leading to the development of new fine-grained structure. It is concluded that the dynamic grain formation can result from a kind of continuous reactions taking place during deformation, i.e. continuous dynamic recrystallization.

3:00 PM

Principles of Grain Refinement in Processing by ECAP: *Cheng Xu*¹; *Minoru Furukawa*²; *Zenji Horita*³; *Terence G. Langdon*¹; ¹University of Southern California; ²Fukuoka University of Education; ³Kyushu University

Equal-channel angular pressing (ECAP) may be used to achieve very significant grain refinement in bulk materials. Typically, the materials processed by ECAP have ultrafine grain sizes within the submicrometer range. This paper examines the homogeneity and the microstructural characteristics of pure aluminum and aluminum-based alloys processed by ECAP. Emphasis is placed on the development of a homogeneous ultrafine-grained microstructure with increasing numbers of passes through the ECAP die. The experimental observations are used to develop a representative model that provides a satisfactory explanation for grain refinement in ECAP.

3:15 PM

Bottom Up Fabrication of Bulk Nanocrystalline Materials Using Severe Plastic Deformation (SPD): Consolidation of Nanoparticles via Equal Channel Angular Extrusion (ECAE): *Ibrahim Karaman*¹; *Mohammed Haouaoui*¹; *Hans J. Maier*²; ¹Texas A&M University; ²University of Paderborn

SPD techniques can be used to refine grains of pure elements down to submicron range, however, achieving grain sizes below 100 nm in bulk (all dimensions in cm range) with considerable ductility is still a challenge. Other available methods of fabricating nanocrystalline materials also suffer from the difficulty of producing bulk samples. In this study, we utilize ECAE as a consolidation technique for controlling grain size from tens of nanometer to micron range by controlling the initial particle size. With this method, we obtained near full density Cu samples with grain

sizes below 100 nm, diameters more than 1.5 cm and lengths of 8 cm and longer. The preliminary results showed UTS levels as high as 800 MPa with fracture strains on the order of 5 to 8%. In this presentation, the challenges and opportunities for utilizing ECAE as a powder consolidation technique and our recent findings will be discussed.

3:30 PM

Consolidation of Nanostructured and Ultrafine Grained Metal Powders Using Equal Channel Angular Pressing: *Deliang Zhang*¹; *Peng Cao*¹; *Hongbao Yu*¹; *Kenong Xia*²; *Xiaolin Wu*²; *Stiliana Raynova*¹; ¹University of Waikato; ²University of Melbourne

Nanostructured and ultrafine grained metal powders such as Cu, Al and Ti were produced by using high energy mechanical milling. These powders have been consolidated using a typical severe plastic deformation process, equal channel angular pressing (ECAP) to utilise the large amount of shearing in ECAP to enhance the sintering effect. Microstructural characterisation, microhardness testing and tensile testing of the bulk samples are conducted to investigate the effects of ECAP conditions such as temperature, forward pressure and back pressure on the grain sizes and quality of the bulk samples produced. The fracture surfaces of the tensile test samples and the shape change of powder particles that occurs during ECAP are also examined to determine the degree of atomic bonding between powder particles achieved by ECAP and to establish the factors which affect it. This paper is to report and discuss the major findings of this study.

3:45 PM

ECA Pressing up to Failure of Oxygen-Free Copper: Structure, Properties, Effect of the Route: *Sergey Dobatkin*¹; *Jerzy Szpunar*²; *Alexander Zhilyaev*³; *Artem Kuznetsov*¹; ¹A.A.Baikov Institute of Metallurgy and Materials Science; ²McGill University; ³Institute of Metals Superplasticity Problems

Structure and mechanical properties of oxygen-free copper depending on the route of ECA pressing at very high strain were studied. Deformation was performed at an angle of 90° between the channels. The maximum number of passes upon deformation by routes A, Bc, and C was N=25. The TEM and EBSD examination revealed the appearance of subgrains and sub-micron grains. The average size of structure elements was 200-300 nm (by TEM) and 250-450 nm (by EBSD). The fraction of high-angle boundaries at N=4 is between 69 and 77%. The equiaxed structure is formed most rapidly upon deformation by route Bc. All strength characteristics have the maximum values after route Bc. Elongation decrease at the early stage of ECA pressing, but then it is stabilized or grow. An increase in plasticity is most pronounced upon deformation by route Bc after sufficiently high strain.

4:00 PM Break

4:10 PM Invited

Plastic Strain-Induced Grain Refinement at the Nanometer Scale in Cu: *Ke Lu*¹; ¹Institute of Metal Research, Chinese Academy of Sciences

Formation of ultrafine grains via severe plastic deformation in various metals has been studied extensively. Nevertheless, strain-induced grain refinement in the nanometer scale has not yet been fully understood. Plastic deformation mechanism and corresponding dislocation activities in nano-sized grains differ significantly from those in coarse grains. A different underlying mechanism for formation of nano-size grains is anticipated. In the present talk, microstructural evolution of pure Cu processed by means of surface mechanical attrition treatment (SMAT) was investigated by means of TEM observations. Grain refinement processes varying from micro- to nano-scale have been examined systematically within the SMAT sample in which a gradient microstructure is achieved with an average grain size of about 10 nm in the top surface layer. Detailed microstructure features together with analysis of the refinement mechanism of nano-sized grains will be presented. Both dislocation activity and mechanical twinning play a key role in the refinement process.

4:30 PM Invited

Scaling Analysis of Boundary Spacing in Nanostructured Metals: *Xiaoxu Huang*¹; *Niels Hansen*¹; ¹Riso National Laboratory

In the last symposium on Ultrafine grained materials (UFG III), we illustrated the importance in the selection of observation planes for pre-

cise characterization of ultrafine grained or nanostructured metals produced by severe plastic deformation. In this study we quantify the boundary spacing on appropriately selected sample planes as a function of plastic strain. Pure Ni samples deformed by HPT to strains above 10 and commercial purity Al samples deformed by cold rolling to strains above 5 are observed in transmission electron microscopy. The distribution of boundary spacing at different strains is measured and analysed to understand the scaling behaviour during the plastic deformation. The results are discussed in terms of the principles that govern the structural evolution during the deformation.

4:50 PM Invited

Experimental Study and Computer Modeling of High Pressure Torsion: Igor V. Aleksandrov¹; Gyorgy Krallics²; Jan Bonarski³; Marina Zhilina¹; Anna Dubravina¹; Irina Shaimardanova¹; ¹Ufa State Aviation Technical University; ²Budapest University of Technology and Economics; ³Polish Academy of Sciences

High pressure torsion (HPT) is one of most wide-spread schemes for severe plastic deformation. This scheme is often applied for analysis of scientific aspects, connected with formation of bulk ultrafine-grained (UFG) and nanostructured states. At the same time the investigation of the HPT process is a topical issue. This is connected with its multiple-factor character. In this work we present the results of experimental investigations and computer simulation of processes, accompanying HPT of pure copper. Analysis of the material flow features was made in frames of the developed analytical model and the finite element method. The process of the preferred orientations' formation was studied in frames of the viscous-plastic self-consistent model. The interrelation between the components of the stress-strain state and the features of structure- and texture-formation in bulk billets, subjected to HPT, was revealed.

5:10 PM Invited

FEM Analysis of Different Aluminum Alloys Severely Strained by Multipass ECAP: Material Properties and Geometry Effects on Deformation Behavior: Emanuela Cerri¹; Paola Leo¹; Pier Paolo De Marco¹; ¹University of Lecce

Three-D FEM simulations of both one and four ECAP passes of different aluminium alloys were performed in order to investigate the deformation state of processed workpiece and, moreover, the effect of different Strain Hardening Rate (SHR) and die geometry (in term of variation of outer angle die) on deformation behaviour. FEM analysis showed a lower equivalent plastic strain on outer side of both cross and longitudinal sections of billets after one and four passes. These results were confirmed both by HV hardness and microhardness test on the same sections of ECAP processed specimens and by microstructural investigations. Moreover FEM analysis indicated that as alloys SHR increases a greater strain inhomogeneity is obtained on cross section of processed specimen. The same effect was observed as the outer angle die increases.

5:30 PM

Influence of Die Features on the ECAP Process: Ralph J. Hellmig¹; ¹Clausthal University of Technology

It has been demonstrated earlier that using a dislocation density based constitutive model is suitable for determining the evolution of microstructure, mechanical properties and texture due to ECAP processing^{1,2}. Using FEM simulation, it is also possible to investigate the homogeneity of deformation due to various processing conditions. In this work, the influence of typical ECAP die features (channel geometries; cross-section reduction; various pressure conditions inside the channel, for example due to homogeneous and inhomogeneous backpressure) is investigated using FEM simulation based on the mentioned constitutive model. The aim of this study is to evaluate the advantages/disadvantages of typical ECAP die designs and processing conditions. ¹Baik SC, Hellmig RJ, Estrin Y, Kim HS: Z. Metallkd. 94 (2003) 754-760. ²Baik SC, Estrin Y, Hellmig RJ, Jeong HT, Brokmeier HG, Kim HS: Z. Metallkd. 94 (2003) 1189-1198.

Wechsler Symposium on Radiation Effects, Deformation and Phase Transformations in Metals and Ceramics: Irradiation Microstructure/ Microchemistry

Sponsored by: The Minerals, Metals and Materials Society, ASM International, TMS Structural Materials Division, ASM Materials Science Critical Technology Sector, TMS Materials Processing and Manufacturing Division, TMS/ASM: Mechanical Behavior of Materials Committee, TMS/ASM: Nuclear Materials Committee, TMS/ASM: Phase Transformations Committee

Program Organizers: Korukonda L. Murty, North Carolina State University; Lou K. Mansur, Oak Ridge National Laboratory; Edward P. Simonen, Pacific Northwest National Laboratory; Ram Bajaj, Bettis Atomic Power Laboratory

Monday PM Room: 208
March 13, 2006 Location: Henry B. Gonzalez Convention Ctr.

Session Chairs: Steven J. Zinkle, Oak Ridge National Laboratory; Roger E. Stoller, Oak Ridge National Laboratory

2:00 PM Invited

Effects of Irradiation on Stress Corrosion Cracking of Austenitic and Ferritic-Martensitic Steels in Supercritical Water: Gary S. Was¹; Sebastien Teyssyre¹; Jiao Zhijie¹; Gaurav Gupta¹; ¹University of Michigan

This paper presents the effect of irradiation on the stress corrosion cracking behavior of irradiated austenitic and ferritic-martensitic (F-M) alloys in supercritical water, in support of the supercritical water reactor concept. Austenitic alloys 304L, 316L, 690 and 800H and F-M alloys T91, HCM12A and HT-9 were irradiated with 2-3 MeV protons to doses between 3 and 10 dpa over the temperature range 400-500°C and tested in constant extension rate mode in deaerated supercritical water at temperatures of 400 and 500°C. Results showed that the austenitic alloys exhibited a substantial increase in IG cracking over the unirradiated condition. Of the F-M alloys, only HT-9 exhibited IG cracking in the irradiated condition. The dependence of IASCC on dose, temperature and the correlation with microstructure will be presented in an effort to identify the microstructure changes responsible for enhanced IGSCC in supercritical water.

2:25 PM

Thermal and Radiation-Induced Segregation in Model Ni-Base Alloys: Todd R. Allen¹; Lizhen Tan¹; Gary S. Was²; ¹University of Wisconsin; ²University of Michigan

Generation IV nuclear energy systems will operate at higher temperatures than current light water reactors and Ni-base alloys are receiving attention as core materials. One aspect of the radiation response of Ni-base alloys to radiation that is not well understood is grain boundary segregation. In this work, three alloys, specifically Ni-18Cr, Ni-18Cr-9Fe, and Ni-18Cr-0.08P were given a series of thermal treatments and quenching to understand the development of thermal non-equilibrium segregation. Additionally, they were irradiated using 3.2 MeV protons at temperatures from 200-500°C to doses up to 1 dpa. Grain boundary segregation was measured with Auger Electron Spectroscopy and Scanning Transmission Electron Microscopy with Energy Dispersive Spectroscopy. Under irradiation, the addition of iron to Ni-18Cr reduced the grain boundary chromium depletion, while the addition of phosphorus to Ni-18Cr increased the grain boundary chromium depletion. Chromium enriches in Ni-18Cr and Ni-18Cr-0.08P due to thermal treatment, but depletes in the Ni-18Cr-9Fe.

2:45 PM

Radiation Stability of Oversize Solute Additions in Austenitic Stainless Steels: Micah J. Hackett¹; Gary S. Was¹; Jeremy T. Busby²; ¹University of Michigan; ²Oak Ridge National Laboratory

The addition of oversize solutes, such as hafnium or zirconium, to austenitic stainless steel may delay or reduce radiation damage through the trapping and enhanced recombination of point defects. Previous work has

shown reductions in void swelling and radiation-induced segregation in addition to a change in the dislocation microstructure. Varying levels of Zr have been added to Fe-14Cr-14Ni and Hf to Fe-17Cr-14Ni and irradiated with 3.2 MeV protons up to doses of 10 dpa at temperatures of 400°C. Void swelling was measured from the void size distribution using transmission electron microscopy. Dark field TEM imaging was used to determine the dislocation size and density, and RIS was measured using STEM-EDS. Improvements in microstructure and microchemistry of the irradiated oversize solute alloys are demonstrated relative to reference 316SS. Void swelling is delayed until higher doses and radiation hardening is reduced for the Hf alloys. A reduction in RIS is also observed.

3:05 PM

Role of Grain Boundary Engineering in Mitigating IASCC in F-M Alloy HT-9: *Gaurav Gupta*¹; Gary S. Was¹; ¹University of Michigan

Ferritic-martensitic alloys have been identified as candidate core structural alloys for the supercritical water reactor (SCWR). Studies have shown that F-M alloys experience high oxidation rate in SCW. They exhibit low susceptibility to SCC, except HT-9 which has shown evidence of cracking in SCW at 400-500°C. HT-9 was irradiated at 400 and 500°C using 2 MeV protons to a dose of 7 dpa and tested in constant extension rate mode at 400 and 500°C in deaerated SCW. Proton irradiation enhanced cracking susceptibility in 400°C SCW with the lower irradiation temperature exhibiting more cracks and a higher maximum crack depth. Grain boundary engineering (GBE) is being explored as a means of reducing the susceptibility of HT-9 to SCC/IASCC in SCW. GBE has already proved beneficial in improving creep properties of T91. Results of CERT tests conducted on unirradiated/irradiated HT-9 in argon and SCW will be presented.

3:25 PM Break

3:45 PM

The Change in the Hardness of LCAC, TZM, and ODS Molybdenum in the Post-Irradiated and Annealed Conditions: *Brian Vern Cockeram*¹; Richard W. Smith¹; Lance L. Snead²; ¹Bechtel-Bettis; ²Oak Ridge National Laboratory

An indirect measure of defects and recovery can be obtained using hardness measurements. Hardness measurements were performed on wrought Low Carbon Arc Cast, TZM, and ODS molybdenum in the post-irradiated and annealed condition to determine the kinetics for defect mobility. Irradiations performed in HFIR at 270C to 600C were shown to result in relatively large increases in hardness (54-100%), while small increases in hardness (-11% to 18%) were observed for irradiations at 870-1100C. The kinetics for hardness recovery for irradiations at 270-605C were determined by performing isochronous anneals. Recovery is observed to begin at about 600C and was completed at 1100C for both LCAC and ODS. The activation energy for recovery was determined to be about 4 eV for LCAC and ODS, which is comparable to values reported in literature for molybdenum self-diffusion. TZM exhibits much slower recovery kinetics, which can be explained by the presence of carbon in solution.

4:05 PM

Effect of Self-Irradiation on Bulk Swelling of Plutonium Alloys: *Christophe Thiebaud*¹; Nathalie Baclet¹; Pierre Giraud¹; Pascale Julia¹; Brice Ravat¹; ¹CEA Centre De Valduc

Several studies show that plutonium alloys present bulk swelling. More precisely, length (as measured by dilatometry) and cell parameter (as measured by X-ray diffraction) increase with time and reach a saturation after a few months. This is very comparable to the phenomenon observed on both ceramics and metallic alloys exposed to radiation. This bulk swelling can be correlated to self-induced radiation due to the decay of the different plutonium isotopes (238Pu, 239Pu, 241Pu and 242Pu) which also induce helium that tends to forms clusters, then bubbles. Many experimental and theoretical results have already been published. The goal of this paper is to review some of the results and to propose a strategy for both experiments and modelling to try to answer some of the remaining questions regarding swelling and more generally self-irradiation defects in plutonium alloys.

2006 Nanomaterials: Materials and Processing for Functional Applications: Nanoscale Electronics

Sponsored by: The Minerals, Metals and Materials Society, TMS Electronic, Magnetic, and Photonic Materials Division, TMS: Nanomaterials Committee

Program Organizers: W. Jud Ready, GTRI-EOEML; Seung Hyuk Kang, Agere Systems

Tuesday AM Room: 214C
March 14, 2006 Location: Henry B. Gonzalez Convention Ctr.

Session Chairs: Seung Hyuk Kang, Agere Systems; W. Jud Ready, GTRI-EOEML

8:30 AM Introductory Comments

8:35 AM Invited

Performance Modeling for Metallic Single Wall Carbon Nanotube Interconnects for Gigascale Integration (GSI): *Azad Naeemi*¹; James D. Meindl¹; ¹Georgia Institute of Technology

In this presentation, after reviewing the circuit models for single wall carbon nanotubes (SWCN), their potential application as interconnects in gigascale chips is evaluated. The results offer important guidance regarding the nature of carbon nanotube technology development needed for improving interconnect performance. For short local interconnects whose resistances are dominated by their drivers, monolayer nanotube interconnects offer latencies smaller than those of their copper counterparts due to significantly smaller lateral capacitances. Significant decreases in power dissipation, crosstalk, and dynamic delay variation are other advantages of replacing copper wires with monolayer nanotube interconnects. For longer lengths, however, bundles of densely packed single wall nanotubes are needed to outperform copper interconnects in terms of resistance and to adequately improve the wave propagation speed. The impact of electron-phonon scattering on the performance of carbon nanotube interconnects is demonstrated to be negligible. This is in sharp contrast with the transistor application of carbon nanotubes.

9:00 AM Invited

Controlled Positioning of Nanoparticles in a Wafer-Level: *Seong Jin Koh*¹; ¹University of Texas, Arlington

Precise positioning of nanoscale objects (such as nanoparticles, carbon nanotubes, nanowires, DNAs, proteins, etc) onto exact substrate locations is one of the key requirements for the realization of nanoscale functional devices. Combining wet chemistry and CMOS fabrication technology, we have developed a technique which enables wafer-level positioning of nanoparticles with nanoscale precision. In this approach, self-assembled monolayers (SAMs) of organic molecules are formed on selected areas of a lithographically patterned silicon wafer. Gold nanoparticles in the range of 20-250 nm selectively attach to the areas functionalized with SAMs, enabling one-dimensional alignment of nanoparticles along the predefined patterns. This technique can be applied to the alignment of other nanoscale objects in general. The application of this technique to the fabrication of single electron devices and carbon nanotube devices will be discussed. Supported by ONR (N00014-05-1-0030) and NSF CAREER (ECS-0449958).

9:25 AM Break

9:35 AM

Fabrication and Characterization of Novel InGaN/GaN Multiple Quantum Disk Nanocolumn Light Emitting Diodes: *Akihiko Kikuchi*¹; Makoto Tada¹; Katsumi Kishino¹; ¹Sophia University

Novel device structure feasible for current injection into nanocolumns (nanorods) is presented. GaN nanocolumns; self-organized columnar nanocrystals grown normal to substrate with diameter of 20-200nm, have superior optical quality due to dislocation-free nature. But only a few re-

ports on LED application have been reported, because formation of electrical contact was difficult. In this study we give a novel technique to solve this problem. Following to the growth of n-GaN and InGaN/GaN multiple quantum disk nanocolumns on n-Si(111), p-GaN nanocolumns were grown with gradually increasing their diameter and finally connected to neighboring nanocolumns. Consequently, the nanocolumn device had a continuous surface without chasms. This novel structure enables to make electrodes on the top of nanocolumn devices. The room temperature bright electro-luminescence of the InGaN/GaN nanocolumn LEDs from violet to red was successfully demonstrated. This technique is attractive to realize practical nano-crystal devices and applicable to various nanocolumn materials such as ZnO.

9:55 AM

Structural Characterization of InAs/GaAs Quantum Dot Molecules: Coupling and Strain Effects: *Anup Pancholi*¹; Valeria G. Stoleru¹; ¹University of Delaware

The growth of quantum dot molecules, defined by a pair of electronically coupled quantum dots, represents a major step in tailoring the electronic properties of nanostructures. Besides great flexibility, the vertical coupling between the dots allows one to shift optical transitions to a specific spectral range, such as the Terahertz regime. Drastic modifications of the basic features of single layer dot assemblies occur as soon as the thickness of the GaAs barrier layer is reduced to a few nanometers, so as to induce strong coupling between vertically adjacent dots. The strain distribution in the InAs/GaAs quantum dot molecule is calculated by taking into account the material intermixing, as well as the shape and the size of the dots, as obtained from cross-sectional high-resolution transmission electron microscopy. The influence of the coupling strength and the strain effects on the properties of quantum dot molecule are further analyzed.

10:15 AM

Characterization of Conductive Inks Deposited with Maskless Mesoscale Material Deposition (M3D): *Jacob M. Colvin*¹; Michael Carter¹; Jan A. Puszynski¹; James W. Sears¹; ¹South Dakota School of Mines and Technology

Direct Write Technologies are being utilized in antennas, engineered structures, sensors, and tissue engineering. One form of Direct Write Technology is Maskless Mesoscale Material Deposition (M3D). The M3D process is a Direct Write Technology that uses aerosol formation, transport and deposition. Conductive inks for the M3D process utilize metal nanoparticles in suspension for deposition. Several different conductive inks were deposited with the M3D process and the deposits characterized for electrical resistivity and microstructure. Physical properties of the deposited inks are also measured and reported. This paper will report on the results obtained after sintering conductive nano-particle inks. Sintering was performed with a 2W frequency doubled Nd:YAG CW laser and a conventional muffle furnace. Sample thickness, microstructural details and sintering characteristics are also examined for the depositions of various conductive ink.

10:35 AM Break

10:45 AM

Modeling of Dielectric Nanocomposites: *Thomas K. H. Starke*¹; Clair Hincliff¹; Colin Johnston¹; Peter Dobson¹; Patrick S. Grant¹; ¹Oxford University

Polymer-ceramic composites are gaining in popularity as candidate materials for lightweight dielectric films in capacitor applications. A large number of theoretical studies have sought to express the relationship between the volume fraction of the ceramic materials and the resulting effective properties of the composite film. Due to their strong van der Waals and electrostatic forces, the behavior of nanosized ceramic particles in these films may be markedly different from larger micron-sized counterparts. With a decrease in diameter particle clustering increases significantly giving rise to morphologies that cannot easily be described by the widely used classical effective medium theories. We propose a model for the dielectric constant of nanocomposites and compare resulting predic-

tions with experimental results from the literature, in-house measurements as well as standard EMT formulations. The physical principles in practical nanoscale systems will be discussed in order to guide further experimental approaches in the field.

11:05 AM

Nanomaterials in Novel Circuit Production Methods: *Alan Rae*¹; ¹Nanodynamics Inc

As nanomaterials become more available the number of novel deposition techniques is increasing to exploit their unique processing characteristics such as low temperature reactivity and self-assembly. This paper outlines developments in three application areas for nanomaterials; materials in inkjet circuit development; thermal transfer of novel silver-palladium internal electrode material for ceramic capacitors; and atomic cluster deposition to prepare lithographically defined nanowires for sensor and other applications.

11:25 AM

Characterization of Diffusion Barrier in Nanometer Range Cu Interconnects: *Dongmei Meng*¹; Choong-Un Kim¹; Nancy Michael¹; ¹University of Texas, Arlington

With the miniaturization of Cu interconnects integrated with low-k dielectrics, the thickness of the diffusion barrier must be just a few nanometers to maintain the advantage of the low resistance of Cu, yet it has to be good enough to prevent Cu diffusion from the Cu trenches. Extensive studies are being conducted to enable the nano-scale barrier, however, the progress has been slow due to the lack of an effective characterization method. In this paper, a new methodology based on conventional two-electrode electrochemical cell is developed to evaluate the quality of the barrier, in which two interconnects are used as electrodes and electrolyte is infiltrated into the low-k forming the electrochemical cell. The method is found to be extremely sensitive to defects in the barrier, with the potential to be extended to evaluation of porosity and pore distribution in the low-k materials by measuring diffusivity of the electrolyte.

11:45 AM Break

11:55 AM

Nonlinear Optical Dynamics of Glass-Embedded Silver Nanoparticles: *Sergiy Lysenko*¹; Jose A. Jimenez¹; Guangjun Zhang¹; Huimin Liu¹; ¹University of Puerto Rico

The nonequilibrium carrier dynamics in Ag nanoparticles (NP) was explored by femtosecond optical pump-probe spectroscopy. Metal-dielectric nanocomposite materials with different sizes of Ag NP were prepared by thermal treatment of aluminophosphate glasses. Laser-induced nonlinear optical response of NP was observed in transient reflection and degenerate-four-wave-mixing measurements. The third-order susceptibility is observed in a nonlinear holographic experiment. The ultrafast relaxation dynamics of electron-phonon coupling on the 10⁻¹³-10⁻¹¹ sec temporal-scale shows size- and pump power-dependent properties. Dependencies of electron-phonon coupling rate and coherent acoustic oscillations on NP size will be discussed in terms of a two-temperature model and stress generation by optical absorption. Kinetics study suggests that the nonequilibrium optical excitation of the NP ensemble leads to coherent acoustic oscillations of NP with different eigenfrequencies in the nanocomposite. Complete relaxation of nanocomposite materials occurs on a ~10⁻⁹sec time scale and can be assigned to phonon system thermalization.

3-Dimensional Materials Science: X-Ray Methods

Sponsored by: The Minerals, Metals and Materials Society, TMS Structural Materials Division, TMS: Advanced Characterization, Testing, and Simulation Committee
Program Organizers: Jeff P. Simmons, U.S. Air Force; Michael D. Uchic, Air Force Research Laboratory; Dorte Juul Jensen, Riso National Laboratory; David N. Seidman, Northwestern University; Anthony D. Rollett, Carnegie Mellon University

Tuesday AM Room: 205
March 14, 2006 Location: Henry B. Gonzalez Convention Ctr.

Session Chairs: Dorte Juul Jensen, Riso National Laboratory; Ulrich Lienert, Argonne National Laboratory

8:30 AM Invited

3D Synchrotron Imaging Techniques: Current State and Perspectives: *Wolfgang Ludwig*¹; ¹INSA Lyon

State of the art synchrotron imaging techniques are powerful tools for the non-destructive characterization of 3D microstructures, applicable to a variety of engineering materials. In particular X-ray microtomography, conventionally used in absorption mode, has seen major improvements and offers now complementary contrast mechanisms exploiting either the coherence of 3rd generation synchrotron beams (phase contrast) or the extinction contrast in crystalline materials (diffraction contrast tomography). In terms of spatial resolution this technique covers the range from 10 down to 0.1 micrometers and consequently allows to address a variety of problems in materials science. The possibilities of synchrotron X-ray microtomography will be presented by discussing selected examples of recent applications, including in-situ fatigue crack propagation and 3D grain mapping experiments in Al alloys.

8:55 AM

3D Characterization of Titanium Alloys Using Phase-Contrast Tomography: *Erik M. Lauridsen*¹; Richard W. Fonda²; Wolfgang Ludwig³; George Spanos²; ¹Center for Fundamental Research: Metalstructures in Four Dimensions; ²U.S. Naval Research Laboratory; ³European Synchrotron Radiation Facility

Knowledge of the 3-dimensional spatial arrangement and morphology in multi-phase materials are essential for a full understanding of the processes taking place during thermal-mechanical processing. As a result 3D characterization techniques plays an increasingly important role in material science. This presentation will focus on some recent results utilising phase-contrast tomography to reveal the detailed 3D microstructure of alpha and beta phase in two different titanium alloys with a spatial resolution of ~1 micron. The differences in microstructure between the two alloys are investigated both qualitatively by 3D renderings of the morphologies and quantitatively using relevant 3D microstructural descriptors.

9:15 AM

3D Grainmaps from X-Ray Diffraction Data with the Algebraic Reconstruction Technique: *Erik Knudsen*¹; Henning F. Poulsen¹; ¹Riso National Laboratory

In this paper we explore methods for generating 3-dimensional maps of the crystallographic structure of monophase materials from x-ray diffraction data. In particular, we focus on applying the algebraic reconstruction technique (ART), to data obtained by 3-dimensional x-ray diffraction microscopy (3DXRD). Although originally designed for applications in medical imaging, ART is a general algorithm for producing solution estimates to underdetermined systems of equations. The non-destructive experimental procedure of 3DXRD, provides a unique ability to study grain morphology in-situ. It also poses a challenge for data-analysis tools to process the vast amounts of data associated with high-resolution 3d maps on minute-scale time resolution. We present result indicating that the ART-formalism is a practical, efficient and reliable procedure for producing high-resolution grain maps. Furthermore, we show that the framework also holds exciting prospects for furthering the analysis beyond grain boundary mapping.

TUESDAY AM

9:35 AM

4D Measurements of Grain Growth: *Soeren Schmidt*¹; Dorte Juul Jensen¹; ¹Center for Fundamental Research: Metal Structures in Four Dimensions

Data showing the simultaneous evolution of hundreds of grains during grain growth in AlMn is presented. Before annealing and following each annealing step a cylindrical volume with a diameter of 700 microns and height of 350 microns was fully characterized, i.e. the morphology as well as the crystallographic orientation was determined for each grain in the volume. The measurements were collected non-destructively utilizing the Three Dimensional X-ray Diffraction microscope (3DXRD). After 5 annealing steps few tens of grains were left. The talk will also present the reconstruction algorithm applied to this data and the potential of the method is discussed.

9:55 AM

3 Dimensional Characterization of Inhomogeneous Plastic Deformation during Friction Stir Processing via Polychromatic Microdiffraction: *Rozaliya I. Barabash*¹; Gene E. Ice¹; Wenjun Liu¹; Oleg M. Barabash¹; Z. Feng¹; S. A. David¹; ¹Oak Ridge National Laboratory

Plastic deformation and structural changes of the Ti surface after Friction Stir Processing (FSP) were analyzed by means of SEM, EBSD and advanced 3D polychromatic X-ray micro diffraction at the synchrotron. Spatially resolved 3D Laue diffraction allowed understanding the changes in dislocation arrangement with depth in different regions of the FSP Ti. Formation of two specific zones was established: friction stir zone (FSZ), with the size of 300 microns, and thermal mechanical affected zone (TMAZ) with the size of 800 microns. It was shown that FSP generates a large number of dislocations. Maximal dislocation density is located within the TMAZ. Dislocation density gradually decreases and reaches the value typical for base metal. Within the TMAZ dislocations are distributed inhomogeneously. Inhomogeneity of plastic deformation and dislocations arrangement is found in 3D both within the individual grains and between separate grains.

10:15 AM Break

10:35 AM Invited

3-Dimensional Characterization of Polycrystalline Materials Using High Energy Synchrotron Radiation at the APS: *Ulrich Lienert*¹; Jon Almer¹; Dean Haeflner¹; Bo Jakobsen²; Wolfgang Pantleon²; Henning Friis Poulsen²; Daniel Hennessy³; Changshi Xiao³; Robert Suter³; ¹Argonne National Laboratory; ²Risø National Laboratory; ³Carnegie Mellon University

The use of high-energy synchrotron x-rays provides a unique combination of bulk penetration power with high spatial and temporal resolution. Their potential to characterize polycrystalline materials under thermo-mechanical processing has recently been demonstrated. The Advanced Photon Source (APS) at the Argonne National Laboratory is one of the three existing high energy, 'third-generation' synchrotron facilities worldwide where the described experiments can be performed. A dedicated experimental station is currently under development at the APS 1-ID beamline. The beamline status and preliminary work will be presented. Case studies include 3-dimensional strain/texture mapping, the mapping of the orientation and boundary topology of individual grains, and the evolution of dislocation structure during plastic deformation by measuring diffraction peaks from grains and subgrains with high reciprocal space resolution.

11:00 AM

Characterization of Dislocation Structures during Deformation of Polycrystals by 3DXRD: *Rozaliya I. Barabash*¹; H. F. Poulsen²; U. Lienert³; W. Pantleon²; ¹Oak Ridge National Laboratory; ²Risø National Laboratory; ³Argonne National Laboratory

As supplement to a 3DXRD setup at beam line 1-ID at APS, the possibility for measuring individual diffraction peaks with high resolution has been established. Several reflections of an individual grain in the bulk of a polycrystalline specimen have been recorded during in-situ tensile loading. The diffraction peaks have been analyzed and related to the deformation microstructure. From the spread perpendicular to the scattering vector, the orientation distribution function of the grain is inferred and information on the non-redundant dislocations is obtained. Additionally, asym-

metries in the radial profile (along the scattering vector) are interpreted in terms of internal stresses and strains developing in the dislocation boundary structure.

11:20 AM

A System for Measuring Lattice Strain Pole Figures Using Synchrotron X-Rays: *Matthew Miller*¹; Joel Bernier¹; Jun-Sang Park¹; Alexander Kazimirov¹; ¹Cornell University

This talk describes a system for mechanically loading test specimens in situ at the A2 experimental station at the Cornell High Energy Synchrotron Source (CHESS) for the determination of lattice strains and their evolution in multiphase alloys via powder diffraction. Relatively thin (0.5mm) iron/copper specimens were axially strained using an electro-mechanical load frame beyond the macroscopic yield strength of the material. The loading was halted at multiple points during the deformation to conduct a diffraction experiment using a 50 keV. Entire Debye rings of data were collected for multiple {hkl}s in both copper and iron using a MAR345 online image plate detector. Strain Pole Figures (SPFs) were constructed by rotating the loading frame about the specimen transverse direction (TD). The CHESS data were validated using in situ data from neutron diffraction experiments. Use of the 3 dimensional SPF data as a material model validation tool is discussed.

11:40 AM

Micro-Laue Diffraction Study of Fatigue Crack Wake Plasticity: *Vipul K. Gupta*¹; Yun Jo Ro¹; Judy WL Pang²; Richard P. Gangloff¹; Sean R. Agnew¹; ¹University of Virginia; ²Oak Ridge National Laboratory

Micro-Laue diffraction was used to investigate crack wake plasticity in aluminum alloy 2024 fatigue cracked in vacuum and saturated water vapor environments. The experiments involved differential aperture depth resolved line scans and automatic indexing software was used to produce orientation image maps showing the grain morphology beneath the sample surface. Such images tomographically reveal the sub-surface crack as well. Crystal defects associated with plasticity were evidenced by streaking of the Laue diffraction peaks in the crack wake and the plastic damage was quantified in terms of peak width and the crystal misorientation within each measurement voxel. The measurements verify the theoretical expectation that the cyclic plastic zone size is a function of stress intensity range, rather than the maximum stress intensity (constant for all the measurements.) The effect of environment is more subtle, yet it appears that there is more localized plastic damage within the moist environment.

12:00 PM

Microtomography and 3-Dimensional Stresses of Compressed Low-Density Amorphous Metal Foam: *Jay C. Hanan*¹; Jin Ma¹; Chris Veazey²; Marios D. Demetrio²; Hongbing Lu¹; Ersan Ustundag³; William L. Johnson²; ¹Oklahoma State University; ²California Institute of Technology; ³Iowa State University

Low density metallic foams of consistent controlled morphology offer unique material and mechanical properties, yet they have eluded traditional metallurgical engineering methods. New metallic foam, processed by thermo-plastic expansion, has recently been discovered and its mechanical properties characterized using microtomography combined with in-situ compression. The new foaming process enables porosities unachievable through traditional metallurgical processes. The metal foams exhibit excellent morphological characteristics as evidenced by the microtomography analysis. The high porosities, exceeding 85%, contribute to enhanced plastic yielding. Microtomography of the amorphous metal foam during in-situ compression reveals the 3-dimensional deformation. The stress in all directions was modeled using the generalized interpolation material point method applied in continuous 3-D space and compared to the deformations observed in tomography. Localized regions of failure were observed allowing the foam to absorb significant energy during deformation. The deformation mechanisms for these foams are discussed.

7th Global Innovations Symposium: Trends in Materials R&D for Sensor Manufacturing Technologies: Session II

Sponsored by: The Minerals, Metals and Materials Society, TMS Materials Processing and Manufacturing Division, TMS: Global Innovations Committee

Program Organizers: Hamish L. Fraser, Ohio State University; Iver E. Anderson, Iowa State University; John E. Smugeresky, Sandia National Laboratories

Tuesday AM Room: 204A
March 14, 2006 Location: Henry B. Gonzalez Convention Ctr.

Session Chair: Iver E. Anderson, Iowa State University

8:30 AM Invited

Controlled Growth of Oriented Nanostructures and Their Applications: *M. Meyyappan*¹; ¹NASA Ames Research Center

Carbon nanotubes (CNTs) exhibit unique electronic properties for sensors applications. However, a lack of selectivity between metallic vs. semiconducting tubes has limited progress in nanoelectronics. Nevertheless, there has been much progress in sensor applications that use multiwalled structures. We report here a carbon nanofiber (CNF) based nanoelectrode array for biosensor and neural interfacing applications. The CNTs are grown using PECVD. The gap between CNFs is filled with SiO₂. This nanoelectrode array (NEA) has been successfully used for developing a biosensor and also as a neural interface for deep brain stimulation applications. Inorganic nanowires have been emerging as an adequate candidate in areas envisioned for application of CNTs, based on the publications we have seen in the literature in the last five years. Here, the growth is reported of well-aligned, vertical nanowires of ZnO, In₂O₃, silicon and germanium and their applications in electronics and optoelectronics.

9:00 AM Invited

Structural Iron-Based Magnetostrictive Alloys for Sensor Applications: *Thomas A. Lograsso*¹; A. E. Clark²; M. Wun-Fogle³; J. Restorff³; ¹Iowa State University; ²Clark Associates; ³Naval Surface Warfare Center

Fe_{1-x}Ga_x alloys offer relatively high magnetostriction along with combination of high mechanical strength, good ductility, low saturation fields, high blocking stress, and low cost. Substituting Ga for Fe in the α -Fe structure, increases the tetragonal magnetostriction, λ_{100} , over 10-fold above that of pure α -Fe. Experimentally it has been shown that single crystalline 3/2 λ_{001} increases monotonically with the Ga concentration to approximately 400 microstrain for $x < 0.19$, decreases thereafter for $0.19 < x < 0.23$, and increases again to the same level at $x \sim 0.29$. Further because of its relatively good mechanical properties, built-in stress anisotropies allow for use in both compressive and tensile regimes, opening up device design space not allowed by other, brittle smart materials. An overview of the magnetic and mechanical properties will be presented.

9:25 AM Break

9:45 AM

Al-Sb Nanoelectrode Arrays for Radiation Detection: *Krishnan S. Raja*¹; Manoranjan Misra¹; Susant Mohapatra¹; Thulasidharan Gandhi¹; ¹University of Nevada, Reno

Stoichiometric single crystal Al-Sb compound semiconductor shows excellent electronic properties that can be tailored for radiation sensing applications. Al-Sb semiconductors can be used for detecting low-medium energy radiation at room temperature. These detectors will have higher resolution and lower noise levels than those of CdZnTe. Al-Sb crystals are manufactured, in general, by Bridgman technique. This investigation reports an electrochemical synthesis of stoichiometric Al-Sb semiconductor nanowires in non-aqueous solutions at room temperature. Suitable electrochemical window for deposition of stoichiometric Al-Sb nanowires were determined by conducting cyclic voltammetry. The nanowires were characterized by determining composition, electronic band gap, and electrical resistivity.

10:10 AM

Characterization of Piezoelectric Aluminum Nitride Thin Film by RF Magnetron Sputtering: Shih-Jeh Wu¹; Ting-Wei Shen¹; *Chen-Ming Kuo*¹; ¹I-Shou University

Surface Acoustic Wave Filter devices have been the main stream of filters in last generation of communication industry under 2GHz. However, for the new specification of mobile telecomm the frequency requirement can be higher than 3GHz. Film Bulk Acoustic Resonator becomes the mainstream of duplexer and filter in communication industry. Aluminum nitride thin film is the best piezoelectric material for the above applications. It has hexagonal crystal structure and is a covalent bonded material. It has high dielectric constant, acoustic speed (high Young's modulus), melting point, energy band gap, good thermal insulation, and low thermal expansion. The piezoelectricity depends on good <002> crystalline structure. In this study, we use RF magnetron sputtering to deposit AlN thin film on different substrates and the film are characterized by several means e.g., SEM, TEM, XRD, and AFM. Also simple devices are fabricated and the piezoelectric properties are also well demonstrated by network analyzer.

Advanced Materials for Energy Conversion III: A Symposium in Honor of Drs. Gary Sandrock, Louis Schlapbach, and Seijirau Suda: Complex Hydrides I

Sponsored by: The Minerals, Metals and Materials Society, TMS Light Metals Division, TMS: Reactive Metals Committee

Program Organizers: Dhanesh Chandra, University of Nevada; John J. Petrovic, Petrovic and Associates; Renato G. Bautista, University of Nevada; M. Ashraf Imam, Naval Research Laboratory

Tuesday AM Room: 214B
March 14, 2006 Location: Henry B. Gonzalez Convention Ctr.

Session Chairs: Craig Jensen, University of Hawaii; Carole Read, U.S. Department of Energy

8:30 AM Plenary

Monitoring of Defect Complexes Arising in the Dehydrogenation of Sodium Aluminium Hydride by Anelastic Spectroscopy: *Craig Jensen*¹; Rosario Cantelli²; Orielle Palumbo²; Annalisa Paolone²; Sessa Srinivasan¹; ¹University of Hawaii; ²Universita di Roma

The mechanism of the reversible, solid-state dehydrogenation of Ti-doped NaAlH₄ has been a topic of considerable recent interest. We have probed this phenomenon through anelastic spectroscopy and found that dehydrogenation of the hydride can be monitored through its effects on the elastic constants. We have also obtained evidence for the formation of highly mobile, stoichiometric defects in Na₃AlH₆ that arise at temperatures much lower temperatures in the Ti-doped samples. These species "jump" at a rate of 1000/s at 70 K corresponding to an activation energy of 0.126 eV and which is typical of point defect relaxation. The results of these studies will be presented and discussed in terms of a model in which this mobilized population of hydrogen plays a fundamental role in the dehydrogenation process that is kinetically enhanced by Ti acting to decrease its migration energy in the crystal lattice.

8:55 AM Invited

Mechanochemical Synthesis and First-Principles Simulations of Mg-Based Hydrogen Storage Materials: Z. X. Guo¹; C. X. Shang¹; Y. Song¹; ¹Queen Mary, University of London

A systematic investigation of the structural stability, evolution and hydrogen-storage properties of Mg-based hydrides and nanostructures was carried out, involving experimental mechanical milling and chemical alloying, and electronic structural simulations of hydrogen-metal interactions. The effects of milling on particle size, lattice parameters, microstructure, and phase composition of the powder mixtures were characterised using SEM, X-Ray diffraction analyses. Mechanical milling was shown to be an effective method of refining the particle size, particularly when MgH₂ is involved. The influences of the selected chemical elements, in-

cluding transition metals, on hydrogen desorption of various milled mixtures were clearly identified using coupled Thermogravimetry (TG) and Differential Scanning Calorimetry (DSC). The as-received MgH₂ shows an onset desorption temperature of 420°C. Mechanical milling reduces the onset temperature to 330°C. Chemical alloying, via surface catalysis and/or solid-solutioning, further increases the desorption kinetics and reduces the desorption temperature down to 250°C. The degree of such effect decreases from Ni, Al, Fe, Nb, Ti, to Cu. A multi-component mixture of (MgH₂+Al+Ni+Y+Ce) exhibits relatively fast desorption kinetics and the lowest desorption temperature at about 200°C. Electronic structural simulations further clarify the effects of alloying elements on the stability and bonding of modified hydride systems. The coupled experimental and theoretical approach has laid a valuable foundation for continued development of new and cost-effective hydrogen storage systems with a high capacity, a low desorption temperature and rapid kinetics.

9:20 AM Invited

Preparation of LiH_{0.5D0.5} Using Isotopic Exchange of Lithium Hydride: *Joseph R. Werner*¹; Steven N. Paglieri¹; Blake P. Nolen¹; John T. Gill¹; Jane Poths¹; ¹Los Alamos National Laboratory

Lithium hydride (LiH) powder and compacts were exchanged with flowing deuterium (2H₂) at temperatures from 300–550°C and pressures of 600–1400 mm Hg (torr) to obtain lithium-hydride deuteride (LiH_{0.5D0.5}). The kinetics of the exchange reaction increased with temperature so that a complete exchange in powder (equimolar composition of hydrogen and deuterium) occurred after 0.5 h at 450°C. Powder exchanged more quickly than partial density LiH compacts, as indicated by real-time analysis on a mass spectrometer connected to the system. The samples were assayed by amalgamating the Li(H,D) with tin and analyzing the released gases with high-resolution mass spectrometry. For example, the offgas from LiH powder exchanged with deuterium at 450°C was composed of 48.9% hydrogen and 51.1% deuterium, indicating that the exchange with deuterium was complete. Analysis of Li(H,D) taken from the core of a sintered compact exchanged with deuterium at 350°C for 24 hours indicated that essentially complete exchange had occurred (LiH_{0.52D0.48}). Experiments are continuing with higher density solid compacts to determine whether exchange is practical in compacts with >70% theoretical density.

9:40 AM Invited

Reversible Hydrogen Storage in Mixtures of Mg(NH₂)₂ and LiH Studied by X-Ray and Neutron Diffraction: Yan Gao¹; Job Rijssenbeek¹; Ji-Cheng Zhao¹; ¹General Electric Company

Mixtures containing various ratios of LiH and Mg(NH₂)₂ theoretically release up to 9 wt % H₂ and are therefore attractive as hydrogen storage materials. An in-situ synchrotron X-ray diffraction (XRD) study was performed on mixture of LiH and Mg(NH₂)₂ at ratios of 2:1, 8:3 and 4:1 to examine similarities and differences in the reaction pathways and products. Detailed analysis indicates that the products consist of mixed Li/Mg imides, whose structures have not been determined previously. For the 2:1 ratio, the product is Li₂Mg(NH)₂ which displays three different crystal structures as a function of temperature: an orthorhombic structure at low temperature (alpha), a primitive cubic structure at intermediate temperature (beta), and a fcc-based structure at high temperature (gamma). The crystal structures were identified based on a combination of high-resolution XRD and neutron diffraction.

10:00 AM

High Pressure Raman Spectroscopy Studies on LiAlH₄: *Raja S. Chellappa*¹; Dhanesh Chandra¹; Yang Song²; Steve Gramsch²; Russell Hemley²; ¹University of Nevada; ²Carnegie Institution of Washington, DC

LiAlH₄ (10.6wt% hydrogen) belongs to a class of light metal complex hydride is a potential candidate for hydrogen storage due to its high theoretical hydrogen weight content. Hydrogen desorption from LiAlH₄ has been generally successful in the presence of catalysts (with some loss of hydrogen content), however reversibility and enhancing the hydriding kinetics is still an active area of research. Recent theoretical calculations predicted a pressure induced phase transformation at room temperature from ambient pressure (α -LiAlH₄) monoclinic (P21/C) structure to a high pressure (β -LiAlH₄) phase (structure not known, predicted tetragonal)

around ~3GPa. It is also predicted that the high pressure (β -LiAlH₄) phase undergoes a huge volume collapse of about ~17% at phase transformation pressure. If this high pressure dense phase can be stabilized at ambient pressures, it can be very attractive for hydrogen storage (due to gravimetric as well as volumetric efficiency). Our recent in-situ high pressure Raman spectroscopy studies on LiAlH₄ suggests a α -LiAlH₄ to β -LiAlH₄ transition beyond ~3GPa. We were also successful in retaining the high pressure (β -LiAlH₄) phase by “pressure quenching” (rapid reduction in pressure) to a lower pressure of about ~1.2GPa. Raman spectra characteristics of the quenched sample do not change even after 6 days. The stabilization of the high pressure phase at ambient pressure holds promise for developing novel hydrogen storage materials that are both volumetrically as well as gravimetrically efficient. The crystal structure determination of the “pressure quenched” high pressure phase will be performed to conclusively establish the retention of the high pressure dense phase. The changes in vibrational mode characteristics as a function of pressure will be discussed in detail.

10:20 AM Invited

Li-C-H Systems as a Novel Family of Hydrogen Storage Media: *Takayuki Ichikawa*¹; Hiroki Miyaoka¹; Yong Zhong¹; Shigehito Isobe¹; Hiroobu Fujii¹; ¹Hiroshima University

Hydrogen storage properties of ballmilled mixtures composed of the hydrogenated nano-structured carbon (C^{nano}H_x) and lithium hydride (LiH) were examined by thermal and optical spectroscopic analyses. Actually, LiH needs higher temperature than 600°C for thermal decomposition even under vacuum condition, while C^{nano}H_x, which was mechanochemically synthesized from graphite powder by ballmilling under hydrogen atmosphere, reveals hydrogen and hydrocarbons desorption in wide range from 300 to 800°C. Nevertheless, the mixtures of C^{nano}H_x and LiH mainly desorb hydrogen around 350°C. These phenomena indicate that the thermally liberated hydrocarbon radicals immediately react with LiH and release hydrogen instead of hydrocarbons, because C^{nano}H_x contains hydrocarbon groups at the edge of nanosized graphene, which are recognized as IR active C-H stretching mode, and LiH is well-known as an ionic crystal. Furthermore, it is of interest that the mixtures keep a nanostructural feature even after annealing at 350°C revealed excellent cycle properties as hydrogen storage media.

10:40 AM Break

10:55 AM Keynote

Materials for Hydrogen Storage: From Nanostructures to Complex Hydrides: *Puru Jena*¹; ¹Virginia Commonwealth University

The limited supply of fossil fuels, its adverse effect on the environment, and growing worldwide demand for energy has necessitated the search for new and clean sources of energy. The possibility of using hydrogen to meet this growing energy need has rekindled interest in the study of safe, efficient, and economical storage of hydrogen. The current methods for storing hydrogen as a compressed gas or liquid are not suitable for practical applications. An alternate method for hydrogen storage involves metal hydrides. Although conventional intermetallic hydrides can store hydrogen reversibly at around room temperature, the relative weight of stored hydrogen in these materials is rather low (1–3 wt %) and do not meet the requirements of the transportation industry (~10 wt %). For this the host materials have to consist of light elements such as Li, Be, B, C, Na, Mg, and Al. Unfortunately, the bonding of hydrogen in these materials is rather strong (covalent or ionic) and the thermodynamics and kinetics are poor. Ways must, therefore, be found to weaken the hydrogen bond strength so that light metal complex hydrides can be used as effective hydrogen storage materials. This talk will discuss the issues and challenges in storing hydrogen in light complex hydrides and discuss the role of nanostructuring and catalysts that can improve the thermodynamics and kinetics of hydrogen. In particular, I will discuss storage of hydrogen in Boron Nitride and Carbon nanocages and demonstrate that metallization of these nanostructures is necessary to store hydrogen with large gravimetric density. I will also discuss the properties of a class of materials called alanates which have the chemical composition [Mn+(AlH₄)_n], M=Li, Na, K, Mg] and can store up to 18 wt % hydrogen, although the temperature where hydrogen desorbs is rather high. It was recently discovered that doping of Ti-based catalysts in NaAlH₄ can significantly lower

the hydrogen desorption temperature, but why and how Ti accomplishes this task remains a mystery. Using first principles calculations, I will provide a fundamental understanding of the electronic structure and stability of sodium alanates and how it is affected due to Ti doping. The role of Ti based precursors in introducing vacancy like defects and their influence on hydrogen desorption will be highlighted. It is hoped that the understanding gained here can be useful in designing better catalysts as well as hosts for hydrogen storage.

11:15 AM Invited

Light Metal Hydrides Studied by High Pressure Techniques: S. Doppiu¹; A. Comin¹; S. Sartori²; G. Principi²; *Oliver Gutfleisch*¹; ¹IFW Dresden; ²Università di Padova

The application of high hydrogen pressure techniques, such as high-pressure ball milling (HP-BM, up to 90 bar) and high-pressure differential scanning calorimetry (HP-DSC, up to 140 bar), is advantageous to synthesize novel hydrides for hydrogen storage under non-equilibrium conditions and to characterize their complex thermodynamic and kinetic properties. In the present study, two different classes of hydrides were investigated: (a) Mg and Mg-based alloys, (b) lithium alanates and modified lithium alanates. It is shown that milling Mg at high hydrogen pressure allows to shorten the time for the complete conversion into the hydride with the formation of a very fine nanometric powder. The hydride synthesised in this way shows better desorption kinetics than nanocrystalline MgH₂ obtained by milling under argon atmosphere. The thermal stability of LiAlH₄ under different hydrogen pressure has been studied. Work is in progress to elucidate with further experiments the observed behaviour.

11:35 AM Invited

Recent Developments of Dopants for Hydrogen Exchange in Alanates: *Maximilian P. Fichtner*¹; ¹Forschungszentrum Karlsruhe

One of the major obstacles to the application of complex hydrides in mobile devices is the slow hydrogenation kinetics of the materials. Therefore, a number of attempts have been undertaken to develop both fast and cost-effective catalysts. This contribution will give a short review on the state of the art as outlined in literature. Furthermore, the properties of new dopants for alanates and the results of recent attempts to drastically reduce costs of Ti-based catalysts will be presented.

11:55 AM Invited

Amorphization of Laves Phase Hydride: *Dhanesh Chandra*¹; Ricardo B. Schwarz²; ¹University of Nevada; ²Los Alamos National Laboratory

Crystalline GdFe₂ Laves phase are formed at relatively low temperatures; for example GdFe₂H_{4.8} is formed at room temperature, which is reversible, with a H/M ratio of 1.6. However, at this temperature desorption of all the hydrogen is difficult because of slow kinetics. An amorphous GdFe₂H_x phase forms at intermediate temperatures and pressures. The absorption isotherm is quite unusual, as the crystal-to-amorphous transformation is accompanied by either a gain or a loss of hydrogen and is temperature dependent. Absorption isotherms taken below 475K showed that there is an abrupt decrease in the hydrogen capacity of the alloy during the crystalline-to-amorphous hydride phase transformation. Whereas the absorption isotherms taken above 475K showed that there is an abrupt increase in the hydrogen capacity during amorphization. At temperatures above 525 K, hydrogen absorption causes to the disproportionation of the GdFe₂ crystal into a two-phase mixture of GdH₂ and bcc α -Fe. The formation of the crystalline and amorphous GdFe₂H_x phases, phase stability regions, disproportionation of the hydride will be presented.

12:15 PM Keynote

Aluminum Trihydride Studied by Powder Synchrotron X-Ray Diffraction: Crystal Structure and Thermal Decomposition: *Volodymyr A. Yartys*¹; Jan Petter Maehlen¹; ¹Institute for Energy Technology

Aluminium hydride is considered as a prospective solid H storage material for transport applications, having high gravimetric (10 wt.% H) and volumetric density of H (2 times higher compared to LH₂) and, also, a convenient range of thermal stability (below 170°C, dependant on synthesis and storage conditions). Achieving sufficiently rapid and controllable decomposition of AlH₃ and proposal of efficient synthesis routes to make the system Al-AlH₃ reversible are focused in ongoing research. This work was aimed on studies of crystal structure of AlH₃ and phase-structural transformations in the system Al-AlH₃ during decomposition of the

hydride by application of in situ synchrotron X-ray powder diffraction (SR-XRD). The SR-XRD studies were performed at the Swiss-Norwegian Beam Line (SNBL) at the European Synchrotron Radiation Facility (ESRF), Grenoble, France. A specially designed cell for performing studies in controlled atmosphere was used. The studied sample is placed inside a quartz glass capillary, which is attached to a remote controlled gas distribution system providing either high-purity hydrogen at convenient pressures from a metal hydride hydrogen storage unit developed at IFE, or vacuum. During the present study of AlH₃, a high-resolution data set (at room temperature) was first obtained, followed by an in-situ measurement by heating with a constant heating rate under secondary vacuum. The high-resolution SR XRD pattern was indexed in the trigonal unit cell; a = 4.44994(5) Å, c = 11.8200(2) Å, V = 202.701(4) Å³; space group R \bar{c} (No.167). The hydrogen sublattice was successfully located from the refinements of the powder XRD pattern started with Al placed in a special position 6a [0,0,0]. This yielded the Al-H bonding distance of 1.712(3) Å and an octahedral coordination of Al in the AlH₆ units. Furthermore, the refinements indicated a small charge transfer from Al to H corresponding to the formation of Al^{+0.15} and H^{-0.05}. This charge distribution can be observed in the Fourier transform of the observed XRD pattern. We note a good correspondence between the data of this XRD work and the results of the powder neutron diffraction study of AlD₃ [2], where the Al-D bond distance of 1.715 Å in the AlD₆ octahedra was reported.

Advances in Furnace Integrity: Advances in Furnace Integrity and Pyrometallurgical Processes

Sponsored by: The Minerals, Metals and Materials Society, TMS Extraction and Processing Division, TMS: Copper and Nickel and Cobalt Committee, TMS: Lead and Zinc Committee, TMS: Pyrometallurgy Committee

Program Organizers: Robert L. Stephens, Teck Cominco Metals Ltd; Christopher J. Newman, Chris Newman Metallurgical Consulting

Tuesday AM
March 14, 2006

Room: 7D
Location: Henry B. Gonzalez Convention Ctr.

Session Chair: Robert L. Stephens, Teck Cominco Metals Ltd

8:30 AM

CONSCAN, A Laser Measurement System for Furnaces Which Are Operating on High Temperatures: *Oliver Zach*¹; ¹RHI Non Ferrous Metals Engineering GmbH

To know as much as possible about the condition of the refractory material (lining thickness, slag layer, build ups, ...) in an high temperature furnace is very important due to the safety and economic impacts. The new CONSCAN system offers the possibility to measure the inner surface of a furnace, and based on this results to calculate the thickness of the refractory lining, slag layer, build ups,.... The CONSCAN System provides this results as figures and graphics. This system is also working under hot conditions so it is not necessary to cool down the furnace. Based on these results the process control and the refractory lining concept could be optimized for maximum campaign life of the furnace.

8:55 AM

Innovative Taphole and Launder Design Using Computer Assisted Engineering Tools: *Hugo Joubert*¹; Bernice Leong¹; Russel Tomlinson¹; ¹Pyromet Technologies Pty Ltd

Tapholes and launders experience high temperature fluctuations during operating cycles, resulting in thermal stresses and thermal fatigue. This is true for all components including refractory materials and water-cooled copper elements. The technology supplier needs to design tapholes and launders, and select materials, to cope with these temperature fluctuations, not only during normal operating cycles, but also under extreme operating conditions. This paper discuss the use of advanced Computer Assisted Engineering (CAE) tools to assist in the design of tapholes and launders to achieve safe operation, increase campaign life, and limit maintenance cost and downtime. As an example the design of matte and slag

TUESDAY AM

tapholes for a PGM slag cleaning furnace is discussed, as well as an innovative water-cooled copper launder design that is inherently safe during, and re-usable after, damage caused by superheated metal or matte. Feedback on the operational performance of both the tapholes and copper launders is presented.

9:20 AM

Recent Improvements in Evaporative Cooling Technology for Copper Tapholes and Launderers: *Pietro Navarra*¹; Frank Mucciardi¹; Tim Van Rompaey²; ¹McGill University; ²Umicore Research

A great deal of effort has been expended on how to optimize conventional water cooling circuits in furnace cooling elements, and the results have been largely satisfactory. However, there is a general agreement that the proximity of high-pressure water passages to the flow of molten furnace products is a safety concern. Nonetheless there exists little alternative to the formula: increasing furnace integrity implies the incorporation of more extensive forced-convection water cooling systems. Recent developments in evaporative cooling technology have resulted in the development of a high-capacity heat pipe capable of operating under the thermally intense environments of metallurgical furnaces. The system functions using several kg of a working fluid (water) in total, has no moving parts, and allows for a significant reduction in cooling water requirements. Full-scale pilot tests of a copper taphole and slag launder were done in 2003 and 2005, with detailed results given in this paper.

9:45 AM Break

10:05 AM

Hacer Castillos en el Aire: Development of Oil Shale Retorting (Esta Fiesta se ha Preparado a Tontas y a Locos): *Larry M. Southwick*¹; ¹LM Southwick & Assoc

The doubling of oil prices over the last two years has generated renewed interest in producing petroleum from oil shales and tar sands. This interest extends even to mining and metals companies, where many of the technologies used are similar. While tar sands processing is an economic reality, brought about primarily by improved and larger scale mining techniques, satisfactory economics have yet to be achieved with oil shale. Thermal processing of minerals is required, involving volatilization of the product in a retort and external condensation. The process is much like zinc smelting, some being very similar to the Imperial Smelting Process shaft furnaces. These oil shale plants involve multiple trains, each of fairly small size. As with tar sands, the route to achieving economic viability in oil shale processing must be through larger processing units. The one technology that offers such potential for large size is fluid bed retorting. In this paper, a review and critique will be provided of previous development efforts. A design will then be described which eliminates many of the problems experienced with earlier fluid bed configurations.

10:30 AM

Acoustic-Pulsation-Based Intensification of Heat Transfer in Continuous Furnace: *Alexey N. Lozhko*¹; Olena V. Sorokina¹; ¹National Metallurgical Academy of Ukraine

The technical-and-economic furnace exploitation indices are considerably influenced by the system of heat utilization. In the situation of total output decrease works are forced to exploit furnaces at the partial loading, sometimes even at the idle running for the sake of steam production. The furnace exploitation in this regime is known to cause the increase of the heat portion, taken away together with waste flue gases. The losses can be partially compensated at the expense of heat exchange efficiency development in the recuperator or heat-exchanger. One of the well-known methods, characterized by high efficiency and low expenditures is the intensification of the heat exchange process by the means of pulsation method.

Alumina and Bauxite: Joint Session of Alumina and Bauxite & Aluminum Reduction Technology

Sponsored by: The Minerals, Metals and Materials Society, TMS Light Metals Division, TMS: Aluminum Committee

Program Organizers: Jean Doucet, Alcan Inc; Dag Olsen, Hydro Aluminium Primary Metals; Travis J. Galloway, Century Aluminum Company

Tuesday AM
March 14, 2006

Room: 7A
Location: Henry B. Gonzalez Convention Ctr.

Session Chair: Renaud Santerre, Alcan Primary Metal

8:30 AM Introductory Comments by Renaud Santerre, Jean Doucet and/or Steve Lindsay

8:40 AM Invited

Smelter/Refinery Teaming for Alumina Supply: *Peter Bailey*¹; ¹Sherwin Alumina Company

The speaker will address procedures and mechanisms necessary to ensure that Refineries and Smelters team to optimize the supply of alumina.

9:05 AM

FLUIDCON – A New Pneumatic Conveying System for Alumina: *Andreas Wolf*¹; Peter Hilgraf¹; ¹Claudius Peters Projects GmbH

Alumina is transported by mechanical and pneumatic systems. The primary disadvantage of pneumatic conveying systems is the high-energy demand versus the mechanical processes. FLUIDCON is pneumatic conveying technology combining the advantage of airlift conveying and pneumatic pipe transport. The operating characteristic of the FLUIDCON is an extremely low transport velocity and low energy requirement. The advantages of the FLUIDCON system are discussed with the aid of the results of comprehensive systematic measurements performed in the research centre of Claudius Peters Technologies GmbH and in operating plants.

9:30 AM

Fundamentals of Crust and Alumina Powder Dissolution in Smelter Electrolytes and Their Impact on Cell Feeding: *Barry J. Welch*¹; ¹University of New South Wales and Welbank Consulting Limited

The blend of knowledge derived from fundamental studies of the physics and science of alumina dissolution help understand the roles of key properties of smelter grade alumina - especially those impacting the operating disturbances linked with alumina "solubility". More important, the information also provides guidelines for good feeding practice and hence feeder design. The knowledge also presents a warning light on issues linked with the accessible bath volume when retrofitting larger anodes and operating at higher line currents.

9:55 AM

Evolution of Microstructure and Properties of SGA with Calcination of Bayer Gibbsite: *Scott Powell*¹; Tania Groutso¹; Margaret M. Hyland¹; *James B. Metson*¹; ¹University of Auckland

The microstructure of smelter grade alumina is relevant to smelter performance in a number of critical areas. The connection between the degree of calcination, the residual structural hydroxide content and HF generation, has recently been explored,¹ and impacts on alumina dissolution have also been reported. A critical parameter of relevance to both of the above, and particularly to dry-scrubber performance, is the evolution of surface area and its relationship to the progression of transition alumina phases.² The relationship of surface area and microstructure with equilibrium heating of gibbsite has been explored in the laboratory and results compared with those from several industrial calciner technologies. For the equilibrium samples, it is possible to accurately represent the transition alumina structure with the γ , γ' , θ model previously developed,³ and to correlate the evolution of phase with changes in surface area. The relative rates of hydroxyl loss versus loss of surface area are of critical importance in understanding the balance between HF generation at the cell and HF capture in the scrubber. ¹M.M. Hyland, E. Patterson, and B.J. Welch.

Light Metals 2004 Edited A.T. Tabereaux, The Minerals, Metals & Materials Society p.361-366 (2004). ²K. Wefers and C. Misra, Alcoa Laboratories, Technical paper No. 19 Revised (1987). ³J. B. Metson, M. M. Hyland and T. Groutso. Alumina Phase Distribution, Structural Hydroxyl And Performance Of Smelter Grade Aluminas In The Reduction Cell. Light Metals 2005 Edited by Halvor Kvande. The Minerals, Metals & Materials Society), p. 127-131, (2005).

10:20 AM Break

10:30 AM

Optimizing the Alumina Feeding Strategy for Different Pot Technologies, Work Practices, and Pot Process Parameters: *Pablo R. Navarro*¹; ¹Aluar Aluminio Argentino

This presentation emphasizes the need to optimize the alumina feeding strategy for each combination of pot technology, lining design, work practices, and process parameters. The evolution of Aluar's alumina feeding algorithm is presented together with the resultant improvements in alumina content control and anode effect frequency.

10:55 AM

Alumina Requirements of Soderberg Smelters: *Alton T. Tabereaux*¹; ¹Alcoa Inc

This presentation addresses the key physical and chemical properties required for side-break and point feeder Soderberg cells. Issues regarding the use of various types of side break operations using wheels, bars, hammer and point feeders on crust breaking and dissolving alumina in Soderberg operations are discussed. Strategy and countermeasures have been developed to reduce the impact of using alumina that have problematic particle size distributions (PSD) and other properties to improve alumina management in Soderberg cells.

11:20 AM

Beryllium Mass Flow in Pot Room Bath: *Stephen Joseph Lindsay*¹; Charles L. Dobbs; ¹Alcoa Inc

Concentration of beryllium in pot room bath has become an issue of concern in more than one country during recent years. In this paper the author discusses the mass flow mechanisms that permit beryllium to become concentrated in pot bath as well as those factors that control reductions in beryllium concentrations when the source of contamination is removed. Some rules of thumb are proposed regarding decay rates in pot room bath.

11:45 AM

Automated Crystal Optical Technique for Quantitative Determination of Phase and Particle Size Composition of Alumina: *Alexander Gennadievich Suss*¹; Andrey Vladimirovich Panov¹; ¹VAMI-RUSAL

For many years specialists of VAMI have been involved in developing of automated techniques and new equipment arrangement for determination of phase and particle size composition of products in alumina manufacture. Crystal optical analysis being a complicated technique requiring professional background however is not free from subjective estimation as far as the quantitative analysis is concerned. Modern advances in computer diagnostics and processing allow overcoming these problems. At present at several alumina refineries a technique for automated quantitative determination of alumina phase composition using «Image Analysis System» is tested. The following automated techniques were developed with the help of «Image Analysis System»: 1. determination of alpha-modification content in alumina of all grades irrespectively of method of production of alumina and way of its formation; 2. determination of quantitative phase composition of smelter grade alumina; 3. automated determination of particle size distribution of aluminium hydroxide containing fine particles.

Aluminum Reduction Technology: Joint Session of Alumina and Bauxite & Aluminum Reduction Technology

Sponsored by: The Minerals, Metals and Materials Society, TMS Light Metals Division, TMS: Aluminum Committee

Program Organizers: Jean Doucet, Alcan Inc; Dag Olsen, Hydro Aluminium Primary Metals; Travis J. Galloway, Century Aluminum Company

Tuesday AM
March 14, 2006

Room: 7A
Location: Henry B. Gonzalez Convention Ctr.

Session Chair: Renaud Santerre, Alcan Primary Metal

See the Alumina and Bauxite Symposium on page 102 for presentations.

Amiya Mukherjee Symposium on Processing and Mechanical Response of Engineering Materials: Mechanical Behavior of Materials

Sponsored by: The Minerals, Metals and Materials Society, TMS Materials Processing and Manufacturing Division, TMS Structural Materials Division, TMS/ASM: Mechanical Behavior of Materials Committee, TMS: Shaping and Forming Committee

Program Organizers: Judy Schneider, Mississippi State University; Rajiv S. Mishra, University of Missouri; Yuntian T. Zhu, Los Alamos National Laboratory; Khaled B. Morsi, San Diego State University; Viola L. Acoff, University of Alabama; Eric M. Taleff, University of Texas; Thomas R. Bieler, Michigan State University

Tuesday AM
March 14, 2006

Room: 217C
Location: Henry B. Gonzalez Convention Ctr.

Session Chairs: Khaled B. Morsi, San Diego State University; Viola L. Acoff, University of Alabama

8:30 AM Invited

Microstructure and Mechanical Properties of Commercial Grade Aluminium as a Function of Welding Speed Using Friction Stir Welding: *Jyoti Mukhopadhyay*¹; G. S. Sengar¹; T. Sakhivel¹; ¹JNARDDC

The weld properties remain an area of uncertainty with respect to the effect of different speeds of Friction Stir Welding (FSW). For this purpose, a FSW tool was designed in such a way that the shoulder of the tool not only provides additional heat generated by friction, but also prevents plasticised material to escape. Infact, the weld was formed by the deformation of materials at temperature below the melting point. The simultaneous rotation of welding tool and the translational motion of the work piece during the welding process produced a high quality weld joint. In the present investigation, an aluminium weld was made using FSW technique. The mechanical properties and microstructural aspects of welded areas were investigated. It is observed that a good correlation exists between the mechanical properties and welding speeds. The main objective of this investigation is to evaluate the mechanical properties and microstructures at different welding speeds.

8:50 AM

Void Nucleation at Grain Boundary Triple Points in AA6022-T43 Aluminium Alloy Sheet: *Joseph Querin*¹; Judy Schneider¹; Mark F. Horstemeyer¹; ¹Mississippi State University

The design and optimization of processing parameters for forming stamped sheet metal components can be expedited by using accurate material models that take into consideration the relationship between microstructure and mechanical properties. One such genre is damage modeling, where the degradation of material properties is attributed to void nucleation, growth, and coalescence. In monotonic tensile testing of 1-mm thick sheet AA6022-T43, microscopic void nucleation was found to first occur at grain boundary triple points (GBTPs). The grain orientations at various

GBTPs in the strained specimens were determined using electron back-scattered diffraction. These orientations were used in conjunction with a crystal plasticity model implemented into a finite element analysis code to reveal that a state of hydrostatic tensile stress surrounded the GBTPs where voids nucleated and a state of hydrostatic compressive stress surrounded those GBTPs that did not nucleate voids.

9:10 AM Invited

The Effect of Silicon on the Deformation and Fracture of Molybdenum: Daniel Sturm¹; Joachim H. Schneibel²; Holger Saage¹; Martin Heilmair¹; ¹Otto-von-Guericke-University Magdeburg; ²Oak Ridge National Laboratory

Mo-Si-B intermetallic alloys are finding interest as structural materials for ultra-high temperature applications. One of their phases, the Mo-Si solid solution, is of paramount importance for the fracture toughness. In general, Si was found to reduce the lattice parameter, slow down grain growth, reduce the room temperature fracture toughness, and increase the tensile strength at temperatures up to 1100°C. Small Si concentrations (e.g., 0.3 at%) actually cause solid solution softening at room temperature which may be attributed to a reduced Peierls stress for screw dislocations. Finally, a model is presented which accounts for the effect of Si on the yield strength. The authors appreciate experimental support from Plansee AG, Reutte, Austria. JHS acknowledges support by the Division of Materials Sciences and Engineering, U.S. Department of Energy, under Contract DE-AC05-00OR22725 with UT-Battelle, LLC, and by the Schiebold Guest Professorship at the University of Magdeburg.

9:30 AM

Co-Continuous Composites for High Temperature Service: Glenn S. Daehn¹; Eduardo del Rio Perez¹; James C. Nash¹; James C. Williams¹; ¹Ohio State University

In principle it would be desirable to create metal-ceramic composites for high temperature service, because the ceramic can reduce density and give strength. However, strain mismatch associated with differential thermal expansion typically make these materials very weak or prone to accumulating damage in thermal cycling. Here we look at a different approach. We evaluate interpenetrating phase composites of alumina and aluminum as well as alumina and NiAl. Experiments compare the thermal cycling induced damage in these materials to traditional discontinuously-reinforced composites. These show that the co-continuous morphology is much more resistant to thermal cycling induced damage. Lastly we will detail a technique whereby large volumes of near-single crystal reticulated alumina can be created. These composites can have exceptional damage tolerance, good high temperature creep resistance and reduced density versus refractory metals.

9:50 AM Invited

High Heat Flux Exposures of NiCrAlY-Coated GRCop-84 Substrates: Sai V. Raj¹; Louis J. Ghosn²; Raymond C. Robinson³; ¹NASA Glenn Research Center; ²Ohio Aerospace Institute; ³QSS, Inc.

An advanced Cu-8(at.%)Cr-4%Nb alloy developed at the Glenn Research Center, and designated as GRCop-84, is currently being considered for use as liners in combustor chambers in NASA's exploration vehicles. Protective overlay coatings alloys are being developed for GRCop-84 to prevent environmental degradation. The creep, tensile and thermophysical data obtained on the monolithic NiCrAlY top and copper alloy bond coats were used to evaluate the stresses in the coating. Coated and uncoated specimens were exposed to a high heat flux hydrogen-oxygen combustion flame in NASA's Quick Access Rocket Exhaust (QARE) rig to evaluate the performance of the coatings. The measured temperatures and heat fluxes were compared with those predicted from finite element analyses (FEA), and it is shown that the experimental and the theoretical results are in excellent agreement. The expected coating performance in a rocket engine chamber is modeled.

10:10 AM

Experimental Techniques for the Characterization of Thermal Barrier Coating Bond Coats: Robert J. Thompson¹; J. C. Zhao²; Kevin J. Hemker¹; ¹Johns Hopkins University; ²GE Global Research Center

Thermal barrier coatings (TBCs), commonly used in modern gas turbines and jet engines, are dynamic, multi-layered, metallic-ceramic structures consisting of a superalloy substrate, an aluminum-rich bond coat, a

thermally grown oxide (TGO), and a ceramic top coat. Many (Ni,Pt)Al bond coats exhibit a strain-inducing B2 to L1₀ martensitic phase transformation that occurs during thermal cycling. Knowledge of this transformation and its effects on the bond coat's mechanical properties are essential to modeling the behavior of a TBC. In this study, combinatorial methods are employed to examine the effect of ternary elements on the martensitic transformation and microsample tensile testing techniques are developed to characterize the elevated temperature mechanical behavior of these alloys. The influence of bond coat composition on the martensitic transformation, high temperature strength, and overall performance of TBC systems will be discussed.

10:30 AM

Overview of the Processing and Properties of Hafnium-Based Ultra High Temperature Ceramics: Matthew J. Gasch¹; Mike Gusman¹; Donald T. Ellerby²; Ed Irby²; Sylvia M. Johnson²; ¹ELORET Inc; ²NASA Ames Research Center

Hafnium diboride-based materials are being investigated at NASA Ames as part of ongoing research aimed at developing superior heat resistant materials for use in extremely high temperature applications. For example, the exceptionally high melting temperatures of hafnium diboride (>3000°C) make it a suitable candidate for the extreme conditions experienced during atmospheric re-entry. Significant work on the manufacture of dense monolithic ceramics has resulted in the development of processing techniques specific to HfB₂-SiC based materials. Powder handling, die configuration, and hot pressing schedule are all aspects that greatly affect the final product. Processing methods found to optimize the uniformity of the material and produce dense billets are addressed, as are the temperature dependant mechanical and thermal properties of monolithic HfB₂-SiC materials.

10:50 AM Break

11:00 AM Invited

Atomistic Modeling of Dislocations in HCP Metals: M. I. Baskes¹; Srinivasan G. Srivilliputhur¹; ¹Los Alamos National Laboratory

In the first part of our talk we will discuss our atomistic calculations, in a generic hexagonal close packed (HCP) metal, wherein we systematically vary the (c/a) ratio and the basal stacking fault energy and explore its effects on the dislocation glide properties. This will be followed by a description of our atomistic calculations of dislocation motion in HCP zirconium metal (Zr). The stresses to move basal, prism, and pyramidal edge and screw dislocations in single crystal Zr are computed as a function of temperature. We find that at low temperature the basal dislocations move much easier than the prism dislocations. The stress needed to move the prism dislocation decreases significantly at higher temperature. For both these studies we use a semi-empirical modified embedded atom method potential that includes angular forces, to describe the interatomic interactions.

11:20 AM

Refinement of the VPSC Model for Deformation of Zirconium: Gwenaelle Proust¹; Carlos N. Tome¹; Deformation C. Kaschner¹; Irene J. Beyerlein¹; ¹Los Alamos National Laboratory

Hexagonal materials plastically deform by activating various families of slip and twin systems depending on diverse processing parameters such as temperature and strain rate. In this work, we propose to further elucidate the balance between the diverse twinning and slip deformation modes as a function of temperature for high purity zirconium. We propose here a new version of the visco-plastic self consistent (VPSC) model to simulate the deformation of this material. In this new version, twinning is accounted for using a composite-grain twin model which has been shown to better reproduce strain path changes than the previously developed Predominant Twin Reorientation (PTR) scheme. We use tensile and compressive experimental data at diverse temperature regimes varying between 76K and 450K to adjust the constitutive parameters of the VPSC model. The experiments were realized on in-plane and through-thickness samples obtained from a clock-rolled zirconium plate.

11:40 AM

The Importance of Slip and Twinning within Deformation Twins in Zirconium: *Rodney J. McCabe*¹; Ellen K. Cerreta¹; Amit Misra¹; Carlos N. Tome¹; George C. Kaschner¹; ¹Los Alamos National Laboratory

Zirconium exhibits ductile deformation behavior at liquid nitrogen (LN) temperature largely due to the operation of deformation twins. Deformation within the first generation of deformation twins can have significant impacts on microstructures, developing textures, and stress strain responses, particularly for uniaxial compressive strains greater than around 10% and for changes in strain path. In addition, our polycrystal constitutive simulations (VPSC) predict activities inside twins that need to be confirmed experimentally. In the present study we examine the role of slip and twinning within deformation twins using OIM and TEM. The results are used to explain both stress strain responses and developing textures in zirconium samples compressed either parallel or perpendicular to an initially strong c-axis texture.

12:00 PM Invited

Exploring the Dislocation/Twin Boundary Interactions in Zirconium: *George C. Kaschner*¹; Carlos N. Tome¹; Ellen K. Cerreta¹; Rodney J. McCabe¹; Amit Misra¹; Sven Vogel¹; ¹Los Alamos National Laboratory

We have shown in previous work that deformation of zirconium is a competing/complementary blend of twinning and slip. At moderate strains and cold temperatures, the twinned structure is sufficiently dense in forest dislocations that TEM observation of dislocation/twin interactions is obscured. We have employed in situ neutron diffraction to study the kinetics of recovery and recrystallization to produce a substructure that retains the deformation twin structure yet with a greatly reduced dislocation density. That product is then reloaded in compression and observed using TEM to study the interactions of dislocations with the deformation twin boundaries.

12:20 PM

Exploring the Dislocation-Twin Boundary Interactions in Zirconium: A TEM Investigation: *Cynthia D. Smith*¹; Henry A. Padilla¹; Ian M. Robertson¹; John Lambros¹; Armand J. Beaudoin¹; George Kaschner²; ¹University of Illinois; ²Los Alamos National Laboratory

Deformation in zirconium, as in all HCP materials, involves a competition between twinning and slip under most deformation conditions. When deforming previously rolled material, twinning is observed in both in-plane compression samples, which show an increasing hardening rate, and through-thickness compression samples, which show a constant hardening rate. The mechanical behavior of zirconium is probed using interrupted high strain rate tests, post-mortem TEM characterization and dynamic straining in the TEM. High strain rates produce a mixed response with some grains containing a high density of dislocations and others twins. The twins are predominately of the tension type. The dynamics of the interaction of twins with pre-existing grain boundaries are being investigated by re-loading the interrupted material in the TEM. In this talk, these observations will be correlated to bulk mechanical properties.

Biological Materials Science: Biological Materials

Sponsored by: The Minerals, Metals and Materials Society, ASM International, TMS Structural Materials Division, TMS: Biomaterials Committee, TMS/ASM: Mechanical Behavior of Materials Committee
Program Organizers: Andrea M. Hodge, Lawrence Livermore National Laboratory; Chwee Teck Lim, National University of Singapore; Richard Alan LeSar, Los Alamos National Laboratory; Marc Andre Meyers, University of California, San Diego

Tuesday AM
March 14, 2006

Room: 212A
Location: Henry B. Gonzalez Convention Ctr.

Session Chairs: Marc A. Meyers, University of California; Masaaki Sato, Tohoku University

8:30 AM Invited

The Organic Layer within Abalone Nacre: *Marc A. Meyers*¹; Albert Y. M. Lin¹; Julie Muyco¹; Kenneth S. Vecchio¹; ¹University of California, San Diego

In this study, we focus on the thin viscoelastic layers between the aragonite tiles in abalone shell and on their role in the growth of tiles as well as on the mechanical properties. AFM shows that the thin layer is comprised of linear chains forming a random planar network. This network contains small holes that expand, upon stretching of the film. They play a pivotal role in growth and enable the maintenance of the same crystallographic relationship for tiles grown sequentially in the 'terraced cone' mode. TEM analysis is carried out to establish the size and spacing of bridges between adjacent tile layers, corresponding to the holes in organic layer. The growth of nacre in abalone was interrupted after periodic times in order to observe the formation of the organic layer. The transition between spherulitic/columnar and tile growth is identified and characterized. Research Support: NSF DMR.

9:00 AM Invited

A Step-Specific Model for Shape Control of Biomineral Phases: *Roger Qiu*¹; Andrzej Wierzbicki²; Germaine Fu³; Chris Orme¹; John Hoyer⁴; George Nancollas⁵; Dan Morse³; Jame De Yoreo¹; ¹Lawrence Livermore National Laboratory; ²University of South Alabama; ³University of California, Santa Barbara; ⁴University of Pennsylvania; ⁵University at Buffalo

Biomineralized structure often exhibit shapes that are different from crystals grown from pure solutions. Understanding the underlying principles by which biomolecules modify the shape can shed light on biomineral processes and suggest strategies for bio-inspired materials design. We use *in situ* atomic force microscopy and molecular modeling to investigate stereochemistry and molecular scale growth modification of calcite and calcium oxalate monohydrate by small molecules, polypeptides, and proteins. We find in all systems that the resulting growth kinetics and crystal habit are modified by interaction to specific atomic steps on existing crystal faces. Moreover, changes in macroscopic crystal shape mimic the modifications seen at the atomic level. Molecular modeling calculating the modifier-crystal interaction energy supports these conclusions in that binding energies are greatest at the step edges and in accordance with the step-specificity observed in the experiments. These results argue for a model of shape modification recognizing the role of steps.

9:30 AM

On the Measurement of Cell Mechanical Properties and Cell Adhesion: *Yifang Cao*¹; Jianbo Chen¹; Monica E. Bravo¹; Randy Bly¹; Alberto M. Cuitiño²; Wole Soboyejo¹; ¹Princeton University; ²Rutgers University

This paper presents a range of experimental techniques for the measurement of the interfacial strengths between human-osteosarcoma (HOS) cells and titanium and poly-dimethyl-siloxane (PDMS) surfaces. The interfacial strengths are measured using shear assay experiments. These involved the laminar flow of cell culture fluid over cells that were cultured onto titanium and PDMS surfaces. In-situ images of cell deformation were also obtained during the shear assay experiments. These were analyzed using digital image correlation (DIC) techniques, which were used to extract the local strain distributions. The results were then incorporated into a finite element model for the extraction of cell modulus. Subsequently,

TUESDAY AM

the cell lift-off strengths were determined using micro-pipette aspiration strengths. The implication of the results are then discussed for the surface design of implantable microelectronics, bioMEMS structures and orthopedic/dental structures.

9:50 AM

Lobster Cuticle as an Example of Smart Anisotropic Material: *Patricia Romano*¹; Helge Fabritius¹; Christoph Sachs¹; Dierk Raabe¹; ¹Max Planck Institute for Iron Research

Many biological materials are composed of fibrils arranged according to well defined three-dimensional patterns. These materials often show a strong anisotropy. The composite microstructure, comprising hard inorganic and soft organic materials, plays a key role in enhancing the toughness, strength, and hardness of cuticles by restricting crack growth and delocalizing deformation fields. An essential characteristic of biological materials is their hierarchical organization, at the nanometer-to-millimeter scale. Lobster cuticle is a good example of this. We studied the exoskeleton of the American lobster (*Homarus americanus*) using optical, scanning and transmission electron microscopy. The results show that the structure is more complex than the commonly assumed model. The structure of the chitin-protein planes creates the twisted plywood pattern characteristic of the arthropod cuticle. However, these planes are not simple arrays of parallel chitin-protein fibers, but interconnected fibers forming planar honeycombs rotating around continuous lenticular cavities.

10:10 AM Break

10:30 AM Invited

Molecular Interaction and Modification in Human Diseased Cells: *ChweeTeck Lim*¹; Ang Li¹; Kevin Shyong Wei Tan¹; ¹National University of Singapore

A key feature of the pathophysiology of *Plasmodium falciparum* malaria is the increased rigidity and stickiness of infected red blood cells (RBCs) which can cause serious impairment of blood flow through narrow capillaries. Proteins released from the parasite induce alterations to the membrane resulting in these changes. These proteins manifest as knob-like structures on the membrane surface of the RBC. Here, we report an atomic force microscopy (AFM) study of malaria-infected RBCs. We first obtain high resolution AFM images of the nanosized knob structures on the surface of infected RBCs to determine the 3-D structure, size and density of the knobs. Next, we quantitatively measure the stickiness or cytoadherence of infected RBCs by identifying and measuring the molecular interaction forces of the various ligand-receptor pairs contributing to cytoadherence. AFM is used to systematically measure the single bond strength between these ligand-receptor pairs occurring between endothelial cells and the infected RBCs.

11:00 AM Invited

Mechanical Properties of Isolated Internal Organs of Vascular Cells: *Masaaki Sato*¹; ¹Tohoku University

Mechanical properties of isolated stress fibers and nuclei were measured using a newly designed micro tensile tester and a micropipette technique. Stress fibers isolated from smooth muscle cells were elongated more than two-fold of the initial length and the resistance to elongation increased with increasing the tensile load. The estimated average value of the initial elastic modulus was 2.5 MPa, which value was much lower than that of synthesized single actin filaments, 1.8 GPa. Isolated nuclei from endothelial cells remained almost rounded shape under static conditions. However, the nuclei were supposed to be compressed state in the cells by observing the 3-D topography. When we applied shear stress, the nuclei showed elongated shape. Elastic modulus measurements with pipette aspiration test showed that nuclei hardened significantly from 0.42±0.12 kPa to 0.62±0.15 kPa with the fluid shear stress.

11:30 AM

Buckling Resistance of Slender, Nano-Scale Components in Biological Materials: Baohua Ji¹; Huajian Gao¹; *K. Jimmy Hsia*²; ¹Max Planck Institute for Metals Research; ²University of Illinois

Biological materials such as bone, tooth and sea shell exhibit a generic nanoscale composite structure consisting of mineral crystals with very large aspect ratios embedded in a soft protein matrix. It is not clear how the slender components in biological materials solve the problem of buck-

ling under compressive loading. In the present study, a simple analytical model is developed to show that the protein matrix in the biocomposites plays a critical role in stabilizing mineral crystals under compression. It is especially interesting in view of the three orders of magnitude difference in the elastic moduli of protein and mineral. The critical load for buckling is derived as a function of aspect ratio and volume concentration of mineral. A unique feature for biocomposite structure is that there exists a lower threshold value for the critical load below which the mineral crystals become stable against buckling no matter how slender they are.

11:50 AM

Toucan and Hornbill Beaks: A Comparative Study: *Yasuaki Seki*¹; Bimal Kad¹; David J. Benson¹; Marc A. Meyers¹; ¹University of California

The structure and mechanical behavior of a Toco toucan and two species of hornbill beaks (wreathed and wrinkled hornbills) were examined. The beaks are comprised of a sandwich composite with an exterior of multiple layers of keratin scales and a core composed of fibrous network of closed cells made of bone. The weight of hornbill beaks is significantly higher than the toucan beak and the internal foam is fused to the keratin shell. A distinctive feature of the hornbill beak is its *casque* formed from the keratin layers. The *casque* has an acoustic function. Both toucan and hornbill beaks have a hollow region in the center of the foam. Tensile and compression tests were applied to determine the mechanical properties of external shells and internal foams. Micro and nanoindentation hardness measurements were used to corroborate these values. The compressive behaviors of the foams were modeled by the Gibson-Ashby constitutive equations.

12:10 PM

Influence of Absorbed Amino Acids on Hydroxyapatite Crystallization and Properties: *Olga Alexandrovna Golovanova*¹; *Elena Vladimirovna Rosseyeva*¹; *Anna Alexandrovna Ogneva*²; *Olga Victorovna Frank-Kamenetskaya*¹; ¹St. Petersburg State University; ²Omsk State University

Ca-deficit hydroxyapatite is the main inorganic phase in human organism. The study of the interaction of hydroxyapatite with organic molecules is only in progress. We have synthesized the crystalline hydroxyapatite powders with molar Ca/P ratio 1.57–1.67 at physiological condition (37°C, phosphate concentration 0.02 mol/l, pH 7.4, 24 hour = 7.5±0.1). The effect of amino acids (L – forms of glutamic acid, aspartic acid, glycine and lysine) on electrokinetic properties and particle size of synthesized material has been estimated. The determination of zeta-potential allow to shown, that the absorption of glycine and lysine result in overcharge of the hydroxyapatite (Ca/P = 1.58±0.01) surface and absorption decrease as the charge on the absorbing species become more negative. It was established, that the greatest decreasing of hydroxyapatite particle size (Ca/P = 1.67±0.01) has been occurred in the presence aspartic acid, overcharging the surface of crystals also.

Bulk Metallic Glasses: Atomic Study and Processing

Sponsored by: The Minerals, Metals and Materials Society, TMS Structural Materials Division, TMS/ASM: Mechanical Behavior of Materials Committee

Program Organizers: Peter K. Liaw, University of Tennessee; Raymond A. Buchanan, University of Tennessee

Tuesday AM
March 14, 2006

Room: 217B
Location: Henry B. Gonzalez Convention Ctr.

Session Chairs: Christopher A. Schuh, Massachusetts Institute of Technology; Michael Atzmon, University of Michigan

8:30 AM Keynote

Atomistic Mechanism of Atomic Transport in Metallic Glasses: *Takeshi Egami*¹; ¹University of Tennessee

Atomic transport and mechanical properties in metallic glasses are often discussed in terms of the free-volume model. However, in glasses the Stokes-Einstein relationship that connects diffusivity and viscosity does

not work, and in addition to free-volume sinks have to be introduced as an additional parameter. At the same time the validity of the free-volume model has been seriously questioned by computer simulations. We propose an alternative model based upon the fluctuation and exchange of atomic bonds, defined by the nearest neighbor atoms. The topology of atomic connectivity is related to the local energy landscapes through the atomic-level stresses, and then translated into thermodynamics. We discuss how glass transition, viscosity, diffusion and mechanical deformation can be elucidated by this model.

9:00 AM Invited

Application of the Dense Cluster Packing Model: *Daniel B. Miracle*¹; ¹U.S. Air Force

The Dense Cluster Packing (DCP) atomic structural model for metallic glasses has recently been established. This structural model is derived from the requirement to efficiently fill space in a system of unequal spheres. Solute-centered clusters are proposed from the relative atomic sizes of solute and solvent atoms, and these atomic clusters are densely packed to efficiently fill space. This structural arrangement provides a number of predictions that can be compared with experiment. The purpose of this presentation will be to explore the implications of this model with respect to topological and chemical effects known to be important in the stability of metallic glasses. Successes of this model, as well as unanswered questions, will be discussed.

9:25 AM Invited

Challenges in Metallic Glass Research: From Atomic-Level Structures to Inch-Diameter Ingots: *Evan Ma*¹; ¹Johns Hopkins University

We discuss two issues of strong current interest in MG research. The first is a fundamental question for the science of glasses. Unlike the well-defined long-range order that characterizes crystalline metals, the details of atomic arrangements in amorphous alloys remain mysterious (although short-range order is considered ubiquitous and medium-range order likely). We use a combination of the state-of-the-art experimental and computational techniques to elucidate exactly how the atoms pack themselves in 3D, in several model MGs with different chemistry and atomic size ratios. On the application side, one of the challenges is to be able to cast BMGs of large sizes using only ordinary, inexpensive metals (e.g., free of Be or Pd), and locate compositions with extraordinary glass forming ability (e.g., critical size > 1 inch). We have come up with a search strategy that will be shown to be up to the task in 3D composition space.

9:50 AM Invited

Concentration Dependence of the Glass Forming Ability in Ternary Ca-Mg-Zn and Ca-Mg-Cu Systems: *Oleg N. Senkov*¹; James Michael Scott¹; Daniel B. Miracle²; Stephane Gorsse³; ¹UES Inc; ²Air Force Research Laboratory; ³Bordeaux Institute of Condensed Matter Chemistry

Several Ca-Mg-Zn and Ca-Mg-Cu bulk metallic glasses with the thickness of at least 10 mm were produced by a Cu mold casting method. The glass transition, crystallization, solidus and liquidus temperatures, as well as the heats of crystallization and melting were determined for these glasses using differential scanning calorimetry. Glass forming ability was determined as a function of the alloy composition and correlated with the driving force of crystallization of different phases at a near glass transition temperature. The compositions having a minimum driving force for crystallization showed better glass forming ability.

10:15 AM

Maximum Critical Thickness in Al-La-Ni Metallic Glasses: W. S. Sanders¹; J. S. Warner¹; *Daniel B. Miracle*¹; ¹U.S. Air Force

The stability of Al-rich glasses in the Al-La-Ni system has been measured. Glasses with critical thicknesses ranging from 270 μm to 780 μm have been achieved. An in-situ two-phase amorphous region containing as much as ~10% by volume of nanocrystals was also observed with critical thicknesses ranging from 420 μm to 950 μm. Measurements of T_g, T_x and T_l, as well as other empirical measures of thermal stability based on these quantities, confirm the unusual thermal stability of these glasses. These results suggest that bulk Al-based glasses with a maximum critical thickness exceeding 1 mm may be possible in alloys based on this system.

10:35 AM Break

10:45 AM

Observation of Structural Effects after Mechanical and Thermal Treatment of BMG: *Wojciech Dmowski*¹; Cang Fan¹; Peter K. Liaw¹; Takeshi Egami¹; ¹University of Tennessee

We have examined atomic structure of several Zr-based metallic glasses that have been heat treated below the glass transition temperature or mechanically deformed by an uniaxial tension and cold rolling. The atomic structure of these materials was compared to the as cast state. Structural studies on the annealed samples were performed using time-of-flight neutron diffraction and followed by the atomic pair distribution function (PDF) analyses. X-ray diffraction studies were carried out on the mechanically deformed samples using high energy synchrotron source and area detector and the data was analyzed assuming non isotropic scattering. The annealed samples exhibited structural relaxation consistent with the elimination of short and long inter-atomic distances in the first coordination shell. The mechanically deformed glasses showed evidence of induced structural anisotropy.

11:05 AM

Local Structural Fluctuations and the Glass Transition: *Rachel Aga*¹; Jamie Morris¹; Takeshi Egami²; Valentin Levashov²; ¹Oak Ridge National Laboratory; ²University of Tennessee

The local structural properties of an amorphous system are examined using molecular dynamics simulations. These local properties include pressure, bulk modulus, shear modulus, volume strain and shear stress. Starting from the low temperature glass, the system starts to show fluctuations of these structural properties upon warming toward the glass transition. Further, we find that the change in the scaling factor for the diffusion and the shear viscosity in the Stokes-Einstein relation is correlated with the change in behavior of the structural fluctuations. By including the many-body effects to the initial pair potential used, we are able to examine model systems with different Poisson's ratios.

11:25 AM

Toward Fine Structures in Metallic Glasses: P. Zetterström¹; *Yandong Wang*²; P. Jónvári³; Y. Ren⁴; H. F. Zhang⁵; R. Delaplane¹; H. Choo⁶; P. K. Liaw⁶; L. Zuo²; ¹Uppsala University; ²Northeastern University; ³Hungarian Academy of Sciences; ⁴Argonne National Laboratory; ⁵Chinese Academy of Sciences; ⁶University of Tennessee

The local structure in metallic glassy materials, including whether the icosahedral short-range order exists and, if so, in what detailed arrangements, is of fundamental interest, but still remains a mystery in materials science. Here, we use the Reverse Monte Carlo (RMC) method to obtain the three-dimensional discrete distributions of constitutional atoms in melt-spun CuZr and CuZrTi metallic glasses from neutron and X-ray scattering data. It was found that the topological short- and medium- range orders are dominated in the rapid-liquid-cooling metallic glasses, and the icosahedral short-range order is less stable in the CuZr binary alloy than in the Ti-doped ternary alloy. The analysis method is generally applicable to other metallic glasses, and the obtained results provide the insightful information on packing of atoms in glassy metals, which can be used as fundamental experimental inputs for modeling mechanical behaviors by the molecular-dynamics simulations and establishing quantitative models to predict the forming abilities of bulk-metallic glasses. The present work is supported by the Swedish Research Council in the frame of the SIDA project (Grant No. 348-2004-3475), the Ministry of Education of China (with the New-Century Outstanding Scholars Fund), the National Natural Science Foundation of China (Grant No. 50471026), and the National Science Foundation International Materials Institutes (IMI) Program with Dr. Carmen Huber as the Program Director.

11:45 AM

Local Atomic Structure and Size Distribution Study on Cu₆₀Zr₃₀Ti₁₀ Metallic Glasses: *Cang Fan*¹; D. M. Nicholson²; T. Proffen³; R. P. Hjelm³; W. Zhang⁴; C. Hammeter³; H. Choo⁵; P. K. Liaw¹; Akihisa Inoue⁴; T. Egami⁵; ¹University of Tennessee; ²Oak Ridge National Laboratory; ³Los Alamos National Laboratory; ⁴Tohoku University; ⁵University of Tennessee and Oak Ridge National Laboratory

It has been reported that the Cu₆₀Zr₃₀Ti₁₀ bulk-metallic glass contains nano-particles that likely contribute to the material's good mechanical properties. There is no report on the particle size distributions and local

atomic structures (short-range to medium-range order), which can help us further understand the mechanism of the nanocrystallization. To study the local atomic structures, we performed neutron diffraction on as-cast and partially crystallized samples to determine pair distribution functions (PDF). The PDF analysis indicated that the peaks of the Zr-Cu pair bond-lengths are in the range of 2.82 and 3.08 angstroms in as-cast samples. The coordination numbers of Cu-Cu and Zr-Cu are increased after partial crystallization. The atomic bonding is discussed on the basis of first principles calculations of the electronic and atomic structure of instantaneously quenched liquid samples. We also performed small angle neutron scattering (SANS) on the as-cast samples to investigate the nano-particle size distributions.

12:05 PM

Optimizing Chemistry of Bulk Metallic Glasses for Improved Thermal Stability: *George S. Dulikravich*¹; Igor N. Egorov-Yegorov²; ¹Florida International University; ²IOSO Technology Center

We propose a novel methodology for predicting concentration of each of the important alloying elements in BMGs so that the new alloys will have improved thermal stability and glass forming ability. Specifically, we are concentrating on maximizing Tliquidus and $Trg = Tg/Tliquidus$. The method is based on computational algorithms rather than on traditional experimentation, expert experience, and intuition. Specifically, the proposed alloy design method combines an advanced stochastic multi-objective evolutionary optimization algorithm based on self-adapting response surface methodology and another algorithm that performs accurate prediction of thermo-mechanical properties from given concentrations of alloying elements. During the iterative computational design procedure, a few judiciously chosen new BMG alloys need to be manufactured and experimentally evaluated for their properties in order to continuously verify the accuracy of the entire design methodology. This BMG alloy design optimization method thus minimizes the need for costly and time-consuming experimental evaluations of new BMG alloys.

Carbon Technology: Greenmill/Rodding

Sponsored by: The Minerals, Metals and Materials Society, TMS Light Metals Division, TMS: Aluminum Committee

Program Organizers: Morten Sorlie, Elkem Aluminium ANS; Todd W. Dixon, Conoco Phillips Venco; Travis J. Galloway, Century Aluminum Company

Tuesday AM
March 14, 2006

Room: 8A
Location: Henry B. Gonzalez Convention Ctr.

Session Chair: Marilou McClung, Century Aluminum of West Virginia

8:30 AM

Anodes Plant – The Next Step: Jean-Christophe Rotger¹; Yann El Gahoui¹; Magali Gendre¹; Andre Pinoncelly²; Jean-Francois Andre²; Jerome Morfoise²; *Andre Molin*²; ¹Alcan - LRF; ²Solios

Investors in greenfield primary aluminium smelters nowadays often contemplate the construction and operation of one 300kA (or more) potline as a first phase followed by a second identical potline a few years later for a targeted metal production of 600 000 T/year. Alternatively the 2 potlines can be built in one single phase. In such situation there is a strong economic incentive, both CAPEX and OPEX, to consider a high capacity green anode plant, 60 t/h or more, rather than two “standard” 35t/h paste plants. This is now feasible thanks to the two major developments achieved in the last few years: the SCAP Rhodax® process for dry mix preparation and the IMC process for paste mixing and cooling. The start-up early 2005 of these 2 processes at 35t/h at respectively ALBA line 5, Bahrain and AOSTAR, China confirmed the high standard of operating and anode quality performance achieved. The equipment are already available for the design of one single line of 70 t/h capacity achieving the same performance standards.

8:55 AM

Dynamic Process Optimization(DPO) in Greenmill: *Raja Javed Akhtar*¹; Saleh Ahmad Rabba¹; Markus W. Meier²; ¹DUBAL; ²R&D Carbon

Dubai Aluminium Company(DUBAL)is one of the largest single site aluminium smelters in the world producing 761000MT/year. It has its own carbon manufacturing plant with a production capacity of 370,000 anodes/year. As a management drive to optimise the current assets an exercise of Dynamic Process Optimisation was carried out in the Greenmill. R&D Carbon was chosen as the technical partner and worked along with DUBAL operational personnel during the three phases of the DPO. The process parameters were optimised systematically to reduce pitch content, increase paste throughput and increase anode density. A mobile pilot press was utilised to prepare samples for evaluation during the optimisation process. The optimised parameter settings were implemented on both the two anode production lines in the Greenmill following a successful 15 cell trial in the Potrooms. This paper describes the DPO methodology, highlights the results achieved in the Greenmill together with the subsequent improvement in anode quality and performance.

9:20 AM

Improve Carbon Plant Operations through Better Use of Data: *Keith Sinclair*¹; Barry Sadler²; ¹Sinclair Associates, Inc.; ²Net Carbon Consulting Pty Ltd.

Most Carbon Plants collect an enormous amount of data for control and improvement of plant operations, reporting and to characterize and assess anode quality for the customer. However, in the experience of the Authors, the way that data is used can be improved considerably - full value is rarely extracted from the information and several “data traps” are common: *Control decisions and actions are based only on comparisons to arbitrary specifications; *Averages are used inappropriately, e.g. with a lack of attention to variability in the data; *Data is over-aggregated; *Data is over-extrapolated; *Insufficient attention is given to the impact of sampling methods on the usefulness of data. This paper will demonstrate these data traps, describe their implications and suggest ways of avoiding these pitfalls using examples based on information from the sampling and testing of anode cores.

9:45 AM

Experience Report - Aostar Aluminium Co Ltd, China: Anode Paste Preparation by Means of a Continuously Operated Intensive Mixing Cascade (IMC): *Berthold Hoh*¹; Youlai Wang²; ¹Maschinenfabrik Gustav Eirich GmbH and Company KG; ²Aostar Aluminium Company Ltd

In 2003, Aostar Aluminium started the construction of a 250 000 t/y greenfield smelter near Meishan in Central China. The smelter uses GAMI 320 kA electrolysis cells. The affiliated anode plant was put into operation in January 2005. It is based on the newly developed Intensive Mixing Cascade (IMC) technology for anode paste preparation, combined with a vacuum vibrocompactor for anode forming. Design figures and current results of the plant operation are given. Typical features like self-adaptation to low raw material qualities and fluctuations of properties are described and discussed. Based on the experiences gathered at Aostar, the IMC process does not only significantly reduce both the investment (Capex) and operating costs (Opex) of an anode paste plant but also allows for the production of more than 60 t/h of anode paste in one single line. This perfectly fulfils the future requirements of the primary aluminium smelting industry.

10:10 AM Break

10:25 AM

A Study on the Quality Assessment of ETP Copper Anode Bars Used in Aluminium Reduction Process to Improve Their Life Cycle Time: *Y. V. Ramana*¹; Rajnish Kumar¹; ¹Hindalco Industries Ltd

Hindalco consumes about 1600 MTPA of ETP copper for production of 350,000 MTPA of aluminium metal. To reduce the consumption patterns several possible control measures were studied. The present paper deals with the study on quality parameters. Copper bars, in the aluminium reduction process are continuously exposed to different physico-chemical environments like flue gases emanating from pots, load bearing, exposure to high temperature, hot and cold working. To meet the demanding requirement of the complex environment, a comprehensive testing of physical, chemical, mechanical and metallographic properties has been introduced and narrowed down the impurities to trace levels. These measures have resulted in improving the life cycle time of the copper bar to a significant extent. The results have established significant relationships be-

tween different physico-chemical and mechanical properties, the patterns of different impurities, especially oxygen and their role in controlling the life cycle time.

Cast Shop Technology: Melt Treatment, Quality and Product Properties

Sponsored by: The Minerals, Metals and Materials Society, TMS Light Metals Division, TMS: Aluminum Committee

Program Organizers: Rene Kieft, Corus Group; Gerd Ulrich Gruen, Hydro Aluminium AS; Travis J. Galloway, Century Aluminum Company

Tuesday AM
March 14, 2006

Room: 7C
Location: Henry B. Gonzalez Convention Ctr.

Session Chair: Benoit Commet, Alcan Centre de Recherches de Voreppe

8:30 AM

Jetcleaner: The Lower Cost Alternative for Degassing Metal: *Ghislain Henry Le Roy*¹; Jean-Marie Bertrand Chateau¹; ¹Novelis

"Jetcleaner" is an aluminum in-trough refining system recently developed by Novelis PAE. This paper reviews industrial performances, in particular using data gathered on extrusion billets casting at the BON-L casthouse in Pickering, Ontario and expert appraisalment by Research Centre engineers: 1) efficient hydrogen removal, linked with some inclusion removal, as measured by Alscan and PodFa; 2) low investment and operating costs, thanks to a simple design, especially in the case of frequent alloy changes; 3) user friendliness features: *the Jetcleaner fits easily with reduced space requirement and fast installation; *little maintenance is required; *there is little metal retention between two casts; *environment constraints are respected. Starting from a concept patented in 1998, then developed in close collaboration with customers, the Jetcleaner has been well received by operators and cost-conscious casthouse managers in North America and Europe.

8:55 AM

Experimental and Numerical Study of Ceramic Foam Filtration: *Emilie Laé*¹; Hervé Duval²; Carlos Rivière²; Pierre Le Brun¹; Jean-Bernard Guillot²; ¹Alcan Centre de Recherches de Voreppe; ²Laboratoire de Génie des Procédés et Matériaux, École Centrale Paris

Ceramic foam filtration is widely used to remove non metallic inclusions from liquid aluminium. Its performances have been largely studied in the literature and some discrepancies remain amongst the published results. Consequently, a research program was deployed to evaluate the performances of a range of CFF used under various conditions and to understand the inclusions capture mechanisms. On the first hand, laboratory trials were run on a filtration pilot under controlled thermal and hydrodynamic conditions. The filtration efficiency of the CFF was assessed by LiMCA measurements. Microscopic observations of the filter impregnated with solidified metal were carried out to know the repartition of the inclusions within the filter and their capture sites. On the other hand, the initial filtration efficiency as well as the inclusion capture sites were calculated by a two-dimension lattice-Boltzmann filtration model on different CFF, for various inclusion sizes. Results of this work are presented and discussed.

9:20 AM

A Novel Metal Treatment Process in Crucibles for Impurity Removal in Secondary Aluminum: *Gaston Riverin*¹; Jean-François Bilodeau¹; Claude Dupuis¹; ¹Alcan Inc

Treatment of aluminium in crucible is well established in the smelter industry as the most efficient technology to remove alkali element such as lithium. The utilization of crucibles is common in Remelt and Recycling plants to transport metal recovered from dross recycling and scrap melting operations. In these cases, the metal is often contaminated with alkali elements, undesired contaminants. This paper presents the development work of an improved crucible treatment better adapted for metal recovered from remelt and recycling operations. This method, which involves

utilization of flux to improve metal cleanliness and alkali elements removal, is specially designed to promote efficient dispersion of the reactant in the melt to achieve optimal performance. Laboratory work is explained covering new impeller design and dispersion methods to meet specific requirements for alkali, oxides and inclusions removal. Results from an industrial demonstration are detailed, including metal cleanliness measured by PoDFA and alkali removal efficiency.

9:45 AM Break

10:00 AM

Kinetics of an AlF₃ Aluminium Filter: *Harald Gorner*¹; Thorvald Abel Engh¹; Martin Syvertsen²; ¹Norwegian University of Science and Technology; ²SINTEF

Kinetic models are proposed for the removal of Na and Ca by an active AlF₃ filter for aluminium melts. Experiments have been carried out using a setup and filter material that have shown its efficiency previously. Pure Al melts containing different levels of Na or Ca have been filtered to reveal the kinetics of the AlF₃ filter material. The surface area of the filter and the temperature of filtration have been varied in addition to the concentrations of Na and Ca. Changing only one parameter at a time in a series of three experiments while keeping the other parameters constant gave a good reproducibility. The removal of Ca and Na in the AlF₃ filter follows zero order kinetics with a transition to first order kinetics for low levels of Na and Ca. At low levels the removal rate becomes proportional to the concentration of Na and Ca.

10:25 AM

Gas Fluxing of Aluminum; Comparison of Computational Fluid Dynamics Models and Experiments: *Autumn Fjeld*¹; *James W. Evans*¹; Corleen Chesonis²; ¹University of California; ²Alcoa Inc

Chlorine fluxing is an essential purification step in aluminum processing in which impurities such as Ca, Na, Li, and Mg are removed by bubbling a mixture of chlorine and argon gas through molten aluminum. The efficiency of impurity removal and control of toxic chlorine and chloride emissions are dependent upon the extent of gas dispersion or mixing, residence time of the bubbles, and surface area of the bubbles. Clearly, these gas phase parameters cannot be directly observed in molten aluminum, thus there are details of the fluxing process which are not fully understood. To gain further insight, two computational models have been developed to simulate the complex two-phase fluid dynamics of a rotary gas injection system. The results of these two modeling approaches are presented and analyzed and compared to experimental bubble measurements gathered using a capacitance probe, which detects bubbles in molten aluminum.

10:50 AM Break

11:05 AM

The Role of B Element on Refining Purity Aluminum: *Henghua Zhang*¹; ¹Shanghai University

The effect of B element on the macrostructure and property of purity aluminum has been studied with Optical Microscopy and MTS. It is shown that although the single B element has little or none refining effect on the purity aluminum, it will obviously increase the refining effect and prolong the fading time when it was simultaneously added into the molten aluminum with Ti element. It is found from the analysis of SEM and thermodynamics that the refining mechanism of salts containing Ti and B elements on the purity aluminum are mainly contributed to the heterogeneous nuclei of TiAl₃ particles reacted and dispersed in the melting. While the reacted (Al, Ti) B₂ particle plays little or none role in refining purity aluminum. However, the fine (Al, Ti) B₂ particle will reduce the size of TiAl₃ since the TiAl₃ nucleates and grows along the (Al, Ti) B₂ particle.

11:30 AM

A Method for Measurement and Control of Boride Agglomeration in Grain Refinement of Aluminum: *Rein Vainik*¹; John Courtenay²; Holm Boettcher³; Lennart Backerud¹; ¹Opticast Aluminium AB; ²MQP Limited; ³AMAG

The method for grain size control during casting of billets and slabs, as developed by Opticast Aluminium AB, is now applied at several cast houses. Apart from savings and increased quality of the cast product, several effects have been encountered, which have a large impact on the grain

refinement efficiency. Grain refining performance between rods from different manufacturers varies considerably. The structure of the master alloy is important, and determines whether the particles present in the master alloy will have enough time to disintegrate/dissolve. The rod addition point in relation to melt flow conditions are other important factors. A new method has been developed that shows the degree of agglomeration of borides and that can be used routinely in the cast house to evaluate this effect. This is used to optimise the casting process to render a fine grained structure in the castings at the lowest possible addition rate.

Characterization of Minerals, Metals and Materials: Structural Engineering Materials I

Sponsored by: The Minerals, Metals and Materials Society, TMS Extraction and Processing Division, TMS: Materials Characterization Committee

Program Organizers: Jiann-Yang James Hwang, Michigan Technological University; Arun M. Gokhale, Georgia Institute of Technology; Tzong T. Chen, Natural Resources Canada

Tuesday AM Room: 206A
March 14, 2006 Location: Henry B. Gonzalez Convention Ctr.

Session Chairs: Toru H. Okabe, University of Tokyo; Ann M. Hagni, CTL Group

8:30 AM

Adiabatic Shear Bands Associated with Plug Formation and Penetration in Ti-6Al-4V Targets: Formation, Structure, and Performance: *Fabiola Martinez*¹; Erika V. Esquivel¹; Maribel I. Lopez²; Sarah M. Gaytan¹; David A. Lopez¹; Amanda Ramirez¹; Diana A. Ramirez¹; Priscilla A. Guerrero¹; Larry E. Murr¹; B. E. Schuster²; ¹University of Texas; ²U.S. Army Research Laboratory

A series of electron beam, cold hearth, single melt Ti-6Al-4V plates (nominally 2.5 cm thick) impacted by 2 cm diameter, 4340 steel projectiles (with 54 g nominal mass) at velocities ranging from 0.633 to 1.027 km/s were sectioned along the impact axis and examined by optical metallography, SEM, and TEM to characterize the formation, growth, and microstructure of adiabatic shear bands which facilitate plug formation and projectile perforation by dynamic recrystallization (DRX) within the shear bands; allowing for solid-state flow. The localized DRX of the projectile and projectile-target interaction phenomena were also examined using elemental X-ray mapping of the targets and projectiles in the SEM. Near ballistic limit velocities, the shear bands propagate towards the rear of the target where they coalesce and grow to provide a cylindrical (DRX) flow regime for the plug volume (Supported by ARL Prime Contract DATM05-02-C-0046, Amendment 16).

8:55 AM Invited

Some Aspects of Free-Machining Stainless Steel with Low Carbon: *Julian Ciupitu*¹; *Dana Daisa*¹; ¹METAV

This paper-work shows some aspects regarding the obtaining, structure and properties of a free-machining Cr-Ni stainless steel using as reference AISI 304 (annealed condition). Better machinability is the result of adding Sulphur up to 0,10% and restriction of Carbon content to a maximum of 0,03%. Sulphur was added into the melt as Fe-S master alloy, in a vacuum induction furnace. Secondary structures were examined with SEM microscope and RX diffraction. The electrochemical properties were investigated by cyclic voltametry in sulphuric acid 1N, at 22°C and a polarization rate of 100mV/sec. The tensile properties were determined. The presence and the distribution of sulphides (mainly MnS), almost no carbides in a γ matrix, have a double effect on machining processes: chip-breaking and lubrication at high cutting speeds. The obtained free-machining stainless steel presents a good combination of technological (machinability) and functional (corrosion resistance) properties without major lowering of tensile strength.

9:20 AM

Laser Generation of Acoustic Waves in Different Laser Power Regions from Rene 77 Superalloy: *Shih-Jeh Wu*¹; *Chen-Ming Kuo*¹; *Chun-Hung Lin*¹; *Shian-Ching Jason Jang*¹; *Dong-Yih Lin*¹; ¹I-Shou University

It is well known that the amplitude of laser generated ultrasonic signals can be significantly enhanced by increasing the power density in the laser pulse such that material ablation occurs. This leads to a direct increase in the signal-to-noise ratio of laser-based systems for the remote generation and detection of ultrasound. In this research an Nd-Yag pulsed laser (532 and 1064 nm wave length) will be used to generate ultrasonic waves from Rene 77 superalloy for the idea power region (either thermal-elastic or lower ablative) to be used to remote characterization of mechanical material properties in terms of the signal-to noise ratio and frequency response. The ultrasound signal is picked up by a Fabry-Perot interferometer and ultrasonic transducer. There were also some modeling works for the laser-acoustics under different power regions. The experimental results will also be compared to these analytical models.

9:45 AM

Ultrasonic Detection of Hydride Blisters in Zr-2.5Nb Pressure Tube: *Yong-Moo Cheong*¹; *Young-Suk Kim*¹; ¹Korea Atomic Energy Research Institute

Since Zr-2.5Nb pressure tubes have a high risk for the formation of blisters during their operation in pressurized heavy water reactors, there has been a strong incentive to develop a method for the non-destructive detection of blisters grown on the tube surfaces. However, because there is little mismatch in acoustic impedance between the hydride blisters and zirconium matrix, it is not easy to distinguish the boundary between the blister and zirconium matrix with conventional ultrasonic methods. This study has focused on the development of the ultrasonic method to detect the hydride blisters formed on Zr-2.5Nb pressure tubes. Hydride blisters were grown on the outer surface of the Zr-2.5Nb pressure tube using a cold finger attached to a steady state thermal diffusion equipment. An ultrasonic velocity ratio method as well as conventional ultrasonic parameters with immersion technique was developed to detect small hydride blisters on the Zr-2.5Nb pressure tubes.

10:10 AM Break

10:20 AM

Iron Oxide Reduction with Conventional and Microwave Heating under CO and H₂ Atmospheres: *Jiann-Yang James Hwang*¹; *Xiaodi Huang*¹; *Shaolong Qu*¹; *Yongqing Wang*¹; *Gerard T. Caneba*¹; ¹Michigan Technological University

Microwave heating has been proved an effective method to rapidly heat and reduce iron oxide with carbon. However, potential use of microwave heating for iron oxide reduction in the steel industry may include the use of coal, CO and/or H₂ as the reducing agent. Other heating method may be required to combine with the microwave heating to provide the total energy need. A special microwave device has been designed and built to facilitate the investigation. With this device, iron oxides can be heated by an electric resistance heating, microwave heating, or their combinations. The incoming CO and/or H₂ also can be preheated to simulate a potential utilization of recovered heat. The iron oxide weight and temperature can be monitored during an entire reduction period. A series of reduction experiments have been conducted. The results will be presented and discussed.

10:45 AM

Development of Ore-Coal Composite Pellets for Sponge Ironmaking: *B. B. Agrawal*¹; *G. I.S. Chauhan*¹; ¹RDCIS, SAIL

Iron ore fines are one concern for Indian economy and ecology. A possible avenue is to use these fines for sponge ironmaking. Work has been carried out to pelletize these fines with coal and a suitable binder, and cure them in ambient atmosphere to retain in-situ reductant. Pellets were characterized for physical-strength and metallization. Critical factors were granulometry of pellet-mix and percentage of coal and binder. In laboratory tests, pellets got metallized faster compared to lump-ore. Large-scale trials were conducted in a 12-meter long rotary- kiln plant. For 90% metallization, required residence time was only 60 minutes against 240 minutes for lump-ore. Coal requirement also decreased. Investigations established the fast reduction nature of pellets. This is due to reduction-reac-

tions occurring simultaneously at many sites within composite pellets, along with diffusion of reducing gases from-surface-to-core. The developed process is a value addition in the conventional pelletmaking, and is environment-friendly.

11:10 AM

Microstructural and Textural Characterization of Brazilian Iron Ores for Quality Control in Ironmaking—A Geometallurgical Approach:

Claudio Batista Viera¹; Varadarajan Seshadri¹; Carlos Alberto Rosiere¹; ¹Universidade Federal de Minas Gerais

In this paper, the structures and textures of some of the iron ores from Quadrilátero Ferrífero of the Minas Gerais state of Brazil are presented. The correlation between structure and characteristics important for suitability as charge in the blast furnace, such as decrepitation, degradation, and reducibility based on microstructure as well as the importance of magnetic susceptibility tests in the evaluation is emphasized. It is demonstrated that granoblastic, mainly martitic ores occurring in geological low strain areas from this region display low decrepitation and degradation during reduction. On the other hand, lepidoblastic ores with strong orientation in the structure, anisotropic ores and those consisting of substantial specularite display higher indices of decrepitation and degradation during reduction. These structural and geological characteristics are also important in agglomeration processes such as sintering and pelletizing.

11:35 AM

Characterization of Softening Behavior of Pellets, Sinters and Lump Ores in Ferrous Smelting Processes: Florian Kongoli¹; I. McBow¹; S. Llubani¹; Robert D. Budd¹; ¹FLOGEN Technologies Inc

One of the most important properties of pellets, sinters and lump ores in ferrous smelting processes is their softening behavior along with temperature increase. A good pellet or sinter need to have an optimal softening behavior in order to respond the strict requirements for a process without problems and high productivity. This behavior becomes even more important when various new minor components come with the primary materials and influence it in various ways that could potentially cause several problems. In this work it is discussed the characterization of the softening behavior of some pellets and sinters through a unique physical modeling that reflect the physical properties of the matter and predict their softening behavior as a function of various furnace parameters and conditions.

Computational Thermodynamics and Phase Transformations: Atomic Modeling of Solid-Liquid Structures

Sponsored by: The Minerals, Metals and Materials Society, TMS Electronic, Magnetic, and Photonic Materials Division, TMS Materials Processing and Manufacturing Division, TMS Structural Materials Division, TMS: Chemistry and Physics of Materials Committee, TMS/ASM: Computational Materials Science and Engineering Committee
Program Organizers: Dane Morgan, University of Wisconsin; Corbett Battaile, Sandia National Laboratories

Tuesday AM
March 14, 2006

Room: 210A
Location: Henry B. Gonzalez Convention Ctr.

Session Chairs: Christopher Mundy, Lawrence Livermore National Laboratory; Anton Van der Ven, University of Michigan

8:30 AM Invited

Using Molecular Dynamics Simulation to Study Nucleation Kinetics:

David T. Wu¹; ¹Yale University

Nucleation is important for phase transformations and microstructural evolution, but a predictive theory for its rate requires detailed understanding of the interfacial free energy (γ), which is difficult to measure for liquid-solid interfaces but can be estimated, e.g., by analyzing molecular dynamics (MD) simulations at equilibrium or fitting nucleation theory to experimental results. Both approaches have pitfalls, however: in the former, γ for a planar interface may not be applicable to critical nuclei with large curvature, while in the latter, different assumptions about γ 's dependence

on temperature or curvature may influence the fit. An alternative, brute-force approach is to simulate nucleation kinetics using MD, but this also has limitations due to possible interaction of nucleation with growth or coarsening; thus its success depends on how the computational results are interpreted. In this talk, I will discuss recent advances in designing and interpreting MD runs to study nucleation kinetics.

9:00 AM Invited

The Properties of Steps at Faceted Crystal-Melt Interfaces from Molecular-Dynamics Simulations: Dorel Buta¹; Mark D. Asta¹; Jeffrey J. Hoyt²; ¹Northwestern University; ²Sandia National Laboratories

The morphologies and growth rates of crystals grown from the melt are highly sensitive to the anisotropies of solid-liquid interfacial free energies and mobilities. In systems with faceted crystal-melt interfaces these anisotropies are governed by the intrinsic properties of steps, and their interactions. Molecular-dynamics simulations have been employed to study the properties of steps at 111 faceted solid-liquid interfaces for the Stillinger-Weber model of Si. Step mobilities are derived from non-equilibrium isothermal crystallization simulations and the resulting mobilities are found to be in good agreement with measured values for large step separations. The step mobility is found to decrease with decreasing step separations, an effect attributed to a reduction in step width resulting from step interactions. Step fluctuations are measured in equilibrium simulations and analyzed in an effort to determine the magnitude of the step stiffness and interaction parameters.

9:30 AM

Crystal-Melt Interfacial Properties in Lennard-Jones Alloys: Chandler A. Becker¹; Mark D. Asta¹; Jeffrey J. Hoyt²; David L. Olmsted²; Stephen M. Foiles²; ¹Northwestern University; ²Sandia National Laboratories

A primary factor in determining alloy solidification rates and morphologies is the magnitude of the crystal-melt interfacial free energy and its associated crystalline anisotropy. Much of the detailed information concerning these interfacial properties in metals comes from atomic-scale computer simulations, focused primarily on elemental systems. Factors controlling compositional dependencies of crystal-melt interface properties in alloys are far less developed. We are using Molecular Dynamics and Monte-Carlo simulation techniques to extract the stiffness and structure of crystal-melt interfaces in model Lennard-Jones alloys at several compositions. Interface stiffnesses at several interface orientations are extracted from equilibrium simulations of interface fluctuations, from which the anisotropic interfacial free energy is computed. The simulations are analyzed using the Gibbs-adsorption theorem to better understand the compositional dependence of interfacial free energies in these model alloy systems.

9:50 AM

Liquid Metal Embrittlement of Grain Boundaries in Metallic Alloys: A Systematic Simulation Investigation: Ho-Seok Nam¹; Mikhail I. Mendeleev II²; David J. Srolovitz¹; ¹Princeton University; ²Ames Laboratory

There are many examples in which a liquid metal in contact with a polycrystalline solid develops a deep liquid groove at the intersections of the grain boundaries and the solid-liquid interface. In some cases such as Al-Ga and Cu-Bi, the liquid film penetrates deep into the solid along the grain boundary and leads to brittle fracture under the influence of even modest stresses. We have performed a series of molecular dynamics simulations using a set of binary embedded atom method potentials that were tuned to reproduce phase diagrams characteristic of systems exhibiting liquid metal embrittlement. We report on a series of molecular dynamics simulations of how liquid films propagate into grain boundaries at the atomic-level scale as a function of thermodynamic properties of the liquid species such as solubility, diffusivity, and melting point. These results are compared with general trends gleaned from a series of experimental studies in the literature.

10:10 AM Break

TUESDAY AM

10:30 AM Invited

Simulating Fluid Phase Equilibria of Water from First Principles:*Christopher Jay Mundy*¹; J. Ilja Siepmann²; Matthew McGrath²; I.-F. Will Kuo¹; ¹Lawrence Livermore National Laboratory; ²University of Minnesota

Efficient Monte Carlo algorithms and a mixed-basis set electronic structure program were used to compute from first principles the vapor/liquid coexistence curve of water. A water representation based on the Becke-Lee-Yang-Parr exchange and correlation functionals yields a saturated liquid density of 900 kg/m³ at 323 K, and normal boiling and critical temperatures of 350 and 550 K, respectively. An analysis of the structural and electronic properties of the saturated liquid phase shows an increase of the asymmetry of the local hydrogen-bonded structure despite the persistence of a four-fold coordination, and decreases of the molecular dipole moment and of the spread of the lowest unoccupied molecular orbital with increasing temperature.

11:00 AM Invited

The Effect of Stress on Melting and Freezing in Nanopores:*Jeffrey J. Hoyt*¹; ¹Sandia National Laboratories

Liquids contained in open porous materials generally exhibit a melting point depressed from the bulk equilibrium value. By contrast, for fluids entrapped in closed pores, such as those formed during ion implantation, a melting point elevation is usually observed. In this work the thermodynamics of stressed solids is used to explain the melting point elevation in enclosed, spherical nanopores. The model includes the effects of liquid pressure, the elastic strain energy in both the pore solid and the surrounding matrix material, the volume change on solidification and the phenomenon of premelting. Results from the analysis agree favorably with experimental observations of melting point elevation in ion implanted Pb droplets in Al.

11:30 AM

Comparison of Grain Boundary and Solid-Liquid Interface Migration:*Mikhail I. Mendeleev*¹; Hao Zhang²; David J. Srolovitz²; James R. Morris³; ¹Ames Laboratory; ²Princeton University; ³Oak Ridge National Laboratory

The goal of this study was to compare the mechanism of the solid-liquid interface (SLI) and grain boundary (GB) migrations in the same pure system. In order to do this, we performed molecular dynamics simulation of the SLI and GB motion in pure Al and Ni. Elasticity was used as driving force in both cases. In order to test the reliability of our results in the case of the solid-liquid interfaces we also used overheating/overcooling as source of driving force. We found that both GB and SLI mobility are strong functions of the interface inclination. Surprisingly, the comparison of these two mobilities showed that the GBs move faster in pure system than SLIs. We will discuss possible explanations for this effect.

Deformation and Fracture from Nano to Macro: A Symposium Honoring W. W. Gerberich's 70th Birthday: Nanoscale Materials

Sponsored by: The Minerals, Metals and Materials Society, TMS Materials Processing and Manufacturing Division, TMS Structural Materials Division, TMS/ASM: Mechanical Behavior of Materials Committee, TMS: Nanomechanical Materials Behavior Committee
Program Organizers: David F. Bahr, Washington State University; James Lucas, Michigan State University; Neville R. Moody, Sandia National Laboratories

Tuesday AM
March 14, 2006

Room: 214D
Location: Henry B. Gonzalez Convention Ctr.

Session Chairs: Robert Keller, National Institute of Standards and Technology; C. Barry Carter, University of Minnesota

8:30 AM Invited

Modeling Size Effects in Micropillar Samples:*Peter Martin Anderson*¹; Julia R. Greer²; William D. Nix²; ¹Ohio State University; ²Stanford University

Compression testing of gold pillars with submicron diameters shows flow strengths as large as 50 times that of bulk counterparts. Corresponding stress-strain traces at uniform strain rate show rapid build-up to a peak stress, followed by repeated release and build-up of stress. A cellular-automaton model is proposed to determine if these results can be explained by the evolution of dislocation content inside a deforming micropillar. The model is based on discretizing pillars into cells with prescribed initial dislocation density and distribution of dislocation source lengths. The dislocation density in each cell evolves due to source operation, dislocation breeding, exchange of dislocation content, and load shedding. Smaller pillars are inherently different due a distribution of source lengths that is truncated by the pillar size and also the inability to contain bursts of dislocation activity. The model predictions and assumptions are assessed in light of recent experimental stress-strain data.

8:50 AM

Flow and Fracture of Isolated Nanostructures:*William Mook*¹; Julia Deneen¹; Michael S. Lund¹; Andrew M. Minor²; Steven L. Girshick¹; C. Barry Carter¹; William W. Gerberich¹; ¹University of Minnesota; ²Lawrence Berkeley National Laboratory

Characterizing the mechanical response of isolated nanostructures is vitally important to fields such as microelectromechanical systems (MEMS) where the behavior of nanoscale contacts can in large part determine system reliability and lifetime. To address this challenge directly, both scanning probe microscope (SPM) and transmission electron microscope (TEM) based nanoindenters have been used to compress structures such as spherical nanoparticles and lithographed nanodots between the substrate and a diamond tip. The tested materials, which include both metals and semiconductors, initially exhibit an elastic response followed by plastic flow during compression. Further compression induced fracture in semiconductor structures. The flow stress and, where applicable, fracture toughness of the structures as a function of shape, size and stress state will be presented and modeled.

9:05 AM

Indentation of Nanoparticles, Nanowires and Nanotubes:*Antonio Rinaldi*¹; Veronica Salgueirino-Maceira¹; Miguel Correa-Duarte¹; Yen T. Yeh¹; *Pedro Peralta*¹; Karl Sieradzki¹; Cody Friesen¹; ¹Arizona State University

This talk reports preliminary experimental results and observations concerning selected elementary nanostructures. Nanoindentation is used to investigate the mechanical properties of composite Co-SiO₂ nanoparticles between 100nm and 300nm in diameter. Metallic nanowires and nanotubes made of Cu or Ni and having 100nm average diameter and variable length between 500nm and 1000nm were also synthesized and tested. In many tests it was possible to use the nanoindenter to image the nanoelements after indenting, which provided extra information about the contact. Data analysis is crucial to filter out the effect of the substrate from the load-penetration curve. Experimental data capture "structural" properties. For example, the Co-SiO₂ nanoparticles appear to have a characteristic load penetration curve, whose shape reflects the composite structure and consists of three distinct zones marked by sharp and consistent slope changes during loading. More experiments and simulations are being conducted to validate and explain the results.

9:20 AM

Deformation Behavior of Nanoporous Gold:*Erica T. Lilleodden*¹; Cynthia A. Volkert¹; ¹Forschungszentrum Karlsruhe

Here we present a combined nanoindentation and microcompression study of the deformation behavior of nanoporous gold. This material is made by electrochemical dissolution of AuAg sheets with a nominal grain size of 100 μ m and results in a structure with pore and wall size on the order of 20 nm. The relevant mechanisms of plasticity in this fine-structured, coarse-grained material have been ascertained from the load-displacement measurements, in combination with microstructural characterization. The observed behavior will be discussed in terms of dislocation mechanisms and the availability of sources and sinks due to the high surface area and small cell wall size. Additionally, the measured elastic modulus and the relative brittle versus ductile behavior will be described in terms of the loading configuration and size of the deforming volume.

9:35 AM

Deformation Mechanisms in Incoherent Nanolayered Metallic Composites: *Srinivasan G. Srivilliputhur*¹; R. G. Hoagland¹; A. Misra¹; ¹Los Alamos National Laboratory

A metallic multilayer composite of soft metals like Cu and Nb possess near theoretical strength when the layer thickness are less than 20nm. Deformation of these materials involves single dislocation crossing the incoherent Cu-Nb interface, which is responsible for the extraordinary strength these multilayers can achieve. Rolling experiments in these multilayers show that large reductions in thickness (> 100%) are possible but become negligible when the individual layer thickness is reduced to 4nm or less. We describe results of molecular dynamics simulations that explore the mechanisms of slip transfer through incoherent Cu-Nb interfaces. These results suggest a mechanism for shear instabilities in very thin-layered composites. (This research was sponsored by Office of Basic Energy Sciences, US Department of Energy).

9:50 AM

Tensile Strength and Ductility of Cu/Nb Multilayered Films: *J. Greg Swadener*¹; Amit Misra¹; Yun-Che Wang¹; Xinghang Zhang²; ¹Los Alamos National Laboratory; ²Texas A&M University

Multilayered thin films exhibit enhanced mechanical properties, such as ultra-high yield strength, but limited tensile ductility and fracture toughness. Tensile tests were conducted to examine the work hardening behaviour and the underlying deformation mechanisms. Free standing films of alternating Cu and Nb layers were synthesized by sputter deposition. The individual layer thickness was controlled for each film and varied from 5 to 100 nm. For decreasing layer thickness, an increase in yield strength was measured. The strength increase and work hardening was not in accordance with the Hall-Petch relation, but was consistent with confined single dislocation slip. For films with 100 nm layers, 4% tensile elongation was achieved. However, tensile ductility decreased with decreasing layer thickness. In addition, the elastic modulus of each film was determined from strain measurements using a laser extensometer. The modulus agrees with expectations for a composite of textured Cu and Nb layers.

10:05 AM **Invited**

Nanomechanical Characterization on Piezoelectric Nanowires: *Scott X. Mao*¹; Minhua Zhao¹; Chuanbing Jiang²; Shouxin Li²; ¹University of Pittsburgh; ²Institute of Metal Research

Piezoelectric ZnO nanobelts were successfully synthesized by evaporating the ZnO powders at high temperatures without the presence of catalyst. Morphology analysis shows the nanobelts have a rectangle-like cross section with typical widths of several hundred nanometers, width-to-thickness ratios of 5 to 10, and lengths of hundreds of micron meters. Nanoindentations were made on the ZnO single nanobelt by using AFM indenter probe with radius < 25nm (Digital Instruments Nanoscope IIIa, tapping mode) and cubic corner tip with radius < 40nm (Hysitron Triboscope, STM mode). It was shown that the indentation size effect was still obvious for the indentation depth under 50nm. Besides, the sharper the indentation tip, the higher the nanoindentation hardness. It is also demonstrated that nanomachining is possible on nanobelt using AFM tip. Piezoelectricity measurement was carried on the single piezoelectric nanobelt under electric force microscope. Scaling effect on piezoelectricity was found.

10:25 AM **Break**

10:45 AM

Deformation Mechanisms in Fine-Grained Niobium: *Alexis C. Lewis*¹; David van Heerden²; Timothy P. Weihs³; ¹Naval Research Laboratory; ²Reactive NanoTechnologies, Inc; ³Johns Hopkins University

Creep rates in fine-grained Nb were measured at 600°C using free-standing Cu/Nb polycrystalline multilayered films. For specimens with grain sizes ranging from 0.5 μm to 5 μm, two distinct regimes were observed. At high stresses, the stress dependence, grain size dependence and activation energy for creep are consistent with Power Law creep, with an average stress exponent of 3.5. At low stresses, creep rates exhibited a linear dependence on stress, and an inverse linear dependence on grain size. A model is presented for a vacancy generation-controlled creep mechanism, whereby deformation rates are controlled by the rate of vacancy generation at or near grain boundaries. The proposed model is consistent

with experimental observations of stress and grain size dependence, as well as the activation energy measured for creep.

11:00 AM

Deformation Behavior of Nanolayered Metal-Ceramic Laminated Composites: Xin Deng¹; *Nikhilesh Chawla*¹; M. Koopman²; Krishan K. Chawla²; J. Bai³; Camden R. Hubbard³; Jinn P. Chu⁴; ¹Arizona State University; ²University of Alabama at Birmingham; ³Oak Ridge National Laboratory; ⁴National Taiwan Ocean University

Small-length scale multilayered structures are attractive materials because of their extremely high strength and flexibility, relative to conventional laminated composites. In this talk we present results on nanolayered laminated composites of Al and SiC. The laminated composites were fabricated by physical vapor deposition (magnetron sputtering) of alternate layers of Al and SiC. The microstructure of the multilayered structures was characterized by scanning and transmission electron microscopy. Residual stresses were characterized by x-ray diffraction using a high-energy x-ray synchrotron source. The mechanical properties of the layered materials were characterized by nanoindentation and tensile testing. The influence of layer thickness on hardness and Young's modulus of individual layers was quantified by nanoindentation. Finite element modeling was conducted to elucidate the stress state under indentation. The important implications of the heterogeneous stress state, during indentation, to measurements of modulus and hardness will be discussed.

11:15 AM

Mechanical Behavior of Severely Deformed NbZr and Ti Using Equal Channel Angular Extrusion (ECAE): *Guney Guven Yapici*¹; Ibrahim Karaman¹; Ralph Dieckmann²; Gagan Singh¹; Hans Maier²; ¹Texas A&M University; ²University of Paderborn

Apart from being technologically important materials for the biomedical industry, NbZr (bcc) and Ti (hcp) are suitable for investigating the deformation mechanisms during severe plastic deformation. Equal channel angular extrusion (ECAE) is applied by extruding bulk billets through two perpendicular channels of equal cross section achieving simple shear in a thin layer at the crossing plane of the channels. Deformation mechanisms of the extruded samples are investigated through extensive TEM analysis exhibiting the microstructure at the nano to micro regime. Post-processing mechanical response of the extruded samples is investigated to reveal the processing-microstructure-property relationships. Series of experiments are conducted with the aim of capturing the yield locus evolution during and after ECAE processing. This enables us to demonstrate the effect of ECAE on the yield surface evolution compared to conventional deformation methods. It will also help in developing accurate hardening models to predict the mechanical properties of severely deformed materials.

11:30 AM

Advanced Nanoparticle-Reinforced Composite Materials in Air-Blast and Vibration Damping Protection: *Liya Bochkareva*¹; ¹University of Sheffield

This paper relates to vibration damping and air-blast protection issues in engineering structures by nanotechnology-based solutions through the utilization of nanomaterials that dissipate a substantial fraction of the vibration energy that they receive. The mechanisms involved in such materials are analyzed and the relevance to damping is identified via both computational and experimental benchmarks. Computational work is concentrated on hierarchical multiscale modelling of damping/friction behavior as a function of frequency, amplitude and temperature. The novel concept of nanoparticle-based damping technology shows that a molecule-level mechanism can considerably enhance vibration damping and dynamic of aerospace components (fan blades) via enhanced energy dissipation because of large surface-to-volume aspects in nanoparticle-reinforced composite material, large damping energy sources for friction and slip-stick motion at interfaces of matrix and nanoparticle. The materials offer the potential to further reduce the mass and dimension, increase performance, and reduce vibrations in wide-ranging applications in areas of transportation.

11:45 AM

Mechanical Behavior of Mg-Alloys Subjected to Severe Plastic Deformation: Grigoreta M. Stoica¹; *Liang Wu*¹; Hao Hsiang Liao¹; Andrew E. Payzant²; Sean R. Agnew³; John E. Spruiell¹; Lijia Chen⁴; Peter K. Liaw¹; ¹University of Tennessee; ²Oak Ridge National Laboratory; ³University of Virginia; ⁴Shenyang University of Technology

The influence of severe plastic deformation [SPD] on the mechanical behavior of Mg alloys, ZK60 and AZ31, was investigated under monotonic and cyclic loading. The extruded material was severely deformed through equal-channel-angular processing [ECAP] at 260°C and 200°C, respectively, or axially compressed at room and intermediate temperatures. Some microstructural-characterization techniques, including X-ray diffraction [XRD], the optical and electronic scanning microscopy [SEM] were used to study the influence of SPD on the grain sizes refinement, the elastic-microstrains, and textures evolution. The tensile properties and fatigue lives were found to be dependent on preferential orientations of the grains. The microstrain build up in the samples deformed by compression at room temperature has a detrimental effect on mechanical behavior, relative to the ECAP-ed samples. On the other hand, the microstrain relaxation in ECAP-ed samples indicates that the recovery/recrystallization processes compete with the plastic deformation, enhancing the ductility.

Fatigue and Fracture of Traditional and Advanced Materials: A Symposium in Honor of Art McEvily's 80th Birthday: Fatigue and Fracture III

Sponsored by: The Minerals, Metals and Materials Society, TMS Structural Materials Division, TMS/ASM: Mechanical Behavior of Materials Committee

Program Organizers: Leon L. Shaw, University of Connecticut; James M. Larsen, U.S. Air Force; Peter K. Liaw, University of Tennessee; Masahiro Endo, Fukuoka University

Tuesday AM Room: 216
March 14, 2006 Location: Henry B. Gonzalez Convention Ctr.

Session Chairs: James M. Larsen, U.S. Air Force; Winston Oluwole Soboyejo, Princeton University

8:30 AM Invited

Fatigue Crack Nucleation in Metals and Alloys: Morris E. Fine¹; *Shrikant P. Bhat*²; ¹Northwestern University; ²Mittal Steel

Over the years, many theories and models have been proposed to explain how fatigue cracks nucleate over many cycles of applied load (strain). In the model originally proposed by Mura and coworkers, fatigue crack initiation is considered a nucleation process in that an energy barrier due to the formation of new surfaces must be overcome. Therefore, by minimizing the Gibbs free energy change, the critical number of cycles required to nucleate fatigue cracks can be estimated. In a previous contribution, the present authors demonstrated the validity of this model with data from commercial purity iron and a high strength low alloy steel. The present paper extends these concepts to other metals and alloys and in particular, explores the applicability to fcc metals, metal-metal oxide composites, influence of temperature and environment, and to subsurface nucleation of fatigue cracks.

8:55 AM

Mechanics Based Probability Modeling for Minimum Life Estimation of S-N Data: *D. Gary Harlow*¹; ¹Lehigh University

Fatigue life prediction has historically been a challenging problem analytically as well as experimentally. Current analyses are predominantly statistical and do not adequately reflect long-term operating conditions. Recent observations of giga cycle fatigue have suggested that there may be multiple mechanisms for nucleation and growth of fatigue cracks. One has been associated with surface damage and another with internal inclusions. These mechanisms make accurate estimation and prediction of the stress dependent minimum life difficult. A simple crack growth based probability model is used to account for plausible, readily identifiable con-

tributors to the observed minimum life, e.g., manufacturing and material properties. A connection between the proposed crack growth model and S-N response is shown. The effect on the minimum life from the contributions of multiple damage mechanisms is examined. The methodology is demonstrated through the analysis of two extensive sets of S-N data, 2024 aluminum alloy and SUJ2 bearing steel.

9:20 AM

Microstructure-Based Modeling of Crack Growth in Particle Reinforced Composites: *Adarsh Ayyar*¹; Nikhilesh Chawla¹; ¹Arizona State University

The crack growth behavior of particle reinforced composites is determined by several factors, such as volume fraction, particle size, and particle morphology. Numerical modeling, such as finite element modeling, can be used to simulate and understand crack growth behavior. In SiC particle reinforced Al matrix composites, for example, it is customary to represent the complex morphology of the SiC particles with simple shapes such as circles and ellipses. Because crack growth is significantly influenced by the morphology of the reinforcement particles, such approximations may lead to erroneous results. In this paper, the effect of SiC particle morphology on crack growth was studied. Two dimensional linear elastic fracture mechanics principles were used to propagate the crack and obtain the local stress intensity values. In addition, the effect of particle fracture on crack growth was also studied. Results from these analyses are compared with experimental observations of crack growth in these systems.

9:45 AM

A Physics-Based Creep-Fatigue Crack Growth Model for a Ni-Base Superalloy: Vikram Bhamidipati¹; *Robert Tryon*¹; ¹Vextec Corporation

A physics-based creep-fatigue intergranular crack growth model is proposed for a Ni-base superalloy at elevated temperature. An intergranular crack nucleation model under fatigue and a short crack growth model are described. The creep short crack model is two dimensional and captures changes in microstructural properties like grain size, defect spacing and grain boundary orientations as the crack grows. A HRR-type stress field solution is assumed to hold good in the region ahead of the crack tip. The principle damage mechanisms include cavity nucleation, growth and coalescence and grain boundary sliding.

10:10 AM Break

10:25 AM Invited

The Effect of Seismic Loading on the Fatigue Strength of Welded Joint: *Yoshiyuki Kondo*¹; Kazuhiko Okuya²; ¹Kyushu University; ²Kyushu Polytechnic College

Earthquakes sometimes give damages to steel structures. The structures which were not seriously damaged are still used after earthquake. The fatigue strength of these structures, however, might have been decreased due to the large cyclic loadings during an earthquake. In order to clarify the effect of seismic loading on the fatigue strength of welded joint, high cycle fatigue test after large straining in gross plasticity was performed. The cyclic application of large strain substantially decreased the fatigue strength. The large straining initiated a short crack at weld toe in low cycle fatigue manner, which acted as a trigger for the high cycle fatigue after seismic loading. The reduction of fatigue limit depended on the crack size. Although the short crack was formed by large straining in gross plasticity, the high cycle fatigue limit of short-cracked welded joint after large straining was determined by the ΔK_{th} considering short crack effect.

10:50 AM

Characterization of the Fatigue Crack Initiation Process in an $\alpha + \beta$ Titanium Alloy: *Christopher Szczepanski*¹; Sushant K. Jha²; James M. Larsen³; J. Wayne Jones¹; ¹University of Michigan; ²Universal Technology Corporation; ³AFRL/MLLMN

Low stress, long lifetime fatigue behavior of the alpha-beta titanium alloy, Ti-6Al-2Sn-4Zr-6Mo, has been characterized using ultrasonic fatigue. Fatigue lifetimes in the range of 10^6 - 10^9 for load ratios of $R=0.05$ were determined at 20 kHz and significant scatter, as much as three orders of magnitude, in the fatigue lifetimes was observed for this material. Fractographic analysis revealed that initiation occurred at one or more

primary α grains. Across specimens, the crack initiation region varied in diameter from approximately 10 to 70 μm . No correlation between life-time and size of the crack initiating region was observed, suggesting that crack initiation may play a significant role in very long fatigue lifetimes. Detailed microstructural analyses of crack initiation regions and observations of the microstructural dependence of crack initiation from ultrafast laser machined micronotches will be described in terms of the mechanisms of crack initiation in the very high cycle lifetime regime.

11:15 AM Invited

On the History of Fatigue Life Diagrams: From August Woehler till Today: *Hael Mughrabi*¹; ¹University Erlangen-Nuernberg

Since August Woehler performed the first systematic fatigue tests one and a half centuries ago, the S-N curve (with a fatigue limit) has been the most widely used fatigue life diagram, extending, typically, to 10 million cycles. Interestingly enough, August Woehler never published a fatigue life diagram but only tables. Since then, different forms of fatigue life diagrams, based on strain rather than on stress, such as the Coffin-Manson plot or the total strain fatigue life diagram (which frequently exhibit a plastic strain fatigue limit), have become equally important. Through the cyclic stress-strain curve, these different types of fatigue life diagrams can be mutually transformed into one another. Currently, fatigue life diagrams extending into the ultrahigh cycle regime (more than a billion cycles) are of particular interest. These developments will be reviewed.

Fatigue and Fracture of Traditional and Advanced Materials: A Symposium in Honor of Art McEvily's 80th Birthday: Fatigue and Fracture IV

Sponsored by: The Minerals, Metals and Materials Society, TMS Structural Materials Division, TMS/ASM: Mechanical Behavior of Materials Committee

Program Organizers: Leon L. Shaw, University of Connecticut; James M. Larsen, U.S. Air Force; Peter K. Liaw, University of Tennessee; Masahiro Endo, Fukuoka University

Tuesday AM Room: 215
March 14, 2006 Location: Henry B. Gonzalez Convention Ctr.

Session Chairs: Morris E. Fine, Northwestern University; Reinhold H. Dauskardt, Stanford University

8:30 AM Invited

Mechanisms of Fatigue Damage Formation and Evolution in Zr-Based Bulk Metallic Glass: *Reinhold Dauskardt*¹; Peter Hess¹; Brian Menzel¹; ¹Stanford University

The mechanisms of fatigue damage initiation and evolution in bulk metallic glasses are not well understood, limiting their use in structural applications. We present experimental and computational studies of initiation of fatigue damage obtained from stress-life experiments, and the growth of fatigue cracks measured under stable and transient cyclic loading conditions. The early stages of damage initiation and propagation resulting in the anomalously low reported fatigue endurance limits are discussed. To further elucidate the underlying shear processes, simulations of the effects of cyclic loading on the nature and propagation of shear bands was conducted using molecular dynamics computational models of a multi-component Leonard-Jones solid. The formation of shear bands and their evolution under the influence of alternating loads will be described. The evolution of fatigue damage was experimentally characterized in terms of both "small" and "long" fatigue crack growth rate behavior to elucidate the detailed mechanism of fatigue crack growth.

8:55 AM

Effect of Age-Hardening Condition on HCF Performance of Mechanically Surface Treated Al 2024: Tomasz Ludian¹; *Wagner Lothar*¹; ¹Clausthal University of Technology

The present work was aimed at evaluating the effects of shot peening and roller-burnishing on the fatigue performance of the well known age-hardening aircraft aluminium alloy Al 2024 (T6). Shot peening to full coverage was performed using spherically shot (SCCW14) with an aver-

age shot size of 0.36 mm and an Almen intensity of 0.20 mmA. Roller-burnishing was done using a conventional lathe and a hydraulically driven device with a 3 mm diameter hard metal ball pressed onto the specimen surface at a constant rolling force. After applying the various mechanical surface treatments, the changes in the surface and near-surface layer properties such as surface topography, micro-hardness and residual stress-depth profiles were determined. In addition to the mechanically surface treated specimens, electrolytically polished conditions were used to serve as reference. The fatigue results will be interpreted in terms of the process-induced changes in the resistances to crack nucleation and micro-crack growth.

9:20 AM

Effect of Localized Precorrosion on Initial Fatigue Damage Process in Al 7075-T6511: *Sang-Shik Kim*¹; James Burns²; Richard P. Gangloff²; ¹Gyeongsang National University; ²University of Virginia

In the present study, detailed micrographic and fractographic analyses were conducted on Al 7075-T6511, pre-corroded on L-S and L-T plane, respectively, in EXCO solution for 6 h, and fatigued at σ_{max} of 150 and 240 MPa (R=0.1), respectively, in a controlled-moist environment with intermittent marker band cycling. The AFGROW fracture mechanics based program was used to predict the corrosion modified (CM)-equivalent initial crack size (EIFS), and the predicted CM-EIFS was compared with the measured CM-EIFS. The fatigue cracks in pre-corroded Al 7075-T6511 specimen were found to be initiated from the semi-elliptical shaped pit clusters with low a/c ratios. The AFGROW modeling of the fatigue life of pre-corroded Al 7075-T6511 specimens could provide reasonable CM-EIFS and full S-N relationships with account taken for varying a/c ratio of initial semi-elliptical surface crack during fatigue crack propagation and the initiation cycles, Ni, required to form a sharp crack from the precorrosion damage.

9:45 AM

Density of Fatigue Weakest-Links in an Al-Li Alloy: *Tongguang Zhai*¹; ¹University of Kentucky

A hot cross-rolled Al-Li 8090 alloy was fatigued in different orientations at 20 Hz, room temperature, R=0.1, in air, using a self-aligning four-point bend rig. It was found that the number of cracks initiated on the sample surface varied with the maximum stress level applied in the fatigue tests and was a Weibull distribution function of this stress. Such a Weibull function represented the distribution of the strength of fatigue weakest-links (i.e., the preferred sites for crack initiation) under certain applied stress level in this alloy. This weakest-link strength distribution and the density of the fatigue weakest-links can be used as a material property. It was found that they were different when measured in different orientations in the 8090 alloy.

10:10 AM Break

10:25 AM Invited

Fatigue-Property Enhancements by Glass-Forming Metallic Films: *F. X. Liu*¹; C. L. Chiang²; D. Smith¹; J. P. Chu²; P. Rack¹; P. K. Liaw¹; ¹University of Tennessee; ²National Taiwan Ocean University

Zr- and Cu-based glass-forming metallic films were deposited onto different substrates by magnetron sputtering. Four-point-bending fatigue tests were conducted on these coated materials. It was shown that the fatigue life and the fatigue-endurance limit of the materials could be considerably improved, depending on the films, the substrates, and the maximum applied stresses. Fractographic studies indicated the good adhesion between the film and the substrate. Surface-roughness measurements showed the improved surface conditions after film deposition. Residual stresses were determined by the curvature measurement. Analyses showed that the good adhesion of the film to the substrate, the improved surface conditions, and the compressive residual stress were the main reasons for the enhancement of the fatigue properties. The high strength and moderate bending ductility of the glass-forming metallic films might also play beneficial roles, revealing the deposition of the films as a novel and effective method to improve fatigue properties of structural materials.

10:50 AM

Fatigue and Fracture of LIGA Ni MEMS Thin Films: *Winston O. Soboyejo*¹; ¹Princeton University

This paper presents the results of an experimental study of fracture and fatigue in LIGA Ni MEMS thin films. The mechanisms of crack nucleation and crack growth are elucidated under monotonic and cyclic loading. In-situ crack-tip strain measurements are also used to identify the extent to which traditional crack-tip fields can be used to characterize the crack driving forces. The results suggest that the crack-tip fields for LIGA Ni films should include a plasticity length scale to account for strain gradient plasticity effects. The fracture resistance curves and fatigue crack growth rate data are presented along with the underlying fatigue and fracture modes. These reveal that the mechanisms of crack growth behavior are influenced by stress state and microstructure effects. The nucleation of fatigue cracks is shown to be dominated by persistent slip band (PSB) induced oxide thickening mechanisms that give rise to surface/near-surface crack formation.

11:15 AM

Investigation of Fatigue in Nano-Layered Cu/Nb Thin Films: *Yun-Che Wang*¹; John Greg Swadener¹; Tobias Hoehbauer¹; Tim Darling¹; Richard Hoagland¹; Amit Misra¹; ¹Los Alamos National Laboratory

It has been shown nano-layered thin films exhibit ultra-high yield strength and large plastic deformation without formation of dislocation cell structures. Fatigue properties of these films are of interest. Multilayered Cu/Nb thin films with a nano-size individual layer thickness were manufactured via sputter deposition. We developed a novel experimental method for fatigue measurements with $R = -1$. Our experimental method employed a bimorph piezo actuator to drive a cantilever beam sample in a moderate vacuum environment. A feedback system using fiber optic measured displacement was utilized, and stress was determined. Resonant frequency shifts and SEM images of fatigued samples were studied to determine fatigue crack propagation. We obtained S-N curves for thin films with various individual layer thicknesses. By systematically studying the S-N curves versus individual layer thickness and comparing results from bulk materials, the effects of nano-size layers on fatigue endurance in thin films were obtained.

General Abstracts: Extraction and Processing Division: Copper and Nickel Hydrometallurgy

Sponsored by: The Minerals, Metals and Materials Society, TMS Extraction and Processing Division, TMS: Aqueous Processing Committee, TMS: Copper and Nickel and Cobalt Committee, TMS: Lead and Zinc Committee, TMS: Precious Metals Committee, TMS: Process Fundamentals Committee, TMS: Process Modeling Analysis and Control Committee, TMS: Pyrometallurgy Committee, TMS: Recycling Committee, TMS: Waste Treatment and Minimization Committee, TMS: Materials Characterization Committee
Program Organizers: Thomas P. Battle, DuPont Company; Michael L. Free, University of Utah; Boyd R. Davis, Kingston Process Metallurgy

Tuesday AM
March 14, 2006

Room: 203A
Location: Henry B. Gonzalez Convention Ctr.

Session Chair: Corby G. Anderson, Montana Tech of the University of Montana

8:30 AM

Fundamental Kinetics of the Ferrous Regeneration for Alternate Anode Reaction Technology in Copper Hydrometallurgy: *Emily A. Sarver*¹; Maurice Fuerstenau²; Scot Sandoval³; Gregory Adel¹; ¹Virginia Polytechnic Institute and State University; ²University of Nevada, Reno; ³Phelps Dodge Mining Company

The Fe(II) regeneration process is an important aspect of Alternate Anode Reaction Technology (AART) using a Fe(II)/Fe(III)-SO₂ (FFS) for copper hydrometallurgy. The process is basically Fe(III) reduction by SO_{2(aq)}, which is catalyzed by activated carbon particles. For the current work, experiments have been conducted to examine the fundamental kinetics of the process, including the primary reaction mechanism and the effects of

four variable factors – carbon particle size, flow rate, and initial Fe(III) and SO₂ concentrations – on the Fe(II) regeneration rate. As expected, the regeneration reaction is mass transfer-controlled, and the rate is limited by the diffusivity of Fe(III), which is 1.1×10^{-7} cm²/s under the tested conditions. Carbon particle size and initial Fe(III) are the most influential factors under the conditions tested. Additionally, initial SO₂ concentration has been determined to be insignificant to the reaction rate, and flow rate affects the reaction rate via its effects on diffusivity.

8:55 AM

Development of a Hydrometallurgical Process for Copper Concentrate Treatment by Sumitomo Metal Mining: Masaki Imamura¹; Kenji Takeda¹; Koji Ando¹; Noriyuki Nagase¹; Yasuo Ojima¹; ¹Sumitomo Metal Mining

A novel hydrometallurgical process for copper concentrate treatment has been developed in Niihama Research Laboratories of Sumitomo Metal Mining Co., Ltd. The process has numerous advantages with respect to operational and environmental aspects. For example, copper is leached effectively from chalcopyrite concentrates by chlorine gas under atmospheric pressure. Then copper in the leach solution is separated from iron and silver by solvent extraction and electrowinning to produce highly pure copper metal without further purification. Iron metal can be produced by electrowinning from the purified raffinate to avoid generating a large volume of goethite or hematite, which is a solid waste for iron rejection in common hydrometallurgical processes. This process also enables significantly efficient recovery of precious metals. Results in batch and continuous testworks are presented in the paper.

9:20 AM

Effect of Additives on the Electrolytic Processing of Dilute Effluents Containing Copper: Ran Ding¹; Daniel Chapman¹; James W. Evans¹; Fiona M. Doyle¹; ¹University of California

The use of copper as the interconnect material in integrated circuits has resulted in the generation of increasingly complex copper-bearing effluents in the semiconductor industry. Those effluents associated with copper electrodeposition or electroless deposition are usually concentrated, with extreme pH. Organic additives are present to allow superfilling of trenches and control the deposit quality. Effluents from chemical mechanical planarization usually contain only trace levels of copper, but may contain significant amounts of complexing agents. In principle, electrodeposition, especially with porous and particulate electrodes, is an attractive means for recovering copper from these effluents, to allow either recycling of the process streams or safe discharge. However, the effect that additives can have on the kinetics of electrodeposition has important ramifications on cell design. Here we report studies on the effect of additives such as polyethylene glycol and glycine, and the sensitivity of their effects to the presence of other electrolyte components.

9:45 AM Break

10:00 AM

The Effect of Additives on Morphology of Copper Electrodeposits from Halide Media: *Aphichart Rodchanarowan*¹; Michael L. Free¹; ¹University of Utah

The effect of organic additives on surface morphology of copper electrodeposit from halide media (0.10 mol/L CuCl, 4.0 mol/L NaCl, and 0.010 mol/L HCl) was studied under current controlled conditions. The copper was electrodeposited on a rotating disc electrode made from 99.999% pure copper. Surface roughness was characterized by a series of CCD camera images combined with computer analysis of the images. The effect of additives was analyzed for C10 TAB, Triton X 100, thiourea, polyethylene glycol, and gelatin. It was found that gelatin gave more uniform deposits compared to those obtained without any additives. Surface roughness evaluations were carried out by varying electrodeposition time, current density, and concentration for gelatin. The addition of gelatin helped to achieve smooth electrodeposit at long deposition time. The surface roughness in solution containing gelatin slightly increased with the increase in i/L ratio. Gelatin concentration did not affect the change in the surface roughness.

10:25 AM

Electrodeposition of Copper from Halide Media: *Ravindra J. Bhide*¹; Michael L. Free¹; ¹University of Utah

The effect of mass transport on the surface roughness of copper electrodeposits, obtained from a bath containing 0.1 mol/L CuCl₂, 4.0 mol/L NaCl and 0.01 mol/L HCl was studied under controlled current conditions. Copper was electrodeposited on a rotating disc electrode made of 99.999% pure copper. Surface roughness was characterized using CCD camera images combined with their computer analysis. The roughness of the electrodeposits was examined as a function of rotational speed of the electrode, current density and pulsed current transients. It was found that the roughness of the deposit decreased with increase in rotational speed of the electrode. Applied current transients also affected the morphology of electrodeposits. For current controlled transients, lower i/i_L values gave electrodeposits with lower surface roughness where i is applied current and i_L is the limiting current density for given experimental conditions. Pulsing also gave smoother electrodeposits compared to those obtained under direct current conditions.

10:50 AM

High Aspect Ratio Nickel Structures Fabricated by Electrochemical Replication of Hydrofluoric Acid Etched Silicon: *Xi Zhang*¹; K. N. Tu¹; ¹University of California, Los Angeles

A technique for fabricating free-standing high-aspect-ratio Ni structures has been developed using wet Si processing. Si (100) was initially etched in HF solution to form macropores with micron-sized diameter. The aspect ratio can exceed 200:1. Immersed in aqueous Ni solution containing no reducing agent but fluoride, metallic Ni was rapidly reduced onto the sidewalls by oxidizing the Si. With longer duration, the Si sidewalls were gradually converted to become total Ni while the deep macropore structure was still maintained. Electron microscopic analyses reveals that fluoride in solution helps dissolve the fully oxidized Si and leave the Ni deposits on the sidewall loosely arranged during the process, which can explain the replication. It is known that close-packed sub-micron Si pillars can be formed by oxidizing and subsequent etching of the macropore sidewalls. Treated in the same Ni solution, high-aspect-ratio Ni pillars were correspondingly emerged by replicating the original Si structure.

General Abstracts: Materials Processing and Manufacturing Division: Novel Processing Methods

Sponsored by: The Minerals, Metals and Materials Society, TMS Materials Processing and Manufacturing Division, TMS; Nanomechanical Materials Behavior Committee, TMS/ASM; Phase Transformations Committee, TMS; Powder Materials Committee, TMS; Process Modeling Analysis and Control Committee, TMS; Shaping and Forming Committee, TMS; Solidification Committee, TMS; Surface Engineering Committee, TMS; Global Innovations Committee, TMS/ASM; Computational Materials Science and Engineering Committee
Program Organizers: Thomas R. Bieler, Michigan State University; Ralph E. Napolitano, Iowa State University; Fernand D. Marquis, South Dakota School of Mines and Technology

Tuesday AM Room: 211
March 14, 2006 Location: Henry B. Gonzalez Convention Ctr.

Session Chairs: Thomas R. Bieler, Michigan State University; Robert E. Barber, Texas A&M University

8:30 AM

Spectral Methods for Capturing Crystallographic Texture Evolution during Large Plastic Strains in HCP Metals: *Xianping Wu*¹; Surya Kalidindi¹; ¹Drexel University

Recently Kalidindi et al. [Acta Materialia 2005; 53: 3613-3623] explored the novel concept for capturing and simulating crystallographic texture evolution during large plastic strains on metals using an efficient spectral representation of the orientation distribution function. The good prediction and efficiency of this new method was evaluated by using fcc

metals in the same publication. In this paper, the similar concept was extended to simulate the crystallographic texture evolution at large deformation on hcp metals where both slip and deformation twinning are plastic deformation modes. Good predictions of the overall texture evolution in a number of different deformation paths were obtained using this newly developed framework.

8:50 AM

Electroless Copper Plating on Graphite Powder Surface: *Liu Wei*¹; Guangchun Yao¹; Yihan Liu¹; ¹Northeastern University

In order to solve the wetting quantity of graphite/copper interface and improve the capability of graphite/copper composite material, we adopted bluestone as main salt, zinc as reductant to plate copper on graphite powder surface. The results indicate that there is only copper but zinc in the electroless plating and the electroless plating is hard to be oxidated. This paper emphasize studied the factors such as the pro-treat process, main salt, reductant, temperature, loading capacity and reaction time that effect the electroless plating in order to confirm the optimizing process. Through the optimizing process without additive the copper-coated graphite assumes rose color, and the electroless plating unites tightly with graphite power by analysis of SEM technique.

9:10 AM

Modeling of Deformation and Bonding of Composite Particle during Cold-Spray Deposition: *Ivica Smid*¹; Gaurav Aggarwal¹; Albert Segall¹; ¹Pennsylvania State University

Cold-gas spray is a low temperature coating process by which coatings can be produced without significant heating of substrate or powder, therefore permitting the use of thermally vulnerable lubricants. Nickel, nickel coated boron nitride and molybdenum disulphide, and granulated nickel-solid lube mixes were cold-spray deposited on Ti-6Al-4V substrates. The thermo-mechanical response has been modeled using finite elements. This allowed the estimation of the maximum impact pressures, deformation rates, and deformation kinetics during the impact. The velocity of the impacting particles was taken into account by applying a transient force along the particle equator; the resulting strains were converted to temperature. Local heating and deformation were experimentally validated. The modeling results were assessed with respect to thickness of composite particle encapsulation, critical particle velocity, bonding success and its quality, and deposition efficiency. On the basis of this criterion, optimum particle design and the respective critical velocities can be predicted.

9:30 AM

Non-Isothermal Shearing in Friction Stir Welding: *Patricio F. Mendez*¹; Thomas J. Lienert²; ¹Colorado School of Mines; ²Los Alamos National Laboratory

A coupled model of the deformation and heat transfer in Friction Stir Welding (FSW) is presented and general expressions are obtained. These expressions are useful to understand FSW in well known alloys such as aluminum-base ones and extrapolate that understanding to higher temperature alloys. The methodology consists of determining asymptotic regimes from which to generate scaling laws. In the analysis of this problem, a threadless pin is considered and the effects of the pin and shoulder are separated. The thickness, temperature, and shear rate of the region surrounding the rotating pin are predicted using an ordering analysis inspired in the boundary layer analysis in fluid mechanics. The model presented helps understand the torque, temperatures, and deformation history of the material near the rotating pin, but it does not address the mechanical mixing occurring behind the pin. Predictions of torque, temperature, and shear region thickness agree with experiments.

9:50 AM Invited

Friction Stir Processing TiB₂ into the Surface of Class 40 Grey Cast Iron to Improve the Wear Resistance: *Uma Ramasubramanian*¹; William J. Arbogast¹; Glenn J. Grant²; Glen A. Stone³; ¹Advanced Material Processing Center; ²Pacific Northwest National Laboratory; ³South Dakota School of Mines and Technology

The objective of this work is to use Friction Stir Processing (FSP) to improve the wear resistance of class 40 grey cast iron. FSP is used to process TiB₂ particulate into the surface of the cast iron to produce a wear resistant layer. The optimization of the process was achieved by placing TiB₂ powders on the surface of a cast iron plate then covering the powder

with a 0.080 in thick mild steel sheet and subsequently plunging and translating a stir tool across the surface. Microstructural characterization of the optimized welds was carried out using optical and SEM. Comparison before and after the process show significant wear and deformation of the PCBN step spiral pin tool. Data on the wear characteristics and friction coefficient of Friction Stir Processed, TiB₂ reinforced cast iron will also be presented.

10:10 AM Break

10:30 AM

Performance Improvement with Advanced Materials at High Temperatures in the Hot Zone Components of Gas Turbines: *Ramarao Adapa*¹; D. N. Reddy²; K. V. Sharma³; ¹VNR VJIE; ²Osmania University; ³Jawaharlal Nehru Technological University

Gas Turbine (G.T) is basically a prime mover for power generation. To get enhanced performances, this Product Research work with F – Technology is presented which means to increase the Fire Point which in turns to increase the Turbine Inlet Temperature (TIT) there by Heat Energy (HE) is increased in the combustion chambers and converts increased Kinetic Energy (K.E) to Mechanical Energy (M.E). To withstand the very high temperatures in the hot zone compartments in the G.T, the advanced materials like Hastalloy in combustion chambers, FSX 414 for Nozzles, IN 738 for Turbine buckets, ASTM A336 and AISI 316 with plasma coating for shrouds and Ni Cr Mo V forged steels for Rotor discs and for guide blades in the stator 403-SS with Ni Cd Coating are preferred. The improved performance are recorded and presented with the practical results.

10:50 AM

An Electroplating Technique to Obtain Copper Coating on Carbon Fibers: *Zhuokun Cao*¹; Yihan Liu¹; Guangchun Yao¹; ¹Northeastern University of China

Carbon fibers coated with copper are widely using in many fields because of its special qualities. In this study, carbon fibers were pretreated in both air at high temperature and HNO₃, and the change of the fibers' surface was detected by X-ray photoelectron spectroscopy (XPS). A simple electroplating technique in a sulfate bath was used. Through changing the concentration of H₂SO₄ and CuSO₄ and adding in addition agents, uniform and smooth copper coating were obtained on carbon fibers. And the effects of H₂SO₄ and addition agents were discussed. Different thickness of copper coating was also obtained by change the compositions of the solution and technological parameters. And the copper coating was characterized by scanning electron microscope (SEM) and X-ray diffraction (XRD).

General Abstracts: Structural Materials Division: Advances in Steel

Sponsored by: The Minerals, Metals and Materials Society, TMS Structural Materials Division, TMS: Alloy Phases Committee, TMS: Biomaterials Committee, TMS: Chemistry and Physics of Materials Committee, TMS/ASM: Composite Materials Committee, TMS/ASM: Corrosion and Environmental Effects Committee, TMS: High Temperature Alloys Committee, TMS/ASM: Mechanical Behavior of Materials Committee, TMS/ASM: Nuclear Materials Committee, TMS: Product Metallurgy and Applications Committee, TMS: Refractory Metals Committee, TMS: Advanced Characterization, Testing, and Simulation Committee, TMS: Superconducting and Magnetic Materials Committee, TMS: Titanium Committee

Program Organizers: Rollie E. Dutton, U.S. Air Force; Ellen K. Cerreta, Los Alamos National Laboratory; Dennis M. Dimiduk, U.S. Air Force

Tuesday AM
March 14, 2006

Room: 218
Location: Henry B. Gonzalez Convention Ctr.

Session Chair: Warren M. Garrison, Carnegie Mellon University

8:30 AM

Compact Strip Production - Challenges and Solutions: *Carl-Peter Reip*¹; Tilmann Böcher¹; Rolf Hagmann¹; Wolfgang Hennig¹; Joachim Ohlert¹; ¹SMS Demag Aktiengesellschaft

It has been particularly in recent years that owners of CSP plants have made considerable efforts to significantly expand their product range in response to changing market demands. In addition to steel grades, the focus now is also on ensuring the product quality in terms of microstructure, mechanical properties and strip surface, as well as the reproducibility of these parameters. Much attention has been paid to the introduction of the melting and casting technology and the pass-schedule design and cooling strategy for materials such as dual-phase steel, TRIP and API grades up to X80. For the large-scale production of TWIP, the metallurgical basis and process parameters have been worked out for the CSP technology and an initial test production prepared. New findings have been processed to achieve the best surface quality by means of a change in the oscillation strategy, casting powder and cleaning of the thin slabs.

8:55 AM

A Discussion of the Spacing of Inclusions and the Spacing of Inclusion Nucleated Voids on the Fracture Surfaces of Ultra-High Strength Steels: *Warren M. Garrison*¹; ¹Carnegie Mellon University

For some steels increasing the inclusion spacing at constant inclusion volume fraction is believed to increase the toughness. This work considers a series of low alloy medium carbon martensitic steels in which high toughness has been achieved by increasing the inclusion spacing. The objectives of this work were to determine the spacing of inclusion nucleated voids on the fracture surface and to determine how this spacing related to the spacing of the inclusions in the volume and to assess the degree to which inclusions were actually retained on the fracture surface. While the spacing of the inclusion nucleated voids is comparable to the spacing of the inclusions in the volume the spacing of the inclusions on the fracture surface is much greater than would be observed if half of the inclusion nucleated voids contained inclusions. This suggests that not all inclusions are retained on the fracture surface.

9:20 AM

Dry Sliding Friction and Wear in High Nitrogen Austenitic 18Cr-18Mn-2Mo-0.9N Steel: *Yong-Suk Kim*¹; Seung Duk Kim¹; Sung-Joon Kim²; ¹Kookmin University; ²Korea Institute of Machinery and Materials

Dry sliding friction and wear characteristics of a high nitrogen austenitic 18Cr-18Mn-2Mo-0.9N steel has been investigated at room temperature. Wear tests of the steel were carried out using a pin-on-disk wear tester against AISI 52100 bearing steel balls. Two different heat treatments (solution treatment alone and isothermal aging after solution treatment) were performed on the steel and the effect of the heat treatments on the wear were investigated. The wear rate of the solution-treated steel was low initially, but increased abruptly at loads above a critical value. Wear rates of the isothermally aged specimen were low and increased gradually with the applied load. Worn surfaces, their cross sections, and wear debris of the steel specimens were examined with an SEM. Phases of the wear debris were identified using XRD to explore wear mechanism of the steel. Effects of strain-induced phase transformation and Cr₂N precipitates on the wear were discussed.

9:45 AM

Effect of Water Vapor on Metal Dusting Behavior of Ferrous Alloys: *Aditya Putrevu*¹; Shailendra K. Varma¹; Zuotao Zeng²; K. Natesan²; ¹University of Texas; ²Argonne National Laboratory

The metal dusting behavior of ferrous alloys T22, T91 and 800 in a H₂+CO₂+CO+x.H₂O atmosphere was investigated. The transition from a combination of accelerated metal dusting and/or extensive pitting to delayed metal dusting attack as vapor content in the atmosphere was increased from 2.3% to 23% was observed. Decreasing H₂O content in the gas increases the carbon activity leading to accelerated carbon deposition. While the increased carbon deposition in the low chromium alloys (T22 and T91) leads to rapid surface and mechanical degradation of the alloys, in high chromium alloys it is more localized in the form of pitting (800). XRD, AES, XPS and EDS have been used to characterize the metal dusting products at micro and nanoscale. Optical microscopy, SEM and TEM were used to study the microstructural issues. The role of alloying elements and mechanisms of growth of carbon nanotubes during metal dusting will also be discussed.

10:10 AM Break

10:25 AM

The Effects of Nickel, Chromium and Carbon on the Strength and Toughness of a Martensitic Precipitation Strengthened Stainless Steel: *Warren M. Garrison¹; Aytekin Hitit²; Piyamane Komolwit¹; ¹Carnegie Mellon University; ²Afyon Kocatepe University*

The effects of nickel, chromium and carbon content on the strength and toughness of a martensitic precipitation strengthened stainless steel having a composition (in wt. %) of 0.005C/12Cr/12Co/5Mo/4.5Ni have been investigated. All alloys were solution treated, oil quenched, refrigerated in liquid nitrogen and then aged. Nickel, chromium and small additions of carbon all increase the strength substantially after aging in the range 500°C to 550°C. Also, these additions all increase the room temperature Charpy impact energy. These additions all result in a marked decrease in the martensite start temperature and an increase in the retained austenite content. Fractography suggests that these additions improve the room temperature toughness because the increase in retained austenite content lowers the ductile-to-brittle transition temperature.

10:50 AM

Influence of Microstructural Anisotropy on Shear Localization in 1080 Eutectoid Steel: *Qing Xue¹; George T. Gray¹; ¹Los Alamos National Laboratory*

The influence of microstructural anisotropy on adiabatic shear localization in 1080 rail steel has been studied. A forced shear technique and “hat-shaped” specimens were utilized on a compression split-Hopkinson pressure bar to generate localized deformation. The microstructure was examined using both optical and transmission electron microscopy (TEM). Elongated MnS stringers are observed to be resident within the crystallographically isotropic eutectoid steel. The orientation of these inclusion stringers relative to the shear band direction was found to substantially affect the shear localization behavior. The debonding between the inclusions and the matrix appears to strongly influence the formation of shear bands. The TEM results indicate that the substructure within the shear bands consists of nanoscale subgrains. The fine pearlitic substructure in the steel constrains the dislocation motion and thus increases the propensity of instable deformation.

11:15 AM

On the Correlation of Fracture Toughness and Yield Strength in (15-5PH) Stainless Steel: *Mina Samir Abdelshehid¹; Kosha Mahmodieh¹; Kyle Mori¹; Leo Chen¹; Omar S. Es-Said¹; John Ogren¹; Richard Clark²; ¹Loyola Marymount University; ²College of the Canyons*

Stainless Steel 15-5 PH (UNS number S15500) was thermally exposed and tested for fracture toughness and yield strength. The specimens were received in blank form. They were then austenized to Condition A form (1900°F (+/-25°F) for 1 hour), and then tempered at 925°F (+/-10°F) for 2 hours. 36 samples were machined as round-threaded tensile bars and 18 C(T) (compact tension) specimens for fracture toughness testing. The round tensile bars were tested using a Tinius Olsen frame. The C(T) specimens were analyzed on an MTS hydraulic frame and all had FFC(T) (front-face compact tension) geometry and an L-T (longitudinal-transverse) crack plane orientation. It was found that if the tolerances for austenization and tempering temperatures are not strictly controlled, the K_{IC} value decreases significantly, while the yield strength remains virtually unaltered.

11:40 AM

The Effect of Cobalt Additions on the Strength of a Martensitic Precipitation Strengthened Stainless Steel: *Warren M. Garrison¹; Piyamane Komolwit¹; ¹Carnegie Mellon University*

The effect of cobalt additions of 3, 6, 9 and 12 wt. % cobalt on the strength of a martensitic precipitation strengthened stainless steel having a nominal composition (in wt. %) of 0.005/12Cr/9Co/5Mo/1.5Ni has been investigated. All alloys were solution treated, oil quenched and then refrigerated in liquid nitrogen and then aged. None of the alloys contained retained austenite or delta ferrite. The tensile properties of these alloys have been determined for the as-quenched condition and for aging temperatures from 200°C to 600°C. The aging temperature of peak yield strength was 550°C to 575°C for all of the alloys. Cobalt additions can substantially increase the strength of these materials and the increase in yield strength per wt. % cobalt increases with increasing cobalt content.

At the highest cobalt level yield strengths of over 1800 MPa can be achieved.

Granulation of Molten Materials: Session II

Sponsored by: The Minerals, Metals and Materials Society, TMS Extraction and Processing Division, TMS: Copper and Nickel and Cobalt Committee, TMS: Lead and Zinc Committee, TMS: Pyrometallurgy Committee

Program Organizers: Cameron L. Harris, HG Engineering Ltd; Hani Henein, University of Alberta

Tuesday AM

Room: 7B

March 14, 2006

Location: Henry B. Gonzalez Convention Ctr.

Session Chair: Anthony E. M. Warner, HG Engineering Ltd

8:30 AM **Introductory Comments by Tony Warner**

8:35 AM

Common Granulation System Problems with a Focus on Non-Ferrous Applications: *Art Cooper¹; ¹Carlingview Technologies Ltd.*

Granulation systems are customarily viewed as problem areas in metallurgical operations. The inherent risk of explosion when combining a high temperature melt with water creates a safety hazard. Separation of the granulated material from the quenching medium generally involves equipment that can have significant maintenance and operating costs. Granulation systems' reliability and availability can negatively affect the plant production. Against this background, granulation systems have been treated by design firms and producers as an add-on and a necessary evil. The technology is becoming better understood and solutions to common problems are being found. This paper will discuss typical problems in common systems, and some of the improvements that have been made, with particular reference to non-ferrous applications.

9:00 AM

Atomisation as Solidification Process Alternative from Pyrometallurgy to Hydrometallurgy and as a One Step Process for Flash Furnace Feed: *David Norval¹; ¹Bateman Engineering*

In the Smelting of Ni, Co, Cu and Pt, mattes are a common material that requires granulation of the molten matte and milling of resultant granules for further processing. This route is fine if the material is brittle (friable) which is a property associated with the higher sulphur mattes. For lower sulphur levels, where the matte is less amenable to milling, the costs of the milling increases. This paper will compare water granulation with certain dry granulation processes and the downstream processes required for Hydrometallurgy. It will further introduce and expand on atomisation which offers a further safety benefit in the control of the metal flow into the ‘wet zone’ with the use of a tundish flow control also reducing the conversion from the matte to powder in one fairly straightforward operation.

9:25 AM

The Generation of Mono-Dispersed Granules from Melts: *Hani Henein¹; ¹University of Alberta*

Recent innovations in atomization of melts have occurred in the area of single fluid atomization. Impulse Atomization (IA), one of the single fluid techniques, provides unique capabilities to study different regimes of atomization in a controlled environment. It has been observed that by changing processing variables, a mono-dispersed distribution of droplets above one millimeter in diameter can be produced. This is accomplished through proper characterization of the forces influencing the process. This paper will discuss the approach and illustrate results for various metallic melts.

9:50 AM **Concluding Comments by Hani Henein**

TUESDAY AM

Hume Rothery Symposium: Multi-Component Alloy Thermodynamics: Alloy Thermodynamics I: Experiment and Modeling

Sponsored by: The Minerals, Metals and Materials Society, TMS Electronic, Magnetic, and Photonic Materials Division, TMS: Alloy Phases Committee

Program Organizers: Y. Austin Chang, University of Wisconsin; Rainer Schmid-Fetzer, Clausthal University of Technology; Patrice E. A. Turchi, Lawrence Livermore National Laboratory

Tuesday AM Room: 202A
March 14, 2006 Location: Henry B. Gonzalez Convention Ctr.

Session Chair: Rainer Schmid-Fetzer, Clausthal University of Technology

8:30 AM Invited Phase Modeling and Thermodynamic Simulations in the Y-Si-C-O System: Hans J. Seifert¹; ¹University of Florida

Recent experimental information was used for the thermodynamic phase modeling in the quaternary Y-Si-C-O system and a new dataset with Gibbs free energy descriptions was developed. The dataset can be used for the simulation of complex multi-component, multiphase reactions in the system. The development of yttrium silicate coatings for the oxidation protection of C/SiC-based composites and the liquid phase sintering of SiC with yttria as an additive will be discussed. Besides the liquid and the gas phases, the following binary and ternary solid phases were taken into account: Y₃Si₃, Y₅Si₄, YSi, Y₃Si₅ (α, β), YSi₂ (α, β), γ yttrium carbide, YC₂, Y₂C₃ (α, β), Y₁₅C₁₉ (α, β), Y₂O₃ (α, β), SiC (α, β), SiO₂ (cristobalite, tridymite, quartz), Y₅Si₃C₂, Y₂Si₂O₇ (α, β, γ, δ), Y₂SiO₅ (A, B) and γ-Y₂CO.

9:00 AM Invited Thermodynamic Modeling of Ni-Based Alloys for Superconducting Coated Conductor Tapes: Alexander Pisch¹; Jiasong Wang²; Jean-Louis Jorda²; ¹Institut National Polytechnique de Grenoble/Centre National de la Recherche Scientifique; ²Universite de Savoie

Superconducting coated conductor tapes have a layered structure including a metallic substrate, an oxide buffer layer, the superconducting layer and a cap layer. To get good superconducting properties, the corresponding layer has to be highly textured. This can be achieved by texturing the substrate. A buffer layer is additionally introduced to prevent any reaction between the superconducting material and the metallic substrate. The substrate is a Ni-based alloy and the texture is achieved by rolling. The buffer layer is deposited by classical thin film deposition techniques. Another possibility is to obtain the buffer layer directly by oxidizing a substrate which contains the oxide forming element. In order to control the process, the relevant multi-component phase diagrams and the underlying equilibria have to be known. A thermodynamic modeling of the Ni-Cu-Ce and the Ni-Cu-Y system has been performed based on literature information to evaluate the feasibility of this in-situ oxidation process.

9:30 AM Invited Thermodynamics of the Pt-Modified γ-Ni+γ'-Ni₃Al System and Resulting Implications on the Development of Novel High-Temperature Alloys and Coatings: Brian M. Gleeson¹; Takeshi Izumi¹; Chao Jiang¹; Daniel Sordellet¹; Shigenari Hayashi²; ¹Iowa State University; ²Hokkaido University

This presentation will discuss the role of platinum addition in promoting the formation a highly adherent, slow-growing Al₂O₃ scale on γ'-Ni₃Al+γ-Ni alloys during high-temperature oxidation. It will be shown that this beneficial effect can be primarily ascribed to the fact that platinum is non-reactive and its addition decreases the chemical activity of aluminum in γ+γ' alloys. Related to the latter, Pt partitions almost solely to the Ni sites in the L1₂ crystal structure of γ', which has the effect of increasing the Al:Ni atom fraction on a given crystallographic plane containing both Al and Ni. Moreover, intensive first principles calculations showed that Pt segregation on (100) and (111) surfaces is energetically favorable. The tendency of Pt to surface segregate and to have a Ni-site

preference has the contributing effect of kinetically favoring the formation of Al₂O₃ relative to NiO on the γ' surface.

10:00 AM Break

10:20 AM Invited Contribution to Phase Relationship Study in the Si-Tb-Ti System: Jean-Claude Tedenac¹; Marina Bulanova²; Henri Noel³; Anton Samelyuk²; A. Pudovkina⁴; ¹Laboratoire de Physique de la Matière Condensée; ²I.N. Frantsevich Institute for Problems of Materials Science; ³Laboratoire de Chimie du Solide et Inorganique Moléculaire- UMR-CNRS6511; ⁴National Technical University of Ukraine

The silicon-terbium-titanium phase diagram system is still unknown. It present a double interest: on the titanium rich side possible cold and hot structural materials and on the silicon rich side possible materials of electronics. The problem which limits all these applications is the brittleness of these silicides which limits the structural properties but also the other applications. Constitution of materials in term of microstructure (study of phase diagrams, crystal structure determination of phases), properties of alloys obtained by solidification, heat treatment and powder techniques need to be determined. Concerning the phase stabilities, the only information available in this system is the existence of two ternary compounds – TiTbSi and Tb₂Ti₃Si₄. By using differential thermal analysis, metallography, microprobe and X-ray analysis of some sections of the Ti-Tb-Si system, the phase transformations are determined.

10:50 AM Lattice Monte Carlo Simulations of Y-Ti-O Nanoclusters in Ferritic Alloys: Matthew J. Alinger¹; Brian D. Wirth¹; G. Robert Odette¹; ¹University of California

Lattice-based Monte Carlo (LMC) simulations of the formation and stability of nanometer-scale Y-Ti-O clusters (NC) in ferritic alloys, with a nominal composition in the range of Fe-(14)Cr-(0-1)W-(0.25-1)Ti-(0.1-0.25)Y-(0.15-0.40)O are presented. The LMC simulations use pair bond energies calculated from the mixing enthalpies in a regular-solution thermodynamics model and validated by ab-initio calculations and are performed on a bcc lattice, with oxygen on an octahedral interstitial sublattice. The results show NC structure and composition evolution in terms of temperature and alloy composition, starting from random super-saturated solutions. The resulting precipitate compositions are compared to an extensive experimental database of transmission electron microscopy, small angle neutron scattering, atom probe tomography and positron annihilation spectroscopy. Combined, these results provide atomic-level insight into the NC structure and chemistry and provide a basis for optimizing alloy development as well as understanding the thermal and radiation stability of the NCs.

11:10 AM Thermodynamic Assessment of the Nb-Mo-Si-B System: Yali Li¹; Zhihong Tang¹; Mufit Akinci¹; Matthew J. Kramer¹; ¹Iowa State University

Mo-Si-B system intermetallics have a great potential for high temperature application due to their good oxidation resistance. In order to improve mechanical properties, Nb is considered as a favorable addition because of excellent strength of Niobium silicides based alloys and the complete solid solution between Mo and Nb. A thermodynamic description of Mo-Nb-Si-B quaternary system is assessed to help design alloy composition with CALPHAD method using Thermo-Calc. First, a thermodynamic description for Nb-Si-B ternary system is assessed using all the existing phase diagram and experimental data. Then, the Mo-Nb-B and Mo-Nb-Si systems are developed with the similar method. Finally, the Nb-Mo-Si-B quaternary system is critically optimized by extrapolating thermodynamic data of four constituent ternary systems. Comparison between experimental phase equilibria data and the predictions based on the assessed data is discussed.

11:30 AM Solute-Solvent Interactions in fcc-Ni: Tao Wang¹; Long-Qing Chen¹; Zi-Kui Liu¹; ¹Pennsylvania State University

The effect of solutes on the structural and thermodynamic properties of an alloy is determined by the solute-solvent interactions. In this work, we used first-principles approach to study the effects of various solute

atoms (Al, Co, Cr, Hf, Mo, Nb, Re, Ru, Ta, Ti and W) on fcc-Ni. The partial formation energy as well as the lattice distortions (macroscopic and local) of different solutes were calculated and compared with experimental data in literature. By analyzing the charge density distributions around the solute atoms, the effects of atomic size, electronic interaction, and magnetic spin direction on lattice distortion were discussed. By neglecting the interactions between different solute atoms, the formation energy and the lattice parameters in multi-component Ni-base superalloys were predicted using a phenomenological model. A comparison of predicted results with available experimental measurements shows and good agreements at relatively low solute concentrations.

Lead Free Solder Implementation: Reliability, Alloy Development, and New Technology: Interfacial Reactions and Role of Intermetallics

Sponsored by: The Minerals, Metals and Materials Society, TMS Electronic, Magnetic, and Photonic Materials Division, TMS: Electronic Packaging and Interconnection Materials Committee
Program Organizers: Nikhilesh Chawla, Arizona State University; Srinivas Chada, Medtronic; Sung K. Kang, IBM Corporation; Kwang-Lung Lin, National Cheng Kung University; James Lucas, Michigan State University; Laura J. Turbini, University of Toronto

Tuesday AM Room: 214A
March 14, 2006 Location: Henry B. Gonzalez Convention Ctr.

Session Chairs: C. R. Kao, National Central University; Andre Lee, Michigan State University

8:30 AM

Whisker and Hillock Formation on Sn, Sn-Cu and Sn-Pb Electrodeposits: William J. Boettinger¹; Gery R. Stafford¹; Christian E. Johnson¹; Maureen E. Williams¹; Kil-Won Moon¹; Leonid A. Bendersky¹; ¹National Institute of Standards and Technology

Bright Sn, Sn-Cu and Sn-Pb layers, 3, 7 and 16 μm thick were electrodeposited on phosphor bronze cantilever beams in a rotating disk apparatus. In several days, the surfaces of the Sn-Cu deposits, which have the highest compressive stress, develop contorted hillocks and whiskers, pure Sn deposits develop compact conical hillocks, and Sn-Pb deposits, which have the lowest compressive stress, remain unchanged. The differences between the initial compressive stresses is due to the rapid precipitation of Cu_6Sn_5 or Pb particles, respectively, within supersaturated Sn grains produced by electrodeposition. Over longer time, analysis of beam deflection measurements indicates that the compressive stress is augmented by the formation of Cu_6Sn_5 on the bronze/Sn interface. Uniform creep occurs for Sn-Pb because it has an equiaxed as-plated grain structure. Localized creep in the form of hillocks and whiskers occurs for Sn and Sn-Cu because both have columnar as-plated structures.

8:50 AM

Effect of Cu_6Sn_5 Doping on Microstructure and Strength for the Sn-Ag-Cu Solder Joint with Al/Ni UBM: Guo-Jyun Chiou¹; Jenq-Gong Duh¹; ¹National Tsing Hua University

Intermetallic compound of Cu_6Sn_5 plays an important role in the interfacial reaction between SnAgCu solder and Al/Ni UBM during reflowing in electronics packaging. In this study, Cu_6Sn_5 -contained SnAgCu solder paste was produced by mixing Cu_6Sn_5 nano powder into commercial SnAg solder paste. The Al/Ni UBM was first deposited onto the silicon wafer, and the Cu_6Sn_5 -contained solder paste was then stencil printed on the UBM and reflowed at 240°. The interfacial microstructure and elemental distribution were evaluated was studied with FE-SEM and FE-EPMA. During different reflow times, the thickness of IMCs in Cu_6Sn_5 -contained solder joints was thinner than that of commercial SnAgCu solder. To realize the effect of Cu_6Sn_5 nano powder doping, the shear strength of the joint was further investigated. In addition, the fracture mode of SnAgCu solder joints was probed with the aid of the fracture surface, interfacial morphology, and shear strength.

9:10 AM

Effect of Phosphorus Content on Cu/Ni-P/Sn-3.5Ag Solder Joint Strength under Multiple Reflow: Zhong Chen¹; Aditya Kumar¹; M. Mona¹; ¹Nanyang Technological University

Electroless Ni-P with three different P contents (6.1, 8.8, and 12.3 wt%) was deposited on copper substrates. Sandwiched specimens of Cu/EN/Au/Sn-3.5Ag/Au/EN/Cu were prepared and were subjected to multiple reflows at 250°C. Tensile test was performed to investigate the effect of P content on the joint strength. It was found that the low-P samples exhibited the highest joint strength after multiple reflows, while the strengths of the medium and high-P samples decreased more rapidly. From cross sectioned views, Ni-Sn IMC formed at the interface of the low-P sample was found to be more stable, while the one of the medium and high-P samples spalled into the molten solder. The IMC spallation speeded up Ni-P consumption, leading to the formation of Cu-Sn IMCs. Fractographic and microstructural analyses showed that the degradation was due to full consumption of EN and the formation of Cu-Sn IMCs at the interface.

9:30 AM

Effects of the Interfacial Reactions of Sn-8Zn-3Bi Solder Joints on Their Electrical and Mechanical Properties: Won Kyoung Choi¹; Changyool Moon¹; Sung K. Kang²; Da-Yuan Shih²; ¹Samsung Advanced Institute of Technology; ²IBM Corporation

Sn-8Zn-8Bi solder has been reported to show improved their joint properties in terms of interfacial reactions, wetting and mechanical properties and long-term reliability comparing to the Sn-Zn binary system. In this study, the effects of the interfacial reactions on the joint properties of Sn-8Zn-3Bi were investigated as a function of reflow time, aging time, and surface finish (Cu vs Ni). The interfacial microstructure was investigated using EPMA and XRD to identify the phases of the interfacial intermetallic compounds formed. The electrical and mechanical properties were measured using a model joint made of two L-coupons. These properties revealed a unique behavior comparing to other Pb-free solder joints. The changes in the electrical and mechanical properties of Sn-8Zn-3Bi joints were also explained based on their interfacial reactions with a corresponding surface finish.

9:50 AM

Elemental Diffusion Behavior for the Sn-3.0Ag-(0.5 Or 1.5) Cu Solder Bump with Cu/Electroless Ni-P/Immersion Au Bonding Pad during Aging: Guh-Yaw Jang¹; Yung-Chi Lin¹; Jenq-Gong Duh¹; Mysore A. Dayananda²; ¹National Tsing Hua University; ²Purdue University

Isothermal interdiffusion in Sn-3.0Ag-(0.5 or 1.5)Cu solder joints with electroless Ni/immersion Au surface finish after aging at 150°C was investigated. The diffusion structures and concentration profiles were examined with a newly developed Field-Emission Electron Probe Microanalyzer. Intermetallic compounds of $(\text{Cu}_{1-y}\text{Ni}_y)_6\text{Sn}_5$, $(\text{Ni}_{1-x}\text{Cu}_x)_3\text{Sn}_4$ and P-rich layer formed between the solder and the EN layer in both Sn-Ag-Cu joints during aging. For the Sn-3.0Ag-0.5Cu joints after more than 2000 h aging, $(\text{Ni}_{1-x}\text{Cu}_x)_3\text{Sn}_4$ IMC gradually grew. The interdiffusion fluxes and effective interdiffusion coefficient of Cu, Ni, and P were calculated from the concentration profile with the aid of Matano plane evaluation. Values of J_{Cu} , J_{Ni} and J_{P} decreased with increasing aging time. The average effective interdiffusion coefficients in the order of 10^{-14} cm^2/s were also evaluated within the diffusion zone. In addition, the effect of Cu content in solders on diffusion behaviors of Cu in Sn-3.0Ag-(0.5 or 1.5)Cu joints were probed and discussed.

10:10 AM Break

10:25 AM

Fracture Mechanics Approaches to the Interfacial Fracture of a Solder Joint and a Solder Bump: Woong Ho Bang¹; Choong-Un Kim¹; Myung-Woon Moon²; Kyu Hwan Oh²; ¹University of Texas at Arlington; ²Seoul National University

Using finite element methods, we have analyzed the interfacial fracture mode of a solder joint in a tensile test and that of a solder bump in a ball-shear test. The cracking site has been defined at interfacial IMC layer (Cu_6Sn_5) between solder and Cu metallization, where we have estimated stress intensity factors 'K' under those specific testing methodologies. Analysis of the tensile test has shown that tensile load applied to a solder joint develops both crack-opening KI mode and crack-shearing KII mode

at crack tip in IMC layer. Through the FEM simulation on a bump shear test, a crack-opening KI has been observed as a dominant mode of the bump fracture. The present talk will discuss in detail current results.

10:45 AM

Revealing the Interfacial Reaction of Novel Solders Developed from Sn-3.5Ag-0.5Cu Nanoparticles on Electroless Ni-P/Al UBM: *Li-Yin Hsiao*¹; Jenq-Gong Duh¹; ¹National Tsing Hua University

To meet the requirements for future electronic packaging technology, an ultrasmall solder bump is a tendency. With the reduced size of solder bumps, finer grain in solder paste is crucial for fine pitch bumping. Currently, near-eutectic SnAgCu alloys are developed as the lead-free solder. In this study, the Sn-3.5Ag-0.5Cu nanoparticles synthesized by chemical reduction method were introduced to prepare the lead-free solder. The secondary particle size of Sn-3.5Ag-0.5Cu nanoparticles was in the range of 40 nm. The detailed interfacial reaction of lead-free solders derived from the Sn-3.5Ag-0.5Cu nanoparticles on EN(P)/Al under bump metallization (UBM) was investigated after reflows. After morphological observation and quantitative analysis with a field-emission electron probe microanalyzer, the influence of the particle size for solders on the formation of IMCs at SnAgCu solder/electroless Ni-P interface was probed and discussed.

11:05 AM

Study of Coupling Effect by Using Sandwich Structures of Ni/Sn/Cu and Au/Sn/Cu: *Snen-Jie Wang*¹; Cheng-Yi Liu¹; ¹National Central University

The coupling effects between Cu-Sn and Ni-Sn soldering reactions have been investigated in this study. The interfacial Ni-Sn reaction would strongly be affected by the interfacial Cu-Sn reaction in the opposite side. The preliminary results did show that an unusual growth of ternary Cu-Ni-Sn compound at the Sn/Ni interface and a huge consumption of Cu in the opposite side. FE-EMPA results showed that the content of Ni in the Cu-Ni-Sn ternary phase varied along its thickness. The detail kinetics model for the ternary Cu-Ni-Sn phase formation will be presented in this talk. Beside, we will also report the coupling effect between Cu-Sn and Au-Sn interfacial reactions by using the Au/Sn/Cu sandwich structures. Again, we observed that the interfacial Cu-Sn reaction would be significantly influenced by the opposite Au-Sn interfacial reaction. The detail experimental observation on the microstructure and phase formation at both interfaces will be reported.

11:25 AM

Study of the Reactions between CuxNiy Alloy UBM and Sn-Ag (-Cu) Solder: *Hun Han*¹; Y. C. Sohn¹; Jin Yu¹; ¹Korea Advanced Institute of Science and Technology

A reaction study of CuxNiy alloy ($x=0.2\sim 0.95$) under bump metallization (UBM) with Sn-Ag-zCu solder ($z=0\sim 0.7$) was conducted. Formation and separation of intermetallic compounds (IMCs), effect of Cu addition to the CuxNiy alloy and the solders, and compatibility of reaction products with currently available phase diagrams are intensively investigated. Optimum range of Cu concentration, over which thick IMCs formed at interface without separation, was found for IMC separation behavior. Addition of Cu to the solder fasten IMC growth and CuxNiy ($x=0.2\sim 0.4$) consumption though the reverse trend was true of most solder reactions in literature. The amounts of Ni and Cu dissolved to the solders were calculated, and the reaction products were compared with Cu-Ni-Sn ternary phase diagrams available. Experimental results in the present study suggest a need for modification of the Cu-Ni-Sn diagrams.

11:45 AM

Cu Content and Size Effects upon the Reaction Layer Detachment in the Sn-Cu/Ni Couples: *Chao Hong Wang*¹; Sinn-Wen Chen¹; ¹National Tsing Hua University

The effects of Cu contents and the size of solder volumes upon the reaction layer detachment are investigated. Sn-Cu/Ni couples are reacted at 250°C and the alloys are with 0.4, 0.7, 1.0 and 2.0wt% Cu. The amounts of Sn-Cu alloys are 2g and 10g. Except for the 0.4wt%Cu couples, the product in the beginning is the Cu₆Sn₅. The Cu₆Sn₅ reaction layer detaches in the 2g Sn-Cu couples after 2-hour reaction. The detached layer decomposes in the molten solder, and Ni₃Sn₄ forms after a prolonged reaction time. Higher amount of Cu and larger amount of solders delay

the layer detachment. Microstructural analysis reveals the detached and the attached layers have different morphologies. The Cu contents in the solders also influence the morphologies of the Cu₆Sn₅ phase. The detachment is related with the formation of the Ni₃Sn₄ phase, and is influenced by both the Cu contents and the amounts of solders.

12:05 PM

Morphology of Intermetallic Compounds Formed between Lead-Free Sn-Zn Based Solders and Cu Substrate: *Chia-Wei Huang*¹; *Kwang-Lung Lin*¹; ¹National Cheng Kung University

The morphologies of intermetallic compound formed between Sn-Zn based solders and Cu substrate were investigated in this study. The investigated solders were Sn-9Zn, Sn-8.55Zn-0.45Al, Sn-8.55Zn-0.45Al-0.5Ag solders in the weight percent. The experimental results indicated that the Sn-9Zn solder formed the Cu₅Zn₈ and Cu₅Zn₅ compounds on Cu substrate, while the Al-containing solders formed the Al₄.2Cu₃.2Zn_{0.7} compound. The addition of Ag to the Sn-8.55Zn-0.45Al solder resulted in the AgZn₃ compound formed at the interface between Al₄.2Cu₃.2Zn_{0.7} compound and solder. Furthermore, it was found that the cooling rate of the specimen after soldering had an effect on the quantity of AgZn₃ compound formed at the interface. The AgZn₃ compound with air-cooling condition exhibited rougher surface and larger size than with water-quenched condition. It was believed that the formation of AgZn₃ compound at the interface was enhanced by heterogeneous nucleation during solidification.

Magnesium Technology 2006: Casting and Solidification II

Sponsored by: International Magnesium Association, TMS Light Metals Division, TMS: Magnesium Committee

Program Organizers: Alan A. Luo, General Motors Corporation; Neale R. Neelameggham, US Magnesium LLC; Randy S. Beals, DaimlerChrysler Corporation

Tuesday AM
March 14, 2006

Room: 6A
Location: Henry B. Gonzalez Convention Ctr.

Session Chairs: David H. St. John, University of Queensland; John E. Allison, Ford Motor Company

8:30 AM

Characterization of Cavity Pressure in Squeeze Casting of Magnesium Alloys: *Fang Alfred Yu*¹; Naiyi Li²; Henry Hu¹; ¹University of Windsor; ²Ford Motor Company

In squeeze casting processes, cavity pressures directly affects the heat transfer coefficients between casting and mold, and subsequently the solidification behavior of castings. For process optimization, it is very important to understand the distribution of applied pressure in a die cavity. Very often in the past, the distribution of the cavity pressure in either process design or numerical simulation of squeeze casting was considered uniform in the die cavity. Rare experimental work on measuring the cavity pressure has been conducted. In this study, an attempt has been made in characterizing the pressure distribution in the die cavity. A piezoelectric quartz pressure transducer was integrated into a die cavity with different geometrical shapes. The experiments have been carried out to reveal that the pressure distribution changes with the cavity geometry. Also, the change of the local cavity pressure at various locations in the duration of casting solidification was observed.

8:50 AM

Effect of Power Ultrasound on Grain Refinement of Magnesium AM60B Alloy: *Xiaogang Jian*¹; Thomas Tom Meek¹; Qingyou Han²; ¹University of Tennessee; ²Oak Ridge National Laboratory

In the past decades, several grain-refining techniques have been reported for magnesium – aluminum based alloys, namely superheating, carbon inoculation, and Elfinal process. This article describes an experimental attempt to refine the solidification structure of magnesium AM60B alloy using high intensity ultrasonic vibrations. Ultrasonic energy up to 1500 W was injected into the alloy during its solidification. Casting tem-

perature was varied in order to obtain the optimal effect on grain refinement. The experimental results indicated that grain refinement was readily achievable for this alloy with ultrasonic vibrations. When the casting temperature was 675°C, globular grains were obtained. The grain size can be as small as 30 to 40 µm, which was over an order of magnitude smaller than the dendritic grains obtained without using ultrasonic vibrations.

9:10 AM

Heat Treatments and Mechanical Properties of a Rheocast AM60 Magnesium Alloy: *Emanuela Cerri*¹; Pasquale Cavaliere¹; Pier Paolo De Marco¹; Paola Leo¹; ¹University of Lecce

A study on the heat treatment response and the mechanical properties of a rheocast AM60 magnesium alloy was performed. The alloy was aged in the as-rheo condition and after high temperature exposure (395 and 415°C). The aging temperatures were in the range of 170-220°C. The hardness values and electrical conductivity measurements of aged samples show no substantial difference between solution treated and as-rheo specimens. Tensile tests on samples heat treated in different conditions according to solution and aging temperatures presented above were also investigated. The mechanical properties like yield strength, ultimate tensile strength and strain to failure are discussed as a function of solution and aging temperature and time. The grain size remains stable when the material is exposed at high temperature (395 and 415°C).

9:30 AM

Microstructural Refinement of Magnesium Alloy by Electromagnetic Vibrations: *Kenji Miwa*¹; Yoshiki Mizutani¹; Takuya Tamura¹; ¹National Institute of Advanced Industrial Science and Technology

We have developed the new process for refinement of metallic materials during solidification without addition of refiners or without rapid cooling. This process uses electromagnetic body force based on the vibrations caused by simultaneous imposition of direct magnetic field and alternative electric current on the alloy melt during solidification. The vibrations create cavitation in the melt and it breaks out during growth of it. Then explosive force is released toward the surroundings such as the primary solid particles and they are fractured finely. Finally fractured solid particles solidified as very fine grains. This process was applied to AZ91D alloy. Primary magnesium dendrite particles decreased from about 1800 micron to about 100 micron. This process was also useful to refinement of primary particle in pure magnesium.

9:50 AM

Microstructure and Mechanical Properties of Die Cast Magnesium Alloy AM50 with Varying Section Thicknesses: Ming Zhou¹; Henry Hu¹; *Naiyi Li*²; Alfred Yu¹; ¹University of Windsor; ²Ford Motor Company

Understanding of the effect of section thicknesses on mechanical behavior of AM50 is critical for proper design of different applications with varying cross-section thicknesses due to its extensive use in automobiles. In the present study, magnesium alloy AM50 was high pressure die cast into rectangular coupons with section thicknesses of 2, 6 and 10 mm. The prepared coupons were tensile tested at room temperature. Microstructure analysis and porosity measurement were performed on the representative specimens. The results show that their tensile properties decreases with an increase in section thicknesses of die cast AM50. Microstructure and porosity analyses indicate that the tensile behavior of die cast AM50 is primarily attributed to the level of porosity which resulted from entrapped gases during die casting process. The preliminary results of numerical simulation on mold filling imply that the porosity content of casting coupons is significantly influenced by the design of gating systems.

10:10 AM Break

10:30 AM

On Liquidus and Solidus Temperatures in AZ and AM Alloys: *Munekazu Ohno*¹; Djordje Mirkovic¹; Rainer Schmid-Fetzer¹; ¹Clausthal University of Technology

The liquidus and solidus data reported for commercial AZ and AM alloys are generally based on thermal analysis. In the present study, the following two points have been clarified by performing own experiments and Calphad-type thermodynamic calculations: (i) The measured 'liquidus' temperature generally does not represent the actual equilibrium one, in

other words, the primary precipitate for these Mg-alloys cannot be detected in the thermal analysis. (ii) The measured "solidus" does not correspond to the equilibrium solidus and not even to the end of non-equilibrium solidification process. The measured "solidus" is often associated with the precipitation of Mg₁₇Al₁₂ phase and, importantly, the solidification process of these Mg-alloys ends at much lower temperature. This work is supported by the German Research Foundation (DFG) in the Priority Programme "DFG-SPP 1168: InnoMagTec."

10:50 AM

Vertical Direct Chill (VDC) Casting of a Novel Magnesium Wrought Alloy with Zr and RE Additions (ZK10): Alloying Issues: *Michael Kettner*¹; Franka Pravidic¹; Werner Fragner¹; Karl Ulrich Kainer²; ¹ARC Leichtmetallkompetenzzentrum Ranshofen GmbH; ²GKSS Research Center

The present paper describes the microstructure of a new magnesium wrought alloy (ZK10) in as cast condition. Furthermore the experimental procedures and the evaluation of the results are presented. Zirconium master alloys of two different suppliers were analyzed in alloying experiments in laboratory scale. The master alloy showing better qualities was subjected to a VDC casting trial in industrial scale at LKR. Billets of the alloy containing zirconium and rare earth metals were cast in a diameter of 185 mm and a length of 2000 mm for further extrusion trials. The master alloys, the samples from the alloying experiments as well as the cast billets were investigated using metallography, scanning electron microscopy and segregation analysis.

11:10 AM

Warm Water Scale Model Experiments for Magnesium Die Casting: Mohamed Hassan¹; Kazunori Kuwana¹; Valerio Viti¹; *Adrian S. Sabau*¹; Kozo Saito¹; ¹University of Kentucky

High Pressure Die Casting (HDCP) involves the filling of a cavity with the molten metal through a thin gate. High gate velocities yields jet break-up and atomization phenomena. In order to improve the quality of Mg parts, the mold filling pattern, including atomization phenomena need to be understood. The goal of this study was to obtain experimental data on jet break-up characteristics for conditions similar to that of a Mg HDCP, and measure droplet velocity, size and size distribution. A scale analysis is first presented in order to identify appropriate analogue Mg materials. Based on the scale analysis, warm water was chosen as a suitable analogue and different nozzles were manufactured. A 2-D component Phase Doppler Particle Analyzer (PDPA) and 2-D component Particle Image Velocimetry (PIV) were then used to obtain fine particle diameter and velocity distributions in 2-D plane.

11:30 AM

Mechanical Properties of Lost Foam Cast Magnesium Alloys AZ91E, AM50 and ZE41: *Festus A. Fasoyinu*¹; Peter Newcombe¹; Mahi Sahoo¹; ¹Materials Technology Laboratory

As part of an ongoing research program at CANMET (Canada Centre for Minerals and Energy Technology) Materials Technology Laboratory (MTL) to develop a viable lost foam casting technology for magnesium-base alloys, the mechanical properties of test bars machined from foam pattern castings were evaluated. This paper provides tensile properties data in the as-cast condition and after heat treatment, and the issues encountered during the casting trials are also described.

Magnesium Technology 2006: Microstructure and Properties I

Sponsored by: International Magnesium Association, TMS Light Metals Division, TMS: Magnesium Committee

Program Organizers: Alan A. Luo, General Motors Corporation; Neale R. Neelameggham, US Magnesium LLC; Randy S. Beals, DaimlerChrysler Corporation

Tuesday AM Room: 6B
March 14, 2006 Location: Henry B. Gonzalez Convention Ctr.

Session Chairs: Jian-Feng Nie, Monash University; Menachem S. Bamberger, Technion

8:30 AM

Effect of Hot Torsion Deformation on Microstructure in AZ31 Magnesium Alloy: Faramarz M. Zarendi¹; Stephen Yue¹; Ravi Verma²; ¹McGill University; ²General Motors

Strength and ductility are desired characteristics in sheet materials for applications in the auto industry. Such characteristics are developed during hot and cold rolling of thick as cast materials. Therefore, it is important to understand the evolution of microstructure during rolling. In terms of large strains and high strain rates applied during rolling, torsion could be an adequate laboratory deformation process to simulate the industrial rolling practice. In this work, an as cast AZ31 magnesium alloy was deformed in torsion under different thermomechanical conditions and the resultant microstructures were examined. At high temperatures, discontinuous recrystallization is the principal mechanism for microstructure evolution with nucleation of new grains at as cast grain boundaries. On the contrary, continuous recrystallization contributes to the evolution of microstructure at low temperatures. It is observed that the effect of strain rate on the microstructural development is not as important as those of temperature and strain.

8:55 AM Cancelled

Microstructure and Mechanical Property of Extruded Mg-Zn-Cu-Gd Based Alloy Reinforced by Quasicrystals and Laves Phases

9:20 AM

Microstructure Study of Magnesium Alloys at Various Stages of Creep Using EBSD: Takanori Sato¹; Barry L. Mordike²; Jian-Feng Nie³; Milo V. Kral¹; ¹University of Canterbury; ²TU Clausthal; ³Monash University

Magnesium and common Mg-Al based alloys exhibit constant creep rates during secondary creep stage, typically described as power law creep. Diffusion-induced dislocation motion and grain boundary sliding are believed to be the key mechanisms of creep in magnesium. Furthermore, with addition of aluminum, the development of coarse intergranular and fine coherent intragranular β ($Mg_{17}Al_{12}$) precipitates is known to affect the creep rate at temperatures over 150°C. In this research, wrought pure magnesium and binary Mg-Al alloys were creep tested at various conditions of temperature and stress. The tests were interrupted periodically and sample surface microstructure was characterized using orientation microscopy via SEM/EBSD to provide a sequential microstructural analysis. This enabled an historical observation of deformation accumulation, precipitation, and grain boundary interactions as creep progressed.

9:45 AM

Design Perspectives for Creep Resistant Die-Cast Magnesium Alloys: Bimal Kadl¹; Qingyou Han²; Srinath Viswanathan³; ¹University of California-San Diego; ²Oak Ridge National Laboratory; ³Sandia National Laboratories

Die cast magnesium alloy design for elevated temperature creep is evaluated from the perspective of the particular contributions of alloying, the nonuniform microstructure and eutectic constituents. Thermodynamic simulations provide the necessary insight into solute segregation, solidus temperature, and the corresponding homologous temperature distribution in the a(Mg) phase for Mg-Al alloys with ternary additions. Experimental and computational results suggest that significant creep deformation occurs in the a(Mg) phase in and adjacent to the eutectic regions with the

low solidus constituent while deformation in the primary a(Mg) dendrites is less pronounced. Microstructural design efforts that increase the homologous temperature, reduce eutectic volume or reinforce the eutectic a(Mg) phase hold significant promise towards increasing the creep resistance of magnesium alloys. This approach is then applied to predict and validate a ranking of the creep performance of current die-cast alloys under development. REF: Han, Kad and Viswanathan (2004) Philos Mag, Vol.84, p.3843-60.

10:10 AM Break

10:30 AM

Creep Transition Behavior of Pure Magnesium Poly and Single Crystals: Jaesin Park¹; Youngwon Chang¹; ¹Pohang University of Science and Technology

The purpose of this study is to investigate the effect of barrier structure on the dislocation motion in hcp crystal, which is in turn believed to determine the permeability parameter(p) of plastic equation of state. It has also been intended to verify whether there exists a mechanical equation of state for Mg single and poly crystals. Mg single crystals with random orientations were grown from a commercial purity Mg poly-crystal using modified Bridgman furnace. A series of load relaxation tests was then conducted on these single and poly-crystal Mg. In addition, tests at various temperatures were performed to investigate the temperature effect on the flow behavior. The test results are then analyzed using the recently proposed internal variable theory, based on dislocation kinematics, which has been successfully applied to many other materials.

10:55 AM

Precipitations Hardening and Phase Formation in Mg-Sn-Zn-Al Alloys: Shlomo Haroosh¹; Ginat Goren-Muginstein¹; George Levi¹; Menachem S. Bamberger¹; ¹Technion

Based on a previous research, Mg-Zn-Sn alloys do not show promising behavior at higher temperatures. In order to increase the structural stability, 1%wt MM (50%Ce-25%La-20%Nd-5%Pr) was added. At the as-cast condition, SEM micrographs indicate a very fine micro-structure (DAS below 12 μ m). The study focuses on the precipitation hardening, phase formation and structural stability during aging at elevated temperatures, of solution treated samples. After solution treatment (450 C) and aging at 225 C, Vickers hardness measurements show that this alloy maintains an increase of 30% in hardness for periods up to 32 days. Very fine homogeneously distributed precipitations (less than 500nm) were found. EDS, XRD and Auger characterization methods were employed in order to identify the phase structure of the alloy and the origin of precipitates. There is no evidence for the presence of the deleterious γ -Al₁₂Mg₁₇ phase. EDS and Auger spectroscopy study showed that the RE precipitates are MgREAlZn.

11:20 AM

The Influence of Y Addition on Precipitation Sequence in Mg-Zn-Sn Based Alloy: Anton Gorny¹; Ginat Goren-Muginstein¹; Gerhard Dehm²; Boriana Rashkova²; Menachem S. Bamberger¹; ¹Technion; ²Max Plank Institute fuer Metallforschung

The main goals of this research are to investigate the precipitation sequence in Mg-Sn-Zn based alloy with the addition of Y. Further, the changes in mechanical properties during the precipitation process were studied. The results showed a huge difference between the alloys. New Mg-Sn-Y phase/compound appeared in the as-cast state. This phase/compound does not dissolve in the a-Mg during the solution treatment (440°C for 96 hrs) and aging up to 16 days at 225°C. The alloy exhibits high hardness levels for a long time at high temperature, i.e. it does not overage in contrary to the base alloy. It seems that the precipitates are Y free, however Y slows down the over aging process. In order to elucidate the contribution of Y to the structural stability of Mg-Sn-Zn based alloy, XRD, TEM, SEM and EDS analyses will be detailed.

Materials Design Approaches and Experiences II: Superalloys

Sponsored by: The Minerals, Metals and Materials Society, TMS Structural Materials Division, TMS: High Temperature Alloys Committee

Program Organizers: Michael G. Fahrman, Special Metals Corporation; Yunzhi Wang, Ohio State University; Ji-Cheng Zhao, General Electric Company; Zi-Kui Liu, Pennsylvania State University; Timothy P. Gabb, NASA Glenn Research Center

Tuesday AM
March 14, 2006

Room: 202B
Location: Henry B. Gonzalez Convention Ctr.

Session Chairs: Michael Fahrman, Special Metals Corporation; Ji-Cheng Zhao, General Electric Company

8:30 AM Introductory Comments by M. Fahrman, Special Metals Corporation

8:40 AM Invited

Accelerated Insertion of Materials and Processes for Aircraft Engine Applications: *Deborah DeMania Whitis*¹; Andrew P. Woodfield¹; J. Pfandner¹; S. Srivatsa¹; David P. Mourer¹; D. Wei¹; Michael F. Henry²; L. Jiang²; ¹GE Aircraft Engines; ²GE Global Research Center

Material and process development for aircraft engines has, in the past, required long and costly experimental programs, imposing a significant barrier to the insertion and exploitation of new materials. With the advent of computer modeling and simulation of materials processing, and the accelerated insertion of materials (AIM) approach, we have begun to provide the tools to industrial materials designers that they need to increase productivity and reduce cost of alloy development. This presentation will provide an overview of the implementation of the AIM approach at GE Aircraft Engines. The integration of materials models, historical databases, and analysis tools have allowed us to more rapidly downselect new alloys and manufacturing processes, responding quickly to the design requirements of a particular component and engine environment. Current progress in applying these techniques to nickel-based superalloys and titanium alloys will be reviewed.

9:05 AM Invited

Transport Phenomena and Macrosegregation in VAR and ESR: *Matthew John M. Krane*¹; Shawn A. Cefalu¹; Kent J. VanEvery¹; Dymtro Zagrebelnyy¹; ¹School of Materials Engineering, Purdue University

The heat, mass and momentum transfer and electromagnetics present during electroslog and vacuum arc remelting (ESR and VAR) are modeled and sump profiles, macrosegregation patterns and local solidification times are predicted. These results are studied as functions of process parameters and ingot geometry. During ESR of superalloys, a maximum in macrosegregation is found as a function of filling velocity in the flow regime dominated by buoyancy, and the growing influence of electromagnetics at higher melt rates is discussed. Comparisons are made to experimental data from industrial ingots. During VAR of titanium alloys, DC current levels are generally much higher than the AC current in ESR, so the sump flow is controlled by Lorenz forces leading to different segregation patterns. Scaling analyses of the fluid flow in the sump give some insight into the effect of process parameters on the fluid velocities and the tendency to segregate.

9:30 AM

Semi-Experimental Approach of Optimizing Castability and Homogenisation of Ni-Base Superalloy: *Muthiah Ganesan*¹; David Dye¹; Peter D. Lee¹; ¹Imperial College London

Increased creep rupture life and strength with acceptable scrap rates and cost are just some of conflicting requirements presently facing designers of heavily alloyed Ni-base superalloy single crystals. Both component castability and solution heat treatability have become increasingly difficult. We have recently proposed an improved statistical approach for accurately characterizing microsegregation in multicomponent alloys. Here, we demonstrate how applicability of this new approach can be further extended via predictive methods (e.g. thermodynamic and regression

modeling) to help make improvements in the processing of existing and new alloys. Examples provided include assessment for thermosolutal convection and thus freckle formation, predictions of incipient melting temperatures and alloy susceptibility to topologically closed packed phase formation in a segregated alloy. Empirical equations predicting non-equilibrium phase transformation temperatures and segregation parameters are also provided and compared to CALPHAD-based thermodynamic predictions. Interactive effects between alloying elements are identified and the implications for alloy design discussed.

9:50 AM Invited

Phase Field Modeling Qualitative and Quantitative Microstructural Evolution in Ni-Base Alloys: *Jeff P. Simmons*¹; Youhai Wen²; B. Wang³; Y. Wang³; ¹U.S. Air Force; ²UES Inc; ³Ohio State University

The Phase Field method has been an important and popular method in academia for simulating realistic microstructures because of its relative simplicity and its striking similarity to actual experimental observations. Recently, Phase Field methods have begun to be applied to phase transformations problems of industrial import. This presentation discusses successes and difficulties in applying the Phase Field method towards qualitative behavior and quantitative kinetic predictions in Ni-base alloys of practical interest. In particular, diffusion-limited transformations behavior, bimodal particle size distributions, quantitative mean particle sizes and number density evolution in time have been successfully modeled, as has microstructures formation under non-isothermal heat-treat conditions, where nucleation, growth, and coarsening all occur concurrently. Computations in this work were accomplished with the OpenPF open source Phase Field code, originally developed under contract to DARPA under the AIM program.

10:10 AM Invited

Integrated Modeling for the Manufacture of Ni-Based Superalloy Discs from Solidification to Final Heat Treatment: *Sammy Tin*¹; Ahmad Keramanpur²; Peter D. Lee²; Malcom McLean²; Martin A. Rist³; ¹University of Cambridge; ²Imperial College; ³Open University

Process models of the various stages of gas turbine disc manufacture have been integrated to simulate the physical and microstructural transformations occurring within a nickel-based superalloy throughout the entire manufacturing route. Production of these critical rotating structural components requires several distinct processing stages: vacuum induction melting, vacuum arc remelting, homogenization heat treatment, cogging, forging, final heat treatment and machining. During the course of these consecutive manufacturing stages, the various thermal and thermo-mechanical processes lead to significant changes in both the microstructural characteristics and internal stresses in the alloy. Although separate models have previously been developed to simulate the individual processing stages, this talk describes how these models can be integrated to simulate the entire manufacturing process from secondary melting through to the final forging and heat treatment. The implications of such integrated modeling for quality assurance through process control are discussed.

10:35 AM Break

10:55 AM

Application of JMatPro in Alloy Design at ATI Allvac: *Wei-Di Cao*¹; Ramesh Minisandram¹; ¹ATI Allvac

The experience of applying JMatPro in alloy design at Allvac will be introduced in this presentation. JMatPro has been applied to the design of new Ni-base superalloy AllvacTM 718PlusTM and new ultrahigh stainless steel AllvacTM S240TM. The methodology was to trace the change of alloy behaviors by systematically changing the chemistry of model alloys. The behaviors include: 1. Type, Chemistry and quantity of alloy phases as function of temperature. 2. Precipitation and coarsening kinetics of various alloy phases. 3. Prediction of thermo-physical and mechanical properties of model alloys. Experiment works were carried out to validate the results, giving an opportunity to evaluate this tool. Examples of successful and unsuccessful experiences will be presented. Improvements desired will be suggested.

11:20 AM

Initial Assessments of Wrought Nickel-Base Superalloys for Space Applications: *Timothy P. Gabb¹*; John Gayda¹; ¹NASA Glenn Research Center

Plate superalloys which can be formed, brazed, and welded have potential applications in space, for ducts and heat exchangers in power generation systems. Some proposed applications would require sufficient strength and creep resistance for long term service at 800-930C, with service times to 10,000 h or more. Such long term service can severely tax alloy creep and phase stability, to the potential detriment of other mechanical properties. Several wrought plate superalloys including Hastelloy X and Inconel 617 are being screened with tensile and creep tests to compare their capabilities for these applications. Conventional tensile and creep tests were performed at temperatures up to 930C on specimens extracted from wrought plates. Microstructure and phase evaluations were then undertaken. The results will be discussed along with supporting comparative predictions of a modern alloy design tool.

11:40 AM

A Validation Study of the Predictive Capabilities of the Materials Properties Simulation Software JMatPro: *Michael G. Fahrmann¹*; ¹Special Metals Corporation

JMatPro is one of the modern computational tools that allows for the simulation of selected thermodynamic, physical, and mechanical properties of various families of alloys. Based on computational thermodynamics and the best available composite models for the material's effective properties, it employs only a few adjustable parameters derived from benchmark alloys of industrial relevance. For an industrial user, the accuracy of the predictions and the range of validity are of paramount importance when utilizing this tool in actual alloy or process development. This paper presents the outcome of a validation study exercised on wrought Ni-base and Ni-Fe-base superalloys. Special emphasis is placed on JMatPro's predictive capabilities for yield strength, minimum creep rate, and stress rupture life. The importance of equilibrium assumptions and a detailed knowledge of microstructural features and length scales is stressed by parametric studies. JMatPro is a registered trademark of Sente Software, U.K.

Materials in Clean Power Systems: Applications, Corrosion, and Protection: Corrosion in Clean Coal Power Plants and Fuel Cells

Sponsored by: The Minerals, Metals and Materials Society, TMS Structural Materials Division, TMS/ASM: Corrosion and Environmental Effects Committee

Program Organizers: Zhenguo Gary Yang, Pacific Northwest National Laboratory; K. Scott Weil, Pacific Northwest National Laboratory; Michael P. Brady, Oak Ridge National Laboratory

Tuesday AM

Room: 212B

March 14, 2006

Location: Henry B. Gonzalez Convention Ctr.

Session Chairs: Peter Tortorelli, Oak Ridge National Laboratory; K. Scott Weil, Pacific Northwest National Laboratory

8:30 AM Keynote

Simultaneous Oxidation and Carburisation of Chromia Forming Alloys: *David John Young¹*; ¹University of New South Wales

Chromium forms both carbides and oxide at moderate and elevated temperatures. Because the carbides are less stable than Cr₂O₃, they form only when the chromia scale is permeable to a carbonaceous species, or when any scale is removed. On the other hand, because carbon has a much higher permeability in austenitic alloys than does oxygen, internal carburisation is much faster than internal oxidation. Reactions of chromium metal and model binary alloys with mixed gases at 900°C were used to identify conditions under which chromia scales are permeable to carbon. Reactions of commercial alloys at 600-700°C with CO/CO₂ gases demonstrated simultaneous internal precipitation of oxide and carbides.

9:15 AM Invited

Fireside and Steamside Corrosion of Alloys for USC Plants: *Ken Natesan¹*; Jong-Hee Park¹; ¹Argonne National Laboratory

A program on fireside and steamside corrosion, in support of ultrasupercritical (USC) plants, was conducted to evaluate the performance of several structural alloys in the presence of mixtures of synthetic coal ash, alkali sulfates, and alkali chlorides and in a steam environment. Experiments address the effects of deposit chemistry, temperature, and alloy chemistry on the corrosion response of alloys at temperatures in the range of 650-800°C. Materials selected for the study included intermediate-Cr ferritic steels, high-Cr austenitic alloys, and Ni-base alloys. Data were obtained on weight change, scale thickness, internal penetration, microstructural characteristics of corrosion products, mechanical integrity of the scales, and cracking of scales. Based on acquired corrosion information, we have proposed a mechanism for accelerated corrosion in the presence of a NaCl-containing oxidizing environment. Corrosion test data will be used to assess the corrosion performance of candidate materials for long-term service in USC plant environments.

9:45 AM

Deposition of Al-Si Precursor onto Mo-Si-B Turbine Materials: *Joshua E. Jackson¹*; David LeRoy Olson¹; Brajendra Mishra¹; Ian Michael Solomon¹; ¹Colorado School of Mines

The interfacial reactions of Mo-Si-B with Al-Si during processing to achieve mullite high-temperature corrosion protective coating for advanced turbine materials are discussed. Al-Si was deposited on the Mo-Si-B substrate material by both cathodic deposition and cryogenic immersion in liquid Al-Si alloy to achieve adhesion and compositional gradients across the interfacial region. This interfacial region, with Al-Si deposition, is the precursor to the formation of mullite by annealing and then oxidation. The optimum Al-Si content of this metallic layer, which is attained by deposition and silicon diffusion from Mo-Si-B, will be described. Characterization of the constitution and gradients across the interfacial region will be reported. Transport modeling of this precursor layer will be discussed.

10:10 AM

Control of Metal Dusting Corrosion in Fe- and Ni-Base Alloys: *Zuotao Zeng¹*; ¹Argonne National Laboratory

Metal dusting is a major issue in plants used in the production of hydrogen, methanol-reformer systems, and syngas (H₂/CO mixtures) systems that are pertinent to the chemical and petrochemical industries. Usually, metal dusting corrosion has two stages: incubation and growth resulting in propagation of metal dusting pits. The two stages were studied by scanning electron microscopy and Raman scattering to evaluate the scale of the surface oxide in the initiation and propagation of metal dusting attack. The initiation is dictated by the presence of defects and the propagation is determined by the diffusion of carbon into the alloy. These carbon diffusion pathways can be blocked by periodically oxidizing the surface of alloys at moderate temperatures in controlled atmospheres. It was concluded that metal dusting degradation by selecting an alloy with a long incubation time and subjecting it to intermediate oxidation steps.

10:35 AM Break

10:50 AM Invited

The Effects of Dual Environments and Chromia Vaporization on Metallic Interconnect Behavior: *Frederick S. Pettit¹*; Wes Jackson¹; Scot Laney¹; Gerald H. Meier¹; ¹University of Pittsburgh

In solid oxide fuel cells, metallic interconnects are exposed at 800°C to air at the cathode and fuel (hydrogen) at the anode. Moreover, in the case of metallic alloys that rely upon Cr₂O₃ for oxidation resistance, the vaporization of Cr₂O₃ has been shown to poison the cathode electrode. This paper is concerned with the effects of dual environments on the oxidation of alloys, as well as approaches that may be used to inhibit the adverse effects of Cr₂O₃ vaporization. The studies concerned with dual environments will use silver exposed to air on one side and an argon-hydrogen gas mixture on the other. Inhibition of Cr₂O₃ vaporization will be described by using nickel and iron base alloys containing chromium and titanium.

11:20 AM

High Temperature Corrosion Behavior of Metals and Alloys under Influence of a Hydrogen Gradient: Z. Gary Yang¹; Gregg Coffey¹; Dean M. Paxton¹; Prabhakar Singh¹; Jeff W. Stevenson¹; Gordon G. Xia¹; ¹Pacific Northwest National Laboratory

In clean power systems, components such as the metallic interconnects in high temperature fuel cells are often exposed simultaneously to a hydrogen or hydrogen-rich fuel at one side and air at the other, i.e. in a "dual" environment. Recently it has been found that the oxidation and corrosion behavior of the metals and alloys under the dual exposures can be significantly different from that in a single exposure, either an oxidizing or reducing atmosphere. The anomalous corrosion behavior that is attributed to hydrogen diffusion from the fuel side to the airside is a function of alloy composition and affected by thermal history and water vapor level in surrounding environments. This paper will present the details of our study on different group of metals and alloys, and discuss mechanistic understanding on the corrosion behavior of the metallic materials under the dual exposure conditions.

11:45 AM

Silver-Aluminum Based Air Braze for High Temperature Electrochemical Devices: Jin Yong Kim¹; John S. Hardy¹; K. Scott Weil¹; ¹Pacific Northwest National Laboratory

Recently, reactive air brazing (RAB) technique has been developed as an effective alternative for high temperature electrochemical devices such as solid oxid fuel cells. One of the concerns related to the silver-based RAB is its endurance under the dual atmosphere such as hydrogen on one side and oxygen on the other side. Since aluminum would be expected to work as an oxygen getter by forming oxides, aluminum was added to the silver-based reactive air braze (RAB) in order to improve the mechanical properties as well as dual atmosphere tolerance of the braze. In this study, the effects of aluminum content and processing conditions on the microstructure and mechanical properties have been investigated. The detailed results to date will be discussed.

Multicomponent-Multiphase Diffusion Symposium in Honor of Mysore A. Dayananda: Metals and Alloys

Sponsored by: The Minerals, Metals and Materials Society, ASM Materials Science Critical Technology Sector, ASM-MSCTS: Atomic Transport Committee

Program Organizers: Yong-Ho Sohn, University of Central Florida; Carelyn E. Campbell, National Institute of Standards and Technology; Richard Dean Sisson, Worcester Polytechnic Institute; John E. Morral, Ohio State University

Tuesday AM
March 14, 2006

Room: 203B
Location: Henry B. Gonzalez Convention Ctr.

Session Chairs: Hiroshi Numakura, Kyoto University; Carelyn E. Campbell, National Institute of Standards and Technology

8:30 AM Invited

Analysis of Interdiffusion Data in Multicomponent Alloys to Extract Fundamental Diffusion Information: Irina V. Belova¹; Graeme E. Murch¹; ¹University of Newcastle

There is a very large quantity of interdiffusion data existing for multi-component metallic systems but rather little has been done so far to extract from it fundamental atomistic diffusion information, e.g. defect-atom exchange frequencies, vacancy-wind factors and tracer correlation factors. This potentially rich source of information could be used to provide a sound foundation from which to tailor the microstructure by means of additives and heat treatment. In this paper, we review the new methods available and the recent progress that has been made to extract fundamental diffusion information from interdiffusion data. We focus on two ternary alloy systems Fe-Ni-Cr and Cu-Ni-Fe, both of which also have some tracer diffusion coefficients available for consistency checking.

9:00 AM

Self- and Interdiffusion Studies in Ternary Cu-Fe-Ni Alloys: Robert Filipek¹; Marek Danielewski¹; Sergiy V. Divinski²; F. Hisker²; Christian Cherzig²; ¹AGH University of Science and Technology; ²University of Münster

Interdiffusion in ternary Cu-Fe-Ni system was studied using diffusion couple technique and Darken model for multi-component systems. Nernst-Planck's flux formula assuming a chemical potential gradient as a driving force for the mass transport was used for computation of the diffusion flux in non-ideal multi-component systems. Lattice diffusion of ⁶⁴Cu, ⁵⁹Fe and ⁶³Ni radiotracers has been measured in Cu-Fe-Ni alloys of different compositions at 1271 K. Most of the measured penetration profiles show both extended grain boundary-induced part and the initial bulk diffusion induced part. Grain boundary diffusion contribution was consistently taken into account when determining the bulk diffusivities of the components. For the computations the measured tracer diffusion coefficients of Cu, Fe and Ni and the literature data on thermodynamic activities for the Cu-Fe-Ni system were used. The calculated interdiffusion concentration profiles (diffusion paths) are compared with the experimental results.

9:25 AM

Multi-Component, Multi-Phase Diffusion in Metallic Nuclear Fuels: Dennis D. Keiser¹; ¹Argonne National Laboratory

Multi-component, multi-phase diffusion is commonly observed in nuclear fuels during irradiation in nuclear reactors. This diffusion results in the formation of a variety of different phases that directly impact the performance of the fuel. Diffusion occurs within the nuclear fuel materials themselves (driven by things like temperature gradients), and also between the fuel alloy constituents and the cladding alloy constituents. To better understand the diffusion that occurs within these fuels during reactor operation, out-of-reactor studies have been conducted with various fuel and cladding alloys. These studies have generated useful information about the diffusion kinetics in specific fuel systems and about the types of phases that can form as a result of the diffusion. This paper will discuss results from some out-of-reactor studies that have been conducted to look at diffusion in metallic nuclear systems. Results from these studies will be compared with what has actually been observed in irradiated fuel.

9:50 AM

Interdiffusion in Ni-Cr-X (Al, Si, Ge or Pd) Alloys: Narayana Garimella¹; Michael P. Brady²; Yong-Ho Sohn¹; ¹University of Central Florida; ²Oak Ridge National Laboratory

Interdiffusion in Ni-Cr (fcc γ phase) alloys with small addition of Al, Si, Ge, or Pd was investigated using solid-to-solid diffusion couples. Ni-Cr-X alloys having compositions of Ni-22at.%Cr, Ni-22at.%Cr-6.2at.%Al, Ni-22at.%Cr-4.0at.%Si, Ni-22at.%Cr-1.6at.%Ge and Ni-22at.%Cr-1.6at.%Pd were cast using arc-melt. The diffusion couples were assembled in Invar steel jig, encapsulated in Ar after several hydrogen flush, and annealed at 900°C in a three-zone tube furnace for 168 hours. Experimental concentration profiles were determined from polished cross-section of these couples by using electron probe microanalysis with pure standards. Interdiffusion fluxes of individual components were calculated directly from the experimental concentration profiles, and the moments of interdiffusion fluxes were examined to determine average ternary interdiffusion coefficients. Effects of ternary alloying additions on the diffusional behavior of Ni-Cr-X alloys are presented in the light of the formation and adhesion of protective Cr₂O₃ scale. This work was financially supported by CAREER award from National Science Foundation (DMR-0238356).

10:15 AM Break

10:25 AM Invited

Three-Dimensional Interdiffusion under a Stress Field in Fe-Ni-Cu and Fe-Ni-Cr Alloys: Marek Danielewski¹; Bartłomiej Wierzba¹; ¹AGH University of Science and Technology

The model of interdiffusion under the stress field base on the Darken concept of the drift velocity. Regardless of the common acceptance of the original Stokes interpretation, we propose that the velocity appearing in Newton's viscosity law should be the drift velocity. The key results lie in modification of the Navier-Lamé equations for systems, where the concentrations are not uniform and diffusion occurs. The presented coupling

of the Darken method with mass and momentum balance equations allows for quantitative analysis of the transport processes. The diffusion of components depends on the chemical potential gradient and on the stress that can be induced by the diffusion and by the boundary conditions. The energy, momentum and mass transport are diffusion controlled and the fluxes are given by the Nernst-Planck formulae. It is shown that the Darken method is effective for modeling transport processes in Fe-Ni-Cu and Fe-Ni-Cr alloys.

10:55 AM

Diffusion in the Ir-Nb System: *Hiroshi Numakura*¹; Tatsuru Watanabe¹; Makoto Uchida¹; Yoko Yamabe-Mitarai²; Eisuke Bannai²; ¹Kyoto University; ²National Institute for Materials Science

The diffusion behaviour of Ir-rich Ir-Nb alloys has been studied by interdiffusion experiments. The chemical diffusion coefficient has been measured in the Ir-rich fcc solid-solution and the L1₂ ordered compound Ir₃Nb has been measured in the temperature range between 1750 and 1950°C, using Ir / Ir-8%Nb and Ir-26%Nb / Ir-28%Nb single-phase diffusion couples, respectively. While the diffusion coefficient in the solid-solution phase turns out to be similar in magnitude to the tracer self diffusion coefficient in pure iridium, the diffusion in the L1₂ compound has been found to be extremely slow: the diffusion coefficient is about 1/20. The low diffusion rate in the compound phase must be beneficial for high-temperature performance of refractory superalloys based on the Ir-Nb system.

11:20 AM

Diffusion in Al₈₀Ni₂₀-Melts: Experiments and Simulation: *Axel Griesche*¹; Michael-Peter Macht¹; Günter Froberg²; S. M. Chathoth³; Andreas Meyer³; S. K. Das⁴; Jürgen Horbach⁴; ¹Hahn Meitner Institute; ²Technical University Berlin; ³Technical University Munich; ⁴University Mainz

In this contribution we report about the comparison between diffusion measurements and molecular dynamic simulations (MDS) in Al-Ni melts. The direct long-capillary method was used to measure Ni self diffusion and to measure interdiffusion in liquid Al-Ni alloys. Convective contributions to the diffusion measurements were detected and could be corrected by measuring the time dependence of the diffusion coefficients. In addition the indirect quasi-elastic neutron scattering was used to measure convection-free Ni self diffusion. MDS were used to determine self diffusion of Al and to determine also interdiffusion. The comparison between experiment and simulation shows an excellent agreement of the interdiffusion coefficients as a function of temperature. The simulation results reflect also the experimentally found phenomenological relation between self diffusion, interdiffusion and thermodynamic forces in Al₈₀Ni₂₀, which was described originally by L.S. Darken.

11:45 AM

Diffusional Reaction Layers in the Rod-Type U-Mo/Al Dispersion Fuel during the Irradiation: *Ho Jin Ryu*¹; Jong Man Park¹; Chang Kyu Kim¹; Yeon Soo Kim²; Gerard L. Hofman²; ¹Korea Atomic Energy Research Institute; ²Argonne National Laboratory

U-Mo/Al dispersion fuel has been developed as one of the most promising candidates for a high performance research reactor fuel. Although a diffusional reaction between the U-Mo fuel and Al matrix results in complicated phenomena, it is necessary to understand the reaction layer growth behavior for the estimation of thermal performance and swelling behavior of the dispersion fuel. Reaction layers in rod-type U-Mo/Al dispersion fuels were observed after irradiation in the HANARO research reactor in this study. Scanning electron microscopy and electron probe microanalysis were used to observe microstructures and compositional profiles. The results from the in-reactor irradiation test were compared with out-of-pile results from diffusion couple tests and annealing tests. The effect of reaction layer on the thermal conductivity was analyzed for the calculation of the temperature profile of a fuel element.

Phase Stability, Phase Transformation and Reactive Phase Formation in Electronic Materials V: New Process for Cu Interconnects and Semiconductor Materials

Sponsored by: The Minerals, Metals and Materials Society, TMS Electronic, Magnetic, and Photonic Materials Division, TMS Structural Materials Division, TMS: Alloy Phases Committee

Program Organizers: Katsuaki Suganuma, Osaka University; Douglas J. Swenson, Michigan Technological; Srinivas Chada, Jabil Circuit, Inc.; Sinn Wen Chen, National Tsing-Hua University; Robert Kao, National Central University; Hyuck Mo Lee, Korea Advanced Institute of Science and Technology; Suzanne E. Mohney, Pennsylvania State University

Tuesday AM
March 14, 2006

Room: 213B
Location: Henry B. Gonzalez Convention Ctr.

Session Chairs: Douglas Swenson, Michigan Technological; Masanori Murakami, Kyoto University

8:30 AM Invited

Reduction of Electrical Resistivity of Cu Interconnects: *Masanori Murakami*¹; Miki Moriyama²; Susumu Tsukimoto¹; Kazuhiro Ito¹; Takashi Onishi³; ¹Kyoto University; ²Toyoda Gosei Company, Ltd.; ³Kobe Steel, Ltd.

Although Cu was found to be attractive as interconnect materials for ultra-large scale integrated (ULSI) Si devices, the electrical resistance of Cu films was found to increase significantly when the film thickness was thinner than 70nm. In this talk we will first review our recent results on (1) determination of the primary factor to increase the electrical resistivity of nano-scale Cu films, (2) development of a fabrication technique for low resistance Cu films, and (3) formation of extremely thin diffusion barriers between Cu films and insulators by adding a small amount of a second element to Cu interconnects. Then, we will propose a new fabrication process of Cu interconnects using a sputter-deposition and high temperature reflow technique.

9:05 AM

Good Thermal Stability Cu Films for Advanced Barrierless Metallization: Jinn P. Chu¹; C. H. Lin²; ¹National Taiwan Ocean University; ²Chin-Min Institute of Technology

Copper has a lower electrical resistivity and better reliability to electromigration than aluminum. Therefore, Cu and its alloys have been widely used for metallization in microelectronics and TFT-LCD. However, Cu diffuses readily into Si and SiO₂, and copper silicide forms at low temperatures. Our prior studies showed that doping with a small amount of the insoluble elements such as W increased the thermal stability of Cu films. In this study, Cu films with dilute amounts of insoluble substances, such as WC and WNx, prepared using co-sputtering were characterized. It is found that the thermal stability of Cu has been greatly improved without a barrier layer on Si up to 600°C while maintaining the low resistivity. Various characterization techniques including XRD, FIB, SIMS, TEM, XPS, electrical resistivity and current-voltage (I-V) curve measurements are employed to evaluate the thermal stability of Cu films. The results are discussed.

9:30 AM

Structural and Passivative Behaviors of Cu(In) Thin Film: Jau Shiung Fang¹; Hsin Yi Hsieh¹; ¹National Formosa University

Self-passivated copper as a gate electrode in the form of In₂O₃/Cu/In₂O₃/SiO₂ has been obtained by annealing Cu (In) alloy film in this study. The deposition of a Cu (In) thin alloy film to cause the formation of a In₂O₃/Cu/In₂O₃ trilayer and nano structure with low Cu resistivity, good adhesion to SiO₂, and excellent passivation capability. Studied Cu (In) films were prepared by a cosputtering method on Corning Eagle²⁰⁰⁰ glass substrate, and annealing under ambient from 200-500°C for 10-30 min. Structural analyzing were performed by XRD, SEM and TEM. Only copper diffraction peaks can be detected for the as-deposited film. However, annealing the film at an elevated temperature induced a formation of In₂O₃

phase. Resistivity was decrease with increasing annealing temperature, thus induced a low resistivity below $5 \mu\Omega\text{-cm}$. Results of the preliminary study can be potentially adopted in the application of TFT-LCD gate electrode and copper metallization in integrated circuits.

9:55 AM

Atomic Bond and Property of Al-Cu Alloy with (Al₂Cu): *Gao Yingjun*¹; ¹Guangxi University

Atomic bond of (Al₂Cu) in Al-Cu alloy is calculated by using empirical electron theory (EET) in solid. The results are showed that the Cu-Cu bond in phase is the strongest, while the second strongest bond is the Al-Cu bond. They were all stronger than the strongest Cu-Cu bond in pure Cu metal. These are the reason that only precipitation in Al-Cu thin-film alloy can be find when fewer vacancy being in the alloy in higher temperature. The electromigration lifetime of Al-Cu thin-film alloy for interconnects is concerned with the strong atomic bonding in particles which dispersed in matrix of alloy. The precipitation in Al-Cu thin-film alloy can enhance the strength of alloy and increased the electromigration lifetime for interconnects.

10:20 AM Break

10:30 AM

Metal-Semiconductor Amorphous+Nanoscale Ge Phase Composites Produced by Rapid Solidification and by Devitrification of an Amorphous Matrix: *Dmitri Louzguine*¹; *Akihisa Inoue*¹; ¹Tohoku University

Ge-rich alloys containing up to 70 at.% Ge were produced in Ge-Al-Cr-RE (RE-rare earth elements) systems while Si-based amorphous alloys containing up to 60 at.% Si were produced in S-Al-TM systems (TM-transition metals) by the melt-spinning technique. The samples are ribbons of 10-100 μm in thickness. In the present work we summarize our findings on the formation of the nanocrystal-amorphous composites containing nanoscale semiconductive Ge or Ge(Si) solid solution particles homogeneously distributed in the conductive amorphous matrix. Nanocomposites in Si-Al-TM-Ge (TM-transition metals) and some Ge-Al-Cr-RE alloys were produced directly by rapid solidification while in the Ge₅₅Mg₃₅Y₁₀ alloy they were produced by devitrification of the glassy phase on heating. The semiconductive nanoparticles exhibit homogeneous distribution and their size is varied from about 5 to 20 nm. The structure, phase transformations and properties of the samples will be discussed.

10:55 AM

Insulator to Metal Phase Transformation of VO₂ Films upon Femtosecond Laser Excitation: *Sergiy Lysenko*¹; *Valentin Vikhnin*¹; *Armando Rua*¹; *Zhang Guangjun*¹; *Felix Fernandez*¹; *Huimin Liu*¹; ¹University of Puerto Rico

The laser induced insulator-to-metal (I-M) phase transition in VO₂ thin films was explored by femtosecond optical pump-probe spectroscopy. The 130 femtosecond laser pulses were applied to study of transient reflection and relaxation processes in VO₂ films with different concentration of oxygen vacancies, deposited by laser ablation on amorphous and crystalline substrates. I-M transition was observed on a 10^{-11} - 10^{-9} sec temporal-scale where phase transition can be considered as a competitive process between thermal and light-induced phase transition mechanisms. The laser excitation is able to produce Frenkel and Wannier-Mott vibronic excitons in VO₂. Excited state dynamics in such a system are strongly dependent on the concentration of structural defects and excitation laser power. Analysis of transient reflectivity properties of qualitatively different VO₂ films allows suggesting the excitonic-controlled light-induced insulator to metal phase transition mechanism in VO₂ via an intermediate state.

11:20 AM

Photoinduced Reflectivity Transients in Vanadium Dioxide: *Sergiy Lysenko*¹; *Valentin Vikhnin*¹; *Armando Rua*¹; *Guangjun Zhang*¹; *Felix Fernandez*¹; *Huimin Liu*¹; ¹University of Puerto Rico

Vanadium dioxide is phase transition functional material which exhibits first order insulator-to-metal phase transition (PT) at the temperature about 340 K or under optical photoexcitation. The ultrafast pump-probe optical spectroscopy can provide unique information about transient structural and electronic properties of solid. We summarize the results of transient reflectivity for VO₂ thin films in semiconductor and metallic phases; the VO₂ reflectivity data for 130 femtosecond laser pulses was recorded

at 295 K and 410 K. It was found that the relative reflectivity changes after photoinduced and thermally-induced PT are different. Such a difference can be related to formation of an excited state during photoinduced PT. Pump-probe reflectivity measurements of VO₂ in metallic phase shows nonlinear optical response with the two-stage relaxation process on the 10^{-9} and 10^{-6} temporal-scales. Structural and carrier dynamic in VO₂ will be discussed in the framework of excitonic model.

11:45 AM

High Reflection and Low Contact Resistance of Ni/Ag(Al) Contact to Thin-GaN LED: *Chiahshien Chou*¹; *Cheng-Yi Liu*¹; ¹National Central University

A high reflective and low contact resistance p-GaN electrode contact is required for n-side up thin-GaN LED structure. Conventionally, Ni-O/Au/Al or Ag metallization scheme was used as p-GaN contact, in which Al or Ag reflector served as a high reflective layer. However, it has been reported that this contact scheme would be significantly degraded during the chip and packaging processes. Especially, Au and Ni-O layer have high absorption coefficient for the ultraviolet region. In this study, we design a Ni/Ag(Al) metallization scheme for the p-GaN electrode contact. Our preliminary results show that this contact scheme has high thermal stability in reflectivity and contact resistance in UV regime. Also, this metal scheme can be used as the electrode contact for n-GaN.

Phase Transformations in Magnetic Materials: Magnetic Nanocrystals and Nanoparticles

Sponsored by: The Minerals, Metals and Materials Society, TMS Materials Processing and Manufacturing Division, TMS/ASM: Phase Transformations Committee

Program Organizers: Raju V. Ramanujan, Nanyang Technological University; William T. Reynolds, Virginia Tech; Matthew A. Willard, Naval Research Laboratory; David E. Laughlin, Carnegie Mellon University

Tuesday AM
March 14, 2006

Room: 213A
Location: Henry B. Gonzalez Convention Ctr.

Session Chairs: Robert D. Shull, National Institute of Standards and Technology; Vincent G. Harris, Northeastern University

8:30 AM Introductory Comments Raju V. Ramanujan, M. Willard, W. T. Reynolds, Jr. and D. E. Laughlin

8:35 AM Invited

Microstructural Development and Influence on the Properties of Nanocrystalline Soft Magnets: *Matthew A. Willard*¹; *Todd Heil*¹; *Ramasis Goswami*²; ¹Naval Research Laboratory; ²Geo-Centers

Soft magnetic materials consisting of nanocrystallites surrounded by a residual amorphous matrix provide excellent properties, including both low coercivity and high magnetization. They are produced by rapid solidification processing with devitrification by isothermal annealing. Ultimately, to obtain the highest permeability and lowest core losses, the microstructure must be successfully optimized, with grain diameters less than 10 nm and retained amorphous matrix. Typically, this microstructure is developed during an isothermal anneal between 450 and 650°C. This study will examine the influence of composition, kinetics, and microstructure on the magnetic properties of (Fe,Co,Ni)-Zr-B-Cu alloys. Differential thermal analysis, thermomagnetic analysis, x-ray diffraction, and transmission electron microscopy will be used to describe the phase transformations and the resulting structure/property relationships.

9:10 AM Invited

Microstructure-Property Relationships of Rare Earth Nanophase Magnets: *Kazuhiro Hono*¹; ¹National Institute for Materials Science

Higher performance permanent magnetic materials are strongly desired for electric vehicles and aerospace applications. Candidates are either Nd-Fe-B or Sm-Co based rare earth magnets, the former is widely used for motors but the current sintered magnets do not have sufficient coercivity for the applications at 200C. The latter is for a higher temperature specifications for aerospace applications. In both systems, the control of nanoscale

microstructures are essential to improve the properties. One approach is to develop exchange coupled nanocomposite magnets. We will be presenting some examples of microstructure-property studies of melt-spun Fe/Nd₂Fe₁₄B nanocomposite magnets, but due to their isotropic nature, high performance cannot be achieved. To demonstrate the possibility of achieving higher performance magnets, we have fabricated an anisotropic Sm(Co,Cu)₅/FeCo exchange coupled thin films. In addition, we will comment on the controversies on the phase transformation and coercivity in Sm(Co,Cu,Fe,Zr)_{7.5} based magnets based on our recent microstructural investigations.

9:45 AM Invited

Structural Evolution and Process Refinement of Nanocrystalline Exchanged-Coupled Magnetic Films: Shashidhar Joshi¹; Soack Dae Yoon¹; Aria Yang¹; Nian X. Sun¹; Carmine Vittoria¹; Ramarsis Goswami²; Matthew Willard²; *Vincent G. Harris*¹; ¹Northeastern University; ²Naval Research Laboratory

Nanocrystalline exchanged-coupled alloys represent the latest development of soft magnetic materials for inductor applications. Although these alloys have been refined for power electronic applications, little work has been done on the processing of these alloys as films. In this paper, we report on the processing and refinement of nanocrystalline exchange-coupled films having compositions (Ni,Co,Fe)₈₈Zr₇B₄Cu_x (x=0,1). Films were processed at a range of temperatures and gas pressures using PLD. The softest magnetic properties (i.e. H_c <0.5 Oe) coincided to a deposition at 300°C in which an fcc grain size (D) was 6-8 nm separated by an amorphous phase of ~ 1 nm. A power law relationship is observed where H_c ∝ D^{3.5} for Cu containing alloys and H_c ∝ D² for the alloy without Cu. These results are consistent with the nanostructure being dominated by an uniaxial anisotropy. The addition of Cu appears to play a minor role in the crystallization.

10:20 AM Invited

Phase Transformations in High Density Magnetic Nanoarrays: *Raju V. Ramanujan*¹; Akhilesh Srivasatava¹; ¹Nanyang Technological University

The development of high density periodic nanoarrays composed of magnetic nanoparticles has several applications in the areas of information storage devices, biosensors and photonics. XRD, SEM, TEM and VSM techniques were utilized in this study of the nanoarrays. Nanowires and nanobowls of cobalt have been prepared by chemical synthesis techniques using porous alumina and polystyrene sphere templates, respectively. Cobalt nanoparticles were synthesized using the reverse micelle technique, vacuum assisted infiltration in the presence of an external magnetic field was used to infiltrate cobalt nanoparticles within the template. Heat treatment of the nanoarrays was then utilized to produce the morphology, size and crystal structure of the array elements possessing the desired magnetic properties. A systematic study of the role of phase transformations occurring during heat treatment was conducted, these results will be presented and discussed.

10:55 AM Break**11:05 AM**

Shape Effects in Magnetic Nano-Particles: Marco Beleggia¹; *Marc J. DeGraef*²; ¹Brookhaven National Laboratory; ²Carnegie Mellon University

It is well known that magnetostatic interactions between nano-particles are sensitive to the shape(s) of these particles. In this talk, we review recent progress in the description of magnetostatic interactions between uniformly magnetized particles of arbitrary shape. The assumption of a uniform magnetization state is justified by the fact that in the small particle limit, magnetic domain walls are energetically unfavorable. The uniformly magnetized state is, hence, a good first order approximation. A Fourier space representation of the particle shape leads to an explicit expression for the magnetometric tensor field, which takes the place of the conventional dipolar interaction field in energy computations. We will provide examples using cylindrical disks and rectangular prisms. It will be shown that, in a triangular array of three thin circular disks, shape-dependent interactions modify the ground state of the array.

11:25 AM Invited

The Effects of Processing Conditions on Chemically Prepared Magnetic Nanoparticles and Nanorods: *Lynn Kurihara*¹; Michael M. Miller¹; Marc P. Raphael¹; David J. Pena¹; Meghan P. McHenry¹; ¹Naval Research Laboratory

Chemical routes have been used to prepare magnetic nanoparticles and nanorods. Nanoparticles of Fe, Co, Ni, Fe_xCo_{100-x}, Fe_xPt_{100-x}, Fe_xNi_{100-x} and Co_xNi_{100-x}, were prepared using the polyol method or a modified polyol method. Using the polyol process we are able to produce monodispersed particle sizes from a few nanometers to microns in diameter. Depending upon their size and composition, these particles can span a range of magnetic behavior from superparamagnetic to ferromagnetic. Cobalt nanorods were prepared by electrodepositing the cobalt into alumina membranes. By varying the process conditions, cobalt nanorods can be prepared so that they are c-axis textured such that the hard magnetic axis is parallel to the principal axis of the rods. The phase purity and structure of the nanoparticles and rods were characterized using XRD. Morphologies were determined by AFM, SEM and TEM. Magnetic properties were measured using VSM and magnetic force microscopy (MFM).

Point Defects in Materials: Bulk Metal Diffusion

Sponsored by: The Minerals, Metals and Materials Society, TMS Electronic, Magnetic, and Photonic Materials Division, TMS Structural Materials Division, TMS: Chemistry and Physics of Materials Committee

Program Organizers: Dallas R. Trinkle, U.S. Air Force; Yuri Mishin, George Mason University; David N. Seidman, Northwestern University; David J. Srolovitz, Princeton University

Tuesday AM
March 14, 2006

Room: 210B
Location: Henry B. Gonzalez Convention Ctr.

Session Chair: David N. Seidman, Northwestern University

8:30 AM Invited

Recent Progress in the Theory of Diffusion Kinetics in Materials: *Graeme E. Murch*¹; Irina V. Belova¹; ¹University of Newcastle

Diffusion kinetics is that part of diffusion theory that deals with models where the defect-atom exchange frequencies are specified and produces, as its main result, tracer and chemical diffusion coefficients and ionic conductivities. The theory can be used where the input defect-atom frequencies come from various types of simulations and diffusion coefficients are then derived or it can be used in reverse in order to extract defect-atom exchange frequencies and correlation factors from experimentally measured diffusion coefficients. In this paper, we review recent findings on a number of such models including the five-frequency solute model, the random alloy model, vacancy-pair model and the four-frequency interstitial model with examples drawn from metallic alloys, intermetallics, ceramic oxides/silicates and alkali halides.

9:00 AM

A Self-Consistent Mean-Field Model for Diffusion in Concentrated Alloys: *Vincent Barbe*¹; Maylise Nastar¹; ¹Commissariat à l'Energie Atomique, Service de Recherches en Métall. Phys.

Building a diffusion model for interacting concentrated alloys based on an atomic scale description of the jump mechanism remains a current challenge. The SCMF theory* calculates the transport coefficients of an alloy through a Master Equation and a self-consistent estimation of a non-equilibrium distribution function expressed in terms of an effective Hamiltonian. Successive upgrades recently proved their efficiency in strongly correlated systems and dilute alloys** for the vacancy mechanism, for which the effective Hamiltonian is directly related to the return paths of the vacancy. Diffusion by the dumbbell mechanism is also addressed, including a realistic description of the set of jump frequencies. The results of the SCMF are discussed on the basis of Monte Carlo simulations in interacting systems. *Nastar et al., Phil Mag A 80 (2000) 155, PCCP 6 (2004) 3611; **Nastar, Phil Mag, 2005, in press.

9:20 AM

Formation Volume of Vacancies in Metals - Correlation with Poisson's Ratio: *Hiroshi Numakura*¹; ¹Kyoto University

The formation volume of atomic vacancies is an important parameter, particularly in diffusion, but experimental evaluation remains rather difficult. We have calculated the vacancy formation volume in some metals of the cubic structure by molecular statics simulation using embedded-atom potentials. The formation volume is found to be well correlated with Poisson's ratio. For bcc transition metals, it is close to 1 atomic volume in materials with Poisson's ratio close to 1/4, while it decreases almost linearly to 0.6 times atomic volume for those with Poisson's ratio of about 0.4. The simple relation may be utilized to estimate an approximate value for which experimental data are not available.

9:40 AM **Invited**

Stability and Mobility of Vacancy- and Interstitial-Clusters in Iron from First Principles: *François Willaime*¹; Chu-Chun Fu¹; ¹Commissariat à l'Énergie Atomique

The properties of point-defect clusters, with up to five vacancies or five interstitials, in iron are studied by DFT-GGA calculations performed on 128 atom supercells using the SIESTA code. The structure of the mono-interstitial is the <110> dumbbell in agreement with experiments and the migration energies of mono-vacancies and mono-interstitials are 0.67 and 0.34 eV against 0.55 and 0.30 eV experimentally. The structures of vacancy clusters are similar to that proposed from empirical potentials - with a second-neighbor configuration for the di-vacancy - and unexpected low migration energies are predicted for the tri- and quadri-vacancies (0.35 and 0.48 eV). Interstitial clusters are made of parallel <110> dumbbells, up to the quadri-interstitial, and of <111> dumbbells at larger sizes. Up to the tri-interstitial, they migrate by the translation-rotation Johnson mechanism. When used as input data in a Kinetic Monte Carlo simulation, these results successfully account for the kinetics of defects in irradiated iron.

10:10 AM **Break**

10:25 AM **Invited**

On the Diffusion of Substitutional Solutes in Nickel: *Roger C. Reed*¹; Chong Long Fu²; Maja Kremer²; ¹Imperial College; ²Oak Ridge National Laboratory

Nickel alloyed with solutes from the d-block of transition metals form the basis of the superalloys - as used for jet engine and industrial gas turbine applications. Vacancy-assisted diffusion controls a number of important phenomena: dislocation creep, precipitate coarsening, oxidation. In this paper, we will report on recent experimental and theoretical work which has aimed to identify patterns of behaviour inherited from the periodic table. Our experimental work rests on the traditional approach of Boltzmann-Matano for the quantification of interdiffusion rates. The theoretical work - using first principles methods - has helped us to rationalise our results. Elements from the centre of the d-block (such as Re) diffuse slowly because of a high activation energy for solute/vacancy exchange. Correlation effects are important only for solutes from the far west and far east of the d-block, e.g. Hf and Au. Predictions for the 3d solutes will also be presented.

10:55 AM

Ab Initio Calculations of Point Defect Formation and Migration in FCC Metals: *Julie D. Tucker*¹; Dane D. Morgan¹; Todd R. Allen¹; Reza Najafabadi²; ¹University of Wisconsin - Madison; ²Lockheed Martin Corporation

Point defects in metals, such as those created in radiation environments, can cause severe degradation of mechanical properties and changes in grain boundary compositions. While vacancy formation and migration mechanisms are well established, quantitative studies on interstitial configurations and migration paths in FCC metal alloys are quite limited. In this work we study the Fe-Ni-Cr alloy system. For each pure element *ab initio* calculations were performed for vacancies and multiple possible interstitial configurations. The most probable diffusion mechanisms have been further investigated to locate the minimum energy migration paths and associated energy barriers for vacancies and interstitials. Many of these values are not available experimentally and *ab initio* calculations allow us to generate a consistent set of diffusion barriers for use in a kinetic model to simulate radiation induced segregation in Fe-Ni-Cr alloys.

11:15 AM

Point Defect Properties in bcc Fe from an Ab Initio Point of View: *Christophe Domain*¹; Charlotte S. Becquart²; Edwige Vincent¹; ¹Electricite De France; ²University of Lille 1

Under ageing or irradiation, the changes of the macroscopic properties such as the hardness or the brittleness are partly due to the evolution of the microstructure, which is governed by the formation and diffusion of point defects (vacancies and interstitials). In order to model the defect evolution, with for instance kinetic Monte Carlo, the knowledge of these elementary properties is required. In this work, point defects as well as small point defect clusters in bcc Fe have been studied and characterised, in terms of their formation and migration energies using density functional theory calculations. The effect of solute atoms will also be discussed. The results are analysed in terms of diffusion properties in order to compare with experimental data and to get input data for upper scale simulations such as kinetic Monte Carlo. Furthermore, point defects properties in bcc Fe are compared to those in other bcc transition metals.

11:35 AM

Diffusion of Small Interstitial Clusters in Fe: *Napoleon Anento*¹; *Anna Serra*¹; Yuri N. Osetsky²; ¹Politechnical University; ²Oak Ridge National Laboratory

Small clusters of self interstitial atoms (SIAs) in Fe can be stable as both <110>-dumbbells and <111>-crowdions. They are mobile and depending on the temperature and size may perform one-dimensional (1D) or three-dimensional (3D) diffusion. We present here the results of modeling of motion of clusters up to 7 SIAs over a wide temperature range. Particular attention was paid to the transition from 3-D to 1-D motion as a function of cluster size. Jump frequency, correlation factors, diffusion coefficient and activation energies for different mechanism were obtained. The results are discussed in application to microstructure evolution of neutron irradiated Fe. This change in orientation has implications in the global microstructure evolution. In this work we study the diffusion of small clusters by atomic computer simulation and we compare the results obtained with two potentials that show different stability for the single dumb-bell interstitial.

Polymer Nanocomposites: Session I

Sponsored by: The Minerals, Metals and Materials Society
Program Organizer: Devesh K. Misra, University of Louisiana at Lafayette

Tuesday AM
March 14, 2006

Room: 217A
Location: Henry B. Gonzalez Convention Ctr.

Session Chair: Hilmar Koerner, University of Dayton Research Institute

8:30 AM **Invited**

3-D Morphology Control of Polymer Nanocomposites Using Electric Fields: *Hilmar Koerner*¹; Evangelos Manias²; Wei Lu³; Devesh Misra⁴; Richard Vaia⁵; ¹University of Dayton Research Institute; ²Pennsylvania State University; ³University of Michigan; ⁴University of Louisiana at Lafayette; ⁵Air Force Research Laboratory/MLBP

The term 'nano-composites' invokes parallels to traditional fiber reinforced composite technology and the ability to spatially 'engineer, design and tailor' materials performance for given applications. At present, minimal methodologies exist to realize this degree of control of nanoparticle dispersion in polymers. Herein, AC electrokinetics will be discussed as an approach to provide non-invasive, spatial and orientational control of organically modified layered silicates in polymers. Experimentally, electric fields smaller than 0.5 V/microns align nanoparticles parallel to the applied field direction in an uncured epoxy matrix. Theoretical simulations reveal remarkably rich dynamics. Alignment and exfoliation behavior is significantly affected by particle shape and dielectric properties of nanoparticles and medium. As predicted, thermal coefficient of expansion, tensile strength and dynamic mechanical response depend on nanoparticle orientation and particle/matrix interface. These results present

TUESDAY AM

new possibilities for investigating mechanical and transport properties at interfaces and provide the initial step to a 'true' nano-composite paradigm.

9:00 AM Invited

Limitations of Mechanical Improvement for High-Stiffness Polymers Layered-Inorganic Nanocomposites: *Evangelos Manias*¹; George Polizos¹; Matthew Heidecker¹; ¹Pennsylvania State University

Nanometer-thin inorganic fillers are currently being explored for the improvement of the mechanical properties of various polymers. Although the nanocomposite structure offers generally-applicable principles for such enhancements across all polymers, there exist realistic limitations for the extent of improvement that can be achieved. A comparative discussion, across several polymers reinforced by the same layered inorganic fillers, aims in revealing these limitations and tracing their molecular origins to the polymer/filler interactions and the filler characteristics. Simple theoretical arguments quantifying the relevant dependencies will also be discussed.

9:30 AM Cancelled

Catalyzing Carbonization of Polypropylene/Clay Nanocomposites for Synthesizing CNTs and Improving Fire Retardancy

9:55 AM

Development and Characterization of Nanocomposite Films for Extended Lunar and Mars Explorations: Iris V. Rivero¹; Mark S. Paley²; Benjamin G. Penn³; Donald O. Frazier³; *Keith Jones*¹; ¹Texas Tech University; ²AZ Technology; ³NASA/Marshall Space Flight Center

Gas barrier, chemical resistant, non-toxic ethylene-vinyl alcohol copolymer (EVOH) has been a subject of research at NASA for devising materials useful as liners in habitat structures for extended Lunar and Mars explorations. Specifically, the innate gas barrier property of this copolymer is attractive for habitat structures to secure the high level of hermeticity required in these extreme environments. In addition, factors such as the abrasiveness of Lunar and Martian regolith, micrometeorite showers, and launch and landing exhaust plume introduce the requirement for the liner material to be able to absorb impact-energy and to be tear resistant. An alternative to impart strength to EVOH while retaining its film flexibility is to embed EVOH with single-wall carbon nanotubes (SWCNTs) due to their high strength-to-weight ratio property. This research will present a methodology for dispersing SWCNTs in EVOH films followed by an evaluation of the resultant nanocomposite's mechanical and microstructural properties.

10:20 AM

Effect of Stylus Radius on the Scratch Resistance of Polymer Nanocomposites: *Qiang Yuan*¹; Devesh K. Misra¹; ¹University of Louisiana at Lafayette

The effect of stylus radius and temperature on the scratch resistance of various polymer nanocomposites is studied. Electron microscopy is used to study the micromechanism and the corresponding theoretical explanation is proposed. Moreover, the results are compared with that of the effect of notch radius on the toughness of the polymers and their blends.

10:45 AM Break

10:55 AM

Essential Fracture Work of Polymer-Silicate Nanocomposites: *Yu Qiao*¹; Jigar K. Deliwala¹; ¹University of Akron

In a fracture experiment, it was discovered that, when the cooling rate was increased, the fracture toughness of a polyamide 6-silicate nanocomposite increased by 50-100% in a broad range of silicate content up to about 4 wt.%. According to the x-ray diffraction analysis, a high cooling rate would promote the formation of gamma phase and suppress the growth of spherulites. The final failure was dominated by the microvoiding induced by intercalated nanolayer stacks. Further investigation showed that, while the background energy dissipation was strongly dependent on the morphology, the essential near-field fracture work was quite constant. Thus, the dependence of the fracture resistance on the cooling rate should be attributed to the variation in viscosity, instead of the change in crack-tip plastic deformation mechanisms.

11:20 AM

Hierarchical Structure, Properties, and Scratch Resistance of Melt Intercalated Polymer-Clay Nanocomposites: *Anand Mudaliar*¹; Raghunath Rao Thridandapani¹; Q. Yuan¹; Devesh K. Misra¹; ¹University of Louisiana at Lafayette

The addition of nanoparticles or nanoclays to polymers has been extensively studied in recent years to examine the benefit of their addition in enhancing mechanical and thermal barrier properties. However, only a few studies have been devoted towards understanding the deformation behavior. In the present study the hierarchical structure of melt-intercalated polymer nanocomposites and the interaction of clay with the polymer matrix studied by high resolution transmission electron microscopy (HRTEM), x-ray diffraction, and Fourier-transform infrared spectroscopy (FTIR) is combined to establish relationships among scratch/mar resistance and deformation mechanism.

11:45 AM

Effects of Filler and Temperature on the Stability of B-Crystal of Glass Bead Filled Polypropylene: *Qiang Yuan*¹; Wei Jiang²; Lijia An²; Devesh K. Misra¹; ¹University of Louisiana at Lafayette; ²Changchun Institute of Applied Chemistry

The effects of crystallization temperature (T_c), filler content and filler size on the b-crystal and structural stability of original b-crystal of glass bead filled polypropylene (PP) are studied. Differential scanning calorimetry (DSC) measurements indicate that the amount of b-crystal in PP crystals is a function of T_c as well as glass bead content. Additionally, disorder parameter deduced from DSC data is defined for the characterization of structural stability of original b-crystal. The results indicate that the increase of glass bead size would decrease the content and stability of b-crystals.

Sampling, Sensors and Control for High Temperature Metallurgical Processes: Session I

Sponsored by: The Minerals, Metals and Materials Society, TMS Extraction and Processing Division, TMS: Process Fundamentals Committee, TMS: Process Modeling Analysis and Control Committee, TMS: Pyrometallurgy Committee
Program Organizer: Robert L. Stephens, Teck Cominco Metals Ltd

Tuesday AM
March 14, 2006

Room: 8B
Location: Henry B. Gonzalez Convention Ctr.

Session Chair: Thomas P. Battle, DuPont Company

8:30 AM

Advanced PC Programmed Level Control for Quality Casting Using Precimeter Control System - Part I: Principle and Devices for Flow Control: *Masao Suzuki*¹; Hans Wilhelm¹; Jan Strombeck¹; ¹AI Tech Associates

In order to cast aluminum and its alloys or other metals, it is necessary to accurately control the flow of the metal out of the furnace. This is achieved by measuring and controlling the level of the molten metal surface downstream. Precimeter Control AB has studied and developed intelligent and affordable solutions to make these operations automatic for implementation in automated facilities and quality assurance processes. This principal is based on laser triangulation using digital camera technology. This combination is unique and it features many advantages like a high accuracy and reliable function in difficult industrial environments. The Precimeter Control System consists of a ProH digital camera sensor and incorporates an actuator equipped with a control unit of a tap-out rod, pin-plug rod and or gate-valve. First, the ProH sensor measures the level or height displacement. This measured signal is then converted to a control signal of 4-20mA.

8:50 AM

Advanced PC Programmed Level Control for Quality Casting - Part II: Examples for Casthouse Application Using Precimeter Control System: *Masao Suzuki*¹; Hans Wilhelm¹; Jan Strombeck¹; ¹AI Tech Associates

In order to cast aluminum and its alloys or other metals, it is necessary to accurately control the flow of the metal out of the furnace. This is achieved by measuring and controlling the level of the molten metal surface downstream. Precimeter Control AB has studied and developed intelligent and affordable solutions to make these operations automatic for implementation in automated facilities and quality assurance processes. This principal is based on laser triangulation using digital camera technology. This combination is unique and it features many advantages like a high accuracy and reliable function in difficult industrial environments. The Precimeter Control System consists of a ProH digital camera sensor and incorporates an actuator equipped with a control unit of a tap-out rod, pin-plug rod and or gate-valve. First, the ProH sensor measures the level or height displacement. This measured signal is then converted to a control signal of 4-20mA.

9:10 AM

Challenges in Sampling, Metallurgical Accounting and Reconciliation of Primary Smelting Furnaces: *Jacques J. Eksteen*¹; Chris Cutler¹; ¹University of Stellenbosch

Primary smelting furnaces pose unique difficulties in the sampling and materials mass flow and inventory measurement. This paper reviews the requirements for good sampling practice, and how conflicting requirements for good furnace operation and design often makes reliable closure of the metallurgical balance tenuous at best. Design and smelter operation requirements for metallurgical accountability will be reviewed. Typical physical causes of variance and bias will be identified together with methods to eliminate or minimize them.

9:30 AM

Development and Field Testing of a Prototype Aluminum Tapping Camera: *David L. Death*¹; Luke J. Pollard¹; Craig A. Rogers¹; Paul Gwan²; Simon Maunder²; Flavio Giurco³; Peter Herd⁴; Andrew Johnston⁵; ¹CSIRO Minerals; ²CSIRO Industrial Physics; ³Aloca; ⁴Tomago Aluminium; ⁵Comalco

The Tapping Camera Prototype (TCP) is a prototype instrument developed to record and analyse video of the molten metal stream entering the tapping crucible as it is tapped from an aluminium reduction cell. The TCP mounts a wireless camera and periscope to view the molten metal stream via a peephole in the tapping crucible. Real time video is recorded to either digital video tape or computer disk for subsequent video analysis to quantify the bath material drawn into the tapping crucible with the molten aluminium. The images transmitted by the camera are available on a handheld LCD video screen. A peephole in the back of the periscope assembly allows the operator to directly view the tapping stream.

9:50 AM

Local Temperature Control for Die Casting Processes: *Tiebao Yang*¹; Henry Hu¹; Xiang Chen¹; Yeou-Li Chu²; Patrick Cheng²; ¹University of Windsor; ²Ryobi Die Casting (USA), Inc.

In high pressure die casting processes, a die plays a critical role in removing heat from the molten metal during the cavity filling and solidification stages. Proper control of die temperature is essential for producing superior quality components and yielding high production rates. This paper proposes a local temperature control scheme for die thermal management based on a computerized intelligent real-time monitoring and control system (IRMCS). In this scheme, cooling water lines are controlled by a pump and solenoid valves. A controller is designed according to the law of die temperature fluctuations. The results obtained from the experiments carried out on a laboratory die casting process simulator indicate that the controller can limit the local die insert temperatures in a given band. Hence, the desired thermal pattern of the die insert becomes achievable.

10:10 AM

Sensors, Laboratory Results and Modern Automatic Control Techniques: *Florian Kongoli*¹; I. McBow¹; R. Budd¹; S. Llubani¹; ¹FLOGEN Technologies Inc

The data provided by high temperature sensors as well as laboratory results are indispensable for an effective control of high temperature smelting processes. However the difficulty with sampling, the lack of timely laboratory measurements and the availability of proper sensors has impeded the effective use of these data for an efficient control. As a result,

the control has been carried out mostly in a classical and static way. It has been always attempted to find the best unique set of feed composition and conditions where the process could run smoothly. However this is associated with natural difficulties and some times has proven impossible due to various reasons. In this work a new approach for an effective control of these processes has been discussed. This not only allows a better control but also a continuous optimization of the processes and can serve as an adequate means for automation.

10:30 AM

Variance and Heterogeneity in Melt Samples from Industrial Ferro-Alloy Furnaces: *Jacques J. Eksteen*¹; Elton L. Thyse¹; Makiwe Nkohla¹; ¹University of Stellenbosch

Any effort to improve the metallurgical control of industrial furnaces employed in the primary extraction of high carbon ferroalloys are bound to fail unless the variability of the melt is not fully accounted for. A number of sampling campaigns were performed on both 3phase AC submerged arc and single phase DC open arc furnaces at different smelter sites in South Africa where High Carbon Ferrochrome is produced. It was found that the heterogeneity between multiple samples during a single taps were much higher than for heterogeneity found within a sample. Moreover, this heterogeneity (as quantified by the relative standard deviation per tap) varied with the operating conditions of the furnace, the element monitored and the type of furnace. A relationship was found between the relative standard deviation of certain elements and the degree of subcooling of the melt.

10:50 AM

Modeling and Control of Magnetite Behavior in Copper Isasmelt Smelting Slag: *Pengfu Tan*¹; Pierre Vix¹; ¹Xstrata Copper

One copper Isasmelt furnace has been operated in Xstrata Copper at Mount Isa in Australia since 1992. A thermodynamic model has been developed to simulate the magnetite behavior in copper Isasmelt furnace. The effects of the process parameters on the content of magnetite in copper slag have been predicted and discussed. These process parameters includes SiO₂/Fe, matte grade, coke or coal, size of coke or coal, temperature, slag concentrate in the feed, oxygen enrichment, and CaO content in slag.

11:10 AM

Modeling of SEMTECH OPC Signals in P-S Converter: *Pengfu Tan*¹; Pierre Vix¹; ¹Xstrata Copper

The SEMTECH OPC system, developed by Semtech AB in Sweden, provides an indication of the endpoints in both converting stages by use of on-line spectroscopy. SEMTECH OPC measures the levels of PbO and PbS emission in the gaseous flame created during the slag and copper making stages of copper conversion. A telescope positioned in the line of sight of the flame detects PbO/PbS emissions. Focused light is transmitted by fiber-optic cable to the server cabinet that contains the spectroscopy hardware. Spectroscopic information is processed, stored, and sent to client screens in the converter control cabins. A thermodynamic mode has been developed to model the SEMTECH signals, in order to determine the slag chemistry, and skimming operations. Some useful information to the operators has been presented.

11:30 AM

Modeling, Control and Optimization of Chemistry and Viscosity of Copper Converter Slag: *Pengfu Tan*¹; Pierre Vix¹; ¹Xstrata Copper

The control of converter slag chemistry and viscosity has played an important role in optimizing converter operations. A thermodynamic model of copper P-S converter and a viscosity model of converter slag have been used to predict the chemistry and viscosity of converter slag. The effect of fluxing strategy, the ratio of SiO₂/Fe in slag, copper and anode skim charges, and temperature on viscosity and skimming operation of converter slag has been discussed. Some improvements of the industrial operations have been presented.

TUESDAY AM

Simulation of Aluminum Shape Casting Processing: From Alloy Design to Mechanical Properties: Alloy Design and Treatment

Sponsored by: The Minerals, Metals and Materials Society, TMS Light Metals Division, TMS Materials Processing and Manufacturing Division, TMS Structural Materials Division, TMS: Aluminum Committee, TMS/ASM: Mechanical Behavior of Materials Committee, TMS: Process Modeling Analysis and Control Committee, TMS: Solidification Committee, TMS/ASM: Computational Materials Science and Engineering Committee

Program Organizers: Qigui Wang, General Motors Corporation; Matthew Krane, Purdue University; Peter Lee, Imperial College London

Tuesday AM Room: 6D
March 14, 2006 Location: Henry B. Gonzalez Convention Ctr.

Session Chair: Y. Austin Chang, University of Wisconsin

8:30 AM Invited

Atomistic and Microstructural Modeling in Aluminum Cast Alloy Applications: *Christopher M. Wolverton*¹; ¹Ford Motor Company

The role of atomic-scale computations in the Integrated Computational Materials Science methodology applied to Al castings at Ford will be described. First-Principles atomic-scale computational methods are becoming increasingly used in industry due to their predictive power. However, their computational complexity often limits their use to relatively simple systems. Hence, we have focused on coupling first-principles methods with other computational approaches such as phase-field microstructural evolution models, computational thermodynamics or CALPHAD methods, and cluster expansion methods and kinetic Monte Carlo. The resulting combined models have been applied to alloys in the Al-Si-Cu-Mg system, and applications to precipitation, heat treatment, microstructural evolution, and yield strength have proved fruitful.

8:55 AM Invited

Multi-Scale Structural Design and Processing for Increased Strength in Aluminium Alloys: *Barry C. Muddle*¹; Jian-Feng Nie¹; Christopher R. Hutchinson¹; ¹ARC Centre of Excellence for Design in Light Metals, Monash University

A design protocol for optimizing structural parameters that may be manipulated to maximize strength in aluminium alloys will be outlined. Attention will be directed to alloy composition, grain size, inclusion content and distribution, and dispersed strengthening constituents. In the case of heat-treatable alloys, recent work in wrought materials to rationalize the roles of precipitate identity, form, crystallography and distribution, and the control of dispersed phases will be reviewed. The potential for extending the strategies utilized for strengthening wrought alloys to existing and emerging cast alloys will be examined. The design analysis will be accompanied by a review of existing and emerging approaches to materials processing that permit implementation and control of desired structural changes. Emphasis will be given to multi-stage heat treatments and to the potential for achieving efficiencies in thermal treatment utilising continuous processing. Issues associated with structural stability and the maintenance of property profiles will be discussed.

9:20 AM Invited

Advances in Computational Modeling of Microstructure Evolution in Solidification of Aluminum Alloys: *M. F. Zhu*¹; C. P. Hong²; D. M. Stefanescu³; Y. A. Chang⁴; ¹Southeast University; ²Yonsei University; ³Ohio State University; ⁴University of Wisconsin-Madison

During the last decade, extensive efforts have been dedicated to explore simulation models of microstructure formation in solidification of alloys. Numerical simulation of microstructure evolution can provide us the information for predicting and controlling solidification microstructures, and also the information for improving the fundamental understanding of solidification mechanism. This paper presents an overview of cellular automaton based models and of derived front tracking models, for the simulation of microstructure evolution in solidification of aluminum alloys. The models can be used for modeling meso-scale and micro-scale

solidification microstructures. The main achievements in this field are addressed by presenting examples encompassing a wide variety of problems including dendritic growth in binary and ternary alloys, dendritic growth with melt convection, and eutectic and peritectic solidification. Particular emphasis is made on the quantitative aspects of simulations. Finally, future prospects and challenges of solidification microstructure modeling are also discussed.

9:45 AM Invited

CALPHAD/First-Principles Hybrid Approach: The Study of Phase Equilibria and Solidification Behavior of the Al-Ni-Y System: *Dongwon Shin*¹; William Golumbfskie¹; Raymundo Arroyave¹; Zi-Kui Liu¹; ¹Pennsylvania State University

Al-Ni-Y alloys show excellent glass forming ability and are very promising for structural materials. In order to study the phase equilibria of this ternary system the CALPHAD (Computer Coupling of Phase Diagrams and Thermochemistry) approach is combined with results from first-principles calculations coupled with experimental data and existing CALPHAD models for the constituent binaries. The finite temperature thermodynamic properties including both enthalpy and entropy of ten ternary compounds in this system have been obtained through harmonic and quasi-harmonic approximations. The calculated formation enthalpy and lattice parameters showed good agreement with experiments. From the constructed thermodynamic database, phase equilibria and the liquidus projections were calculated. The solidification sequences for several alloys in this system were also studied through Scheil simulations and were compared with available experimental information.

10:10 AM Break

10:25 AM

Evolution of the Morphology of the Remaining Liquid Pool during the Last Stages of Solidification: *Hongbiao Dong*¹; Helen Atkinson¹; ¹University of Leicester

The morphology of the remaining liquid pool at the last stages of solidification is a critical factor affecting the formation of casting defect, such as hot tears. The evolution of morphology has been related to the dihedral angle ($2q$) in previous studies. In this paper, the effect of solute diffusion in solid phase on the morphology of the remaining liquid and the area fraction of solid phase covered by liquid phase is described for a two dimensional hexagonal network, by assuming a constant dihedral angle. Predicted microsegregation using a numerical model including the proposed description shows a better fit with experimental observation in Al-Cu alloys.

10:50 AM

Modeling of Hydrogen in Aluminum Foundry Melt Treatment Operations: Christian Simensen¹; Oyvind Nielsen¹; Jan Ove Løland²; Steinar Sælid³; ¹SINTEF; ²Alcoa Automotive Castings; ³Prediktor

Variations in hydrogen content in aluminium melts due to variations in weather, alloy, and process conditions constitute a significant part of the large variability of properties in shaped castings. On one hand, it is well-known that the combination of hydrogen and oxide inclusions promotes the formation of gas porosity in castings, which has a negative impact on mechanical properties. On the other hand, a stable "non-zero" hydrogen content may significantly reduce the reject rate in structural castings by dispersing the macroshrinkage in poorly feed regions into micropores. Thus, the prediction of the hydrogen content in the melt to be cast would be useful for reducing the variability in foundry processes. In the present work, a semi-empirical model describing the evolution of hydrogen in various foundry melt treatment operations is presented. Furthermore, the implementation of this model in an online processes simulation installed at a LPDC foundry is described.

11:15 AM

Validation of Microsegregation Models by the Point-Matrix Approach: *Muthiah Ganesan*¹; David Dye¹; Peter D. Lee¹; ¹Imperial College London

Experimental characterization by the point-matrix approach has proven to be an effective means of validating microsegregation models. The accuracy of this method however depends strongly in the manner in which measured data are subsequently treated to yield segregation profiles. Here, an improved alloy-independent data treatment algorithm recently proposed

by the authors for the treatment of randomly sampled data has been applied to accurately examine and validate CALPHAD-type Scheil-Gulliver model predictions of the influence of grain refinement and/or Sr-modification on elemental segregation in an A319-type aluminum alloy. Comparison is also made to other available data sorting strategies and it is demonstrated that the normal procedure of independently sorting elemental data leads to inaccurate estimation of the solidification path of multi-component alloys. The influence of non-equilibrium interdendritic particles on the consequent sorted profiles is examined.

11:40 AM

Pressure Losses during Pressure Filtration Tests of Liquid Aluminium Alloys: *Xinjin Cao*¹; ¹Institute for Aerospace Research

There has been an increasing tendency to determine liquid metal quality using the pressure filtration methods in casting industry. However, little has been known about the pressure losses and the distributions as well as their influence on the structures of formed cakes. In this work, the pressure losses across the cakes and filter media during the Prefil Footprinter tests of liquid aluminium alloys have been calculated. The pressure losses and their distributions at the three phases (i.e. initial transient, steady and terminal transient stages) are discussed in details.

Solidification Modelling and Microstructure Formation: A Symposium in Honor of Prof. John Hunt: Columnar to Equiaxed Transition

Sponsored by: The Minerals, Metals and Materials Society, TMS Materials Processing and Manufacturing Division, TMS: Solidification Committee

Program Organizers: D. Graham McCartney, University of Nottingham; Peter D. Lee, Imperial College; Qingyou Han, Oak Ridge National Laboratory

Tuesday AM
March 14, 2006

Room: 6C
Location: Henry B. Gonzalez Convention Ctr.

Session Chairs: P. Lee, Imperial College; G. Lesoult, Ecole des Mines de Nancy

8:30 AM Invited

Columnar-to-Equiaxed Transition Revisited: Selim Mokadem¹; *Wilfried Kurz*¹; ¹Swiss Federal Institute of Technology

The original Hunt model on the columnar to equiaxed transition (CET) from 1984 allowed for the first time an understanding of this important microstructure transition. In experiments on laser repair of SX superalloys it became evident that even using more precise dendrite models Hunt's approach did not always lead to the right results. Two cases will be presented: (i) Dendritic growth: in off heat flow axis growth a columnar to columnar transition may occur, i.e. the new columnar structure reorients itself by competition into the heat flow direction; (ii) Cellular growth: even if no CET is expected when growth is in the heat flow direction, in off heat flow axis growth nucleation ahead of a divergent front is often observed. These two cases will be analysed and modelled. A model for the CET accompanied by a phase change will also be presented.

8:55 AM Invited

Influence of Macroseggregation on Developing Grain Structures: A Comparison of Predictions with Experimental Observations: Gildas Guillemot¹; *Charles A. Gandin*¹; ¹Ecole des Mines de Paris

Following Hunt's model to predict the extent of columnar and equiaxed grain structures in casting, deterministic approaches have been developed. The main limitation of the deterministic models is yet due to the grain shape approximations. Thus the impingement of an equiaxed grain with a growing front and its further preferred development in the direction of the temperature gradient is not accounted for. This limitation is overcome by considering the development of each individual grain. This is possible using stochastic models in which the growth front of each crystal is considered. Comparison between predictions and in-situ observations of the solidification of a binary alloy in the casting configuration proposed by Hebditch and Hunt is presented. The effect of macrosegre-

gation on the development of the structure is demonstrated. The model offers the possibility to quantify the approximation of using a model in which no consideration of the grain structure is accounted for.

9:20 AM

Recent Developments on Deterministic Models for the Description of the Columnar-to-Equiaxed Transition (CET): *Menghui Wu*¹; Andreas Ludwig¹; ¹University of Leoben

Since the first analytical model of J.D. Hunt in 1984, the so-called columnar-to-equiaxed transition (CET) has become one of most important subjects in solidification research. Today, there exist stochastic and deterministic models for CET predictions. In the present paper an overview on recent developments on deterministic models is given. It is demonstrated that with appropriated multi-phase volume-averaging approaches it is possible to account for nucleation and growth of equiaxed grains ahead of a growing columnar front in the presence of shrinkage-induced feeding flow, thermo-solutal buoyancy driven flow and grain sedimentation. Special modeling assumptions ensure that both CET mechanisms namely 'hard' and 'soft' blocking are described. It is demonstrated that although these models are highly sophisticated, under special conditions they still get similar results as Hunt's classical approach.

9:45 AM

Analysis of Columnar – Equiaxed Transition and Equiaxed Growth of Al – 3.5 Wt% Ni Alloys by In Situ Synchrotron X-Ray Radiography: *Guillaume Reinhart*¹; Henri Nguyen-Thi¹; Nathalie Mangelinck-Noël¹; Thomas Schenk²; Joseph Gastaldi³; Bernard Billia¹; Jürgen Härtwig⁴; José Baruchel⁴; ¹L2MP (Laboratoire Matériaux et Microélectronique de Provence); ²Laboratoire de Physique des Matériaux; ³CRMCN; ⁴ESRF

Physical mechanisms involved during grain growth and Columnar to Equiaxed Transition (CET) are related to dynamical events during solidification. Therefore, in situ and real time studies are required to improve our understanding of those phenomena. For metallic alloys, the use of X-ray sources provided by 3rd generation synchrotron allows such study. In this communication, we present results of x-ray radiography performed during experiments at the European Synchrotron Radiation Facility (ESRF). Directional solidifications of Al-Ni alloys were analysed to determine growth conditions of dendritic columnar or equiaxed regime. CET was studied by following the microstructure evolution and its characteristics induced by successive jumps of the pulling rate on refined samples. Several outstanding results are obtained: i) blocking mechanism of the columnar structure by equiaxed grains nucleation, ii) propagation of an effective front for fully equiaxed growth, iii) influence of the pulling velocity on the fully equiaxed microstructure morphology and grain density.

10:10 AM Break

10:25 AM Invited

Aspects of Nucleation Mechanisms on the CET in Al Alloys: *Peter Schumacher*¹; ¹University of Leoben

The columnar to equiaxed transition is central to the casting behaviour of foundry alloys. In particular the phenomenon of grain refinement is best described with the CET. Within the models of CET assumptions on the nucleation mechanism are contained which need to reflect the nucleation mechanism on added heterogeneous substrates. This paper will give an overview of nucleation mechanism observed in aluminium alloys on added grain refining particles and discusses their effect on the CET.

10:50 AM Invited

Two Versus Three Dimensional Simulation of the Columnar-to-Equiaxed Transition: *Hongbiao Dong*¹; Peter D. Lee²; ¹University of Leicester; ²Imperial College London

The influence of simulating the solute fields in the primary dendrite tip region during the transition from columnar to equiaxed growth in two dimensions versus three is investigated. A mesomodel that combines a cellular automaton description of solid growth together with a finite difference computation of solute diffusion was used. The variations in solute concentration and tip undercooling between 2D and 3D simulations is compared and contrasted to data from prior experimental observations and models. The importance of stereological effects on solute diffusion and the undercooling are discussed.

11:15 AM

Modelling Convection and Grain Impingement in Alloy Solidification Using Front-Tracking: Jerzy Banaszek¹; Shaun A. McFadden¹; David J. Browne¹; ¹University College Dublin

Modelling of columnar and equiaxed growth into undercooled metallic liquid is carried out using a front-tracking technique. The methodology is a 2D variant of the models of John Hunt and Steve Flood developed in the 1980s, and here progress on the inclusion of natural convection and grain impingement is reported. Via solution of the flow field occurring due to natural thermal convection in interdendritic and bulk liquid, it is predicted that such flow affects undercooling ahead of the growing columnar front and therefore changes the conditions created for equiaxed solidification. Modelling the growth of such equiaxed grains, both hard and partially soft impingement is simulated. In hard impingement there is no interaction with the solutal or thermal fields of neighbouring grains, but in semi-soft impingement the effects of latent heat evolving from nearby grains is simulated. It is shown that the interaction of such thermal fields alters dendritic growth conditions.

11:40 AM

Influence of Solidification Thermal Parameters on the Columnar to Equiaxed Transition of Al-Zn and Zn-Al Alloys: Alicia Esther Ares¹; Sergio Fabian Gueijman²; Ariane Bonczok²; Adriana Candia²; Miguel Angel Alterach²; Rubens Caram³; Carlos Enrique Schvezov²; ¹CONICET/UNAM; ²University De Misiones; ³DEMA-FEM-UNICAMP

The prediction of the columnar to equiaxed transition (CET) is of great interest for the evaluation and design of the mechanical properties of castings products. Experiments are conducted to analyze the CET during the upward unsteady state directional solidification of Al-Zn and Zn-Al alloys, under different conditions of superheat and heat transfer efficiencies at the metal/mould interface. A combined theoretical and experimental approach is developed to quantitatively determine the solidification thermal parameters: transient heat transfer coefficients, growth rates, thermal gradients and cooling rates. A numerical procedure combined with experimental results does not give support to CET criteria based either on growth rate or on temperature gradients. Rather, the analysis has indicated that a more convenient criterion should encompass both thermal parameters through the cooling rate. The effects of solidification parameters like cooling rate, growth rate, temperature gradient, melt superheat and solute concentration on the CET position are investigated.

Surfaces and Interfaces in Nanostructured Materials II: Nano-Structured Metals and Oxides

Sponsored by: The Minerals, Metals and Materials Society, TMS Materials Processing and Manufacturing Division, TMS: Surface Engineering Committee

Program Organizers: Sharmila M. Mukhopadhyay, Wright State University; Narendra B. Dahotre, University of Tennessee; Sudipta Seal, University of Central Florida; Arvind Agarwal, Florida International University

Tuesday AM
March 14, 2006

Room: 209
Location: Henry B. Gonzalez Convention Ctr.

Session Chair: Narendra B. Dahotre, University of Tennessee

8:30 AM

A Cross-Strip Comparison Study of Cu Surface/Interface Electromigration: Jee Yong Kim¹; Nancy Michael¹; C.-U. Kim¹; ¹University of Texas at Arlington

With the use of Cu interconnects in integrated circuits, several new technical and theoretical challenges are emerging. One of these is the effect of the interface on Cu electromigration. In this study, the effect of interface materials on electromigration rate at the Cu surface/interface is investigated using a simple cross-strip configuration which enables a direct comparison of interface and surface electromigration rates. Surprisingly, the polarity of void and hillock formation appears to indicate a higher electromigration rate at the Cu/Ta interface than at the Cu/Si₃N₄ interface, with both being higher than that of the adjacent Cu/ambient surface.

Variation in cross-strip configuration, material, thickness, length, test ambient, temperature and current density affect marker formation and indicate that competing mechanisms are active.

8:50 AM Invited

The Secret Life of Nanoparticles: Characteristics of Nanoparticles and Nanostructured Materials that are Frequently Forgotten or Ignored: Donald Baer¹; M. H. Engelhard¹; A. S. Lea¹; D. G. Gaspar¹; K. Pecher¹; C.-M. Wang¹; J. E. Amonette¹; A. A. El-Azab²; S. Kuchibhatla³; Sudipta Seal³; ¹Pacific Northwest National Laboratory; ²Florida State University; ³University of Central Florida

The literature is increasingly filled with images of nanoparticles and nanostructured materials and along with descriptions of their synthesis and aspects of their properties. Properties of nanoparticles are often influenced by particle size. However, it is possible to read many papers on nanoparticles before learning that many nanoparticles are structurally unstable and that aspects of their history, environment and even proximity to other nanoparticles may also alter their physical or chemical properties. The dynamic properties of these particles can explain some altered chemical properties. Although it is generally accepted that nano-structured materials are mostly surface or interface, the impacts of the nature of that surface are often ignored or minimized. The properties of individual nanoparticles or isolated nanoparticles can also be altered when they are assembled or packed into aggregate systems. Some of these effects will be described based on studies of iron oxide and ceria oxide nanoparticles.

9:30 AM

N-Implantation Induced Phase Separation in Zr-Cu Film: Hirono Naito¹; Shinji Muraishi¹; ¹Tokyo Institute of Technology

The phase-transition, -separation in proportion to N has been investigated for Zr-Cu alloy by means of N-implantation. Since Zr shows negative enthalpy change with N, whereas Cu shows positive, the different sign of formation and mixing enthalpy would yield selective nitriding of Zr against Cu and simultaneous phase-separation structure consisting of ZrN with metallic ZrCu phase. The 200 nm thick of Zr and Zr-10at%Cu films have been prepared and N-implantation has been conducted with beam energy of 100keV and dose of 1.0x10¹⁷ ions/cm². Selective nitriding behavior in Zr-Cu has been made by XPS chemical shift analysis. The evolution structure with lattice constant change in proportion to N has been observed by TEM to evaluate phase separation sequence in Zr-Cu-N system.

9:50 AM Invited

Nickel Nano-Interlayers for CrN Coatings on Steels: Ray Y. Lin¹; Pravahan Salunke¹; ¹University of Cincinnati

Effects of nickel nano interlayers on the property of CrN coated steels were investigated. The nickel interlayer was prepared with electroless plating to various thicknesses of up to 100 nm. CrN coatings were sputter deposited over the nickel interlayer. The coating crystal structures, microhardness, and scratch resistance were determined. Results showed that the nickel interlayer improved the microhardness and scratch resistance of CrN coated steels. To further enhance coating performance, an infrared heat treatment at 400°C and 2 minutes was carried out. With infrared heat treatments, the beneficial effect of the Ni interlayer was clearly exhibited. Without the Ni interlayer, after heat treating the CrN coated steel, severe cracks on coatings were observed. Heat treatment induced cracks on the CrN coatings were completely eliminated with a thin Ni interlayer.

10:30 AM

Oxidation of Ta at Low Temperatures and Its Implications for Cu Interconnect Technology: Nancy L. Michael¹; Dongmei Meng¹; Choong-Un Kim¹; ¹University of Texas at Arlington

Ta is considered a stable material and is commonly used as a barrier for nanometer range Cu interconnects. While it is true that the Cu/Ta interface shows little intermixing under normal conditions, the presence of oxygen leads to formation of Ta_xCu_yO compounds and degradation of Cu. Because low dielectric constant materials allow ambient gasses to reach the Ta barrier, Ta degradation through oxidation is possible within the structure. The ability of nanoscale Ta films (~20nm) to protect Cu in the presence of oxygen is the subject of this study. Using both blanket wafers and real interconnect structures, the influence of oxygen on Ta and the Ta/

Cu interface is investigated at temperatures below 350°C. In this study we find that even at these low process temperatures Ta is readily oxidized beyond its native oxide thickness. Using XPS and TEM, the sequence of Ta film oxidation and Cu degradation is developed.

10:50 AM

Surface Amorphization in Zr Alloy Films via Ni Implantation: *Shinji Muraishi¹; Hirono Naito¹; Tatsuhiko Aizawa²; ¹Tokyo Institute of Technology; ²Asia SEED*

Multi component Zr based glassy alloy is promising candidate for structural material and protective coating because of its high strength and good surface roughness. The good fabrication nature and stability is derived from enhanced mixing enthalpy and radius differences between selected constituents. Present work focuses on surface amorphization behavior in Zr and Zr-Cu films in proportion to Ni implantation. TEM observation revealed that Ni-implantation induced surface amorphization of Zr alloy films with thickness of 100nm. Compositional gradient of penetrated Ni has been measured by XPS to exhibit critical concentration for c-a transition is 20at%Ni for pure Zr, 10at%Ni for Zr-10at%Cu. The decrease of Ni concentration in Zr-Cu film for c-a transition indicates that induced amorphization is mainly attributed to chemical interaction between constituents with large negative enthalpy of mixing.

11:10 AM

Void Formation at Aluminum-Spinel Interface under the Influence of an Electrical Field at 620°C: *Gurpreet Singh¹; Myongjai Lee¹; Rishi Raj¹; Yeonseop Yu²; Jeremy Mark²; Frank Ernst²; ¹University of Colorado at Boulder; ²Case Western Reserve University*

We show that voids can be formed at an aluminum-spinel interface by the application of an electrical potential difference. The mechanism is related to the change in the vacancy potential at the interface when an electrical field is applied. The polarity of the applied electrical potential can either enhance or weaken the vacancy potential. Accordingly, the voids are nucleated when the aluminum film is the positive electrode. The experimental findings will be followed by a unified model for void nucleation which articulates the equivalence of electrical potentials as well as mechanical stress. The pathway for the unified model is the use of electrochemical potential of the atomic and defect species at interfaces.

11:30 AM Invited

Polar-Surface Induced Novel Growth Configurations of Piezoelectric Nanobelts: *Zhong Lin Wang¹; ¹Georgia Institute of Technology*

The wurtzite structure family has a few important members, such as ZnO, GaN, AlN, ZnS and CdSe, which are important materials for applications in optoelectronics, lasing and piezoelectricity. The two important characteristics of the wurtzite structure are the non-central symmetry and the polar surfaces. The structure of ZnO, for example, can be described as a number of alternating planes composed of tetrahedrally coordinated O²⁻ and Zn²⁺ ions, stacked alternatively along the c-axis. The oppositely charged ions produce positively charged (0001)-Zn and negatively charged (000-1)-O polar surfaces, resulting in a normal dipole moment and spontaneous polarization along the c-axis. This polar surface gives rise a few interesting growth features. In this presentation, we will focus on a few growth phenomena that are closely related to the polar surface. Some details will be given about the analysis of the nanobelt based materials.

12:10 PM

AFM Characterization and Surface Modification of Nanocrystalline Ni Films: *Kevin Stevenson¹; Frederic Sansoz¹; ¹University of Vermont*

Electroplated Ni for thin films and nanowires exhibit improved mechanical properties due to the increased volume fraction of crystal interfaces and surfaces. Advanced mechanical testing at the nanoscale requires a comprehensive understanding of the relation between fabrication and surface properties. The objective of this paper is to obtain a correlation between electrodeposition parameters and grain size using high-resolution atomic force microscopy (AFM). The surface structure of electroplated Ni films was investigated to determine the ideal electrochemical environment to produce grain sizes between 8-80 nm. Pulsed-current deposition and organic additives were critical for obtaining grain sizes less than 30 nm. Standard AFM cantilevers (tip radius~10nm) were found to be insufficient for imaging grains smaller than 30 nm. However, high-resolution AFM cantilevers (tip radius~1nm) enabled accurate surface and

grain analysis over the range of produced sizes. This non-destructive approach provided additional insight into the structure-property relationship of thin films at the nanoscale.

The Brandon Symposium: Advanced Materials and Characterization: Atom Probe

Sponsored by: The Minerals, Metals and Materials Society, Indian Institute of Metals, TMS Extraction and Processing Division, TMS: Materials Characterization Committee

Program Organizers: Srinivasa Ranganathan, Indian Institute of Science; Wayne D. Kaplan, Technion; Manfred R. Ruhle, Max-Planck Institute; David N. Seidman, Northwestern University; D. Shechtman, Technion; Tadao Watanabe, Tohoku University; Rachman Chaim, Technion

Tuesday AM
March 14, 2006

Room: 206B
Location: Henry B. Gonzalez Convention Ctr.

Session Chairs: David Seidman, Northwestern University; Danny Shechtman, Technion - Israel Institute of Technology

8:30 AM Invited

3-D Atomic-Scale Analysis of Interfaces in Thin-Film Materials and Devices: *Alfred Cerezo¹; ¹University of Oxford*

The 3-dimensional atom probe (3DAP) permits the nanochemistry of materials to be observed in 3 dimensions with near-atomic spatial resolution. Although the primary application of the technique has been to the study of engineering alloys, developments in specimen preparation and the use of laser pulsing allow analysis of thin-films and semiconductor devices. With the 3DAP, asymmetry has been observed in the atomic-scale roughness and interdiffuseness of the interfaces in CoFe/Cu/CoFe structures, similar to those used as giant magnetoresistance (GMR) read heads in hard disks. Molecular dynamics (MD) simulations have shown a good match to the atomic-scale chemical data from the 3DAP. The chemistry and morphology of barrier layers in tunnel magnetoresistance (TMR) films has also been investigated as a function of oxidation and annealing, again showing good agreement with MD modelling. Preliminary results have also been obtained on composition fluctuations and interface sharpness in III-V semiconductor multiple quantum-wells.

8:55 AM Invited

Atomic Scale Characterization of Advanced Materials Using 3D Atom Probe: *Muraleedharan Kuttanellore¹; Balamuralikrishnan Ramalingam¹; Mohan P. Pathak¹; Konduri Satya Prasad¹; ¹DMRL, Hyderabad India*

Our laboratory is engaged in the development of several advanced materials for structural applications at ambient and at high temperatures. These include high strength aluminium alloys, ultra high strength high toughness steels and nickel base superalloys. In each of these classes of materials, a significant contribution to the understanding of the microstructure-property-processing correlations can be made by the use of the unique atomic-scale characterization capability of the 3D atom probe: the morphology and composition of fine precipitates and nano-scale clusters in modified 7010 high strength aluminium alloys; the evolution of the fine carbides and their chemical composition as a function of tempering temperature and times in the ultra high strength high toughness steel; and the alloy partitioning behaviour between γ and γ' in multi-component nickel base superalloys. The presentation will provide an overview of our efforts at addressing these issues.

9:20 AM

A Comparison of the Early-Stages of γ' -Precipitation in Two Ni-Al-Cr Superalloys: *Chantal K. Sudbrack¹; Jessica A. Wening¹; Chris Booth-Morrison¹; Ronald D. Noebe²; David N. Seidman¹; ¹Northwestern University; ²NASA*

Atom-probe tomography (APT) is a direct-space post-mortem imaging and chemical analysis technique that characterizes chemical heterogeneities with sub-nanometer resolution in 3D. The nanostructural evolution in two model Ni-base superalloys, Ni-5.2 Al-14.2 Cr and Ni-7.5 Al-8.5 Cr atomic %, with similar solute supersaturations is followed tempo-

TUESDAY AM

rally with APT, as the alloys decompose isothermally at 873 K for times varying from 0.17 to 1024 hours. Particular emphasis is placed on the influence of solute composition on the nanostructural properties and phase compositions as they evolve temporally. Small spheroidal precipitates with radii ranging from < 1 nm to 10 nm are observed at a high number density (ca. 10^{23} - 10^{24} m $^{-3}$). Over the time scale investigated, nucleation, growth and coarsening of the γ' -phases is observed. The decomposition behavior is analyzed with established models utilizing nondilute thermodynamics.

9:35 AM

Microstructural Evolution of Nanoscale Precipitation-Strengthened Aluminum Alloys: *Keith E. Knippling*¹; David C. Dunand¹; David N. Seidman¹; ¹Northwestern University

This research is toward developing a new castable and heat-treatable precipitation-strengthened aluminum alloy having coarsening- and creep resistance beyond 375°C. Decomposition of supersaturated Al(Zr) solid solutions occurs initially by the formation of metastable cubic L1₂ Al₃Zr precipitates, which are small (ca. 20 nm), coherent, and resist coarsening at temperatures up to 425°C. However, segregation incurred during peritectic solidification results in an inhomogeneous dendritic distribution of Zr, creating a network of interdendritic precipitate-free zones in the precipitated microstructure. By adding a eutectic ternary solute, we exploit the natural tendency for solute partitioning during solidification to obtain a homogeneous dispersion of strengthening precipitates. Specifically, Sc is added which forms nanoscale L1₂ Al₃Sc precipitates. Moreover, in the presence of Zr, Al₃(Sc,Zr) precipitates form with substantially improved thermal stability compared to binary alloy, α -Al plus Al₃Sc. Relationships between the microstructure (precipitate size, morphology, distribution, and chemistry) and the observed mechanical properties are discussed.

9:50 AM Break

10:20 AM Invited

Recent Applications of Field Ion Microscopy and 3D-Atom Probe Analysis: *Reiner Kirchheim*¹; Talaat Al-Kassab¹; ¹Institut Fuer Materialphysik

(1) Nucleation and growth have been studied in supersaturated Cu-Co alloys using the 3d-atom probe (TAP). Besides the known spherical nuclei cylindrically shaped particles with an aspect ratio of more than 10 were found. The long axis is directing in the soft (100) direction. These findings are supported by 3d-field ion microscopy. (2) Using TAP data and a statistical evaluation of atomic positions in the intermetallic alloy Ti(Nb)Al revealed that Nb-atoms are occupying sites of the Ti-sublattice. (3) Growth and coarsening of oxide particles was studied in internally oxidized Ag-Mg and Ag-Mn alloys by using both TAP and SANS. It could be shown that growth and coarsening are strongly affected by the composition of the oxide/Ag-interface. (4) By using a Cu-Bi bicrystal and a focussed ion beam a TAP-sample containing the corresponding grain boundary was prepared and the Bi-excess of the boundary was measured with the 3d-atom probe.

10:45 AM Invited

Atom-Probe Tomographic Studies of the Temporal Evolution of Nanostructures in Multicomponent Alloys: *David N. Seidman*¹; ¹Northwestern University

Atom-probe tomographic (APT) and transmission electron microscopy (TEM) studies of the temporal evolution of nanostructures of multicomponent nickel-based alloys, Ni-Al-Cr, are studied in concert with lattice kinetic Monte Carlo (LKMC) simulations. Additionally, Al-Sc-X (X = Mg, Zr or Ti) are studied employing APT, TEM and high-resolution electron microscopy (HREM). The experimental studies involve temporally following the mean radius of precipitates (second phase), number density of precipitates, mean compositions of the precipitates and the matrix, volume fraction of precipitates, and precipitate morphologies; thereby obtaining a complete experimental description of how a multicomponent alloy evolves towards its thermodynamic equilibrium state when aged in a two-phase region. The experimental results are compared with predictions of extant models for nucleation, growth or coarsening, and with LKMC simulation results. It is shown that LKMC simulations in concert with the experimental results allows for a deeper physical understanding of the temporal evolution than either approach alone.

11:10 AM Invited

Solute Segregation at Crystal Lattice Defects Studied by 3-D Atom Probe Analysis: *George David William Smith*¹; ¹Oxford University

The segregation of solute atoms at crystal defects such as dislocations and grain boundaries can have a profound effect on the properties of materials. Until recently, the techniques available to characterise these segregation processes have been extremely limited. The development of the 3-D atom probe has enabled valuable new information to be obtained regarding the atomic-scale distribution of solute species, including interstitial atoms such as boron, carbon and nitrogen. This presentation will review recent work carried out at Oxford University on the segregation of carbon to dislocations in iron, the segregation of phosphorus to grain boundaries in nanocrystalline nickel, and the segregation of interstitial and substitutional solutes to grain boundaries in iron. Applications to the design and development of new advanced engineering materials will be emphasised.

11:35 AM Invited

Atom Probe Tomography Characterization of Solute Segregation to Dislocations and Interfaces: *Michael K. Miller*¹; ¹Oak Ridge National Laboratory

The level and extent of solute segregation to individual dislocations and interfaces may be visualized and quantified by atom probe tomography. The large volume of analysis and high data acquisition rate of the local electrode atom probe (LEAP) enables the solute distribution in the region of and along the core of dislocations to be estimated. Solute segregation along and normal to interphase interfaces and grain boundaries may also be estimated. Solute segregation at precipitate-matrix interfaces of precipitates as small as 2 nm diameter may be quantified. Examples will be presented of solute segregation in superalloys, neutron irradiated pressure vessel steels and mechanically alloyed, oxide dispersion strengthened (MA/ODS) ferritic alloys. Research at the SHaRE User Facility was sponsored by the Division of Materials Sciences and Engineering, U. S. Department of Energy, under Contract DE-AC05-00OR22725 with UT-Battelle, LLC.

The James Morris Honorary Symposium on Aluminum Wrought Products for Automotive, Packaging, and Other Applications: Fundamental Studies

Sponsored by: The Minerals, Metals and Materials Society, TMS Light Metals Division, TMS: Recycling Committee

Program Organizers: Subodh K. Das, Secat Inc; Gyan Jha, ARCO Aluminum Inc; Zhong Li, Aleris International Inc; Tongguang Zhai, University of Kentucky; Jiantao Liu, Alcoa Technical Center

Tuesday AM
March 14, 2006

Room: 207A
Location: Henry B. Gonzalez Convention Ctr.

Session Chairs: Subodh K. Das, Secat Inc; Tongguang Zhai, University of Kentucky

8:30 AM Introduction to Prof. Morris by Dr. Subodh Das

8:40 AM Invited

Anisotropy of Aluminum and Aluminum Alloys: *William F. Hosford*¹; ¹University of Michigan

A Taylor-Bishop & Hill model describes the plastic anisotropy of aluminum single crystals under constrained deformation. A yield criterion with an exponent of eight describes the anisotropy and is useful in metal forming analyses of aluminum. Anisotropy has less effect on the limiting drawing ratio in cupping than predicted by the quadratic Hill yield criterion. The effect of texture on forming limit diagrams is negligible. Predictions of strain-path changes on forming limit curves of aluminum alloy sheets are in reasonable agreement with experiments. Second phase precipitates greatly modify the form of plastic anisotropy. In age-hardened Al-4% Cu single crystals the anisotropy of hardening caused by thin θ' platelets on {100} planes is explained by their rotation as well as deformation. Tension during ageing causes the precipitates to form primarily

on the {100} planes normal to the stress whereas compression causes precipitation on the other two sets of {100} planes.

9:05 AM Invited

Recrystallization Kinetics and Texture Development in Aluminum: *Anthony D. Rollett¹; Mohammed Alvi¹; Abhijit Brahme¹; Hasso Weiland²; Jaakko Suni²; ¹Carnegie Mellon University; ²Alcoa Technical Center*

Both automated EBSD and computer simulation has been used to study the recrystallization behavior of several aluminum alloys including both kinetics and texture development. In Al-1050, the kinetics are dominated by nucleation and growth from sites close to boundaries in the deformed structure, which has highly elongated grains. These characteristics, combined with site saturated nucleation conditions, leads to exponents in KJMA plots close to unity. The texture development is dominated by strong growth in the cube component, which is found to nucleate in cube oriented bands. The cube grains grow most strongly into the S deformation component, whereas the brass deformation component is the slowest to recrystallize. Computer simulation demonstrated that several factors were significant to texture development. In approximate decreasing order of importance were oriented nucleation, stored energy varying with component, oriented growth (anisotropic boundary mobility), and anisotropic boundary energy. Results for 3003 and 5005 will also be reported.

9:30 AM Invited

Recrystallization Kinetics in Cold-Rolled Aluminum: *Dorte Juul Jensen¹; ¹Riso National Laboratory*

This presentation focuses on crystallographic orientation aspects of growth during recrystallization. By the electron back scattering pattern method it is shown that cube grains may grow faster than grains with other orientations and that this growth advantage cannot be explained a 40° $\langle 111 \rangle$ misorientation relationship. 3 Dimensional X-ray Diffraction (3DXRD) microscopy confirms that cube grains on average grow the fastest but also that there is a large variability in growth rates even among grains with the same orientation. This can strongly affect the overall recrystallization kinetics. Besides, in-situ recording of the kinetics of individual bulk grains, 3DXRD can also be used to map the complete 3D grain shape evolution while annealing the sample on-line in the x-ray beam. These measurements are also presented and used for an analysis of orientation relationships for grain boundary migration during recrystallization.

9:55 AM Invited

Simulation of Microstructure and Texture in Al-Mg-Mn Sheet: *Juergen R. Hirsch¹; ¹Hydro Aluminium AS*

The microstructure and texture evolution during industrial production of Al-Mg-Mn alloy sheet and the resulting properties are shown and analyzed, based on recently developed integrated process simulation tools. This alloy group is used for beverage cans where anisotropy is strictly controlled, but also for many other applications where optimum forming conditions are required and sophisticated forming simulation methods – including detailed microstructure information - is often applied. The characteristic texture effects and related deep drawing cup (“earing”) profiles are analyzed systematically for various initial hot band microstructures achieved by different rolling reductions. Method for the evaluation of the characteristic forming behaviour and earing profiles in Al-sheet are applied which allow the description of cup profiles and their transition in a simple quantitative way. The variation of initial cube texture and the cold rolling texture evolution, incl. minimum rolling strain are predicted to ensure optimum strength and anisotropy.

10:20 AM

Sheet Metal Formability for Anisotropic Materials Based on Stress-Based Forming Limit Curve: *Jeong Whan Yoon¹; Thomas B. Stoughton²; Robert E. Dick³; ¹Alcoa Technical Center; ²General Motors R&D Center; ³Alcoa Rigid-Packaging*

Since the trend today is to utilize models with full anisotropy in order to more accurately capture the physics of material behavior, the issue of anisotropy of forming limits must also be addressed. A solution to assess formability for an anisotropic material is proposed that rescales the stresses by a factor so that the scaled stresses have the same relationship to a single forming limit curve in a 2D plot in stress-space, as the actual stresses have to the true anisotropic forming limit in 3D space. The rescaling enables engineers to accurately view the formability of all the elements at the

same time for a given finite element analysis of an application. Several applications in rigid-packaging are presented to show the validity of the suggested model.

10:40 AM Break

10:50 AM

Rolling History Microstructure-Property Relations of 6022 Aluminum Sheet: *Christina Burton¹; ¹Mississippi State University*

This paper covers the microstructure analysis and correlating mechanical properties of 6022 aluminum alloy at various stages of the rolling process. The history effect will provide a database for material modeling. The rolling steps comprise reductions of a 6-inch billet to a 3-inch billet to a 1/8-inch sheet, an annealing process of the 1/8-inch sheet, and finally a reduction to the 1/32-inch finish gauge sheet. The microstructural content will be obtained through scanning electron microscope (SEM) analyses, optical microscopy (OM) analyses, and X-ray tomography. Mechanical tensile tests and microhardness tests will be performed on specimens retrieved from the various stages in the rolling direction and short and long transverse directions of the material. 6022 aluminum sheet is used in the automotive industry primarily in closure panel applications.

11:15 AM Invited

The Effects of Transition Metal Element Additions on Concurrent Precipitation and Recrystallization in Al Alloys: *Tongguang Zhai¹; Qiang Zeng¹; Xiyu Wen¹; Jin Li²; ¹University of Kentucky; ²Beijing Jiaotong University*

Continuous cast Al alloys, such as AA5083, AA5754, high Fe-containing AA5754 and AA3004, were studied in this work in terms of their recrystallization behaviors, especially the effects of transition metal element additions in these alloys. Concurrent precipitation occurred during recrystallization, which gave rise to the formation of special textures in these deformed alloys that had a high level of solid solution. It was found that Mn resulted in a strong P {011} $\langle 122 \rangle$ texture, Cr led to a strong texture of {113} $\langle 110 \rangle$, and Fe had no significant effect on the concurrent precipitation in these alloys. The recrystallized grain structure was elongated in the rolling direction because of the concurrent precipitation effect in these alloys. TEM observations revealed that fine precipitates pinning dislocations was likely to be the mechanism for the formation of these special textures in these alloys.

11:40 AM Invited

Anisotropic Ultrasonic Attenuation in an AA 5754 Aluminum Hot Band: *Chi-Sing Man¹; Zhiqiang Cai¹; Kevin D. Donohue¹; ¹University of Kentucky*

Ultrasound resonance spectroscopy of through-thickness stress waves is an emerging technique for in-line monitoring of texture and microstructures in sheet metals. In this paper a simple phenomenological theory involving an effective viscosity tensor is adopted for the analysis and interpretation of spectroscopic data of through-thickness resonance. Ultrasonic attenuation of through-thickness shear and longitudinal waves in sheet samples of a continuous-cast AA 5754 aluminum hot band and its O-temper counterpart was measured at room temperature with resonance EMATs (electromagnetic acoustic transducers). The frequency range in question was 2 to 10 MHz. For the hot band, the attenuation of each mode was found to be predominantly proportional to the square of the frequency. The dissipation constant pertaining to the fast shear mode was about 4 times that of the slow shear mode, which suggests the presence of a highly anisotropic dislocation structure that resulted from the hot rolling.

12:05 PM

Nanoindentation Study of Strain Gradient Plasticity in Aluminum Alloy 2024: *Yun Jo Ro¹; Matthew R. Begley¹; Sean R. Agnew¹; ¹University of Virginia*

This study was motivated by the hypothesis that strain gradients play an important role in determining the crack growth resistance. Fatigue crack growth resistance of AA2024 within inert vacuum environments degrades with aging. Therefore, the effect of aging on the so-called length-scale parameter, which governs the impact of strain gradients on the plastic flow stress, has been studied using nanoindentation. Measured hardness vs. depth data are plotted according to the Nix and Gao model, and the results show a specific trend in the length-scale parameter with aging. The

length scale is large at short aging conditions (< 1 hour at 190°C) and decreases rapidly with increasing aging, until essentially reaching a plateau at the peak aged condition (~ 6 hours.) Speculations as to why an increase in strain gradient effects would correlate with increased crack growth resistance will be offered.

12:25 PM

Modelling Recovery, Recrystallization and Precipitation in AA6111: *Johnson Go*¹; Warren J. Poole¹; Matthias Militzer¹; Mary A. Wells¹; ¹University of British Columbia

A systematic study has been carried out to examine the microstructure evolution in cold rolled AA6111 during isothermal annealing. Prior to cold rolling, the alloys was severely overaged for 7 days at 250 and 325°C. Experimental results indicate the recrystallization kinetics is controlled by the spatial distribution of precipitates and the extent of recovery in the deformed matrix. At lower annealing temperatures, an extensive amount of recovery occurs before the onset of recrystallization. In addition, clusters of precipitates were found to pin grain boundaries during recrystallization. A model was subsequently developed by combining models for recovery, recrystallization and precipitation. Particular attention was taken to capture the interaction between the three phenomena. The precipitation model takes into account the dissolution or growth and coarsening of precipitates. It will be demonstrated that the model is capable of describing the softening response of the alloys which has been cold rolled 40% thickness reduction.

12:45 PM

Thermodynamic Investigation of the Effect of Na on High Temperature Embrittlement of Al-Mg Alloys: *Shengjun Zhang*¹; Qingyou Han²; Zi-Kui Liu¹; ¹Pennsylvania State University; ²Oak Ridge National Laboratory

Sodium is an undesired impurity element in Aluminum-Magnesium alloys. Despite trace amounts of content, it leads to high temperature embrittlement (HTE) due to intergranular fracture which is prone to edge cracking during hot rolling. In the present work, thermodynamic investigation was carried out to reveal the correlations between HTE, phase relations, temperature and Na content of the Al-Mg alloys. The HTE sensitivity and safe zones of the Al-Mg alloys were determined. The effect of Na on hot ductility loss was also studied. It was found: (i) The liquid miscibility gap associated with Na is closely related to HTE; (ii) HTE ascribes the formation of the intergranular Na-rich liquid phase which significantly weakens the strength of the grain boundary; (iii) The Na content should be controlled below the critical content and different proper hot-rolling temperature should be chosen with different Na content in order to suppress HTE and avoid cracking.

The Rohatgi Honorary Symposium on Solidification Processing of Metal Matrix Composites: Processing and Microstructure of MMCs - II

Sponsored by: The Minerals, Metals and Materials Society, TMS Materials Processing and Manufacturing Division, TMS Structural Materials Division, TMS/ASM: Composite Materials Committee, TMS: Solidification Committee

Program Organizers: Nikhil Gupta, Polytechnic University; Warren H. Hunt, Aluminum Consultants Group Inc

Tuesday AM

Room: 207B

March 14, 2006

Location: Henry B. Gonzalez Convention Ctr.

Session Chairs: David C. Dunand, Northwestern University; Adam Loukus, GS Engineering, Inc

8:30 AM Invited

Structure and Properties of Pressure-Infiltrated Aluminum/Mullite-Microsphere Syntactic Foams: Dorian K. Balch¹; Olivier Couteau²; *David C. Dunand*²; ¹Sandia National Laboratory; ²Northwestern University

Aluminum syntactic foams with densities of 1.4-1.6 g/cm³ are fabricated by liquid metal infiltration of aluminum into a packed bed of hol-

low mullite-silica spheres with diameters of about 50 micrometers. The foam structure is first presented, e.g. matrix/sphere interface, infiltration of spheres and chemical reaction between spheres and matrix. The foam compressive behavior measured at room temperature is then discussed in terms of stiffness, strength, damage, energy absorption and load transfer between matrix and spheres. Finally, the foam thermal expansion and creep behavior are presented and discussed within the framework of metal matrix composites.

8:55 AM

Effects of Interfacial Reactions during Solidification on Mechanical Properties in Short Fiber Reinforced AlSi12CuMgNi Composites: Yuanding Huang¹; *Norbert Hort*¹; Karl Ulrich Kainer¹; ¹GKSS Research Centre

The addition of short fibers to AlSi12CuMgNi matrix alloys causes interfacial reactions between fiber and matrix during casting. These reaction products are influencing the matrix composition as well as the physical metallurgy of the matrix, such as microstructure, aging behavior and mechanical properties. The present work investigates the interfacial reactions of Saffil®- and Kaowool®-fiber reinforced AlSi12CuMgNi composites by means of SEM and TEM techniques. It is shown that the interfacial reaction largely depends on the fiber composition, especially the content of SiO₂ in the fiber. The reaction occurring during solidification can drastically influence the subsequent mechanical behavior of the investigated composites. The relationship between the interfacial reaction and mechanical behavior in accordance to ageing is discussed based on the obtained experimental results. The ageing hardening is deteriorated due to the depletion of the alloying element magnesium caused by the interfacial reaction.

9:20 AM

Microstructure Characterization of Al-7%Si-10%B4C Die Casting Composite: *Zhan Zhang*¹; X.-G. Chen²; A. Charette¹; ¹University of Quebec at Chicoutimi; ²Alcan International Limited

Recently, Alcan has developed a liquid mixing process to economically produce Al-B4C particulate reinforced composites. Al-7%Si-10%B4C is a composite developed for shape casting. On the microstructure characterization of a die casting part (a box type) with optical and electron microscopies, attention is particularly focused on the distribution of particulates and interactions between B4C particles and matrix. Quantitative analysis results show that solidification process affects the distribution of the reinforcement particulates. Basically, more particulates are located on final solidified zones, such as the section center of the part. However, in this case, the filling mould process seems not to significantly impact on the distribution of particles. Moreover, a reaction layer containing titanium and silicon is detected on the surface of boron carbide particulates. This layer would play an important role in the limitation of interfacial reactions. The mechanism of interfacial reactions and their prevention in this composite will be discussed.

9:45 AM

Solidification Structures and Properties of Zinc-Aluminum/SiC(MMC) Alloys: Alicia Esther Ares¹; Rubens Caram²; *Carlos Enrique Schvezov*³; ¹CONICET/UNaM; ²DEMA-FEM-UNICAMP; ³UNaM

The Zinc-Aluminum (ZA) alloys can be cast using a variety of casting methods; they can also be forged, extruded and laminated. The fabrication cost is competitive and at present it is used in some vehicle components in transmission and suspension systems. In the present investigation Zinc - Aluminum alloys containing Silicon, Copper and reinforcing particles of Silicon Carbide were cast and analyzed. The analyses were done performing hardness test (HV), quantitative metallography, and dimensional stability tests. Composition analysis of the different alloying elements along the cast samples were done by SEM (Scanning Electron Microscopy) and EDAX (Energy Dispersive X-Ray Microanalysis). Several correlations between properties, structures and compositions were found, showing the increase in hardness with the increase in the volume fraction of SiC particles. The alloys tested for dimensional stability during 1000 hr at 165 ± 2,5°C were very stable.

10:10 AM

Aluminum Composite Castings Incorporating Used and Virgin Foundry Sand as Particle Reinforcements: *Michael A. Belger*¹; Pradeep

Rohatgi²; Nikhil Gupta³; ¹Citation Corporation; ²University of Wisconsin - Milwaukee; ³Polytechnic University

Incorporating virgin and used sand from foundries into aluminum castings serves as a means toward recycling waste sand, reducing the cost of castings, and improving selected mechanical properties of castings. The research conducted differs from other researcher's prior experimentation in this field because higher volume percentages of finer silica particles were incorporated in aluminum alloys in the virgin and used state. Stir mixing can be used to incorporate up to twenty volume percent of sand and pressure infiltration can be used to incorporate above fifty volume percent of sand. SEM and XRD show some of the silica in the sand is converted to alumina, leading towards higher hardness, stiffness, and abrasion resistance in the castings. Simulations of the compositions used in these studies were conducted using ProCAST to further understand the dispersed sand particle's influence on fluidity of the melt, thermodynamic changes in the system, and fill characteristics.

10:35 AM Break

10:50 AM

Microstructural Analysis of Ni Coated Carbon Fiber Reinforced Al-2014 Composites: Pradeep Rohatgi¹; *Vindhya Tiwari*¹; Nikhil Gupta²; ¹University of Wisconsin-Milwaukee; ²Polytechnic University

Ni coated carbon fibers were infiltrated with Al-2014 melt using conventional and a modified squeeze cast process. The process modification involved extending the fibers out of the mold and being air cooled during solidification. The process modification was aimed at reducing the damage to the Ni-coating during the infiltration process. The mismatch between the coefficient of thermal expansion of Ni-coating and carbon fiber was found to be the primary reason leading to the damage, which was minimized by adjusting the cooling rates. This process resulted in significant improvement in retention of the Ni-coating compared to the unmodified process. The solidification pattern in the matrix was established by measuring the copper and nickel contents at various distances from the fiber surface. The contents for both nickel and copper in the matrix decreased with increase in the distance from fiber surface suggesting that solidification of primary α -Al started in the interfiber region.

11:15 AM

Reactions in Cast Aluminum/Silica Composites and Their Effect on Physical and Mechanical Properties: *J. B. Ferguson*¹; Ben Schultz¹; Pradeep Rohatgi¹; Simon Alaraj²; ¹University of Wisconsin - Milwaukee; ²Birzeit University

In order to gain a better understanding of the reactions and strengthening mechanisms in cast aluminum/silica composites synthesized by stir mixing, a critical review of recent work was undertaken and experiments were conducted to incorporate virgin foundry sand into aluminum composites by stir mixing with the use of Mg as a wetting agent. It was determined that composite density increased with increasing reaction time and SiO₂ content. Reactions between the particles and both the wetting agent and the matrix result in extensive conversion of SiO₂ to MgAl₂O₄ and some Al₂O₃ releasing Si into the matrix. The change in mechanical properties with composition and time is also described. A reaction mechanism is proposed to account for these changes which indicates that both physical and mechanical properties can be controlled by controlling the Base Alloy/SiO₂/Mg chemistry and reaction times.

11:40 AM Invited

Development of Innovative Magnesium Based Composite Formulations Using Disintegrated Melt Deposition Methodology: *Manoj Gupta*¹; S. F. Hassan¹; Wai Leong Eugene Wong¹; ¹National University of Singapore

Magnesium based materials are subject of extensive research investigations due to their ability to significantly reduce the weight of engineering devices. For example, magnesium has the capability to reduce 35% of the weight if it replaces aluminium in engineering applications. To make inroads in the weight-critical area currently dominated by aluminium based materials, it is important that new magnesium based materials to be developed with comparable or better properties than aluminium based materials and conventional magnesium alloys. To realize that, experimental investigations were made to reinforce magnesium with metallic particles such as copper, nickel, titanium and molybdenum. Disintegrated melt deposition coupled with hot extrusion was used as the processing meth-

odology to produce near dense samples. Primary focus was to make matrix-reinforcement interface relatively more compatible and to enhance the properties as a result of that. Very interesting and promising results were obtained from these formulations.

12:05 PM

Microstructural Evolution of TiC Particulate Reinforced Mg-13.5Al-0.6Zn Matrix Composite during Partial Remelting: *Hui-Yuan Wang*¹; Lin Huang¹; Qi-Chuan Jiang¹; ¹Jilin University at Nanling Campus

Microstructural evolutions during partial remelting of Mg-13.5Al-0.6Zn alloy and TiC/Mg-13.5Al-0.6Zn composite are investigated by the isothermal treatment at the temperature of 510°. Compared with the unreinforced matrix alloy, the remaining liquid dramatically decreases in the composite; furthermore, also the solid α -Mg grain size in the composite significantly reduces in the partial remelting microstructure. The addition of cerium (Ce), which is combined with Al to form AlxCe compounds during solidification, has little contribution to the entrapment of TiC by the α -Mg grains during partial remelting process. As a result, in addition to very small amount of them eventually entrapped within the α -Mg grains, most of the TiC particulates are present in the remaining liquid phases distributing at the grain boundaries after partial remelting process.

Titanium Alloys for High Temperature Applications - A Symposium Dedicated to the Memory of Dr. Martin Blackburn: Processing of High Temperature Titanium Alloys

Sponsored by: The Minerals, Metals and Materials Society, TMS Structural Materials Division, TMS: Titanium Committee

Program Organizers: Michael W. Peretti, Lyondell Chemical Company; Daniel Eylon, University of Dayton; Ulrike Habel, Munich; Guido C. Keijzers, Del West USA; Michael R. Winstone, DSTL

Tuesday AM
March 14, 2006

Room: 201
Location: Henry B. Gonzalez Convention Ctr.

Session Chairs: Andrew P. Woodfield, GE Transportation; Daniel Eylon, University of Dayton

8:30 AM Invited

Processing to Maximize High Temperature Performance of Titanium Alloys: *Stephen P. Fox*¹; ¹TIMET

The high temperature performance of titanium alloys is a function of chemistry and microstructure, which are in turn a function of the alloy formulation, melting, conversion and heat treatment. Optimization of these processes can be quite different for an application where a balance of strength, fatigue and creep resistance is required, as compared to optimization for ultimate creep performance. Similarly where the critical requirements are oxidation performance, a very different approach to alloying and processing can be required depending on the specific requirements of the application. The different approaches used will be discussed and placed in context of aerospace and automotive applications comparing the different characteristics of TIMETAL®834, TIMETAL®1100, TIMETAL®21S and TIMETAL®XT.

9:00 AM

Microstructural Development and Modeling the Relationships between Microstructure and Tensile Properties of Timetal 550 Using Bayesian Neural Networks: Eunha Lee¹; *Gopal B. Viswanathan*¹; Sujoy Kar¹; Santosh Kaduri¹; Peter Collins¹; Hamish L. Fraser¹; ¹Ohio State University

Alloy Timetal-550 is heat-treated using the Gleeble thermal-mechanical simulator to obtain various microstructures. Samples from each heat-treated condition were tested in tension at RT. Various microstructural features of the tested samples, spanning large length scales, are quantified using stereological procedures. The database consisting of these quantified microstructural features together with the corresponding tensile properties are used to develop a Bayesian Neural Network (BNN) model to predict the relationship between microstructure and RT mechanical properties: yield strength, ultimate tensile strength and elongation. Results in-

TUESDAY AM

dicating that α lath thickness has the most influence on tensile properties considered. The prior β grain size has a smaller effect on UTS and YS, but has a significant effect on the elongation. Grain boundary α layer-width has a significant effect on the UTS and YS. The model will be presented and the effect of individual microstructural features on the RT tensile properties will be discussed.

9:30 AM

A Combinatorial Approach to the Elemental Optimization of a Beta Titanium Alloy Using Directed Laser Deposition: *Ben Peterson*¹; Peter C. Collins¹; Dan Evans²; Pat Martin²; James Williams¹; Hamish Fraser¹; ¹Ohio State University; ²Air Force Research Laboratory

The composition of the alloy Timetal 21S has been selected as a baseline for the development of a new high temperature beta titanium alloy. A combinatorial approach employing directed laser deposition of elemental powders has been used to develop rapidly the new alloy. Subsequently, the tensile properties are assessed in a rapid manner for simulated high-temperature exposures, and the associated microstructures are characterized. These data populate the databases used to train and test fuzzy logic based models for predicting the mechanical properties. In addition to the base elements (Ti, Mo, Nb, Al, and Si), neutral elements (Zr and Sn), β -stabilizers (W), and dispersoid formers (B, C, Ge) are being tested as alloying additions. The most promising alloying additions have been identified. Based on the results of the coupled mechanical tests and computer models, a new group of alloys for application in high temperature thermal protection systems are being developed.

10:00 AM Break

10:30 AM Invited

The Burn-Resistant Alloy Ti-25Cr-15V-2Al-0.2C and Its Potential Application in Aeroengines: *Xinhua Wu*¹; Michael Loretto²; Wayne Voice¹; ¹Rolls-Royce plc; ²University of Birmingham

The burn-resistant alloy Ti-25Cr-15V-2Al-0.2C(wt%) was developed in the Materials IRC and has a tensile strength >1200MPa, ductility >20% and is thermally stable up to 500°C. The alloy is commercially competitive because vanadium and chromium are introduced using aluminium-containing master alloys rather than using expensive pure elements. The material has been used to manufacture aeroengine components through forging and powder processing and some examples of applications will be given. Extensive work has been carried out to understand the effect of various elements on the microstructure and mechanical properties. It has been found that too much aluminium gives rise to embrittlement associated with the formation of B2. Carbon reduces oxygen matrix content and grain boundary segregation through transformation of Ti₂C carbide that subsequently retards the precipitation of alpha thus conferring thermal stability. The resultant Ti(CO) carbide also leads to a finer grain size after thermo-mechanical processing and higher creep resistance.

11:00 AM

The Role of Jominy Tests in Understanding Transformations in TiAl-Based Alloys: *Michael H. Loretto*¹; David Hu¹; Xinhua Wu¹; Aijun Huang¹; ¹University of Birmingham

The influence of composition and of grain size on the transformation of the high temperature alpha phase during cooling a number of TiAl-based alloys has been studied using standard end-quench Jominy tests. Longitudinal sections of these quenched samples provide information over a wide range of cooling rates of the influence of composition and of the alpha grain size on the solid state transformations which lead either to two phase structures (lamellar, Widmanstatten, feathery) or to single phased structures (massive gamma or retained alpha). The alloys which have been studied include alloys such as Ti46Al8Nb with and without addition of boron. The observations will be discussed in terms of the factors which favour the massive transformation over those transformations which result in two phase microstructures of gamma and alpha and on the response of the massive microstructure to subsequent aging.

11:30 AM

Development of Damage Tolerant Titanium Aluminides by Equal Channel Angular Extrusion Processing: *Shankar M. Sastry*¹; Rabindra N. Mahapatra¹; ¹Washington University

Equal Channel Angular Extrusion (ECAE) processing was used to produce fine grained microstructures in several titanium aluminides including the most recent iterations of the commercial titanium aluminide compositions. ECAE was performed successfully below the eutectoid isotherm which resulted in the conversion of gamma+alpha₂ grains into fine, equiaxed grains. The lamellar microstructure was the most difficult to break down. Upon ECAE processing, the intense shearing during BECAE produced duplex grains of size 0.5-2mm. Annealing the ECAE processed alloys at temperatures in the lower a+g region resulted in the formation of fine, duplex grains. Room temperature ductility values, as measured by the percentage elongation before fracture, were 50-90% higher than in conventionally processed alloys. Furthermore, an increase in room temperature yield strength of up to 50% was observed the ECAE processed alloys.

Ultrafine Grained Materials - Fourth International Symposium: Processing and Microstructures II

Sponsored by: The Minerals, Metals and Materials Society, TMS Materials Processing and Manufacturing Division, TMS Structural Materials Division, TMS/ASM: Mechanical Behavior of Materials Committee, TMS: Shaping and Forming Committee

Program Organizers: Yuntian T. Zhu, Los Alamos National Laboratory; Terence G. Langdon, University of Southern California; Zenji Horita, Kyushu University; Michael Zehetbauer, University of Vienna; S. L. Semiatin, Air Force Research Laboratory; Terry C. Lowe, Los Alamos National Laboratory

Tuesday AM
March 14, 2006

Room: 217D
Location: Henry B. Gonzalez Convention Ctr.

Session Chairs: Ruslan Z. Valiev, UFA State Aviation Technical University; Kazuhiro Hono, National Institute for Materials Science; Zenji Horita, Kyushu University; K. Ted Hartwig, Texas A&M University

8:30 AM Invited

The New SPD Processing Routes to Fabricate Bulk Nanostructured Materials: *Ruslan Z. Valiev*¹; ¹UFA State Aviation Technical University

Since the mid-1990's the fabrication of bulk nanostructured metals using severe plastic deformation (SPD) has been evolving as a rapidly advancing direction of modern materials science that is aimed at developing materials with new mechanical and functional properties. The principle of these developments is based on grain refinement down to nanoscale level by various SPD techniques. However, within recent years SPD techniques have been applied for producing bulk nanomaterials using some other principles, namely, SPD-consolidation of powders, including nanostructured ones, as well as SPD-induced nanocrystallization of amorphous alloys. This paper is focused on investigations and development of these new trends in SPD processing enabling fabrication of fully dense bulk nanocrystalline metals with a mean grain size of 20-30 nm and homogenous microstructures. We consider physical principles of these routes and present results on the microstructural characterization of several nanocrystalline materials produced as well as on studies of their unique properties.

8:50 AM Invited

TEM Study of the Strain-Induced Low- and High-Angle Boundary Development in ECA-Pressed Commercial Purity Al: *Enrico Evangelista*¹; Marcello Cabibbo¹; M. E. Kassner²; ¹Polytechnic University Marche; ²University of California

Cell, subgrain and high-angle boundary evolution under equal channel angular (ECA) pressing was investigated in commercial-purity aluminum using transmission electron microscopy (TEM). Bc route pressing to a strain of about 8 at ambient temperature was investigated. TEM allowed the examination of cells and subgrains with misorientations less than 2-4°. High-angle boundaries (HABs) accounted for about 70% of the boundary population at the highest strain (8 passes). The HABs appear to be substantially formed through the formation of geometrically necessary boundaries (GNBs). The substructural evolution appeared similar to that

observed in an earlier study by other investigators on cold rolling of similar purity aluminum. These two processes appear to have similar grain refining potential.

9:10 AM Invited

Microstructure and Texture Development of Al-7034 and 2024 Alloys Processed by ECAP: *Nong Gao*¹; Marco J. Starink¹; Shun Cai Wang¹; Cheng Xu²; Terence G. Langdon²; ¹University of Southampton; ²University of Southern California

The evolution of microstructure and texture during equal channel angular pressing (ECAP) of a spray-cast Al-7034 alloy and an Al-2024 alloy were studied through TEM, EBSD and DSC. Microstructural examination showed the grain sizes of both alloys were reduced to the range of 0.3–0.5 μm through ECAP. There is a relatively rapid increase in the fraction of low-angle boundaries during the initial ECAP passes and a subsequent more gradual increase in the fraction of high-angle grain boundaries in subsequent passes. The crystallographic textures and their rotations during ECAP were analysed. The DSC analysis identified the occurrence of several thermal effects involving the formation, coarsening and dissolution of the precipitation phases, and concurrent recrystallization. The heating and ageing response of post-ECAP were studied by microhardness testing of the samples after interrupted heating and ageing treatment to allow a comparison of their respective hardening/softening behaviour between the as-received and ECAP materials.

9:30 AM

3D Atom Probe Investigation of the Nanostructure of a Commercial 6061 Aluminum Alloy Processed by SPD: *Xavier Sauvage*¹; Gulnaz Nurislamova¹; Ruslan Valiev²; Maxim Murashkin²; ¹GPM-CNRS; ²Institute of Physics of Advanced Materials

Aluminum alloys processed by SPD usually exhibit a significant increase of the mechanical strength and even superplasticity due to the strong grain size reduction. The 6061 commercial aluminum alloy is heat treatable and its remarkably high hardness after aging is due to a fine distribution of nanoscaled precipitates containing Mg and Si. It was shown however that its hardness could be significantly increased thanks to ECAP processing before the aging treatment. The aim of this work is to investigate such nanostructure resulting from SPD to understand these unusual mechanical properties. A solutionized 6061 aluminum alloy was processed by ECAP and aged. Then, the distribution of alloying elements (Mg and Si) was mapped out in 3D at the atomic scale thanks to the 3D Atom Probe technique. In this paper, we would like to discuss the precipitation kinetics induced by SPD and deformation mechanisms leading to high mechanical properties of the alloys.

9:45 AM

Microstructural Analyses of Deformation Induced Crystallization Reactions in Amorphous Al88Y7Fe5 Alloy: *Rainer J. Hebert*¹; John H. Perepezko¹; Harald Rösner²; Gerhard Wilde²; ¹University of Wisconsin-Madison; ²Forschungszentrum Karlsruhe in der Helmholtz Gemeinschaft

Cold-rolling experiments with amorphous Al88Y7Fe5 ribbons reveal characteristics of crystallization reactions under driven conditions. During initial deformation, Al nanocrystals develop in shear bands. The development of dislocations in deformation induced Al nanocrystals exceeding a size of approximately 11 nm x 5 nm along with a fragmentation of thermally induced dendrites offers a novel approach to tailor the size distribution of the nanocrystals. Autocorrelation images of high-resolution TEM images demonstrate that correlations in the amorphous phase develop not only in the shear bands, but also in the matrix during deformation at near-ambient temperatures. Annealing experiments with deformed and undeformed samples underline the notion of shear transformation zones and demonstrate their influence on thermally induced crystallization. The results highlight novel options for microstructure control in marginal glass formers under driven conditions. The support of the ARO is gratefully acknowledged (JHP, DAAD-19-02-1-0245).

10:00 AM

Torsion Process for Creation of Severe Strain and Ultrafine Grains: *Zenji Horita*¹; Terence G. Langdon²; ¹Kyushu University; ²University of Southern California

The process of severe plastic deformation (SPD) leads to a significant reduction in grain size in many metallic materials. The SPD may be attained through a torsion process as it is an endless process when a disk is rotated around the center or when a circular rod is rotated about the longitudinal axis. High Pressure Torsion (HPT) is a typical process making use of torsion strain and producing ultrafine grains in the submicrometer or nanometer range. Although the HPT process has been applied to disk samples, recent studies demonstrated that HPT is also applicable to bulk samples. The principle of the torsion process was also used recently in developing the Severe Torsion Straining (STS) process where a rod is moved in the longitudinal direction while introducing torsion strain through rotation. This presentation reviews grain sizes and microstructure features including mechanical properties after these SPD processes.

10:15 AM Break

10:25 AM Invited

Microstructure of Severely Deformed Fe-C Eutectoid Steel and Its Application: *Kazuhiro Hono*¹; H. W. Zhang¹; S. Ohsaki¹; ¹National Institute for Materials Science

Recent studies of cold drawn pearlite steel wires reported fragmentation and substantial decomposition of cementite. Many literatures reported that nanocrystalline microstructure as the typical feature of the white etching layer on pearlite rail tracks. A model experiment by mechanical milling of pearlite demonstrated that the cementite decomposes after long time milling forcing carbon to dissolve in ferrite and to segregate at the grain boundaries. Here, we report the microstructural features of these severely deformed pearlite steels examined by TEM and 3DAP and discuss the mechanism of nanocrystalline structure formation. We found the nanocrystalline ferrite is quite resistant against grain growth, which motivated us to consolidate the power by spark plasma sintering (SPS) to fabricate bulk nanocrystalline Fe-C alloy, which exhibited yield strength of 1,800 MPa, ultimate strength of 3,500 MP with plastic strain of 40% in a compression mode. The microstructural feature of the bulk nanocrystalline Fe-C will be reported.

10:45 AM Invited

Ultrafine-Grained Aluminium Alloys Produced by Accumulative Roll Bonding: *Mathias Göken*¹; Irena Topic¹; Johannes May¹; Heinz-Werner Höppel¹; ¹University Erlangen-Nürnberg

Accumulative roll bonding (ARB) has been used in recent years to produce ultrafine-grained materials by severe plastic deformation. The ARB process is especially attractive due to its simplicity and technological relevance. Superior mechanical properties, as an increase in strength and in the fracture strain by a factor of two, have been found for technical purity ARB-Al in comparison with cold rolled Al. The surface condition before rolling has a strong influence on the microstructure and on the interlayer bond strength of the material. High roughness and friction show a positive influence on refining the microstructure. The ARB process has been applied on different Al alloys from the 6000 series, as for example AA6016, where also an increase in strength and ductility has been found. The properties of these precipitation hardened alloys will be compared with that of technical purity Al and discussed in terms of microstructure and processing conditions.

11:05 AM Invited

The Effect of Purity Level and Die Cross-Section Geometry on Microstructure Evolution during ECAE of Aluminum: *Ayman A. Salem*¹; Terence G. Langdon²; Terry R. McNelley³; Zenji Horita⁴; S. L. Semiatin¹; ¹Air Force Research Laboratory; ²University of Southern California; ³U.S. Naval Postgraduate School; ⁴Kyushu University

Microstructure and texture evolution during room temperature ECAE of several lots of aluminum was investigated to establish the effect of purity level and die geometry (i.e., circular vs square) on grain refinement. Aluminum with different purity levels (99.998%Al, 99.99% Al and 99%Al) were subjected to four ECAE passes via route Bc in a 90° square die. Furthermore, the 99.99%Al was deformed in three dies with different cross-sections: a 10-mm diameter circular die, a 50x50-mm square die, and a 6x6-mm square die. The 99%Al showed an ultra-fine microstructure with a grain size of ~1.5-μm and no signs of discontinuously-recrystallized grains. The 99.998%Al, on the other hand, exhibited large discontinuously-recrystallized grains (~20-μm). The 99.99%Al revealed a

bimodal microstructure with both ultra-fine grains (~1.5- μm) and moderate-size discontinuously-recrystallized grains (~10- μm). The inhomogeneity of the microstructure was greatest for deformation in the die with circular cross-section and least for material deformed in the square die.

11:25 AM Invited

Microstructure Evolution in Copper during Large - Strain Machining: Alexander H. King¹; Srinivasan Chandrasekar¹; Dale Compton¹; Kevin P. Trumble¹; Travis L. Brown¹; Lawrence F. Allard²; ¹Purdue University; ²Oak Ridge National Laboratory/High Temperature Materials Laboratory

A study has been made of the microstructure and mechanical properties of machining chips created from pure copper. Varying levels of large shear strain, shear strain rate, and deformation temperature were induced during chip formation by systematically varying the tool geometry and cutting speed. The machining chips were characterized for microstructure and Vickers hardness to map the microstructure evolution over the selected machining-parameter space. Results at low cutting speeds (~1 m/min) show chips composed of ultrafine-grained (UFG) structures with enhanced hardness up to the highest shear strain achieved. At higher cutting speeds, deformation twinning was observed along with elongated UFG structures, and where critical strain values were reached, catastrophic dynamic recrystallization occurred causing a loss in UFG structure and enhanced hardness. These results lead to a processing map for the development of ideal microstructures. We will use this to discuss the prospects for large scale production of UFG copper.

11:45 AM Invited

Influence of Processing Parameters and Annealing on Texture and Microstructure in ECAP'ed Aluminum: Alexander P. Zhilyaev¹; Keiichi Oishi¹; Georgy I. Raab²; Terry R. McNelley¹; ¹Naval Postgraduate School; ²UFA State Aviation Technical University

The influence of ECAP parameters such as relief angle, backpressure and number of passes during equal-channel angular pressing (ECAP) on texture and microstructure in commercially pure aluminum has been studied. Recrystallization behavior during subsequent annealing has also been considered. Material was processed using a 90° die and examined by orientation imaging microscopy (OIM) and transmission electron microscopy (TEM) methods after the initial pressing operation and after four passes by route BC. The microtexture data indicate that the distortion during ECAP corresponds to a simple shear in a direction approximately parallel to die-channel exit and on a plane perpendicular to the flow plane. The OIM data reveal a prominent simple shear texture and deformation bands at a meso scale. Lattice orientations in each band correspond to a texture orientation. High-angle boundaries in the structure correspond to interfaces between the bands. These features may influence recrystallization.

12:05 PM

Structural Peculiarities of UFG Metal after Severe External Influences: Victor N. Varyukhin¹; Borys M. Efros¹; Vladimir A. Ivchenko¹; Natalya B. Efros¹; ¹Donetsk Physics and Technology, Institute of NAS of Ukraine

Nowadays, the problem of producing UFG materials with 10-200 nm grain size is among actively developing scientific problems. In our experiments we took Iridium, Nickel, Tungsten and Copper pretreated with severe plastic deformation and ion implantation. Some interesting results have been obtained by field ion microscopy method. For example, it has been revealed that in Iridium influenced by severe plastic deformation a UFG structure is formed (the grain size of 20-30 nm), but in the bodies of grains there are practically no defects of structure, however, after implantation of argon ions a sub-UFG structure, (sub-grain size of 3-5 nm) is formed, and in the bodies of subgrains there are defects. The sub-UFG structure was also revealed in Nickel and Copper after severe plastic deformation effect (sub-grain size of 3-15 nm), but in the latter case the observed boundary region is broader and the ultra dispersive sub-grain are highly misorientation.

Wechsler Symposium on Radiation Effects, Deformation and Phase Transformations in Metals and Ceramics: Dislocations/Obstacles/Channeling

Sponsored by: The Minerals, Metals and Materials Society, ASM International, TMS Structural Materials Division, ASM Materials Science Critical Technology Sector, TMS Materials Processing and Manufacturing Division, TMS/ASM: Mechanical Behavior of Materials Committee, TMS/ASM: Nuclear Materials Committee, TMS/ASM: Phase Transformations Committee

Program Organizers: Korukonda L. Murty, North Carolina State University; Lou K. Mansur, Oak Ridge National Laboratory; Edward P. Simonen, Pacific Northwest National Laboratory; Ram Bajaj, Bettis Atomic Power Laboratory

Tuesday AM
March 14, 2006

Room: 208
Location: Henry B. Gonzalez Convention Ctr.

Session Chairs: Gary S. Was, University of Michigan; Ram Bajaj, Bechtel Bettis Inc

8:30 AM Invited

Deformation and Fracture in Irradiated Metals: Steven J. Zinkle¹; Meimei Li¹; ¹Oak Ridge National Laboratory

Neutron irradiation at low and intermediate temperatures can cause large increases in the strength of metals. As reviewed by Wechsler and others, heterogeneous deformation in the form of coarse slip bands (dislocation channels) often occurs during mechanical testing of these irradiated metals. This presentation will summarize deformation and fracture mechanisms in irradiated metals. The deformation behavior of irradiated metals can be conveniently represented by radiation-modified Ashby deformation mechanism maps. Dislocation channeling can be considered to be a specialized case of the normal dislocation glide deformation mechanism, whereas irradiation creep represents a deformation mechanism not observed in unirradiated materials. Most of the fracture modes observed in irradiated metals can be directly related to unirradiated fracture mechanisms (transgranular cleavage, ductile intergranular fracture, etc.). One unresolved issue is whether high matrix helium levels can induce new fracture modes in steels irradiated at low temperatures.

8:55 AM

Dislocation Interactions with Stacking Fault Tetrahedron and Frank Loops: Hyon-Jee Lee¹; Lucie Saintoyant¹; Brian D. Wirth¹; ¹University of California

Molecular dynamics simulations of the interaction between gliding dislocations and faulted Frank loops or stacking fault tetrahedron are presented. An examination of various factors, including dislocation type (edge, screw and mixed), temperature, SFT size, stacking fault energy, dislocation velocity and the interaction geometry lead to the conclusion that SFT are very strong obstacles to dislocation motion. Regardless of dislocation character, the trailing Shockley partial detaches by an Orowan type mechanism, suggesting that shearing of the SFT, and not annihilation or absorption, is the most common result of dislocation interaction. Complete SFT annihilation and absorption into the dislocation core, which is believed to govern the onset of plastic flow localization, may be possible, but only for specific interactions. Dislocation interactions with Frank loops have been observed to produce shear of the loop, or the transformation into a perfect, prismatic loop.

9:15 AM

Microstructural Analysis of Deformation in Neutron-Irradiated Zirconium and Zircalloy-4: Naoyuki Hashimoto¹; T. S. Byun¹; ¹Oak Ridge National Laboratory

The effects of neutron-irradiation near 80°C on the deformation behavior of hexagonal close packed (hcp) materials, zirconium and zircalloy-4, were investigated by transmission electron microscopy (TEM). Particular emphasis is placed on the deformation microstructure responsible for the changes in mechanical behavior. Neutron irradiation at low temperature up to 1 displacement per atom (dpa) induced a high number den-

sity of defect clusters, which resulted in irradiation-induced hardening. Dislocation channel deformation is observed for doses greater than 0.1 dpa, and is coincident with prompt plastic instability at yield. TEM analysis suggests that the loss of work hardening capacity in irradiated zirconium and zircalloy-4 at higher doses is mainly due to dislocation channels that are formed under a high local resolved shear stress, leading to the observed localized deformation.

9:35 AM

Atomic-Scale Mechanisms of Cleared Channels Formation in Neutron-Irradiated Low Stacking Fault Energy fcc Metals: *Yuri Osetsky*¹; Roger E. Stoller¹; Steven Zinkle¹; ¹Oak Ridge National Laboratory

Clusters of self-interstitial atoms (SIAs) and vacancies are formed directly in high-energy displacement cascades in all metallic structural materials. In low stacking fault energy metals they can be faulted and perfect interstitial loops (IL) which are sessile and glissile, respectively, and stacking fault tetrahedra (SFTs). These defects are obstacles for dislocation motion and sources for strengthening, hardening and loss of ductility of irradiated metals. These effects are often accompanied with plastic instability when significant plastic deformation occurs in shear bands which can also be cleared of radiation induced defects, leading to so called cleared channels. In this paper we present results of large-scale atomistic modeling of edge and screw dislocations interaction with IL and SFTs in model Cu crystals. We report a number of different mechanisms and suggest a possible scenario for how shear bands can be cleared of radiation defects. The results are discussed and compared with experimental observations.

9:55 AM

Atomistic Simulations and Dynamic Observations of Dislocation-Defect Interactions: *Brian D. Wirth*¹; Hyon-Jee Lee¹; Joshua S. Robach²; Ian M. Robertson³; C. M. Li³; ¹University of California; ²Northwestern University; ³University of Illinois, Urbana-Champaign

In the early stages of deformation of irradiated materials, dislocations emitted from grain boundaries and other localized regions of high stress concentration interact with and destroy radiation-induced defects, creating defect-free channels. Although the presence of channels in a wide range of materials is well documented, the atomistic processes responsible for defect annihilation have not been experimentally verified. We present a study of dislocation interactions with defect clusters in copper and gold performed by combining molecular dynamics simulations with dynamic transmission electron microscope studies. Interaction of a dislocation with a stacking-fault tetrahedron can result in shearing of the tetrahedron into two defects, conversion of the tetrahedron to another defect type, as well as unfaulting and annihilation of the tetrahedron. These observations provide insight into irradiation hardening and defect interaction and annihilation mechanisms.

10:15 AM Break

10:35 AM

Deformation Microstructure of Proton-Irradiated Stainless Steels: *Zhijie Jiao*¹; Gary S. Was¹; ¹University of Michigan

The deformation microstructure of proton-irradiated stainless steels may play a key role in explaining their irradiation-assisted stress corrosion cracking (IASCC) susceptibility. In the present study, three model alloys (UHP-304, 304+Si, 304+Cr+Ni) with different stacking fault energies (SFEs) were irradiated with 3.2-MeV protons at 360°C to 5.5 dpa and then strained to 12% in 288°C Ar atmosphere. The deformation microstructures of the strained samples were investigated using transmission electron microscopy (TEM). The interaction between dislocations and irradiation-induced defects, characteristics of dislocation channels and dislocation pile-ups and the interaction between dislocation channels and grain boundaries will be reported. The effect of SFE on deformation microstructures, and thus on IASCC susceptibility of stainless steels will be discussed.

10:55 AM

Flow Localization and Fracture in Irradiated FCC Materials: *Xianglin Wu*¹; Xiao Pan¹; *James F. Stubbins*¹; ¹University of Illinois at Urbana-Champaign

Irradiated material exhibits sharp increases in yield strength and associated reductions in ductility at low to intermediate temperatures, up to 0.4 Tm. Reductions in ductility are troubling since metal alloys are se-

lected for reactor structural applications due to their ability to flow plastically and redistribute stresses. This property also results in high values of fracture toughness. Flow localization is shown to be associated with a critical stress for tensile failure in fcc metals and alloys. The critical stress is the largest stress the material can withstand prior to necking. As the yield strength increases with irradiation exposure, the difference between the material yield strength and the critical stress decreases, leading to an early onset of necking or localized flow. The dependence of the flow localization process on deformation mechanisms, temperature and irradiation exposure is discussed in this paper. Experimental and modeling studies show the related influence on fracture toughness.

11:15 AM

Dose Dependence of True Stress Parameters in Irradiated fcc, bcc, and hcp Metals: *Thak Sang Byun*¹; ¹Oak Ridge National Laboratory

The metallic materials after irradiation to high doses often experience prompt necking at yield. Such unstable deformation without preceding stable deformation makes it difficult to evaluate the radiation effects on the necking and fracture properties. A method to calculate the true stress-true strain behavior for necking deformation is proposed using experimental evidence and theoretical assumptions. The true fracture stress was calculated for a dozen irradiated fcc, bcc, and hcp polycrystalline metals, and the results are discussed focusing on the dose dependence of the true fracture stress and on the relationship with other true stress parameters such as plastic instability stress or strain hardening rate during necking. In most of the test materials the true fracture stress was nearly independent of dose as was the plastic instability stress, while a few bcc metals experience significant embrittlement, with which it failed before yield, and therefore the fracture stress decreased with dose.

2006 Nanomaterials: Materials and Processing for Functional Applications: Nanoscale Magnetics

Sponsored by: The Minerals, Metals and Materials Society, TMS Electronic, Magnetic, and Photonic Materials Division, TMS: Nanomaterials Committee

Program Organizers: W. Jud Ready, GTRI-EOEML; Seung Hyuk Kang, Agere Systems

Tuesday PM
March 14, 2006

Room: 214C
Location: Henry B. Gonzalez Convention Ctr.

Session Chairs: Robert D. Shull, National Institute of Standards and Technology; W. Jud Ready, GTRI-EOEML; Seung Hyuk Kang, Agere Systems

2:00 PM Introductory Comments

2:05 PM Invited

Computer Simulation of Domain Structures in Nanoferroics: *Long Qing Chen*¹; Y. L. Li¹; S. Choudhary¹; J. X. Zhang¹; ¹Pennsylvania State University

This presentation will discuss the phase-field computational approach to ferroic domain structures that involve multiple long-range interactions. It involves the simultaneous solutions to Landau-Lifshits-Gilbert equation for ferromagnetic domains and time-dependent Ginzburg-Landau equations for ferroelectric and ferroelastic domains. The contributions from long-range interactions are obtained by solving the mechanical, electrostatic, and magnetostatic equilibrium equations. Examples to be discussed include ferroelectric domain structures in epitaxial thin films, domain formation and switching in polycrystals of nanoscale grain size, as well as domains and magnetoelectric coupling in nanoscale composites of ferroelectric and ferromagnetic crystals.

2:30 PM

Tailorable Fe₃O₄ Nanocrystals for Use as T₂ Contrast Agents in Magnetic Resonance Imaging: *Alex J. Barker*¹; Brant Cage²; Stephen Russek²; Craig Lanning³; Robin Shandas³; Conrad Stoldt¹; ¹University of Colorado, Boulder; ²National Institute of Standards and Technology; ³Children's Hospital, Denver

TUESDAY PM

Monodisperse Fe₃O₄ nanocrystals of various sizes (10-20 nm) are size controlled synthetically for use as target specific magnetic resonance imaging (MRI) contrast vectors. The crystals are synthesized by time varied thermal decomposition of Fe(III) acetylacetonate (Fe(acac)₃) in the presence of trioctylamine (TOA) and heptanoic acid (HA). The conjugation of 2,3-dimercaptosuccinic acid (DMSA) to the surface of the Fe₃O₄ improves the biostability and aqueous solubility, in addition to supplying a bonding site target molecules. The material and magnetic properties of the Fe₃O₄ ensembles are examined by transmission electron microscopy (TEM), X-Ray diffraction (XRD), superconducting quantum interference device magnetometry (SQUID), and nuclear magnetic resonance (NMR). The particle size, crystal symmetry, magnetic anisotropy, and T₁, T₂ times in de-ionized water are reported. MRI images of 1.5 mL phantoms and aqueous phase T₁, T₂ shortening indicate that the magnetically optimized Fe₃O₄ nanocrystals hold promise for use as size-tailorable contrast agents.

2:50 PM Break

3:00 PM

Magnetic Properties of Mechanically Alloyed and Annealed Fe-40 at. % Al: Q. Zeng¹; Ian Baker¹; ¹Dartmouth College

This presentation will describe the production and characterization of metastable, nanostructured, disordered b.c.c. Fe-40 at. % Al solid solution from elemental powders using a high-energy ball mill. The effects of milling and subsequent annealing on the formation of disordered nanocrystals, changes in the lattice parameter and grain size, the disorder-to-order transformation, and ferromagnetic-to-paramagnetic transformation were studied by x-ray diffraction, differential scanning calorimetry and magnetic measurements. This work was supported by NIST grant 60NANB2D0120.

3:20 PM

Nanostructured High-Energy Permanent Magnets: Xiangxin Rui¹; Jeffrey E. Shield¹; ¹University of Nebraska

Two-phase permanent magnets consisting of hard and soft magnetic phases assembled at the nanoscale are the most promising class of high-energy permanent magnets. The magnetic behavior critically depends on the scale of the structure, particularly the grain size of the soft magnetic phase. In this paper, we report on the structure and magnetic properties of two types of cluster-assembled nanocomposite permanent magnets. In the first, ~10 nm Fe clusters are imbedded in an FePt matrix. The fine-scale Fe clusters allows effective exchange coupling, resulting in energy products of 22 MGOe, which are near-record values for isotropic materials. In the second, individual ~10 nm clusters with compositions in the Fe₃Pt/FePt two-phase field have been fabricated. Phase decomposition leads to nanoscale phase separation resulting in complete exchange coupling. Here, energy products close to 20 MGOe have been achieved. These results provide insight into optimum nanostructural features in exchange coupled nanostructured permanent magnets.

3:40 PM

The Effect of Alloying Elements on the Microstructure and Soft Magnetic Properties of Nanocrystalline Fe-Si-B-Cu-Nb Alloys: Raju V. Ramanujan¹; Yanrong Zhang¹; ¹Nanyang Technological University

Nanostructured magnetic materials are used in novel applications in bioengineering, electronics, data storage and other industries. Soft nanomagnetic materials have been intensively studied following the success of the Fe-Si-B-Cu-Nb nanocrystalline alloys. Copper and niobium are essential alloying elements, they bring about a dramatic change in the microstructure obtained on crystallization of the amorphous alloys. However, the mechanisms by which this change is effected is still unclear. A study using DSC, XRD, CTEM, EDX, VSM and hot stage in situ TEM was conducted, focusing on the synergistic effects between the Cu and Nb atoms. The crystallization mechanisms of amorphous Fe-Si-B alloys was compared to those of Fe-Si-B-Cu, Fe-Si-B-Nb and Fe-Si-B-Cu-Nb alloys. Synergistic composition changes of Cu and Nb at the crystal:matrix interface were found to play a key role in determining the crystal morphology, crystal size and nucleation density. These results and the associated change in magnetic properties will be discussed.

4:00 PM Break

4:10 PM

Polymer-Metal Nanocomposites for Functional Applications: Vladimir Zaporozhchenko¹; Ulrich Schuermann¹; Henry Greve¹; Haile Takele¹; Christian Pochstein¹; Abhijit Biswas¹; Michael Frommberger²; Eckhard Quandt²; Rainer Podschun³; Franz Faupel¹; ¹Kiel University; ²Center of Advanced European Studies and Research; ³Kiel University Hospital

Recently, there is much interest in hybrid materials consisting of metal nanoparticles dispersed in a dielectric matrix due to their novel functional properties offering hosts of new applications. Polymers are particularly attractive as matrix. Consequently, various approaches have been reported to incorporate metal nanoparticles into polymers. The present talk is concerned with the preparation of polymer-based nanocomposites by vapor phase co- and tandem-deposition and the resulting functional properties. The techniques involve evaporation and sputtering, respectively, of metallic and organic components and inter alia allow the preparation of composites which contain alloy clusters of well defined composition. Emphasis will be placed on soft-magnetic and optical composites, but antibacterial coatings will also be addressed. In particular, a novel approach to produce magnetic nanorods for potential applications in high-density data storage and other fields will be presented.

4:30 PM

TEM and APT Investigations of Nanocrystalline MRE-Fe-B (MRE = Y, Nd, Dy) Hard Magnets with TiC Additions: Y. Q. Wu¹; W. Tang¹; M. K. Miller²; Iver E. Anderson¹; R. W. McCallum¹; K. W. Dennis¹; M. J. Kramer¹; ¹Iowa State University; ²Oak Ridge National Laboratory

Nanocrystalline hard magnets with multi-rare earth (MRE) elements are of interest for their high temperature performance (>200°C). A (MRE₂Fe₁₄B)_{1-x}(TiC)_x (MRE=Y, Nd, Dy) base alloy with TiC additions (mole fraction, x=0.00-0.03) was investigated using transmission electron microscopy (TEM) and atom probe tomography (APT) to ascertain whether the partitioning of the various RE occurs during solidification, the segregation behavior of elements to the grain boundaries, and the effectiveness of the TiC grain refiner. The TiC additions significantly refine microstructure from an average grain size of >200nm (x=0.01) to ~20nm (x=0.03), to alter magnetic properties. APT investigations reveal the selective behavior of MRE and TiC in the alloys. This work was supported by DOE-EE-FCVT Program, Freedom Car Initiative, through Contract No. W-7405-ENG-82 at Ames Laboratory (USDOE). Research at the SHaRE User Facility was sponsored by the Division of Materials Sciences and Engineering, U.S. Department of Energy, under Contract DE-AC05-00OR22725 with UT-Battelle, LLC.

4:50 PM Break

5:00 PM

Characterization of Soft Magnetic Nano-Material Deposited with M3D Technology: Michael Carter¹; Jacob M. Colvin¹; James W. Sears¹; ¹South Dakota School of Mines and Technology

Direct Write Technologies are being utilized in antennas, engineered structures, sensors, and tissue engineering. One form of Direct Write Technology is Maskless Mesoscale Material Deposition (M3D). The M3D process is a Direct Write Technology that uses aerosol formation, transport and deposition. Inks for the M3D process utilize nano-particles in suspension for deposition. Soft magnetic material was formulated as an ink suspension, deposited and characterized. This paper will report on the results obtained after depositing the soft magnetic material. The results of the permeability are calculated from magnetic structures created with the deposition. These results are compared to conventional methods of soft magnetic material formation and construction.

5:20 PM

Nano Structured Garnet Films Suitable for Magneto Optic Devices: Pragati Mukhopadhyay¹; ¹Indian Institute of Technology

The rapid development of the technologies of the communication and network has increased the need of high density recording for the storage of the information. Bismuth substituted rare earth iron garnet (Bi: RIG) films are potential materials for magneto-optic devices and efforts are being made to make films by various methods to enhance magneto-optic properties and make low cost viable devices. These types of films are mainly

prepared by sputtering, laser ablation, liquid phase epitaxy etc. which can be expensive, need high growth temperature and time. By Sol-gel method nano-structured garnet films suitable for magneto optic devices can be prepared at very low costs and with ease to solve these limitations. We have made bismuth substituted rare earth iron garnet films by sol gel method and compare their preparations and characterizations with other rare earth substituted films grown by us by LPE method showing good magneto optic properties.

5:40 PM

The Role of Inversion Symmetry on the Magnetisation Reversal of Array of Ni Nanobars: *Prabeer Barpanda*¹; Takeshi Kasama²; Rafal Dunin-Borkowski²; ¹Rutgers University; ²University of Cambridge

Ni nanobars are quite promising for MRAM application, as they possess stable and higher coercivity owing to their shape anisotropy. Nanobars possess a special domain structure with an 'inversion symmetry' feature. Any magnetisation process essentially deals with movement and breaking of this symmetry. This high-energy process leads to higher coercivity. The current work investigates the effect of inversion symmetry (in Ni nanobars) on the overall magnetisation behaviour of an array of closely-spaced nanobars using 3-dimensional micromagnetic simulations. We studied arrays of Ni-nanobars (spaced 10 nm apart) of varying length (20~200 nm) and diameter (10~50 nm). The longitudinal magnetisation reversal revealed the formation of symmetric inversion state, which gradually formed a Neel wall at the central cross section of nanobars before switching to the other direction. This was true both for single domain and vortex state bearing Ni nanobars. The results were compared with corresponding electron holographs and analytical calculations.

3-Dimensional Materials Science: X-Ray Methods II/Quantitative Characterization

Sponsored by: The Minerals, Metals and Materials Society, TMS Structural Materials Division, TMS: Advanced Characterization, Testing, and Simulation Committee

Program Organizers: Jeff P. Simmons, U.S. Air Force; Michael D. Uchic, Air Force Research Laboratory; Dorte Juul Jensen, Riso National Laboratory; David N. Seidman, Northwestern University; Anthony D. Rollett, Carnegie Mellon University

Tuesday PM Room: 205
March 14, 2006 Location: Henry B. Gonzalez Convention Ctr.

Session Chairs: Julie A. Christodoulou, U.S. Navy; Matthew Miller, Cornell University

2:00 PM

3DXRD Investigations of Recrystallization: *Dorte Juul Jensen*¹; ¹Riso National Laboratory

By 3 Dimensional X-ray Diffraction (3DXRD) it is possible non-destructively to make complete 3D maps of the microstructure and to follow the kinetics in-situ while deforming and/or annealing the sample. 3DXRD results on recrystallization of cold rolled fcc materials are presented. It is shown that nuclei can be registered when they have a size of about 1.4 μm, that nuclei can develop with crystallographic orientations different from the parent phase and that nucleation kinetics vary significantly from nucleus to nucleus. The growth kinetics can be monitored either by fast measurements of only the increase in volume or by slower measurements mapping the complete 3D grain shape evolution. Based on the map-type measurements growth rates are quantified and related to the crystallographic orientations of the growing grains and the surrounding deformed microstructures. Finally an outlook for the planned upgraded 3DXRD is presented.

2:20 PM

Effects of Laser Shock Peening (LSP) on the Microstructure and Residual Stress Distributions in Titanium Alloys: *Yixiang Zhao*¹; Seetha R. Mannava¹; Todd J. Rockstroh²; Vijay K. Vasudevan¹; ¹University of Cincinnati; ²GE Aircraft Engines

The present study was undertaken to develop a fundamental understanding of the effects of Laser shock peening parameters on the residual stress distributions and microstructural changes in Ti-6Al-4V alloy. Coupons of the alloy with and without a sacrificial/ablativ layer were LSP-treated with varying laser energy density using the GEN IV system at GEAE. In addition Ti-6Al-4V fan blades that had been LSP-treated were also studied. Depth-resolved characterization of the macro residual strains, stresses and degree of cold work in the peening direction and transverse to it was achieved using high-energy synchrotron x-ray diffraction at the Advanced Photon Source. The near-surface and through-the-depth changes in strain, texture and microstructure were also studied using EBSD in an SEM and by TEM, whereas local property changes were examined using micro- and nano-indentation measurements. The results showing the relationship between LSP processing parameters, the microstructure and residual stress distribution in the Ti alloy samples.

2:40 PM

Effects of Laser Shock Peening (LSP) on the Microstructure and Residual Stress Distributions in IN718 Superalloy: *Anrinder Singh Gill*¹; Vijay K. Vasudevan¹; S. R. Mannava¹; ¹University of Cincinnati

LSP enhances service lifetimes of critical metal parts like aircraft engine fans and compressor blades. LSP dramatically improves fatigue strength, life and crack propagation resistance with shock wave-induced generation of deep compressive residual stress and microstructural changes. This study aims to understand effects of LSP parameters on residual stress distributions and microstructural changes in an important aero-engine material, IN718. Coupons of alloy with and without sacrificial layer were LSP-treated with varying energy densities using the GENIV system at GE Aircraft Engines. Depth-resolved characterization of macro residual strains and stresses and degree of cold work in peening direction and transverse to it was achieved using high-energy synchrotron x-ray diffraction at the Advanced Photon Source. Property changes were also studied using EBSD in SEM and TEM. Local property changes were examined using micro and nano-indentation measurements. Results show dominant effects of sacrificial layer and energy density on residual stress distributions and microstructure.

3:00 PM Invited

Topology of 3-D Grain Structures: *Burton R. Patterson*¹; Alan P. Sprague¹; ¹University of Alabama

This presentation reviews several aspects of the topology of 3-D grain structures, such as the frequency distributions of the numbers of faces on grains and the numbers of edges on grain faces. Much data has been obtained from separation of grains by liquid metal penetration as well as by serial sectioning. Also reviewed is the path of topological change that grains must traverse during grain growth and the different arrangements of faces experimentally observed and the relative affinities between faces of n and m sides. Frequency distributions and affinities from 2-D structures are compared.

3:25 PM

Microstructure of a Shocked Tantalum Plate: *John F. Bingert*¹; Benjamin L. Henrie¹; ¹Los Alamos National Laboratory

The nature of the three-dimensional damage characteristics in a polycrystalline metal are difficult to ascertain from two-dimensional sections. The heterogeneous nature of such a structure leads to uncertainties regarding the true tableau of voids and strain localization. The term 'microstructure' has been used to describe the stereological quantification of a microstructure in terms of its geometry, and its subsequent relationship to microstructural evolution. This approach was applied to understand the correlation between the underlying microstructure and the evolution of damage within a shocked tantalum plate. A three-dimensionally reconstructed microstructure measured from serially sectioned images was used to explore the geometric state of the material. In particular, the relationship between the formation and topology of the cavitation damage and the initial microstructural defect network are investigated at the mesoscale. The evolution of shear localization with respect to the cavitation network is also considered with the aid of the reconstruction.

TUESDAY PM

3:45 PM

Determination of the Lattice Strain Tensor as a Function of Orientation from Three Dimensional Diffraction Data: *Joel Bernier*¹; Matthew Miller¹; ¹Cornell University

One of the manifestations of anisotropy in polycrystalline materials is the non-homogenous partitioning of elastic strains over the aggregate. The distributions of these strains have a strong functional dependence on crystallite orientation. In this talk, a versatile and robust method for determining a Lattice Strain Distribution Function (LSDF) from Strain Pole Figure (SPF) data is presented in the context of in situ loading/diffraction experiments. The LSDF is basically the mean lattice strain tensor as a function of crystal orientation. The determination of the LSDF relies on solving an inverse problem using optimization. Inter-granular stresses may be recovered from the LSDF via a constitutive relation, such as anisotropic linear elasticity. With this information in hand, orientations in the aggregate that are susceptible to localization or void growth may be identified. Additionally, knowledge of the evolution of these stresses and strains with deformation provides a robust tool for validation of polycrystal simulations.

4:05 PM Break

4:25 PM

Reconstruction and Characterization of 3D Microstructures: An Unbiased Description of Grain Morphology: *Michael Groeber*¹; Michael Uchic²; Dennis Dimiduk²; Yash Bhandari¹; Somnath Ghosh¹; ¹Ohio State University; ²Air Force Research Laboratory

The Dual Beam Focused Ion Beam-Scanning Electron Microscope (DB FIB-SEM) has proved to be a powerful instrument for collecting crystallographic data at a sub-micron level in 3D. The crystallographic data collected by the DB FIB-SEM system can be processed by customized codes in both 2D (Micro-Imager) and 3D (Micro-Imager3D). Micro-Imager is capable of automatically delineating grain boundaries and calculating characterization parameters for the segmented grain structure. Micro-Imager3D can be used to reconstruct the 2D orientation maps obtained during the serial-sectioning experiment into a true 3D microstructure. Once the data is reconstructed a host of statistical descriptions of the 3D structure can be made and compared to their 2D counterparts coupled with conventional stereological methods. These statistical descriptions are anticipated to be especially useful in accurately representing and model grain-level microstructures. This talk will briefly review the serial-sectioning methodology, and will focus primarily on the statistical description and representation of microstructure.

4:45 PM

The 3-Dimensional Characterization and Digitization of Complex Microstructures over Various Length Scales: *Robert Williams*¹; Santhosh Koduri¹; Peter C. Collins¹; Gopal B. Viswanathan¹; Hamish Fraser¹; ¹Ohio State University

It is necessary to fully characterize materials for inclusion in accurate neural network and fuzzy logic models relating microstructure-property relationships. Previous methods of characterizing 2-D representations of the microstructures using rigorous stereological procedures have been useful, but new techniques to characterize the microstructure in 3-dimensions are expected to yield more accurate representations of microstructure. Additionally, it is required to characterize complex microstructures at a range of length scales, from meso-scale structures (e.g., grain size) to nano-scale features (e.g., secondary α in Ti-based alloys). Titanium alloys such as Ti-6-2-4-6, an α/β alloy, offer microstructures rich in a variety of microstructural features, and this alloy has been heat-treated to produce a variety of these features. Three different 3-dimensional characterization techniques, each optimized for a specific length scale, will be shown, and the results will be discussed as they relate to the digitization of the microstructure.

7th Global Innovations Symposium: Trends in Materials R&D for Sensor Manufacturing Technologies: Session III

Sponsored by: The Minerals, Metals and Materials Society, TMS Materials Processing and Manufacturing Division, TMS: Global Innovations Committee

Program Organizers: Hamish L. Fraser, Ohio State University; Iver E. Anderson, Iowa State University; John E. Smugeresky, Sandia National Laboratories

Tuesday PM
March 14, 2006

Room: 204A
Location: Henry B. Gonzalez Convention Ctr.

Session Chair: John E. Smugeresky, Sandia National Laboratories

2:00 PM

On True Sedimentation in Liquid Phase Sintering: *Lei Xu*¹; *Shu Zu Lu*¹; *Thomas H. Courtney*¹; *Jong K. Lee*¹; ¹Michigan Technological University

When a binary alloy such as Ni-W is liquid phase sintered, heavy solid W particles sedimentate to the bottom of the container, provided that their volume fraction is less than a critical value. The sintering process evolves typically in two stages, diffusion-driven macrosegregation sedimentation followed by "true" sedimentation. During sedimentation, the overall solid volume fraction decreases concurrently with elimination of liquid concentration gradient. However, in the second stage of true sedimentation, the average solid volume fraction in the mushy zone increases with time, and oddly, no concentration gradient is necessary in the liquid zone. For the mechanism, there are several possibilities such as solid state sintering, preferential coarsening, or packing rearrangement of the solid particles. In this presentation, we will first present the experimental results of three alloy systems, Cu-Fe, Ni-W, and Pb-Sn, and then discuss theoretical analyses including a modelling work for understanding the driving force for true sedimentation.

2:25 PM

Master Decomposition Curve for Binders in PM Processing: *Gaurav Aggarwal*¹; *Seong Jin Park*¹; *Ivi Smid*¹; *Randall M. German*¹; ¹Pennsylvania State University

Thermal debinding is one of the crucial steps in powder processing. In order to systematically analyze and design the thermal debinding step, the master decomposition curve (MDC) has been formulated and constructed based on intrinsic kinetics of organic pyrolysis. The Kissinger method is used to estimate the activation energy from TGA experiments. Overall thermal decomposition was synthesized from MDCs of individual components of binder systems with experimentally good agreement, which can help process designers to change the composition without additional experiments and can predict the remaining amount of each binder component during the debinding process. The input data are obtained from industrial debinding practice. In addition, the catalytic effect of metal powders has been investigated in terms of different powders, shapes and sizes. When extrapolating to very small particle size, this approach is of particular interest for predicting the behavior of nano-particulates.

2:50 PM

Characterization of Engineering Materials Utilizing Thermoelectric Power Measurements: *Joshua E. Jackson*¹; *Angelique N. Lasseigne*¹; *David LeRoy Olson*¹; *Brajendra Mishra*¹; *Victor I. Kaydanov*¹; ¹Colorado School of Mines

Advanced thermoelectric power sensors have been developed for numerous applications to guarantee material integrity by providing a non-destructive electronic property correlation to material microstructure, phase stability, specific solute addition, lattice strain, and assessment during material processing will be discussed. These properties can be correlated to the thermoelectric power coefficient using classical electron model descriptions of the electronic state of the alloy. How the electron concentration, the effective mass, and the dominating scattering mechanisms allow for non-destructive evaluation of materials will be described. Because thermoelectric power is dependent upon numerous variables, additional non-

destructive techniques are necessary to further characterize or classify the material. The use of additional collaborative NDE technologies will be described.

3:15 PM Break

3:35 PM

Overview of the Use of Direct Write Technologies for Use in Sensor Developments and Fabrication: *James W. Sears*¹; ¹South Dakota School of Mines and Technology

Direct Write Technologies (DWT), like the ones developed under the DARPA MICE program, provide a tool for the novel manufacturing of various sensors (e.g. thermocouples and pressure transducers). DWT are also being used in electronics, engineered structures, and tissue engineering. Many of the precursors materials used as inks and pastes for the Direct Write technologies are comprised of nano-scale particles (i.e., Ag, Au, Pt). Various formulations are used to carry the nano-particles during the Direct Write processing. The Direct Write processes deliver these inks and pastes to a surface where they are then post processed to form functional devices. This presentation will provide an overview of these technologies and provide a examples of some of the sensors that have been fabricated.

4:00 PM Invited

Composite Magnetostrictive Materials for Advanced Automotive Magnetomechanical Sensors: *R. William McCallum*¹; *K. W. Dennis*¹; *D. C. Jiles*¹; *J. E. Snyder*¹; *Y. H. Chen*¹; ¹Ames Laboratory

Co-ferrite and metal-bonded Co-ferrite composites have been investigated by the authors as an alternative to existing materials competing for use in automotive and other torque sensing applications. The materials are inexpensive and non-corroding, and the metal-bonded Co-ferrite composites are mechanically robust and can be attached (e.g. by brazing) to metal parts. They show a steep slope of magnetostriction at low applied fields, $(d\lambda/dH)\sigma$, which contributes to a high sensitivity of magnetic induction to stress, hence giving high signal-to-background noise ratios in sensor applications.

Advanced Materials for Energy Conversion III: A Symposium in Honor of Drs. Gary Sandrock, Louis Schlapbach, and Seijirau Suda: Metal Hydrides II

Sponsored by: The Minerals, Metals and Materials Society, TMS Light Metals Division, TMS: Reactive Metals Committee
Program Organizers: Dhanesh Chandra, University of Nevada; John J. Petrovic, Petrovic and Associates; Renato G. Bautista, University of Nevada; M. Ashraf Imam, Naval Research Laboratory

Tuesday PM
 March 14, 2006

Room: 214B
 Location: Henry B. Gonzalez Convention Ctr.

Session Chairs: James Wang, Sandia National Laboratory; John J. Petrovic, Petrovic and Associates; M. Ashraf Imam, Naval Research Laboratory

2:00 PM Invited

Defects Formation in LaNi_5 and Its Related Alloys with Hydrogenation and Dehydrogenation: *Etsuo Akiba*¹; *Kouji Sakaki*¹; *Yumiko Nakamura*¹; ¹AIST

With hydrogenation and dehydrogenation, lattice of hydrogen absorbing alloys expands and contracts in 20 to 30% in volume. Defects are expected to be introduced into the lattice to relax the strain energy that is generated by volume expansion and contraction. We have studied defect formation into the lattice of LaNi_5 and related alloys using in-situ diffraction and positron life time measurements. In the lattice of LaNi_5 , a large amount of defects such as dislocations and vacancies was introduced at the first hydrogenation. Once defects were introduced, they were not relaxed at the working temperature of the alloys. Using diffraction method, we measured the size of crystallite before and after hydrogenation. The crystallite size did not changed with hydrogenation in all the alloy stud-

ied; LaNi_5 and $\text{LaNi}_{5-x}\text{M}_x$ ($\text{M}=\text{Al}, \text{Sn}$). Volume expansion and contraction can be accepted by introducing defects in the lattice without reducing the crystallite size.

2:25 PM Invited

Kinetics of Hydrogen Absorption and Desorption in Magnesium: Role of the Structure and of Catalysts: *Antonio Miotello*¹; ¹Università di Trento

Among the light metals forming hydride phase, magnesium is one of the most interesting for application in hydrogen storage technology because of the very high capacity, close to 7.6 wt. % : unfortunately, the very slow kinetics in hydrogenation and dehydrogenation reactions requires the addition of a proper catalyst even at temperatures as large as 673 K. The catalyst, typically in form of metallic nanoparticles (Nb, PdFe₃, Pd) dispersed at the Mg surface, favours the H₂ dissociation and the jump of H atoms towards the subsurface layers of the Mg matrix by the formation of the metastable Nb-H phases or by the transfer of H atoms to Mg after the H migration through the Mg-Nb interface. MgD₂ film samples with microcrystalline structure containing 5 at. % Nb as metallic additive (prepared by r.f. magnetron sputtering) show an improved D₂ desorption kinetics compared to the pure MgD₂ film samples, as evidenced by thermal desorption spectroscopy (TDS) analysis: the D₂ desorption spectra of the Nb doped deuteride show a maximum of the D desorption rate at 440 K compared to a maximum at 630 K for the pure MgD₂ sample. The evaluated values of the effective activation energies for desorption were 141 ± 5 and 51 ± 5 kJ mol⁻¹H for the pure and the Nb- doped hydride, respectively. It is relevant to note that the activation energy for H diffusion in a-Mg is 40 kJ mol⁻¹. To understand the role of catalyst in enhancing kinetics, Nb K-edge Extended X-ray Absorption Fine Structure spectroscopy (EXAFS), X-ray diffraction (XRD) and Transmission Electron Microscopy (TEM) were used to analyse the Nb coordination and phase formation in Nb-doped (5 at. %) h-Mg film samples. Results show that the catalytic effect of the Nb doping in the H₂ absorption and desorption kinetics is connected with the formation of Nb nano-clusters dispersed in the host matrix. In particular, while the Nb atoms are dispersed into the Mg matrix upon sputtering deposition, H-containing Nb nanoclusters (-NbH_{0.89}) are present in the film upon H₂ absorption, while Nb single metal clusters remain upon the H₂ desorption process. From the above results, we may conclude that Nb clusters act as efficient catalysts, through a number of mechanisms which include: i) a reduced stability of the hydride due to elastic stresses produced by the -NbH_{0.89} nanoclusters distributed in the matrix, ii) the presence of Mg-Nb interfaces where the transfer of H atoms preferentially occurs. This last mechanism is justified on the basis of the activation energy for diffusion, as well as the kinetics order, being ~1. On the contrary, when clusters are not formed, kinetics is low and of order ~ 4. The different kinetics orders are discussed in terms of structure and of dissociation mechanisms.

2:50 PM Invited

Storing Hydrogen with Metal Perhydrides: *Jiann-Yang James Hwang*¹; *Shangzhao Shi*¹; *Bowen Li*¹; *Xiang Sun*¹; ¹Michigan Technological University

Research on hydrogen storage materials has been pursued for many years, and has proved to be a tough task. The key problem is perhaps that most of the candidate materials are much heavier than carbon but their capabilities to bind hydrogen (in atomic ratios) are lower. In addition, the host materials cannot contribute to the energy content. It becomes more and more apparent that the hydrogen storage materials so far developed cannot meet their application goals. In recent years, the U.S. Department of Energy sponsored a number of projects exploring new materials and concepts for hydrogen storage. This article briefs a project being currently pursued at Michigan Technological University. The project is exploring a novel kind of materials that contain hydrogen clusters in their molecules. The novel materials are termed as metal perhydrides, which are anticipated to have sufficient content of hydrogen and are promising for high-efficiency hydrogen storage.

3:10 PM

Suppression of the Martensitic Transformation in Ti-Ni-Cu Alloys with Shape Memory Properties: Specific Impact of Hydrogenation: *Nataliya Skryabina*¹; *Daniel Fruchart*²; *Aleksandr Shelyakov*³; *Dmitrii*

TUESDAY PM

Gunderov⁴; ¹Perm State University; ²Centre National de la Recherche Scientifique; ³Moscow Physical-Technical Engineering Institute; ⁴Institute of Physics of Advanced Materials

Two possibilities were known to suppress the thermo-elastic martensite phase transformation in alloys based on the Ti-Ni-Cu system. The first one route can operate via a refinement of the grain size up to 10 to 15 nm from fast quenching treatments from the melt. The second route results from severe plastic deformation (SPD) or high pressure torsion (HPT) methods developed at room temperature. We have discovered a new possibility to suppress the martensite B2-B19 transformation by hydrogenation of amorphous then nano-crystallised alloys. This results in a two step process of the grain growth promoted by hydrogenation and subsequent heat treatments of the nano-crystallized materials. The nucleation of the nano-grains at a first step of crystallization has made impossible the B2-B19 transformation due to a reduced size of the grains. In this contribution, we compare the merits of the different process as mentioned here above.

3:30 PM

Investigations on Light Metal Hydrides at Padova, the City of San Antonio: *Gianni Principi*¹; P. Palade¹; S. Sartori¹; A. Maddalena¹; F. Agresti¹; S. Lo Russo¹; ¹Università di Padova

The activity of the "Hydrogen Group" of Padova University, addressed to the study of materials for solid state hydrogen storage, is illustrated. Various Mg-based materials have been considered and are being studied: a) MgH₂ and 0.5% mol Nb₂O₅ mixture ball milled under argon atmosphere; b) Mg-Ni-Fe intermetallic compounds prepared by short time ball milling of ribbons obtained by melt spinning and by long time ball milling of a mixture of MgH₂, Ni and Fe powders; c) MgH₂ ball milled in argon with Ni-Al and Zr-Cr-Fe catalyst alloys. All the samples have been structurally characterized by X-ray diffraction (Rietveld refinement) before and after hydrogen absorption/desorption cycling and tested with a Sievert apparatus as regarding their thermodynamic and kinetic properties. Investigations are also in progress on complex hydrides as alanates and Li amides modified with transition metal based catalysts.

3:50 PM Break

4:05 PM Keynote

Is High Weight H Intake in Pseudobinaries Still an Option?: *Issac Jacob*¹; ¹Ben Gurion University of Negev

Pseudobinary intermetallic compounds constituted the backbone of hydrogen storage research for tens of years. This is because they present versatile hydrogenation properties, and some of them form reversible hydrides under moderate hydrogen pressures near room temperature. However, a current limit of about 2% hydrogen weight causes a shift of the research interest to other hydrogen absorbers. We overview here the conditions and the factors, determining hydrogen absorption in intermetallic compounds. A special attention is given to recently found differentiation and divergence of elastic properties in intermetallics upon pseudobinary substitution. The possibility to form superior intermetallic compound for hydrogen storage is considered.

4:25 PM

Hydrogen Short-Long Range Dynamics in Nano-MgH₂ a Mechanical Spectroscopy Approach: *Ennio Bonetti*¹; Annalisa Fiorini¹; Luca Pasquini¹; Amelia Montone²; Marco Vittori Antisari²; ¹University of Bologna; ²ENEA Centro Ricerche Casaccia

The technological applications of MgH₂ hydrides for hydrogen storage demand the overcoming of some critical issues: an improvement of the reaction kinetics and a reduction of the desorption temperature. The synthesis of nanocrystalline MgH₂ by reactive milling and inert gas condensation and proper catalysts addition, are recently employed strategies. In the investigation of the hydrogen short and long range dynamics, the sorption kinetics and the nanostructure stability, the mechanical spectroscopy offer some specific advantages. In the present research this technique was employed with other experimental approach XRD, TEM, to investigate relaxational and structural damping processes in nanocrystalline MgH₂ with different added catalysts. Time temperature variation of the dynamic elasticity moduli and mechanical quality factor are correlated to hydrogen anelastic relaxation processes and concomitant structural transformation of MgH₂ to Mg during long range diffusion. Results are dis-

cussed with reference to microstructural modification strategies able to assist hydrogen release.

4:45 PM

Characterization of Hydrogen Storage Capabilities of the Two-Phase Region of LaNi₅: *Angelique N. Lasseigne*¹; M. Ashraf Imam²; Brajendra Mishra¹; David LeRoy Olson¹; ¹Colorado School of Mines; ²Naval Research Laboratory

Hydrogen storage capabilities of LaNi₅ intermetallic compounds are investigated utilizing the combination of thermoelectric power, Beeghy Ester-Halogen digestion, and Leco hydrogen determination. Thermoelectric power has demonstrated a rapid hydrogen assessment capability and can achieve the equivalent of the pressure-composition-temperature (activity) diagram. Effective use of hydrogen storage materials occurs in the (alpha+beta)-phase plateau region of the PCT diagram. A thorough assessment of the content of each phase in this two-phase region to optimize performance of the hydrogen storage materials will be described. Practices using the combination of these three analytical practices for rapid characterization of LaNi₅ intermetallic alloys will be discussed.

5:05 PM

Improving a Rechargeable Hydrogen Storage Capacity of BCC Alloy by Eliminating Internal Defects: *Toshiki Kabutomori*¹; Kazuya Kubo¹; Hironobu Arashima¹; Hideaki Itoh¹; Takanori Suda²; Somei Ohnuki²; Keizo Onisi¹; ¹Japan Steel Works, Ltd.; ²Hokkaido University

Although a Ti-Cr-V hydrogen storage alloy having a BCC structure can absorb about 4wt% hydrogen, a rechargeable hydrogen storage capacity is only about 2.6 wt% because the alloy has a wide hydrogen solid solution. On the other hand, many internal defects are introduced by the volume expansion (> 40 %) at the hydriding of the Ti-Cr-V BCC alloy. Due to hydrogen trapping to the defects, it is expected that hydrogen solid solution increase, resulting to decrease a plateau width in the P-C-T diagram. In this study, we examined an influence of the internal defects produced by hydriding affects the P-C-T characteristic of a Ti₂₄Cr₃₆V₄₀ BCC alloy. After annealing at 1,000°C for 10 min, a Ti-Cr-V BCC alloy shows increase in the plateau width from 2.4 to 3.3wt%. Accordingly, it is thought that a rechargeable hydrogen capacity of the BCC alloy can be largely improved by eliminating the internal defects.

5:25 PM

Low Pressure Hydriding of V-0.5 at% C Hydrides: *Joshua H. Lamb*¹; Dhanesh Chandra¹; Michael Coleman¹; Joseph R. Werner¹; Stephen N. Paglieri¹; ¹University of Nevada

The properties of vanadium (V) hydride formation at low pressures have significance in hydrogen transport membranes. Low pressure hydriding characteristics of V-0.5 at% C alloy using gas phase hydrogen has been performed in this study. There are few prior reports on the stability and low pressure isotherms of (pure) vanadium 1 phase pure V and some with alloying elements (transition elements), but no reports on V-C alloys. The V-0.5% C has many advantages from strengthening of the alloy as well as structural integrity of the membranes. In our study, van't Hoff plots were plotted and enthalpies of the low pressure plateau region of the V-0.5% C and pure V are compared.

Alumina and Bauxite: Bauxite and Bauxite Characterization

Sponsored by: The Minerals, Metals and Materials Society, TMS Light Metals Division, TMS: Aluminum Committee

Program Organizers: Jean Doucet, Alcan Inc; Dag Olsen, Hydro Aluminium Primary Metals; Travis J. Galloway, Century Aluminum Company

Tuesday PM
March 14, 2006

Room: 7B
Location: Henry B. Gonzalez Convention Ctr.

Session Chair: Milind V. Chaulal, Sherwin Alumina Company

2:00 PM Introductory Comments

2:10 PM

Cross Country Bauxite Slurry Pipeline Transportation: *Ramesh L. Gandhi¹; Yueguang Che¹; Jay Norwood¹; ¹Pipeline Systems Incorporated*

Over the last four decades, slurry pipelines have proven themselves to be a safe, reliable and cost effective way to transport large tonnages of minerals over long distances. A variety of minerals have been successfully transported over distances ranging from a few kilometers to 400 km. However, no long distance bauxite pipelines have been built to date. Bauxite has developed a reputation for being difficult to pump. This is about to change with the first long distance slurry pipeline. The 250 km long 10 MT/y capacity pipeline is designed by PSI. Several other pipelines are currently being considered for transportation of bauxite. It will be shown that a properly designed hydro-transport system is an economically viable alternative for the long distance transport of bauxite ore. The focus of this paper is on how to integrate a pipeline into an existing facility.

2:35 PM

The Future of Alumina/Bauxite Mining in Guinea: *Koulibaly Siafa¹; ¹Ministry of Geology and Mines*

Guinea is one of the richest countries in Africa in view of its bauxite mining and energy potential. It has nearly one-third of the world's bauxite reserves and it is the second world producer of this mineral, coming after Australia. The mining sector plays a key role in the Guinean economy. The state will continue to depend highly on this sector's fiscal revenue and foreign exchange for the coming years at least. Guinea is currently facing serious economic problems. It is therefore of prime importance that government should adopt effective policies with regard to management and making viable regulation to govern the alumina/bauxite industry, as well as acquire strong capacity to implement them. This paper will survey the basic parameters such as resources and competitiveness, Guinea's prospective in terms of efficiency of technology, and environmental considerations. The article will emphasize Guinea's bauxite position in the market, increasing production, and opening new alumina plants.

3:00 PM

Occurrence and Characterization of Zn and Mn in Bauxite: *Frank Roman Feret¹; Jeannette See¹; ¹Alcan Inc*

Zinc is one of the secondary elemental constituents occurring in Caribbean bauxite and the associated non-bauxitic material. It is generally believed that Zn in bauxite could either occur in gahnite or sphalerite, or substitute for Fe in goethite. Manganese represents an appreciable impurity in Caribbean bauxites and is identified on diffractograms as lithiophorite (Li,Al)MnO₂(OH)₂. Because Zn was observed to increase with the MnO content the objective of this work was to better understand the mineralogical nature of Zn and Mn compounds. Data representative of 340 bauxite samples of different origin was assembled. It was found that Zn in bauxite cannot substitute for Fe in goethite or hematite. Strong evidence was obtained that Zn occurs in the same compound as Mn. The application of the Rietveld-XRD method to the quantification and characterization of a new mineral called zincophorite Al(Zn_xMn_{1-x})O₂(OH)₂ is discussed. Caustic solubility of ZnO in bauxite is also assessed.

3:25 PM Break

3:45 PM

Beneficiation of High Quartz Content Bauxite from Los Pijiguao: *Jean-Marc Rousseaux¹; Perdo Flores²; Stefan Buntentbach³; Hans Verschuur¹; ¹Alcan; ²CVG Bauxilum; ³AKW Apparate und Verfahren*

At Los Pijiguao, the economic bauxite horizon attains an average thickness of 7.6 m. Below this layer, High Quartz Content bauxite can be found. The aim of this study was to investigate the possibility to extract quartz from High Quartz Content bauxite of LP, with a minimum of Al₂O₃ losses. The beneficiation process studied in this work is carried out in several steps. The first step is an elutriation, operated in a washing drum, aiming at liberating quartz particles. The second step is a classification process, aiming at obtaining different grain sizes according to the quartz content. Part of the study was to investigate if the finest fractions could further be beneficiated using such technologies as cyclones and shaking tables. This paper describes tests carried out and results obtained. Characteristics of beneficiated bauxite and beneficiation recovery are also detailed. Conclusions and perspectives delineate pilot test strategies.

4:10 PM

Thin Layer Chromatography of Bauxite: Instrumental Characterization and Quantification by Scanning Densitometry: *Mohamed Najari¹; Ramana Rao Kondapalli¹; ¹Jawaharlala Nehru Aluminium Research Development and Design Centre*

Thin layer chromatography (TLC) was successfully used for the detection and characterisation of various elements present in bauxites. The chromatographic characteristics have been evaluated on silica gel and cellulose layers developed with double distilled water and aqueous sodium chloride solutions. The densitometric evaluations of chromatograms of Al, Fe, Ti and Si in bauxites have shown a percentage recovery of 98 ± 2. The method developed was successfully extended to the characterisation of organic impurities (<0.2%) in bauxites by coupling TLC with FTIR spectroscopy. The characteristic functional groups for some organic compounds were identified in the IR spectra. The advantages of these methods over the conventional methods of characterisation were also presented.

Aluminum Reduction Technology: Cell Development and Operations - Part II

Sponsored by: The Minerals, Metals and Materials Society, TMS Light Metals Division, TMS: Aluminum Committee

Program Organizers: Stephen Joseph Lindsay, Alcoa Inc; Tor Bjarne Pedersen, Elkem Aluminium ANS; Travis J. Galloway, Century Aluminum Company

Tuesday PM

March 14, 2006

Room: 7A

Location: Henry B. Gonzalez Convention Ctr.

Session Chair: Yousuf Ali Mohammed Alfarsi, Dubal Aluminium Company Ltd

2:00 PM

Paradox in Cell Temperature Measurement Using Type K Thermocouples: *Xiangwen Wang¹; Gary P. Tarcy¹; Mike Slangenaupt¹; Susanne L. Albright¹; ¹Alcoa Inc*

Type K (Chromel-Alumel) thermocouples or temperature probes are widely used in routinely measuring cell temperature because they are readily available and economical while offering the kind of accuracy and precision for smelter operations. However, the popular usage does not mean there are no issues. More often than not, we, as an end user of the thermocouples, are not aware of the existence of several alloys available in the market in making the Type K thermocouples. Accordingly, some confusions or ignorance in selecting proper thermocouples and their proper accessories causes inaccurate temperature measurements or temperature measurement bias. Sometimes, a temperature bias as high as 10C may be observed. This paper discusses our smelter operating experience in dealing with the temperature bias issues in using Type K thermocouples and probes. Selection from various suppliers and proper use of the Type K thermocouples are discussed.

2:25 PM

The Liquidus Enigma Revisited: How it Could Be Solved: *Bjorn P. Moxnes¹; Asbjørn Solheim²; Trond Store¹; Bjorn Erik Aga¹; Lisbet Støen²; ¹Hydro Aluminium; ²SINTEF*

The superheat calculated from bath analyses often show negative values, although measurements made with the superheat-sensor from Heraeus Electro-Nite show positive values. Aiming at coming up with an explanation, the bath temperature and superheat were measured in different cells at the Hydro Aluminium Sunndal plant and at the Research Centre in Årdal. Simultaneously, bath samples were taken for Al₄C₃ analysis, XRF, XRD and ICP analyses, as well as alumina analysis on LECO and thermal analysis. It turned out that Al₄C₃ content was very low. By comparing all measured temperatures, it could be concluded that the Heraeus probe in some cases gave 4-5°C too high superheat. The key factor, however, appeared to be the precision of the standard bath analysis. Furthermore, it is likely that the some of the trace elements in the bath lower the liquidus temperature more in an acidic bath than in pure cryolite.

TUESDAY PM

2:50 PM

Rate of Metal Cooling in Aluminum Reduction Cell Removed from Line Current – Method and Model: *Kayron F. Lalonde*¹; H. Wayne Cotten; Richard M. Beeler; ¹Alcoa Inc

A method was established for obtaining temperatures of molten aluminum as it solidifies in a reduction cell after the cell has been removed from line current (a “dead” cell). The temperatures were used to develop cooling curves, so the time at which the metal pad solidifies can be estimated and demolition of the lining can begin. The effect on the cooling rate of removing all the anodes in the cell at 24 hours was assessed. Mathematical modeling including the heat of fusion of aluminum was developed to explain the effect of anode removal and to provide predictive capability based on several input variables.

3:15 PM

Method for Automated Adjustment of Alumina Feeding Times in Smelting Pots: Constantin Radulescu¹; Puiu Chirimbu¹; *Cristian T. Stanescu*¹; Mihail Atanasiu¹; Ioan Cojocaru¹; Gheorghe C. Dobra¹; ¹ALRO SA

This paper presents a method for automated adjustment of alumina feeding times in smelting pots with a continuous control of alumina concentration in the bath. The method performs a recalculation, each 4 - 8 hours, of the feeding frequency for theoretical, over and underfeeding in order to keep an alumina concentration in the bath in the range of 1.6 - 2.2%. The basis for recalculation is the connection of the main pot parameters with the theoretical feeding frequency. This allows keeping optimal condition for alumina dissolution and counteracts the time variation of the weight of alumina doses. Moreover this method limits the sludge accumulation on the pot bottom and prevents the occurrence of anode effects resulting from temporary failures of equipment.

3:40 PM Break

3:50 PM

CVG Venalum Potline Supervisory System: *Carlos Abaffy*¹; Jesús Lárez¹; Rafael Aique¹; Jesús González¹; ¹CVG Venalum

This paper describes architecture and features of CVG-Venalum aluminum reduction Cell Supervisory System (SSC) which, besides the standard characteristics of a supervisory system (real-time parameters display, historic trends, operation tracking, etc.), allows effective (easy interpretation), accurate (allows quantitative evaluation) and adaptable (serves multiple needs) data visualization and analysis of potlines. The SSC has an outstanding performance compared with other supervisory systems. It's been installed in 4 CVG-Venalum potlines of 180 cells each, where a desktop PC serves each line with no impact on performance. In addition, the potlines have been integrated in a high-level system for visualize the whole plant. The SSC is part of the V-350 cell technology and it will be used in CVG-Venalum and CVG-Alcansa expansion plans. The system was developed using free software platform: LAMP (Linux-Apache-MySQL-Php) and C++. The Human-Computer Interface is mainly web, allowing the user interact easily with the system using a web browser.

4:15 PM

300 KA Pre-Baked Cells Start-Up at the “Sual” JSC: *Viatcheslav Veselkov*¹; Yury Bogdanov¹; Boris Ayushin¹; ¹Sibvami JSC

In May 2005 the Test Site of six 300 KA (design amperage) pre-baked cells was put in operation at the Ural Aluminium smelter. All calculations and Test Cell Project was developed by “SibVAMI” JSC, Irkutsk. The Site consists of the Reduction Pot Room, “Dry” Scrubber Unit, and injecting Silicon Rectifier. Power for the Test Site is supplied from two sources: the existing Pot Line (165 KA) and the injecting SR (135 KA). The cell shows highly stable behavior, MGD-noise in the cell is under 15-20 mV. Test cell bottom firing was carried out using gas-flame unit for 72 hours. The competitive up-to-date electrolyzer was developed. These cells are intended for operation at 330 – 350 KA.

4:40 PM

Investigation of the Failure of a 300kA Prebaked Anode Reduction Cell: *Zhongning Shi*¹; Bijun Ren¹; Hongtao Zhang²; Quanhong Cao²; Tiejun Wen²; Hui Li²; Zhuxian Qiu¹; ¹Northeastern University; ²Yichuan Aluminum Smelter Plant

Because of the failure of side lining and cathode, some 300kA prebaked anode aluminum reduction cells were shut down in Yichuan aluminum smelter plant. Combining with actual observations, the samples of side lining and cathode were analyzed from different locations of the cell, and the failure reasons of the Si₃N₄-SiC side lining and cathode were investigated. Also, the influencing factors of cathode and side lining failure were summarized as superheat temperature, anode effect coefficient, interval from anode edge to the sidewall, anodic current density and the operating parameters. Some suggests are offered to solve these problems occurring in large scale prebaked anode reduction cell in China.

5:05 PM

Production of Refined Aluminum and High-Purity Aluminum: *Huimin Lu*¹; Yongheng Wang¹; Zongren Liu²; Xinsheng Zhai²; Jie Liu²; Tao Hong²; ¹University of Science and Technology Beijing; ²Xinjiang Joinworld Company, Ltd.

Xinjiang Join-world Co. Ltd. is the largest producer in China and an important one in the world for refined aluminum and high-purity aluminum. At present, 99.99~99.9999% refined aluminum is produced by 80kA three-layer electrolysis cells (XJ-80) with the Gadeau process electrolyte system and solid refined aluminum cathode, the current efficiency is up to 99%, DC power consumption 14000kWh/t refined aluminum, the XJ-80 cell is also the largest one in aluminum refining industry in the world; 99.999~99.99999% high-purity aluminum is yielded by the combined technique of three-layer electrolysis and segregation method; high-purity aluminum in excess of 99.9999% is produced by the new combined technique of ionic liquid electrolysis and zone refining method. This paper introduces these characteristics of the XJ-80 three-layer electrolysis cell, the combined technique of three-layer electrolysis and segregation method and the new combined technique of ionic liquid electrolysis and zone refining method for producing high-purity aluminum.

5:30 PM End

Amiya Mukherjee Symposium on Processing and Mechanical Response of Engineering Materials: Processing of Materials

Sponsored by: The Minerals, Metals and Materials Society, TMS Materials Processing and Manufacturing Division, TMS Structural Materials Division, TMS/ASM: Mechanical Behavior of Materials Committee, TMS: Shaping and Forming Committee
Program Organizers: Judy Schneider, Mississippi State University; Rajiv S. Mishra, University of Missouri; Yuntian T. Zhu, Los Alamos National Laboratory; Khaled B. Morsi, San Diego State University; Viola L. Acoff, University of Alabama; Eric M. Taleff, University of Texas; Thomas R. Bieler, Michigan State University

Tuesday PM
March 14, 2006

Room: 217C
Location: Henry B. Gonzalez Convention Ctr.

Session Chairs: Donald R. Lesuer, Lawrence Livermore National Laboratory; George C. Kaschner, Los Alamos National Laboratory

2:00 PM Invited

A Microtexture Investigation of Recrystallization during Friction Stir Processing of As-Cast NiAl Bronze: Keiichiro Oishi¹; Alexander P. Zhilyaev¹; *Terry R. McNeley*¹; ¹Naval Postgraduate School

OIM and TEM methods were used to obtain microtexture data in an NiAl Bronze subjected to FSP. Random textures, grains 1 – 2 μm in size and annealing twins indicated recrystallization in the phase inside the stir zone; subgrains near the plate surface apparently formed after passage of the tool. Distinct shear textures and texture gradients were apparent in the thermomechanically affected zone (TMAZ) outside and along the periphery of the stir zone. The TMAZ texture gradient was steeper on the advancing side and under the stir zone center than on the retreating side. Grain refinement in the a phase reflects dynamic recrystallization and particle stimulated nucleation at undissolved particles during FSP. Random stir zone textures reflect recrystallization textures for materials expe-

riencing warm deformation in shear during FSP as well as contributions from PSN and the twin chaining.

2:20 PM

Aspects of Thermomechanical Processing Controlling the Austenite Transformation in Si-Mn TRIP Steel: *Jozef Zrnik*¹; Ondrej Stejskal²; Zbysek Novy¹; Peter Hornak³; ¹COMTES FHT; ²West Bohemian University; ³Technical University of Kosice

The main emphasis of this study has been placed on thermomechanical processing simulations of TRIP steel performed by using forging. The choice of applied strain and thermal parameters modified austenite conditioning and consequently affected its transformation kinetics and resulted in variety of final structure characteristics in time of two step transformation process. The development of multiphase structure consisted of ferrite, bainite and retained austenite had strong impact on the transformation induced plasticity effect of steel. The complex relationship among the volume fraction of the retained austenite, the morphology and distribution of phases, and mechanical properties of TRIP steel was revealed. The tensile tests were conducted and due to TRIP effect functionality good combination of tensile strength and ductility was found. The results proved that TM processing conducted in intercritical temperature region significantly effected forming and refinement of convenient multiphase structure, providing sufficient ductility at increased strength of bulky forgings.

2:40 PM

Design of High-Strength Steels by Microalloying and Thermomechanical Treatment: *Patricia Romano*¹; Araz Ardehali Barani¹; Dirk Ponge¹; Dierk Raabe¹; ¹Max Planck Institute for Iron Research

Steels with higher strength, ductility and improved fatigue behaviour are required for light-weight structures in the automotive industry. It is shown that for ordinary steels the combination of microalloying and an optimized thermomechanical treatment results in increased strength and improved ductility. Proper conditioning of the austenite by a sequence of deformation steps refines the austenitic grains and generates a dislocation substructure that is inherited to the martensite structure. In contrast to simply quenched and tempered martensite with no prior deformation, the thermomechanically processed martensite exhibits a more refined structure and is free of grain boundary carbides. Addition of vanadium is beneficial for the stabilization of the austenite defect structures that are produced by deformation. In this study an increase of more than 600MPa in the ultimate tensile strength and an improvement of 40% in the reduction area are reported. A general thermomechanical treatment for high-strength martensitic steels is proposed.

3:00 PM

Development of the Surface Structure of TRIP Steels Prior to Hot-Dip Galvanizing: *Erika Bellhouse*¹; Anne Mertens¹; Joseph McDermid¹; ¹McMaster University

Focusing on improving the galvanizability of TRIP steels, the effect of the alloying elements; manganese, silicon and aluminum on the surface state prior to galvanizing were studied. A C-Mn steel was used to determine the effect of manganese, and TRIP steels with varying amounts of Si and Al were used to determine the effect of the silicon and aluminum. Different dew points and reducing atmospheres were tested during annealing in a galvanizing simulator in order to improve the wettability of liquid zinc on the steel surface. This paper will present the kinetics and development of the surface structure prior to galvanizing as a function of annealing atmosphere, temperature and time.

3:20 PM

Effect of Annealing Atmosphere on Galvanizing Behavior of Dual Phase Steel: *Rubaiyat Khondker*¹; *Anne Mertens*¹; Joseph R. McDermid¹; ¹McMaster University

Selective surface oxidation of alloying elements such as Mn can cause DP wettability problems by liquid Zn during continuous galvanizing. It is well known that process parameters, such as annealing atmosphere %H₂ and dew point, can affect surface and subsurface oxidation. The purpose of the paper is to study the effect of annealing atmosphere to find the desired DP steel surface that could produce better wetting by zinc. In particular, the evolution of the surface phases and structures during the continuous galvanizing annealing cycle were studied. It will be shown that the internal/external oxidation behavior of the alloying elements of DP

steel (e.g. Mn, Si, and Mo) at the surface and subsurface demonstrate that segregation can be controlled by changing process parameters (dew point and H₂/N₂ ratio) and that some segregation of elements is unavoidable but can produce good wetting by liquid galvanizing alloys.

3:40 PM

New Aqueous Metal Feedstock Materials for Injection Molding Process: *Mohammad Behi*¹; Kamal Shahrabi¹; Ahmad Shohadaee¹; ¹Kean University

A new water-based stainless steel 17-4 feedstock material has been developed for the injection molding process. Fine stainless steel 17-4 powder (10-25 microns) is mixed with a binder system at about 85-90°C to make the feedstock. The binder comprises 98-99% de-ionized water and 1-2wt% polysaccharide binder. A conventional injection molding machine is used to mold the feedstock into articles of various shapes at temperatures between 80-90°C and injection pressures of 500-900 psi. The flowability of the feedstock material was evaluated at 500 and 1000 psi injection pressures. Unlike the polymer based metal feedstock, there is no thickness limitation and no debinding process associated with this new material upon sintering. The molded parts are sintered at 1300-1350°C in hydrogen atmosphere. The feedstock material is user friendly and environmentally safe.

4:00 PM Break

4:10 PM Invited

Nano-Subgrain Strengthening in Ball-Milled Iron: *Donald R. Lesuer*¹; Chol Syn¹; Oleg Sherby²; ¹Lawrence Livermore National Laboratory; ²Stanford University

Recent studies of ball-milled iron have shown that nano-scale subgrains can form during the early stages of ball milling. In this paper we evaluate the strength and strengthening mechanisms of these ball-milled materials containing nano-subgrains. The results are compared with the strength and strengthening mechanisms resulting from larger-scale subgrains in iron and iron-base alloys produced by traditional mechanical working. The data covers over 2 orders of magnitude in subgrain size (from 30 nm to 6 µm). For all materials studied, at the larger grain sizes the strength varied as λ^{-1} , where λ is the subgrain size. In addition, the ball-milled materials showed significant strengthening contributions from nano-scale oxide particles. The data shows deviation from the λ^{-1} relation and a breakdown in subgrain strengthening at about 150 nm. The results are interpreted in terms of changes in the dominant strengthening mechanism with subgrain size and oxide particle spacing.

4:30 PM

Deformation Mechanisms of Cryomilled Al Alloys with Bimodal Microstructure: *Bing Q. Han*¹; David B. Witkin¹; Riqing Ye¹; Enrique J. Lavernia¹; ¹University of California

Cryomilling is one of several synthesis techniques that is capable of producing engineering materials with grain sizes in the 10-500 nm ranges. In the present study, processing of several bimodal nanostructured Al alloys from cryomilled nanostructured powders is reviewed briefly, followed by a discussion of mechanical behavior and the underlying deformation mechanisms. Particular emphasis is placed on strategies aimed at the development of materials with a balance of properties, i.e., strength and ductility. In one such strategy, as the volume fraction of submicron grains is increased, tensile ductility increased and strength decreases. Enhanced tensile ductility is attributed to the occurrence of crack bridging as well as delamination between nanostructured and submicron-grained interfaces during plastic deformation. The finite element simulation on the deformation behavior and failure process of cryomilled bimodal Al alloys via a unit-cell model is also presented. The numerical results are in good agreement with tensile experimental data.

4:50 PM

Effect of Degassing on Mechanical Properties, Density and Porosity in Cryomilled Nanostructured Al-Mg Alloys: *Byungmin Ahn*¹; Piers Newbery²; Enrique J. Lavernia²; Steven R. Nutt¹; ¹University of Southern California; ²University of California

5083 Al powders were ball-milled in a cryogenic temperature to accomplish nanocrystalline grains, and then degassed to remove residual gaseous phases at different temperatures and time. The degassed powder

was consolidated using CIP (Cold Isostatic Pressing) followed by forging to produce bulk nanostructured materials. The mechanical properties, such as yield strength and elongation, of the bulk materials were enhanced relative to 5083 Al with conventional grain size. The mechanical properties of these materials tended to vary with respect to different degassing conditions, which also correlated with the density and porosity of the resulting bulk materials. The relation between the mechanical properties and microstructures also will be discussed in detail. In the present study, the variation of microstructure, porosity and density was investigated using optical microscope, SEM, TEM and density measurements. The quantitative analysis of density and porosity provides insight and a basis for optimizing the degassing conditions and production procedures.

5:10 PM

Characterization of Mechanical Alloying Processed Ti-Si-B Nanocomposite Consolidated by Spark Plasma Sintering: H. B. Lee¹; I. J. Kwon¹; *Young-Hwan Han*²; ¹Myong-Ji University; ²University of California, Davis/Sungkyunkwan University, Korea

The microstructure and mechanical properties of TiB₂/Si nanocomposites based on the Ti-Si-B system, consolidated by spark plasma sintering of mechanically alloyed activated nanopowders, have been characterized. Mechanical Alloying was carried out in a planetary ball mill for 180 min with 350 rev min⁻¹. The powders were pressed in vacuum at a pressure of 60 MPa, generating a maximum temperature in the graphite mould of 1400°C. Analysis of the synthesized nanocomposites by SEM, XRD and TEM showed them to consist of TiB₂ second phase, sub-micron in size, with no third phase. Composites consolidated from powders mechanically alloyed from an initial elemental powder mix of 0.3 mol Si, 0.7 mol Ti, and 2.0 mol B achieved the best relative density (97%) and bending strength (774 MPa); the highest Vickers hardness of 14.7 GPa was achieved for the 0.1-0.9-2.0 mol starting composition.

5:30 PM

Processing Ti-Al-Nb Sheet Materials by Accumulative Roll Bonding and Reaction Annealing from Ti/Al/Nb Elemental Foils: *Rengang Zhang*¹; Viola L. Acoff¹; ¹University of Alabama

The Ti-46Al-9Nb (at%) was produced using accumulative roll bonding followed by two-stage annealing from elemental foils. Well-bonded sheet materials were successfully obtained with the initial rolling reduction of 50%. Two-stage annealing of 600°C and 1400°C was employed to promote the formation of intermetallic compounds. The SEM and XRD analysis indicated that there were no room temperature solid-state reactions between Ti/Al/Nb foils, even at high cycles. Besides the annealing time and temperature, rolling strain also has a significant effect on the production of the intermetallic compound. Differential thermal analysis (DTA) was used to characterize the effect of rolling strain on the solid-state reaction and phase formation in the composites during annealing. It is clear that the first annealing stage did promote the complete reaction of the Al layers to form the intermetallic compounds TiAl₃ and NbAl₃. After the second stage annealing, the desired intermetallic compounds, composition and lamellar structure were achieved.

5:50 PM

High Strength and Ductility of Nanostructured Al-Based Alloy Prepared by High Pressure Technique: *Nikolay Krasilnikov*¹; ¹Ulyanovsk State University

The structure and mechanical properties of Al-based alloy 2024 after high-pressure torsion (HPT) was investigated. Alloy 2024 with homogeneous structure and grain size about 70 nm was obtained using HPT at 6 GPa pressure and 5 turns of anvils at room temperature. The nanostructured alloy at room temperature demonstrated very high UTS above 1100 MPa, and superplastic behavior at temperature higher than 300°C. The microhardness of nanostructured alloy after superplastic deformation (1.5 GPa) was more than after standard treatment of coarse-grained alloy (1.2 GPa). The influence parameters of HPT and heat treatment on structure and deformation behavior of alloy were studied. Opportunity of achievement in metals and alloys of combination high strength and good ductility opens perspectives of its application in industry, particularly, for microsystems and for high-strength details with complex geometry obtained due to superplastic forming.

Amiya Mukherjee Symposium on Processing and Mechanical Response of Engineering Materials: Poster Session: Processing and Mechanical Response of Engineering Materials

Sponsored by: The Minerals, Metals and Materials Society, TMS Materials Processing and Manufacturing Division, TMS Structural Materials Division, TMS/ASM: Mechanical Behavior of Materials Committee, TMS: Shaping and Forming Committee

Program Organizers: Judy Schneider, Mississippi State University; Rajiv S. Mishra, University of Missouri; Yuntian T. Zhu, Los Alamos National Laboratory; Khaled B. Morsi, San Diego State University; Viola L. Acoff, University of Alabama; Eric M. Taleff, University of Texas; Thomas R. Bieler, Michigan State University

Tuesday 5:15-7:00 PM
March 14, 2006

Room: 217C
Location: Henry B. Gonzalez Convention Ctr.

Comparative Analysis of Microstructural Defects Obtained by Quasi-Isentropic Compression of Copper via Gas-Gun and Laser Driven Loading: *Hussam Nassib Jarmakani*¹; J. M. McNaney²; M. S. Schneider¹; D. Orlikowski²; J. H. Nguyen²; B. Kad¹; M. A. Meyers¹; ¹University of California, San Diego; ²Lawrence Livermore National Laboratory

This current effort aims at understanding the differences in microstructural defects in copper obtained by quasi-isentropic loading achieved using two different methods: gas-gun loading and laser-driven loading. Although the pressures reached in both cases are the same, the strain-rates achieved are approximately three orders of magnitude higher in the laser experiments (10⁷ 1/s as compared to 10⁴ 1/s for gas-gun experiments). Dislocation activity at lower pressures in both cases are compared, and the transition of the defect substructure into stacking faults and twins is discussed. A constitutive model describing the slip-twinning transition for both cases is also introduced.

Effect of Competing Deformation Mechanisms on the Plastic Anisotropy of Zr Severely Deformed by Equal Channel Angular Extrusion (ECAE) at Room Temperature: *Guney Guven Yapici*¹; Irene J. Beyerlein²; Ibrahim Karaman¹; Carlos N. Tome²; ¹Texas A&M University; ²Los Alamos National Laboratory

Recent findings have shown that a number of materials exhibit plastic anisotropy after large strain deformation. Huge strains and various routes applied during ECAE alter the microstructure and crystallographic texture significantly leading to considerable flow stress anisotropy. High purity Zr billets with different initial textures are successfully extruded at room temperature. Post-processing compressive response up to 30% strain along three orthogonal directions are reported along with microstructural and textural evolution at intermediate strain steps. This extensive experimental approach will shed light on the governing deformation mechanisms, namely slip and twinning and their interactions. Also, it will help in developing accurate single crystal hardening formulations that take into account the interaction between dislocation substructures and the operative deformation modes. A visco-plastic self consistent model predicting the texture and shape evolution of individual grains is utilized to relate these single crystal hardening models to the anisotropy in the deformation of polycrystalline Zr.

Finite Element Simulation of Selective Superplastic Forming of Friction Stir Processed 7075 Al Alloy: *Yanwen Wang*¹; Rajiv S. Mishra¹; ¹University of Missouri-Rolla

For many superplastic formed components, only some regions undergo superplastic deformation. In these cases, instead of choosing expensive superplastic materials for the entire sheet, conventional materials can be chosen and friction stir processing (FSP) can be performed in the selected regions to make them superplastic. This is called "selective superplastic forming" (US Patent #20020079351). In this study, finite element simulation of superplastic forming of bowl shape component has been conducted. We chose commercial 7075 Al alloy and FSP was used to generate fine grained regions with different grain sizes. The pressure schedule, the overall forming time and the final thickness distribution in the formed component were calculated. These simulations demonstrate the design possibili-

ties with this new concept. The authors gratefully acknowledge the support of National Science Foundation through grant # 0323725.

Fracture Mechanism of Bimodal Structured Nanocrystalline Al-Mg Alloys: *Zonghoon Lee*¹; *Velimir Radmilovic*¹; *Enrique J. Lavernia*²; *Steven R. Nutt*³; ¹Lawrence Berkeley National Laboratory; ²University of California at Davis; ³University of Southern California

Bimodal structured bulk nanocrystalline Al-Mg alloys, which were comprised of nanocrystalline grains separated by coarse grains, show balanced mechanical properties of enhanced ultimate strength and reasonable ductility/toughness compared to conventional Al-Mg alloys and other nanocrystalline metals. Our previous investigation of tensile test, TEM and FEM analyses had proposed unusual deformation mechanisms and interactions between ductile coarse grains and nanocrystalline regions. However, the direct evidence of the deformation and fracture has not been fully provided. In this work, embedded cracks and voids in the tensile fractures were revealed using FIB, SEM and analytical TEM, which gave explanations of the relation between the improved mechanical properties and the fracture mechanism. The findings suggested that cracks nucleated in nanocrystalline region during tensile loading were arrested at coarse grains. The incorporation of ductile coarse grains, which effectively blunted advancing cracks and impeded crack growth by bridging crack wakes, resulted in enhancing the toughness.

Mechanical Behavior of Bulk Nanocrystalline Ti Alloys Produced by Cryomilling: *Alejandro Zúñiga*¹; *Fusheng Sun*¹; *Paula Rojas*²; *Bing Q. Han*¹; *Enrique J. Lavernia*¹; ¹University of California, Davis; ²Pontificia Universidad Católica de Valparaíso

The influence of the microstructure and chemical composition on the mechanical behavior of Ti alloys consolidated from cryomilled powders is described. The powders were cryomilled in liquid nitrogen and liquid argon, and then consolidated using Spark Plasma Sintering. The microstructure of the consolidated samples consisted of an α matrix with some retained β phase. The chemical analyses showed that the amount of nitrogen in the nitrogen-milled sample was higher than that of the argon-milled sample. The tensile properties of the argon-milled sample were 825 MPa of yield stress and 17% of elongation; whereas the compression properties of the nitrogen-milled sample were 2650 MPa of UTS and 0.11 of strain to failure. The compression behavior of nitrogen-milled samples after annealing at 500, 600 and 700°C was also investigated. The low ductility-high strength observed in the nitrogen-milled sample may be attributed to the large amount of nitrogen incorporated in solid solution.

Mesoscale Effects on the Mechanical Behavior of Inertial Confinement Fusion Ablator Materials: *Eric N. Loomis*¹; *Pedro Peralta*²; *Damian Swift*¹; *Shengnian Luo*¹; *Tom Tierney*¹; *Ken McClellan*¹; ¹Los Alamos National Laboratory; ²Arizona State University

The mechanical behavior of inertial confinement fusion (ICF) ablator materials is being studied to determine mesoscale shock effects during the implosion of spherical capsules. Specifically, plastic wave and grain boundary effects on macroscopic deformation are being considered. Laser shock and recovery experiments with peak applied pressure between 5 and 15 GPa have been performed on ~200 micron thick (5 mm diameter) planar specimens of a model anisotropic material, nickel aluminide (NiAl). Cross-section transmission electron microscopy (XTEM) was performed on shocked samples to characterize the degradation of the plastic wave along the shock direction. Post-shock characterization has shown that defect production and large lattice rotations are confined to within 30 microns from the ablation surface of single crystal NiAl. Be-Cu alloys have also been tested under shock conditions with in-situ velocity diagnostics to measure variations in shock breakout time at the free surface as a way of quantifying implosion symmetry.

Microstructure and Mechanical Behavior of Liquid Metal Cooling Single Crystal Ni-Based Superalloy, N5: *Ganjiang Feng*¹; *Steve Balsone*¹; *Andrew Elliott*¹; *Jon Schaeffer*¹; ¹General Electric

The increased firing temperature and the thermal efficiency of industrial gas turbines (IGT) demand sound castings and improved mechanical properties for hot gas path components. In the past ten years, the liquid-metal cooling (LMC) high gradient casting process has emerged as the most promising technology that produces single crystal (SC) and directionally solidified (DS) castings with substantially refined dendrite

arm spacing and homogeneous microstructure. In the present study, the microstructures of LMC and conventional radiation cooled single crystal N5 castings were compared. Microstructural features such as dendrite arm spacing, phase segregation, carbides, and gamma prime morphology were analyzed. The effect of the refined microstructure under different heat treatment conditions on low-cycle fatigue and creep properties was also discussed.

Microstructure and Mechanical Properties of Hot and Cold Deformed Ti-6Al-4V: *Mehmet N. Gungor*¹; *Lawrence S. Kramer*¹; *Hao Dong*¹; *Ibrahim Uçok*¹; *Wm. Troy Tack*¹; ¹Concurrent Technologies Corporation

The microstructures and mechanical properties of seamless Ti-6Al-4V tubes manufactured by various deformation processes, including hot extrusion, hot rotary piercing and cold flowforming, were studied. Tensile and fatigue tests were conducted on extruded and rotary pierced tubes in the annealed condition, and on flow formed tubes in the stress relieved condition. Microstructure development in the tubes was examined via metallography, texture analysis, scanning electron microscopy and transmission electron microscopy techniques. This paper compares and discusses the mechanical testing and microstructural examination results for tubes produced by different manufacturing methods. This work was prepared by the National Center for Excellence in Metalworking Technology, operated by Concurrent Technologies Corporation (CTC), under Contract No. N00014-00-C-0544 to the Office of Naval Research as part of the U. S. Navy Manufacturing Technology Program.

Modeling the Anomalous Flow Behavior of Ni₃Al Single Crystals: *Yoon S. Choi*¹; *Dennis M. Dimiduk*²; *Michael D. Uchic*²; *Triplicane A. Parthasarathy*¹; ¹UES Inc; ²Air Force Research Laboratory

In the present study we developed a new comprehensive crystallographic constitutive model for Ni₃Al and Ni₃(Al,X) intermetallic single crystals. This model aims at capturing important thermo-mechanical features of Ni₃Al, such as anomalous flow stress and work-hardening rate (WHR) variations with temperature, the strain dependence of these anomalous behaviors, tension-compression asymmetries over a stereographic projection triangle and the Cottrell-Stokes type two-step (at T₁ and T₂) deformation behavior. The framework of the model was structured based on two major contributions to the plastic flow of Ni₃Al, the motion of the macro-kinks (MKs), and the repeated cross-slip exhaustion and athermal defeat of the screw dislocation segments. The contribution of the irreversible obstacle storage was also incorporated in the constitutive formulations as a resistance against the glide of MKs. The model was implemented in the FEM framework, and the simulation results showed a qualitative agreement with experimental observations.

Modeling the Metal Deformation Path during Friction Stir Welding: *Judy Schneider*¹; *Arthur C. Nunes*²; ¹Mississippi State University; ²NASA-Marshall Space Flight Center

In friction stir welding (FSW), a rotating threaded pin tool is inserted into a weld seam, literally stirring the edges of the seam together. To determine the optimal pin tool design and processing parameters to produce a defect free weld, a better understanding of the resulting metal deformation flow path or paths is required. In this study, wire markers are used to trace the streamline flow paths of the metal. X-ray radiographs are used to record the post weld segmentation and position of the wire. The post weld position of markers are used to evaluate the effect of the weld parameters on the entrainment of the metal into the different flow paths. This data is being used to validate a kinematic based model to describe the metal deformation path as a function of the weld parameters and pin tool design.

Primary Creep in Equiaxed (Duplex) TiAl Alloys: *Thomas R. Bieler*¹; ¹Michigan State University

Primary creep in TiAl is of significant importance for heat engine applications. Though lamellar microstructures usually have better creep resistance and toughness than duplex microstructures, some applications need the better ductility afforded by duplex microstructures. Primary creep in duplex alloys is characterized by a two stage primary creep process, consisting of a viscous glide process that exhausts itself, where a diffusional based dislocation creep process is observed. Much of this initial glide process occurs by either mechanical twinning parallel to the existing lamella in lamellar grains or by a shear transformation process by which metastable alpha phase is transformed to gamma phase, in some alloys.

The influence of several alloying elements including C on primary creep properties is summarized.

Synthesis and Mechanical Properties of Ultrahard AlMg₁₄/TiB₂ Composite: *Xuezheng Wei*¹; Bruce Cook¹; ¹Iowa State University

AlMg₁₄/TiB₂, the second hardest (hardness around 46GPa) bulk material only after diamond, has recently attracted some attention due to its superior wear resistance compared with cemented carbide and cubic BN. This compound was fabricated by high energy ball milling and subsequent hot pressing. One problem encountered in this process is the existence of agglomerate in mechanical milled powder lowered the density and mechanical properties of hot pressed ceramic compound. In this study, process control agent (PCA) was added during mechanical milling and the effects of PCA on agglomerate, powder yield, particle size, and the density of hot pressed ceramic were investigated. XRD, SEM, and TEM were used for phase identification and microstructure, particle size analysis. It was found that with optimum amount of PCA, agglomerate-free powders were obtained; and the density and mechanical properties including hardness, toughness, and wear resistance of ceramic prepared with agglomerate-free powders were significantly increased.

Wear Behavior of AA1060 Reinforced with Alumina under Different Loads: *Mario Roberto Rosenberger*¹; Romina Borelli¹; Alicia Ares¹; Elena Forlerer²; Carlos Schvezov¹; ¹National University of Misiones; ²National Commission of Atomic Energy

The wear behavior of samples of AA1060 aluminum matrix reinforced with 15% of alumina particles in a range of loads between 4.9 N and 130.5 N, were determined using a pin-on-ring machine. The tests were performed at a velocity of 2.7 m/s up to achieve the steady-state. The counterface was a carbon steel ring of 280 HB in hardness. Optical and electronic microscopy, X-Ray energy analysis and hardness measurement were performed in order to characterize the worn samples. A mild wear mechanism is present for loads lower than 80 N and at larger loads changes to severe wear mechanism. In the mild wear regime a Mechanically Mixed Layer (MML), with Iron from the counterface and material of the composite, was formed. This MML was responsible of the wear resistance of the composite. At larger load the conditions produced large instabilities which prevent the formation of the protective Mechanically Mixed Layer.

Process-Structure-Property Relationships in LENS® Processed PH13-8Mo Steel: *John E. Smugeresky*¹; Baolong Zheng²; Yizhang Zhou²; Enrique J. Lavernia²; ¹Sandia National Laboratories; ²University of California, Davis

The LENS® additive manufacturing processing of PH13-8 Mo has been evaluated for a range of conditions to establish process-structure-property relationships. Since LENS is also a tool for repair and modification, the interfaces between wrought material and laser deposited replacement features were also investigated. The effect of processing parameters on resultant shape and microstructure was determined using statistically designed experiments where melt pool volume was chosen as input variable. Powder feed rate was adjusted to insure a constant melt pool volume during part fabrication. The experiments were assisted with feedback control of the melt pool size. Microstructural homogeneity, mechanical property variation, and dimensional uniformity were determined for 10 mm by 10 mm by 50 mm parts. Tensile testing, Metallographic and electron optical analytical techniques, including fractography and EDS analysis were used to characterize the relationship between processing conditions, microstructure, and properties.

Biological Materials Science: Biological Materials Science

Sponsored by: The Minerals, Metals and Materials Society, ASM International, TMS Structural Materials Division, TMS: Biomaterials Committee, TMS/ASM: Mechanical Behavior of Materials Committee
Program Organizers: Andrea M. Hodge, Lawrence Livermore National Laboratory; Chwee Teck Lim, National University of Singapore; Richard Alan LeSar, Los Alamos National Laboratory; Marc Andre Meyers, University of California, San Diego

Tuesday PM
March 14, 2006

Room: 212A
Location: Henry B. Gonzalez Convention Ctr.

Session Chairs: Andrea M. Hodge, Lawrence Livermore National Laboratory; Robert O. Ritchie, University of California

2:00 PM Invited

Biological Issues in Materials Science and Engineering: Interdisciplinarity and the Biomaterials Paradigm: *Lawrence E. Murr*¹; ¹University of Texas

Biological systems and processes have had, and continue to have, important implications and applications in materials extraction, processing, and performance. This presentation will illustrate some of the important interdisciplinary, biological issues in materials science and engineering. These will include metal extraction (especially copper) involving bacterial catalysis; galvanic couples and bacterial-assisted corrosion of materials; antibacterial metals and other materials (particularly metal colloids and nanoparticle regimes); metal and material implants and prosthetics and the bio/materials interface; metal and material (particularly nanomaterial) toxicities and related health effects; materials as drug delivery systems (aerosol cages and controlled release configurations); biomimetics and biologically inspired materials developments. These examples will provide compelling evidence for emphasizing biology in materials science and engineering curricula, and the implementation of a biomaterials paradigm to facilitate the emergence of interdisciplinarity involving the biological sciences and the materials sciences and engineering. Supported by SCERP Projects A-04-1 and A-05-1, and a Murchison Endowment.

2:40 PM Keynote

From Concept to Patient - Materials Solutions for Bone Replacement: *William Bonfield*¹; ¹University of Cambridge

Materials derived from engineering practice have provided the foundation for a wide spectrum of first generation skeletal implants and prostheses, based on an acceptable biological response in the host tissue. However, it is now well recognised that a controlled and enhanced biological response, such as to produce bone apposition rather than fibrous encapsulation on an implant surface, can result in an extended device lifetime in vivo. As a consequence, there has been a major drive to innovate novel second generation biomaterials for specific clinical applications, with appropriate bio- and mechanical-compatibility. An early example of this approach was the innovation of hydroxyapatite reinforced polyethylene composite (HAPEX(TM)) as a bone analogue. Modelled on the structure of cortical bone, HAPEX(TM) was tailored to provide matching deformation characteristics and superior fracture toughness to cortical bone, together with a favourable bioactive response. This research has culminated in a major clinical application as a middle ear prosthesis.

3:20 PM Invited

Failure of Human Cortical Bone: Aspects of Fracture Mechanics and Crack Propagation: *Robert O. Ritchie*¹; Ravi K. Nalla¹; Jamie J. Kruzic²; John H. Kinney³; ¹University of California; ²Oregon State University; ³Lawrence Livermore National Laboratory

The origins of the toughness of human cortical bone are examined by considering the salient micro-mechanisms of failure over a range of characteristic nano to macroscopic length-scales. It is argued that the structure of bone at the hundreds of microns, specifically the osteon structures, is most important in determining the fracture resistance. These mechanisms act to toughen bone by lessening the magnitude of stresses at the tip of

any cracks. Although crack deflection along cement lines provides a source of toughening in the transverse orientation, crack bridging by intact regions in the crack wake provides for toughening in the medial-lateral and proximal-distal orientations. We show that biological aging, and certain disease states, which cause a deterioration in “bone quality” and hence raise the fracture risk, can be attributed to a degradation in the potency of crack bridging, a phenomenon that we believe is associated with excessive remodeling.

3:50 PM Break

4:10 PM Invited

The Ever Changing Materials Science and Engineering Curriculum: *Mark C. Hersam¹; Morris E. Fine¹; ¹Northwestern University*

In 1950, materials science and engineering did not exist as a university department. Instead, one found that the different classes of materials (e.g., metals, ceramics, polymers, and electronic materials) were taught in different departments. During the following 10 to 15 years, many universities initiated educational programs in materials science and engineering. The curricula were based on principles that apply to all classes of materials rather than separate introductory courses for each. Such core course sequences covered solid state theory, thermodynamics, phase transformations, kinetics, diffraction, microscopy, structure, and properties. The history of this development will be discussed. The current challenge is to introduce biological materials into the curriculum on the same basis. Strategies for meeting this challenge will also be outlined.

4:50 PM Invited

Mechanotransduction in Cells is Conducted by Supramolecular Complex: *Masahiro Sokabe¹; ¹Nagoya University*

Mechanotransduction is an important cell function to convert mechanical stimuli into electrical/chemical signals leading to important responses such as hearing, touch, proprioception or regulation of blood pressure. It also plays a crucial role in the regulation of cell-volume, -shape and -motility. In the past decade, we have partially understood the molecular mechanism of mechanotransduction based on the molecular identification of a certain class of mechanosensors such as mechanosensitive (MS) ion channels. The best known example is bacterial MS channels that can be activated simply by cell inflation upon hypotonic shock. However, eukaryotic cells have evolved more complicated mechanosensor systems. We found that some of their MS channels are associated with cytoskeletons and adhesion molecules, by which they obtain increased mechanosensitivity and force-direction sensitivity. Cytoskeleton would be a more efficient force transmitter than the membrane by its larger elastic modulus and adhesion molecules would provide stiffer base to generate stronger forces.

5:20 PM

Microstructure and Properties of Biocompatible TiO₂/Ti: *Grant A. Crawford¹; K. Das²; Nikhilesh Chawla¹; S. Bose²; A. Bandyopadhyay²; ¹Arizona State University; ²Washington State University*

Titanium oxide coatings have been shown to exhibit desirable properties as biocompatible coatings. In this talk we report processing and characterization of nanoporous TiO₂ grown on commercially pure titanium substrates through anodic oxidation. Characterization of the as-processed coatings was conducted using scanning electron microscopy. Nanoindentation was used to probe mechanical properties such as Young’s modulus and hardness. In addition, nanoindentation was used to measure the adhesion strength between the oxide coating and titanium substrate. Nano-scratch testing was employed as an additional method of testing adhesion strength. By changing processing conditions, both coating thickness and porosity were varied, and these variables related to mechanical behavior. Coatings were also immersed in simulated body fluids (SBF) up to 21 days to study apatite growth on coated surfaces. In vitro cell-materials interaction was studied using OPC1 human osteoblast cells to understand the influence of coating microstructure on cell attachment and proliferation.

5:40 PM

Cytotoxic Response and Cell Death Mechanisms for Carbon Nanotubes and Other Nanoparticle Aggregates: The Role of In Vitro

Biological Assays in Nanomaterials Evaluations: *Karla F. Soto¹; K. M. Garza¹; L. E. Murr¹; ¹University of Texas*

Over the past years, research in nanotechnology has increased significantly. Carbon nanotubes and nanoparticulates have become a key component in this research. As there is a high demand and interest for these materials, there should also be a need to investigate their potential health and environmental aspects. The present study deals with cytotoxicity assays performed on an array of commercially manufactured nanoparticulate materials such as: Ag, TiO₂, Fe₂O₃, Al₂O₃, ZrO₂, Si₃N₄, carbonaceous nanoparticulate materials: single-walled and multi-walled carbon nanotube aggregates, black carbon; and naturally occurring chrysotile asbestos. The nanomaterials were characterized by TEM; the aggregates ranged from 25 nm to 20µm. Cytotoxicological assays of these nanomaterials were performed utilizing a murine alveolar macrophage cell line and human macrophages as well as a human epithelial lung cell line as a comparator. The mechanism of cell death induced in these cell lines will also be discussed.

Bulk Metallic Glasses: Processing and Characterization

Sponsored by: The Minerals, Metals and Materials Society, TMS Structural Materials Division, TMS/ASM: Mechanical Behavior of Materials Committee

Program Organizers: Peter K. Liaw, University of Tennessee; Raymond A. Buchanan, University of Tennessee

Tuesday PM
March 14, 2006

Room: 217B
Location: Henry B. Gonzalez Convention Ctr.

Session Chairs: Daniel B. Miracle, U.S. Air Force; Katharine M. Flores, Ohio State University

2:00 PM Invited

Synthesis of High-Density Refractory Metal/Metallic Glass Nanocomposites: *Daniel Sordellet¹; Min Ha Lee¹; ¹Ames Laboratory*

Shear localization of bulk metallic glasses makes them candidates for some specific applications such as kinetic energy penetrators, but densities are in general too low for consideration. One possible solution is to introduce tungsten into a BMG matrix to achieve the required combination of density and deformation behavior. However, the use of body-centered cubic metals to increase the density presents another problem as they are notoriously resistant to shear localization because of their strong strain-rate sensitivity. We have expanded on the recent discovery that certain bcc metals exhibit a decrease in their strain rate sensitivity and show adiabatic shear-localized flow when deformed under uniaxial dynamic compressive loading conditions. Uniformly-layered nanometer-scale tungsten/metallic glass composite particles were fabricated by a milling process and subsequently consolidated by warm extrusion into fully dense rods. Deformation during quasistatic compression tests exhibited highly localized shear flow in these novel tungsten/metallic glass composites.

2:25 PM Invited

The Boson Peak in Pd₄₀Cu₄₀P₂₀: *D. J. Safarik¹; Ricardo B. Schwarzl¹; M. F. Hundley¹; F. Trouw¹; ¹Los Alamos National Laboratory*

A low-temperature hump in C_p/T^3 vs. T (commonly known as the “Boson Peak”) is ubiquitous to amorphous solids and is attributed to an excess of low-frequency vibrational modes not accounted for by the Debye model. We have measured the low-temperature heat capacity, the elastic constants, and the phonon density of states of both glassy and single-phase crystalline Pd₄₀Cu₄₀P₂₀ (the elastic constants and the specific heat were measured in a Pd₄₀Cu₄₀P₂₀ single crystal). The C_p/T^3 vs. T hump in crystalline Pd₄₀Cu₄₀P₂₀ was of comparable amplitude and peak temperature as for the Boson peak measured in Pd₄₀Cu₄₀P₂₀ glass. Inelastic neutron scattering measurements show that both materials have similar phonon density of states spectra, which deviate markedly from the Debye model assumption [$g(\omega) \sim \omega^2$] at low frequencies. These densities of states are used to compute the specific heat, which we compare to our direct specific heat measurements.

TUESDAY PM

2:50 PM Invited

Nanocrystallization Pathways in Ternary Zr-Based Bulk Metallic Glass: *Xun-Li Wang*¹; Ling Yang²; Alexandru D. Stoica¹; Jon Almer³; Peter K. Liaw⁴; ¹Oak Ridge National Laboratory; ²University of Cincinnati; ³Argonne National Laboratory; ⁴University of Tennessee

High-energy synchrotron x-ray was used to study the nanocrystallization pathways in a Zr-based ternary bulk metallic glass. The experiment was conducted in-situ by making simultaneous time-resolved measurements of wide-angle diffraction and small angle scattering data under isochronal and isothermal heating conditions. Two successive phase transitions were observed during nanocrystallization, where an intermediate phase of icosahedral symmetry was identified. This result is similar to that observed in multi-component Zr-Ni-Cu-Ti-Al alloys. The implication of the intermediate phase on nanocrystallization behaviors will be discussed. This research was supported by Division of Materials Sciences and Engineering, Office of Basic Energy Sciences, U.S. Department of Energy under Contract DE-AC05-00OR22725 with UT-Battelle, LLC. Use of the Advanced Photon Source was supported by the U. S. Department of Energy, Office of Science, Office of Basic Energy Sciences, under Contract No. W-31-109-Eng-38. The financial support by the National Science Foundation's International Materials Institutes (IMI) program at the University of Tennessee; with Dr. C. Huber, as the Program Directors; is also gratefully acknowledged.

3:15 PM Invited

Recent Advances in Development of Bulk Metallic Glasses: *O. N. Senkov*¹; Daniel B. Miracle²; ¹UES, Inc.; ²U.S. Air Force

Over the past several years, a number of new specific criteria for the selection of bulk metallic glass alloy compositions have been introduced. These new criteria include specification of the elastic properties of solute and solvent atoms, the relative and absolute values of atomic size and compositional ranges. The rules are based on topological and thermodynamic models of metallic glass stability and a new structural model for metallic glasses, and have led to discovery of a number of new metallic glasses. An overview of these selection criteria is provided, along with a brief discussion of the structural and thermodynamic models from which they are derived. These new theoretical developments allow accurate prediction of concentrations of a wide range of simple and complex metallic glasses. Properties of several new Ca-based metallic glasses, which have recently been produced based on these developments, are also presented.

3:40 PM Invited

Atom Probe Tomography Characterization of a Gas Atomized Bulk Metallic Glass: *Michael K. Miller*¹; Shankar Venkataraman²; Jurgen H. Eckert²; L. Schultz²; Daniel J. Sordelet³; ¹Oak Ridge National Laboratory; ²Technical University of Darmstadt; ³Ames National Laboratory

An atom probe tomography characterization of gas atomized powder particles of a bulk metallic glass has been performed. The needle-shaped specimens required for the local electrode atom probe were fabricated from individual 10-40 micron diameter particles with the use of a dual beam focused ion beam miller. Details of the specimen preparation process and the microstructure of the as-atomized powder and the powder after different isothermal annealing treatments will be presented. Research at the SHaRE User Facility was sponsored by the Division of Materials Sciences and Engineering, U. S. Department of Energy, under Contract DE-AC05-00OR22725 with UT-Battelle, LLC.

4:05 PM Break**4:15 PM**

Glass-Forming Ability, Fragility, and Fracture Toughness in Various Bulk Metallic Glass Forming Systems: *Guojiang Fan*¹; W. H. Jiang¹; D. C. Qiao¹; Hahn Choo¹; P. K. Liaw¹; ¹University of Tennessee

Understanding the glass-forming ability as well as their inherent fragility of bulk metallic glass (BMG) forming liquids has been actively pursued. More recent studies indicate that the fracture toughness of BMG alloys is closely related to their Poisson's ratio, and, thereby, to their kinetic fragility, which measures the steepness of the viscosity change at the glass transition. The relationship among the glass-forming ability, the fragility, and the fracture toughness for various BMG forming systems will be presented. The glass-forming ability of liquids is controlled both by the thermodynamic driving force and kinetic factor. The implications of ther-

modynamic and kinetic factors controlling the glass-forming ability on the fracture toughness of BMG alloys will be discussed. This work was supported by the National Science Foundation (NSF) International Materials Institutes (IMI) Program (DMR-0231320) with Dr. C. Huber as the Program Directors.

4:35 PM

Processing of Amorphous Zr_{52.5}Cu_{17.9}Ni_{14.6}Al₁₀Ti₅ (VIT-105) with High Oxygen Contents Using Microalloying: *James Wall*¹; Peter K. Liaw¹; Hahn Choo¹; ¹University of Tennessee

One of the obstacles that needs to be overcome to facilitate a wide-scale industrial acceptance of bulk metallic glasses as structural materials is their stringent processing requirements. Very small amounts of oxygen and other impurities can destabilize the supercooled liquid and lead to crystallization during cooling from the melt. Recently, a new microalloying scheme, which allows relatively high amounts of oxygen to be retained within the glass forming alloy Zr_{52.5}Cu_{17.9}Ni_{14.6}Al₁₀Ti₅ (VIT-105), has been developed. Preliminary processing results are presented along with characteristic x-ray diffraction and differential scanning calorimetry analyses. Furthermore, preliminary results on fracture strengths of the materials with different oxygen/dopant levels are presented.

4:55 PM

Effect of Processing on Stability and Structure of Amorphous/Nanocrystalline Aluminum Alloys: *Timothy W. Wilson*¹; Hahn Choo¹; Cang Fan¹; Alex C. Hannon²; Peter K. Liaw¹; Laszlo J. Kecskes³; ¹University of Tennessee; ²Rutherford Appleton Laboratory; ³U.S. Army Research Laboratory

Understanding how the role processing affects the structure and in turn, the properties of amorphous and nanocrystalline aluminum alloys is vital for the future consolidation of ribbon and powder samples into bulk specimen. In this study, two types of Al₈₅Y₇Ni₈, Al₈₅Y₇Fe₃Ni₃, and Al₈₁Y₇Fe₃Ni₇ alloys were examined. One set was produced by rapidly solidifying melt-spun ribbons, and another set was prepared by mechanical alloying of elemental powders. The thermal stability of these two sets of materials was examined, and the studies revealed that powder samples show a higher thermal stability than the ribbon samples. In an effort to gain further insight on the structure-properties-processing relationship, the local atomic structures of Al-Y-Fe-Ni and Al-Y-Ni amorphous/nanocrystalline alloys were examined using neutron scattering. From this, atomic pair distribution function (PDF) analyses were performed on these alloys. Results showed that small changes in the composition and processing conditions affect the local atomic environment.

5:15 PM

Effects of Electrodes and Frequency of the Electromagnetic Vibrations on Glass-Forming Ability in Fe-Co-B-Si-Nb Bulk Metallic Glasses: *Takuya Tamura*¹; Daisuke Kamikihara¹; Yoshiki Mizutani¹; Kenji Miwa¹; ¹National Institute of Advanced Industrial Science and Technology

It is known that cooling rate from the liquid state is an important factor for producing the bulk metallic glasses. However, almost no other factors such as electric and/or magnetic fields were investigated. The present authors reported in Nature Materials 4(2005)289 that a new method for producing Mg-Cu-Y bulk metallic glasses by using electromagnetic vibrations is effective in forming the metallic glass phase. Moreover, the present authors have reported that the glass-forming ability of Fe-Co-B-Si-Nb alloys also enhances with increasing the electromagnetic vibration force. This study aims to investigate effects of electrodes and frequency of the electromagnetic vibrations on glass-forming ability in Fe-Co-B-Si-Nb bulk metallic glasses in order to investigate further. It was found that the enhancement of the glass-forming ability by the electromagnetic vibrations is not affected by electrodes.

Carbon Technology: Anode Baking

Sponsored by: The Minerals, Metals and Materials Society, TMS Light Metals Division, TMS: Aluminum Committee

Program Organizers: Morten Sorlie, Elkem Aluminium ANS; Todd W. Dixon, Conoco Phillips Venco; Travis J. Galloway, Century Aluminum Company

Tuesday PM
March 14, 2006

Room: 8A
Location: Henry B. Gonzalez Convention Ctr.

Session Chair: Trygve Foosnas, Norwegian University of Science and Technology

2:00 PM

Thermal Dilation of Green Anodes during Baking: *Juraj Chmelar*¹; Trygve Foosnas²; Harald Armljot Øye²; ¹SINTEF; ²Norwegian University of Science and Technology

Pilot scale anodes were made using three single source and one blended coke to determine how the green anode properties affect the final baked anode. Testing was performed in an improved vertical dilatometer using samples 50 mm in diameter and 50 mm long to determine the effect of different heating rates. No sample support was used, however the effect of different packing materials was evaluated. A number of samples were prebaked to 450°C to reduce the initial volatile release and the subsequent sample swelling during dilatometric measurements. The sample shrinkage was calculated from the dilatometric data as the difference between the expansion at 550°C and 950°C. Dilatometric data for anodes prepared identically and with the same composition show differences due to varying mechanical properties of the cokes.

2:25 PM

New Process Control System Applied on a Closed Baking Furnace: *Inge Holden*¹; Frank Heinke²; Frank Aune¹; ¹Hydro Aluminium AS; ²Innovatherm, Prof. Dr. Leisenberg GmbH+Co.KG

In 2004 the Årdal Carbon plant increased total baked anode production with 30% through retrofit of Furnace #3. Using the latest technology of the Hydro baking furnace design, annual capacity of a two fire-zone furnace was increased from 45.000 to 100.000 tons. The closed top furnace technology has traditionally higher tar content in the off-gas than furnaces of the open type design. At plants with electrostatic precipitators the major part of uncombusted volatiles are collected as tar which has been dealt with either by deposition, recycling or combustion. With this retrofit, flue gas treatment is now based on the technique of regenerative thermal oxidation. The paper demonstrate the improvements achieved with a new process control system and evaluate the most relevant parameters of the baking process such as combustion of volatiles, energy consumption and quality consistency.

2:50 PM

The Equivalent Temperature Method for Measuring the Baking Level of Anodes: *Lorentz Petter Lossius*¹; Inge Holden¹; Hogne Linga¹; ¹Hydro Aluminium AS

The main use is for monitoring anode quality, but the method is also effective for mapping the baking level in entire sections of baking furnaces and for controlling laboratory scale anode preparation. Examples will be given from Hydro Aluminium baking furnaces and pilot anode plants. The method has been established as an ISO method, ISO 17499: "Carbonaceous materials used in the production of aluminium — Determination of the baking level expressed by the equivalent temperature". The background for the ISO method will be described, including the 2003 round robin for determining the precision which resulted in a repeatability of 9°E and reproducibility (between laboratories) of 14°E. The method is based on a calibration linking the equivalent temperature to L-sub-c crystallite height of a reference coke material. The principle including use of sets of calibration reference materials will be described.

3:15 PM

New Requirements and Solutions for the Fume Treatment at Paste Mixing and Anode Baking Plants: *Matthias Ernst Hagen*¹; ¹LTB

The new IPPC regulation as well as local legislation forces manufacturers of anodes to improve their existing fume treatment center. The most critical emissions are Benzene and other PAH. Generally a regenerative thermal oxidiser (RTO) would be the best applicable solution. But the first systems installed, had huge problems with heavy tar and soot. The new RTO-based technology should avoid problems due to condensibles like heavy tar and soot and use the calorific value of the tar. For this task a new test plant was installed at a closed type baking furnace. The results of this test confirmed the basic design of the RTO but also caused a totally new design of the inlet valves. Furthermore a ceramic prefilter is required to avoid condensations at the inlet of the RTO. The result of the test and a plant in operation at a mixer will be shown.

3:40 PM Break

3:55 PM

Integrated Technology for Baking Furnace and Fume Treatment Plant: *Wolfgang K. Leisenberg*¹; ¹Innovatherm GmbH

In the state of art anode plants baking furnace and fume treatment are regarded as isolated stand alone plants. But fume treatment starts in the baking furnace. The treatment begins as preheated air in the cooling area of the baking furnace and ends at the stack. We regard this process as an integrated one; we will find hidden potentials for both plants. Special situations as moving procedure or pitch burn can be anticipated in the FTP as feed forward information, while flue gas parameters can help to improve the baking process as feed back information. The paper also deals with the energy situation of the process including the use of free heat content of the flue gases. Last but not least a concept of the optimisation of the flue gas cleaning is presented, using the furnace as precipitator of VOC and condensable tar emissions.

4:20 PM

Flue Condition Index – A New Challenge to Increase Flue Lifetime, Operational Safety and Fuel Efficiency in Open Pit Anode Baking Furnaces: *Detlef Maiwald*¹; Wolfgang Leisenberg¹; ¹Innovatherm GmbH

The condition of the flue walls in open pit anode baking furnaces is an important factor in terms of production efficiency. The flue walls change their physical properties in terms of flow resistance, leakages and even mechanical stability due to the continuous heating/cooling cycle. Therefore the flue walls have to be observed regularly by maintenance staff and exchanged in average after a lifetime of 150 fire cycles. With the introduction of a flue condition index, each flue in a furnace is evaluated continuously. An on-line mathematical model detects the actual condition of each flue by correlation of the relevant process data available in the firing system. As a consequence the firing properties like the maximum fuel input or the draft can be adapted or limited to the actual condition of the flue. This prevents critical situations, avoids hot spots which increases operational safety, flue wall lifetime and fuel efficiency.

Cast Shop Technology: Shape Casting and Foundry Alloys

Sponsored by: The Minerals, Metals and Materials Society, TMS Light Metals Division, TMS: Aluminum Committee

Program Organizers: Rene Kieft, Corus Group; Gerd Ulrich Gruen, Hydro Aluminium AS; Travis J. Galloway, Century Aluminum Company

Tuesday PM
March 14, 2006

Room: 7C
Location: Henry B. Gonzalez Convention Ctr.

Session Chair: Mahi Sahoo, National Research Council of Canada

2:00 PM

Factors Influencing the Mechanical Properties of B206 Alloy Castings: *James F. Major*¹; Geoffrey K. Sigworth²; ¹Alcan International Ltd; ²GKS Engineering Services

The AA 206 family of Aluminum casting alloys includes some of the strongest, toughest, aluminum foundry alloys in current use. Primarily limited to aerospace and military applications, because of their tendency

towards hot shortness, these alloys are also seeing increased interest as candidates for automotive suspension components. This paper will outline the results of studies carried out under the auspices of USCAR aimed at more fully characterizing and understanding the mechanical performance of the alloys as a function of composition, casting process, and temper. The results of a statistically designed experiment covering the allowable range of alloy elements and impurities within the AA 206 system will be interpreted in terms of the quality factor for both the T4 and T7 tempers.

2:25 PM

Characterization and Application of Novel 300-Series Die Casting Alloys: Adam Kopper¹; Raymond Donahue¹; ¹Mercury Marine

High pressure die casting is widely utilized in aluminum casting because of its economic benefits derived from high productivity, inexpensive alloys, and near-net shape part geometry. One important feature of the die casting process not yet fully exploited is the fine grain structure; a result of rapid cooling rates typical of the process. This is largely due to the negative impact of iron content and porosity. Iron offers solder resistance; but iron-containing precipitates are of a morphology which behaves as a stress riser resulting in brittle castings. Two new alloys are introduced which, through specific alloy composition, eliminate the need for iron and manganese in die casting alloys. Results show marked improvements in impact strength and elongation over standard die casting alloys.

2:50 PM

Effects of Sr and B Interactions in Hypoeutectic Al-Si Foundry Alloys: Liming Lu¹; Arne K. Dahle²; ¹CSIRO; ²University of Queensland

Strontium is the most widely used and a very effective element for modifying the morphology of eutectic silicon, while boron is commonly present in the commercial grain refiners used for Al-Si alloys. Recent work on the combined additions of Sr and Al-B master alloys and of Sr and Al5Ti1B master alloy has suggested that negative interactions occur between Sr and B added through the grain refiners. However, the effects and mechanisms for such negative interactions are not fully understood. This paper documents the experimental work and results aimed at determining the effects of Sr and B interactions on the solidification of hypoeutectic Al-Si foundry alloys. The mechanisms responsible for such negative interactions are further discussed.

3:15 PM Break

3:35 PM

Influence of Ca on Properties of Hypoeutectic Silumins Type AlSi7Mg: Tomasz Stuczynski¹; Marzena Lech-Grega¹; Zbigniew Zamkotowicz¹; Boguslaw Augustyn¹; ¹Institute of Non-Ferrous Metals

Paper presents results of investigations defining the role of Ca in range 0-500 ppm on properties and structure of hypoeutectic silumins AlSi7Mg0.4. The following properties were characterized: tensile strength, elongation, castability, gas ability, corrosion resistance for material with variable contents of Fe=0.2-0.6%. Paper also presents the influence of Ca as modifier of eutectic (a+Si) and intermetallic phases.

4:00 PM

Behaviour of the Solid-Liquid Interface at the Moment of Quenching during the Solidification of Aluminium Alloys: Demian Ruvalcaba¹; D. Eskin¹; L. Katgerman²; ¹Netherlands Institute for Metals Research; ²Delft University of Technology

The fraction of solid phase is a key parameter studied in order to understand how the microstructure evolves during solidification of alloys. The quenching technique is widely employed to understand microstructural changes during solidification by freezing the microstructure. However, it has been found that the results obtained by the quenching technique overestimates the solid fraction when comparing to solidification models (e.g. lever rule and Scheil approximation). Therefore, it is important to understand how the microstructure develops during quenching in order to overcome in some way the overestimation of solid fraction when employing the quenching technique. In the present study aluminium alloys (i.e. Al-3 wt.% Si and Al-7 wt.% Cu) were solidified and quenched at different temperatures within the solid-liquid region. The microstructure is analyzed by optical microscopy and Electron Probe Microanalysis (EPMA). Overestimation of solid fraction was found in samples quenched

at high temperature, while those quenched close to the eutectic reaction did not show overestimation of solid fraction compared to the lever rule and Scheil approximation. The existence of instabilities was found in those samples that show overestimation of solid fraction. The formation of instabilities away from the solid-liquid interface may be due to the formation and detachment of an instability at the very beginning of quenching. A discussion based on line-scan measurements and optical analysis is made for the existence of overestimation of solid fraction due to the formation of instabilities. The present research provides an insight in understanding the overestimation of solid fraction in order to overcome the problem when reconstructing the real microstructure that was present before quenching.

Characterization of Minerals, Metals and Materials: Structural Engineering Materials II

Sponsored by: The Minerals, Metals and Materials Society, TMS Extraction and Processing Division, TMS: Materials Characterization Committee

Program Organizers: Jiann-Yang James Hwang, Michigan Technological University; Arun M. Gokhale, Georgia Institute of Technology; Tzong T. Chen, Natural Resources Canada

Tuesday PM
March 14, 2006

Room: 206A
Location: Henry B. Gonzalez Convention Ctr.

Session Chairs: Arun M. Gokhale, Georgia Institute of Technology; Junji Shibata, Kansai University

2:00 PM

Reconstruction, Visualization, and Characterization of Three-Dimensional Microstructure of High-Pressure Die-Cast AE44 Magnesium Alloy: Jacqueline Milhans¹; Soon Gi Lee²; Arun Gokhale²; ¹Carnegie Mellon University; ²Georgia Institute of Technology

High-pressure die-cast Mg-alloys are of significant interest in the automotive industry due to potentials of weight savings and fuel efficiency. Visualization, characterization, and representation of three-dimensional (3D) microstructures are of significant interest for understanding and modeling processing-microstructure-properties relationships. In this contribution, an efficient and unbiased montage serial sectioning technique is applied for reconstruction of large-volume high-resolution (~ 1 μm) 3D microstructure of high-pressure die-cast AE44 Magnesium alloy. The 3D reconstruction reveals the morphology and geometry of the eutectic constituent as well as of Mg-rich dendrites. The surface rendering as well as volume rendering techniques is used for three-dimensional microstructure visualization.

2:25 PM

Magneto-Thermo-Mechanical Characterization of NiMnGa Single Crystals to Reveal Guidelines to Increase Actuation Stress by Magnetic Field Induced Phase Transformation and Variant Reorientation: Haluk Ersin Karaca¹; Burak Basaran¹; Ibrahim Karaman¹; Yuriy Chumlyakov²; Hans Maier³; ¹Texas A&M University; ²Siberian Physical-Technical Institute; ³University of Paderborn

Magnetic shape memory alloys (MSMAs) have the ability to combine large strain output of conventional shape memory alloys with high frequency response of magnetostrictive materials. However, their operation range under stress is limited to a few megapascals. In this work, an extensive experimental program was undertaken on NiMnGa single crystals using a unique magneto-thermo-mechanical (MTM) testing system in quest for identifying physical and microstructural parameters critical in increasing the magnetic actuation stress. The present paper will discuss guidelines to increase the actuation stress considering the coupled effects of magnetocrystalline anisotropy energy, detwinning stress, operating temperature, phase transformation temperatures and Curie temperature. Few specific experimental results will be presented in which one to two orders of magnitude increase was achieved in the magnetic actuation stress. This giant increase will be shown to be a consequence of field induced phase transformation which has been observed for the first time in these alloys.

2:50 PM

Comparison of Dislocation and Other Deformation Microstructures in As-Grown, Compression Tested, and Ballistically Penetrated W Single-Crystal Rods: *Micah T. Baquera*¹; Lawrence E. Murr¹; Carlos Pizaña¹; Thomas L. Tamoria²; H. C. Chen²; S. J. Cytron³; ¹University of Texas; ²General Atomics; ³U.S. Army TACOM-ARDEC

A comparison of microstructures associated with W single-crystal ([001], [011], [111]) rods prior to deformation (as grown), and after quasi-static compression (at a strain rate of $\sim 1/s$) by transmission electron microscopy (TEM) shows a more than 10-fold difference in dislocation density. Dislocation substructures were not significantly different in the deformed samples. In contrast, [001] W rods penetrated into steel targets, at impact velocities of ~ 1.3 km/s, exhibited heavy dislocation densities and dynamic recrystallization as very distinct microstructural regimes. Twinning on {112} also occurred as a precursor to these microstructures near the projectile head. These results suggest that deformation accommodating the extreme strains and strain rates associated with the penetration of a single-crystal rod into a metal target is not adequately represented by conventional deformation as envisioned within the realm of room temperature strain-strain-rate deformation. (U.S. Army TACOM-Picatiny Prime Contract W15QKN-04-M-0267, Project No. 1A4CFJERIANG).

3:15 PM

Engineering Analysis of Subway Rolling Stocks for Safety Evaluation: *Jeongguk Kim*¹; Jung-Won Seo¹; Sung-Tae Kwon¹; ¹Korea Railroad Research Institute

The safety assessment of subway rolling stocks was performed with various types of engineering analysis techniques for the understanding of the current wear status. The car body and bogies were characterized by the employment of nondestructive evaluation techniques, corrosion testing, and three-dimensional measurements. In braking system, degradation and performance tests were conducted, and functional and degradation tests for electrical system in order to identify the actual performance of the system. Moreover, stress and structural analyses using commercial finite element method software provided important information on stress distribution and load transfer mechanisms, and the FEM results were compared with running safety testing results. In this investigation, various advanced engineering analysis techniques for the safety analysis of subway rolling stocks have been introduced and the analysis results have been used to provide the critical information for the criteria of safety assessment.

3:40 PM Break

3:50 PM

Characterization and Modeling of 3-Dimensional Damage Progression of Laser-Deposited Iron-Based Materials Using X-Ray Tomography: *Paul T. Wang*¹; Haitham El Kadiri¹; Gabriel Pontimiche¹; Mark F. Horstemeyer¹; ¹Mississippi State University

LENSTM is one of the direct digital manufacturing techniques for fabricating high strength, near net shape metallic components. To understand and be able to virtually predict the service performance of LENSTM components, i.e., ductility, fatigue, and fracture strength, three-dimensional CT becomes a vital characterization tool for measuring initial and as-deformed states of material. In this case, dual X-ray tubes representing fine and finer resolutions of measurement were used to trace the evolution of damage state and assist the development of damage models. At the macro-scale, an internal state variable constitutive theory representing plasticity and hardening behavior is adopted for its ability of tracing deformation history; at the micro-scale, a 3-dimensional void-cell model is introduced where void growth and coalescence are validated by the dual-tube X-ray tomography. Results of 3-dimensional reconstruction of void images and its connection to modeling are discussed.

4:15 PM

Characterization of Aged U-Nb Alloys by X-Ray Diffraction: *Heather M. Volz*¹; Robert E. Hackenberg¹; Robert D. Field¹; Andrew C. Lawson¹; W. Larry Hulst¹; Ann Kelly¹; David F. Teter¹; ¹Los Alamos National Laboratory

Uranium alloys exhibit many different stable and metastable phases, including martensite. It is desirable to understand any long-term changes in the structure of these materials in order to better predict behavior over

time, but changes may be subtle and elude standard metallographic techniques. To this end, several U-Nb alloys have been quenched and artificially aged for various times at temperatures up to 300C. Powder diffraction patterns were collected on a laboratory X-ray diffractometer along with a ceria standard, and analyzed using full pattern Rietveld analysis with GSAS. As surface condition is a critical issue in obtaining meaningful diffraction patterns in uranium alloys, sample preparation issues related to these materials and their effects on structural refinement and precision lattice parameters will be discussed. Aging-induced changes (or lack thereof) in lattice parameters, unit cell volume, atomic positions in the crystal structure, and phases will be also presented and interpreted.

4:40 PM

EDXRF Analysis of Alloys and Corrosion Products of Metallic Pre-Hispanic Pieces of the Museum of Ethnology and Archaeology of University of Sao Paulo: *Augusto Camara Neiva*¹; Jérémie Nicolae Dron¹; Hercilio Gomes de Melo¹; Silvia Cunha Lima²; ¹Escola Politecnica da Universidade de Sao Paulo; ²Museu de Arqueologia e Etnologia da Universidade de Sao Paulo

An energy-dispersive x-ray fluorescence spectrometer was assembled with the aim of analysing alloys and corrosion products of artistic, ethnological and archaeological pieces. The spectrometer is semiportable and consists basically of an 60kV/2mA x-ray tube with W anode and a Si-drift x-ray detector with Peltier cooling, with no need of liquid nitrogen. It was used for the analysis of the alloys and occasional corrosion products of several metallic pre-Hispanic pieces of the Museum of Ethnology and Archaeology of the University of Sao Paulo. Special care was taken to account for the contribution of spurious radiation from both the Pb primary collimator and the Zr detector collimator. The main components of most alloys were Au, Ag and Cu, but Pb, Ca, Fe and other elements were also identified. The characterization of the alloys and corrosion products is important for the subsequent conservation of the collection.

5:05 PM

Corrosion Processes and Mineral Formation on the Surface of Bronze Monuments in Urban Environments: *Olga Frank-Kamenetskaya*¹; Evgenii Treivus¹; ¹Saint Petersburg State University

The experimental results of study of corrosion processes on Saint-Petersburg bronze monuments surface, received in situ and by means of simulating experiments, have been discussed. Influence of the time factor on corrosion film (patina) mineral composition has been analyzed. Direct dependence between patina mineral composition and environmental conditions has been proved. The sequence of patina phases crystallization has been established. Effect of the chemical composition and heterogeneity of artistic bronze and also monument surface structure on the rate of corrosion process has been regarded. The time variations of mass of the crystallized in the hydrochloric acid vapor phases have been investigated. The kinetic laws of their development at the initial stage of formation, indicating simple (non chain) reactions, have been revealed.

TUESDAY PM

Computational Thermodynamics and Phase Transformations: Alloy Models and Thin Films

Sponsored by: The Minerals, Metals and Materials Society, TMS Electronic, Magnetic, and Photonic Materials Division, TMS Materials Processing and Manufacturing Division, TMS Structural Materials Division, TMS: Chemistry and Physics of Materials Committee, TMS/ASM: Computational Materials Science and Engineering Committee
Program Organizers: Dane Morgan, University of Wisconsin; Corbett Battaile, Sandia National Laboratories

Tuesday PM Room: 210A
 March 14, 2006 Location: Henry B. Gonzalez Convention Ctr.

Session Chairs: Vidvuds Ozolins, University of California; Michael I. Baskes, Los Alamos National Laboratory

2:00 PM Invited

Calculated Properties of Pu-Ga Alloys Using the Modified Embedded Atom Method: *Michael I. Baskes*¹; Shenyang Hu¹; Marius Stan¹; ¹Los Alamos National Laboratory

The Pu-Ga system is perhaps the most complicated binary alloy system in nature. Not only does this system have important technological importance, but also scientifically it is extremely challenging. Previously we have used the Modified Embedded Atom Method (MEAM) to describe the behavior of both Pu and Ga. This method, though semi-empirical, is able to capture most of the important unusual behavior of both of these elements. In this presentation we show the results of recent calculations using MEAM for various alloys (phases and composition) in this complex system. Results presented will include simple bulk thermal and mechanical properties such as specific heat, thermal expansion, and elastic constants for the solid phases. Two-phase equilibrium will be discussed with respect to melting and the predicted phase diagram. Predictions will be compared with experiment when available.

2:30 PM Invited

Theoretical and Experimental Studies of Metastable Phases in Devitrification of the Glass Forming System Zr₂(Pd,Cu): *James R. Morris*¹; Yiying Ye²; Matthew J. Kramer²; Min Xu²; ¹Oak Ridge National Laboratory; ²Ames Laboratory

Zr₂Cu_xPd_{1-x} is a glass forming system that shows a composition-dependent devitrification pathway. We have used ab initio calculations and x-ray diffraction to examine the competition between the phases, as a function of composition. Calculations reveal that Cu and Pd mix nearly ideally in the ground state structure. However, in the closest competing metastable phase, Cu and Pd preferentially mix. Supporting this calculation, this metastable phase is clearly observed in the experiments only when for equal Cu and Pd concentrations. For Pd-containing compounds, a metastable quasicrystalline phase is the first observed devitrification product. Contrary to existing suggestions, our calculations demonstrate that this phase is not related to the NiTi₂ structure, which is destabilized by Pd additions. This research has been sponsored by the Division of Materials Sciences and Engineering, Office of Basic Energy Sciences, U.S. Department of Energy under contract DE-AC05-00OR-22725 with UT-Battelle, LLC, and Contract W-7405-ENG-82 with Iowa State University.

3:00 PM

A Modified Embedded Atom Method Interatomic Potential for the Fe-C System: *Byeong-Joo Lee*¹; Young-Min Kim¹; ¹POSTECH

For an elaborate control of microstructures and materials properties, it is desired to understand the materials behavior from more fundamental level, e.g. the atomic level. A semi-empirical interatomic potential for the Fe-C binary system has been developed based on the Modified Embedded Atom Method formalism. The potential describes various fundamental physical properties of pure carbon and iron well, as well as known physical properties of carbon as an interstitial solute element in bcc- and fcc-Fe (dilute heat of solution of carbon, vacancy-carbon binding energy and its configuration, location of interstitial carbon atoms and migration energy of carbon atoms). The applicability of the potential to atomistic approaches

to investigate the interactions between carbon interstitial solute atoms and other defects such as vacancies, dislocations and grain boundaries, etc., will be presented. Some atomistic simulation results on the effects of carbon on various deformation and mechanical behavior of iron will also be presented.

3:20 PM

Building Empirical Interatomic Potentials to Describe C Interstitials in Fe: *Diana Farkas*¹; Margarita Ruda²; ¹Virginia Tech; ²Centro Atomico Bariloche

In this work, thermodynamic and lattice expansion data for C in Fe were used to develop an empirical potential that can describe small amounts of C interstitials in Fe. The potentials were tested for the prediction of martensitic structures and successfully predict the stability of the martensitic phase. They were also compared with first principle calculations for the effect of interstitial C in the cohesive energy of grain boundaries, where the correct trend is predicted. The results for lattice relaxation and energetics for the structure of the interstitial sites in the bulk are also compared with first principles results and the limitations of the technique are discussed.

3:40 PM

Molecular Dynamic Simulations of Thermodynamic Properties and Stability of Precipitates in Al-Cu Alloys: *Shenyang Hu*¹; Michael Baskes¹; Marius Stan¹; Longqing Chen²; ¹Los Alamos National Laboratory; ²Pennsylvania State University

Precipitate strengthening is one of the main mechanisms responsible for the improved mechanical properties of alloys. The thermodynamic stability of precipitates and mobility of precipitate/matrix interfaces control the rates of nucleation, growth and coarsening, and hence the precipitate volume fraction, morphology, size distribution, and the mechanical properties. The plate-like theta-prime precipitate is one of the main strengthening precipitates in Al-Cu alloys. In this work, molecular dynamics (MD) simulations are employed to calculate thermodynamic properties of various phases: alpha solid solution, theta prime, and theta phases. The free energy and entropy differences between a reference state and an Einstein solid were calculated using the method of adiabatic switching in a MD formalism. Analytic free energy functions were constructed as a function of temperature and Cu composition. In addition, Interface energies, interface structure and critical nuclei were obtained, and compared with those from first principles calculations and experimental measurements.

4:00 PM Break

4:10 PM Invited

Strain Contributions to Phase Transitions in Epitaxial Thin Films: *Y. L. Li*¹; *Long Qing Chen*¹; ¹Pennsylvania State University

Many applications of materials require the growth of thin films on a substrate. It is known that the interface between an epitaxial film and a substrate is coherent when a film thickness is small, i.e. below the critical thickness for nucleation of interfacial dislocations. There are increasing evidences that the thermodynamics of phase transitions in such epitaxial films can be profoundly affected by the strain imposed by a substrate. For example, it has been experimentally determined that ferroelectric phase transition temperatures in epitaxial thin films can be hundreds of degrees higher than the corresponding bulk. It will be shown that the observed huge shifts in phase transition temperatures can be rationalized using continuum thermodynamics taking into account the strain effect. It is suggested that significant changes in phase transition temperatures should be expected for any phase transition whose order parameter is coupled to strains.

4:40 PM Invited

Ab Initio Modeling of Pattern Formation in Bulk-Immiscible Heteroepitaxial Alloy Films: *Vidvuds Ozolins*¹; Tejodher Muppidi¹; ¹University of California

Formation of two-dimensional (2D) nanoscale patterns (stripes and disks) has been observed in several surface alloy systems composed of bulk-immiscible species. These 2D structures occur due to competition between short-range chemical bonds favoring phase separation and long-range elastic forces favoring intermixing. We present an accurate theoretical framework that incorporates interatomic interactions obtained from

first-principles electron-structure methods. The central role in this formalism belongs to a Fourier transform of long-ranged pair interactions, which include both alloying and elastic strain effects. This formulation enables rapid screening for new alloy/substrate systems with strong energetic tendencies to form long-period ordered patterns. Applications to several metallic alloy systems on Ru(0001) and Mo(110) substrates and rare-earth disilicide nanowires on Si(100) will be shown.

5:10 PM

A New Model of Stress Generation during Thin Film Growth: *Edmund B. Webb*¹; Steven C. Seel¹; J. J. Hoyt¹; Jonathan A. Zimmerman¹; ¹Sandia National Laboratories

Residual stress in a material influences microstructure evolution. This is particularly true for thin films, which support higher stresses than bulk material due to restricted geometry. During Volmer-Weber thin film growth, discrete islands grow until their separation distance becomes small. Islands then elastically deform to close the gap between them, trading surface energy for strain energy. Island coalescence is believed to generate stress during thin film growth; however, details are only qualitatively understood - especially for nanometer islands since experiments are challenged to probe this scale. We present results from an analytical coalescence model that predicts, contrary to prior models, significantly reduced stress as a function of island size. Our model improves agreement with experiment by evoking a reasonable mechanism for island coalescence. Results are supported by atomistic and continuum models; however, the former reveal inelastic behavior for very small islands that cannot be predicted from analytical or continuum approaches.

Deformation and Fracture from Nano to Macro: A Symposium Honoring W. W. Gerberich's 70th Birthday: Length Scales

Sponsored by: The Minerals, Metals and Materials Society, TMS Materials Processing and Manufacturing Division, TMS Structural Materials Division, TMS/ASM: Mechanical Behavior of Materials Committee, TMS: Nanomechanical Materials Behavior Committee
Program Organizers: David F. Bahr, Washington State University; James Lucas, Michigan State University; Neville R. Moody, Sandia National Laboratories

Tuesday PM Room: 214D
March 14, 2006 Location: Henry B. Gonzalez Convention Ctr.

Session Chairs: James Perry Lucas, Michigan State University; Maarten P. de Boer, Sandia National Laboratories

2:00 PM Invited

Cyclic Contact Deformation of Nanocrystalline Ni: *Ruth Schwaiger*¹; Joerg Knyrim¹; Subra Suresh²; ¹Forschungszentrum Karlsruhe, IMF2; ²Massachusetts Institute of Technology

Nanocrystalline materials show potential for high performance applications due to their improved mechanical properties, such as higher strength and hardness, and enhanced resistance to wear. Understanding the damage behavior and the microstructural changes due to repeated contact loading is critical to assess the usefulness of nanocrystalline materials. Cyclic contact deformation was studied by repeatedly indenting the surface of Ni specimens of different grain size and by repeatedly sliding a tip over the surface. A systematic series of experiments under well-controlled conditions were performed using instrumented indenters. We studied the microstructural changes and changes in the mechanical response to the cyclic contact. We observed prominent changes of the grain structure during these experiments. This microstructural instability is most apparent in materials with a very fine initial grain size and represents a threat to the use of fine-grained materials in many applications. Effects of microstructural and experimental length scales will be described.

2:20 PM

Indentation Size Effect in Metallic Material: From Pop-In to Macroscopic Size Independent Hardness: Karsten Durst¹; Björn Backes¹; *Mathias Göken*¹; ¹University Erlangen-Nürnberg

In this paper, size effects observed during indentations with Berkovich and cube corner indenters are discussed in terms of geometrically necessary dislocations (GND). Considering the plastically deformed volume underneath the indenter, a modified Nix/Gao model of the ISE is used for describing the depth dependence of hardness. For the formation of a permanent hardness impression, the necessary dislocation density must be nucleated. The transition from elastic to plastic deformation generally occurs in a pop-in event. After the pop-in, the hardness of the material is described by the Taylor relation for dislocation hardening, where the geometrically necessary dislocations are the dominant factor. At higher depth, the density of the statistically stored dislocations, at a certain representative strain, controls the deformation resistance. An excellent agreement is found between the modeled depth dependence of hardness and indentation experiments on Al, W, Cu, Ni at indentation depths from the pop-in to 3000 nm.

2:35 PM

Characterization of the Dislocation Substructure beneath Nanoindentations in hcp α and bcc β Phases in Ti-V Based Alloys: *Gopal B. Viswanathan*¹; Eunha Lee¹; Dennis Maher¹; Srikumar Banerjee¹; Hamish L. Fraser¹; ¹Ohio State University

The hardness of α and β phases in the alloys Ti-6Al-4V and Ti-22V are assessed using nanoindentation technique. Results indicate that the hardness varied with the depth of indentation and the orientation of grains in both alloys. Dislocation substructures are characterized by TEM analysis of the thin-foil membranes cut through specific indents with a focused-ion-beam instrument. Regarding the orientation dependence of hardness in the α phase, the nature of statistically stored dislocations and that of geometrically-necessary dislocations is identified. The occurrence of former dislocations are predicted from Schmid's Law, while noting the presence of minor densities of other dislocations required presumably because of the shape change imposed by the nanoindenter. The geometrically-necessary dislocations are identified as appropriate combinations of slip dislocations such that an overall-displacement parallel to the direction of the indentation results. Detailed dislocation-substructure analysis in the β phase is currently underway. These results will be presented and discussed.

2:50 PM

Correlating Changes in Dislocation Substructures to Plasticity Size-Effects in Ni, Ni₃Al, and Ti-6242: *Dave M. Norfleet*¹; Steven Polasik¹; Dennis M. Dimiduk²; Michael D. Uchic²; Michael J. Mills¹; ¹Ohio State University; ²Air Force Research Laboratory

Recently much attention has been given to mechanical size effects at the micron size scale. However, the specific details of how dislocation micro-mechanisms are affected by sample volume are still unresolved. Using current micromechanical fabrication and testing methods, micron-sized compression samples of Ni, Ni₃Al, and single colony Ti-6Al-2Sn-4Zr-2Mo-0.1Si were tested at room temperature. The pure Ni and Ni₃Al alloys displayed strong size effects (a marked increase in strength) as the sample volumes were reduced. In comparison, the Ti-6242 material exhibited opposite behavior, displaying a reduction in strength as the sample volume approached micron size scales. Subsequent FIB-based TEM foils were prepared along active slip bands and along the gauge length to study the dislocation dynamics and deformation homogeneity. Dislocation analysis was performed on each of these materials to gain an understanding as to the micro-mechanisms that control plasticity at this size scale.

3:05 PM

Slip Behavior in Single Crystal Ni-Base Superalloys: *Fereshteh Ebrahimi*¹; Eboni Westbrooke¹; ¹University of Florida

It has been shown that single crystal Ni-base superalloys do not comply with the Schmid's law, i.e. the critical resolved shear stress depends on the loading orientation. Furthermore, the slip bands do not follow the predicted slip traces and their appearance depends on the loading orientation. In this study, the room temperature plastic deformation of two Ni-base superalloys in HIP'ed and un-HIP'ed conditions was investigated. Optical, scanning and transmission electron microscopy techniques were employed to investigate the evolution of deformation bands as functions of strain and loading orientation. Detailed analysis of the results revealed that geometrical arrangements of precipitates, pores (or eutectic pools) and dendrites affect the plastic deformation at nano-, micro-, and macro-

scales, respectively. It is shown that the development of local tri-axial stresses owing to these inhomogeneities influence the path of deformation bands as well as the level of remote stress needed for yielding.

3:20 PM

Dislocation Nucleation and Source Activation through Yield Point Phenomena during Nanoindentation: *Ali Zbib*¹; David F. Bahr¹; ¹Washington State University

Experimental studies on single crystal tungsten were performed using indentation to examine yield point phenomena with respect to dislocation nucleation and source activation. Macroindentation was used to create a spatially distinct array of dislocations in the single crystal. Nanoindentations which exhibited a yield point indicative of the onset of plasticity were then performed at various positions, corresponding to different dislocation densities identified using dislocation etch pitting techniques. The maximum shear stresses underneath the indenter at which yielding occurs was then compared to dislocation densities, and found to relate inversely with dislocation density. The maximum shear stress reached 1/11 of the shear modulus at a dislocation density of 1.81 per square micron and 1/9 the shear modulus at a dislocation density of 0.0035 per square micron. The effects of tip radius on the stress field under the tip, and the volume in which a pre-existing dislocation is activated, will be discussed.

3:35 PM Break

3:55 PM Invited

Deformation and Patterning in the Micro- and Nano- Scale: *Elias C. Aifantis*¹; Daniel Walgraef²; ¹Michigan Technological University; ²Free University of Brussels

Various spatiotemporal patterning phenomena of strain and dislocation populations are discussed. A self organization approach is employed to describe the relevant instabilities in small volumes, surfaces and interfaces. The competition of strain, interaction and surface energies are considered in both linear and nonlinear regimes. The results of the analysis are compared with experimental observations.

4:15 PM

Analytic Treatment of Metallic Multilayer Strength at All Length Scales: *Lei Fang*¹; Lawrence H. Friedman¹; ¹Pennsylvania State University

Metallic multilayers can be used as ultra-high strength coatings. They exhibit a very pronounced size-effect where the mechanical strength depends on the layer thickness. Traditionally, the Hall-Petch relation from dislocation pileup theory is used to describe the size effect. However, more rigorous application of dislocation pileup theory as applied to multilayers predicts significant deviation from the Hall-Petch relation due to elastic inhomogeneity, discreteness of dislocations and dislocation source operation. The necessary modifications to the Hall-Petch Relation are presented. An analytic formula accounting for these effects can only be obtained in a piecewise fashion. The variation of strength with layer thickness must be broken down into four length-scale regimes, and a simple analytic formula is obtained for each regime. This formulation allows one to bridge the length scales and predict multilayer strength from microscopic parameters (interface strength and dislocation source characteristics) and fundamental material parameters (elastic moduli and crystal structure).

4:30 PM

Thickness Effects on the Plasticity of Gold Films: *Megan J. Cordill*¹; Neville R. Moody²; David P. Adams²; David F. Bahr³; Alex A. Volinsky⁴; William W. Gerberich¹; ¹University of Minnesota; ²Sandia National Laboratories; ³Washington State University; ⁴University of South Florida

Gold films are used in advanced applications where limited film thickness can affect the film's mechanical properties. It has been shown that as film thickness decreases the energy required for film delamination also decreases. This decrease is most likely due to the amount of plasticity available for deformation. To examine these effects, nanoindentation was employed to simulate a sharp crack on the film's surface. The indenter tip will cause deformation by dislocation nucleation. The time dependent elastic recovery of the indents will be monitored using scanning probe microscopy techniques. Gold films (40 nm and 200 nm) were indented using three tips: a blunt berkovich, a sharp berkovich, and an ultra sharp cube corner. Each tip demonstrates different behavior as a function of

film thickness and initial indentation depth. Experimental results are compared to existing dislocation shielding models. This work funded by the United States Department of Energy through contract DE-AC04-94AL85000.

4:45 PM

Relating Gradient Plasticity with Dislocation Mechanics through the Use of Nanoindentation: *Katerina E. Aifantis*¹; Jeff T. H. DeHosson¹; John R. Willis²; ¹University of Groningen; ²University of Cambridge

During the past twenty years strain-gradient plasticity has been used extensively to capture deformation features at the micron/nanometre scale, such as the development and persistence of dislocation patterns, and the occurrence of size effects that classical plasticity could not describe. A key material parameter that comes into play in all gradient theories is the internal length. From a mathematical point of view it is required for dimensional consistency; nevertheless it has not yielded to precise physical interpretation. In the present talk by relating a theoretical gradient plasticity formulation to experimental results obtained through nanoindentation the internal length is investigated and interpreted within a dislocation mechanics framework. In the experiments on bi-crystals of bcc metals, the deformed volume is limited to a submicron length scale by the indenter on the one side and the grain-boundary on the other side, resulting in a significant size effect on the strain bursts observed.

5:00 PM

Deformation Behavior of Metal-Matrix Nanocomposites Reinforced by Carbon Nanotubes: *Donghyun Bae*¹; ¹Yonsei University

Deformation behavior of nanocrystalline (nc) aluminium and its alloys (the grain size < 100nm) reinforced by carbon nanotubes (CNTs) at room temperature has been systematically investigated. Nc powders and nanocomposite powders with randomly embedded CNTs are produced via mechanical milling. And the rods (diameter: 6mm, length: 300mm) are fabricated by hot-extrusion. Nanocomposites show yield strength more than 10 times higher than that of the starting sample due to the effects of nanograins, the presence of nano-particles and solute atoms distributed in the nc matrix, and the incorporation of uniaxially aligned CNTs. Furthermore, nanocomposites exhibit high elongation around 8% under uniaxial tension mainly due to the resistance of neck growth. High resolution transmission electron microscopy analyses reveal that twins and partial dislocations are frequently observed in the matrix and the interface between CNTs and the matrix is strongly bonded. The detailed deformation mechanisms of such nanocomposites will be presented.

Fatigue and Fracture of Traditional and Advanced Materials: A Symposium in Honor of Art McEvily's 80th Birthday: Fatigue and Fracture V

Sponsored by: The Minerals, Metals and Materials Society, TMS Structural Materials Division, TMS/ASM: Mechanical Behavior of Materials Committee

Program Organizers: Leon L. Shaw, University of Connecticut; James M. Larsen, U.S. Air Force; Peter K. Liaw, University of Tennessee; Masahiro Endo, Fukuoka University

Tuesday PM

March 14, 2006

Room: 216

Location: Henry B. Gonzalez Convention Ctr.

Session Chairs: David L. McDowell, Georgia Institute of Technology; Johannes Weertman, Northwestern University

2:00 PM Invited

Corrosion Fatigue Crack Initiation and Propagation Process of 12 PCT Chromium Stainless Steel: *Ryuichiro Ebara*¹; ¹Kagawa University

Corrosion fatigue failure of steam turbine blades has been a big concern in the world for more than these thirty years. In this paper characteristics of corrosion fatigue failures of steam turbine blades learned from failure analysis are summarized. Then influencing variables on corrosion fatigue crack initiation and propagation process of 12 pct chromium stainless steel are briefly reviewed. The emphasis is focused upon initiation and propagation of corrosion pit in corrosion fatigue crack initiation pro-

cess. A recent investigation of early stage of corrosion pit initiation process by use of electrochemical noise method is demonstrated. Finally future problems should be solved in corrosion fatigue crack initiation and propagation process of 12 pct chromium stainless steel.

2:25 PM

Creep-Fatigue-Environment Interactions in INCONEL 617: *Terry Craig Totemeier¹; Hongbo Tian¹; ¹Idaho National Laboratory*

Wrought nickel-base alloys are being considered for use in very-high temperature gas-cooled nuclear reactors as piping, heat exchangers, and reactor internals, with operating temperatures in the range of 850-950°C. Creep-fatigue damage will play an important role in determining component lifetimes. The results of initial work on clarifying the separate and synergistic roles of creep, fatigue, and environment in INCONEL alloy 617 are presented. Creep-fatigue tests have been performed at 1000°C and 800°C; the effect of tensile hold time on cycles to crack initiation and failure was determined for total strain ranges of 1.0 and 0.3% at both temperatures. Tests were performed in air and a purified He inert gas environment.

2:50 PM

Fatigue Behavior of a C-2000 Superalloy with a Nanostructured Surface Layer: *J. W. Tian¹; K. Dai²; D. Fielden¹; D. L. Klarstrom³; J. C. Villegas²; L. L. Shaw²; P. K. Liaw¹; ¹University of Tennessee; ²University of Connecticut; ³Haynes International, Inc.*

A series of C-2000 superalloy samples were treated with different times and/or ball sizes using a newly developed surface nano-crystallization and hardening (SNH) process. After the treatment, a nanostructured surface layer with thicknesses of several tens of microns was found, and four-point-bending fatigue tests were conducted. The results show that a nanolayer with moderate thickness can effectively improve the fatigue limit, while with the further increase of the thickness of the nanolayer, the fatigue behavior was severely deteriorated. Therefore, nanostructured surface layers do not necessarily improve the fatigue properties of this material. A possible mechanism involved with the competitive relations among the residual stresses, nanograin strengthening, and surface defects is proposed to illustrate the effect of the nanostructured surface layer on the fatigue behavior. The present work is supported by the National Science Foundation (NSF) with the grant number of DMR-0207729.

3:15 PM

High-Cycle Fatigue of a Nickel-Base Single-Crystal Superalloy: *Jianzhang Yi¹; Chris J. Torbet¹; Tresa M. Pollock¹; J. Wayne Jones¹; ¹University of Michigan*

The fatigue behavior of a second-generation nickel-base superalloy with a platinum aluminide coating was investigated using an ultrasonic fatigue testing system, operating at a frequency of approximately 20kHz. Single crystals were stressed along the <001> orientation with a stress ratio of 0.2 at a temperature of 982°C (1800°F) up to 10⁹ cycles. For the testing conditions investigated, multiple types of initiation sites were observed: the Pt/Al coating layer, solidification porosity and Ta-rich carbides within inter-dendritic region. Cracks initiating at or near specimen surfaces propagated macroscopically along the (001) plane with the crack tip influenced by oxidation, creep and/or cyclic deformation processes. Conversely, cracks initiating from interior carbides or porosity tended to propagate along (111) planes.

3:40 PM Break

3:55 PM Invited

Effects of Microstructure on Dwell Fatigue Crack Growth in Ti-6242: *Winston O. Soboyejo¹; ¹Princeton University*

This paper presents the results of a combined experimental and mechanistic modeling approach to the study of dwell fatigue in Ti-6242. Crack shape evolution, depth and surface crack growth rates are established using beachmarking, acoustic emission and scanning electron microscopy (SEM) techniques. The differences between the dwell crack growth rates and pure fatigue crack growth rates in the short regime are attributed to possible creep effects that give rise to a mean stress estimation of fatigue life in the three microstructures. The implication of the predictions are discussed for the modeling of dwell fatigue.

4:20 PM

The Effect of Porosity on the HCF of a Model Carbon-Containing Ni-Base Superalloy: *Elyssa R. Cutler¹; Gerhard E. Fuchs¹; Adam W. Haskins¹; ¹University of Florida*

A carbon-containing single crystal Ni-base superalloy was tested in high cycle fatigue (HCF) in a hot isostatically pressed (HIPed) and unHIPed condition. Eighty samples were tested at five carbon levels and four conditions. The HIPing reduced porosity significantly and greatly improved creep properties. However, the fatigue lives of the HIPed alloys were not improved and in most cases, decreased. Failure in the unHIPed samples was initiated by internal defects such as porosity and carbides, while most HIPed samples failed due to persistent slip bands. To separate the effects of carbide morphology and gamma prime size, a third and fourth set were given a 1000°C/1000hr thermal exposure, with the fourth set being re-HIPed and heat treated. As expected, the third set showed decreased fatigue lives due to overaging. The fourth set had improved fatigue lives, but not near the order of magnitude expected.

4:45 PM

Influence of Cyclic Loading on the Residual Stress Profile in High Strength Steel Wires: *Jesús Toribio¹; Miguel Lorenzo¹; Diego Vergara¹; ¹University of Salamanca*

This paper deals with the influence of cyclic (fatigue) loading on the residual stress profile in high strength steel wires. To this end, wires with several residual stress profiles (of tensile and compressive nature) were analysed, and different sinusoidal loads with diverse values of maximum loading level and number of cycles were applied on the wires. The evolution of the residual stress profile was numerically evaluated throughout the loading sequence, in particular at the instants of maximum and minimum load during the fatigue cycle. Results of the simulations showed no significant variation with the fatigue loading sequence of the key parameters of the residual stress profile, neither its original shape nor the boundary values at the external surface of the wire. Thus fatigue loading does not affect the residual stress profile in high-strength steel wires (introduced into the material during the manufacturing process by wire drawing through different dies).

TUESDAY PM

Fatigue and Fracture of Traditional and Advanced Materials: A Symposium in Honor of Art McEvily's 80th Birthday: Fatigue and Fracture VI

Sponsored by: The Minerals, Metals and Materials Society, TMS Structural Materials Division, TMS/ASM: Mechanical Behavior of Materials Committee

Program Organizers: Leon L. Shaw, University of Connecticut; James M. Larsen, U.S. Air Force; Peter K. Liaw, University of Tennessee; Masahiro Endo, Fukuoka University

Tuesday PM

Room: 215

March 14, 2006

Location: Henry B. Gonzalez Convention Ctr.

Session Chairs: Richard P. Gangloff, University of Virginia; James C. Williams, Ohio State University

2:00 PM Invited

Effect of Material Microstructure on Fatigue Behavior of AZ31 Magnesium Alloy: *Sotomi Ishihara¹; Zhenyu Nan¹; Takahito Goshima¹; ¹University of Toyama*

Fatigue experiments were carried out using an extruded magnesium alloy, AZ31. In the alloy, a lamellar structure which is parallel to the extruded direction exists. Two kinds of specimens with axial directions, parallel (EP) or tangential (ET) to the lamellar structure, were used. By comparing the S-N curves and crack generation and propagation characteristics of both specimens, effects of the lamellar-structure of the AZ31 magnesium alloy on the fatigue characteristics was studied. In the specimen EP, fatigue life was almost occupied with a fatigue propagation period. Crack retardations or arrests due to the lamella structure were observed. Therefore, a sharp bend in the S-N curve was observed. In the specimen ET, many cracks were generated and propagated as compared to the speci-

men, EP. The rate of fatigue crack growth in the specimen, ET was faster than in the specimen, EP and led reduction in fatigue lives of the former.

2:25 PM

Effect of Porosity and Frequency on Very Long Life Fatigue of Cast Aluminum Alloys: Xiaoxia Zhu¹; Jianzhang Yi¹; John E. Allison²; J. Wayne Jones¹; ¹University of Michigan; ²Ford Motor Company

The fatigue behavior of a cast Al-Si-Cu alloy was investigated for lifetimes up to 10^8 cycles using ultrasonic fatigue instrumentation at 20 kHz and at lifetimes up to 10^7 cycles using conventional fatigue testing at 30 Hz. Fatigue cracks predominantly initiate from microshrinkage pores at or near the specimen surface. The growth rates of fatigue cracks was measured at 20 kHz and at 30 Hz. Fatigue lifetime was accurately predicted, even in the gigacycle regime, by a model that assumed lifetime to be dominated by crack growth from porosity, and neglecting crack initiation. Porosity size and spatial distribution has been quantified and correlated with fatigue life and the fatigue limit. A comparison of the crack growth behavior at ultrasonic and conventional frequencies and the implications for the use of ultrasonic fatigue in examining the behavior of very long life fatigue in cast aluminum alloys will be described.

2:50 PM

Fatigue Crack Growth in Al-Si-Mg Cast Alloys: Microstructural and Processing Considerations: Diana A. Lados¹; Diran Apelian¹; Peggy E. Jones²; Fred J. Major³; ¹Worcester Polytechnic Institute; ²General Motors Corporation; ³Alcan International Ltd.

The fatigue crack growth behavior of long and small cracks was investigated for hypoeutectic and eutectic Al-Si-Mg cast alloys. Microstructure related mechanisms were used to explain the near-threshold behavior and the crack growth response in Regions II and III for alloys with different Si composition/morphology, grain size level, and matrix strength. The effect of SDAS was qualitatively assessed using the developed knowledge. The thresholds of long cracks reflect combined effects of global residual stress induced and microstructure/roughness induced closure. The threshold behavior of small cracks is explained through closure unrelated mechanisms, specifically through the barrier effects of characteristic microstructural features specific to each alloy. In Regions II and III the observed changes in the fracture surface appearance were associated to changes in crack growth mechanisms at the microstructure scale. The extent of the plastic zone ahead of the crack tip was successfully used to explain the changes in growth mechanisms.

3:15 PM Invited

Analysis of the Effect of the Cold-Working of Rivet Holes on the Fatigue Life of an Aluminum Alloy: Paulo T. de Castro¹; Paulo F. P. de Matos¹; Pedro M. G. P. Moreira¹; ¹Universidade do Porto

The understanding of fatigue crack propagation requires the link between the micro and macro structural problem. Results of quantitative microfractography are presented to quantify the crack growth rate in a detail of an aircraft structure. The structural detail under analysis is represented by open-hole specimens in Al-alloy 2024-T3, with and without residual stresses due to hole expansion. The residual stress field created by the cold expansion was experimentally assessed by using the X-ray technique and predicted by FEA. Fatigue tests at several stress levels were supplemented by fatigue striation spacing measurements along the longitudinal crack surface of each specimen. The rates of fatigue crack propagation were deduced from a determination of striation spacing measured by scanning electron microscopy. The approach proposed by McEvily et al. was used to analyze the results. A novel feature of the present analysis was the use of ΔK dependent, plasticity-induced crack closure.

3:40 PM Break

3:55 PM

Analysis of Fatigue Resistance Improvements via Surface Nanocrystallization and Hardening Process: Kun Dai¹; Jiawan Tian²; Juan C. Villegas¹; Leon L. Shaw¹; Peter K. Liaw²; Dwaine Leroy Klarstrom³; ¹University of Connecticut; ²University of Tennessee; ³Haynes International Inc

Numerical simulations have been performed to analyze the work hardening and residual compressive stresses induced by the surface nanocrystallization and hardening (SNH) process. The contributions of

work hardening and nano-grains at the surface region are separated from that of residual compressive stresses. The study suggests that work hardening and nanoscale grains at the surface layer play a significant role in enhancing the fatigue resistance of a nickel-based alloy achieved via the SNH treatment. In comparison, less contribution is provided by residual compressive stresses.

4:20 PM

Effects of Shot-Peening and Re-Shot-Peening on Four-Point Bend Fatigue Behavior of Ti-6Al-4V: Xiuping Jiang¹; Jinxia Li¹; Chi-Sing Man¹; Michael J. Shepard²; Tongguang Zhai¹; ¹University of Kentucky; ²U.S. Air Force

The effects of shot peening and re-shot peening treatment on four-point bend fatigue strength of Ti-6Al-4V were investigated at room temperature and 150°C. The maximum compressive residual stress produced by shot peening was measured by XRD to be around 800 MPa, which improved the fatigue strength from about 65%_{sy} to 71%_{sy}. A step-test method was applied to determine the fatigue strength of the shot-peened and re-peened specimens at different conditions. Re-peening recovered the residual stress, which was relaxed due to bending fatigue at 150°C, and significantly enhanced the fatigue strength both at room temperature and 150°C. Intergranular fracture was also observed in the crack initiation region of shot-peened and re-peened samples.

4:45 PM

Cyclic Plastic Deformation of GTA Welds in Titanium Alloys: Shing-Hoa Wang¹; Ming-De Wei¹; ¹National Taiwan Ocean University

The effects of strain amplitude and strain rate on the low cycle fatigue are investigated in three kinds of aerospace applied Ti alloys and their welds. Sheets of commercially pure titanium (CP-Ti), alpha + beta titanium alloy (Ti-6Al-4V, Ti-64) and beta titanium alloy (Ti-15V-3Al-3Cr-3Sn, Ti-153) in 0.3 mm thick were melted using the TIG welding process. The microstructures of the fusion zones for CP-Ti and Ti-64 consisted of needle-like martensite with maximum hardness. LCF tests of the received titanium alloys and welds were performed. The fatigue strength increased with the strain rate. The strength of Ti-153 β phase titanium alloy demonstrated more sensitivity to strain rate changes than the CP-Ti and Ti-64 alloys. The fatigue strength of Ti-153 welds was slightly superior to that for the received metal, even though it failed in the fusion zone. The fatigue strengths of CP-Ti and Ti-64 welds were inferior to that for the received metal.

General Abstracts: Materials Processing and Manufacturing Division: Surface Modification and Properties

Sponsored by: The Minerals, Metals and Materials Society, TMS Materials Processing and Manufacturing Division, TMS: Nanomechanical Materials Behavior Committee, TMS/ASM: Phase Transformations Committee, TMS: Powder Materials Committee, TMS: Process Modeling Analysis and Control Committee, TMS: Shaping and Forming Committee, TMS: Solidification Committee, TMS: Surface Engineering Committee, TMS: Global Innovations Committee, TMS/ASM: Computational Materials Science and Engineering Committee
Program Organizers: Thomas R. Bieler, Michigan State University; Ralph E. Napolitano, Iowa State University; Fernand D. Marquis, South Dakota School of Mines and Technology

Tuesday PM
March 14, 2006

Room: 211
Location: Henry B. Gonzalez Convention Ctr.

Session Chair: D. Graham McCartney, University of Nottingham

2:00 PM

Interaction of Nanofluids with Heat Transfer Surface: Satyanarayana Kuchibhatla¹; Denitsa Milanova¹; Swanand D. Patil¹; Keith E. Rea¹; Sameer A. Deshpande¹; Sudipta Seal¹; Ranganathan Kumar¹; ¹University of Central Florida

Nanofluids are a new category of heat transfer fluids, where nano particles are dispersed in a conventional heat transfer fluid, imparting very

high heat transfer rates. One major aspect that is less focused is the interaction of these nano dispersions with heat transfer surfaces that interact with nanofluids. Pool boiling experiments were carried in Ceria, silica and alumina nano fluids with NiCr wire. The NiCr wires, before and after the experiments, were characterized with Scanning Electron Microscope (SEM) and Transmission Electron Microscope (TEM) and Energy Dispersive Spectroscopy (EDS) measurements have clearly shown that the oxide formation is relatively low in the presence of ceria, alumina when compared to the conventional fluid and also the nanofluid with silica. Various possible reasons for the differences in interaction of the other nanoparticles with the heat transfer surface and their role in the over all nanofluid performance shall be discussed critically.

2:20 PM

Investigating Functionally Graded Materials to Improve the High Temperature Operating Characteristics of Industrial Tools and Dies and Processing Equipment: *Sudip Bhattacharya*¹; Jerrod A. Roalstad¹; Aaron C. Costello¹; Stanley M. Howard¹; James W. Sears¹; ¹South Dakota School of Mines and Technology

The goal of this ongoing investigation is to obtain a five times improvement in the service life of industrial tools and dies by laser depositing functionally graded materials on their working surfaces. Ni and Co based superalloys like Inconel® and Stellite® and conventional alloys like NiTung60, DM21 and CCW+ have been deposited onto H13 surfaces and actual tools and dies. The initial work on hot forging tools clad with NiTung60 has shown slight improvement in service life while those clad with CCW+ have almost doubled. Alloys similar to AeroMet 100 and Co-WC are also being evaluated. However, it is also felt that cladding refractory metal alloys onto tool surfaces may be necessary to achieve the stated program goals. Therefore in a parallel effort, pairs of metals such as; H-13/Cr, H-13/Ni, Ni/Cr, Cr/V, Cr/Nb, V/Ta, Nb/Ta and Nb/W are being investigated.

2:40 PM

Load and Friction Issues in Sliding Wall ECAE Tooling: *Robert E. Barber*¹; Karl Ted Hartwig¹; ¹Shear Form, Inc.

Load influencing factors and friction issues in sliding wall equal channel angular extrusion tooling are discussed. Analysis of the load curves produced while extruding several different materials and billet sizes shows that billet upsetting, starting material texture, lubrication efficiency and billet surface to volume ratio all influence extrusion force and load efficiency. The benefits of a sliding-wall tool design are reduction of the coefficient of friction between all sliding surfaces, the possibility of variable backpressure, and punch face stress reduction. These benefits translate into the ability to extrude longer billets at lower loads. Friction forces in sliding wall tooling can be sufficiently low so as to allow discrimination of the main factors that influence punch load including material flow stress and texture, lubrication efficiency and billet geometry.

3:00 PM

Integrity of Spark Eroded Surfaces: *Laxminarayana Pappula*¹; Ramesh Nagabhushana Nunna¹; Sudhakar Kasoju¹; ¹Osmania University

Electrodischarge machining involves material erosion by high frequency electrical sparks. The tool and work piece form a pair of electrodes separated by a small gap through which a dielectric liquid circulates to facilitate sparking, quenching of eroded metal in liquid form and flushing away the resultant debris. The associated thermal cycle is quite severe which results in considerable metallurgical changes involving high inducement of tensile residual stresses, microhardness and interelectrode material diffusion. This study presents the differing nature and severity of these effects with different process parameters, particularly spark energies, type of dielectrics and type of workmaterial. Spark energy depends on the current and pulse durations. The dielectrics selected are kerosene and distilled water whereas the work materials employed are stainless steel and aluminium. Not only they have significant influence by themselves but also in association with each other exhibiting both direct and interaction effects.

3:20 PM

Thermal Stability of Various Alloys Clad on H-13 Tool Steel by Laser Powder Deposition: *Jerrod A. Roalstad*¹; *Sudip Bhattacharya*¹; *Stanley*

*M. Howard*¹; *James W. Sears*¹; ¹South Dakota School of Mines and Technology

Thermal stability investigations were performed under research to improve high temperature wear resistance of industrial tools and dies. The commercial alloys CCW+®, DM21®, and NiTun60® were deposited onto H13 tool steel using a 3-KW Nd:YAG laser. The samples were heat treated at 1200°C for 1, 10, and 100 hours. Optical microscopy was performed to identify if any phase transformation had taken place during the heat treatment. DM21® samples revealed precipitate growth within the clad. SEM analysis showed the composition of the precipitates observed within the clad to contain Titanium, Tantalum, and Tungsten. Compositions of the precipitates were compared with published phase diagrams to identify the possible phases. Dictra® computational software was used to theoretically determine the extent of the growth of the phases present. Good bonding was observed for all deposited materials.

3:40 PM Break

4:00 PM

Microstructure and Properties of Thermally Sprayed Al-Sn Based Alloys for Automotive Journal Bearings: *D. Graham McCartney*¹; *Tiziana Marrocco*¹; *Samuel J. Harris*¹; ¹University of Nottingham

Al-Sn automotive journal bearings traditionally comprise a multilayer structure manufactured by casting the Al-Sn alloy and roll-bonding to steel. Recently, high velocity oxy-fuel (HVOF) thermal spraying has been employed as a novel manufacturing route to produce coatings, approx 250 µm thick, on steel substrates which are subsequently annealed to achieve the desired microstructure. The present research extends work on ternary Al-Sn-Cu alloys to quaternary systems with specific additions for potentially enhanced properties. Al-20wt.%Sn-1wt.%Cu-2wt.%Ni and Al-20wt.%Sn-1wt.%Cu-7wt.%Si alloys were studied and we will describe the microstructure formation and wear behaviour of the deposits. Starting powders and coatings were investigated by scanning electron microscopy and X-ray diffraction. Deposit microhardness was measured in both as-sprayed and heat treated conditions, and the wear behaviour in hot engine oil determined using an industry standard test. The results will be interpreted in terms of non-equilibrium microstructure formation and the influence of key microstructural features on mechanical behaviour.

4:20 PM

Improvement of Corrosion Resistance of Plain Carbon Steel Bars by Friction Induced Surface Coating with Aluminum: *Pravash Chandra Maity*¹; *B. RaviKumar*¹; ¹National Institute of Foundry and Forge Technology

A novel technique of surface modification of plain carbon steel by Rotational Pressure Friction (RPF) has been developed to improve its corrosion resistance. The technique involved movement of a pressurized cylindrical alloying tool (Al) over rotating round steel substrate. Rpm of steel specimen, composition of the coating alloy, feed of coating alloy over rotating specimen and no. of passes over 25 mm dia., 75 mm long specimens. 1 Mpa pressure was used in all the experiments. Selected uniformly coated samples were tested for corrosion resistance using potentiodynamic polarization technique (ASTM G5) with 3.5 % NaCl solution as a corrosive medium. Coated steel specimens showed substantial improvement in corrosion resistance from 5.37 mpy for uncoated steel to as low as 0.125 to 0.30 mpy for coated steel specimens.

General Abstracts: Structural Materials Division: Processing and Properties of Light Metals

Sponsored by: The Minerals, Metals and Materials Society, TMS Structural Materials Division, TMS: Alloy Phases Committee, TMS: Biomaterials Committee, TMS: Chemistry and Physics of Materials Committee, TMS/ASM: Composite Materials Committee, TMS/ASM: Corrosion and Environmental Effects Committee, TMS: High Temperature Alloys Committee, TMS/ASM: Mechanical Behavior of Materials Committee, TMS/ASM: Nuclear Materials Committee, TMS: Product Metallurgy and Applications Committee, TMS: Refractory Metals Committee, TMS: Advanced Characterization, Testing, and Simulation Committee, TMS: Superconducting and Magnetic Materials Committee, TMS: Titanium Committee

Program Organizers: Rollie E. Dutton, U.S. Air Force; Ellen K. Cerreta, Los Alamos National Laboratory; Dennis M. Dimiduk, U.S. Air Force

Tuesday PM Room: 218
March 14, 2006 Location: Henry B. Gonzalez Convention Ctr.

Session Chair: Rollie E. Dutton, U.S. Air Force

2:00 PM

A Group of New Ti-Based Composite Alloys: *Faolang Guo*¹; Joe Poon¹; Gary Shiflet¹; ¹University of Virginia

New Ti-based composite alloys with amorphous phases plus a/b Ti(Zr) solid solution have been discovered, which show superior mechanical properties. Both compression and tension tests of the prepared Ti alloys exhibit a 1.6 % of elastic strain limit. A plastic deformation of around 10% was obtained from compression test while a plastic elongation of ~ 4% was found in the tension test experiment. The Ti composite alloys yield at about 1200 MPa, showing steady work-hardening during deformation, and finally fracture at a strength of about 1700 MPa. These Ti composite alloys have already been ready to be used as structural materials in terms of mechanical properties.

2:25 PM

Dynamics of Twinning in Beta-Titanium Alloys: *Paul G. Oberson*¹; Sreeramamurthy Ankem¹; ¹University of Maryland

Recently it has been shown that in the beta-Ti-14.8 wt.%V alloy, twins of the type {332}<113> form and grow slowly at a stress level of 95% yield stress at room temperature. In this investigation a crystallographic model has been developed for the slow-growth of twins. It is shown that the octahedral interstitial sites at the twin-matrix interface, where oxygen resides, are not conserved. The measured activation energy for twin-growth is compared with the activation energy for the diffusion of oxygen in this material and the correlation was very good. The ramification of these findings and the details of the investigation will be presented. This work is being supported by the National Science Foundation under grant number DMR-0513751.

2:50 PM

Friction and Electronic Properties of Al-Based Complex Phases: *Jean-Marie Dubois*¹; ¹CNRS Institut Jean Lamour

A throughout study of many Al-based intermetallics, including compounds with complex (or giant) unit cells and quasicrystals, was performed using a pin-on-disk tribology set-up housed in a vacuum chamber. The riding counterpart was a hard-steel ball, loaded with a 2N force. Our data show a direct relationship between friction observed in such conditions and the filling of the electronic bands at the Fermi energy, with a small, if not negligible, contribution of the plowing component to friction. The case will be exemplified, especially using data obtained with a decagonal, anisotropic quasicrystal. Furthermore, after proper calibration of the experiment, an estimate of the upper limit of the surface energy of the samples may be derived. These measurements are assessed in the light of partial electronic densities of states, with the view that chemical bonding at the pin-sample interface dominates friction in vacuum on such Al-based compounds.

3:15 PM

Hydrogen Diffusion in Ti-45 Nb and ATI-425: Brian James Sarraill¹; Shake Babakhanyan¹; Charles Schrupp¹; Richard Clark¹; Omar Es-Said¹; *John Organ*¹; ¹Loyola Marymount University

The objective of this project was to determine the conditions needed to "contaminate" two alloys, Ti-45 Nb and ATI-425, with known and uniform levels of hydrogen. Alloying Ti-based alloys with hydrogen is used to modify the microstructure and improve mechanical properties. The design of Ti-based alloys can be made more efficient through the use of hydrogen as a temporary alloying element since both manufacturing temperatures and stresses can be decreased. The uniform target hydrogen concentration levels are 50, 100, 200, 300, 400 and 500 ppm. Samples of both alloys were annealed in a hydrogen furnace at 12% hydrogen with a 5 psi chamber pressure for 1, 2, and 4 hours at 450°C and 600°C. The concentration profiles were then determined.

3:40 PM Break

3:55 PM

Mechanical Properties of Ti-6Al-4V Castings for Ground Vehicle Applications: *Ibrahim Ucok*¹; Mustafa Guclu¹; Hao Dong¹; Joseph R. Pickens¹; ¹Concurrent Technologies Corporation

There is a strong interest in reducing weight of combat vehicles because of an increased need for air transportability and reduced logistical support. Titanium alloys are candidates for ground vehicle applications because they combine high specific strength and excellent corrosion resistance. In the present study, gun pod and elevation arm castings for the Stryker - Mobile Gun System (MGS) were made by investment and rammed graphite casting methods using alloys Ti-6Al-4V and Ti-4Al-2.5V-1.5Fe at different oxygen levels. Redesigning the gun pod to exploit titanium and replace steel reduced weight by 28%. Tensile and fatigue properties, as well as the microstructures of the castings, were evaluated. This work was conducted by the National Center for Excellence in Metalworking Technology, operated by Concurrent Technologies Corporation, under Contract No. N00014-00-C-0544 to the Office of Naval Research as part of the U.S. Navy Manufacturing Technology Program. Approved for public release; distribution is unlimited.

4:20 PM

Property Investigation of Laser Cladded TiAl6V4: *Johannes Vlcek*¹; Sven Orban²; ¹European Aeronautic Defense and Space Company; ²IWS Dresden

Laser cladding is an interesting process technology for structural repair or overhaul of engine components. In order to evaluate the technology for structural repair or direct component manufacturing the properties under dynamic loading and fracture toughness values are of interest. Laser cladded TiAl6V4 material was produced at the Fraunhofer IWS Dresden with a 3 KW Nd:YAG laser and the IWS coaxial cladding head type COAX8. The material was tested in the as sintered and mill annealed condition after a 2 hour vacuum anneal at 850°C. Ultimate tensile strength of maximum 1100 MPa with an elongation greater than 11% was measured. The fatigue resistance can be assumed around 475 MPa, but needs further investigation. A fracture toughness value of 63 MPa m^{0.5} was measured. The investigation focused on micro-structural features, the influence of vacuum annealing and fracture behaviour depending on the previous and specimen orientation.

4:45 PM

Quenching Effects on Ti-325 Alloy: Brian James Sarraill¹; Charles Schrupp¹; Shake Babakhanyan¹; Richard Clark¹; Omar Es-Said¹; *John Organ*¹; ¹Loyola Marymount University

Ti-325 is a near alpha alloy with 3 wt% aluminum as an alpha stabilizer and 2.5 wt% vanadium as a beta stabilizer. This alloy is most widely used in its seamless tubing form. This study determined the effects of two different cooling procedures on the room temperature mechanical properties of the alloy. Samples were machined from a seamless tube and quenched either in water or furnace-cooled at temperatures ranging from 1170°F to 1230°F. The yield strength and ultimate strength were measured as a function of quenching medium. In addition, S-N curves were developed for this alloy.

5:10 PM

The Effect of RRA Treatment on Corrosion and Corrosion Wear Performance of 7175 Aluminum Alloy: *Ozgur Celik*¹; Ilke Dagli¹; Murat Baydogan¹; Eyup Sabri Kayali¹; Huseyin Cimenoglu¹; ¹Istanbul Technical University

This study aims to compare the corrosion and wear responses of a 7175 alloy after conventional aging (T6 temper) and retrogression and reaging (RRA) treatments. Corrosion tests were conducted in HCl and H₂O₂ solutions, according to ISO 11846 and ASTM G 110 standards, respectively. Wear test were made under dry sliding and corrosion (in HCl and H₂O₂ solutions) wear testing conditions. Among the examined retrogression temperatures, 260°C yielded the superior corrosion resistance, when compared to T6 temper. RRA treated alloy (retrogressed at 260°C) exhibited higher dry sliding wear resistance than T6 tempered alloy. In HCl and H₂O₂ solutions wear resistance of the alloys dramatically decreased without leading any considerable difference in the corrosion wear resistance of T6 temper and RRA treatment. Although HCl is more aggressive than H₂O₂ solution, the progress of corrosion wear is more severe in H₂O₂ solution.

Hume Rothery Symposium: Multi-Component Alloy Thermodynamics: Alloy Thermodynamics II: Experiment and Modeling

Sponsored by: The Minerals, Metals and Materials Society, TMS Electronic, Magnetic, and Photonic Materials Division, TMS: Alloy Phases Committee

Program Organizers: Y. Austin Chang, University of Wisconsin; Rainer Schmid-Fetzer, Clausthal University of Technology; Patrice E. A. Turchi, Lawrence Livermore National Laboratory

Tuesday PM
March 14, 2006

Room: 202A
Location: Henry B. Gonzalez Convention Ctr.

Session Chair: Adolf Mikula, University of Vienna

2:00 PM **Invited**

Experimental Thermodynamic Methods to Determine Partial Properties: Examples: *Herbert Ipsen*¹; Klaus Richter¹; ¹University of Wien

Among the various experimental methods to determine partial thermodynamic properties, there are two main groups: those depending on the measurement of electromotive forces (emf), and those that determine the vapor pressure of one or several components, in both cases as a function of composition and/or temperature. Whereas the value of emf or vapor pressure at a given temperature yields the partial Gibbs energy (thermodynamic activity) itself, its temperature dependence can be used to derive the partial enthalpy and entropy. Two of these methods will be presented here with various examples. The first are emf measurements with solid oxygen conducting electrolytes that were used to determine partial thermodynamic properties of indium in Pt₃In and in ternary Ag-In-Pd alloys. The second are isopiestic vapor pressure measurements that served to determine partial thermodynamic properties of zinc in solid Pt-Zn alloys and partial thermodynamic properties of antimony in ternary Fe-Ni-Sb and In-Ni-Sb alloys.

2:30 PM **Invited**

Integrating First-Principles Calculations and Thermodynamic Modelling: *Zi-Kui Liu*¹; Stefano Curtarolo²; Aleksey Kolmogorov²; Raymundo Arroyave¹; Dongwon Shin¹; ¹Pennsylvania State University; ²Duke University

Results from first-principle calculations are becoming more and more important in thermodynamics modeling of multi-component systems. Enthalpies of formation of stable compounds are routinely predicted by first-principles calculations. However, calculations are more difficult for phases with homogeneity ranges of compositions, which are typically represented by sublattice models. In this presentation, we will discuss following challenging issues: 1. Lattice stability, i.e. the energy difference between two structures of an element; 2. Stability issues related to the end-members in sublattice models; 3. Application of special quasirandom

structures for solution phases; 4. Contribution of vibrational entropy on structure stability.

3:00 PM **Invited**

Potential of Knudsen Effusion Mass Spectrometry for Multi-Component Alloy Thermodynamics: *Klaus Hilpert*¹; ¹Research Centre Julich

Knudsen effusion mass spectrometry (KEMS) is the most versatile method for the analysis of high temperature equilibrium vapors. It offers the following potential: •Vaporisation studies up to temperatures above 2500 K; •Identification of the gaseous species; •Determination of their partial pressures in the range 10 to 10⁻⁵ Pa; •Evaluation of thermodynamic data. This potential can be efficiently used in the determination of thermodynamic data of the condensed phase and the gas phase. For the condensed phase thermodynamic activities and Gibbs energies of formation can be determined with high accuracy and precision as primary data. Moreover, partial and integral enthalpies of formation can be obtained. For the gas phase numerous intermetallic molecules can be identified and their Gibbs energies and enthalpies of formation determined. The fundamentals of modern KEMS will be given and recent results on alloy thermodynamics and gas phase chemistry will be reported.

3:30 PM **Break**

3:50 PM **Invited**

Thermodynamics of Roses: *Marius Stan*¹; ¹Los Alamos National Laboratory

In one of his talks, Alan Oates presented a calculated ternary equilibrium phase diagram that looked much like a rose. He explained that he did that to demonstrate the versatility of the software and to show how, in principle, one can get any diagram they want. This presentation reviews results, benefits, and challenges of making thermodynamics a less descriptive and more predictive science. It builds upon the work of Hume-Rothery and Alan Oates and emphasizes the importance of turning electronic structure calculations into trusted sources of information for thermodynamic models and simulations. The proposed multi-scale and multi-physics approach is illustrated with calculations of equilibrium phase diagrams.

4:20 PM **Invited**

Thermodynamics of Pd Alloy-H Systems: *Ted B. Flanagan*¹; Suifang Luo¹; ¹University of Vermont

The thermodynamics of Pd binary alloy-H systems have been investigated by many workers using mainly equilibrium H pressure measurements which give the relative H chemical potentials. From the T-dependence of these potentials, the partial enthalpies and entropies can be obtained as a function of H content. Alternatively, these quantities can be obtained by simultaneous measurements of enthalpies from calorimetry and equilibrium pressures as function of H contents. The latter gives the partial entropies from the enthalpies and relative H chemical potentials. In this research such calorimetry has been carried out at a moderate temperature where many of the alloys form hydride phases. Some binary Pd alloys which have been investigated are: Pd-Ag(-Au, -Cu, -Sn, -Fe, -Mn).

4:50 PM **Invited**

Thermodynamic Interaction between Pt, Ni and Al in β -NiAl, γ' -Ni₃Al and β -Ni(Al) in the Ni-Al-Pt-O System: *Evan H. Copland*¹; ¹NASA Glenn Research Center

The addition of Pt to Ni-Al alloys is generally seen to improve oxidation behavior but little is understood about the reasons for this improvement. Determining how Pt affects the thermodynamic activity of Al and Ni in β -NiAl, γ' -Ni₃Al and γ -Ni(Al) is fundamental to understanding this behavior. As part an investigation into the solution behavior of the Ni-Al-Pt-O system the activities of Ni, Al, Al₂O, O and Al₂O₃ have been measured directly by the vapor pressure technique with a multiple effusion-cell vapor source coupled to mass spectrometer (multi-cell KEMS). Measurements were made over a wide range of compositions and focused on the { β -NiAl + Al₂O₃(s)}, { β -NiAl + γ' -Ni₃Al + Al₂O₃(s)} and { γ -Ni₃Al + γ -Ni(Al) + Al₂O₃(s)} phase fields with increasing Pt content. These results are discussed together with a series of measurements made in the Au, Al-O and Ni-Al-O systems that are used as reference states for activity measurements.

TUESDAY PM

Lead Free Solder Implementation: Reliability, Alloy Development, and New Technology: Microstructure Evolution

Sponsored by: The Minerals, Metals and Materials Society, TMS Electronic, Magnetic, and Photonic Materials Division, TMS: Electronic Packaging and Interconnection Materials Committee

Program Organizers: Nikhilesh Chawla, Arizona State University; Srinivas Chada, Medtronic; Sung K. Kang, IBM Corporation; Kwang-Lung Lin, National Cheng Kung University; James Lucas, Michigan State University; Laura J. Turbini, University of Toronto

Tuesday PM Room: 214A
March 14, 2006 Location: Henry B. Gonzalez Convention Ctr.

Session Chairs: Jin Yu, MSE Korea Advanced Institute of Science and Technology; Iver E. Anderson, Iowa State University

2:00 PM Invited

Near-Single Crystal Character of Sn-3.5Ag Eutectic Solder Joint Specimens: *Thomas R. Bieler*¹; Telang Adwait²; Sven Vogel³; ¹Michigan State University; ²Intel Corporation; ³Los Alamos National Laboratory

Tin-based solder joints are frequently near single or multi-crystalline rather than polycrystalline, as determined by comparing orientations measured using OIM on opposite sides of two solder joints and by volumetric measurements of crystallographic texture using neutrons (HIPPO beam line). Comparisons among more than 20 joints indicated no preferred solidification orientation, though there is a tendency for tin <110> vector to be roughly aligned with the heat flow (crystal growth) direction, but any rotation about this axis leads to a wide range of observed preferred orientations. This implies that the properties of all lead free solder joints may be different, implying that one of the two joints will deform preferentially in service.

2:25 PM

Effect of Reflow and Thermal Aging on Microstructure Evolution and Microhardness of Sn-3.7Ag-xBi Solder Alloys: *Min He*¹; Viola L. Acoff¹; ¹University of Alabama

This work investigates effect of reflow and thermal aging process on microstructure evolution and microhardness of five types of Sn-Ag based lead-free solder alloys: Sn-3.7Ag, Sn-3.7Ag-1Bi, Sn-3.7Ag-2Bi, Sn-3.7Ag-3Bi, and Sn-3.7Ag-4Bi. Microhardness and microstructure of the solders under different reflow time at 250°C and different thermal aging durations at 150°C have been studied. The effect of Bi is discussed based on the experimental results. It was found that the microhardness increases with increasing Bi addition to Sn-3.7Ag solder regardless of reflow or thermal aging process. SEM images show the formation of Ag₃Sn particles, Sn-rich phase and precipitation of Bi-rich phase in different solders. The increase of microhardness with Bi addition is due to the solution strengthening and precipitation strengthening provided by Bi in the solder. The trend of decrease in microhardness with the extension of reflow time and thermal aging duration for the same solder alloy was observed.

2:45 PM

Flux Effect on Wetting Behavior of SnZnAl Lead-Free Solder Balls: *Cho-Liang Chung*¹; Haoyin Tsai²; Alex Lu²; De-Shin Liu³; S. L. Fu³; ¹I-Shou University; ²ChipMOS Technologies Inc.; ³National Chung Cheng University

Effects of two different fluxes (A6 and B6) on wetting performance of Sn-37Pb, Sn-3.5Ag-0.5Cu and Sn-7.0Zn-100ppmAl lead-free solder balls were investigated during melting process. Solder ball wetting behavior in-real time via an optical microscope coupled with a video recorder during the reflow process was studied. The lead-free solder balls started to melt and wet below normal melting point by using A6. Wetting performance of the lead-free solder ball was dramatically enhanced by using A6. The wettability test indicated that the height of the solder ball after the reflow process with flux A6 was significantly lower than that with B6. It was also observed that strong fluxing capability caused these phenomena.

3:05 PM

Interaction of Pb Free Solder Alloys and Package Pad Finish on Drop/Impact Reliability of CSP Packages: *Ahmer R. Syed*¹; Tae Seong Kim¹; Jae Hyeon Shin¹; Sang Hyun Ryu¹; Min Yoo¹; ¹Amkor Technology

Both Sn4.0Ag0.5Cu and Sn3.0Ag0.5Cu solder do not perform as good as SnPb solder under drop/impact loading experienced by CSP packages in handheld electronic applications. This study focuses on finding alternate Pb free solder alloys which can perform similar or better than SnPb solder under board level drop testing. Eight (8) SnAgCu based alloys were considered for this evaluation using both NiAu and Cu OSP surface finish on package ball pads. The alloys included various versions on ternary SnAgCu as well as quaternary alloys with the addition of Co, Ni, and Sb in basic SnAgCu system. Intermetallic analysis and package and board level tests were performed for each solder alloy-pad finish combination. The results show that changes in SnAgCu composition and additional elements in SnAgCu based solder can significantly improve the drop performance, primarily because of differences in IMC formation and the strength of solder alloys.

3:25 PM

A Nano-Structured Approach in Lead-Free Electronic Solders: *Andre Lee*¹; K. N. Subramanian¹; ¹Michigan State University

The nano-structured materials technology based on polyhedral oligomeric silsesquioxanes (POSS), with appropriate organic groups, can produce suitable means to promote bonding between nano-reinforcements and the metallic matrix. The microstructures of lead-free solder reinforced with surface-active POSS tri-silanols were evaluated using SEM technique. Steady-state deformation of solder joints made of eutectic Sn-Ag solder containing varying amounts of POSS of different chemical moieties were evaluated at different temperatures. Mechanical properties such as shear stress versus simple shear-strain relationships, peak shear stress as a function of rate of simple shear-strain and testing temperature for such nano-composite solders are reported. The service reliability of joints made with these newly formulated nano-composite solders was evaluated using a realistic thermomechanical fatigue test profile. Evolution of microstructures and residual mechanical property after different extents of TMF cycles were evaluated and compared with joints made of un-modified eutectic Sn-Ag solder.

3:45 PM Break

4:00 PM

Synchrotron Radiation X-Ray Microdiffraction Study on Orientation Distribution of Cu₆Sn₅ Intermetallic Compound Scallop in Solder Joint: *Jong-Ook Suh*¹; Albert T. Wu¹; King-Ning Tu¹; Andriy M. Gusak²; ¹University of California, Los Angeles; ²Cherkasy National University

Formation and growth of intermetallic compound layer in solder joint is one of the most fundamental issues in solder joint reactions. While intermetallic compound formation provides adhesion in the joint between the solder and the metal, growth of the intermetallic compound layer by solder wetting reaction is also responsible for spalling when the metal is a thin film. Final thickness of the intermetallic compound layer affects mechanical strength and thermal fatigue reliability of the solder joint, especially for solder joints with very a fine pitch. The intermetallic compound growth is a unique interfacial parasitic reaction because each intermetallic compound scallop undergoes non-conservative ripening during the growth. In this talk, we present experimental results of morphological transition and size distribution of intermetallic compound scallops, followed by orientation distribution of the scallops characterized by synchrotron radiation x-ray microdiffraction. Comparison to theoretical model of flux-driven ripening will be made.

4:20 PM

Ternary Additions in the Ag-Sn System: Determination of Phase Equilibria: *Evgueni Dobrev*¹; Gueorgui P. Vassilev¹; *Jean-Claude Tedenac*¹; ¹Laboratoire de Physique de la Matière Condensée

Isothermal sections of the Ag-Sn-In were studied by X-ray diffraction, DSC, SEM, microhardness and metallographic studies. The calculation of phase equilibria by thermocalc software in the ternary have been made in order to determine the region were composition of lead free solder alloys can be defined.

4:40 PM

The Effect of Ag Content on the Formation of Ag₃Sn Platelet in Sn-Ag-Cu Lead Free Solder: *Huann-Wu Chiang*¹; *Kendi Chang*¹; *Jeffrey C. B. Lee*²; ¹I-Shou University; ²Advanced Semiconductor Engineering, Inc.

The formation of Ag₃Sn platelet at the Sn-Ag-Cu lead-free solder joints for various Ag content solder balls will be investigated in WL CSP (wafer level chip scale package). After appropriate SMT (surface mount technology) reflow process on PCB (printed circuit board), samples will be subjected to 150°C HTS (high temperature storage) 1000 hours aging or -40 to 125°C 1000 cycles thermal cycling test (TCT). Sequentially, the cross-section analysis is scrutinized by SEM/EDX (scanning electron microscope/energy dispersive spectrometer) and to observe metallurgical evolution of the amount of the Ag₃Sn platelets in the interface and solder buck itself. Pull and shear tests will also be performed on samples. The relationship among the solder ball Ag content, the amount of Ag₃Sn platelet and the joint strength will then be analyzed and discussed.

5:00 PM

The Structural Analysis of the Immersed-Au between a Sn-Zn Based Lead Free Solder and a Substrate: *Nobuhiro Ishikawa*¹; ¹National Institute for Materials Science

The microstructure of the interface between a Sn-Zn based Pb-free solder and a substrate by packaging of ball grid assembly (BGA) process has been studied. The several disadvantages, for example low wettability and low corrosion resistance and so on, put off the spread of the Sn-Zn based alloys. Immersion of Au on the surface of the substrate is sometimes necessary to promote the adhesion properties of soldering especially in case of using Sn-Zn based alloys. But Au forms brittle intermetallic compounds with Zn. The effects of the thickness of immersed Au have been investigated in this study. Angle lapping method was employed to analyze the Au-layer between solder and substrate three dimensionally. The cracks at the Au-layer became smaller with the thinning of the immersed Au. But they spread all directions even having thinner layer of Au and this result was found by using angle lapping method.

5:20 PM

Thermodynamic Models for the Bi-Ga-In-Sn-Zn Lead-Free System: *Raymundo Arroyave*¹; *Joel Williams*²; *Thomas W. Eagar*²; ¹Pennsylvania State University; ²Massachusetts Institute of Technology

In the past decade, considerable effort has been made in the development of lead-free soldering techniques due to environmental concerns. In general, the process of alloy development is costly and time consuming; however, the development process can be greatly simplified by the use of computational thermodynamics. Issues such as topology of the liquidus surface, solidification sequence, driving force for precipitation of intermetallic compounds and so forth can be addressed with this technique. In this work, we present a thermodynamic database for the Bi-Ga-In-Sn-Zn system, which is a modification of a previous model for the Bi-In-Sn-Zn quaternary system. The thermodynamic models for the ternary systems formed by the components of this quaternary system and Ga are obtained through the use of the available experimental data. Some examples on the application of this database on the characterization of alloys in this quinary system are also presented.

5:40 PM

Sedimentation of Intermetallics in Liquid Lead-Free Solders: *Jenn-Ming Song*¹; *Yu-Lin Shen*¹; *Zong-Mou Wu*¹; ¹National Dong Hwa University

Since Sn-Ag-Cu and Sn-Zn alloys, which are regarded as promising lead-free solders, exhibit a lower density than the Sn-Pb solder, the sedimentation of intermetallic dispersoids may occur during multi-reflow or wave soldering processes due to gravity effect. This is usually viewed as having a harmful influence on soldering quality. This study examined microstructural evolution of intermetallics induced by alloying in isothermal liquid solders. The test materials include Sn-Ag-Cu alloys doped with small amounts of transition metals, Co, Fe or Ni, and Sn-Zn alloys with Ag or Cu. Experimental results show that the behavior of intermetallics was closely related to the temperature of the melt. Except for Cu-Zn compounds in some Sn-Zn-Cu solders, most of the heterogeneous intermetallics tended to coarsen and settle at the bottom of the molten solder when

isothermally heated at 250°C. This can be ascribed to the difference in buoyancy and crystallizing temperature of the intermetallic compounds.

Magnesium Technology 2006: Microstructure and Properties II

Sponsored by: International Magnesium Association, TMS Light Metals Division, TMS: Magnesium Committee

Program Organizers: Alan A. Luo, General Motors Corporation; Neale R. Neelameggham, US Magnesium LLC; Randy S. Beals, DaimlerChrysler Corporation

Tuesday PM
March 14, 2006

Room: 6B
Location: Henry B. Gonzalez Convention Ctr.

Session Chairs: Bob R. Powell, General Motors Corporation; Xiaoqin Zeng, Shanghai Jiao Tong University

2:00 PM

Effect of 2nd Phases on the Strength and Formability of Twin-Roll Strip Cast Mg-Zn-X Alloys: *Sung S. Park*¹; *Jung G. Lee*¹; *Geun T. Bae*¹; *Nack J. Kim*¹; ¹Pohang University of Science and Technology

In spite of increasing demand for light-weight vehicle, application of Mg alloy sheets in transportation systems is rather limited since few Mg alloy sheet products fulfill the strength and formability requirements of automobile industry. Recent development of twin-roll strip casting technology has shown that it can efficiently produce low cost, high performance wrought Mg alloy sheets. One of the main advantages of twin-roll strip casting is that novel microstructure can be developed due to its relatively fast solidification rate. Therefore, microstructure of recently developed twin-roll strip cast Mg alloys is usually characterized by the presence of fine second phase particles. In the present study, effect of second phase particles on the strength and formability of twin-roll strip cast Mg-Zn-X alloys has been investigated. Types of second phase particles include precipitates, primary dispersoids as well as quasicrystalline particles. Effects of alloying elements and thermo-mechanical treatment will also be discussed.

2:20 PM

Effect of Grain Size and Solute Distribution for Enhancing Strength-Ductility Balance in Wrought Magnesium Alloys: *Toshiji Mukai*¹; *Hidetoshi Somekawa*¹; *Kazuhiro Hono*¹; *Tetsuya Shoji*²; *Takumi Hiji*²; ¹National Institute for Materials Science; ²Toyota Motor Corporation

Magnesium alloys are the lightest commercial alloys and have great potential for weight reduction of automobiles to save the natural resources and to reduce the exhaust. As well as the development of the cast alloys for the power train components, production of the wrought alloys at low cost is attractive owing to the thinning of structural components. It has been demonstrated that wrought processing, i.e., extrusion or rolling, effectively enhances the strength by means of the grain refinement of materials. The effect of solute has not been, however, fully understood yet to enhance the mechanical properties in the fine-grained alloys. In this study, kinds of solute, i.e., Al, Zn, Y, etc., are investigated for the microstructure modification and enhancing the strength-ductility balance. Concentration of solute atoms inspected with high resolution TEM and EDS correlates with the grain refinement and mechanical properties in tension.

2:40 PM

Effect of Grain Size and Texture on Fracture Toughness in Magnesium and Magnesium Alloy: *Hidetoshi Somekawa*¹; *Toshiji Mukai*¹; ¹National Institute for Materials Science

For structural applications, it is important to examine the mechanical properties of magnesium materials whether satisfied with both reliability and safety or not. One of the distinction methods is the investigation of fracture toughness. However, it has been reported that the fracture toughness in magnesium materials are lower than that in commercial aluminum materials. Therefore, it needs to develop the improvement method of fracture toughness for the future applications. Recently, the grain refinement has been used to improve the mechanical properties such as strength and elongation-to-failure in magnesium materials. In addition, it has been re-

TUESDAY PM

ported that the controlling of texture is another effective method. However, these effects on fracture toughness in magnesium materials have not been investigated yet. In this study, the effect of grain size and texture were discussed to the enhancement of fracture toughness in commercial pure magnesium and magnesium alloy, AZ31, which produced by severe plastic deformation.

3:00 PM

Fatigue Behavior of High-Pressure Die-Cast Magnesium Alloys: *Oren Bar-Yosef*¹; Nir Nagar¹; Nir Moscovitch¹; Boris Bronfin¹; German Gertsberg¹; ¹Dead Sea Magnesium

Diecasting magnesium alloys offer excellent opportunities for achieving high performance, low weight, cost efficient, and fully recyclable solutions to complex engineering design challenges. Magnesium alloys that are being widely used in safety related parts and other applications are mainly subjected to complicated repetitive or fluctuating dynamic stresses at service conditions. Thus, the fatigue behavior that to large degree depends on the component soundness and particularly surface conditions is becoming one of crucial factors that may pave the way for expanding magnesium alloy applications in the automotive industry. The present paper addresses fatigue behavior of several HPDC magnesium alloys dependent on percentage of porosity and surface conditions that were varied via shot peening treatment. The effect of the above parameters on the fatigue life is discussed in terms of Goodman diagram approach.

3:20 PM

Fracture Characteristics of Die Cast Magnesium Alloy AM60B Determined from High-Resolution X-Ray Tomography under Tensile Loading: *Jon Weiler*¹; J. T. Wood¹; R. J. Klassen¹; E. Maire²; J. Adrien²; R. Berkmortel³; G. Wang³; ¹University of Western Ontario; ²INSA de Lyon; ³Meridian Technologies

In this work, fracture characteristics of a die casting magnesium alloy AM60B sample under tensile loading were studied. A high-resolution X-ray tomography analysis was performed at four different loading levels on a 1 mm x 1 mm x 11.5 mm sample cut from a die casting corrosion plate. The differences in distribution, volume, shape and fraction of pores at each loading level are analyzed. It was found that pore growth and coalescence resulted in the fracture of the AM60B sample. The data was applied to a previously reported "critical strain model" to predict the mechanical properties of the magnesium die-casting. This study indicates that mechanical properties of magnesium die castings could be potentially predicted through the unstrained X-ray tomography data.

3:40 PM

Mechanical Behavior of Wrought Mg-Zn-Y(-Mn) Alloys: *Ju Yeon Lee*¹; Tae Eung Kim¹; Hyun Kyu Lim¹; Jun Hyun Han²; Won Tae Kim³; Do Hyang Kim¹; ¹Yonsei University; ²Korea Institute of Science and Technology; ³Ceongju University

The room temperature mechanical behavior of Mg-Zn-Y(-Mn) alloys has been investigated. Earlier, it has been reported that the Mg-Zn-Y alloys (Mg96Zn3.4Y0.6) reinforced by icosahedral-phase particles show better mechanical properties than AZ31 alloy mainly due to strengthening effect by I-phase particles and stable I-phase/matrix interface at elevated temperature. In order to understand the mechanical behavior in more detail, the grain size of the rolled plate has been controlled in two ways: by controlling the reduction ratio during rolling and by adding alloying elements such as misch-metal (Mn). The grain size in Mg-Zn-Y alloys decreases with addition of Mn due to increased volume fraction of secondary solidification phase which accelerates the dynamic recrystallization during rolling. The mechanical properties of Mg-Zn-Y(-Mn) alloys have been investigated, and compared with those of commercial AZ31 alloys. In particular, the elongation of Mg-Zn-Y(-Mn) alloys is better than that of AZ31 alloy due to the stable I-phase/matrix interface.

4:00 PM Break

4:20 PM

Study of Rolling, Heat Treatment Characteristics and Mechanical Properties of Superlight Mg-Li-Zn Alloys: Hong Bin Li¹; Guang Chun Yao¹; Yi Han Liu¹; Hai Bin Ji¹; ¹Northeastern University

Cold-rolling workability, and mechanical properties of Mg-5~22wt%Li-2wt%Zn wrought alloys were studied. The limit of reduction for cold roll-

ing of the β phase alloys at 16 and 22wt%Li exceeds 90% at room temperature. High strength and good elongation can be obtained by quenching at 300°. The tensile strength of both as-rolled specimens increase with decrease in lithium content. Additionally, age-hardening at room temperature occurs in the specimens of (α + β)phase(9 wt% Li)and β phase (16,22 wt% Li) alloys quenched after isothermal holding at 300° for 1h. A remarkable decrease in elongation is encountered for the β phase alloys having the maximum hardness. The appearance of side-bands in the results of X-ray diffraction patterns suggests that the hardening may be attributed to spinodal decomposition.

4:40 PM

The Tensile and Creep Behavior of Mg-Zn Alloys with and without Y and Zr as Ternary Elements: *Carl J. Boehlert*¹; ¹Michigan State University

The microstructure, tensile, and tensile-creep behavior (100-200°C) of Mg-Zn alloys ranging from 0-5.6wt%Zn were investigated. The greatest tensile-creep resistance was exhibited by Mg-3.6Zn. In addition the effect of Y and Zr as ternary elements was evaluated. The effect of 1.5-2.9wt%Y was minimal on the creep and tensile strength. The greatest tensile strength and elongation was exhibited by Mg-5.6Zn-0.6Zr, which also exhibited the finest grain size and the poorest creep resistance. The measured creep exponents and activation energies suggested that the creep mechanisms were dependent on stress. For applied stresses greater than 40MPa, the creep exponents were between 4-8. For applied stresses less than 40MPa, the creep exponent was 2.2. The activation energies were dependent on temperature where the Q values between 100-150°C (65kJ/mol) were half those between 150-200°C for the same applied stress value (30MPa). Deformation observations indicated that grain boundaries were susceptible to cracking in both tension and tension-creep.

5:00 PM

Improvement in Creep Resistance of Mg-Sn Based Alloys by Microstructural Modification: *Dae H. Kang*¹; Sung S. Park¹; Yoon S. Oh¹; In-Ho Jung²; Nack J. Kim¹; ¹Pohang University of Science and Technology; ²Research Institute of Industrial Science and Technology

Mg alloys are the lightest commercially available structural alloys developed so far and have great potential for high performance automotive applications. However, current commercial Mg alloys cannot be used for elevated temperature applications such as powertrain due to their poor creep resistance. In the present research, Mg-Sn based alloys which have thermally stable second phase particles along grain boundaries and within matrix have been studied. Effects of alloying elements and cooling rates on the microstructure of the alloys were investigated. Tensile and creep properties were analyzed with emphasis on the role of second phase particles. It shows that the creep resistance of Mg-Sn based alloys can significantly be improved by the incorporation of thermally stable second phase particles within matrix. To understand the effect of second phase particles within matrix, load relaxation behavior was also analyzed in the context of internal variable theory.

Magnesium Technology 2006: Wrought Alloys and Forming Processes I

Sponsored by: International Magnesium Association, TMS Light Metals Division, TMS: Magnesium Committee

Program Organizers: Alan A. Luo, General Motors Corporation; Neale R. Neelameggham, US Magnesium LLC; Randy S. Beals, DaimlerChrysler Corporation

Tuesday PM
March 14, 2006

Room: 6A
Location: Henry B. Gonzalez Convention Ctr.

Session Chairs: Amit Ghosh, University of Michigan; Sean R. Agnew, University of Virginia

2:00 PM

A Study on the Static Recrystallization of Cold Rolled Magnesium Alloy AZ80: *Jayant Jain*¹; Warren J. Poole¹; Chad W. Sinclair¹; ¹University of British Columbia

Recently, there has been substantial interest in refining the grain structure of as-cast magnesium alloys using deformation processing. The majority of this work has focused on deformation at elevated temperatures where dynamic recrystallization is the dominant softening mechanism. On the other hand, relatively little literature is available on static recrystallization. In this work, the magnesium alloy AZ80 was chosen due to the possibility of examining situations where grain refinement can be combined with precipitation hardening to produce interesting microstructures and mechanical properties. AZ80 in a supersaturated solid solution was rolled 10-30% at room temperature and then annealed in the temperature range of 200-400°C. The evolution of microstructure was systematically studied using optical microscopy and EBSD. It was observed that static recrystallization of the samples occurred in the temperature range of 325-400°C and that the possibility of concurrent precipitation may exist.

2:20 PM

Deformation Anisotropy of High Purity Magnesium and AZ31B Magnesium Alloy: *Veronica Livescu*¹; Carl M. Cady¹; Ellen K. Cerreta¹; Benjamin L. Henrie¹; George T. Gray¹; ¹Los Alamos National Laboratory

The deformation in compression of pure magnesium and AZ31B alloy, both with a strong basal pole texture, has been investigated as a function of temperature, strain rate, and specimen orientation. The mechanical response of both metals is highly dependent upon the orientation of loading direction with respect to the basal pole. Specimens compressed along the basal pole direction have a high sensitivity to strain rate and temperature and display a concave down work hardening behavior. Those loading perpendicularly to the basal pole have a yield stress that is relatively insensitive to strain rate and temperature and a work hardening behavior that is parabolic and then linearly upwards. Post mortem characterization was conducted on a subset of specimens to determine the microstructural and textural evolution during deformation and these results are correlated with the observed work hardening behavior.

2:40 PM

Deformation Characteristics of AZ31 Alloy at the Elevated Temperature: *Yong Nam Kwon*¹; Y. S. Lee¹; S. W. Kim¹; J. H. Lee¹; ¹Korea Institute of Machinery and Materials

Since magnesium alloy has a limited formability at room temperature, forming should be carried out at the elevated temperature. Forming between 473-573K is known to be successful due to active dynamic recrystallization. If the initial grain size is small, superplasticity could be expected over 623K. Deformation assisted grain growth becomes evident at superplastic temperature of AZ31 alloy. It is quite natural to assume that deformation mechanisms could evolve with temperature, which means that deformation proceeds with dislocation and grain boundary sliding depending on temperature. However, the initial (0001) fiber texture remained strong after deformation irrespective of temperature. In the present study, the deformation characteristics of AZ31 is studied to understand several features of elevated temperature deformation behavior. For this purpose, a series of tensile and relaxation tests were performed along with microstructural observations including texture measurement. Grain growth and compatibility problems after grain boundary sliding are discussed.

3:00 PM

Deformation Mechanisms and Ductile Failure of Magnesium AZ31: *Matthew Barnett*¹; Zohreh Keshavarz¹; X. Ma¹; ¹Deakin University

A series of tensile tests were carried out at different temperatures and strain rates using commercial AZ31 over a range of grain sizes. Experiments were performed in a conventional load frame and these tests were complemented with a number of tensile measurements carried out in-situ in a Scanning Electron Microscope. Careful measurements of twin populations were made. These enabled the relationship between deformation conditions and the frequency of c-axis compression twins to be determined. The uniform and total elongations are rationalized in terms of the twinning frequencies. A simple model is constructed on the assumption that compression twins are "soft" with respect to the matrix. This model is used to identify the importance of suppressing twinning for improved ductility.

3:20 PM

Ductility and Low Temperature Superplasticity of Ultrafine Grain Mg Alloys: *Amit K. Ghosh*¹; Qi Yang¹; Xiang Li¹; ¹University of Michigan

Current interest to develop Mg alloys formable at low to warm temperatures has led to exploration of grain refinement of several alloys by severe deformation process. Alloys containing Al and Zn as solid solution elements are investigated in wrought and thixomolded conditions. The paper will discuss the evolution of microstructure during processing and mechanical behavior after the processing steps. Impressive gains in strength and strain rate sensitivity of flow stress are achieved through fine grain processing. The effect of crystallographic anisotropy is significantly reduced in grain sizes between 3 micron and 0.3 micron. This paper will discuss results on the variations in strain hardening rate and available tensile elongations when mechanical twinning is present vs. when it is absent. Some results on biaxial formability will be reported. (Project supported by NSF-DMR Project Award 0314218).

3:40 PM

Hardening Evolution of AZ31B-O Mg Sheet: Xiaoyuan Lou¹; Min Li¹; Richard K. Boger¹; *Robert H. Wagoner*¹; ¹Ohio State University

The monotonic and cyclic mechanical behavior of O-temper AZ31B Mg sheet was measured in large-strain tension/compression and simple shear. Metallography, acoustic emission (AE), and texture measurements revealed twinning during in-plane compression and untwinning upon subsequent tension, producing asymmetric yield and hardening evolution. Plastic straining occurs preferentially by basal slip, which provides two independent slip systems with low critical resolved shear stress. The macroscopic flow stress is determined by the required activation of higher-stress mechanisms to accommodate arbitrary deformation: predominantly non-basal slip for initial tension, twinning for initial compression, and untwinning for tension following compression. The nucleation stress for twinning is larger than that for untwinning. Increased accumulated hardening increases the twin nucleation stress, but has little effect on untwinning. Multiple-cycle deformation tends to saturate after a few cycles of +/- 0.02 strain, but does not saturate for +/-0.035 strain cycles by the time fracture intervenes at 10 cycles.

4:00 PM Break

4:15 PM

Study on Microstructures Evolution, Tensile Mechanical Properties and Forming Techniques of AZ31 Alloy Sheets: *Yan Yunqi*¹; ¹Suzhou Institute for Nonferrous Metal Research

Better properties of magnesium alloys make it as a natural choice for use as 3C materials. However, the magnesium alloy thin sheets used in this field were difficult to be obtained and punched, whereas the homogeneous microstructures without any textures, the better ductility were needed. AZ31 alloy was investigated using rolling and punching techniques in this paper. Various rolling experiments were carried out to make fine-grained Mg sheets. Microstructures were observed using optical and scanning electron microscope with EBSD device. Tensile tests were conducted at the temperatures ranged from 150 to 300°C for as-rolled AZ31 alloy. The analysis revealed that there is an excellent warm forming temperature for as-rolled AZ31 alloy. A warm deep punching tool setup using heating elements was designed and manufactured to produce the cell phone. The certain type cell phone was produced using this tool and method in the temperature range 250-350°.

4:35 PM

A Study of Damping Properties of Mg-Zr Alloys after Rolling and Annealing: *Chuming Liu*¹; Jia Zhang¹; Haitao Zhou¹; ¹Central South University

The effect of hot rolling and annealing on the damping behavior of Mg-Zr alloys was investigated. It was found that rolling lead to a significant grain refinement, and hence improved their tensile properties. In cast condition damping was strain dependent. However, the damping of the hot rolled alloys weakly depended on strain, which indicates that the damping capacity decreases after hot rolling. In contrast, annealing for the rolled alloy made the damping capacity increasing, but it didn't reach the as-cast level. The varieties of damping behavior can be explained by dislocation model of Granato and Lücke.

5:00 PM

Direct Chill Casting and Plastic Deformation of Magnesium Alloys:*Gady Isaac Rosen*¹; Menachem S. Bamberger²; Christoph Honsel³; ¹Alubin Ltd; ²Technion; ³RWP GmbH

To be able to produce sound, repeatable and reliable plastic deformation in magnesium alloys, high quality billets are required. Usually extrusion or hydroforming at elevated temperature is used. This is since they have hexagonal close packed structure, which shows limited ductility at room temperature. In order to be able to deform the low ductility magnesium alloys, premium quality billets and well-defined parameters and conditions are crucial. Therefore, in-depth understanding of the influence of direct chill casting conditions on the production quality and safety, and on micro-structure, properties and workability are of high importance. Efficiency of the production can be improved by utilizing advanced process-simulation in the production floor. The proposed research will be focused on these issues. Extensive simulation will be used in order to model the underlying physics of casting so that process improvement variables can be identified and controlled, resulting in significant benefits. The aim of modeling, the filling and solidification of a casting is to: Provide temperature profiles during, and at the end of filling for a more accurate solidification analysis. Predict the pattern of solidification, indicating where shrinkage cavities and other solidification defects, such as hot tearing. And, predict solidification time and the effect of cooling system on the solidification.

5:20 PM

Effects of Microstructural Changes on Tensile Properties of AZ31 Magnesium Alloy up to Localized Necking: *Ravi Verma*¹; Louis G. Hector¹; Manuel Marya²; ¹General Motors R&D Center; ²Colorado School of Mines

An AZ31 magnesium alloy was investigated for effects of microstructural modifications on room temperature mechanical properties. Three distinct microstructures were generated through heat-treatments: (1) single-phase, fine grains; (2) single-phase, coarse grains with twins; (3) fine grains decorated with Mg₁₇(Al,Zn)₁₂ grain-boundary precipitates. Small coupons fabricated from each microstructure were then tested to failure in a miniature tensile stage. True stress – true strain curves were computed with the digital image correlation (DIC) technique and strain accumulation in the necking region of each coupon was quantified with two-dimensional strain maps. The initial yield points, ultimate tensile strengths and maximum elongations prior to failure were taken as measures of room temperature tensile properties of each microstructure. These values are examined within the context of key features of each microstructure in order to infer the mechanism of plastic deformation in tension and whether or not the potential for improved room temperature formability exists.

Materials Design Approaches and Experiences II: Light Alloys

Sponsored by: The Minerals, Metals and Materials Society, TMS Structural Materials Division, TMS: High Temperature Alloys Committee

Program Organizers: Michael G. Fahrman, Special Metals Corporation; Yunzhi Wang, Ohio State University; Ji-Cheng Zhao, General Electric Company; Zi-Kui Liu, Pennsylvania State University; Timothy P. Gabb, NASA Glenn Research Center

Tuesday PM

Room: 202B

March 14, 2006

Location: Henry B. Gonzalez Convention Ctr.

Session Chairs: Ingo Steinbach, RWTH-Aachen Access EV; Qigui Wang, General Motors Corporation

2:00 PM

Effect of Moderate Pressures (to ~5GPa) on Phase Equilibria in Some Al-Based Alloys: *Joanne L. Murray*¹; ¹Alcoa Technical Center

Moderate pressure affects solidification, melting, and solid solubility of Al alloys to an extent great enough that the effect must sometimes be taken into account when optimizing alloy composition and processing. Moreover, pressure can play a role in development of qualitatively new

alloys. So far little has been done, to model the effect of pressure on the phase equilibria of Al-base alloys. Minamino et al.* have made a start at introducing thermal expansion, modulus and molar volumes as parameters of the Gibbs energies. In the present study, a methodology is developed for assessing the physical property data needed to model the pressure dependence of phase diagrams. The systems Al-Ag, Al-Cu, Al-Ge, Al-Li, Al-Mg, Al-Si, Al-Zn will be modeled. *Y. Minamino, T. Yamane, T. Sato, Journal of Japan Institute of Light Metals. Vol. 38, no. 12, pp. 800-806 (1988).

2:25 PM Invited

The Latest Development of Computational Tools for Virtual Casting of Aluminum Components: *Qigui Wang*¹; ¹General Motors Corporation

The increasing use of cast aluminum components in critical structures has required improved quality, with more reliable and quantifiable performance. Aluminum shape casting processing is very complex and often involves many competing mechanisms, multi-physics phenomena, and potentially large uncertainties. The only effective way to optimize the processes and achieve the desirable mechanical properties is through the development and exploitation of robust and accurate computational models. Numerous modeling and simulation techniques have been developed and applied in practice for aluminum casting and subsequent processing that enable both casting designers and process engineers to better design and develop sound shape cast components with minimum lead time and cost. This talk will review the latest development of computational tools for aluminum shape casting processing from alloy design to mechanical properties. Some suggestions for future development will be presented.

2:50 PM Invited

Prediction of Porosity Defects and Mechanical Properties of a High Pressure Die Cast A380 Aluminum Alloy Component: *Mei Li*¹; Jacob W. Zindel¹; Larry A. Godlewski¹; John E. Allison¹; ¹Ford Motor Company

Cast aluminum alloys are increasingly being utilized by automotive industry for manufacturing chassis and powertrain components to reduce vehicle weight and consequently increase fuel economy and reduce emissions. High pressure die casting process provides tremendous cost saving opportunities in manufacturing these components. Development of Virtual Casting tools for HPDC aluminum will lead to fast prototyping and tooling, thus fast final products with reduced cost. Porosity is a commonly found defect in high pressure die cast components which affects both the ductility and fatigue properties. This talk describes the development of an algorithm which can predict porosity defects in HPDC A380 component and the correlation of defects to fatigue property in the component. The prediction can be used to design and optimize casting component and process.

3:15 PM

Study on Preparation of Ceramic Particles Reinforced Aluminum Foam: *Wang Yong*¹; Yao Guang-Chun¹; Li Bing¹; ¹Northeastern University

In this work, fly ash was selected as reinforcement in melt-foaming process. The most component are quartz and mullite was observed by XRD in the fly ash, therefore it's a kind of hardness ceramic particles. Fly ash particles act as viscosity increaser and increase stabilization of bubble wall in the aluminium foam. Put fly ash into melting aluminium, suitable stir and add in frothing agent, after foaming and cooling, then obtain particles reinforced aluminium foam. Through compression strength test, compare aluminium foam which fly ash particles as viscosity increaser with Ca as viscosity increaser. Experimental results indicate: fly ash has not only viscosity increase function, but also particles reinforced function, because of Al₂O₃ and mullite in the fly ash, in which the Al₂O₃ particle is quartz and melting aluminium have happened in-situ reaction.

3:35 PM Break

3:55 PM Invited

CalPhad and Phasefield Modeling for the Development of New Mg-Base Alloys: *Ingo Steinbach*¹; Janin Eiken¹; Bernd Boettger¹; Muneakazu Ohno²; Rainer Schmid-Fetzer²; Gerald Klaus¹; Andreas Buehrig-Polaczek¹; ¹RWTH-Aachen; ²TU Clausthal

The solidification behaviour of Mg-base alloys is investigated by CalPhad and Phase Field modelling. The investigation starts from a criti-

cal reassessment of the Mg-Al system with special care on micro alloying elements. Equilibrium and Scheil calculations serve to identify candidates for new alloy compositions. Subsequently Phase Field calculations for the equiaxed solidification of the Mg-phase are performed taking into account nucleation on primary precipitates, growth with hexagonal surface anisotropy reflecting the Mg lattice structure and eutectic termination of solidification. The Phase Field simulations reveal the influence of alloy composition and casting conditions on the phase morphology. Phase distribution and morphology together define quality criteria for the as cast structure, dependent on alloy composition and process conditions. The presentation discusses the prospect and limitation of the numerical approach in comparison with experimental results.

4:20 PM

The Mg-Zn-Zr System: From First Principles to Grain Refining - An Integrated Approach to Materials Design: *Raymundo Arroyave*¹; Dongwon Shin¹; Axel van de Walle²; Zi-Kui Liu¹; ¹Pennsylvania State University; ²Northwestern University

In this work we show how, by integrating first-principles techniques with the CALPHAD method, it is possible to address practical problems in materials manufacturing. The thermodynamic models of the Zn-Zr and Mg-Zr binaries are obtained through the CALPHAD approach with the aid of first-principles methods including state of the art calculations of the finite temperature thermodynamic properties of intermetallic phases in which vibrational degrees of freedom are taken into account, as well as the energetics of special quasirandom structures, utilized to mimic the behavior of random solid solution phases. The two binary models obtained in this work are combined with the existing description for the Mg-Zn system to predict the thermodynamic behavior of the Mg-Zn-Zr ternary. This thermodynamic description is then used to address important issues regarding the grain refining behavior and solidification sequences observed in cast Mg-Zn-Zr alloys.

4:40 PM

Balanced Alloy Design for 6000 Series Al-Mg-Si Alloys: Malcolm J. Couper¹; *Barbara Rinderer*¹; Mark Cooksey²; ¹Comalco Aluminium Ltd; ²CSIRO Minerals

In 6000 series Al-Mg-Si alloys the optimum strength, with minimum alloy content, can be achieved using a "balanced" alloy composition with respect to Mg_xSi precipitates, with x close to 1. Al-Mg-Si alloys with a wide range of Mg and Si contents were VDC cast as billet, extruded and the tensile properties in T1, T4, T5 and T6 heat treatment condition evaluated. Balanced alloys can be designed with strengths that increase with increasing total alloy content, for example SF6060 and SF6063. The performance of 6061 alloys with additions of Cu, have also been investigated.

Materials in Clean Power Systems: Applications, Corrosion, and Protection: Interconnection and Sealing in Fuel Cells I

Sponsored by: The Minerals, Metals and Materials Society, TMS Structural Materials Division, TMS/ASM: Corrosion and Environmental Effects Committee

Program Organizers: Zhenguo Gary Yang, Pacific Northwest National Laboratory; K. Scott Weil, Pacific Northwest National Laboratory; Michael P. Brady, Oak Ridge National Laboratory

Tuesday PM
March 14, 2006

Room: 212B
Location: Henry B. Gonzalez Convention Ctr.

Session Chairs: Frederick S. Pettit, University of Pittsburgh; Lorenz Singheiser, Forschungszentrum Jülich

2:00 PM Keynote

Interconnect Performance in SOFC Environments: *Peggy Y. Hou*¹; Hideto Kurokawa¹; Craig Jacobson¹; Steven Visco¹; Lutgard De Jonghe¹; ¹Lawrence Berkeley National Laboratory

For medium temperature solid oxide fuel cells (SOFCs) operating at 600-800°C, ferritic steels can be successful interconnect or support struc-

ture materials due to their low cost, compatible thermal expansion with the electrode and electrolyte ceramics and the ability to develop a relatively slow growing and conductive Cr₂O₃ surface layer under SOFC operating conditions. This paper gives an overview of the current status of the development of such interconnect materials and discusses important issues concerning their usage. These include the effect of alloying elements and coatings on the growth and evaporation rates of these thermally grown Cr₂O₃ scales, the boundary conditions on scale adherence and the effect of applied current on Cr₂O₃ growth in typical oxidizing and reducing SOFC environments. Experimental data performed under short term exposures will be presented along with models predicting long term behaviors.

2:45 PM Invited

Metallurgical and Geometrical Parameters Affecting the Oxidation of Ferritic Steels as Interconnector Materials in Solid Oxide Fuel Cells: *W. J. Quadackers*¹; ¹Forschungszentrum Jülich

High-Cr ferritic steels are presently being considered as SOFC interconnect materials because they fulfil most of the requirements for SOFC application. In the present paper the oxidation behaviour a number of high-Cr, ferritic steels in the temperature range 700 to 900°C in dry air, wet air and H₂/H₂O-mixtures will be described. Thereby the effect of main alloying elements (e.g. Cr) as well as minor alloying additions (Mn, Si, Al, Ti, La) on the oxidation properties will be treated. Considering the envisaged possible application of SOFC's (stationary as well as mobile), special emphasis is given to the effect of interconnect geometry (mainly component thickness) on the oxidation behaviour. It will be shown, that oxidation data derived from experiments using thick components (of a few millimetres in thickness) cannot straightforwardly be used to describe the oxidation properties of thin walled (a few tenths of a millimetre) components considered for SOFC-APU application.

3:15 PM

Continuous Improvements in the Commercial Development of Alloy 22APU for Interconnect Applications in Solid Oxide Fuel Cells (SOFC): *Larry Paul*¹; Rajj Hojda¹; ¹ThyssenKrupp VDM USA Inc.

Several years ago a new material was introduced for use as an interconnect material for solid oxide fuel cell (SOFC) application. The development of this material was the joint effort of Forschungszentrum Jülich and ThyssenKrupp VDM. Crofer 22APU has unique properties that make it an ideal choice in application as an interconnect material. The key properties are the coefficient of thermal expansion (CTE), which closely matches the ceramic materials used in the SOFC stack, the good electrical conductivity of the protective oxide scale that is formed during operation of the fuel cell stack and the outstanding oxidation resistance at operating temperatures. Several lessons were learned during the development, scale-up, and production of the Crofer APU material. The end result is a commercially available material that meets the technical requirements for interconnects in SOFC application.

3:40 PM

Influence of Minor Alloy Elements on the Performance of Crofer 22APU: *Paul D. Jablonski*¹; David E. Alman¹; ¹U.S. Department of Energy

Crofer 22APU, a ferritic stainless steel which contains 22 weight percent chrome, was developed at Jülich specifically for application as an interconnect material in solid oxide fuel cells (SOFC). Thyssen-Krupp has taken on the task of manufacturing this alloy. Two commercial heats of Crofer 22APU were evaluated for use in the SOFC temperature range of 700 to 800C. It was observed that the heat which contained higher levels of the aluminum and silicon, presumably either from alloy make-up or furnace practices, was less resistant to oxidation. Furthermore, these minor differences appeared to also impact the performance of a surface treatment we have developed for enhanced oxidation resistance. We will discuss the impact of these minor impurities in terms of long term component stability.

4:05 PM Break

TUESDAY PM

4:20 PM Invited

SnO₂:F Coated Stainless Steels for PEM Fuel Cell Bipolar Plates:John A. Turner¹; Heli Wang¹; ¹National Renewable Energy Laboratory

The corrosion resistance and the interfacial contact resistance are the major challenges for stainless steels operating as bipolar plates in a polymer electrolyte membrane fuel cell (PEMFC). Modification of the surface of the steels so as to have a lower contact resistance and better corrosion resistance is necessary. Conducting oxides, used as current collectors for solar cells, can carry currents up to 1A/cm² and may offer protection against corrosion and additionally give high interfacial conductivity. These oxides can be applied at high-speeds during production and are of interest for fuel cell coatings. Films of SnO₂:F are of particular interest due to their known high stability in a variety of aqueous solutions. In this report we will describe our work with SnO₂:F coatings on stainless steels.

4:50 PM

Oxidation Behavior of Fe-Cr-Al Alloy: Metallic Interconnects for Solid Oxide Fuel Cell Applications:Venkateswarulu Kamavaram¹; Ramana G. Reddy¹; ¹University of Alabama

Solid oxide fuel cells (SOFCs) are developed to meet the energy requirements of the society. Due to high operating temperatures (800-1000°C), the material selection for SOFC is an important aspect of its design and development. Among the four essential components of SOFC; anode, cathode, electrolyte, and interconnect, materials selection for interconnects is a critical factor. Iron based alloy (Fe; Cr: 22%; Al: 5%; Zr: 0.1% and Y: 0.1%) was investigated as metallic interconnect material. Oxidation behavior of Fe-Cr-Al alloy in the temperature range 650-850°C under air and oxygen atmospheres was investigated. Both short-term (50 hrs) and long-term (1000 hrs) oxidation of the FeCrAl alloy was studied using thermogravimetric analysis (TGA). Effect of thermal cycling on the stability of FeCrAl alloy also was investigated. Short-term oxidation kinetics of the alloy followed parabolic rate law in the temperature range 600-850°C with an Arrhenius activation energy of 196 kJ/mol.

5:15 PM

Effect of Ceramic Coating on Chemical Stability of a Composite Seal for Solid Oxide Fuel Cells:Srivatsan Narasimhan¹; Kristoffer Ridgeway¹; Xinyu Huang¹; ¹University of Connecticut

The interconnects in planar solid oxide fuel cells (SOFC) require stable hermetic sealing to their adjacent components to maintain efficiency and longevity. The seal material, typically glass, has to be chemically compatible with the Fe-Cr based ferritic stainless steel commonly used as interconnect for intermediate temperature SOFCs. A novel multilayered composite seal structure that consists of layers of intermetallic bondcoat, a ceramic topcoat, and a filler glass, has been investigated by the authors as an alternative to traditional glass seals, where glasses are in direct contact with Fe-Cr interconnects. One advantage to use a ceramic layer in the composite seal is to mitigate the undesirable chemical interaction. In this study, high temperature aging tests of SOFC seal samples with and without a ceramic inter-layer were conducted. After aging, the degrees of interfacial chemical interactions were characterized by SEM/EDX and the results for the two types of samples were compared.

Materials Processing Fundamentals: Smelting and Refining

Sponsored by: The Minerals, Metals and Materials Society, TMS Extraction and Processing Division, TMS: Process Fundamentals Committee, TMS: Process Modeling Analysis and Control Committee
Program Organizers: Princewill N. Anyalebechi, Grand Valley State University; Adam C. Powell, Massachusetts Institute of Technology

Tuesday PM
March 14, 2006

Room: 203A
Location: Henry B. Gonzalez Convention Ctr.

Session Chair: Princewill N. Anyalebechi, Grand Valley State University

2:30 PM

Mechanisms of Oxygen Partial Lead Softening:Daryl Vineberg¹; Sadegh Firooz²; Ralph Harris²; ¹Ontario Ministry of the Environment; ²McGill University

Simultaneous kinetic studies and visual observations of the oxidation of static and/or agitated baths of lead containing arsenic, antimony and tin as impurities were conducted. Their purpose was to further the understanding of the mechanisms of partial lead softening with pure oxygen as practiced at Teck Cominco Ltd. The visual observations of the melt/gas interface between 500 and 600°C saw the formation of a solid oxide layer on pure lead and lead-tin alloys and formation of liquid oxides during the oxidation of lead-arsenic and lead-antimony alloys. Thermogravimetric measurements showed that the rate of oxygen uptake was strongly influenced by the form of oxides being generated at the melt/gas interface. Tin was most effective in retarding the rate of oxidation. Arsenic increased the rate of oxygen uptake throughout the temperature range and antimony showed a moderate increase in the rate of oxygen uptake at 600°C as compared to arsenic.

2:55 PM

Prevention of Resulfurization in Magnesium Desulfurization Process of Molten Iron:Jian Yang¹; Mamoru Kuwabara¹; Keiji Okumura²; Zhongzhu Liu¹; Masamichi Sano¹; ¹Nagoya University; ²Nagoya Institute of Technology

There are two kinds of mechanisms of resulfurization in magnesium desulfurization process of molten iron. One is decomposition of the desulfurization product of MgS under the inert atmosphere. The other is oxidation of MgS under the oxidative atmosphere. In the desulfurization process with magnesium vapor produced in-situ by aluminothermic reduction of MgO, lowering operating temperature and oxygen partial pressure in the atmosphere, and adding more pellets containing magnesium oxide and aluminum could effectively prevent the resulfurization. The resulfurization took place more markedly by using Al₂O₃ crucible than by using MgO or C crucible. Adding CaO onto the melt surface was an effective method for preventing the resulfurization due to transformation of the desulfurization product of MgS into the more stable compound of CaS. Since addition of the activated charcoal powders greatly decreased the transfer rate of oxygen in the atmosphere to the melt surface, it also reduced the resulfurization remarkably.

3:20 PM

Carbothermal Reduction Study of Kaolin and Two Different Silica Sources:Sutham Niyomwas¹; ¹Prince of Songkla University

Synthesis of Al₂O₃-nSiCw composite was obtained in situ by carbothermal reduction of a mixture of kaolin and two different silica sources. The carbothermal reduction was carried out in a horizontal tube furnace under flow of argon gas. The standard Gibbs energy minimization method was used to calculate the equilibrium composition of the reacting species. The synthesized products were mixtures of alumina and silicon carbide in the form of whiskers. The effects of adding two different silica sources of rice husk ash and silica powder to the mixture of kaolin and activated carbon were investigated. XRD and SEM analyses indicate complete reaction of precursors to yield Al₂O₃-nSiC as product powders, with the SiC having whisker morphology.

3:45 PM

Increase in Concentration of a Zn-Containing Volatile Complex by UV Irradiation of a Target for ZnO Films Synthesis: *Emma Rubenovna Arakelova*¹; V. G. Parvanyan¹; F. A. Grigoryan¹; G. G. Asatryan¹; G. G. Petrosyan¹; ¹State Engineering University of Armenia

An increase in concentration of a Zn-containing volatile complex for synthesis of ZnO films was investigated when processing their target by ultraviolet radiation emitted by mercury lamp. The experiments were carried out using a flow-type quartz reactor. ZnO tableted target was preliminarily irradiated during 2 to 7 hours. H₂O₂ (98 %) vapor at 25 Pa passed through the reactor with ZnO target at 373 K. As substrate material, five subsequent quartz cylinders were used at 423 K. The experiment lasts 4 hours. H₂O₂ decomposition on ZnO surface was accompanied by formation of a Zn-containing volatile complex which passed in gas phase and decomposed on the substrates with isolation of final ZnO. The concentration of the Zn-containing volatile complex (N) in gas phase increases with UV pre-irradiation time (t) (without irradiation N=1,05 •10¹¹ particles / cm³; after t = 2 hours, N=5,19 •10¹¹ particles / cm³, after t = 4 hours, N=9,95 •10¹¹ particles / cm³, after t = 7 hours, N=1,86 •10¹² particles / cm³.

4:10 PM Break

4:25 PM

Preparation of SmCo₅ Alloy by Chemical Co-Deposition and Reduction and Diffusion Method: *Guo Xueyi*¹; ¹Central South University

This SmCo₅ powder was prepared by chemical co-precipitation followed by improved reduction and diffusion method. In the chemical co-precipitation, the thermodynamic equilibrium analysis was conducted, then the precipitation were done to address all the factors on the behaviors of the precursor particle. The optimum conditions were determined, and the precursor particles with narrow size distribution, spherical shape or quasi-sphere were prepared. In the high temperature process, the precursor powder was treated to produce the SmCo₅ alloy by the improved reduction and diffusion method. First, the Sm-Co oxide powder was produced by controlling the calcining temperature, atmosphere and time. Then, the Sm-Co oxide powder was treated to obtain the SmCo₅ alloy under the hydrogen atmosphere, precise reduction and diffusion temperature and the rate for temperature rise. The effects of all the parameters on the high temperature process were addressed.

4:50 PM

Electrical Field Effects on Reactive Sintering: *Dat V. Quach*¹; Lia A. Stanciu²; Vladimir Y. Kodash¹; Joanna R. Groza¹; ¹University of California; ²Purdue University

Field-assisted sintering technique (FAST) is a novel processing method to process powder materials at lower temperature and in shorter time. The application of an external field can increase the mobility of atoms/ions involved in the diffusion process, thus enhancing not only neck formation and growth but also the rate of chemical reaction. Aluminum titanate (Al₂TiO₅) was prepared by FAST sintering of a mixture of amorphous sol-gel Al₂O₃ and TiO₂ powders at 1300°C in 10 minutes. Compared with conventional sintering that requires a longer sintering time (2 hours), FAST gives a higher yield of Al₂TiO₅ formation. To further investigate the effects of electrical field/current on the reaction between Al₂O₃ and TiO₂, basic diffusion couple studies were performed and the results will be reported.

Multicomponent-Multiphase Diffusion Symposium in Honor of Mysore A. Dayananda: Intermetallics and Ceramics

Sponsored by: The Minerals, Metals and Materials Society, ASM Materials Science Critical Technology Sector, ASM-MSCTS: Atomic Transport Committee

Program Organizers: Yong-Ho Sohn, University of Central Florida; Carelyn E. Campbell, National Institute of Standards and Technology; Richard Dean Sisson, Worcester Polytechnic Institute; John E. Morral, Ohio State University

Tuesday PM
March 14, 2006

Room: 203B
Location: Henry B. Gonzalez Convention Ctr.

Session Chairs: Marek J. Danielewski, AGH University of Science and Technology; Dennis D. Keiser, Idaho National Laboratory

2:00 PM Invited

Diffusion in Binary Intermetallic Compounds: *H. Mehrer*¹; ¹Universität Münster

Diffusion studies on binary intermetallics including silicides and aluminides are reviewed. Particular attention is given to ⁹⁹Mo, ³¹Si, and ⁷¹Ge diffusion in single crystals of tetragonal MoSi₂. Si and Ge diffuse six or more orders of magnitude faster than Mo suggesting that diffusion in the Si and Mo sublattice is decoupled. Diffusion is in all cases significantly faster perpendicular to the tetragonal axis than parallel to it. Monte Carlo simulations of correlation effects and anisotropy ratio of vacancy-mediated diffusion in the Si-sublattice lead to their rationalization. Diffusion in aluminides is reviewed with particular attention to iron-aluminides: interdiffusion coefficients were measured on binary diffusion couples. Tracer diffusivities of Al were deduced using the Darken-Manning equation, ⁵⁹Fe tracer diffusivities, and theoretical values of thermodynamic factors. Al and Fe diffusion are closely coupled in B2 structured FeAl. The diffusion of ternary alloying elements in FeAl and self-diffusion in NiMn is also discussed.

2:30 PM

Interdiffusion in Mo₅SiB₂ (T₂) Synthesized in a Mo₅Si₃/Mo₅B Diffusion Couple: *Sungtae Kim*¹; John H. Perepezko¹; ¹University of Wisconsin

Diffusion couples based upon Mo₂B and Mo₅Si₃ were used to determine the diffusion kinetics of T₂ phase development and the relative diffusivities controlling the kinetics. During the growth of the T₂ phase, Si and B atom movements were found to be coupled and driven by the Si concentration gradient. The activation energy for interdiffusion in the T₂ phase was evaluated to be larger than that for layer growth of Mo₅Si₃ in both Mo/Si and MoSi₂/T₂ diffusion couples. This larger activation energy in T₂ may result from the restricted jump possibilities in T₂ due to the coupled nature of Si and B atom movements. The relatively slow diffusion of the T₂ phase due to this high activation energy explains the improvement in the high-temperature creep properties of the Mo-Si-B alloy systems. The support of the AFOSR (F49620-03-1-0033) is gratefully acknowledged.

2:55 PM

Reactive Interdiffusion in the Binary System Ni-Si: Morphology of the Ni₃Si₂ Phase: *Delphine Borivent*¹; Jérôme Paret¹; Bernard Billia¹; ¹L2MP

In binary multi-phase diffusion, it is generally admitted that interfaces between phases are necessarily plane. However, a few cases exist, as the binary diffusion couples Ni-Si, Mo-Si and Fe-Al, for which an intermediate phase of each system grows with an irregular needle-like morphology. To characterize the nonplanar growth of Ni₃Si₂, we have studied the behaviour of intermetallic compounds formation in Ni/Si bulk samples by in-situ X-ray microtomography, for different annealing times. Studying evolution of needles curvature radii with time, we show that these radii grow proportionally to the square-root of time. This result is compatible with an anisotropic diffusion model of the origin of this peculiar microstructure.

TUESDAY PM

3:20 PM Invited

Defect Interactions in Binary Compounds of Transition Metals at High Temperatures: *Ewa Maria Fryt¹*; ¹AGH University of Science and Technology

In highly defective solids in which concentration of point defects is higher than 0.1%, interactions between defects become important influence on diffusion in its crystallographic lattices and many properties. For description of interactions between defects in highly defective solids it is necessary to introduce new terms in diffusion theory characterizing the influence of interactions between defects especially for temperature and pressure dependencies of activity and mobility, and hence on diffusivity. The above mentioned function is characteristic for a crystallographic lattice of a given compound, different types of defects and their relative concentrations, attractive or repulsive interactions between defects and for a given diffusion mechanism. This approach will be discussed using different examples of determined free energy of defect interactions and interpretation of its influence on many macroscopic properties of binary compounds of some transition metal oxides, sulphides and carbides at high temperatures.

3:50 PM Break**4:10 PM**

Irradiation Enhancement of Interdiffusion in the Interaction Zone of U-Mo or U3Si2 Dispersion Fuel in Al: *Yeon Soo Kim¹*; Gerard L. Hofman¹; Steve Hayes²; Ho Jin Ryu³; M. R. Finlay²; ¹Argonne National Laboratory; ²Idaho National Laboratory; ³Korea Atomic Energy Research Institute

The main issue in the process of developing dispersion fuel containing U3Si2 or U-Mo particles in an Al Matrix is the interdiffusion zone growth at the interface between the fuel and matrix. To predict the zone width during irradiation, extrapolated values of the out-of-reactor correlation based on diffusion-couple test data at 350-550°C to reactor operation temperature (~150°C) must be enhanced to account for irradiation effect. The irradiation enhancement factor varies due to the changes in fission density and in deposition of fission fragment damage in the zone. Using the TRIM code, enhancement factors as a function of zone width were assessed for U-Mo/Al and U3Si2/Al dispersion fuels. These factors were compared to measured irradiation data. In addition, diffusion enhancement for ion beam irradiation in U-Mo/Al was measured. Comparison to the analytically obtained results showed that the ion beam test results were in line with those of analytical results.

4:35 PM

Interdiffusion in Ilmenite Solid Solutions of (Ni,Co)TiO₃: *Srinivasa Reddy¹*; Lowell B. Wiggins¹; Brian Sundlof¹; ¹IBM Corporation

This paper reports the results of interdiffusion studies in (Ni_xCo_{1-x})TiO₃ solid solutions in the temperature range of 1473-1623K. In the ilmenite structure, the divalent (Ni,Co) cations and the tetravalent Ti occupy separate sub-lattice and the diffusion of ions in different sub-lattice are not strongly correlated with each other. At 1573 K, the interdiffusion co-efficient increases by more than an order of magnitude when the composition changes from NiTiO₃ to CoTiO₃. This indicates that the concentration of point defects responsible for diffusion increases with increasing Co in the solid solution. However, no data is available regarding the point defects or tracer diffusion of individual cations in these solid solutions and hence the applicability of Darken type relation is not known.

5:00 PM

Diffusional Analysis of a Multiphase Oxide Scale Formed on a Mo-Mo₂Si-Mo₅Sib₂ Alloy: *Voramon S. Dheeradhada¹*; David Johnson¹; Mysore A. Dayananda¹; ¹Purdue University

Diffusional analyses were performed to understand the oxidation at 1300°C of a multiphase Mo-13.2Si-13.2B (at%) alloy. During oxidation, a protective glass scale formed with an intermediate layer of (Mo+glass) between the base alloy and external glass scale. Compositional profiles across the (Mo+glass) layer and the external glass scale were determined, and interdiffusion fluxes and effective interdiffusion coefficients were calculated by using "MultiDiFlux©" software. Interdiffusion coefficients for the various component in the Mo and glass phases were estimated on the basis of Mishin's analysis. The motion of the (alloy/Mo+glass) and (Mo+glass/glass) interphase boundaries after passivation was examined.

Additionally, vapor-solid diffusion experiments at 1300°C were performed with multiphase Mo-10Si-10B(at.%) and single phase Mo₃Si or T2 specimens. These specimens were exposed to vacuum to induce silicon loss resulting in the formation of a Mo layer. An average effective interdiffusion coefficient of silicon in molybdenum at 1300°C was estimated at about 10⁻¹⁷ m²/s.

5:25 PM

Oxygen Diffusion through Aluminum-Containing Amorphous Silica: *Yiguang Wang¹*; Yi Fan²; Ligong Zhang²; Yong-Ho Sohn¹; Linan An¹; ¹University of Central Florida; ²Chinese Academy of Science

Oxygen diffusion through vitreous silica has attracted extensive attention in last decades due to its scientific interests and practical importance. The process is the rate-control step for the thermal growth of dielectric silica thin film on silicon, which enabled technology for modern microelectronics and optoelectronics. The same process also determines the degradation of silicon-based ceramics (e.g. SiC and Si₃N₄) when they are used in high-temperature oxidizing environments. Oxygen diffusion through amorphous silica doped with small amount of aluminum is investigated using SIMS to profile the diffusion of ¹⁸O tracer. We demonstrate that aluminum-doping can significantly inhibit both interstitial transportation and network diffusion of oxygen. The activation energy of oxygen network diffusion for aluminum-doped silica is two times higher than that for pure silica. Contrary to conventional understanding, these results suggest a small amount of aluminum-doping could decrease oxygen diffusion by strengthening the network structure of otherwise pure silica.

Phase Stability, Phase Transformation and Reactive Phase Formation in Electronic Materials V: 3D, Fine Pitch and High Temperature/Low Temperature Interconnects in Electronics Packages

Sponsored by: The Minerals, Metals and Materials Society, TMS Electronic, Magnetic, and Photonic Materials Division, TMS Structural Materials Division, TMS: Alloy Phases Committee

Program Organizers: Katsuaki Suganuma, Osaka University; Douglas J. Swenson, Michigan Technological; Srinivas Chada, Jabil Circuit, Inc.; Sinn Wen Chen, National Tsing-Hua University; Robert Kao, National Central University; Hyuck Mo Lee, Korea Advanced Institute of Science and Technology; Suzanne E. Mohney, Pennsylvania State University

Tuesday PM
March 14, 2006

Room: 213B
Location: Henry B. Gonzalez Convention Ctr.

Session Chairs: Hyuck Mo Lee, Korea Advanced Institute of Science and Technology; Jae-Ho Lee, Hong Ik University

2:00 PM Invited

Interconnection Process and Electrical Properties of the Interconnection Joints for 3D Stack Package with Cu Via: *Kwang-Yong Lee¹*; Hye-Jin Won¹; Teck-Su Oh¹; *Jae-Ho Lee¹*; Tae-Sung Oh¹; ¹Hong Ik University

Stack specimen with three dimensional interconnection structure through Cu via of 75µm diameter, 90µm height and 150µm pitch was successfully fabricated using subsequent processes of via hole formation with Deep RIE (reactive ion etching), Cu via filling with pulse-reverse electroplating, Si thinning with CMP, photolithography, metal film sputtering, Cu/Sn bump formation, and flip chip bonding. Contact resistance of Cu/Sn bump and Cu via resistance could be determined from the slope of the daisy chain resistance vs the number of bump joints of the flip chip specimen containing Cu via. When flip-chip bonded at 270°C for 2 minutes, the contact resistance of the Cu/Sn bump joints of 100X100µm size was 6.7 mΩ, and the Cu via resistance of 75µm diameter, 90µm height was 2.3 mΩ.

2:30 PM

Electro and Electroless Copper Plating on Flexible Substrate for CoF Applications: *Jae-Ho Lee¹*; Sung-Sup Byun¹; Jung-Eun Kang¹; ¹Hong Ik University

As electronic devices are getting smaller and lighter, the density of copper lines on flexible circuit board (FCB) is getting higher. Subtractive method is cost effective and most widely used method in copper line formation, however, as the line pitch is getting smaller, the lateral etching of copper cause serious problem. To replace the subtractive method, semi-additive method was used for fine pitch copper line. Lithography and copper electroplating are two key factors in this process. Polyimide film was used as flexible substrate and copper seed layer was deposited on polyimide film by magnetron sputtering method. For copper electroplating bath, low residual stress bath was used since flexibility of copper line is very important. The feasibility of electroless plating to replace sputtered copper seed layer was also investigated. The adhesion strength between polyimide and copper was improved by treating the polyimide surface with amines.

2:55 PM

Decapsulation Method for Flip Chip with Ceramics in Microelectronic Packaged Devices: T. I. Shih¹; *Jeng-Gong Duh*¹; ¹National Tsing Hua University

Decap of flip chip with ceramics in microelectronic devices is an arduous work especially accompanied by polishing techniques. Current processing for flip chip with ceramics is limited due to the ability of human and capability of equipment. After decap of flip chip package, the destructiveness of pad and clean level of samples are primary concerns that should be focused for any possible improvement. This study is aimed to provide an alternative methodology to decap the flip chip package of semiconductor microelectronic device by manual method and chemical reaction of selective acids. A novel processing approach is developed to well prepare the flip chip sample consistently and accurately. It can be demonstrated that this way of process suffices to increase sample through put and also to improve surface finishes with reduced consumables and preparation time.

3:20 PM

Deposition of Conductive Films on Electronic Substrates by Using Gold Nanopowders: *Tzu-Hsuan Kao*¹; Jenn-Ming Song²; In-Gann Chen¹; ¹National Cheng Kung University; ²National Dong Hwa University

Since nano-sized metals exhibit a dramatically low melting point compared to bulk materials, nano-metallic particle fluid suspensions (NPFS) can be deposited and cured to obtain electric conductors at a relative low processing temperature. This implies that fabrication of micro-interconnects without using the conventional lithography-etching process is possible. In this study, gold particles with an average size of 5nm were selected to prepare NPFS. Utilizing spin coating and ink-jet printing, the NPFS was deposited onto several commonly used electronic substrates, Cu, Ni and Al. After a proper curing treatment, the degree of continuity and adhesion strength of the coated film on the Ni substrate was better than that on the Cu substrate, which is in turn better than Al substrate. Electrical resistivity of the gold film thus produced and the interfacial reactions between the films and the substrates were also examined. Finally, the optimal processing parameters were recommended.

3:45 PM

Study of Au-Si Wafer Bonding Technology for GaN/Si Wafer Bonding: *Hsiang-En Chiu*¹; Cheng-Yi Liu¹; ¹National Central University

A void-free and thermally stable wafer bonding is required for the fabrication of the state-of-the-art thin-GaN LED device. To meet this criteria, Au-Si bonding is one of good techniques to bond GaN wafer with Si wafer. However, it has been reported that a lot of voids formed at the interface between Au bonding layer and Si(111) surface due to the serious inter-diffusion between Si and Au. In this study, the GaN/Ti/Ni/Au wafers were bonded with Si substrates. By adjusting the process temperatures, bonding time, and thickness of Au bonding layer, a void-free Au-Si eutectic layer can be achieved. In this talk, we will also compare Au-Si bonding interface microstructure by using different Si substrates, such as, n-type and p-type high-doping (111) Si. The detail Au-Si reaction analysis will be given.

4:10 PM Break

4:20 PM

Development of Bi-Based High Temperature Pb-Free Solders with Second Phase Dispersion: Microstructure, Interfacial Reaction and Thermal Fatigue: *Yoshikazu Takaku*¹; Ikuro Ohnuma¹; Ryosuke Kainuma¹; Yasushi Yamada²; Yuji Yagi²; Yuji Nishibe²; Kiyohito Ishida¹; ¹Tohoku University; ²Toyota Central R&D Laboratory, Inc.

Bi based alloys are candidates of high temperature Pb-free solder which can be substituted for conventional Pb-rich Sn-Pb solders. However, inferior properties such as brittleness should be improved for practical use. In this study, the microstructure of Bi-based alloys was designed by thermodynamic database, ADAMIS (Alloy Database for Micro-Solders), and their applicability for high temperature solder was investigated. Bi-based alloys were prepared by a rapid quenching method. The microstructure was controlled through liquid-phase separation to exhibit an in-situ composite of fine dispersed particles in the Bi-based matrix. Other composite samples which consist of Cu-based alloy powder in the Bi-based matrix were also fabricated. Semiconductor chips and substrates were soldered with the Bi-based composite alloys. After the soldering, the interfacial reaction was examined by SEM. Thermal cycles between -40°C and 195°C were subjected to soldered samples. The effect of the second phase dispersion on thermal fatigue properties was investigated.

4:45 PM

Thermal and Humidity Stability of Zn-xSn and Zn-30In Alloys as High Temperature Lead-Free Solder: *Jae-Ean Lee*¹; Keun-Soo Kim¹; Katsuaki Suga¹; ¹Osaka University

The potential of the newly designed Zn-xSn(x=20, 30 and 40mass%) and Zn-30 mass%In alloys as a high temperature lead-free solder have been evaluated, especially focusing on the thermal and humidity stability. The hypereutectic solders showed two endothermic peaks in DSC, these peaks are well associated with the eutectic and liquidus temperature, and little undercooling was observed on cooling. In the Zn-Sn alloys, primary α -Zn grains were surrounded with β -Sn/ α -Zn eutectic phase, in which fine Zn platelets disperse in a β -Sn/ α -Zn matrix. The Zn-30In alloy did not find out Zn platelets in a porous β -In/ α -Zn matrix. From the tensile test of alloys, UTS and 0.2% proof stress were not much difference but the elongation was slightly decreased as increasing Zn contents in the Zn-Sn alloys, showing ductile fracture mode. The Zn-30In alloy show lower tensile properties and seriously degraded as time goes under thermal and humidity conditions.

5:10 PM

Interfacial Reactions in the Joint of 80Au-20Sn/58Bi-42Sn Combination Solder: Chang Joon Yang¹; Moon Gi Cho¹; *Hyuck Mo Lee*¹; ¹KAIST

The 80Au-20Sn/58Bi-42Sn combination solder is proposed for multi-chip module packaging. The bonding process between the 80Au-20Sn solder bump and the 58Bi-42Sn solder has been conducted at 200°C for 2 min. The intermetallic phases of (Au,Ni)₃Sn₂, Ni₃Sn₄ and AuSn₄ were observed to form at the interface between solder and Ni UBM, and the AuSn₂ phase together with a thin inner layer of AuSn was observed at the combination interface. The interfacial reactions were explained through thermodynamic considerations. The ball shear and lap shear tests after multiple reflows have also been performed and their behavior will be explained.

5:35 PM

Comparison of Sn-2.8Ag-20In and Sn-10Bi-10In Solders for Intermediate Step Soldering: *Sun-Kyoung Seo*¹; Hyuck Mo Lee¹; ¹KAIST

Sn-2.8Ag-20In and Sn-10Bi-10In (in wt.%) have been chosen as Pb-free solder materials for intermediate step soldering. Reactions between two solders and under bump metallurgy (UBM) Au/Ni (Au: 1.5 μ m, Ni: 3 μ m) were investigated at 210, 220, 230 and 240°C for up to 4 min. All of the Au UBM was dissolved into the solder matrix as soon as the reaction started and resulted in formation of Au(In,Sn)₂ in the case of SnAgIn and Au(In,Sn)₂ as well as Au(In,Sn)₄ in SnBiIn. The exposed Ni layer reacted with the solder and formed Ni₃(In,Sn)₄ in both solders. The formation mechanism of intermetallic phases was thermodynamically explained. The growth rate of the interfacial Ni₃(In,Sn)₄ phase in SnBiIn was faster than that in SnAgIn. In the shear strength test, the shear strength values of both solders were similar.

TUESDAY PM

Phase Transformations in Magnetic Materials: Magnetic Shape Memory Alloys

Sponsored by: The Minerals, Metals and Materials Society, TMS Materials Processing and Manufacturing Division, TMS/ASM: Phase Transformations Committee

Program Organizers: Raju V. Ramanujan, Nanyang Technological University; William T. Reynolds, Virginia Tech; Matthew A. Willard, Naval Research Laboratory; David E. Laughlin, Carnegie Mellon University

Tuesday PM Room: 213A
March 14, 2006 Location: Henry B. Gonzalez Convention Ctr.

Session Chairs: Michael McHenry, Carnegie Mellon University; Gernot Kostorz, ETH Zurich

2:00 PM Invited

Magnetic and Martensitic Transformation of Ni-(Co,Fe)-(Al,Ga) β Alloys: *Katsunari Oikawa*¹; Ryosuke Kainuma¹; Kiyohito Ishida¹; ¹Tohoku University

Magnetic and martensitic phase transformation of the Ni-Co-Al, Ni-Fe-Al, Ni-Co-Ga and Ni-Fe-Ga systems were systematically investigated. The composition region of the β phase showing the shape memory effect in the ferromagnetic state of these systems was clarified. The spontaneous magnetization of these ferromagnetic shape memory alloy systems showed linear dependence with the magnetic valence introduced in the generalized Slater-Pauling curve. The β phase transformed from B2 to 2M structures in the Ni-Co-Al, Ni-Fe-Al and Ni-Co-Ga systems, and from L₂ to 10M or 14M structures in Ni-Fe-Ga systems. In addition, the plastic workability of these alloy systems could be improved by the introduction of a small amount of the ductile γ (fcc structure) phase with control of the chemical composition and annealing temperature because the composition region of the ferromagnetic shape memory alloys in these systems appears near the $\beta+\gamma$ two-phase region. This characteristic is one of advantage for practical application.

2:35 PM

Martensite Transformation in Ni-Mn-Ga Ferromagnetic Shape-Memory Alloys: *Marc L. Richard*¹; Jorge C. Feuchtwanger¹; Patricia Lázpita²; Samuel M. Allen¹; Robert C. O'Handley¹; Manu Barandiarán²; ¹Massachusetts Institute of Technology; ²Universidad del País Vasco/EHU

The crystal structure of Ni-Mn-Ga ferromagnetic shape-memory alloys is extremely sensitive to composition. Several martensitic structures including tetragonal (5-layered), orthorhombic (7-layered) and non-modulated tetragonal have been observed. A systematic exploration of the composition-structure relationship has been performed using x-ray diffraction on several single crystals with different compositions. Temperature-dependent magnetic measurements have revealed markedly different transformation behavior in the tetragonal and orthorhombic materials. The orthorhombic material shows a much larger difference between the martensite start and finish temperatures as compared to tetragonal martensite. The martensitic transformation processes have been observed with in-situ TEM and the defect structure present in each phase has been explored. Single-crystal and powder neutron diffraction have been employed to study the chemical ordering in the austenite and martensite phases. The difference in transformation character can be explained with a thermodynamic model by including the difference in the strain energy contribution for the two different martensite phases.

3:00 PM Invited

Influence of Composition and Microstructure on the Magnetic Properties of Ni-Fe-Ga Ferromagnetic Shape Memory Alloys: *Todd M. Heil*¹; Matthew A. Willard²; William T. Reynolds¹; ¹Virginia Tech; ²Naval Research Laboratory

The martensite and magnetic transformations in Ni-Fe-Ga ferromagnetic shape memory alloys are very sensitive to alloy chemistry and thermal history. A series of Ni-Fe-Ga alloys near the prototype Heusler composition (X₂YZ) were prepared, and a Ni₅₃Fe₁₀Ga₂₈ alloy was subsequently annealed at various temperatures below and above the B2/L₂ ordering

temperature. Calorimetry and magnetometry were employed to measure the martensite transformation temperatures and Curie temperature. Compositional variations of only a few atomic percent result in martensite start temperatures and Curie temperatures that differ by about 230 K degrees and 35 K degrees, respectively. Various one-hour anneals of the Ni₅₃Fe₁₀Ga₂₈ alloy shift the martensite start temperature and the Curie temperature by almost 70 K degrees. Transmission electron microscopy investigations were conducted on the annealed Ni₅₃Fe₁₀Ga₂₈ alloy. The considerable variations in the martensite and magnetic transformations in these alloys are discussed in terms of microstructural differences resulting from alloy chemistry and heat treatments.

3:35 PM Invited

Analysis of Magnetoelastic Composites: *Perry H. Leo*¹; ¹University of Minnesota

We consider the properties of high volume fraction magnetoelastic composites. Our analysis depends on new results related to Eshelby's inclusion problem. Specifically we prove the existence of special inclusions that induce uniform magnetic fields when they are uniformly magnetized under periodic boundary conditions. Similar properties hold for linear elasticity. These inclusions are in some sense the high volume fraction equivalent to isolated ellipsoidal inclusions under uniform magnetic field (or, in the elastic case, eigenstrain). By using these special inclusions we are able to estimate the properties of high volume fraction composites. We discuss the implications of our results to the Eshelby conjecture and to the construction of energy minimizing microstructures. This work is joint with R. D. James and Liping Liu.

4:10 PM Break

4:25 PM Invited

Martensitic and Magnetic Transformations of the Ni-Mn-Based Ferromagnetic Shape Memory Alloys: *Ryosuke Kainuma*¹; Yuji Sutou¹; Katsunari Oikawa¹; Kiyohito Ishida¹; ¹Tohoku University

Ferromagnetic shape memory alloys (FSMAs) such as Ni₂MnGa and NiCoAl have attracted considerable attention as a new type of magnetic actuator materials. Recently, the present authors have reported some Ni-Mn based FSMAs in NiMnX (X: In, Sn and Sb) systems¹. In the present paper, characteristic features on the martensitic and magnetic transformations of these NiMn-based FSMAs will be reported. ¹Sutou et al., Appl. Phys. Lett., 85(2004)4358.

5:00 PM Invited

Martensitic Transformations and Magnetic Shape Memory in Heusler Alloys: Gernot Kostorz¹; Myriam Aguirre¹; Debashis Mukherji¹; *Peter Mullner*²; ¹ETH Zurich, Applied Physics; ²Boise State University, Materials Science and Engineering

In L21-type ordered body-centered cubic alloys (Heusler alloys), martensitic transformations lead to various low-symmetry, non-modulated (tetragonal) or long-periodic modulated (10M and 14M) structures. Twinning rather than dislocation motion provides the lattice-invariant shear in most cases. Alloys around the stoichiometric composition Ni₂MnGa have recently attracted major interest because of their ferromagnetic order. Ferromagnetism in the martensitic phase provides a magnetically-induced mechanism for shape change (also called magnetic shape memory), if the crystal anisotropy leads to a sufficient driving force to move twin boundaries. Details of the size and reproducibility of shape changes under the influence of magnetic fields depend very sensitively on the microstructure. Polysynthetically twinned single crystals and polycrystals have been investigated, with a maximum strain of 10% for the 14M structure. Results on magnetomechanical properties will be presented and related to microstructural features obtained from electron diffraction and conventional as well as high-resolution electron microscopy.

5:35 PM

Phase Field Modeling and Simulation of Microstructure Evolution in Ferromagnetic Shape Memory Alloys: *Yongmei M. Jin*¹; ¹Texas A&M University

The unusually large magnetomechanical responses of ferromagnetic shape memory alloys are correlated with the coupled magneto-elastic domain evolutions in these multiferroic materials. The ferromagnetic and ferroelastic domain structures actively respond to the change in external

magnetic field, applied stress, and temperature. The kinetic pathways of domain evolutions play the key role in determining the materials properties. Even the basic mechanism of magnetic-field-induced shape memory effect is understood, little quantitative details of the processes are known. Phase Field model could be a valuable tool to understand these processes. It takes into account the strain and magnetic coupling of the structural and magnetic domains and their interactions with external magnetic field and applied stress. This method can be employed to investigate the quantitative details of magnetic and strain responses to the applied fields and to determine the main factors affecting the ferromagnetic shape memory effect. Ongoing computational effort will be discussed.

Point Defects in Materials: Other Diffusion

Sponsored by: The Minerals, Metals and Materials Society, TMS Electronic, Magnetic, and Photonic Materials Division, TMS Structural Materials Division, TMS: Chemistry and Physics of Materials Committee

Program Organizers: Dallas R. Trinkle, U.S. Air Force; Yuri Mishin, George Mason University; David N. Seidman, Northwestern University; David J. Srolovitz, Princeton University

Tuesday PM Room: 210B
 March 14, 2006 Location: Henry B. Gonzalez Convention Ctr.

Session Chair: Irina V. Belova, University of Newcastle

2:00 PM Invited

Diffusion and Viscous Flow in Bulk Glass Forming Alloys: *Franz Faupel*¹; Volker Zoellmer¹; Alexander Bartsch¹; Klaus Raetzke¹; ¹Kiel University

We review radiotracer diffusion and isotope measurements in bulk glass forming alloys from the glassy state to the equilibrium melt and compare diffusion and viscous flow. In the glassy as well as in the deeply supercooled state below the critical temperature T_c , where the mode coupling theory predicts a freezing-in of liquid-like motion, very small isotope effects indicate a highly collective hopping mechanism. Even in the supercooled state below T_c the temperature dependence is Arrhenius-type with an effective activation enthalpy, and diffusion is clearly decoupled from viscosity. Above T_c the onset of liquid-like motion is evidenced by a gradual drop of the effective activation energy and by the validity of the Stokes-Einstein equation. This strongly supports the mode coupling scenario. The isotope effect measurements show atomic transport up to the equilibrium melt to be far away from the regime of uncorrelated binary collisions.

2:30 PM

Kinetic Monte Carlo Simulation of Cesium Migration in UO₂: *Thomas A. Patten*¹; Chaitanya S. Deo²; Blas P. Uberuaga²; S. G. Srivilliputhur²; James F. Stubbins¹; Stuart A. Maloy²; ¹University of Illinois; ²Los Alamos National Laboratory

The migration of Cs in uranium dioxide, and its consequent segregation, is important to understand the operational containment of fission products. We have developed a kinetic Monte Carlo (kMC) model to study the long time evolution of Cs migration and defect clustering. In this model, the fission product Cs migrates on the Uranium sub-lattice with assistance of vacancy type defects. Atomistic models based on the Buckingham potential are used to obtain the catalog of Cs mechanisms, the energy barriers to their diffusion, as well as other point defect migration and cluster binding energies, in stoichiometric and non-stoichiometric UO₂. Using our kMC model, we calculate the self-diffusion coefficient for point defects and the survival rate of defect clusters. The Cs self-diffusion coefficient is predicted for various system temperatures.

2:50 PM Invited

Defects and Self-Diffusion Mechanisms on SiO₂: An Ab-Initio Study: *Yves Limoge*¹; Guido Roma¹; ¹Commissariat à l'Energie Atomique

Either as a pure material or as the main component of oxides alloys, SiO₂ plays an increasing role in various properties demanding technological fields. Here the atomic scale understanding of material properties becomes more and more the required level. In this work we will present the

results of a study of defect formation and migration energies in crystalline and amorphous SiO₂, using ab-initio methods in the framework of Density Functional Theory. We review the difficulties in predicting the absolute equilibrium concentration and charges of each type of defect (Si/O vacancies and interstitials) in real materials as a consequence of impurity concentrations. We discuss also the main self-diffusion mechanisms that, from our calculations, turn out to be dominant in specific conditions.

3:20 PM

Microscopic versus Macroscopic Activation Barriers for Diffusion in Solid Solutions: *Ramanathan Krishnamurthy*¹; Mikhail Mendeleev²; David J. Srolovitz¹; Roberto Car¹; ¹Princeton University; ²Ames Laboratory

Diffusion in solid solutions is rich with varied physical effects, occurring on disparate length/time scales. At a microscopic level, individual atom/vacancy exchanges depend intimately on the local environment surrounding the exchanging pair. An accurate calculation of the activation energy for this exchange requires the use of density functional theory methods (or molecular statics where reliable potentials are available). The relevant length/time scale is nm/ps. Several atom-vacancy exchanges with differing microscopic energy barriers combine to give macroscopic diffusion, the activation energy for which is generally different from any of the exchange energies. Depending on the type of solid solution under investigation, the simulation size/time required to accurately predict long-time diffusivities is 10-1000 nm / 100 - 10⁶ ns or even more. Kinetic Monte Carlo methods, with only the microscopic rates as input are eminently suited to address these time/length scale requirements. Here, we present two technologically important examples, oxygen diffusion in yttria stabilized zirconia and Fe impurity diffusion in Al where such a combination of simulation techniques has been employed to successfully predict modeling complex diffusion phenomena. Interesting physical effects that occur as the disparate time/length scales are bridged and their relevance in explaining experimental observations will be discussed.

3:40 PM Break

3:55 PM Invited

Using Molecular Dynamics Techniques for Simulations of Grain Boundary Diffusion and Mobility: *Diana Farkas*¹; ¹Virginia Tech

In this talk we will discuss the use of large scale molecular dynamics techniques to study the mechanisms of diffusional transport along grain boundaries as well as grain boundary migration. Results are presented of molecular dynamics simulations of the diffusion process in ordered B2 NiAl at high temperature using an embedded atom interatomic potential. In this material, diffusion occurs through a variety of cyclic mechanisms that accomplish the motion of the vacancy through nearest neighbor jumps restoring order to the alloy at the end of the cycle. MD allows the study of the detailed time evolution of the jump sequence in these cyclic mechanisms, both in the bulk and along the grain boundary. A similar technique is used to study the process of grain boundary motion in a pure Ni digital sample containing initially 15 grains.

4:25 PM

Vacancy Formation and Migration Energies in Nonequilibrium Grain Boundaries: *Airat A. Nazarov*¹; Ramil T. Murzaev²; ¹Ufa State Aviation Technical University; ²Russian Academy of Sciences

Grain boundaries (GBs) in plastically deformed metals have a nonequilibrium structure characterized by the presence of extrinsic dislocations and disclinations. Such GBs are important elements of the structure of nanocrystals prepared by severe plastic deformation. In order to understand underlying mechanisms of diffusion along nonequilibrium GBs, vacancy formation and migration energies in these GBs are calculated by atomistic simulations based on the embedded atom method. Two types of nonequilibrium GBs containing (a) extrinsic grain boundary dislocations (EGBDs) and (b) wedge disclinations are studied. GBs subjected to uniform tensile stress are also considered. The uniform tensile stress and long-range stresses of extrinsic dislocations are shown not to influence significantly the characteristics of vacancies. Up to about 0.2 eV change of both the vacancy formation and migration energies is caused by disclinations on a large distance from the disclination core. Implications of the results to the diffusion in nanocrystals are discussed.

TUESDAY PM

4:45 PM Invited

Segregation, Pre-Melting, and Melting Phenomena in the Cu-Bi System Studied by Radiotracer Grain Boundary Diffusion: *Sergiy V. Divinski*¹; Christian Herzig¹; Maik Lohmann¹; Boris Straumal²; ¹University of Muenster; ²Institute of Solid State Physics

Copper embrittlement by Bi is a typical example of a severe detrimental phenomenon in materials science. Strong segregation of Bi can induce significant changes in grain boundary structure and even cause a liquid-like film at the grain boundaries. The recent results on grain boundary diffusion of Cu-64 and Bi-207 in Cu-Bi alloys are presented. The measurements are performed in the single-phase (solid solution) as well as in the two-phase (solid + liquid) regions of the equilibrium phase diagram. Above certain temperature, the grain boundary diffusivities of both Cu and Bi in the two-phase region are by orders of magnitude higher than those in pure Cu. An abrupt increase of the diffusivities was observed at certain Bi contents which are unequivocally in the single-phase region. The present results convincingly showed the occurrence of the premelting phase transition in GBs of the Cu-Bi system.

Polymer Nanocomposites: Session II

Sponsored by: The Minerals, Metals and Materials Society

Program Organizer: Devesh K. Misra, University of Louisiana at Lafayette

Tuesday PM

Room: 217A

March 14, 2006

Location: Henry B. Gonzalez Convention Ctr.

Session Chairs: Jyoti Prakash Jog, National Chemical Laboratory; Quan Yuan, University of Illinois

2:00 PM Invited

Polymer Nanocomposites: Crystallization and Polymorphism Studies: *Jyoti Prakash Jog*¹; ¹National Chemical Laboratory

Polymer nanocomposites is an emerging area of research and is of particular interest to scientists because of the molecular level interaction of the fillers with polymer chains. The nanocomposites may be comprised of nanoparticles, nanotubes or nanoclays. The dimensions of the second phase are close to the chain dimensions, and a number of studies are aimed to elucidate the effect of nano size filler on the crystallization of polymers. An attempt is made to address the few aspects of crystallization in polymer nanocomposites. We will be discussing the effect of the second phase in nano- dimension on the various aspects of crystallization such as isothermal crystallization, non-isothermal crystallization, spherulitic growth, phase transformation, polymorphism etc. The polymers, which are studied, include Polybutene and Polyvinylidene fluoride. The effect of type of filler and its concentration is investigated through isothermal crystallization, optical microscopy and X-ray diffraction.

2:30 PM Invited

Structural and Mechanical Characterization of Polymer Nanocomposites: *Xiaodong Li*¹; ¹University of South Carolina

The extremely small dimensions of nanoscale reinforcements in polymer nanocomposites such as carbon nanotubes, nanoclays, and nanoparticles impose a great challenge for many existing characterization techniques and instruments. To understand and establish the reinforcing mechanisms for polymer nanocomposites, the morphology, dispersion and orientation of the reinforcements as well as the bonding between the reinforcements and matrix need to be well characterized. The nanoscale structure of single-walled carbon nanotube-reinforced epoxy composites, nanoclay-reinforced agarose composites, bamboo-like polymer/silicon nanocomposites, and natural seashell nanocomposites such as the shells of red abalone and pectinidae was studied by atomic force microscopy (AFM), scanning electron microscopy (SEM), and transmission electron microscopy (TEM). Their mechanical properties were measured by nanoindentation, nanoscratch, and tensile and bending tests. The reinforcing mechanisms are discussed in conjunction with their structure and mechanical properties such as hardness and elastic modulus. The strength-

ening and toughening mechanisms of natural nanocomposites are also presented.

3:00 PM

Photocatalytic and Antimicrobial Active Polymer Nanocomposites Membrane for Water Purification: *Subhasis Rana*¹; Jagdish Rawat¹; Melinda Sorensson¹; Devesh K. Misra¹; ¹University of Louisiana at Lafayette

Titania-coated nickel ferrite nanoparticles have been successfully dispersed in a porous polymer membrane with consequent formation of a hybrid polymer nanocomposite structure. This porous polymeric membrane acts as a filter for water purification characterized by photocatalytic and antimicrobial activity. Titania contributes to antimicrobial activity, while nickel ferrite facilitates removal of the membrane with the help of small magnetic field. The performance of the hybrid structure and the factors that influence its performance are discussed.

3:25 PM

Micromechanism of Stress Whitening during Tensile Deformation in Polymer Nanocomposites: *Raghunath R. Thridandapani*¹; Harish Nathani¹; Jyoti Prakash Jog²; Devesh K. Misra¹; ¹University of Louisiana at Lafayette; ²National Chemical Laboratory

The micromechanism and susceptibility to stress whitening during tensile deformation of polymer nanocomposites is studied by electron microscopy and compared with the unreinforced neat polymer. Mineral-reinforced composites exhibit significantly reduced susceptibility to stress whitening, and are characterized by lower gray level in the plastically deformed stress whitened zone. This behavior is attributed to the effective reinforcement of polymer by the mineral and the nucleating effect. Additionally, reinforcement of polymer alters the primary micromechanism of stress whitening.

3:50 PM

Processing and Property Optimization of Polycarbonate Matrix-Carbon Nanotube Reinforced Composites: *Jerimiah E. Robbins*¹; ¹New Mexico Institute of Mining and Technology

We investigate multi-walled carbon nanotubes as reinforcement in polycarbonate matrix composites. Experimental data show relevant processing-property relationships via glass transition measurements, tensile testing, TEM imaging and SEM fractography. Addressed are processing issues such as dispersion, interfacial adhesion, and forming operations. Based on statistical data from designed experiments, we will discuss optimum processing parameters of the polymer nanocomposites.

4:15 PM Break

4:25 PM

The Relaxation Behavior of Polymer Nanocomposites: A Study of Dynamic Mechanical Analysis: *Qiang Yuan*¹; S. Awate¹; Devesh K. Misra¹; ¹University of Louisiana at Lafayette

The effects of nanoparticles on the relaxation behavior of polymer matrix are studied with dynamic mechanical analysis (DMA). In order to elucidate the mechanism of the effect of nanoparticles on the mechanical properties of polymer nanocomposites, the results of DMA combined with micromorphology of SEM and TEM are presented.

4:50 PM

Thermal and Mechanical Properties of PMMA/SiO₂ Nanocomposites with Controlled Particle/Matrix Interfaces: *Sarah L. Lewis*¹; Chunzhao Li¹; Robert G. Shimmin²; Brian C. Benicewicz¹; Paul V. Braun²; Linda S. Schadler¹; ¹Rensselaer Polytechnic Institute; ²University of Illinois at Urbana-Champaign

In polymer/nanoparticle composites particle size and surface chemistry control the mechanical and thermal properties. Previous work has suggested that the addition of small particles can change the glass transition temperature and the addition of larger particles alters the ductility of the final composite. The "strength" of the interface controls the direction of change of the properties relative to the neat PMMA. To test these hypotheses and hence to better understand the physics of polymer chains adjacent to nanoparticle surfaces, SiO₂/PMMA composites have been made using monodisperse particles of two sizes, 15 and 150 nm. Different nanoparticle surface treatments to provide different "strengths" of particle/matrix interface were used. Preliminary results show that composites

made with smaller particles with a weak interface (fluorinated) have a lower T_g than the neat polymer whilst those made with larger particles with the same surface chemistry show no change in T_g but do increase the ductility.

5:15 PM

On the Impact Strength of Clay Reinforced Polymer Nanocomposites:

Mahesh Tanniru¹; Raghunath Rao Thridandapani¹; Samrat Awate¹; Q. Yuan¹; Devesh K. Misra¹; ¹University of Louisiana at Lafayette

The micromechanism of plastic deformation during impact loading of polymer nanocomposites is investigated through electron microscopy and atomic force microscopy and the behavior compared with the un-reinforced polymer under identical conditions of processing. The impact strength of composites is linked to structural studies by X-ray diffraction and atomic force microscopy observations. The adoption of clay in polymers has two primary effects: the reinforcement and the nucleating effect. The reinforcement effect generally increases the bulk crystallinity and modulus, while the nucleating effect decreases the spherulite size. The extent to which impact strength is retained on reinforcement depends on the polymer matrix.

Recycling - General Sessions: Electronics Recycling

Sponsored by: The Minerals, Metals and Materials Society, TMS Extraction and Processing Division, TMS Light Metals Division, TMS: Recycling Committee

Program Organizers: Gregory K. Krumdick, Argonne National Laboratory; Cynthia K. Belt, Aleris Intl

Tuesday PM Room: 8B
 March 14, 2006 Location: Henry B. Gonzalez Convention Ctr.

Session Chair: Gregory K. Krumdick, Argonne National Laboratory

2:30 PM Introductory Comments

2:35 PM

Metallurgical Recycling of Electronic Scrap: Birgit Matl¹; Helmut Antrekowitsch¹; Christine Wenzl¹; Franz Prior²; Walter Spruzina²; ¹University of Leoben; ²Centre of Excellence for Electronic Scrap Recycling and Sustainable Development

Nowadays, the pyrometallurgical treatment in copper smelters is the common process for the recycling of metals from the electronic scrap. The European Directive on the Waste from Electrical and Electronic Equipment (WEEE) and the Directive on the Restriction of Hazardous Substances (RoHS), increase the importance of electronic scrap recycling. A high amount of plastic and inert materials in these materials leads to problems at the processing. An optimisation concerning the internal recovery and the high amount of plastic is necessary to reach the recycling quota of the European directive. The majority of scrap is treated mechanically in order to separate plastics from metals. The quality of the different fraction often rather low and further treatment leads to higher costs. The Christian Doppler Laboratory for Secondary Metallurgy of Nonferrous Metals and the Institute of Nonferrous Metallurgy at the University of Leoben carried out investigations concerning the optimisation of the metallurgical recycling.

3:00 PM

Examining the Eco-Efficiency of Recycling Alternatives: A Case Study on End-of-Life Cathode Ray Tubes: Jeremy Gregory¹; Jennifer Atlee¹; Jaco Huisman²; Ab Stevels²; Randolph E. Kirchain¹; ¹Massachusetts Institute of Technology; ²Delft University of Technology

The disposal of end-of-life electronics is an issue receiving increasing scrutiny. This paper evaluates several alternatives for recycling cathode ray tubes (CRTs) within monitors and televisions with particular emphasis on their leaded glass. The primary recycling options for the glass, reuse in new CRTs or as a smelter flux, are examined from economic and environmental standpoints. The economics are modeled using a process-based cost model (PBCM) and include dependencies on processing technolo-

gies, transportation logistics, and incoming material composition. The environmental consequences are modeled using several methods including QWERTY, a framework that has been developed specifically to examine the recyclability of electronic products. Results are presented mapping out preferred processing alternatives across a range of technological and operational conditions using several evaluation methods. The modeling framework and results provide insights useful to stakeholders such as original equipment manufacturers, recyclers, and policy-makers.

3:25 PM

Filtration of Solar Cell Silicon Scrap: Anne Kvithyld¹; Dilip Chithambaranadhan¹; Arjan Ciftja¹; Eivind Johannes Øvrelid²; Thorvald Abel Engh¹; ¹Norwegian University of Science and Technology; ²SINTEF

Silicon solar cells are attractive sources of energy. Recycling scrap from top and sides of ingots of multi crystalline silicon is addressed. SiC and Si₃N₄ inclusions are a major problem. Scrap from Scan Wafer ASA is melted in a high vacuum furnace at around 1500°C. The filters, from commercial producers, are C and SiC with 10, 20 and 30 ppi. Characterisation of inclusions before and after filtration, and in the filter itself, is performed by microscopy. Dissolution of silicon in acid and counting of the un-dissolved inclusions is also carried out. In the filter Si₃N₄ needles and SiC inclusions were identified. The amount of these inclusions in the filtered silicon is much less than in the input. In conclusion, filtration using SiC and C filters in vacuum system in argon atmosphere removes SiC and Si₃N₄ inclusions from solar cell scrap. Flow of metal through the filters is not a problem.

3:50 PM

Leaching of Copper from Waste Printed Circuit Boards Using Electro-Generated Chlorine in Hydrochloric Acid Solution: Eun-Young Kim¹; Min-Seuk Kim²; Jae-Chun Lee²; Jin-Ki Jeong²; Byung-Su Kim²; ¹University of Science and Technology; ²Korea Institute of Geoscience and Mineral Resources

Electro-generated chlorine leaching of waste printed circuit boards was investigated in hydrochloric acid solutions. The pulverized printed circuit board contained about 45% of metal component, in which copper was about 84%. The current efficiency of chlorine generation was calculated by measuring the volume and composition of the generated gas. The leaching rate of copper was greatly affected by current density and agitation speed. The Leaching of copper up to 98% was achieved at 20 mA/cm², 50°C, 180 minutes, and 600 rpm in 1M HCl solution. Increasing agitation and lowering current density enhanced utilization efficiency of electro-generated chlorine. Leaching of copper was suppressed at the initial stage, while the minor metal elements, such as aluminum, lead, and tin, were dominantly leached out.

4:15 PM Break

4:30 PM

Recovery of Tellurium from Retired Cadmium Telluride Photovoltaic Modules and Other Sources: Wenming Wang¹; Vasilis M. Fthenakis¹; ¹Brookhaven National Laboratory

Recycling of retired cadmium telluride (CdTe) photovoltaic (PV) modules has attracted attention due to new European environmental regulations. Recycling tellurium from CdTe PV modules makes economical sense because of the low availability of this metal. We investigated several possible treatment paths for reclaiming tellurium from leaching solution generated from processing CdTe PV modules. Our experiments showed that conventional neutralization/hydrolysis methods recovered only 50–60% of tellurium. However, by appropriately combining neutralization and sulfide precipitation, all the tellurium present in the leaching solution was precipitated and recovered, and the concentration of tellurium in the processed solution was reduced from 900–1000 mg/L to less than 5 mg/L, yielding a tellurium recovery of more than 99%. This method can be incorporated in the scheme of recycling spent CdTe PV modules and manufacturing wastes. It may be also an alternative to the current operations for removing tellurium from copper slimes leaching solutions.

TUESDAY PM

4:55 PM

Recovery of Metals from Spent Batteries: Masao Miyake¹; Masafumi Maeda¹; ¹University of Tokyo

A recovery process of metals from spent nickel-metal hydride batteries was investigated. The batteries contain nickel hydroxide as positive electrode and hydrogen storage alloy comprising rare earth metals, nickel, cobalt, manganese, and aluminum as negative electrode. A leaching treatment with an ammoniacal solution was developed to remove the hydroxide and recover the alloy from their mixture. By the leaching treatment, only the hydroxide was dissolved in the solution and the alloy could be recovered without decomposition.

5:20 PM

A Clean-Lead Factory for Lead Batteries Recycling is Available by Means of the "Cleanlead" Process: Carlos Frias¹; Nuria Ocaña¹; Gustavo Diaz¹; Tony Piper²; Brunon Bulkowski³; Andrzej Chmielarczyk⁴; Peter A. Claisse⁵; Steve Hemmings⁶; Luisa M. Abrantes⁷; Herman J. Jansen⁸; Joost van Erkel⁹; Ton Franken¹⁰; Zdenek Kunicky¹¹; Teodor Velea¹²; ¹Tecnicas Reunidas S.A.; ²Britannia Refined Metals Limited; ³Orzel Bialy, S.A.; ⁴Institute of Non-Ferrous Metals; ⁵Coventry University; ⁶Lafarge Plasterboard Ltd; ⁷Universidade de Lisboa; ⁸Magneto Special Anodes B.V.; ⁹TNO - MEP; ¹⁰Membraan Applicatie Centrum Twente; ¹¹Kovohute Pribram a.s.; ¹²Institute for Non-Ferrous and Rare Metals

The lead-battery recycling is a major industrial activity (more than four million tonnes recycled lead per year) that generates large amounts of toxic wastes such as lead slag, mattes and acidic sludge, besides airborne emissions. This is a waste-producer industry that needs a definitive solution to avoid its negative environmental impact and getting a sustainable lead production. That is the principal aim of the CLEANLEAD technology, which properly combines both hydrometallurgical and pyrometallurgical routes aiming to get zero-waste production, reducing the use of energy and resources in all phases of battery reprocessing, and consequently greatly decreases the operating cost. There will be no toxic emissions to land, water or air, and obtained products are pure lead or pure lead oxide, and commercial gypsum instead of waste sludge. Obtained results and achievements at pilot plant level are very satisfactory, opening the way to further developments and potential applications.

5:45 PM

Cost Analysis of Used Battery Recycling in Taiwan: Esher Hsu¹; Chenming Kuo²; ¹National Taipei University; ²I-Shou University

In Taiwan, around 9,000 tons of batteries are consumed per year but only 10% of which were collected and transported to oversea for recovery. The dumping used batteries have become a potential environment problem. How to increase the collection efficiency of used batteries becomes an important issue for EPA in Taiwan. Besides, some treatment plants are on process to get permission for recovering used batteries. The objective of this study is to estimate the recycling cost of spent consumer battery and explore the feasibility of recovering used consumer batteries in Taiwan based upon the principle of cost-efficiency. The recycling cost including collection cost and recovery is estimated based on a survey. Results would provide some suggestions to Taiwan EPA regarding feasibility of recovering used batteries in Taiwan.

6:10 PM **Concluding Comments**

Simulation of Aluminum Shape Casting Processing: From Alloy Design to Mechanical Properties: Through Process Modeling

Sponsored by: The Minerals, Metals and Materials Society, TMS Light Metals Division, TMS Materials Processing and Manufacturing Division, TMS Structural Materials Division, TMS: Aluminum Committee, TMS/ASM: Mechanical Behavior of Materials Committee, TMS: Process Modeling Analysis and Control Committee, TMS: Solidification Committee, TMS/ASM: Computational Materials Science and Engineering Committee

Program Organizers: Qigui Wang, General Motors Corporation; Matthew Krane, Purdue University; Peter Lee, Imperial College London

Tuesday PM
March 14, 2006

Room: 6D
Location: Henry B. Gonzalez Convention Ctr.

Session Chair: John T. Berry, Mississippi State University

2:00 PM **Invited**

Virtual Aluminum Castings: The Ford Experiment in Integrated Computational Materials Engineering: John E. Allison¹; ¹Ford Research and Advanced Engineering, Ford Motor Company

This talk will describe Virtual Aluminum Castings, a comprehensive, integrated and experimentally verified suite of CAE tools for optimization of cast aluminum components and processes. Using VAC castings can be designed and virtually cast, heat treated and tested for durability, all on a workstation long before components are fabricated. VAC represents the Ford experiment in a new approach to component engineering, Integrated Computational Materials Engineering (ICME). ICME seeks to unify analysis of manufacturing, design and materials into a holistic system and to unify materials models across length and time scales and knowledge domains. This talk will review recent progress in ICME and, more specifically, our ability within VAC to integrate models for the Al-Si-Cu alloys typically used in automobile engine structures, including models for phase equilibria and microsegregation, aging response, and the influence of microstructure on properties.

2:25 PM **Invited**

Study on Macro and Micro-Modeling of Solidification Process of Aluminum Shape Casting: Baicheng Liu¹; Shoumei Xiong¹; Tao Jing¹; Qingyan Xu¹; ¹Tsinghua University

Numerical methods to improve the computational efficiency and to extend the computational scale of the mold filling and solidification of aluminum die casting process were studied. For molding filling simulation, parallel computation method was studied, while for solidification simulation, an implicit finite difference scheme and a transient surface layer concept were studied. Three-dimensional simulation of the dendritic growth of multiple grains for aluminum alloy was studied by using phase field method coupling with thermal noise. In addition, modified cellular automaton (MCA) method was used to simulate the microstructure formation and evolution of Al alloy, including the grain structure and the dendritic microstructure and arm branching. Based on microstructure simulation, the mechanical properties were also predicted. The experimental results show that the models in the paper are reasonable for describing the formation and evolution of the dendritic microstructure.

2:50 PM **Invited**

A Mathematic Model to Predict the Cyclic Stress State of an A356 Automotive Wheel and Its Application to Fatigue Life Evaluation: Peifeng Li¹; Daan M. Maijer²; Peter D. Lee¹; Trevor C. Lindley¹; ¹Imperial College; ²University of British Columbia

Fatigue life is a key consideration in the design of cast aluminium alloy automotive wheels which offer both improved strength-to-weight ratio and fuel efficiency. The cyclic in-service (applied load and residual) stress distribution within a wheel is a limiting factor determining a wheel's fatigue performance. In this investigation, a through-process modelling methodology was applied to predict the cyclic stress state of an A356 automotive wheel subject to a bending moment. The predicted residual stresses arising during heat treatment and released through machining were

validated by a destructive strain measurement technique. With the residual stress state used as an initial condition, the variation of the in-service stress state during a bending test was predicted. The measured strain variations within the wheel for a series of different bending loads was found agree with the predictions. The through process modelling approach is completed by assessing the fatigue performance of the wheel.

3:15 PM Invited

Modeling and Simulation of Semisolid Casting: *Gilmer R. Burgos*¹; ¹Polytechnic University of Puerto Rico

Processing of metal alloys in their mushy state represents a new trend in metal processing. The process produces components with low porosity, high crack resistance, and superior mechanical properties. However, its implementation to industrial applications is hampered by technical problems due to the complex rheology of the material. The material behaves differently under slow and rapid transients and its response is time-dependent. In the present study, the thixotropic behavior of semisolid slurries is modeled using conservation equations and the Herschel-Bulkley fluid model. The model is implemented into a computer code to predict die filling. Results show that the final quality of the products depends on the processing conditions and the geometry of the die.

3:40 PM Break

3:55 PM Invited

Development and Applications of OPTCAST - A Thermal Boundary Conditions and Casting Process Optimization Tool: *Mei Li*¹; John E. Allison¹; ¹Ford Motor Company

OptCast is an integrated thermal/optimization tool coupling commercial casting simulation software MagmaSoft and ProCAST with optimization software iSIGHT. Two types of optimizations are realized in OptCast: one is using an inverse modeling approach to determine boundary conditions such as interfacial heat transfer coefficient, and the other is optimizing casting process variables by minimizing cycle time while maintaining casting quality. With OptCast heat transfer coefficients were developed from simple test casting and applied to V8 engine block for thermal analysis, microstructure and mechanical properties predictions and I4 block for porosity defect study. Heat transfer coefficients were also optimized for quenching process of cylinder head for residual stress analysis.

4:20 PM

Novel Solver Strategies for the Computational Modeling of Mould Filling in Very Complex Geometries: *Mark Cross*¹; Nick Croft¹; Diane McBride¹; ¹University of Wales Swansea

Simulation of shape casting processes involves the simultaneous capture of the rapidly developing metal-air free surface and the liquid-solid moving boundary in the metal phase. Although a wide range of techniques have been developed to address this problem, there are occasions where existing techniques are limited, especially in very complex geometries where the mesh quality may inevitably be relatively poor at some key locations. These poor quality cells can seriously inhibit convergence. Here we describe a finite volume approach over unstructured meshes where the flow is solved at the cell or element vertex, and all other variables are solved at the cell centre (as in conventional CFD tools). This flow solver strategy is much more tolerant of meshes with poor quality elements and enables the solution of simultaneous free surface flows coupled with solidification in very complex meshes, thus enabling the capture of such behaviour in arbitrarily complex geometrical structures.

4:45 PM

A Thermal Model of the Low-Pressure Die-Casting (LPDC) Process and Its Application to Predict Porosity Formation in Aluminum Alloy Wheels: *Bin Zhang*¹; Steve Cockcroft¹; Daan Maijer¹; Jindong Zhu¹; ¹University of British Columbia

A mathematical model of the Low Pressure Die Casting process for the production of A356 aluminum alloy wheels has been developed to predict the evolution of temperature and the porosity formation in the wheel. The model was validated against temperatures measured at numerous locations in the die and wheel during production. A modified Niyama parameter has been employed to estimate the critical solid fraction (fsc) for liquid encapsulation and in turn, this has been used to estimate the volume fraction of porosity. Comparison of the predicted and measured porosity

content within the wheel shows that the predicted porosity formation agrees reasonably well with the measurements. The application of LPDC pressurization sequence has also been discussed with respect to enhancing mass feeding to reduce porosity.

5:10 PM

Squeeze Casting Quality Control through Process Simulation: *Yun Xia*¹; ¹SPX Contech

Squeeze casting process, because of availability of heat treatment, minimum metal flow turbulence and gas entrapment by steady bottom shot velocity, and minimum volumetric shrinkage by directional and spot solidification, has advantage over HPDC casting. It has been a very competitive process in the automotive industry. The casting quality is sensitive to the process control and gate and runner design. Usual defects found in squeeze casting production can occur during both the die-filling phase and the metal solidification phase of the process. These defects can be directly attributed to improper adjustment or lack of control for the following process parameters: metal filling velocity, temperature, dwell time, cooling pattern and casting design, etc. Some special techniques with process simulation have been used, which include pressurized runner and gate design, casting layout in the die, squeeze pin application, high thermal conductivity inserts and casting design and castability, spray and lubricant techniques.

Solidification Modelling and Microstructure Formation: A Symposium in Honor of Prof. John Hunt: Eutectic Growth

Sponsored by: The Minerals, Metals and Materials Society, TMS Materials Processing and Manufacturing Division, TMS: Solidification Committee

Program Organizers: D. Graham McCartney, University of Nottingham; Peter D. Lee, Imperial College; Qingyou Han, Oak Ridge National Laboratory

Tuesday PM
March 14, 2006

Room: 6C
Location: Henry B. Gonzalez Convention Ctr.

Session Chairs: W. Kurz, Swiss Federal Institute of Technology; J. Perepezko, University of Wisconsin

2:00 PM Invited

Modeling of Cast Iron Solidification – The Defining Moments: *Doru Michael Stefanescu*¹; ¹Ohio State University

There are many to contend that today human civilization has reached the age of engineered materials, yet the importance of iron castings continues to support the thesis that we are still in the Iron Age. Cast iron, the first man-made composite, is at least 2500 years old. It remains the most important casting material, with over 70% of the total world tonnage. This paper is a review of the mathematical models that describe the fundamentals of solidification of iron-base materials, from the seminal paper by Oldfield, the first to attempt modeling of microstructure evolution during solidification, to the prediction of mechanical properties. The latest analytical models for irregular eutectics such as cast iron as well as numerical models with microstructure output are discussed. Because of space limitations, the emphasis is on model performance rather than model formulation. The impact of solidification simulation on defect control is also discussed.

2:25 PM Invited

Columnar and Equiaxed Growth of the Eutectic in Al-Si Alloys: *Arne K. Dahle*¹; Kazuhiro Nogita¹; S. D. McDonald¹; ¹University of Queensland

The Al-Si eutectic is an irregular eutectic with silicon being a faceted phase. During solidification, silicon is the leading phase of the eutectic interface. It has been shown that this eutectic system often displays equiaxed growth, such as in unmodified commercial alloys. Adding certain elements causes columnar eutectic growth to occur instead. The nucleation rate of the eutectic is expected to directly influence the eutectic spacing through its effect on the solid/liquid interfacial area, and thus the growth rate of the eutectic. Modification treatment, undertaken to refine the Al-Si

eutectic in common foundry alloys, typically also changes the eutectic nucleation conditions. This paper analyses the solidification mechanisms in unmodified and modified Al-Si alloys from the perspective of columnar and equiaxed growth, particularly focussing on the roles of potent nucleant populations and solidification conditions.

2:50 PM

Secondary Ion Mass Spectroscopy Analysis of Trace Element Distribution during the Al-Si Eutectic Reaction: *Oyvind Nielsen*¹; Christian Simensen¹; ¹SINTEF

Additions of trace elements like Sr, Na, Sb, Ca, etc are well known to modify the plate-like Si-particles in Al-Si alloys into a beneficial morphology. However, such additions have been shown to increase the amount of porosity and change the porosity distribution. Reviewing the extensive literature on this topic in the last years, it is evident that the mechanisms for nucleation and growth of the Al-Si binary eutectic is still a matter of controversy, although a significant progress has been made in the understanding of the effect of modifying elements on the eutectic grain size. In the present work, Secondary Ion Mass Spectroscopy has been used to quantify the distribution of elements like Sr, Na, Ca, and P in Al-Si alloys with different nominal trace element contents. The results constitute new knowledge about the solubility of trace elements in Si particles and other intermetallic phases and the local segregation behaviour.

3:15 PM Invited

Spacing Selection in Ternary Eutectic Alloys: Experiments and Computer Simulations: *Markus Apel*¹; Ingo Steinbach¹; ¹RWTH Aachen, Access e.V.

The 1966 paper of Jackson and Hunt about eutectic growth is the fundamental work in understanding eutectic microstructures. Tying in with this tradition we will present our recent progress in understanding lamellar growth pattern formation in a ternary eutectic alloy Bi-In-Sn. In-situ observations of pattern formation in thin metallic films are performed using light microscopy. In a wide range of parameters a γ -Sn/BiIn₂/β-In/BiIn₂ lamellar sequence forms as a steady state growth mode. A scaling relation $\lambda^2 \sim 1/v$ holds even for this ternary lamellar structure. This particular stacking sequence was selected from a planar solid/liquid growth front by a series of nucleation events. The final sequence is independent of the phase of the initial planar growth front. By a combination of the in-situ technique and phase field simulations, nucleation undercooling for γ -Sn and β-In and the diffusion coefficients of Bi and Sn in the melt can be extracted from the experimental data.

3:40 PM Break

3:55 PM Invited

Phase-Field Modeling of Rapid Eutectic Growth: *Andrew Martin Mullis*¹; James R. Green¹; ¹University of Leeds

As the cooling rate (or conversely undercooling) is increased it becomes progressively more difficult for a eutectic front to adapt to the increasing growth rate. At high growth velocity this will lead to a breakdown of the eutectic front, often by the emergence of dendrites. However, a number of studies of undercooled bulk samples have shown that it is also possible for an anomalous, unstructured, eutectic to be formed. Structures reminiscent of this anomalous eutectic have been observed by Nestler et al. [Physica D 138 (2000) 144] using phase field models. However, their model lacked anisotropy it was suggested that this was an artefact of the model and that if anisotropy were included dendrites would be observed instead. In this study we use phase-field modelling to analyse the effect anisotropy has upon the breakdown of eutectic solidification at enhanced growth velocities and comment upon the formation of anomalous eutectic.

4:20 PM

Modification of Semiconductor Phases in Metallic Alloys: *Simon N. Lekakh*¹; Carl Loper²; ¹University of Missouri-Rolla; ²University of Wisconsin-Milwaukee

A number of metallic alloys contain phases with semiconductor properties. A small amount of some additives can modify the shape faceted semiconductor phases into fibrous form in eutectics and into compact shape in hypereutectic alloys. The possible mechanism responsible for modification of semiconductor phases by donor type additives was de-

scribed in this article. A possibility of decreasing latent heat and increasing electro conductivity of the semiconductor phases modified by donor elements follows from this mechanism. The decrease of latent heat by the addition of Na and P in Al-Si alloys was experimentally confirmed. The electro-conductivity of primary Si crystals was qualitatively analyzed by EBIC method. The suggested mechanism predicts the composition of additives which could produce the modification of semiconductor phases in different metallic alloys. The possibility of changing the shape of the primary AlSb phase in hypereutectic Al-Sb alloys by donor type additive of Te was demonstrated.

4:45 PM

Microstructural Evolution during Laser Resolidification of Fe3Ge Alloy: *Krishanu Biswas*¹; Kamano Chattopadhyay¹; ¹Indian Institute of Science

The microstructural evolution of concentrated alloys is relatively less understood both in terms of theory and experiments. Laser remelting represents a powerful technique to study the solidification behaviour under controlled growth conditions. We have utilized this technique to experimentally probe the solidification and microstructural selection during solidification of concentrated Fe—25at%Ge alloys. Under equilibrium solidification condition, the alloy undergoes a peritectic reaction between B2 α_2 and it liquid leading to the formation of ordered hexagonal intermetallic phase e (DO19). In general microstructure consists of e phase and e-β eutectic that forms due to incomplete peritectic reaction. We shall show that with increasing velocity, the solidification front undergoes a change leading to the selection of microstructure corresponding to metastable α_2/β eutectic to α_2 dendrite + α_2/β eutectic to non steady state double growth of the dendrite and finally compact seaweed patterns. We'll discuss the underlying basis for such microstructural selection.

5:10 PM

Characterization of Hypereutectic Al-Si Powders Solidified Far-From-Equilibrium: *Eren Yunus Kalay*¹; Scott L. Chumbley¹; Iver E. Anderson¹; ¹Ames Laboratory, Iowa State University

Gas atomization was used to produce rapidly solidified hypereutectic Al-Si powders; Al-15Si, Al-18Si, Al-25Si, and Al-50Si (wt %), which were characterized by scanning and transmission electron microscopy (SEM, STEM) and x-ray diffraction (XRD). XRD revealed two phases (i) Si and (ii) supersaturated Al solid solution, with a comparison of measured and calculated lattice parameters. The sample powders exhibited four distinct microstructures with increasing particle diameter: microcellular Al grains, Al dendrites, coupled eutectic growth of Al and Si, and primary Si. TEM revealed a distinct nanocrystalline zone for small particles (<1 μm) which may indicate solute rejection ahead of the solidification front after recalescence. The microstructures of Al-25Si particles with diameters of 2-3 μm consisted of Al cells, which were separated by thick boundaries rich in Si. Large faceted Si and fine eutectic structures were also resolved for different compositions by TEM. Support from DOE-BES, contract no. W-7405-ENG-82.

Surfaces and Interfaces in Nanostructured Materials II: Liquid Phase and Biological Interactions

Sponsored by: The Minerals, Metals and Materials Society, TMS Materials Processing and Manufacturing Division, TMS: Surface Engineering Committee

Program Organizers: Sharmila M. Mukhopadhyay, Wright State University; Narendra B. Dahotre, University of Tennessee; Sudipta Seal, University of Central Florida; Arvind Agarwal, Florida International University

Tuesday PM Room: 209
March 14, 2006 Location: Henry B. Gonzalez Convention Ctr.

Session Chair: Sharmila M. Mukhopadhyay, Wright State University

2:00 PM

Chitosan-Hydroxyapatite Nanocomposite Coatings for Biomedical Applications: Igor Zhitomirsky¹; Xin Pang¹; ¹McMaster University

New method has been developed for the fabrication of nanocomposite chitosan-hydroxyapatite (HA) coatings. The method is based on the electrophoretic deposition of HA nanoparticles, prepared by a chemical precipitation technique, and electrochemical deposition of chitosan macromolecules. The deposit composition can be varied by the variation of HA concentration in chitosan solutions. X-ray studies revealed the preferred orientation of HA nanoparticles in the nanocomposites. Nanocomposite coatings were obtained on stainless steel, Ti and Pt foils, Ti wires, Ti meshes and graphite substrates. Deposition yield can be controlled by the variation of the deposition time. Coatings of various thickness in the range up to 50 μm were obtained. The method enables the formation of dense, adherent and uniform deposits on substrates of complex shape. Obtained coatings provide corrosion protection of stainless steel and Ti and can be utilized for the fabrication of advanced biomedical implants.

2:20 PM

Diffusion of Aqueous Solutions into Hydrophobic Nanoporous Thin-Films: Implications for Fracture: Eric Guyer¹; Reinhold Dauskardt¹; ¹Stanford University

Nanoporous organosilicate thin-films are being developed for use in a range of novel technologies ranging from biological to microelectronic devices. However, they are mechanically fragile and are prone to environmentally assisted cracking when exposed to aqueous environments. In this presentation, we demonstrate using novel diffusion studies that aqueous solutions can diffuse into highly hydrophobic nanoporous films containing interconnected porosity. The solution chemistry and presence of organic buffering agents significantly affects the ability of the solution to permeate into the nanoporous film. We further show that the diffusion of aqueous solutions into films can alter the films' stress state by changes in the surface stress of the internal pore surfaces. The resulting change in stress state has a profound effect on crack growth rate and has important consequences for reliability. Implications for the integration of nanoporous thin-films into advanced devices are considered.

2:40 PM Invited

Improvement of the Surface Bioactivity of Titanium Implants: Mei Wei¹; Haibo Qu¹; ¹University of Connecticut

Titanium has been widely used in orthopedic applications owing to its superior mechanical properties and higher corrosion resistance. However, as a bioinert material, titanium implants cannot bond directly to living bone as bioactive ceramics can, such as hydroxyapatite and Bioglass. As a result, there has been increasing interest in the recent years in the formation of a bioactive surface layer directly on titanium substrates, which will induce apatite formation in the living environment or simulated body fluid. In the present study, nano-hydroxyapatite was formed on the surface-modified titanium surface. The effects of both surface modification and simulated body fluid immersion conditions on the hydroxyapatite formation rate and the bonding strength between the hydroxyapatite and titanium substrate were investigated. A dense, strong hydroxyapatite layer

was formed on the surface-modified titanium substrate within a short period.

3:20 PM

Ion Adsorption Behavior on SiO₂ and Al₂O₃ Nanoparticles in Aqueous Electrolytes: Gabriele Vidrich¹; Oliver Moll¹; Hans Ferkel²; ¹Technical University Clausthal; ²Volkswagen AG

The ion adsorption behavior on nanoparticles in aqueous electrolytes for deposition of dispersion-strengthened nickel was investigated. Measurements of the hydrogen formation during plating from pure nickel sulfamate electrolyte, electrolyte containing either 1.5 wt.-% SiO₂ or Al₂O₃ nanoparticles with particle diameter around 30 nm were carried out. These results were correlated with earlier investigations on the Zeta potential as well as on the dispersion behavior of the nanoparticles in diluted electrolytes. It was found that in case of pure electrolyte and dispersions containing SiO₂ nanoparticles the amount of H₂ collected at the cathode is nearly the same whereas in case of electrolyte containing Al₂O₃ about 3 times less H₂ evolves during plating. In conjunction with overpotential measurements, these results indicate that hydrogen is probably bonded on the co-deposited Al₂O₃. In case of SiO₂ the adsorption site on the particle surface are preferentially occupied by Ni²⁺ ion as discussed in earlier publications.

3:40 PM

Photo-Synthesis of Nano Gold Particles for Drug Delivery: Yung-Chin Yang¹; Jun-Ying Lin¹; Chang-Hai Wang²; Yeukuang Hwu²; ¹National Taipei University of Technology; ²Institute of Physics, Academia Sinica

We reported a simple approach to generate gold colloidal from HAuCl₄ containing aqueous solution by synchrotron x-ray irradiation at room temperature, without a reducing agent. Gold colloidal were readily formed by the exposure of HAuCl₄ aqueous solution to synchrotron x-ray. It was also observed that the addition of NaHCO₃ tremendously modified the size and size distribution of gold nanoparticles. Under optimal conditions, the precipitated nanoparticles were well dispersed and with uniform size, ~10 nm. The Au nanoparticle solution prepared with this simple, clean and very fast process without toxic reductant is biocompatible – and could be used for surface modification and drug attachment procedures in the same bath. Our preliminary drug carrying experiment showed that thus produced gold nanoparticles could successfully carry anti-tumor drug and possess potential for drug delivery applications. Further studies on accessing the capacity of drug loading, delivery and release characteristics are currently underway.

4:00 PM

Energy Exchange in Nanopores: Yu Qiao¹; Falgun B. Surani¹; Xinguo Kong¹; ¹University of Akron

According to a recent experimental study, with appropriate porous structure and surface properties, a nanoporous material can be infiltrated by a nonwetting liquid when the pressure is sufficiently high. As the pressure is reduced, for reasons that are still under investigation, the confined liquid would remain in the nominally energetically unfavorable nanopores, and thus the excess solid-liquid interface energy can be considered as being "absorbed", leading to a significant hysteresis of absorption isotherm. Due to the ultrahigh specific surface area of the nanoporous material that usually ranges from 100-1000 m²/g, the energy absorption effectiveness of such a system can be higher than that of conventional energy absorption materials by orders of magnitude. The infiltration pressure can be adjusted by using chemical admixtures in the range of 0-20 MPa. The system recovery ratio can be as high as 75%.

4:20 PM

Investigation of Nanostructured Cadmium Sulfide in the Presence of Copper and Silver Salts: Christopher Ryan Lubeck¹; T. Yong-Jin Han²; Alexander E. Gash²; Fiona M. Doyle¹; ¹University of California, Berkeley; ²Lawrence Livermore National Laboratory

Polymeric and oligomeric molecules have been used to template inorganics. In particular, nanostructured cadmium sulfide has been synthesized via a direct templating method in which self-assembled amphiphiles create structure within precipitated inorganic particles. Cadmium sulfide forms in the hydrophilic portion of the water/amphiphile liquid crystal and is excluded from the hydrophobic portion as particles grow. We investigate the transformation of this cadmium sulfide structure

in the presence of silver and copper salts. Due to the high interfacial area of the nanostructured material, the rate of transformation is significantly faster than for bulk material. This method has allowed for the exchange of cadmium ions with copper and silver ions yielding silver sulfide and copper sulfide of different structures.

The Brandon Symposium: Advanced Materials and Characterization: Interfaces

Sponsored by: The Minerals, Metals and Materials Society, Indian Institute of Metals, TMS Extraction and Processing Division, TMS: Materials Characterization Committee

Program Organizers: Srinivasa Ranganathan, Indian Institute of Science; Wayne D. Kaplan, Technion; Manfred R. Ruhle, Max-Planck Institute; David N. Seidman, Northwestern University; D. Shechtman, Technion; Tadao Watanabe, Tohoku University; Rachman Chaim, Technion

Tuesday PM Room: 206B
March 14, 2006 Location: Henry B. Gonzalez Convention Ctr.

Session Chairs: Tadao Watanabe, Tohoku University; Yuichi Ikuhara, University of Tokyo

2:00 PM Invited

Thin Films in Ceramic Grain Boundaries: *C. Barry Carter*¹; Jessica L. Riesterer¹; Arzu Altay¹; Jeffrey K. Farrer²; N. Ravishanker³; ¹University of Minnesota; ²Brigham Young University; ³Indian Institute of Science

Thin amorphous films are so often present along interfaces in polycrystalline ceramics that it is frequently assumed that such films are always present, similar in thickness in all ceramics, and in an equilibrium form. These assumptions are not generally valid and may be misleading. Classic liquid-phase sintering relies on the wetting of ceramic powder compacts by glass-forming additives with lower melting points. How the secondary phase wets the interface, how glass permeates these interfaces, and how this influences interface migration during processing is unclear. This talk will present results from two systems using a combination of microscopy techniques. Thin films of the second phase (anorthite or silica) are deposited onto sapphire or rutile substrates and then heated to 1400°C–1650°C. The second phase may dewet or continue to wet the surface. Particular attention will be paid to considering the importance of kinetics, and how they combine to control the wetting process.

2:25 PM Invited

Role of Interface on Structure and Properties of Multifunctional Epitaxial Oxides: *Xiaoqing Pan*¹; Darrell Schlom²; Chang-Beom Eom³; ¹University of Michigan; ²Pennsylvania State University; ³University of Wisconsin

In this talk the effect of lattice mismatch (epitaxial strain), crystal defects, and chemistry at the film/substrate interfaces on the microstructure and properties of different systems will be addressed. The interfacial atomic structure and defects of the films were investigated by high-resolution transmission electron microscopy (HRTEM). The structure and formation mechanisms of misfit dislocations and their significance for the relaxation of epitaxial strain were systematically investigated. Quantitative HRTEM analysis of strained BaTiO₃ predicts the enhancement of spontaneous polarization by 200%, which is consistent with the direct measurements of strained BaTiO₃ thin films using epitaxial SrRuO₃ electrodes. Furthermore, the effect of atomic steps on the substrate surface due to vicinal cutting on the epitaxial growth, microstructure and properties of perovskite oxide films will be described. It will be demonstrated that the existence of the atomic step flow on miscut substrate eliminates the formation of pyrochlore phases in epitaxial PMN-PT films.

2:50 PM Invited

Contact Deformation and Failure in Single Layer and Multi-Layer Columnar Hard Coatings: *Vikram Jayaram*¹; S. K. Biswas¹; ¹Indian Institute of Science

Hard, columnar films of TiN are used extensively in applications ranging from cutting tools to decorative coatings. When subject to contact

loading, the films display one of two extreme responses: thin coatings on hard substrates display a mode of inter-columnar sliding in which the two phases deform compatibly, while thick coatings on hard substrates display extensive cracking, characteristic of a large strain mis-match between film and substrate. This presentation will address the rationale behind this behaviour, the influence of multi-layering at the nanometric level and the implications for the design of hard coatings, through qualitative arguments as well as an analytical treatment of the problem of Hertzian contact deformation of a bi-material system using integral transforms.

3:15 PM Invited

Equilibrium Amorphous Films at Metal-Ceramic Interfaces: *Wayne David Kaplan*¹; Amir Avishai¹; ¹Technion-Israel Institute of Technology

Intergranular amorphous films (IGF) with a thickness of ~1nm exist in many ceramic systems. In this work the nature of IGF's at metal-ceramic interfaces was investigated via detailed microstructural characterization of model metal-alumina nanocomposites, and wetting/dewetting experiments. Cu-alumina and Ni-alumina composites, with and without glass-forming additives, were produced and characterized. The composites doped with glass-forming additives contained amorphous pockets at the triple junctions, as well as IGF's at all of the metal-alumina interfaces. No amorphous phase was observed in the undoped composites. In the doped composites the metal particles were found at triple junctions, grain boundaries, and as occluded particles within the alumina grains. Calculation of Hamaker constants for the metal-ceramic interfaces resulted in a stronger attractive force for IGF's at metal-alumina interfaces, compared to alumina grain boundaries, correlating to the film thickness measured in this work.

3:40 PM Break

4:00 PM

The Role of Partial Grain Boundary Dislocations in Grain Boundary Sliding: *Diana Farkas*¹; Brian Hyde²; ¹Virginia Tech; ²Northwestern University

Atomistic computer simulations were performed to investigate the mechanisms of grain boundary sliding in bcc Fe using molecular statics and dynamics with embedded atom method interatomic potentials. For this study we have chosen the $\Sigma=5, (310)[001]$ symmetrical tilt boundary with tilt angle $\theta = 36.9^\circ$. Sliding was determined to be governed by grain boundary dislocation activity with Burgers vectors belonging to the DSC lattice. The sliding process was found to occur through the nucleation and glide of partial grain boundary dislocations, with a secondary grain boundary structure playing an important role in the sliding process. Interstitial impurities and vacancies were introduced in the grain boundary to study their role as nucleation sites for the partial grain boundary dislocations. While vacancies and H interstitials act as preferred nucleation sites, C interstitials do not. The role of pre-existing grain boundary dislocations in the sliding behavior will also be discussed.

4:25 PM Invited

Grain Boundary Excess Free Volume – Direct Thermodynamic Measurement: *Lazar Simhovich Shvindlerman*¹; Günter Gottstein¹; ¹RWTH Aachen

Grain boundary excess free (BFV) volume along with surface tension belongs to the major thermodynamic properties of grain boundaries. Unfortunately, our knowledge about grain boundary excess free volume is completely restricted by data of computer simulation, which, in its turn, is strictly limited by grain boundaries in the vicinity of special misorientation. However, for the grain boundaries due to the availability of the additional degree of freedom there is a way for correct thermodynamic measurement of this physical property. The special technique developed makes it possible to measure the BFV for practically any grain boundary and provides a way of estimating grain boundary excess free volume for grain boundaries of different classes with rather high accuracy. The knowledge of BFV is especially important for fine grained and nanocrystalline systems where it opens up new possibilities to control and design the physical properties and microstructure of such polycrystals.

4:50 PM Invited

Grain Boundary Populations as a Function of Disorientation and Boundary Normal: *Anthony D. Rollett*¹; Jason Gruber¹; Chang-Soo Kim¹;

Tricia Bennett¹; Gregory Rhorer¹; Nathalie Bozzolo²; ¹Carnegie Mellon University; ²University of Metz

Studies of grain boundary populations that take account of the full five degrees of freedom, that is to say misorientation and boundary normal, reveal many interesting trends. Although the coincident site lattice (CSL) theory that is linked to Prof. Brandon's name has been a very useful tool for understanding interfaces, the grain boundary population data point to a much stronger connection to the properties of the two surfaces comprising the boundary. This connection is reinforced by computer simulation of grain growth that demonstrates the existence of a steady-state anisotropy in the population directly linked to the anisotropy of the grain boundary energy. This view is illustrated by reference to recent results for a variety of materials, including zirconium and iron.

The James Morris Honorary Symposium on Aluminum Wrought Products for Automotive, Packaging, and Other Applications: Automotive Alloys

Sponsored by: The Minerals, Metals and Materials Society, TMS Light Metals Division, TMS: Recycling Committee

Program Organizers: Subodh K. Das, Secat Inc; Gyan Jha, ARCO Aluminum Inc; Zhong Li, Aleris International Inc; Tongguang Zhai, University of Kentucky; Jiantao Liu, Alcoa Technical Center

Tuesday PM Room: 207A
March 14, 2006 Location: Henry B. Gonzalez Convention Ctr.

Session Chairs: Subodh K. Das, Secat Inc; Jiantao Liu, Alcoa Technical Center

2:00 PM Invited

Implementation of Continuous Cast (CC) AA5754 Aluminum Alloy in Automotive Stampings and Hydroforms: *SooHo Kim*¹; Anil K. Sachdev¹; Alan A. Luo¹; Raja K. Mishra¹; ¹General Motors R&D Center

This study demonstrates that low-cost continuous cast (CC) aluminum alloys have slightly lower press formability than current production direct chill (DC) cast aluminum sheet, but the formability is sufficient for many automotive stampings like hood reinforcements, heat shields, skid plates etc. Tubes made of CC 5754 sheet showed similar forming strains in bending and hydroforming compared to conventional DC 5754 seam-welded and 6063 extruded tubes. The talk will describe the microstructures, post-forming properties of the hydroformed tubes and EBSD measurements of the texture distribution/evolution during deformation.

2:25 PM Invited

The Role of Microstructure on the Formability on Automotive Aluminum Alloy Sheet: *David S. Wilkinson*¹; Xinjian Duan¹; Jidong Kang¹; Mukesh Jain¹; Raj Mishra²; Anil Sachdev²; Sooho Kim²; ¹McMaster University; ²General Motors R&D Center

We have studied the effect of microstructure on formability of aluminum alloys sheet (primarily AA5755, DC and CC variants). Fe-based intermetallic particles, found as isolated particles and in stringers, lower the ductility and formability of these alloys. They may also contribute to the lower ductility of CC alloys. These materials are very resistant to damage until just before fracture, so that this is not a particle-induced damage effect. We have studied the role of particles in the development of shear localization. I will outline a set of experiments and models which demonstrate the link between shear instability and fracture and the role played by hard particles. I will show how local strain mapping using digital image correlation helps to understand PLC band development and shear localization, while FEM calculations demonstrate the effect of particle density and morphology on shear localization. The aim is a new model that couples micro/macro effects.

2:50 PM

Study of Microstructure and Aging Behavior of Continuous Cast 6111 Aluminum Alloy: *Zhong Li*¹; Steve Kirkland¹; Shixi Ding¹; Dave Thompson¹; Paul Platek¹; ¹Aleris International, Inc

Aleris International, Inc. has been developing continuous cast (CC) aluminum alloy sheets for different automotive applications over the last several years. Aleris has cast 5754, 5182, 5083 and 6111 using twin-belt casting technology for the research and development work towards automotive applications. In this paper, microstructures and aging behavior of continuous cast 6111 aluminum alloy after different routes of processing were studied and discussed.

3:15 PM

The Bauschinger Effect in Aluminum Alloy AA6111: *Henry Proudhon*¹; Warren Poole¹; David Lloyd²; ¹UBC; ²Novelis Inc.

There is considerable current interest in developing mechanical property models which describe the yield stress and work hardening of 6000 series alloys which are used in automotive applications. This study examines the contribution of long range internal elastic stresses on the macroscopic hardening response. Internal stresses have been evaluated by a series of Bauschinger tests on alloys with different states of precipitation. It has been observed that there are significant differences between underaged and peak aged material compared to highly overaged material. This is attributed to the transition in the nature of the dislocation-precipitate interaction. For underaged and peak aged materials, precipitate shearing dominates and there are relatively small internal stresses. On the other hand, for the case of overaged samples with non-shearable precipitates, significant internal stresses are observed due to the storage of dislocations around the precipitates.

3:40 PM

AA6082 Feedstock Production for Thixoforming: *Yücel Birol*¹; Ugur Bozkurt²; Mehmet Onsel²; ¹Marmara Research Center; ²Bosphorus University

Thixoforming offers the possibility of forming complex aluminum parts with an exceptional quality and a reduction of processing steps. The production of a fine, equi-axed, globular microstructure is a must for the success of the thixoforming process. Strain induced melt activation (SIMA) process produces such a microstructure through recrystallization of heavily deformed billets and a subsequent heat treatment in the mushy zone. In the cooling slope (CS) route, on the other hand, molten metal with a suitable superheat is cast over a water-cooled, inclined surface into a permanent mould to produce the thixotropic billet. Both SIMA process and the CS casting route were employed to produce AA6082 thixotropic feedstock in the present work. The effect of cold work and heat treatment conditions and the effect of cooling length, casting temperature and reheating conditions on the final microstructures were investigated for the SIMA process and CS casting route, respectively.

4:05 PM Break

4:15 PM

A Microstructural Examination of Aluminum Alloys Subjected to Incremental Forming: *Albert Krause*¹; William T. Donlon¹; Alan Gillard¹; Sergey Golovashchenko¹; ¹Ford Motor Company

Improvements in formability of certain aluminum alloys is required for utilization by the automotive industry for complex shaped body panels to reduce vehicle weight. One possible approach to increase formability is through incremental forming; a process of deforming the aluminum sheet in separate steps, with the sheet being subjected to a quick recovery heat treatment between each forming step, in order to partially undo the effects of work hardening. This process can significantly increase the total amount of deformation before fracture. The purpose of this work was to determine if the structural mechanism responsible for the partial recovery of both aging and non-aging aluminum alloys could be determined. The microstructure was examined through both optical and transmission electron microscopy for alloys subjected to a variety of temperatures and deformations.

4:40 PM

Characterization of AA 5754-O Sheet Metal Deformed under In-Plane Stretching: *Stephen W. Banovic*¹; Mark A. Iadicola¹; Tim Foecke¹; ¹National Institute of Standards and Technology

Material behavior data for use in constitutive equations is often lacking to properly model material flow during stamping operations and accurately predict the material's response (limiting strains; surface roughness;

friction; springback). In an effort to better understand the processing-structure-properties relationship of aluminum sheet, AA 5754-O is deformed under in-plane stretching, with measurement of true stress-true strain curves using a unique in situ X-ray diffraction system. Subsequent characterization is conducted using light optical and scanning electron microscopy. Diffraction techniques are used to measure the change in crystallographic texture. The results of this work are discussed with respect to implementation in existing and developing constitutive laws.

5:05 PM

Improving the Characterization of the Surface Morphology Generated in Deformed Aluminum Sheet: *Mark R. Stoudt*¹; Joseph B. Hubbard¹; ¹National Institute of Standards and Technology

Numeric predictions of mechanical behavior during forming are central to the automotive design process. Discrepancies between the predicted roughness and what is measured on real surfaces signify that improved predictive accuracy requires a better understanding of the fundamental relationships between deformation and the morphology of the free surface. Inaccurate predictions of surface character also imply limitations in the conventional surface roughness characterization methods. Most surface roughness assessments utilize tacit assumptions about the distributions of surface features within the roughness data. The validity of these assessments is further degraded by compressing complex surface information into singular quantities that are too coarse with respect to the length-scales of the relevant features. A different approach, based on ensemble averaging and rigorous statistical protocols, is being developed to improve the fidelity between roughness measurements and the original surface. Results from efficacy determinations performed on strained 6022 aluminum surfaces are presented and discussed.

5:25 PM

Overview of 5000-Series Aluminum Materials for Hot Forming in the Automotive Industry: *Eric M. Taleff*¹; ¹University of Texas

Hot gas-pressure forming of 5000-series aluminum materials has recently been implemented for the mass production of automotive components by two major automobile producers. Product shapes used in these forming operations include both sheet, for body closure panels, and tubing, for subframe components. This presentation provides an overview of the important aspects of microstructure and mechanical behavior in 5000-series aluminum materials for these hot-forming operations. The elevated-temperature deformation mechanisms of grain-boundary sliding and solute-drag creep enable the large tensile ductilities necessary for hot-forming operations. Failure under forming conditions can be by either cavitation or flow localization. Cavitation is strongly influenced by the volume and size distribution of intermetallic particles. Aspects of microstructure which influence deformation and failure behaviors are discussed.

The Rohatgi Honorary Symposium on Solidification Processing of Metal Matrix Composites: Properties of MMCs

Sponsored by: The Minerals, Metals and Materials Society, TMS Materials Processing and Manufacturing Division, TMS Structural Materials Division, TMS/ASM: Composite Materials Committee, TMS: Solidification Committee

Program Organizers: Nikhil Gupta, Polytechnic University; Warren H. Hunt, Aluminum Consultants Group Inc

Tuesday PM
March 14, 2006

Room: 207B
Location: Henry B. Gonzalez Convention Ctr.

Session Chairs: Darrell R. Herling, Pacific Northwest National Laboratory; Somuri V. Prasad, Sandia National Laboratories

2:00 PM Invited

Friction and Wear Mechanisms in Aluminum Alloy Metal-Matrix Composites: *Somuri V. Prasad*¹; Rajiv Asthana²; ¹Sandia National Laboratories; ²University of Wisconsin-Stout

The major drawback of aluminum alloys in tribological (friction and wear) applications is their poor resistance to seizure and galling. The pio-

neering work of Rohatgi in the late 1960's has enabled us to synthesize a variety of cast aluminum alloy metal-matrix composites (MMCs) dispersed with solid lubricants, or ceramics (particulates, whiskers, or short fibers), or a combination of these to achieve the desired balances in physical, mechanical and tribological properties required for a tribocomponent. In this paper, we shall critically examine the mechanisms of lubrication in self-lubricating MMCs (e.g., Al alloy-graphite) and material removal mechanisms in abrasion-resistant MMCs (e.g., Al alloy-ceramic composites). Current and emerging applications of Al MMCs in aerospace and automotive industries will be discussed. *Sandia is a multiprogram laboratory operated by Sandia Corporation, a Lockheed Martin Company, for the United States Department of Energy under contract DE-AC04-94AL85000.

2:25 PM Invited

Short-Fiber Cast Aluminum MMCs: Properties and Value: *Gerald A. Gegel*¹; David Weiss²; ¹Materials and Process Consultancy; ²Eck Industries, Inc.

Metal matrix composite alloys combine the attributes of metals and ceramic reinforcements to provide materials engineered with low density and high specific mechanical properties. Most components do not require the high performance capability of aluminum MMCs throughout their entirety. Selective reinforcement, the reinforcement of only the high stress regions of a component, will reduce manufacturing costs. Pressure infiltration casting was used to produce test specimens from three short-fiber ceramic reinforcements. The measured mechanical properties of these materials and comparative cost analysis were used to accomplish a value analysis for each ceramic reinforcement. These property and value data may be used to facilitate component design and manufacture of selectively reinforced aluminum MMC components.

2:50 PM

Effects of Particle Size and Volume Fraction on Wear Behavior of A356 Aluminum Alloy/SiC Particles Composites: *Martin Duarte*¹; *Jose Miguel Molina*¹; *Javier Narciso*¹; *Enrique Louis*¹; ¹Alicante University

The wear resistance of A356/SiC composites with different particle sizes and volume fractions has been evaluated in the as-cast condition. The composites were fabricated through direct mixing of the ceramic particle and the liquid metal. Wear experiments were carried out in a ball-on-disk machine. In an attempt to determine the wear mechanisms, the morphology of the wear track was examined by scanning electron microscopy. As found in previous studies, the wear performance increases with the particle size and volume fraction. The tribological properties of these materials are analyzed and compared against theoretical wear models. The power spectrum of the friction signal is analyzed by means of Fast Fourier Transform Algorithms. It turns out that the power spectrum shows a 1/f behavior. The fractal dimension of the signal is determined by means of a modified Counting Box Method. The results are compared with those obtained for steel and matrix alloy.

3:15 PM

Damping Characteristics of Al-Li-SiCp Composites: *Mirle Krishnegowda Surappa*¹; *Ranjit Bauri*¹; ¹Indian Institute of Science

Damping characteristics of 8090 Al alloy and its composites reinforced with 8, 12, and 18 vol pct SiC particles were investigated using a dynamic mechanical analyzer (DMA). Tests were done at different frequencies over a temperature range of 27°C to 300°C. Composites show higher damping capacity than the unreinforced alloy. Damping capacity is found to increase with decreasing frequency. An equation relating damping capacity with frequency has been proposed. The damping data are analyzed in the light of matrix microstructure and different operative mechanism.

3:40 PM

The Effect of Si and Mg Addition on Microstructure and Mechanical Properties of Al-60% SiC Composites Produced by Pressure Infiltration Technique: *Huseyin Cimenoglu*¹; *Ercan Candan*²; *Hayrettin Ahlatci*²; ¹Istanbul Technical University; ²Zonguldak Karaelmas University

In this study, effect of Si and Mg addition on the microstructure and mechanical properties of the Al-60 vol.% SiCp composites, produced by pressure infiltration, technique were investigated. Si and Mg content of Al matrix varied 0-8 wt.% while SiC particles had 23µm mean diameter. Mechanical properties of the composites were characterized by uniaxial

compression, three point bending and impact tests. Si and Al₃C₄ intermetallics were present in the Al-Si matrix composites and whereas Mg₂Si was also present in Al-Mg alloy matrix composites in addition to Si and Al₃C₄ intermetallics. Mechanical test revealed that maximum bending and compression strengths were achieved in Al-1.0 Si alloy/SiC composite. Impact resistance of Al-Si/SiC composites decreased with increasing Si content. As compared to Al-Si alloy matrix composites, Mg addition to Al matrix increased both bending and compression strengths whereas toughness was reduced notably. Fractured surfaces were examined by SEM after the mechanical tests.

4:05 PM Break

4:20 PM

Use of Dynamic Low Load Micro Hardness Indentation Technique in Studying Serrated Flow in Al-Si₃C₂ Composites: *Mirle Krishnegowda Surappa*¹; Ranjit Bauri¹; ¹Indian Institute of Science

Occurrence of plastic instabilities during depth sensing indentation in 8090 Al alloy and 8090 Al-SiCp composites containing 8 and 15 vol.% of SiC particles have been investigated by dynamic ultra low load micro hardness (DUH) technique. The unreinforced alloy shows instabilities (serrations) in the load-displacement curve in the as-extruded (AE) and solution-treated conditions. However, the magnitude of serrations becomes negligible after ageing. Al-Li-8% SiC composite shows signs of serrations in the solution-treated condition. On the other hand, Al-Li-15% SiC composite shows almost no or negligible serrated flow in all the conditions (as-extruded, solution-treated, and aged).

4:45 PM Invited

Laser Deposition of Metal Matrix Composites: *John E. Smugersky*¹; Baolong Zheng²; David Gill¹; Yizhang Zhou²; Enrique J. Lavernia²; ¹Sandia National Laboratories; ²University of California

Laser deposition via the Laser Engineered Net Shaping (LENS®) process is being used to explore the potential for in-situ synthesis of metal matrix composites. LENS® is a layer additive metal shaping process, that employs solidification as a mechanism for synthesizing materials with variations in compositions coupled with process parameter (e.g., substrate temperature, laser power, substrate traverse speed) modifications as a means to control microstructures and properties. With cooling rates in the 10³ K per second, the LENS process enables the achievement of microstructure refinement and metastable phases. In this paper, we evaluate the effect of increasing additions of fine dispersoids into a metal matrix over a range of compositions and processing conditions on the microstructure and properties of the matrix metal. Characterization of the resultant microstructure includes metallographic analysis, composition profiles, and hardness using optical, SEM, EDS, XRD, and micro-hardness techniques. Mechanical properties of selected compositions will also be presented.

5:10 PM

Wear and Friction Behavior of Near Eutectic Al-Si +ZrO₂ or WC Particle Composites: *Atef Awad Doud*¹; Pradeep Rohatgi²; ¹CMRDI; ²University of Wisconsin-Milwaukee

Dry sliding wear and friction behavior of cast near eutectic Al-Si alloy and composites containing 5 vol% WC or ZrO₂ particles were studied by means of a three pins-on-disk (steel) apparatus. The results showed that the composites exhibited a superior wear resistance in comparison to the unreinforced alloy at load range of 18-180 N. The coefficients of friction for all the tested materials decreased with increasing applied load from 18 N to 90 N. However, at load levels of 90-180 N, the coefficients of friction increase as the load increases. SEM investigations revealed that in the load range of 18-90 N, the worn surfaces of the composites reinforced either by WC or ZrO₂ were covered by iron oxides, which provided in situ lubrication. At load above 90 N, the WC or ZrO₂ particles fractured and lose their ability to support the load. Therefore, the wear rates of the composites significantly increased.

5:35 PM Invited

Wear of Lead Free Cast Copper Alloy-Graphite Particle Composite: *Deo Nath*¹; N. Prasad¹; Pradeep Rohatgi²; ¹Banaras Hindu University; ²University of Wisconsin - Milwaukee

Copper alloy-graphite particle composite (60Cu - 37.5Zn, 1.75 Graphite, 0.75Ti) was developed as a substitute for leaded copper alloy used in

plumbing and bearings and wear tested under cast and extruded conditions. The wear volume and rate were determined as a function of sliding distance and lead. Optical and Scanning Electron Microscopy was used to study the wear debris and worn surfaces respectively. The wear volume and rate of the composite increased with increasing lead and sliding distance and was comparable to those of leaded copper alloy (60Cu - 37.5Zn, 1.75Pb, 0.75Sn) at higher loads. The size of wear debris decreased with increasing load. SEM studies indicated adhesive wear to operate.

Titanium Alloys for High Temperature Applications - A Symposium Dedicated to the Memory of Dr. Martin Blackburn: Microstructure and Properties of High Temperature Titanium Alloys

Sponsored by: The Minerals, Metals and Materials Society, TMS Structural Materials Division, TMS: Titanium Committee

Program Organizers: Michael W. Peretti, Lyondell Chemical Company; Daniel Eylon, University of Dayton; Ulrike Habel, Munich; Guido C. Keijzers, Del West USA; Michael R. Winstone, DSTL

Tuesday PM
March 14, 2006

Room: 201
Location: Henry B. Gonzalez Convention Ctr.

Session Chairs: Ulrike Habel, Munich; Michael H. Loretto, University of Birmingham

2:00 PM Invited

Microstructure and Properties of High-Temperature Titanium Alloys after Rapid Heat Treatment: *Orest Ivasishin*¹; Vadym Bondarchuk¹; ¹Institute for Metal Physics, NAS of Ukraine

Enhancement of high-temperature strength and creep resistance of titanium alloys is an important issue that would allow to extend the field of their application. Mechanical properties of titanium alloys are to a great extent determined by a microstructure. The present paper addresses Rapid Heat Treatment (RHT) as an effective method to improve microstructure of titanium alloys and thus their high temperature performance. The RHT comprises fast (tens to hundreds degrees per second) heating into the single-phase beta field and results in a formation of a specific fine-grained beta-transformed microstructure unachievable with conventional heat treatments. This microstructure possesses a high creep resistance inherent to the conventional beta-transformed condition, but is free from drawbacks of the latter such as low ductility or fatigue resistance. The advantages of RHT over conventional treatments are discussed from the standpoint of microstructure/properties relationship and high temperature deformation mechanisms.

2:30 PM

Creep Behavior of TIMETAL®1100 at Elevated Temperatures and Its Automotive Applications: *Yoji Kosaka*¹; Stephen P. Fox¹; ¹Timet

TIMETAL®1100 (Ti-6Al-2.7Sn-4Zr-0.5Mo-0.45Si) was developed to maximize creep resistance with adequate strength and fatigue performance in aircraft jet engine applications. The combination of weight saving and the excellent high temperature properties of this alloy has opened an opportunity for the application of this alloy as exhaust valves of automotive and motorcycle engines. The service temperature for the alloy in this application appears to be much higher than the 1100°F (600°C) for which the alloy was originally designed. The present paper will introduce the application of TIMETAL®1100 for automotive engine valves and discuss the creep behavior up to 760°C or 1400°F.

3:00 PM

Creep and Recovery at Lower Temperatures in Titanium-Aluminum Alloys: *M. Brandes*¹; Michael J. Mills¹; ¹Ohio State University

Although titanium alloys are widely known to undergo a variety of creep and recovery processes at temperatures above 0.4 T_m, these types of phenomena occurring at lower temperatures are not well documented. Remarkably, it has been found that these materials, when deformed at lower temperatures, can exhibit recovery processes at temperatures as low as room temperature. This work addresses observations of the recovery of

TUESDAY PM

strain hardening in creep deformed Ti-6 wt% Al and Ti-6242 with the variation of several factors including plastic strain level, time spent in the unloaded state, exposure temperature, loading direction, and microstructure. It is proposed that the formation of intense $b = \langle 11\bar{2}0 \rangle$ dislocation pile-ups at grain and/or phase boundaries, which stem from the planarity in these alloys, provide the driving force for a thermally activated, dislocation level recovery mechanism.

3:30 PM

Roller-Burnishing Effects on HCF Performance of Notched Ti-6242 at Ambient and Elevated Temperatures: *Tomasz Ludian*¹; Wagner Lothar¹; ¹Clausthal University of Technology

In Ti-6Al-2Sn-4Zr-2Mo-0.1Si, fully lamellar and duplex microstructures were processed through thermal and thermo-mechanical treatments, respectively. Resulting microstructures and textures were evaluated. Mechanical testing was performed at 20°C as well as 500°C. Fatigue tests were done in axial loading ($R=-1$) at roughly 100 Hz. Unnotched ($kt = 1.0$) and circumferentially slightly notched ($kt = 1.5$) as well as heavily notched ($kt = 3.0$) specimens were tested. In ball-burnishing, a hydraulically driven device utilizing various ball sizes and rolling forces was used. After burnishing, the changes in surface and near-surface properties such as surface topography, surface layer micro-hardness and residual stress-depth profiles were determined. For comparison, electrolytically polished conditions were prepared to serve as reference. The fatigue results are interpreted in terms of cyclic and thermal stability of the ball-burnishing-induced near-surface high dislocation densities and residual compressive stresses and their effects in turn on fatigue crack nucleation and micro-crack propagation.

4:00 PM Break

4:30 PM

Comparing Residual Stresses in Linear Friction Welded α - β and Near- α Ti Alloys: *Philipp G. Frankel*¹; Mallikarjun Karadge¹; Michael Preuss¹; Greg Johnson¹; Philip J. Withers¹; Axel Steuwer²; Simon Bray³; ¹University of Manchester; ²ESRF - ILL; ³Rolls Royce Plc.

Residual stresses in linear friction welded (LFW) Ti-6Al-4V and Ti-6242 have been determined using high energy synchrotron X-ray diffraction. The chemical induced shift is accounted for by using the biaxial $\sin^2\Psi$ -technique with a collimated laboratory X-ray source on thin slices cut from the centre region of a LFW sample of each material. Use of the Contour Method and hardness profiling also provide valuable information, as texture from the LFW process limits the effectiveness of diffraction based techniques directly at the weld line. Results show stresses near the weld line for the as-welded samples, with higher peak stresses in the Ti-6242 sample. After post weld heat treatment (PWHT) effective for stress relief in Ti-6Al-4V, stresses remain in the Ti-6242. Increasing the temperature by 100°C significantly lowers these stresses. This demonstrates that alloys designed for creep resistance at higher temperature, produce higher residual stresses during friction welding, requiring modified PWHT for effective stress relief.

5:00 PM

Heat-Resistant Titanium with Intermetallic Frame-Dispersion Strengthening: *Yaroslav Yuriyevich Kompan*¹; Alexander Tarasovych Nazarchuk¹; Igor Viktorovych Protokovilov¹; ¹Paton Electric Welding Institute

The present paper is devoted to the magnetohydrodynamic and technological peculiarities of refining and homogenization of a cast structure of solid-solution multi-component heat-resistant titanium alloys with intermetallics. Round and rectangular ingots of these alloys were produced in magnetically-controlled electroslog melting (MEM). The key in the creation of the magnetically-controlled technology of melting of heat-resistant alloys of the new class is the different nature of hydrodynamic control of metal melting and ingot crystallization. The control is realized by external magnetic fields of different directivity, discrete cyclic action of melting electric current, and also by an integrated action of external fields and discrete electric currents. Alloy with a uniform frame and dispersion strengthening was melted on the solid-solution base of alloy VT22 with additions of tin intermetallics. Heat-resistance of this alloy is 330-400 MPa in heating up to 750-800°C.

5:30 PM

Visualization of Three-Dimensional Microstructures Reconstructed from Serial Sections in Ti-6Al-4V-TiB: *Scott I. Lieberman*¹; Arun M. Gokhale¹; Sesh Tamirisa²; ¹Georgia Institute of Technology; ²Ohio University

Discontinuously reinforced titanium matrix composites (DRTi) and modified titanium alloys containing in-situ formed titanium boride whiskers (TiB_w) enhance the mechanical properties relative to unreinforced Ti-6Al-4V at room and elevated temperatures. In the development of these materials, characterization and visualization of the three-dimensional (3D) microstructure is of significant theoretical and practical interest. The properties and performance of the resultant material depend on the attributes of the 3D microstructural geometry. A recently developed montage-based serial sectioning technique has been utilized to visualize and recreate large volumes of 3D microstructure on a millimeter length scale at sub-micron resolution. This technique is useful for detecting and characterizing both short-range and long-range spatial patterns in non-uniform microstructures, and is of relevance for the increasingly diverse potential applications of Ti-6Al-4V-TiB materials.

Ultrafine Grained Materials - Fourth International Symposium: Microstructures and Properties

Sponsored by: The Minerals, Metals and Materials Society, TMS Materials Processing and Manufacturing Division, TMS Structural Materials Division, TMS/ASM: Mechanical Behavior of Materials Committee, TMS: Shaping and Forming Committee

Program Organizers: Yuntian T. Zhu, Los Alamos National Laboratory; Terence G. Langdon, University of Southern California; Zenji Horita, Kyushu University; Michael Zehetbauer, University of Vienna; S. L. Semiatin, Air Force Research Laboratory; Terry C. Lowe, Los Alamos National Laboratory

Tuesday PM
March 14, 2006

Room: 217D
Location: Henry B. Gonzalez Convention Ctr.

Session Chairs: Terry R. McNelley, U.S. Naval Postgraduate School; Hael Mughrabi, Universitaet Erlangen-Nuernberg; David Morris, CENIM; David J. Alexander, Los Alamos National Laboratory

2:00 PM Invited

Microstructural Mechanisms Governing the Fatigue Performance of Ultrafine-Grained Materials: *Hael Mughrabi*¹; Heinz Werner Hoepfel¹; Martin Kautz¹; ¹University Erlangen-Nuernberg

The fatigue behaviours of different ultrafine-grained (UFG) metals and alloys (pure copper, commercial purity aluminium, alpha brass, an age-hardenable aluminium alloy) that were produced by the equal channel angular pressing technique, will be reviewed. Aside from details characteristic of the material considered, one important common finding is that the fatigue life of UFG materials, compared to materials of conventional grain (CG) size, is enhanced in the high-cycle fatigue (HCF) regime but lowered in the low-cycle fatigue (LCF) range. This behaviour is easily understood in a total strain fatigue life diagram. The LCF performance of UFG materials can be improved by a suitable annealing treatment (enhancing the ductility, retaining sufficient strength). However, the LCF performance generally remains below that of the CG materials. The dominant microstructural features of fatigue damage in different UFG materials will be reviewed and discussed with respect to fatigue life.

2:20 PM Invited

Microstructure and Texture Evolution in Commercial Purity Aluminum during High-Pressure Torsion Studied by OIM: *Alexander P. Zhilyaev*¹; Keiichi Oishi¹; Terry R. McNelley¹; ¹Naval Postgraduate School

An investigation was conducted to evaluate the microstructural evolution occurring in disks of commercial purity aluminum processed by high-pressure torsion (HPT) under constrained conditions. Microhardness measurements were taken to assess the variation in hardness across the diameters of disks subjected to different imposed strains and the microstructures were observed at the edges and in the centers of the disks using

transmission electron microscopy. The results show the microhardness is lower and there is less grain refinement in the central regions of the disks in the initial stages of torsional straining but the microstructures become reasonably homogeneous across the disks at high-imposed strains. Thorough OIM study has been performed to reveal a relationship between microstructure and texture forming during high-pressure straining. Comparison with the results of OIM study of ECAP aluminum has been discussed.

2:40 PM Invited

Density of Stacking Faults and Twin Boundaries in Ultrafine-Grained Materials Determined by X-Ray Line Profile Analysis: *Tamás Ungár¹; Levente Balogh¹; Gábor Ribárik¹; Yuntian T. Zhu²; Zenji Horita³; Terence G. Langdon⁴; ¹Eötvös University; ²Los Alamos National Laboratory; ³Kyushu University; ⁴University of Southern California*

It has been reported that planar faults can play an important role in the defect structure in ultrafine-grained materials. The planar fault character (i.e. intrinsic- or extrinsic stacking faults or twin boundaries) can be distinguished by X-ray line profile analysis. Planar faults are crystal defects of "size" character in the sense that the line broadening caused by them is globally diffraction order independent. Line broadening and line shift caused by planar faults is highly anisotropic as a function of the hkl indices. This makes it possible to distinguish the line broadening components corresponding to planar faults, dislocations and subgrain-size. The numerical procedures developed so far for the determination of dislocation structures and subgrain-size are extended for determining planar faults. The defect structure of high pressure torsion specimens is presented with special emphasis on the planar fault structure.

3:00 PM

Effect of Grain Size Refinement and Particle Redistribution on the Mechanical Properties of an Al-7%Si Alloy Processed by Severe Plastic Deformation at Different Temperatures: *Maria Antonia Muñoz-Morris¹; Ivan Gutierrez¹; David Gareth Morris¹; ¹CENIM-CSIC*

The microstructural evolution of an Al-7%Si alloy has been analysed after severe plastic deformation processes carried out both by equal channel angular pressing (ECAP) and forging at 20°C and 200°C. The as-cast microstructure is coarse and has a cellular distribution of Si particles which are broken and redistributed by the severe deformation processes at the same time as the reduction in grain size occurs. The two processes produce, however, different effects with respect to the particle redistribution and morphology of grains and particles which determine the final grain size. The latter reaches values ranging between 150-250 nm in the materials processed at room temperature but are slightly larger at a processing temperature of 200°C. The increase in strength produced by the microstructural refinement has been analysed considering the different parameters leading to hardening in terms of their effectiveness as obstacles for dislocation motion.

3:15 PM

Low-Temperature Consolidation of Ultrafine Grained Al 6061-T6 Produced by Machining: *Balkrishna Rao¹; Richard McMillen¹; W. Dale Compton¹; Srinivasan Chandrasekar¹; Kevin P. Trumble¹; ¹Purdue University*

Plane-strain machining has been used to produce Al6061-T6 particulate having grain sizes less than 100 nm and ~1.5 times higher hardness than bulk 6061-T6. Retaining the ultrafine structure through consolidation to bulk forms requires low-temperature densification/bonding routes. The presentation will focus on two main routes under investigation: room-temperature powder extrusion and polymer bonding. Extrusion of 1:1 blends of Al6061-T6 machining chip particulate and pure Al at room temperature and extrusion ratios up to 42 yielded densities greater than 97%, with intimate bonding as revealed by metallography. Preliminary tensile testing showed little or no plastic elongation, but tensile strengths of 150 to 200 MPa. Several routes for densifying and bonding the chip particles with various epoxy resins will also be presented. Metal fractions greater than 90 vol % have been achieved with no loss of hardness during the epoxy cure. Preliminary modeling on the hardness of these composites.

3:30 PM

Medium Carbon Steel Processed by Warm Equal Channel Angular Pressing: *Jozef Zrník¹; Jaroslav Drnek¹; Ondrej Stejskal²; Sergej*

Dobatkín³; Zbyšek Nový¹; ¹COMTES FHT; ²West Bohemian University; ³MISIS Moscow

In present study, the evolution ultrafine ferrite-pearlite microstructure during thermomechanical(TM)processing and subsequent warm severe deformation ECAP of medium carbon steel AISI 1045 was investigated. In preliminary step of straining very fine microstructure with high degree of strengthening has been achieved by means of a multistep open die forging. Fine dynamically recrystallized structure of ferrite and pearlite mixture with grain size of ~2 µm resulted from hot press forging. The further grain refinement was obtained during severe warm deformation of preliminary forged specimens using ECAP following route Bc. The ECAP was performed with channel of 90 deg at temperature of 400°C and in two cycles (N=2). After the second ECAP pass the substructure was locally depended and presence polygonized substructure and submicrocrystalline structure was observed in strongly extended ferrite grains, and/or areas with desintegrated pearlite. The final mechanical properties of TM treated and ECAP processed specimens were designed.

3:45 PM

Scale-Up Experiments Demonstrate Benefits of ECAE Processing: *Karl T. Hartwig¹; Shabib J Kadri¹; Robert E. Barber¹; ¹Texas A&M University*

The ability of ECAE to induce equivalent plastic strain irrespective of work-piece size is demonstrated. Square cross-section bars of large-grained as-cast CDA 101 Cu having columnar grains of 1-5 mm diameter and 10-20 mm length, and billet widths of 19 mm, 25 mm and 50 mm were extruded at room temperature through routes A, B, C and E for up to eight passes in sliding-wall 90° tooling. Characterization of as-worked and recrystallized microstructures via hardness and microscopy show independence from billet size. Fully worked material exhibits elongated grain fragments with widths of 100-150 nm and lengths of 200-300 nm. The fully-worked/recrystallized material has an average grain size of 4-5 microns. It is concluded that a larger billet cross-section gives greater load efficiency during ECAE processing, and that extrusion routes which incorporate a 90° rotation between passes lead to an increase in load as a result of texture affects.

4:00 PM Break

4:10 PM Invited

The Influence of Coarse Second-Phase Particles and Fine Precipitates on Microstructure Refinement, Structural Stability on Annealing, and Mechanical Properties of a Severely Deformed Al-Mg-Si Alloy: *Maria A. Muñoz-Morris¹; Ivan Gutierrez-Urrutia¹; David G. Morris¹; ¹CENIM-CSIC*

An Al-Mg-Si alloy in various solutionised and aged states was severely plastically deformed. Materials were subsequently annealed and mechanical behaviour examined. Microstructural refinement and strengthening occur faster in the presence of particles. Coarse particles remain unaffected by severe deformation, and help stabilise the deformation microstructure, while fine precipitates dissolve. Microstructural refinement and strengthening depends more on solute content than on particle distributions. Solute precipitates on annealing, irrespective of the initial material state, but these particles play only a small role in stabilising deformation substructure. After significant particle and grain coarsening occurred, discontinuous grain coarsening may occur. Material strength is examined in terms of the contributions of loosely-arranged dislocations, many grain boundaries, and dispersed particles. Dislocation strengthening is significant in as-deformed and lightly annealed materials, with grain boundary strengthening providing the major contribution thereafter. Particle strengthening is not generally as important here as the other two strengthening contributions.

4:30 PM Invited

Formation Mechanism of Dimpled Fracture Surfaces of Nanocrystalline Materials: *Zhiwei Shan¹; J. A. Knapp²; D. M. Follstaedt²; Jorg Michael Wieszorek¹; Eric A. Stach³; Scott X. Mao¹; ¹University of Pittsburgh; ²Sandia National Laboratories; ³Purdue University*

Dimple features much larger in size than the average grain size are often observed at the fracture surface of three dimensional nanocrystalline materials, but their formation mechanism is currently unclear. This study demonstrates that the in situ tensile straining transmission electron microscopy (TEM) technique can be used to reveal the underlying physical mechanism for the formation of the dimple features. At the onset of defor-

TUESDAY PM

mation of nanocrystalline Ni, we found that grain agglomerates with sizes much larger than the average grain size formed very frequently and rapidly in many locations, apparently independently of one another. HRTEM observations suggested that the grains in those grain agglomerates are most probably separated by low angle grain boundaries. Furthermore, both inter- and intra- grain agglomerate fractures were observed. Sandia is a multiprogram laboratory operated by Sandia Corporation, for the United States DOE's National Nuclear Security Administration under contract DE-AC04-94AL85.

4:50 PM Invited

Parameters Influencing the Limits of Microstructural Fragmentation during Severe Plastic Deformation: *Andreas Vorhauer*¹; Reinhard Pippan¹; ¹Austrian Academy of Sciences

Severe Plastic Deformation (SPD) is an effective method to produce ultra fine grained materials in bulk dimensions. In certain cases, many authors reported about the possibility to obtain submicrometer or even nanometer scaled microstructures in initially recrystallized, coarse grained base materials. This phenomenon is now well known since about more than ten to fifteen years. However, despite the continuously growing number of publications aimed to this topic and the increasing number of institutes, which are engaged in this field of materials science, the parameters, which are influencing the limits of microstructural fragmentation during severe plastic deformation at large strains, are still not fully understood. The aim of this paper is to gain a better understanding of such parameters, which are may be influencing the microstructural fragmentation and its saturation at large strains. Therefore, SPD by means of a high quality High Pressure Torsion tool was applied at different temperatures (between 77K and 723K), strain rates (between 2.5×10^{-3} and 6.5×10^{-2} s⁻¹), hydrostatic pressures (between 0.85 and 5.4 GPa) on a wide range of different materials (pure metals: copper, iron, titanium, aluminium, molybdenum, nickel; technical relevant high alloyed steels: austenitic and ferritic steel). Measurements of flow curves in-situ during SPD have shown that a saturation of flow stress without any further work hardening is obtained at large strains, when SPD is performed at low homologous temperatures. At higher processing temperatures, the flow curves show a distinct maximum followed by a drop when strain exceeds the peak strain. These results, together with microstructural investigations in the scanning electron microscope (capturing of back scattered electron micrographs and orientation maps) at peak strain (maximum stress or plateau stress) have clearly shown, that the properties obtained by SPD are significantly dependant on parameters such as the homologous temperature and strain rate of materials processing and the purity of the material itself, whereby the applied hydrostatic pressure affects the results only for a small extent.

5:10 PM Invited

Preparing Multi-Component Hard Materials through Severe Plastic Deformation: *Jacob Chih-Ching Huang*¹; C. J. Lee¹; C. H. Chuang¹; ¹National Sun Yat Sen University

It is intended to prepare much harder materials of multi-elements or multi-components through friction stir processing (FSP) or accumulative roll bonding (ARB). The first trial is to add 1-10% nano ceramic particles into the soft AZ61 Mg alloy via four FSP passes. The Hv hardness of the resulting nano-composites reaches over 110. The second trial is to fabricate multi-element intermetallic alloys of Mg50-80Al10-25Zn10-40 by three FSP passes. The Hv hardness of the resulting intermetallic alloys varies from 140 to 350. The third trial is to prepare the nanocrystalline and amorphous Zr based alloys through room temperature ARB from various elemental foils. After 40-100 ARB cycles, the elemental foils are refined into nanocrystalline phases and eventually transformed into amorphous alloys. The Hv hardness varies from 200 to over 500. The characterization of microstructures and mechanical properties of the resulting hard materials will be presented.

5:30 PM

Production of Ultrafine-Grained Copper by Cryogenic Torsion: *David J. Alexander*¹; ¹Los Alamos National Laboratory

High-purity copper was strained at cryogenic temperatures by performing torsion of samples immersed in liquid nitrogen. The samples had a gage length of 51 mm and a diameter of 12.7 mm. Up to 16 rotations were applied before failure. Several combinations of forward and reversed tor-

sion with a cumulative strain equivalent to 16 complete forward rotations were examined, including no reversals, a single reversal, and 8 reversals. Thin slices were taken from the deformed gage section, and heat-treated for various combinations of time and temperature. The resultant microstructures were examined by optical and scanning microscopy, and orientation imaging microscopy was used to determine the texture. The effect of strain, the number of strain reversals, and heat treatment conditions on the texture and grain size distribution will be discussed.

5:45 PM

Microstructural Development of "Recycled-Like" Alloys during ECAP – Particle Break-Up, Phase Transformations and Mechanical Properties: *Przemyslaw Szczygiel*¹; Hans J. Roven¹; ¹Norwegian University of Science and Technology

As a part of a comprehensive research program on recycling of aluminium, the present work deals with microstructural development of two generic alloys with recycled-like chemistries during severe plastic deformation (ECAP). Influence of deformation routes A and B were investigated, i.e. the microstructure evolution under different shearing patterns. Particle behaviour under complex stress conditions in the die corner was investigated and both qualitative and quantitative descriptions of the particle break-up processes are presented. Size distributions of different phases are given based on 2D image analysis and 3D measurements of particles extracted from the matrix using the "buthanol method". Some indications of possible pressure induced phase transformations are discussed. The influence of particles on deformation mechanisms, grain size distribution and evolution of grain boundaries was characterized applying HR-SEM and TEM. Post ECAP mechanical properties are examined and correlated with observed microstructure characteristics.

Ultrafine Grained Materials - Fourth International Symposium: Poster Session

Sponsored by: The Minerals, Metals and Materials Society, TMS Materials Processing and Manufacturing Division, TMS Structural Materials Division, TMS/ASM: Mechanical Behavior of Materials Committee, TMS: Shaping and Forming Committee

Program Organizers: Yuntian T. Zhu, Los Alamos National Laboratory; Terence G. Langdon, University of Southern California; Zenji Horita, Kyushu University; Michael Zehetbauer, University of Vienna; S. L. Semiatin, Air Force Research Laboratory; Terry C. Lowe, Los Alamos National Laboratory

Tuesday 5:15-7:00 PM

Room: 217D

March 14, 2006

Location: Henry B. Gonzalez Convention Ctr.

Influence of Equal Channel Angular Extrusion Processing Routes on Consolidation of Intermetallics: *Anumalasetty Venkata Nagasekhar*¹; *Yip Tick-Hon*¹; ¹Nanyang Technological University

Equal channel angular extrusion is the most promising severe plastic deformation technique for the fabrication of bulk ultrafine grain materials, and for consolidation of ultrafine powders. Thus, it has potential to enhance both physical and mechanical properties of the processed materials. In the current study an attempt was made to consolidate the recently invented intermetallic superconductor, magnesium boride (MgB₂). By using commercial MgB₂ powder as core and low carbon steel tube as the sheath, ECAE consolidation was carried at room temperature up to four passes via different processing routes: Route A, Route BC, Route BA, and Route C. Influence of processing route on consolidation was characterized in terms of density, and micro-hardness measurements. Consolidation force requirements for different passes were also calculated. Higher densification was achieved via Route A, and lower densification was achieved via Route BC. The result shows that ECAE offers a new possibility for the consolidation of intermetallic superconductors.

Deformation Resistance of Ultrafine-Grained Copper at Elevated Temperature: *Yujiao Li*¹; *Rajeev Kapoor*¹; *Jingtao Wang*¹; *Wolfgang Blum*¹; ¹University of Erlangen

The deformation resistance (flow stress, creep rate) of ultrafine-grained (UFG) Cu produced by equal channel angular pressing on route B_C at

room temperature is investigated at elevated temperature (100 to 200 °C). Compared to coarse-grained (CG) Cu the UFG Cu is stronger at small strains, but softer at large strains, due to its large content of high-angle grain boundaries. The virtual absence of small-angle grain boundaries in UFG Cu is apparent from TEM observation as well as from the absence of the pronounced transients upon change of deformation conditions. There is a distinct softening of UFG Cu with strain during deformation at elevated temperature beyond the maximum deformation resistance. The microstructural reasons for this softening and the resistance of UFG Cu against creep and stress relaxation are addressed.

Deformation Resolution of Aluminidies of Transition Metals by Severe Plastic Deformation: *Irina Grigorjevna Brodova*¹; Irina Gennadjevna Shirinkina¹; Irina Petrovna Lennikova¹; Valery Aleksandrovich Shabashov¹; ¹Institute of Metal Physics

A special interest for studies has a deformation resolution of stable and metastable aluminidies of twice phase Al alloys with transition metals (Zr, Fe, Cr) by severe plastic deformation. It was determined a kinetic of deformation dissolution of the Al7Cr and Al13Fe4 stable aluminidies and the Al3Zr and Al6Fe metastable intermetallic-compound crystals. It was established that metastable crystals of Al3Zr fully dissolved in Al matrix and super saturated Al-base solid solution with ultra microcrystalline structure was formed in the Al-Zr alloy. Another aluminidies destroyed and only partly dissolved in Al matrix. After HPT these sizes decreased up to 10–20 nm and they regular distributed in ultra microcrystalline Al matrix. The hardness of these materials very high – 2000–3000 GPa. According the Mössbauer spectroscopy data, HPT results to changes in the phase composition of structure constituents in the Al-Fe alloys.

Effect of Severe Plastic Deformation on Internal Friction in Fe3Al, AZ31 and Titanium Alloys: *Igor Stanislavovich Golovin*¹; ¹Technical University

In the past, several attempts were undertaken to study anelastic properties of metals whose ultra fine grain structure was produced by severe plastic deformation (SPD). With rare exceptions, in most of them grain boundary effects were considered at elevated temperatures. Here we present mechanical spectroscopy data on low-temperature dislocation- and point-defect-related anelasticity of three materials: Fe-26Al and Ti deformed by high pressure torsion and Mg alloy AZ31 deformed by equal channel angular pressing. Several internal friction peaks with the activation energy in the range of 0.35–0.55 eV were found to be introduced or significantly enhanced by SPD. At least some of these peaks can be classified as Hasiguti peaks. Since the internal friction peaks observed are caused by different crystal lattice imperfections, which have different thermal stability, the mechanical spectroscopy provides a useful tool for studying early annealing stages of SPD processed alloys.

Effect of Very High Straining on the Stress-Strain Behavior of a Zinc-Aluminum Alloy: *Praveen Kumar*¹; Cheng Xu¹; Terence G. Langdon¹; ¹University of Southern California

Specimens of the Zn–22% Al eutectoid alloy were processed by equal channel angular pressing (ECAP) through various numbers of passes up to a maximum of 24 passes at 473 K. Tensile specimens were cut from the unpressed and as-pressed billets and they were tested at strain rates of 1.0×10^{-2} and $1.0 \times 10^{-3} \text{ s}^{-1}$ at room temperature. The tensile tests show that higher elongations are recorded in the specimens processed by ECAP. However, samples processed through a very large number of passes show neither more strain hardening nor higher fracture strain than the samples processed through a small number of passes. This result is attributed to the relatively low melting temperature of the alloy since room temperature corresponds to a homologous temperature of about 0.4.

Effects of the Number of Equal-Channel Angular Pressing Passes on the Strain Rate Sensitivity of Ultrafine Copper: *Alexander Korshunov*¹; Lev Polyakov¹; Irina Vedernikova¹; Tamara Kravchenko¹; Irina Korotchenkova¹; Andrey Smolyakov¹; Vyacheslav Soloviev¹; ¹RFCN-VNIEF

Annealed tough-pitch copper was processed by eight passes of equal-channel angular pressing (ECAP) using two routes, BC and C. Pressed samples had a square section with a side length of 8 mm. Tensile tests were performed at static loading with strain rate variation by three orders. The material was examined in the as-received condition and after 1, 4 and

8 passes. All standard mechanical properties (conventional yield strength, tensile strength, elongation and contraction) were determined, and conditional and true deformation curves were plotted. Strength properties (conventional yield strength and tensile strength) in all cases grow as the strain rate increases, and plastic properties (elongation and contraction) remain practically the same, except for contraction after 8 ECAP passes, which grows as the strain rate increases. The strain rate sensitivity coefficient was found to grow with the number of ECAP passes.

Experimental Study and Computer Modeling of SPD Shape Forming Process of UFG CP Ti: *Vladimir Latysh*¹; Gyorgy Krallics²; Irina Semenova³; A. Fodor²; Igor V. Aleksandrov³; ¹INTC; ²Budapest University of Technology and Economics; ³Ufa State Aviation Technical University

Numerous experimental studies proved the efficiency of severe plastic deformation (SPD) realized by equal channel angular pressing (ECAP) used for producing bulk ultrafine-grained (UFG) CP Ti billets. However, the successful implementation of the method into the commercial production implies the satisfaction of various requirements to the technological processes. In particular, the most important parameters to be achieved are the decrease in the number of ECAP passes, fabrication of billets with the increased relation between the length and the size of the cross section, enhancement of structure and properties' homogeneity over the whole volume of processed billets. This report presents the results of experimental studies and computer modeling, aimed at the optimization of SPD regimes realized by the combination of ECAP and further broaching. The described approach enabled to find the optimal regimes and produce bulk billets with homogeneous UFG structure and extraordinary properties.

Fatigue Properties of Forged AA6061 after Severe Plastic Deformation: *Balakrishna Cherukuri*¹; Prabir Kanti Chaudhury²; Rob Mayer³; Raghavan Srinivasan¹; ¹Wright State University; ²Orbital Sciences Corporation; ³Queen City Forging Company

Severe plastic deformation (SPD) has emerged as a promising technique for creating ultra fine grained metals and alloys, with grain sizes of a micrometer or less. Mechanical properties of forged AA 6061 after severe plastic deformation was investigated. AA 6061 samples in solutionized (W) condition and in annealed (O) condition are severely deformed by Equal Channel Angle Pressing to produce ultrafine grain material of the order of 0.5 micron grain size. The SPD processed material was successfully forged at 650F and 700F as compared to the conventional forged material at 850F. Tensile, hardness and fatigue properties of the forged SPD material is compared against the conventional material. The results show marked difference between the starting material and the severely deformed ultrafine grain material. The results of this investigation will be presented in the light of enhanced properties and processing cost savings for industrial application of SPD material.

High Energy Milling as a Route for Obtaining Ultrafine Grained Duplex Stainless Steel: *Oswaldo Mitsuyuki Cintho*¹; Cleverson Moinhos¹; Evaldo Toniolo Kubaski¹; José Deodoro Trani Capocchi¹; Eduardo Franco Monlevade¹; ¹State University of Ponta Grossa

In the present study, Iron, Chromium and Nickel powders were mixture (Fe-19.5%Cr-5.0%Ni) and submitted to high energy milling in an Attritor type mill, with a ball-to-powder ratio was 50:1. Millings were conducted for 5, 9 and 15 hours under Argon atmosphere. After milling, even for long times, particles have a plate-like morphology. For longer milling times, microscopic platelike particles group into equiaxial agglomerates. The milled samples were then uniaxially pressed into pastilles form and heat treated for 1 hour at 900, 1050 and 1200°C. A complete dissolution reaction of Chromium and Nickel was only observed in the 15 hour milling samples. As a result, an ultra-fine grained (ca. 1 mm) duplex stainless steel sample was obtained in the samples treated at 1200°C. For shorter milling times, Chromium dissolution was shown to be substantially delayed when compared to Nickel dissolution in Iron.

Inhomogeneous and Anisotropic Deformation Behavior and Strain Hardening of Ultrafine-Grained Aluminum by ECAE: *Stijn Poortmans*¹; Fouad El Houdaigui²; Anne-Marie Habraken²; Bert Verlinden¹; ¹Katholieke Universiteit Leuven; ²University of Liège

Hot-rolled AA1050 commercial pure aluminum was deformed by ECAE at room temperature following route BC for 8 passes. Mechanical testing

at room temperature on both hot-rolled aluminum and aluminum after ECAE consisted of uniaxial tension, axisymmetric compression and shear by torsion. The phenomenological Hill's criterion identified from texture data accounts for the observed tension-compression asymmetry due to ECAE and predicts torsion yielding close to measurements. FE simulations of the compression tests are performed with Hill model or Minty micro-macro model and coupled with an isotropic Voce saturation hardening law. These simulations compute the inhomogeneous behavior due to barreling, the observed sample anisotropy and the force-displacement curve. Comparisons of numerical and experiments results provide a first identification of the hardening parameters and the friction coefficient during compression tests. Finally a general hardening model is proposed accounting for the softening during tensile tests and stress saturation in compressive and torsion tests.

Mechanical Alloying and Related Solid-State Flow and Mixing of Single-Crystal Tungsten Ballistic Penetrator and Steel Target Material: Carlos Pizana¹; Lawrence E. Murr¹; Aditya Putrevu¹; Thomas L. Tamoria²; H. C. Chen²; S. J. Cytron³; ¹University of Texas; ²General Atomics; ³U.S. Army

In this study optical metallography and SEM analysis (including elemental X-ray mapping) in combination with microhardness maps have elucidated the dynamically recrystallization (DRX)-facilitated flow and interaction of steel targets with penetrating, clad and unclad [001] single-crystal W long rods impacting at initial velocities ranging from 1 to 1.3 km/s. The ultra-fine DRX regime composing adiabatic shear zones in both the penetrator and target allows for mechanical mixing of the W and Fe in complex flow regimes which, in the extreme, melt in localized regions at the projectile/target interface, creating intermetallic phases within the intercalated flow zones. Optical metallographic observations also suggest that the addition of clad material to the projectile could contribute to the penetration deformation and to the projectile/target interaction and therefore the overall performance of the ballistic penetrator. (Supported by the U.S. Army-Picatinny Arsenal, prime Contract No. W15QKN-04-M-0267, project No. 1A4CFJER1ANG).

Mechanical Behavior and Microstructural Evolution in ECAP Copper: Anuj Mishra¹; Bimal Kad¹; Fabienne Gregori²; Robert Asaro¹; Morgana Martin³; Naresh N. Thadhani³; Marc A. Meyers¹; ¹University of California; ²Laboratoire des Propriétés Mécaniques et Thermodynamiques des Matériaux - CNRS; ³Georgia Institute of Technology

Microstructural evolution during ECAP has been investigated using TEM and EBSD techniques. Results on quasi-static compression and tensile tests, dynamic compression using Hopkinson bar and Reverse Taylor tests on ECAP samples after different number of passes (initial, 2, 4 and 8 passes) are presented. Saturation in hardness after 10 ECAP passes is shown to exist indicating a lower limit to the grain size that can be achieved using this technique. Deformation mechanisms in ultra-fine grained materials (grain size >100 nm) as produced by ECAP are discussed and compared with the ones that operate in the nanocrystalline regime (grain size < 100 nm).

Effect of Temperature on the Mechanical Properties of Bulk Nanocrystalline Ni Prepared by Electrodeposition: Anna Torrents¹; Manish Chauhan¹; Farghalli A. Mohamed¹; ¹University of California

Variation in the hardness as a function of temperature in bulk nanocrystalline Ni having an average initial grain size of 20 nm, prepared by an electrodeposition technique, has been investigated by nano and microindentation. Hardness measurements were conducted on these 20 nm samples which were annealed at different temperatures, ranging from 323–1173 K, for various annealing times. It has been found that the hardness of the material increases with an increment in the annealing temperature and reaches its maximum value at 493 K, and decreases thereafter with further increase in the annealing temperature. This increase in the hardness until 493 K can be attributed to the relaxation of internal stresses around grain boundaries and triple junctions, and the bimodal grain size distribution obtained at this low annealing temperature.

Microstructure and Tensile Properties of Ultrafine Grained Pure-Ti: Young Gun Ko¹; Dong Hyuk Shin²; Chong Soo Lee¹; ¹Pohang University Science and Technology; ²Hanyang University

A study was made to investigate microstructural evolution and mechanical properties of ultra-fine grained (UFG) pure-Ti produced by equal channel angular (ECA) pressings. The deformed structures were analyzed by finite element method and transmission electron microscopy with the increment of straining. After 4 isothermal ECA pressings, initial coarse grains (30 μ m) were significantly refined to ~0.3 μ m with homogeneous distribution of microstructure which was resulted from 180° rotation of the sample between pressings. UFG pure-Ti exhibited the considerable improvement in yield strength while losing strain hardening capacity as compared to coarse grained microstructure at ambient temperature, which was mainly attributed to ultra-fine grain microstructure with non-equilibrium grain boundaries. Such high strength and unusual strain hardening behavior of UFG pure-Ti were discussed in relation with two dislocation models based on dislocation bow-out and dynamic recovery associated with trapped lattice dislocations.

Modeling of Grain Refinement and Texture Evolution during Equal-Channel Angular Pressing by Means of Combined Visco-Plastic Self Consistent/Disclination Model: Airat A. Nazarov¹; Igor V. Aleksandrov¹; Irene J. Beyerlein²; Nariman A. Enikeev¹; Tatiana S. Orlova³; Alexei E. Romanov³; ¹Ufa State Aviation Technical University; ²Los Alamos National Laboratory; ³Ioffe Physico-Technical Institute, Russian Academy of Sciences

Disclination model of grain subdivision incorporated into the viscoplastic self-consistent (VPSC) modeling of plastic deformation is used to simulate the grain refinement during equal-channel angular pressing (ECAP). Strain incompatibilities between a homogeneous effective medium and a grain calculated by VPSC are assumed to result in an accumulation of disclinations at the grain junctions. The stresses of these disclinations are then relaxed by growth of low-angle dislocation boundaries from the junctions. These boundaries split the grain into smaller, mis-oriented volumes which, with further deformation, can lead to its subdivision into new grains. The applied ECAP deformation histories are given by either a simple shear model, a fan model, or by finite element method calculations. The corresponding evolution of microstructure and texture during different ECAP routes are simulated. The calculated texture and intragrain misorientations evolution are found to be in good agreement with experimental data.

Modelling of Stress-Strain Distribution in ECAE by Analytical-Experimental Method: Georgy Iosifovich Raab¹; Rimma Lapovok²; ¹UFA State Aviation Technical University; ²Monash University

It is believed, that uniform simple shear is realized during ECAE resulting in uniformity of the stress-strain distribution and mechanical properties. However, some experimental facts as well as Finite Element (FE) simulation confirm a more complicated and non-uniform strain mode. Despite increased efficiency of FE packages accounting for temperature, friction condition, tooling configuration and complicated constitutive models, the finite shear strain can not be precisely simulated by plastic flow or incremental models. The simple and precise analytical-experimental method for direct evaluation of strain distribution during shear deformation, namely the combined grid method was adopted in this study. This paper describes the theoretical principles, the grid patterns and the calculation of the strains based on the grid node displacements and calculation of stress resulting on integration of equilibrium equations along flow lines. Results are compared with those of FE simulation.

Nanostructure Formation Induced by Explosively Driven Friction: Hong Jin Kim¹; Andrew Emge¹; Karthikeyan Subramanian¹; David Rigney¹; Peter Keightley²; Ron Winter²; ¹Ohio State University; ²Atomic Weapon Establishment

There has been a surge of interest in ultrafine and nanograin microstructures formed by severe plastic deformation (SPD) methods such as Equal Channel Angular Pressing (ECAP), High Pressure Torsion (HPT), Repetitive Corrugation and Straightening (RCS) and even simple sliding. Explosively driven friction testing is a novel technique developed at the Atomic Weapon Establishment to produce large plastic strains in a short time. These tests involve driving a pair of metals obliquely against each other in a confined sleeve at velocities of 50-200 m/s. The metal-pair used here is aluminum/steel. Post-test characterization techniques such as Scanning Electron Microscopy (SEM), Focused Ion Beam (FIB) imaging and

Transmission Electron Microscopy (TEM), conducted at The Ohio State University, revealed SPD occurring on the aluminum side. The bending of fiducial line markers suggest large plastic strains (>14) adjacent to the sliding interface and this is structurally manifested by the formation of nano-scale structure.

Numerical Simulations of the ECAE Process Multi Pass: *Andrey Smolyakov*¹; Alexander Korshunov¹; Vyacheslav P. Solovyev¹; ¹RFNC-VNIIEF

Numerical simulations of ECAE process carried using DRACON code (VNIIEF) based on variation-difference method of solving continuum mechanics equations have shown that satisfactory agreement between experimental and numerical data on deformed billet state can be achieved by using experimental data in the development of physical model. Issued analysis of passes number influence on uniform state in ECAE.

Processing of Long-Length Rods of TiNi Alloys with the UFG Structure and Increased Properties Using Multi-Step SPD Processing: *Dmitry Valerievich Gunderov*¹; Vladimir Latysh²; Vladimir Pushin³; Alexander Lukyanov¹; Irik Kandarov²; Ruslan Valiev¹; ¹Ufa State Aviation Technical University; ²INTC "Iskra"; ³Institute of Physics of Metals

As the investigations have shown, formation of UFG structure by ECAP allows increasing strength and instrumental properties of TiNi alloys with shape memory effect (SME). But ECAP allows to process only cylindrical samples with the diameter 20-40 mm and the length up to 200 mm. However TiNi alloys are most widely used in medicine as pieces of thin rods and wire. Multi-step SPD processing that consists of the combination of ECAP, forging and drawing was applied to Ti49.4Ni50.6 alloy. As a result integral rods with the length up to 800 mm, diameter 6 mm and NC structure were successfully obtained. The given results show that the chosen treatment modes allowed to change the shape of an ECAP-billet and process integral long-length rods of NC TiNi alloy with high level of strength - 1400 MPa, that respectively implies high level of instrumental characteristics of SME.

Production of Ultrafine Grained Ferrite Structure through Multi-Pass Warm Caliber Rolling: *Venkata Suryanarayan Susarla Murty*¹; Shiro Torizuka¹; Akio Ohmori¹; Kotobu Nagai¹; ¹National Institute for Materials Science

Ultrafine grained steel bars having a cross section of 18mm square were fabricated through a multi-pass warm caliber rolling for a 0.15%C-0.3%Si-1.5%Mn steel. Average ferrite grain sizes of 0.43 μm, 0.70 μm and 1.2 μm were obtained in the isothermal rolling processes at 773K, 823K and 873K respectively. Even though caliber rolling results in inhomogeneous strain distribution, multi-pass caliber rolling to large accumulated strains of 2 or 3 can be uniformly introduced in to bar samples. Strain accumulation due to multi-pass warm deformations was confirmed by comparing microstructural evolution through multi-pass deformation with that of single pass deformation. The hardness and the evolved grains size of the ultrafine grained structures formed through severe warm deformation depend on the Zener-Hollomon parameter. The similarity of the microstructural evolution with single pass deformation reveals that the multi-pass warm deformation is an effective method to obtain ultrafine grained ferrite structure in bulk materials.

Structure of Ti-5Al-5Mo-5V Alloy Deformed by Heat Twist Extrusion: *Tatyana Alexeevna Ryumshyna*¹; G. K. Volkova¹; L. V. Loladze¹; T. E. Konstantinova¹; V. N. Varyukhin¹; ¹Donetsk Physics and Technology Institute

X-ray, optic metallography, has investigated features of the structure formed under heat twist extrusion in Ti-5Al-5Mo-5V alloy. The twist extrusion was realized after annealing of samples in one-phase state (100% β). After a heat annealing at same conditions the a - phase precipitations were obtained in number 49% and one had an elliptical form 5 μm in size. The morphology of structure had been changed essentially after twist extrusion. The part of the precipitated a - phase was 55%. Two types of precipitations had observed: thin layers of deformation martensite and fine dispersed precipitations up to 300 nm in size. The forming by twist extrusion the structure with ultra fine precipitations of a - phase in β - grain leads to a reduction of strength and to a rise plasticity.

Microstructural Refinement of Ti Billets by Equal Channel Angular Pressing: *Vladimir Latysh*¹; Gulnaz Salimgareeva²; Irina Semenova²; Irek Kandarov¹; Ruslan Valiev²; Yuntian Theodore Zhu³; ¹Innovative Scientific Technological Centre "Iskra"; ²Ufa State Aviation Technical University; ³Los Alamos National Laboratory

Preliminary deformation is one of the ways to increase the efficiency to refine bulk billets microstructure at equal channel angular pressing (ECAP). In the present paper preliminary deformation by isothermal forging in special heads has been used for CP Ti Grade 2 billets with diameter 40 mm. The investigations of microstructure evolution and mechanical properties of the billets during the forging and further ECAP after 1, 2, 3, and 4 passes have been carried out. It has been shown that decrease in the initial grain size from 50 to 1 μm already after 2 ECAP passes makes it possible to form a uniform equilibrium ultrafine-grained structure with average grain size of a-phase 0.6 μm compared to the grain size after 8 ECAP passes without the preliminary deformation. Moreover, this kind of treatment has allowed increasing Ti strength up to 750 MPa in contrast to 680 MPa after 8 ECAP passes.

Superplastic Behavior of Ultrafine-Grained Ti-6Al-4V ELI Processed by Severe Plastic Deformation: *Irina Semenova*¹; Liliya Saitova¹; Georgy Raab¹; Ruslan Valiev¹; Terry C. Lowe²; ¹Ufa State Aviation Technical University; ²Los Alamos National Laboratory

The present paper considers the investigation results of the Ti-6Al-4V ELI alloy mechanical behavior in both coarse-grained and ultrafine-grained (UFG) state at elevated temperatures (500-800°C). It has been shown that combined severe plastic deformation induced by equal-channel angular pressing in combination with the further extrusion resulted in a considerable enhancement of Ti-6Al-4V ELI superplastic behavior. The Ti-6Al-4V ELI alloy demonstrates the superplastic characteristics even at 600°C. The following elongation parameters have been processed at relatively low temperatures and high strain rates: 286% at T = 700°C, strain rate = 10⁻² s⁻¹ and 516% at T = 800°C, strain rate = 10⁻² s⁻¹. It has been established that UFG Ti-6Al-4V ELI after superplastic deformation demonstrates the extraordinary strength value of 1500 MPa at room temperature.

Theory of Non-Equilibrium Grain Boundaries and Its Application for Nano- and Microcrystalline Materials: *Vladimir N. Chuvil'deev*¹; ¹Physical-Technical Research Institute of Nizhny Novgorod State University

Basic principles and methods of non-equilibrium grain boundary theory are considered. Concepts according to which the non-equilibrium grain boundary state depends on the grain boundary free volume changes caused by their interaction with lattice defects, in particular with dislocations, are in the basis of the theory. Non-equilibrium states of the grain boundaries in microcrystalline metals and alloys processed by equal channel angular pressing were analyzed. It was shown that non-equilibrium grain boundary state in microcrystalline materials can be provided by initial non-equilibrium state, as well as by non-equilibrium state caused by embedding dislocations into the boundary during grain boundary migration and/or materials deformation. Influence of the non-equilibrium grain boundary state on recovery, recrystallization, grain boundary sliding, solid solution decomposition and second phase particles precipitation in microcrystalline Al-Mg-Sc, Al-Zn-Mg-Sc, Mg-Al-Zn and Cu-Cr alloys is investigated. This research was supported by International Scientific and Technical Center (Grant No. 2809).

Ultrafine Grained Magnetic Shape Memory Ni2MnGa – Based Alloys: *Vladimir Pushin*¹; Nikolay Kourov¹; Alexander Korolev¹; Ludmila Yurchenko¹; Dmitry Gunderov²; Ruslan Valiev²; Yuntian Theodore Zhu³; ¹Institute of Metal Physics; ²Ufa State Aviation Technical University, Institute of Physics of Advanced Materials; ³Los Alamos National Laboratory

In this work we report the results of investigations of ferromagnetically ordered Heusler Ni2MnGa-based alloys. Our recent studies have shown that superrapid solidification (SRS) from melt and severe plastic torsion deformation (SPD) under high pressure could be effectively used for formation of homogeneous ultrafine grained structures (nano- and submicrocrystalline) and even amorphous state in alloys. For the first time nanostructured alloys were produced using complex combined methods (SRS+SPD+thermotreatment). Structural states and their thermal stabil-

ity, and also martensitic transformations have been analyzed by X-ray and neutron diffraction and transmission electron microscopy. We identify in submicro-SRS and nano-SPD alloys a premartensitic state, structures of the low-temperature 5M and 7M martensites and their temperature evolution. The physical properties were determined by measuring of electrical resistance, magnetic susceptibility and dilatometry. We also demonstrate in this work that mechanical and shape memory properties can be enhanced essentially by forming ultrafine grained structures in these alloys.

Thermomechanical Conditions of Nanocrystalline Structure Formation and Functional Properties of Severely Deformed Ti-Ni Shape Memory Alloys: Sergey Prokoshkin¹; Irina Khmelevskaya¹; Sergey Dobatkin²; Irina Trubitsyna¹; Evgeny Tatyannin²; Sylvain Turenne³; Vladimir Brailovskii⁴; Vladimir Stolyarov⁵; Egor Prokofiev⁵; ¹Moscow State Steel and Alloys Institute; ²Baikov Institute of Metallurgy and Material Science of RAS; ³Ecole Polytechnique de Montreal; ⁴Ecole de Technologie Supérieure; ⁵Institute of Physics of Advanced Materials

Structure formation under conditions of high pressure torsion in dependence on deformation temperature, pressure and post-deformation annealing in Ti-Ni-based alloys were studied. The tendency to form an amorphous structure under SPD conditions depends on relative positions of the deformation temperature and M_s temperature. The upper limiting deformation temperatures for amorphous and nanocrystalline structures formation were determined for aging and non-aging Ti-Ni alloys. To obtain a nanocrystalline structure under equal-channel angular pressing (ECAP), the ECAP temperature should be below 350°C. As a result of ECAP of Ti-Ni alloys at 350-500°C in 6-8 passes, a submicrocrystalline austenite structure was obtained with the grain size of 0.1-0.2 microns after ECAP at 350°C, 0.2-0.4 microns after ECAP at 450°C and 0.3-0.5 microns after ECAP at 500°C. The highest functional properties were obtained after ECAP at 350°C which exceed the properties provided by traditional thermomechanical treatment.

Combined Reaction Processing of FePd Intermetallics with UFG Microstructure: Anirudha R. Deshpande¹; Andreas Kulovits¹; Vincent M. Sokalski¹; Paul Ohodnicki²; Jorg Michael Wieszorek¹; ¹University of Pittsburgh; ²Carnegie Mellon University

It has been shown in numerous works that ordering heavily deformed Fe-50at%Pd via a combined reaction transformation mode leads to a ultra-fine grained equiaxed structure with enhanced magnetic properties as compared to the polytwinned micro - constituent that forms upon conventional ordering of undeformed γ Fe-50at%Pd. In this study a Fe-50at%Pd alloy was severely plastically deformed in the austenitic γ - FePd state by an equal channel angular pressing or ECAP operation. The structural evolution of the phase - transformation was investigated by means of XRD, SEM and TEM and compared to the combined reaction product of heavily rolled Fe-50at%Pd. The differences in texture evolution during the solid state reactions after different processing routes were measured. The change in magnetic properties during the phase - transformation mode was monitored via VSM. The magnetic domain structure was measured and correlated to the underlying microstructure by means of MFM and AFM.

Effect of Strain Path on Grain Refinement of Aluminum Sheet: Tetsuo Sakai¹; Koki Mori¹; Hiroshi Utsunomiya¹; Eimei Nakayama¹; ¹Osaka University

It is known that recrystallization behaviors of work hardening materials are influenced by not only the amount of strain but also the mode of strain. In the present study, 3 different modes of deformation - only compression, only shear, and the combination of compression and shear - are introduced into commercially pure aluminum sheet, and then we studied about the effects of deformation mode on recrystallization temperature, recrystallization grain size, and texture. In the case of constant annealing temperature, compared with only shear and only compression of single strain mode, material of combination strain mode has smaller recrystallization grain size. According to this result, combination strain sample has lowest annealing temperature in the three samples. These results show that the deformation of different strain mode promotes the refinement of recrystallization grain.

Grain Refinement Limit during ECAP-Deformation: Vladimir I. Kopylov¹; Vladimir N. Chuvil' deev²; ¹Physico-Technical Institute, Na-

tional Academy of Sciences of Belarus; ²Physical-Technical Research Institute of Nizhny Novgorod State University

The purpose of the present investigation is to determine minimum grain size which can be achieved using intensive plastic deformation. The investigations of the grain refinement limit D_m , which can be attained by ECAP-deformation, were carried out for pure metals, Al-alloys, Fe-Ni alloys and other materials. The experiments have shown the magnitude D_m for metals is varied in the interval 80-200 nm and depends mainly on the ECAP-deformation temperature, strain rate and diffusion parameters of materials. The model of grain refinement limit based on the theory of the nonequilibrium grain boundaries and the classical theory of fragmentation during severe plastic deformations, is developed. According to the model, the process of fragmentation is considered as one of the accommodation processes leading to increasing the power of defects, which are accumulated on the grain boundaries during deformation. The authors thank International Scientific-Technical Center (ISTC grant No. 2809) for support.

Influence of Multi-Step SPD Processing by ECAP, Cold-Rolling and Subsequent Annealing on the Structure of Ti-50.2%Ni Alloy: Dmitry Valerievich Gunderov¹; Vladimir Pushin²; Alexander Lukyanov¹; Egor Prokofiev¹; Georgy Raab¹; Ruslan Valiev¹; ¹Ufa State Aviation Technical University; ²Institute of Physics of Metals

The titanium nickelide alloys (TiNi) have high strength, ductility, corrosion resistance and such a property as shape memory effect (SME). This makes them important for application in technology and medicine as long-lasting materials implanted into a body. Equal-channel angular pressing (ECAP) allows to process bulk TiNi samples with UFG structure (grain size \approx 250nm) and enhanced strength and instrumental properties. The investigations have also shown that rolling after ECAP allows to additionally refine the structure and enhance the properties of TiNi. As a result of rolling mode optimization integral band samples were processed. The alloy structure after rolling with the strain level of 80%-90% may be described as amorphous-nanocrystalline. The following controlled annealing of these states allows forming homogeneous nanocrystalline structures. With the degree of rolling increasing dislocation yield stress and strength increase, reaching 2000 MPa. The processed samples are materials with high reactive stress - up to 1500 MPa.

Advanced ECAP Techniques with Higher Intensity of Strain per One Pressing Cycle: Georgy Iosifovich Raab¹; ¹UFA State Aviation Technical University

Severe plastic deformation (SPD) by equal channel angular pressing (ECAP) makes it possible to considerably enhance mechanical properties of commercial metals and alloys by forming a submicrograined (SMG) structure in billets for 4-12 processing cycles. However this process has a number of disadvantages. Among them are: a low materials utilization rate which is less than 0.5 and high labour intensity caused by high-cycle treatment. In this connection in the paper a number of ECAP methods has been investigated that allows to reach true strain $\Sigma \geq 1,5$ for one processing cycle and therefore intensifies the structure-forming process. Peculiarities of both flow and material strain state of the suggested ECAP techniques have been studied by experimental and finite element (FE) simulation. The examples of high-efficiency solutions to form a SMG structure during SPD have been shown. Recommendations for applications of the given investigations are presented.

Development of ECAP-Conform to Produce Ultrafine-Grained Ti: Georgy Iosifovich Raab¹; Fidis Safin¹; Yuntian Zhu²; Terry Lowe³; Ruslan Valiev¹; ¹UFA State Aviation Technical University; ²Los Alamos National Laboratory; ³Metallicum

Recently we have shown an ability to process submicrograined aluminum rods with enhanced properties by the new technique that is ECAP-conform. However the production of long-length rods from ultrafine-grained Ti is of great interest, for example for medical applications. In the present work finite element (FE) simulation of a stress-strain state, the influence of tribological regimes, temperatures and some other processing parameters on a material flow and on strain uniformity in the long-length rods have been studied that enables us to design a new die-set for processing Ti by ECAP-conform. The most effective ways for a commercial development of ECAP-conform are discussed as well.

The Influence of ECAP on Microstructure and Mechanical Properties of AM60 - Magnesium Alloy: *Rinat Islamgaliev*¹; Olga Kulyasova¹; Bernhard Mingler²; Erhard Schafner²; Georg Korb³; Hans Karnthaler²; Michael Zehetbauer²; ¹Ufa State Aviation Technical University; ²University of Vienna; ³Austrian Research Center Seibersdorf GmbH

The AM60 alloy has been processed by ECAP at different temperatures (150–350°C), and the resulting microstructures have been investigated by means of TEM, DSC and XRD. ECAP reduced the grain size of cast alloy down to 2 μm. The majority of Mg₁₇Al₁₂ precipitates with a size of 0.05–0.2 μm were observed to be situated close to the grain boundaries, whereas precipitates with a size of 10–20 nm were found in the interior of the grains. The ECAP processing at 150°C led to enhancement of strength from 120 MPa to 310 MPa while the original ductility (15%) has been retained. Observations of deformation relief suggest processes of dislocation slip and grain boundary sliding to be responsible for the considerable ductility. Experimental results indicate that in the ECAPed materials the phase transition from solid solution to the two-phase region occurs at lower temperatures than in the undeformed material.

Initial Observations of the Effects of Sample Size on Microstructure and Properties of HPT Processed Titanium: *Rinat Islamgaliev*¹; Vladimir Latysh²; Maxim Murashkin¹; Askar Kilmametov¹; Ruslan Valiev¹; Yuntian Zhu³; ¹Ufa State Aviation Technical University; ²Innovation Scientific Technical Center “ISKRA”; ³Los Alamos National Laboratory

High pressure torsion (HPT) is a well established severe plastic deformation method to produce nanostructured states in metallic materials. This work presents the new developments of HPT technique to produce larger samples from various metals and alloys under higher imposed pressure. Using this new installation we revealed that SPD leads in pure Ti not only to structure refinement with increase of both the dislocation density and mean-root-squared strains but also to a-w phase transition at room temperature. In the case of Al-based alloys through refining microstructure up to 60–80 nm and precipitation hardening we could reach extraordinary strength and ductility needed for practical application of SPD produced materials.

On the Evolution of Microstructure of Tantalum Induced by Severe Plastic Deformation: *Qiuming Wei*¹; K. T. Ramesh²; K. T. Hartwig³; Ruslan Z. Valiev⁴; Laczlo J. Kesckes⁵; ¹University of North Carolina at Charlotte; ²Johns Hopkins University; ³Texas A&M University; ⁴Ufa State Aviation University; ⁵Army Research Laboratory

We have investigated the evolution of microstructure of a body-centered cubic refractory metal, tantalum, induced by equal channel angular press (ECAP). Commercial purity tantalum bars have been subjected to different number of ECAP passes and different type of routes. The grain refinement, grain boundary nature, etc. have been studied as a function of route type and number of passes of ECAP processing. It was found that even after 16 passes of ECAP, the grain refinement was still not saturated. We observed ghost diffraction spots and rings from the severely deformed state the smallest {h,k,l} indices of which are {0,1/2,1/2}. The interpretation of the appearance of such ghost diffractions calls for further work. It was also found that the ghost diffraction intensity in the selected area electron diffraction increases with number of passes. This ghost diffraction is absent in the undeformed, annealed state.

Anisotropic Mechanical Properties of Ultra-Fine Grained Aluminum Alloy: Gyorgy Krallics¹; Arpad Fodor¹; Ahmed Ajina Agena¹; ¹Budapest University of Technology and Economics

Bulk materials, subjected to SPD, are considered to be semi-finished components. They are subjected to additional processing in order to create different kinds of products. The present paper is focused on the workability and anisotropy parameters, required for the subsequent plastic forming processes. Samples for testing were prepared from work pieces subjected to the ECAP process, using various pass schedules. The tensile samples were taken in the longitudinal direction while the samples for upsetting were taken in longitudinal and two perpendicular directions. The mechanical investigations indicated fairly good measurable anisotropic behaviour of the material. Using continuum mechanics, the parameters of the constitutive equation were determined, assuming the material to be rigid-plastic. Complementary investigations, using special specimens to determine the formability limits in different stress states, were

also performed. The fracture criteria of isotropic materials were thus modified.

Characterization of Nano and Ultra-Fine Grains Formed during Friction Stir Processing of Ti: *Oleg M. Barabash*¹; Zhili Feng¹; Stan A. David¹; Joe A. Horton¹; Rozaliya Barabash¹; ¹Oak Ridge National Laboratory

Microstructural changes of commercially pure Ti due to Friction Stir Processing (FSP) were analyzed by means of optical, electron (TEM), orientation imaging microscopy, mono- and polychromatic X-ray micro diffraction. It was established that after FSP a surface layer with nanocrystalline structure is formed in which the grain size is between 20–60nm. Beneath the nanocrystalline grain layer is a thermomechanically affected zone (TMAZ). The grain size increases sharply (by two orders of magnitude) from nanocrystalline surface region to TMAZ, reaching micron size (5–30 micron) in the TMAZ. Possible causes and mechanisms for the formation of the nanocrystalline and ultra-fine grains will be discussed in light of the microstructure analysis results.

Texture Evolution and Monotonic and Cyclic Response of ECAE Processed Interstitial Free (IF) Steel at Room Temperature: Guney Guven Yapici¹; Steven Sutter¹; Ibrahim Karaman¹; Hans Jurgen Maier²; ¹Texas A&M University; ²University of Paderborn

Interstitial Free steel is commonly utilized in automotive industry for producing large body panels and other structural components due to its high formability. Apart from high strength levels, improved fatigue performance is a prerequisite for some applications. Present work focuses on the severe plastic deformation of IF steel using ECAE. IF steel was processed up to 16 passes using various ECAE routes to investigate the processing-microstructure-property relationships. An extensive program was undertaken to characterize microstructure, crystallographic texture and mechanical properties of successfully extruded billets. Eight pass extrusion following route Bc resulted in yield strengths close to 700 MPa exhibiting a ten-fold increase compared to the annealed materials. Low cycle fatigue experiments on the eight pass sample demonstrated a more than two-fold increase in both the cyclic strength and number of cycles to failure. Effect of ECAE texture on the monotonic and cyclic response is discussed together with cyclic microstructural evolution.

Characterization of Severe Plastic Deformation Processed Commercially Pure Al-2024: Andreas Kulovits¹; Anirudha R. Deshpande¹; Brian Webler²; Jorg Michael Wieszorek¹; ¹University of Pittsburgh; ²Carnegie Mellon University

Nano-crystalline microstructures with average grain sizes below 100nm have been produced for an Al-Cu-Mg base high strength age hardening aluminum alloy (commercially pure Al-2024) by severe plastic deformation processing. High reductions in thickness were achieved by cold-rolling and subsequent cold-rolling and stacking of the deformed sheets. This variation of the accumulated roll bonding (ARB) method resulted in locally bonded layered compacts. Changes in hardness and microstructure have been carefully monitored by means of micro-hardness measurements, XRD and TEM. The microstructural investigations indicated a truly nanocrystalline microstructure in the locally bonded sections of the layered compact. Microstructural changes associated with the SPD processing of this Al-alloy have been studied with a special focus on the nature of precipitation products and are discussed.

Effect of Severe Plastic Deformation via Equal Channel Angular Extrusion on Shape Memory Response of a Ti-Ni-Pd High Temperature Shape Memory Alloy: *Jae Il Kim*¹; Ibrahim Karaman¹; Benat Kockar¹; Jeff Sharp²; ¹Texas A&M University; ²Marlow Industries

In order to extend the utility of TiNi shape memory alloys for high temperature applications, higher martensitic transformation temperatures (M^*) than 100°C, lower temperature hysteresis, and better cyclic reversibility are required. The addition of Pd is effective in increasing the M^* and decreasing the temperature hysteresis, however, it also leads to the degradation of thermal cyclic response under stress at elevated temperatures. In this study, the effect of severe plastic deformation (SPD) via equal channel angular extrusion (ECAE) on shape memory properties of a TiNiPd alloy was investigated. Multi-pass extrusions using several different ECAE routes were performed at temperatures as low as 300°C. Shape memory properties were investigated before and after ECAE. Thermal cycling under constant stress levels revealed that cyclic reversibility was

significantly improved and critical stress for slip was increased after ECAE. TEM observations revealed that this improvement is caused by ultrafine and nano-scale grains (<300nm).

Design of Microstructure and Texture in NbZr and Ti Using Severe Plastic Deformation for Desired Mechanical Properties in Biomedical Applications: *Guney Guven Yapici*¹; Ibrahim Karaman¹; Gagan Singh¹; Ralph Dieckmann²; Hans Jurgen Maier²; ¹Texas A&M University; ²University of Paderborn

NbZr and Ti are widely used in biomedical applications ranging from cardiovascular stents to bone implants due to their high corrosion resistance and excellent biocompatibility. These applications require high strength and elastic modulus combined with enhanced ductility. This talk will summarize findings on the ECAE of NbZr and Ti to achieve target mechanical properties by engineering microstructure and texture. NbZr was processed up to 16 passes at room temperature while Ti was processed up to 12 passes at 300C without any shear localization. Post-processing of extruded billets with conventional forming techniques assisted by low temperature annealing treatments led to the formation of microstructures yielding both high tensile strengths and uniform strains. Series of experiments are conducted with the aim of capturing the yield locus evolution during ECAE. This enables us to demonstrate the effect of ECAE on the yield surface evolution and help developing models to predict the mechanical behavior.

Influence of Ultrafine Grain Size on Yield Strength of Ball-Milled Iron Alloys: *Chol K. Syn*¹; Donald R. Lesuer¹; Oleg D. Sherby²; ¹Lawrence Livermore National Laboratory; ²Stanford University

Extended ball millings of iron powders have been shown in recent studies to generate ultrafine grains, as small as 5 nm, and create nano-sized iron oxide particles, leading to extraordinary hardness. Detailed analyses of these studies on ball-milled powders and the consolidated powders show that nano-oxide particles are the major contributors to the strength of ball-milled iron. Ultra-fine grains, although stabilized by the presence of the nano-oxide particles, do not seem to contribute significantly to the strength. This is because grain boundary sliding of the high-angle boundary ultra-fine grains prevent dislocation pile-up and the Hall-Petch mechanism becomes less effective at grain sizes below 2 μm. It will be shown that the particles' contribution to the yield strength can be predicted by the surface-to-surface inter-particle spacing. It is proposed that adiabatic shear banding and phase transformation are the basis for creation of the ultrafine oxide particles.

Effects of ECAP Processing on the Recrystallization of FCC Copper and BCC Tantalum: *Joel W. House*¹; James M. O'Brien²; Philip Flater¹; Robert DeAngelis³; William F. Hosford⁴; ¹U.S. Air Force; ²O'Brien and Assoc; ³University of Florida; ⁴University of Michigan

Deformation by Equal Channel Angular Pressing (ECAP) has been used to develop ultra-fine grain structures in metals. Generally these metallic structures are associated with increases in strength and/or ductility depending on the specific deformation mechanism. Previously we have reported the hardness of ECAP processed OFE Copper and Tantalum (99.95%) after 1, 2, 4, 8 and 16 passes using route BC. No hardness increase was observed after eight passes for either of these two metals. Studies of the effects of extensive plastic strain on metallic structures have correlated an increase frequency of high angle grain boundaries with increasing strain. The present study investigates the effects that the increase frequency of high angle grain boundaries has on the recrystallization of Copper and Tantalum. Detailed comparisons of the recrystallization characteristic of these metals following ECAP processing to eight and 16 passes will be presented.

Microstructural Evolution of Inconel-718 Alloy during Equal Channel Angular Extrusion Processing—Simulation and Experimental Validation: Padma Dhulipala¹; Vadim Protasov¹; *Shankar M. Sastry*¹; ¹Washington University

Inconel-718 alloy was processed by equal channel angular extrusion (ECAE) at 900°C and 925°C for micro structural refinement and mechanical property modifications. Finite element method based DEFORM 3D code was used to simulate the ECAE process and microstructural evolution during ECAE. The simulation predictions of strain distribution in the ECAE processed samples, the extent of metadynamic recrystallization

and the recrystallized grain size were in good agreement with the experimental measurements. Fully recrystallized microstructure with an average grain size of 3μm was obtained by ECAE processing the alloy at 925°C at an extrusion rate of 0.4 inch/min. further grain refinements are possible by using multiple pass ECAE processing.

Residual Stresses in Ultrafine Grained Flowformed Ti-6Al-4V: *Ibrahim Ucak*¹; Gabriel J. Hostetter¹; Hao Dong¹; Lawrence S. Kramer¹; Mehmet N. Gungor¹; Troy Tack¹; ¹Concurrent Technologies Corporation

The flowforming (FF) is a novel method for manufacturing near-net-shape tubes. FF is generally performed at room temperature and provides a thickness reduction up to 80%, which yields enhanced tensile properties in the as-flowformed material. However, the large amount of cold work also generates significant residual stresses that may cause problems during final manufacturing processes, such as machining, cutting and welding. In this study, Ti-6Al-4V structural tubes in both the as-flowformed and stress relieved conditions were subjected to residual stress measurement by X-ray diffraction method. The effect of heat treatment on the magnitude of residual stresses, resultant microstructure and mechanical properties will be presented and discussed. This work was conducted by the National Center for Excellence in Metalworking Technology, operated by Concurrent Technologies Corporation, under Contract No. N00014-00-C-0544 to the Office of Naval Research as part of the U.S. Navy Manufacturing Technology Program. Approved for public release; distribution is unlimited.

Microstructure and Strength of Ultrafine Grained fcc Metals Produced by Severe Plastic Deformation: *Jeno Gubicza*¹; Nguyen Quang Chinh¹; Tamas Ungar¹; Terence G. Langdon²; ¹Eotvos Lorand University; ²University of Southern California

Nanostructured materials produced by equal channel angular pressing (ECAP) have very high strength owing to their small grain sizes and high dislocation densities. To understand the mechanical behavior of materials produced by ECAP it is necessary to characterize their microstructure. In this work the microstructure of ultrafine-grained face centered cubic (fcc) metals (e.g. Cu, Ni, Al and its alloys) produced by ECAP was studied by X-ray diffraction line profile analysis. High resolution X-ray diffraction experiments were performed using a special double-crystal diffractometer with rotating Cu anode. The crystallite size distribution and some characteristic parameters of the dislocation structure (e.g. density, character and arrangement of dislocations) were obtained from the fitting. The correlation between the parameters of the microstructure and the mechanical behavior is studied and discussed. The effect of alloying and precipitation on the evolution of microstructure during ECAP was also investigated.

Microstructure and Mechanical Properties of an Ultrafine Grained Dual-Phase Steel: *Hongwei Song*¹; Bi Shi¹; Junbao Zhang¹; Xiufang Wang¹; ¹Baosteel Iron and Steel Company, Ltd.

The tensile ductility of ultrafine grained (UFG) steels grow rapidly worse when the grains is refined down to less than 5 microns. When this happens, the UFG steels appear to lose the capacity for strain hardening or uniform deformation. On the other hand, dual-phase (DP) steels consisting of ductile ferrite matrix and martensite islands show superior mechanical properties, such as continuous yielding, high work hardening rate, and high uniform elongation. It is reasonable to combine UFG with DP microstructure. In the present work, an UFG DP steel was produced by means of severe intercritical-rolling. The results indicate that the grains of ferrite and martensite are equiaxed or polygonal with average grain diameters of 4 and 2 microns, respectively. The steel exhibits both high strength and good ductility, which have been attributed to the grain refining effect and the DP microstructure, respectively.

New Concepts for Severe Plastic Deformation: *David J. Alexander*¹; ¹Los Alamos National Laboratory

Several concepts for new methods of severe plastic deformation have been devised at Los Alamos National Laboratory. Some of these are simple extensions of conventional methods, such as equal channel angular extrusion (ECAE). This includes ECAE of long billets, or ECAE of flat plates. Some are primarily surface-deformation techniques, while others are bulk deformation processes. The new methods will be described, along with efforts to reduce the methods to practice. Possible benefits and shortcomings of the new concepts will be discussed.

Mechanical Anisotropy due to Microstructural Morphology and Bauschinger Effect in Equal Channel Angular Extrusion (ECAE)

Processed Cu: *Mohammed Haouaoui*¹; Ibrahim Karaman¹; Hans J. Maier²; ¹Texas A&M University; ²University of Paderborn

The effect of strain path and level on the flow stress anisotropy and Bauschinger effect (BE) in UFG OFHC copper was investigated considering grain morphology, dislocation mean free path and texture evolution. The material was deformed via multipass ECAE using a 90° square die to different strain levels following several routes (A, B, C, C' and E). The room temperature experiments were conducted under tension and compression along three perpendicular directions in each billet. Bauschinger experiments were conducted in both forward tension/reverse compression and forward compression/reverse tension modes. The strong anisotropy in flow stress, softening and BE were correlated to grain morphology and texture. It was found that as opposed to previous observations in which UFG materials have higher strength under compression, the observed stronger tension and tension/compression asymmetry is not only due to the effect of hydrostatic pressure on dislocations and it is also a function of grain morphology.

Deformation Microstructure and Grain Stability in Al-RE Alloys Produced by ECAP: *Michael Ferry*¹; Nanang Burhan¹; ¹University of New South Wales

This paper describes the evolution of microstructure in Al-RE alloys generated by equal channel angular pressing (ECAP) and the subsequent microstructural changes associated with elevated temperature annealing. As expected, the alloys develop a submicron grain (SMG) structure during severe plastic deformation with the amount of RE additions strongly influencing the stability of the deformation substructure. It was shown that nanosized RE dispersoids have a strong influence on grain stability with discontinuous grain coarsening suppressed at high annealing temperatures despite the general non-uniformity of the grain boundary character associated with the deformation microstructure. A simple analytical model is proposed that takes into account the effect of both fine particles and orientation gradients on grain coarsening in SMG alloys with the model confirming the observed coarsening behaviour.

Structure and Properties of Ni-20Cr Produced by Severe Plastic Deformation: *Judson S. Marte*¹; Richard DiDomizio¹; P. R. Subramanian¹; Dheepa Srinivasan¹; Michelle Othon¹; ¹GE Global Research

Nanostructured and ultrafine grained materials have been receiving attention because of their superior mechanical properties. This paper will examine two severe plastic deformation (SPD) processes for producing nanostructured and ultrafine grained materials: multi-axis forging and equal channel angular extrusion (ECAE). The two processes were applied to a Ni-20 wt.% Cr alloy to determine the extent of grain refinement achievable via SPD. The multi-axis forging process resulted in an equiaxed microstructure with an average grain size of 1 micron. The ECAE process resulted in a heavily dislocated structure with shear bands and sub-grain sizes of approximately 100-300 nm. Heat treatment of the ECAE'd material resulted in dislocation-free structures and substantial grain growth. The evolution of microtexture was examined by electron backscatter diffraction. Low levels of microtexture were observed after heat treatment. Tensile tests were performed on the SPD processed Ni-20Cr. A significant increase in tensile strength was observed after SPD.

Wechsler Symposium on Radiation Effects, Deformation and Phase Transformations in Metals and Ceramics: Irradiation Pressure Vessel

Sponsored by: The Minerals, Metals and Materials Society, ASM International, TMS Structural Materials Division, ASM Materials Science Critical Technology Sector, TMS Materials Processing and Manufacturing Division, TMS/ASM: Mechanical Behavior of Materials Committee, TMS/ASM: Nuclear Materials Committee, TMS/ASM: Phase Transformations Committee

Program Organizers: Korukonda L. Murty, North Carolina State University; Lou K. Mansur, Oak Ridge National Laboratory; Edward P. Simonen, Pacific Northwest National Laboratory; Ram Bajaj, Bettis Atomic Power Laboratory

Tuesday PM
March 14, 2006

Room: 208
Location: Henry B. Gonzalez Convention Ctr.

Session Chairs: Ram Bajaj, Bechtel Bettis Inc; Roger E. Stoller, Oak Ridge National Laboratory

2:00 PM

Local Electrode Atom Probe Characterizations of Neutron Irradiated RPV Steel Welds: *Michael K. Miller*¹; Kaye Russell¹; Randy K. Nanstad¹; Mikhail A. Sokolov¹; ¹Oak Ridge National Laboratory

An atom probe tomography characterization of the microstructure of two high copper, high nickel, high manganese alloys was performed with particular emphasis on the nature of the copper-enriched precipitates. The materials studied were a 0.20 wt% Cu 1.27% Mn, 1.20% Ni weld from the Palisades reactor that was irradiated to fluences of 1.4 and 3.4 x 10²³ m⁻² at 288°C and a 0.56 wt% Cu, 1.36% Mn, 1.66% Ni Rolls Royce weld (WV) that was irradiated to a fluence of 1.6 x 10²³ m⁻² at 290°C. Phosphorus and carbon were detected at different segments of the dislocations in the Palisades weld. The extents of the manganese, nickel and silicon distributions in the precipitates were larger than the extent of copper. Nickel and manganese were preferentially located at the precipitate-matrix interface. Silicon was uniform within the precipitate. Phosphorus was located both within the precipitate and at the interface.

2:20 PM

Positron Annihilation Characterization of Nanostructural Features in Reactor Pressure Vessel Steels and Model Alloys: *Brian D. Wirth*¹; Stephen C. Glade¹; G. Robert Odette¹; Michael K. Miller²; ¹University of California; ²Oak Ridge National Laboratory

Irradiation embrittlement of reactor pressure vessel (RPV) steels results from formation of a high density of nm-scale precipitates. In RPV steels with >0.1%Cu the dominant hardening features are copper-rich precipitates (CRPs) alloyed with manganese, nickel and silicon. But as theoretically predicted long ago, manganese-nickel(-silicon) rich precipitates (MNPs) can form in both copper bearing and copper free alloys, containing large amounts of these elements. Large volume fractions of so-called late blooming MNPs (LBP), cause severe hardening and embrittlement. The presence LBP-MNPs and large hardening in low copper and copper free alloys has been demonstrated recently by a variety of techniques. We present positron annihilation spectroscopy results of neutron irradiated model alloys and welds that provide insight into CRPs and MNP behavior, as well as their composition and magnetic properties. The positron results are compared to corresponding small angle neutron scattering, combined electrical resistivity-Seebeck coefficient and atom probe tomography data.

2:40 PM

Irradiation Induced Precipitates in Model Fe-Cu-Mn Alloys: A Unified Cross Comparisons of Multiple Characterization Techniques: Mike Miller¹; Brian D. Wirth²; G. Robert Odette³; ¹Oak Ridge National Laboratory; ²University of California, Berkeley; ³University of California, Santa Barbara

Cu rich precipitates (CRPs) in iron alloys are important in several technological applications and are of fundamental scientific interest. Copper precipitation in both thermally aged and irradiated Fe-0.80Cu and Fe-

TUESDAY PM

0.78Cu-1.05Mn alloys was characterized by several complementary microanalytical techniques, including: atom probe tomography, small angle neutron scattering, combined electrical resistivity-Seebeck coefficient measurements and positron annihilation coincidence Doppler broadening orbital electron momentum spectroscopy. A major objective was to help resolve the controversy about Fe in the CRPs, found or not found, by various methods. Detailed inter-comparisons showed very good overall consistency in the CRP volume fractions, sizes, number densities and even compositions. Unification of the results suggest nearly pure solute CRP cores are surrounded by shells with dilute concentrations of Cu and, especially, Mn. Significant thermal precipitation occurs at 290°C in only 7200h, indicating anomalously fast solute diffusion. Irradiation slightly enhances the solute content of the interface shell, perhaps by cascade mixing.

3:00 PM

A Unified Constitutive Model for Irradiated RPV Steels: Increases in Intrinsic Strain Hardening: *Takuya Yamamoto*¹; G. Robert Odette¹; ¹University of California, Santa Barbara

RPV steels irradiated at ~300°C up to 0.1 dpa harden due to a high density of nanometer-scale Cu-Mn-Ni coherent precipitate and defect-solute cluster complex dislocation obstacles. Higher yield stress is accompanied by modest reductions in strain hardening and uniform strains, usually assumed to be due to dislocation cutting-destruction of the obstacles. A unified constitutive model is developed that properly combines all strength contributions (grain boundary, stress fields, pre-irradiation precipitates, obstacles and dislocation structures) between linear and root sum square superposition limits, and accounts for dislocation storage and annihilation mechanisms. Notably, although the net observed strain hardening is lower, due to superposition effects the intrinsic dislocation hardening (and density) is actually higher after irradiation, even assuming no obstacle destruction, probably due to reductions in the annihilation rate by suppressed cross slip. The database, novel experiments to measure flow stress at high strains and microstructural characterizations underpinning the model are described.

3:20 PM

Modeling Cascade Aging and Dose Rate Effects in Ferritic Alloys: *Brian D. Wirth*¹; Paul Monasterio¹; G. Robert Odette¹; ¹University of California

Fundamental understanding of defect production in displacement cascades is required to model and predict long-term neutron irradiation induced microstructural evolutions. Defect production is generally treated in terms of primary events, occurring in cascades over time scales of less than 100 ps. We describe the development of advanced kinetic lattice Monte Carlo (KMC) methods to simulate the long-term rearrangement (aging) of displacement cascades as well as cascade aging effects on overall damage accumulation in neutron irradiated Fe, Fe-Cu and Fe-Cu-Ni alloys. Special algorithms have been developed to model self-interstitial atom-vacancy recombination in cascades and long-range point defect and solute diffusion. The simulations reveal the formation of a continuous distribution of three dimensional cascade vacancy-solute cluster complexes and demonstrate the critical importance of spatial, as well as short and long-time, correlated processes, that mediate the effect of dose rate on microstructural evolution under conditions relevant to fusion reactor materials.

3:40 PM Break

4:00 PM Invited

Synergistic Effects of DSA and Radiation Defects on Mechanical and Fracture Characteristics of Pure Iron and Steels: *Indrajit Charit*¹; Chang-Sung Seok²; K. Linga Murty¹; ¹North Carolina State University; ²Sungkyunkwan University

Ferritic steels commonly used for pressure vessels and reactor supports in light water reactors (LWRs) are known to exhibit radiation embrittlement in terms of decreased toughness and increased DBTT following exposure to neutron radiation. The superimposed effects of dynamic strain aging (or Portevin LeChatelier effect) on radiation embrittlement were considered first by Wechsler, Hall and others. We summarize here some of our work on these aspects with emphasis on synergistic effects of interstitial impurity atoms (IIAs) and radiation induced point defects, that result in interesting beneficial effects of radiation exposure

at appropriate temperature and strain-rate conditions. A variety of ferritic steels are considered including pressure vessel steels as well as relatively pure (Armco) iron using tensile, 3 point bend and CT specimens. The superimposed effects of radiation on these steels and iron will be presented along with studies on fast vs. total (thermal+fast) neutron spectra that revealed unexpected results.

4:25 PM

On the Effects of Alloy Chemistry on the Composition of Copper and Manganese-Nickel Rich Precipitates in Irradiated Reactor Pressure Vessel Steels: *G. Robert Odette*¹; Jonathan Smith¹; Takuya Yamamoto¹; Brian D. Wirth²; ¹University of California, Santa Barbara; ²University of California, Berkeley

Irradiation embrittlement of reactor pressure vessel steels is primarily due to hardening caused by a high number density of Cu or Mn-Ni rich nm-scale precipitates. Modeling embrittlement requires understanding the thermodynamic relation between the alloy chemistry and the corresponding composition of the Cu-Mn-Ni-Si precipitates that form under irradiation. Predictions of both mean field and atomistic thermodynamic models, accounting for non-equilibrium effects of the interface at the nm-scale, are in good general agreement with observation, but they have not been rigorously verified by systematic experiment. In this work, we develop an experimental non-equilibrium Fe-Mn-Ni-Cu phase diagram for coherent transition phase precipitates at around 290°C, from both small angle neutron scattering and combined electrical resistivity-Seebeck coefficient measurement data on a large matrix of irradiated alloys with systematic variations in composition. The roles of Si and irradiation temperature are also discussed. The experimental phase diagram is used to fine-tune the thermodynamic models.

4:45 PM

Interaction of Plastic Deformation and Phase Transformations in Zr-Based Alloys at Temperatures of ($\alpha+\beta$)-Region of Phase Diagram Zr-Nb: *Yuriy Perlovich*¹; *Margarita Isaenkova*¹; *Sergey Kropachev*²; *Mikhail Shtutca*²; *Vladimir Filippov*²; *Oleg Bocharov*³; ¹Moscow Engineering Physics Institute (State University); ²Chepetckiy Mechanical Plant; ³All-Russia Research Institute of Inorganic Materials

Development of plastic deformation in Zr-based alloys at temperatures of β - and ($\alpha + \beta$)-regions of phase diagram Zr-Nb was studied by X-ray methods. Mechanisms, responsible for plastic deformation development by different temperature-rate regimes, were determined by texture changes, taking place in deformed samples. Among these mechanisms there are crystallographic slip in grains of β -Zr and α -Zr as well as diffusion displacements of crystallites along interphase boundaries. The latter mechanism becomes more intense under conditions of phase transformations and lies in the basis of superplasticity. Both α -Zr and β -Zr by deformation at temperatures of ($\alpha + \beta$)-region show a phase instability, which can result in repeated phase conversions, accompanied by fragmentation of crystallites and intensifying of intergranular slippage. The latter leads to scattering of the texture, formed by operation of crystallographic slip. The greater is the input of slippage by interphase boundaries, the more uniform is the deformation of samples.

WEDNESDAY

2006 Nanomaterials: Materials and Processing for Functional Applications: Nanomaterial Formation and Manufacture

Sponsored by: The Minerals, Metals and Materials Society, TMS Electronic, Magnetic, and Photonic Materials Division, TMS: Nanomaterials Committee

Program Organizers: W. Jud Ready, GTRI-EOEML; Seung Hyuk Kang, Agere Systems

Wednesday AM Room: 214C
 March 15, 2006 Location: Henry B. Gonzalez Convention Ctr.

Session Chairs: Seung Hyuk Kang, Agere Systems; W. Jud Ready, GTRI-EOEML

8:30 AM Introductory Comments

8:35 AM

Dispersion and Alignment of Single Walled Carbon Nanotubes in Ceramic Slurries by Pot Milled Method: *Alok Vats*¹; *Haiping Hong*¹; *Fernand D. Marquis*¹; *James W. Sears*¹; ¹South Dakota School of Mines and Technology

Single walled carbon nanotubes have shown promising electronic, mechanical and thermal properties due to their unique structures and bonds. In this abstract, we report our attempts to understand the behavior of SWCNT in ceramic slurries modified through pot milling, sonification and other chemical routes. Since ball milling operations on SWCNT's show reduction in size and introduction of defect on the sidewalls, depending on the duration of milling which contribute to change the morphology and properties of single wall nanotubes, we tried to incorporate and disperse nanoscale ceramics onto the SWCNT through the above techniques. The preliminary results of the Transmission Electron Microscopy (TEM) show that SWCNT are dispersed very well by the treatment of pot milled method. More interesting electrical and thermal properties are expected by using these kinds of materials. It may open the new route towards better utilizing the SWCNT.

8:55 AM

Synthesis of Carbon Nanocapsules by an Electric Plasma in Ultrasonic Cavitation Field of Liquid Ethanol: *Ruslan Sergiienko*¹; *Etsuro Shibata*¹; *Zentaro Akase*¹; *Hiroyuki Suwa*¹; *Takashi Nakamura*¹; *Daisuke Shindo*¹; ¹Tohoku University

Nanoparticles of iron carbides wrapped in multilayered graphitic sheets (carbon nanocapsules) were synthesized by a newly developed method in which an electric plasma was flashed in an ultrasonic cavitation field in liquid ethanol. Ultrasonic cavitation causes a very highly localized high temperature and pressure field where tiny bubbles are collapsing. An ultrasonic cavitation field, with its many activated tiny bubbles, enhances electrical conductivity due to the radicals and free electrons formed within it. Thus, an electric plasma can be generated at relatively low power, even in insulating organic liquid mediums. The size of the carbon nanocapsules ranged between 5 and 600 nm. The crystal structures of the spherical cores were found to be orthorhombic Fe₃C and monoclinic χ -Fe_{2.5}C. Some spherical particle cores were discovered in the amorphous state. The magnetic hysteresis loop of the nanocapsules at room temperature showed the saturation magnetization of 51.36 Am²/kg and coercivity of 3.4 kA/m.

9:15 AM Break

9:25 AM

Formation of Bulk Nanocrystalline Grains in Titanium by Friction Stir Processing: *Zhili Feng*¹; *Oleg M. Barabash*¹; *Stan A. David*¹; *Joe A. Horton*¹; ¹Oak Ridge National Laboratory

We report the formation of bulk nanocrystalline grains in commercially pure Titanium by friction stir processing (FSP). In the FSW experiment, a specially designed rotating refractory tool induces severe plastic deformation near the surface of the Ti specimen, accompanied by a con-

siderable temperature rise as the result of high-strain rate deformation and friction. The translational movement of the rotating tool makes it possible to process a large surface area of the material. The hardness in the processed region exceeds 300 Hv, compared to the base metal value of less than 200 Hv. Transmission electron microscopy (TEM) analysis revealed that the grain size in the processed region is in the range of 20 to 60 nanometers (nm). The basic principles of FSW as applied to producing nanocrystalline grains will be described, as well as the microstructural features of the processed region.

9:45 AM

Nanostructures and Mechanical Properties Developed in Copper by Severe Plastic Deformations: *Michal Besterčí*¹; ¹Institute of Materials Research of Slovak Academy of Sciences

The development of the nanostructure in Cu and the strength and ductility after severe plastic deformation (SPD) with the technology of equal channel angular pressing are analyzed. Results showed strength and ductility can be increased simultaneously by SPD. The changes in grain size and yield strength followed in some range the Hall-Petch equation. The grain size decreased with the increase of deformation, after 10 passes to 100-300 nm. The stress-strain curve of the deformed test piece after 10 passes showed a "plateau", showing the presence of superplastic like deformation mechanism, we suppose sliding and rotations of grains, and the same can explain the increase of the reduction of area after severe deformation. TEM analysis suggested the possible nanostructure formation mechanism by the formation of cellular grain structure, forming of subgrains and then forming of large angled nanograins with random orientation.

10:05 AM

Bulk Nanomaterials through Powder Consolidation by Twist Extrusion: *Victor Varyukhin*¹; *Yan Beygelzimer*¹; *Viktor Tkach*¹; *Viktor Maslov*¹; *Sergey Synkov*¹; *Aleksandr Sergeevich Synkov*¹; *Viktor Nosenko*¹; ¹DonFTI

We propose a theory of powder consolidation by twist extrusion. It is based on the continuum model of powder body with representative volume element which satisfies the quadratic yield condition. We show that intensive shear under high pressure at the end points of the twist channel and the intensity of material flow in the cross-sections of the billet provide favorable conditions for powder consolidation. The TE technique has been used for consolidation of macroscopically ductile amorphous Al86Ni6Co2Gd6 ribbons produced by melt-spinning processing. The fully billets with dimensions of 14×23×40 mm³ were produced at extrusion temperatures above 523 K, while the maximum microhardness (550 kgf/mm²) was reached for the bulk billet consolidated at 513 K with the nanocomposite structure consisted of about 57% of Al-nanocrystals with size about 13 nm embedded in residual amorphous phase.

10:25 AM Break

10:35 AM

Nanostructure Materials Fabricated by Ion Beam Mixing: *Sufian Abedrabbo*¹; *Dia-Eddin Arafah*¹; *Nuggehalli Ravindra*²; ¹University of Jordan; ²New Jersey Institute of Technology

Special nanostructure materials and thin films/alloys are processed utilizing the novel technique of Ion Beam Mixing (IBM). Examples include shallow alloy formation of engineered band gap Si-Ge for solar cell applications and GeO₂ islands and continuous nano-dimensional films by subsequent annealing. Characterization processes include investigations of the structural variations noted due to Argon beam irradiation to various fluences by Rutherford Backscattering (RBS), shallow defects and deep trapping level states by Thermo luminescence (TL), X-ray Diffraction (XRD) are performed.

10:55 AM

Self-Assembly of Amphiphilic Triblock Copolymers into Various Nanostructures: *Wei Jiang*¹; ¹Institute of Applied Chemistry

Self-assembly of ABA (P4VP-b-PS-b-P4VP) and ABC (PS-b-P2VP-b-PEO) amphiphilic triblock copolymers in selective dilute solution were

investigated and various novel nanostructures, such as ring-shaped aggregates, biomimetic segmented worm-like micelles, ring-ring nesting micelles, among others were obtained. Micellar morphology formation mechanism was explored by combining experimental and computer simulative method. Moreover, the micellar morphologies of ABA triblock copolymer in dilute solution were tuned by using many facile methods, including changing common solvent properties, hydrogen coupling between one of the block of copolymers and small molecular surfactants, binary blending of copolymers and homopolymer of core-forming blocks (PS blocks) addition method. The micellar morphologies can be conveniently tuned into spheres, rods, vesicles, et al by using these methods. Finally, we have successfully fabricated various metallized nanostructures by coating metallic nanolayers onto the copolymer micellar templates through simple electroless plating methods. In particular, bimetallic nanostructures have been obtained by using simple methods.

11:15 AM

Architectural Transformation on Nanoparticles to Nanowires in Applied Field: Harish Nathani¹; Jagdish Rawat¹; Devesh K. Misra¹; ¹University of Louisiana at Lafayette

We present a novel room temperature fabrication of nanowires of about 8-10 micrometers in length and about 100-200 nm in diameter. The magnetic behavior was studied by Superconductivity Quantum Interface Device (SQUID) magnetometer. Most importantly, the nanowires exhibit higher coercivity at 2K and are paramagnetic. This behavior is in contrast to nanoparticles that indicated high remanence and low coercivity.

11:35 AM Break**11:45 AM**

Optical Characterization of Ag Nanoparticles Embedded in Aluminophosphate Glass: Sergiy Lysenko¹; Jose A. Jimenez¹; Guangjun Zhang¹; Huimin Liu¹; ¹University of Puerto Rico

The physical properties of small metal particles, including their optical properties are strongly dependent on local structural and geometric parameters of particles caused by the preparation process. Silver nanoparticles (NP) embedded in aluminophosphate glass were prepared by melt and heat treatment processes. A red shift of the surface plasmon resonance (SPR) peak is observed as particle size increases, with the quadrupolar plasmon excitation being prominent for the more intensely heat treated samples. Low-temperature photoluminescence studies of Ag NPs embedded in the glass matrix show a broad band emission at ~410 nm with a dip which has a minimum at wavelength corresponded to dipole SPR mode in spherical Ag NP. Such a dip is assigned to reabsorption of Ag₂O emission by NPs. Time-resolved femtosecond pump-probe reflectivity measurements have shown the particle size-dependent nonlinear optical dynamics on a picosecond time scale. The relaxation mechanism of the electron-phonon system will be discussed.

12:05 PM

Experimental Study on Particle Size and Crystalline Phase of Titania Synthesized by Vapor Phase Oxidation Route: Wang Zhi¹; Yuan Zhangfu¹; Guo Zhancheng¹; ¹Chinese Academy of Sciences

Crystalline TiO₂ particles were produced in a tubular flow reactor by chemical vapor reaction using titanium tetrachloride as a starting material in oxygen containing atmospheres. The resulting powders were characterized by scanning electron microscope, transmission electron microscope and x-ray diffraction. The influence of temperature rules on titania showed that the particles size was controlled by the reaction temperature, the oxygen preheated temperature and the cooling fashion, but the particle crystalline phase was predominately anatase and hardly changed with the variation of the temperature, which was supposed due to the short residence time.

3-Dimensional Materials Science: 3-D Atom Probe

Sponsored by: The Minerals, Metals and Materials Society, TMS Structural Materials Division, TMS: Advanced Characterization, Testing, and Simulation Committee

Program Organizers: Jeff P. Simmons, U.S. Air Force; Michael D. Uchic, Air Force Research Laboratory; Dorte Juul Jensen, Riso National Laboratory; David N. Seidman, Northwestern University; Anthony D. Rollett, Carnegie Mellon University

Wednesday AM
March 15, 2006

Room: 205
Location: Henry B. Gonzalez Convention Ctr.

Session Chairs: David N. Seidman, Northwestern University; Chantal K. Sudbrack, Northwestern University

8:30 AM Invited

Applications of the Leap Tomograph to Three-Dimensional Materials Science: Thomas F. Kelly¹; David J. Larson¹; ¹Imago Scientific Instruments

Atom probe tomography provides 3-D atomic-scale structural and compositional analysis of materials that complements and supersedes other high-performance techniques such as TEM and SIMS. With recent developments in Local Electrode Atom Probe or LEAP® technology by Imago Scientific Instruments, the atom probe's compositional imaging capabilities are now available for a wide spectrum of materials. The materials to be analyzed can be prepared in either the traditional needle-shaped geometry or in the form of microtips residing on planar surfaces. Imago's LEAP technology also enables a cross-sectional area up to 100 nm and requires only minutes of data collection. The end result is that much larger volumes of material may be rapidly accessed with the atom probe microscope than has previously been possible or practical. In this talk, application of atom probe tomography to a wide range of materials studies including magnetic storage materials, semiconductor materials, and metals will be discussed.

8:55 AM Invited

The Benefits of 3D Microscopy at the Atomic Scale: Alfred Cerezo¹; ¹University of Oxford

The 3-dimensional atom probe (3DAP) permits analysis of the nanochemistry of materials with near-atomic spatial resolution, and was one of the first 3D-microscopy techniques in materials science. With 3-dimensional data, it is far easier to interpret complex microstructures and not only investigate the shape and orientation of features but also determine the proximity between different phases and the degree of interconnectivity. Other types of topological characterisation also become possible, such as the fine-scale roughness or the fractal dimension of an interface. 3D shape information is important in making an accurate determination of interface segregation, and may also give some indication of relative surface energies. This paper will review a number of studies in which the 3-dimensional nature of the data from the 3DAP has been important in the study of nanostructured engineering materials.

9:20 AM Invited

Atom-Probe Tomographic Studies of the Temporal Evolution of Nanostructures in Multicomponent Alloys: David N. Seidman¹; ¹Northwestern University

Atom-probe tomographic (APT) and transmission electron microscopy (TEM) studies of the temporal evolution of nanostructures of multicomponent nickel-based alloys, Ni-Al-Cr, are studied in concert with lattice kinetic Monte Carlo (LKMC) simulations. Additionally, Al-Sc-X (X = Mg, Zr or Ti) are studied employing APT, TEM and high-resolution electron microscopy (HREM). The experimental studies involve temporally following the mean radius of precipitates (second phase), number density of precipitates, mean compositions of the precipitates and the matrix, volume fraction of precipitates, and precipitate morphologies; thereby obtaining a complete experimental description of how a multicomponent alloy evolves towards its thermodynamic equilibrium state when aged in a two-phase region. The experimental results are compared with predictions of extant models for nucleation, growth or coarsening, and with

LKMC simulation results. It is shown that LKMC simulations in concert with the experimental results allows for a deeper physical understanding of the temporal evolution than either approach alone.

9:45 AM

Atom-Probe Tomography Study of Precipitation-Strengthened Aluminum Alloys: *Keith E. Knippling*¹; David N. Seidman¹; David C. Dunand¹; ¹Northwestern University

We seek to develop new castable and heat-treatable, precipitation-strengthened aluminum alloys with coarsening- and creep resistance beyond 375°C. Decomposition of supersaturated Al(Zr) solid solutions occurs initially by the formation of nanoscale metastable L1₂ Al₃Zr precipitates. However, segregation during peritectic solidification results in an inhomogeneous dendritic distribution of Zr, creating interdendritic precipitate-free zones in the precipitated microstructure. By adding Sc, a eutectic solute which forms L1₂ Al₃Sc, solute partitioning occurring during solidification improves the inhomogeneous dispersion of precipitates. Furthermore, in the presence of Zr, Al₃(Sc,Zr) precipitates form with improved thermal stability compared to binary Al₃Sc. We analyze via atom-probe tomography the temporal evolution during thermal exposure of the structure and chemistry of the complex precipitate structure formed from the nonuniform initial solute distribution. We compare our results with previous work on Al(Sc,Zr) alloys with low Zr/Sc ratios.

10:05 AM

3D Characterization of the Carbon Distribution in a Medium Carbon Steel: *Donald H. Sherman*¹; Michael K. Miller²; Sudarsanam Suresh Babu³; Nan Yang¹; ¹Caterpillar Inc; ²Oak Ridge National Laboratory; ³Edison Welding Institute

The microstructure of a medium carbon (0.26 wt% C), low alloy steel has been characterized by atom probe tomography. The microstructure of this predominantly martensitic steel was characterized in the water quenched and the quenched and tempered at 215C conditions. The carbon distribution was determined in a local electrode atom probe. This wide angle instrument enables significantly larger samples to be obtained more rapidly than in previous generations of three-dimensional atom probes. A discussion of the local variations in carbon level and formation of ultrafine carbides will be presented. Research at the SHaRE User Facility was sponsored by the Division of Materials Sciences and Engineering, U.S. Department of Energy, under Contract DE-AC05-00OR22725 with UT-Battelle, LLC.

10:25 AM Break

10:45 AM

Temporal Evolution of the Sub-Nanometer Compositional Profiles across the γ/γ' -Interface in a Model Ni-Al-Cr Superalloy: *Chantal K. Sudbrack*¹; Ronald D. Noebe²; David N. Seidman¹; ¹Northwestern University; ²NASA

Combining atom-probe tomography (APT) and lattice kinetic Monte Carlo (LKMC) simulations is a robust technique to analyze in 3D the earliest stages of solid-solid phase separation; that is, the genesis, microstructural evolution and compositional development of nanometer-sized precipitates. Employing sophisticated computer-based analytical methods, the early-stage phase separation in a Ni-5.2 Al-14.2 Cr atomic % superalloy, isothermally decomposing at 873 K, is investigated with APT. Sub-nanometer scale compositional profiles across the $\gamma(\text{fcc})/\gamma'(L1_2)$ interfaces demonstrate that both the γ -matrix and the γ' -precipitate compositions evolve temporally. Observed chemical gradients of Al-depletion and Cr-enrichment adjacent to the γ' -precipitates are initially transient, consistent with well-established model predictions for time dependent diffusion-limited growth, and mark the first detailed observation of this phenomenon. Furthermore, it is shown that Cr atoms are kinetically trapped in the growing γ' -precipitates.

11:05 AM Invited

Local Electrode Atom Probe Characterization of Crept CMSX-4 Superalloy: *Michael K. Miller*¹; Roger C. Reed²; ¹Oak Ridge National Laboratory; ²Imperial College

The solute distribution in crept and annealed single crystal CMSX-4 nickel-based superalloy has been characterized from multi-million atom, three-dimensional data sets obtained with the local electrode atom probe.

Solute-depleted and solute-enriched regions are evident on both sides of the $\gamma-\gamma'$ interface. Rhenium partitioned to the γ matrix and acts as a solid solution strengthener. Ultrafine (~1 nm diameter) rhenium clusters containing up to ~10% Re were evident in the 10-nm wide Re-enriched region in the matrix close to the $\gamma-\gamma'$ interface. No evidence of nanometer size Re clusters was observed in the central region of the matrix in any of the crept or annealed materials. Research at the SHaRE User Facility was sponsored by the Division of Materials Sciences and Engineering, U. S. Department of Energy, under Contract DE-AC05-00OR22725 with UT-Battelle, LLC.

11:30 AM Invited

GP Zones Structures in Al-Ag Alloys: *Emmanuelle A. Marquis*¹; ¹Sandia National Laboratories

In the phase-separating Al-Ag system, intermediate metastable precipitates (Guinier Preston zones) are formed. However, the exact structure of the GP zones (ordering, Ag concentration) and the existence of temperature-dependent phases (ordered at low T and disordered at high T) is still matter of debate. Recent experimental observations have indicated that in the initial stages of decomposition, precipitates form with a surprising morphology consisting of a Ag-rich shell surrounding an Al-rich inner core. This particular structure had been hypothesized from SAXS experiments, but the exact crystallographic nature and Ag concentrations have not yet been determined. Through transmission electron microscopy and atom probe tomography measurements, the temporal evolution of the local Ag concentration in three-dimensions is investigated. These measurements provide key information for connecting to theoretical predictions of the faceting and interfacial sharpness, and provide a basis for explaining the interesting morphologies observed in this system.

11:55 AM

Dilute Al-Sc-Yb Alloys Studied by Atom-Probe Tomography: *Marsha E. Van Dalen*¹; David C. Dunand¹; David N. Seidman¹; ¹Northwestern University

Small additions of Sc to Al lead to greatly improved mechanical properties due to the formation of nano-size Al₃Sc precipitates. In the present study, ytterbium was added as a ternary alloying element to further improve the mechanical properties of Al-Sc-X alloys. Utilizing LEAP atom-probe tomography, it is found that Yb forms precipitates in Al more rapidly than Sc, upon aging at 300°C. Initially, Al₃Yb precipitates form with radii of 1-2 nm. Al₃Yb precipitation is followed by slower diffusion of Sc to these precipitates. The resulting Al₃(Sc_{1-x}Yb_x) precipitates show interfacial segregation of Sc to the a-Al/Al₃(Sc_{1-x}Yb_x) heterophase interface. The number density of Al₃(Sc_{1-x}Yb_x) precipitates formed is higher than that of binary Al-Sc alloys of similar volume fraction, thereby leading to higher hardness values.

Advanced Materials for Energy Conversion III: A Symposium in Honor of Drs. Gary Sandrock, Louis Schlapbach, and Seijirau Suda: Complex Hydrides II

Sponsored by: The Minerals, Metals and Materials Society, TMS Light Metals Division, TMS: Reactive Metals Committee
Program Organizers: Dhanesh Chandra, University of Nevada; John J. Petrovic, Petrovic and Associates; Renato G. Bautista, University of Nevada; M. Ashraf Imam, Naval Research Laboratory

Wednesday AM
March 15, 2006

Room: 214B
Location: Henry B. Gonzalez Convention Ctr.

Session Chairs: Craig Jensen, University of Hawaii; Carole Read, U.S. Department of Energy; Ragaïy Zidan, Savannah River National Laboratory

8:30 AM Invited

Materials Properties of Complex- and Perovskite-Hydrides: *Shin-Ichi Orimo*¹; Yuko Nakamori¹; Kazutaka Ikeda¹; ¹Tohoku University

Complex hydrides have been regarded as potential candidates for advanced hydrogen storage media. Currently, two effective methods, 'par-

WEDNESDAY AM

tial substitution by elements with larger electronegativities' and 'preparation of appropriate combinations', are investigated with the primary aim of destabilizing the complex hydrides for promoting their dehydrogenating reactions. On perovskite hydrides, fundamental properties such as formation abilities and dehydrogenating mechanisms are studied experimentally. We have then confirmed the occurrence of the dehydrogenating (and also rehydrogenating) reactions of the perovskite hydrides, similar to the reactions of the complex hydrides.

8:55 AM Invited

Synthesis, Stability and Crystal Structure of Al-Based Complex Hydrides: *H. W. Brinks*¹; *B. C. Hauback*¹; *A. Fossdal*¹; *M. S. Sorby*¹; *C. M. Jensen*²; ¹Institute for Energy Technology; ²University of Hawaii

Alانات, metal hydrides based on the AlH_4^- unit, is one of the most promising groups of metal hydrides for reversible hydrogen storage at moderate temperatures, with possibilities of reaching 5 wt% reversible storage capacity. The pioneering work of Bogdanovic et al. in 1997¹ revealed that Ti additives increased the desorption kinetics of $NaAlH_4$ and furthermore made re-hydrogenation possible. In order to get a better understanding of the reactions, detailed studies of the structure is essential. In particular, it is important to understand the nature of the additive in order to be able to improve the kinetics by design. Most of the Ti additive was after cycling found to be present as $Al_{1-y}Ti_y$ with $y \approx 0.15^2$. Structural studies and stability measurements will be shown for a number of other alانات, including bialkali-alانات like Na_2LiAlH_6 and K_2NaAlH_6 . ¹B. Bogdanovic and M. Schwickardi, *J. Alloys Comp.* 253 (1997) 1. ²H.W. Brinks, B.C. Hauback, S.S. Srinivasan, C.M. Jensen, *J. Phys. Chem. B* (2005) In press.

9:20 AM Invited

Physicochemical Pathway to Reversible Hydrogen Storage in Complex Hydrides: *Jun Wang*¹; *Armin B. Ebner*¹; *James A. Ritter*¹; ¹University of South Carolina

The use of hydrogen as a renewable and clean energy source is one of the most exciting news items to hit this country in a long time. President Bush, during his State of the Union Address in February of 2003, pronounced 1.2 billion dollars to jump-start the Hydrogen Economy. The Hydrogen Economy represents not only freedom from the US dependence on foreign oil, which is a national security issue, but also a necessary step toward improving the environment by eliminating the release of carbon dioxide into the atmosphere due to the burning of fossil fuels. However, hydrogen storage is proving to be one of the most important issues and potentially biggest roadblock, when it comes to implementation of the hydrogen economy. Of the three options that exist for storing hydrogen, i.e., in a solid, liquid or gaseous state, hydrogen storage in a solid matrix is becoming more and more accepted as the only method to have any expectation of meeting the gravimetric and volumetric densities of the recently announced FreedomCar goals; and of all the known hydrogen storage materials, complex hydrides are showing considerable promise. To this end, a physicochemical pathway that facilitates reversible H_2 storage in complex hydrides has been developed. The products of this physicochemical pathway represent perhaps the highest capacity, reversible H_2 storage material known to date in low temperature ranges. This new pathway was utilized to create a 5 to 6 wt% reversible H_2 storage material at less than 150°C from the complex hydride, lithium aluminum hydride. Moreover, this material reversibly stores approximately 3 to 4 wt% H_2 at around 100°C. The unique feature of this off-board, physicochemical route is that it enables regeneration of this complex hydride material that to date has resisted regeneration through more conventional on-board routes that are being pursued with, for example, sodium aluminum hydride. This physicochemical pathway, or variations thereof, may also be amenable to fostering the reversibility of other higher capacity complex hydrides, like other alانات and boronates. With reversibility of the lithium aluminum hydride being achieved through this physicochemical pathway, optimization of this process is currently being studied, as is the applicability of this technique to other complex hydrides. The objective of this study is to present the most recent results obtained from the author's laboratory on the dehydrogenation and rehydrogenation properties and kinetics of lithium aluminum hydride and possibly other complex hydride systems.

9:45 AM Invited

Reaction of Hydrogen with DPB Organic Hydrogen Getter: *George L. Powell*¹; ¹BWXT Y-12, L.L.C.

DPB (diphenyl butyldiene typically mixed with 25 wt% C – 1 wt% Pd) is made into a hydrogen getter as porous pellets by Honeywell Federal Manufacturing and Technologies Kansas City Plant. The gettering reactions are very effective, and irreversible since the H_2 is converted into a hydrocarbon. A 2-volume system was used to titrate DPB pellets, as a series of pressure drop curves, from which the reaction rate was determined as a function of H_2 pressure and DPB reaction extent at ambient temperature. Methods are described for measuring and modeling reaction rate as a function of pressure and reaction extent, and the results compared to that for another organic hydrogen getter. Managed by BWXT Y-12 L.L.C. for the U. S. Department of Energy under contract DE-AC05-00OR22800.

10:05 AM Invited

AES and RBS Study of the Deactivation Mechanism of Palladium Coated Vanadium Alloy Membranes: *Stephen N. Paglieri*¹; *Venhaus J. Thomas*¹; *Yongqiang Wang*¹; *David R. Pesiri*²; *Robert C. Dye*¹; *Craig R. Tewell*³; *Ronny C. Snow*¹; ¹Los Alamos National Laboratory; ²SDC Materials; ³Sandia National Laboratory

Metal membranes based on highly permeable metals such as vanadium may be used to purify hydrogen for use in fuel cells, compound semiconductor manufacturing, or the chemical industry. Foils of V-Cu coated with thin films of palladium or palladium alloy were fabricated and tested for hydrogen permeability and stability during operation at temperatures from 320-450°C. The vanadium alloy foils (~75 microns thick) were ion-milled and palladium coatings between 50 and 200 nm thick were applied to both sides in-situ, via electron beam evaporation PVD. The membranes were completely permselective for hydrogen. The rate of hydrogen flux decline at 400°C was gradual but accelerated quickly at higher temperatures. Hydrogen flux decrease was caused by metallic interdiffusion between the palladium coating and the vanadium alloy foil. Interdiffusion between various surface coatings and foils tested at different temperatures was characterized with AES depth profiles and RBS.

10:25 AM

Liquid Organic Hydrides for Hydrogen Storage: *Shinya Hodoshima*¹; *Yasukazu Saito*¹; ¹Tokyo University of Science

Liquid organic hydrides such as decalin, methylcyclohexane and tetralin have been proposed as hydrogen carriers for on-board or stationary application in this study. Both decalin and methylcyclohexane, which can store hydrogen with high capacities: decalin (7.3 wt%, 64.8 kg- H_2 / m^3); methylcyclohexane (6.2 wt%, 46.5 kg- H_2 / m^3), are suitable for operating hydrogen vehicles. Though the storage densities of tetralin are relatively low (3.0 wt%, 28.2 kg- H_2 / m^3), the rates of absorbing and desorbing hydrogen are much faster than the others, suggesting that tetralin is another choice for stationary use. Efficient hydrogen supply from organic hydrides under moderate conditions could be accomplished with the carbon-supported metal catalysts in the "superheated liquid-film states". Superheated catalyst layers gave high reaction rates and conversions at 210-280°C only under liquid-film conditions. Serious coke formation over the catalyst surface and excessive exergy consumption were therefore prevented simultaneously.

10:45 AM Break

11:00 AM Invited

Multiscale Heat and Mass Transfer Modeling and Optimization of Hydrogen Solid Storage Systems: *Eustathios S. Kikkindes*¹; *Maria Konstantakou*¹; *Michael C. Georgiadis*²; *Theodore Steriotis*³; *Thanos Stubos*³; ¹University of Western Macedonia; ²Imperial College London; ³National Center for Scientific Research, Demokritos

The operation of hydrogen solid storage tanks presents distinct challenges in process modeling and optimization. In order to make the method viable, the adsorption capacity of the absorbent must be such so as to allow storage of a sufficient amount of hydrogen at a relatively short filling time. Thermal limitations may need to be considered during the charging/delivery process to take account of potential safety and operational concerns. This work presents an integrated approach that formally exploits the benefits of material design and process design. Systematic simu-

lation and optimization studies are performed at two different length scales, adsorbent pore level and fixed bed adsorber level. A detailed mathematical model is developed, describing the hydrogen storage in the bed using as example a carbon-based material. The model is validated against experimental and theoretical literature results. Heat, mass and momentum transfer effects are modeled in detail.

11:20 AM Invited

Novel Organometallic Nanomaterials for Room-Temperature Reversible Hydrogen Storage: A First-Principles Prediction: *Shengbai Zhang*¹; ¹National Renewable Energy Laboratory

First-principles total energy calculations reveal the mechanism for non-dissociative H₂ adsorption on various organometallic nanomaterials ranging from (yet-to-be synthesized) transition metal-coated buckyballs and carbon nanotubes to (already-existing) metal carbide nanocrystals. Our study reinforces the notion that the relatively light-weighted 3d transition metal (TM) atoms are potential absorbers for H molecules, as the empty d orbital can bind dihydrogen with exceptionally high capacity at an energy range ideal for room temperature vehicular applications. However, upon H release, a collection of isolated TM atoms is unstable against spontaneous cohesion. We show that this difficulty may be overcome by “embedding” the TM atoms into various carbon-based organometallic nanostructures. In particular, the amount of H₂ adsorbed on an Sc-coated C₄₈B₁₂ [ScH]₁₂ could approach 9 wt%, with 30-40 kJ/mol binding energies. TM-coated carbon nanotubes also show similar binding characteristics although important differences do sometimes exist. Metallo-carbohedrenes and TM carbide nanocrystals are different from the above TM coated carbon structures in that the TM atoms are coordinated into the carbon backbone. Still, a similar non-dissociative H₂ binding mechanism is identified. These studies demonstrate the adaptiveness of the overall mechanism to different local chemical environments. Work was in collaboration with Y. Zhao, Y.-H. Kim, A. Dillon, & M. Heben and supported by the U.S. DOE/EERE under contract No. DE-AC36-99GO10337.

11:40 AM Invited

Characterization of Hydrogenation Behavior of NaAlH₄ Utilizing Thermoelectric Power and Magnetic Analyses: *Angelique N. Lasseigne*¹; M. Ashraf Imam²; Brajendra Mishra¹; David LeRoy Olson¹; ¹Colorado School of Mines; ²Naval Research Laboratory

Hydrogenation behavior of the NaAlH₄ intermetallics is investigated utilizing thermoelectric power and magnetic analyses. Using both thermoelectric power and magnetic susceptibility measurements on these intermetallics allows for confirmation and further insight into hydrogen's role in altering the material's electronic structure. Electron concentration changes with variations in stored hydrogen content, thus altering the filling of the electronic d-band and slope of the plot of the paramagnetic susceptibility as a function of the thermoelectric power coefficient. The electronic and magnetic property correlations to indicate the direction for further alloy development to optimize hydrogen storage will be discussed.

12:00 PM

Mechanism of Hydrogen Desorption in Li-N-H Hydrogen Storage System Catalyzed by Titanium Compounds: *Shigehito Isobe*¹; Takayuki Ichikawa¹; Satoshi Hino¹; Hironobu Fujii¹; ¹Hiroshima University

A solid-solid reaction between LiH and LiNH₂ catalyzed by a titanium compound proceeds with desorption of ~6mass% hydrogen and a quite small amount of ammonia. In this work, hydrogen desorption mechanism in the reaction from LiH+LiNH₂ to Li₂NH+H₂ under He flow atmosphere as a non-equilibrium condition was clarified by TDMS, TG and FT-IR analyses for the products replaced by LiD or LiND₂ for LiH or LiNH₂, respectively. The results suggested that the reaction progressed through two-step elementary reactions mediated by ammonia. Moreover, from the practical point of view, we carefully determined the amount of the ammonia contained in desorbed hydrogen for the Li-N-H system in a closed system. The results indicated that a quite small of ammonia thermodynamically coexisted in the desorbed hydrogen from the product although the ammonia could not be detected as emitted gas by TDMS under the non-equilibrium condition.

Alumina and Bauxite: Bayer Digestion Technology

Sponsored by: The Minerals, Metals and Materials Society, TMS Light Metals Division, TMS: Aluminum Committee
Program Organizers: Jean Doucet, Alcan Inc; Dag Olsen, Hydro Aluminium Primary Metals; Travis J. Galloway, Century Aluminium Company

Wednesday AM
March 15, 2006

Room: 7B
Location: Henry B. Gonzalez Convention Ctr.

Session Chair: Steve Healy, Alcan Queensland Research and Development Centre

8:30 AM Introductory Comments

8:40 AM

New Design for Digestion of Bauxites: *Rob Kelly*¹; Dirk Deboer¹; Mark Edwards¹; Peter McIntosh¹; ¹Hatch Associates

A number of process technologies are available for digestion of bauxites. Typically the major conceptual differences in these revolve around the design of the heating section employed to heat liquor and bauxite slurry to the desired digestion temperature, and in the design of the pressure vessels for extraction of alumina from the bauxite. However, the energy efficiency, operating and maintenance characteristics are determined by the overall design of the unit. This paper reviews technologies commonly used for both low and high temperature digestion. It then presents new designs that utilise tubular heating technology. Safety, technical, operational and cost attributes of the new designs are discussed.

9:05 AM

Digester Design Using CFD: *Jennifer Woloshyn*¹; Lanre Oshinowo¹; John Rosten¹; ¹Hatch

In the Bayer process, dissolution of gibbsite and kaolinite and continued dissolution of desilication products occur in the digester train. Understanding the hydrodynamics of the digester is key to improving the extent of dissolution, and thus the extraction of alumina and re-precipitation of silica. Deviation from ideal plug flow results in a miscalculation of the slurry retention time, leading to losses of bauxite in the red mud, or an over-sized digester. To address this issue, the hydrodynamics of a digester train were modeled using computational fluid dynamics (CFD). The impact of column aspect ratio and inlet configuration on the slurry residence time distribution (RTD) were investigated. The RTD was used to estimate reaction extents and evaluate the effect of design parameters on performance. The modeling approach allows the inclusion of the digestion chemistry to directly evaluate the yield. Results show that the choice of slurry inlet configuration significantly impacts performance.

9:30 AM

Oxalate Removal by Occlusion in Hydrate: *Valérie Esquerre*¹; Philippe Clerin¹; Benoît Cristol¹; ¹Alcan

Occlusion plays a significant role in the removal of oxalate at Alcan's Gardanne refinery. Up to 50% of the oxalate purge can be ensured by occlusion. This study investigates the occlusion phenomenon and identifies the action parameters that facilitate the control of the occlusion process. Successive precipitation cycle laboratory tests have been conducted in different operating conditions to ascertain the key factors. The addition of CGM appears to completely inhibit oxalate occlusion, whereas an increase in caustic concentration enhances the process. The impact of temperature is not clear, suggesting a counteracting effect of productivity and hydrate growth. Having a high level of precipitated oxalate doesn't ensure a high level of occluded oxalate. Possible mechanisms are proposed. The new operating instruction to maintain a high caustic concentration in the spent liquor has led to a high and lasting level of occluded oxalate.

9:55 AM

Organic Carbon in Indian Bauxites and Its Control in Alumina Plants: *Ramana Rao Venkata Kondapalli*¹; Ram Nivas Goyal¹; ¹Jawaharlal Nehru Aluminium Research Development and Design Centre

The organic build up in alumina plants is known to cause not only various plant operational problems but also reduces the productivity and

quality of product hydrate. The organic situation in Indian alumina plants is still not alarming for the reason that the bauxites contain low organic carbon. However, every plant feels the impact of the organic build up as it becomes old. The rate of organic build up is plant specific and depends upon the digestion conditions such as digestion temperature and pressure, caustic concentration, TOC values and nature of organic compounds in the mineral. In this paper the influence of digestion parameters, TOC in Indian bauxites and influence of special additives on organic build up in Indian alumina plants are discussed. The details of various control methods investigated for removal of oxalates, humates and TOC for Indian plants are also presented.

10:20 AM Break

10:40 AM

Reaction Behavior between Calcium Silicate Hydrate and Aluminate

Solution: Zhuo Zhao¹; Qingjie Zhao¹; Xiaobin Li¹; ¹Chaclo

Calcium silicate hydrate is an important hydrate product of Portland cement. And it is also a very important substance in alumina production. If the silicate compound with no alumina, C-S-H, can be formed in the process of alkaline alumina production, aluminum and silicon will be separated completely. Using calcium hydroxide and sodium silicate as starting materials, two kinds of calcium silicate hydrates, $\text{CaO}\cdot\text{SiO}_2\cdot\text{H}_2\text{O}$ and $2\text{CaO}\cdot\text{SiO}_2\cdot 1.17\text{H}_2\text{O}$, were hydrothermally synthesized at 120°C. The reaction rule of calcium silicate hydrate in aluminate solution has been investigated. The result shows that the reaction between calcium silicate hydrate and aluminate solution is mainly through two routes. Firstly Al replaces partially Si in calcium silicate hydrate. Secondly calcium silicate hydrate can react directly with aluminate solution, forming hydrogarnet and $\text{Na}_2\text{O}\cdot\text{Al}_2\text{O}_3\cdot 2\text{SiO}_2\cdot n\text{H}_2\text{O}$. The concentration of Na_2CO_3 and NaOH have less influence on the stability of calcium silicate hydrates; meanwhile the $\text{Al}(\text{OH})_4^-$ concentration in aluminate solution affects those remarkably.

Collaboration between Alcoa and UC, Berkeley has resulted in further experiments on of wireless sensors at Eastalco during 2004-5. The sensors were designed to measure the gas temperature in the pot exit duct and the heat flux through the pot shell. Dando (Light Metals 2004) has shown that the former (with wired sensors) signals open holes in the pot cover. Wireless measurements were intended to signal the same cell difficulty without the problems of making wired connections. The heat flux from the shell indicates the presence of sufficient ledge to ensure sidewall life. Sensors were connected to Crossbow MPR400 wireless motes running the TinyOS operating system. Early results were in a previous paper (Schneider et al. Light Metals 2005); the present paper reports on recent campaigns where duct temperatures and heat fluxes were measured over several days with results logged by a laptop and relayed by e-mail to the Alcoa Technical Center.

9:20 AM

Stability Analysis of Electrolysis Cells with MISTRAL: Morgan Le Herve¹; Thierry Tomasino¹; ¹Alcan

The control of the electrolysis cell stability represents a major stake. For this reason, many numerical models were developed by considering a linear stability approach. The stability of the electrolysis cell was studied with an unsteady 3D model (MISTRAL) strongly coupling the equations of fluid mechanics and induction. Then, two specific magnetic configurations were analysed: one known to be stable, the other known to be unstable. From the evolution in time of the interface deformation associated to a spectral analysis (FFT), the stable case from the unstable one could be differentiated. A comparison with the linear stability model (ALUCCELL) made it possible to bring up the differences as well as the advantages and disadvantages of the two numerical approaches.

9:45 AM

Busbar Sizing Modeling Tools: Comparing an ANSYS® Based 3D Model with the Versatile 1D Model Part of MHD-Valdis: Marc Dupuis¹; Valdis Bojarevics²; ¹GeniSim Inc; ²University of Greenwich

The main goal of a cell stability MHD model like MHD-Valdis is to help locate the busbars around the cell in a way that leads to the generation of a magnetic field inside the cell that itself leads to a stable cell operation. Yet, as far as the cell stability is concerned, the uniformity of the current density in the metal pad is also extremely important and can only be achieved with a correct busbar network sizing. This work compares the usage of a detailed ANSYS® based 3D thermo-electric model with the one of the versatile 1D model part of MHD-Valdis to help design a well balanced busbar network.

10:10 AM Break

10:20 AM

Comparison of MHD Models for Aluminum Reduction Cells: Valdis Bojarevics¹; Koulis Pericleous¹; ¹University of Greenwich

The self sustained waves at the aluminium-electrolyte interface, known as 'MHD noise', are observed in the most of commercial cells under certain conditions. The instructive analysis is presented how a step by step inclusion of different physical coupling factors is affecting the wave development in the electrolysis cells. The early theoretical models for wave development do not account for the current distribution at the cathode. When the electric current is computed according to the actual electrical circuit and if a sufficient dissipation is included, the waves can be stabilised. The inclusion of the horizontal circulation-generated turbulence is essential in order to explain the small amplitude self-sustained oscillations. The horizontal circulation vortices create a pressure gradient contributing to the deformation of the interface. The full time dependent model couples the nonlinear fluid dynamics and the extended electromagnetic field that covers the whole bus bar circuit and the ferromagnetic effects.

10:45 AM

Neural Model of Electric Resistance in Reduction Cells of Aluminum to be Applied on the Process Control: Marcos Castro¹; ¹ALBRAS

This work describes the development and the implementation of a electrical resistance model for application in the control of voltage of aluminium Reduction cells. For the system modeling, and aiming to surpass the difficulties and limitations of using physical equations for the behavior of the system, it was considered the use of the Artificial Neural Net tech-

Aluminum Reduction Technology: Pot Control and Modeling

Sponsored by: The Minerals, Metals and Materials Society, TMS Light Metals Division, TMS: Aluminum Committee

Program Organizers: Stephen Joseph Lindsay, Alcoa Inc; Tor Bjarne Pedersen, Elkem Aluminium ANS; Travis J. Galloway, Century Aluminum Company

Wednesday AM
March 15, 2006

Room: 7A
Location: Henry B. Gonzalez Convention Ctr.

Session Chair: Gary P. Tarcy, Alcoa Inc

8:30 AM

The New Development of the ALPSYS® System Related to the Management of Anode Effect Impact: Sylvain Fardeau¹; ¹Alcan

The development of automated process control has allowed aluminium producers to improve cell and potline control strategy. One of the features of the ALPSYS® system developed by Aluminium Pechiney is to manage and to correct abnormal or exceptional cell or potline situations. This particular point has already led to very significant improvements in anode effect rates. Given the impact of greenhouse gas (GHG) emissions from the aluminium industry, the ALPSYS® continuous improvement plan is now focusing on achieving even greater reductions in the frequency and duration of anode effects. This study compares the situation before and after ALPSYS® implementation at the St-Jean-de-Maurienne plant. It also shows the impact of feeding device crustbreaker chisel-bath contact equipment, optimized control cycle, and anticipated anode effect detection algorithms.

8:55 AM

Further Results from the Wireless Instrumentation of Hall-Héroult Cells: Micheal Schneider¹; James W. Evans¹; Paul Wright¹; Donald Ziegler¹; ¹University of California

niques, that is capable to identify the variable through the acquisition of input and output signals of the process. Moreover, the model acts with equipment that is specific for tests called "JIGA", making possible the development, simulation and implementation of new control strategies without any direct interference in the process. This becomes system much more flexible and, with more trustworthy adjustments.

11:10 AM

PIV Measurements on Physical Models of Aluminium Reduction Cells: *Mark A. Cooksey*¹; William Yang¹; ¹CSIRO

A full-scale room temperature model of part of an aluminium reduction cell was used to study bubble behaviour and gas induced liquid flows. The model consisted of three industrially-sized anodes so that the effects of the walls did not dominate. The bubbles were generated by forcing air through a porous polymer that formed the base of each anode. The liquid flows were characterised using particle image velocimetry (PIV). The effect of a longitudinal slot in each anode was investigated and was shown to have a significant effect on the liquid flows.

11:35 AM

Numerical Analysis of the Collector Bar Current Distribution of a Reduction Cell: *Dariusz Kacprzak*¹; Marcus Gustafsson¹; Liren Li¹; Mark Taylor¹; ¹University of Auckland

The paper presents modelling results of current distributions in reduction cells. The work examines an idealised reduction cell to determine the design features responsible for non-uniformities in the collector bar currents and considers design modifications to improve the current distribution. The analysis showed that non-uniformity in the collector bar currents is often caused by unsuitable resistances connected in series and that the dominant role is played by the cathode bus bar and its connecting flexes. The upstream/downstream balance is influenced by longer and shorter current paths. The design work was aimed to reduce this first-order-effect. Further analysis showed that it is important to reduce the variation in the current distribution along each side. To reduce this second-order-effect, modifications of the flex geometries were required. A before and after comparison of the cell electrical design and its impact on the riser currents and the magnetic fields is presented.

12:00 PM End

Amiya Mukherjee Symposium on Processing and Mechanical Response of Engineering Materials: Steady State Deformation of Materials - Part I

Sponsored by: The Minerals, Metals and Materials Society, TMS Materials Processing and Manufacturing Division, TMS Structural Materials Division, TMS/ASM: Mechanical Behavior of Materials Committee, TMS: Shaping and Forming Committee
Program Organizers: Judy Schneider, Mississippi State University; Rajiv S. Mishra, University of Missouri; Yuntian T. Zhu, Los Alamos National Laboratory; Khaled B. Morsi, San Diego State University; Viola L. Acoff, University of Alabama; Eric M. Taleff, University of Texas; Thomas R. Bieler, Michigan State University

Wednesday AM Room: 217C
March 15, 2006 Location: Henry B. Gonzalez Convention Ctr.

Session Chairs: Thomas R. Bieler, Michigan State University; Eric M. Taleff, University of Texas

8:30 AM Invited

The History of the Bird-Mukherjee-Dorn (BMD) Equation: *Avraham Rosen*¹; ¹Mississippi State University

The talk will outline the scientific career of Prof. Amiya K. Mukherjee from the time he was a post doctoral fellow in the lab of Prof. John E. Dorn. The author of this contribution knows him since then and cooperated with him on various research projects. Special emphasis will be given to the BMD equation that was presented for the first time at the Haifa 69' conference in Israel. In this equation the authors demonstrate, probably the first time, the importance of the structure and the sub-structure during steady state creep at high temperatures.

8:50 AM Invited

Comparisons and Contrasts in Creep Behaviour: *Geoffrey Wilson Greenwood*¹; ¹University of Sheffield

Creep rate and ductility are uniquely related to stress, temperature and structure and correlations to assist in predicting the behaviour of many widely differing materials have emerged, particularly in the past 4 decades. Progress has also been made in the evaluation of anisotropic materials, on the influence of multi-axial stresses and of the influence of temperature changes. The extent and value of these correlations will be examined together with the identification of situations, especially in creep fracture, where chemical and microstructural features make predictive capability less reliable. The nucleation and development of creep damage continue to pose problems but useful information can be derived from experimental studies of notched specimens and from materials containing gas bubbles.

9:10 AM Invited

Inverse Problems in Stochastic Modeling of Mixed Mode Power-Law and Diffusional Creep for Variable Grain Size: *Rishi Raj*¹; Jie Bai¹; ¹University of Colorado

Analytical results for two kinds of inverse problems in mixed-mode creep are presently where the material behavior is strongly influenced by grain size distribution. In one problem the measurement of the power-law stress exponent is used to predict the grain size exponent. In the second problem the measurement of the stress exponent at two different strain rates, that are one to four orders of magnitude apart, is analyzed to estimate: (i) the standard deviation, and (ii) the median value of the grain size probability density function. Thus, for the first time, we have analytical methods for deducing the variability parameters of the microstructure from phenomenological measurements of material behavior.

9:30 AM Invited

Constitutive Modelling of Creep of Metallic Materials: Some Simple Recipes: *Yuri Estrin*¹; ¹IWW, TU Clausthal

An approach to modelling dislocation glide controlled creep is presented. It is based on the evolution of dislocation density treated as an internal variable. The general constitutive modeling frame permits inclusion of microstructural features, such as grain size, volume fraction and size of second-phase particles, lamellae spacing in lamellar materials, etc. Examples of modeling creep in single-phase and particle reinforced metallic materials will be given. In the latter case, in situ evolution of particle population will also be considered. Finally, in addition to average quantities, effects of particle arrangement on the creep deformation will be discussed. A simple and transparent architecture of the models presented makes them to easy-to-use creep modeling tools.

9:50 AM Invited

On the Negligible Effect of Microstructural Variations Occurring during Steady-State Deformation on the Flow Stress: *Hael Mughrab*¹; ¹University Erlangen-Nuernberg

Experimental evidence shows that non-negligible microstructural variations occur during seemingly steady-state deformation in high-temperature creep and in cyclic deformation. These microstructural variations apparently have no significant effect on the flow stress. The experimental evidence will be reviewed. Reasons will be given why the flow stress is rather insensitive to these microstructural variations. It is proposed that, in steady-state deformation, there is a slow persistent increase of the overall dislocation density which occurs mainly in the form of geometrically necessary dislocations, giving, e.g., rise to increasing misorientations between neighbouring dislocation cells separated by cell walls which become increasingly thinner and sharper. In the Taylor flow-stress law, the increase of the dislocation density is more or less compensated by the lowering of the "arrangement" factor α , related to the reduced stress effectiveness of the dislocations.

10:10 AM Invited

On the Nature and Origin of Harper-Dorn Creep: *Farghalli A. Mohamed*¹; ¹University of California

Harper-Dorn creep refers to the anomalous high-temperature deformation behavior first reported by Harper and Dorn in their studies on the creep of Al at very low stresses and temperature near the melting temperature. Experimental data obtained on Al under the condition of small strains

(~ 0.01) indicated that Harper-Dorn creep in Al was characterized by: (a) a creep rate that was linearly proportional to stress (Newtonian behavior), (b) an activation energy for creep that was nearly equal to that for self-diffusion, and (c) a creep rate that was independent of grain size. However, the results of recent experiments performed on Al under the condition of large strains (> 0.1) have revealed two important findings. First, Harper-Dorn creep is observed in Al only when the dislocation density in annealed samples is low. Second, Harper-Dorn creep not only is accompanied by boundary activities but also is influenced by purity level.

10:30 AM Break

10:40 AM Invited

Interfacial Creep in Thin Film Structures and Application to Interconnects in Microelectronic Devices: *Indranath Dutta*¹; Michael Burkhard¹; Chandrasen Rathod¹; Vijay Sarihan²; ¹U.S. Naval Postgraduate School; ²Freescale Semiconductor

Thin film structures in microelectronic devices can deform via unusual, scale-sensitive phenomena due to thermo-mechanical loads sustained during processing, or during service as part of a microelectronic package. In particular, large shear stresses may develop at interfaces during thermo-mechanical excursions, allowing the interface to slide via diffusional processes (i.e., creep). Such interfacial creep can be further augmented by superimposed electric currents (via electromigration) as the thin film features shrink to the nanometer regime in modern microelectronic devices, potentially causing severe reliability problems. In this paper, we will present experimental and modeling approaches for deriving constitutive laws for this phenomenon, discuss the potential role of interaction between electromigration and interfacial sliding, and present experimental and modeling results to provide insight into the effect of this phenomenon on potential damage/failure mechanisms within a microelectronic device. Supported by NSF grants DMR 0075281 and DMR 0513874.

11:00 AM

Transition of Creep Behavior in BCC, FCC and HCP Solid Solution Alloys of Binary Systems: *Hirokyu Sato*¹; Hiroshi Oikawa²; ¹Hirosaki University; ²College of Industrial Technology

Creep behavior of binary solid solutions of cubic and hexagonal alloys are summarized and discussed in detail. Alloys which are strengthened by size misfit and show type-M (metal type) and type-A (alloy type) behavior, are compared with each other at the temperature range around 0.6Tm. Conditions of change in creep characteristics from type-A to type-M is overviewed from view points of both normalized critical stress and critical normalized strain rate. Concentration dependence of steady state creep rates, obtained experimentally by the authors in aluminum-magnesium (fcc and hcp), titanium-aluminum (hcp), titanium-vanadium (bcc) and iron-molybdenum (bcc) systems, are compared and discussed. Transition conditions between type-A and type-M are reasonably classified by either size-misfit parameter or non-dimensional normalized strain rate. Concentration dependence in type-M conditions is still inconsistent with investigators. Peculiar concentration dependence in alloys in type-M in high concentration solid solutions is also pronounced.

11:20 AM

Non-Contact Measurements of Creep Properties of Refractory Materials: *Jonghyun Lee*¹; Richard C. Bradshaw¹; Robert W. Hyers¹; Jan R. Rogers²; Thomas J. Rathz³; James J. Wall⁴; Hahn Choo⁴; Peter K. Liaw⁴; ¹University of Massachusetts; ²NASA MSFC; ³University of Alabama; ⁴University of Tennessee

State-of-the-art technologies for hypersonic aircraft, nuclear electric/thermal propulsion for spacecraft, and more efficient jet engines are driving ever more demanding needs for high-temperature ($> 2,000^\circ\text{C}$) materials. At such high temperatures, creep rises as one of the most important design factors to be considered. Since conventional measurement techniques for creep resistance are limited to about $1,700^\circ\text{C}$, a new technique is in demand for higher temperatures. This paper presents a non-contact method using electrostatic levitation (ESL) which is applicable to both metallic and non-metallic materials. The samples were rotated quickly enough to cause creep deformation by centrifugal acceleration. The deformation of the samples was captured with a high speed camera and then the images were analyzed to estimate creep resistance. Finite element analyses (FEA) were performed and compared to the experiments to verify the

new method. Results are presented for niobium and tungsten, representative refractory metals, at $2,300^\circ\text{C}$ and $2,700^\circ\text{C}$ respectively.

11:40 AM

Effects of Microstructure on Creep Properties of Commercial-Purity Molybdenum: *James R. Cui*¹; Eric M. Taleff¹; ¹University of Texas

The tensile creep behavior of commercial-purity, powder-metallurgy molybdenum sheet was determined using short-term creep tests at slow to moderate true-strain rates of 10^{-6} to 10^{-4} s^{-1} and temperatures between 1300°C and 1700°C . Standard strain-rate change (SRC) creep tests were used to measure the activation energy for creep (Q_c) and the steady-state stress exponents within these ranges. Creep flow stresses at these temperatures were affected by dramatic microstructural changes that occurred during testing, resulting in sudden decreases in flow stress. Elongation-to-failure (EF) tests at constant strain rate illustrate this effect. The dramatic microstructural changes causing this behavior are attributed to dynamic abnormal grain growth (DAGG). The DAGG process is found to be temperature dependent and to require an initiation strain.

12:00 PM

High Temperature Microsample Characterization of Creep in Ruthenium Nickel Aluminide Alloys: *Daniel T. Butler*¹; Brian Tryon²; Budhika Mendis¹; Tresa M. Pollock²; Kevin J. Hemker¹; ¹Johns Hopkins University; ²University of Michigan

Modern thermal barrier coatings (TBCs) consist of four distinct layers: superalloy substrate, aluminide bond coat, thermally grown oxide (TGO) and ceramic top coat. Failure of the TBC is caused by spallation of the top coat. Bond coat plasticity has been shown to play an important role in this failure process, and the high melting temperature and increased dislocation activity observed in ruthenium aluminides make them promising candidates for bond coat applications. Here, we report on micro-tensile experiments conducted to measure the elevated temperature properties of (Ni,Ru)Al and (Ni,Ru)AlCoCr. Dramatic improvements in elevated temperature tensile strength, as compared to platinum modified nickel aluminide bond coats, have been realized. Stress relaxation experiments confirm similar enhancements in creep strength and have been successfully modeled using the Dorn description of power-law creep. The measured stress exponent ($n=3$) and activation energies ($Q=150-250 \text{ kJ/mol}$) will be discussed in light of TEM observations of the underlying dislocation structure.

12:20 PM

Characterization of Stress Rupture Behavior of Zr and Ti Alloys via Burst Testing: *Gollapudi Srikanth*¹; Brian Marple¹; Indrajit Charit¹; K. Linga Murty¹; ¹North Carolina State University

An understanding of the stress rupture behavior of Zr and Ti alloy tubings is of primary importance in structural applications in energy technology. The stress rupture properties were evaluated using burst testing of closed-end thin-walled tubing at varied test temperatures and internal pressures. The rupture data are correlated using the Larson-Miller parameter. The uniform hoop strains were also measured along with rupture times from which the strain-rates were calculated. These results will be fit to Monkman-Grant relation with the aim of extrapolating to in-service stress levels. The activation energy for deformation will also be determined and the data correlated using Dorn parameters. Wherever possible, the results will be correlated with the biaxial creep data. Plans include investigation of deformation microstructures using TEM and the results to-date will be presented. This work is supported by the National Science Foundation grants DMR0101309 and DMR0412583.

Biological Materials Science: Bioinspired Materials

Sponsored by: The Minerals, Metals and Materials Society, ASM International, TMS Structural Materials Division, TMS: Biomaterials Committee, TMS/ASM: Mechanical Behavior of Materials Committee
Program Organizers: Andrea M. Hodge, Lawrence Livermore National Laboratory; Chwee Teck Lim, National University of Singapore; Richard Alan LeSar, Los Alamos National Laboratory; Marc Andre Meyers, University of California, San Diego

Wednesday AM Room: 212A
March 15, 2006 Location: Henry B. Gonzalez Convention Ctr.

Session Chairs: Mehmet Sarikaya, University of Washington; Chris Orme, Lawrence Livermore National Laboratory

8:30 AM Invited

Molecular Biomimetics: Genome-Based Materials Science and Engineering: *Mehmet Sarikaya*¹; ¹University of Washington

Functions of organisms are carried out by billions of proteins through predictable and self-sustaining interactions via molecular specificity and high efficiency leading to formation and self-assembly of controlled functional constructs, structures, tissues, and systems, at all scales of dimensional hierarchy. Through evolution, Mother Nature developed molecular recognition via successive cycles of mutation and selection. Structural control of inorganic materials at the molecular-scale is a key to synthesis of novel, practical material systems. With the recent developments of nanoscale engineering and the advances in molecular biology, we are now able to combine genetic tools with synthetic nanoscale constructs, and create a hybrid methodology, Molecular Biomimetics. We have adapted bioschemes, combinatorial biology, post-selection engineering, bioinformatics, and modeling to select and tailor inorganic-binding short, 7-60 aas, polypeptides, for use as nucleators, catalyzers, growth modifiers, molecular linkers and erector sets, fundamental utilities for nano- and nanobio-technology. Supported by ARO-DURINT and NSF-MRSEC Programs.

9:00 AM Invited

Printing Biological and Biomimetic Materials: *Paul Calvert*¹; David Kaplan²; ¹University of Massachusetts; ²Tufts University

Inkjet printing can be used to pattern layers of material on a substrate with a thickness of about 100 nm and a lateral resolution of about 20 microns. It can be seen as comparable to the building of biological tissue, layer by layer, by a sheet of cells. This talk will cover printing of materials by chemical reaction between layers of different inks, by self-assembly and by direct printing of proteins. The printing of yeast and human cells will also be discussed.

9:30 AM

Biocompatible, Osteoconductive, and Resorption Properties of Synthetic Bone Substitutes Derived from Marine Structures: *Kenneth Scott Vecchio*¹; Xing Zhang¹; Jennifer Massie¹; Mark Wang¹; Choll Kim¹; ¹University of California, San Diego

This project is focusing on optimizing the hydrothermal process to convert the aragonite/calcite to hydroxyapatite HAP or β -tricalcium phosphate (β -TCP), while maintaining the architecture of the marine structures, making the possibility of dense, well-structured, synthetic bone or strong, porous bone structures a realizable goal. Three important features of bone substitutes are their biocompatibility, osteoconductivity, and bioresorption properties, to facilitate bone in-growth and achieve a resorption rate comparable to the bone growth rate. Results from an in-vivo study using distal femur defects filled with the synthetic bone samples will be presented. Radiographically the position of the implants, possible absorption and evidence of fibrosis tissue can be determined during the implant period. Following the in-vivo implant period, electron microscopy and histology are used to establish new bone growth around and through the implant material, as well as the ability of the implants to serve as bone growth scaffolding.

9:50 AM

Biomimetic Syntheses of Inorganic Optical Materials Directed by Specific Peptides Isolated from a Phage-Displayed Library: *Matthew B. Dickerson*¹; Gul Ahmad¹; Ye Cai¹; Kenneth H. Sandhage¹; Nils Kroger¹; Rajesh R. Naik²; Morley O. Stone²; ¹Georgia Institute of Technology; ²Air Force Research Laboratory

Growing attention is being paid to the preparation of nanostructured oxide materials through biogenic or biomimetic approaches. Proteins isolated from biomineralizing organisms, or biological analogues (i.e., poly-L-lysine) to such proteins, have been used to direct the formation of silica or calcium carbonate. Although study of these naturally-occurring materials is certainly important, other oxide materials are often desired for advanced optical applications. In this work, a combinatorial phage-displayed peptide library was used to isolate and identify peptides exhibiting a binding affinity for selected inorganic optical materials, such as germania. Synthetically-produced peptides identified from the phase-displayed library, and the peptide-expressing phage, have been used to direct the nucleation and growth of optical oxides from precursor solutions. Correlations between the amino acid sequences of isolated peptides, and the nanoscale to microscale morphologies of oxide structures produced under their influence, will be discussed. The optical properties of the peptide-assembled oxides will also be presented.

10:10 AM Break

10:30 AM Invited

A Molecular View of Adsorbate Effects during Biomineralization: *Chris Orme*¹; Jennifer Giocondi¹; Molly Darragh¹; Roger Qiu¹; Jim De Yoreo¹; ¹Lawrence Livermore National Laboratory

Recent research has shown that biologically inspired approaches to materials synthesis and self-assembly, hold promise of unprecedented atomic level control of structure and interfaces. With the advent of in situ probes such as atomic force microscopy, surface processes can be imaged in real-time, providing an unprecedented view of how organic molecules modulate growth. Direct measurables such as the atomic step velocity and the critical length for step motion, can be used to distinguish whether adsorbates induce energetic changes (for example by modifying the step-edge free energy or acting as surfactants) or whether adsorbates change kinetics (for example, by pinning the step motion or acting as catalysts). Using examples from calcium carbonate and calcium phosphate crystallization we show that the organic molecules that modulate biomineral formation exhibit all of these behaviors and collectively can be used to control macroscopic crystal shape and growth rate through step-specific interactions.

11:00 AM Invited

Tailoring of Inorganic Specific Polypeptides via Post Selection Genetic Engineering: *Candan Tamerler*¹; Mehmet Sarikaya²; ¹Istanbul Technical University; ²University of Washington

It is now well established that inorganic-specific polypeptides can be selected using combinatorial biology protocols, such as cell surface and phage display methods. While the first generation peptides selected as such can directly be used in biofabrication and assembly of inorganics, we now have adapted genetic engineering protocols to further tailor polypeptides with enhanced functionalities. In this process, combinatorially selected peptides are characterized experimentally and their molecular structures, sequence similarities are evaluated using computational modeling and bioinformatics. Similar to the natural evolution process, where recursive cycle of mutation and selection resulting in the progeny with improved features, these adapted procedures and second generation libraries are used iteratively for identification of binding domains critical in dictating the recognition mechanism. Example applications engineered polypeptides in nano- and nanobiotechnology include: i. Inorganic biofabrication through catalysis; ii. Molecular erectors, and iii. Synthetic/peptide hybrids. Supported by US-ARO-DURINT, and NSF-MRSEC program and State Planning Organization of Turkey.

11:30 AM

Effect of Polyethylene Pretreatments on the Biomimetic Deposition and Adhesion of Bone-Like Calcium Phosphate Films: *Kevin C. Baker*¹; Jaroslaw Drelich¹; ¹Michigan Technological University

Improving the deposition characteristics of biomimetic calcium-phosphate (CaP) films on polymeric substrates has the potential to enhance the lifetime and performance of many orthopedic devices on the market today. The effect of increasing the hydrophilic nature of polyethylene substrata on the deposition and adhesion of calcium-phosphate (CaP) films will be discussed. Ultrasonically cleaned samples undergo oxidation via either ultra-violet (UV) treatment, corona discharge (CD) processing, or immersion in chromic acid for specified times and conditions. After the conversion of predominantly hydrophobic polyethylene to a more hydrophilic surface, the samples are immersed in a supersaturated calcium phosphate solution (SCPS) to grow porous CaP coatings. The CaP coating coverage and morphology are examined with scanning electron microscopy (SEM). Coating compositions are determined by x-ray diffraction (XRD), Fourier transform infrared spectroscopy (FTIR) and energy dispersive x-ray spectroscopy (EDS). Substrate-coating adhesion is studied by performing scratch tests with a nanoindenter.

11:50 AM

Shock-Induced Index of Refraction Changes and Dynamic Cavitation Threshold in Water: *J. Michael Boteler*¹; ¹NSWC-Indian Head

Applications of cavitation within the medical community range from lithotripsy to the use of bubble collapse jetting to penetrate cell sites for the purpose of drug delivery. As the physical understanding of micro-bubble collapse matures, emphasis for new experimental diagnostics and improved precision of existing diagnostic techniques becomes paramount. Specifically, many optical scattering techniques (Raman and IR spectroscopy etc.) require a precise understanding of the index of refraction (IOR) of the medium under investigation. Shock waves are known to alter the IOR and thus play a critical role. Modeling the complex phenomena of bubble nucleation, collapse, and jetting has proved difficult. A precise, dynamic value for the cavitation threshold is integral to the modeling effort. Purified water is examined in this study to quantify its dynamic cavitation threshold, shock-wave induced IOR, and the feasibility of using bubble collapse and micro-jetting to react with dispersed 5 micron oxidized aluminum powder.

Bulk Metallic Glasses: Physical Properties

Sponsored by: The Minerals, Metals and Materials Society, TMS Structural Materials Division, TMS/ASM: Mechanical Behavior of Materials Committee

Program Organizers: Peter K. Liaw, University of Tennessee; Raymond A. Buchanan, University of Tennessee

Wednesday AM
March 15, 2006

Room: 217B
Location: Henry B. Gonzalez Convention Ctr.

Session Chairs: Robert W. Hyers, University of Massachusetts; Matthew J. Kramer, Iowa State University

8:30 AM Invited

Finding New Fe Based Bulk Amorphous Alloys with Minimum Number of Components: *J. Zhang*¹; *H. Tan*¹; *Yi Li*¹; ¹National University of Singapore

Fe based bulk amorphous alloys have tremendous potential either as a structural material or as a magnetic material for functional application. Most of the large sized Fe based bulk metallic glasses discovered so far are multi-component with at least 6 elemental components and most of them are based on Fe, B and Rare earth. Starting from the simplest ternary Fe-B-Y system, new bulk metallic glass up to 1 mm was discovered using our recently developed pinpointing strategy. More importantly by carefully monitoring the microstructure changes, amorphous alloys with critical size large than 5 mm in Fe-B-Y based quaternary alloys have been discovered, which has never been reported before in a quaternary system. These alloys also have exceptional high fracture strength. We will discuss how these have been systematically found using our simple and practical strategy and the potential for further findings in Fe based alloys.

8:55 AM Invited

Measuring the Thermophysical and Structural Properties of Glass-Forming and Quasicrystal-Forming Liquids: *Robert W. Hyers*¹; *Richard C. Bradshaw*¹; *Jan R. Rogers*²; *Anup Gangopadhyay*³; *Kenneth F. Kelton*³; ¹University of Massachusetts; ²NASA MSFC; ³Washington University

The thermophysical properties of glass-forming and quasicrystal-forming alloys show many interesting features in the undercooled liquid range. Some of the features in the thermophysical property curves are expected to reflect changes in the structure and coordination of the liquid. These measurements require containerless processing such as electrostatic levitation to access the undercooled liquid regime. An overview of the state of the art in measuring the thermophysical properties and structure of undercooled liquid glass-forming and quasicrystal-forming alloys will be presented, along with the status of current measurements.

9:20 AM Invited

Anisotropic Free Volume Creation in a Metallic Glass during High Temperature Creep: *R. T. Ott*¹; *Matthew J. Kramer*¹; *S. Bulent Biner*¹; *M. F. Besser*¹; *D. J. Sordelet*¹; ¹Iowa State University

Zr41.2Ti13.8Cu12.5Ni10Be22.5 metallic glass was homogeneously deformed under isothermal uniaxial tensile loading at 598 K, 25° below the glass transition temperature. Total strain exceeded 80% for nominal tensile stresses of 250 and 400 MPa. High-energy synchrotron X-ray scattering and differential scanning calorimetry were used to examine strain-induced structural disordering. 2D detector allows for accurate measurements of the total scattering function in the longitudinal and transverse direction. The diffraction data and reduced radial distribution function demonstrate that the free volume parallel to the loading axis increases with increasing macroscopic strain. The free volume in the direction normal to the loading axis remained essentially constant for smaller strains. When the total strain exceeds 60%, the stress state becomes more triaxial due to the necking, resulting in an increase in the free volume in the transverse direction. DSC confirms that the amount of excess free volume is dependent on the gradient in plastic strain.

9:45 AM

Critical Analysis of Al-RE-Ni Glasses Using a Wedge-Casting Technique: *W. S. Sanders*¹; *J. S. Warner*¹; *Daniel B. Miracle*¹; ¹U.S. Air Force

The critical thickness of Al glasses with rare earth (RE) and Ni additions has been established. Twelve RE additions were studied including Ce, Dy, Er, Eu, Gd, Ho, La, Nd, Pr, Sc, Sm, and Zr. A wedge-casting technique was used to ascertain maximum glass-forming ability of each composition and differential scanning calorimetry and TEM were used to evaluate glass thermal and structural characteristics. A strong linear correlation is found between the atomic radius of the RE element and the maximum amorphous thickness obtained in each ternary system. The maximum amorphous thickness ranges from <100 µm for Al-Zr-Ni to 780 µm for Al-La-Ni. These results reveal new insights into possible mechanisms of glass formation and structure, and offer a refinement of glass-forming criteria in Al-based glasses. New metallic glasses have been discovered in the Al-Ho-Ni, Al-Eu-Ni, and Al-Sc-Ni systems. The results obtained will be reported and discussed.

10:05 AM

Fabrication of Amorphous Alloy Surface Composites by High-Energy Electron-Beam Irradiation: *Kyuhong Lee*¹; *Sunghak Lee*¹; *Nack J. Kim*¹; ¹Postech

Surface composites were fabricated with amorphous alloy powders by high-energy electron-beam irradiation, and their microstructure, hardness and wear resistance were investigated. Amorphous powders were deposited on a metal substrate, and then electron-beam was irradiated on these powders to fabricate one-layered surface composites. Two-layered surface composites were also fabricated by irradiating electron beam again onto the powders deposited on the one-layered surface composites. The microstructural analysis results indicated that a number of coarse crystalline phase particles were formed in the one-layered surface composite layers, whereas a small amount of fine and hard crystalline particles were homogeneously distributed in the amorphous matrix of the two-layered surface composite layers. Owing to these fine and hard crystalline particles, the hardness and wear resistance of the two-layered surface com-

posite layers improved over the one-layered surface composite layers. These findings suggested the possibility of applying amorphous alloy surface composites to wear- and thermal-resistant coatings or parts.

10:25 AM Break

10:35 AM

Metallic Glass Layers Produced by High Power Lasers – Applications and Opportunities: *David T. A. Matthews*¹; Vasek Ocelik¹; Jeff T. H. DeHosson¹; ¹University of Groningen

The concepts surrounding glassy metallic alloys have been directed towards the production of thick (= 250 micrometer) amorphous surface layers on light metals such as aluminium and titanium, by harnessing the processing power of high power Nd:YAG lasers to achieve the inherently high cooling rates required to form many of today's bulk metallic glasses. Microstructural and chemical observation techniques include secondary electron microscopy, transmission electron microscopy, and X-ray diffraction, which reveal fully amorphous layers are attainable. Coating to substrate adherence is achieved by virtue of a functionally graded, often amorphous matrix, interlayer around 50 micrometer in depth. Thermo-dependant properties have been explored by differential scanning calorimetry and in-situ heating with transmission electron microscopy. Hardness and nano-indentation profiles reveal hardnesses up to 13 GPa over the full depth of a coating, coupled with elastic modulus around 150 GPa. Tribological tests have also been conducted and possible applications explored.

10:55 AM

Numerical Prediction and Experiments on Casting Fe-Based Bulk Amorphous Strips on a Twin Roll Caster and a Horizontal Single Belt Strip Caster: *Roderick I. L. Guthrie*¹; Donghui Li¹; Mihaiela Isac¹; Roderick I. L. Guthrie¹; Jim Wright²; Caian Qiu²; Francois G. Hamel³; Serge Turcotte⁴; ¹McGill University; ²QuesTek Innovations LLC; ³National Research Council of Canada; ⁴IMI

The purpose of this work was to investigate the possibility of casting Fe-based bulk amorphous strip material using either twin roll and/or horizontal belt strip casting processes. Three kinds of Fe-based alloy were studied: ORNL-A1 (Fe-15B-7Co-7Mo-2Y-8Zr At.%), Darva101 (Fe-6B-15C-15Cr-14Mo-2Er At.%) and Darpa-Q21 (Fe-20B-2Zr-2Nb-1.5Cr-4.5V-2Y At.%), respectively. Maximum thicknesses of amorphous strip cast were predicted for various operating conditions for the two processes, and compared with corresponding experiments. Strip samples of 0.2~2mm thick were obtained. Darva101 alloy were cast on pilot-plant-scale twin roll caster. The strip samples' microstructures were analyzed by microscope, X-ray diffraction and SEM. Helium atmospheres were considered to be essential for enhancing cooling rates and lowering melt temperatures below the T_g values noted above. The possibility of casting Fe-based amorphous strip via the two casting processes was confirmed.

11:15 AM

Production of Bulk Metallic Glass Components by Low-Pressure Injection Die Casting: *Kevin Laws*¹; Bulent Gun¹; Michael Ferry¹; ¹University of New South Wales

This study applies a repetitive low-pressure die-casting technique for optimizing the processing parameters for producing amorphous Mg-base alloy samples of cross section 3mm x 7mm and length 125mm for use in studies of elevated temperature mechanical behaviour. The aim of the present work is to establish the optimal combination of casting parameters to generate high quality cast components and, hence, reduce the variation in quality from a minimum number of experiments. In particular, the work investigates the effects of various die-casting parameters, including melt temperature, injection pressure and injection velocity on maximum cast length, porosity and internal microstructure of Mg-base alloys. The work has generated a comprehensive set of processing maps showing the optimized casting conditions for the production of these amorphous alloys.

11:35 AM

Recent Advances in Developing Large BMGs by the MANS Research Team: J. Xu¹; C. L. Dai¹; H. Ma¹; Q. Zheng¹; Y. Li²; *Evan Ma*³; ¹IMR, CAS; ²National University of Singapore; ³Johns Hopkins University

Encouraged by our recent success in developing inch-diameter Mg-based BMGs, the MANS research team has launched a new round of ex-

plorations to locate large BMGs in other systems. Cu-based systems, due to their strong potential for ductilization, are singled out as the next group worthy of special attention. Concurrently, the team has been striving to derive decent plasticity from the large BMGs discovered. The over-riding theme is to invent BMGs that not only are large and inexpensive (based on engineering metals), but also possess mechanical properties (strength and ductility) that are practically useful in structural applications. This talk highlights some of the recent progress in these directions.

11:55 AM

Solidification Behavior of Fe-Base Amorphous Alloys during Twin-Roll Strip Casting: *Yoon S. Oh*¹; Jung G. Lee¹; Nack J. Kim¹; ¹Pohang University of Science & Technology

Bulk amorphous alloys usually possess ultra-high strength, which are quite desirable for application as structural components. However, there are several obstacles which prevent their widespread applications such as high costs due to exotic alloying elements and limited fabrication methods and limited plasticity. In the present study, Fe-base bulk amorphous alloys were fabricated by twin-roll strip casting, which has been shown to be a cost efficient method for fabricating bulk amorphous alloy sheet products. Fe-base bulk amorphous alloys are interesting in that they are relatively inexpensive as compared to other bulk amorphous alloys. To improve the plasticity, microstructure of the alloys was modified to contain second phase of crystalline particles within amorphous matrix by control of alloy compositions and twin-roll strip casting conditions. Cooling sequence during twin-roll strip casting and continuous cooling transformation (CCT) diagram were simulated to determine the optimum process conditions at which desirable microstructures could be achieved.

Carbon Technology: Cathode Properties/ Refractory Materials

Sponsored by: The Minerals, Metals and Materials Society, TMS Light Metals Division, TMS: Aluminum Committee

Program Organizers: Morten Sorlie, Elkem Aluminium ANS; Todd W. Dixon, Conoco Phillips Venco; Travis J. Galloway, Century Aluminum Company

Wednesday AM
March 15, 2006

Room: 8A
Location: Henry B. Gonzalez Convention Ctr.

Session Chair: Glen Goeres, Alcoa Aluminum

8:30 AM

Influence of Internal Cathode Structure on Behavior during Electrolysis Part III: Wear Behavior in Graphitic Materials: *Pretesh Mahendrabhai Patel*¹; Margaret Hyland¹; Frank Hiltmann²; ¹University of Auckland; ²SGL Carbon GmbH

An extensive laboratory study has been undertaken to determine the effect of changes in internal structure on graphitized and graphitic cathode blocks used in aluminium reduction cells. Research has focused on sub-surface chemical and electrochemical wear. Previous work on graphitized material (published in Light Metals 2005) showed increasing the total porosity leads to uneven wear with pitting due to particle detachment becoming a noticeable feature of the surface topography. Results also showed that wear is dependant on the combined interaction of multiple variables, in particular the interaction between current density, bath chemistry and porosity. This paper focuses on recent work with a graphitic material. Compared to the graphitized materials, the graphitic cathodes show even wear phenomena with less surface pitting; this is due to the reduction in porosity in the graphitic material. The effect of variables such as current density, bath chemistry and porosity will also be addressed.

8:55 AM

A Study on the Property Changes of Cathode Blocks during Aluminium Smelting: *Fengqin Liu*¹; Yexiang Liu²; ¹Zhengzhou Research Institute of Chalco; ²Central South University

The properties of the waste cathode samples from the reduction cells with different working life have been studied in this paper. The chemical and mineralogical compositions of the waste cathodes and their physical

WEDNESDAY AM

properties and microstructures have been analysed by SEM and XRD etc. The study results show that the volume density, compressive strength of the cathode samples are enhanced, and their conductivity is even increased by 30-50% after undergoing aluminum reduction process. It is found from SEM and XRD analysis that there appears a large amount of graphite in the waste cathodes and some cryolite, fluorides and metal aluminum penetrate into the gaps in the cathodes. It is suggested that the cathode blocks with higher strength and electrical conductivity and lower porosity and permeation property should be used in order to prolong the cathode working life.

9:20 AM

Wetting and Cryolite Bath Penetration in Graphitized Cathode Materials: Nikolai Shurov¹; Nina Kulik¹; Leonid Sitnikov¹; Larissa Babushkina¹; Victor Stepanov¹; Yurii Zaikov¹; Andrei Khramov¹; Vyacheslav Malkov¹; Alexander Gusev²; Anton Frolov²; ¹Institute of High Temperature Electrochemistry; ²RUSAL

The special electrochemical cell was used in order to measure angles of wetting on different materials depending on cathode current density. Wetting of all samples was found to improve with cathode current rise. The dynamics of contact angles decrease depends on a type of material and the open porosity value. The investigation of bath penetration was carried out at 960°C under argon atmosphere in a special closed container made of the same cathode materials. Penetration depth was found to depend on open porosity. At the same conditions impregnated materials have lower penetration depth. The distribution of electrolyte components depending on distance from interface boundary has been investigated by local microspectral analysis method. The conclusions on different elements absorption mechanism were made on the basis of electrolyte components concentration in pores.

9:45 AM

Sodium Penetration into Carbon-Based Cathodes during Aluminum Electrolysis: Jilai Xue¹; Qingsheng Liu¹; Jun Zhu¹; ¹University of Science and Technology Beijing

Sodium penetration into carbon-based cathodes during aluminum electrolysis was investigated in a laboratory cell. The sodium penetrations into the cathode specimens were determined against electrolysis time, electrolyte composition and current density. The results show the sodium penetration varies as various additives present in the carbon-based cathodes.

10:10 AM Break**10:25 AM**

SiC in Aluminium Electrolysis Cells: An Update: Rudolf P. Pawlek¹; ¹TS+C Technology Information Services and Consulting

The physical and chemical properties, the bond types and the resistance to bath, aluminium, carbon dioxide and air attack of SiC are reviewed, outlining especially the use of non-oxide bonded SiC refractories as sidewall materials for aluminium electrolysis cells. This type of SiC sidewall lining material is particularly suitable for the operation of modern electrolysis cells equipped with point feeders for automatic alumina feeding to the bath.

10:50 AM

A New Test Method for Evaluating Si₃N₄-SiC Bricks' Corrosion Resistance to Aluminum Electrolyte and Oxygen: Xiaozhou Cao¹; Bingliang Gao¹; Zhaowen Wang¹; Xianwei Hu¹; Zhuxian Qiu¹; ¹North-eastern University

In the paper a new test method was applied to evaluate the bath resistance and oxygen resistance of silicon nitride bonded silicon carbide bricks that were used for sideling in aluminum electrolysis pots. In test, carbon dioxide gas was input to the molten electrolyte in which part of sample was immersed in order to simulating the factual operating conditions of cells. Based on the method the bath resistance and oxygen resistance of refractory bricks from several Chinese refractory factories were tested. The method was also used to evaluate the bath resistance of different parts of one brick. The test result showed that the inside of the brick had worse bath resistance than the outside, which may be caused by lower content of Si₃N₄ and higher content of impurities in the inner part of the brick.

11:15 AM

Test Method for Resistance of SiC Materials to Cryolite: Junguo Zhao¹; Zhiping Zhang¹; Wenwu Wang¹; Guohua Liu¹; ¹Luoyang Institute of Refractories Research

To obtain a stable and reliable test method for determination of the resistance of SiC materials to cryolite. This 'Rotating-CO₂-Cryolite' test method has been designed by LIRR. The test specimens are being rotated in molten bath and CO₂ and then placed in the test furnace to simulate the actual working conditions in reduction cells (pots). The influences of test temperature, holding time, CO₂ flow rate and atmosphere inside the furnace (CO₂, air and argon gas) on the cryolite resistance of Si₃N₄-SiC materials have been studied. The initial study shows that the optimized test parameters are 1000°C, holding time 24h, CO₂ flow rate 1.0 L/min and rotating speed 30 rpm.

Cast Shop Technology: Casting, Solidification and Cast Defects

Sponsored by: The Minerals, Metals and Materials Society, TMS Light Metals Division, TMS: Aluminum Committee

Program Organizers: Rene Kieft, Corus Group; Gerd Ulrich Gruen, Hydro Aluminium AS; Travis J. Galloway, Century Aluminum Company

Wednesday AM

March 15, 2006

Room: 7C

Location: Henry B. Gonzalez Convention Ctr.

Session Chair: Steve Cockcroft, University of British Columbia

8:30 AM

Heat Fluxes at Metal-Mold Interface during Casting Solidification: Adrian S. Sabau¹; ¹Oak Ridge National Laboratory

In this study, the heat transfer at the metal-mold interfaces is investigated using a sensor for the direct measurement of heat flux. Casting experiments were conducted using graphite molds for aluminum alloy A356. Several casting experiments were performed using a graphite coating and a boron nitride coating. The temperature of the mold surface was provided by the heat flux sensor while the temperature of the casting surface was measured using a thermocouple. Results for the heat transfer coefficients were obtained based on measured heat flux and temperatures. Four stages were clearly identified for the variation in time of the heat flux. Values of the heat transfer coefficient were in good agreement with data from previous studies.

9:00 AM

An Integrated Approach to Control Hot Tearing in Sheet Ingot DC Casting: Benoit Commet¹; André Larouche²; ¹Alcan CRV; ²Alcan ARDC

Among other defects, hot tearing is responsible for an important proportion of production losses. This paper presents an integrated approach to tackle this problem. The approach relies on fundamental understanding, experimental casting, mathematical modelling and application on particular situations. Simple, but promising hot tearing criteria are described. Criteria evaluate cracking sensitivities of alloys and provide an estimation of the castability in new product conception. Presentation of industrial cases is made. Also, realistic process conditions of application of the criteria are presented. Tuning of casting practices and/or development of new technology using this approach are highlighted. Various examples show that a rigorous approach integrating physical and numerical modelling provide an efficient tool to improve DC-cast slab quality and to reduce ingot defects increasing production recovery.

9:30 AM

Comparison of Experiments with Computer Simulations of Constant Unidirectional Melt Flow along Solidification Front: Andrey Turchin¹; Dmitry G. Eskin¹; Laurens Katgerman²; ¹Netherlands Institute for Metals Research; ²Delft University of Technology

Effects of melt flow on structure formation during solidification were studied experimentally using a specially designed setup consisting of an electromagnetic pump and a melt transfer system with a built-in chill with the aim to correlate the structure and process parameters under conditions

of constant melt flow. In the present paper, CFD simulations of melt flow and solidification are applied as a tool to interpret the structure development under conditions of linear flow. Different geometries of the chill are tested in order to achieve laminar flow conditions in the widest possible flow velocity range. The computational results are validated against experimentally measured temperatures. The experimental and computational results show that flow parameters such as velocity and temperature affect the grain morphology, size and growth direction in a binary Al–Cu alloy.

10:00 AM

Studies in the Casting of AA6111 Strip on a Horizontal, Single Belt, Strip Casting Simulator: *Roderick I. L. Guthrie*¹; ¹McGill University

Strips of AA6111 automotive alloy were cast on a horizontal single belt strip casting simulator. Chill substrates of pure copper and carbon steel were sprayed with various coatings for improving the strips' surface quality. The microstructures of the strip samples were studied by microscope and Scanning Electron Microscopy (SEM). The effects of casting parameters, including casting temperature and strip thickness, on interfacial heat fluxes, cooling rates and microstructures, were investigated. Very fine equiaxed grains were obtained for both 1.2mm and 2.5mm thick strips thanks to the rapid extraction of heat, and effective grain refinement procedures.

10:30 AM Break

10:45 AM

Billet Quality Assessments and Investigation of Fine Oxides in 6000 Series VDC Cast Product: *Malcolm J. Couper*¹; *Barbara Rinderer*¹; *Ben Cumerford*²; ¹Comalco Aluminium Ltd; ²University of Queensland

The assessment of homogenised billet quality is routinely carried out for random samples from a range of billet diameters and alloys produced in the casthouse. The results of the assessments are tracked to confirm quality and process control. The laboratory evaluation includes ultrasonic and dye penetrant testing for inclusions and defects, hardness, macro etching for grain size and chill zone, as well as microstructural examination of intermetallics at the surface mid-radius and centre of the slices. The presence of fine oxides within the butt region of the billet have been investigated to determine their number, size and distribution. Factors influencing the occurrence of these oxides are discussed.

11:15 AM

Remelt Ingot Mould Heat Flow and Deformation: *John Francis Grandfield*¹; ¹CSIRO

A study of mould heat transfer, air gap formation and mould deformation has been made with pure aluminum cast in a 22.5 kg ingot mould. A rig was built which casting machine conditions were replicated for a single ingot allowing thermocouples to be placed in the ingot and the mould. Displacement transducers were used to measure the ingot and mould displacements. Thermal and stress modeling were conducted. The heat flow across the ingot/mould interface was found to be controlled by the formation of an air gap between the ingot and the mould. The air gap dimension is in turn a function of mould distortion and ingot contraction.

Characterization of Minerals, Metals and Materials: Structural Engineering Materials III

Sponsored by: The Minerals, Metals and Materials Society, TMS Extraction and Processing Division, TMS: Materials Characterization Committee

Program Organizers: Jiann-Yang James Hwang, Michigan Technological University; Arun M. Gokhale, Georgia Institute of Technology; Tzong T. Chen, Natural Resources Canada

Wednesday AM
March 15, 2006

Room: 206A
Location: Henry B. Gonzalez Convention Ctr.

Session Chairs: Jian Li, Natural Resources Canada; Donato Firrao, Politecnico Di Torino

8:30 AM

Blunt Notch Specimens Fracture Behavior in Quenched and Tempered Tool Steels with and without Surface Treatment: *Donato Firrao*¹; *Daniele Ugues*¹; ¹Politecnico Di Torino

A comparison of fracture modes on impact tested quenched and tempered blunt notch die steel samples with varying notch root radii are described. Fracture mechanisms occurring on such samples is compared with that of nitrided specimens. On the basis of a previously developed model, different zones of the fracture surface are identified: (I) a "stress free zone", where multiple cracking formation at notch root provides a stress release in subsurface layers and actually creates a virtual larger notch radius; (II) a zone where the crack propagates along logarithmic spirals of a slip line field; (III) a zone where the crack finally rapidly propagates along the reduced section. The metallurgical structure of the surface layer is correlated with the aforementioned zones, considering the case of quench and tempered tool steels, where only mechanical working affected structures can be present, and of surface treated tool steel, where compound and diffusion layers exist.

8:55 AM

Characterization of Surface-Treated and Cold-Worked Nickel-Base Superalloys: *Hyojin Song*¹; *Peter B. Nagy*¹; *Vijay K. Vasudevan*¹; ¹University of Cincinnati

The intentional introduction of near-surface compressive residual stresses, using method like laser shock peening (LSP), is well known for enhancing the resistance to fatigue crack nucleation and growth of turbine engine parts. Recently, nondestructive quantitative eddy current conductivity measurements have been successfully utilized to measure the state and degree of residual stress in shot-peened and cold worked nickel-base superalloys. However, the difficulty in separating the macro residual stress (elastic) and cold work (plastic) contributions to the conductivity has militated against the achievement of a complete analysis of the measured frequency-dependent apparent eddy current conductivity (AECC) results, and, furthermore, there is a lack of basic understanding of how intrinsic and extrinsic factors like microstructural changes brought about by surface and/or cold-work treatments affect the conductivity. The present study combines measurements of electrical resistivity/conductivity with detailed characterization of microstructure, residual stress distributions and quantitative analysis of surface-treated and cold worked Ni-base superalloys.

9:20 AM

Effect of Retrogression and Re-Aging Treatment on Stress Corrosion Cracking Resistance of 7075 Aluminum Alloy: *Murat Baydogan*¹; *Hüseyin Çimenoglu*¹; *Sabri Kayali*¹; *Jahan Rasty*²; ¹Istanbul Technical University; ²Texas Tech University

Effect of retrogression and reaging (RRA) treatment on hardness and stress corrosion cracking resistance of 7075 aluminum alloys was investigated. As received 7075 alloys in T6 tempered condition were retrogressed at 170, 220, 240 and 380°C for different durations between 15 s and 60 min. Subsequent re-aging was made at the T6 ageing condition. Treated materials exhibited higher hardness and better stress corrosion cracking resistance than T6 temper in a wide range of retrogression temperature and time. The highest hardness was obtained after retrogression at 170°C

for 210 s followed by re-aging, corresponding to 20% hardness improvement. Improvements in stress corrosion cracking resistance of the alloy by as much as 85% was also observed. Stress corrosion cracking resistance of the alloy was also improved dramatically. In this paper, improvements in hardness and stress corrosion cracking resistance are discussed on the basis of the microstructural changes during RRA treatment.

9:45 AM

Microstructural Characterization of Mg Based Alloys: Apóstolos Jean Sideris Junior¹; Ana Lucia Diegues Skury¹; Gueroold Sergevitch Bobrochnitchii¹; Sergio Neves Monteiro¹; ¹UENF

It is known that Mg can act as a catalyst/solvent in the high pressure-high temperature diamond synthesis. However, above pressure levels of the order of 7 GPa, and temperatures from 1700-1800°C, it was not possible yet to use Mg for the industrial diamond production. A possible alternative in the use of MgNi based alloys. Moreover, owing to the great Mg reactivity, it was consider, so far, a difficult task to deal with such alloys. The present work presents successful results regarding the application of MgNi alloys, with different composition, at high pressure conditions. The behavior of the alloys and their microstructured characterization is analysed.

10:10 AM Break

10:20 AM

Texture Evolution and Monotonic and Cyclic Response of Interstitial Free (IF) Steel after Severe Plastic Deformation at Room Temperature: Guney Guven Yapiçi¹; Steve Sutter¹; Ibrahim Karaman¹; Hans J. Maier²; ¹Texas A&M University; ²University of Paderborn

Present work investigates the mechanical behavior and texture evolution of severely deformed IF steel using equal channel angular extrusion. ECAE is applied by extruding bulk billets through two perpendicular channels of equal cross section achieving a simple shear deformation in a thin layer at the crossing plane of the channels. IF steel was processed up to 16 passes using various ECAE routes to investigate the processing-microstructure-property relationships. An extensive program was undertaken to characterize microstructure, crystallographic texture and mechanical properties of successfully extruded billets. Eight pass extrusion following route Bc resulted in yield strengths close to 700 MPa exhibiting a ten-fold increase compared to the annealed materials. Low cycle fatigue experiments on the eight pass sample demonstrated a more than two-fold increase in both the cyclic strength and number of cycles to failure. Effect of ECAE texture on the monotonic and cyclic response is discussed together with cyclic microstructural evolution.

10:45 AM

The Characterization of the Intermetallic Fe-Al Layer of Steel-Aluminum Weldings: Michael Potesser¹; Thomas Schoeberl¹; Helmut Antrekowitsch¹; Juergen Bruckner²; ¹University of Leoben; ²Fronius International GmbH

One of the main targets in the automotive industry and supplying industry is the weight reduction of the vehicle for decrease the fuel consumption. For that reason combinations of different kinds of materials and connections for example steel and aluminium are developed or are already successfully field-tested. A determining factor concerning the quality assessment of the welded joint during hybrid welding is the characterisation of the intermetallic Fe-Al layer regarding strength, hardness, morphology and mainly the different phases in which Fe occurs together with the aluminium (FeAl, Fe₂Al₅, FeAl₃). A combination of conventional light microscopy, SEM - EDX - analysis, the usage of an atomic force microscope including a nanointender and theoretical thermodynamic calculations turned out to be highly effective. Based on the attained results the intermetallic FeAl layer, influenced by silicon, manganese and zinc, can be predicted.

11:10 AM

Microstructure of Nb-Si-Ti-Al-Cr-X Alloys for High Temperature Aeroengine Applications: Hyojin Song¹; Raghvendra Tewari¹; Amit Chatterjee²; Vijay K. Vasudevan¹; ¹University of Cincinnati; ²Rolls-Royce Corporation

Advanced intermetallic materials, in particular the refractory Nb-based silicides, possess a good combination of properties like high strength at

elevated temperatures, high stiffness, low density, etc., which make them potential candidate materials for high temperature applications. However, the binary material exhibit low room temperature ductility and poor oxidation at elevated temperature. A multi element approach, which produces these silicides in equilibrium with the soft β -matrix, appears to provide a solution to the aforementioned problems. The present paper reports microstructures of as-cast and heat treated Nb-Si-Ti-Cr-Al based multi component system. The microstructural investigation has revealed the presence of four distinct phases, namely, the matrix β phase, the Cr₂(Nb,Ti) Laves phase, which had dissolved and re-precipitated during various heat treatments, and Nb- and Ti- 5-3 silicides, in these alloys

11:35 AM

Local Thermal Property Analysis by Scanning Thermal Microscopy of Ultrafine-Grained Surface Layer in Copper and Titanium Produced by Surface Mechanical Attrition Treatment: Fuan Guo¹; Nathalie Tranno¹; ¹Suzhou Institute for Nonferrous Metal Research

Ultrafine-grained surface layers were obtained by surface mechanical attrition treatment (SMAT) in copper and titanium samples, the thermal properties of the deformed layers were then characterized using a scanning thermal microscopy that allows thermal conductivity to be mapped down to the submicrometer scale. It is found that the microstructures obtained by SMAT show different thermal conductivities that strongly depend on the grain size: the thermal conductivity of the nanostructured surface layer decreases substantially if compared with that of the coarse-grained matrix of the sample. A theoretical approach, based on this investigation, was used to calculate the heat flows from the probe tip to the sample and then estimate the thermal conductivities at different scanning positions. Experimental results and theoretical calculation demonstrate that the SThM analyses open a new way for the thermal property and microstructural analysis of ultrafine-grained microstructures.

Computational Thermodynamics and Phase Transformations: Phase Field Models I

Sponsored by: The Minerals, Metals and Materials Society, TMS Electronic, Magnetic, and Photonic Materials Division, TMS Materials Processing and Manufacturing Division, TMS Structural Materials Division, TMS: Chemistry and Physics of Materials Committee, TMS/ASM: Computational Materials Science and Engineering Committee
Program Organizers: Dane Morgan, University of Wisconsin; Corbett Battaile, Sandia National Laboratories

Wednesday AM
March 15, 2006

Room: 210A
Location: Henry B. Gonzalez Convention Ctr.

Session Chairs: Jeffrey J. Hoyt, Sandia National Laboratories; Nikolas Provatas, McMaster University

8:30 AM Invited

Phase Field Simulations of Microstructural Development: Topology and Topological Singularities: R. Mendoza¹; S. Hao¹; K. Thornton²; P. W. Voorhees¹; ¹Northwestern University; ²University of Michigan

The evolution of microstructures using three-dimensional reconstructions and computations is investigated. Three-dimensional phase field calculations are employed along with three-dimensional reconstructions of microstructure to follow the evolution of a topologically complex dendritic microstructure during coarsening in two-phase mixtures, and grain structures in Ti alloys. By using the experimentally measured microstructures as initial conditions in the phase field calculations it is possible to compare quantitatively the experimentally measured microstructure with the calculations. For systems undergoing coarsening, phase field calculations are used to compute the average time rate of change of a given pair of principle interfacial curvatures at a point on the surface. The calculations also show the important role topological singularities play in the evolution of dendritic structures during coarsening. The results of calculations of grain growth that employ experimentally measured grain structures will also be presented.

9:00 AM Invited

Mixed Stress: An Approach to Mixing Fluids and Solids in Phase Field Models: *Adam C. Powell*¹; ¹Massachusetts Institute of Technology

The Mixed Stress method combines elastic stress in a solid with viscous stress in a fluid in order to model phase transformations involving solids which move in response to fluid flow around them. The local weighting of the elastic and viscous stresses is a function of the local phase: in the fluid, only the viscous stress applies; in the solid, only the elastic stress (unless the solid is viscoelastic); in between, an interpolation function combines the two to produce smooth variation across a diffuse fluid-solid interface. This method is not optimal for all fluid-solid phase transformations; for example, liquid metals near their melting point behave more like very viscous fluids than elastic solids. This talk will therefore focus on application of mixed stress to other phenomena, such as electrochemistry and polymer crystallization, and discuss avenues for further development and application.

9:30 AM

Three-Dimensional Simulation and Characterization of Coarsening in Complex Microstructures Following Order-Disorder Transformation: *Yongwoo Kwon*¹; *Katsuyo Thornton*²; *Peter W. Voorhees*¹; ¹Northwestern University; ²University of Michigan, Ann Arbor

Order-disorder transformation is observed in a variety of materials ranging from polymers to metals. This process frequently produces a complicated and highly interconnected 3D interfacial morphology possessing both positive and negative curvatures. Such a microstructure cannot be fully described by information obtained from its two-dimensional cross-sections. Characterizing the morphology of these structures in three-dimensions has proven challenging. We employ analyses of the three-dimensional curvature and the genus in two-phase microstructures obtained by large-scale phase-field simulations using the Allen-Cahn equation. The simulations are conducted in a high-performance parallel computing environment. We investigate the evolution of microstructures using quantifiable measures such as the interfacial shape distribution (the probability of finding a patch of interface with a given pair of principal curvatures) and topological quantities like the genus of the microstructures. We will discuss quantitatively the microstructural evolution and the presence of scaling using these characteristics.

9:50 AM

Phase Field in Polymeric Membrane Formation: *Bo Zhou*¹; *Adam C. Powell*¹; ¹Massachusetts Institute of Technology

A ternary phase field model is applied to simulate the polymeric membrane formation by phase inversion techniques. A ternary Cahn-Hilliard formulation incorporating a Flory-Huggins homogeneous free energy function is used. The Water/DMF/PVDF ternary system with a two-layer polymer-solvent/nonsolvent initial condition and with a mass-transfer boundary condition is used to simulate actual membrane fabrication conditions. 2D and 3D simulation results show the membrane morphology evolution during the spinodal decomposition. The simulated final morphologies in 2D show an asymmetric structure of membranes with a top layer, while 3D simulation results show a more symmetric structure. Simulations with different initial compositions show membrane morphology changes from isolated droplets to bi-continuous patterns. The effects of concentration-dependent polymer mobility are studied in both 2D and 3D. Different formula of variable mobility are adopted. In addition, the Navier-Stokes equations are coupled with this ternary Cahn-Hilliard to model hydrodynamic effects in 2D and 3D.

10:10 AM Break

10:30 AM Invited

Confronting Atomistic and Continuum Models of Solid-Liquid Interfaces: *Alain S. Karma*¹; *Kuo-An Wu*¹; *Mark D. Asta*¹; *Jeffrey J. Hoyt*²; ¹Northeastern University; ²Sandia National Laboratories

Major advances in both atomistic and continuum modeling of solid-liquid interfaces have been made over the last few years. On the one hand, the advent of the capillary fluctuation method has yielded an accurate determination of energetic and kinetic interface properties for a wide range of potentials. On the other, the phase-field crystal method inspired from density functional theory has emerged as a potentially powerful continuum simulation tool that enables simulations on much larger time scale than

atomistic simulations, and naturally describes anisotropic interfacial properties related to crystal structure. The phase-field crystal method is also closely related to older Ginzburg-Landau theories of solid-liquid interfaces based on order parameters that are the amplitudes of density waves corresponding to principle reciprocal lattice vectors. This talk explores the quantitative relationship between atomistic simulations, phase-field crystal models, and Ginzburg-Landau theories in the context of a detailed comparison of solid-liquid interface structure and excess free-energy for body-centered-cubic forming systems. Hopes and perils of respective continuum approaches are emphasized.

11:00 AM Invited

Phase Field Crystal Modeling: *Ken Elder*¹; ¹Oakland University

Over the past several years a relatively simple phase field model has been developed to study elastic and plastic deformations in crystal growth phenomena. This simple model was used to study many interesting phenomena including epitaxial growth, yield strength in nanocrystals, grain growth, reconstructive phase transitions and ductile fracture. In this talk I would like to discuss recent developments in this modeling technique such as the incorporation of specific atomic potentials, extensions to three dimensions and binary systems.

11:30 AM

Finding the Critical Nucleus of Martensite with Phase Field Method: *Chen Shen*¹; *Ju Li*¹; *Yunzhi Wang*¹; ¹Ohio State University

A mechanistic description of nucleation of martensite was proposed more than two decades ago by Olson and Morris, where a martensitic nucleus is formed from dissociation of a group of pre-existing lattice dislocations and the nucleation barrier is evaluated in a classical nucleation framework. This picture is adopted in a new phase field model originated from a treatment for dislocations at microscopic length scales. The model includes both dilatational and shear strain components and uses *ab initio* generalized stacking fault energy for quantitative calculations. The activation energy and morphology of a critical nucleus is sought in a non-classical nucleation scheme by finding the saddle point of the total energy consisting of a self-consistently described stacking fault energy and elastic energy.

11:50 AM

Analysis of Nucleation and Interfacial Mobility for Polygonal Ferrite Formation Using Phase Field Simulations: *Maria Mecozzi*¹; *Matthias Militzer*²; *Jilt Sietsma*³; *Sybrand van der Zwaag*³; ¹Netherlands Institute for Metals Research; ²University of British Columbia; ³TU Delft

2D and 3D phase field simulations of the austenite (g) to ferrite (a) transformation during continuous cooling at different cooling rates were performed for a Fe-0.10 C- 0.49 Mn (wt%) steel. The initial austenitic microstructure and the nuclei density are input data based on experimental observations. Ferrite nuclei are assumed to form continuously over a temperature range of ΔT . The model considers carbon diffusion and employs an effective interfacial mobility with an activation energy of 140kJ/mol and a pre-exponential factor, m_0 , that, together with ΔT , is used as fitting parameter to optimise the agreement between the predicted and measured ferrite fraction. The best fitting combinations (m_0 , ΔT) have then been concluded by considering the ferrite grain size distribution that depends on ΔT as selection criterion. The model provides a reasonable description of the experimental data when ΔT and m_0 are increased with cooling rate.

12:10 PM

A Novel Approach to the Calculation of Energy and Lattice Resistance to Sliding of Small-Angle Twist Boundaries: *Chen Shen*¹; *Ju Li*¹; *Yunzhi Wang*¹; ¹Ohio State University

Grain boundary properties including grain boundary energy and sliding under stresses have been extensively studied with atomistic models such as molecular dynamics. At small angles the simulation becomes increasingly expensive with the size of the periodic cell. A recently developed phase field model for dislocations at microscopic length scales is extended to study twist grain boundaries via atomic disregistry fields in the boundary plane, which at small twist angles give rise to well defined dislocation networks. The model makes use of first principles γ -surface for quantitative study. It is first validated by comparing with Peierls model the calculated core structures of straight dislocations, and then applied to

WEDNESDAY AM

simulating dislocation core structures of small-angle twist boundaries and to calculate their energies. Following the Peierls-Nabarro scheme the lattice friction for grain boundary sliding is calculated from the Peierls stress of constituent screw dislocations.

Deformation and Fracture from Nano to Macro: A Symposium Honoring W. W. Gerberich's 70th Birthday: Macroscopic Mechanical Behavior

Sponsored by: The Minerals, Metals and Materials Society, TMS Materials Processing and Manufacturing Division, TMS Structural Materials Division, TMS/ASM: Mechanical Behavior of Materials Committee, TMS: Nanomechanical Materials Behavior Committee
Program Organizers: David F. Bahr, Washington State University; James Lucas, Michigan State University; Neville R. Moody, Sandia National Laboratories

Wednesday AM Room: 214D
March 15, 2006 Location: Henry B. Gonzalez Convention Ctr.

Session Chair: Kumar V. Jata, U.S. Air Force

8:30 AM Invited

Fatigue Crack Initiation in Supergrains in Waspaloy at 20°C: *David L. Davidson*¹; R. Tryon²; Michael E. Oja³; K. S. Ravi Chandran³; ¹Consultant; ²VEXTEC; ³University of Utah

Orientation microscopy (EBSP) was used to measure the Euler angles for grains that initiated fatigue cracks and for grains surrounding the initiating grain. It was hypothesized that cracks initiated preferentially in clusters of grains having similar orientations so that slip could be more easily transmitted across grain boundaries, thus making it appear as if these grain clusters were effectively one large grain (supergrain). Analysis of the results supports this hypothesis. Supergrain criteria were not satisfied in two non-crack regions used as controls. Grains in an area where a crack initiated from a void did not satisfy the supergrain criteria. A basis for predicting the sites for crack initiation in clean alloys has been established.

8:50 AM

Elevated Temperature Low-Cycle-Fatigue Behavior of HAYNES® 188® Superalloy: *Yulin Lu*¹; L. J. Chen¹; G. Y. Wang¹; M. L. Benson¹; P. K. Liaw¹; S. A. Thompson²; J. W. Blust²; P. F. Browning²; A. K. Bhattacharya²; J. M. Aurrecochea²; D. L. Klarstrom³; ¹University of Tennessee; ²Solar Turbines, Inc.; ³Haynes International, Inc.

Total strain controlled low cycle fatigue (LCF) tests with and without hold times were performed at temperatures ranging from 816 to 982°C in laboratory air on a cobalt-based superalloy, HAYNES 188. The influence of hold time on the cyclic-stress response and fatigue life was studied. Fracture surfaces and metallographic sections were evaluated in terms of the crack initiation and propagation modes, i.e., transgranular or intergranular. The introduction of a hold time led to a decrease in fatigue life. An increase in temperature and/or the introduction of a hold time decreased the stress hardening rate and increased the softening rate. Within the two phases of the fatigue process, crack initiation was more severely influenced by the change of hold time and/or temperature.

9:05 AM

Low-Cycle Fatigue Behavior of an As-Extruded AM50 Magnesium Alloy: *Lijia Chen*¹; Chunyan Wang¹; Wei Wu¹; Zheng Liu¹; Grigoreta M. Stoica²; *Peter K. Liaw*²; ¹Shenyang University of Technology; ²University of Tennessee

The low-cycle fatigue behavior of an as-extruded AM50 magnesium alloy has been investigated. The cyclic stress response of the alloy strongly depends on the imposed strain amplitude. It is also noted that at the higher total strain amplitudes, the alloy exhibits a pronounced anisotropic behavior in the direction of tension and compression, where the width of the hysteresis loop in the tensile direction is greater than that in the compressive direction. At the total strain amplitude of 1.5%, a serrated flow can be observed in the compressive direction of the hysteresis loop. It means that the dynamic strain aging takes place during fatigue deformation. The re-

lation between elastic and plastic strain amplitudes with reversals to failure shows a monotonic linear behavior and can be well described by the Basquin and Coffin-Manson equations, respectively. In addition, crack initiation and propagation modes are suggested, based on SEM observations on the fracture surfaces.

9:20 AM

Remarkable Dynamic Mechanical Properties of a "Trimodal" Al 5083/B4C Composite: *Haitao Zhang*¹; *Shailendra P. Joshi*¹; *K. T. Ramesh*¹; *Jichun Ye*²; *Julie M. Schoenung*²; *Ernest S. C. Chin*³; ¹Johns Hopkins University; ²University of California, Davis; ³Army Research Laboratory

We have examined the mechanical behavior of a "tri-modal" Al5083/B4C composite in compression at both low and high strain rates. The material is tri-modal in that it incorporates (through cryomilling) a boron carbide particulate reinforcement within a nanostructured Al 5083 matrix, which is subsequently blended with unmilled (coarse grained) Al 5083. The composite powder is consolidated via cold isostatic pressing (CIP) and hot extrusion. The mechanical properties are evaluated through a combination of low strain rate testing with a servohydraulic testing machine and high strain rate testing using a compression Kolsky bar. The resulting mechanical properties are remarkable for an aluminum-based material, in that very high strengths and substantial ductility are both observed at both low and high strain rates. Very little rate sensitivity is observed. The primary failure mode in compression appears to be through shear band development. We discuss the deformation mechanisms that may produce the observed behavior.

9:35 AM

The Elastic and Plastic Strain Formation Near the Crack Tip of Stainless Steel During Fatigue by Neutron Diffraction: *Yinan Sun*¹; *R. Barabash*²; *H. Choo*¹; *P. K. Liaw*¹; *Y. Lu*¹; *K. An*²; *F. Tang*²; *C. Hubbard*²; ¹University of Tennessee; ²Oak Ridge National Laboratory

The deformation in the vicinity of the crack tip during fatigue tests was studied with neutron diffraction. Formations of large dislocation densities together with high residual stresses were observed. The inhomogeneous plastic deformation was determined. The anisotropic line broadening and lattice strain were observed at different distances from the crack tip. The dislocation density and arrangement were studied from the line-width and profile behavior. Lattice strains and stresses were analyzed by the Rietveld-refinement technique. The comparison of the results and line-profile analyses facilitate the understanding of the change of dislocation densities and strains in the plastic zone. The dislocation density was found to decrease with the distance from the crack tip.

9:50 AM

Tensile Damage Evolution and Fracture Mechanisms of Nicalon/CAS Composites: *Jeongguk Kim*¹; *Peter K. Liaw*²; ¹Korea Railroad Research Institute; ²University of Tennessee

Infrared (IR) thermography was employed to study the tensile fracture behavior of Nicalon fiber reinforced calcium aluminosilicate (CAS) glass-ceramic matrix composites (Nicalon/CAS) with two different types of samples; cross-ply and unidirectional specimens. During tensile testing, an IR camera was used for in-situ monitoring of progressive damages of Nicalon/CAS samples in terms of the temperature evolution. Microstructural characterization using scanning electron microscopy (SEM) was performed to investigate fracture mechanisms of Nicalon/CAS composites. In this investigation, a thermographic NDE technique was used to facilitate a better understanding of fracture mechanisms of Nicalon/CAS composites during tensile testing.

10:05 AM

Structural Health Monitoring Research for Thermal Protection, Cryo and Hot Structures with Emphasis on Materials Aspects: *Kumar V. Jata*¹; ¹U.S. Air Force

One of the major goals of our current research at the Air Force Research Laboratory is to develop structural health monitoring capability for real time interrogation of material and damage state awareness in thermal protection, cryo and hot structures. This talk will discuss various proposed material concepts and potential failure modes in these structures. Sensing methodologies required to perform real time interrogation of material and damage state awareness will be discussed using a few examples.

10:20 AM Break

10:40 AM Invited

Marine Forensics and Shipwreck Preservation: USS Arizona and RMS Titanic: *Tim Foecke*¹; Jennifer Hooper-McCarty¹; ¹National Institute of Standards and Technology

An important historical legacy lies with historically significant shipwrecks scattered around the globe. In conjunction with the National Park Service, Navy and NOAA, the Metallurgy Division of NIST provides technical assistance and finite element models of wrecks currently under preservation. This talk will detail work over the last 9 years investigating the sinking and deterioration of the RMS Titanic in the North Atlantic and the past 3 years work on the USS Arizona, a war memorial at Pearl Harbor in Hawaii. Results presented will include corrosion and bioencrustation studies, geological analyses, metallurgical studies and model predictions of wreck stability and predicted lifetimes.

11:00 AM

Fracture Toughness of a Zr-2.5Nb Tube with Temperature: *Young Suk Kim*¹; ¹Korea Atomic Energy Research Institute

Fracture toughness tests were conducted on curved compact tension (CCT) specimens taken from a cold-worked and stress relieved Zr-2.5Nb tube at temperatures ranging from RT to 300°C. The CCT specimens were subjected to electrolytic charging of hydrogen to 200 ppm at a maximum. The as-received Zr-2.5Nb with no additional charging of hydrogen had an increased fracture toughness resistance, dJ/da with an increasing temperature with the maximum dJ/da around at 180°C, which corresponds to the α to δ hydride transformation temperature. The Zr-2.5Nb tube with hydrogen of 100 to 200 ppm had a ductile-to-brittle transition at around 150 to 180°C and became as ductile as the as-received one at temperatures in excess of 180°C. The ductile-to-brittle transition behavior for the Zr-2.5Nb tube with hydrogen concentration and heat treatment conditions is discussed in association with the α to δ hydride phase transition.

11:15 AM

Fracture Morphology Study of Hastelloy®2000®: *Rejanah V. Steward*¹; Chang Kyong Choi¹; Gongyao Wang¹; Peter K. Liaw¹; Raymond A. Buchanan¹; Dwaine Leroy Klarstrom¹; ¹University of Tennessee

Hastelloy® C2000® Alloy is a commercially designed superalloy manufactured to function in reducing and oxidizing corrosive solutions. Its industrial applications have tremendous potentials in automotive, structural, aviation, and storage components. Albeit its good reducing and oxidizing traits in extremely aggressive media are attractive features of its chemistry, changes in the mechanical properties are believed to be insignificant due to its strong propensity to passivate under corrosive conditions. The ductility behavior and corrosion properties of C2000® are superior to that of stainless steels. The objective of this study is to thoroughly examine the fracture morphology of C2000® and understand the damage evolution from incipient crack-initiation to final fracture after subsection to fatigue in air and 3.5 wt. % NaCl solutions. Electron microscopy and in-situ macro-visualization were used to monitor crack initiation and propagation behavior of C2000®. The fatigue life was drastically reduced under maximum stress conditions and decreasing frequencies.

11:30 AM

Nondestructive Evaluation and Tension Behavior of Nicalon/SiC Composites: *Jeongguk Kim*¹; Peter K. Liaw²; ¹Korea Railroad Research Institute; ²University of Tennessee

The tension behavior of Nicalon fiber reinforced silicon carbide matrix composites (Nicalon/SiC) was investigated with the aid of nondestructive evaluation (NDE) techniques. The NDE techniques include ultrasonic testing (UT), X-ray computed tomography (CT), and infrared (IR) thermography. UT C-scans were developed to investigate defect distributions and to detect variations in the internal flaws. X-ray CT was used to characterize the type of defects and the location of flaws in composites to compare with UT C-scan results. IR thermography was conducted to generate thermal diffusivity maps for the samples. This paper also investigated the feasibility of using NDE techniques as integrity assessment means for Nicalon/SiC composites. IR thermography was also employed to measure temperature evolution during tensile testing. The tensile testing results showed quite reasonable agreement with previous NDE results. Microstructural characterization was performed using SEM to investigate

failure mechanisms of Nicalon/SiC composites, and the results were compared with NDE data.

11:45 AM

An Overview of the Effects of Dispersed Particles on the Creep of Granular Ice: *Ian Baker*¹; Min Song¹; David M. Cole²; ¹Dartmouth College; ²U.S. Army Cold Regions Research and Engineering Laboratory

Over 20 yrs ago, Professor Gerberich studied the effects of both crystal size and solid inclusions on the creep strain rate and activation energy for creep of ice [RW Baker and WW Gerberich, J. Glaciology 24 (1979), 179]. In this paper, we present an overview of the current understanding of the effects of inclusions on the creep of ice, and outline our recent findings on the effects of silt-sized particles upon the compressive creep rate and activation energy for creep of polycrystalline ice at temperatures from -20°C to -2°C. We have examined the situations when the particles are distributed only along the grain boundaries and when the particles are dispersed throughout the material. How the particles affect the dislocation densities present (as determined from cyclic loading tests), dynamic recrystallization and texture evolution will also be presented. Supported by NSF Office of Polar Programs, Arctic Natural Sciences Program OPP 011737.

12:00 PM

Microstructural Control of Ti-Al-Nb-W-B Alloys: *Lan Huang*¹; Peter K. Liaw¹; Chain T. Liu¹; ¹University of Tennessee

TiAl alloys have been considered as promising candidates for structural-materials applications at around 800°C. But TiAl alloys are quite brittle at room temperature and have relatively low fracture toughnesses. In this work, new TiAl alloys containing W, B, and Nb have been developed. Fine uniform microstructures, with the colony size smaller than 50 μ m, can be conveniently developed after HIPing the as-cast alloys without any hot deformation process. Microstructural evolution of the alloys at temperatures ranging from 900°C to 1,310°C, were investigated. The α -phase transus temperature, T_α , has been determined. Different microstructures can be developed with the addition of alloying elements and related heat treatments. The effects of boron and tungsten on the microstructural evolution of the TiAl alloys were analyzed. The research is supported by the Fossil Energy Materials Program, with Dr. R. Judkins and Dr. J. Zollar as program managers.

Fatigue and Fracture of Traditional and Advanced Materials: A Symposium in Honor of Art McEvily's 80th Birthday: Fatigue and Fracture VII

Sponsored by: The Minerals, Metals and Materials Society, TMS Structural Materials Division, TMS/ASM: Mechanical Behavior of Materials Committee

Program Organizers: Leon L. Shaw, University of Connecticut; James M. Larsen, U.S. Air Force; Peter K. Liaw, University of Tennessee; Masahiro Endo, Fukuoka University

Wednesday AM

Room: 216

March 15, 2006

Location: Henry B. Gonzalez Convention Ctr.

Session Chairs: Masahiro Endo, Fukuoka University; K. S. Ravi Chandran, University of Utah

8:30 AM Invited

Effects of Volume Fraction of Alumina Short Fiber on High Cycle Fatigue Property in Al-MMCs and Mg-MMCs: *Yasuo Ochi*¹; Kiyotaka Masaki¹; Takashi Matsumura¹; Mitsushi Wadasako²; ¹University of Electro-Communications; ²Nitias Company, Ltd

Rotating bending fatigue tests in high cycle region were carried out on alumina short fiber reinforced aluminum alloy composites (Al-MMCs) and magnesium alloy composites (Mg-MMCs). The matrix materials of an aluminum alloy A6061 and a magnesium alloy AZ91D, and both MMCs with three kinds of volume fraction of 10%, 18% and 25% of alumina short fiber were prepared. It was found that the fatigue strength increased with an increase of volume fraction of alumina short fiber in both MMCs, and also, the fatigue strength in Al-MMCs at elevated temperature was

improved by reinforcement of alumina short fibers. The crack initiation sites were large size alumina short fibers, cluster of short fibers and large size alumina particles in both MMCs. The crack propagation rates of MMCs decreased with an increase of volume fraction of alumina short fibers.

8:55 AM

Fatigue Crack Growth of Particle Reinforced Metal Matrix Composites: *Nikhilesh Chawla*¹; V. V. Ganesh¹; ¹Arizona State University

The fatigue crack growth (FCG) behavior of SiC particle reinforced 2080 Aluminum alloy was examined. The influence of matrix microstructure, particle volume fraction and size, and R-ratio on the FCG behavior of MMCs will be discussed. A fundamental relationship exists between ΔK_{th} and K_{max} , which is influenced by the interaction between the fatigue crack, the SiC particles, and the size of the plastic zone ahead at the crack tip. In particular, the SiC particles induce significantly different damage mode than in the unreinforced alloy, particularly under compressive loading. The evolution of damage during fatigue crack growth will be demonstrated from in situ optical measurements of crack growth and the analysis of fracture morphology. The effects of particle morphology and distribution (homogenous and clustered) on crack growth were studied using a continuum-based approach. Predictions from this analysis correlated well with experimental observations of crack growth in these systems.

9:20 AM

The Role of SiC Particle Distribution Heterogeneity in the Very High Cycle Fatigue Behavior of Discontinuously-Reinforced Aluminum Metal Matrix Composites: *James K. Huang*¹; Jonathan Edward Spowart²; J. Wayne Jones¹; ¹University of Michigan; ²U.S. Air Force

The role of microstructure heterogeneity on fatigue behavior of two extruded 2009/SiC/15p-T4 DRA composites has been examined in the very high cycle fatigue (VHCF) regime where $10^6 = N_f = 10^7$ cycles. Ultrasonic fatigue was used to achieve the very high cycle counts. Both composites were carefully processed using identical powder blending and consolidation methods. One material was extruded to a 400:1 ratio and the other was extruded to a 14:1 ratio. Processing yielded materials with nearly identical compositions: a very homogeneous particle distribution with minimal clustering was produced in the 400:1 extrusion and a more heterogeneous of SiC particles was produced in the 14:1 extrusion. Crack initiation in the homogeneous, high extrusion ratio material was observed almost exclusively at AlFeCu inclusions while initiation at particle clusters was frequently observed in the material subjected to the lower extrusion. In all cases, fatigue lives at a given stress level exhibited very minimal scatter and subsurface crack initiation was observed in all cases. The role of microstructure variations in the fatigue behavior will be described.

9:45 AM

Fatigue of Titanium Alloys and Composites: *Winston O. Soboyejo*¹; ¹Princeton University

This paper presents an overview of the fatigue of titanium alloys and composites. These include near $\alpha + \beta$ and β titanium alloys and composites reinforced with whiskers and fibers. The underlying mechanisms of fatigue crack growth and crack-tip shielding are elucidated using a combination of experimental techniques and theoretical models. The studies suggest that the effects of stress ratio can be explained largely as a result of crack closure phenomena. In particular, the role of roughness-induced closure is shown to be important, as identified in the original work of Art McEvily. The shielding contributions from roughness-induced crack closure are then quantified using fracture mechanics models. Subsequently, the mechanisms of fatigue are reviewed for crack growth in in-situ TiB whisker-reinforced and SiC fiber-reinforced composites. The crack/microstructure interactions observed in these composites are presented along with their effects on fatigue crack growth rates and fatigue life.

10:10 AM Break

10:25 AM Invited

Growth of Small Cracks and Prediction of Lifetime in High Temperature Alloys: *Luc Rémy*¹; ¹Ecole des Mines de Paris

The lifetime to initiate an engineering crack is usually predicted from of S-N curves in high cycle fatigue or Coffin-Manson curves for low cycle

fatigue. Furthermore, the engineering life to initiate an engineering crack could be mostly spent in the growth of small cracks. This paper intends to show a few examples, which have been investigated in our laboratory for various high temperature applications involving superalloys, stainless steels or CMMs. The examples provided include small crack initiation from PM superalloys, and small crack growth under large scale yielding in stainless steels and CMMs. A damage model based on the propagation of microcracks originating at casting defects has been developed. The model gives satisfactory life predictions on various single crystal superalloys for isothermal LCF tests with or without dwell, for variable temperature TMF tests with dwell period, as well as for thermal transient tests on a wedge-shaped structure.

10:50 AM

Fatigue Crack Growth from Small to Long Cracks in VHCF with Surface and Internal "Fish-Eye" Failures for Ferrite-Perlitic Low Carbon Steel SAE 8620: *Israel Marines Garcia*¹; Paul C. Paris¹; Hiroshi Tada¹; Claude Bathias²; ¹Washington University in St Louis; ²CNAM-ITMA

In recent years, the importance of knowing the materials behavior under Very High Cycle Fatigue (VHCF), has been pointed out by many research laboratories around the world. An important failure phenomenon has been seen between 10^6 and 10^8 cycles, where, the failure initiation switched location from the specimen surface to an interior "fish-eye". As used before, the Paris-Hertzberg-McClintock crack growth rate law, will demonstrate that crack growth is not of significant portion of total life if over 10^7 cycles for a low carbon steel SAE 8620, with ferrite-perlitic microstructure. In this discussion, the presence of closure will be explored for a range of transition sizes from small to long crack as well as various load ratios. Crack initiating at both surface and internal sites will also be considered. Finally, the K at final failure for internal failure will be estimated to see its impact.

11:15 AM

Fatigue Crack Propagation in Cold Drawn Steel: *Jesús Toribio*¹; Beatriz González¹; Juan Carlos Matos¹; ¹University of Salamanca

This paper deals with the influence of the manufacturing process on the fatigue behaviour of pearlitic steels with different degrees of cold drawing. The fatigue crack growth rate (da/dN) is related to the stress intensity range (ΔK) by means a compliance method to evaluate the crack depth a in the samples at any instant during the tests. The analysis is focussed on the region II (Paris) of the fatigue behaviour in which $da/dN = C(\Delta K)^m$, measuring the constants (C and m) for the different degrees of drawing. From the engineering point of view, the manufacturing process by cold drawing improves the fatigue behaviour of the steels, since the fatigue crack growth rate decreases as the strain hardening level in the material increases. In particular, the coefficient m (slope of the Paris laws) remains almost constant and independent of the drawing degree, whereas the constant C decreases as the drawing degree rises.

11:40 AM

In-Situ Studies of Local Stresses and Textures in Bulk Nanocrystalline Metals under Large Plastic Deformation Obtained by the Four-Points Bending Device: *Yandong Wang*¹; G. Fan²; H. Q. Li²; Y. Ren³; H. Choo²; P. K. Liaw²; L. Zuo²; ¹Northeastern University; ²University of Tennessee; ³Argonne National Laboratory

Of those various mechanisms to control the plastic deformation in bulk nanocrystalline metals (BNMs), the diffusion-assisted grain-boundary sliding and/or diffusion-assisted grain rotation are the common ones, instead of the dislocation-motion-mediated grain rotation in the coarse-grained materials. However, it is an open question whether the deformation mechanism will change during the large plastic deformation (over a 10% strain) in the BNMs. Stimulated by the recent experimental finding on the appearance of strain-hardening in the gold nanowires over a large deformation [Wu, et. al., Nature Materials 4, 525-529(2005)], we think that the above mechanisms are not unique in BNMs. In this experiment, we used a four-point bending device, instead of the usual tensile frame, for studying the distributions of various stresses and grain orientation as a function of the depth from the bending tensile surface of a nano crystalline Ni-Fe alloy. Thus, at least over a 10% tensile strain was produced on the bottom side of the bended BNM samples. A micro-beam high-energy X-ray was

used to map the lattice strain/orientation distributions with a resolution of 5 μ m along the compression axial. The type I, II and III stresses, and grain-orientation distribution function (ODF) were determined and modeled for elucidating the detailed deformation mechanisms of BNMs during the large plastic deformation. The present work is supported by the National Science Foundation International Materials Institutes (IMI) Program with Dr. Carmen Huber as the Program Director and the National Natural Science Foundation of China (Grant No. 50471026).

Fatigue and Fracture of Traditional and Advanced Materials: A Symposium in Honor of Art McEvily's 80th Birthday: Fatigue and Fracture VIII

Sponsored by: The Minerals, Metals and Materials Society, TMS Structural Materials Division, TMS/ASM: Mechanical Behavior of Materials Committee

Program Organizers: Leon L. Shaw, University of Connecticut; James M. Larsen, U.S. Air Force; Peter K. Liaw, University of Tennessee; Masahiro Endo, Fukuoka University

Wednesday AM Room: 215
March 15, 2006 Location: Henry B. Gonzalez Convention Ctr.

Session Chairs: Jaroslav Polak, Institute of Physics of Metals; Yasuo Ochi, University of Electro-Communications

8:30 AM Invited

Microstructurally Induced Fatigue Variability and Life Prediction of Turbine Engine Materials: *Sushant K. Jha*¹; Michael J. Caton²; James M. Larsen²; Reji John²; Andrew Henry Rosenberger²; ¹Universal Technology Corporation; ²U.S. Air Force Research Laboratory

A more physically based life prediction coupled with a real-time damage-state monitoring may be the key to removing some of the uncertainties in the current approach to life management of fracture critical turbine engine components and therefore, increasing their utilization potential. In this paper, we examine the factors contributing to the variability in fatigue lifetimes of turbine disk materials including a+b titanium alloys and nickel-base superalloys. The effect of microstructure, surface residual stress, and the loading variables on the scale and the nature of fatigue variability will be discussed. A worst-case life prediction methodology applicable to the materials in this study will be presented and its physical basis will be discussed. The implications of this approach for the assessment of the role of microstructure and loading variables in the worst-case lifetime distribution and reducing the uncertainty in life prediction will also be addressed.

8:55 AM

Orientation Imaging Microscopy of Fatigue Crack Nucleation and Growth in Waspaloy: *Michael E. Oja*¹; K. S. Ravi Chandran¹; Robert G. Tryon²; ¹University of Utah; ²VEXTEC

The effects of grain orientation on fatigue crack nucleation and growth in a polycrystalline nickel-base superalloy, known as Waspaloy, were investigated. Specimens were from a used forged compressor disk from an aircraft engine. Fatigue tests were conducted at 85-95% of the yield stress of the material, at R = 0.1. Multiple nucleations of cracks of the order of a few grain diameters and propagation of the dominant crack were documented. Orientation Imaging Microscopy (OIM) was used to investigate orientations of grains in the cracks' nucleation and adjacent areas. Cracks nucleated in either larger grains or in groups of similarly-oriented grains, collectively called as a "supergrain" due to the closeness of Schmid factors between the grains. The "supergrain" effect was seen in 8 of the 10 cracks investigated. The nature of small crack growth, crack path and the benefits of applying OIM to the study of fatigue cracks are discussed.

9:20 AM

Propagation of Small Surface Crack in Nickel Base Superalloy ME3: *Yong Gao*¹; Mukul Kumar¹; Robert Ritchie¹; ¹University of California

High-cycle fatigue (HCF), involving the premature initiation and/or rapid propagation of cracks to failure due to high-frequency cyclic loading, has been identified as one of the leading causes of turbine engine

failures in aircraft. Under HCF conditions, small crack propagation is of great importance for nickel-base superalloys used as turbine engine components. In this paper, details of small surface fatigue crack propagation in the surface stress (75~95% yield stress) of a nickel base superalloy ME3 and the effect of grain-boundary-engineering processing on small fatigue crack behavior have been studied using Optical Microscopy (OM), Scanning Electron Microscopy (SEM), Focused Ion Beam (FIB), and Electron Backscattered Diffraction (EBSD) techniques.

10:10 AM Break

10:25 AM Invited

Simulation-Based Strategies for Microstructure-Sensitive Fatigue Modeling: *David L. McDowell*¹; ¹Georgia Institute of Technology

Efforts to develop microstructure-sensitive fatigue life estimation methods for alloy systems must consider various factors that are not presently addressed by conventional fatigue design tools such as the strain-life curve, the stress-life curve, the modified Goodman diagram, fatigue limit concepts, or by traditional linear elastic fracture mechanics (LEFM) approaches. In this work, relations between remote loading conditions and microstructure-scale plasticity and crack behavior are considered as a function of stress amplitude, stress state and microstructure. Based on multiscale modeling that employs computational micromechanics, influences of microstructure-scale heterogeneities are characterized in terms of cyclic microplastic strain, shakedown, percolation limits for microplasticity through polycrystals and two phase microstructures, fatigue at inclusions (micronotches), and driving forces for microstructurally small cracks. Treatment of grain boundary strength relevant to the distribution of grain boundary type is also explored. Some applications involving materials design and material prognosis are briefly described.

10:50 AM

Microstructure Variability and the Very Long Life Fatigue Behaviors of Rene' 88 DT: *J. Miao*¹; Tresa M. Pollock¹; J. W. Jones¹; ¹University of Michigan, Ann Arbor

Elevated temperature ultrasonic fatigue techniques have been used to examine the fatigue behaviors of the Ni-base superalloy Rene' 88 DT in the lifetime regime of 10⁵ to 10⁹ cycles at 593°C for a load-ratio of 0.05. The results obtained from ultrasonic fatigue test and conventional fatigue test are comparable and fatigue crack initiation location changes from surface to interior at longer lifetimes/lower stresses. At low loading stress, fatigue cracks are found to initiate from large grains. The correlation between microstructure, fatigue crack initiation behavior and fatigue lifetime has been examined. These observations are used to describe a mechanism for very long life fatigue crack initiation in this alloy.

11:15 AM

Life Prediction of Fretting Fatigue with Advanced Surface Treatments: *Patrick Golden*¹; Michael Shepard¹; ¹Air Force Research Laboratory

Fretting fatigue tests were performed on dovetail specimens with and without advanced surface treatments. Laser shock processing and low plasticity burnishing have been shown to produce deep compressive residual stresses with relatively little cold work. Testing showed these advanced surface treatments improved fretting fatigue strength by approximately 50%. In addition to advanced surface treatments, several specimens were also coated with diamond like carbon applied through a non-line-of-sight process capable of coating small dovetail slots in an engine disk. Testing with this coating also significantly improved fretting fatigue strength due to low friction. This work presents a mechanics based lifing analysis of these tests that takes into account the local plasticity and the redistribution of residual stresses due to the contact loading. Local changes in the coefficient of friction due to coatings and wear were also carefully considered. Comparisons were made using different fracture mechanics software tools.

General Abstracts: Light Metals Division: Session I

Sponsored by: The Minerals, Metals and Materials Society, TMS Light Metals Division, TMS: Aluminum Committee, TMS: Magnesium Committee, TMS: Reactive Metals Committee, TMS: Recycling Committee

Program Organizers: Jim McNeil, Novelis Inc; Neale R. Neelameggham, US Magnesium LLC

Wednesday AM Room: 7D
March 15, 2006 Location: Henry B. Gonzalez Convention Ctr.

Session Chairs: Neale R. Neelameggham, US Magnesium LLC; Sivaraman Guruswamy, University of Utah

8:30 AM

Microstructural Evolution in Titanium 5%Mo-5%V-5%Al-3%Cr upon Aging: *Roque Panza-Giosa*¹; Zhirui Wang¹; David Embury¹; ¹McMaster University

This paper presents optical, SEM and TEM characterization of the microstructure of Ti-5553 after solution heat treatment and four aging cycles. The response to ageing was established based on changes in mechanical properties and hardness with ageing time. The four aging times selected represent inflection points in the ageing time/hardness curve. The relationship between microstructure and mechanical properties resulting from these ageing cycles is explored in light of decomposition of Beta phase during ageing.

8:55 AM

Titanium Production through Electrolysis of Consuming TiCxOy Anode: *Hongmin Zhu*¹; Shuqiang Jiao¹; Xiaotong Hu¹; ¹Beijing University of Science and Technology

Titanium oxide can be reduced by carbon forming titanium carbide or oxygen doped titanium carbide (TiCxOy). It was found that the product sintered at temperatures higher than 1573K is electronic conductor like a metal. A series of researches has been performed on the possibility of titanium electrolysis using carbon doped titanium oxide (TiCxOy) as an anode. Carbon monoxide CO was monitored at the anode during the electrolysis when the potential was kept at a certain value. The product on the cathode was investigated by scanning electrode microscopy (SEM) with EDS and X-ray diffraction (XRD) technique. High purity titanium, with the oxygen content of less than 300 ppm, was obtained, and the current coefficient was higher than 90%.

9:20 AM

High Grade Titania from Rutile: *David Freeman*¹; Graham Sparrow¹; ¹CSIRO Minerals

One aim of the Light Metal Flagship initiative in CSIRO is to cut the cost of production of titanium metal in half. Several processes being developed for the production of titanium metal use a titania feedstock. It is considered that the removal of impurities during the preparation of the titania, rather than during the processing of the titanium metal, is likely to be a less expensive processing option and so the preparation of a high grade titania material from titaniferous feedstocks may provide a significant economic advantage. Simple processing involving physical separations of ilmenite concentrates, synthetic rutile and rutile concentrates using electrostatic and magnetic techniques gave products containing 97-98% TiO₂. A product with 98.5 wt% TiO₂ was obtained from commercial rutile concentrates by physical separations, heating with a flux and leaching the heated product. Potential processing conditions are discussed.

9:45 AM

Lithium Peroxide Production: *Javad Khosravi*¹; Ralph Harris¹; ¹McGill University

Lithium peroxide can be utilized as final product in space projects as an oxygen source or as an intermediate product for production of pure lithium metal by vacuum reduction. Different procedures for production of lithium peroxide were reviewed and the manufacture of lithium peroxide by leaching with organic solvents and utilizing hydrogen peroxide as a reactant was experimentally studied in an attempt to establish the mecha-

nisms and kinetics of the process. The solubility of lithium hydroxide monohydrate as a precursor material in the organic mediums was measured. The conversion rate of lithium hydroxide monohydrate into lithium peroxide was seen to be high and vary as a function of the test parameters, notably the kind of organic solvent and oxidant. The effects of temperature and time on conversion also were studied.

10:10 AM

A Global View on Aluminium Recycling: *Marlen Bertram*¹; ¹Organisation of European Aluminium Refiners and Remelters and European Aluminium Association

In 2004, almost 15 million tonnes of recycled aluminium were used globally compared to 30.2 million tonnes of primary aluminium. Aluminium scrap is utilised all over the world, but the solid recycling industry is centred in the traditional recycling areas such as Europe, North America and Japan. Recently fast growing recycling activities have been recognised in China and other North Asian countries. The talk will give an overview of the global aluminium flow based on latest studies of the Global Aluminium Recycling Committee and will show the development of aluminium recycling in the different regions of the world. It will also describe how the aluminium industry is improving the transparency of global scrap flows, analysing weak points in the aluminium value chain and forecasting scrap availability. A further subject of the presentation is the importance of aluminium recycling in the context of sustainable development.

General Abstracts: Materials Processing and Manufacturing Division: Powder Processing

Sponsored by: The Minerals, Metals and Materials Society, TMS Materials Processing and Manufacturing Division, TMS: Nanomechanical Materials Behavior Committee, TMS/ASM: Phase Transformations Committee, TMS: Powder Materials Committee, TMS: Process Modeling Analysis and Control Committee, TMS: Shaping and Forming Committee, TMS: Solidification Committee, TMS: Surface Engineering Committee, TMS: Global Innovations Committee, TMS/ASM: Computational Materials Science and Engineering Committee
Program Organizers: Thomas R. Bieler, Michigan State University; Ralph E. Napolitano, Iowa State University; Fernand D. Marquis, South Dakota School of Mines and Technology

Wednesday AM Room: 211
March 15, 2006 Location: Henry B. Gonzalez Convention Ctr.

Session Chair: Hyungsik Chung, Ajou University

8:30 AM

Mechanical Alloying and Reactive Processing of Ni3Al Intermetallics: *K. Morsi*¹; Satyajit Shinde¹; E. A. Olevsky¹; ¹San Diego State University

The current paper investigates the effect of mechanical alloying (MA) of mixtures of aluminum and nickel (with different nickel particle sizes) on the dispersion and cold compaction of the composite powders. The concepts of the theory of plasticity of porous bodies are also employed to assess the influence of MA on the yield stress of the composite powder. The influence of processing parameters on the combustion synthesis of optimised compositions is also discussed

8:50 AM

Processing and Properties of Armstrong Process Ti and Ti6Al4V Powders: *Aditya Sathaye*¹; Adam Benish²; Philip Nash¹; ¹Illinois Institute of Technology; ²International Titanium Powder

Titanium and Titanium alloys have desirable properties for applications in the transportation and biomedical fields. Reduction in the price of feedstock and processing would widen the market for titanium products. In this paper, we report on the processing and properties of Grade 4 CP Titanium powder and pre-alloyed Ti6Al4V powders synthesized by the Armstrong process developed by ITP. A conventional cold-press and sinter process was selected for consolidation of the powders. Pre-processing of the powder by ball or jet milling was necessary to improve the apparent density. The effect of using blended elemental powders was also investi-

gated. The sintering kinetics for the different powder combinations were determined by dilatometry. The effect of sintering parameters and heat treatment on the mechanical properties will be reported.

9:10 AM

Development of a Cu-W Composite by a Powder Metallurgical Technique: *Debajyoti Maitra*¹; Ravinder Kumar Dube²; Ajit Kumar Roy¹; ¹University of Nevada; ²Indian Institute of Technology Kanpur

A powder metallurgical route has been proposed for making tungsten dispersed copper composite strips used as electric contact materials. Composition of 80Cu-20W has been considered in this study. The route consists of high energy milling of a mixture of Cu₂O and WO₃ powders in the required ratio in a high-energy ball mill which is then co-reduced in hydrogen at a suitable temperature. It is then compacted and sintered at suitable temperature. The strips are then subsequently hot rolled. The resulting grain size of co-reduced powder was found to be ~25 nm. 93% theoretical density of the Cu-20%W composite strip was achieved. The results indicate that this composite was capable of maintaining appreciably high electrical conductivity, strength and microhardness. The overall data indicate that the enhanced metallurgical and physical properties may be attributed to the fine dispersion of W in Cu due to the combined effect of milling and co-reduction.

9:30 AM

Rapid Prototyping of Biofouling Resistant ABS: *Mario H. Castro-Cedeno*¹; ¹Rochester Institute of Technology

A surface coating of silver nanoparticles added to ABS rapid prototyping material was successful in increasing the biofouling resistance of the parts produced. Surfaces treated with silver-ion nanoparticles have been shown to resist the growth of bacteria and mold and are not hazardous to humans. By treating the material used for rapid prototyping with silver-ion particles, we can produce prototype parts or small production runs of parts that can be used in environments where biofouling is a problem.

9:50 AM Break

10:10 AM

Preparation of Ag Powders by Mechanochemical Reaction in AgCl-Cu System: *Jaeryeong Lee*¹; Ikkyu Lee¹; Jonggwan Ahn¹; Dongjin Kim¹; Jae-Chun Lee¹; Hun S. Chung¹; ¹Korea Institute of GeoScience and Mineral Resources

Silver powders have been widely used as for conductive paints, inks and paste to making films due to good thermal/electrical conductivity, anti-oxidation and catalysis. In accordance with these purposes, its specific morphology is strongly desired. Especially, plate-shaped Ag powders are widely used as fillers for isotropic conductive adhesives. For this reason, many processes have been researched to prepare the Ag powder. Among them, mechanical grinding is the most common and popular process for the production of Ag powders with a shape of plate, although there are two problems due to the intensive grinding; one is the impurity caused by wearing of pot and balls, and the other is the defect of crystal structure. In the present work, a noble technique was proposed. Plate-shaped Ag powders were prepared by mechanochemical reaction in AgCl-Cu system, and the effect of additives was investigated on morphological and structural properties of the Ag powders.

10:30 AM

Effects of Alloying Elements on the Sintered Properties of Mixed Elemental Aluminum Powder Alloys: *Hyungsik Chung*¹; Jae-Hwan Ahn¹; Moon-Tae Kim¹; ¹Ajou University

The effects of Cu, Mg and Zn on the sintering of elemental aluminum powder mixtures were studied. In binary aluminum mixtures, copper was most effective for raising sintered density and properties. Higher strength could be obtained with Al-6 to 10% Cu than those of commercial powder blends. A small amount of magnesium was also effective for improving the sintering to some extent. Too much magnesium over 1%, however, resulted in coarse pores after sintering due to the transient nature of the liquid phase formed, and lowered the overall sintered properties. The Al-Zn also formed a transient liquid phase during sintering but yielded much lower sintered properties than Al-Cu. The addition of Mg or Zn to Al-Cu altered the sintered structure significantly and produced some improve-

ments of the sintered properties. Zn addition, however, was much more effective for raising the sintered properties than Mg.

10:50 AM

Measurement Method for Cell Gap and Twist Angle of Reflective LCD: *Zou-Ni Wan*¹; Chia-Fu Chang¹; Si-Wen Wan¹; ¹Kun Shan University of Technology

A polarization insensitive, electrically tunable Gooch-Tarry's first minimum condition is demonstrated. When the light passes through the TN medium an even number of times. Furthermore, some properties of this method are discussed and an analysis by theoretical calculation is undertaken. We proposed a cell gap measurement method to determine the cell thickness by simulation values of the transmitted light for arbitrary wavelength regions.

11:10 AM

Morphological Characterization of Diamond Particles Synthesized at High Pressure and High Temperature: *Ana Lucia Diegues Skury*¹; Sergio Neves Monteiro¹; ¹UENF

The performance of synthetic diamond used in wear resistant tools or abrasive pastes depends on many factors such as the mechanical strength, crystallinity, size and morphology of the particles. Diamond powders synthesized in different solvent/catalyst systems at high pressure and high temperature conditions, contains crystals that could be separated into groups of distinct sizes and defect morphology. These groups can be differing by their mechanical strength. In general the strength of diamond particle is affected by its surface condition, shape, defect concentration and other factors. In this work results on the morphological characterization of diamond particles, obtained at 4.3 GPa and 1200C from a mixture of graphite and NiMn alloy, are presented.

General Abstracts: Structural Materials Division: Microstructure and Properties of Materials I

Sponsored by: The Minerals, Metals and Materials Society, TMS Structural Materials Division, TMS: Alloy Phases Committee, TMS: Biomaterials Committee, TMS: Chemistry and Physics of Materials Committee, TMS/ASM: Composite Materials Committee, TMS/ASM: Corrosion and Environmental Effects Committee, TMS: High Temperature Alloys Committee, TMS/ASM: Mechanical Behavior of Materials Committee, TMS/ASM: Nuclear Materials Committee, TMS: Product Metallurgy and Applications Committee, TMS: Refractory Metals Committee, TMS: Advanced Characterization, Testing, and Simulation Committee, TMS: Superconducting and Magnetic Materials Committee, TMS: Titanium Committee

Program Organizers: Rollie E. Dutton, U.S. Air Force; Ellen K. Cerreta, Los Alamos National Laboratory; Dennis M. Dimiduk, U.S. Air Force

Wednesday AM
March 15, 2006

Room: 218
Location: Henry B. Gonzalez Convention Ctr.

Session Chair: Donna Ballard, U.S. Air Force

8:30 AM

Cu-SiC_p Composites with Interpenetrating Network Structure for Thermal Management and Electrical Contact Applications: *Aditya Putrevu*¹; V. V. Bhanu Prasad²; Veerredhi Vasudeva Rao³; ¹University of Texas; ²Defense Metallurgical Research Laboratory; ³Sreenidhi Institute of Science and Technology

Copper matrix composites reinforced with varying content of particulate SiC (0-30% by volume) were processed by vacuum hot pressing and press-sinter routes. No reaction products were detected in any of the composites. Density and porosity of the composites reduced considerably with increasing SiC content and there is an evolution of an interpenetrating network structure with increasing SiC content. Significant strengthening of the composites took place with increasing reinforcement content with an increase in hardness, strength and elastic modulus. Coefficient of thermal expansion of the composites reduced with SiC content. In spite of lower thermal and electrical conductivity of SiC compared to copper, the conductivity of the composites was considerable. Superior mechanical

WEDNESDAY AM

properties, lower density, cheaper SiC reinforcement without foregoing much of the conductivity makes Cu-SiC_p composites potential materials for thermal management and electrical contact applications.

8:55 AM

Numerical Modeling of Stress Concentration on Clustered Porosity: *Yi Cheung Lok*¹; Adam C. Powell¹; ¹Massachusetts Institute of Technology

The effect of stress concentration on a single spherical cavity is well understood. This study models numerically the stress concentration on a cluster of cavities and compared with that on a single cavity. The effect of the number of cavities, their relative location and the distance between cavities on stress concentration will be discussed. The result will be used to validate the applicability of Saint Venant's principle and can possibly act as a guideline for evaluating clustered porosity.

9:20 AM

On the Sensitivity and Uniqueness Issues in Determining the Elasto-Plastic Properties of Materials through Indentation: A Comparative Analysis: *Hongzhi Lan*¹; T. A. Venkatesh¹; ¹Tulane University

Instrumented indentation as a technique for extracting the fundamental mechanical properties of materials has recently received considerable attention. Issues concerning the uniqueness and robustness of the extracted properties to variations in experimentally measured quantities have been recognized as being important. In the present study: (i) A uniform framework for assessing the uniqueness and sensitivity of the forward and reverse analyzes, for all the principal methods that have been developed so far, will be identified. (ii) Within a broad range of homogeneous, isotropic, power-law hardening materials, domains where the indentation method is applicable for an unambiguous identification of elasto-plastic properties will be distinguished. (iii) The differences in the nature of the sensitivity of the indentation analyzes, as a function of the nature of the indentation method, will be characterized. (iv) Guidelines for selecting appropriate methods for accurate and robust determination of elasto-plastic properties will be provided.

9:45 AM

In-Situ Internal Strain Measurement in Polytetrafluoroethylene by Neutron Diffraction: *Eric N. Brown*¹; Philip J. Rae¹; Dana M. Dattelbaum¹; George T. Gray¹; Donald W. Brown¹; ¹Los Alamos National Laboratory

Measurements of internal strain development during in-situ deformation of polytetrafluoroethylene (PTFE) have been performed utilizing neutron diffraction measurements with the SMARTS diffractometer at Los Alamos National Laboratory. While PTFE is known to be semi-crystalline in nature, the effect of mechanical deformation on this structure has received limited attention. The chemical structure of PTFE, (C₂F₄)_n, makes it ideally suited for investigation by neutron methods as it is free of the H that results in limited penetration depths and poor diffraction acquisition in most polymers. Internal strains have been measured in tension and compression for well pedigreed PTFE 7C with accurate temperature control to ensure the phase IV crystalline structure. Six primary diffraction peaks have been identified. For compression the (210) and (300) helical lattice orientations exhibit the largest strains (~0.5% internal strain at 60% bulk true strain) and closely parallel the bulk imposed stress.

10:10 AM Break

10:25 AM

Shock and Recovery of Polytetrafluoroethylene through the Phase II-III Transition: *Eric N. Brown*¹; Philip J. Rae¹; Carl P. Trujillo¹; Neil K. Bourne²; George T. Gray¹; ¹Los Alamos National Laboratory; ²University of Manchester

Polytetrafluoroethylene (PTFE) is semi-crystalline in nature with its linear chains forming complicated temperature and pressure dependent phases. Experimental studies on pressure-induced phase transitions using shock-loading techniques and the resulting changes in crystalline structure are presented. Disks of pedigreed PTFE 7C have been shock loaded in momentum trapped assemblies using a 80 mm gas launcher, and recovered in a density graded polymer network. Experiments were performed with impact pressures from 0.4 to 0.85 GPa to investigate the material response above and below the phase II to phase III crystalline transition.

Recovered samples were planar with residual strains of less than 5%. Changes in crystalline structure of the recovered materials were quantified using dynamic scanning calorimetry (DSC) and density, both indicating decreased crystallinity with increased impact pressure.

10:50 AM

Characterization of Grain Boundary Liquation in Inconel 718 Subjected to GTAW: *Shenavia Wilkerson Howell*¹; Viola L. Acoff¹; ¹University of Alabama

Inconel 718 is a high-strength precipitation hardenable nickel-based superalloy that is used for many high temperature applications. During welding of this alloy, the area immediately adjacent to the fusion zone is subjected to partial melting along the grain boundaries. This phenomenon is termed liquation. Extensive studies have shown that constitutional liquation of grain boundary precipitates results in intergranular microfissuring in the weld heat-affected zone. In the present study, bead-on-plate welds were made on specimens using gas tungsten arc welding (GTAW). The resulting welds were characterized using electron backscattered diffraction patterns and transmission electron microscopy. The liquation of grain boundaries is a heterogeneous process. This means that some grain boundaries liquate while others do not. Therefore, the purpose of this study is to investigate the crystallographic orientations of grain boundaries in the liquated region, and the conditions under which liquation occurs.

11:15 AM

Annealing Effects on the Grain Growth of ZR-702: Brian James Sarraill¹; Shake Babakhanyan¹; Charles Schrupp¹; Richard Clark¹; Omar Es-Said¹; *John Ogren*¹; ¹Loyola Marymount University

Zirconium is a hard, shiny, grayish white metal. With its superior corrosion resistance capabilities, it has increasingly become the material of choice in the fabrication of chemical processing equipment and nuclear reactors. This project determined the intermediate annealing step that will avoid the growth of very large crystallites in the metal during the final material annealing step. In addition, the effect of cold work on grain growth was analyzed. The amount of cold work was varied from 0% to 15%, and a T-5 radius bend test also used. These samples were then annealed in air and the microstructure was examined. No significant grain growth was found to occur.

11:40 AM

Influences of Different Copper Coatings on Microstructure of C/Cu/Al Composites: *Zhuokun Cao*¹; Guangchun Yao¹; ¹Northeastern University of China

Different copper coatings whose thickness varies between 0.5 μm to 2 μm were deposited on carbon fibers using both electroless and electroplating method. The fibers with copper coating were chopped and fabricated composites with melting aluminum. Influences of different copper coatings on distribution and interface bonding condition of carbon fibers in aluminum matrix were studied by scanning electron microscope (SEM). The role of the copper layer on the microstructure in the system was also discussed. The results indicate that 0.7 μm thick copper coating deposited using electroplating technique performs the best effects in the matrix and that copper layer reacts with aluminum matrix, results to the formation of intermetallic compound CuAl₂ which can protect the fibers at a high temperature and help to improve the mechanical properties of the composites.

12:05 PM

The Effect of Thermal Exposure on the Mechanical Properties of 2099-T6 Die Forgings, 2099-T83 Extrusions, 7075-T7651 Plate, 7085-T7452 Die Forgings, 7085-T7651 Plate, and 2397-T87 Plate Aluminum Alloys: Joseph Jabra¹; J. Lai¹; E. Lee¹; M. Setiawan¹; *Eui W. Lee*²; Jeffrey J. Witters³; Nabil Abourialy²; Michael Romios¹; John R. Ogren¹; Omar S. Es-Said¹; ¹Loyola Marymount University; ²Naval Air Systems Command; ³Alcoa Aerospace Applications Engineering

Aluminum alloys 2099-T6 die forgings, 2099-T83 extrusions, 7075-T7651 plate, 7085-T7452 die forgings, 7085-T7651 plate, and 2397-T87 plate were thermally exposed at temperatures of 180°C (350°F), 230°C (450°F), and 290°C (550°F) for 0.1, 0.5, 2, 10, 100, and 1000 hours. The purpose of this study was to determine the effect of thermal exposure on the mechanical properties and electrical conductivity of these alloys. The data show that higher temperatures and longer exposure times generally

resulted in decreased strength and hardness and increased percent elongation and electrical conductivity.

Hume Rothery Symposium: Multi-Component Alloy Thermodynamics: Alloy Design and Properties

Sponsored by: The Minerals, Metals and Materials Society, TMS Electronic, Magnetic, and Photonic Materials Division, TMS: Alloy Phases Committee

Program Organizers: Y. Austin Chang, University of Wisconsin; Rainer Schmid-Fetzer, Clausthal University of Technology; Patrice E. A. Turchi, Lawrence Livermore National Laboratory

Wednesday AM Room: 202A
 March 15, 2006 Location: Henry B. Gonzalez Convention Ctr.

Session Chair: Fan Zhang, CompuTherm LLC

8:30 AM Invited

Phase Diagram and Design of Cobalt-Base Alloy Systems: *Kiyohito Ishida*¹; ¹Tohoku University

Cobalt-base alloys are widely used in various applications such as magnetic materials, corrosion and heat-resistant alloys, wear-resistant alloys, prosthetic alloys in medical parts etc., where the phase diagrams play a key role in material development. This paper presents recent progress on the phase diagrams and design for Co-base alloys, focusing on magnetic recording media, ferromagnetic Co-Ni-Al-base shape memory alloys and Co-base superalloys. The calculated miscibility gap between ferromagnetic and paramagnetic states in the Co-X(X: Cr, Mo, W) systems was found to agree well with the experimental results, strongly implying that the magnetic induced phase separation is responsible for the compositional heterogeneity in Co-base magnetic recording media. New ferromagnetic Co-Ni-Al shape memory alloys were also developed based on phase diagrams. The introduction of γ (Al structure) to the β (B2) matrix was found to drastically improve the ductility. Finally, the possibility of potent strengthening of Co-base superalloys upon precipitation of γ' (L12) is presented.

9:00 AM Invited

Thermodynamic Modelling of Multi-Component Oxide Systems: *Ling Zhang*¹; Shouyi Sun¹; Sharif Jahanshahi¹; ¹CSIRO Minerals

The cell model originally proposed by Kapoor and Froberg for simple silicate melts was later extended to multi-component liquid slags by Gaye and Welfringer. CSIRO has extended the application of this model to describing the behaviour of numerous oxide species commonly found in metallurgical slags. The developed database includes the following species; SiO₂, Al₂O₃, Cr₂O₃, TiO₂, Ti₂O₃, Fe₂O₃, FeO, CaO, MgO, MnO, CrO, PbO, NiO, CoO, ZnO, Na₂O and Cu₂O in the liquid slag and oxide solid solutions. Recent enhancements to the model will be discussed with particular focus on the behaviour of Al₂O₃ containing ternary and higher order systems. As a structurally based model, the cell model calculates parameters related to the degree of polymerisation in silicate melts. These parameters have been used in a model for calculating the viscosity of silicate melts. Examples on viscosity of silicate slags with alumina and other oxides will also be presented.

9:30 AM Invited

Application of Thermodynamic Modeling Tool to Commercial Titanium Alloys: *Fan Zhang*¹; Shuanglin Chen¹; ¹CompuTherm LLC

Materials are developed and improved by adjusting both the alloy chemistry and the processing conditions to achieve desired microstructures and properties. Traditionally, these improvements have been made by a slow and labor-intensive series of experiments. Today, thermodynamic modeling has become an essential tool in understanding the effect of alloy chemistry on the final microstructure of a material. Implementation of such a tool to improve material processing via parameter optimization has resulted in significant cost savings through the elimination of shop/laboratory trials and tests. In this study, a thermodynamic modeling tool developed at CompuTherm is being utilized to predict properties of commercial

titanium alloys, such as beta transus, phase proportions, phase chemistries and so on. This tool includes Pandat, software for multi-component phase equilibrium calculations, and PanTitanium, a thermodynamic database for titanium alloys. Model predictions are compared to experimental results for number of alpha-beta alloys.

10:00 AM Break

10:20 AM

Determination of Thermodynamic Properties and Calculation of Viscosity and Phase Diagrams of Various Ternary Lead-Free Solder Materials: *Adolf Mikula*¹; *Sabine Knott*¹; *Zuoan Li*¹; *Peter Terzieff*¹; ¹University of Vienna

The target of our thermodynamic investigations was to determine a complete set of partial and integral quantities of ternary systems as a function of temperature and molar weight. Surface tension and viscosity directly affects the solder fluidity characteristic and the ability to wet a substrate surface. The thermodynamic measurements and calculations were done in the framework of the European COST 531 action. Little information about the thermodynamic properties and viscosity data of the ternary Ag-Bi-Sn, Ag-Cu-Sn and Bi-In-Sn systems are known. We carried out thermodynamic measurements of these systems in the liquid state using two different methods: calorimetric and an EMF method with a liquid electrolyte. The integral Gibbs free energy of the system at 1000 K was calculated by Gibbs-Duhem integration. The results of the thermodynamic investigations were used to calculate the viscosity and the phase diagrams. The results of these measurements and the calculations will be presented.

10:45 AM

Experimental Studies and Scheil Simulations of Microstructure in Nb-Ti-Hf-Si Alloys: *Bernard P. Bewlay*¹; *Ying Yang*²; *Laurent Cretegy*¹; *Y. Austin Chang*³; ¹General Electric; ²CompuTherm LLC; ³University of Wisconsin

Nb-silicide based in-situ composites are promising materials for future high-temperature structural applications. Nb-silicide composites are typically alloyed with Hf, Ti, Cr and Al to provide a balance of mechanical and environmental properties. Solidification processing can play a critical role in the control of the final microstructure of these composites. In this study, thermodynamic modeling of the Nb-Ti-Hf-Si system was performed using the CALPHAD approach; in conjunction with this approach, Scheil and global-equilibrium simulations of solidification paths were then performed based on the optimized thermodynamic description for the Nb-Hf-Ti-Si system. These simulations can serve as a guide in the selection of alloy compositions for microstructure optimization, and a range of examples will be described. Experimental observations for selected directionally solidified alloys will be compared with simulation results. These experimental results are also used in the validation of the thermodynamic descriptions.

11:10 AM

Multicomponent Alloy Thermal Physical Property Prediction Coupled Computational Thermodynamics with Back Diffusion Consideration: *Jianzheng Guo*¹; *Mark T. Samonds*¹; ¹ESI U.S. R&D

Simulation technologies are applied extensively in casting industries to understand the aspects of heat transfer and fluid transport phenomena and their relationships to the microstructure and the formation of defects. It is critical to have accurate thermo-physical properties as input for reliable simulations of the complex solidification and solid phase transformation processes. The thermo-physical properties can be calculated with the help of thermodynamic calculations of phase stability at given temperatures and compositions. A comprehensive multicomponent alloy solidification model, coupled with a Gibbs free energy minimization engine and thermodynamic databases, has been developed. The thermal physical properties can be calculated. A back-diffusion model is integrated so that the solidification conditions, such as cooling rate, can be taken into account.

WEDNESDAY AM

Lead Free Solder Implementation: Reliability, Alloy Development, and New Technology: Electromigration

Sponsored by: The Minerals, Metals and Materials Society, TMS Electronic, Magnetic, and Photonic Materials Division, TMS: Electronic Packaging and Interconnection Materials Committee
Program Organizers: Nikhilesh Chawla, Arizona State University; Srinivas Chada, Medtronic; Sung K. Kang, IBM Corporation; Kwang-Lung Lin, National Cheng Kung University; James Lucas, Michigan State University; Laura J. Turbini, University of Toronto

Wednesday AM Room: 214A
 March 15, 2006 Location: Henry B. Gonzalez Convention Ctr.

Session Chairs: Sinn-Wen Chen, National Tsing Hua University; Kwang-Lung Lin, National Cheng Kung University

8:30 AM

Effect of UBM Consumption on Failure Mechanism in Flip Chip Solder Joints during Current Stressing: *Yen-Liang Lin¹; C. Robert Kao¹; Yi-Shao Lai¹; ¹National Central University*

The electromigration failure mechanism in flip chip solder joints through the rapid depletion of UBM was investigated. The solder used was 63Sn37Pb and the joints had a nominal diameter of 125 μm . The UBM on the chip had a Cu/Ni(V)/Al metallization, and the surface finish on the substrate side was Au/Ni. Our results showed that Ni UBM adhered well after 300 hours at 150°C when no electric current was applied. However, under current stressing, a rapid consumption of Ni UBM occurred and the joints failed due to UBM exhaustion and de-adhesion. In other words, electric current accelerated the Ni UBM consumption, and eventually resulted in the failure of the solder joints. In this presentation, the effect of UBM consumption on flip chip solder joint failure will be discussed.

8:50 AM

Effect of Electromigration on Mechanical Property of Lead-Free Solder Joints Studied by Nano-Indentation Continuous Stiffness Measurement: *Fei Ren¹; King-Ning Tu¹; Luhua Xu²; John H. L. Pang²; Zhong Chen²; ¹University of California, Los Angeles; ²Nanyang Technological University*

Tensile test structures of a solder ball connected by two Cu wires of 300 to 500 μm diameter were prepared and tested. The ultimate tensile strength decreases with longer time or higher current density of electromigration. To study the effect of electromigration on mechanical property of lead-free SnAgCu solder joints, a nano-indentation continuous stiffness measurement (CSM) was used. In electromigration at 100°C, the applied current density was from 1.5 \times 10³ A/cm² to 1 \times 10⁴ A/cm² and the time from 3 to 144 hrs. An array of 50 nm indentations was created by the nano-indenter from the cathode area, across the bulk of the solder, to the anode area. The change of Young's modulus and hardness from the cathode to the anode was analyzed from the CSM. Combined with the microstructure study of intermetallic compound formation at the interfaces, the effect of electromigration on mechanical property of the solder joint will be discussed.

9:10 AM

Electromigration Effect on Intermetallic Growth and Young's Modulus in SAC/ENIG Solder Joint: *Luhua Xu¹; John H. L. Pang¹; Fei Ren²; K. N. Tu²; ¹Nanyang Technological University; ²University of California, Los Angeles*

The impact of electromigration on growth of interfacial IMC in ENIG/SAC/ENIG single ball solder joint was studied. When solder joint was subjected to a current density of 5000A/cm² at 125C, IMC layer growth on anode interface is faster than cathode interface, and both are faster than isothermal aging. Young's modulus and hardness were measured by nanoindentation CSM (continuous stiffness measurement) on these interfacial IMCs after 86 hrs EM test. Different value was observed on anode and cathode sides. Young's modulus for the IMC at anode side is around 180-190 GPa, while the value at cathode side is only 130-140 GPa. EDS

Line Scan was conducted at interface from Ni(P) substrate to SAC solder, showing that the copper concentration at anode IMC is about 25-35%, while less than 10% at cathode side IMC. This indicates composition and crystal structure of IMC at anode and cathode is affected by EM.

9:30 AM

Electrochemical Migration of the Sn-9Zn-0-4Ag Reflowed on Cu/Ni/Au Substrate: *Jing Chie Lin¹; Yi-Fang Hong¹; Sheng-Long Lee¹; ¹National Central University*

The electrochemical migration of the lead-free solders Sn-9Zn-0-4Ag reflowed on Cu/Ni/Au substrate was investigated. A term t_{cm} is defined as the duration from null to a sudden rise of current to evaluate the reliability of the system. Reliability of the solders Sn-9Zn-0-4Ag decreases with increasing the silver content from 0 to 4 wt%. Failure is caused by a connection of the dendrites that extend from cathode to anode. Chemical analysis of the dendrites by XPS depicts that the concentration ratio of Zn/Sn decreases with migration time. Investigation of anodic potentiodynamic polarization benefits the delineation of the electrochemical migration. The solders contain higher silver content shifts their open circuit potential (OCP) to noble. Anodic current is greater for the solder containing higher silver concentration at any potential higher than OCP. Galvanic corrosion induced by Ag and Ag₂Zn₃ leads to this failure.

9:50 AM

Electromigration in Cu Column Flip Chip Joints: *Jae-Woong Nah¹; Jong-Ook Suh¹; King-Ning Tu¹; Vempati Srinivasa Rao²; Seung Wook Yoon²; Vaidyanathan Kripesh²; ¹University of California, Los Angeles; ²Institute of Microelectronics*

When size of solder bumps decreases for fine pitch, stand-off height between chips and substrates also decreases. The low stand-off height is of concern in mechanical fatigue life. Also, as size of solder bumps decreases, current density through the joint increases and electromigration reliability becomes an issue. Therefore, new packaging concept is required for flip chip with fine pitch, high stand-off height, and high current density capability simultaneously. In this study, we introduce a new flip chip technology by using Cu columns which has 100- μm pitch and 60- μm stand-off heights. We investigate electromigration in solder part of the Cu column flip chip joints. When we compare electromigration resistance between conventional solder flip chip joints and Cu column flip chip joints, we found that the latter has better electromigration resistance than the former. The reason will be explained. The effect of Cu columns on current distribution has been confirmed by simulation.

10:10 AM Break

10:25 AM

Electromigration Study Using Kelvin Bump Structure: *Yuan-Wei Chang¹; Shih-Wei Liang¹; Chih Chen¹; ¹National Chiao Tung University*

Electromigration of flip-chip solder joints has been studied extensively in recent years. Voids formed at the solder in the vicinity of the entrance point of the Al trace for solder joints with thin film UBM. However, the nucleation and propagation of the voids is still not clear. For Al and Cu interconnects, void nucleation and propagation during electromigration is monitored by resistance change. But the bump resistance is quite small compared with the resistance of the metallization traces. Therefore, daisy-chain structure cannot detect the slight changes in microstructure in the solder joint. In this study, we designed and fabricated Kelvin bump probe, and used it to monitor the bump resistance change during electromigration successfully. Three-dimensional (3D) finite element modeling was also performed to simulate the bump resistance increase due to void formation. This approach facilitates the systemic study of failure mechanism due to electromigration in flip-chip solder joints.

10:45 AM

Electromigration Study of Pd-SnAgCu Solder-Pd Structure Using V-Groove Lines: *Annie T. Huang¹; King-Ning Tu¹; ¹University of California*

The use of Pb-free solders is gradually replacing the Pb-containing solders due to environmental concern. However, high temperature Pb-free solder with melting point around 300°C has not yet been developed. Because the trend of increasing I/O density in interconnect technology, size of flip chip solder joints has to be reduced. It is anticipated that interme-

tallic compound (IMC) will gradually replace the bulk part or the entire bump of a solder joint in the near future as the solder joint size decreased. The element Pd was reported to have ultra-fast IMC formation with Sn-containing solders. Fast IMC formation between Pd and Sn may function as high temperature solder joint due to the higher melting point of IMC. In this talk, we report the fast formation of IMC between Pd electrode and SnAgCu solder, and electromigration behavior across Pd-SnAgCu solder-Pd lines in v-grooves on Si wafers.

11:05 AM

Mechanism of Void Formation in Flip-Chip Solder Joints: *Shih-Wei Liang¹; Yuan-Wei Chang¹; Tung-Liang Shao¹; Chih Chen¹; ¹National Chiao Tung University*

Redistribution of current density and temperature due to void formation in flip-chip solder joints during electromigration was investigated using three-dimensional thermo-electrical coupled modeling, in which the current density and temperature redistribution were simulated at different stages of void growth for solder joints with thin-film UBM. After the void formation near the entrance point of Al trace, the current may drift through the UBM layer to the periphery of the solder joint, leading to the void formation in the periphery of the solder joint, which was low current density region before the void formation. This proposed mechanism successfully explained our experimental results. In addition, the temperature change due to the void formation will be presented in this meeting.

11:25 AM

Prevention of EM-Induced Cu Dissolution by an Effective Ni Barrier Layer: *Yu-Hsiang Hsiao¹; Cheng-Yi Liu¹; ¹National Central University*

EM(Electromigration)-induced dissolution of Cu UBM in eutectic SnPb has been reported, which is a crucial issue for the flip-chip solder bump. By next few years, Sn-rich Pb-free solders would replace SnPb solder in C4 bumps. Those promising Sn-rich Pb-free solders are known to have higher Cu solubility than that of SnPb solder. Therefore, much serious EM-induced Cu dissolution would be expected for Sn-rich Pb-free solders. In this study, a Ni barrier layer was deposited on the Cu metal bond pad to retard EM-induced Cu dissolution. Our preliminary results show that the Ni thin layer, indeed, can retard EM-induced Cu dissolution. In this talk, we will also report EM behaviors of three different Pb-free solders, i.e., Sn, Sn0.7Cu, Sn3.0Cu on Ni/Cu substrates.

11:45 AM

The Combined Effects of Electromigration Flux and Cross-Interaction Flux in SnAg Flip-Chip Solder Joints: *Chiaming Tsai¹; Yi-Shao Lai²; C. R. Kao¹; ¹National Central University; ²Advanced Semiconductor Engineering, Inc.*

In a solder joint with the Cu layer on one side and the Ni layer on the other, there is a net Cu flux from the Cu side to the Ni side, which is known as the cross-interaction flux. When an current passes through a solder joint, the current could produce the EM(electromigration) flux. In this study, the combined effects of EM flux and cross-interaction flux in flip-chip solder joints was studied. The UBM had a Ti/Cu/Ni triple-layer structure, and the surface finish on the board side was SOP Cu. When the direction of electron flow was from board side to chip side, Cu cross-interaction flux and Cu EM flux were in the same direction, but when the direction of electron flow was from chip to board, these two fluxes were in the opposite direction. Effects generated from such configuration were reported.

12:05 PM

Heat Effect and Impact Resistance during Electromigration on Cu-Sn Interconnections: *Tae-Kyu Lee¹; J. W. Morris, Jr.¹; Fay Hua²; ¹University of California, Berkeley; ²Intel Corporation*

The influence of electron current on the diffusion of Sn and Cu in simply designed Cu-Sn-Cu diffusion couples was investigated. The diffusion couples were designed to permit in situ studies of the progress of diffusion. Initial tests were done in various temperature in air with a current density over $1 \times 10^4 \text{ A/cm}^2$. The results showed Cu movement into Sn in the direction of the electron current with accompanying grain boundary sliding of the Sn grains. A continuous intermetallic compound formation was observed at the anode side, simultaneously with an intermetallic dissipation at the cathode side. Temperature measurements at the interconnection using thermo-couples and IR(Infra Red) camera showed a con-

tinuous temperature increase during current stressing. A series of results on impact resistivity of the Cu-Sn interconnections during current stressing were also achieved by using a modified Micro-Chardy impact testing method.

Magnesium Technology 2006: Thermodynamics and Fundamental Research

Sponsored by: International Magnesium Association, TMS Light Metals Division, TMS: Magnesium Committee

Program Organizers: Alan A. Luo, General Motors Corporation; Neale R. Neelameggham, US Magnesium LLC; Randy S. Beals, DaimlerChrysler Corporation

Wednesday AM
March 15, 2006

Room: 6B
Location: Henry B. Gonzalez Convention Ctr.

Session Chairs: Zi-Kui Liu, Pennsylvania State University; Rainer Schmid-Fetzer, Clausthal University of Technology

8:30 AM

Finite-Temperature Thermodynamic Properties of Intermetallics in the Mg-Ca-Sn System via First-Principles Methods: *Raymundo Arroyave¹; Munekazu Ohno²; Zi-Kui Liu¹; Rainer Schmid-Fetzer²; ¹Pennsylvania State University; ²Clausthal University of Technology*

In recent years, interest in the use of Magnesium alloys in automotive applications has increased significantly due to economic, political and environmental factors. Accordingly, a considerable effort has been put into the development of a complete thermodynamic database for Mg alloys, based on the CALPHAD approach. This methodology requires the existence of experimental data to determine the values of the parameters in the models describing each phase. In this work, first-principles methods are used to calculate the total free energies of most intermetallic phases in the Mg-Ca-Sn system so they can be eventually used in CALPHAD models of this ternary system. Vibrational and electronic degrees of freedom are taken into account, as well as the contributions due to lattice thermal expansion. To illustrate how one can use the finite-temperature, first-principles thermodynamic properties in CALPHAD modeling, the Mg-Ca binary system is re-modeled. The results are then compared with previous CALPHAD models.

8:50 AM

Investigation of the Liquidus Surface in the Mg-Rich Corner of the Mg-In-Ce Ternary System: *Elvi C. Dalgard¹; Dmytro Kevorkov¹; Mihriban O. Pekguleryuz¹; ¹McGill University*

The liquidus surface in the ternary Mg-In-Ce system was studied in the composition range 1 to 3% In and 0.1 to 1.5% Ce. Thermal analysis was used to determine the liquidus points in order to construct polythermal sections of the ternary phase diagram. Metallography and x-ray techniques were used to examine phases present at the compositions studied. A triple point presumed to represent a peritectic was discovered at 580°C. In addition, FACTSage was used to confirm thermodynamic agreement of the new data with existing literature on the system.

9:10 AM

Linking Meso- and Macroscale Simulations: Crystal Plasticity of HCP Metals and Plastic Potentials: *Dirk Steglich¹; ¹GKSS Research Center*

Due to its hexagonal crystallographic structure, magnesium alloys show a strong tension-compression asymmetry, which have to be accounted for by advanced material models. The untypical mechanical behaviour of magnesium can be explained and reproduced with the help of a viscoplastic model for crystal plasticity. The study of single crystal specimens subjected to channel die compression tests reveals the active slip and twinning systems. In order to describe the mesoscopic behaviour of a polycrystal, texture is incorporated into polycrystalline RVEs and mechanical properties of extruded bars and rolled plates can be predicted. In order to extend the modelling potential, a phenomenological yield surface accounting for anisotropy and tension/compression asymmetry has been developed and implemented in a finite element code and compared with crystal plasticity calculations. This allows for a direct comparison of simulation

strategies on different length scales and thus for a calibration of model parameters.

9:30 AM

Study of Phase Equilibria in Magnesium-Cerium Binary System via the Diffusion Couple Technique: *Xin Zhang*¹; Dmytro Kevorkov¹; Mihriban Pekguleryuz¹; ¹McGill University

A liquid-solid diffusion couple method was implemented to investigate the magnesium-cerium binary system. Pure Mg and Ce contact was vacuum-encapsulated in quartz tube and the Mg and Ce inter-diffused at 400°C. All the four single-phase zones corresponding to the Mg-Ce phase diagram were observed. The solid solubility ranges of the phases at magnesium-rich side were investigated by means of SEM line-scan. The phase identification was carried out by electron microprobe analysis (EMPA), X-ray diffraction and SEM. In order to investigate the composition range of the intermetallic compounds and clarify data in existing phase diagrams, alloys containing target phases were prepared, cast and annealed at a temperature range of 400-550°C. The room-temperature and elevated-temperature (quenched) microstructures of these alloys were observed and the lattice parameters of the intermetallics were determined via XRD.

9:50 AM

Study of Thermal Evolution of the Mg Solid Solution in the Mg-Al-Li-Zn System: *Dmytro Kevorkov*¹; Carl Fuerst²; Mihriban Pekguleryuz¹; ¹McGill University; ²General Motors R&D

The modification of commercial AZ alloys with Li requires precise knowledge concerning solubility ranges in the Mg-Al-Li-Zn solid solution. The study of solubility range variations with temperature (thermal evolution) is extremely important for the prediction of solidification behavior in multicomponent alloys. The Mg solid solution in the Mg-Al-Li-Zn system has a complex shape and has never been studied in detail. The two, three and four phase samples were annealed at the temperatures of 250, 300, 350 and 400°C, and quenched in liquid nitrogen. The crystal structures of intermetallic phases and the maximum solubilities of elements in Mg were determined by powder x-ray diffraction (Rietveld analysis). Alloy microstructures were studied with SEM and the compositions of the intermetallic phases were determined by quantitative EDX. The shapes of the Mg-Al-Li-Zn solid solution were constructed at various temperatures and their thermal evolution was analyzed.

10:30 AM Break

10:10 AM

The Effect of Solute Elements on the Lattice Parameters of Binary Solid Solutions of Magnesium: *Ana Maria Becerra*¹; Dmytro Kevorkov¹; Carlton D. Fuerst²; Mihriban O. Pekguleryuz¹; ¹McGill University; ²General Motors of Canada

The influence of solute elements on the lattice parameters of magnesium has been studied. Binary solid solutions of Mg-Ce, Mg-In, Mg-Zn, and Mg-Li alloys were cast in copper moulds and homogenized at temperatures between 375°C and 400°C. Filings were then taken under protective atmosphere, encapsulated under argon and then annealed at 275°C to remove residual stress. Lattice parameter measurements were carried out with a Philips PW 1710 powder diffractometer with Cu- α radiation. The experimental XRD results were refined and analyzed using the Rietveld method. Alloys were also characterized using optical and scanning electron microscopy. The effects of solutes on lattice parameters were explained on the basis of atom size differences, and the change in electron overlap of magnesium due solute additions.

10:50 AM

Thermodynamic Modeling of the Mg-Sn-Zn-Al System and Its Application to Mg Alloy Design: *In-Ho Jung*¹; Woo Jin Park¹; Sangho Ahn¹; Daehoon Kang²; Nack J. Kim²; ¹Research Institute of Industrial Science and Technology; ²POSTECH

Recently Mg-Sn-Zn-Al alloy system has been investigated actively in order to develop new magnesium alloy which satisfies a stable structure and good mechanical properties at high temperatures. In the present study, available thermodynamic and phase diagram data of the Mg-Sn-Zn-Al quaternary system have been critically evaluated and all reliable data have been simultaneously optimized to obtain one set of model parameter for the Gibbs energy of the liquid and all solid phases as functions of compo-

sition and temperature. The optimized database was applied to new alloy design. All calculations were performed using FactSage thermochemical software.

11:10 AM

Dissolution Kinetics and Recovery of Manganese Additions into Liquid Magnesium: *Zhi Li*¹; *Stavros A. Argyropoulos*¹; Timothy J. Kosto²; ¹University of Toronto; ²Milward Alloys Inc

This paper will focus primarily on the dissolution of various Manganese compacts in liquid magnesium. A unique experimental procedure has been developed, using cylindrical compacts with various Manganese compositions. The various temperatures of the addition and magnesium bath, as well as the apparent weight of the addition were measured simultaneously during the immersion of the addition into the magnesium bath. The exothermicity level of these additions during their dissolution in liquid magnesium was determined. The relation of the exothermicity level with the dissolution kinetics was also examined. In addition, SEM and EDX work was conducted for additions, which were withdrawn from the Magnesium bath. Finally, the recovery of these additions was estimated by taking samples from the Magnesium bath and conducting ICP analyses.

11:30 AM

Two-Stage Thermodynamic Modeling of a Thixoforming Process: *Rainer Schmid-Fetzer*¹; Mile B. Djurdjevic¹; ¹Clausthal University of Technology

A two-stage thermodynamic calculation is proposed as a tool to analyze the alloy related aspects in semisolid forming processes. The two process stages are identified as (i) equilibration in semisolid state, and (ii) subsequent fast solidification of the material. For the example of Mg-Al-Zn-Ca alloys the results and limitations of this modeling approach are given. The wealth of information provided, such as process temperature and sensitivity, freezing ranges and the detailed constitution of the processed material, is suggested to assist in alloy development. This work is supported by the German Research Foundation (DFG) in the Priority Programme "DFG-SPP 1168: InnoMagTec".

11:50 AM

Tensile Properties and Microstructures of the Mg-13Li-9Al-1Zn Alloy Prepared in Air by Electrolytic Diffusing Method: *Meng-Chang Lin*¹; Jun-Yen Uan¹; ¹National Chung Hsing University

The Mg-Li-Al-Zn alloy was successfully produced in air by electrolytic diffusing method at 500°C. In electrolysis cell, Mg-9Al-1Zn (AZ91) alloy plate with 3mm in thickness was used as cathode and graphite was as anode. The mixtures of 55wt%KCl - 45wt%LiCl were employed as the electrolyte. The microstructure was investigated by optical microscopy, scanning electron microscopy, X-ray diffraction and transmission electron microscopy. After electrolysis experiments, the Mg-13Li-9Al-1Zn alloy plate can be obtained, the hexagonal-closed-pack AZ91 plate (3mm in thickness) was converted to the mixture of α -Mg and BCC Mg phase (thickness changed to 4.6mm). The Mg-13Li-9Al-1Zn alloy plate could be cold rolled easily into 1.5mm strip. After heat treatment, the Mg-13Li-9Al-1Zn alloy strip exhibits yield strength ~ 148MPa. The elongation can reach ~ 22%, which is much better than AZ91D alloy.

Magnesium Technology 2006: Wrought Alloys and Forming Processes II

Sponsored by: International Magnesium Association, TMS Light Metals Division, TMS: Magnesium Committee

Program Organizers: Alan A. Luo, General Motors Corporation; Neale R. Neelameggham, US Magnesium LLC; Randy S. Beals, DaimlerChrysler Corporation

Wednesday AM
March 15, 2006

Room: 6A
Location: Henry B. Gonzalez Convention Ctr.

Session Chairs: Karl U. Kainer, GKSS Research Center; Ravi Verma, General Motors Corporation

8:30 AM

Development of CaO Added Wrought Mg Alloy for Cleaner Production: *Jin-Kyu Lee*¹; *Hyung-Ho Jo*¹; *Shae K. Kim*¹; ¹Korea Institute of Industrial Technology

Magnesium alloys are attractive for structural components in transportation industries. At present, magnesium components for structural applications are mainly produced by the die casting process. It is, however, commonly acknowledged that structural components made from wrought alloys through a metal forming process have great advantage in terms of obtainable strength and toughness. In addition, most of the wrought magnesium alloys are heat treatable and thus allow their strengths to be further improved or their mechanical performance to be tailored by adjusting the parameters of heat treatment. The wrought process route of melting, ingot casting/continuous casting, forming and heat treatment is carried out under protective cover gas to prevent oxidation and ignition. In order to eliminate cover gas during forming process, the aim of present study is to investigate the effect of CaO additions on surface oxidation of extrudate without protective cover gas and properties of CaO added AZ31 alloys.

8:55 AM

Development of Thixoextrusion Process for AZ31 Magnesium Wrought Alloy: *Young-Ok Yoon*¹; *Hoon Cho*¹; *Hyung-Ho Jo*¹; *Shae K. Kim*¹; ¹Korea Institute of Industrial Technology

Magnesium and magnesium alloys are used in a wide variety of structural applications. Recent developments in the field of magnesium wrought alloys are opening up diverse industrial applications, especially, in the field of extrusion process. Various extrusion processes such as rapid cooling extrusion, isothermal velocity extrusion, alternative section extrusion and thixoextrusion, have been developed for improving extrudability of AZ31 magnesium wrought alloy. Especially, thixoextrusion process has advantages of high productivity, reduced extrusion pressure and homogeneous internal microstructure compared with conventional extrusion processes. The aim of this study is to investigate feasibility of thixoextrusion for AZ31 magnesium wrought alloy through simple partial remelting. Microstructural evolution on globular solid particle size and distribution with respect to isothermal holding temperature and time will be discussed.

9:20 AM

Drawing Formability of Magnesium Alloy (AZ31) Sheet with Conical Cup Test: *Hee Taek Lim*¹; *Jeong Hun Kang*¹; *Seong Ho Cho*¹; *Jeong Whan Han*¹; ¹Inha University

The drawing forming has considerable potential because of its competitive productivity and performance. Though die-casting process has been widely used in magnesium forming, unavoidable poor surface qualities are major obstacles for applying to electronic housing components. In the present study, a conical cup test was made to evaluate drawing formability of magnesium alloy (AZ31) sheet. Sheets fabricated by extrusion and rolling were examined and effects of punch speed and temperature were investigated as major process parameter. Drawing Formability was evaluated by using CCV (conical cup value) designated in the standard, which is the arithmetical mean of maximum and minimum diameter. In order to investigate microstructure, the examined specimens were sectioned in the middle vertically and observed microstructure locally. It was found that the CCV increase with the increase of punch speed. This means

high punch speed has poor drawing formability. The CCV reaches to a minimum value at 573K.

9:45 AM

Effect of Extrusion Temperature on Formability and Tensile Properties of AZ31B Extrusions: *Weinan Ding*¹; *Jiang Li*¹; *Dongchang Jiang*¹; *Changbao Ren*¹; ¹SinoMaG-GRM

This study investigated the extrusion formability and mechanical properties of AZ31B extrusions at various extrusion temperatures from 2000C to 4500C. A vertical direct chill casting equipment was set up in GRM for semi-continue casting ϕ 110 mm AZ31B billets and a horizontal 630-ton extrusion press was used to extrude AZ31B extrusions. Extrusion die, holding tube and F95x350 billets were all heated to specified temperature before extrusion. Microstructure and tensile properties of ϕ 25 mm round bars extruded with different extrusion temperatures were investigated. Extrusion experiments indicated that the lowest extrusion formable temperatures are variable with different section profiles and extrusion rates. Extrusion surface tearing defects become worse with extrusion temperature increasing. The proper extrusion temperature range is optimized by the consideration of metal formability and extrusion surface quality. The strength and ductility of extrusions were obviously improved in respect with billet material. Extrusion temperatures significantly influence metal recrystallization performance and tensile properties.

10:10 AM Break

10:30 AM

Effect of Strain Rate on Deformation Behavior of a Mg-9Li-2Zn Alloy Sheet at Room Temperature: *Hong Bin Li*¹; *Guang-Chun Yao*¹; *Yi Han Liu*¹; ¹Northeastern University

A two-phase Mg-9Li-2Zn alloy sheet is made by cold-rolling at room temperature and the formability of it at room temperature is investigated in this study. Uniaxial tension tests are carried out for various strain rates between 0.5mm/min and 250mm/min, and the microstructural changes during the tests are observed. The sheet has high formability at comparatively low strain rates. Maximum elongation amounts to 40%. However, ductility decreases with the increase in strain rate. Even at room temperature, the stress is also sensitive to the strain rate. There are many large dimples at comparatively low strain rates, and small dimples occur at high strain rates, it shows fine sub-grains come into being.

10:55 AM

High-Speed Heavy Rolling of Magnesium Alloy Sheets: *Hiroshi Utsunomiya*¹; *Tetsuo Sakai*¹; *Satoshi Minamiguchi*¹; *Hiroaki Koh*¹; ¹Osaka University

As Mg alloys are well known difficult-to-work alloys, they are mostly processed by die-casting or thixo-moulding. The lower deformability is due hcp crystal structure and inactiveness of basal slip at low temperature (<500K). Sheets are produced by rolling. Rolls are often heated and multi-pass low reduction rolling with intermediate annealing are frequently employed to suppress edge cracks or fracture. The authors propose a high-speed heavy-reduction rolling for manufacturing of Mg alloy sheets. Commercial AZ31B sheets were processed at high-speed (~2000m/min) between RT and 623K. It is found that the thickness can be reduced 60% by one-pass operation even at room temperature without fracture. The sheets processed at 473K showed the finest recrystallized microstructure with a mean grain size of 2.2 microns. The fine-grained sheets show superior mechanical properties than conventional sheets. It has been concluded that the high-speed heavy rolling is promising for industrial manufacturing of Mg sheets.

11:20 AM

Hot Rolling of AM50 for Sheet Production: *Jürgen Göken*¹; *Norbert Hort*²; *Kurt Steinhoff*²; *Karl Ulrich Kainer*²; ¹University of Kassel; ²GKSS Research Center

In the past magnesium cast alloys have been successfully developed and are fairly good introduced to vehicles even in power train applications with service temperatures up to 150°C and more. But there is still a lack of information's regarding the use of magnesium alloys as wrought materials especially in sheet applications. This concerns both the availability of alloys and the processing parameters of a chosen wrought process. In the present work AM50 has been used to produce sheet by hot

rolling. Preheated material has been deformed in several steps until the sheet reached a final thickness of 0.3 mm. Further deformation was applied on the sheets by deep drawing to obtain information's of the materials behavior after a secondary deformation process. The paper describes the rolling and deep drawing experiments and the microstructure obtained in the different steps of processing with a special regard to recrystallization behavior.

Materials Design Approaches and Experiences II: Steels and Titanium Alloys

Sponsored by: The Minerals, Metals and Materials Society, TMS Structural Materials Division, TMS: High Temperature Alloys Committee

Program Organizers: Michael G. Fahrman, Special Metals Corporation; Yunzhi Wang, Ohio State University; Ji-Cheng Zhao, General Electric Company; Zi-Kui Liu, Pennsylvania State University; Timothy P. Gabb, NASA Glenn Research Center

Wednesday AM
March 15, 2006

Room: 202B
Location: Henry B. Gonzalez Convention Ctr.

Session Chairs: Timothy P. Gabb, NASA Glenn Research Center; Yunzhi Wang, Ohio State University

8:30 AM Invited

Computational Systems Design of Hierarchically Structured Materials: *Gregory B. Olson*¹; ¹Northwestern University and QuesTek Innovations LLC

A systems approach integrates processing/structure/property/performance relations in the conceptual design of multilevel-structured materials. Using examples of high performance alloys, numerical implementation of materials science principles provides a hierarchy of computational models defining subsystem design parameters which are integrated via computational thermodynamics in the comprehensive design of materials as interactive systems. Recent initiatives integrate materials science with quantum physics and applied mechanics, and address the acceleration of the full materials design, development and qualification cycle. Principal barriers to the adoption of the new paradigm of science-based materials engineering are primarily cultural, and will require substantial reform of undergraduate materials education.

9:00 AM Invited

The Application of Computational Thermodynamics to Materials Design: *John M. Vitek*¹; Ron L. Klueh¹; ¹Oak Ridge National Laboratory

Computational thermodynamics provides the basis for identifying phase stability in multi-component systems, such as ferrous and nickel-based alloys, by considering the free energy of phases as a function of composition and temperature. This tool can be used effectively to model the influence of composition and heat treatment on the phases that form during solidification, thermal processing and service exposure. Consequently, it can lead to improved alloy design by tailoring alloy compositions to meet specific needs. This presentation will describe several examples in which calculations provided guidance in terms of identifying alloy modifications or heat treatment schedules to optimize material performance. This research was sponsored by the Laboratory Technology Research Program of the Office of Science, U. S. Department of Energy, under contract DE-AC05-00OR22725 with UT-Battelle, LLC.

9:30 AM

Carbon Diffusion and Phase Transformations during Gas Carburizing of High Alloyed Stainless Steels: Experimental Study and Theoretical Modeling: *Thierry Turpin*¹; Jacky Dulcy²; Michel Gantois²; ¹Aubert and Duval; ²Ecole des Mines de Nancy

Gas carburizing of high alloyed stainless steels increases surface hardness, as well as the overall mechanical characteristics of the surface. The growth of chromium rich carbides during carbon transfer into the steel causes precipitation hardening in the surface, but decreases the chromium content in solid solution. In order to maintain a good corrosion resistance in the carburized layer, the stainless steel composition and the carburizing

process need to be optimised. To limit the experimental work a methodology using software for modeling the thermodynamic and kinetic properties in order to simulate carbon diffusion and phase transformations during gas carburizing is presented. Experimental carbon profiles were determined by WDS-EPMA analyses, while carbide compositions were measured by EDS_X analyses. A good agreement between calculated and experimental values was observed for the Fe-13Cr-5Co-3Ni-2Mo-0.07C and the Fe-12Cr-2Ni-2Mo-0.12C (wt pct) martensitic stainless steels at 955°C and 980°C.

10:00 AM Break

10:20 AM Invited

Use of Modeling Tools for Forging and Heat Treat Process Design: *David U. Furrer*¹; Gangshu Shen¹; Vikas Saraf¹; ¹Ladish Company Inc

Modeling and simulation has been advancing at a rapid rate. The use of deformation and thermal simulations, along with microstructure evolution modeling tools is now advancing to the point where virtual process design is possible from component configuration to final component microstructure and properties. Combined simulation tools are being used for a variety of materials, including steel, titanium and nickel-base superalloy forgings. The future will continue to demand more rapid process design and increased component capabilities, which will require further advancements in the development and use of computer-based simulation tools.

10:50 AM Invited

Design Tools for Predicting Microstructure/Property Relationships in Ti Alloys: *Hamish L. Fraser*¹; ¹Ohio State University

There has been a significant effort aimed at integrating computational methods with critical experiment to produce design tools for structural materials. This paper describes the work that has been focused on the development of such tools for prediction of the interrelationship between microstructure and properties for Ti alloys. This has been done by a number of researchers within our group who will be gratefully acknowledged during the presentation. The methods for quantification of microstructure will be detailed, including new ways in which 3-D representations of microstructure may be determined. These data together with measurements of mechanical properties are used to populate databases that become the basis for the development of neural network models capable of predicting the desired interrelationships. The ways in which these neural networks are used to perform virtual experiments, leading to increased mechanistic understanding, and to develop design tools which operate on PC computers will be demonstrated.

11:20 AM

Phase Field Modeling of Microstructural Evolution in Ti-6Al-4V: *Ning Ma*¹; Yunzhi Wang¹; ¹Ohio State University

Phase transformation and microstructural evolution in commercial titanium alloys are extremely complex. In this presentation we discuss our recent effort in integrating thermodynamic modeling and phase field simulation to develop computational tools for quantitative prediction of phase equilibrium and spatiotemporal evolution of microstructures during thermal processing. The models account explicitly for precipitate morphology, spatial arrangement and anisotropy. The models developed were validated against experimental observations using optical metallography, SEM, and TEM, with microstructural features quantified by a set of rigorous procedures based on stereology. The rendering of the predictive capabilities of the phase field models as fast-acting design tools through the development of constitutive equations is also demonstrated.

11:40 AM

Neural Networks for Mechanical Property Predictions – Example of Fracture Toughness in Ti Alloys: *Sujoy Kar*¹; Thomas Searles²; Jaimie Tiley³; Brian Welk¹; Joshua Tuggle¹; Santhosh Koduri¹; Gopal Babu Viswanathan¹; Hamish L. Fraser¹; ¹Ohio State University; ²Rolls-Royce Corporation; ³Air Force Materials Laboratory

The accelerated insertion of titanium alloys in component application requires the development of predictive capabilities for property-microstructure relationships. This paper discusses the development of Neural Network (NN) Models based on Bayesian statistics to predict the fracture toughness at room temperature. The microstructural data are obtained by stereological procedures. These data along with the measurements of frac-

ture toughness constitute the database. This database is used to train and test the NN to predict the fracture toughness. In addition, the trained NN models are successfully used to identify the functional dependence of fracture toughness on individual microstructural features via virtual experiments, which in turn can assist in the development of physically based models. Comparative fractography analysis is performed to understand the fracture behavior of extreme fracture toughness samples. Development of web based design tool for online prediction of fracture toughness using NN model is demonstrated.

Materials in Clean Power Systems: Applications, Corrosion, and Protection: Interconnection and Sealing in Fuel Cells II

Sponsored by: The Minerals, Metals and Materials Society, TMS Structural Materials Division, TMS/ASM: Corrosion and Environmental Effects Committee

Program Organizers: Zhenguo Gary Yang, Pacific Northwest National Laboratory; K. Scott Weil, Pacific Northwest National Laboratory; Michael P. Brady, Oak Ridge National Laboratory

Wednesday AM
March 15, 2006

Room: 212B
Location: Henry B. Gonzalez Convention Ctr.

Session Chairs: Jeffrey W. Fergus, Auburn University; Anthony Petric, McMaster University

8:30 AM Invited

Spinel Coatings for Solid Oxide Fuel Cell Interconnects: *Anthony Petric¹; Ping Wei¹; M. Reza Bateni¹; ¹McMaster University*

Chromia scale-forming alloys have adequate corrosion protection as SOFC interconnects but the electrical resistance becomes a problem with time. In addition, volatile chromia species can poison the cathode reaction. One possible solution is to apply a compatible coating to the interconnect surface. We surveyed the electrical and thermal properties of spinel compounds. Spinel based on Al₂O₃ and Cr₂O₃ exhibit low values of conductivity and thermal expansion. CuFe₂O₄, CuMn₂O₄ and Co₂MnO₄ were found to have the most compatible properties for interconnect coatings. Our measurements showed that conductivities range from 10 to 100 S/cm at 800°C and thermal expansion coefficients are 10-12 ppm/K. Spinel coatings up to 50 μm thick were grown by electroplating the metals individually onto UNS430 ferritic stainless steel, followed by oxidation at 750°C for 1 day. The coatings were dense and showed good adhesion to the substrate. Testing of the performance of these coatings at fuel cell conditions is underway.

9:00 AM

Development of (Mn,Co)3O4 Protection Layers on Ferritic Stainless Steels for SOFC Interconnect Applications: *Zhenguo Gary Yang¹; Gordon Xia¹; Gary Maupin¹; Shari Li¹; Prabhakar Singh¹; Jeff Stevenson¹; ¹Pacific Northwest National Laboratory*

Due to their excellent oxidation resistance and thermal expansion match to the other stack components, stainless steels are among the most promising candidate materials for interconnect applications in intermediate-temperature planar SOFC stacks. For this particular application, however, there remain some issues in their long-term surface stability and the electrical resistance arising from the oxide scale growth, as well as chromia evaporation and potential poisoning of cells. Application of (Mn,Co)₃O₄ spinel protection layers on the ferritic stainless steels appears to be a promising solution to overcome these issues. To optimize the spinel protection layers for maximum performance, the spinel materials were systematically studied; different fabrication approaches and parameters have also been investigated. This paper will present details of this work and give an overview on the materials and different approaches of fabricating the spinel protection layers on ferritic stainless steel SOFC interconnects.

9:25 AM

Dual Atmosphere Tolerance of Ag-CuO Based Air Braze: *Jin Yong Kim¹; John S. Hardy¹; K. Scott Weil¹; ¹Pacific Northwest National Laboratory*

Silver-based reactive air braze (RAB) is an effective alternative for hermetic sealing of high temperature devices such as solid oxide fuel cells (SOFCs). Since the seal in the SOFCs (especially the cell-to-frame seal) is exposed to the dual atmosphere such as hydrogen on one side and oxygen on the other side, the dual atmosphere tolerance is one of the critical requirements for this application. Exposure to the dual atmosphere can initiate degradation such as hydrogen embrittlement after long term operation. We will discuss the microstructure after dual atmosphere exposure and apparent mechanisms of the degradation.

9:50 AM

Enabling Inexpensive Metallic Alloys as SOFC Interconnects: An Investigation into Hybrid Coating Technologies to Deposit Nanocomposite Functional Coatings on Ferritic Stainless Steels: *Paul Gannon¹; Max C. Deibert¹; Richard Smith¹; Asghar Kayani¹; Z. Gary Yang²; Jeffery Stevenson²; Steven Visco³; Craig Jacobson³; H. Kurokawa³; Stephen Sophie⁴; ¹Montana State University; ²Pacific Northwest National Laboratory; ³Lawrence Berkeley National Laboratory; ⁴NASA-Glenn Research Center*

Reduced operating temperatures (600-800°C) of Solid Oxide Fuel Cells (SOFCs) may enable the use of inexpensive ferritic steel interconnects. Due to the demanding SOFC operating environment, protective coatings are gaining attention to increase long-term interconnect stability. In this study, large area filtered arc deposition (LAFAD) and hybrid filtered arc-assisted EB-PVD (FA-EB-PVD) technologies were used for deposition of two-segment coatings with Ti-Cr-Co-Al-Y-O-N based bottom sublayer and Mn-Co-O top layer. Coatings were deposited on ferritic steel and subsequently annealed in air for various time intervals. Surface oxidation was investigated using RBS and SEM/EDS analyses. Cr-volatilization was evaluated using a transpiration apparatus and ICP-MS analysis of the resultant condensate. Area Specific Resistance was studied as a function of time using the four-point technique. The oxidation behavior, Cr volatilization rate, and electrical conductivity of the coated and uncoated samples are reported. Transport mechanisms for various oxidizing species and coating diffusion barrier properties are discussed.

10:15 AM Break

10:30 AM Invited

Evaluation of Fe-Ni Alloys for Reduced-Temperature SOFC Interconnect Application: *Jiahong Zhu¹; S. J. Geng¹; M. P. Brady²; I. G. Wright²; X. D. Zhou³; H. U. Anderson³; ¹Tennessee Technological University; ²Oak Ridge National Laboratory; ³University of Missouri-Rolla*

Current standard solid oxide fuel cell (SOFC) interconnect materials, ferritic Fe-Cr alloys, have the Cr volatility problem, which leads to the poisoning of the cathode and subsequent degradation in SOFC performance over long-term stack operation. A new generation of Fe-Ni base alloys which are either free of Cr or have low Cr content is under development to mitigate the Cr volatility problem. This talk will summarize our recent alloy design efforts on Cr-free or low-Cr Fe-Ni alloys with different Ni levels as interconnect materials for reduced-temperature SOFC. Evaluation of these alloys includes their coefficient of thermal expansion (CTE), oxidation resistance, oxide scale area specific resistance (ASR), and interaction/compatibility with cathode materials. The promises of the Fe-Ni alloys as SOFC interconnect will be highlighted and alloy design strategies to address the remaining issues related to these alloys will be discussed.

11:00 AM

Investigation of Clad Materials for Use in PEMFC Bipolar Plates: *K. Scott Weil¹; Z. Gary Yang¹; Gordon Xia¹; Jin Yong Kim¹; ¹Pacific Northwest National Laboratory*

We are currently investigating clad materials for potential use as bipolar plates in PEMFCs. In our present approach the thin metal laminate sheet consists of a middle filler layer sandwiched between two transition metal alloy layers that can be thermally nitrided or carbided to form a conductive, yet corrosion-resistant (i.e. passivating) barrier layer. Ideally the material selected for the filler, which will form the thickest of the three layers, is chosen based primarily on material cost, formability, durability, and thermal conductivity. The cladding material, on the other hand, is selected based on the ease of nitriding or carbiding, the corrosion resistance and electrical transport properties of the resulting nitride or carbide,

WEDNESDAY AM

formability, and cost. In this way, the bipolar plate can be tailored to take advantage of the merits of each material, while minimizing material and processing costs.

11:25 AM

Nitrided Stainless Steels for PEM Fuel Cell Bipolar Plates: *Bing Yang*¹; Michael P. Brady¹; David Young²; Peter Tortorelli¹; Heli Wang³; John Turner³; ¹Oak Ridge National Laboratory; ²University of New South Wales; ³National Renewable Energy Laboratory

This paper will overview efforts to form electrically conductive and corrosion resistant Cr-nitride surfaces on commercial and developmental stainless steel alloys for use as proton exchange membrane fuel cell (PEMFC) bipolar plates. Emphasis will be placed on the details of the nitridation reaction for both austenitic and ferritic alloy substrates, and the possible role of oxygen impurities in the nitriding environment in aiding establishment of the external nitride layer. Results of interfacial contact resistance measurements and polarization screenings in simulated PEMFC environments will also be presented.

Materials Processing Fundamentals: Powders and Composites

Sponsored by: The Minerals, Metals and Materials Society, TMS Extraction and Processing Division, TMS: Process Fundamentals Committee, TMS: Process Modeling Analysis and Control Committee
Program Organizers: Princewill N. Anyalebechi, Grand Valley State University; Adam C. Powell, Massachusetts Institute of Technology

Wednesday AM
March 15, 2006

Room: 203A
Location: Henry B. Gonzalez Convention Ctr.

Session Chair: Princewill N. Anyalebechi, Grand Valley State University

8:30 AM

Effects of Temperature and Precursors on Preparation of Fe-TiC Composite from Ilmenite: *Sutham Niyomwas*¹; ¹Prince of Songkla University

The Fe-TiC composite powder was synthesized in situ by carbothermal reduction of ilmenite. The standard Gibbs energy minimization method was used to calculate the equilibrium composition of the reacting species. The effects of The reaction temperature (1400°C - 1600°C) and milling time of precursors on the Fe-TiC conversion and powder morphologies were investigated using XRD and SEM method. The synthesized products showed that composite with iron matrix and titanium carbide as a reinforced phase was formed.

8:55 AM

Production of Titanium Powder Directly from Titanium Ore by Preform Reduction Process (PRP): *Haiyan Zheng*¹; Toru H. Okabe¹; ¹University of Tokyo

The preform reduction process (PRP) based on the calciothermic reduction of titanium ore was investigated. To develop a new process for producing metallic titanium powder directly from titanium ore, thermodynamic analyses for removing iron from the ore by selective chlorination were conducted before the experimental work. Titanium feed preform was fabricated at room temperature by casting slurry, which is a mixture of titanium ore (rutile TiO₂ with impurities, e.g., iron), flux (CaCl₂), and binder. The fabricated preform was calcined at elevated temperatures and iron was removed by selective chlorination. The obtained preform was then reduced using metallic calcium vapor as the reductant, and the reduced preform was subject to leaching to remove CaO, Ca, and other impurities. When de-ironized rutile ore mixed with CaCl₂ flux was reduced, metallic titanium powder with 99% purity was obtained. Thus, the PRP is feasible to produce titanium powder directly from titanium ore.

9:20 AM

EMF Studies on Nb-Al Intermetallics: *Pratheesh George*¹; Ramana G. Reddy¹; ¹University of Alabama

Niobium-Aluminum alloys are of great interest due to its high temperature properties. Nb is also used as an alloying element with Ti-Al

alloys to improve properties like oxidation resistance. In this investigation, Gibbs energy of mixing of NbAl₃ was determined using EMF method in the temperature range of 933 to 1098 K. The construction and design of the cell used for EMF measurement was also discussed. The cell reaction is as follows: Pt /Al, Ca₂AlF₇ ||CaF₂||Al (Nb-Al alloy), Ca₂AlF₇/Pt. Experimental results showed that a linear relationship between EMF and temperature was obtained. The partial Gibbs energy of formation was calculated using the Nernst equation. The thermodynamic properties like activity, activity coefficient and partial Gibbs energy of mixing was determined in the temperature range of 933 to 1098 K for NbAl₃. These experimentally determined thermodynamic properties of Nb-Al alloys were compared with other aluminides.

9:45 AM

In Situ Synthesis of Al-TiC-Al₂O₃ and Al-SiC-Al₂O₃ Composites: *Napisorn Memongkol*¹; Sutham Niyomwas¹; ¹Prince of Songkla University

Syntheses of Al-TiC-Al₂O₃ and Al-SiC-Al₂O₃ composites were obtained in situ by combustion assisted synthesis (CAS) of mixtures of Al powder, TiO₂ powder and activated carbon powders and Al powder, SiO₂ powder and activated carbon powders. The reactions were carried out in a horizontal tube furnace under flow of inert gas. The standard Gibbs energy minimization method was used to calculate the equilibrium composition of the reacting species. The synthesized products were mixtures of aluminum matrix reinforced with titanium carbide and alumina and aluminum matrix reinforced with silicon carbide and alumina. The effect of the quantity of the matrix powder (Al powder) was investigated using XRD and SEM method. The synthesized products showed those composites with aluminum matrix and titanium carbide and alumina as reinforced phases and aluminum matrix and silicon carbide and alumina as reinforced phase were formed.

10:10 AM Break**10:25 AM**

Ti Product from the Reaction of TiCl₄ Gas with Droplets of Molten Mg: *Akio Fuwa*¹; *Masashi Tsumura*¹; ¹Waseda University

Presently, sponge titanium metal product is produced through Kroll process where TiCl₄ reactant gas is reacted and reduced with molten Mg reactant in a batch reactor. This reduction reaction may be limited taking place at these reactants interfacial area, so that higher reduction rate may be limited as well. This research investigates the reduction reaction of TiCl₄ with molten Mg metal droplets, and titanium product situation and morphology. Molten Mg droplets have larger interfacial area so that the higher reaction rate can be expected. Here, molten Mg droplets are continuously formed by flowing Mg through a nozzle with small hole at a heated, holding crucible, introduced in a reactor and reacted with TiCl₄ gas, fed continuously into the reactor. The reduction reactions are studied with the following experimental parameters; temperature, droplet size, Mg/TiCl₄ feed ratio, and etc.

10:50 AM

Titanium Subchloride Synthesis by Reaction of Titanium with TiCl₄: *Osamu Takeda*¹; Toru H. Okabe¹; ¹University of Tokyo

In order to establish a new semi-continuous/high-speed titanium production process based on the magnesiothermic reduction of titanium subchlorides, a novel synthetic process of titanium subchlorides (TiCl_x, x = 2, 3) by reacting titanium metal with TiCl₄ was investigated. Titanium metal powder placed on a molybdenum tray was heated to 1273 K in a stainless steel reactor filled with argon gas, and TiCl₄ liquid was supplied into the reactor by a pump at a rate of 0.12~0.64 g/min. Deposits recovered from the trays after the experiment were identified to be TiCl₂. Under certain conditions, a trace of TiCl₃ was also observed in the TiCl₂ deposit. Currently, a more efficient method for titanium subchloride production using a molten salt medium is under investigation. Some results on the reduction of synthesized TiCl₂ by magnesium will also be shown.

11:15 AM

Study of Decomposition Regularities for a Zn-Containing Volatile Complex Used in ZnO Film Synthesis: *Emma Rubenovna Arakelova*¹; *Fridrikh Akopovich Grigoryan*¹; *Vergine Gagikovna Parvanyan*¹; *Goarik Gagikovna Asatryan*¹; ¹State Engineering University of Armenia

H₂O₂ (98%) vapor passed through a reactor at 25 Pa where a ZnO target was placed at 273K-373K. Experiments were carried out on a flow-type vacuum device. H₂O₂ decomposition on ZnO surface accompanied by formation of a Zn-containing volatile complex which transferred to the gas phase, and ZnO deposited on a substrate at condensation. As the substrate, five sequentially located quartz cylinders were used at 293K-423K (TII). Decomposition of the Zn-containing complex on quartz substrates carried out as a first-order reaction. The complex decomposition constant (K_p) increased with the substrate temperature (TII = 293 K, K_p = 7.05 sec⁻¹; TII = 373 K, K_p = 87 sec⁻¹; TII = 423 K, K_p = 158 sec⁻¹). The complex decomposition constant did not practically vary when the target temperature increased; the complex formation rate increased slightly.

11:40 AM

Preparation of Mono-Dispersed Co₃O₄ Particles by Homogeneous Precipitation with Urea Followed by Decomposition: *Guo Xueyi*¹; ¹Central South University

The mono-dispersed Co₃O₄ precursor particles were prepared by homogeneous precipitation from the high Co²⁺ concentration with urea, the main factors were investigated on the homogeneous precipitation, which include the Co²⁺ concentration, the initial pH of the solution, the temperature and the reacted time for the reaction, the use of the urea, the agitation pattern, It is determined that the precursor particles were cobalt hydroxyl-carbonate with fine crystalline. Then, the precursor was decomposed at high temperature and the mono-dispersed Co₃O₄ particles with 2μm in average particle size and special micrograph, fine crystalline were obtained. The effects of the temperature, the time for decomposition were addressed.

12:05 PM

The Formation of Misty Band near the Substrate during Contact Angle Measurement: Wu Linli¹; Yao Guangchun¹; Tianjiao Luo¹; Zhang Xiaoming¹; ¹Northeastern University

During measuring contact angle there was a misty band near the substrate. Hsien-Nan Ho and Shinn-Tyan Wu thought this was because the oxygen atoms on the interface migrate to the droplet surface to form an oxide band near the substrate. But from our experiments misty band appeared before the drop reach to the substrate. Theoretically speaking, the oxygen partial was the same everywhere in the vacuum furnace. So there was no condition to provide enough oxygen forming oxide. This appearance would be explained more reasonably with the optics principle. Most reflect light would be absorbed by the substrate and light cannot reach the observation area, so the misty band formed.

Multicomponent-Multiphase Diffusion Symposium in Honor of Mysore A. Dayananda: Industrial Applications

Sponsored by: The Minerals, Metals and Materials Society, ASM Materials Science Critical Technology Sector, ASM-MSCTS: Atomic Transport Committee

Program Organizers: Yong-Ho Sohn, University of Central Florida; Carelyn E. Campbell, National Institute of Standards and Technology; Richard Dean Sisson, Worcester Polytechnic Institute; John E. Morrall, Ohio State University

Wednesday AM Room: 203B
 March 15, 2006 Location: Henry B. Gonzalez Convention Ctr.

Session Chairs: Sungjin Koh, University of Texas at Arlington; John E. Morrall, Ohio State University

8:30 AM

Carbon Diffusion in Steels – An Analysis Based on Direct Integration of the Flux: *Olga Karabelchchikova*¹; Richard D. Sisson¹; ¹Worcester Polytechnic Institute

In the early 1970s Professor Dayananda developed a technique of direct integration of fluxes over distance from the concentration profiles in vapor-solid diffusion couples. This integration allowed determination of concentration dependent atomic mobilities and diffusion coefficients. As

part of a project to control and optimize the industrial carburization process in mild and low-alloyed steels, this analysis was applied to several commercial grade carburized steels to determine the effect of alloy composition on their atomic mobility and carbon diffusion in the Austenitic phase. While carbon flux and therefore surface carbon content vary with time during single-stage carburizing even with a fixed carbon potential in the atmosphere, a mass balance at the gas-solid interface must serve as boundary condition. Furthermore, the analysis was applied to determine the characteristic surface mass transfer coefficient and carbon mobilities in several grades of steel. The results were compared with previous determinations and predictions reported in literature.

8:55 AM

Carbon Diffusion in Austenite: A Reassessment: *Irina V. Belova*¹; Graeme Murch¹; ¹University of Newcastle

We re-analyse carbon tracer and chemical diffusion in austenite at low carbon compositions using a very general four-frequency model first formulated by McKee. Our re-analysis makes use of the almost exact formalism of Okamura and Allnatt. In the re-analysis of the carbon diffusion and making use of the carbon activity data we confirm the general finding of McKee that the increase of both tracer and chemical diffusivities with carbon composition at 1000 C is largely a result of a much higher rate of rotation of carbon interstitial pairs compared with isolated carbon interstitials. We find however that the carbon atoms move almost twice as fast as a rotating pair than found originally by McKee. We also extrapolate information on the ratios of exchange frequencies to temperatures between 800 C and 1000 C using available experimental data on the carbon chemical diffusion and activity.

9:20 AM

Comparative Studies of Boron Diffusion in Low Carbon Steel, High Strength Alloy Steel and Stainless Steel: *Naruemon Suwattananon*¹; Roumiana Petrova¹; Boris Goldenberg¹; ¹New Jersey Institute of Technology

Comparative studies of boron diffusion in low carbon steel (AISI 1018), high strength alloy steel (AISI 4340) and stainless steel (AISI 304) are reported. The steel samples were boronized by using powder mixture method in temperature range of 600-1000°C for 2, 4, 6, 8 and 10 hours, respectively. Boron diffusion, morphology and types of borides were analyzed by optical microscopy, XRD, SEM and EDS. The growth kinetics of MeB, Me₂B phases was investigated as a function of treatment time and temperature as well as the effect of alloying element concentration on the kinetics process. Diffusion coefficient and activation energy were calculated from the distribution profiles of alloying elements and the thickness of the boride layers. The experimental results show the diffusion coefficient and activation energy of boronizing process are dependent on the concentration of the alloying elements in steel as well as treatment time and temperature.

9:45 AM

Diffusion Phenomena Related to Carburization Resistant Ablation Coatings for Ethylene Pyrolysis Coils: *Alok P.S. Chauhan*¹; Henry J. White¹; Weidong Si²; ¹State University of New York; ²Brookhaven National Laboratory

Wholly austenitic heat resistant materials have been the workhorse for the outlet pass of ethylene pyrolysis tubing for many years. Higher operating temperatures (>1100 C) and the presence of both oxidizing (on the outer diameter side) and carburizing (process side) environments have reduce tube life significantly (by 4-6 years). We will present the diffusion related phenomena (carburization and oxidation related events in the material at 1100 C; conversion of the inherent Cr₂O₃ surface protective coating to Cr₂₃C₆ and Cr₇C₃; paramagnetic to ferromagnetic transformation; etc.) associated with our efforts to reduce catalytic coke formation (i.e. increase tube life) by coating the inner diameter of ethylene pyrolysis tubing using pulsed deposition carburization resistant coatings. Diffusion controls the structure, properties, processing, and performance of the material. Thus, a complete understanding of diffusion related phenomena will result in a coating/substrate system with limited deleterious microstructures, excellent coating/substrate adhesion, and improved performance.

WEDNESDAY AM

10:10 AM Break

10:30 AM

Assessment of Superalloy-Dependent Lifetime of a NiCoCrAlY Coating Based on Understanding of Interdiffusion in NiAl vs. Superalloys Diffusion Couples: *Emmanuel Perez*¹; Travis Patterson¹; Yong-Ho Sohn¹;

¹University of Central Florida

Superalloy-dependent lifetime of a NiCoCrAlY coating was examined with several solid-to-solid diffusion couples consisting of NiAl vs. various commercial superalloys (i.e., CM247, GTD-111, IN-939, IN-718, and Waspalloy). The couples were assembled, encapsulated in Ar with quartz capsule, and annealed at 1050C for 96 hours. Concentration profiles measured by EPMA in single-phase NiAl region were employed to determine interdiffusion fluxes and effective interdiffusion coefficients of individual components in single-phase NiAl region. The interdiffusion fluxes and effective interdiffusion coefficients determined experimentally in single-phase NiAl region were employed to predict effective interdiffusion coefficients in multi-phase superalloy region. Microstructural and concentration stability of a NiCoCrAlY coating as a function of superalloys are presented based on effective interdiffusion coefficients predicted from diffusion couple studies. This work was financially supported by CAREER award from National Science Foundation (DMR-0238356).

10:55 AM

Copper Diffusion into Silicon Substrates through TaN and Ta/TaN Multilayers Barriers: Florent Bernard¹; *Nicole Fréty*¹; Joël Sarradin¹; Jean-Claude Tedenac¹; ¹Université de Montpellier II

The progress of the ultra large scale integration (ULSI) device technology is strongly dependent on the development of new wiring materials exhibiting a lower electrical resistivity and a higher resistance to electromigration compared with those of aluminium-based alloys. Copper has then become the most attractive material. However the copper diffusion into the silicon-based substrates during the device fabrication leads to a degradation of the reliability of the ULSI devices. Various barrier layers, such as tungsten and titanium nitride, have then been developed to prevent the copper diffusion, the thickness of which being of about 100 nm. This thickness needed to be reduced, novel barrier layers have to be developed. The aim of this project was to study the potentiality of thin TaN and Ta/TaN multilayer barriers in the diffusion mechanisms of copper into silicon substrates. The diffusion mechanisms were determined from microstructural characterizations (XRD, SEM, AFM) associated to SIMS analyses.

11:20 AM

Diffusion Path and Interdiffusion Structure in the Flip-Chip Eutectic Sn-Pb Solder Bump with Ni/Cu UBM during Reflow and after Aging: Guh-Yaw Jang¹; Li-Yin Hsiao¹; Su-Yueh Tsai²; *Jeng-Gong Duh*¹; Mysore A. Dayananda³; ¹National Tsing Hua University; ²Ming Hsin University of Science and Technology; ³Purdue University

In the current flip-chip technology, Ni-based under-bump metallurgy (UBM) is widely used, and the formation and growth of intermetallic compounds (IMC) between solders and UBM play a critical role in the solder joint reliability. In this study, solder joints of eutectic Pb-Sn/Ni-UBM were employed to investigate the IMC formation during reflows at 220°C and after aging at 150°C. The interfacial microstructures were revealed with FE-SEM through special etching technique. The quantitative analysis and elemental redistribution were obtained by EPMA, and FE-EPMA. Various types of IMC, such as (Cu,Ni)₆Sn₅, (Ni,Cu)₃Sn₄ and (Cu,Ni)₃Sn were observed. With the aid of X-ray color mapping technique, the measured compositions were mapped onto the ternary isotherm of Sn-Ni-Cu. Series of diffusion paths were then constructed, which should help to interpret the phase transformation among related IMCs.

11:45 AM

Interdiffusion Coefficients Extraction from Multicomponent Diffusion Couples: *Liang Jiang*¹; Jing Lu¹; Srikanth Akkaram¹; ¹GE Global Research

The behavior of multicomponent diffusion can be complex due to the inter-dependence of diffusion among multiple elements. Interdiffusion coefficients are critical to characterize diffusion in multicomponent systems. Multicomponent diffusion couples are typically used to extract the interdiffusion coefficient. In the present study, various procedures for de-

termining interdiffusion coefficients are reviewed and a numerical inverse method is proposed. The numerical inverse method is utilized to extract interdiffusion coefficients from experimental data of various binary and ternary diffusion couples.

Phase Stability, Phase Transformation and Reactive Phase Formation in Electronic Materials V: Electromigration in Leaded and Lead-Free Solder Joints

Sponsored by: The Minerals, Metals and Materials Society, TMS Electronic, Magnetic, and Photonic Materials Division, TMS Structural Materials Division, TMS: Alloy Phases Committee

Program Organizers: Katsuaki Suganuma, Osaka University; Douglas J. Swenson, Michigan Technological; Srinivas Chada, Jabil Circuit, Inc.; Sinn Wen Chen, National Tsing-Hua University; Robert Kao, National Central University; Hyuck Mo Lee, Korea Advanced Institute of Science and Technology; Suzanne E. Mohny, Pennsylvania State University

Wednesday AM

March 15, 2006

Room: 213B

Location: Henry B. Gonzalez Convention Ctr.

Session Chairs: Sinn Wen Chen, National Tsing-Hua University; Katsuaki Suganuma, Osaka University

8:30 AM Invited

Electromigration Study in Flip Chip Pure Sn Solder Joints: *Jae-Woong Nah*¹; Jong-Ook Suh¹; King-Ning Tu¹; Yong-Min Kwon²; Kyung-Wook Paik²; ¹University of California, Los Angeles; ²KAIST

Electromigration is serious reliability issue in flip chip technology because design rule in devices requires high current density through solder joints. Many papers have reported that the general failure mode induced by electromigration in flip chip solder joints is the loss of UBM and the interfacial void formation at the cathode contact interface between the interconnect line and the solder bump. However, the effect of electromigration on the change of stress distribution in flip chip solder joints has not been studied. In this study, we have prepared pure Sn flip chip samples and used synchrotron radiation white beam x-ray microdiffraction to measure the stress distribution in the pure Sn samples driven by electromigration. The stress analysis on the basis of the in-situ change of lattice parameters was obtained from the diffracted Laue patterns during electromigration. The electromigration induced failure mechanism in flip chip pure Sn solder joints will be presented.

9:00 AM

Current Direction Effects upon Interfacial Reactions in the Sn-In/Cu and Sn-In/Ni Joints: Sinn-Wen Chen¹; *Shih-Kang Lin*¹; ¹National Tsing Hua University

Sn-In alloys are promising low melting point Pb-free solders. Cu and Ni are commonly used substrate materials. At the Sn-In/Cu and Sn-In/Ni joints in electronic products, both electromigration and Joule heating contribute significantly to the interfacial reactions. Sn-20at.%In/Cu and Sn-20at.%In/Ni couples are prepared, and they are reacted at 160 and 140°C with and without the passage of DC currents. It is found that the current directions have a strong effect upon the interfacial reactions. When the electrons are from the solder to the substrate, the reaction products are η-Cu₆Sn₅ and Ni₃Sn₄ in the two different couples, respectively. The IMCs' formation and their morphologies are similar to those without passing through of electric currents. However, when the electrons are from the substrate into the solder side, very significant interfacial reactions are observed. It is likely that the liquid phase is formed from interfacial reactions and the substrate is consumed seriously.

9:25 AM

Effect of Aging on Electromigration of Flip-Chip Solder Joints: *Che Cheng Chang*¹; Chih Chen¹; ¹National Chiao Tung University

Electromigration has become an important reliability issue in flip chip technology. In this study, effect of aging on electromigration of flip-chip solder joints was investigated. Eutectic Sn63Pb37 solder bumps were aged

at 150°C for different aging times, and then electromigration test were performed. Both solder bumps with thin-film and thick-film under Bump Metallurgy (UBM) were examined. It is found that electromigration life time decreased when the aging time increased for solder bumps with thin-film UBM, whereas the life time increased as the aging time increased for the solder bumps with thick-film UBM. It is speculated that the intermetallic compound layer played critical role during the electromigration test. The reasons that caused the different behaviors will be presented in the conference.

9:50 AM

Electromigration Effects on Intermetallic Growth Trends: *Helen T. Orchard*¹; A. Lindsay Greer¹; ¹University of Cambridge

Microelectronic device structures continue to be miniaturised, allowing improvements in performance, but also introducing new reliability issues. Of interest are bimetallic interfaces across devices, such as wire bonds and solder joints. Intermetallic compounds form at these interfaces, and excessive growth can cause device failure. Theoretical work shows that when a direct current is passed through a bimetallic couple, an electromigration effect can occur, resulting in a change in the rate of intermetallic thickening [Orchard and Greer, Appl. Phys. Lett. 86 (2005) 231906, 1-3]. When the electromigration flux augments the diffusion flux the intermetallic thickening is accelerated. If the electromigration flux opposes the diffusion flux the intermetallic thickening is slowed and the intermetallic reaches a limiting thickness. In this paper we compare the predicted growth regimes to experimental observations of intermetallic thickening with a direct current. The model is extended to include multiphase intermetallic compounds and alternating current conditions.

10:15 AM

Electromigration Effects upon Microstructural Evolution and Interfacial Reaction of Eutectic SnBi Solder on Au/Ni Metallization: *Chih-Ming Chen*¹; Long-Tai Chen¹; ¹National Chung Hsing University

Eutectic SnBi alloy is one of the most potential candidates for low-temperature lead-free solders. Electromigration is one of the most important reliability concerns in solder systems. This study investigated electromigration effects on microstructural evolution of eutectic SnBi solder and interfacial reaction between eutectic SnBi solder and Au/Ni metallization. Eutectic SnBi solder ball was placed in between two Au/Ni metallization pads, and by conducting a reflow a sandwich-type reaction couple was fabricated. Experiments were conducted by passing through a constant current in the reaction couples. Current density was $5 \times 10^3 \text{ A/cm}^2$ and temperature was 70°C. Accumulation of Bi at the anode side was observed, and by measuring the accumulation rate of Bi the apparent effective charge was estimated. Different intermetallic growth and interfacial morphology were also observed at the anode and cathode sides. Current distributions inside the solder and at the joint interface were simulated and correlated with the experimental observations.

10:40 AM Break

10:50 AM

In-Situ Electromigration Studies on Sn-Ag-Cu Solder Joint by Digital Image Speckle Analysis: *John H. L. Pang*¹; Luhua Xu¹; ¹Nanyang Technological University

The phenomenon of electromigration in Pb-free Sn-Ag-Cu solder joint specimen subject to high current density was characterized by in-situ test. Digital Image Speckle Analysis (DISA) was used to measure the in-situ micro-deformation of a cross sectioned solder joints, which is subject to electromigration with a current density of 5000 A/cm^2 under a constant temperature of 125°C. The tests were conducted on specimen with different geometry, lapshear specimen and wired specimen. It was recognized in this study that EM can cause strain gradient effects from cathode to anode. High strain concentration was found near pre-existed void. Void growth is anticipated at current crowding regions and this can be measured by in-situ digital image measurements and correlation analysis.

11:15 AM

In-Situ Observation of Pb and Sn Migration during Electromigration-Induced Drift of Eutectic SnPb Lines: *Young-Bae Park*¹; Min-Seung Yoon²; Oh-Han Kim¹; Min-Ku Ko²; Yong-Duk Lee¹; Ja-Young Jung¹;

Young-Chang Joo²; ¹Andong National University; ²Seoul National University

Flip chip packages with smaller size are likely to have higher current densities through their solder bumps, which has given rise to electrical failure due to solder electromigration. Since the eutectic SnPb solder bump consists of two major elements, it is necessary to take both the migration of Sn and that of Pb into consideration. In this study, we have investigated the distinct migration behavior of both Sn and Pb in the eutectic SnPb solder lines as a function of temperature and current density by using in-situ SEM. It was of interest that an incubation stage for the edge drift was observed during electromigration of the eutectic SnPb solder lines. It was clearly confirmed by in-situ observation that Pb migrated dominantly at 110°C while Sn migrated dominantly at 50°C. The existence of incubation stage for edge drift and the temperature dependence of migration elements will be discussed in detail.

11:40 AM

Redistribution of Pb-Rich Phase during Electromigration in Eutectic SnPb Solder Stripes: *Cheng-Chang Wei*¹; Chung-Kwang Chou¹; Chih Chen¹; ¹National Chiao Tung University

By using Blech structure, we studied the EM behaviors on SnPb solder stripes. The thickness of the solder stripes varied from 3 to 8µm and the width of the stripes was 100µm. In order to investigate the microstructure evolution in the eutectic SnPb solder, we applied high current density to stripes. It is found that Pb-rich phase ripened and aligned along the direction of electron flow after the current stressing of $9.7 \times 10^3 \text{ A/cm}^2$ at 80°C for 24 hours. It is very interesting that this phenomena became more significant with the stressing time or current density increased. Simulation results shows that the resistance of the solder stripes may be reduced when the Pb-rich phase aligns along the direction of the electron flow. This reduction of the total resistance provides the driving force for the Pb-rich phase to align along the direction of the electron flow.

12:05 PM

Thermomigration in Composite High Pb - Eutectic SnPb Flip Chip Solder Joints: *Annie T. Huang*¹; King-Ning Tu¹; ¹University of California

High current density in the Al interconnect can cause a large joule heating in flip chip solder joints. Because Silicon is a much better thermal conductor than a polymer substrate, temperature across a silicon chip differs only by a few degrees whereas a large temperature change occurs across a polymer substrate side from the bump with current stressing to no-current bumps. Temperature gradient thus exists across the bumps located on the same chip regardless if the bumps have current or not. Composite solder consists of 97Pb3Sn and eutectic SnPb. Because of the difference in the diffusion rate between Sn and Pb, its unique structure can be utilized to study thermomigration based on the redistribution of Sn and Pb. In this talk, we report the thermomigration and failure mode of composite solder bumps without current stressing by a thermal gradient induced by joule heating from the neighboring bumps with current stressing.

Phase Transformations in Magnetic Materials: Magnetic Shape Memory Alloys and Information Storage

Sponsored by: The Minerals, Metals and Materials Society, TMS Materials Processing and Manufacturing Division, TMS/ASM: Phase Transformations Committee

Program Organizers: Raju V. Ramanujan, Nanyang Technological University; William T. Reynolds, Virginia Tech; Matthew A. Willard, Naval Research Laboratory; David E. Laughlin, Carnegie Mellon University

Wednesday AM Room: 213A
March 15, 2006 Location: Henry B. Gonzalez Convention Ctr.

Session Chairs: Marc J. DeGraef, Carnegie Mellon University; Lynn Kurihara, Naval Research Laboratory

8:30 AM Invited

Formation and Evolution of Domain Structures in Ferromagnetic Shape Memory Alloys: Jingxian Zhang¹; Long Qing Chen¹; ¹Pennsylvania State University

Ferromagnetic shape memory alloys undergo both ferromagnetic and ferroelastic (martensitic) phase transformations. This presentation will discuss a computational model for predicting formation and evolution of both the ferroelastic and ferromagnetic domain structures in ferromagnetic shape memory alloys. It combines the phase-field approach with micromagnetics and microelasticity theory. As an example, the Ni₂MnGa ferromagnetic shape memory alloy is considered. The emphasis is on the overall strain response and associated evolution of magnetic domain structure and martensite microstructure under an applied stress or a magnetic field with different initial conditions. The interactions between martensite twins and magnetic domain walls will be discussed. The energetic contributions that are responsible for the experimentally observed reorientation of magnetic domain walls during martensite plate growth will be analyzed. Finally, the effects of defects on the formation of tweed structures as well as on the twin boundary mobility under a stress or magnetic field are investigated.

9:05 AM Invited

Interfacial Phase Formation during Growth of Ferromagnetic CdCr₂Se₄ on AlGaAs/GaAs: Ramasis Goswami¹; George Kioseoglou²; Aubrey T. Hanbicki²; Berend T. Jonker²; George Spanos²; ¹Geo-Centers Inc.; ²Naval Research Laboratory

Ferromagnetic semiconductors (FMS) provide an opportunity to control spin dependent behavior and study spin injection and transport in semiconductor heterostructures. A key element of semiconductor-spintronics technology is the quality of heterointerfaces that affect the injection of polarized carriers. This presentation is centered about the overall microstructural evolution, interfacial phase formation, and magnetic properties of ferromagnetic off-stoichiometric CdCr₂Se₄ thin films deposited on AlGaAs/GaAs LED structures. High Resolution Transmission Electron Microscopy (HRTEM), Z-contrast imaging, Electron Energy Loss Spectroscopy (EELS), and Energy Dispersive Spectroscopy (EDS) were used to characterize the films. Z-contrast imaging revealed that Cr-rich nano-islands ~2 nm thick formed epitaxially at the AlGaAs side of the CdCr₂Se₄/AlGaAs interface. Z-contrast imaging and HRTEM studies suggest that the possible interfacial phase is CrAs, which is a half-metallic ferromagnet. Detailed microstructural analysis of the interface and comparison with near stoichiometric CdCr₂Se₄ on AlGaAs/GaAs (LED), and on ZnSe/AlGaAs/GaAs (LED), will be presented.

9:40 AM

Phase Transformation in Nonstoichiometric Ni₄₉Mn₂₃Ga₂₈: Peng Zhao¹; Liyang Dai¹; James Cullen¹; Manfred Wuttig¹; ¹University of Maryland, College Park

The martensitic phase transformation in a nonstoichiometric alloy, Ni₄₉Mn₂₃Ga₂₈, with M_s=273 K and T_c=383 K has been studied. The martensitic phase is a tetragonal with a c/a ratio of 1.33 and lattice distortion of about 6.1%, determined by high resolution neutron diffraction. Hence,

it shows potential capability to exhibit ferromagnetic shape memory effect (FSME) because the FSME depends largely on the tetragonality. The temperature dependence of magnetization shows a temperature hysteresis of about 10 K, demonstrating that the martensitic phase transformation is reversible. The low field thermal magnetization curve shows that the alloy also undergoes a pre-martensitic transformation at around 333 K, corresponding to the anomalies displayed by the temperature dependence of elastic constants C₄₄ and C'. This intermediate, pre-martensitic state is believed to have a micro-modulated structure that develops prior to the transformation of the parent cubic phase to the tetragonal phase.

10:15 AM Invited

Magnetic Nanostructures for Spintronics Applications: Adekunle Olusola Adeyeye¹; Navab Singh²; Sarjoosing Goolaup¹; Chenchen Wang¹; Debashish Tripathy¹; Jun Wang¹; ¹National University of Singapore; ²Institute of Microelectronics

There has been considerable interest in magnetic nanostructures in the last decade due to advances in nanofabrication and nanocharacterization techniques. From an application point of view, nanomagnets are the building blocks of magnetic random access memory cell and also patterned magnetic media. In this talk, we will present a large area nanofabrication technique for synthesizing ferromagnetic nanostructures using deep ultraviolet lithography at 248 nm exposing wavelength. One unique advantage of this technique is that unlike e-beam lithography, thicker resists can be used to make high aspect ratio nanostructures. Ferromagnetic nanostructures of different shapes and sizes were fabricated. The magnetic properties were characterized using vibrating sample magnetometer, magnetic force microscopy and magnetotransport measurements. We observed that the magnetic properties of the nanostructures are strongly dependent on the size and shape of the nanostructures. We have also used micromagnetic modeling to aid our understanding of the magnetization reversal process in the nanomagnets.

10:50 AM Break

11:00 AM

Micromagnetism in the Ultrathin Limit: Danilo Pescia¹; Oliver Portmann¹; Andreas Vaterlaus¹; ¹ETH Zurich

We derive some results concerning the static and dynamic micromagnetic behaviour of magnetic elements in the ultrathin limit. In this limit, a most remarkable logarithmic correction of the magnetostatic energy appears. Experimentally observed phenomena such as the quenching of the precessional motion at boundaries and the multi-to-single domain transition in ultrathin elements with perpendicular magnetization are ascribed to this logarithmic singularity. Because of the competition between the very weak but long ranged dipolar interaction and the strong but short ranged exchange interaction, perpendicularly magnetized ultrathin films are unstable against stripe domain formation. This competition completely changes the pattern of the phase transition: the stripe system is forced out of the Landau-Ginzburg-Wilson universality class and becomes a Coulomb frustrated ferromagnet (CFF). Because of its complexity, the phase transition in a CFF is presently a subject of strong controversy. Here we discuss some theoretical and experimental aspects of a CFF.

11:25 AM Invited

Short Range Order, Long Range Order and Phase Miscibility of Nanostructured CoCrPt and FePt Media Films: Gan Moog Chow¹; ¹National University of Singapore

The properties of nanostructured magnetic films are controlled by composition, dopants, structure, microstructure, texture and interfaces. Nanostructure alloying may not necessarily follow conventional phase diagrams that ignore the effects of surfaces and interfaces. The composition of a textured long range order, which may differ from the global average composition, needs to be controlled to provide optimum texture-dependent properties. In this talk, selected examples of some of our work on nanostructured CoCrPt and FePt films for high density magnetic recording are discussed. The effects of seedlayer and underlayer, long range order, short range order, compositions of textured Bragg peak and dopants were investigated using high resolution x-ray scattering, anomalous x-ray scattering, extended x-ray absorption fine structure, transmission electron microscopy and vibrating sample magnetometry. Correlations of magnetic properties with structures, phase miscibility and dopants are addressed.

Point Defects in Materials: Thermodynamics

Sponsored by: The Minerals, Metals and Materials Society, TMS Electronic, Magnetic, and Photonic Materials Division, TMS Structural Materials Division, TMS: Chemistry and Physics of Materials Committee

Program Organizers: Dallas R. Trinkle, U.S. Air Force; Yuri Mishin, George Mason University; David N. Seidman, Northwestern University; David J. Srolovitz, Princeton University

Wednesday AM Room: 210B
March 15, 2006 Location: Henry B. Gonzalez Convention Ctr.

Session Chair: David J. Srolovitz, Princeton University

8:30 AM Invited

Short-Range Ordering, Clustering, and Early-Stage Precipitation in a Model Ni-Al-Cr Superalloy: *Chantal K. Sudbrack*¹; *Zugang Mao*¹; *Ronald D. Noebe*²; *David N. Seidman*¹; ¹Northwestern University; ²NASA

Short-range ordering (SRO) and clustering in substitutional alloys occurs by solute diffusion, which is mediated by a vacancy mechanism. These processes have been primarily characterized in binary alloys with small-angle scattering in reciprocal-space, as meaningful quantification is difficult for multicomponent alloys (technologically important systems). A radial distribution function analysis of direct-space atom-probe tomography images allows these processes to be studied in detail in a Ni-Al-Cr superalloy, where L1₂-ordered Ni₃(Al_xCr_{1-x}) precipitates form via a first-order transformation. The fast diffusion of Al leads to the observation of L1₂-Ni₃Al SRO domains (<R> = 0.6 nm), after the initial quench to room temperature from the single phase regime. Congruent SRO precedes phase separation, where phase separation is established by compositional fluctuations that are small in spatial extent (<R> = 0.75 nm) and large in amplitude. The observed pathways are considered in light of classical nucleation theory and compared to lattice kinetic Monte Carlo simulations.

9:00 AM

Effect of a Ternary Addition on Ordering Kinetics in L1₂-Ordered Quasi-Binaries: *Ewa Partyka*¹; *Rafal Kozubski*¹; ¹Institute of Physics Jagiellonian University

Studies of the influence of admixing a ternary element on long-range ordering kinetics in quasi-binary systems with L1₂ superstructure were carried out. The intermetallic Ni₃Al_{1-x}Fe_x system showing a decrease of the ordered phase stability upon alloying with Fe was examined by means of quasi-residual resistometry and positron lifetime spectroscopy. It has been found out that the previously reported decrease of the activation energy for ordering kinetics with increasing Fe concentration is due to a decrease of the vacancy formation energy. It suggests an increase of the "vacancy availability" in the neighbourhood of Fe atoms with an increase of the Fe content and easier diffusion of Fe atoms than Al atoms within Ni-sublattice. Applied Monte Carlo simulations revealed the atomistic mechanism of the ordering process in L1₂-ordered quasi-binaries which is controlled mainly by the migration of a ternary component within the majority sublattice.

9:20 AM Invited

Thermodynamics of Impurities in Vanadium: *Oliver Delaire*¹; *Tabitha Swan-Wood*¹; *Max Guy Kresch*¹; *Brent T. Fultz*¹; ¹California Institute of Technology

We investigated the effects of dilute alloying on the lattice dynamics and electronic structure of bcc vanadium. Using inelastic neutron scattering, we have measured the phonon density of states and vibrational entropy of random solid solutions of vanadium with transition metal impurities. Group IVa elements caused a softening of the V phonons, while elements to the right of V induced a gradually increasing stiffening. The stiffening observed for 6% Pt impurities is very large and induces a decrease of vibrational entropy that is larger than the gain in configurational entropy, resulting in a negative entropy of mixing. Using density functional theory, we calculated the electronic structure for all alloys and found that the electronic entropy of alloying follows the same trend as the vibra-

tional part, although it is smaller in magnitude. We discuss the consequences of these findings on the thermodynamics of impurities in vanadium.

9:50 AM

Inelastic Neutron Scattering Studies on the Formation Entropy of Vacancies in FeAl: *Tabitha L. Swan-Wood*¹; *Olivier Delaire*¹; *Max Kresch*¹; *Brent Fultz*¹; ¹California Institute of Technology

Inelastic neutron scattering spectra of B2 FeAl with quenched vacancies were measured giving the vibrational entropy of vacancy formation. Born von Karman calculations indicate that point defects change the phonon dispersions. The vibrational entropy of vacancy formation is measured to have an upper bound of -0.75 kB/vacancy. Inelastic neutron scattering spectra also measured anharmonic vibrational entropy of B2 FeAl between temperatures 10K to 1323K. We postulate that this anharmonicity is caused by vacancies and Fe anti-site defects in the alloy.

10:10 AM Break

10:25 AM Invited

The Kinetics of Crystallization: Role of Point Defects: *Yinon Ashkenazy*¹; *Robert S. Averbach*²; ¹Hebrew University of Jerusalem; ²University of Illinois at Urbana Champaign

The common model for crystallization speeds in metals assumes that the velocity of the crystal-liquid interface in metals at deep under-coolings is limited by the rate at which liquid atoms collide with the crystalline interface. We show here by MD simulations that in contrast to current models, crystallization of under-cooled liquids and metallic glasses is controlled by diffusion, in accordance with recent experiments. The big surprise, however, is that the relevant diffusion coefficient appears to be that of self-interstitial atoms in the crystalline state. For the three metals, Fe, Ni and Cu, we find the activation energies of crystallization, from both the liquid and glass states, are precisely those found for the migration energy of self-interstitial atoms. These measurements give new credence to the model attributed to Frenkel that liquids are crystals with high concentrations of point defects, and more specifically to Granato's interstitial theory of liquids.

10:55 AM

Impact of Vacancy Diffusion on the Early Decomposition Stages of Alloys and the Role of Heterophase Interfaces on Coarsening: *Zugang Mao*¹; *Chantal K. Sudbrack*¹; *Kevin E. Yoon*¹; *Georges P. Martin*¹; *David N. Seidman*¹; ¹Northwestern University

The kinetic pathway for nucleation and growth is commonly thought to be dictated by the initial supersaturation of solutes in the solid solution undergoing phase separation. We demonstrate that the details of the diffusion mechanism, in the solid solution affect deeply the early stage morphologies of precipitates. Our argument is based on a combined use of atomic-scale observations, with atom-probe tomography (APT) and lattice kinetic Monte Carlo simulation of a Ni(Al,Cr) alloy. By an optimized choice of thermodynamic and kinetic parameters we first reproduce the experimental APT observations. We then modify only the long-range vacancy-solute binding energy, without altering the thermodynamic driving force for phase separation, thereby demonstrating that the microstructural evolution changes from a coagulation to an evaporation-condensation coalescence mechanism. The changes can only be accounted for with non-zero values for the vacancy chemical potential and off-diagonal terms of the Onsager matrix, at variance with classical models.

11:15 AM

Effect of the Antisite Defects on the Temperature Dependence of the Lattice Misfit in γ/γ' Alloys: *Oleg Y. Kontsevoi*¹; *Yuri N. Gornostyrev*¹; *Arthur J. Freeman*¹; ¹Northwestern University

The magnitude of the lattice misfit δ between the γ matrix and γ' precipitate phases is one of the key parameters determining the mechanical behavior and microstructure morphology of two-phase high temperature superalloys. The two main contributions to the temperature dependence $\delta(T)$ are under intense investigation: (i) the difference in thermal expansion of the two phases, and (ii) the redistribution of alloying components between γ and γ' which creates the substitutional and antisite defects. We explore the role of both contributions for the Ni-Al and Ir-Nb two-phase

alloys based on first principles calculations of the phonon spectra and antisite defects. We demonstrate that the $\delta(T)$ behavior depends on the shape of the $\gamma - \gamma'$ gap on the phase diagram. The redistribution of the alloy components gives the main contribution to $\delta(T)$ for Ni/Ni₃Al, in contrast with Ir/Ir₃Nb where the thermal expansion dominates. Supported by the AFOSR (grant FA9550-04-1-0013).

11:35 AM

Formation of Topologically Close Packed Impurity Locked Phases in Mo and Cr Base Alloys: Nadezhda I. Medvedeva¹; Oleg Y. Kontsevoi²; Yuri N. Gornostyrev²; Arthur J. Freeman²; ¹Institute of Solid State Chemistry; ²Northwestern University

The application of bcc refractory metals is limited by their room temperature brittleness, which is caused by interstitial impurities (C, N, O) that form brittle carbides, nitrides and oxides. Alloying with rhenium dramatically increases ductility, and the proposed mechanism of this effect connects the increase of the solubility of impurities with the appearance of topologically close packed (TCP) particles. By means of first-principles calculations, we investigated the cumulative effect of both Re alloying and light interstitial impurities on the structural stability of the A15 phase of Mo and Cr, assumed as the the prototype TCP phase. We demonstrate that the metastable A15 M₃Re (M=Mo,Cr) is stabilized by the interstitial impurities. The precipitates of this impurity locked phase may serve as scavengers of interstitials, prevent the formation of brittle phases and grain boundary segregation, and thus improve the ductility of Mo and Cr alloys. Supported by the AFOSR (grant FA9550-04-1-0013).

11:55 AM

Effect of Vacancy on Al-Li Alloy in Earlier Aging Condition: Gao Yingjun¹; ¹Guangxi University

Al-Li alloys are very attractive in the aerospace industry. Binary Al-Li alloys are strengthened by the solute segregation zone and Al₃Li particles. Solute segregation zone models are used to calculate the atomic bonding of the solute segregation zone with a vacancy defect of Al-Li alloy in earlier aging condition. Three kinds of atomic bond order are given by bonds of Al-Al, Al-Li and Al-Li-vacancy in the solute segregation zone according to the empirical electron theory (EET) in solid. The strongest covalent bond in the segregation zone with vacancy defect, formed in quenching state of alloy, are the main strengthening reason for alloy in earlier aging condition. These results explain the experimental findings.

Recycling - General Sessions: Aluminum Recycling

Sponsored by: The Minerals, Metals and Materials Society, TMS Extraction and Processing Division, TMS Light Metals Division, TMS: Recycling Committee

Program Organizers: Gregory K. Krumdick, Argonne National Laboratory; Cynthia K. Belt, Aleris International

Wednesday AM
March 15, 2006

Room: 8B
Location: Henry B. Gonzalez Convention Ctr.

Session Chair: Cynthia K. Belt, Aleris International

8:30 AM Introductory Comments

8:35 AM

Emerging Trends in Aluminum Recycling: Reasons and Responses: Subodh K. Das¹; ¹Secat Inc

The growth in aluminum usage in transportation applications, the decline in aluminum beverage can recycling, and the increasing reliance of the domestic fabrication industry on secondary aluminum have combined to create new needs in both the materials design and processing space. This presentation will detail the history and future projections for aluminum recycling, emphasizing the increasing importance of mixed scrap streams in the makeup of secondary aluminum. To most economically utilize these scrap streams, new approaches to developing acceptable materials processed to control properties suitable for an expanded range of applications are needed. How the aluminum enterprise, including indus-

try, academia, and government can work together to meet these important but aggressive targets and transform recycling from strictly an environmental imperative to an economic development opportunity will be discussed.

9:00 AM

Raw Material Usage Strategies under Conditions of Uncertain Alloy Demand: Gabrielle Gaustad¹; Preston Li¹; Randolph Kirchain¹; ¹Massachusetts Institute of Technology

Operational uncertainties are the source of much inefficiency in metal alloy production. Past work has shown that recourse model based optimization can identify raw materials acquisition strategies that mute the effects of at least one form of uncertainty - variation in product demand. These models suggest that additional scrap purchase and usage, referred to as purchase hedging, provides financial advantage for remelters across a range of operating conditions. This paper investigates the correlation of production and raw materials characteristics to preferred hedging strategy. In this study, cases are presented involving available scrap materials used in production of both cast and wrought products. Early results indicate that hedging strategy is correlated to the diversity of the production portfolio and the versatility of scrap types.

9:25 AM

Material Selection and the Impact on Recyclability, Green Purchasing and Corporate Social Responsibility – The Manganese Metal Case: John E. Heinzel¹; Karen Hagelstein²; ¹Environmental Health Research Foundation; ²Times Limited

Manganese metal is widely used as an alloying agent in the aluminum industry and is available from two distinct production processes. The environmentally preferred process uses sulfur as the catalyst and results in a typical purity of 99.9%. The other process, favored by many Chinese manufacturers, uses selenium as the catalyst with the result that the manganese metal contains up to 0.15% selenium but is produced at a lower cost. This has resulted in 75% of the global market in recent years consisting of selenium-contaminated manganese. A recent case study demonstrates that use of this material has an impact on the recyclability of the aluminum dross and scrap, where recyclers face metal dust exposure issues and may not even be aware of the selenium content that likely triggers hazardous solid waste disposal requirements. This illustrates downstream recycling is an important consideration of green purchasing and corporate social responsibility.

9:50 AM Break

10:05 AM

Recycling Wastes in the Alumina Industry: N. Ilyoukha¹; V. Timofeeva²; ¹Aleris International; ²Academic Ceramic Center

Main wastes of the alumina and aluminum industries are not used at present and are being stored after partial treatment in special places. The paper will discuss the technology of treatment wastes as an additive for the cement industry. The solution of this complex problem will be of great importance for the purification of aerial, earth and waste region in whole. Besides this, as a result of waste treatment there will be special cements: high strength, extensible, gas-water proof, self-stressing needed in the road and runway construction, in building tunnels and pits, and in nuclear wastes burial.

10:30 AM

State of the Art in Recovery of Aluminum from Aluminum Dross: Lifeng Zhang¹; ¹University of Illinois

The paper reviews the current research and development of Aluminum recovery from aluminum dross, including dross types and dross properties, and methods for metal Al recovery from dross, such as reducing metal loss during cooling, separation of metal from dross, and remelting of the metallic fraction. Techniques to separate Al metal from the dross, such as stirring hot dross, crushing and screening cold dross, bubble flotation, and leaching process, are discussed. Several remelting methods are summarized, such as reverberatory furnace, rotary furnaces, salt-free thermal plasma furnaces, and salt-free rotary Arc furnace with graphite electrodes. Fundamentals related to these dross recovery processes are reviewed too, such as thermodynamics and kinetics, lab experiments, and numerical simulation on the fluid flow, electromagnetic field and forces, chemical

reactions, combustion, multiphase flow, heat transfer, radiation, melting, and top surface phenomena. This review provides clear research directions for the Al recovery from Aluminum dross.

10:55 AM Concluding Comments

Simulation of Aluminum Shape Casting Processing: From Alloy Design to Mechanical Properties: Casting Defect Simulation and Validation

Sponsored by: The Minerals, Metals and Materials Society, TMS Light Metals Division, TMS Materials Processing and Manufacturing Division, TMS Structural Materials Division, TMS: Aluminum Committee, TMS/ASM: Mechanical Behavior of Materials Committee, TMS: Process Modeling Analysis and Control Committee, TMS: Solidification Committee, TMS/ASM: Computational Materials Science and Engineering Committee

Program Organizers: Qigui Wang, General Motors Corporation; Matthew Krane, Purdue University; Peter Lee, Imperial College London

Wednesday AM Room: 6D
 March 15, 2006 Location: Henry B. Gonzalez Convention Ctr.

Session Chairs: Mei Li, Ford Motor Company; David Robert Poirier, University of Arizona

**8:30 AM Invited
 Modeling of Entrainment Defects:** *John Campbell*¹; ¹General Motors Corporation

The enfolding action of the liquid surface involved in surface turbulence, and sometimes in laminar surface flow, usually enfolds air inside the surface oxide film, creating both bubbles, and unbonded double oxide interfaces in the liquid that act as cracks. To fully understand and predict casting defects, it is essential that such events are included in computer models since such defects are now known to be numerous in liquid Al alloys. For instance up to 85% or more of casting defects are entrainment defects, or defects that are initiated by and grown from entrainment defects. Over the past few years the modeling of such bubbles and bifilm creation events has begun to be tackled with some success. These successes are examined and future challenges for models will be assessed.

**8:55 AM Invited
 Modeling of Porosity Formation in Aluminum Alloys:** *Christoph Beckermann*¹; Kent D. Carlson¹; Zhiping Lin²; ¹University of Iowa; ²Caterpillar

A new approach based on microsegregation of gas dissolved in the melt is used to model pore formation during the solidification of aluminum alloy castings. The model predicts the amount and size of the porosity in the solidified casting. Computation of the gas species transport in the melt is coupled with the simulation of the feeding flow and calculation of the pressure and temperature fields. The rate of pore growth is calculated based on the local level of gas supersaturation in the melt. The effects of the dendritic and eutectic microstructure on pore formation are also taken into account. Parametric studies for one-dimensional solidification under an imposed temperature gradient and cooling rate illustrate that the model captures all important phenomena observed in porosity formation in aluminum foundry alloys. Comparisons between predicted porosity distributions and experimental measurements show good correspondence.

**9:20 AM Invited
 Modeling of Porosity Formation in Multicomponent Alloys in the Presence of Several Dissolved Gases and Volatile Solute Elements:** Gael Couturier¹; *Michel Rappaz*¹; ¹Ecole Polytechnique Fédérale de Lausanne

Although microporosity is a critical issue for the mechanical properties of cast parts, modeling of such defects is still not yet fully satisfactory. The present contribution addresses the problem of multicomponent alloys and multigas systems including volatile solute elements. The effects of all solute elements on the activity of gas elements (hydrogen in the case of

aluminum alloys) are first taken into account, together with the partial vapor pressure of volatile elements such as zinc. After writing an overall mass balance for each element contributing to porosity formation, a linearized system of equations can be solved to relate the increment of porosity to the local pressure. This general formalism has been implemented in a program that calculates the pressures drop in the mushy zone using Darcy's equation and an adaptive refined mesh. Examples related to aluminum alloys will be shown in order to emphasize the various contributions to porosity formation.

**9:45 AM Invited
 A Porosity Simulation for High Pressure Die Casting:** *Chung-Whee M. Kim*¹; Kimio Kubo¹; Ken Siersma¹; ¹EKK Inc.

High pressure die castings have a tendency to have small size porosity defects, which are caused by gas holes and shrinkage. The origin of the gas holes is considered to be mainly hydrogen or nitrogen. Hydrogen evolves from liquid during solidification and nitrogen is a part of the trapped air during filling. This air trapped porosity reduces the quality of the die castings and prevents the use of heat treatment. Shrinkage porosity in the die castings is caused by hot spots just like the other casting processes. A model of the initialization and growth of porosity in the high pressure die castings is proposed. First, trapped air porosity forms during filling. Some of these porosity become large size porosity during solidification. The calculated results of size and distribution of porosity in magnesium die casting plates are compared favorably with the experiments.

10:10 AM Break

**10:25 AM
 Computational Analysis of Oxide Inclusions in Aluminum Castings:** *Gerald P. Backer*¹; Chung Whee Kim²; Ken Siersma²; Qigui Wang¹; ¹General Motors; ²EKK, Inc

Computer simulations of mold filling and solidification behavior have been used by foundries for years to optimize casting design. However, one aspect of the casting process that has not yet been carefully considered by simulation is the formation of oxides during filling. It is well known that oxides are very detrimental to the microstructure and mechanical properties, as they are often sites for nucleation of shrinkage porosity. In this paper, oxide formation during mold filling is studied computationally and experimentally with 319 and A356 aluminum alloys in both gravity pour and low pressure fill conditions. The simulation results and computational techniques will be discussed.

**10:50 AM Invited
 Study on Improvement of Casting Design System Based on John Campbell's Casting Design Rules:** Henry Hu¹; Zhaoxia Li¹; Jean Kor¹; *Qigui Wang*²; Wenyang Yang²; ¹University of Windsor; ²GM - Powertrain Engineering HQ

Casting design has a direct influence on the quality and cost of cast components. A full casting design includes design of components, a gating system and casting process parameters. At all times, many efforts have been done to improve quality of castings and at the same time to reduce cost and lead time. However, there are still many problems exist for the casting design process. In this paper, the improvement of casting design system, especially the design of gating system based on John Campbell's casting design rules has been studied. Under the guide of John Campbell's casting design rules, a preferable gating system has been designed. The filling process and the quality of the casting have been simulated using the software Magmasoft[®]. The result shows, with the improved gating system, the filling process and the quality of castings have been greatly improved.

**11:15 AM
 Microporosity Modeling in Aluminum Castings:** *Gerald Backer*¹; Qigui Wang¹; ¹General Motors Corporation

A new computational method for predicting microporosity in aluminum alloys is described. The method was calibrated against literature data for binary Al-7%Si alloys, and subsequently applied to a chill plate test casting in A356 alloy. The new method allows spherical micropores to nucleate and grow by hydrogen diffusion from a material volume surrounding the pores. This differs from a state of the art interdendritic-flow computational model for calculating porosity that assumes spherical pores

WEDNESDAY AM

have a diameter given by the secondary dendrite arm spacing. The pore growth method predicts larger pore diameters and a volume fraction of microporosity that is in better agreement with experimental observations than the interdendritic-flow model.

11:40 AM

Study of Micro Defects in Aluminum Casting Using X-Ray Computed Tomography: *Kaname Sasaki*¹; *Harsha Badarinarayan*¹; *Hitachi America, Ltd.*

Using X-ray Computed Tomography (CT), an aluminum casting specimen was scanned to quantify the amount of the micro defects present. Due to the enormous file size of the X-ray CT raw data, the specimen was limited to 10 x 10 x 180mm in dimension. The pixel resolution was 30micron, and the actual observable defect size was approximately 70 micron. This was done in order to eliminate noise and artifacts that were present in the raw scanned data. The specimen was divided equally into 15 vertical sections. The count and volume of the defects in each section increased from the base to the top section. This was because the casting was in contact with a copper chill at the base and opened to the atmosphere at the top. The defects were more prominent in the top region where a number of small voids (with an approximate diameter 80 micron) were detected.

Solidification Modelling and Microstructure Formation: A Symposium in Honor of Prof. John Hunt: Solidification Defects

Sponsored by: The Minerals, Metals and Materials Society, TMS Materials Processing and Manufacturing Division, TMS: Solidification Committee

Program Organizers: D. Graham McCartney, University of Nottingham; Peter D. Lee, Imperial College; Qingyou Han, Oak Ridge National Laboratory

Wednesday AM
March 15, 2006

Room: 6C
Location: Henry B. Gonzalez Convention Ctr.

Session Chairs: A. Dahle, University of Queensland; M. Rappaz, Ecole Polytechnique Fédérale de Lausanne

8:30 AM Invited

Microporosity in Cast Alloys: Contributions to the Understanding of Its Formation and Consequences: *Gérard Robert Lesoult*¹; *Ecole des Mines de Nancy*

A few examples of microporosity patterns are selected first on the basis of the significance of their effects on the solidification or post-solidification behaviour and properties of cast products. This first part is completed by a list of the main casting conditions that affect microporosity. The second part summarises the various research programmes that were carried out in Paris and Nancy to study the formation of microporosity in different types of cast alloys: nickel-based alloys in investment casting, spheroidal graphite cast iron, and aluminium-based alloys. The third part of this paper presents the most useful and comprehensive physical ideas that allow understanding of the formation of microporosity for various cast alloys and various casting processes. Emphasis is put on alloy chemistry, hydrostatic pressure in the liquid, microstructure and mechanical state of the solid in the mushy zone. Similarities and differences between microporosity and hot tearing are tentatively drawn.

8:55 AM Invited

Phase-Field Simulation of Microporosity Formation in Solidification: *Christoph Beckermann*¹; *Ying Sun*¹; *University of Iowa*

Direct numerical simulations on a microscopic scale are presented of porosity formation due to gas evolution during alloy solidification. The gas bubbles nucleate and grow in the supersaturated liquid ahead of the solidification front. Flows are induced by the interaction of the bubbles with the solid and the large density contrast between the bubbles and the melt. A phase-field method is used to model the interface and triple-junction motions in the present three-phase system. The flows and species transport in the gas and liquid phases are solved using a diffuse interface model for two-phase flows with surface tension and phase change. The

pore growth, solid-pore interactions, and final shape of the pores are investigated as a function of the initial gas concentration, the nucleation supersaturation, and important solidification parameters. The interactions of the pores with cellular and dendritic microstructures are examined in detail and compared to experimental observations.

9:20 AM

Permeability Gradient Model for Predicting Shrinkage Porosity Formation: *Danylo Oryshchyn*¹; *Omer Dogan*¹; *U.S. Department of Energy/Albany Research Center*

This model examines porosity formation in castings as a function of the ability of liquid to fill voids in the densest region of the mushy zone. These voids occur as the final interdendritic liquid freezes, shrinking. A minimum liquid flow rate is required to fill voids before final solidification. This minimum flow is accompanied by a pressure drop across the mushy zone. Driving pressure must match or exceed this drop. The permeability gradient model tests the impact of interdendritic channel constriction on liquid flow in a casting. The model examines two regimes: (i) Dendritic solidification: permeability dominated by liquid volume fraction and dendrite arm spacing, and (ii) Eutectic solidification: flow dominated by eutectic viscosity. The cooling eutectic mixture is assumed to behave like a slurry with increasing solid fraction. It is envisioned that this model can be developed into a tool that can be very useful for metal casters.

9:45 AM

Migration of Bubbles in the Mushy Zone: *Qingyou Han*¹; *Oak Ridge National Laboratory*

Bubbles usually form during solidification of alloys having a large solubility of gas in the liquid but a negligible solubility of gas in the solid. These bubbles become pores in a solidified casting. Lee and Hunt observed the formation of worm-like bubbles during solidification of aluminum alloys using X-ray. We observed, in transparent organic materials, that this worm-like morphology occurred at certain conditions. More often, bubbles migrate or jump from locations to locations in the mushy zone. It is the migration of bubbles that determine the final distribution and size of the pore in an solidifying casting.

10:10 AM Break

10:25 AM Invited

Dendrite Growth and Stability: Implications for Defect Control in Single Crystal Superalloy Castings: *Peter D. Lee*¹; *Barbara A. Shollock*¹; *Malcolm McLean*¹; *Imperial College London*

The potential of single crystal superalloy castings can only be achieved through routine control of the crystal orientation and avoidance of defects such as stray grains. Relaxation of the quality specifications has design implications, while stringent quality control can reduce yield with obvious economic consequences. Solidification of SX components invariably occurs dendritically; understanding the characteristics of dendrite growth in these complex materials is required for effective quality control. A range of defects observed in SX castings are considered, including: (i)Sensitivity of range of orientations produced to alloy chemistry and solidification rate, (ii)Effect of changes in mould cross-section on dendrite growth and (iii)Origins of stray grains during seeding of specific crystal orientations. The research has involved experimental studies by both controlled/quenched directional solidification and observation of industrial castings in conjunction detailed microstructural characterization. These have been complemented by novel multiscale modeling of solidification processing.

10:50 AM Invited

Solidification in Spray Forming: *Patrick Grant*¹; *University of Oxford*

Initially regarded as a rapid solidification process for the manufacture of small near-net shapes, spray forming has found commercial success in the production of specialized billet materials on a semi-continuous basis. In this arrangement, the spray forming solidification conditions comprise two distinct regimes: in-flight rapid solidification of a substantial fraction of the alloy droplets; and much slower solidification of the residual liquid in the billet once droplets/particles are reconstituted at deposition. This paper will focus on the events immediately prior, during and after deposition and show how the resulting solidification conditions lead to the characteristic spray formed microstructure comprising equiaxed grains with

low levels of microsegregation, as well as the possibility for the onset of macrosegregation and porosity. The use of non-intrusive process diagnostics and process modelling to reveal critical process physics will be described, and specific examples will include spray formed Si-Al alloys and ultra lightweight aerospace alloys.

11:15 AM Invited

Quest for a New Hot Tearing Criterion: *Laurens Katgerman*¹; Dmitry G. Eskin²; ¹Delft University of Technology; ²Netherlands Institute for Metals Research

Hot tearing remains a major problem of casting technology despite decades-long efforts to develop working hot tearing criteria and to implement those into casting process computer simulation. Existing models allow one to calculate the stress-strain situation in a casting (ingot, billet) and to compare it with the chosen hot tearing criterion. In most successful cases, the simulation shows the relative probability of hot tearing and the sensitivity of this probability to such process parameters as casting speed, casting dimensions, and casting recipe. None of the existing criteria, however, cannot give the quantitative answer on whether the hot crack will appear or not and on the extent of hot cracking (position, length, shape). This paper outlines the requirements for a modern hot tearing criterion as well as the future development of hot tearing research in terms of mechanisms of hot crack nucleation and propagation.

11:40 AM

A Tensor Phase Field Approach to Crystallization with Moving Solids: *Adam C. Powell*¹; Jorge Vieyra¹; ¹Massachusetts Institute of Technology

The Phase Field method can model crystal solidification in two and three dimensions by representing order parameter and orientation in multiple fields. For example, Kobayashi and Warren use an SO(3) tensor field to describe orientation in three dimensions; this tensor can be thought of as three orthogonal unit vectors representing directions of the local crystalline axes. Here the constraints of orthogonality and unit length are relaxed to allow this tensor to store local elastic strain information in addition to orientation. This information can provide for coupling between mechanics and phase for example giving complex behavior at a crack tip, or can provide the strain field used in the Mixed Stress method for fluid-structure interactions during solidification with moving elastic solids.

12:05 PM

Thermo-Mechanical Effects and Microstructure Formation near the Meniscus during Continuous Casting of Steels: *Joydeep Sengupta*¹; *Brian G. Thomas*¹; ¹University of Illinois

Initial solidification is significantly affected by local changes in heat transfer, fluid flow, pressure forces, and thermal stresses that arise near the liquid steel meniscus during mold oscillation in the continuous casting of steel. These phenomena govern both the mechanical behavior of the initial shell and the sub-surface microstructure. They lead to the formation of periodic oscillation marks and hooks, which are detrimental to the final surface quality. To investigate the formation of these defects, this paper first uses a transient finite-element model (CON2D) to compute temperature, stress development, and the shape of the distorted steel shell during the initial stages of solidification. The model incorporates temperature-dependent properties, phase transformations, thermal shrinkage effects and a creep-type elastic-viscoplastic constitutive equation. The effect of steel grade on the initial shell shape during sudden metal level fluctuations near the meniscus is investigated.

Surfaces and Interfaces in Nanostructured Materials II: Nanoscale Powders, Tubes and Composites

Sponsored by: The Minerals, Metals and Materials Society, TMS Materials Processing and Manufacturing Division, TMS: Surface Engineering Committee

Program Organizers: Sharmila M. Mukhopadhyay, Wright State University; Narendra B. Dahotre, University of Tennessee; Sudipta Seal, University of Central Florida; Arvind Agarwal, Florida International University

Wednesday AM
March 15, 2006

Room: 209
Location: Henry B. Gonzalez Convention Ctr.

Session Chair: Arvind Agarwal, Florida International University

8:30 AM

Advanced FEM-Based Computational Modeling of CNT-Reinforced Damping Composite Materials: *Liya Bochkareva*¹; Vladimir Kompis²; ¹NAS of Belarus; ²University of Zilina

The focus in this paper is directed toward to the investigation into carbon-based nanoparticle/fibre/tube-reinforced composite materials and their advanced computational FEM-based dynamic/damping characterization. Structural micro to nanomechanical approach has been developed to predict damping behavior of the CNT-reinforced polymer matrix material. The model is based on interface motion to address the damping characteristics of CNT-reinforced composite material. It is worth noting that SWNT can be represented as a shell hollow frame-like structure with a simple nanoscale damping spring characteristics so as to enable multiscale modelling and validation of the assembled computational workbench. Experiments are also performed to investigate the damping characteristics of the CNT-reinforced composite materials and validate the model predictions as a function of a number of various factors, including the magnitude of critical bonding stress, nanotube weight ratio, structure deformation (strain), and CNT properties. Dr. Bochkareva pursues her research work under EU INTAS 2005-2007 fellowship Ref. Nr 04-83-3067.

8:50 AM Invited

Controlling and Modeling the Interphase in Polymer Nanocomposites: *Catherine Brinson*¹; T. Ramanathan¹; H. Liu¹; ¹Northwestern University

Polymeric nanocomposites made by incorporating small amount of nanoscale inclusions into polymer matrices exhibit dramatic changes in thermomechanical properties over the pure polymers. Because the properties of the nanoscale fillers can be extraordinary, even small volume fractions can result in significant changes. Enhancing the effect is the extremely significant role that the interphase plays in these systems. Given the enormous surface to volume ratio for nanoparticles, the interphase volume fraction can dwarf that of the inclusions themselves. In this talk, experimental evidence of the existence of this interphase region are presented. We show that by properly controlled functionalization of the nanoscale inclusions, we can impact the properties of the interphase region and consequently control the properties of the nanocomposites. In conjunction with the experimental results, the viscoelastic behavior of multi-phase polymeric nanocomposites is modeled using a novel hybrid numerical-analytical modeling method that can effectively take into account the existence of the interphase region. This hierarchical modeling approach couples the finite element technique and micromechanical approach and operates at low computational cost. Comparison between experimental and modeling results is reported.

9:30 AM

Effect of Sintering on Thermally Sprayed Carbon Nanotube Reinforced Aluminum Nanocomposite: *Tapas Laha*¹; Arvind Agarwal¹; ¹Florida International University

Multi-walled carbon nanotube (MWCNT) reinforced hypereutectic Al-Si nanocomposites were synthesized by high velocity oxyfuel and plasma spray techniques. Post processing sintering of these nanocomposites at 400°C for different periods under inert atmosphere has been carried out for further consolidation. Scanning electron microscopy and quantitative

microscopy has been performed to study the microstructural alteration viz. change in size and volume fraction of pores and primary silicon particles in the nanocomposites. The effect of sintering for prolonged time has been investigated by microhardness testing and nanoindentation technique. The counter effect of grain growth and residual stress on microhardness has been critically studied. Interfacial structure between Al-Si alloy and CNT has been examined by transmission electron microscopy.

9:50 AM Invited

Interfaces and Properties of TiC/a-C:H Nano-Composite Coatings: Jeff T. H. DeHosson¹; Yutao Pei¹; Damiano Galvan¹; ¹University of Groningen

TiC/a-C:H nanocomposite coatings, deposited with closed-field unbalanced magnetron sputtering, have been scrutinized with high-resolution transmission electron microscopy focusing on the role of the various heterophase interfaces. These coatings consist of 2-5 nm TiC nanocrystallites embedded in an amorphous hydrocarbon (a-C:H) matrix. The toughening of the nanocomposite coatings has been achieved effectively on two different scales, namely by restraining the formation of columns on a micro-scale and by manipulating the nanostructure on a nano-scale. The hardness (H) and elastic modulus (E) of the coatings are found to increase monotonically with increasing substrate bias whereas the H/E increases with C content. Tribo-tests confirm that the nanocomposite coatings possess superior self-lubrication effects with a coefficient of friction as low as 0.05 in ambient air and below 0.02 in dry air. Physical arguments are presented to explain the toughening mechanism and the ultra-low friction.

10:10 AM

Plasma Sprayed Aluminum Oxide-Carbon Nanotube Nanocomposite Coating: Kantesh Balani¹; Arvind Agarwal¹; ¹Florida International University

Al₂O₃ being ceramic is extremely brittle, hence incorporation of carbon nanotube (CNT) as reinforcement is utilized to study the fracture toughness of the composite. Plasma spraying is used to synthesize Al₂O₃-CNT nanocomposite coating. Phase identification is carried out using X-ray diffraction analysis and Raman Spectroscopy. Scanning electron microscopy has been employed to study dispersion and retention of CNT in the coating after plasma spraying. Preliminary mechanical properties of Al₂O₃-CNT nanocomposite coating is compared with Al₂O₃ coating without CNT reinforcement towards evaluating the effect of reinforcement.

10:30 AM

Preparation and Characterization of Alumina-Titania Composite Membranes on Alumina Substrates: Sandra Fernandes Quaresma¹; Mei Sen¹; Yang Juan¹; José Maria da Fonte Ferreira¹; ¹University of Aveiro

High porosity titania-alumina washcoatings were successfully deposited by dip-coating onto alumina substrates for the manufacture of honeycomb type-catalysts via sol-gel method. The thermal behavior of the as-prepared films was investigated by DTA, DTG. The evolution of crystalline phases after heat-treating at different temperatures (650°C, 800°C and 950°C) was determined by XRD. The microstructural and morphology evolution of the membranes was investigated by SEM. It was found that the molar ratio of alumina-titania in the precursor sols plays a determinant role and membranes with high homogeneous distribution of pores were obtained from an alumina-titania molar ratio of 1:11. For this ratio, anatase was the only crystalline phase identified after heat treating up to 650°C. Higher temperatures gave rise to the appearance other minor phases and to a decrease of porosity.

10:50 AM Invited

Modification of the Stiffness and Q-Factor of Micromechanical Structures Using Carbon Nanotubes: Srinivas Tadigadapa¹; ¹Pennsylvania State University

High frequency mechanical resonators operating in the frequency range of 1GHz and higher are of great interest in RF applications. However, even using the torsional mode of operation, micron sized resonators are typically limited to a maximum frequency of ~1 GHz. Carbon nanotubes (CNT) have been measured to have very high axial modulus of elasticity ~1 TPa. Incorporation of the high modulus CNT into MEMS thin films is expected to improve the elastic properties of deposited thin films. By in-

corporating CNTs in MEMS structures we have observed an increase in the stiffness of the micromechanical structures. Further, implicit in the miniaturization of mechanical resonators is the maintenance of Q-factor of the resonator necessary for achieving the required frequency stability. We also report the observation of the increase in the quality factor of an AT-cut quartz resonator through deposition of thin layers of SWNTs on its electrodes.

11:30 AM

Behavior of Impurity Elements in Powder Aluminium: Sergey Lipko¹; Vladimir Tauson²; Vladlen Akimov²; Vecheslav Veselkov¹; Boris Zelberg¹; ¹Siberian Research and Design Institute for Aluminium and Electrode Industry JSC; ²Institute of Geochemistry, Siberian Branch of the Russian Academy of Sciences

It is considered the influence of various chemical components on powder aluminium composition, produced using the method of gas dispersion of aluminium melt in nitrogen atmosphere and then annealed in different conditions. Powders with particles of different size 5-7 and about 20 mkm were examined. The presence of W makes better the structure of a film and promotes the formation of less strained nitride coating that was seen during comparative analysis of XPS width, pick no. 1s at half of maximum height after aluminium powder annealing in the presence of W in a sealed test-tube with air. It is anticipated that W has catalytic effect promoting the formation of nitric radicals that interact with particles' surface. W belongs to the group of elements with effect of integral accumulation in fine fractions of spray like Zn, Zr and some others.

The Brandon Symposium: Advanced Materials and Characterization: Small Length-Scales and Microstructures

Sponsored by: The Minerals, Metals and Materials Society, Indian Institute of Metals, TMS Extraction and Processing Division, TMS: Materials Characterization Committee

Program Organizers: Srinivasa Ranganathan, Indian Institute of Science; Wayne D. Kaplan, Technion; Manfred R. Ruhle, Max-Planck Institute; David N. Seidman, Northwestern University; D. Shechtman, Technion; Tadao Watanabe, Tohoku University; Rachman Chaim, Technion

Wednesday AM
March 15, 2006

Room: 206B
Location: Henry B. Gonzalez Convention Ctr.

Session Chairs: Sheldon Wiederhorn, National Institute of Standards and Technology; Xiaoqing Pan, University of Michigan

8:30 AM Invited

Electron Microscopy: Does it Solve Nano-Materials Problems?: Jeff T. H. DeHosson¹; ¹University of Groningen

The actual linkage between the microstructure studied by microscopy on one hand and the physical property of a material is almost elusive. The reason is that various physical properties are determined by the collective dynamical behavior of defects rather than by the behavior of an individual static defect. We argue that for a more quantitative evaluation of the structure-property relationship of (nano)structured materials extra emphasis on in-situ measurements is necessary and that will be the topic of this contribution to honor David Brandon. These points will be illustrated with our recent work on nanostructured metal clusters. Various in-situ TEM observations as a function of temperature appeared to be in contrast with classical thermodynamics. In addition, it will be shown that dynamical properties, mechanical as well as magnetic, can be studied with in-situ TEM indentations and with electron holography.

8:55 AM Invited

Predicting Interface-Limited Growth Morphologies with Minimal Experimental Input: David J. Srolovitz¹; Danxu Du¹; ¹Princeton University

Interesting and useful growth morphologies are routinely observed in covalently and ionically-bound materials. In the limit, where these morphologies are dictated by attachment or reaction kinetics rather than dif-

fusional fields, these morphologies can be predicted from knowledge of the growth velocity as a function of surface normal. Convexification of such a velocity plot yields an asymptotic growth shape known variously as the kinetic Wulff shape or idiomorph. Unfortunately, such velocity plots are rarely known. In this talk, we discuss how to deduce sufficient features of the velocity plot from observations of selected area growth morphologies. We then present an efficient numerical approach that uses such input to predict both asymptotic as well as transient growth morphologies. As an example, we will focus on GaN islands grown using the epitaxial lateral overgrowth technique.

9:20 AM Invited

Superfast Densification by Spark Plasma Sintering of Nanocrystalline Oxide Powders: *Rachman Chaim*¹; ¹Technion - Israel Institute of Technology

Spark plasma sintering (SPS) is a newly discovered old technique which recently has been used for superfast densification of ceramic powders. Simultaneous application of pulsed DC high current densities and load is the necessary condition for full densification by SPS. Commercial nanocrystalline MgO and yttrium aluminum garnet (YAG) powders were densified to optical transparency using spark plasma sintering at distinctly different homologous temperatures (0.3 for nc-MgO versus 0.7 for nc-YAG). The microstructure and density evolutions versus the SPS parameters were characterized and determined. Although a debate still exists about the exact mechanisms for the enhanced densification rate, an existing hot-isostatic pressing (HIP) model with conventional densification mechanisms was successfully used for the description of the densification of nanocrystalline MgO. Theoretical and experimental results both emphasize the importance of the ultrafine powder character as well as its mechanical and physical properties at high temperatures.

9:45 AM Invited

Tailoring of Multiferroic Nanostructures in Epitaxial Films: *Igor Levin*¹; ¹National Institute of Standards and Technology

Multiferroic materials which display a coexistence of ferroelectric (FE) and ferromagnetic (FM) responses attract particular interest because of their potential for several novel applications. The present study combined experimental and theoretical work to determine the transferable principles of engineering of self-assembled multiferroic heterophase nanostructures in epitaxial films. The study was conducted on the nanostructures consisting of the epitaxial ferroelectric PbTiO₃ and ferrimagnetic CoFe₂O₄ phases on differently oriented SrTiO₃ substrates. Regardless of substrate orientation, the nanostructures consisted of vertical columns of CoFe₂O₄ dispersed in the PbTiO₃ matrix, or vice versa. However, the morphologies of these columns, and their spatial arrangements, exhibited a marked dependence on the substrate orientation. Phase-field modeling of these nanostructures succeeded in reproducing even fine morphological details and revealed that the nanostructure morphologies are determined by the in-plane elastic anisotropy of the films. The implications of these results for a design of multifunctional epitaxial nanostructures will be discussed.

10:10 AM

Nanostructure and Mechanical Properties of Precipitation-Strengthened Al-Sc Alloys with Rare Earth Additions: *Marsha E. Van Dalen*¹; David N. Seidman¹; David C. Dunand¹; ¹Northwestern University

Currently, most precipitation-strengthened aluminum alloys are limited to usage at relatively low temperatures (<460 K), because of the rapid coarsening and/or dissolution of their precipitates. Al-Sc alloys are an exception, because they contain nanometer diameter, coherent Al₃Sc precipitates (L1₂ structure) with relatively low coarsening rates. Rare earth (RE) elements (Gd or Yb) are being added to Al-Sc alloys as ternary additions and are found to increase the hardness of the alloys by a factor of three over binary Al-Sc alloys. Transmission electron microscopy and atom-probe tomography are utilized to analyze the morphology and coarsening kinetics of the precipitates. The heterophase interface between α -Al and Al₃(Sc_{1-x}Yb_x) exhibited segregation of Sc. The resulting creep properties of Al-Sc-RE alloys are also presented.

10:25 AM Break

10:35 AM Invited

Some Structure-Property-Function Connections for Healthy and Diseased Human Red Blood Cells: John Mills¹; Ming Dao¹; *Subra Suresh*¹; ¹Massachusetts Institute of Technology

Changes to the biomolecular structure and cytoskeleton network of human red blood cells due to various disease states can result in significant changes in mechanical, chemical and biological responses. In this work, we explore some such connections for human red blood cells where structural changes arise from either infectious or hereditary diseases. We use biomechanical measurements and force-displacement responses to characterize progressive changes in mechanical response due to the diseased state. These experiments are supplemented with detailed computational simulations so as to develop mechanistic insights into the changes in properties with specific references to red blood cells and human diseases.

11:00 AM Invited

Characterization of Ceramics Using Luminescence and Piezospectroscopy: *David Clarke*¹; ¹University of California

Because most ceramic materials are transparent in the visible portion of the spectrum, optical tools, such as luminescence and spectroscopy, can be used in their characterization. In this talk I will describe two principal tools, the characterization of local stresses using piezospectroscopy and the characterization of temperature in doped zirconia coatings using luminescence. Piezospectroscopy involves the determination of strain from the frequency shift, and broadening, of characteristic spectral lines excited by either a laser beam or electron beam. The technique is particularly useful for studying alumina ceramics as chromium, a well-known dopant in alumina, occurs naturally in all alumina ceramics. The basic principles and applications will be described. In the second part of the talk I will describe recent work in doping zirconia, and related ceramics, to facilitate photo-stimulated luminescence and its use in non-contact measurement of temperature in coatings. So far, temperatures up to 1250°C have been measured.

11:25 AM Invited

Twin Quintuplets in CVD Diamond Films: *Dan Shechtman*¹; ¹Ames Laboratory

Five fold twins have been observed in a large number of crystals, and in nanoparticles in particular. However, these twin quintuplets have been rarely thoroughly studied. Presented here is a crystallographic study of the formation of twin quintuplets in CVD diamond crystals. The quintuplets form during the initial growth process of the film, and at the onset of nucleation crystals with icosahedral shape are often created. The shape of some other CVD diamond crystals is also related to twin quintuplets. Observations by high resolution TEM and surface studies by SEM identify the surface crystallography of the diamond film. Twin quintuplets may consist of four $\Sigma=3$ and one $\Sigma=81$ boundaries, but in some cases they consist of only three $\Sigma=3$ and two general grain boundaries.

11:50 AM Invited

New Dimensions in Structural Metallurgy: *Srinivasa Ranganathan*¹; ¹Indian Institute of Science

Metals are characterized by the metallic bond based on free electrons. This leads to a few close packed structures. The rich variety of atomic configurations seen in the larger class of inorganic materials with covalent and ionic bonding has long remained the envy of metallurgists. However, over the past few decades non-equilibrium processing has led to new configurations of quasicrystalline and noncrystalline phases, rivaling in complexity other inorganic structures. These studies have also revealed deep connections between the structure of intermetallics and clathrates and even biological materials with helices. The icosahedral order linking many of these structures will be emphasized.

12:15 PM

Finite Size Effects on Grain Boundary Structures and Interactions with Dislocations: *Emmanuelle A. Marquis*¹; John C. Hamilton¹; Douglas L. Medlin¹; Francois Leonard¹; ¹Sandia National Laboratories

Grain boundary structures in nanocrystalline materials, which by deviating from their ideal structures in infinitely long bicrystals, may impact

WEDNESDAY AM

the operating deformation mechanisms. We examine the relaxation of $\Sigma 3$ {112} grain boundary structures of nanometer length scale, and address the interactions with dislocation focusing on the forces and interactions that drive the emission of extended defect structures from grain boundaries. This issue has become increasingly important in nanostructured materials in which distances between interfaces are sufficiently small that individual interfaces cannot be considered in isolation. Of broader significance, simulations and experiments in the literature have indicated that the emission of extended defects plays a role in the deformation of nanocrystalline materials. The detailed connection of such emission processes to the properties and structure of the emitting interfaces, however, remains unclear. This work points out the relative importance of interfacial and elastic energies in controlling the equilibrium structures of such configurations.

The James Morris Honorary Symposium on Aluminum Wrought Products for Automotive, Packaging, and Other Applications: Continuous Casting and Related Technologies

Sponsored by: The Minerals, Metals and Materials Society, TMS Light Metals Division, TMS: Recycling Committee

Program Organizers: Subodh K. Das, Secat Inc; Gyan Jha, ARCO Aluminum Inc; Zhong Li, Aleris International Inc; Tongguang Zhai, University of Kentucky; Jiantao Liu, Alcoa Technical Center

Wednesday AM Room: 207A
March 15, 2006 Location: Henry B. Gonzalez Convention Ctr.

Session Chairs: Subodh K. Das, Secat Inc; Zhong Li, Aleris International Inc

8:30 AM

Texture Evolution of Continuous Casting AA5052 Aluminum Alloy Sheet during Closed to Equi-Biaxial Stretching: *Xiyu Wen*¹; Zhengdong Long¹; Weimin Yin²; Tongguang Zhai¹; Zhong Li³; Subodh Das²; ¹University of Kentucky; ²Secat, Inc.; ³Aleris International, Inc

In this study, texture evolution in a 0.080" gauge hotband of continuous casting AA5052 aluminum alloy sheet after annealing at 750°F for 4 hours was investigated by X-ray through thickness of the sheet. In the three different strain levels from equi-biaxial stretching, the deformed samples were prepared for texture measuring. The major and minor strains were measured. The texture evolution in the different layers through thickness of the three samples was obtained during the closed to equi-biaxial strain state. It was found that cube component rotates to Goss orientation ((110)<001>) during equi-biaxial deformation. The Goss component gradually changes to Brass orientation ((110)<112>) and penetrates to (110)<hhl> position. The part of Brass component also rotates to S orientation ((213)<364>). In addition, the (110)<111> component was found on the surface.

8:55 AM Invited

Quantitative Analysis of Texture Evolution of Aluminum Alloys during Cold Rolling: A Review: *Wenchang Liu*¹; Zhong Li²; Chi-Sing Man¹; James G. Morris¹; ¹University of Kentucky; ²Aleris International Inc.

The texture evolution of various aluminum alloys during cold rolling was investigated by X-ray diffraction. The rotation paths and stability of the cube and rotated cube orientations were determined based on the variation in the three-dimensional orientation distribution function (ODF) with rolling reduction. Texture volume fractions were calculated by an improved integration method. The relationship between the texture volume fractions and true strain was described quantitatively by mathematical formulae. The effect of alloy composition, initial microstructure and texture, and processing method (CC vs. DC) on the texture evolution during rolling was determined.

9:20 AM

Microstructure, Crystallographic Texture, and Plastic Anisotropy of a Continuous Cast Al-Mn-Mg Alloy Sheet: *Jiantao Liu*¹; Robert E. Dick¹; Thomas N. Rouns¹; Stephen W. Banovic²; Richard J. Fields²; James G.

Morris³; ¹Alcoa Technical Center; ²National Institute of Standard and Technology; ³University of Kentucky

The microstructure, crystallographic texture, and plastic anisotropy of a continuous cast Al-Mn-Mg alloy sheet was investigated. It was found that the cold rolling reduction and initial heat-treatment of hot rolled sheet had a significant effect on the microstructure and mechanical properties of the sheet, respectively. For the sheet specimens without the initial heat-treatment, a severely elongated grain structure was found in which the texture was dominated by a strong P orientation {011}<566> regardless of the fact that the specimen was completely recrystallized. In contrast, specimens receiving the same cold rolling and annealing conditions but with the initial heat-treatment had an equiaxed grain structure with a Cube orientation {001}<100>. The R values were predicted using Hosford-Backofen model as well as continuum mechanics of texture polycrystals (CMTP) method. The predicted R values were compared with the measured results. The effect of initial heat-treatment on the plastic anisotropy of the specimens was discussed.

9:45 AM Invited

Analysis of Deformed Microstructures in AA5005 and AA6022: *David P. Field*¹; Reza S. Yassar¹; ¹Washington State University

Dislocation generation and motion is the primary mechanism of plastic deformation in polycrystalline materials. Strain hardening of these materials is a function of dislocation interactions with one another, and with various additional obstacles or defects in the crystallite. Measurement of the local plastic strain state requires analysis of the dislocation structure. A non-unique correlation between the lattice curvature and plastic strain in polycrystalline aluminum is demonstrated using a variety of microstructural measures. Measurements in aluminum alloys 5005 and 6022 deformed by channel die compression are discussed in the context of structural evolution as measured by lattice curvature and geometrically necessary dislocations. Evolution of the dislocation structures is assumed to be dependent on Taylor factors of individual grains, but little evidence to support this supposition is found. It is shown that non-local factors, such as interactions with neighboring grains, are of importance in describing structural evolution.

10:10 AM Break

10:20 AM

Quantitative Texture Evolution in a Continuous Cast AA5052 Aluminum Alloy during Hot Rolling: *Qiang Zeng*¹; Tony Zhai¹; Xiyu Wen¹; ¹University of Kentucky

In order to investigate the influence of hot rolling on the texture and microstructure evolution in commercial continuous cast Aluminum alloys, a continuous cast (CC) AA5052 slab bitten by the first hot rolling mill at an entry temperature of 465°C and an exit temperature of 370°C was made. The rolling reduction in thickness varied from 8.6 mm to 21.5 mm across the sample along the rolling direction. Textures were measured by XRD at cross-sections perpendicular to the rolling direction in this sample. The evolution of all the texture components during hot rolling was quantified using Johnson-Mehl-Avrami-Kolmogorov type equations in terms of the rolling true strain. Orientation hardening during hot rolling was also calculated based on the texture measurement in the alloy. The microstructure evolution was studied in the sample.

10:45 AM

Thermal Stability of Selected 5000 Series Al Alloys: *Catherine Wong*¹; Alicia Field¹; ¹NSWCCD

Due to the propensity of the 5000 series Al alloys containing more than 3% Mg to sensitize it was undertaken to empirically produce the time temperature curve for sensitization of three common alloys. The alloys studied included 5383, 5454 and 5456. They were heated above 100°F and below 400°F for up to 80 days and the degree of sensitization was measured using ASTM G 66 and ASTM G 67. Image analysis was employed to form a relationship between the resulting volume fraction of the beta phase and the weight loss in recrystallized 0.25" plate of these three alloys.

11:10 AM

Heating Rate Effect on Microstructure Evolution during Annealing of Twin Roll Cast AA3105: *Naiyu Sun*¹; Burton R. Patterson¹; Jaakko P.

Suni²; Eider A. Simielli²; Hasso Weiland²; Puja Kadolkar³; Craig Alan Blue³; Gregory B. Thompson¹; ¹University of Alabama; ²Alcoa Inc; ³Oak Ridge National Laboratory

Rapid solidification and cooling of twin roll cast (TRC) AA3105 traps excess solute that precipitates as fine dispersoids during conventional annealing. These particles inhibit recrystallization by Zener pinning of subgrain boundaries, resulting in a coarse, elongated grain structure. Prior studies have shown that a rapid heating rate to the annealing temperature produces a much finer and more equiaxed recrystallized grain structure. The present study examines the effects of three constant heating rates on the resulting precipitation and recrystallization behavior. The two highest rates, 50 and 3°C/s, were achieved in an infrared furnace at the ORNL Materials Processing Lab, while the slowest rate, 0.01°C/s, was obtained in a conventional programmable lab furnace. The time-temperature-transformation diagrams for dispersoid precipitation and recrystallization were determined via conductivity measurements and optical microscopy. The relative positions of these curves were used to explain the effects of heating rate on recrystallization kinetics and grain size.

11:35 AM

Effect of Texture and Second Phase Particle Distribution on Formability of Continuous Cast and Direct Chill Cast 5754 Al-Mg Sheet: Asim Tewari¹; Shashank Tiwari¹; *Raja Mishra*¹; Anil Sachdev¹; ¹General Motors

Continuous casting (CC) offers an opportunity to decrease the cost of sheet aluminum, however, the formability of CC sheets is slightly lower than sheet made from the Direct Chill cast (DC) process. A systematic study of the texture and microstructure in DC and CC 5754 aluminum sheet was performed using electron back scattered diffraction (EBSD) and digital imaging. Stereological tools were employed to characterize the second phase particles in three dimensions, and unbiased robust values of particle size, particle fraction, interfacial-area and mean free path were estimated. Differences in the size distribution and spatial scatter were also quantified. It is seen that the random components of texture are nearly identical in DC and CC sheet, but individual FCC rolling components differ from one material to the other. It is shown that differences in texture and spatial arrangements of particles correlates with differences in the ductility and fracture properties observed.

12:00 PM

Application of Rapid Infrared Heating for Processing Aluminum Forgings: *Gowreesan Vamadevan*¹; Frank F. Kraft¹; Puja Kadolkar²; Howard (Rob) Mayer³; ¹Ohio University; ²Oak Ridge National Laboratory; ³Queen City Forging Company

Infrared (IR) heating has the potential to be used for solutionizing of aluminum forgings with benefits of reduced energy consumption, and improved microstructure and mechanical properties. Standard procedures to take advantage of rapid IR for solutionizing are not currently available. Thus, a primary objective of this work was to determine optimum solutionizing cycles for four aluminum alloys; AA 2014, AA 2618, AA 6061 and AA 7075. A second objective was to demonstrate the mechanical property improvements possible with optimized rapid IR solutionizing cycles. Laboratory experiments on aluminum coupons were performed to establish optimum solutionizing thermal cycles for each alloy. Upset forgings were then produced via conventional production means and “optimized” IR thermal processing. The results of lab and production testing are presented, and the microstructure and mechanical properties of conventionally heat treated parts and rapid IR treated parts are compared.

The Rohatgi Honorary Symposium on Solidification Processing of Metal Matrix Composites: Modeling and Nanocomposites

Sponsored by: The Minerals, Metals and Materials Society, TMS Materials Processing and Manufacturing Division, TMS Structural Materials Division, TMS/ASM: Composite Materials Committee, TMS: Solidification Committee

Program Organizers: Nikhil Gupta, Polytechnic University; Warren H. Hunt, Aluminum Consultants Group Inc

Wednesday AM
March 15, 2006

Room: 207B
Location: Henry B. Gonzalez Convention Ctr.

Session Chairs: Daniel B. Miracle, U.S. Air Force; Anil Kumar Gupta, National Physical Laboratory

8:30 AM Invited

Microstructure-Based Modeling of Particle Reinforced Metal Matrix Composites: *Nikhilesh Chawla*¹; Krishan K. Chawla²; ¹Arizona State University; ²University of Alabama at Birmingham

It is well recognized that microstructure controls the physical and mechanical properties of a material. Several analytical and numerical techniques have been employed extensively to predict and characterize the behavior of multiphase materials. Analytical models provide reasonable predictions for relatively simple configuration of the phases. Numerical models can extend the realm of problems that can be modeled, but they still make some simplifying assumptions about the inherent microstructure of heterogeneous multiphase materials. Microstructure-based modeling of particle reinforced metal matrix composites (MMCs) involves use of microstructural data in finite element modeling, in two and three dimensions, with a view to predict the properties such as elastic, plastic, or thermal behavior of the composite. It can also be used as a tool to understand the mechanical and physical behavior of the composite. We provide examples from important particulate MMCs such as SiC/Al and WC/Co.

8:55 AM

Measurement and Modeling of Damage in Cast Al-Si Alloys: B. Ye¹; M. Erukullu¹; Stephen J. Harris²; Somnath Ghosh³; *Bhaskar S. Majumdar*¹; ¹New Mexico Tech; ²Ford Motor Company; ³Ohio State University

In this presentation, we report on damage mechanisms and ductility prediction of cast A356 and A319 Al-Si alloys. These materials may indeed be considered a subset of cast metal matrix composites, which were pioneered by Professor Rohatgi approximately 4 decades ago. Our observations indicate that although the Al-Si alloys were Sr-modified, the brittle Si-particle shapes have complex 3-D morphological features that are generally not known in such alloys. Tensile specimens were incrementally loaded to different strains, and microstructurally examined to measure particle cracking and matrix damage. In addition, neutron and Raman-shift measurements were conducted to estimate stresses in Si particles. Analytical and computational modeling involved homogenization methods to include particle cluster effects. Results of predicted particle stresses are compared with measured data, and our attempts to predict ductility in such systems are discussed. We acknowledge support from NSF contract CMS 0309519 for conducting this research.

9:20 AM

Numerical Modeling of Interaction of Particles with Solidifying Interfaces: *Mario Roberto Rosenberger*¹; Eliana Mabel Agalotis¹; Carlos Enrique Schvezov¹; ¹National University of Misiones

The thermal fields of a moving solidification interface towards a spherical particle were dynamically modeled in order to study the deformation of the interface in relation with different thermal properties of particle and matrix. Finite element methods were employed in an axi-symmetric model of the system. The degree of deformation when the particle has different thermal conductivity than the matrix is presented and discussed. The drag force on a particle being pushed by a crystal was calculated with a fluid flow model. The force was calculated for different pushing configurations and the results compared with the values given by the modified Stokes equation; which show that the model value are slightly larger than those

WEDNESDAY AM

calculated with the equation. This difference predicts an equilibrium separation for pushing lower than the computed by modified Stokes equation when a Lifshitz-Van der Waals model for the repulsion force is used.

9:45 AM

Multiscale Approach to Modeling Particle-Solidification Front Interactions: *Justin W. Garvin*¹; *Yi Yang*¹; *H. S. Udaykumar*¹; ¹University of Iowa

Predicting microstructures of metal-matrix composites (MMC) requires an understanding of how solidification fronts interact with particles. The particle-solidification front interaction is a multiscale process as the dynamics at the micro-scale hinges on the interactions between the front and the particle, which occurs across a nano-scale gap. In these systems, the solution of the Navier-Stokes equations including the nano-scale gap between their interacting surfaces would be impossible due to resolution demands placed on the mesh. Therefore an embedded model for solution in the gap is needed. This model takes the form of a lubrication equation with disjoining pressure acting as a body force and is coupled to the solution outside the gap that is solved using the Navier-Stokes equations. A sharp-interface method is used to track the interfaces. This method illustrates a new way of predicting the critical velocity and allows for an in-depth analysis of the physics that cause particle pushing/engulfment.

10:10 AM

Influence of Processing Parameters on the Structure and Mechanical Properties of Lightweight Aluminum and Magnesium-Nanoparticle Metal Matrix Nanocomposites: *Benjamin F. Schultz*¹; *Pradeep Kumar Rohatgi*¹; *J. B. Ferguson*¹; *Nikhil Gupta*²; ¹University of Wisconsin-Milwaukee Center for Composites; ²Brooklyn Polytechnic

Metal matrix nanocomposites (MMNC) reinforced with dispersed nanosized ceramics have the potential of ultra high strength and improved tribological properties. To date, most of the developments and research in the synthesis of metal matrix nanocomposites have focused on powder metallurgy techniques and deformation processing. Researchers at the University of Wisconsin have developed cast lightweight aluminum and magnesium MMNC's through solidification processing techniques. Applications and optimization of vortex mixing, ultrasonic agitation and squeeze infiltration processes to produce lightweight metal matrix nanocomposites are discussed. The synthesis parameters were varied and analyzed using statistical design of experiments. Selected mechanical and physical properties and microstructures of cast metal matrix nanocomposites will be presented.

10:35 AM Break

10:50 AM

Sharp Interface Simulation of Interactions of Dendrites with Solid Particles: *Yi Yang*¹; *J. W. Garvin*¹; *H. S. Udaykumar*¹; ¹University of Iowa

The behaviour of growing dendrites when approaching particles in the melt determines the particle distribution in the finished metal-matrix composites (MMCs). A sharp interface level-set based numerical method is employed to study dendrite-particle interactions. The simulation of the interaction between particles and dendrites grown from pure material shows that for a particle to melt thermal conductivity ratio $\lambda = k_p/k_r < 1$ (typical for MMCs), the dendrite does not approach the particle close enough to activate particle pushing. Instead, the dendrite chooses to go around the particle and eventually the particle is engulfed by sidebranches. Thus the entrapment mode is the likely outcome. The simulation of interaction of particles with dendrites grown from a binary alloy is also carried out. A local mesh refinement technique is used along with the sharp-interface methodology to enable the simulation of interactions of multiple dendrites and multiple particles, so the prediction of the particle distribution in MMC microstructures is also attempted.

11:15 AM Invited

Polymeric Route for Processing NanoScale Aluminum Matrix Ceramic Composites for High Temperature Applications: *Scott Patrick*¹; *Atanu Saha*¹; *Rishi Raj*¹; ¹University of Colorado

Recent research on polymer-derived ceramics whereby ultrahigh temperature silicon-carbonitride materials are made by controlled pyrolysis of highly cross-linked polysilazane polymers is extended to the insertion of the ceramic phase into an aluminum matrix by in-situ pyrolysis. Since

the pyrolysis temperature lies above the melting point of aluminum, the polymer is introduced into the aluminum melt and then pyrolyzed in the liquid metal environment near 1000°C. The results show that in-situ pyrolysis is viable and that it leads to enhanced mechanical properties (the experiments are being done with pure aluminum). The mechanical properties do not degrade with elevated temperature anneals implying that the hard phase introduced by pyrolysis does not coarsen. This process raises new issues: the elimination of hydrogen from the melt, the fragmentation of the polymer particles during pyrolysis, and the constitution of the ceramic phases produced within the liquid metal and their adherence to the metal.

11:40 AM Invited

Nanostructured Ceramic Thin Films: Their Structures, Mechanical Properties, and Applications to Microfabrication: *Wen J. Meng*¹; *Dong Mei Cao*¹; *Jing Jiang*¹; ¹Louisiana State University

Our recent results on two-phase nanocomposite thin films based on amorphous hydrogenated carbon (a-C:H) and amorphous silicon nitride (a-Si₃N₄), synthesized by plasma assisted vapor phase deposition, will be summarized. Detailed nanoscale structural characterization was achieved by combining X-ray spectroscopy with high resolution electron microscopy. Mechanical properties of the films, such as modulus, hardness, and residual stress, were characterized with instrumented nanoindentation and substrate curvature measurements. Structure - mechanical property correlations will be discussed. Applications of nanostructured ceramic thin films to microscale molding replication of metal-based high-aspect-ratio microscale structures will be illustrated.

Titanium Alloys for High Temperature Applications - A Symposium Dedicated to the Memory of Dr. Martin Blackburn: Titanium Alloys for High Temperature Oxidation Resistance

Sponsored by: The Minerals, Metals and Materials Society, TMS Structural Materials Division, TMS: Titanium Committee

Program Organizers: Michael W. Peretti, Lyondell Chemical Company; Daniel Eylon, University of Dayton; Ulrike Habel, Munich; Guido C. Keijzers, Del West USA; Michael R. Winstone, DSTL

Wednesday AM
March 15, 2006

Room: 201
Location: Henry B. Gonzalez Convention Ctr.

Session Chairs: Guido C. Keijzers, Del West USA; Yoji Kosaka, TIMET

8:30 AM Invited

Improvement of High Temperature Environmental Resistance of Titanium Alloys and Titanium Aluminides - Recent Trends: *Christoph Leyens*¹; *Reinhold Braun*¹; *Maik Froehlich*¹; *Olaf Schroeter*²; ¹German Aerospace Center (DLR), Institute of Materials Research; ²Technical University of Brandenburg at Cottbus

The use of high temperature titanium alloys and aluminides at moderately elevated and high service temperatures is a strong challenge to their environmental resistance. The paper will review the most recent trends in surface modification techniques for these light weight high temperature materials while focusing on the development of protective overlay coatings. Metallic coatings typically provide good oxidation resistance at high temperatures by the formation of protective oxide scales while the coatings themselves remaining "ductile". Nitride coatings can combine good oxidation resistance with high hardness, thus additionally providing protection against wear and erosion, however, typically at the expense of coatings adhesion and potential adverse effects on the fatigue behavior of the structural material. For highest operating temperatures the use of thermal barrier coatings on gamma titanium aluminides has been explored recently. Very promising results were achieved when zirconia top coatings were applied using the EB-PVD deposition technique.

9:00 AM

Recent Development of Titanium and Its Alloys in Automotive Exhaust Applications: *Yoji Kosaka*¹; *Stephen P. Fox*¹; ¹TIMET

There has been a significant growth in the application of titanium and its alloys to automotive exhaust systems over the last decade. CP Ti has been used for dual exhaust systems of Corvette Z06 in recent years. Exhaust pipes and mufflers for high performance motorcycles have been a prime target of titanium, since the visual appearance of titanium as well as performance with titanium attracts users. There has been notable progress in material side as well. Ti-1.5%Al and TIMETAL®Exhaust XT (Ti-0.45%Si-0.25%Fe) have been developed to meet more stringent requirement in terms of oxidation resistance at higher temperatures where CP Ti cannot be used. This paper will review high temperature titanium and its alloys for automotive exhaust applications. Metallurgical factors that control oxidation resistance will also be discussed primarily focusing on TIMETAL®Exhaust XT.

9:30 AM

Investigation of Ductility Loss in a Thermally Exposed Near-β Ti Alloy: *Frederic Sansoz*¹; Hamouda Ghonem²; ¹University of Vermont; ²University of Rhode Island

We studied the effects of thermal exposure in air on the plastic elongation of Ti-15Mo-2.7Nb-3Al-0.2Si (Timetal-21S) alloy. Sheet specimens (0.12-1.0 mm in thickness) were exposed in air to temperatures between 482°C and 693°C. Tensile tests conducted on these specimens at room temperature show a reduction of plastic elongation along with a change in the failure mode into a quasi-brittle fracture in the near-surface region. The kinetics of embrittlement is studied through theoretical considerations of gas diffusion into metal. This approach shows that two distinct embrittlement mechanisms operate in this alloy depending on the temperature range. Above 545°C, the embrittlement activation energy is 41.2 kcal.mol⁻¹, indicating that the embrittlement process is governed by an enhanced diffusion of oxygen into Timetal-21S. Below this transitional temperature, the activation energy approaches zero, a characteristic of slow kinetics transformation. The role of solid-solution hardening, precipitation-hardening mechanisms, and alloying-element partitioning on this effects are also discussed.

10:00 AM

Aluminum Clad Titanium for High Temperature Applications: *Lichun Leigh Chen*¹; Yoji Kosaka²; Mike Hardy¹; ¹Engineered Materials Solutions Inc; ²TIMET Henderson Technical Laboratory

The addition of aluminum increases the oxidation resistance of titanium at elevated temperatures. There is interest in cladding aluminum to titanium or titanium alloys for elevated temperature applications. A study was conducted to roll-bond aluminum sheet over Ti substrate to form Al/Ti clad metal and then to anneal the clad metal for diffusion-alloying. TIMETAL Exhaust-XT was selected as a Ti substrate. Three different thicknesses of aluminum were used to make Al/Ti clad metals. The processes were investigated for ideal microstructure and properties. The metallurgical views behind the process design are discussed. Microstructural examination revealed the effects of the annealing temperature on microstructure evolutions. Aluminum-titanium intermetallic compounds were formed during diffusion-annealing. Ti was well diffused into the original Al surface clad layer while the diffusion of Al into the Ti substrate was insignificant. Mechanical testing showed the optimal processing for forming. Oxidation weight gain at 800°C followed the parabolic law.

10:30 AM Break

Titanium Alloys for High Temperature Applications - A Symposium Dedicated to the Memory of Dr. Martin Blackburn: Titanium Based Intermetallic Alloys for High Temperature Applications - Alpha 2 and Orthorhombic

Sponsored by: The Minerals, Metals and Materials Society, TMS Structural Materials Division, TMS: Titanium Committee

Program Organizers: Michael W. Peretti, Lyondell Chemical Company; Daniel Eylon, University of Dayton; Ulrike Habel, Munich; Guido C. Keijzers, Del West USA; Michael R. Winstone, DSTL

Wednesday AM
March 15, 2006

Room: 201
Location: Henry B. Gonzalez Convention Ctr.

Session Chairs: Patrick L. Martin, U.S. Air Force; John J. Schirra, Pratt & Whitney

11:00 AM Invited

The Emergence of the Orthorhombic Aluminides: *Dipankar Banerjee*¹; ¹Defense Research and Development Organization

The development of aluminides based on the intermetallic phases in the Ti-Al system consumed almost three decades of intensive research through the seventies and eighties, and into the nineties. Martin Blackburn played a central role in this effort. The alloying of Ti3Al was examined in the sixties, but engineering plasticity in this class of alloys appears to have emerged from programs directed by Blackburn through the late seventies and eighties at the United technologies Research Centre. The Ti-24Al-11Nb and the supera2 alloy (with about 15at% beta stabilizers) emerged from this effort. In the late eighties, Rowe at GE,CR&D observed significantly improved properties in Ti3Al alloys containing Nb upto 25at %. Almost simultaneously, we discovered that alloys with Nb contents greater than about 15at% Nb were based on a ternary intermetallic, Ti2AlNb that we christened the O phase. In the following years we defined the physical metallurgy of the higher Nb alloys covering phase equilibria and transformations, mechanical behavior and processing. In the mid nineties, working together with the School of Materiaux, Ecole des Mines and Snecma Moteurs, we significantly improved the properties of this class of alloys through extensive studies on compositional effects on processing, structure and properties. We summarize the totality of this effort in our presentation in a tribute to Martin Blackburn's pioneering work.

11:30 AM

Microstructure, Tensile, and Creep Behavior of Ti-15Al-33Nb and Ti-21Al-29Nb Orthorhombic+BCC Alloys: *Christopher J. Cowen*¹; Carl J. Boehlert¹; ¹Michigan State University

In this work the creep and elevated temperature tensile behavior of two orthorhombic (O)+body-centered-cubic (BCC) alloys, specifically Ti-15Al-33Nb (at%) and Ti-21Al-29Nb (at%), were evaluated in order to determine the effect of alloy composition and microstructure on mechanical properties and deformation behavior. Tensile tests, performed at RT and 650°C, indicated that the Ti-21Al-29Nb alloy exhibited significantly lower elongation-to-failure values than the Ti-15Al-33Nb alloy. Heat-treatments used to precipitate greater volume fractions of the O-phase resulted in greater strength levels, while the BCC phase provided ductility. The measured creep stress exponents (1.1<n<6) and apparent activation energies (99 kJ/mol<Qapp< 317 kJ/mol) suggested that different mechanisms were active dependent on temperature and applied stress level. Overall, the Ti-15Al-33Nb alloy was shown to exhibit a greater balance of RT and elevated-temperature properties than the Ti-21Al-29Nb alloy, and this presentation will discuss the implications of this result in terms of microstructure-property relationships for O+BCC alloys.

12:00 PM

Property Enhancement of Ti₂AlNb-Based Intermetallic Alloys for High Temperature Use: *Satoshi Emura*¹; Masuo Hagiwara¹; ¹National Institute for Materials Science

In order to improve the mechanical properties of orthorhombic Ti₂AlNb-based titanium intermetallic alloys for temperatures above 650°C, we have been conducting following researches. To improve room temperature prop-

WEDNESDAY AM

erties without sacrificing high temperature properties, grain-size refinement was attempted using the pinning effect of second phase particles. The finer-grained materials showed a good combination of room and high temperature properties. To improve tensile and creep strength at temperatures above 650°C, substitution of transition metal elements such as W, Mo, V, Fe or Cr for a portion of Nb was conducted. Substitution of W for Nb in a Ti-22Al-27Nb alloy substantially increased the high temperature tensile and creep strength. To further improve high temperature mechanical properties, fine TiB or TiC particulate reinforced Ti₂AlNb-based composite was produced using a gas atomization P/M method. Most of the mechanical properties such as tensile strength and creep properties were superior to those of the unreinforced matrix alloy.

12:30 PM

Oxidation Studies on Ti3Al-Mo Alloys: Ramana G. Reddy¹; *Dusti Livingston*¹; Divakar Mantha¹; ¹University of Alabama

The Ti3Al-Mo oxidation studies were conducted in oxygen gas using TGA. Three alloys containing 1.7 at. %Mo, 2.2 at.% Mo and 4.0 at. %Mo was studied from 800°C to 1100°C. The effects of time, temperature, and composition affect on the oxidation of the alloys were investigated. For each given alloy, weight gain per unit surface area vs. time plot was made, and reaction rate constants were used to calculate the activation energies. Reaction products were characterized using optical microscope, scanning electron microscope (SEM), X-ray diffraction, and energy dispersive spectrometer (EDS). The results showed that alloys that contain Molybdenum were higher resist to oxidation than the binary alloys. The alloy that contains 2.2 at.% Mo has lower activation energy than other alloys containing 2.6 at.%Nb. A possible oxidation mechanism of the alloys in oxygen was proposed.

Ultrafine Grained Materials - Fourth International Symposium: Mechanical Properties

Sponsored by: The Minerals, Metals and Materials Society, TMS Materials Processing and Manufacturing Division, TMS Structural Materials Division, TMS/ASM: Mechanical Behavior of Materials Committee, TMS: Shaping and Forming Committee

Program Organizers: Yuntian T. Zhu, Los Alamos National Laboratory; Terence G. Langdon, University of Southern California; Zenji Horita, Kyushu University; Michael Zehetbauer, University of Vienna; S. L. Semiatin, Air Force Research Laboratory; Terry C. Lowe, Los Alamos National Laboratory

Wednesday AM Room: 217D
March 15, 2006 Location: Henry B. Gonzalez Convention Ctr.

Session Chairs: Michael Josef Zehetbauer, University of Vienna; Jingtao Wang, Nanjing University of Science and Technology; Irene J. Beyerlein, Los Alamos National Laboratory; Hyoung Seop Kim, Chungnam National University

8:30 AM Invited

Effect of ECAP on the Mechanical Properties of Mg Alloys: *Yuri Estrin*¹; Ralph J. Hellmig¹; Milos Janecek²; Torbjorn T. Lamark¹; Mikhail V. Popov¹; ¹IWW, TU Clausthal; ²Charles University

We present results on the effect of equal channel angular pressing (ECAP) on several Mg alloys, including AZ31, AS21X, and Mg-Ni. The enhancement of the yield strength and variations in ductility, as well as the effect on the fatigue life will be discussed. In addition, the influence of ECAP on the acoustic emission will be reported. The microstructures observed in ECAP-processed Mg alloys by TEM differ significantly from those in fcc metals. In the Mg alloys studied, a pronounced small grain structure was shown to develop 'precipitously', already after a single ECAP pass. A residual strain hardening capacity (albeit relatively small) associated with the microstructure produced provides sufficient – and sometimes enhanced – ductility of the ECAP-processed Mg alloys.

8:50 AM Invited

Optimization of Strength, Ductility and Properties of Ultra-Fine-Grained Copper with Nano-Scale Twins: Lei Lu¹; Ming Dao²; *Subra*

*Suresh*²; ¹Institute of Metal Research, Chinese Academy of Sciences; ²Massachusetts Institute of Technology

Tensile and nanoindentation experiments at room temperature show the pulsed-electrodeposited copper samples with high density nanoscale twins have an ultrahigh strength (1.0 GPa) and considerable ductility. Moreover, significantly enhanced rate sensitivity of plastic flow and work hardening rate are also observed in these tests. With an increase in twin density (or a decrease in twin lamellar spacing), rate sensitivity, strength and ductility increase as well. The concept of Twin Boundary Affected Zone (TBAZ) is introduced into a physically-motivated crystal plasticity model to study strength, rate sensitivity and ductility. The orientation and size dependent plastic behavior parallel (plastically softer) and perpendicular (plastically harder) to the twin boundaries is specifically modeled. Parametric studies show that the proposed TBAZ model correctly captures the experimentally observed trend. Possible deformation and failure mechanisms are discussed. Strategies for the optimization of strength and ductility as well as of electrical and mechanical responses will also be addressed.

9:10 AM Invited

Enhanced Mechanical Properties in Ultrafine Grained 7075 Al Alloy: *Yonghao Zhao*¹; Yuntian Zhu¹; ¹Los Alamos National Laboratory

The high strength and high ductility for 7075 Al alloy were obtained by combining the equal-channel angular (ECAP) and natural aging. The tensile yield strength and ultimate strength of the ECAP processed and naturally aged sample were 103% and 35% higher, respectively, than those of the coarse-grained 7075 Al alloy counterpart. The tensile elongation to failure is about 12%. The enhanced strength resulted from high densities of the 2nd-phase particles (G-P zones and meta-stable phase) and dislocations. The origin of the high ductility of the ECAP processed and aged 7075 Al alloy will be discussed. This study shows that severe plastic deformation has the potential to significantly enhance the mechanical properties of precipitated hardening 7000 series Al alloys.

9:30 AM Invited

On Tension/Compression Asymmetry of an Extruded Nanocrystalline Al-Fe-Cr-Ti Alloy: *Leon L. Shaw*¹; Hong Luo¹; ¹University of Connecticut

The tension/compression asymmetry of nanocrystalline materials has been the subject of intensive study in recent years. In this study, a multiphase nanocrystalline Al93Fe3Cr2Ti2 alloy containing 30 vol.% intermetallic particles was prepared via mechanical alloying, followed by hot extrusion. Tensile and compressive tests at ambient and elevated temperatures were performed. The alloy exhibited significant difference in deformation behavior between tension and compression at 25°C, 200°C and 300°C. However, the strengths obtained in tension and compression were similar at 400°C. Systematic microstructure examinations and deformation mechanism analyses indicate that the asymmetry of this nc Al93Fe3Cr2Ti2 alloy is related to its dislocation mediated plastic deformation mechanism, its nanoscale grain microstructure, and premature brittle failure in tension tests.

9:50 AM

Fatigue and Fracture in Bimodal Al 5083: *Peter S. Pao*¹; Harry N. Jones¹; C. R. Feng¹; David B. Witkin²; Enrique J. Lavernia³; ¹Naval Research Laboratory; ²University of California at Irvine; ³University of California at Davis

The fatigue crack growth and fracture resistance of ultrafine-grained (UFG) Al 5083 having a bimodal grain size were investigated. The bimodal Al 5083 was prepared by mixing ball-milled particulates with various amounts of larger grained powders and then extruded into rods. The bimodal Al 5083 thus produced consists of UFG grains and coarse grain bands. With increasing larger grained material, the yield strength of the bimodal Al 5083 is lowered progressively while its tensile ductility and fracture toughness are increased significantly. Fatigue crack growth rates of bimodal Al 5083 are lower than those of all-UFG Al 5083. The higher fatigue crack growth rates in the all-UFG Al 5083 may be attributed to the much smoother fracture surface and lower crack deflection. The fracture toughness and fatigue crack growth of the bimodal and UFG Al 5083 will be discussed in terms of the differences in underlying microstructure and deformation mechanisms.

10:05 AM

Microstructure and Deformation Behavior of Nc Pd: *Julia Ivanisenko*¹; Juergen Markmann²; Harald Roesner¹; Heinz Schiels³; Hans J. Fecht³; Ruslan Z. Valiev⁴; Jorg Weissmueller¹; ¹Forschungszentrum Karlsruhe; ²University of Saarlands; ³University of Ulm; ⁴UFA State Aviation Technical University

A novel method for the preparation of bulk nanocrystalline materials with a grain size <30 nm using the combination of inert gas condensation and subsequent high pressure torsion (hpt) was developed. Here we present results on a comprehensive investigation of the microstructure and mechanical properties of fully dense Pd with a mean grain size of 15 nm. After hpt consolidation, texture measurements have not revealed any preferential orientations, and HRTEM investigations demonstrated the presence of stacking faults inside the nanocrystalline grains. By the contrast, a pronounced texture and developed sub-granular dislocation structures were developed in the Pd specimens with a grain size of 75 nm processed in a similar way. These observations suggest that the operating deformation mechanisms in materials with a grain size of the order of 15 nm include emission of partial dislocations along with grain rotations instead of the slip of full lattice dislocations in coarse-grained materials.

10:20 AM Cancelled

The Effect of Grain Size on the Mechanical Behavior in AA1050

10:35 AM Break

10:45 AM Invited

Intrinsic or Extrinsic Plastic Strain Gradients Enhance the Effectiveness of SPD Processes: *Javier Gil Sevillano*¹; ¹CEIT and TECNUN, University of Navarra

The nanostructuring ability and strengthening effects of severe plastic deformation (SPD) processes significantly differ when comparison is made at equal equivalent strains and homologous temperatures. For instance, large strain wire drawing of BCC or HCP alloys, high pressure torsion (HPT) and accumulative roll bonding (ARB) systematically are quoted to be more effective than equal channel angular extrusion (ECAE), reciprocating extrusion or constrained groove pressing. HPT and ARB induce sample size-dependent extrinsic (macroscopic) plastic strain gradients; BCC or HCP wire drawing induce intense intrinsic (microscopic, associated to the grain microstructure) ones. In both cases those gradients are to be accommodated by an extra storage of geometrically necessary dislocations (GND) absent in other SPD processes. Such extra GND density can explain the superior effectiveness of HPT, ARB or BCC-WD as SPD processes. New SPD process should be designed with enhanced intrinsic or extrinsic plastic strain gradient development ability.

11:05 AM Invited

Modeling the Mechanical Response of fcc Materials Processed by ECAE: *Irene J. Beyerlein*¹; Carlos N. Tome¹; David J. Alexander¹; ¹Los Alamos National Laboratory

In this work we study the asymmetry in the tension versus compression response observed in fcc materials processed by equal channel angular extrusion (ECAE). The substantial difference in the response between these two tests is attributed to a combination of the texture evolution and the grain and subgrain microstructural evolution induced by ECAE. To predict this response we incorporate a recently developed single crystal hardening model into a Visco-Plastic Self Consistent (VPSC) polycrystal model. The hardening law captures the directional anisotropy in the single crystals that is induced by the formation of planar dislocation walls. It also captures the effects of new substructure that dissolves and builds upon previously developed substructure when the strain path changes from ECAE to uniaxial deformation.

11:25 AM Invited

Softening in Constitutive Relationship of Pure Copper at High Strain Level: *Jingtao Wang*¹; Wei Wei¹; Yue Zhang¹; Guang Chen¹; ¹Nanjing University of Science and Technology

To study the constitutive relationship of pure copper at high strain levels, equal channel angular pressing (ECAP) was used to impose high levels into the pure copper samples, and tensile testing was used to estimate the yield stress after ECAP. It is found that the Stress - Strain (accumulated through ECAP) constitutive relationship shows softening as the ac-

cumulated ECAP strain level beyond an equivalent strain of ~4. This behavior could not be described by the existing constitutive relationship models of the Hollomon power-law relationship at low strains, or the Voce exponential relationship at high strains. An new constitutive equation was deduced to describe this softening behavior. And this softening behavior is discussed considering the microstructural evolution during ECAP.

11:45 AM Invited

Strain-Rate Dependence of Tensile Ductility of Cryomilled 5083 Al Alloys: *Bing Q. Han*¹; J. Y. Huang²; Y. T. Zhu³; E. J. Lavernia¹; ¹University of California; ²Boston College; ³Los Alamos National Laboratory

The mechanical properties of nanostructured or ultrafine-grained (UFG) materials have engendered increased interest for the past two decades. Inspection of numerous published studies reveals that there is a strong effect of strain rate on the mechanical properties of nanostructured or UFG materials. In many cases, it is found that the tensile ductility increases with increasing strain rate and the strain rate sensitivity exponent is larger than that in their counterpart coarse-grained materials. In the present study, the mechanical properties and microstructural characterization of several bimodal nanostructured 5083 Al alloys processed from cryomilled nanostructured powders are investigated. It is noted that there are higher values of ultimate tensile strength and ductility as well as compression flow strength at slower strain rates in the cryomilled 5083 Al alloys. The relationships among mechanical properties at different strain rates, microstructural characteristics and deformation mechanisms of these materials are thus explored in the present study.

12:05 PM

Deformation Behavior of Cryomilled Al-Mg Alloy Consolidated via ECAP: *Jichun Ye*¹; Bing Q. Han¹; Dong H. Shin²; Enrique J. Lavernia¹; Julie M. Schoenung¹; ¹University of California; ²Hanyang University

Mechanically alloying in liquid nitrogen (cryomilling) has been proven to be an effective approach to produce nanostructured aluminum powders. Recently, several nanostructured/ultrafine-grained aluminum alloys have been consolidated from cryomilled nanostructured aluminum powders and the mechanical properties have been investigated. It is generally observed that there is a stress drop after a brief work-hardening region and the necking deformation is dominant in the plastic deformation of cryomilled aluminum alloys. Inspection of previous investigation indicates that the consolidation routes have a significant influence on the mechanical performance of aluminum alloys. In the present study, the cryomilled Al-7.5%Mg alloy powders are consolidated using hot isostatic pressing followed by equal channel angular pressing. Tensile properties and microstructural characterization of the consolidated Al-Mg alloy are investigated and compared with those processed via other routes. The influence of intrinsic microstructural characterization arising from different processing routes on deformation mechanisms of cryomilled aluminum alloys is discussed.

12:20 PM

Mechanical Behavior of Nanocrystalline Ni: *Indranil Roy*¹; Manish Chauhan¹; Farghalli A. Mohamed¹; ¹University of California

In the present study, the mechanical behavior of Ni with an average grain size of 100 nm has been investigated. Tensile tests have been performed on the material in the temperature range of 393 to 473 K and strain rate of 10⁻⁵ to 10⁻² s⁻¹. The experimental data reveal high strength, low-strain hardening and a defined yield point. Observations regarding ductility and fracture will be discussed.

Wechsler Symposium on Radiation Effects, Deformation and Phase Transformations in Metals and Ceramics: Irradiation Facilities and Techniques

Sponsored by: The Minerals, Metals and Materials Society, ASM International, TMS Structural Materials Division, ASM Materials Science Critical Technology Sector, TMS Materials Processing and Manufacturing Division, TMS/ASM: Mechanical Behavior of Materials Committee, TMS/ASM: Nuclear Materials Committee, TMS/ASM: Phase Transformations Committee

Program Organizers: Korukonda L. Murty, North Carolina State University; Lou K. Mansur, Oak Ridge National Laboratory; Edward P. Simonen, Pacific Northwest National Laboratory; Ram Bajaj, Bettis Atomic Power Laboratory

Wednesday AM Room: 208
March 15, 2006 Location: Henry B. Gonzalez Convention Ctr.

Session Chairs: Gary S. Was, University of Michigan; Steven J. Zinkle, Oak Ridge National Laboratory

8:30 AM Invited

Materials Issues for High Power Accelerators: *Louis K. Mansur*¹; ¹Oak Ridge National Laboratory

High power accelerators present numerous research issues. Some questions are unique, others are similar to considerations for fission and fusion reactors. There may be conditions for which there are little or no data. Materials research may reduce risk or even establish a new concept's viability. High power accelerators are applied to neutron scattering research and radiation materials science, and proposed for waste transmutation. Others produce radioactive ion beams, or are used for particle physics. Applications are mentioned; spallation neutron sources are emphasized. The design of the Spallation Neutron Source (SNS), a new US materials research facility, is described. The target suffers the highest displacement damage; somewhat lower are beamline windows and a beam dump, where the beam is transferred between accelerators. Other components experience high ionization damage; they also must be designed for radiation resistance. Questions that require future materials research are discussed.

8:55 AM Invited

Materials Irradiation Facilities at the High-Power Swiss Proton Accelerator Complex: *Werner Wagner*¹; *Yong Dai*¹; *Heike Glasbrenner*¹; ¹Paul Scherrer Institute

At the Swiss proton accelerator complex and spallation neutron source SINQ irradiation facilities are operated to investigate materials behaviour under high-dose irradiation conditions. In the frame of STIP (SINQ Target Irradiation Program) hundreds of samples, mainly austenitic and ferritic/martensitic steels like 316L, T91 or F82H, were irradiated under realistic spallation conditions, i.e. in a mixed spectrum of 570 MeV protons and spallation neutrons, to doses up to 20 dpa. As well, solid metals in contact with liquid Hg and liquid lead bismuth eutectic (LBE) were part of the program. In complement, in LiSoR (Liquid Solid Reaction) loop T91 steel was irradiated with 72 MeV protons while being in contact with flowing LBE at elevated temperatures and under tensile stress. The post-irradiation examinations yield valuable information for safety assessments and lifetime predictions of high-power accelerator driven systems using liquid lead alloys as target and coolant material.

9:20 AM Invited

A Comparison of Microstructure in Martensitic and Austenitic Steels Irradiated in SINQ Targets: *Yong Dai*¹; *Xuejun Jia*¹; ¹Paul Scherrer Institut

Martensitic steels F82H and T91 and austenitic steel SA316LN have been irradiated in SINQ targets up to 20 dpa in a temperature range of 80-400°C. TEM observations have been performed. For F82H and T91 the results show: (1) the formation of dense defect clusters and dislocation loops at ≈350°C; (2) the formation of high-density visible He bubbles (> ~1 nm) at temperatures above 170°C; (3) bubbles (or voids) up to 60 nm

large formed in a sample irradiated to 20 dpa / 1790 appm He at 400°C, and a bimodal size distribution was observed; (4) in this sample, the martensite lath structure disappeared accompanied with the formation of new M23C6. For SA316LN steel, high-density small defect clusters and large frank loops were observed. High-density tiny helium bubbles were observed in samples irradiated at >350°C. The difference of microstructure in martensitic and austenitic steels will be discussed.

9:45 AM

In Situ Neutron Diffraction Studies of Artificial Aging in Uranium-Niobium Alloys at LANSCE: *Donald Brown*¹; *Mark A. Bourke*¹; *Robert E. Hackenberg*¹; *Larry Hulst*¹; *David F. Teter*¹; *Dan J. Thoma*¹; ¹Los Alamos National Laboratory

Niobium is soluble in uranium at high temperature, in the body-centered cubic phase, but not at room temperature. The diffusion of Nb in U is rather slow, and if the alloy is quenched at moderate rates a metastable monoclinic phase is produced at room temperature. The properties that make U-Nb attractive, such as enhanced ductility, are a strong function of the Nb content and are optimized in this metastable phase at 6 weight percent. This study was aimed at understanding the stability of the alloy through in-situ neutron diffraction measurements during accelerated aging. Samples were heated in-situ to temperatures between 100°C and 400°C and the development of the interatomic spacings monitored over roughly one-day aging times by taking diffraction patterns at 5-20 minute intervals. The observed changes in the lattice parameter are related to the decreased Nb in solution with time at temperature.

10:05 AM Break

10:20 AM

Topological Model of Martensitic Transformations in Ferrous Alloys: *Xiao Ma*¹; *Robert C. Pond*¹; ¹University of Liverpool

The Phenomenological Theory of Martensite Crystallography is based on the hypothesis that the habit plane is an invariant plane of the shape transformation. Experimental observations of the crystallography of a range of transformations are consistent with this notion, but several instances, including some ferrous alloys, are not. Recently, a topological model of martensitic transformations has been presented wherein the habit plane is a semi-coherent structure, as is observed using TEM, and transformation mechanism is shown explicitly to be diffusionless. The transformation crystallography predicted using the topological approach differs systematically from the classical approach, reflecting the differing compatibility criteria at interfaces between atomic solids, as represented in the former, and continua, as in the latter. Experimental observations of ZrO₂ and Ti alloys are in excellent agreement with the topological model; the objective of the present work is to apply the topological method to ferrous alloys and compare with the phenomenological predictions.

10:40 AM

Kinetic Pathways of Temperature- and Field-Dependent Structural Phase Transitions in Ferroelectric PMN-PT and PZN-PT near Morphotropic Phase Boundaries: *Yu U. Wang*¹; ¹Virginia Tech

Thermodynamic analysis and kinetic modeling are developed to explain recent experimental observations of the structural phase transition sequences, phase stabilities, polarization rotations, crystallographic data, and ultrahigh electromechanical responses of PMN-PT and PZN-PT ferroelectric/ferroelastic perovskites. It is shown that the fascinating while puzzling phase behaviors in such multiferroic oxides can be understood from the perspectives of self-accommodation of spontaneous ferroelastic strain and ferroelectric polarization and self-assembling of ferroelastic and ferroelectric domains at nanometer length scale. Extensive experimental data supporting this theory are presented. Ongoing computer simulation effort to gain better quantitative insight into this problem is also discussed.

11:00 AM Invited

Deformation Dynamics Studies Using Stress Relaxation: *Placid Rodriguez*¹; ¹Indian Institute of Technology

When a tensile or compression test (normally performed at constant extension or strain rate) is interrupted, stress-relaxation occurs since plastic deformation continues to take place as long as the applied stress is sufficiently high for the dislocations to move. Analysis of the load/stress Vs. time data leads to valuable information on the relationship between

stress and plastic strain rate and important parameters like activation area, strain rate sensitivity and the thermal component of the flow stress. Monroe Wechsler's group at Oak Ridge was one of the first to use the technique particularly for studies on irradiation hardening. This paper makes a review of the deformation dynamics results using stress relaxation in a variety of materials; a few examples are also discussed in which the technique has been used to study the kinetics of stain ageing and dynamic recovery.

11:25 AM

The NCSU Radiation Damage Database: Proton-Induced Helium Production Cross Sections: *Wei Lu*¹; Monroe Wechsler²; ¹Oak Ridge National Laboratory; ²North Carolina State University

A radiation damage database is completed at NCSU. It contains damage energy, displacement, helium, and hydrogen cross sections for 23 elemental targets by proton and neutron projectiles up to 3.2 GeV. As a part of the database, proton-induced helium cross section is described in this paper. The cross section calculation runs on CEM2k with default options and on Bertini with three level densities and multistage pre-equilibrium model (MPM) on and off. The calculation results were compared to the experimental data so far available. Such an evaluation suggests that, depending on the target mass, different intranuclear cascade (INC) models or different level densities within the INC model may be chosen for the proton-induced helium production cross section. The database indicates which cross sections give best agreement with experimental data. The criteria derived from the evaluation could be applied to neutrons as well as protons. Neutron and proton cross sections are approximately equal at high energies.

11:45 AM

Monte Carlo Simulations of Stray Neutron Radiation Exposures to Proton-Beam Radiotherapy Patients: *Yuanshui Zheng*¹; Jonas Fonteno¹; Nicholas Koch¹; Wayne Newhauser¹; ¹UT MD Anderson Cancer Center

Radiation therapy is one of the major treatment options for cancers, and proton radiation therapy is gaining increased interest around the world because it offers more normal tissue sparing when compared to conventional radiation therapy. However, second neutron production is of greater concern in proton therapy due to the presence of stray and leakage neutrons that are produced by proton interactions in both the beamline and the patient. The authors predicted the neutron doses to a typical patient receiving proton therapy at the University of Texas M. D. Anderson Cancer Center (Houston) using the Monte Carlo method simulation. The resulting risk of secondary cancer for a patient was also estimated.

2006 Nanomaterials: Materials and Processing for Functional Applications: Carbon Nanostructures

Sponsored by: The Minerals, Metals and Materials Society, TMS Electronic, Magnetic, and Photonic Materials Division, TMS: Nanomaterials Committee

Program Organizers: W. Jud Ready, GTRI-EOEML; Seung Hyuk Kang, Agere Systems

Wednesday PM
March 15, 2006

Room: 214C
Location: Henry B. Gonzalez Convention Ctr.

Session Chairs: W. Jud Ready, GTRI-EOEML; Seung Hyuk Kang, Agere Systems

2:00 PM Introductory Comments

2:05 PM

Microstructural Observations of Deformation Mechanisms in Nanoindented DLC Coatings on Silicon Substrates: *Ayesha Jabeen Haq*¹; *Paul Richard Munroe*¹; Mark Hoffman¹; Phil Martin²; Avi Bendavid²; ¹University of New South Wales; ²CSIRO Telecommunications and Industrial Physics

The surface and subsurface microstructural changes resulting from deformation induced by nanoindentation have been studied in a number

of diamond-like carbon (DLC) coatings on silicon substrates. A range of amorphous hydrogenated carbon films (a-C:H) were deposited onto silicon substrates using a plasma assisted chemical vapour deposition technique. The compositions of the as-deposited coatings were characterised by Raman spectroscopy and transmission electron microscopy (TEM). The coatings were indented to loads up to 500 mN using a 5 µm spherical indenter. Detailed microstructural studies were performed on the indented regions using atomic force microscopy, focused ion beam milling and TEM. The planned presentation will correlate features observed in the load-displacement curves, such as pop-ins and pop-outs, to observed microstructural events, such as the onset of slip on {111}, cracking, delamination and localised phase transformations in the silicon substrate.

2:25 PM

Conductivity Predictions in Carbon-MMC's Based on Contact Resistance Considerations: *Ivica Smid*¹; Erich Neubauer²; ¹Pennsylvania State University; ²Austrian Research Centers

Metal Matrix Composites (MMCs) based on carbon based reinforcements exhibit a high potential for applications as heat sink materials. From theoretical considerations the thermal properties can be tailored by a simple variation of the volume fraction of the reinforcement. An additional parameter of importance in the copper-carbon system is the thermal contact resistance (TCR). By a variation of the TCR the whole range between an insulating interface and a perfect heat transfer can be simulated in theoretical calculations. The realization of the desired experimental values for the TCR, however, is not an easy task. The experimental values of the TCR in the carbon-copper system were determined by the help of photo-thermal methods. The resulting bulk thermal properties have been modeled using finite element methods, allowing a prediction of the maximum achievable conductivity as a function of processing, and filler particle size and shape.

2:45 PM

Grow and Control the Length of Carbon Nanotubes on Silicon Substrates by Chemical Vapor Deposition: *Zhengjun Zhang*¹; Ya Zhou¹; Yang Yue¹; ¹Tsinghua University

Carbon nanotubes were believed not able to grow directly on silicon substrates by chemical vapor deposition from a mixture of ferrocene and xylene, due to the reaction of Fe with Si. Via controlling the growth kinetics to suppress the reaction of Fe with Si, we have successfully deposited carbon nanotubes on silicon substrates. Using the fact that nanosized materials exhibit mostly a lower melting point than the bulk form, we thus used the vaporization of nanosized Au films as a block to suppress nanotubes growth, and established a technique to fabricate arrays of aligned nanotubes on silicon substrates, and to control the length of nanotubes from site to site. This controllable growth of carbon nanotubes on silicon substrates might be further utilized to build large-scale electronic devices, which brings no further contamination to the substrates.

3:05 PM Break

3:20 PM

Carbon Nanotube Deformation - In-Situ SEM Observation and Force Measurement: *Christian P. Deck*¹; Kenneth Scott Vecchio¹; Chi-Nung Ni¹; Prabakar R. Bandaru¹; ¹University of California

Carbon nanotubes (CNTs) have been the subject of great interest in many fields, due to their unique material properties and geometry. In particular, they possess exceptional mechanical strength, which is desirable in many diverse applications, such as field emission, sensing devices, and composite reinforcement. A stage was designed and built to allow in-situ scanning electron microscopy observation of compression, tension, and shear testing of densely-packed mats of well-aligned multi-walled CNTs. These tubes were grown using both thermal and vapor phase chemical vapor deposition (CVD) methods, and different tube lengths and morphologies were investigated. Force measurements were taken during testing, and mechanical properties of the CNT mats were obtained, as well as other properties such as tube-substrate bond strength. The relevance of these results to nanotube-based tactile and flow sensing devices is also discussed.

3:40 PM

Evaluation of the Field Emission Properties of Carbon Nanotubes: Victor Kumsomboone¹; Stephan Turano¹; Brent Wagner¹; Jud Ready¹; ¹Georgia Tech Research Institute

Carbon nanotubes (CNTs) are investigated for field emission (FE) properties for applications in ion electric propulsion and field emission display by altering synthesis parameters. CNTs are grown on quartz and silicon substrates utilizing thermally evaporated Iron (Fe) as a catalyst layer on top of electron-beam evaporated Titanium (Ti) as a conductive layer. CNTs are grown via chemical vapor deposition pyrolysis of hydrocarbon gases at various flow rates. CNTs are observed via scanning electron microscope (SEM). FE properties are evaluated in a diode configuration at a pressure of 10^{-5} Torr, applied voltage ~ 500 V, and cathode/anode separation (CAS) $\sim 500\mu\text{m}$. Electrons flow from the voltage source through the CNTs cathode, across the CAS, and illuminate a layer of phosphor at the anode. Qualitative results include SEM images and macroscopic images of illuminated phosphor. Quantitative results include percentage illumination of the anode, current across the anode, and graphs modeling each vs. various growth controls.

4:00 PM

Growth of Self-Organized Carbon Nanotubes Using Anodic Aluminum Oxide Template on a Si Substrate: Ching-Jung Yang¹; Jia-Min Shieh²; Chang-Hsuan Lee¹; Chih Chen¹; Fu-Ming Pan¹; Bau-Tong Dai²; ¹National Chiao Tung University; ²National Nano Device Laboratories

In this study, we report the development of a carbon nanotube using a thin film of anodic aluminum oxide template on a Si wafer. We sputter 20 nm TiN followed by 10 nm Ni. The TiN layer acts as a diffusion barrier to prevent silicidation of the Ni, which is needed as the catalyst for CNT growth. For the preparation of the AAO template, 1.5 μm Al film was deposited on the Ni layer by thermal evaporation. The nanopores feature a uniform size with a hexagonal pattern. By using the AAO template, the CNTs of a very high density of 1.7×10^{10} tubes/cm² can be grown. The turn-on electric field was 2.8 V/ μm and emission current density was 80 mA/cm² at 8 V/ μm . Our fabrication technique enables us to control the tube diameter, length and density easily. This approach offers a potentially elegant technique for fabricating cold-cathode flat panel displays.

4:20 PM Break

4:35 PM

Thermo-Gravimetric Analysis of Synthesis Variation Effects on CVD Generated Multi-Walled Carbon Nanotubes: Gregg S. B. McKee¹; Kenneth S. Vecchio¹; ¹University of California

The unique properties of carbon nanotubes have suggested a myriad of applications in a variety of fields. However, consistent and optimal growth of high purity, high quality nanotubes has proven to be a challenge. Small variations in synthesis conditions have significant effects upon the final nanotube product. We examine changes in the thermo-gravimetrically determined oxidation behaviors of CVD-grown multi-walled carbon nanotubes with varying synthesis conditions. Catalyst type and synthesis temperature are found to have a measurable impact upon nanotube stability, suggesting differing levels of crystalline perfection in the resulting nanotubes. The results provide evidence showing the catalytic effects of nanotube catalyst particles and their oxides upon the oxidation of nanotube carbon and graphite. The significance of thermo-gravimetric analysis as a characterization tool for carbon nanotubes is discussed.

4:55 PM

Oxidation Activation Energy Determination and Comparison for CVD Grown Multi-Walled Carbon Nanotubes: Gregg S. B. McKee¹; Kenneth S. Vecchio¹; ¹University of California

Oxidation rates are measured and an activation energy determined for several length ranges of as-grown and treated chemical vapor deposition grown nanotubes within a range of 725K to 900K. The activation energy barrier is found to be within the range calculated in the literature and may not change significantly with synthesis method or with changing nanotube length. The results show that the oxidation of carbon nanotubes need not originate in the nanotube caps alone, but may originate in other areas of increased strain energy.

5:15 PM

Energetic Comparison of Single-Walled Carbon Nanotube Computer Simulations: Shalayna L. Lair¹; Lawrence E. Murr¹; William Herndon¹; Stella Quinones¹; ¹University of Texas

An easily applied graphical approach for facilitating precise tailoring during computational construction of modeled uncapped or capped carbon nanotubes or fullerenes is delineated and utilized in this paper. The main enabling concept is nucleation of single and multi-walled carbon nanotubes from end cap structures. A novel construction protocol is used to rapidly create any type of armchair, zigzag or chiral defect-free nanotube. Any feasible combination of length and diameter, along with specific placement of hexagonal and pentagonal rings in end caps, can be controlled. The suggested methodology is used to systematically model heats of formation of a variety of carbon nanotubes and related fullerenes using AM1 semiempirical calculations. The main factors affecting the calculated physical properties, other than size, are the structures of the various base and terminating end caps. The possible relationship of the construction methodology to mechanisms for carbon nanotube nucleation will also be commented on.

3-Dimensional Materials Science: Serial Sectioning

Sponsored by: The Minerals, Metals and Materials Society, TMS Structural Materials Division, TMS: Advanced Characterization, Testing, and Simulation Committee

Program Organizers: Jeff P. Simmons, U.S. Air Force; Michael D. Uchic, Air Force Research Laboratory; Dorte Juul Jensen, Riso National Laboratory; David N. Seidman, Northwestern University; Anthony D. Rollett, Carnegie Mellon University

Wednesday PM
March 15, 2006

Room: 205
Location: Henry B. Gonzalez Convention Ctr.

Session Chairs: George Spanos, Naval Research Laboratory; Michael D. Uchic, Air Force Research Laboratory

2:00 PM Invited

Automated Serial Sectioning: An Enabling Technology for 3D Microstructural Analysis: Jonathan Edward Spowart¹; Herbert M. Mullens²; ¹U.S. Air Force; ²UES, Incorporated

The aim of this presentation is to introduce some of the tools and techniques that have been developed at AFRL for performing automated serial sectioning of advanced materials. These techniques are seen as enabling for many 3D microstructural analysis problems. The presentation will draw from selected examples, spanning a broad range of materials science areas and illustrating the current state of the art in automated serial sectioning. In addition, projections for both the near-term and long-term development of the technology will be provided, highlighting the limitations of current practices and exploring the potential for future enhancements in terms of higher throughput, greater fidelity and increased access to the 3D data.

2:25 PM

Three-Dimensional Characterization of Damage in Shocked Tantalum: Benjamin L. Henrie¹; John F. Bingert¹; ¹Los Alamos National Laboratory

Tantalum plate subjected to shock loading was serially sectioned to interrogate the effect of shock parameters on damage accumulation. A primary goal was to determine correlations between microstructural details and damage in the form of voids and strain localization. Serial sectioning was performed at 5 μm increments using optical microscopy and electron backscatter diffraction (EBSD) as characterization tools. Image segmentation resulted in the reconstruction of void networks that allowed for insight into their nucleation and growth characteristics, and spatial relationships. In addition, the interaction of voids was investigated with regards to the role of strain localization and their connectivity with the void network. Crystallographic orientation data was also applied to enhance the reconstructed data set with anisotropic information. Relevant

microstructural statistics regarding feature distributions were also calculated.

2:45 PM

Visualization of Three-Dimensional Microstructures Reconstructed from Serial Sections in Modified Ti-6Al-4V Alloys with TiB Whiskers: *Scott I. Lieberman*¹; Arun M. Gokhale¹; Sesh Tamirisa²; ¹Georgia Institute of Technology; ²Ohio University

In the development of modified titanium alloys containing in-situ formed titanium boride whiskers (TiB_w), characterization and visualization of the three-dimensional (3D) microstructure is of significant theoretical and practical interest. The properties and performance of the resultant material depend on the attributes of the 3D microstructural geometry. A recently developed montage-based serial sectioning technique has been utilized to visualize and recreate large volumes of 3D microstructure on a millimeter length scale at sub-micron resolution. This technique is useful for detecting and characterizing both short-range and long-range spatial patterns in non-uniform microstructures, and is of relevance for the increasingly diverse potential variations of Ti-6Al-4V-TiB materials.

3:05 PM

Recovery of the Grain Boundary Character Distribution through Oblique Double-Sectioning: *Eric R. Homer*¹; Brent L. Adams¹; ¹Brigham Young University

A new method for the retrieval of the complete grain boundary character distribution (GBCD) by a new oblique double-sectioning (ODS) method is presented. Section cuts taken from the sample at oblique angles are prepared by performing a pair of parallel material removals and their corresponding OIM scans. In this manner an incomplete GBCD, including grain boundary inclination, is measured for each double section. The overall GBCD of the material is then obtained from the set of oblique double-sections in a manner similar to that applied for recovery of orientation distributions from incomplete pole figures. Comparison of ODS with calibrated serial sectioning and the L_v/S_v stereology will be presented along with the solution to the fundamental equations of ODS in the Fourier space. Implementation of the method for rolled and annealed alloy 304 stainless steel will be presented.

3:25 PM

Three-Dimensional Reconstruction of Alpha Laths in Alpha/Beta Ti Alloys: *Robert E. A. Williams*¹; Michael Uchic²; Dennis Dimiduk²; Hamish L. Fraser¹; ¹Ohio State University; ²Air Force Research Laboratory/MLLMD

Alpha/beta titanium alloys have a complex microstructure involving features spanning a wide range of size scales that can vary from sub-micron to millimeters depending on thermo-mechanical history. Recent advances in stereology and microscopy have made quantification of titanium microstructures possible, but in order for stereology to be validated a physical three-dimensional understanding of the features is necessary. 2-D images provide limited information regarding the 3-D nature of the microstructure and can often be misleading. In order to gain a better understanding and reduce error due to stereological measurements, a FEI NOVA 600 microscope was used to section serially through alpha/beta titanium microstructures for digital reconstruction of morphological features. EBSD patterns were also collected in order to visualize and validate the values measured by stereology. The 3-D reconstruction also provides a physical representation of interactions between microstructural features.

3:45 PM Break

4:05 PM Invited

Statistical Microstructural and Crystallographic Analysis in 3D: *Alexis C. Lewis*¹; Andrew B. Geltmacher¹; David J. Rowenhorst¹; George Spanos¹; ¹Naval Research Laboratory

Three-dimensional microstructural measurement, modeling, and analysis techniques are being applied to large datasets which contain the spatial and crystallographic data for statistically representative volumes comprising hundreds of grains. These 3D volumes contain experimental data derived from serial sectioning, Electron Backscatter Diffraction (EBSD), Focused Ion Beam (FIB) characterization, and X-ray tomography. Properties which have been quantified in three dimensions include grain volume, true 3D grain shape (aspect ratio, and number of faces, edges and

corners for each grain), crystallographic orientation, 3D grain boundary networks and populations, and distributions of grain boundary crystallographic normals. This data is input into 3D Image-Based Finite Element Models for analysis of stress and strain evolution in the microstructure. In addition to analytical results, 3D measurement and visualization techniques will be discussed.

4:30 PM

3D Analysis of Early Stages of Creep Void Development: Azmi Abdul Wahab¹; *Milo V. Kral*¹; ¹University of Canterbury

Hydrogen reformer tubes fail by a sequence of creep void nucleation, growth and coalescence. Previous 3D analysis by serial sectioning and computer reconstruction on a severely crept reformer tube indicated that creep voids occurred at grain edges and corners and voids were always found adjacent to chromium-rich M₂₃C₆ precipitates. However, due to the extensive nature of the damage, it was not possible to determine the precise nucleation site. In the present work, samples have been taken at various positions along the length of an ex-service tube (operating different service temperatures) in order to analyze the progress of creep damage. By examining a single reformer tube in various stages of creep, early stages of creep void development can be better understood. Comparisons to interrupted creep test samples and as-cast material will also be presented.

4:50 PM

Three Dimensional Visualisation of Splat-Substrate Interactions in Plasma Spray Coated Systems: Damien McGrouther¹; *Paul Munroe*¹; William Trompeter²; Margaret Hyland³; ¹University of New South Wales; ²Institute of Geological and Nuclear Sciences; ³University of Auckland

A series of coated substrates were prepared by high velocity oxy-fuel (HVOF) spray processing. In this case, nickel powders were sprayed over an aluminium substrate. Spray parameters were controlled such that the powders were sprayed under conditions where their velocity is high, but temperature is low. The particles remain solid, or semi-solid, in flight and their high momentum means that they become embedded in the substrate. Of particular interest is the nature of the interaction between the particle (or splat) and substrate and whether their interaction is solely mechanical or results in partial melting. In this study dual-beam focused ion beam instrumentation has been used to acquire and generate three-dimensional sections through these splats. It is shown that these visualisations allow the degree of melting of the splat to be readily discernable, in addition to the extent of the plastic deformation of the unmelted portions of the splat.

5:10 PM

The Influence of Material Type and Milling Parameters on the Generation of High Quality EBSD Patterns for 3-D Orientation Mapping by FIB Tomography: *Michael Ferry*¹; Nora Mateescu¹; Robin Ma¹; ¹University of New South Wales

The present paper describes the influence of both material type and milling parameters on the quality of electron backscatter diffraction (EBSD) patterns produced by focussed ion beam (FIB) milling. A sound understanding of the influence of these parameters is necessary for accurate three dimensional reconstruction of EBSD orientation maps for generating crystallographic information in small volumes of material. Samples studied in this study include single crystals of a range of metals and inter-metallic compounds with FIB milling parameters and EBSD conditions varied to optimise EBSD pattern recognition. It was found that a reasonable correlation exists between EBSD pattern quality and atomic number of the material with the FIB milling parameters needed to be adjusted accordingly. The work indicates that rapid generation of EBSD orientation maps by FIB milling is most difficult in low atomic number materials.

WEDNESDAY PM

Advanced Materials for Energy Conversion III: A Symposium in Honor of Drs. Gary Sandrock, Louis Schlapbach, and Seijirau Suda: Magnets, Superconductors, Thermoelectrics and Energy Materials I

Sponsored by: The Minerals, Metals and Materials Society, TMS Light Metals Division, TMS: Reactive Metals Committee

Program Organizers: Dhanesh Chandra, University of Nevada; John J. Petrovic, Petrovic and Associates; Renato G. Bautista, University of Nevada; M. Ashraf Imam, Naval Research Laboratory

Wednesday PM
March 15, 2006

Room: 214B
Location: Henry B. Gonzalez Convention Ctr.

Session Chairs: Donald Anton, United Technologies Research Center; Dag Noreus, Stockholm University; Renato G. Bautista, University of Nevada

2:00 PM Invited

Very Fine Controlled Nd-Fe-B Microstructure for High Performances Magnets: *Daniel Fruchart*¹; P. de Rango¹; J. Luo²; S. Miraglia¹; I. Popa¹; S. Rivoirard¹; ¹Centre National de la Recherche Scientifique; ²North Western Institute for Non-Ferrous Metals

Hydrogen Decrepitation (HD) and Hydrogenation Disproportionation Dehydrogenation Recombination (HDDR) are recognized techniques allowing both to deliver very fine microstructures for the design of high performances Nd-Fe-B magnets. HD permits to refine the size of powder particles thus exhibiting the same level of coercivity as the precursor alloy, but interestingly large remanence level were achieved provide a texture was first installed, e.g. via high temperature fast forging. HDDR leads to very high level coercivity but the remanence remains generally low. Introduction of very small amounts of Zr, Nb, Ga etc (e.g. less than 1 at.%) in the precursor alloys allows to optimize well all intrinsic properties. EXAFS analyses have permitted to localize unambiguously the extra precipitates. Kinetic analyses of hydrogenation/dehydrogenation processes were performed and then fairly fitted via Jander and Avrami's type laws for the best understanding of hydrogen interaction and time diffusion mechanisms via extra precipitates.

2:25 PM

Processing and Study of Magnetic and Magnetostrictive Properties of Fe-Zn and FeGaZn Alloys: *Swieng Thuanboon*¹; Robert P. Corson¹; Sivaraman Guruswamy¹; ¹University of Utah

Zinc has a large solubility in Fe and a completely filled "d" shell. With the discovery of dramatic increase of the magnetostriction in Fe by Ga addition, an examination of element Zinc that is adjacent to Ga in the periodic table is of significant interest. In this work, the effect of binary alloying of Zn with Fe and ternary alloying with FeGa alloy on the magnetic and magnetostrictive properties is examined. The alloys were processed using powder metallurgy and vapor phase synthesis, and Zn contents were varied from 2.5% to 20%. An examination of the influence of different processing parameters and the Zn content on the resulting alloy is properties are presented. The alloys were characterized using X-ray diffraction and SEM. Magnetostriction measurements were carried out at different pre-stress levels. Magnetic properties were measured using a vibrating sample magnetometer.

2:45 PM

Effect of Ordering on the Elastic and Magnetostrictive Properties of Fe-27.5 at% Ga Alloy Single Crystals: *Tanjore V. Jayaraman*¹; Swieng Thuanboon¹; Sivaraman Guruswamy¹; ¹University of Utah

FeGa alloys show large magnetostriction that is attractive in sensor and actuator applications. Fe-Ga alloys with composition around 27.5 at.% Ga can be heat treated to obtain ordered phases based on "alpha" (ordered bcc), DO19 (ordered hexagonal) and LI2 (ordered fcc) structures. Our earlier work using polycrystalline samples had shown that magnetostriction is strongly influenced by ordering in this alloy. A more detailed study of the correlation between ordering and magnetostriction using single crystals of Fe 27.5 at% Ga alloys is reported in this paper. X-ray and electron

diffraction were used to study the ordering in this alloy. Magnetostriction measurements were carried out at different pre-stress levels. Magnetic properties were measured using a vibrating sample magnetometer. Elastic constants were measured using Resonant Ultrasound Spectroscopy.

3:05 PM

Thermoelectric Properties of High Temperature Boron Cluster Materials: *Takao Mori*¹; ¹National Institute for Materials Science

The search for thermoelectric materials is being carried out with great intensity because of the huge possibilities for useful energy conversion of waste heat. There is obviously a particular need to develop materials which can function at high temperatures. Boron-rich cluster compounds are attractive materials for their stability under high temperature typically exhibiting melting points above 2200 K. The framework of new rare earth boron cluster compounds that we have discovered is basically composed of boron clusters while heavy rare earth atoms reside in spaces among the clusters, and we note that they have substantially lower thermal conductivities (favorable for thermoelectric applications) compared to β -boron systems which have been previously investigated. REB₃₀-type compounds exhibit Seebeck coefficients greater than 200 μ V/K at high temperatures and unlike most compounds, the figure of merit shows a steep increase at T>1000 K. Properties of other novel B₁₂ icosahedral cluster-containing compounds will also be presented.

3:25 PM

High Pressure Raman Spectroscopy Studies on Organic "Plastic Crystal" Thermal Energy Storage Materials: *Raja S. Chellappa*¹; Dhanesh Chandra¹; ¹University of Nevada

Alcohol derivatives of neopentane are potential candidates for thermal energy storage applications. The phase transformation temperatures at one atmosphere of pure compounds are well established and these materials typically undergo a solid-solid transition from a low temperature ordered structure to a high temperature orientationally disordered "plastic crystal" cubic phase. Examples of these "plastic crystals" include Pentaerythritol [(PE):C(CH₂OH)₄], and Neopentylglycol [NPG:(CH₃)₂C(CH₂OH)₂]. We are conducting a systematic study to characterize the pressure induced phase transformations in these compounds. We will present results from our high pressure Raman spectroscopy studies conducted at room temperature for PE, and NPG. Based on our analysis of the various Raman modes and pressure induced wavenumber shifts, PE exhibits phase transformations at ~4.8 GPa, ~6.9 GPa, and ~9.4 GPa before amorphization at ~15 GPa.

3:45 PM Break

4:00 PM

Peculiarity of Ternary Stannides and Antimonides Exhibiting Potentially Thermo-Electric Properties: Crystal Structures, Physical Properties, Electronic Structures: L. P. Romaka¹; O. Bodak¹; Yu. Y. Stadnyk¹; M. G. Shelyapina²; E. K. Hlil³; *Daniel Fruchart*³; P. Wolfers³; ¹Ivan Franko Lviv National University; ²St. Petersburg State University; ³Centre National de la Recherche Scientifique

Three different types of new ternary stannides and antimonides have been recently synthesized and investigated for their structural and physical properties, and systematically analyzed in terms of band structure determination. These materials are formed with an early d-metal such as Ti, Zr, Hf (as well as Sc for a part), a late d-metal such as Co, Ni, Cu, and X being Sn or Sb. The crystal structure analyses show that they crystallize either with a derivative Cu₂Sb, or a TiNiSi or mostly with the MgAgAs (semi-Heusler) type structure. Strong covalent bonding are evidenced from this analyses. The band structure calculations reveal that the late d-metal bands do not contribute significantly to the conduction, but the conductivity (if any) issues from the d- or p- type electrons of the early d-metals. This allows to control fairly the opening a gap (or semi-gap) at EF via the VEC, and to initiate interesting thermo-electric properties.

4:20 PM

Polymer Derived Carbon Electrode Materials for Electrochemical Capacitors: Ravinder Reddy Nagireddy¹; *Ramana G. Reddy*¹; ¹University of Alabama

Electrochemical capacitors are charge storage devices. Electrochemical capacitors can be classified into two types, electrochemical double

layer capacitors (EDLC's) and capacitors based on pseudocapacitance. In EDLC, when a high surface area electronic conductor material like carbon is brought in contact with an ionic conducting electrolyte, a charge accumulation is achieved electrostatically on either side of interface, leading to the development of an electrochemical double layer. In this study carbon materials are derived from a polymer source and are studied as electrode material for electrochemical double layer capacitors. The polymer source is dried at high temperatures to yield carbon. Carbon electrode surface is characterized using NOVA 1200 gas sorption analyzer. It is also characterized using XRD and SEM. Carbon electrode was electrochemically characterized using cyclic voltammetry (CV). Modeling results of potential distribution in porous carbon electrode under cyclic voltammetric conditions will be presented.

4:40 PM

Phase Transition and Thermal Studies of Polyalcohols Thermal Energy Storage Solid Solutions: *Wen-Ming Chien*¹; Dhanesh Chandra¹; ¹University of Nevada-Reno

Low temperature X-ray diffraction and thermal property studies of the solid-solid state phase transition for the polyalcohols (pentaerythritol (PE), pentaglycerine (PG) and neopentylglycol (NPG)) thermal energy storage solid solutions have been investigated by using X-ray diffractometry and differential scanning calorimetry (DSC) methods. X-ray diffraction studies on polyalcohols solid solutions, PE-NPG and PG-NPG, are from -10°C to 50°C. XRD results shows the + mixed phase at the related low temperature (-10°C) for both PE-NPG and PG-NPG solid solutions. At high temperature range, XRD results show phase for PG-NPG solid solution and + mixed phase for PE-NPG solid solution. There are only two Bragg peaks, (111) and (200), shown in phase XRD patterns. The polyalcohols solid solutions have been cycled 5 times between -20°C to 100°C at different DSC scan rates to study the phase transition properties. DSC results of both PE-NPG and PG-NPG solid solutions show that the solid-solid state phase transition is near room temperature. Details of low temperature phase transition XRD and DSC results of PE-NPG and PG-NPG solid solutions will be presented.

5:00 PM

Microstructure and Texture of Cast BixSb1-x Alloy Processed by Angular Reduction Extrusion: *Jae-Taek Im*¹; K. Ted Hartwig¹; Jeff Sharp²; ¹Texas A&M University; ²Marlow Industries, Inc.

Multipass Equal Channel Angular Extrusion (ECAE) with an area reduction in the exit channel enables one to produce heavily deformed and textured materials. Such an approach is effective for microstructure breakdown and for developing texture to bulk materials. Cast BixSb1-x alloy was extruded above the recrystallization temperature through 90° die for up to four extrusion passes and with area reduction to 75%. The microstructure is characterized by polarized optical microscopy and SEM, and the texture by X-ray diffraction. The results are reported.

5:20 PM

The Development of Metal Oxide Based Supercapacitors: Beth McNally¹; Nandakumar Nagarajan¹; *David S. Wilkinson*¹; Igor Zhitomirsky¹; ¹McMaster University

The development of a viable power storage system for electric vehicles is gaining importance. The cyclic behaviour caused by repeated acceleration and braking requires a robust system for both short and long term energy storage. A system combining a battery and an electrochemical supercapacitor (ES) has been proposed. The battery provides long-term storage and a constant energy output, with the ES assisting during peak load situations. The discovery of electrochemical capacitance in nickel and cobalt oxides has led to investigation of these materials as alternatives to ruthenium and iridium oxides. Our work with ESs focuses on the recent developments in the cathodic electrolytic deposition of oxide films. Using polyethylenimine we can produce thick, crack-free oxide films after heat treatment. The presence of the polymer also reduces the particle size within the film both as deposited and after heat treatment. Capacitance values of over 100 F/g have been achieved using cyclic voltammetry for both nickel oxide and cobalt oxide.

Alumina and Bauxite: Plant Design, Operation and Maintenance

Sponsored by: The Minerals, Metals and Materials Society, TMS Light Metals Division, TMS: Aluminum Committee

Program Organizers: Jean Doucet, Alcan Inc; Dag Olsen, Hydro Aluminium Primary Metals; Travis J. Galloway, Century Aluminum Company

Wednesday PM
March 15, 2006

Room: 7B
Location: Henry B. Gonzalez Convention Ctr.

Session Chair: Jean-Pierre Riffaud, Alumina Partners of Jamaica

2:00 PM Introductory Comments

2:10 PM

Operating Cost - Issues and Opportunities: *Peter-Hans Ter Weer*¹; ¹TWS Services and Advice BV

The operating cost of a bauxite and alumina project is often regarded as a burden to have to deal with or at best as an unavoidable, sometimes even bureaucratic, management requirement. However in a sense the operating cost and its underlying rationale provide tools to assess the "health" of a project and they may offer improvement opportunities. This paper provides an insight in facets and issues related to the operating cost of a bauxite and alumina project and it explores ways for improvement.

2:35 PM

"Alumina Refineries 21st Century" Computerized Non-Polluting and Green Fields: *Milenko Dracic*¹; ¹Technip

This article is based on practical experience on gibbsite (hydrargillite) and boehmite bauxite processing with worldwide technology. The author gained industrial experience involving feasibility studies, conceptual design, construction, operation and maintenance of alumina refineries worldwide. This paper addresses the best new technical solutions regarding low operating costs and highest quality product, including higher environmental protection. Greenfield equipment used in these technologies is manufactured in various developed countries. The author has tested different technology and equipment successfully in Kombinate Aluminiuma Podgorica - Montenegro and particularly in Brazilian Company of Aluminium - Brazil while working in bauxite processing, power plant, and environmental engineering. This new technology is different regarding all the actual Bayer process technology.

3:00 PM

New Chemistry for Alumina Recovery from Lateritic Ores: *William F. Drinkard*¹; ¹Drinkard Research and Development Corporation

We have been developing new chemistry for the recovery of alumina from lateritic ores for the last seventeen years. This new process chemistry promises the elimination of red mud wastes, the ability to use a wider range of alumina containing ores because of superior silica and organic rejection, reduction of operating costs by not requiring settling, and possible elimination of the costliest and most energy-intensive operations in alumina refining, "calcination".

3:25 PM

Digital Fieldbus Implementation for Mineral Processing: *Manoj Pandya*¹; ¹Alcan Engineering

This paper talks about the implementation of digital communication for process control equipment from concept through to commissioning. The topics include the technology migration plan, associated risk management, engineering design process, and commissioning including benefits gained and the tips and traps for a successful project implementation. A technological change is emerging in the process control and monitoring environment. The enormous economic benefits of the application of digital communication for instrumentation equipment are influencing the decision to abandon the conventional point-to-point technology making the shift to digital technology imminent. To date the large-scale use of this technology has been limited to the petro-chemical sector; however, Alcan has taken the step to keep abreast of this technological change with

WEDNESDAY PM

the introduction of the Foundation Fieldbus and Profibus as part of the A\$2.2bn expansion of Alcan Gove's alumina refinery.

3:50 PM Break

4:10 PM

Maximizing Bauxite Grinding Mill Capacity to Sustain Plant Production: *Pierre G. Cousineau*¹; Jean Larocque¹; Colin Thorpe²; ¹Alcan Bauxite & Alumina; ²Alcan Engineering Pty, Ltd

In 2002, a new bauxite wet grinding circuit was commissioned in Alcan's Vaudreuil alumina plant. It replaced the original 60-year-old dry grinding circuit. The former circuit restricted the type of bauxite that could be processed. The new installation, consisting of two rod and ball mills, enabled the plant to improve alumina recovery, process ores with higher moistures and reduce bauxite supply costs. In March 2004, important premature equipment damage was noticed on both mills. In order to avoid significant production losses, it was necessary to upgrade each mill to handle full plant needs, as the repairs on each mill were estimated to last about 6 weeks. A task force was formed with the aim of identifying quick and efficient solutions. Alcan Engineering's milling model was used to evaluate various options. Conclusions and recommendations coming out of the study and plant results are presented.

4:35 PM

Upgrade of Existing Circulating Fluidized Bed Calciners at CVG Bauxilum without Compromizing Product Quality: *Hans W. Schmidt*¹; Michael Missalla¹; Vladimir Hartmann²; Guzman Lugo²; Olivier Hennequin³; Andrew Carruthers⁴; ¹Outokumpu Technology GmbH; ²CVG Bauxilum; ³Alcan Bauxite & Alumina/Alcan Engineering Gardanne; ⁴Alcan Bauxite & Alumina Montreal

To date 50 Circulating-Fluidized-Bed-Calciners have been installed in the alumina industry worldwide or are under construction. They represent a production capacity of 28 million tpa. Over the years, 17 existing calciners were upgraded. Recently, the capacities of the 3 initial CVG-Bauxilum calciners in Puerto-Ordaz, Venezuela were increased to over 2,000 tpd from 1500 tpd, using new concepts. The paper presents performance figures from the existing calciners before and after the upgrade as well as relevant product data. Particle breakage achieved with the upgraded calciners was reduced, while the capacity was increased by approximately 30%. All other product quality data, e.g. LOI, BET, remained unchanged. The specific energy consumption was reduced. Particle emissions of the calciners were reduced by adding a third ESP-field. The close co-operation between Owner, Contractor, and Designer, during the project resulted in a major success: Project schedule was met without compromising high safety standards. Guaranteed performance characteristics were fulfilled.

5:00 PM

Influence of Variables of Process in the Agglomeration Phase on the Attrition of the Hydrate and Its Relationship with Its Morphology: *Erik Farias*¹; ¹CVG Bauxilum

Considering attrition and granulometric distribution an important part in the quality of alumina and the small amount of morphologic information on this produced in CVG Bauxilum, the following work has shown the effects of the independent variables on dependent variables (productivity, agglomeration, attrition) of the process in the agglomeration phase in relation to its morphology. The contribution of this research will help to initiate the appropriate changes in the process to obtain a product of high quality.

5:25 PM

Crystal Growth Modifying Reagents; Nucleation Control Additives or Agglomeration Aids?: *James A. Couter*¹; ¹Nalco Australia

Crystal growth modifiers are commonly used in the Bayer process to increase the average gibbsite particle size and improve the particle size distribution during crystallisation from supersaturated sodium aluminate solutions. With respect to the mechanism of action there has been much debated as to whether this result could be due to the additives aiding agglomeration or reducing the number of secondary nuclei. Presented here is work completed on both synthetic and Bayer plant liquors, over various experimental conditions, in order to study the mechanism of action of CGM additives. Crystallisation kinetics, secondary electron microscopy (SEM), molecular modeling and atomic force microscopy (AFM) data are

collected to examine the impact that these surface active additives have on the precipitation process.

5:50 PM

Plantwide Replacement of the Existing Control Equipment by a New DCS at AOS: Joerg Ruester¹; Holger Grotheer¹; *Rolf Arpe*¹; ¹Aluminium Oxide Stade GmbH

Since the start-up of the plant in 1973 AOS has been running with single loop process control equipment. The majority of the controllers need to be replaced, since there is no more support available. Therefore, AOS decided to install a modern DCS. Along with the implementation of the system a reduction of staff is supposed to be achieved by means of centralization of the current eleven control rooms and by a higher level of automatization. This paper describes the experience with the hot cut-over of the DCS in a running system, the opportunities of a DCS at AOS and the design of a new central control room.

Aluminum Reduction Technology: Cell Development Part III and Emerging Technologies

Sponsored by: The Minerals, Metals and Materials Society, TMS Light Metals Division, TMS: Aluminum Committee

Program Organizers: Stephen Joseph Lindsay, Alcoa Inc; Tor Bjarne Pedersen, Elkem Aluminium ANS; Travis J. Galloway, Century Aluminum Company

Wednesday PM

March 15, 2006

Room: 7A

Location: Henry B. Gonzalez Convention Ctr.

Session Chair: Joaquín J. Fernández Fernández, Alcoa

2:00 PM

Experiences with Long Power Interruption Periods and Lower Amperage Operation in a VS Soderberg Potline: *Jean Yamamoto*¹; Leonardo Paulino¹; Carlos Eduardo Zangiacomi¹; ¹Alcoa Aluminum Inc, Brazil

On December 27th, fuses failed in three rectifier units of Potline #1 in an Alcoa Smelter causing a long and dangerous power interruption. This paper presents the efforts made to reestablish full control of pots with imminent bath freezing process after spending a long period without current and operating with only 70% of nominal amperage. The presentation will focus on two main issues: 1) Actions to reestablish the full pot control after power interruption; 2) Procedures implemented to operate pots at lower amperage level during scheduled switchyard rectifier/transformer maintenance. Actions taken to reestablish pot control during longer power-off period will be presented to operate pots with a risk of freezing electrolyte. Additionally, some strategies will be presented to minimize the risks involved during the successive amperage reduction adopted for switchyard maintenance. Finally, some recommendations will be given to foresee and prevent transformers and rectifiers from unexpected failure mode.

2:25 PM

Influence of Thermo-Hydraulic Fields on Structural Mechanics of Aluminum Reduction Cells: *Yasser Safa*¹; Michel Flueck¹; Michel Rappaz¹; ¹Swiss Federal Institute of Technology EPFL

The elasto-thermal deformation in pot shell of aluminum reduction cell is obtained by solving a stationary elasticity problem with thermal expansion effect as an applied force. The temperature distribution in the whole smelting cell is obtained by two approaches, the first one is based on electro-thermal model without velocity fields, an artificial thermal conductivity is thus used in the heat equation. The second approach is based on a coupled model involving thermal, electromagnetic and hydrodynamic fields. An elasto-thermal calculations corresponding to these two approaches is carried out. The results show the influence of thermal convection on the heating of side walls of the cell. They also exhibit a correlation between velocity fields and mechanical deformation. Strain and stress fields are also presented.

2:50 PM

Towards a Proper Understanding of Sideledge Facing the Metal in Aluminium Cells: *Asbjørn Solheim*¹; ¹SINTEF

Existing calculation models and hypotheses concerning the sideledge facing the metal in aluminium electrolysis cells are critically examined. It can be concluded that the commonly used heat transmittance theory for heat transfer and growth of ledge is not correct, although the existence of the sideledge can probably only be explained by a bath film between metal and sideledge. Most likely, the bath film is maintained by a source of liquid bath at the bottom of the cell, and the film is alumina-saturated at a temperature close to the metal temperature. An alternative conceptual model for the formation of sideledge facing the metal is briefly outlined. According to the model, formation and removal of sideledge at the metal level will be slow, and the dynamic behaviour can not be directly related to the superheat or to the heat transfer coefficient.

3:15 PM

Technoeconomic Assessment of the Carbothermic Reduction Process for Aluminum Production: Established versus Future Technologies: *Bill Choate*¹; John A. S. Green²; ¹BCS, Inc.; ²JASG Consulting

In pursuit of the aluminum industry Vision and Roadmap goals, the Department of Energy has partially supported a consortium of Alcoa and Elkem in the development of the Aluminum Carbothermic Technology – Advanced Reduction Process (ACT-ARP), which promises significant energy and emission reductions. This report explores the progress of the ACT-ARP as a potential replacement for the Hall-Héroult process in the context of several evolving Hall-Héroult development scenarios. Considerable progress has been made and demonstrated, including new furnace wall designs integral to successful operation of Stage 1 reactor, operational characteristics of vapor recovery reactor and aluminum de-carbonization reactor, as well as significant modeling and simulation. Despite these considerable accomplishments, there are still formidable technical and economic challenges to overcome before the ACT-ARP can replace the conventional Hall-Héroult process, such as slag and scale formation, metal and carbon quality issues, mini-mill operation, etc. All these and other issues will be discussed.

3:40 PM Break

4:00 PM

Ionic Liquids Electrowinning of Aluminum in Batch Mode Cells: *Mingming Zhang*¹; Ramana G. Reddy¹; ¹University of Alabama

A batch-recycle electrowinning cell system was developed to deposit aluminum from 1-hexyl-3-methylimidazolium chloride and aluminum chloride mixture (ionic liquids) at low temperatures. In this system, two types of laboratory cells were used to recycle electrolyte in batch mode: one was cylindrical while the other was in rectangular geometry. During the course of batch experiments, the behavior of current density, current efficiency, cell voltage, aluminum ion concentration, specific energy consumption and process time on both types of cells were analyzed. The results showed the rectangular cell was superior to the cylindrical cell in terms of electrolyte recycling efficiency and cell current efficiency. Energy consumption for rectangular cell system was less than 3 kWh/kg aluminum at current densities up to 350 A/m² and cell current efficiencies ranged from 80-90%. Based on these results, the development of large scale Electrowinning Cells for the production of aluminum at low temperatures was also discussed.

4:25 PM

Size Distribution of the Bubbles in the Hall-Héroult Cells: *Sandor Poncsak*¹; Laszlo Istvan Kiss¹; Dominic Toulouse¹; Alexandre Perron¹; Sebastien Perron²; ¹Universite du Quebec a Chicoutimi; ²Alcan International Ltd.

Bubbles in the Hall-Héroult cells act as a momentum source, but they also represent an additional electrical resistance. In order to understand how bubbles play their role, the evolution of the bubble layer structure – namely the number, size and spatial distribution of the bubbles – need to be known. As direct observation is not possible, we have little information about bubble sizes. Neither small scale electrolysis cells nor real scale water-air models can reproduce correctly the morphology of the bubble layer in the electrolysis cell. A mathematical model using the Lagrangian description of the bubble layer has been built and presented in earlier papers. The simulator was first validated with industrial scale air-water systems then the bubble size distribution was calculated using physical

properties of a real cell. This paper presents the impact of cell design on the structure of the bubble layer as computed with our simulator.

4:50 PM

Study on Bubble Behavior on Anode in Aluminum Electrolysis-Part I: *Zhaowen Wang*¹; Bingliang Gao¹; Haitao Li¹; Zhongning Shi¹; Xiaodong Lu¹; Zhuxian Qiu¹; ¹Northeastern University

A tailor made data recorder was used to continuously measure cell voltage fluctuation status during electrolysis in lab scale. Anode gas bubbles generation and departure process that causes cell voltage fluctuation was analyzed. Average values of the voltage peaks were calculated. The effects of anode current density and anode size on bubble size and bubble departure rate were discussed. It was found that bubble size changed largely at different anode current density and also affected by anode sizes. The bubble departure rate was also affected by anode current density and anode size. The bubble-releasing rate became stable at a special current density for certain size of anode.

5:15 PM

Study on Bubble Behavior on Anode in Aluminum Electrolysis-Part II: *Bingliang Gao*¹; Xianwei Hu¹; Junli Xu¹; Zhongning Shi¹; Zhaowen Wang¹; Zhuxian Qiu¹; ¹Northeastern University

The see-through cell was used to investigate the bubble behavior on carbon anode and inert anodes. The observation confirmed that the bubble generation process on metal anode could be divided into three steps: anode oxidation and oxygen generation and bubble departure. The bubbles generated on the carbon anode coalesced into a big bubble before suddenly releasing from the anode. According to the time-cell voltage trace during electrolysis and see-through cell tests, the bubble behavior under the anode showed many differences among three types of anodes, and probably linked to the wettability of the materials by the electrolyte. The see-through cell is a very effective method in studying bubble behavior even at high anode current density.

5:40 PM End

Amiya Mukherjee Symposium on Processing and Mechanical Response of Engineering Materials: Steady State Deformation of Materials - Part II

Sponsored by: The Minerals, Metals and Materials Society, TMS Materials Processing and Manufacturing Division, TMS Structural Materials Division, TMS/ASM: Mechanical Behavior of Materials Committee, TMS: Shaping and Forming Committee
Program Organizers: Judy Schneider, Mississippi State University; Rajiv S. Mishra, University of Missouri; Yuntian T. Zhu, Los Alamos National Laboratory; Khaled B. Morsi, San Diego State University; Viola L. Acoff, University of Alabama; Eric M. Taleff, University of Texas; Thomas R. Bieler, Michigan State University

Wednesday PM
March 15, 2006

Room: 217C
Location: Henry B. Gonzalez Convention Ctr.

Session Chairs: Norman Ridley, University of Manchester; K. Ted Hartwig, Texas A&M University

2:00 PM Invited

Creep Mechanism for Grain Growth: *James C. M. Li*¹; Bhakta B. Rath²; ¹University of Rochester; Naval Research Laboratory

Grain growth is usually a diffusion process across grain boundaries. It can be accompanied by subgrain rotation (Li, J. Appl. Phys. 33, 2958 (1962)) or nanograin rotation (Haslam, et al. Mat. Sci. Eng. A318, 293 (2001)). However, grain boundary migration can be achieved also by dislocation motion or creep. (Li, Trans. TMS-AIME 245, 1591 (1969)) The evidence is the power law relationship between driving force and boundary velocity and an activation energy which approaches that of self diffusion at low driving forces and decreases with increasing driving force. (Rath and Hu, Trans. TMS-AIME, 245, 1577 (1969)). The creep mechanism may involve grain rotation (Li, et al. Acta Metall. 1, 223 (1953)) or may not. (Rath and Hu, cited above). When grain rotation is involved, it

provides a mechanism for the coupling between grain boundary migration and grain rotation. (Cahn and Taylor, Acta Mat. 52, 4887 (2004)).

2:20 PM

Assessment of the Creep Behavior of Molybdenum Silicide Alloys for Ultra-High Temperature Applications: Pascal Jehanno¹; Martin C. Heilmair²; Holger Saage²; Mike Boening¹; Heinrich Kestler¹; ¹Plansee AG; ²Otto Von Guericke University

Due to their outstanding mechanical and creep properties refractory metal silicide alloys may be first choice candidates for ultra-high temperature applications in oxidizing environment beyond Ni-base superalloys. The creep behavior of a 3-phase Mo-9Si-8B (at.%) alloy was characterized by tensile and compressive tests with volume fractions of about 15% of Mo₃Si and 30% T2 phase and the remainder being a Mo_(ss) solid solution. Two processing variants possessing either an intermetallic compound or a Mo_(ss) matrix were comparatively assessed. Values for the stress exponent *n* and for the activation energy of creep *Q* were determined showing that material with the continuous and ultra-fine Mo matrix (grain size around 1 μm) exhibits superplastic behavior with a (record-breaking) strain to failure of more than 400%. Annealed material with a coarsened microstructure, however, yields promise for satisfactory high temperature creep resistance at temperatures up to 1300°C.

2:40 PM

Microstructure and Damage Tolerance of Al-Cu-Mg-Li Alloys for Age Forming: Marco J. Starink¹; Nong Gao¹; Nicolas Kamp²; Shun Cai Wang¹; Ian Sinclair¹; ¹University of Southampton; ²University of Manchester

Age forming of Al based alloys for damage tolerant applications requires an alloy with good age formability and good post-forming mechanical properties. To investigate optimisation of this balance, several newly designed Al-Cu-Mg-Li (Mn,Zr,Sc) alloys were subjected to artificial ageing representative of age-forming. It was seen that combinations of yield strength and fatigue crack growth resistance could be achieved that are at least comparable to the incumbent damage tolerant material for such applications, whilst creep rates at the ageing temperatures applied were better than those achieved in commercially applied age forming processes of heat treatable Al based alloys. Coarse grain structure and high Li content are associated with good fatigue crack growth resistance but reduce age formability. The underlying physical aspects responsible for the balance between creep rates and resulting properties are discussed.

3:00 PM Invited

A New Approach to Grain Boundary Engineering for Ceramics: Tadao Watanabe¹; Sadahiro Tsurekawa¹; Varanasi Sri Rama Chandra Murthy¹; ¹Tohoku University

In recent years, the potential and the usefulness of the grain boundary engineering for polycrystalline and nanocrystalline materials have been well demonstrated for metallic materials by several groups including the authors'. This paper will introduce a new approach and challenge of the grain boundary engineering for ceramics which the authors have recently performed to develop high performance structural ceramics. It was found that the control of oxidation brittleness and improvement in wear resistance of SiC were achieved by controlling the grain boundary microstructure, defined by the grain boundary character distribution (GBCD), the grain boundary connectivity, and the grain boundary density (grain size), at least. A new processing of the grain boundary microstructure based on Reactive Metal Penetration (RMP) was found to produce an extremely high fraction of low-energy fracture resistant grain boundaries, which may result in an improvement of mechanical properties of Al/Al₂O₃ composites.

3:20 PM Invited

Superplasticity as Scientific and Practical Challenges: Oskar A. Kaybyshev¹; ¹Institute for Metals Superplasticity

The review on the nature of superplastic deformation is presented. The possibilities of low temperature high rate superplasticity occurrence and microstructure refinement as means for converting commercial alloys into superplastic state are analyzed. Data on manufacturing large size billets with nano, submicro and microcrystalline structures are presented. Examples of practical use of superplasticity are provided.

3:40 PM Invited

Diffusion-Controlled Processes on the Grain Boundaries and Plasticity/Superplasticity of Polycrystalline and Nanostructured Metals and Alloys: Yury R. Kolobov¹; Ilya V. Ratochka²; ¹Belgorod State University; ²Institute of Strength Physics and Materials Science Sb RAS

The main both original and literature research results of the peculiarities of the effect of grain boundary diffusion atom flow on structure evolution and mechanical properties of metals and alloys as well as during superplastic deformation have been reviewed. The interconnection and intereffect of diffusion processes, sliding and grain boundary migration as factors, determining the development of plastic deformation at examined conditions are analyzed. The peculiarities of grain boundary diffusion of substitution from impurity environment (coating) in nanostructured metals and alloys relative to the respective ones in coarse grained metals and alloys have been investigated. The physical reasons for considerable (by some orders of magnitude) increase of diffusion penetration of grain boundaries in nanostructured state are discussed. The features of manifestation of low temperature and/or high-strain rate superplasticity in nanostructured metals and alloys have been considered.

4:00 PM Break

4:10 PM Invited

Effect of High Temperature Pre-Straining on Superplastic Properties: Bhagwati Prasad Kashyap¹; ¹Indian Institute of Technology, Bombay

Typical quasi-single phase and two-phase superplastic grade materials were subjected to pre-straining over wide ranges of temperatures and strain rates, including that which belongs to superplastic region. There occurred, texture evolution, grain growth, grain-morphological changes, cavitation etc., some of which were subsequently found to have deleterious effects while others were found to improve superplastic properties. The nature of stress-strain and log(stress)-log(strain rate) curves were analyzed towards quantifying and generalizing the correlations between flow behaviour and microstructural evolution during pre-straining. Superplastic deformation of the pre-strained tensile specimens was found to ascertain steady state flow behaviour to limited extent but, deformation to large strains, once again resulted in strain sensitive flow stress or pseudo-steady state. The effects of pre-straining and non-steady nature at large strains were examined vis-à-vis steady state flow property in order to evolve an indirect measure of microstructural parameters.

4:30 PM Invited

Effect of Strain Rate Path on Cavitation in Superplastic AA5083: Norman Ridley¹; P. S. Bate¹; B. Zhang¹; ¹University of Manchester

Previous work on aluminium alloys has demonstrated that rapid pre-straining can lead to enhancement of superplastic (SP) behaviour. Both experimental and modelling studies have shown that the rapid pre-strain is often associated with a reduction in flow stress and an increase in strain rate sensitivity, *m*, in the later stages of deformation, relative to constant strain rate deformation. The higher value of *m* leads to a greater uniformity of thickness in a formed part. However, aluminium alloys are prone to cavitation during superplastic flow, and metallographic observations suggest that cavities are most likely to develop at grain boundary particles. The present work investigates the effect of rapid pre-strain on cavitation behaviour in SP AA5083 deformed under both uni-axial and bi-axial conditions, and compares cavity density, size distribution and cavity shape, with that for material deformed under constant strain rate conditions. The mechanism(s) of cavity growth are also examined.

4:50 PM

Grain Boundary Processes in High Temperature Deformation: Atul H. Chokshi¹; ¹Indian Institute of Science

High temperature plastic deformation may occur by intragranular dislocation processes or intergranular processes that depend on grain sizes. Grain boundary sliding is an important mode of deformation in fine grained materials, and it is requirement for superplastic deformation. The occurrence of grain boundary sliding can also lead to premature failure by the nucleation, growth and interlinkage of cavities. Grain boundary processes are also of current interest in examining plastic deformation in nanocrystalline materials. Professor Amiya Mukherjee has made several important contributions to evolution and scientific examination of high

temperature plastic flow and fracture, and this report will highlight current understanding of such phenomena.

5:10 PM Invited

Transformation Superplasticity of Cast Ti and Ti-6Al-4V with Coarse Grain Size: Qizhen Li¹; Edward Y. Chen²; Doug R. Bice²; *David C. Dunand*¹; ¹Northwestern University; ²TiTech, International, Inc.

Unlike fine-structure superplasticity which relies on grain-boundary sliding and necessitates fine, stable grains below about 10 micrometers, transformation superplasticity relies on internal stresses produced during thermal cycling around an allotropic transformation temperature, and is thus expected to be active even for very large grain sizes. We test this prediction by subjecting as-cast, coarse-grained CP-Ti and Ti-6Al-4V to thermal cycling under stress, and demonstrate superplastic deformation under both uniaxial deformation and multiaxial dome forming. We compare superplastic properties for the present cast, coarse-grain CP-Ti and Ti-6Al-4V to previous results on powder-metallurgy CP-Ti and Ti-6Al-4V with intermediate grain size.

5:30 PM

Superplasticity and Cooperative Grain Boundary Sliding in Nanocrystalline Ni₃Al: *Nathan A. Mara*¹; Alla V. Sergueeva¹; ¹University of California

Cooperative grain boundary sliding (CGBS) has shown to account for the majority of macroscopic strain seen in microcrystalline metallic systems undergoing superplastic deformation. While CGBS has been observed on the surface of microcrystalline samples deforming superplastically through the shifting of diamond scribe lines, there have been no TEM results showing occurrence in the bulk of the material, and the details behind the micromechanism of CGBS. In this work, nanocrystalline Ni₃Al produced via High Pressure Torsion is deformed superplastically in the TEM. High-temperature (~700°C) in-situ tensile testing shows the nature of CGBS at the nanoscale through direct observation of this phenomenon. This investigation is funded by National Science Foundation grant: (NSF-DMR-0240144).

5:50 PM

Constitutive Modeling of Superplastic Deformation of AZ31 Mg Alloy: *Marwan K. Khraisheh*¹; Fadi Abu-Farha¹; ¹University of Kentucky

As the lightest constructional metal on earth, magnesium (and its alloys) offers a great potential for weight reduction in the transportation industry. Many automotive components have been already produced from different magnesium alloys, but they are mainly cast components. Production of magnesium outer body components is still hindered by the material's inferior ductility at room temperature. Magnesium alloys are usually warm-formed to overcome this problem; however, it was found that magnesium exhibits superior ductility and superplastic-like behaviour at higher temperatures. In this work, the deformation behaviour of Magnesium Alloy AZ31 is investigated under a wide range of forming temperatures and true strain rates. The results of the mechanical and microstructural tests are used to develop a microstructure-based constitutive model that can capture the behaviour of the material under the various forming conditions. The model is based on the viscoplasticity theory and includes a microstructure-based overstress function.

Biological Materials Science: Functional Biomaterials and Devices

Sponsored by: The Minerals, Metals and Materials Society, ASM International, TMS Structural Materials Division, TMS: Biomaterials Committee, TMS/ASM: Mechanical Behavior of Materials Committee
Program Organizers: Andrea M. Hodge, Lawrence Livermore National Laboratory; Chwee Teck Lim, National University of Singapore; Richard Alan LeSar, Los Alamos National Laboratory; Marc Andre Meyers, University of California, San Diego

Wednesday PM
March 15, 2006

Room: 212A
Location: Henry B. Gonzalez Convention Ctr.

Session Chair: Roger Jagdish Narayan, University of North Carolina

2:00 PM Invited

Nanoporous Materials for Biosensors: *Alex V. Hamza*¹; Juergen Biener¹; Andrea M. Hodge¹; Joel R. Hayes¹; Sergei O. Kucheyev¹; Thomas Huser¹; Chad E. Talley¹; ¹Lawrence Livermore National Laboratory

The optical properties and chemical stability of noble metal nanoporous materials make them ideal for studying biological systems. The morphology of nanoporous metals allows for an efficient excitation of surface plasmons by photons in the visible spectral range. These surface plasmons are also responsible for the increase in the Raman scattering observed in surface-enhanced Raman scattering (SERS). SERS makes it possible to exploit the chemical specificity inherent in Raman spectroscopy for chemical sensing with low detection limits. Examples of the control over the nanoporous materials that can be achieved and the relationship between the nanoporous structure and SERS signal will be presented. This work was performed under the auspices of U.S. Department of Energy by the Lawrence Livermore National Laboratory under Contract No. W-7405-Eng-48.

2:30 PM

Towards Protein-Based Bio-Electronic Circuit Components: *Jack Adam Tuszynski*¹; John M. Dixon¹; ¹University of Alberta

The surface of tubulin molecules exposes a pattern of amino acid residues that provides active sites for nucleation, organization, and binding of metal particles. Under appropriate conditions, every tubulin molecule is able to nucleate silver, gold, platinum and palladium nanoparticles thus forming regular arrays reflecting the tubulin array patterns. This provides a potential approach to develop electronic devices with novel I-V characteristics and attractive physical and biochemical properties such as self-organization and ease of manipulation. Electronic conductivity calculations for the bare MT structure have been based on the Hubbard model in which the dynamic conductivity matrix has been determined using the Kubo formalism in conjunction with the periodic square well approximation. We have investigated MTs decorated with metallic nanostructures using a percolating resistor network approach where metallic wires are interconnected with protein segments represented as insulators with resistance values we have calculated earlier.

2:50 PM

Laser Processing of Advanced Bioceramics: *Roger Jagdish Narayan*¹; ¹Georgia Institute of Technology

Lasers are also finding greater use in processing biomaterials processing. A relatively new concept in biomaterials is the use of advanced biomaterials, which contain "value-added" features or components. Novel laser processes for creating advanced bioceramics, including diamondlike carbon-metal nanocomposites, hydroxyapatite-osteoblast composites, tissue engineering scaffolds, and microneedles will be discussed. Pulsed laser deposition, matrix assisted pulsed laser deposition-direct write, and two photon induced polymerization processes provide these advanced bioceramics with unique structures and added functionalities for next generation medical and dental applications.

WEDNESDAY PM

3:10 PM

Nanoindentation of Biomaterials – Novel Applications and Challenges in the Biological Field: *Michelle E. Dickinson*¹; ¹Hysitron Inc.

Nanoindentation is an accurate and established method for obtaining the nanomechanical properties of traditional homogenous materials. As this technique moves into the biological world, new challenges such as viscoelasticity, heterogeneity and hydration become important considerations. Results from nanoindentation of highly diverse biomaterials ranging from red blood cells and contact lenses to teeth and bones will be discussed. Focus will be given to the specific environmental conditions used to create testing conditions realistic of those *in vivo*. Fixation techniques such as functionalized substrates and hydrated chambers will be described as will different fluid solutions for specialized applications. By discussing the challenges that biomaterials bring to nanomechanical testing and presenting some of the newest solutions to these issues, accurate testing conditions can be developed for future experimental research.

3:30 PM

Nanotechnology-Based Water-Filtering and Purification Solutions for Emerging Biomedical Applications and Advanced Health Benefits: *Ion Nemerenco*¹; ¹Nanowater

The idea presented in this paper is a novel concept of kremen-activated water-filtering and purification technology shows that a molecule-level mechanism can considerably enhance purity and quality of drinking water via biocatalyzed nanostructuring, positive energizing, and purification of processed water (“nanowater”) from any microorganisms or contaminations. It provides normal water with emerging biomedical applications and unique health benefits. The water cleaning technology is based on the bio-catalyst properties of black flint mineral stone (“kremen”) found in certain parts of the world. The observed positive effects of nanowater result from its unique capabilities of saturating the human body with oxygen (O₂), distributing water molecules evenly across the human body, and increasing the organism’s antioxidant complex through better assimilation of regulated nanowater particles which contain health-boosting elements. The health benefits acquired by nanowater create an easy to apply the benefits in areas of human health, agriculture and medicine.

3:50 PM Invited

Effects of Loading Rate on the Mechanical Behavior of a Natural Rigid Composite: *S. G. Walter*¹; *B. D. Flinn*¹; *George Mayer*¹; ¹University of Washington

The effects of loading rate variations on the stress-strain behavior, failure mechanisms, and fracture modes of the spicules of the sponge *Euplectella aspergillum* have been investigated. Comparisons were made with similar measurements on a silicate glass. The influence of very thin (5-10 nm layers) of protein that are interspersed with thicker layers of hydrated glass in the concentric ring structure of the spicules provide strong influence on the mechanical behavior. Ramifications for building synthetic composites with similar architecture are discussed.

Bulk Metallic Glasses: Processing and Mechanical Behaviors

Sponsored by: The Minerals, Metals and Materials Society, TMS Structural Materials Division, TMS/ASM: Mechanical Behavior of Materials Committee

Program Organizers: Peter K. Liaw, University of Tennessee; Raymond A. Buchanan, University of Tennessee

Wednesday PM
March 15, 2006

Room: 217B
Location: Henry B. Gonzalez Convention Ctr.

Session Chairs: Hahn Choo, University of Tennessee; Yanfei Gao, University of Tennessee

2:00 PM Invited

Ductile Ti-Based Metallic Glass and Composite Alloys: *Faqqiang Guo*¹; *Joe Poon*¹; *Gary Shiflet*¹; ¹University of Virginia

In this talk we present two kinds (in terms of microstructure) of Ti-based alloys, one is monolithic amorphous alloy and the other one is a

composite containing amorphous phase and a/b Ti(Zr) solid solution. These two kinds of alloys share the similar components but differ significantly in individual constituent concentrations. The mechanisms responsible for their respective formation are explored. Mechanical properties, including compressive and tensile test as well as fracture toughness, are evaluated and compared between these two kinds of alloys. Both alloys show impressive plastic deformation under compressive test (up to 10%), especially for the composite alloys, a plastic elongation of around 4% can be readily achieved. These results indicate that both alloys are almost ready-to-be-used as structural materials.

2:25 PM Invited

Two-Glass Phase Formation by Phase Separation and Crystallization Behavior in Ti-Y-Al-Co Alloys: *Do Hyang Kim*¹; *Byung Joo Park*¹; ¹Yonsei University

Recently, it has been shown that phase separation into two-glass phases occurs in several metallic glass forming systems. Since different types of phase separated microstructures have been reported in the previous studies, the research on the effect of alloy compositions on the formation of phase separated microstructures is required. Moreover, crystallization behavior of the phase separated alloys has not been investigated, yet. In the present study, it will be shown that the resulting microstructure after phase separation in (Ti,Y)-Al-Co alloy will appear differently, depending on the alloy composition, i.e. relative amount of two glass phases. If the volume fraction of one glass phase is much higher than the other glass phase, droplet type phase separated microstructure is observed, while if the volume fraction of two glass phases is similar, interconnected type phase separated microstructure is observed. In addition, the crystallization behavior of the phase separated (Ti,Y)-Al-Co alloys will be discussed.

2:50 PM

Development of Low Cost Amorphous Steels: *Justin Lee Cheney*¹; *Kenneth S. Vecchio*¹; *Hesham Khalifa*¹; ¹University of California, San Diego

The role of alloying additions on the formation of iron-based metallic glasses was studied by computational analysis of their influence on the alloy’s liquidus temperature and ideal solution melting temperature. It was found that alloys having a reduced liquidus temperature relative to the ideal solution liquidus temperature, in combination with sufficient atomic size mismatches, produced bulk metallic glasses most readily. Experimentally, solute elements consisting of Cr, Mo, W, C, and B were varied systematically; the resulting glass forming ability of the alloy produced was measured via differential scanning calorimetry. The alloys produced contained above 60 atomic percent iron, and can be made largely from Fe-based scrap materials, such as cast iron, HSLA steels and structural steel scrap. This approach leads to very low cost Fe-based BMGs. The specific contributions of each alloying element were justified in terms of various modeling techniques, which have been created to theoretically describe glass formation.

3:10 PM

Approaching the Universal Yield Point of Bulk Metallic Glasses from Molecular Dynamics Simulations: *Ju Li*¹; *Futoshi Shimizu*¹; *Shigenobu Ogata*²; *Hideo Kaburaki*³; ¹Ohio State University; ²Osaka University; ³Japan Atomic Energy Research Institute

Most bulk metallic glasses yield at about 2% strain in uniaxial tension/compression tests. A careful analysis of the elementary shear behavior in contrast to crystalline concepts such as the generalized stacking fault energy reveals a simple explanation. We perform molecular dynamics simulations on 2-component model systems and a 5-component BMG system, observing and characterizing the nucleation and evolution of shear bands. Despite gross uncertainties in the interatomic interactions and the pre-deformation glass structure, our MD results give a reasonable account of the 2% universal yield point. The general concepts of glass rejuvenation and aging, which we call alienation and recovery processes in the context of intense localized shear, and occurring mainly within a timescale of 1-100 atomic vibration periods, is postulated to play a critical role. This mechanistic model can explain why the yield point is relatively insensitive to the interatomic potential and the structure of the pre-deformed glass.

3:30 PM

Multi-Scale Instrumented Indentation Studies of Deformation in a Zr-Based Bulk Metallic Glass: *Subhaashree Sridharan*¹; *C.*

Suryanarayana¹; Rajan Vaidyanathan¹; ¹University of Central Florida

We report on the use of spherical diamond indenters of different diameters to probe both elastic and inelastic deformation in a fully amorphous Zr-based alloy. The spherical geometry results in a simpler stress distribution under the indenter (when compared to a sharp geometry) and the choice of diameter controlled the location of the maximum stress below the indenter. While the elastic response did not depend on the diameter of the indenter used, the inelastic response was influenced by a geometrical length scale associated with the evolution and interaction of shear bands and their subsequent propagation to the surface of the specimen. The influence of pre-existing shear bands on the indentation response was also investigated. The observations were substantiated with microscopy and finite element modeling. This work was supported by a grant from NSF (DMR 0314212).

3:50 PM Break

4:00 PM

Mechanical Behaviors of Zr-Based Bulk Metallic Glasses at Cryogenic Temperatures: *Hongqi Li¹; Cang Fan¹; Hahn Choo¹; Peter K. Liaw¹; ¹University of Tennessee*

In this study, the effect of low temperature on mechanical properties, such as strength, ductility, deformation, and fracture behaviors will be investigated in Zr-based bulk metallic glasses (BMGs) using uniaxial compression testing. Also, the influence of strain-rate on mechanical response at room and cryogenic temperatures is investigated. The Zr-based BMGs were fabricated via an arc-melting system, and X-ray diffraction analysis showed that their microstructures are fully amorphous. The mechanical behavior, especially ductility of BMGs, is related to the local development of shear bands, whose evolution is believed to be associated with the free volume in materials. That is, the diffusion process could be involved. Therefore, it is anticipated that both temperature and strain-rate will play an important role in governing BMGs' mechanical response under loading. This work was supported by the National Science Foundation (NSF) under the grant No. DMR-0231320, with Dr. Carmen Huber as the Program Director.

4:20 PM

Corrosion Resistance of Cu-Zr-Al-Y Bulk Metallic Glasses: *Uwe Koster¹; Daniela Zander¹; ¹University of Dortmund*

Bulk metallic glasses based on late transition metals, e.g. Ni or Cu have many potential advantages, such as higher elastic limit and strength, in comparison to those based on early transition metals: $Cu_{46}Zr_{42}Al_7Y_5$ exhibits a tensile fracture strength in excess of 2000 MPa and a Young's modulus of about 120 GPa. Electrochemical tests of amorphous $Cu_{46}Zr_{42}Al_7Y_5$ were conducted by potentiodynamic polarization at room temperature in $NaCl_{aq}$. The influence of corrosion on the surface topography was studied by X-ray diffraction, SEM and TEM. Electrochemical measurements indicate a good corrosion resistance in solutions with low molarity (pH 8) due to the formation of protective oxide films, but no passive layer is formed at high molarity thus resulting in a high susceptibility to pitting. The corrosion mechanisms of formation of oxide films as well as nucleation and growth of pitting were clarified by associating microstructural investigations with the results of the electrochemical measurements.

4:40 PM

Oxidation of Cu-Based Bulk Metallic Glasses: *Uwe Koster¹; Monika Meuris¹; Daniela Zander¹; ¹University of Dortmund*

Excellent mechanical properties combined with good glass forming ability and low cost materials make Cu-based bulk metallic glasses the material of choice for a variety of applications, appropriate oxidation and corrosion behaviour provided. Oxidation reactions were studied in detail in $Cu_{60}Zr_{40}$, $Cu_{50}Zr_{50}$, $Cu_{60}Zr_{30}Ti_{10}$ and $Cu_{46Zr42}Al_7Y_5$ metallic glasses by thermogravimetry and cross sectional scanning and transmission electron microscopy. Since crystallization often interferes with the oxidation, oxidation of already crystallized glasses exhibiting a nanocrystalline structure will be investigated. Whereas the formation of homogeneous oxide scales was observed in many Zr-rich glasses a layered structure was found to develop in Cu-rich glasses with an assembly of Cu-oxide needles at the outer surface and Cu depletion of the inner layer. During ongoing oxidation parts of the scale lose contact due to developing stresses and forma-

tion of voids and start to peel off. This behavior will be compared with that of crystalline Cu.

5:00 PM

Cu-Based Bulk Metallic Glass Composites Containing In-Situ TiC and TiB Particles: *Hao Wang¹; Huameng Fu²; Haifeng Zhang²; Zhuangqi Hu²; ¹University of Queensland; ²Chinese Academy of Sciences*

Cu-based bulk metallic glasses are of relative low cost and high strength, which have been considered to have more potential for engineering applications. Two Cu-based BMGs containing TiC and TiB particles respectively have been successfully developed using copper mould injection casting. TiC and TiB particles with a size of about 4 mm were in-situ formed and uniformly distributed in the BMG matrix. The volume fraction of the reinforcement particles was up to 30%. The two-phase BMG composites exhibited 2% plastic strain after yielding and the hardness of the materials increased by 25%. On the fracture surface, besides of vein patterns, honeycomb-like characteristics were observed, which might be responsible for the plasticity enhancement. The in-situ particle also restricted shear band propagation and changed its direction, which resulted in an increase of compressive fracture strength. However, a high particle level caused stress concentration on the particle agglomeration and liquid droplets were observed.

5:20 PM

A Finite Element Method for Simulating Inhomogeneous Deformation of Amorphous Alloys: *Yanfei Gao¹; ¹University of Tennessee*

Inhomogeneous deformation of amorphous alloys is related to the initiation and propagation of shear bands. Based on Spaepen's free volume model and its generalization to multi-axial stress states, this work develops a finite element scheme to model the evolution of free volume and shear bands. The method follows that of a small-strain rate-dependent plasticity theory. The incremental nonlinear equations are solved by the Newton-Raphson method, while the corresponding Jacobian matrix is obtained from the evolution of internal state variables. This micromechanical model allows us to study the interaction between individual shear bands and background stress fields. Numerical examples will be presented.

Carbon Technology: Cathode Preheating/Wettable Cathodes

Sponsored by: The Minerals, Metals and Materials Society, TMS Light Metals Division, TMS: Aluminum Committee

Program Organizers: Morten Sorlie, Elkem Aluminium ANS; Todd W. Dixon, Conoco Phillips Venco; Travis J. Galloway, Century Aluminum Company

Wednesday PM
March 15, 2006

Room: 8A
Location: Henry B. Gonzalez Convention Ctr.

Session Chair: Ketil Rye, Elkem Aluminium ANS

2:00 PM

Thermo-Chemo-Mechanical Modeling of a Hall-Héroult Cell Thermal Bake-Out: *Daniel Richard¹; Patrice Goulet²; Marc Dupuis³; Mario Fafard²; ¹Hatch Associates Ltd.; ²Laval University; ³GéniSIM Inc.*

Start-up of a Hall-Héroult cell is a delicate task. Modern practices for high amperage cells involve preheating the lining before the molten electrolyte is poured in. The optimum preheating method for a rapid production of metal and a long pot life is elusive. Numerical modeling is an invaluable tool to gain insights into the complex phenomena taking place during start-up. The adequate modeling of the mechanical response of the lining is critical to detect risks of cathode block cracking or the development of gaps where liquids could leak. Taking into account the ramming paste baking, the quasi-brittle nature of carbon and the contact interfaces are examples of key elements to consider. A finite element demonstration cell slice model was built and simulations of different thermal bake-out scenarios were performed using the in-house code FESH++. Potential industrial application of the model is discussed.

2:25 PM

Development of Coke-Bed Preheating Method for 200kA Cells: *Shaher Mohamed*¹; M. M. Megahed²; H. Hashem¹; M. El-Ghonimy¹; ¹Aluminium Company of Egypt; ²Cairo University

Many factors affecting pot life of aluminium reduction cells. Preheating and start-up had been evaluated to be of the most effecting parameters on cathode life. Different methods are used to preheat the cells. Coke bed preheating with shunt rheostat is one of the most popular methods. The Aluminium Company of Egypt (Egyptalum) utilizes coke bed for preheating of aluminium reduction cells since 1991. Several modifications on the preheating process had been done. Coke bed height modified from 50 to 30 to less than 20mm now. To reduce the preheating current different designs of shunting units have been used. This paper describes the different preheating conditions, as well as analysis and discussions of preheating measurements. A finite element model is used to evaluate the different preheating schemes. The results indicate that the best scheme is the one who has less coke bed and smooth current increase.

2:50 PM

Study on the Heating-Up Rate for Coke Bed Preheating of Aluminum Reduction Cell: Jie Li¹; *Qinsong Zhang*¹; Yanqing Lai¹; Yexiang Liu¹; ¹Central South University

Impacts of shunting schedules on the heating-up rate during coke preheating and heating-up rate variation of temperature are of great importance to get the proper heating-up rate and prolong the cell life during and after the preheating process. A nonlinear transient heat transfer model of a 160kA prebaked cell was developed by ANSYS codes. Results show that longer interval and more shunt groups resulted in slower average heating-up rate. The average heating-up rate from 200 to 600°C had the slowest value at some starting current percentage, which was approximate to 50% of the whole current. Concerned with the same cell structure and coke-bed thickness, the heating-up rate of certain period of time was dependent on time, temperature and current but not on the shunting schedules after the current loading moment. A shunting schedules design method was proposed to meet the given requirement of heating-up rate during any temperature intervals.

3:15 PM

Titanium Diboride and Wolfram Silicide Composite Used as Aluminum Electrolysis Inert Cathode Materials: *Huimin Lu*¹; Huanqing Han¹; Ruixin Ma¹; Dingfan Qiu²; ¹University of Science and Technology Beijing; ²Beijing General Research Institute of Mining and Metallurgy

In this paper, various performances of TiB₂-WSi₂ composite with WSi₂ content 10mass%, 30mass%, 50mass% and 70mass% are studied. The results show that WSi₂ can improve TiB₂ sintering performance apparently, when WSi₂ content of TiB₂- WSi₂ composite exceeds 30mass% the compactivity of the composite sintered 1hour at 1900°C is higher than 98%; its conductivity is prior to TiB₂; WSi₂ exhibits significantly better resistance aluminum corrosion but weaker resistance cryolite corrosion than TiB₂. Aluminum corrosion to TiB₂- WSi₂ composite is mainly that Al and TiB₂ reaction becomes TiAl and so on intermetallics, but cryolite corrosion to composite is mainly that WSi₂ dissolves and fractures in the cryolite solution. Because in aluminum electrolysis process, there is a thin aluminum liquid layer on the inert cathode surface, the inert cathode failure is mainly aluminum liquid corrosion, so TiB₂- WSi₂ composite is a better inert cathode material for aluminum electrolysis.

3:40 PM Break

3:55 PM

Stability of TiB₂-C Composite Coatings: *Mohamed Ibrahim*¹; Trygve Foosnaes¹; Harald A. Oye¹; ¹Norwegian University of Science and Technology

Several recipes of pitch-bonded TiB₂ were studied with respect to adherence, cracking and stability during electrolysis. A successful recipe for a crack-free coating was obtained. The coating showed good adherence and stability after 34 hours of electrolysis. The wetting of the coating by aluminium in the presence of cryolite melt was time dependent and almost complete wetting was observed after 120 minutes. Furan resin-based TiB₂ coatings were not wetted by aluminium during electrolysis due to the presence of a carbon layer at the coating surface. Coating samples

were polished by SiC paper after curing. The polished samples showed good stability and aluminium wetting.

Cast Shop Technology: Cast Processes and Chain Analysis

Sponsored by: The Minerals, Metals and Materials Society, TMS Light Metals Division, TMS: Aluminum Committee

Program Organizers: Rene Kieft, Corus Group; Gerd Ulrich Gruen, Hydro Aluminium AS; Travis J. Galloway, Century Aluminium Company

Wednesday PM

March 15, 2006

Room: 7C

Location: Henry B. Gonzalez Convention Ctr.

Session Chair: Bjorn Rune Henriksen, Elkem ASA

2:00 PM

Copper Shells for Twin Roll Casting: *Hans-Guenter Wobker*¹; Gerhard Hugenschuett¹; Dietmar Kolbeck¹; ¹KM Europa Metal AG

The drawback of the twin-roll method of aluminium strip casting as compared with other casting processes has been low productivity. The cause of these productivity limits has been mainly in the difficulty of removing the process heat from the zone of melt/strip – roll contact. Substitution of the steel alloys used today by high-conductivity engineering materials opens up very interesting possibilities of improving the productive capacity of such casting systems. The present paper gives an account of the development, properties and application of Cu based materials for casting roll sleeves. The first part portrays the Cu materials that have been developed and their particular material properties. The second part highlights performance results achieved with Cu alloy casting sleeves when used in actual practice. It describes the casting speeds/productivity levels which have been reached, the wear characteristics of such sleeves, and the properties of the produced cast Al-strip.

2:25 PM

A New Continuous Casting Process: *Hubert Sommerhofer*¹; Peter Sommerhofer¹; ¹Sommerhofer Technologies GmbH

Continuous casting using water as coolant has some important disadvantages. Water is evaporating at low temperatures and causes difficulties in process control and product quality. Furthermore the use of water as cooling material causes the danger of explosions. To prevent these disadvantages, we use liquid metal to cool the strand. Laboratory scale experiments have been done to investigate the possibility to cast an aluminium alloy, a magnesium alloy and copper using a low melting liquid metal as cooling material. Now a pilot scale plant has been constructed by Sommerhofer Technologies. After several tests with the pilot scale plant, results on the castability of Aluminium- and Magnesium alloys are existing now. Advantages of the new process: Much lower crack risk; constant high heat transfer coefficients; higher casting rates; larger process window for the coolant temperatures; nearly no subsurface layer; no explosions; no contaminated cooling water; exchanged heat at usable temperature level.

2:50 PM

Maximizing the Quality of DC Cast Aluminum Billet: *Roger A. P. Fielding*¹; ¹Benchmarks

The quality of DC cast aluminum billet is affected by the control of the incoming materials: smelter ingot, scrap aluminum, and of the alloying and grain refining additions to the melt. The quality of the billet is affected by the preparation and treatment of the incoming materials; by the design and operation of the melting and holding furnaces, the metal treatment systems, the casting and homogenizing equipment, and the training and skills of the operators. Failure to understand the impact of the various factors affecting the quality of the billet results in improperly engineered facilities whose features adversely affect the quality of the billet, increase the cost of converting the incoming materials to billet, and compromise the profitability of the facility.

3:15 PM Break

WEDNESDAY PM

3:30 PM

Turnkey Solutions for the Modern Day Primary Aluminium Casthouse: The Alba Line 5 Experience: *Andrew Haberl*¹; Barry J. Houghton¹; Hussain Hussain Al-Ali²; ¹Solios Thermal; ²Aluminium Bahrain B.S.C.(c)

Placing a turnkey order with one supplier for all the equipment that interfaces together, as on a casting line, is a very cost effective means of providing an efficient and flexible Casthouse Solution. Decisions can be taken more quickly, interface issues can be resolved with minimal recourse to the customer and delays and cost over runs can be minimised. In 2003 ALBA one of the world's leading aluminium producers, gave Solios Thermal the opportunity to demonstrate their ability to deliver when they awarded them the contract for turnkey supply of the casting lines for their Line 5 expansion. The scope of supply included 11 – furnaces, 3 – VDC casters, 1 – Continuous ingot caster, 2 – electromagnetic stirrers and all interconnecting launders, associated degassing and filtration units. Various key stage decisions, layout considerations, and start up together with the benefits to the end user are discussed in this paper.

3:55 PM

Industrial Application of DOE Energy Savings Technologies to Aluminium Melting: *Cynthia K. Belt*¹; Brian M. Golchert²; Paul E. King³; Ray D. Peterson¹; Joseph L. Tessandori¹; ¹Aleris International; ²Fluent Inc; ³U.S. Department of Energy

Aleris International was part of a four-year DOE program on “Improving Energy Efficiency in Aluminum Melting”. Key findings from this work were interpreted and implemented on a corporate-wide basis. 1) Natural gas savings were realized by adjusting burner input based on the bath area for melting and holding furnaces. 2) Modifying burner loading for an asymmetrical and symmetrical reverberatory furnace was investigated. 3) The PHAST program was utilized to understand and quantify the potential of preheated combustion air. Additional modeling was done for this paper to analyze response from a different furnace design. Methods and results will be discussed in this paper.

4:20 PM Break

4:35 PM

A Quick-Change Ceramic Filter Assembly for Filtering Molten Aluminium and Other Metals: *David A. Larsen*¹; Dean Vander Jagt²; ¹Blasch Precision Ceramics; ²New Century Heaters Inc.

A new concept of a quick-change interchangeable ceramic filter assembly for filtration of molten aluminum and other metals is described. The ceramic filter cartridge assembly may be replaced without draining the molten metal filter box, and without permitting unfiltered metal to pass downstream. Oxygen/air is purged from this ceramic filter, and it is preheated before immersion into the molten metal. The purging prevents oxides from forming during priming of the filter, which would plug filter pores, and the preheating prevents thermal shocking. The filter cartridge thus can be easily interchanged without manual removal of surface oxides or corundum, and without contamination of the melt.

5:00 PM

Modeling Methods for Managing Raw Material Compositional Uncertainty in Alloy Production: *Gabrielle Gaustad*¹; Preston Li¹; Randolph Kirchain¹; ¹Massachusetts Institute of Technology

Operational uncertainties create inefficiencies in metal alloy production. One that greatly influences remelter batch optimization is variation in raw material composition, particularly for secondary materials. Currently, to accommodate compositional variation, firms commonly set production targets well inside of the window of compositional specification required for performance reasons. Window narrowing, while effective, does not make use of statistical sampling data, leading to sub-optimal usage of secondary materials. This paper explores the use of a chance constrained optimization method, which allows explicit consideration of statistical information on composition. The framework and a case study of cast and wrought production with available scrap materials are presented. Results show that it is possible to increase scrap consumption without compromising the likelihood of batch errors, when using this method compared to conventional window narrowing.

Characterization of Minerals, Metals and Materials: Composites and Other Materials

Sponsored by: The Minerals, Metals and Materials Society, TMS Extraction and Processing Division, TMS: Materials Characterization Committee

Program Organizers: Jiann-Yang James Hwang, Michigan Technological University; Arun M. Gokhale, Georgia Institute of Technology; Tzong T. Chen, Natural Resources Canada

Wednesday PM
March 15, 2006

Room: 206A
Location: Henry B. Gonzalez Convention Ctr.

Session Chairs: Tzong T. Chen, Natural Resources Canada; Jiann-Yang James Hwang, Michigan Technological University

2:00 PM

Pullout Test of Coir Fiber to Evaluate the Interface Strength in Polyester Composites: *Sergio Neves Monteiro*¹; Janine Feitosa de Deus¹; Regina Coeli Paes Aquino²; Jose Roberto Moraes d'Almeida³; ¹State University of the Northern Rio de Janeiro; ²Federal Center for Technological Education; ³Pontificia Universidade Catolica do Rio de Janeiro

Polymeric composites reinforced with natural fibers are increasingly used in several engineering applications, from automotive parts to building construction elements. In addition to the relatively low cost, the natural fibers are also appraised by their renewable characteristics and biodegradability. Fibers extracted from the crust of coconut fruits, also known as coir fibers, have been investigated for a possible use in composite materials. The present work evaluated the coir fiber/polyester matrix interface shear strength by means of pullout tests. The variation of the pullout tensile stress vs. the embedded coir fiber length permitted to determine the critical fiber length and thus to calculate the interface strength. Observations by SEM complemented the results from pullout tests, indicating that coir fibers have a potential for application in polymeric composites that could replace conventional materials such as wooden and gypsum panels.

2:25 PM

Structural and Morphologic Characterization of the Natural Graphite after Application of High Pressure and High Temperature Treatment: *Ana Lucia Diegues Skury*¹; Sergio Neves Monteiro¹; ¹UENF

In the synthesis of diamond, the precursor graphite must present a degree of crystallinity to assure optimum yield and quality for the transformed crystals. X-ray diffraction, SEM and TEM analyses were carried out to investigate the structural and morphologic transformations produced in natural graphite by high pressure-high temperature (HPHT) treatment. The present study had as its objective to characterize the morphological and structural changes suffered by a natural graphite that was subject to HPHT in the region of diamond thermodynamic stability. The results indicate the material that constitutes the gasket for the reaction capsule, could act as catalyst in the graphite recrystallization observed after the treatments.

2:50 PM

Environmentally Correct Jute Reinforced Polyethylene Composites: *Sergio Neves Monteiro*¹; Amanda Camerini Lima¹; Lucio Jose Terra Petrucci¹; Luiz Augusto Hernandez Terrones¹; Jose Roberto Moraes d'Almeida²; ¹State University of the Northern Rio de Janeiro; ²Pontificia Universidade Catolica do Rio de Janeiro

Wastes generated by our society and the question on how to dispose them is, nowadays, a relevant matter of concern. The objective of the present work was to characterize the technical properties of composites made of discarded jute bags, with their plain weave fabric, serving as reinforcement phase, and polyethylene wastes, collected from city dumps, as continuous matrix. Different amounts, up to 30 wt%, of jute plain weave fabric were press molded at 160°C together with sieved polyethylene particles. The resulting composites showed mechanical properties that could compete with those of low density wooden boards. Both by presenting a solution to, otherwise, disposed wastes and by helping to prevent deforestation, the investigated composite may be considered as an environmentally correct material.

3:15 PM

Microstructural Characterization of Ice: *Ian Baker*¹; R. Obbard¹; K. Seig¹; D. Iliescu¹; C. P. Dahglan¹; ¹Dartmouth College

In this presentation we describe techniques that have been developed to characterize the microstructures of ice and firn from polar ice sheets and seasonal ice from temperate lakes and rivers. Characterization includes controlled sublimation of uncoated ice in an environmental cold-stage-equipped SEM equipped with an energy dispersive x-ray spectrometer to examine impurity locations in ice and an electron backscatter pattern system to map orientations. Confocal scanning optical microscopy coupled with Raman spectroscopy has also been used to determine the compounds present in grain boundaries and triple junctions. The limitations of the techniques are discussed. Supported by ARO contract DAAD 19-03-1-0110 and NSF grant OPP-0440523.

3:40 PM Break

3:50 PM

Mechanical and Structural Characterization of Curaua Fibers: *Sergio Neves Monteiro*¹; Janine Feitosa de Deus¹; Jose Roberto Moraes d'Almeida²; ¹State University of the Northern Rio de Janeiro; ²Pontificia Universidade Catolica do Rio de Janeiro

Natural lignocellulosic fibers are successfully replacing synthetic fibers in many engineering applications. In addition to well known conventional fibers such as cotton, sisal and lax, others with promising properties are now being considered. The present work investigated the mechanical and structural characteristics of a relatively high strength fiber, curaua (*Ananas erectifolius*), from the Amazon region in Brazil. The results obtained from tensile tests confirmed the superior strength while scanning electron microscopy (SEM) analysis displayed features that justify the possibility of using the curaua fibers as an effective reinforcement for polymeric composites.

4:15 PM

Microstructural Characterization of Epoxy Matrix Composites with Dispersed Diamond Particles: *Sergio Neves Monteiro*¹; Ana Lucia Diegues Skury¹; Gustavo Wagner Menezes¹; Ruben Sanchez Rodrigues¹; ¹UENF

Polymeric matrix composites with dispersed hard particles are being used as wear resistant tool in industrial polishing operations. In the present work the microstructure of epoxy composites with different amounts of embedded diamond particles, up to 30%, was investigated for the effect on the fracture characteristics. It was found that introduction of diamond particles promoted an increase in the porosity of the epoxy matrix. Moreover, the particle morphology associate with a non-uniform distribution within the matrix, were responsible for nucleation of cracks, that caused the rupture of the composite.

4:40 PM

Morphological, Mechanical and Optical Characterization of Flyash Filled Nylon-6: *P. A. Mahanwar*¹; Suryasarathi Bose²; H. Raghu¹; ¹Mumbai University; ²Indian Institute of Technology, Bombay

Flyash were melt mixed with nylon-6 at a 30wt% concentration. TYZOR® TPT, a coupling agent, was used to facilitate the link between filler and matrix. The morphological characterization, using SEM, revealed sufficient matrix residue on the filler surfaces thus confirming the strong interfacial bonding between the filler and the matrix on treating. Tensile, impact and the flexural properties of the composites were also improved with the incorporation of coupling agent. As flyash particles tend to impart a grayish color to the plastic, TiO₂ pigment was employed to make the formulations aesthetic. The pigment was added to the filled system in 0.1, 0.5, 1.0, 1.5, 2.0 wt/wt ratios. Scattering of incident light and spectral reflectance was higher for smaller particle size flyash. Moreover an increase in the scattering with increase in pigment concentration indicates better dispersion of the pigment, which again is due to the presence of coupling agent.

5:05 PM

Texture Gradient in OFHC Copper Processed by Equal Channel Angular Extrusion: *Daudi R. Waryoba*¹; P. N. Kalu¹; ¹Florida State University

Most deformation processes such as rolling, forging and extrusion, produce bulk through-thickness microstructure and texture gradient, in addition to the local inhomogeneities. Microstructural and textural gradient that has been observed in wire drawing is attributable to the inhomogeneous deformation along the radial direction. This inhomogeneity in the microstructure is visible as three distinct concentric regions: the inner core, the mid section, and the outer surface. Such microstructural inhomogeneities have been observed to adversely contribute to recrystallization heterogeneity. In the last three decades, equal channel angular extrusion (ECAE) has received a considerable attention as one of the methods for producing ultrafine grain structures. Apart from its effectiveness of producing bulk grain refinement, ECAE results in a homogeneous microstructure and nearly random texture. The goal of this investigation was to study texture gradient in oxygen free high conductivity (OFHC) copper after being deformed by ECAE. Texture gradient is discussed based on electron backscattered diffraction (EBSD) measurements, and results are compared with gradient observed in wire drawn materials.

Computational Thermodynamics and Phase Transformations: Atomic Kinetics Processes - Joint Session with Point Defects in Materials

Sponsored by: The Minerals, Metals and Materials Society, TMS Electronic, Magnetic, and Photonic Materials Division, TMS Materials Processing and Manufacturing Division, TMS Structural Materials Division, TMS: Chemistry and Physics of Materials Committee, TMS/ASM: Computational Materials Science and Engineering Committee
Program Organizers: Dane Morgan, University of Wisconsin; Corbett Battaile, Sandia National Laboratories

Wednesday PM
March 15, 2006

Room: 210B
Location: Henry B. Gonzalez Convention Ctr.

Session Chairs: Adri C. van Duin, California Institute of Technology; Mark D. Asta, University of California

2:00 PM Invited

Materials Analysis at the Atomic Scale: The Role of Atom Probe Tomography in Materials Modeling: *Thomas F. Kelly*¹; David J. Larson¹; ¹Imago Scientific Instruments

Atom probe tomography (APT) provides 3-D atomic-scale structural and compositional analysis of materials. The Local Electrode Atom Probe or LEAP® made by Imago Scientific Instruments, greatly increases the capacity of APT for materials analyses on a wide spectrum of materials types. Because of the close match between the size of APT data sets and the capabilities of materials modeling approaches, they are a natural complement to each other. Materials modeling is of great interest for tracking of structural evolution in time or properties estimation based on atomic-scale information. A selection of materials analyses will be shown and a few examples of this complementarity will be highlighted.

2:30 PM Invited

Impact of Vacancy Diffusion on the Early Decomposition Stages of Alloys and the Role of Heterophase Interfaces on Coarsening: *Zugang Mao*¹; Chantal K. Sudbrack¹; Kevin E. Yoon¹; *David N. Seidman*¹; Georges P. Martin¹; ¹Northwestern University

The kinetic pathway for nucleation and growth is commonly thought to be dictated by the initial supersaturation of solutes in the solid solution undergoing phase separation. We demonstrate that the details of the diffusion mechanism, in the solid solution affect deeply the early stage morphologies of precipitates. Our argument is based on a combined use of atomic-scale observations, with atom-probe tomography (APT) and lattice kinetic Monte Carlo simulation of a Ni(Al,Cr) alloy. By an optimized choice of thermodynamic and kinetic parameters we first reproduce the experimental APT observations. We then modify only the long-range vacancy-solute binding energy, without altering the thermodynamic driving force for phase separation, thereby demonstrating that the microstructural evolution changes from a coagulation to an evaporation-condensation coalescence mechanism. The changes can only be accounted for with non-

zero values for the vacancy chemical potential and off-diagonal terms of the Onsager matrix, at variance with classical models.

3:00 PM Invited

Diffusion in Multicomponent Solids from First-Principles: *Anton Van der Ven*¹; ¹University of Michigan

Atomic diffusion plays an important role in determining both the mechanisms as well as the rates of many phase transformations in multi-component solids. In this talk, I will describe how diffusion coefficients can be calculated from first-principles in multi-component solids. Kubo-Green relations from statistical mechanics provide the link between macroscopic kinetic quantities such as diffusion coefficients and properties of the solid at the atomic scale. Multi-component solids are characterized by differing degrees of short and long-range order and diffusing atoms sample many different local environments along their trajectories. The cluster expansion from alloy theory is ideally suited to extrapolate first-principles energies and activation barriers to describe the activation barriers for any state of configurational disorder. Combined with kinetic Monte Carlo simulations, this approach enables the first-principles calculation of diffusion coefficients as a function of concentration and temperature in multi-component solids.

3:30 PM Invited

Kinetic of Fe Alloys under Aging and Irradiation Based on Ab Initio and Kinetic Monte Carlo Simulations: *Christophe Domain*¹; ¹Electricite De France

Under ageing or irradiation, the changes of the macroscopic properties such as the hardness or the brittleness are partly due to the evolution of the microstructure and of the distribution of the alloying elements. In order to model the evolution of pressure vessel steels under ageing or under irradiation, kinetic Monte Carlo simulations have been performed. The energetic of systems containing Cu, Ni, Mn, Si, P as well as C and the activation barriers for migration (which depend on the local environment) have been derived from ab initio calculations and compared to thermodynamical and as well as diffusion based experimental data. As the link between the ab initio results and the kinetic Monte Carlo parameterisation is not straightforward several strategies have been adopted. The effect of these models on the kinetic pathways is discussed. The simulation results are compared to model experiments on simple model alloys.

4:00 PM Break

4:10 PM Invited

Application of ReaxFF Reactive Force Fields to Chemical Diffusion of Hydrogen and Oxygen through Fuel Cell Membranes: *Adri C. van Duin*¹; *Valeria Molinero*¹; *Xin Zhang*¹; *Boris Merinov*¹; *William A. Goddard*¹; ¹California Institute of Technology

ReaxFF is a bond-order dependent force field that can perform reactive simulations on systems too large to be amenable to quantumchemical (QM) simulations. By fitting ReaxFF parameters to extensive databases, derived from QM simulations on small molecules and condensed phase systems and covering both ground state molecules and full reaction pathways, we have developed reactive potentials for a wide range of materials, including organic compounds, metals/metal oxides and semiconductors and interactions between these material classes. Here we present applications of several recently developed ReaxFF potentials to hydrogen and oxygen diffusion through fuel cell membranes. For the membrane material a wide range of compositions are considered, including imidazoles, water-filled zeolites, yttrium stabilized zirconia and yttrium-doped barium zirconates.

4:40 PM Invited

Abnormal Grain Growth Due to Boundary Mobility Variations: *Elizabeth A. Holm*¹; *Mark A. Miodownik*²; *Kristopher Healey*¹; ¹Sandia National Laboratories; ²King's College London

Abnormal grain growth occurs in many engineered materials and can be desirable or detrimental. Many theories attempt to explain this phenomenon, and it is likely that there are several causes. In pure polycrystals, one mechanism for abnormal growth is the existence of special, high mobility grain boundaries. If such boundaries can persist during evolution, they impart a significant growth advantage to certain grains. We apply highly realistic, microstructural-scale computer simulations to ex-

amine abnormal growth in several systems, including textured polycrystals, deformed polycrystals with spatial orientation gradients, and thermally inhomogeneous polycrystals. We find abnormal events similar in morphology, frequency, and crystallography to those observed in experiments. The key requirement for abnormal growth is the persistence of high mobility boundaries due to crystallographic, spatial, or thermal considerations. In contrast, systems with random high mobility boundaries show no abnormal growth. These simulations provide new insight into one mechanism for abnormal grain growth.

5:10 PM

Computing the Mobility of Grain Boundaries: *Koenraad G. F. Janssens*¹; *Elizabeth A. Holm*¹; *Steven J. Plimpton*¹; *Stephen M. Foiles*¹; *David Olmsted*¹; ¹Sandia National Laboratories

Many modern technical materials are designed and manufactured by controlling the evolution of the microstructure. Most of the solid-state microstructure transformations, like recrystallization, grain growth, phase transformation or precipitation, involve the motion of grain boundaries. The mobility of a solid-state grain or phase boundary is determined by the atomistic mechanisms by which the boundary moves. While uncertainty remains about the exact nature of these mechanisms, it is generally accepted that mobility strongly depends on the crystallographic misorientation between neighboring grains. Current experimental and simulation methods cannot determine the mobility of flat boundaries across the large misorientation phase space. We have developed a new, molecular dynamics method for imposing an artificial driving force on boundaries. This allows us to induce motion in flat boundaries of arbitrary misorientation using considerably smaller systems and shorter times than previously attainable. For different series of boundaries, we find both expected results and unexpected results.

5:30 PM

Spatial and Temporal Analysis of Nonequilibrium Order Fluctuations in Alloys Driven by Energetic Ion Irradiation: *Pascal M. Bellon*¹; *Jia Ye*¹; *Yaofeng Chen*¹; ¹University of Illinois

External driving forces often leads to the self-organization of alloys microstructures. Using analytical models and atomistic simulations, we recently predicted that ion beam processing can lead to the spontaneous formation of nanoscale patterns of the degree of chemical order. One fundamental question relates to the dynamics of order fluctuations in these nonequilibrium states. This would provide new insight on the origin of the stabilization of these patterns, on the selection of length scales, and, more practically, on the stability of these nanostructures when used in engineering materials. Using atomistic kinetic Monte Carlo simulations, we performed a spatial and temporal analysis of the nonequilibrium fluctuations of order in a binary alloy that would form an L12 ordered structure at equilibrium. This analysis provides new and unambiguous criteria for identifying states of pattern of order, both in simulations and experimentally, and it sheds new light on the origin of their formation.

5:50 PM

Precipitation Kinetics in a Cu-4 wt.% Ti Alloy: *Victor Manuel Lopez-Hirata*¹; *Felipe Hernandez-Santiago*¹; *Maribel Leticia Saucedo-Muñoz*¹; ¹Instituto Politecnico Nacional

The precipitation kinetics was studied using SEM, TEM, XRD and Vickers hardness in an isothermally aged Cu-4 wt. % Ti alloy. The XRD and TEM results indicated that the phase decomposition occurred by spinodal decomposition during the early stages of aging. The growth kinetics of composition modulation wavelength is very slow at the early stages of aging. The precipitation of metastable Cu₄Ti phase preceded to that of the equilibrium Cu₃Ti phase, which formed through cellular precipitation. The coarsening process of Cu₄Ti phase followed the LSW theory for diffusion-controlled growth. The activation energy for this coarsening process was determined to be about 190 kJ/mol. The discontinuous precipitation of Cu₃Ti phase has an activation energy of about 207 kJ/mol and an exponent time of about one. The highest hardness and fastest transformation kinetics occurred at aging temperatures of 673 and 873 K, respectively.

WEDNESDAY PM

Computational Thermodynamics and Phase Transformations: Phase Field Models II

Sponsored by: The Minerals, Metals and Materials Society, TMS Electronic, Magnetic, and Photonic Materials Division, TMS Materials Processing and Manufacturing Division, TMS Structural Materials Division, TMS: Chemistry and Physics of Materials Committee, TMS/ASM: Computational Materials Science and Engineering Committee
Program Organizers: Dane Morgan, University of Wisconsin; Corbett Battaile, Sandia National Laboratories

Wednesday PM Room: 210A
March 15, 2006 Location: Henry B. Gonzalez Convention Ctr.

Session Chairs: Ken R. Elder, Oakland University; Adam C. Powell, Massachusetts Institute of Technology

2:00 PM Invited

Multiscale Modeling of Solid-Solid Phase Transformations: *Valery I. Levitas*¹; ¹Texas Tech University

Several approaches to continuum modeling of phase transformations are analyzed. To model martensitic microstructure formation, nanoscale and microscale phase field theories are developed. They are based on the combination of a continuum thermodynamic approach, diffuse interface and a material instability concept. These approaches are applied to the martensite nucleation at various dislocation configurations and formation of multivariant stress-induced martensite in single and polycrystals. An alternative sharp interface approach is developed which takes into account large strains and interaction between phase transformation and plastic straining. A general theory of phase transformations in plastic materials is developed which includes phase transformation criterion and extremum principle for determination of all unknown parameters. Nucleation and growth of martensitic plate and strain-induced nucleation at shear-band intersection is studied.

2:30 PM Invited

Modeling Elastic and Plastic Deformation of Nanostructured Materials: Peter Stefanovic¹; Mikko Haataja²; *Nikolas Provatas*¹; ¹McMaster University; ²Princeton University

A continuum field theory approach is presented for modeling elastic and plastic deformation, free surfaces, and multiple crystal orientations in nano-crystalline systems with both hexagonal and cubic symmetry in two and three spatial dimensions. The model is based on a free energy for the local atomic density, which is minimized by spatially periodic structures. It incorporates both elastic phenomena (deviations from the preferred spatial period cost energy) as well as defects in the form of, e.g., vacancies, dislocations, and grain boundaries. Furthermore, its dynamics is constructed such that it incorporates both diffusive and elastic relaxation phenomena. By introducing a variable elastic time scale, we are able to maintain mechanical equilibrium while simulating microstructural evolution on time scales well beyond those accessible by conventional atomistic MD simulation methods. We apply this model to elucidate the role of dislocations during deformation of nanocrystalline materials.

3:00 PM

Applications of Moving Mesh Method to Phase Field Simulations: *Weiming Feng*¹; Peng Yu¹; Shenyang Hu²; Zikui Liu¹; Qiang Du¹; Longqing Chen¹; ¹Pennsylvania State University; ²Los Alamos National Laboratory

Phase-field simulations have increasingly been used in modeling microstructure evolution during phase transformations and structural coarsening. However, large-scale simulations are still computationally expensive. The semi-implicit Fourier spectral method (FS_implicit) is found to be particularly efficient for this problem. One of the main features for the spectral method is the use of uniform grids that utilizes existing Fast Fourier Transform (FFT) packages. In this presentation, we report our recent progress in making grid points spatially adaptive in the physical domain while maintaining a uniform grid in the computational domain and semi-implicit in time. The new scheme not only provides a more accurate resolution around the interfaces but also retains the numerical efficiency of the FS_implicit method. Numerical examples using the new moving mesh

method will be presented for both two and three space dimensions. We will compare the accuracy and efficiency of our results with those obtained by other methods.

3:20 PM

Solving Phase Transformation Problems with FiPy: *Jonathan E. Guyer*¹; Daniel Wheeler¹; James A. Warren¹; ¹National Institute of Standards and Technology

The solution of coupled sets of partial differential equations (PDEs) is ubiquitous in continuum models of phase transformations, such as in phase field or level set simulations. We have developed a phase transformation modeling framework called FiPy that combines the finite volume method, widely used in fluid dynamics, and the Python scripting language, which has enjoyed considerable attention from the scientific community. The result is a tool that is extensible, powerful, freely available and, most importantly, tailored to the needs of materials scientists. The framework includes terms for transient diffusion, convection, and standard sources, enabling the solution of arbitrary combinations of coupled elliptic, hyperbolic and parabolic PDEs, including higher-order expressions such as Cahn-Hilliard. We will present the representation and results of current models, including phase field and level set treatments of electrochemical, polycrystalline, and multi-component dendritic phase transformations.

3:40 PM Break

4:00 PM

Phase Field Modeling of γ' Rafting in Single Crystal Ni-Base Superalloys: *Ning Zhou*¹; Chen Shen¹; Mike Mills¹; Yunzhi Wang¹; ¹Ohio State University

Rafting of γ' precipitates in single crystal Ni-base superalloys under external load is investigated by computer simulations. The simulation technique is based on an integrated phase field model that characterizes simultaneously spatio-temporal evolution of both precipitate morphology and dislocation structures. The initial γ/γ' microstructure consisting of cuboidal particles and dislocation configuration in the γ -channels are constructed according to experimental observations and phase field simulation of dislocation filling process in the γ -channels. The spatial variation of chemical potential of solute atoms is evaluated based on local concentration and stress, and diffusion fluxes in different γ -channels are analyzed. For a given state (sign and magnitude) of lattice misfit and external load, the predicted morphologies of the rafted γ' precipitates agree well with experiment observations. The kinetics of rafting is also characterized as a function of lattice misfit and external load for a binary Ni-Al alloy with an effective diffusivity calibrated against experiment.

4:20 PM

Phase Field Modeling of High-Temperature Electrochemistry: Application to Subhalide Reduction of Titanium: *Wanida Pongsaksawad*¹; Adam C. Powell¹; ¹Massachusetts Institute of Technology

Phase field model of transport-limited with rapid-charge redistribution electrochemistry is used to simulate magnesiothermic reduction of TiCl₂. This model derived from the Cahn-Hilliard and Poisson equations can capture both electrolysis and electronically-mediated reactions (EMR) which play a major role in this process. For a solid-solid system, the Peclet number, dimensionless electrode separation and metal/electrolyte conductivity ratio control the cathode interface stability; in a liquid-liquid system, modeled by coupling with the Navier-Stokes equations, the Schmidt number and a modified Weber number also play a role as flow provides an additional stabilizing mechanism. Preliminary 2D simulation results of a solid-liquid system with fluid flow are presented and its stability criteria are discussed. Three-dimensional results without flow illustrate formation of the titanium structure. This methodology can be used to model shape and topology changes in any electrochemical system satisfying the above assumptions.

4:40 PM

Phase Field Model of Solid-State Sintering: *Yu U. Wang*¹; ¹Virginia Tech

Sintering is a well-known complicated material process involving multiple diffusion mechanisms (along surface and grain boundary, through lattice and vapor), grain boundary migration, particle rigid-body translation and rotation. The high-diffusivity paths along the solid-solid inter-

faces, i.e. grain boundaries, play a key role in the densification of sintered powder compact. The diffusion of atoms from grain boundaries to nearby high-curvature growing neck surfaces leads to approaching of centers of particles through rigid-body motions. This work develops a phase field model of solid-state sintering, which treats the rigid-body motions of particles and surface diffusion, grain boundary diffusion, volume diffusion, vapor transport, as well as grain boundary migration. Consideration of rigid-body motions results in modifications to both Cahn-Hilliard nonlinear diffusion equation and Ginzburg-Landau (Allen-Cahn) structural relaxation equation. Computer simulations are presented.

5:00 PM

Phase-Field Modeling of Homogenization Process of Binary Aluminum Alloys: Igor Kovacevic¹; Bozidar Sarler¹; ¹Nova Gorica Polytechnic

The simulation of homogenization process of aluminum alloys is made by the phase-field model. The model is focused on the dissolution kinetics of interdendritic eutectic phase in industrial conditions of homogenization. The simulation is performed in two places of the billet, the center and the surface. The realistic industrial direct-chill as-cast microstructure is used as the initial condition for simulation of homogenization. The initial concentration profile of alloying element is obtained by the Scheil-Gulliver solidification model. The thermo physical properties of material are obtained by the thermodynamic database JMatPro for aluminum alloys. The microstructure evolution of Al-5% wt Cu binary alloys during homogenization process in both simulated places is modeled.

5:20 PM

Phase Field Simulations for Grain Growth in Polycrystalline Films: Nele Moelans¹; Bart Blanpain¹; Patrick Wollants¹; ¹K. U. Leuven

Grain size, grain size distribution and grain orientation in polycrystalline films strongly influence their strength, electronic properties and durability. Once the grain size is larger than the thickness of the film, grains become columnar with their grain boundaries perpendicular to the plane of the film. As a result, grain growth shows many 2-dimensional features, although is not really 2-dimensional because of the importance of surface energy. Grooves at the triple lines where grain boundaries meet the surface, formed to balance surface energies and grain boundary energy, hinder grain boundary movement. Furthermore, surface energy of the grains may depend on orientation. As favourably oriented grains have a high driving force for growth, the anisotropy in surface energy may provide the necessary additional driving force for abnormal grain growth (= secondary recrystallization). A phase field model that takes into account surface energy is presented and simulation results are discussed.

Deformation and Fracture from Nano to Macro: A Symposium Honoring W. W. Gerberich's 70th Birthday: Simulations of Mechanical Behavior

Sponsored by: The Minerals, Metals and Materials Society, TMS Materials Processing and Manufacturing Division, TMS Structural Materials Division, TMS/ASM: Mechanical Behavior of Materials Committee, TMS: Nanomechanical Materials Behavior Committee
Program Organizers: David F. Bahr, Washington State University; James Lucas, Michigan State University; Neville R. Moody, Sandia National Laboratories

Wednesday PM Room: 214D
March 15, 2006 Location: Henry B. Gonzalez Convention Ctr.

Session Chair: Erica T. Lilleodden, Forschungszentrum Karlsruhe

2:00 PM Invited

Molecular Dynamics Simulations of Deformation and Fracture Behavior in Nanocrystalline Ni: Diana Farkas¹; ¹Virginia Tech

This talk will discuss large scale atomistic studies of the plastic deformation, fracture and fatigue mechanisms occurring in nanocrystalline metals of various grain sizes. We have studied Ni digital samples with grain sizes from 5 to 12 nm in diameter and randomly generated fully three dimensional microstructures. Using molecular statics and dynamics techniques, we observe various mechanisms of plasticity in these digital

samples. The mechanisms observed include dislocation based mechanisms, grain boundary accommodation of slip and twinning. We observe grain boundary mechanisms of plasticity at the smallest grain sizes. At room temperature these include grain boundary motion as a stress accommodation mechanism. Our results show a distribution of grain boundary mobilities present in the samples, and the role of grain boundary motion in the deformation process at the nano-scale is discussed in detail.

2:20 PM

Dislocation Dynamics Simulations of Rough Surface Contact: Lucia Nicola¹; Alan Needleman¹; Allan Bower¹; Erik Van der Giessen²; ¹Brown University; ²University of Groningen

Due to unavoidable roughness, contact between surfaces is characterized by localized plastic deformation. When the loading is removed this leads to the development of a residual stress state that can promote crack nucleation. Therefore the study of plasticity in rough surface contact is of major importance for understanding friction and wear, as well as contact and fretting fatigue. We carry out simulations of indentation of an infinitely long two dimensional deformable single crystal by a rigid flat indenter. The profile of the crystal surface is taken to be a sinusoidal wave. Plasticity in the crystal occurs by the collective motion of discrete dislocations, modeled as line singularities in an otherwise isotropic linear elastic medium. A set of constitutive rules is supplied for the glide of dislocations as well as their generation, annihilation and pinning at point obstacles. The simulations track the evolution of the dislocation structure during loading and unloading.

2:35 PM

Atomistic Simulation of Metal Surface Indentation Including Interface Friction and Adhesion: Virginie Dupont¹; Frederic Sansoz¹; ¹University of Vermont

At the nanoscale, the plasticity of films and surfaces is strongly influenced by friction and adhesion effects. The present paper investigates the role of these effects on the elastic deformation and defect nucleation of FCC crystals via simulation of mechanical contacts. We simulated the indentation of surfaces with a single crystal cylinder using molecular dynamics and statics. The results are compared to the continuum elastic theories of M'Ewen and Johnson, Kendall and Roberts including friction and adhesion, respectively. Single crystal simulations were performed with different crystal orientations and atomic potentials in order to change the friction and adhesion properties of the contact interface. These simulations agree well with the continuum theory at early deformation stage, but deviate from this theory near the elastic limit. Polycrystal simulations are also addressed and show that friction and adhesion have strong impact on the grain boundary evolution, associated with GB movement and deformation twins.

2:50 PM

Combined MD and Continuum Approaches towards Modeling Inter-Granular Failure Using Cohesive Zone Models: Veera Sundararaghavan¹; Nicholas Zabarvas¹; ¹Cornell University

Molecular dynamics (MD) is a valuable tool to understand GB response to loading conditions and hence, derive accurate cohesive laws for finite element simulations. In a MD study, we carried out a series of simulations on an arrangement of constrained atoms under loading in order to identify traction-separation laws in nanocrystalline GBs. Several dependencies were parametrically studied; these include dependence of grain boundary property on strain rate, mis-orientation, deformation modes (tension or shear), temperature etc. Modified cohesive laws which include thermal, rate dependence and deformation mode effects as provided by MD are presented and bicrystal simulations are initially carried out. These simulations employ a continuum slip theory based model for the interior of the grain. Extension from bicrystals to polycrystals with additional MD studies of cohesive response of tri- and quad- junctions to loading and subsequent incorporation of these effects in cohesive laws will be shown.

3:05 PM

A Molecular Dynamics Study of the Ductile to Brittle Transition in Dilute Iron Alloys: Neeraj S. Thirumalai¹; Peter A. Gordon¹; Michael J. Luton¹; Diana Farkas²; ¹ExxonMobil Research and Engineering Company; ²Virginia Tech

WEDNESDAY PM

Model empirical interatomic potentials were used to study crack tip processes in single crystals of iron containing substitutional nickel and chromium additions. Molecular Dynamics techniques were employed to simulate the atomic level configuration of the crack tip region at temperatures up to 300 K. Various orientations were selected for study, with Ni and Cr additions up to 10 atomic %, in a random solid solution. The configuration of the crack-tip region was found to be dependent on the crystal orientation and the associated activity of $\frac{1}{2}\langle 111 \rangle$ Burgers vector dislocations on the $\{110\}$, $\{112\}$ and $\{123\}$ slip planes. The emission of such dislocations at the crack-tip causes crack blunting and suppression of brittle crack extension. These results are discussed in terms of the effect of solute on the unstable stacking energy and the surface energy. The influence of the use of alternative empirical interatomic potentials on the observations is also discussed.

3:20 PM

Atomistic Simulation and Continuum Mechanics Analysis of the Formation of a Crack in a Disclinated Bicrystalline Nickel Nanowire: *Airat A. Nazarov*¹; Kun Zhou²; Mao See Wu²; ¹Ufa State Aviation Technical University; ²Nanyang Technological University

The stability of a cylindrical bicrystalline nickel nanowire containing a negative wedge disclination is studied via continuum mechanics calculations and atomistic simulations. The continuum theory considers stable and unstable double-ended equilibrium cracks initiating from the disclination in an isotropic cylinder, and takes into account the redistribution of stress due to crack disturbance. It predicts a critical disclination strength above which the disclination is unstable and an equilibrium crack can grow from it. For the atomistic simulations, a disclination is inserted into a cylinder of radius up to containing a special (310) [001] tilt grain boundary. Molecular statics relaxations are then performed starting from structures both without and with an initial interfacial crack. The continuum and atomistic calculations show very close agreement in the critical disclination strength, and general agreement in the stable crack length, the crack opening profile, and the stress field of the disclinated crack in the nanowire.

3:35 PM Break

3:55 PM Invited

Modeling Instrumented Indentation in Linear Viscoelastic Solids: *Yang-Tse Cheng*¹; Che-Min Cheng²; Wangyang Ni¹; ¹General Motors Corporation; ²Institute of Mechanics

Inspired by Professor Gerberich's work on indentation in viscoelastic solids and motivated by the needs for probing small-scale mechanical behavior of "soft" matters, we have recently studied indentation in linear viscoelastic solids using analytical and numerical modeling. In this presentation, we derive the initial unloading slope equation for indentation in linear viscoelastic solids using rigid indenters with arbitrary axisymmetric smooth profiles, including conical and spherical indenters. While the same expression is known for indentation in elastic and elastic-plastic solids, we show that it is also valid for indentation in linear viscoelastic solids, provided that the unloading rate is sufficiently fast. When the unloading rate is slow, a "hold" period between loading and unloading can be used to provide a correction term for the initial unloading slope equation. Finite element calculations are used to illustrate the methods of fast unloading, "hold-at-the-peak-load," and "hold-at-the-maximum-indenter-displacement" for determining instantaneous modulus by instrumented indentation.

4:15 PM

A Numerical Study on the Effect of Grain Morphology on Anelasticity of Polycrystals: *Angelo Simone*¹; Erik van der Giessen¹; C. Armando Duarte²; ¹University of Groningen; ²University of Illinois at Urbana-Champaign

Although the distribution of grain sizes and shapes in real materials is usually far from homogeneous, the importance of grain morphology in polycrystalline materials has been often neglected in theoretical and numerical studies. We present a study on the effect of grain morphology (size, size distribution and shape) on anelasticity of polycrystals caused by free grain boundary sliding. Free sliding is accounted for by means of the 'Generalized Finite Element Method for polycrystals', a novel computational technique developed by the authors. In the GFEM for polycrys-

tals the finite-element mesh does not need to mimic the grain morphology since grain boundaries and junctions are described by means of elements with embedded discontinuities. With this computational tool, we carried out a series of simulations on a wide range of grain morphologies in several arrangements of grains. Realistic polycrystalline aggregates were generated with a vertex dynamics simulation.

4:30 PM

3-D Atomistic Pathways of Slip Transmission across Twin Boundaries: *Ting Zhu*¹; Hyoung Gyu Kim²; Amit Samanta²; Ju Li²; ¹Georgia Institute of Technology; ²Ohio State University

Recent experiments show that the introduction of nano-sized twins within ultrafine crystalline metals leads to significant increases in the strain-rate sensitivity. To understand the role of the nano-scale twins in affecting the rate dependence of plastic flow, we study in this work the 3-D thermally activated dislocation motions near the coherent twin boundaries. Using the reaction pathway sampling scheme of nudged elastic band and dimer methods, we identify the atomistic pathways of slip transmissions of both perfect and partial dislocations across the twin boundaries. The activation energies and activation volumes are quantified, thus making contact with previous continuum analyses and experimental measurements.

4:45 PM

Short Range Ordering and Room Temperature Creep in Metallic Titanium-Aluminum Alloys: *M. Brandes*¹; Peter Anderson¹; Michael J. Mills¹; ¹Ohio State University

Titanium-aluminum alloys are widely known to undergo pronounced creep deformation at low stresses and temperatures. Recently, short range ordering (SRO) of aluminum atoms in the HCP titanium matrix of these materials was found to provide significant creep strengthening. The presence of SRO leads to planar slip and the pairing of $b = \langle 1120 \rangle$ dislocations. In this work, the pairing of these dislocations is observed and measured via transmission electron microscopy in creep deformed Ti-6 wt% Al of several SRO states. Utilizing a combination direct measurement and modeling, the diffuse anti-phase boundary energies, the Peierls stresses, and solid solution strengthening parameters for these alloys are determined.

5:00 PM

A Multi-Scale, Dislocation Mechanics Based Model to Characterize the Transition Region Fracture Toughness Behavior of Ferritic Steels: *Matthew Wagenhofer*¹; Marjorie EricksonKirk¹; Mark EricksonKirk¹; ¹Phoenix Engineering Associates, Inc.

Efforts to characterize the transition region fracture toughness behavior of ferritic steels have primarily been focused on the development of statistical models derived from empirical data sets. Recent work produced a quantitative model of the plastic work local to second phase particles that is required to initiate unstable cleavage fracture. This model captures the temperature dependence of the macroscopic toughness distribution and shows that it is a function of the strength of long range obstacles to dislocation motion. Further development has led to the refinement of a multi-scale, dislocation mechanics-based model to bridge the gap between the local nature of the plastic fracture work and the global nature of the macroscopic toughness values. Results presented here for A533B plate steel show that the multi-scale model is capable of capturing both the transition region temperature dependence as well as the distribution of toughness values across each temperature.

Fatigue and Fracture of Traditional and Advanced Materials: A Symposium in Honor of Art McEvily's 80th Birthday: Fatigue and Fracture IX

Sponsored by: The Minerals, Metals and Materials Society, TMS Structural Materials Division, TMS/ASM: Mechanical Behavior of Materials Committee

Program Organizers: Leon L. Shaw, University of Connecticut; James M. Larsen, U.S. Air Force; Peter K. Liaw, University of Tennessee; Masahiro Endo, Fukuoka University

Wednesday PM Room: 216
March 15, 2006 Location: Henry B. Gonzalez Convention Ctr.

Session Chairs: R. Sunder, BiSS Research; Detlef Lohe, Universität Karlsruhe

2:00 PM Invited

Influence of Residual Stresses and Mean Load on the Fatigue Strength of Case-Hardened Notched Specimens: *Karl-Heinz Lang*¹; Thomas Krug²; Detlef Löhle¹; ¹Universität Karlsruhe; ²Robert Bosch GmbH

Case-hardened gear wheels are cyclically most stressed components. To evaluate the tooth-foot load-capacity, the knowledge of the mean stress and residual stress sensitivity of the fatigue strength of the material conditions at the failure critical sites is necessary. The examinations on hand usually concern homogeneous materials. Systematic analyses for case-hardened conditions are missing. In this work case-hardened notched specimens with different residual stress states are investigated under cyclic bending. The results are analyzed using a local concept and an additional fracture mechanical approach. With the local concept it was possible to determine the crack initiation site which was partly at the surface and partly below the surface. The fracture mechanical approach was necessary to understand the crack stop behavior. A uniform description of the lifetime behavior could be achieved using a modified Haigh diagram which takes into account the local stress state at the failure critical site.

2:25 PM

Effect of Residual Stresses and Relaxation on Fatigue Crack Propagation at Notches: *Dennis Buchanan*¹; Reji John²; Alisha Hutson¹; ¹University of Dayton Research Institute; ²U.S. Air Force Research Laboratory

Fatigue crack propagation at critical locations such as holes and notches in turbine engine components pose many challenges. The presence of residual stresses and residual stress relaxation add considerable complication to these analyses. Baseline (as-machined) and shot peened double edge notch nickel-base superalloy specimens were tested at elevated temperature conditions. Corner crack propagation was monitored using electric potential, optical inspection and acetate replication during testing. FE analysis of corner crack propagation was accomplished using the 3D crack growth code ZENCRACK™ and FE code ABAQUS™. Residual stress depth profiles, measured via XRD on as-machined and shot peened surface finishes, were incorporated into the analyses. Crack propagation predictions with and without residual stresses were performed and compared with experimental measurements. The predicted crack propagation life correlated well with experimental results. A significant increase in crack growth life was observed for shot peened specimens under the imposed test conditions.

2:50 PM

Effects of Drawing Strain on the Bending Fatigue Properties of Hyper-Eutectoid (1.02%) Steel Wires: *Yang Yo Sep*¹; Park Seong Yong¹; Park Chan Gyung¹; Bae Jong Gu²; Ban Deok Young²; ¹POSTECH; ²TrefilARBED Korea

In this study, influences of drawing strain on bending fatigue properties of hyper-eutectoid (1.02%) steel wire with high strength were investigated. A series of the fatigue tests was carried out depending on drawing strain by using Hunter-type tester at a frequency of 60 Hz under the bending stress level of 900 to 1500 MPa. Microstructural changes of the wires were identified in the lateral direction by using transmission electron microscopy (TEM). Increasing drawing strain reduced lamellar spacing and cementite thickness, which effectively increased tensile strength of steel

wires from 4400 to 4600 MPa. However, the fatigue limit gradually decreased from 1450 to 1300 MPa. Overall mechanical properties of the filaments, depending on drawing strain, have been discussed in terms of the microstructural parameter change of lamellar spacing and cementite thickness. In addition, the changes of cementite morphology on the fatigue crack propagation of hyper-eutectoid steel wires will be discussed.

3:15 PM Invited

Fatigue Strength Improvement of Notched Structural Steels: *Shin-Ichi Nishida*¹; Nobusuke Hattori¹; Congling Zhou¹; Shengwu Wang²; ¹Saga University; ²Dalian Jiaotong University

Fatigue tests have been performed using two kinds of specimens made of a conventional structural steel; that is, one is statically pre-strained specimen with changing from 2% until 8% by tension and the other is roller worked one with changing roller working ratio from 0.25mm until 1.50mm in depth. In the case of pre-strained specimen, the fatigue limit decreases under the small pre-strain and gradually increases with the pre-strain. In addition, the increase of fatigue limit is only 5% under the 8% pre-strain in tension. On the other hand, in the case of roller worked specimen, the fatigue limit increases extraordinarily by 120% with increase in the roller working ratio and is gradually saturated and then deteriorates a little. This remarkable increase of fatigue limit would be caused by the existence of large compressive residual stress, work-hardening, elongated micro-scopic structures, etc. in comparison with the case of monotonic tension.

3:40 PM Break

3:55 PM Invited

Isolation of Crack Closure from Residual Stress Effect in Variable Amplitude Fatigue: *R. Sunder*¹; ¹BiSS Research

Residual stress variation is modeled in notch fatigue analysis as the primary variable affecting load sequence sensitivity of metal fatigue. In crack growth modeling, however, closure has emerged as the predominant variable to model sequence effects. This paper reviews recent research that appears to suggest that residual stress and crack closure may in fact qualify as independent variables that operate in synergy. Fractographic evidence from specially designed experiments appears to underscore the different nature of the two mechanisms. Crack closure truncates fatigue driving force, while residual stress moderates material resistance to fatigue driving force. It would follow that the residual stress effect should diminish or disappear altogether in vacuum, a possibility that appears to be indeed supported by available data from different materials.

4:20 PM

Effects of Laser Peening Treatment on High Cycle Fatigue Property of Degassing Processed Cast Aluminum Alloy: *Kiyotaka Masaki*¹; Yasuo Ochi¹; Takashi Matsumura¹; Yuji Sano²; ¹University of Electro-Communications; ²Toshiba Corporation

It is well known that the degassing (DG) process is very useful for decreasing cast defects such as porosity, micro-shrinkage, and inclusions in casting process of metallic alloys. The DG process is also the effective method for improvement of fatigue property of cast aluminum alloy. In this study, a laser peening (LP) treatment is applied to the DG processed cast aluminum alloy to improve the fatigue property. Fatigue tests of rotating bending loading are carried out on the LP treated DG processed cast aluminum alloy. It is found that the fatigue life in the whole range and the fatigue strength at 10⁷ cycles of the DG cast aluminum alloy are improved by the LP treatment. The reasons of the fatigue property improvement by the treatment are decelerated effects of the surface crack growth rate by the compressive residual stress of the surface layer induced by the LP treatment.

4:45 PM

Effects of Residual Stresses on Probabilistic Lifting of Engine Disk Materials: *Harry R. Millwater*¹; James Larsen²; Reji John²; ¹University of Texas at San Antonio; ²Air Force Research Laboratory

Residual stresses are known to be beneficial with respect to fatigue life of metal components. Shot peening or other techniques are routinely used to improve the fatigue performance. This study examines the importance of the residual stress on the fatigue life using a probabilistic methodology. Specifically, the residual stress at a bolt hole in a compressor disk com-

WEDNESDAY PM

posed of a superalloy is modeled as a random variable along with the initial crack size, life scatter and stress scatter. The sensitivities of the predicted probability-of-fracture with respect to the parameters of the random variables are computed and comprise a metric for comparison determining the significance of the residual stress on reducing the probability-of-fracture.

Fatigue and Fracture of Traditional and Advanced Materials: A Symposium in Honor of Art McEvily's 80th Birthday: Fatigue and Fracture X

Sponsored by: The Minerals, Metals and Materials Society, TMS Structural Materials Division, TMS/ASM: Mechanical Behavior of Materials Committee

Program Organizers: Leon L. Shaw, University of Connecticut; James M. Larsen, U.S. Air Force; Peter K. Liaw, University of Tennessee; Masahiro Endo, Fukuoka University

Wednesday PM Room: 215
March 15, 2006 Location: Henry B. Gonzalez Convention Ctr.

Session Chairs: Peter K. Liaw, University of Tennessee; Stan Lynch, DSTO

2:00 PM Invited

The Influence of Soft, Precipitate Free Zones at Grain Boundaries of Ti- and Al-Alloys on Their Fatigue and Fracture Behavior: *Gert Lütjering*¹; J. Albrecht¹; C. Sauer²; T. Krull¹; ¹Technical University Hamburg-Harburg; ²Lufthansa Maintenance

High strength Al-alloys and beta Ti-alloys containing weak precipitate free zones (PFZ) along grain boundaries usually fracture within these soft zones upon monotonic or cyclic loading. In these cases, the fracture properties are mainly influenced by the strength difference between the age-hardened matrix and the soft PFZ. In the case of pancake shaped grains, the mechanical properties are anisotropic. This paper presents results obtained from peak-aged 7475/7075 Al-alloys and from the beta Ti-alloys Ti-6246 and Beta-CEZ for different grain sizes and grain shapes. In case of Ti-6246, the yield stress was varied between 1000 MPa and 1500 MPa to demonstrate the influence of the strength difference between matrix and PFZ on fracture toughness and HCF strength. This influence of the yield stress was studied for small and large equiaxed beta grains (bi-modal and beta-annealed microstructures) as well as for pancake shaped beta grains (beta-processed microstructure).

2:25 PM

Intrinsic Fatigue Crack Propagation Kinetics for Al-Cu-Mg/Li: *Yun Jo Ro*¹; Sean R. Agnew¹; Richard P. Gangloff¹; Gary H. Bray²; ¹University of Virginia; ²Alcoa Technical Center

The composition and aging condition of Al-Cu alloys govern intrinsic fatigue crack propagation for vacuum, but have less effect in the saturation regime of water vapor pressure/frequency, p/f . For Al-Cu-Mg, vacuum growth rate at high K_{MAX} increases dramatically with the transition from clusters to S' precipitation. This increase is large near-threshold and correlates with a slip band to nondescript transgranular crack path transition. Conversely, Al-Cu-Li exhibits outstanding vacuum growth resistance for all aging and ΔK conditions, correlating with slip band cracking in all cases. Water vapor increases growth rates and promotes a brittle mode of transgranular cracking for each alloy. Considering natural aging, Li has no measurable effect on da/dN in vacuum, compared to Mg, but is beneficial (1.5-3 times slower da/dN) for water vapor saturated N_2 . Fatigue experiments with varying p/f test the hypothesized difference in Li vs Mg reaction with water to produce hydrogen at the crack tip.

2:50 PM

Identifying Sources of Fatigue Variability in a Powder Processed Nickel-Base Superalloy for Improved Life Prediction: *Michael J. Caton*¹; Sushant K. Jha²; James M. Larsen¹; K. Li³; William John Porter³; Andrew Henry Rosenberger¹; ¹U.S. Air Force Research Laboratory; ²Universal Technology Corporation; ³University of Dayton Research Institute

In improving life management methods for turbine aircraft engines, a thorough understanding of the sources and scale of fatigue variability in relevant alloys is required. The fatigue behavior of a powder processed IN-100 nickel-base superalloy was examined at 650 C and at a frequency of 0.33 Hz. The influence of a 6 second hold time at peak load was also investigated. Total fatigue life, crack initiation, and long and small fatigue crack growth rates were examined. The maximum observed scatter in fatigue life is over an order of magnitude, and the vast majority of this variability is introduced during initiation and very early crack growth. A critical crack size is identified, above which the relative variability in crack growth behavior from specimen to specimen is almost negligible. A method for predicting worst-case failures based upon a life dominated by crack growth is presented.

3:15 PM

Fatigue Crack Growth at 223K in High Strength Aluminum Alloys: *Cedric Gasqueres*¹; Christine Sarrazin-Baudoux¹; Jean Petit¹; David Dumont²; ¹ENSMA/Centre National de la Recherche Scientifique; ²Alcan CRV

Aluminum alloys aircraft structures are confronted with temperatures ranging from 300K on the ground down to 223K during a fly. This paper deals with a study of the fatigue crack propagation in two high strength 2xxx alloys at 223K. Tests were performed in an environmental chamber with a controlled atmosphere (dew point of 223K). Cooling of the specimen was performed by mean of two blocks fixed on both sides of the C.T. specimens. Crack closure was detected using the compliance method. The crack propagation mechanism in the naturally-aged alloys was shown strongly modified at 223K with an abrupt transition from a stage II propagation at 300K to a retarded crystallographic stage-I like propagation at 223K. But no change was observed on the peak-aged alloys. The data are analyzed in terms of a previous modeling and influence of microstructure, temperature and air dryness is discussed on the basis of scan observations.

3:40 PM Break

3:55 PM

Mixed-Mode I/II Fracture of Polytetrafluoroethylene: *Eric N. Brown*¹; Cheng Liu¹; George T. Gray¹; Dana M. Dattelbaum¹; ¹Los Alamos National Laboratory

In the current work we present on mixed mode I/II fracture in polytetrafluoroethylene (PTFE). Four complex crystalline phases have been reported in PTFE with three crystalline structures (phases II, IV, and I) are observed at atmospheric pressure with transitions at 19 and 30°C. Mode I fracture in PTFE is strongly phase dependence with a brittle-to-ductile transition associated with the room temperature phase transitions. Increases in J integral fracture toughness around room temperature and above result from the onset of stable fibril formation bridging the crack plane and increased plastic deformation. The stability of drawing fibrils is primarily determined by temperature and crystalline phase with additional dependence on loading rate and microstructure anisotropy. Mixed mode I/II loading conditions are achieved using a modified compact tension specimen with Arcan type fixtures and digital image correlation. The bulk failure properties are correlated to failure mechanisms through fractography of the fracture surfaces.

4:20 PM

An Empirical Relationship between Crack Advance and Strains during Stage II Fatigue Crack Growth in a FCC Metal: *Seon-Ho Choi*¹; Pedro Peralta¹; James Gee²; Zhiyong Xie²; ¹Arizona State University; ²University of Pennsylvania Medical Center

An empirical relationship between crack growth via plastic blunting and strain ahead of the crack tip is proposed. Cracks were grown under quasi-constant ΔK in the stage II region using pure polycrystalline nickel CT specimens. Two different sizes of CT specimens were prepared to study geometrical effects. A half cycle of the fatigue load that corresponds to the maximum K was applied during an in-situ loading experiment. The in-plane displacement fields were measured using digital image correlation and the corresponding strains were quantified using large deformation theory. It was found that there is a power law relationship between the maximum opening strain ahead of a crack tip and the applied load, ΔK , which indicates a proportionality between crack advance and plastic strain

at the crack tip. Finite element analysis using hybrid material properties based on hardness change in specimens also confirmed the power law relationship.

4:45 PM

Relationships between Tensile and Fracture Mechanics Properties and Fatigue Properties of Large Plastic Mold Steel Blocks: *Donato Firrao*¹; Paolo Matteis¹; Giorgio Scavino¹; Graziano Uberralli¹; Maria Giuseppina Ienco²; Maria Rosa Pinasco²; Enrica Stagno²; Riccardo Gerosa³; Barbara Rivolta³; Antonio Silvestri³; Giuseppe Silva³; Andrea Ghidini⁴; ¹Politecnico Di Torino; ²Università di Genova; ³Politecnico di Milano; ⁴LucchiniSidermeccanica

Molds for plastic automotive components such as bumpers and dashboards are usually machined from large pre-hardened steel blocks. Due to their dimensions, the heat treatment produces mixed microstructures, continuously varying with the distance from the quenched surface, at which fracture toughness and fatigue properties are not well known and generally lower than those corresponding to a fully quenched and tempered condition. The response of the mold to defects (for example, microcracks due to improper weld bed deposition) and strengths during service depends on steel properties, that in turn depend upon the heat treatment and the microstructure. A pointwise determination of the tensile, Charpy V-notched, fracture toughness and rotating bending fatigue properties was carried out in a large bloc. Infinite fatigue life was investigated by the stair-case method. The samples were obtained from different depths of the blooms. The relationship between mechanical properties, fracture surfaces morphology and microstructure was also investigated.

**Furnace Systems Technology Workshop:
Emerging Technologies and Energy Efficiency:
Energy Efficiency and Emerging Technologies
in Secondary Aluminum Melting**

Sponsored by: The Minerals, Metals and Materials Society, TMS Light Metals Division

Program Organizers: Paul E. King, U.S. Department of Energy; Subodh K. Das, Secat Inc

Wednesday PM
March 15, 2006

Room: Exhibit Floor
Location: Henry B. Gonzalez Convention Ctr.

Session Chair: Paul King, U.S. Department of Energy

2:00 PM Introductory Comments

2:05 PM Invited

Gas-Fired Immersion Melting of Aluminum: Technical Challenges: Shridas T. Ningileri¹; Qingyou Han²; *John A. Clark*³; Arvind Thekdi⁴; ¹Secat Inc; ²Oak Ridge National Laboratory; ³U.S. Department of Energy; ⁴E3M, Inc

Energy efficiency ranging from 55% to 75% is possible if natural gas-fired, immersed tube burners were used to melt aluminum from secondary sources instead of open flames. Currently, recuperated tube burners with capacities to remelt aluminum are available. Some manufacturer claim thermal efficiencies above 80%. Previous efforts by Babcock and Wilcox, under GRI contract in the late 1980's, demonstrated the feasibility of immersion melting of aluminum. However, technological gaps have stalled further full-scale development and application of this melting method. Present furnace geometries hurt efficient transfer of energy from tubes into the aluminum. Traditional refractory tubes are quite porous and promote metal penetration and dross build-up resulting in poor performance. Secat, Inc. is leading an effort on a U.S. Dept. of Energy - Industrial Technologies Program sponsored project to develop a scaleable, natural gas-fired, immersion melter for the secondary aluminum industry with potential to replace traditional open-flame reverberatory furnaces.

2:30 PM Question and Answer Period

2:35 PM

Improved Aluminum Melting Using Pumping: *Brian Golchert*¹; Hossam Metwally¹; Paul King²; Chris Vild³; ¹Fluent, Inc.; ²Albany Research Center; ³Metallux Systems

It has been suggested that stirring of molten aluminum during the melting process would increase the melting efficiency since it would allow the hotter aluminum at the top of the melt to mix with the colder aluminum at the bottom of the melt. Instead of using mechanical stirrers, one could use pumping, either mechanical or electromagnetic. This paper will present the results of a computational fluid dynamics study of the effect of pumping on the energy efficiency of an aluminum melter. How the pumps affect the temperature distribution and heat requirements needed to melt the aluminum will be analyzed. The effect of pump location and pumping power on the furnace efficiency will also be analyzed to determine if there exists an optimal location and size of the pump.

3:00 PM Question and Answer Period

3:05 PM Invited

High Temperature Industrial Furnace Based on Radiative Homogeneous Combustion for Improved Efficiency and Reduced Emissions: *Arvind Atreya*¹; ¹University of Michigan

A solution to the problem of "configuring combustion in industrial furnaces to increase efficiency and reduce emissions" is examined in a laboratory-scale furnace. The incoming oxygen-enriched air and fuel are highly preheated with wasted flue gas enthalpy. While simple, this method increases the NOx production and contributes to heat flux non-uniformities within the furnace. A solution to this problem is proposed where EGR, flame radiation and increased residence time are employed to reduce the flame temperature and thus NO. Nearly homogeneous burning occurs in distributed reaction zones under slightly rich conditions that enable increasing the flame radiation and also promote NO reburn reactions. The aim is to increase flame emissivities at temperatures not exceeding 1900K and provide uniform radiation heat flux at a magnitude exceeding 400kW/m², while maintaining strict constraints on NOx, CO, unburned hydrocarbons and particulate emissions. This enables increasing furnace productivity or decreasing its size and cost.

3:30 PM Question and Answer Period

3:35 PM Break

3:50 PM Invited

Energy Efficient Operation of Secondary Aluminum Melting Furnaces: *Paul E. King*¹; Jarrod J. Hatem¹; Brian M. Golchert²; ¹U.S. Department of Energy; ²Fluent Inc.

It has been shown that re-melted aluminum can be produced at approximately 5% of the energy required of primary production. However, industry wide studies suggest an average melt efficiency of 25% in secondary furnaces. Efficiency improvement of the re-melt process is a challenge that currently faces the industry. Refinement of this process requires analysis of the intricate combustion and heat transfer processes within the furnace. The Department of Energy, Albany Research Center (ARC) has had tremendous success at predicting the performance of industrial secondary furnaces. Through scale modeling and verifiable computational results, the ARC has been able to simulate the processes of industrial furnaces with a high degree of confidence. These methods have suggested small design modifications that improve overall furnace performance. Using the results from previous computational models, the ARC aims to define the design parameters that will result in peak efficiency considering both power input and emission composition.

4:15 PM Question and Answer Period

4:20 PM Concluding Comments

General Abstracts: Light Metals Division: Session II

Sponsored by: The Minerals, Metals and Materials Society, TMS Light Metals Division, TMS: Aluminum Committee, TMS: Magnesium Committee, TMS: Reactive Metals Committee, TMS: Recycling Committee

Program Organizers: Jim McNeil, Novelis Inc; Neale R. Neelameggham, US Magnesium LLC

Wednesday PM Room: 7D
March 15, 2006 Location: Henry B. Gonzalez Convention Ctr.

Session Chair: Michael J. Kaufman, University of North Texas

2:00 PM

Refinement of As-Cast Microstructure of Aluminum 319 Alloy Using High Intensity Ultrasonic Vibration: Xiaogang Jian¹; Thomas Tom Meek¹; Qigui Wang²; Qingyou Han³; ¹University of Tennessee; ²General Motors Corporation; ³Oak Ridge National Laboratory

High intensity ultrasonic vibrations were utilized in an attempt to achieve grain refinement for aluminum-silicon-copper based 319 alloy. Ultrasonic energy up to 1500 W was injected into the alloy during its solidification. Casting temperature was varied in order to obtain optimal grain refinement effect. The experimental results indicated that ultrasonic vibration has a significant effect on the as-cast microstructure of 319 alloy. Small globular grains were obtained instead of large dendritic grains. The morphology of the eutectic phase was also altered.

2:25 PM

Pullout Strengths of Keenserts in High Performance Aluminum Alloys: Alexander Ordonez-Chu¹; Marcus Prieto¹; Magdolna Hugi Haberl²; John Harold Kabisch³; Omar S. Es-Said¹; Richard Clark⁴; John Ogren¹; ¹Loyola Marymount University; ²Los Angeles Valley College; ³Long Beach City College; ⁴College of the Canyons

Numerous structural components on expendable launch vehicles require the use of blind installations for attachment purposes. For this study, a type of insert known as a Keensert was used. Keenserts are permanently installed into one of the structural members and a bolt is used to attach such structure to mating structure. The Keenserts in this study were installed into specimens made from 2219 aluminum alloy and 2099 aluminum-lithium alloy. Both T6 and T8 tempers were tested with Keenserts of three different lubricants and three different diameters. Maximum load was determined by pulling the inserts from their installations.

2:50 PM

Role of Scandium on Mechanical Properties of Al-Zn-Mg Alloys: Pathickal K. Poulouse¹; M. Ashraf Imam²; Jerry Feng²; Krishnan K. Sankaran³; ¹University of the District of Columbia; ²Naval Research Laboratory; ³Boeing Company

The effect of small amounts of scandium on strengthening characteristics of an Al-Zn-Mg alloy was studied. A composition close to aluminum alloy 7055 having 0.1wt% Sc was used (8 wt% Zn-2 wt% Mg-2wt% Cu-0.1wt% Zr-0.1wt% Sc-balance Al). The solution treated and quenched alloy was aged at 120°C in air. Progress of hardening as a function of time was monitored using hardness and impression tests until past peak hardness. Structure, density and homogeneity of distribution of intermetallic phases including Al₃(Sc_{1-x}Zr_x) were studied using transmission electron microscopy and diffraction techniques. Enhancement of stability of the grain structure due to the presence of Al₃(Sc_{1-x}Zr_x) was analyzed. The results are compared with aluminum alloy 7055. Changes in the homogeneous and heterogeneous precipitation characteristics due to scandium, including effect on precipitate-free zones and role of Al₃(Sc_{1-x}Zr_x) in providing nucleation sites for other precipitates, were examined. The relationship between microstructure and mechanical properties are discussed.

3:15 PM

Effect of Microstructural Features on the Mechanical Behavior of A356 Alloy: Yong Nam Kwon¹; Y. S. Lee¹; J. H. Lee¹; ¹Korea Institute of Machinery and Materials

A356 alloy is one of most widely used cast Al alloys for automotive components. Mechanical properties of A356 alloy largely depend on the casting defects, such as gas porosity, oxide film and so on. Recently, there has been an interesting report on the inverse Hall-Petch type relation on A356 alloy, which means the larger primary alpha gives rise to the higher strength. In the present study, the effect of the basic microstructural features of A356 alloy on the mechanical behavior of was studied. Various samples of A356 were prepared with different casting routes. In order to get rid of porosity effect, compressive deformation was applied. The results tell that the overall mechanical behavior is closely related with the porosity level, eutectic Si distribution as well as volume fraction of primary alpha. Discussion of the microstructural effect on deformation mechanism will be given in detail.

3:40 PM

Age Hardening Behavior of Modified Al-Si-Cu Cast Alloys: Junyeon Hwang¹; Herbert Doty²; Michael Kaufman¹; ¹University of North Texas; ²GM Powertrain

Two common cast aluminum alloys used in the automotive industry are alloys 319 (Al-Si-Cu) and 356 (Al-Si-Mg). These alloys have good castability, low density, acceptable mechanical properties and low cost. Slight property improvements are sometimes achieved by (1) alloying additions (modifiers, solid solution strengtheners, etc.), (2) modified heat treatments and (3) improved degassing procedures. In this study, 319 Al modified with Mg, Mn and Sr was examined after peak aging, over aging, step aging, etc. using a variety of advanced analytical characterization methods (e.g., transmission electron microscopy). The results indicate that small additions of Mn have a slightly beneficial effect on the baseline properties whereas larger additions decrease both strength and ductility. These and other effects are correlated with the observed variations in strength in order to clarify their role on structure-property relations in these alloys. [Supported by General Motors through the Powertrain Advanced Materials Engineering Group].

Hume Rothery Symposium: Multi-Component Alloy Thermodynamics: Kinetics and Microstructural Modeling

Sponsored by: The Minerals, Metals and Materials Society, TMS Electronic, Magnetic, and Photonic Materials Division, TMS: Alloy Phases Committee

Program Organizers: Y. Austin Chang, University of Wisconsin; Rainer Schmid-Fetzer, Clausthal University of Technology; Patrice E. A. Turchi, Lawrence Livermore National Laboratory

Wednesday PM Room: 202A
March 15, 2006 Location: Henry B. Gonzalez Convention Ctr.

Session Chair: Shuanglin Chen, CompuTherm, LLC

2:00 PM Invited

CalPhad and Phase Field Modelling: A Successful Liaison: Ingo Steinbach¹; Bernd Boettger¹; Nils Warnken¹; ¹ACCESS

The connection between CalPhad models and Phase Field models is discussed against the background of minimization of the total Gibbs energy of a system. Both methods are based on separation of a multiphase system into individual contributions of the bulk phases, which are described by appropriate models. While the CalPhad method uses a global minimization of the total Gibbs energy, the Phase Field method introduces local interactions, interfaces and diffusion and allows for nonequilibrium situations. As such the Phase Field method is much more general by its concept, however it can profit a lot if realistic thermodynamic descriptions, as provided by the CalPhad method, are incorporated. The present paper discusses details of a direct coupling between the Multi Phase Field method and the CalPhad method. Examples are presented from solidification of technical Mg and Ni base alloys and some problems arising from common practice of thermodynamic descriptions in order-disorder systems.

2:30 PM Invited

Application of Thermodynamic Database to Phase Field Modeling of Microstructural Evolution in Complex Multi-Component and Multi-Phase Alloys: *Yunzhi Wang*¹; Ning Ma¹; ¹Ohio State University

Most engineering alloys are multi-component and multi-phase with complex microstructures. The traditional constitutive models representing microstructural features by their average values without capturing the spatially varying aspects may not be sufficient to quantitatively define the microstructure and hence allow for establishing a robust microstructure-property relationship. The phase field approach has proven to be able to handle complex microstructural patterns. However, quantitative modeling at real length and time scales requires model inputs be linked to thermodynamic and mobility databases. In this presentation we review our recent efforts in developing quantitative phase field models by linking model inputs to multi-component and multi-phase thermodynamic databases. Critical issues related to the formulation of a non-equilibrium free energy as a function of both concentration and long-range order parameters based on the equilibrium free energies of individual phases available from the database will be addressed. Examples of applications will be given for advanced Ti alloys.

3:00 PM Invited

How Far Can We Rely on Multi-Component Equilibrium Thermodynamic Data in Non-Equilibrium Kinetic Simulations?: *Ernst Kozeschnik*¹; Ivan Holzer¹; Bernhard Sonderegger¹; ¹Graz University of Technology

When performing precipitation kinetics simulations in multi-component materials, input data such as chemical potentials or driving forces can be evaluated from equilibrium thermodynamic databases. Even interfacial energies can be estimated from these databases with surprising success, thus reducing the number of critical fit parameters to zero. However, solid-state precipitation is a non-equilibrium process by nature and the path along which the system evolves toward final equilibrium can significantly deviate from any kind of equilibrium state. With a novel model, the authors investigate the predictive potential of precipitation kinetics simulations based on thermodynamic equilibrium databases in a number of alloy systems and for various different materials. It is shown that in systems where the equilibrium thermodynamics is well known, the predictions are reasonably close to experiment.

3:30 PM Break

3:50 PM Invited

Modeling of Microstructure Evolution during Solidification of Multi-Component Alloys: *M. F. Zhu*¹; Weisheng Cao²; Shuanglin Chen³; Chunpyo Hong⁴; Y. Austin Chang²; ¹Southeast University; ²University of Wisconsin-Madison; ³CompuTherm LLC; ⁴Yonsei University

Driven by industrial demand, extensive efforts have been made to investigate microstructure evolution during solidification of multicomponent alloys. This paper briefly reviews the recent progress in modeling of microstructures in multicomponent alloy solidification using various models including phase field, front tracking and cellular automaton approaches. Then a two-dimensional modified cellular automaton (MCA) model coupled with phase diagram software PANENGINE is presented for the prediction of microstructures and microsegregation in solidification of ternary alloys. The model adopts MCA technique to simulate the nucleation and growth of dendrites. The thermodynamic data needed for determining the dynamics of dendritic growth are calculated with PANENGINE. After validating the model by comparing the simulated values with the prediction of the Scheil model for solute concentration profile in the primary dendrites as a function of solid fraction, the model was applied to predict the evolution of microstructure and microsegregation in the directionally solidified Al-rich ternary alloys.

4:20 PM

Thermodynamic and Microstructural Modeling of Nb-Si Based Alloys: *Sundar Amancherla*¹; Bernard Bewlay²; Ying Yang³; Y. Austin Chang³; ¹GE India Technology Center; ²GE Global Research; ³University of Wisconsin-Madison

Nb-Si alloys have gained much attention over the last decade as the next generation alloys for high-temperature aero-engine applications due to their low density and better properties. However the microstructures of

these alloys are quite complex and vary significantly with the addition of elements such as Ti and Hf. Hence an improved understanding of the phase stability and the microstructural evolution of these alloys is essential for rapid alloy design for advanced high-temperature applications. In the present paper we will describe the thermodynamic construction of the Nb-Si-Ti-Hf system and the microstructural evolution modeling results, obtained using a phasefield model. The results of the calculations for these Nb-Si based alloys will be compared with a range of experimental observations.

4:45 PM

Evaluation of Microstructure Evolution in Multiphase TRIP Steels by Thermodynamic and Diffusion Calculations Combined with a Dilatometry Analysis: *Chang-Seok Oh*¹; Dong-Woo Suh¹; Sung-Joon Kim¹; ¹Korea Institute of Machinery and Materials

During the past decades thermodynamic calculations with reliable databases for multicomponent alloy systems have been successfully applied to the development of new materials and understanding processing route thereof. In case of steels, use of thermodynamic calculation in delineation of microstructure evolution during heat treatment can't be fully validated due to the fact that interstitial element usually governs overall kinetics of phase transformation. Recently, methodology based on restricted equilibrium concept, such as para-equilibrium, was widely used in order to put more real factors to the thermodynamic calculation of steels. Meanwhile, in selected cases, numerical simulation of diffusion-controlled phase transformation has shown a sufficient level of accuracy and agreement with experimental observations. In this presentation, few examples are shown how thermodynamic and diffusion calculations combined with a dilatometric analysis can be used to predict microstructure evolution of the multiphase TRIP-aided steels, and limitation and usefulness of the multicomponent thermodynamic calculation are also discussed.

Lead Free Solder Implementation: Reliability, Alloy Development, and New Technology: Electromigration and Reliability

Sponsored by: The Minerals, Metals and Materials Society, TMS Electronic, Magnetic, and Photonic Materials Division, TMS: Electronic Packaging and Interconnection Materials Committee
Program Organizers: Nikhilesh Chawla, Arizona State University; Srinivas Chada, Medtronic; Sung K. Kang, IBM Corporation; Kwang-Lung Lin, National Cheng Kung University; James Lucas, Michigan State University; Laura J. Turbini, University of Toronto

Wednesday PM
March 15, 2006

Room: 214A
Location: Henry B. Gonzalez Convention Ctr.

Session Chairs: K. N. Subramanian, Michigan State University; Laura J. Turbini, University of Toronto

2:00 PM Invited

Electromigration in Pb-Free Flip Chip Solder Joints on Flexible Substrates: *Jae-Woong Nah*¹; Fei Ren¹; King-Ning Tu¹; Sridharan Venk²; Gabe Camara³; ¹University of California, Los Angeles; ²Belton-Group; ³Western Digital

Flexible circuit technology enables smaller, lighter, faster products, and lower cost because flexible circuit can be rolled, bent, and folded to fit a limited space where required. Therefore, flip chip on flex may have a wide application for liquid crystal display (LCD), hard disk drive (HDD), automotive, and medical electronics applications, etc. As the electronics industry continues to push for high performance and miniaturization, electromigration is one of serious reliability issues in flip chip solder joints on flexible substrates. In this study, we report electromigration behavior of flip chip Sn96Ag3.5Cu0.5 solder joints on flexible substrates. The in-situ resistance change of the flex circuit during the electromigration test was measured. And the voids movement inside the solder joints due to electromigration was investigated. This voids movements was matched with the resistance change during the electromigration test.

2:25 PM

Threshold Current Density of Electromigration in Eutectic SnPb and SnAgCu Solder Lines: *Min-Seung Yoon*¹; Min-Ku Ko¹; Young-Chang Joo¹; Oh-Han Kim²; Young-Bae Park²; ¹Seoul National University; ²Andong National University

The flip chip packages with the higher current densities have given rise to the electromigration-induced failure. Threshold current density is defined by the current density in which the electromigration flux is zero, i.e. atomic migration did not occur any longer. Drift velocities of eutectic SnPb and SnAgCu lines with the length of 1000 μm at the various current densities were measured through the interruptive test. From the drift velocities, threshold current density was calculated. The threshold current densities of the eutectic SnPb and SnAgCu lines are 7.4×10^3 A/cm² at 100°C and 1.8×10^4 A/cm² at 140°C, respectively. The threshold current density was measured in the solder lines with the various line lengths. Threshold current density is determined by the balance of the forward flux (electric-wind-force) and the backward flux (the stress-gradient or the atomic-concentration-gradient). Details on the immortal condition of the eutectic SnPb and SnAgCu will be discussed.

2:45 PM

Effects of Solder Volume on the Cross-Interaction between Cu and Ni in Cu/Sn3.5Ag/Ni Solder Joints: *C. E. Ho*¹; S. C. Yang¹; Chien Wei Chang¹; C. Robert Kao¹; D. S. Jiang¹; ¹National Central University

The copper/solder/nickel sandwich structure was one of the most common solder joint configurations for electronic packages. In the past, many studies just focused on the unilateral reaction of solders with Cu or Ni, and didn't take into consideration the possible interaction of the two interfaces. In this study, the interaction between Cu and Ni across the Sn3.5Ag (wt.%) solder was investigated. The Sn3.5Ag spheres used in this study were 760, 500, or 300 microns in diameter. As a result, solder joints with the same configuration but three different volumes were studied. The as-reflowed joints were subjected to high temperature storage at 160°C. The results revealed the Cu₆Sn₅ and the Ni-bearing Cu₆Sn₅ were the predominant reaction products on the Cu-side and the Ni-side of the joints, respectively. Their growth and morphologies were found to be strongly dependent on the solder volume. The kinetics and the underpinning mechanism will be presented.

3:05 PM Break

3:25 PM

Electrical Characteristics for Sn-Ag-Cu Solder Bump with Ti/Ni/Cu Under-Bump-Metallization after Environmental Tests: T. I. Shih¹; S. Y. Tsai²; G. J. Chiou¹; *Jeng-Gong Duh*¹; ¹National Tsing Hua University; ²Ming Hsin University of Science and Technology

Lead free solder bump has been widely used in current flip chip technology (FCT) due to the environment issue. Solder joints after various environmental tests were employed to investigate the interfacial reaction between the Ti/Ni/Cu under-bump metallization (UBM) and Sn-Ag-Cu solders. The environmental tests included highly accelerate stress test (HTST), temperature cycling test (TCT), and high temperature storage test (HTSL). An SEM internal probing system was introduced to evaluate the electric characteristics in the intermetallic compounds after different test conditions. The electric data would be correlated to microstructural evolution due to the interfacial reaction between solder and UBM. In addition, a REBECA-3D software was also used to simulate the corresponding strain and stress distribution in the joints subjected to environmental tests.

3:45 PM

Joule Heating Effect in Flip-Chip Solder Joints for Various Dimension of Al Traces: *Sheng-Hsiang Chiu*¹; Chih Chen¹; S. S. Lin²; C. M. Chou²; Y. C. Liu²; K. H. Chen²; ¹National Chia Tung University; ²MEGIC Technology

The purpose of this paper is to investigate the thermal characteristic of solder bumps with different dimension of Al trace under current stressing in flip-chip package. The thermal characteristic of flip-chip solder joints under different current stressing conditions was measured by infrared technique. The measured temperature increase due to Joule heating, and we also discussed the temperature increase in different dimension of Al trace under current stressing. Because the Al traces on the chip side have much

higher electrical resistance than the total electrical resistance of the flip chip solder joints and the Cu pad on the substrate. The Al trace on the chip side is the major heat source during current stressing. According the results from infrared technique, it was found that the solder joint of with longer Al trace has Joule heating effect than that of solder joint with shorter Al trace.

4:05 PM

Morphology and Growth Pattern Transition of IMCs between Cu and Sn3.5Ag Containing Small Amount of Additives: *Feng Gao*¹; Tadashi Takemoto¹; Hiroshi Nishikawa¹; ¹Osaka University

The morphology and the grain growth pattern of IMCs formed between Cu substrate and Sn3.5Ag solder doped with small amount of additives (0.1mass%), say, Ni or Co, was investigated. The faceted-shape IMCs were observed for outer region of (Cu, Ni)₆Sn₅ or (Cu, Co)₆Sn₅ IMCs. However, the rounded-shape IMCs were identified for inner region of (Cu, Ni)₆Sn₅ or (Cu, Co)₆Sn₅ IMCs. Based on the thermodynamic calculation, the enthalpy change for the outer region IMCs was significantly elevated due to the high concentration of Ni or Co additives. Consequently the increased Jackson parameter value was even larger than 2 to ensure the formation of faceted-shape crystal. The abnormal grain growth (AGG) was demonstrated from the evolution of IMC grain size distribution. With the extended reflow time, the abnormal large grain size of outer region of (Cu, Ni)₆Sn₅ or (Cu, Co)₆Sn₅ IMCs was generated.

4:25 PM

A Study on the Rework Lead-Free Solder Components: *Huann-Wu Chiang*¹; Ming-Chuan Chen¹; Jeffrey Lee²; ¹I-Shou University; ²Advanced Semiconductor Engineering, Inc.

A rework process will be performed on low-profile quad flat package (LQFP) components with various terminal finishes by using Sn-3.0Ag-0.5Cu lead free solder wire on Cu/Ni/Au PCB (printed circuit board). After 3 time rework processes, samples will be subjected to 150°C HTS (high temperature storage) 1000 hours aging or -40 to 125°C 1000 cycles thermal cycling test (TCT). Sequentially, the cross-section analysis is scrutinized by SEM/EDX (scanning electron microscope/energy dispersive spectrometer) and EPMA (energy probe micro analysis) to observe metallurgical evolution in the interface and solder buck itself. Pull test will be performed on the TCT samples. The relationship among interfacial microstructure, the terminal finish and the joint strength will then be analyzed and discussed. Samples by normal SMT process will also be analyzed for comparison.

Magnesium Technology 2006: Alloy Development I

Sponsored by: International Magnesium Association, TMS Light Metals Division, TMS: Magnesium Committee
Program Organizers: Alan A. Luo, General Motors Corporation; Neale R. Neelameggham, US Magnesium LLC; Randy S. Beals, DaimlerChrysler Corporation

Wednesday PM

Room: 6B

March 15, 2006

Location: Henry B. Gonzalez Convention Ctr.

Session Chairs: Gordon Dunlop, Advanced Magnesium Technologies; Kwang S. Shin, Seoul National University

2:00 PM

AM-Lite a New Magnesium Diecasting Alloy for Decorative Applications: Trevor Abbott¹; Morris Murray¹; *Gordon Dunlop*¹; ¹Advanced Magnesium Technologies Pty Ltd

The recently developed magnesium diecasting alloy, AM-lite, has attributes that address many of the issues that restrict the growth of applications for the well known magnesium diecasting alloy, AZ91D. As well as being capable of replacing AZ91D, AM-lite can also replace zinc and aluminium diecasting alloys and plastics in many applications. The most important features of AM-lite relate to its diecastability, its much improved as-cast surface, ability to be electroplated, oxidation and corrosion resistance, improved mechanical properties and recyclability. Improved fluidity of the alloy leads to an ability to reliably diecast very thin sections with

reduced dimensions of runners and overflows. The as-cast surface is much smoother than AZ91D resulting in a reduced need for buffing or polishing as preparation for surface finishing operations. The surface chemistry allows high quality electroplating at a similar cost as for zinc diecastings. Diecast AM-lite has a much higher linear elastic limit than AZ91D and this provides a higher design strength. Because of its resistance to oxidation, the alloy has improved recyclability giving it a potential for in-cell recycling in many diecasting operations.

2:20 PM

Effect of Ca Addition on the Microstructure Evolution of AZ31 Alloy During Thermomechanical Processing: *Elhachmi Essadiqi¹; Jian Li¹; C. Galvani¹; P. Liu¹; R. Varano²; S. Yue²; Ravi Verma³; ¹MTL CANMET; ²McGill University; ³General Motors R&D Center*

The use of Magnesium alloys in auto industry has been limited to diecast parts due to their low ductility and fracture toughness. Grain refinement in wrought magnesium alloy can be produced by thermal-mechanical processing to increase the ductility, fracture toughness and the strength. In this study, the microstructure of two AZ31 alloys during extrusion and hot rolling, one with Ca and one without Ca addition, were compared. The magnesium with small amount of Ca addition produced finer grain size. The grain refinement is attributed to the precipitation of small Ca-rich particles, which reduce the grain boundary mobility and stabilize the fine-grained microstructure during extrusion and subsequent hot rolling.

2:40 PM

Effect of Ca on Microstructure and Mechanical Properties of Mg-Li-Al Alloy: *Hong Bin Li¹; Guang Chun Yao¹; Yi Han Liu¹; ¹Northeastern University*

Mg-9mass%Li-2mass%Zn(-Ca) alloys were cast and rolled to sheet at room temperature. Effect of Ca on microstructure and mechanical properties of the sheet is studied in this study. Uniaxial tension tests are carried out at room temperature. The rise of tensile strength and elongation of sheets is 19% and 6%, respectively, when Ca content being 0.1mass%. While elongation descends largely with Ca content rise. Ca can refine grains and the effect of thinning is the evident test while Ca content being 0.1mass%. It is clarified that adsorption of Ca on the grain boundary makes grains refined and that it changes the mechanical properties of sheets.

3:05 PM

Effect of Ca/Y on Tensile Properties and Damping Capacity of As-Cast Mg-0.6Zr Alloy: *Chuming Liu¹; Ren Feng Ji¹; Haitao Zhou¹; ¹Central South University*

The effect of Ca/Y on tensile properties and damping capacity of Mg-0.6Zr alloy are investigated. It is found that the 0.3%Ca, 0.3%Ca+0.1%Y added into Mg-0.6Zr alloy respectively leads to both grains refinement and improvement of tensile properties which refers to grain strengthening and solution strengthening. In contrast, the damping capacities of the modified alloys measured by DMA decreased slightly. When strain is below 0.014, Q-1 decreases rapidly. While strain is over 0.014, Q-1 decreases slightly. This indicates that it is dependent on strain amplitude. The decrease of damping capacity is due to the hindrance to the motion of dislocations with the element Ca/Y and the increasing number of grain boundaries. The most interesting result is that the addition of Ca/Y suspends the damping peak(P1) of Mg-0.6Zr at 75°C. The damping mechanism of the tested alloys could be analyzed by G-L dislocation damping model.

3:30 PM

Effects of Alloying Elements on Mechanical Properties of Mg-Al-X Alloys at Elevated Temperatures: *Kwang Seon Shin¹; Woo Chul Cho¹; Hwa Chul Jung¹; ¹Seoul National University*

Various new magnesium alloys have been developed in recent years for elevated temperature applications. In the present study, the effects of various alloying elements on mechanical properties of Mg-Al-X alloys were investigated at elevated temperatures. Various alloying elements including Ca, Sr, Mn (Misch metal), etc. were added to Mg-Al alloys in order to either introduce the thermally stable precipitates at grain boundaries as well as in the grain interior or suppress the formation of the Mg17Al12 phase and thus improve the high temperature mechanical properties of magnesium alloys. The specimens were produced on a 320 ton high pressure die casting machine. The microstructures of the specimens were examined by optical and scanning electron microscopy. In addition,

the existence and distribution of second phases were also examined by X-ray and EPMA. The high temperature mechanical properties of the die-cast specimens were examined in the temperature range of 150°C to 200°C.

4:10 PM Break

3:50 PM

Hot Deformation Behaviors of Mg-6Zn-2Nd-0.5Zr Alloy: *Haitao Zhou¹; Zhendong Zhang¹; Chuming Liu¹; ¹Central South University*

Deformation behaviors of Mg-6Zn-2Nd-0.5Zr alloy during hot compression at temperature range from 543 K to 693 K and strain rate from 0.001s⁻¹ to 1 s⁻¹ are investigated. Flow softening is found to occur and all flow curves exhibit a peak with characteristics of dynamic recrystallization and significantly change with temperature and strain rate. As a result of DRX, the grains are greatly refined through dynamic recrystallization, and the mean size of the recrystallized grain decreases with the decrease of temperature or the increase of Z parameter, while the reciprocal of the recrystallized grain has a good linear relationship with the natural logarithm of Z value. After comparison of DRX grain size, it is found 593K is the best deformation temperature. After hot extrusion at 593 K, the yield strength and tensile strength of extruded Mg-6Zn-2Nd-0.5Zr alloy are 320MPa and 370MPa respectively, which are higher than that of ZK60 alloy.

4:30 PM

Influence of Li and Y Alloying Additions on Microstructural Evolution and Texture of Magnesium Alloys: *Luke William Fox Mackenzie¹; Mihriban Pekguleryuz¹; Ravi Verma²; ¹McGill University; ²General Motors*

The influence of alloying additions, Li and Y, on the microstructural and texture evolution of pure magnesium and AZ31 alloys, during thermomechanical processing, has been investigated. Alloy coupons were cast in copper moulds and homogenized at temperatures between 380 and 450°C. As-cast and homogenized microstructures were then characterized, and the homogenized specimens were rolled up to 60% at temperatures between 25 and 400°C. Selected specimens were subsequently annealed at 400°C. Optical microscopy, scanning electron microscopy and electron backscattered diffraction (EBSD) were used to characterize the microstructures and textures of the rolled and annealed alloys. The influence of Li and Y alloying additions on the microstructural evolution and texture of magnesium alloys has been demonstrated.

4:50 PM

Magnesium Alloys with Magnetic Properties: *Martin Bosse¹; Friedrich-Wilhelm Bach¹; ¹University Hanover*

Magnesium is suited especially as construction material for highly accelerated components. In order to increase its field of application, magnesium alloys shall additionally be equipped with ferro-magnetic properties. The main objective of the presented project founded by the German Research Foundation (DFG) is to develop a composite material made of magnetic particles and a magnesium base alloy. The die casting process is used to insert magnetic powders in the outer surfaces of the component. Hence, it is possible to use this part of the component as a storage zone for magnetic encoding. A second goal is the characterization of magnesium alloys which are modified by additions of cobalt in combination with Rare Earth (RE) metals. Previous research at IW has shown that intermetallic phases with magnetic properties can be precipitated controllably. These phases open the possibility to use the reverse magnetostriction effect to measure the mechanical load in the component.

5:10 PM

The Microstructures and Tensile Properties of AZ61-RE Alloy: *Haitao Zhou¹; Zijuan Liu¹; ¹Central South University*

The microstructure and tensile properties of AZ61 and AZ60-RE alloys are investigated. It is found that RE brought about precipitation of a new Al11RE3 phase besides β phase. After hot extrusion, both alloys are refined due to dynamic recrystallization. However, a very finer grain with size of 6μm is obtained in AZ61-RE. This suggests that RE had a great effect on grain refining during dynamic recrystallization. Tensile tests at room temperature suggest that the strength of hot-extruded AZ61-RE is higher than that of AZ61-RE alloy, whilst ductility of hot-extruded AZ61-RE is a little lower. The improvement of tensile properties of AZ61-RE alloy by RE addition is attributed to very finer grains.

5:30 PM

High-Strength Mg-Zn-RE Alloys with Long Period Order Structure: *Yoshihito Kawamura*¹; *Shintaro Yoshimoto*¹; *Michiaki Yamasaki*¹; ¹Kumamoto University

Ingot metallurgy (I/M) alloys with a long period order (LPO) phase had excellent yield strength above 400 MPa, ultimate tensile strength of 450 MPa or more, and elongation of 5% or more. Magnesium alloys in which LPO phase was formed were limited to magnesium with Zn and RE elements added. RE elements forming LPO phase were limited to seven: Y, Gd, Tb, Dy, Ho, Er, and Tm. The Mg-Zn-RE alloys with LPO phase can be divided into two types. Type I is Mg-Zn-(Y, Dy, Ho and Er) alloys, in which LPO phase was formed in an as-cast state. Type II is Mg-Zn-(Gd, Tb and Tm) alloys. In the type II, LPO phase which did not exist in an as-cast state was formed by annealing at 773 K for 5 hours or more. The LPO Mg-Zn-RE alloys are expected to yield a new concept of strengthening in magnesium alloys.

Magnesium Technology 2006: Wrought Alloys and Forming Processes III

Sponsored by: International Magnesium Association, TMS Light Metals Division, TMS: Magnesium Committee

Program Organizers: Alan A. Luo, General Motors Corporation; Neale R. Neelameggham, US Magnesium LLC; Randy S. Beals, DaimlerChrysler Corporation

Wednesday PM
March 15, 2006

Room: 6A
Location: Henry B. Gonzalez Convention Ctr.

Session Chairs: Alan A. Luo, General Motors Corporation; Mihriban O. Pekguleryuz, McGill University

2:00 PM

Low-Temperature Superplasticity of Bulk Microcrystalline Magnesium Alloys: *Vladimir N. Chuvil'deev*¹; *Mikhail Yu. Gryaznov*¹; *Anatoly N. Sysoev*¹; *Vladimir I. Kopylov*²; ¹Physical-Technical Research Institute of Nizhny Novgorod State University; ²Physical-Technical Institute of National Academy of Science

New microcrystalline ZK60, AZ31, and AZ91 magnesium alloys are processed by equal - channel angular pressing (ECAP). Mean grain size of microcrystalline magnesium alloys is equal to 1 micron. The record low-temperature superplastic characteristics are obtained in microcrystalline alloys: ZK60 (elongation to failure is equal to 810%), AZ31 (400%), and AZ91 (380%) at temperature of 250°C and strain rate of 0.003 1/s. Moreover, ECAP technology increases the room temperature elongation of commercial cast magnesium alloys up to 3 times without decreasing tensile strength. The model of superplastic flow rheology of microcrystalline magnesium alloys is developed; it is shown that non-equilibrium state of grain boundaries is the main factor influencing the deformation behavior of microcrystalline magnesium alloys at low-temperature superplasticity. The authors thank International Scientific and Technical Center (Grant #2809) and U.S. CRDF (Grant Y2-P-01-04) for financial and technical support.

2:20 PM

Low Temperature Hydrostatic Extrusion of Magnesium Alloys: *Jan Bohlen*¹; *Jacek Swiostek*¹; *Heinz Günter Brokmeier*¹; *Dietmar Letzig*¹; *Karl Ulrich Kainer*¹; ¹GKSS Research Centre

Semi-finished components from magnesium wrought alloys like extruded profiles are in the focus of present studies in order to improve the properties of final structural parts. The parameter settings during extrusion, e.g. the extrusion temperature, play an important role for the development of the microstructure and therefore the resulting mechanical properties of the extruded component. In this paper hydrostatic extrusion trials using several magnesium alloys will be shown. The extrusion temperatures were varied in a range beginning as low as 100°C which resulted in a better homogeneity of the microstructure compared to trials at 200 – 300°C. A very fine grain size leads to improved mechanical properties. The microstructure and texture of extruded rods will be shown and compared to the mechanical properties. The influence of the extrusion tem-

perature and the mechanisms that play a role during the development of the microstructure will be discussed.

2:40 PM

The Temperature Dependent Role of Twinning in the Ductility of Magnesium Alloy Sheet: *Ashutosh Jain*¹; *Sean R. Agnew*¹; ¹University of Virginia

A polycrystal plasticity simulation code was used to model experimental compression test data obtained from AZ31 sheet over the temperature range $T = 300-473$ K. The resulting model predicts the deformation behavior, including strength and strain anisotropy, as well as deformation texture evolution. The predicted relative activities of deformation modes suggest that excessive twinning is detrimental to ductility, as it causes rapid hardening to stress levels which result in failure. Thermally activated deformation modes, prismatic and pyramidal slip, compete with twinning and promote ductility. Twinning also has a significant impact on the flow stress during a change in strain path, such as compression along the rolling direction followed by compression along the normal direction. Such non-monotonic strain paths are ubiquitous in practical metal forming, which provides an incentive to model their impact. Accurate models could assist forming process designers, and ultimately promote the use of wrought magnesium.

3:00 PM

Microstructure Evolution during Hot Rolling of Magnesium Alloy AZ31 Strip: *Mahmoud Shehata*¹; *Jon Carter*¹; *Claude Galvani*²; *Amjad Javaid*²; *Elhachmi Essadiqi*²; *Ravi Verma*¹; ¹General Motors R&D; ²CANMET-MTL

A series of quenching experiments was designed to follow the evolution of microstructure during the hot rolling of a 5 mm strip into 1.5 mm sheet. The hot rolling schedule consists of three passes (30% reduction each) at 350 C, where the material was reheated between rolling passes so that each reduction pass started at 350 C. Samples were quenched after the passes, and after the reheats so as to monitor the dynamic recrystallization during reduction and the static recrystallization during reheat. Metallography of the quenched samples showed that the large cast grain structure is broken down by segmentation of the cast grain through localized deformation in twin bands, where dynamic recrystallization occurs in these bands as well as in the grain boundaries (necklacing). Quantitative metallography by image analysis was performed to quantify the extent of static and dynamic recrystallization at each processing step.

3:20 PM

Microstructure and Texture Evolution during the Uniaxial Tensile Testing of AM30 Alloy: *Lan Jiang*¹; *Stephane Godet*¹; *John J. Jonas*¹; *Alan Luo*¹; *Anil Sachdev*¹; ¹McGill University

The evolution of microstructure and texture were examined in an AM30 alloy during uniaxial tensile testing under different conditions. This study is part of a systematic analysis of the formability of Mg alloy tubes during warm hydroforming. Samples were cut from extruded AM30 tubes along the extrusion direction. Microstructural and EBSD examination show that double twinning exerts an important influence on both flow and fracture at temperatures below 200°C. Dynamic recrystallization (DRX) was observed even at 150°C. However, it never goes to completion under any set of conditions. The microstructures near fracture surfaces indicate that cracks are readily formed next to twins at high strain rates; such twinning-induced cracks are evident at temperatures up to 250°C. Partial recrystallization also exacerbates the tendency for cavitation. No significant change in the texture occurred during straining along the extrusion direction.

3:40 PM Break

4:00 PM

Numerical Modelling of Large Strain Deformation Phenomena in HCP Metals: *Julie Lévesque*¹; *Kaan A. Inal*¹; *Kenneth W. Neale*¹; *Alan A. Luo*²; *Raja K. Mishra*²; ¹University of Sherbrooke; ²General Motors Corporation

In this paper, a new constitutive framework based on a rate-dependent crystal plasticity theory is presented to simulate large strain deformation phenomena in HCP metals. In this new model the principal deformation mechanisms considered are crystallographic slip and deformation twinning. The new framework is incorporated into in-house finite element

(FE) codes and simulations are performed using two approaches. In the first approach, the Taylor theory of crystal plasticity is adopted to model the behavior of the polycrystalline material. In the second approach, each grain is represented individually using one or more finite elements. Using these two approaches, various large strain phenomena for magnesium alloys at different temperatures are investigated. These include behavior in tension and compression as well as localized deformation failures. In certain cases comparisons are made with experimental results. Limitations of the current modelling approaches will also be discussed.

4:20 PM

Microstructure, Mechanical Properties and Bendability of AM60 and AZ61 Magnesium Alloy Tubes: Yingxin Wang¹; Xiaoqin Zeng¹; Wenjiang Ding¹; Alan A. Luo²; Anil K. Sachdev²; ¹Shanghai Jiaotong University; ²General Motors

Microstructure, mechanical properties and bendability of AM60 and AZ61 magnesium alloy tubes have been investigated. AM60 magnesium alloy tube is extruded with extrusion-temperatures of 643K and 693K and average strain rates of 0.1s⁻¹ and 0.6s⁻¹ successfully and the extrusion-temperature is 683K and average strain rate is 0.1s⁻¹ for AZ61 magnesium alloy tube. Lower extrusion-temperature leads to higher yield strength for AM60 magnesium alloy tube and the strain rate has no effect on the mechanical properties. Meanwhile, extrudability of AM60 alloy is better than that of AZ61 alloy. The results of bendability of AM60 and AZ61 magnesium alloy tubes show that the bendability of AM60 magnesium alloy tube is better than that of AZ61 magnesium alloy tube and lower yield strength results in the well bendability for the two magnesium alloy tubes. Furthermore, compressive stress leads to the more twinings formed during the bending process than tensile stress.

4:40 PM

Warm Formability and Plastic Anisotropy of AZ31B Mg Sheets: W. Bang¹; H. J. Sung¹; I. J. Kim¹; Dong-Kyun Choo¹; Woo Jin Park¹; In-Ho Jung¹; Sangho Ahn¹; ¹Research Institute of Industrial Science and Technology

Due to the limited ductility and the extensive springback at room temperature, warm forming is considered indispensable for the processing of Mg sheets. In this study, the warm formability of Mg sheets has been evaluated, having different fabricating routes such as strip cast and coil rolled, DC cast and sheet rolled, DC cast and extruded. A series of mechanical tests has been conducted to characterize the deformation behaviors of AZ31 sheets at elevated temperatures. Deep drawing tests have also been conducted using the universal drawing machine equipped with an warm toolset. Transition of drawability and failure mode was investigated in terms of measured mechanical properties, i.e. plastic anisotropy.

5:00 PM

High Internal Pressure Forming of Magnesium Tubes: Adi Ben-Artzy¹; A. Spinat²; O. Dahan²; K. Siegert³; S. Jager³; Klaus Bernd Mueller⁴; T. Altan⁵; ¹Rotem Ind; ²Magtech-Magnesium Technologies; ³Stuttgart University; ⁴Technische University; ⁵Ohio State University

High-strength steels, aluminum, and polymers are already being used to reduce the weight of various components in many fields, but much additional reduction could be achieved by greater use of low-density magnesium (Mg) and its alloys. Lightweight components will improve ease of use, performance and structure of many applications, especially where mobility is essential. In transportation (bicycle, vehicle, spacecraft etc.) applications - for example, the steel in a chassis is strong and relatively cheap but is also very heavy. A reduction in vehicle weight will reduce fuel consumption and emission without degrading performance. Magnesium is an attractive material, primarily because of its light weight (Mg density ~ 1.7 g/cm³) - it is 36% lighter per unit volume than Al and 78% lighter than iron (Fe). When alloyed, it has the highest strength-to-weight ratio of all the structural metals, about 65% of that of Aluminum. Furthermore, Mg is the eighth most abundant element; seawater, the main source of supply, contains 0.13% Mg, which represents a virtually unlimited supply. The objective of this research was to develop a method for the manufacturing of lightweight components from magnesium alloys, for all stages of manufacturing up to the semi-finished part, where the rest of the finishing can be done in conventional methods. Internal High Pressure forming (IHP-forming) is a well-known technique for the production of struc-

ture parts in the automotive industry. Especially in the body structure, weight saving is an important design issue, which can be realized by load optimized design and the use of lightweight materials, such as aluminum and magnesium. However, magnesium has a hexagonal lattice structure and shows a low formability at room temperature, as well as different tensile- and compression properties. Beside the strength properties, the formability of the extrusions plays a key role for potential applications. First investigations on hot extruded magnesium tubes show that a maximum hoop strain of 20% can be realized under plane strain condition, if the forming temperature is increased to 350°C. However, the tube does not expand uniformly, which leads to a non-uniform wall thickness reduction of the IHP-formed part. The reasons for the non-uniform expansion might be found in the hot extrusion technique (indirect hot extrusion, direct hot extrusion with moving or fixed mandrel) as well as in differences of the grain size of hot extruded tubes. Some complex magnesium technological demonstrators were formed by Internal High Pressure forming, using hot in-direct extruded Mg-tubes. These tubes were formed in certain parameters and showed a good formability in radial direction, as well as high strength properties, which are required for structure parts.

Materials Design Approaches and Experiences II: New Tools

Sponsored by: The Minerals, Metals and Materials Society, TMS Structural Materials Division, TMS: High Temperature Alloys Committee

Program Organizers: Michael G. Fahrman, Special Metals Corporation; Yunzhi Wang, Ohio State University; Ji-Cheng Zhao, General Electric Company; Zi-Kui Liu, Pennsylvania State University; Timothy P. Gabb, NASA Glenn Research Center

Wednesday PM
March 15, 2006

Room: 202B
Location: Henry B. Gonzalez Convention Ctr.

Session Chair: Gregory B. Olson, Northwestern University

2:00 PM Invited

Integration of Computational Tools for Predicting Thermodynamics and Precipitate Microstructure Evolution: T. Wang¹; Y. Wang¹; C. Ravi¹; S. Y. Hu¹; J. X. Zhang¹; S. H. Zhou¹; Christopher M. Wolverton²; Zi-Kui Liu¹; Long Qing Chen¹; ¹Pennsylvania State University; ²Ford Motor Company

This presentation will report our recent progresses in establishing a MATerials Computation And Simulation Environment (MATCASE) that integrates first-principles calculations, computational thermodynamics (CALPHAD), phase-field models, and object-oriented finite element computation of macroscopic properties. In particular, it will be shown that it has now become a routine practice to rely on first-principles calculations to provide some of the necessary data for constructing thermodynamic, kinetic, and lattice parameter databases using the CALPHAD approach. These databases are necessary for the inputs to phase-field simulations of precipitate microstructure evolution. The advantages and limitations of various models to incorporate CALPHAD thermodynamics within the phase-field formulation will be discussed. Examples to be presented include precipitation reactions in binary and ternary Ni-base superalloys as well as Al-alloys.

2:30 PM Invited

Software Implementation of Computational Materials Dynamics for Accelerated Design of Hierarchical Materials: Herng-Jeng Jou¹; Gregory Olson²; ¹QuesTek Innovations LLC; ²Northwestern University/QuesTek Innovations LLC

Computational materials design and accelerated insertion of materials (AIM) rely on a set of interacting mechanistic process/structure and structure/property models. This presentation will discuss the recent development of PrecipiCalc™ and the Computational Materials Dynamics (CMD) software platform, which provide robust and efficient implementation of accelerated material design. The PrecipiCalc software provides detailed high fidelity precipitation kinetic simulations for material process optimization, as successfully demonstrated under the DARPA AIM initiative on

Ni-based superalloys. Integration with underlying CALPHAD-based tools and with a high-level optimization engine, such as iSIGHT, are critical software components and are fully implemented in the PrecipiCalc and CMD system. In addition, a graphical user interface of the CMD system was developed to unify the operation and accelerate the testing/development of the software tools. Examples of accelerated material developments with these software tools will be discussed.

3:00 PM Invited

Modeling the Material Properties and Behaviour of Multicomponent Alloys: Nigel John Saunders¹; Zhanli Guo²; Alfred Peter Miodownik²; Jean-Philippe Schille²; ¹Thermotech Ltd; ²Sente Software Ltd.

This presentation describes the development of a multi-platform software programme called JMatPro for calculating the properties and behaviour of multi-component alloys. These properties are wide ranging, including: •Thermo-physical and physical properties (from room temperature to the liquid state). •Temperature dependent mechanical properties up to the liquid state. •TTT/CCT diagrams of steels, Al-alloys, Ni-based superalloys, Ti-alloys. •Physical and mechanical properties of steels as a function of time and temperature during quenching. A feature of the new programme is that the calculations are based on sound physical principles rather than purely statistical methods. Thus many of the shortcomings of methods such as regression analysis can be overcome. It allows sensitivity to microstructure to be included for many of the properties and also means that the true inter-relationship between properties can be developed, for example in the modelling of creep and precipitation hardening.

3:30 PM Invited

Development of Modeling Tools for the Prediction of Materials Properties: Fan Zhang¹; S.-L. Chen¹; K.-S. Wu¹; Y. Yang¹; W. Cao²; Y. A. Chang²; ¹CompuTherm LLC; ²University of Wisconsin-Madison

Materials with desired properties are constantly needed in today's world. To achieve desired microstructures and mechanical properties, materials must be improved by adjusting alloy chemistry and processing conditions. Traditionally, these improvements have been made by a slow and labor intensive series of experiments. Today, different modeling tools have been developed that allow the simulation of material properties. Implementation of such tools has been proved to be useful in materials development and improvement and has resulted in significant cost savings through the elimination of shop/laboratory trials and tests. In this talk, we will present the simulation tools developed at CompuTherm with respect to both thermodynamic and kinetic modeling aspects. We will discuss the features of Pandat for multi-component phase equilibrium calculation. We will also show how PanEngine, the calculation engine of Pandat, can be connected with kinetic models for the kinetic simulation. Examples for industrial applications will be demonstrated.

4:00 PM Break

4:15 PM Panel Discussion

State-of-the-Art Modeling and Future Needs: Moderated by M. Fahrman, Special Metals Corporation

Materials in Clean Power Systems: Applications, Corrosion, and Protection: Interconnection and Sealing in Fuel Cells III

Sponsored by: The Minerals, Metals and Materials Society, TMS Structural Materials Division, TMS/ASM: Corrosion and Environmental Effects Committee

Program Organizers: Zhenguo Gary Yang, Pacific Northwest National Laboratory; K. Scott Weil, Pacific Northwest National Laboratory; Michael P. Brady, Oak Ridge National Laboratory

Wednesday PM
March 15, 2006

Room: 212B
Location: Henry B. Gonzalez Convention Ctr.

Session Chairs: Lichun Leigh Chen, Engineered Materials Solutions Inc; Jin Yong Kim, Pacific Northwest National Laboratory

2:00 PM

Development of a Compliant Seal for Planar SOFCs: K. Scott Weil¹; Brian J. Koepfel¹; ¹Pacific Northwest National Laboratory

A critical issue in developing high performance planar solid oxide fuel cell (pSOFC) stacks is appropriate seal design. To date, essentially two standard methods of sealing are used by stack developers: (1) rigid seals (e.g. glass) or (2) compressive seals (typically mica based). Each method has its own set of advantages and design constraints. We are developing an alternative approach that conceptually combines advantages of both techniques, including hermeticity, mechanical integrity, and minimization of interfacial stresses in either of the joint substrate materials, particularly the ceramic. The new sealing concept relies on a plastically deformable metal seal; one that offers a quasi-dynamic mechanical response in that it is adherent to both sealing surfaces. We will present recent experimental data on one version of this seal, as well as results from modeling of a full-scale design.

2:25 PM

Effect of Cathode and Electrolyte Transport Properties on Chromium Poisoning in Solid Oxide Fuel Cells: Jeffrey W. Fergus¹; ¹Auburn University

A major degradation mechanism in solid oxide fuel cells (SOFC) is poisoning of the cathode by chromium from volatilization of the interconnect materials. The chromium deposition is generally considered to occur by an electrochemical reaction, which can only occur where both ions and electrons are available. For a purely ionic conducting electrolyte and a purely electronic conducting cathode, such an electrochemical reaction can only occur at the three-phase gas-electrolyte-electrode interface. However, the introduction of ionic conductivity into the cathode or electronic conductivity into the electrolyte can allow deposition to occur away from this three-phase interface, and thus alter its effect on the fuel cell performance. In this paper, the chromium poisoning of SOFC cathodes will be reviewed, with a focus on the effects of the transport properties of the cathode and electrolyte materials.

2:50 PM

Oxidation Resistance and Mechanical Properties of Experimental Low Coefficient of Thermal Expansion (CTE) Ni-Base Alloys: David E. Alman¹; Paul D. Jablonski¹; ¹U.S. Department of Energy

Energy generation systems must operate at higher temperatures and pressures in order to achieve increased efficiency. This may require the utilization of high temperature, high strength Ni-base alloys. However, the high thermal expansion coefficients (CTE) of commercially available Ni-base alloys relative to low cost ferritic steels, may make it difficult to employ Ni-base alloys in hot sections. Utilizing prior work by Yamamoto et al¹ and the ThermoCalc phase prediction software, a series of Ni-based alloys were developed at the Albany Research Center based on the composition range of Ni-(18-25)Mo-(8-15)Cr-1Ti-0.5Mn, with CTEs similar to ferritic steels. The oxidation behavior was measured at 800C in moist air. The tensile properties were measured at 25C and 750C after aging at 750C for upwards of 1000 hours. The results were compared to Haynes 230 and Haynes 242. ¹Yamamoto et al. Energy and Technology, 21, 2002.

3:15 PM

Development of Clad Metals for Planner SOFC Interconnects: *Lichun Leigh Chen*¹; Z. Gary Yang²; G. G Xia²; Jeff W. Stevenson²; ¹Engineered Materials Solutions Inc; ²Pacific Northwest National Laboratory

Recent research and development in metallic interconnect materials for solid oxide fuel cells (SOFC) at operating temperatures in the range of 650~850°C have focused mainly on two major alloy groups to meet the multiple requirements. That is ferritic stainless steels, and Ni-based heat resistance alloys. Coating is also being studied to improve the material performance. In the present work, a different material option, clad metals, is explored, in order to combine the merits and overcome the shortfalls of different alloys or alloy groups. In addition, the applications of clad metal technologies can allow dealing with the dual environments of the SOFC interconnect separately at each side. Roll-bonded clad metals with a high chromium ferritic stainless steel substrate and Ni-based superalloy surface clad layers were processed and tested under the SOFC interconnect service conditions. This paper will present the details of this developing effort.

Multicomponent-Multiphase Diffusion Symposium in Honor of Mysore A. Dayananda: Surfaces and Interfaces

Sponsored by: The Minerals, Metals and Materials Society, ASM Materials Science Critical Technology Sector, ASM-MSCTS: Atomic Transport Committee

Program Organizers: Yong-Ho Sohn, University of Central Florida; Carelyn E. Campbell, National Institute of Standards and Technology; Richard Dean Sisson, Worcester Polytechnic Institute; John E. Morrall, Ohio State University

Wednesday PM Room: 203B
March 15, 2006 Location: Henry B. Gonzalez Convention Ctr.

Session Chair: Yong-Ho Sohn, University of Central Florida

2:00 PM **Invited**

Single Atom Surface Diffusion: An Atomic View: *Seong Jin Koh*¹; ¹University of Texas at Arlington

The diffusion of single atoms on atomically flat surfaces and the effects of atom-atom interactions on single atom diffusion will be presented. The diffusion of single atoms was studied by tracing the displacement of individual atoms using a field ion microscope (FIM) and model systems of Pd and W on W(110). It was found that for both Pd and W, the adatoms make long jumps in addition to nearest-neighbor jumps. The ratio of long jumps to nearest-neighbor jumps increases as temperature goes higher, indicating that at high temperatures the long jumps would prevail. The effects of adatom interactions on single atom diffusion were studied with Pd and Ir atoms on W(110) as model systems. It was found that the adatom-adatom interactions are long-range and quite anisotropic, which drastically affects the random characteristic of single atom diffusion. Supported by the Department of Energy (DEFG02-96ER-45439).

2:30 PM

Rapid Diffusion in Grain Boundary Triple Junctions: *Alexander H. King*¹; Mysore A. Dayananda¹; Raghavan Narayanan¹; Shashank Shekhar¹; ¹Purdue University

It is well-recognized that grain boundaries act as rapid diffusion paths in polycrystalline materials, and they can dominate mass transport at lower temperatures. In recent years, it has become apparent that the triple lines at which grain boundaries meet (grain boundary triple junctions, or GBTJs) may have distinct properties and behaviors from the grain boundaries themselves. In order to investigate the kinetic effects of GBTJs, we have performed a study of the diffusion of nickel into copper, using controlled tricrystals of copper. This allows us to assess the penetration of nickel into the crystal lattice, the grain boundaries and the GBTJ, independently. The results provide a clear demonstration of enhanced diffusion along the triple junctions, along with a number of other effects. The implications for mass transport in polycrystals will be discussed. Acknowledgement: This work

is supported by the US Department of Energy, under contract number DE-FG01-01ER45940.

2:55 PM **Break**

3:15 PM **Invited**

Ad- and Desorption of Oxygen at Metal-Oxide Interfaces: Two-Dimensional Modelling Approaches: *A. Oechsner*¹; M. Stasiak¹; J. Gracio¹; ¹University of Aveiro

Metal/ceramic phase boundaries are of great importance for many applications in materials science technology, e.g. to thin solid films or coatings. They are also included in microminiature electronic devices, e.g. MOSFETs. The presence of solute atoms at internal metal-oxide interfaces influences the physical properties of the interfaces and this, in turn, may affect the bulk properties. Therefore, it is an important task to predict and measure accurately the level of equilibrium solute-atom segregation at internal interfaces. In the presented work, the segregation of oxygen at Ag/MgO interfaces is numerically simulated whereas a general segregation kinetic which incorporates adsorption and desorption of oxygen is considered. The solution of the coupled system of partial differential equations is based on a two-dimensional finite element scheme for arbitrary oxide distribution. Based on model oxide distributions, the influence of the oxide distribution is numerically investigated and compared with the solution for equidistant arrangements.

3:45 PM

Interface Chemistry of Fe/Al-Si Bimetallic Joints: *Myriam Sacerdote-Peronnet*¹; Jean-Claude Viala¹; ¹University of Lyon

This contribution deals with the chemical reactivity in bimetallic couples resulting from the association of molten Al-Si alloys and ferrous base metals. The applied background concerns the development of various metallic products for the automotive and aeronautic industries. The interface reactivity of the Fe/Al-Si system was studied by two complementary approaches: experimental determination of the phase equilibria in the ternary system at 730°C (isothermal reaction-diffusion and thermal analysis), characterization of the reaction zones formed at the interfaces, depending on the temperature and the silicon content of the aluminium alloy. From the results obtained, a refined Al-Fe-Si section at 730°C and the reaction scheme describing the crystallisation sequence of Al-Fe-Si liquids below 730°C are proposed. We also determined the growth kinetics and mechanism at these interfaces. The diffusion path concept was used to relate the phase diagram of the relevant systems with the reaction layers observed at the interfaces.

4:10 PM

Interface Diffusion Phenomena in Advanced Materials: *Yury R. Kolobov*¹; Maxim B. Ivanov¹; Ilya V. Ratochka²; ¹Belgorod State University; ²Institute of Strength Physics and Materials Science SB RAS

The characteristic regularities of diffusion and diffusion-controlled processes (grain boundary sliding, dislocation accommodation and grain boundary migration) in polycrystalline metals and alloys with bcc and fcc crystal lattice during annealing and simultaneous activity of temperature and loading during creep were considered. The particular features of the effect of grain boundary sliding activation by directed diffusion fluxes of atoms along grain boundaries are discussed. The interaction and interference of diffusion processes - grain boundary sliding and migration - as the factors determining the development of plastic deformation at conditions considered are analyzed. The determining role of diffusion-controlled processes on grain boundaries in grain boundary sliding development during creep and superplastic flow of nanostructured metals and alloys is proved. The regularities of low temperature or/and high-strain rate superplasticity manifestation in the materials indicated were investigated.

4:35 PM **Concluding Comments**

Phase Stability, Phase Transformation and Reactive Phase Formation in Electronic Materials V: Phase Simulation and Interface Reactions in Solder Joints

Sponsored by: The Minerals, Metals and Materials Society, TMS Electronic, Magnetic, and Photonic Materials Division, TMS Structural Materials Division, TMS: Alloy Phases Committee

Program Organizers: Katsuaki Suganuma, Osaka University; Douglas J. Swenson, Michigan Technological; Srinivas Chada, Jabil Circuit, Inc.; Sinn Wen Chen, National Tsing-Hua University; Robert Kao, National Central University; Hyuck Mo Lee, Korea Advanced Institute of Science and Technology; Suzanne E. Mohny, Pennsylvania State University

Wednesday PM Room: 213B
March 15, 2006 Location: Henry B. Gonzalez Convention Ctr.

Session Chairs: C. Robert Kao, National Central University; James W. Morris, University of California, Berkeley

2:00 PM Invited

Melting Point Lowering of the Sn-Sb Alloys Caused by Substrate Dissolution: *Sinn-Wen Chen*¹; Po-Yin Chen¹; Chao-Hong Wang¹; ¹National Tsing Hua University

Sn-Sb alloys are used for the soldering of ceramic devices. The liquidus and solidus temperatures of the Sn-5wt%Sb alloy are 244°C and 240°C, respectively. However, in the step soldering, the Sn-Sb solder melts at temperature lower than 232°C. Dissolution of the Ag and Cu substrates into the molten Sn-Sb alloys are determined by metallographical examinations and atomic absorption. The melting points of the ternary Sn-Sb-Cu and Sn-Sb-Ag alloys are determined using differential thermal analyzer. It is found that the substrate dissolution into the Sn-Sb alloy in the first reflowing process is the primary cause for the melting point lowering phenomenon. During the first reflow, the substrate either Cu or Ag dissolves into the molten solder, and the binary Sn-Sb alloy becomes a ternary melt. The ternary melts are with lowering melting points. Preliminary liquidus projections of the ternary systems are constructed to illustrate the solidifications of the ternary melts.

2:35 PM Invited

Numerical Prediction of Fraction of Eutectic Phase in Sn-Ag-Cu Soldering: *Machiko Ode*¹; Minoru Ueshima²; Taichi Abe¹; Hideyuki Murakami¹; Hidehiro Onodera¹; ¹National Institute for Materials Science; ²Senju Metal Industry Company, Ltd

A combination of macro-scale solidification simulation and phase-field calculation is employed to predict fraction of the eutectic phase in Sn-4.0mass%Ag-XCu solder alloys (X=0.5-1.1mass%). The solidification simulation incorporates the cooling rate in the phase-field simulation. We assume the residual liquid solidifies as eutectic phase when the driving force for the nucleation of Sn₆Cu₅ amounts to a critical value. The driving force is estimated as the free energy difference between that of Sn₆Cu₅ and the undercooled melt adjacent to the primary beta-Sn phase. The driving force criteria are determined based on the force in 4.0mass%Ag-1.1mass%Cu alloy. The obtained ratio of eutectic phase shows good agreement with the experimental data.

3:10 PM

Lead-Free Soldering: The Meaning of Formation Enthalpies of Liquid and Solid Alloys: *Hans Flandorfer*¹; Herbert Ipser¹; ¹University of Wien

Besides its melting temperature, the solidification behavior of a solder and its interfacial reactions with substrate materials are the most important criteria for joining and the reliability of solder joints. Thus, for a systematic design of new solder materials, a comprehensive knowledge of intermetallic phases, phase relations, thermochemical properties, and diffusion is indispensable. Usually, solders are binary or higher-order alloy systems whereas substrate materials are a single component, but very often also binary or higher-order systems. The intermetallic system formed after joining is therefore of ternary or higher-order. Phase diagrams of

such complex systems cannot be treated experimentally only but thermodynamic calculations according to the well established CALPHAD method are necessary. However, their quality depends strongly on experimental data like e.g., the enthalpy of formation of solid and liquid alloys. Furthermore, the formation enthalpy plays an important role for the theoretical prediction of diffusion behavior and various surface phenomena.

3:35 PM

Investigation of the Phase Equilibria of the Sn-Cu-Au Ternary, the Sn-Cu-Au-Ag Quaternary System, and Interfacial Reactions in Sn-Cu/Au Couples: *Yee-Wen Yen*¹; Hsien-Ming Hsiao¹; Chiapng Lee¹; Yu Tseng¹; Yu-Lin Kuo²; ¹National Taiwan University of Science and Technology; ²Case Western Reserve University

Sn-Ag-Cu and Sn-Cu alloys are the commercial Pb-free solders and widely used in electronic industries. The Au is commonly used in FC technology, TAB as UBM and substrate materials in PCB. In this study, the phase equilibria of the Sn-Cu-Au ternary, Sn-Ag-Cu-Au quaternary system, and interfacial reactions in Sn-Cu/Au were experimentally investigated. Results indicate that there exists a complete solid solubility between AuSn and Cu₆Sn₅ at 200°C and three ternary intermetallic compounds are found at 200°C. Three IMCs, AuSn, AuSn₂, AuSn₄ are found in all couples, and (Au,Cu)Sn/(Cu_xAu_{1-x})₆Sn₅ is found in all Sn-Cu/Au couples except the Sn/Au couple. Total thicknesses of reaction layers increase with higher temperature, longer reaction time and lower content of Cu, and the growth mechanism can be described by using the parabolic law. In addition, with increasing reaction time, the IMC AuSn₄ disappears gradually, and turns into (Au,Cu)Sn/(Cu_xAu_{1-x})₆Sn₅.

4:00 PM Break

4:10 PM Invited

Growth and Reconfiguration of Interfacial Intermetallics in Solder Joints: *John W. Morris*¹; Tae-Kyu Lee¹; Kyu-Oh Lee¹; ¹University of California

The bonding of microelectronic solders to the contacts they joined is usually accomplished by the formation of intermetallics between the Sn constituent of the solder and the various metallic constituents of the contact, primarily Cu and Ni. The nature and morphology of the intermetallic is affected by the composition of the solder and the contacts, by the temperature and duration of the reflow and by the temperature and time in subsequent service. The present talk will focus on some anomalous features and effects of intermetallic growth: exaggerated intermetallic development in asymmetric joints, anomalous precipitation in the bulk and massive reconfiguration if intermetallics during service.

4:45 PM

Effect of Co Addition to Sn-Ag Solder on Interfacial Reaction and Joint Strength of Solder with Cu: *Hiroshi Nishikawa*¹; Akira Komatsu¹; Tadashi Takemoto¹; ¹Osaka University

The reaction between Sn-Ag solder added Co and Cu substrate was investigated in order to clarify the effect of the addition of Co to Sn-Ag solder on the formation of intermetallic compound at the interface and the joint strength of the solder with Cu. Sn-3.5mass%Ag-xCo solders (x = 0, 0.1, 0.3, 0.5, 1.0mass%) was specially prepared. As a result, it was shown that the thickness of the intermetallic compound (IMC) at the interface was the thinnest in binary Sn-3.5Ag solder just after reflow process at 250°C for 60s. During aging process at 150°C for 504h, in the case of solder added Co, the growth rate of the IMC layer is lower compared to the case of Sn-Ag solder. On the other hand, during aging process, the degradation of the joint strength for Co added solders is smaller than that for binary Sn-3.5Ag solder.

5:10 PM

Effect of Ni Particles and Nano-Sized Ni₃Sn₄ Powders Addition on the Interfacial Reactions between Sn-Ag-Ni Solders and Cu Substrate: *Hsiang-Yi Lee*¹; *Li-Yin Hsiao*¹; Jenq-Gong Duh¹; Su-Yueh Tsai¹; ¹National Tsing Hua University

Ni and nano-sized Ni₃Sn₄ powders were incorporated into Sn and Ag powders to form 95.5Sn-3.5Ag-1.0Ni solders by mechanical alloying. The morphologies of IMC at Ni-doped and Ni₃Sn₄-doped solders/Cu interfaces after reflows at 240°C were observed. (Cu,Ni)₆Sn₅ IMC in Ni₃Sn₄-doped solder appeared pebble-shape, while scallop-shape (Cu,Ni)₆Sn₅ was

revealed in Ni-doped solder. Due to the difference in thickness of IMC, the reaction was much rapid in the Ni₃Sn₄-doped solder. By quantitative analysis. The variations of Ni concentration in (Cu,Ni)₆Sn₅ were evaluated. The elemental redistributions of (Cu,Ni)₆Sn₅ were discussed and correlated to Ni-Cu-Sn ternary equilibrium.

5:35 PM

Growth of Bulk Cu-Sn Compound by Liquid Phase Electroepitaxy: *Yao-Chun Chuang*¹; *Cheng-Yi Liu*¹; ¹National Central University

Cu-Sn compounds phases, Cu₃Sn and Cu₆Sn₅, play very important roles for the reliability of Sn-based solders jointing with Cu pads. Yet, the physical properties of Cu-Sn compounds are still not very well understood! In the talk, we will report the fabrication of bulk Cu-Sn compounds by using liquid phase electroepitaxy (LPEE) process. Under different process temperatures, Cu₃Sn and Cu₆Sn₅ compounds can be grown, respectively. Also, from X-ray analysis, we found that LPEE-grown Cu₃Sn and Cu₆Sn₅ compounds are nearly single crystal and have the prefer orientation along the direction of the electrical current. The plane of LPEE-grown Cu-Sn compounds, which parallel with the direction of electrical current, was found to have the largest d spacing and the lowest planar density. Besides, physical properties of Cu-Sn compounds, CTE, and electrical resistivity, will be reported in this talk.

Phase Transformations in Magnetic Materials: Information Storage

Sponsored by: The Minerals, Metals and Materials Society, TMS Materials Processing and Manufacturing Division, TMS/ASM: Phase Transformations Committee

Program Organizers: Raju V. Ramanujan, Nanyang Technological University; William T. Reynolds, Virginia Tech; Matthew A. Willard, Naval Research Laboratory; David E. Laughlin, Carnegie Mellon University

Wednesday PM Room: 213A
 March 15, 2006 Location: Henry B. Gonzalez Convention Ctr.

Session Chairs: Kazuhiro Hono, National Institute for Materials Science; Yasukazu Murakami, Tohoku University

2:00 PM Invited

A1 to L10 Transformation in FePt Nanoparticles: *Sara Majetich*¹; *Yi Ding*¹; ¹Carnegie Mellon University

FePt nanoparticle arrays have been proposed for the next generation of data storage media, as made the coercivity is low. When the particles are annealed to induce the transformation, they sinter. Here we describe the mechanism of the A1 to L10 transformation in nanoparticles, in order to understand why the phase transformation is much more challenging in nanoparticle arrays than in thin films. We investigated the switching field distributions in samples with and without sintering. The switching field distributions are related to the volume distributions and show that the larger particles are, on average, more likely to have transformed. By repeating this process for particles of different initial sizes, we demonstrate the importance of grain boundary diffusion and the limitation of the nucleation site density.

2:35 PM Invited

Atomic Ordering in FePt Nano-Particles: *Mihaela Tanase*¹; *Timothy Klemmer*²; *Jian-Gang Zhu*¹; *David E. Laughlin*¹; ¹Carnegie Mellon University; ²Seagate Research

FePt nano-particles are being studied world wide for their potential use as ultra-high density media. The ordering process takes the FCC phase (A1,cF4) into the L10 phase (tP2). We present our recent results on the atomic ordering process in nano-particles of FePt. Of particular interest is the effect of size and shape of the particles on the ordering kinetics and the maximum atomic order parameter obtained. Our investigations include high resolution TEM, selected area electron diffraction and nano-beam electron diffraction. This work is supported by Seagate Research, through the Data Storage Systems Center of Carnegie Mellon.

3:10 PM Invited

Formation of fct-FePt Thin Films with High Coercivity at Low Deposition Temperature: *Jun Ding*¹; *Zeliang Zhao*¹; *Jingsheng Chen*²; ¹National University of Singapore; ²Data Storage Institute

FePt with the fct-phase is very promising as the next generation of high-density magnetic recording media, because of its large magneto-crystalline anisotropy, high coercivity and good chemical stability. However, one of the major problems need to be solved is the high formation temperature of the fct-phase. In general, the phase transformation from soft-magnetic fcc-phase to hard-magnetic fct-phase requires a relatively high temperature (> 600°C). The high formation may lead in formation of large grain and damage of substrate. Therefore, many research groups in the world are investigating how to form fct-phase at low temperature with promising structural and magnetic properties. In our work, we have successfully employed thin Ag layers to promote the formation of the hard-magnetic fct-phase. Nanostructured FePt thin films deposited on MgO at 400°C have shown very promising properties for perpendicular magnetic recording, such as high coercivity of >30 kOe and large perpendicular anisotropy.

3:45 PM

Microstructure Evolution in Fe-Pt Thin Films during Post-Deposition Ordering: *Andreas Kulovits*¹; *Bryan Webler*²; *Anirudha R. Deshpande*¹; *Paul Ohodnicki*²; *Jorg Michael Wiezorek*¹; ¹University of Pittsburgh; ²Carnegie Mellon University

The tetragonal L1₀-ordered intermetallic phase FePt is offers attractive uniaxial hard-ferromagnetic properties for permanent magnet applications. FePt thin films produced by magnetron sputtering without substrate heating usually consist of the disordered FCC-solid solution, stable at higher temperatures and metastable at room temperature, rather than the L1₀-phase. Hence, post-deposition annealing procedures inducing the ordering transformation have to be used. Optimization of processing strategies for FePt based thin films, including alloying schemes, requires a basic understanding of their microstructural response to annealing. Here combinations of X-ray diffraction (XRD), including texture measurements, and imaging and analytical techniques of transmission electron microscopy (TEM) have been used to characterize as-deposited and annealed films in order to study the microstructural responses. The magnetic properties and domain structure of the FePt thin films have been monitored by VSM and MFM experiments.

4:05 PM Break

4:15 PM Invited

Low-Temperature Chemical Ordering in Fe-Pt Nanoparticles by Sb Doping: *Qingyu Yan*¹; *Taegyun Kim*¹; *Arup Purkayastha*¹; *Y. Xu*²; *Mutsuhiro Shima*¹; *Richard Gambino*³; *Ganapathiraman Ramanath*¹; ¹Rensselaer Polytechnic Institute; ²University of Minnesota; ³Stony Brook University

Obtaining the ordered tetragonal L1-sub-0 phase at low temperatures is crucial to achieving high magnetic coercivity in nanoparticles to harness them for ultra-high-density memory devices. This talk demonstrates that Sb doping stabilizes the ordered structure in Fe-Pt nanoparticles, yielding higher magnetic coercivity at lower temperatures, than previously reported. Even as-synthesized 8-nm-diameter nanoparticle assemblies with XSb=0.23 and XSb=0.14 are ferromagnetic at room temperature with coercivity H_c ~120 mT and 10 mT, respectively. Upon annealing to temperatures as low as ~300°C, nanoparticles with XSb = 0.14 show H_c >500 mT, without particle coalescence. The coercivity is >10-times greater than previously reported for similarly-sized FePt nanoparticles and annealing temperature. XRD and TEM analyses suggest that ordering at low temperatures is due to a lattice shuffling effect caused by Sb during annealing. The ordering mechanism and implications of our results on the development of new high-coercivity nanostructures will be discussed.

4:50 PM

Numerical Simulations of Infrared Processing of FePt Nanoparticle Films: *Adrian S. Sabau*¹; *Ronald D. Ott*¹; *Ralph B. Dinwiddie*¹; *Puja Kadolkar*¹; *Craig Alan Blue*¹; ¹Oak Ridge National Laboratory

In order to anneal FePt nanoparticle films, a plasma arc lamp was used in this study. The processing aimed at reaching a peak target temperature for multiple pulses of 550C. Numerical simulations of the heat transfer

WEDNESDAY PM

and infrared measurements for the PTP were carried out to determine the operating power levels for the plasma arc lamp. Infrared measurements were conducted to obtain experimental data for the surface temperature of the FePt nanofilm. Parameters needed for the heat transfer model were identified based on the experimental temperature results. Following the model validation, several numerical simulations were carried out to identify the power levels for each pulse. It was shown that the FePt nanoparticle films were successfully processed using the power levels provided by the heat transfer analysis.

5:15 PM

Pulsed-Thermal-Processing of FePt Thin Films: Amanda C. Cole¹; Gregory B. Thompson¹; J. W. Harrell¹; Ronald Ott²; ¹University of Alabama; ²Oak Ridge National Laboratory

The magnetic anisotropic L1₀ FePt phase is a candidate material for next generation magnetic storage. When FePt is sputter deposited, it adopts a metastable A1 phase that is superparamagnetic. Conventional annealing at 600°C will phase transform FePt into L1₀ but result in grain coarsening and the loss of the narrow granular size distribution. We report pulsed-thermal-processing using a high density infrared plasma arc light source at exposure times of 100 to 250 ms to chemically order 20 nm and 100 nm thick FePt films on Si substrates. Upon ordering, no grain growth in the 100 nm thick films was observed. As the thin film thickness decreased, grain growth became more prevalent for similar processing conditions. Depending on the time, temperature and number of pulses, we are able to control the texture evolution of the film. XRD, TEM and magnetometry characterization have been performed and will be reported for each process.

5:40 PM

The Mechanism of (001) Texture Evolution in FePt Thin Film during Post-Annealing: Jae-Song Kim¹; Yang-Mo Koo¹; Byeong-Joo Lee¹; Seong-Rae Lee²; ¹POSTECH; ²Korea University

We discuss the origin of the (001) texture evolution of FePt thin films during post-annealing, considering order/disorder transformation strain. Strain energies corresponding to transformation strain and in-plane strain were calculated according to crystals having various normal orientations, using Molecular Statics (MS) with Modified Embedded Atom Method (MEAM). In order to confirm the calculated results, residual stress of the FePt thin films was measured with the sin²ψ technique modified by the present author. The theoretic calculations revealed that the transformation strain stabilizes the crystal grains with the (001) crystallographic orientation relative to the surface of the film under in-plane tensile strain and the free normal stress, which was consistent with experimental results from the residual stress measurements. From this, it is suggested that transformation strain generated in the early stages of post-annealing plays an important role in the texture evolution of FePt thin film.

Point Defects in Materials: Atomic Kinetics Processes - Joint Session with Computational Thermodynamics and Phase Transformations

Sponsored by: The Minerals, Metals and Materials Society, TMS Electronic, Magnetic, and Photonic Materials Division, TMS Materials Processing and Manufacturing Division, TMS Structural Materials Division, TMS: Chemistry and Physics of Materials Committee, TMS/ASM: Computational Materials Science and Engineering Committee
Program Organizers: Dane Morgan, University of Wisconsin; Corbett Battaile, Sandia National Laboratories

Wednesday PM Room: 210B
March 15, 2006 Location: Henry B. Gonzalez Convention Ctr.

Session Chairs: Adri C. van Duin, California Institute of Technology; Mark D. Asta, University of California

See Computational Thermodynamics and Phase Transformation Symposium on page 264 for presentations.

Recycling - General Sessions: General Recycling

Sponsored by: The Minerals, Metals and Materials Society, TMS Extraction and Processing Division, TMS Light Metals Division, TMS: Recycling Committee

Program Organizers: Gregory K. Krumdick, Argonne National Laboratory; Cynthia K. Belt, Aleris International

Wednesday PM Room: 8B
March 15, 2006 Location: Henry B. Gonzalez Convention Ctr.

Session Chair: Christopher M. Keller, Aleris International Inc

2:00 PM Introductory Comments**2:05 PM Invited**

Immobilization Process via Solidification of Hazardous Heavy Metals for Recycling Industry Waste: Ji-Whan Ahn¹; Kwnag-Suk You¹; Seung-Hyeon Ahn²; Hwan Kim²; ¹Korea Institute of Geoscience and Mineral Resources; ²Seoul University

The purpose of this study was to investigate the immobilization as a host for metallic pollutants (Cr, Cu, Pb, and Zn) by ettringite phase. Ettringite phase is produced through hydration reaction of calcium aluminate with gypsum. From the XRD patterns, it is known that the distance between spaces in 010 planes in ettringite crystal increase with an increase of ionic radius of heavy metal except Pb; no big difference is shown. For this reason, the d-value of 010 planes in ettringite crystal increased with the substitution of Cr, Cu and Zn having a big Al ionic radius. But in case of Pb, because the substitution occurred at calcium site, it does not influence to increase d-value of 010 planes.

2:30 PM

Effect of Magnetic Separation in Removal of Heavy Metals in Municipal Solid Waste Incineration Bottom Ash: Nam-Il Um¹; Gwang-Suk You¹; Gi-Chun Han¹; Ji-Whan Ahn¹; Hee-Chan Cho¹; ¹Korea Institute of Geoscience and Mineral Resources

Incineration is a commonly used solid waste treatment in many countries and typically 20% of the mass remains as a bottom ash collected as fly ash. Although incineration has merits such as heat recovery, a small volume compared to the volume of waste incinerated, the management of residues have been become a main issue as criteria for use of the residues or landfilling. MSWI bottom ash have been considered as aggregate substitute because MSWI bottom ash consists of slag, glasses, ceramics mainly. And in several countries such as the Netherlands, Denmark, France, MSWI bottom ash have been used as road materials after separating ferrous metals. Separation of ferrous metals from MSWI bottom ash may not only give economical advantage but also removal of heavy metals. Therefore, in this study, the relationship between recovery of ferrous metals and separation of heavy metals from MSWI bottom ash was investigated.

2:55 PM

Repeatedly Utilization of Carbon Fiber Chemistry Copper Plating Waste Liquid: Tianjiao Luo¹; Guangchun Yao¹; Linli Wu¹; Xiaoming Zhang¹; ¹Northeastern University

How to reuse the waste liquid directly was researched in this paper. Firstly, the waste liquid should be filtrated to remove the impurity; then some of H₂O₂ solution was dripped into the waste liquid to pretreat it; finally, CuSO₄ solution was added into the treated waste liquid and the pH was adjusted to about 12, then some HCHO solution was added into it, in which the treated carbon fiber can be plated. The morphology and composition of coatings were investigated by means of Scanning Electron Microscopy and Energy Dispersive X-ray Spectroscopy. The results indicated that, as the new plating solution, and the pretreated solution is stable, and the plating rate is still about 0.8μm/h, and the copper coating is even and combines closely with carbon fiber. According to this way, the waste liquid can be reuse 5~7 times.

3:20 PM

Recycling of Sludge Derived from Cutting and Polishing Natural Stones in Ceramic Formulations: Paula Costa Torres¹; Rodrigues Salvador Manjate¹; Sandra Fernandes Quaresma¹; José Maria da Fonte Ferreira¹; ¹University of Aveiro

The aim of the present work was to study the incorporation of industrial sludges derived from cutting and polishing natural stones (slate, granite, and quartzite) as main components in stoneware compositions and to evaluate the impact on the final properties of the products. The materials were characterized in terms of particles size distribution, chemical (XRF) and mineralogical (XRD) compositions, and thermal behaviour (DTA, AT, Dilatometry) and density. Formulations containing 70 wt.% of residues and 30 wt.% of a plastic ball clay were prepared. The plasticity of all the pastes tested was characterised. The sintered samples were characterised for shrinkage, crystalline phase formation, water absorption, flexural strength, density and microstructure (SEM). The final properties obtained (flexural strength >35 MPa, water absorption <3%) are typical of stoneware products.

3:45 PM Break

4:00 PM

Zinc Vapor Treatment for Precious Metals Recovery: Masao Miyake¹; Junichi Itoh¹; Masafumi Maeda¹; ¹University of Tokyo

Compound formations of precious metals by zinc vapor treatment were investigated to develop a new recovery process of precious metals from scraps. Precious metals were exposed to zinc vapor at constant temperatures of 673-973 K, and compound layers were formed on the surface of the precious metal. The growth rates of the layers followed the parabolic law, indicating that volume diffusion controlled the growth of the layers. Interdiffusion coefficients in the compound phases were derived from concentration-penetration profiles.

4:25 PM

A New Recycle Process of Uranium from Spent Fuel by Selective Sulfurization: Nobuaki Sato¹; Genki Shinohara¹; Osamu Tochiyama¹; ¹Tohoku University

For the recovery of uranium from spent nuclear fuel, sulfide reprocessing process, which consists of voloxidation, selective sulfurization, and magnetic separation or selective dissolution steps, are proposed. In this paper selective sulfurization of rare-earth oxides in the presence of uranium oxides was studied by thermogravimetry and X-ray diffractometry. In case of the mixture with UO₂, the rare-earth oxides R₂O₃ (R=Nd, Eu, etc.) were preferentially sulfurized by CS₂ forming oxysulfides and sulfides, while UO₂ remained at temperatures lower than 500°C. When R₂O₃ was mixed with U₃O₈, first, the reduction of U₃O₈ to UO₂ occurred at low temperatures followed by the sulfurization of R₂O₃. The sulfurization of UO₂ solid solution containing rare-earths was also investigated. The magnetic separation and selective dissolution processes were discussed by the fundamental experiments using the simulated mixture of uranium and rare-earths oxides.

4:50 PM

Recycling of Oxidic Waste from the Ferroalloy Production: Markus Hohenhofer¹; Helmut Antrekowitsch²; Michael Potesser²; Wolfgang Labenbacher¹; ¹Christian-Doppler Laboratory for Secondary Metallurgy of Non-Ferrous Metals; ²University of Leoben

Due to the economic aspects and the environmental regulations recycling of slag and waste from the ferroalloy production is a very important point for the companies. The treatment of slags depends on the composition especially on the valuable metals and impurities. Furthermore the aim is the use of these materials in the industry e.g. cement industry, pig-iron production etc. Therefore the requirements for these applications should be reached by metallurgical processing. The treatment of the slag with a high V-, Mo- and P-content by using a reducing metal bath is one alternative to recover the elements from the materials. Besides phase analysis thermodynamic calculations were done to determine the process parameters. Additionally the Christian Doppler Laboratory for Secondary Metallurgy of Nonferrous Metals at the Institute of Nonferrous Metallurgy at the University of Leoben carried out investigations with different slag compositions to verify the thermodynamic calculations.

5:15 PM Concluding Comments

Simulation of Aluminum Shape Casting Processing: From Alloy Design to Mechanical Properties: Heat Treatment Modeling

Sponsored by: The Minerals, Metals and Materials Society, TMS Light Metals Division, TMS Materials Processing and Manufacturing Division, TMS Structural Materials Division, TMS: Aluminum Committee, TMS/ASM: Mechanical Behavior of Materials Committee, TMS: Process Modeling Analysis and Control Committee, TMS: Solidification Committee, TMS/ASM: Computational Materials Science and Engineering Committee

Program Organizers: Qigui Wang, General Motors Corporation; Matthew Krane, Purdue University; Peter Lee, Imperial College London

Wednesday PM
March 15, 2006

Room: 6D
Location: Henry B. Gonzalez Convention Ctr.

Session Chair: Murat Tiryakioglu, Robert Morris University

2:00 PM Invited

Modeling of Precipitate Free Zone Developing upon Heat Treatment in Industrial Aluminum Casting: Charles A. Gandin¹; Alain Jacot¹; ¹Ecole des Mines de Paris

The formation of precipitate free zone (PFZ) upon heat treatment of industrial aluminum alloys is known to be detrimental to fracture toughness. The width of the PFZ depends on the relative importance of solute diffusion in the vicinity of primary particles as compared with the potency of precipitates to nucleate and grow in the matrix phase. A model to predict the PFZ is presented. It is based on the coupling between a Precipitate Size Distribution method and a Pseudo-Front Tracking method. Coupling with equilibrium thermodynamic calculations is achieved through Thermo-Calc. As a result of the interaction between precipitation and long range diffusion, the PFZ is predicted together with profiles of the compositions of species, the density and the volume fraction of the precipitates. The simulation results are compared with experimental data collected in the literature for an industrial homogenization heat treatment of a 3003 aluminum alloy.

2:25 PM Invited

Modeling the Heat Treatment of Age-Hardenable Cast Aluminum Alloys: Richard Dean Sisson¹; Shuhui Ma¹; Md. Maniruzzaman¹; ¹Worcester Polytechnic Institute

The effects of solutionizing times and quenching rates on the microstructure and mechanical properties of age-hardenable cast aluminum alloys (i.e. 319 and A356) has been experimentally investigated with Jominy End Quench Bars and theoretically analyzed using Quench Factor Analysis. The results indicate that the solutionizing time for metal mold cast alloys can be reduced from 12 hours to less than 4 hours depending on the casting microstructure and secondary dendrite arm spacing. The Jominy End Quench experiments revealed that these alloys are not very quench sensitive with alloy A356 being more quench sensitive than 319. Quench Factor Analysis proved to be applicable to these cast alloys and a good predictor of hardness. The results are discussed in terms of alloy microstructure including Silicon spheroidation and hardening precipitate development.

2:50 PM

Optimization of Load Design and Thermal Recipe Design for Time and Energy Efficient Heat Treatment Processes: Yao Zhou¹; Jinwu Kang¹; Yiming Rong¹; ¹Worcester Polytechnic Institute

Aluminum alloy solutionizing is a time and energy consuming process. Based on the process model built in our previous research, the processes can be simulated, evaluated, and optimized. This research examined two possibilities to reduce cycle time and energy consumption: load design and thermal recipe design. Load arrangement can be quantitatively assessed and determined among several designs to achieve shorter cycle time and lower energy consumption. Thermal recipe can be such designed that the furnace is first heated over the soaking temperature so as to heat the load faster, and then furnace is brought back to the soaking temperature at a proper time so the load finally rises to the soaking temperature

WEDNESDAY PM

without overheat. This "proper time" is critical and is calculated and controlled by the algorithms. Comparative study shows that the proposed optimizations in load design and thermal recipe design yield significant saving on both time and energy.

3:15 PM

Effect of Various Casting Parameters on Air Gap Formation and Interfacial Heat Transfer Coefficient for Various Aluminum Alloys Cast against Different Metal Molds: Stavros A. Argyropoulos¹; Horazio G. Carletti¹; Basil L. Coates¹; ¹University of Toronto

This paper will be focused on the effects of surface roughness and temperature and metallographic head on the heat transfer coefficient at the metal mold interface. The experimental work was carried out in a special apparatus developed to measure heat transfer at the metal mold interface. This apparatus was instrumented with two types of sensors, thermocouples and LVDT's (Linear Variable Differential Transformer). The monitoring of the two types of sensors was carried out simultaneously during solidification of various aluminum alloys. These alloys were cast against different metal molds. Inverse heat transfer analysis was used to estimate the heat transfer coefficient and the heat flux at the metal mold interface. In general, an increase in mold surface roughness results in a decrease in the heat transfer coefficient at the metal mold interface. On the other hand, an increase in metal temperature results in an increase in the heat transfer coefficient.

3:40 PM Break

3:55 PM

Numerical Modeling of the Heat Treatment with Residual Heat of Aluminum-Alloy Castings: He Liang¹; Kang Jinwu¹; Huang Tianyou¹; ¹Tsinghua University

Aluminum-alloy castings are frequently used by the automotive industry in both as-cast and heat-treated conditions. The purpose of heat treatment is to obtain a better combination of strength and ductility, but the heat treatment demands a very large cost of electric energy. The heat treatment with residual heat of aluminum-alloy castings, immediately after their solidification, can reduce reheating, cycle times and energy consumption. A three-dimensional model for the solidification, solution and artificial aging is presented in this study. This model predicts the temperature distribution during the whole heat treatment procedure and can do help on the design of the heat treatment parameters. The model is used for the 319 aluminum-alloy castings and the simulation results are in good agreement with experimental results.

4:20 PM

Thermal Contact in Permanent Molding of Aluminum Alloys: John Trevor Berry¹; Rogelio Luck¹; Robert D. Pehlke²; August Johnson¹; Jeffrey Weathers¹; ¹Mississippi State University; ²University of Michigan

The problem of adequately describing the conditions of thermal contact in casting processes involving metallic molds, especially where a protective coating is in place, has been investigated almost continually over the last quarter century. A recent investigation has coupled both analytical and computational techniques with careful measurement in order to obtain reliable data describing the time/temperature dependant heat transfer coefficients concerned and their relation to current coating practice. Additionally, the invasive nature of temperature sensing devices in the mold and how true time-temperature data might be recovered for use in inverse analysis has been studied. (The work has been supported by the US Dept. of Energy through the Cast Metals Coalition and by Mississippi State's Center for Advanced Vehicular Systems).

4:45 PM

Modeling the Quench Sensitivity of an Al-7wt.%Si-0.6wt.%Mg Alloy: Murat Tiryakioğlu¹; Ralph Shuey²; ¹Robert Morris University; ²Alcoa Technical Center

The quench sensitivity of a cast Al-7wt.%Si-0.6wt.%Mg alloy was characterized by tensile tests and scanning electron microscopy. Samples were cooled from the solution treatment temperature by interrupted and delayed quenches. Mg₂Si was found to nucleate on Si particles as well as in the matrix. The quench sensitivity was modeled by double-C curves following the quench factor analysis methodology.

Solidification Modelling and Microstructure Formation: A Symposium in Honor of Prof. John Hunt: Solidification Processing and Thermophysical Properties

Sponsored by: The Minerals, Metals and Materials Society, TMS Materials Processing and Manufacturing Division, TMS: Solidification Committee

Program Organizers: D. Graham McCartney, University of Nottingham; Peter D. Lee, Imperial College; Qingyou Han, Oak Ridge National Laboratory

Wednesday PM

March 15, 2006

Room: 6C

Location: Henry B. Gonzalez Convention Ctr.

Session Chairs: P. Grant, University of Oxford; L. Katgerman, Delft University of Technology

2:00 PM Invited

Evaluation of Kinetic Competition during Solidification: John H. Perepezko¹; Kjetil Hildal¹; ¹University of Wisconsin

The evolution of an as-cast microstructure is related to the dynamic kinetic competition during solidification. Microstructure morphology transitions from cells to dendrites and the columnar to equiaxed grain transition reflect a kinetics competition that is motivated by a changing interface velocity and interface undercooling. Similarly, the conversion between metastable and stable phase products and the crystal to glass reaction are related directly to a changing melt undercooling. While growth kinetics transitions tend to be sharply defined, nucleation controlled transitions occur over a range. Traditionally, solidification transitions have been examined by multiple directional freezing runs, but with a wedge mold castings can be subjected to a range of solidification rates differing by orders of magnitude. With microstructure analysis, temperature measurements and heat transfer analysis, wedge casting can be used to explore a spectrum of solidification microstructures and provide new insight on the processing conditions as illustrated for bulk glass formation.

2:25 PM

Issues in the Computational Modeling of Solidification and Casting Processes: Mark Cross¹; Nick Croft¹; Diane McBride¹; Alison Jayne Williams¹; Kyriacos A. Pericleous²; ¹University of Wales Swansea; ²University of Greenwich

Solidification modelling of metals casting, whether for shape, (semi-) continuous or in the manufacture of thin strip is now a mature activity. There are now a wide range of software tools addressing all aspects of this family of processes. Indeed, the main challenge here is perceived as being in capturing the micro-structure within the context of a macro-scale process, the area precisely where John Hunt made many of his achievements over his career. In this paper we will focus upon a range of challenges that still remain to enable effective and comprehensive simulation at the macro-scale to ensure the arising computational models are appropriate hosts for capturing micro-structural behaviour. These challenges will include: 1) macro-segregation for multi-component alloys; 2) mould filling and simultaneous solidification in very complex geometries; 3) closely coupled thermo-fluid-structure interaction in the metal-mould context; 4) simulation issues for operating at multiple length and time scales.

2:50 PM

Fractional Latent Heat Data from Heat Flux Differential Scanning Calorimetry: Adrian S. Sabau¹; Wallace D. Porter¹; ¹Oak Ridge National Laboratory

Differential Scanning Calorimetry (DSC) measurements are used to estimate the fractional latent heat release during phase changes. There are instrument temperature lags due to the temperature measurement at a different location than that of the sample and reference materials. Recently, Dong and Hunt (2001) showed that significant improvement in estimating the fractional latent heat can be obtained when a detailed simulations of the heat transfer within the instrument are performed. The Netzsch DSC 404C instrument, with a high accuracy heat capacity sensor, is considered in this study. This instrument had a different configuration that

that studied by Dong and Hunt (2001). The applicability of Dong and Hunt's approach to this instrument is investigated. It was found that the DSC instrument can be described by numerous parameters. It was difficult to identify model parameter. Numerical simulation results are presented and compared with experimental results for the fractional latent heat.

3:10 PM

Determination of Solute Diffusion Coefficient by Droplet Migration

Method: *Shan Liu*¹; *Jing Teng*¹; ¹Iowa State University

Liquid droplets can migrate through a solid matrix in a temperature gradient field. Watson and Hunt employed this method to obtain the solute diffusion coefficient (D_L) in Al-Cu alloys by interrupted experiments in order to determine the position of a band of droplets. In this study, we used transparent SCN base alloys and obtained the solute diffusion coefficient by quantifying the migration behavior of an individual droplet. We find that there is a characteristic migration curve for an alloy at each temperature gradient that all the droplets follow, indicating that the instant velocity of droplets only depends on the position in the temperature field and is independent of the droplet size and shape. The diffusion coefficient is determined through the this characteristic curve, which gives D_L in the SCN-salol system as 0.65×10^{-9} m²/s and D_L in the SCN-camphor system as 0.26×10^{-9} m²/s.

3:30 PM Invited

The Contribution of John Hunt to Measurement of Solid/Liquid Interfacial Energies in Metallic Systems: *Howard Jones*¹; ¹University of Sheffield

Solid-liquid interfacial free energy σ_{SL} plays a key role in a wide range of metallurgical phenomena. Pioneer estimates by Turnbull et al in the 1950's from undercooling measurements were primarily for pure metals on the assumption of homogeneous nucleation and estimates from dihedral angle measurements require an independent measurement or estimate of σ for at least one of the other interfaces involved. Gündüz and Hunt in 1985 reported the first direct measurements of σ_{SL} for three eutectic alloy systems from the profiles of grain boundary grooves stabilised by a known radial temperature gradient, embodying a methodology applied prior to 1985 only to transparent systems or pure metals at or near to ambient temperatures. The significance of these and subsequent measurements and their application to solidification theory will be critically evaluated.

3:55 PM Break

4:10 PM

Measurement of Solid-Liquid Interface Energies in Ternary Alloys:

*Annemarie Bulla*¹; *Carlos Carreno-Bodensiek*¹; *Bjoern Pustal*¹; *Ralf Berger*¹; *Andreas Bührig-Polaczek*¹; *Andreas Ludwig*²; ¹RWTH Aachen University; ²University of Leoben

The solid-liquid interface energy plays a major role in phase transformations. It has a strong influence on solidification morphologies and the final grain structure. The "grain boundary groove in an applied temperature gradient" method developed by J. Hunt/ Oxford was found to be suitable for measuring the solid-liquid interface energy in metal alloy systems. A radial heat flow apparatus was assembled as described by Hunt and Gündüz. This apparatus ensures a stable temperature gradient for hours and thus allow the sample to equilibrate. After rapid quenching, the local curvature of the groove can be analysed. From the graphically measured boundary groove information and the simulated local temperatures, the solid-liquid interface energy can be evaluated indirectly using the Gibbs-Thomson equation. Values for the solid-liquid interface energy and the Gibbs-Thomson coefficient have been obtained for the Al-Cu-Ag ternary eutectic system. The relationship between concentration and solid-liquid interface energy was also investigated.

4:30 PM

Microstructure and Creep Resistance of Lead-Free Solder under Different Solidification Conditions: *Jin Liang*¹; *N. Dariavach*¹; *Dongkai Shangguan*²; ¹EMC; ²Flextronics

Mechanical, metallurgical, thermal and environmental factors all affect the service reliability of solder joints, and are under extensive study for preparation of the transition from Sn-Pb eutectic soldering to lead-free

soldering in the electronic industry. However, there is a general lack of understanding about the effects of solidification conditions on the microstructures and mechanical behavior of lead-free solder alloys. This study attempts to examine the creep resistance of the Sn-Ag-Cu eutectic alloy with a variety of solidification conditions with cooling rates ranging from 10+2C/sec to 10-2C/sec. Although real soldering processes have limited solidification rate variations, an understanding of the mechanical property change with microstructures, which are determined by the solidification conditions, should shed some light on the fundamental deformation and fracture mechanisms of lead-free solders.

4:50 PM

Preparation of AZ91D Slurries for Semi-Solid Forming Using Precipitates and Cast Properties: *Ha Heon Phil*¹; *Byun Ji Young*¹; ¹Korea Institute of Science and Technology

During the solidification of the AZ91D-alloys, the Al₈(Mn,Fe)₅ phase is generally precipitated in the melt in advance of the precipitation of the primary a-Mg. The basic principle for manufacturing AZ91D-alloy slurries for semi solid forming is to use the Al₈(Mn,Fe)₅ precipitates as the heterogeneous nucleation sites for primary a-Mg phases. Al₈(Mn,Fe)₅ precipitate is the effective heterogeneous nucleation site for the primary a-Mg phase. It was also observed that increase of the Mn content in the melt and the cooling rate below to the solid/liquid two-phase region resulted in smaller and more globular primary a-Mg due to the increase of heterogeneous nucleation sites. The cooling rate below to the solid/liquid two-phase region, Mn content in AZ91D alloy, and the holding time and temperature affected on the quality of slurry. After annealing rheo-cast samples, mechanical properties were examined.

5:10 PM

Solid-Liquid Interfacial Energy of Tin in the Cd-Sn Eutectic System:

*Buket Saatçi*¹; *Sevgi Çimen*¹; *Hakan Pamuk*¹; *Mehmet Gündüz*¹; ¹Erciyes University

When the stabilized solid-liquid interface intersects with a planar grain boundary in a temperature gradient, G a shape of the grain boundary groove is formed. The equilibrated groove shapes were directly observed after annealing the sample at just above the eutectic temperature for about 8 days. The thermal conductivities of the solid phase, K_s and the liquid phase K_l for the groove shapes were measured. From the observed groove shapes the Gibbs-Thomson coefficients have been obtained for the solid Sn in Cd-Sn liquid solution by using the measured G, K_s and K_l with a numerical method. The solid-liquid interfacial energy, between solid Sn and Cd-Sn liquid solution has been determined from the Gibbs-Thomson equation. The grain boundary energy for the same material has been collected from the observed groove shapes.

5:30 PM

Measurement of Solid-Liquid Interfacial Energy for Solid Zn in Equilibrium with the Zn-Mg Eutectic Liquid: *Mustafa Erol*¹; *Kazim Keslioglu*¹; *Necmettin Marasli*¹; ¹Erciyes University

The equilibrated grain boundary groove shapes for solid Zn in equilibrium with the Zn-Mg eutectic liquid were observed on rapid quenched samples. The Gibbs-Thomson coefficient for the solid Zn have been determined to be $(10.64 \pm 0.43) \times 10^{-8}$ Km from the observed grain boundary groove shapes with present numerical model and the solid-liquid interfacial energy for the solid Zn in equilibrium with the Zn-Mg eutectic liquid has been obtained to be $(89.16 \pm 8.02) \times 10^{-3}$ Jm⁻² from the Gibbs-Thomson equation. The grain boundary energy for the solid Zn has been calculated to be $(172.97 \pm 20.76) \times 10^{-3}$ Jm⁻² from the observed grain boundary groove shapes. The thermal conductivity of the solid phase and thermal conductivity ratio of liquid phase to solid phase for Zn-0.15wt.%Mg alloy has also been measured.

Surfaces and Interfaces in Nanostructured Materials II: Coatings, Films, Multi-Layers and Arrays

Sponsored by: The Minerals, Metals and Materials Society, TMS Materials Processing and Manufacturing Division, TMS: Surface Engineering Committee

Program Organizers: Sharmila M. Mukhopadhyay, Wright State University; Narendra B. Dahotre, University of Tennessee; Sudipta Seal, University of Central Florida; Arvind Agarwal, Florida International University

Wednesday PM Room: 209
March 15, 2006 Location: Henry B. Gonzalez Convention Ctr.

Session Chair: Sudipta Seal, University of Central Florida

2:00 PM

Deposition, Characterization and Performance Evaluation of Nano-Layered Superlattice Nitride Coatings: *Qi Yang*¹; *Linruo Zhao*¹; ¹National Research Council Canada

Nano-layered superlattice nitride coatings with two or multi-layer constituents were deposited by unbalanced reactive magnetron sputtering technique using metallic targets. The modulation periods of the superlattices were measured according to the reflection peak positions in their low-angle X-ray reflectivity spectra using the modified Bragg law, a technique proven to be accurate by TEM analysis. Superlattice structures can lead to a remarkable higher hardness than monolayered nitride coatings; and hardness enhancement is closely related to the superlattice layer constituents, modulation period and coating crystallographic orientation. Post-annealing tests indicate that nitride superlattices have a high thermal stability. Pin-on-disc dry sliding test shows that the nitride superlattices exhibit lower friction coefficients and markedly higher wear resistances than commercial TiN hard coating. These tribological properties make these superlattice coatings a strong candidate for surface protection against wear in engineering applications.

2:20 PM

Nanoscale Coatings for Surface Modification of Carbon Structures: *Rajasekhar V. Pulikollu*¹; *Pratik Joshi*¹; *Sharmila M. Mukhopadhyay*¹; ¹Wright State University

For nanoscale materials to be implemented in useful devices, control of surface functionality for appropriate bonding or dispersion is very important. It is important that the surface modification is limited to the top few atomic layers and does not degrade the underlying structure. In this project, microwave plasma coatings having thickness less than 5 nm can be applied successfully to modify complex and uneven carbon structures like carbon foam and nanofibers. This talk will focus on silica-like oxide coating that has been successfully developed for enhancing the bond between carbon reinforcements and matrix materials in composites. Characterization techniques such as XPS, SEM, TEM, AFM and mechanical testing are used to study the chemistry, morphology, structure and effectiveness of these coatings. Additionally, the influence of these coatings on nucleation and growth of nanotubes on larger carbon structures (to produce multiscale, multifunctional materials) will be presented.

2:40 PM

Role of Interfaces in Determining Phase Stability in Nanoscale Multilayers: *Arda Genc*¹; *Rajarshi Banerjee*¹; *Mark Yavorsky*²; *Dennis Maher*²; *Hamish L. Fraser*²; ¹University of North Texas; ²Ohio State University

When the layer thickness in a multilayered thin film is reduced to the nanometer scale, the interfaces between the layers dominate the free energy of the system consequently dictating the structure of the individual nanolayers. While the phase stability in these multilayers can be rationalized based on a thermodynamic model, their predictive capability depends critically on the accuracy of input computational parameters such as the interfacial energy. Accurate computation of such interfacial energies in turn depends on the detailed characterization of the atomic-scale structure and chemistry of the interfaces between the nanolayers. This presen-

tation will focus on the application of multiple high-resolution characterization techniques, including, high-resolution TEM, electron-energy loss spectroscopy at a high spatial resolution, and, 3D atom-probe tomography, for the characterization of these interfaces at the atomic-scale.

3:00 PM

Tailoring the Texture of Magnetron Sputtered Ta Films by Self-Assembled Dendrimer Sublayers: *Xiao Li*¹; *Feng Huang*¹; *Shelby F. Shuler*¹; *Shane C. Street*¹; *Mark L. Weaver*¹; ¹University of Alabama

In this study, we demonstrate the use of ultrathin (<5 nm in thick) self-assembled dendrimer monolayers to tailor the texture of the magnetron sputtered Tantalum (Ta) films. As characterized by X-ray diffraction (XRD) techniques, dendrimer-mediated films developed a (330) preferred orientation in the tetragonal β -Ta phase, which is in contrast to the (002) preferred crystalline orientation in the bare Si substrates. Variation of the sputtering conditions and the generation of the dendrimers, alters the ratio of the intensity from the two peaks, yielding weak or strong (330) texture. A discussion of the nucleation and the competitive growth is conducted for the origin of the tailored Ta texture.

3:20 PM

Three Dimensional Imaging of Cracking in Berkovich Indented Thin Film Coatings: *Lok-Wang Ma*¹; *Damien McGrouther*¹; *Paul Munroe*¹; *Julie Cairney*¹; *Mark Hoffman*¹; ¹University of New South Wales

A TiN thin film coating deposited on a ductile steel substrate, was subjected to surface deformation via nanoindentation using a Berkovich indenter. Pop-ins were observed during loading that are characteristic of the onset of cracking and the formation of shear steps at the coating-substrate interface. Focused ion beam microscopy was used to prepare and observe cross-sections through the indentation that revealed the presence of both intercolumnar and inclined cracks. However, the pyramidal nature of the indenter means that the cracks observed in these 2-D sections are strongly dependent on the location of the milled region. In this study we have used dual-beam focused ion beam instrumentation to acquire datasets used to construct 3-D visualisations of the indented regions. These images provide highly detailed images of the morphology of cracks, which were observed to be consistent with theoretical models of plastic deformation of such brittle coatings.

3:40 PM

Synthesis of Nanocrystalline Intermetallic Layer by Mechanical Attrition: *Xiao-Lei Wu*¹; *You-Shi Hong*¹; *Nai-Rong Tao*²; *Xiang-Kang Meng*³; *Jian Lu*⁴; *Ke Lu*²; ¹Institute of Mechanics, Chinese Academy of Sciences; ²Institute of Metal Research, Chinese Academy of Sciences; ³Nanjing University; ⁴University of Technical of Troyes

By means of the technique of surface mechanical attrition treatment, the nanocrystalline (nc) intermetallic compound Co₃Fe₇ was synthesized in the surface layer of bulk cobalt. It was found that diffusion occurred during deformation, leading to the extension of solid solution and a series of phase transformation. Fe contents were significantly higher in the grain boundary and triple junction than in grain interiors. In particular, stacking faults were found to contribute diffusion significantly. The alloying on the atomic level was ascribed to deformation-induced intermixing during deformation. The superimposed effects of deformation at high strain rates on diffusion were analyzed in terms of dislocation solute-pumping mechanism and enhanced mobile vacancy concentration. The mechanism of intermetallic formation was a result of numerous nucleation events followed by limited growth.

4:00 PM

Surface Nanostructuring with Ordered Arrayed Nanoparticles of Tunable Size, Shape and Property: *Yong Lei*¹; *Gerhard H. Wilde*¹; ¹Forschungszentrum Karlsruhe GmbH

Nanoparticle arrays are fabricated on Si and Si/SiO₂ substrates using nanoporous ultra-thin alumina membranes (UTAMs) as evaporation masks. Because the shape and size of the nanoparticles are controllable, it is possible to tune the properties of the nanoparticle arrays, which will be highlighted by selected examples of our recent work. Ordered CdS nanoparticle arrays on Si substrates with tunable photoluminescence properties have been synthesized. Moreover, ordered arrays of In₂O₃ single-crystal nanoparticles were obtained based on a controlled oxidation of In nanoparticles. All In₂O₃ nanoparticles are oriented in the similar lattice

direction, which offers an additional control parameter i.e. a high degree of orientational order. This behavior is thought to be related to the so-called “two-dimensional nucleation and layered growth”. The methods developed here are applicable in a large range of possible processes and applications and serve to develop highly defined nanostructured surfaces that are structured in a massive parallel manner.

The Brandon Symposium: Advanced Materials and Characterization: Microstructure and Properties

Sponsored by: The Minerals, Metals and Materials Society, Indian Institute of Metals, TMS Extraction and Processing Division, TMS: Materials Characterization Committee

Program Organizers: Srinivasa Ranganathan, Indian Institute of Science; Wayne D. Kaplan, Technion; Manfred R. Ruhle, Max-Planck Institute; David N. Seidman, Northwestern University; D. Shechtman, Technion; Tadao Watanabe, Tohoku University; Rachman Chaim, Technion

Wednesday PM Room: 206B
 March 15, 2006 Location: Henry B. Gonzalez Convention Ctr.

Session Chairs: Paul Wynblatt, Carnegie Mellon University; Dominique Chatain, Centre National de La Recherche Scientifique

2:00 PM Invited

Low Temperature Colossal Supersaturation (LTCSS) Surface Hardening of Stainless Steels via Ti Alloys: *Arthur H. Heuer*¹; ¹Case Western University

Attempts to surface harden austenitic stainless steels by traditional carburization processes, without adversely affecting other useful properties, have traditionally failed due to formation of stable Cr-bearing carbides. We have demonstrated that with suitable surface activation, a temperature “window” exists where interstitial carbon diffusion can occur in the absence of substitutional diffusion of solutes such as Cr. Under such conditions, colossal supersaturation of carbon can occur (>10 atomic %), leading to impressive surface hardening and very high surface residual compressive stresses, improved fatigue resistance, and improved corrosion resistance, without serious loss of ductility.

2:25 PM Invited

Do Cavities Form during the Fracture of Silicate Glasses?: *Sheldon Wiederhorn*¹; Jean-Pierre Guin¹; ¹National Institute of Standards and Technology

The topography of surfaces formed by subcritical crack growth was investigated using the atomic force microscope. Our objective was to determine how well the “upper” and “lower” surfaces matched after being formed by a crack moving at a slow velocity. Specifically, were features left in the fracture surfaces of silicate glasses that would indicate cavity formation during the fracture process? Crack growth experiments were performed on silica, or soda-lime-silicate glass, in air and water over a velocity range of 10-10 m/s to 10-2 m/s. Silica glass surfaces “matched” normal to the fracture surfaces to better than 0.3 nm for the entire range of experimental variables. Soda-lime-silicate glass, surfaces “matched” to an accuracy of 0.5 nm to 0.8 nm normal to the fracture surface, depending on crack velocity. Within these limits, no evidence for cavitation was found in either glass.

2:50 PM Invited

Piezoluminescence Phenomenon on Thin ZnS: Metal Film for Smart Structure Applications: *Shuki Yeshurun*¹; Yarden Weber¹; Daniel Schweitzer¹; Jo Amar¹; Erez Hasman²; Haim Gurgov²; Hedva Bar¹; ¹RAFAEL; ²Technion

The phenomenon of light emission from crystals due to mechanical stimulation was known to science for centuries. This phenomenon is known as Piezoluminescence (PL). The main expectation from the PL materials is to be used for production of self-diagnostic materials and smart structures that will dynamically visualize the stress distribution by light emission. This paper gives a short theoretical background of the phenomenon

and mainly presents the influence of different fabrication processes on light emission. The materials which was used in the impact experiment include ZnS:Mn deposited on glass slides and mixture of ZnS:Mn with epoxy. Characteristics of light emission such as intensity and time response to impact stimulation were examined. As for the impact intensity, the experiments show a clear relationship between the impact amplitude and the emission intensity.

3:15 PM Break

3:30 PM Invited

The Physical and Mechanical Properties of Nickel - SiC Metal Matrix Composites: *Pnina Ari-Gur*¹; Seyed Mirmiran²; ¹Western Michigan University; ²DaimlerChrysler Autogesellschaft

Nickel-matrix composites of ceramic nano particles present unique properties that offer potential applications in aerospace, automotive and electronics industries. Electrocodeposition is the least expensive fabrication method. The properties of these composite coatings depend on the electrodeposition parameters, the ceramic nanoparticles concentration in the bath solution; properties of the ceramic nanoparticles (material, size, shape, surface roughness, surface charge), properties of the substrate and the interfaces. These coatings are examined via different tools, including microhardness, MTS, AFM, SEM, TEM and XRD. The optimum properties of these composites are obtained when the ceramic nanoparticles are uniformly monodispersed in the matrix with the smallest obtainable grain size. The influence of these factors on the mechanical and physical properties of such composite coatings was studied. Properties like grain size, crystallographic texture, residual stresses and wear resistance and their relationship to processing parameters, ceramic particle size and concentration were determined and interpreted.

3:55 PM Invited

Fracture Initiation at Interfaces: *Placid Rodriguez*¹; Vaidehi Ganesan²; ¹Indian Institute of Technology; ²Indira Gandhi Centre for Atomic Research

The paper examines fracture initiation at interfaces. The nucleation of a cavity or a crack at an interface results from decohesion at the interface or fracture of a hard and brittle phase across the interface. The most common cause leading to such a decohesion or fracture is either the stress concentration due to the pile-up of dislocations at the interface or a sudden coalescence of dislocations at the head of a pile-up. Impingement by a persistent slip band, intersecting micro-shear bands and intersecting twins also lead to fracture initiation. Sudden unpinning of dislocations leading to localized shear bands is another damage mechanism. All situations lowering grain boundary strength promote intergranular cracking. There are also instances of environment-assisted cracking mechanisms. The various mechanisms of fracture initiation at interfaces are discussed with specific examples from commercial and model alloy systems under both monotonic and cyclic loading conditions.

4:20 PM

Structural and Magnetic Characterization of Li_{0.5}Fe_{2.5-x}Mn_xO₄ Spinel Produced by Combustion Synthesis: *Prabeer Barpanda*¹; Shantanu Behera²; Japes Bera³; Swadesh K. Pratihari³; Shantanu Bhattacharya³; Rakesh Kumar Sinha⁴; ¹Rutgers University; ²Lehigh University; ³National Institute of Technology; ⁴Tata Refractories Limited

Lithium ferrites are key materials to replace yttrium iron garnate (YIG) for applications like microwave devices and memory core. It is due to their low cost combined with high curie temperature, saturation magnetization and hysteresis properties. In the reported work, Li_{0.5}Fe_{2.5-x}Mn_xO₄ (0 < x < 1) spinel samples were prepared by a novel combustion synthesis routes taking metal nitrates as oxidizer and citric acid as fuel. The resulting product was annealed at temperature 300–900°C and the structural evolution was investigated using XRD and Raman spectroscopy. The ordered (α) and disordered (β) spinel phase was quantified using Rietveld analysis and Raman spectra. The structural ordering with temperature was observed using TEM of spinel powder samples. Additionally, the magnetic properties of manganese substituted lithium iron ferrites were measured using vibrating sample magnetometer and Mossbauer spectroscopy. The increasing manganese substitution was marked to enhance the magnetisation and reduce the curie temperature.

WEDNESDAY PM

4:35 PM Concluding Comments Wayne D. Kaplan

The James Morris Honorary Symposium on Aluminum Wrought Products for Automotive, Packaging, and Other Applications: Processing Related Studies

Sponsored by: The Minerals, Metals and Materials Society, TMS Light Metals Division, TMS: Recycling Committee

Program Organizers: Subodh K. Das, Secat Inc; Gyan Jha, ARCO Aluminum Inc; Zhong Li, Aleris International Inc; Tongguang Zhai, University of Kentucky; Jiantao Liu, Alcoa Technical Center

Wednesday PM Room: 207A
March 15, 2006 Location: Henry B. Gonzalez Convention Ctr.

Session Chairs: Subodh K. Das, Secat Inc; Gyan Jha, ARCO Aluminum Inc

2:00 PM

Aging Alloy 7085 Mold Block: Part I, Two-Step Aging: *James T. Staley*¹; ¹North Carolina State University

Aerospace quality 7085 forgings are aged by a multi-step 72 hour aging practice. This treatment was deemed to be too expensive for forged block used for polymer molds, so Alcoa's Cleveland Works asked that we develop a shorter aging treatment. We first determined T_v (GP zones nucleate below this temperature regardless of vacancy content) and T_{ET} (GP zones are unable to nucleate above this temperature). Using these data, we selected a pre-aging temperature of 260°F and explored effects of time at this temperature prior to aging at the standard aging temperature 320°F. We found that 3 hours at this temperature provided a size distribution of GP zones that was stable at 320 F. Alcoa had determined previously that 17 hours at 320°F provided the strength and corrosion characteristics required. We recommended that they precede this treatment by a pre-age of 3 hours at 260°F.

2:25 PM

Aging Alloy 7085 Mold Block: Part II, Continuous Non-Isothermal Aging: *James T. Staley*¹; ¹NC State University

The acceptance of alloy 7085 by the polymer molding industry led to increased demands on the aging furnaces at Alcoa's Cleveland Works, so they asked us to develop an even shorter aging practice. We explored the feasibility of combining the stage that nucleates GP zones with the stage that transforms them into η' and η precipitates. We determined the heating rate that allowed GP zones to grow continuously at a rate sufficient to prevent reversion as the temperature increased. We also determined that the kinetics of overaging during continuous aging could be predicted by integrating effects of isothermal overaging. We determined that a linear heating rate of 25 F/hr. produced target strength in 11.25 hours and that heating rate need not be linear. Depending on the size of the load and the characteristics of the furnace, target properties can be obtained by setting the furnace air temperature above 360 F.

2:50 PM

Future Challenges for Aluminum Packaging Alloys: *Gyan Jha*¹; Weimin Yin²; Randall Bowers²; ¹ARCO Aluminum Inc; ²Secat Inc

The Aluminum packaging industry needs to have cost effective high performance alloys for a sustainable future. The key stakeholders at all parts of the supply chain need to work together to develop new alloys that are competitive in today's economic environment. The alloys used for new packaging need to be expanded beyond the current available selection. The opportunities and framework to create value for the supplier, customer and consumer will be discussed.

3:15 PM

Microstructure and Texture Evolution during Drawing and Ironing Rigid Container Sheet: *Gyan Jha*¹; Weimin Yin²; Randall Bowers²; ¹ARCO Aluminum Inc; ²Secat Inc

The structural evolution during D and I process has been studied in AA3xxx aluminum alloys. The complex changes of microstructure and

texture occur in the process of drawing and ironing because of aggressive deformation and the heat generated in the process. The microstructure at different stages of the process is characterized in comparison with the as-received can sheet regarding particles, texture and dislocations. The insoluble particles and dispersoids have been determined using Scanning Electron Microscopy equipped with Energy Dispersive Spectroscopy. Omnimet Imaging Analysis System attached to Optical Microscopy is employed to measure the size and distribution of the particles and dispersoids. The micro-hardness and formability has also been evaluated at each stage and related to the evolution of texture and microstructure. A fundamental understanding of the alloy behavior during processing will help support the development of future alloys.

3:40 PM Invited

The Influence of Cold Working on Crystallographic Texture Following Solutionization and Quenching in Ti-6Al-4V Wire: *Thomas R. Bieler*¹; Liang Zeng²; ¹Michigan State University; ²Alcoa Fastening System

The evolution of microstructure and crystallographic texture of the alpha phase in titanium alloy were examined before and after the solutionization process. The Ti-6Al-4V wire was worked by extrusion, solution heat-treated and water quenched, then aged. Optical and transmission electron microscopes, as well as serial sectioning X-ray diffraction and texture were used to provide information about solutionization and variant selection kinetics and texture homogeneity. Following solutionization and quenching, the primary <10-10> fiber texture decreased at the expense of an emerging secondary fiber texture with <0001> basal plane normal aligned with the longitudinal axis. This 90° mis-oriented component increased in volume fraction with increasing solutionization temperature and time, due to a higher beta phase volume fraction. The relationship between the variant selections of alpha phase, and the effects of dislocations are discussed in the context of the known physical metallurgy of titanium and other alloys.

4:05 PM Break

4:15 PM

Solidification and Stress Modeling of DC Casting of 5xxx Aluminum Alloys: *Zhengdong Long*¹; Qingyou Han²; Shridas Ningileri³; Subodh Das³; ¹University of Kentucky; ²Oak Ridge National Laboratory; ³Secat, Inc.

The DC casting is the predominant casting process for producing ingot for aluminum sheet. An integrated 3D Direct Chill (DC) casting model was used to simulate the heat transfer, fluid flow, solidification, and thermal stress during casting. The ingot surface temperature dependent heat transfer coefficient was determined by temperature measurements, which were performed in an industrial casting facility. The effects of cooling water flow rate, air gaps caused by mold and bottom block design were also coupled into the model. The heat flux, temperature distribution, solid fraction, and thermal gradients during the casting were analyzed. The stress evolution was compared at various locations and correlated with physical phenomena associated with the casting process.

4:40 PM

Friction Stir Processing of AA5052: Basil Darras¹; *Marwan K. Khraisheh*¹; ¹University of Kentucky

Recently, Friction Stir Processing has emerged as a promising new tool that can produce ultrafine and homogenized structures in sheet metals. Friction Stir Processing is a solid state processing technique that uses a rapidly rotating non-consumable high strength tool steel pin that extends from a cylindrical shoulder. The rotating pin is forced with a predetermined load into the workpiece and moved along the desired direction. Frictional heating is produced from the rubbing of the rotating shoulder with the workpiece, while the rotating pin deforms and stirs the locally heated material. It is a hot working process in which a large amount of deformation is imparted to the sheet. FS processed zone is characterized by dynamic recrystallization which results in grain refinement. In this work, the effects of various process parameters on the resulting microstructure are discussed.

The Rohatgi Honorary Symposium on Solidification Processing of Metal Matrix Composites: Advanced Applications of MMCs

Sponsored by: The Minerals, Metals and Materials Society, TMS Materials Processing and Manufacturing Division, TMS Structural Materials Division, TMS/ASM: Composite Materials Committee, TMS: Solidification Committee

Program Organizers: Nikhil Gupta, Polytechnic University; Warren H. Hunt, Aluminum Consultants Group Inc

Wednesday PM Room: 207B
 March 15, 2006 Location: Henry B. Gonzalez Convention Ctr.

Session Chairs: Nikhilesh Chawla, Arizona State University; B. C. Pai, Regional Research Laboratory, CSIR; Rahul R. Maharsia, Louisiana State University

2:00 PM Invited
Metal Matrix Composites—Commercial Status and Insights: *Daniel B. Miracle*¹; ¹U.S. Air Force

Over the past four decades, metal matrix composites (MMCs) have been transformed from topic of scientific and intellectual interest to a material of broad technological significance. The worldwide MMC markets in 1999 accounted for 2500 metric tons valued at over \$100M. Important MMC applications in the ground transportation, thermal management, aerospace, industrial and recreation industries have been enabled by functional properties that include high structural efficiency, excellent wear resistance, and attractive thermal and electrical characteristics. A suite of challenging technical issues has been overcome, including processing, material design and development, and characterization and control of interface properties. Research, development and transition efforts that led to the successful insertion of MMCs will be described, including insights gained into strategies for successful technology transition in the post-Cold War era. A forward look at the motivating factors and candidate approaches for the next generation of MMCs will be provided.

2:25 PM Invited
Low-Cost Cast Metal Matrix Composites for Ground-Based Vehicles: *Darrell R. Herling*¹; ¹Pacific Northwest National Laboratory

Metal matrix composites (MMC) have found applications in many industries, from aerospace to automotive, sporting-goods and electronics packaging. Many applications have been for military components, where high performance materials are necessary to meet vigorous property challenges. Aluminum and magnesium MMC are attractive due to high specific stiffness and enhanced strength. In the case of most discontinuous reinforced aluminums, wear resistance of these materials is also increased significantly. Regardless of these benefits, high materials costs relative to conventional alloys have limited widespread application of this material family in the ground transportation industry. If the cost associated with production and shape forming methods of MMC can be reduced, this could enable widespread use of particle reinforced composite materials in the automotive and truck manufacturing industries. This paper will highlight the results of a program sponsored by the Department of Energy and USCAR that is focused on developing low-cost options for MMC components.

2:50 PM
Application of Al-B4C Metal Matrix Composites in the Nuclear Industry for Neutron Absorber Materials: *X. Grant Chen*¹; ¹Alcan Inc.

For dry storage and transportation of nuclear fuel in the nuclear industry, the most commonly used neutron absorber are boron-containing metallic materials, in which the element boron possesses a high cross-section for absorbing thermal neutrons. Al-B4C metal matrix composites, recently developed by Alcan, are particularly suitable for manufacturing high quality neutron absorber components due to the flexibility of adding various boron concentrations, the lightweight, and superior thermal conductivity and mechanical properties. In this paper, a series of Al-B4C MMCs with different Al-matrix and B4C loads are presented for both structural and non-structural applications. The process routes for incorporating B4C into metal

and associated downstream fabrication are outlined. The composites can be cast, extruded or rolled to almost any desired size and shape. The microstructure, thermal conductivity and mechanical properties of some Al-B4C products are described. Results of neutron absorptivity based on neutron transmission tests for typical Al-B4C products are presented.

3:15 PM Invited
Hybrid Aluminum Matrix Composites for Brake Applications: *Jason S. H. Lo*¹; ¹CANMET, Natural Resources Canada

Traditionally, automotive brake rotors for both light and heavy vehicles are made with cast iron. Besides having economical advantage, cast iron rotors provide many disadvantages. Disadvantages due mainly to their weight are reduction in fuel efficiency; increase in green house gas emission; and increase in noise, vibration and hardness. Commercial aluminum composite materials with property overcoming most of the drawbacks in cast iron brake rotors has been developed and employed in light vehicles. However, such commercial composite materials suffer a major drawback of poor elevated temperature property. In this paper, the results of the work in developing a novel hybrid composite material specifically for the brake application are described. This material consists of a SiC reinforcement and a modifier to enhance the elevated temperature property of the aluminum matrix alloy. Both the fabrication technology, microstructure, mechanical and physical properties of the hybrid composite being evaluated, are reported.

3:40 PM Invited
High Energy X-Ray Diffraction Measurements and Imaging of Superconducting Mg/MgB2 Composites under Compressive Loading: *Marcus Young*¹; *John D. DeFouw*¹; *Jonathan D. Almer*²; *Kamel Fezzaa*²; *Wah-Keat Lee*²; *Dean R. Haeffner*²; *David C. Dunand*¹; ¹Northwestern University; ²Argonne National Laboratory

In this study, 140 μm diameter boron fibers were pressure infiltrated with liquid Mg metal and the Mg/B composite was subsequently heat treated at 950°C for 2.5 hours to convert B fibers into MgB2 fibers by reaction with liquid Mg. The resulting Mg-73 vol% MgB2 fiber composite was loaded in uniaxial compression, and volume-averaged lattice strains in the Mg and MgB2 phases were measured in-situ at various constant stresses by synchrotron X-ray diffraction up to 500 MPa. Load transfer was observed to occur from the Mg matrix to the MgB2 fibers. Spatially resolved measurements showed variations in load transfer at different positions within the composite for the elastic, plastic, and damage deformation regimes. Using phase-enhanced x-ray imaging, the extent of damage within the composites was also observed.

4:05 PM Break
4:20 PM Invited
Non Destructive Characterization of Metal Matrix and Advanced Composites—A Review: *Phani Surya Kiran Mylavaram*¹; *Eyassu Woldeesenbet*¹; ¹Louisiana State University

Metal matrix composites (MMC) offer wide variety of property advantages over conventional metals and alloys. MMC's can be classified into four types depending upon the type of reinforcement as MMC's reinforced with particles(PMC), MMC's reinforced with short whiskers or fibers (SFRM), MMC's reinforced with continuous fibers(CFM) and MMC's reinforced with mono filaments (MFRM). With the increasing usage of MMC's and advanced composites as realistic candidates for engineering components, quality control and failure monitoring during service in these materials have gained importance. This paper reviews the present non destructive characterization techniques used in the industry for characterizing MMC's and other advanced composites with the challenges behind them.

4:45 PM Invited
Applications of Solidification Processed Discontinuously Reinforced Aluminium Alloy Composites: *Satyabrata Das*¹; *Dehi Pada Mondal*¹; *N. Ramakrishnan*¹; ¹Regional Research Laboratory

Aluminium Composites are engineered combination of aluminium alloy and reinforcing phase capable of providing tailored properties. AACs combine the favorable properties of aluminium and ceramic leading to improved physical, mechanical and tribological properties. Regional Research Laboratory, Bhopal, India has developed liquid metallurgy route to

WEDNESDAY PM

synthesis Al composites. Developed composites are characterized in terms of microstructure, deformation behaviour, tribological properties etc. Efforts are being made to design and develop Al composite prototype components. Such components are field trialed in various sectors and encouraging results are obtained and thus found their way for commercialization. Considerable efforts have been made in transferring the aluminium composite technology developed in the laboratory to automobile industries. Prototype components such as brake drum for automobile are developed. It is found that AMMC brake drums are lighter by 60% and better braking efficiency as compared to existing one. Composite Apex Insert for mining industries is also developed.

5:10 PM Break

5:15 PM Panel Discussion

Future Directions in Micro and Nano Metal Matrix Composites: Moderated by Dr. Warren Hunt, Aluminum Consultants Group Inc

Titanium Alloys for High Temperature Applications - A Symposium Dedicated to the Memory of Dr. Martin Blackburn: Titanium Based Intermetallic Alloys for High Temperature Applications - Gamma

Sponsored by: The Minerals, Metals and Materials Society, TMS Structural Materials Division, TMS: Titanium Committee

Program Organizers: Michael W. Peretti, Lyondell Chemical Company; Daniel Eylon, University of Dayton; Ulrike Habel, Munich; Guido C. Keijzers, Del West USA; Michael R. Winstone, DSTL

Wednesday PM
March 15, 2006

Room: 201
Location: Henry B. Gonzalez Convention Ctr.

Session Chairs: Xinhua Wu, University of Birmingham; Wayne Voice, Rolls-Royce plc

2:00 PM Invited

Development of New Structural Alloys Based on $\beta+\gamma$ TiAl: *Young-Won Kim*¹; Dennis M. Dimiduk²; Christopher F. Woodward²; ¹UES Inc; ²U.S. Air Force

Ongoing research is investigating a titanium-based high-temperature structural alloy system, called beta-gamma Ti, consisting of three phases (γ -TiAl + β -Ti + α_2 -Ti₃Al). Gamma alloys (based on γ -TiAl and α_2 -Ti₃Al) exhibit remarkable creep and oxidation resistance useful up to 900°C. Yet, gamma alloys have not been implemented for aerospace applications, primary due to their low low-temperature ductility, unconventional processing requirements and poor machinability. Experiments were initiated to develop robust beta-gamma alloys, and preliminary experiments show that such alloy compositions exist within the phase fields which are of three phases ($\gamma + \beta + \alpha$) at low temperatures (<1100°C) and of two or three phases ($\beta +$ one or two others) at higher temperatures. Determination of such phase fields is underway through phase/composition analyses of a few selected compositions and ThermoCal calculations and modeling. This accelerated development process will be discussed, along with the initial results of forging behavior, machinability and properties of a selected alloy.

2:30 PM

Synthesis and High Temperature Mechanical Properties of Two Ultrafine Grained Gamma-TiAl Based Alloys: Ti-47Al and Ti-45Al-5.5(Cr,Nb,B,Ta): Hongbao Yu¹; *Deliang Zhang*¹; Peng Cao¹; Yuyong Chen²; Brian Gabbitas¹; ¹University of Waikato; ²Harbin Institute of Technology

In our research on titanium based materials, high quality bulk nanostructured (grain sizes <100nm) and ultrafine grained (100nm<grain sizes<1 μ m) TiAl intermetallic based alloys are produced using a novel powder metallurgy route which combines high energy mechanical milling of mixtures of elemental powders to produce nanostructured powders and consolidation of the powders using various thermomechanical processes including hot isostatic pressing, equal channel angular pressing and forward

extrusion. The fine microstructure renders the alloys with improved formability which is critical for the applications of TiAl based alloys. To determine the capacity of the ultrafine grained TiAl based alloys for high temperature applications, their high temperature mechanical properties such as strength and ductility are studied. This paper will report findings of a study which has been focused on the synthesis and high temperature mechanical properties of two alloys: a binary alloy Ti-47Al and a complex alloy Ti-45Al-2Cr-2Nb-1B-0.5Ta (in at%).

3:00 PM Break

3:30 PM

The Effects of W Additions on the Microstructural and Mechanical Properties of Ti-48Al-2Nb-2Cr Alloys: *Dongyi Seo*¹; Scott Bulmer²; H. Saari²; P. Au¹; P. Patnaik¹; ¹National Research Council of Canada; ²Carleton University

Ti-48Al+2Nb+2Cr powders, with 0%, 0.5% and 1%W (at%), were consolidated by hot isostatic pressing (HIP). A heat treatment, which consisted of slow cooling from 1400°C in the α region to 1280°C in the $\alpha+\gamma$ region at a rate of 20°C/min, followed by air-cooling, was developed to produce fully lamellar microstructures with narrow lamellar spacing. This procedure also produced a microstructure that was free from Widmanstätten or massive γ and β particles. To stabilize the microstructure, the HIP'ed and heat-treated samples were subsequently aged in the $\alpha_2+\gamma$ region for various durations. The resulting microstructures were analyzed in terms of grain size, precipitate size, and interlamellar spacing. Hardness tests were also conducted to assess the strength of the heat-treated materials, and the results were analyzed with respect to W additions. The results from this study will be used to identify heat treatment conditions to optimize the creep resistance of these materials.

4:00 PM

Microstructure and Mechanical Properties of Rolled Sheet and Forged Block Gamma-Titanium Aluminides: *Russell J. Foon*¹; Julius De Rojas¹; Sun Hyung Kim¹; Nicole Sporer¹; Richard Clark²; John Ogren¹; Omar Es-Said¹; Kyle Mori¹; Elizabeth Villalobos¹; Hamid Garmestani³; Dongsheng Li³; Gopal Das⁴; ¹Loyola Marymount University; ²College of the Canyons; ³Georgia Institute of Technology; ⁴Pratt & Whitney

γ -based inter-metallic titanium aluminides are ideal for high temperature structural applications in gas turbine engines and automotive industries. γ -TiAl based alloys have attractive properties such as low density, high modulus, high temperature strength, oxidation resistance, burn resistance, and the potential to replace heavier superalloys for the temperature range 550-850°C. Titanium aluminide samples processed from sheet and forged samples with varying compositions of Cr, Nb, Ta, B, C were heat treated above and below the alpha transus temperature. Microhardness, optical microscopy, texture (preferred crystallographic orientation) and tensile tests were carried out to characterize the material.

Ultrafine Grained Materials - Fourth International Symposium: High Temperature and Physical Properties

Sponsored by: The Minerals, Metals and Materials Society, TMS Materials Processing and Manufacturing Division, TMS Structural Materials Division, TMS/ASM: Mechanical Behavior of Materials Committee, TMS: Shaping and Forming Committee

Program Organizers: Yuntian T. Zhu, Los Alamos National Laboratory; Terence G. Langdon, University of Southern California; Zenji Horita, Kyushu University; Michael Zehetbauer, University of Vienna; S. L. Semiatin, Air Force Research Laboratory; Terry C. Lowe, Los Alamos National Laboratory

Wednesday PM
March 15, 2006

Room: 217D
Location: Henry B. Gonzalez Convention Ctr.

Session Chairs: Terence G. Langdon, University of Southern California; Yuri S. Estrin, Technical University Clausthal; Farghalli A. Mohamed, University of California; Taku Sakai, UEC Tokyo

2:00 PM Invited

Creep Behavior of an Al-7034 Alloy Processed by ECAP: *Cheng Xu*¹; Terence G. Langdon¹; ¹University of Southern California

Processing by equal-channel angular pressing (ECAP) at a temperature of 473 K, an ultrafine grain size of ~0.3 μm was obtained in a commercial Al 7034 alloy and superplastic elongations of =1000% were achieved at high strain rates (=10² s⁻¹) when testing at 673 K. The creep behavior of the as-pressed alloy was investigated at temperatures of 473, 573 and 673 K and the relationship between strain rate and flow stress was examined. The stress exponent was calculated to determine the dominating deformation process and emphasis was placed on the strain rate range where superplastic elongations were achieved. The creep behavior of the alloy in the as-received condition was also examined for comparison.

2:20 PM Invited

Effect of Nano-Scale Dispersion Particles on Thermal Stability and Creep in Bulk Cryomilled Ultrafine Grained 5083 Al: Farghalli A. Mohamed¹; *Manish Chauhan*¹; Indranil Roy¹; ¹University of California

The preparation of Ultra fine grained (UFG) 5083 Al using gas atomization followed by cryomilling leads to introducing oxides (resulting from the breakup of oxide layers that are formed around metal particles during gas atomization), and carbides, nitrides, and other impurities during cryomilling. The results of research in progress show that the presence of these nano-scale dispersion particles affects the behavior of the alloy in several ways. First, the particles enhance thermal stability by suppressing grain growth. Second, they serve as strong obstacles to the movement of dislocations, a process that provides a possible source for a threshold stress during superplastic flow. Finally, they act as sites for cavity nucleation, leading to a loss in ductility.

2:40 PM

A Quantitative Investigation of Cavity Development in an Aluminum Alloy Processed by Equal-Channel Angular Pressing: *Megumi Kawasaki*¹; Cheng Xu¹; Terence G. Langdon¹; ¹University of Southern California

A commercial spray-cast aluminum 7034 alloy was processed by equal-channel angular pressing (ECAP) to produce an ultrafine grain size of ~0.3 μm. Microstructural examination showed the alloy contains MgZn₂ and Al₃Zr precipitates which restrict grain growth at elevated temperatures. Tensile tests were conducted on both as-received and as-pressed specimens at a temperature of 673 K and the results showed the occurrence of high superplastic elongations in the as-pressed material. There was also evidence for the development of extensive cavitation during testing. This paper describes a quantitative examination of cavity development in specimens pulled to failure in both the as-received and the as-pressed conditions. Measurements were taken to record critical parameters including the area of each cavity, the orientations of the long axes

with respect to the tensile axis and the roundness coefficient which is a measure of the shape of each individual cavity.

2:55 PM

Compressive Creep in an Al-3%Mg-0.2%Sc Alloy Processed by Equal-Channel Angular Pressing: Jiri Dvorak¹; Milan Svoboda¹; Zenji Horita²; *Vaclav Sklenicka*¹; ¹Academy of Sciences of the Czech Republic; ²Kyushu University

Creep tests in compression on an Al-3wt%Mg-0.2wt%Sc alloy after processing through equal-channel angular pressing (ECAP) were conducted at temperature 473 K and stress in the range 15-50 MPa. The microstructure of a ternary alloy was examined by transmission electron microscopy. The present results were compared with the results of our earlier work on compressive creep of pure ECAP aluminium with the same imposed strain and the ECAP processing route. The results demonstrate that the creep strength of an Al-Mg-Sc alloy is significantly improved compared to that of pure aluminium. The higher strength observed for the ternary alloy in the high-stress region (>25 MPa) results from the synergism of solid-solution strengthening and precipitate strengthening due to Al₃Sc nanoscale precipitates. The presence of these precipitates dramatically increases the creep resistance in the low-stress region through a threshold stress for creep.

3:10 PM Invited

Creep Regularities and Mechanisms of Ultrafine Grained Ti-6Al-4V Alloy Produced by Severe Plastic Deformation: *Yury R. Kolobov*¹; Galina P. Grabovetskaya²; Yuntian T. Zhu³; Konstanin V. Ivanov¹; Olga V. Zabudchenko⁴; ¹Belgorod State University; ²Institute of Strength Physics and Materials Science SB RAS; ³Los Alamos National Laboratory; ⁴Tomsk State University

A comparative analysis of plastic deformation development regularities at creep of ultrafine grained (0.2-2 μm) Ti-6Al-4V alloy processed by severe plastic deformation (SPD) and its fine grained (3-10 μm) counterpart was carried out. It is shown that the formation of ultrafine grain structure of two-phase Ti-6Al-4V alloy by SPD leads to temperature range shear of superplastic properties manifestation to lower temperatures. The influence of structural state of Ti-6Al-4V alloy on the development of grain boundary sliding (GBS) at creep has been studied. The apparent activation energy of creep was lower for the ultrafine grained Ti-6Al-4V than for its fine grained counterpart. The role of GBS and diffusion mass transfer in the development of plastic deformation at creep is being analyzed.

3:30 PM

Rapid Nanostructuring of Cementite during the Deformation of Pearlitic Steel: *Ian MacLaren*¹; Yulia Ivanisenko²; Xavier Sauvage³; Ruslan Z. Valiev⁴; Hans-Jörg Fecht²; ¹University of Glasgow; ²Forschungszentrum Karlsruhe; ³University of Rouen; ⁴Ufa State Aviation Technical University

It is now well known that the cementite component of pearlitic steel tends to be destroyed and dissolved on deformation, although many details of the process remain unclear. The present study focuses on the early stages of high-pressure torsion deformation of pearlitic steel using TEM and 3D atom probe as the primary characterisation methods. It is found that the ferrite lamellae deform much as expected by slip of lattice dislocations, resulting in the normal cell formation that is common to many ductile materials. In contrast to this, even at this early stage of the deformation, the cementite lamellae are reduced to a nanocrystalline structure. The compositional changes in the cementite as a consequence of the deformation are analysed and the processes that lead to this rapid nanostructuring are discussed.

3:45 PM

Stress Corrosion Cracks Propagation in Ultra-Fine Grain Copper Fabricated by an Equal Channel Angular Pressing: *Hiroyuki Miyamoto*¹; Takuro Mimaki¹; Satoshi Hashimoto²; Alexei Vinogradov²; ¹Doshisha University; ²Osaka City University

The present study aims to assess the susceptibility of ultra-fine grain (UFG) copper produced by Equal channel angular pressing (ECAP) to stress corrosion cracking (SCC) by a ASTM plane strain fracture test with a constant load in an aqueous 1M NaNO₂ solution under a constant applied potential of 100mV(Ag-AgCl). The effect of equilibrium and unequilibrium states of grain boundaries on the susceptibility of SCC has

been focused. Two copper billets of commercial purity were pressed through a ECA-die until eight passes via the so-called route B in order to obtain an UFG structure. One of them was subsequently annealed at 473K for 40 seconds in order to relieve internal stress. It was found that the crack propagation rate of ultra-fine grain copper decreased by a flash annealing. The decrease of SCC sensitivity is attributed to the change of grain boundary structures to equilibrium state during the flash annealing.

4:00 PM Break

4:10 PM Invited

Properties of Ultrafine Grained Conductors: *Ke Han*¹; Jun Lu¹; ¹National High Magnetic Field Laboratory

Codeformation is used to fabricate large quantities of metal matrix composite conductors which possess unique combination of mechanical and physical properties. The properties of those materials are related to the microstructure. A number of Cu matrix conductors have strength levels close to their theoretical strength because the size of the grains reaches nanometer scales. However, the electrical resistance is also increased because of the refined microstructure. The application of these materials requires detailed consideration of the mechanisms of strengthening and electron transport which are operative in materials with ultra fine scale microstructures. In addition, consideration must be given to the fatigue endurance of those composites. Low temperature superconductors are also the composite. The critical current of Nb₃Sn superconductors is related to the mechanical strain to which the materials are exposed. This presentation will address the correlation between the properties (both mechanical and transport) and microstructure of those conductors.

4:30 PM

Texture Gradient in fcc Metals Deformed by ECAP as a Function of Stacking Fault Energy: *Werner Skrotzki*¹; Burghardt Kloeden¹; Nils Scheerbaum¹; Carl-Georg Oertel¹; Satyam Suwas²; Laszlo S. Tóth³; ¹TU Dresden; ²RWTH Aachen; ³University Metz

Different fcc metals (Al, Cu, Ni, Ag) have been deformed by equal channel angular pressing (ECAP) up to 3 passes using route A. The texture with respect to position in the deformed billet has been measured with high-energy synchrotron radiation. It is characterized by texture components typical for simple shear in the intersection plane of the square-shaped 90° bent channel. Intensities of the texture components as well as deviations from their ideal shear positions vary from the top to the bottom of the billet and with the number of passes. The change of the intensity of texture components and the texture gradient within the metals investigated will be discussed. Special emphasis will be put on the influence of stacking fault energy on texture formation during ECAP of fcc metals.

4:45 PM

Non-Equilibrium Processing Routes for Ultrafine Grained or Nanostructured Materials: *Gerhard H. Wilde*¹; Nancy Boucharat¹; Guru Prasad Dinda¹; Harald Rösner¹; Ruslan Valiev²; ¹Forschungszentrum Karlsruhe GmbH; ²Ufa State Aviation Technical University

The sequential combination of different processing routes that drive a material to a different extent, - with different rates - and by different means from thermodynamic equilibrium present new and attractive processing opportunities to obtain bulk nanocrystalline or massive ultrafine grained materials that are widely unexplored. More specifically, processing routes based on rapid quenching or plastic deformation have been combined here such that the initial state is continuously energized and successively driven farther away from thermodynamic equilibrium. Here, different deformation methods with largely different strain and pressure levels have been applied on rapidly quenched metallic glasses, but also on elemental sheet samples. Both processing routes result in a nanocrystalline microstructure with remarkable properties, especially with respect to strength and hardness. The basic underlying mechanisms that lead to ultrafine grained or nanocrystalline microstructures are discussed and the current state of nanostructure control is highlighted by selected examples.

5:00 PM Question and Answer Period, Award Ceremony and Free Style Discussion: Moderated by Terence G. Langdon, University of Southern California

Wechsler Symposium on Radiation Effects, Deformation and Phase Transformations in Metals and Ceramics: Shape Memory Alloys

Sponsored by: The Minerals, Metals and Materials Society, ASM International, TMS Structural Materials Division, ASM Materials Science Critical Technology Sector, TMS Materials Processing and Manufacturing Division, TMS/ASM: Mechanical Behavior of Materials Committee, TMS/ASM: Nuclear Materials Committee, TMS/ASM: Phase Transformations Committee

Program Organizers: Korukonda L. Murty, North Carolina State University; Lou K. Mansur, Oak Ridge National Laboratory; Edward P. Simonen, Pacific Northwest National Laboratory; Ram Bajaj, Bettis Atomic Power Laboratory

Wednesday PM
March 15, 2006

Room: 208
Location: Henry B. Gonzalez Convention Ctr.

Session Chairs: Louis K. Mansur, Oak Ridge National Laboratory; K. Linga Murty, North Carolina State University

2:00 PM

The Effect of Severe Plastic Deformation on the Recoverable Phase Transformation in High Temperature Shape Memory Alloys: *Benat Kockar*¹; Ibrahim Karaman¹; Jae-Il Kim¹; ¹Texas A&M University

NiTi alloys are the most important shape memory alloys due to their superior mechanical and functional properties, however their use is restricted below 100°C. In order to extend their utility in high temperature applications, higher martensitic transformation temperatures than 100°C, lower temperature hysteresis, and better cyclic reversibility are required. The transformation temperatures of NiTi alloys can be increased by the addition of Hf and Pd, however, these additions lead to the degradation of thermal cyclic response under stress due to the decrease in critical stress for slip. In this study, severe plastic deformation via equal channel angular extrusion (ECAE) was used to increase the critical stress for slip by grain refinement down to nanometer range and by designing specific textures in NiTi and NiTi(Pd,Hf) alloys. We will present methods of engineering microstructure and texture using ECAE and resulting thermomechanical response including temperature hysteresis and enhanced cyclic reversibility.

2:20 PM

On the High Strain-Rate Response of Ni-Rich NiTi Shape Memory Alloy as a Function of Aging Temperature: *Raghavendra Adharapurapu*¹; Kenneth Scott Vecchio¹; ¹University of California

The influence of aging on the high strain-rate response of Ni-rich (60 wt%) NiTi shape memory alloy was studied. Aging in Ni-rich NiTi alloys leads to metastable Ti₃Ni₄ precipitates, which promotes the occurrence of R-phase. These precipitates lead to precipitation hardening, and aid the overall shape memory effect and strengthening of B2 matrix. Since precipitates in this alloy affect the shape memory properties and also the transformation temperatures, initial investigations were focused on precipitation using metallographic techniques and a TTT diagram was developed. In order to ascertain their behavior under impact loading conditions for various defense applications, the dynamic response of these alloys was studied as a function of aging and compared with the quasi-static results. A split-Hopkinson bar was utilized for high-strain rate compression tests using a pulse-shaper technique. Preliminary results indicate that a wide range in strength (between 950MPa – 2500MPa) is achievable in these materials.

2:40 PM

Dynamic Response of NiTi Shape Memory Alloys: Influence of Temperature and Strain-Rate on Tension-Compression Asymmetry: *Raghavendra Adharapurapu*¹; Kenneth Scott Vecchio¹; FengChun Jiang¹; ¹University of California

Polycrystalline NiTi shape memory alloys (SMA) are known to exhibit asymmetry in tension-compression behavior at room temperature and low strain rates. In order to fully explore the extent of this asymmetry, the compressive and tensile behavior of NiTi shape memory alloy has been

examined as a function of temperature (-196°C to 400°C) at 10⁻³/s and 1200/s strain rates. A Hopkinson tensile bar and a split-Hopkinson compression bar with a pulse shaper technique were utilized for dynamic tension and compression tests, respectively. The attendant asymmetry between tension and compression behavior was captured in the variation of stress-plateau and the critical stress (as obtained by 0.2% strain offset) with temperature. The critical stress exhibited a three-stage characteristic, with critical stress being higher in compression than in tension. These findings have important implications in the application of SMA towards defense and others applications where understanding the dynamic response of the SMA is essential.

3:00 PM

Neutron Diffraction Studies of Deformation in NiTiFe Shape Memory Alloys at 90 K: *Rajan Vaidyanathan*¹; ¹University of Central Florida

NiTiFe shape memory alloys can undergo transformations between cubic, rhombohedral and monoclinic phases at low temperatures. The low hysteresis associated with the rhombohedral or R phase transformation, coupled with superior fatigue properties, makes them candidates for actuator applications at low temperatures. This talk reports on neutron diffraction measurements from NiTiFe shape memory alloys during mechanical loading at low temperatures, with the objective of probing deformation in the R phase. For this purpose, a low temperature loading capability for in situ neutron diffraction measurements was implemented on the Spectrometer for Materials Research at Temperature and Stress (SMARTS) at Los Alamos National Laboratory. The in situ diffraction measurements, during loading at 90 K, observed twinning in the R phase prior to a reversible martensitic transformation to the monoclinic phase at higher stresses. This work was supported by grants from NASA (NAG3-2751) and NSF (CAREER DMR-0239512).

3:20 PM Break

3:40 PM

Few Guidelines to Increase Actuation Stress in NiMnGa Magnetic Shape Memory Alloys (MSMAs): *Burak Basaran*¹; Haluk Ersin Karaca¹; Ibrahim Karaman¹; Yuriy I. Chumlyakov²; Hans J. Maier³; ¹Texas A&M University; ²Siberian Physical-Technical Institute; ³University of Paderborn

MSMAs have the ability to combine large strain output of conventional shape memory alloys with high frequency response of magnetostrictive materials. However, their operation range under stress is limited to a few megapascals. In this work, an extensive experimental program was undertaken on NiMnGa single crystals in quest for identifying physical and microstructural parameters critical in increasing the magnetic actuation stress. The present paper will discuss few guidelines to increase the actuation stress considering the coupled effects of magnetocrystalline anisotropy energy, phase transformation temperatures and Curie temperature. Few specific results will be presented in which one order of magnitude increase was achieved in the magnetic actuation stress. This giant increase will be shown to be a consequence of field induced phase transformation instead of field induced martensite reorientation which has been the only mechanism reported to be responsible for magnetic shape memory effect.

4:00 PM

An In Situ Study of Martensitic Transformation in Shape Memory Alloys Using PEEM: *Mingdong Cai*¹; Stephen C. Langford¹; J. Thomas Dickinson¹; Gang Xiong²; Timothy C. Droubay²; Alan G. Joly²; Wayne P. Hess²; ¹Washington State University; ²Pacific Northwest National Laboratory

The thermally-induced martensitic transformation in a polycrystalline CuZnAl and NiTi thin film shape memory alloy (SMA) was probed using photoemission electron microscopy (PEEM). Ultra-violet photoelectron spectroscopy (UPS) measurements indicate that the apparent surface work function changes reversibly during transformation, presumably due to the contrasting electronic structures of the martensitic and austenitic phases. *In situ* PEEM images provide information on the spatial distribution of these phases and the microstructural evolution during transformation. The evolution of the photoemission intensities obtained from PEEM images during transformation can provide quantitative information on fractional percentages of austenite and martensite phases as the transformation pro-

ceeds. PEEM offers considerable potential for improving our understanding of martensitic transformations in shape memory alloys in real time.

4:20 PM

New Cobalt Based Ferromagnetic Shape Memory Alloys (SMAs): *Haluk Ersin Karaca*¹; Ibrahim Karaman¹; Yuriy Chumlyakov²; Hans Maier³; ¹Texas A&M University; ²Siberian Physical-Technical Institute; ³University of Paderborn

Ferromagnetic SMAs have attracted increasing interest because of the ability to obtain one order of magnitude higher recoverable magnetic field induced strain than other active materials. A recently discovered ferromagnetic shape memory CoNiAl and CoNiGa alloys have promising shape memory characteristics for conventional and magnetic shape memory applications. We have conducted extensive studies to capture several aspects of the shape memory behavior of both alloys in single and polycrystalline forms. It has been demonstrated that these alloys have low pseudoelastic stress hysteresis even at temperatures higher than 200°C, high strength for dislocation slip, large recoverable strain levels (10%), large pseudoelastic temperature window (>250°C), low stress for martensite reorientation, and stable response to cyclic deformation. They also demonstrate strong orientation dependence and tension/compression asymmetry in shape memory characteristics. Selected experimental findings on single and polycrystals that summarize these findings will be presented and the challenges will be addressed.

4:40 PM

Deformation Mechanisms in U-Nb Shape Memory Alloys: *Robert D. Field*¹; Donald Brown¹; Dan J. Thoma¹; ¹Los Alamos National Laboratory

Alloys with compositions in the vicinity of U-14at%Nb display the shape memory effect (SME), with the maximum recoverable strain associated with a martensitic transformation from the high temperature (bcc) gamma phase to a monoclinically distorted version of the room temperature alpha-U phase, designated as alpha". The martensitic structure, deformation mechanisms, and texture development during uniaxial straining in the SME regime have been explained in terms of a correspondence variant model which describes the martensitic twin relationships derived from gamma/alpha" orientation relationships. This model has been extended to the post-SME regime by considering the texture developed during SME deformation as a starting point for subsequent plasticity. Recent progress will be presented, with particular emphasis on TEM observations of deformation twinning mechanisms and crystallographic texture evolution as determined by in-situ neutron diffraction experiments.

5:00 PM

Deformation Behavior of U-6 Wt% Nb: *Carl M. Cady*¹; George T. Gray¹; Donald Brown¹; Robert D. Field¹; Philip K. Tubesing¹; Denise R. Korzekwa¹; Ellen K. Cerreta¹; ¹Los Alamos National Laboratory

The shape memory effect is well documented in uranium-niobium alloys. The uranium-6 wt. % niobium alloy was investigated to determine the deformation behavior at different strains and loading conditions. Information will also be presented on the effect of strain rate, temperature, and loading orientation on the deformation behavior. Texture and mechanical experiments were conducted in compression, tension and shear to various strain levels to try to determine the active deformation mechanisms. This paper will present evidence as to the deformation mechanisms that occur, when they are activated, and when they saturate.

Advanced Materials for Energy Conversion III: A Symposium in Honor of Drs. Gary Sandrock, Louis Schlapbach, and Sejjirau Suda: Carbon, Borohydrides and Other Materials

Sponsored by: The Minerals, Metals and Materials Society, TMS Light Metals Division, TMS: Reactive Metals Committee

Program Organizers: Dhaneesh Chandra, University of Nevada; John J. Petrovic, Petrovic and Associates; Renato G. Bautista, University of Nevada; M. Ashraf Imam, Naval Research Laboratory

Thursday AM Room: 214A
March 16, 2006 Location: Henry B. Gonzalez Convention Ctr.

Session Chairs: Daniel Fruchart, CNRS; Joseph Wermer, Los Alamos National Laboratory; Bernard Bonnetot, CNRS-University of Lyon France

8:30 AM Invited

A Fuel Cell Actuated by Sodium Borohydride as a Hydrogen Storage Material: *Seiji Suda*¹; ¹MERIT

Abstract not available.

8:55 AM Invited

Hydrogen Storage Using Borohydrides: *Bernard Bonnetot*¹; Laetitia Laversenne¹; ¹University of Lyon-France

Borohydrides, however high hydrogen containing compounds, can hardly be used for hydrogen storage. What ever the solution chosen to recover the stored hydrogen, thermal dehydrogenation or hydrolysis, the regeneration of the borohydride must be operated out of the site of hydrogen utilization. Borohydrides would never be considered as reversible compounds for hydrogen storage. Dehydrogenation yield through thermal decomposition is highly energy consuming because borohydrides, specially alkaline earth derivatives, require high temperatures to be decomposed. More-over the multistep thermolysis of borohydride yield to very stable intermediates as alkaline earth hydrides whose dehydrogenation is rarely performed due to the volatility of the alkaline earth metal. This limitation implies the fact that the announced hydrogen containing must be lowered from 3/4 at least to be realistic. Improvements have been obtained using catalysts which lower the decomposition temperature but they also lower the stored hydrogen amount. The regeneration of the thermolyzed borohydrides would involve a specific chemical treatment which has not been studied up to now because the starting materials of borohydride chemistry are usually oxides. More promising are the developments of hydrogen generation from borohydrides through hydrolyzing process. How ever the hydrogen stored percentage must take into account all the reactants but the technical conditions directed the storage capacity. The hydrogen recovering process involves water as reactant and a key of the "fuel", borohydride plus water, efficiency is the conditions of the reaction of hydrolysis. The amount of recovered hydrogen is fixed by the stoichiometry of the reaction but the ultimate state of the formed borates after hydrolysis fixes the yield of the storage. Water and the borate hydrates formed from borohydrides becomes the most important results of the storage capacity. If all the hydrogen of water can be recovered, the high hydrogen containing of water allows high "fuel" efficiency. If the dehydration conditions of the side products formed after hydrolyze is not possible or required to hard conditions, the storing yield will be lowered. The option of hydrolyzing borohydride-water solution have to face two antagonist conditions: the solution must be as stable as possible to avoid any hydrogen leaking but the hydrolysis reaction must be as fast as possible to feed the fuel-cell with hydrogen. This balance is difficult and choices must be made to favor technical solution. The recycling of the borate resulting of the hydrolysis must be done out of the hydrogen consuming zone and technical points are actually non resolved specially for on board applications.

9:20 AM Invited

Integrated Design of Novel Hydrogen and Ammonia Storage Systems: *Tejs Vegge*¹; Anders Andreassen¹; Allan Schröder Pedersen¹; ¹Risø National Laboratory

Synthesizing new materials and catalysts for hydrogen storage is complex and expensive task, and a rational materials design process is required. Recent computer advances have made it possible to treat many of the essential materials problems, i.e. structural stability, hydrogen ab-/desorption and diffusion, with high accuracy methods like density functional theory (DFT). DFT calculations can be used to, e.g. provide a physical explanation for the catalytic role of the titanium based additives in complex hydrides or to predict the existence of new hydrogen storage structures with optimized thermodynamic properties. At Risø National Laboratory, we utilize the synergy of integrating theoretical work with in situ x-ray diffraction/SAXS, synchrotron/neutron experiments, and advanced materials testing to expedite the development of improved hydrogen and ammonia storage materials. We rely primarily on i) theoretically and experimentally observed trends, ii) improved nano-scale insight, and iii) structural predictions to guide our materials optimization process.

9:40 AM

Synthesis and Characterization of New Complex Borohydrides for Hydrogen Storage: *Sesha Srinivasan*¹; Elias K. Stefanakos¹; ¹University of South Florida

Complex chemical hydrides with high theoretical hydrogen densities have been renewed an interest for hydrogen storage in recent years. The breakthrough discovery of catalyzed sodium alanates for the reversible on-board hydrogen storage may not be the ideal system to realize the 2010 DOE technical targets due to its limited hydrogen storage capacity. On the other hand, sodium borohydride or lithium borohydride is a complex hydride possesses high hydrogen capacity of 10.5 wt.% and 18.2 wt.% respectively. However, the release of hydrogen from sodium borohydride is possible only by hydrolysis (reaction with water) and this process is irreversible. Whereas, the transition metal assisted borohydride derived from NaBH₄ (LiBH₄) undergoes thermal decomposition of molecular hydrogen at low temperatures. Destabilizing the borohydride complexes by reacting with binary compound yields better reversibility with greater hydrogen storage capacity at moderate temperatures. In search of binary metal hydrides with suitable hydrogen decomposition temperature (T_{dec}), the surprising correlation was found between T_{dec} and the standard redox potential (E₀) for the Mnⁿ/M⁰ redox pair in acidic aqueous solutions according to the general equation, Mnⁿ+1 (H-1)_n = M⁰ + n/2 H₂. Several binary and ternary hydrides which have T_{dec} values suitable for incorporating with low temperature fuel cells are known. Such hydrides include ZnH₂ [T_{dec}=90°C], Zn(BH₄)₂ [T_{dec}= 85°C], KSiH₃ [T_{dec}=70°C], CuH [T_{dec}=60°C] and LiGaH₄ [T_{dec}=50°C]. Unfortunately, with the exception of Zn(BH₄)₂ (8.4 wt.% hydrogen capacity), rest of the compounds do not store a sufficient high wt.% of hydrogen to attain the US DOE target of 6.5 wt.%. Keeping these aspects in view, the present work aims to synthesize new complex borohydride, Zn(BH₄)₂ by mechanochemical milling of NaBH₄ and ZnCl₂ under inert atmosphere. The as-prepared complex hydride has been characterized extensively using PXD, FTIR, DSC, TGA and PCT techniques to study the structural, B-H bond environment, thermal and volumetric properties. Powder X-ray diffraction analysis of mechanically milled sample exhibits the presence of zinc borate, NaCl, and unreacted NaBH₄ as well. The FTIR spectra of BH₄⁻ ion in NaBH₄ has a characteristic band at 2290 cm⁻¹, and in Zn(BH₄)₂, it occurs at ~2061 cm⁻¹ (bridging B-H bonds) and ~2451 cm⁻¹ (terminal B-H bonds). It is also interesting to note that Zn(BH₄)₂ exhibits ~6.0 weight percent of gravimetric hydrogen storage capacity at around 100-150°C as demonstrated by thermogravimetric analysis. The reversibility of the constituent elements to complex hydride phase under H₂ atmosphere is presently underway.

10:05 AM

Effect of Catalysts on Hydrogen Sorption Properties of Magnesium:

R. Sundaresan¹; R. Vijay¹; ¹International Advanced Research Centre for Powder Metallurgy and New Materials

Absorption/desorption of hydrogen by magnesium can be enhanced by incorporation of suitable catalysts. Studies have been carried out to evaluate such effects by mechanical alloying (MA) processing of the catalyst addition, when the effects of both grain refinement in Mg and finely distributed catalyst on Mg surface can be combined. Results are presented on the systems (i) Mg-TM (TM = 10-20 wt% Ti), (ii) Mg-IM (IM = 10-50 wt% MmNi₅, Mm = mischmetal) and (iii) Mg-Oxide (Oxide = 5-20 wt% Cr₂O₃), milled in Fritsch P5 planetary mill under toluene cover. With the addition of Ti, Mg could absorb 6.1 and 6.0 wt% of hydrogen at 300 and 200°C, respectively, at 30 bar pressure. The absorption capacity and rate reduced significantly at temperatures below 200°C. There was no desorption of hydrogen at temperatures below 300°C at a pressure greater than 1 bar. With the addition of MmNi₅, Mg was seen to absorb up to 5.0 wt% at 100°C and 15 bar pressure. MmNi₅ does not itself form a hydride at this pressure and its effect appeared to be only catalytic. The amount absorbed appears to be the saturation limit, rising to only 5.1 wt% at 300°C. No desorption occurred at temperatures below 300°C, while at 300°C and 1 bar pressure, the maximum hydrogen desorbed was 3.1 wt%. Magnesium with the addition of Cr₂O₃ absorbed 5.45, 5.3 and 3.8 wt% at 300, 200 and 100°C, respectively, at a pressure of 30 bar. The absorption as well as desorption rates increased with increase in Cr₂O₃ content. Mg-15 wt% Cr₂O₃ composite desorbed maximum quantity of 4 wt% at 300°C and 1 bar pressure. Desorption was marginal at temperatures less than 300°C. In all cases catalysis is evident since Mg with similar grain size within the three systems behaved differently. In terms of catalytic effect on absorption MmNi₅ gave the best results enabling high absorption at temperature as low as 100°C. In terms of quantity of hydrogen absorbed, Ti addition showed the best results with 6.1 wt% of hydrogen absorbed at 300°C. Cr₂O₃ addition indicated maximum desorption with 4 wt% at 300°C and 1 bar pressure. Detailed results are discussed and possible routes in the absorption/desorption processes are considered.

10:30 AM Break

10:45 AM Plenary

Carbon-Based Nanostructured Adsorbents for Hydrogen Storage: J. L. Blackburn¹; C. Curtis¹; A. C. Dillon¹; T. Gennett²; K. E. H. Gilbert¹; Michael Heben¹; K. M. Jones¹; Y.-H. Kim¹; P. A. Parilla¹; L. J. Simpson¹; S. B. Zhang¹; Y. Zhao¹; ¹National Renewable Energy Laboratory; ²Rochester Institute of Technology

Hydrogen is viewed as a clean energy alternative that could one-day replace fossil fuels in powering vehicles. For this vision to become a reality, significant advances will be required in a wide array of hydrogen related technologies. For hydrogen storage, the U.S. Department of Energy has set a goal of achieving system gravimetric and volumetric storage densities exceeding 6 wt% and 45 kg H₂/m³, respectively, to facilitate large scale commercial deployment of hydrogen fuel on several low-demand vehicle platforms by the year 2010. A generic approach to the problem based on nanoscience considerations can offer a new perspective on this problem. In this approach, one considers how suitable binding sites for hydrogen can be designed and arranged in space with sufficient density, using a light host material, to simultaneously achieve high gravimetric and volumetric performance. To minimize energy input requirements during the charge/discharge cycle, and therefore optimize system efficiency, the "suitable" binding sites should stabilize hydrogen with energies in the range of 10 – 50 kJ/mol. We will discuss theoretical and experimental results on carbon nanotubes, fullerenes, and other nanostructured adsorbent materials, and explore the role of composition, doping, and local environment in tuning hydrogen storage properties. We will also describe the research activities of the recently-established DOE Center of Excellence for Carbon-Based Hydrogen Storage Materials which is focused on developing new solutions for hydrogen storage on-board vehicles. The Center is researching systems that reversibly stabilize sufficient hydrogen to meet the DOE targets, and builds on existing experimental and theoretical evidence for (i) dissociative adsorption that is weaker than typical C-H bond formation, and (ii) non-dissociative adsorption that is stronger than pure physisorption. In the first case we consider reversible hydrogen

spillover, while in the second the goal is molecular adsorption via structural/chemical modifications to the physisorption potential as well as complexation of dihydrogen. The Center consists of projects at Air Products and Chemicals, Inc., California Institute of Technology, Duke University, Lawrence Livermore National Laboratory, National Institute of Standards and Technology, National Renewable Energy Laboratory, Oak Ridge National Laboratory, Pennsylvania State University, Rice University, University of Michigan, University of North Carolina (Chapel Hill), and the University of Pennsylvania.

11:05 AM Keynote

Metal-Assisted Hydrogen Storage in Nanostructured Carbons: Nidia Gallego¹; Fred Baker¹; Cristian Contescu¹; ¹Oak Ridge National Laboratory

First-principle calculations at ORNL on interactions between hydrogen and graphite provided the fundamental basis for experimental work on metal-doped, activated carbon fibers (produced at Clemson). Measurements at ORNL revealed that the Pd doped fibers exhibited a hydrogen storage capacity of about 2 wt% at ambient temperature and a pressure of 2 MPa. This represented an order of magnitude improvement over the capacity of the corresponding Pd free fibers. Further modeling work indicated that, provided the high energy barrier for initial sorption could be overcome, hydrogen could be stored by intercalation between graphene layers. On the basis of these preliminary findings, it is hypothesized that metal assisted hydrogen storage in nanostructured carbon is the result of catalytic activation of molecular H₂ and surface diffusion of H atoms, followed by storage on carbon structural defects through either chemical bonding or intercalation. We will present both modeling and experimental results.

11:25 AM Keynote

Low Temperature Hydrogen Adsorption Capacity of Carbon Nanoparticles: Helmut Hermann¹; Melanie Hentsche¹; Andrei Touzik¹; Agnieska Kuc²; Roswitha Wenzel²; Gotthard Seifert²; ¹IFW Dresden; ²TU Dresden

Accurate quantum mechanical calculations have shown that the effective interaction potential between hydrogen molecules and a graphene sheet has minima at a distance of about 0.3nm from the surface of the graphene layer. Thermodynamic considerations based on this result give an estimate of the hydrogen storage capacity of graphene sheets and its dependence on temperature and pressure (for example, 0.5wt% at 100K and approximately 2wt% at 80K at 0.1MPa). To study this effect experimentally, we built up a Sievert's like apparatus allowing temperature variation between 300K and 40K at a maximum pressure of 200 bar. For C₆₀ fullerenes, the results confirm recent data obtained at 77K. We consider also nanometre-scale carbon powders produced by ball-milling of graphite as a cheap and promising material for hydrogen storage. Variation of the milling conditions including milling at low temperatures is shown to be a way to optimise the storage capacity of carbon powders.

11:45 AM

Electrochemical Hydrogen Storage in Assembly of Nanotubular TiO₂ and Carbon Nanotubes: Pradeep Pillai¹; Krishnan S. Raja¹; Manoranjan Misra¹; ¹University of Nevada, Reno

Hydrogen storage behavior of carbon nanotubes (CNTs) has been investigated intensely because of its ultra-light weight and large surface area. In this investigation, hydrogen charging and discharging studies were carried out by electrochemical method using an assembly of nanotubular titanium dioxide and carbon nanotubes. Anodization of Ti foil resulted in formation of ordered nanotubular TiO₂ layer. This nanoporous TiO₂ was used as template for growing carbon nanotubes. Cobalt was the catalyst for chemical vapor deposition of CNTs. Preliminary results indicate a hydrogen discharge capacity of about 1740 mA-h/g(CNT) for the total assembly and 1100 mA-h/g for CNT alone. Hydrogen charging experiments are being carried out by impregnating Mg nanoparticles inside the nanotubular arrays.

Advanced Materials for Energy Conversion III: A Symposium in Honor of Drs. Gary Sandrock, Louis Schlapbach, and Seijirau Suda: Metal, Alloys and Energy Materials

Sponsored by: The Minerals, Metals and Materials Society, TMS Light Metals Division, TMS: Reactive Metals Committee

Program Organizers: Dhanesh Chandra, University of Nevada; John J. Petrovic, Petrovic and Associates; Renato G. Bautista, University of Nevada; M. Ashraf Imam, Naval Research Laboratory

Thursday AM
March 16, 2006

Room: 214B
Location: Henry B. Gonzalez Convention Ctr.

Session Chairs: M. Ashraf Imam, Naval Research Laboratory; Etsuo Akiba, AIST; Ji-Cheng Zhao, General Electric Company

8:30 AM Invited

Fundamental Analysis of the MM'X Phosphides and Arsenides: A Promising Series Exhibiting Potentially High Magneto-Caloric Performances: *Daniel Fruchart*¹; F. Allab²; M. Balli¹; P. de Rango¹; D. Gignoux¹; E. K. Hilli¹; A. Lebouc¹; S. Miraglia¹; C. Rillo³; J. Tobola⁴; M. G. Shelyapina⁵; N. E. Skryabina⁶; P. Wolfers¹; R. Zach⁴; ¹Centre National de la Recherche Scientifique; ²LEG, Institut National Polytechnique de Grenoble; ³Instituto de Ciencias de Materiales de Aragon; ⁴University of Cracow; ⁵St. Petersburg State University; ⁶Perm State University

The pnictides MM'X, phosphides and arsenides of transition metals can exhibit very peculiar (ferro)magnetic properties. Systematic changes of magnetic ordering occur via first order or meta-magnetic transitions, in such a way that marked contribution of entropy with or without magneto-elastic effects are characteristics of these transitions. E.g. for MnFeP1-xAsx compounds, a large magneto-caloric effect (MCE) was realized by application of moderate magnetic fields only. For a long time, we have analyzed the MM'X series for their fundamental characteristics (magnetization, neutron scattering, specific heat, Mössbauer...) as well from systematic band structure calculations. As for the parent series of monpnictides MnAs-MnP (M' ~ vacancy), we better understand the nature of the magnetic forces (polarization, exchange), that mostly proceeds via electronic instabilities. Thus a molecular field model looks not the best approximation to develop MCE analyses.

8:50 AM Invited

Synchrotron X-Ray Absorption Spectroscopy (XAS) Studies for Understanding Dopant Effects in NaAlH₄: *Tabbatha A. Dobbins*¹; Roland Tittsworth²; John Olivier¹; Yuri Lvov¹; ¹Louisiana Tech University; ²Louisiana State University

Transition metal dopant additions to complex metal hydrides enhance hydrogen adsorption/desorption kinetics. The atomic-scale location of dopants has been reported, however, a mechanism for the kinetic enhancements associated with these dopants has not been fully developed. X-ray absorption spectroscopy (XAS) is an element specific probe for local atomic structure determination. This work explores the local bonding environment around Al in Ti-doped NaAlH₄-both before and after dopant additions-using x-ray absorption spectroscopy (XAS). The local bonding environment of Ti is also explored. Layer-by-layer (LbL) nanoassembly is used to catalyze the NaAlH₄ powders. LbL allows a more uniform distribution of dopants. Transmission electron microscopy (TEM) is used to study microstructural development.

9:10 AM

Heat Capacity Determination of Organic "Plastic Crystals" by Adiabatic Calorimetry from 3K to 350K: *Anjali S. Talekar*¹; Raja S. Chellappa¹; Dhanesh Chandra¹; Wen-Ming Chien¹; Alexandra O. Tsokol²; J. A. Sampaio²; ¹University of Nevada; ²Iowa State University

Thermal Energy Storage [TES] systems for passive heating systems and other thermal applications invariably use the latent heat effect of solid state phase change materials. Examples of alcohol and amine derivatives of neopentane include: Pentaerythritol [PE:C(CH₂OH)₄], Pentaglycerin [PG:(CH₃)C(CH₂OH)₃], Neopentylglycol [NPG:(CH₃)₂C(CH₂OH)₂], Neopentylalcohol [NPA:(CH₃)₃C(CH₂OH)], Tris(hydroxymethyl)

aminomethane [TRIS:(NH₂)C(CH₂OH)₃], and 2-amino-2-methyl-1,3-propanediol [AMPL:(NH₂)(CH₃)C(CH₂OH)₂]. Low temperature heat capacities of such organic compounds with unusually high enthalpies of solid-solid transitions have been determined from 3K to 350K using a semi-adiabatic heat pulse calorimeter. These organic compounds undergo solid-solid phase transitions from low temperature ordered polymorphs (tetragonal, monoclinic, etc.) phase to an orientationally disordered high temperature "Plastic Crystal" modulated cubic phase (FCC or BCC). The effect of the number of hydroxyl groups (that provide the hydrogen bonding for the crystal structure framework) on the heat capacities and the dependence of the Debye temperature (TD) on the number of hydroxyl group is also presented in this study.

9:30 AM

Ionic Conductivity Measurement of Orientationally Disordered Crystals: Tris(hydroxymethyl)aminomethane + 2-Amino-2-Methyl-1,3-Propanediol Binary System: *Md S. Rahman*¹; Raja S. Chellappa¹; Suresh Chandra Divi¹; Dhanesh Chandra¹; ¹University of Nevada

The amine derivatives of neopentane (Tris(hydroxymethyl)aminomethane: TRIS and 2-Amino-2-Methyl-1,3-Propanediol: AMPL) belong to special class of organic molecular crystals that undergo solid-solid phase transition from a low temperature ordered phase to an orientationally disordered high temperature phase with an unusually high enthalpy of transition. The ionic conductivity of pure TRIS and AMPL show a noticeable increase in the orientationally disordered phase when compared to the low temperature structure. Such an increase in ionic conductivity makes these materials potential candidates for semiconductor applications. In this work, we will present results from our ionic conductivity measurements for pure as well as binary mixtures of TRIS and AMPL. The effect of temperature as well as compositional dependencies on the ionic conductivity of binary solid solutions will be discussed.

9:50 AM

Heat Capacity Measurement of Organic "Plastic Crystal" Thermal Energy Storage Materials Using Modulated Differential Scanning Calorimetry: Tris(hydroxymethyl)aminomethane-2-Amino-2-Methyl-1,3-Propanediol Binary System: *Suresh Chandra Divi*¹; *Raja S. Chellappa*¹; Dhanesh Chandra¹; ¹University of Nevada

Tris(hydroxymethyl)aminomethane (TRIS) and 2-Amino-2-Methyl-1,3-Propanediol (AMPL) belong to a special class of organic molecular crystals that are potential candidates for thermal energy storage applications. TRIS and AMPL undergo solid-solid phase transitions from a low temperature layered structure (TRIS: orthorhombic, AMPL: Monoclinic) to an orientationally disordered plastic crystal phase (TRIS: BCC, AMPL: BCC). A systematic calorimetric study of organic "plastic crystal" thermal energy storage materials is being conducted using Modulated Differential Scanning Calorimetry (MDSC). The goal of this study is to establish a thermodynamic database of heat capacities of pure as well as binary mixtures of these compounds. Recent calorimetric studies on pure and binary organic "plastic crystals" using MDSC has shown that MDSC is a fast and powerful technique for accurate measurement of absolute heat capacities. In this work, we report the molar heat capacities of ten binary mixtures of TRIS-AMPL from xTRIS=0 to xTRIS=1.

10:10 AM

Comparison of Hydrogen Diffusion Properties of Materials for the Yucca Mountain High Level Waste Repository: *Joshua H. Lamb*¹; Dhanesh Chandra¹; ¹University of Nevada

Various materials intended for use at the Yucca Mountain High Level Waste Repository were studied for hydrogen diffusion and trapping effects using the electrochemical method first proposed by Devanathan and Satchurski. The environment present at repository has the propensity to generate hydrogen at the surface of materials leading to the trapping of hydrogen and detrimental effects on material properties. This study looks at these effects resulting from the electrochemical transport through a membrane sample. The electrochemically obtained permeation current is used to calculate the reversible and irreversible hydrogen diffusion properties. This is then related to the total hydrogen stored in and diffused through the material.

Alumina and Bauxite: Precipitation Fundamentals

Sponsored by: The Minerals, Metals and Materials Society, TMS Light Metals Division, TMS: Aluminum Committee

Program Organizers: Jean Doucet, Alcan Inc; Dag Olsen, Hydro Aluminium Primary Metals; Travis J. Galloway, Century Aluminum Company

Thursday AM
March 16, 2006

Room: 7B
Location: Henry B. Gonzalez Convention Ctr.

Session Chair: Songqing Gu, Zhengzhou Research Institute of Chalco

8:30 AM Introductory Comments

8:40 AM

Influence of Alumina Morphology and Structure on Its Strength:

Songqing Gu¹; Lijuan Qi¹; ¹Zhengzhou Research Institute of Chalco

A study of influences of alumina morphology and structure on its strength has been carried out. It is found that agglomerated alumina hydrate particles have many more opportunities to be strengthened than those particles which grow individually. The strength of the agglomerated alumina particles will be kept higher because the water vapor can be released gradually through the gaps among the agglomerated hydrate particles during calcination so as not to damage the whole structure of the particles. In order to obtain alumina with high strength it seems necessary that some small alumina hydrate crystals should be agglomerated in the first step and further strengthened by following growth in the relatively high supersaturation.

9:05 AM

Study on the Oscillation Phenomena of Particle Size Distribution during the Seeded Agglomeration of Sodium Aluminate Liquors:

Jianguo Yin¹; Qiyuan Chen¹; Zhoulan Yin¹; Jiangfeng Zhang²; ¹Central South University; ²Institute of Technology and Economy in Nonferrous Metals

Chaotic and Fractal theory was used to study the oscillation phenomena of particle size distribution (PSD) in the agglomeration process of sodium aluminate solution. Conclusions were made as follows: PSD of particles is in macroscopic disorder, while it is regular in certain ranges; curves of PSD sometimes appear to oscillate, but particles for a certain range own general rules in the whole process; that is, the curves of PSD oscillating decrease with time for small and median size particles yet oscillating increases for large particles; the minor change of initial conditions can be enlarged in the process, and the particle size information will be affected. As a result, the butterfly effect of the PSD appears; each curve of PSD has the space fractal character for particles of certain range. More precise structure of curves can be identified if smaller divided rule of particle size is adopted.

9:30 AM

Study on the Rate of Crystal Growth and the Phenomena of Template Crystallization during Seed Precipitation from Sodium Aluminate Solutions:

Bai Wanquan¹; Yin Zhonglin¹; Li Wangxing¹; Qi Lijuan¹; Yang Qiaofang¹; ¹Zhengzhou Research Institute Alumimun Corporation of China Ltd.

Seeded, the precipitation from sodium aluminate solutions with high concentration of diasporic bauxite was studied using a laboratory batch crystallizer. The results show that the enhancement of particles is mainly contributed to agglomeration with the speed of 7-8 $\mu\text{m}/\text{hour}$. There are some particles, which are bigger, in the shape of similar sphericity. And the crystallites on the surface are small and identical in size observed by SME. The center of these particles is hollow. It is conjectured that the formation of these particles is based upon some crystal templates, and $\text{Al}(\text{OH})_3$ is precipitated layer by layer on the surface of the template. The template is probably dissolved after the shell of $\text{Al}(\text{OH})_3$ has formed in the precipitation. That is why the center of the particles is hollow. The alumina particles produced remain the same shape as the original $\text{Al}(\text{OH})_3$ particles, and their strength after attrition is still high.

9:55 AM

Effects of Monohydroxy-Alcohol Additives on the Seeded Agglomeration of Sodium Aluminate Liquors:

Jianguo Yin¹; Jie Li¹; Yanli Zhang²; Qiyuan Chen¹; Zhoulan Yin¹; ¹Central South University; ²Zhengzhou Research Institute of Chalco

A series of monohydroxy-alcohol additives were adopted in Bayer process. The effects of dosage and carbon chain length on precipitation ratio of sodium aluminate liquors and particle size distribution (PSD) of gibbsite were investigated. Experimental results indicated that: all three monohydroxy-alcohols can increase precipitation ratio of sodium aluminate liquors at the proper dosage. They can accelerate precipitation process obviously at lower dosage at the beginning and yet last longer effects at higher dosage. Particle size of gibbsite products is enlarged when 1-Octadecanol is added at low dosage, yet the product fines under all other conditions. It can be concluded that: long chain additives with low dosage or short chain additives with high dosage is favorable for the seeded agglomeration of sodium aluminate liquors. The relationship between carbon chain length and its dosage may be complementary. Action mechanism among monohydroxy-alcohol additives, sodium aluminate liquors and gibbsite crystals will be further investigated based on the information mentioned above.

10:20 AM Break

10:35 AM

Study on the Effect of K₂O on Seed Precipitation in Sodium Aluminate Liquors:

Yanli Xie¹; Qun Zhao²; Zhenan Jin³; ¹Georgia Institute of Technology; ²Zhengzhou Research Institute of Chalco; ³Northeastern University

Potassium oxide accumulates during liquor recycling, and its concentration can be up to 55 g/l in pregnant liquor with the total soda 178.4 g/l, which causes negative effects on the seed precipitation procedure. This paper studied the effect of K₂O on precipitation yield and hydrate particle size distribution when the concentration of K₂O is in the range of 0-60 g/l from 160 g/l caustic soda. The results demonstrated that the potassium contaminated sodium aluminate liquor has higher precipitation ratio, but its effect on particle size distribution is complicated, which varied with time and potassium concentration. The mechanism on why potassium affects precipitation procedure is also studied in this paper.

11:00 AM

Influences of Cation and Anion Ions and Some Kinds of Additives on the Aggregation of Seeds:

Lijuan Qi¹; Songqing Gu²; ¹Zhengzhou University; ²Zhengzhou Research Institute Alumimun Corporation of China, Ltd

There have been many works on the precipitation mechanism of sodium aluminate solution. However, due to the complexity of the structure of the solution and many factors affecting the process of precipitation, there is no agreement on the mechanism of nucleation, growth, and aggregation of aluminum hydroxide in the process of precipitation so far. In this paper, the influences of cation and anion ions and some kinds of additives on the superficial charges of seeds are investigated, and then the effects of them on the aggregation of seeds are further studied.

11:25 AM

Effects of Power Ultrasound on Precipitation Process of Sodium Aluminate Solutions:

Jilai Xue¹; Shaohua Li¹; Baoping Song¹; ¹University of Science and Technology Beijing

Sodium aluminate solutions for alumina production have been ultrasound treated to enhance the precipitation seeded in a laboratory Bayer process. The effects of sound power intensity, sonication time, and temperature on the precipitation process were investigated. In this paper the results will be discussed with respect to precipitation efficiency and process kinetics.

Aluminum Reduction Technology: Fundamentals, Emerging Technologies and Inert Anodes - Part II

Sponsored by: The Minerals, Metals and Materials Society, TMS Light Metals Division, TMS: Aluminum Committee

Program Organizers: Stephen Joseph Lindsay, Alcoa Inc; Tor Bjarne Pedersen, Elkem Aluminium ANS; Travis J. Galloway, Century Aluminum Company

Thursday AM
March 16, 2006

Room: 7A
Location: Henry B. Gonzalez Convention Ctr.

Session Chair: Martin Iffert, Trimet Aluminium AG

8:30 AM

On the Entropy Generation in Aluminum Electrolysis Cell: Adam Holda¹; Janusz Donizak¹; Juan Mendez Nonell²; *Zygmunt Kolenda*¹; ¹AGH University of Science and Technology; ²Centro de Investigacion de Quimica Aplicada

Classical thermodynamic analysis of any technological processes is usually based on the First Law of Thermodynamics in the form of energy (enthalpy) balances. However, deeper thermodynamic analysis leads to the conclusion that such approach is not sufficient. The first Law of Thermodynamics guarantees the exact equivalence of the various forms of energy but it does not guarantee interconvertibility. One of the possible solutions comes from the Second Law of Thermodynamics using entropy as the state function describing degree of process irreversibility. There are many effects whose presence during electrolysis process renders it irreversible, most important are: heat transfer, spontaneous chemical reactions, electric current flow. Engineers should be able to recognize irreversibilities, evaluate their influence and develop cost-effective means for reducing them. Paper presents the method of calculation of entropy generation occurring during the aluminum electrolysis elementary processes.

8:55 AM Invited

Effect of Additive V2O5 on Sintering and Corrosion Resistance of Inert Anodes of Cermets: *Xi Jinhui*¹; Yao Guangchun¹; Liu Yihan¹; ¹Northeastern University

The inert anodes of nickel ferrite-based cermets doping V2O5 were prepared. The effect of V2O5 on sintering and corrosion resistance was researched. The results indicate that when the additive V2O5 was added, Ni2FeVO6 was produced, which has low melting point 625–652°C. Ag also became liquid at 961°C, so the sintering is liquid sintering. Doping V2O5 makes the grains of ceramic grow completely with the shape of octahedron and grains become coarse. The corrosion rate of samples with V2O5 is much lower than that of sample without V2O5. Ni2FeVO6 concentrated at grain boundary and it has good corrosion resistance. Ni2FeVO6 reinforces the corrosion resistance of the grain boundary and liquid makes the grains of ceramic grow completely, so the corrosion resistance of the sample with V2O5 was strengthened.

9:20 AM Invited

Effect of Additive V2O5 on Conductivity of Inert Adnodes: *Xi Jinhui*¹; Yao Guangchun¹; Liu Yihan¹; ¹Northeastern University

The inert anodes of nickel ferrite-based cermets were prepared by the powder metallurgy method using NiO, Fe2O3, Ag and a little V2O5 as raw materials. The effect of V2O5 on microstructure and conductivity was researched. The results indicate when V2O5 was added, Ni2FeVO6 was produced. During sintering, Ni2FeVO6 became liquid, and it made metal phase distribute in slender strip form; EDX analysis shows there is ceramic phase in the metal phase. The facts show V2O5 can improve the wettability between Ag and ceramics. At the same time, the conductivity is improved remarkably. When the amount of V2O5 is 2.0%, the conductivity is 7 times of that of the sample without V2O5. Moreover, a remarkable change of conductivity took place from 450°C to 650°C. This must be a change in magnetism induced by the V2O5.

9:45 AM

Study on Corrosion of Cermet Inert Anode Based on Nickel Ferrite Spinel: *Tao Luo*¹; Zhao-Wen Wang²; ¹Sunstone Carbon Technology Center; ²Northeastern University

According to the corrosion comparison of anodes (NiFe₂O₄+NiO+Cu+Ni) under different conditions, the paper discusses the corrosion of metal and ceramic phases. The metals Cu and Ni are present as the Cu_xNi_y alloy in the anode. The Ni of Cu_xNi_y alloy was primarily oxidized in an O₂-atmosphere at 900°C. In the polarization experience, the Ni content of the anode decreased remarkably after electrolysis, and the main residual metal was Cu. For the nickel ferrite spinel, the electrolyte did not corrode the anode matrix at 900°C in the absence of oxygen. After adding O₂ to the electrolyte, the corrosion happened. The SEM of an anode after electrolysis showed that the Fe₂O₃ of nickel ferrite spinel dissolved in the electrolyte and hence resulted in corrosion of the anode matrix.

10:10 AM

On the Corrosion Behavior of NiFe₂O₄-10NiO Based Cermets as Inert Anodes in Aluminum Electrolysis: *Yanqing Lai*¹; Xinzheng Li¹; Jie Li¹; Zhongliang Tian¹; Gang Zhang¹; Yexiang Liu¹; ¹Central South University

NiFe₂O₄-10NiO based cermets of different metallic phase compositions (Ni, Cu, and Cu-Ni alloy) were prepared with cold isostatic pressing-sintering process. All samples were pretreated in nitric acid to remove the metal bled out of the sample surface at high sintering temperature. Electrolysis test results showed that, corrosion resistance was difficult to be differentiated effectively just by comparing external changes, mass loss, impurity content in the bath samples taken from the cell during electrolysis or in the aluminum metal. The cermet components, that corrode into the melt follow the Boltzmann distribution with respect to distance from the inert anode. Such distribution may be identified by gathering the impurity ions near the cathode with electric force under polarization condition. This uneven distribution together with different algorithms has great potential to estimate the corrosion rate of inert anodes. An improved test cell configuration and comprehensive evaluation method were used to differentiate the corrosion resistance of cermets.

10:35 AM

Study on Sintering Technique of NiFe₂O₄/SiC Used as Matrix of Inert Anodes in Aluminum Electrolysis: *Shu-Ting Zhang*¹; Guang-Chun Yao¹; Yi-Han Liu¹; ¹Northeastern University

In order to improve deficiencies of NiFe₂O₄ spinel used as matrix of inert anode in aluminium electrolysis, NiFe₂O₄/SiCw were prepared by the solid state reaction for the first time. Microstructural changes were observed by scanning electronic microscope and phase was determined with x-ray detector. Effect of sintering temperature and times on density, porosity and microstructure were researched, and the reasons that caused the difference were discussed deeply. At the same time the thermodynamical compatibility of NiFe₂O₄ and SiCw was proved under 1200° by DTA. The results showed that the microstructure was more homogeneous when the sintering temperature reached 1180° and the density attained their maximum about 6-hours sintering. The appropriate sintering technique of NiFe₂O₄/SiCw composite materials selected 1180°×6h.

11:00 AM

Electrolysis Test of 1350A Drained Cathode Reduction Cell with TiB₂-Coated Cathode: *Feng Naixiang*¹; Qi Xiquan¹; Peng Jianping¹; ¹North-eastern University

For a new drained cathode cell, detailed operations of cell building, packing, baking, starting-up and normal operations are presented here. Cathode inclination is 10°. TiB₂-coated cathode is adopted. The cell is dryly built, carbon-particulate baked and dryly started up. The average current is 1350A. Feeding, tapping, voltage adjustment, etc. are almost the same as those of commercial cells. After 100 hours of continuous electrolysis, it is found that the cell performs rather steadily. Cell noise is about 9mv. The cell performed exactly like industrial cell. Based on metal production and leftover, current efficiency is found not lower than 86% which closes commercial cells. TiB₂ coating is firm without any damage and hence effects good protection for carbon cathode. It is analyzed that the dissolution speed of TiB₂ is about 1.0g/h-1•m⁻². Test results not only

verified the theoretical analysis beforehand, but also proved the feasibility of such cell structure.

11:25 AM

Producing Aluminum-Silicon Alloys from Andalusite Ore by Carbothermal Reduction Method: *Huimin Lu*¹; *Mingfa Chen*²; *Qiang Liu*²; *Shuang Chen*²; ¹University of Science and Technology Beijing; ²Beijing Yanhuang Investment Management Company Ltd.

A big andalusite ore bed was found in Kuerle District, Xinjiang, China, and its reserves are the largest and quality best in the world. In this paper, the feasibility of producing aluminum-silicon alloys by carbothermal reduction of andalusite is studied. The mix proportion of furnace charge is as follows, andalusite ore 50~80mass% in which the impurities are quartz, calcium oxide and magnesia etc. and the total impurities amount is not in excess of 20mass%; reducer gas coal and petroleum coke 20~40mass%, the mix proportion of gas coal and petroleum coke 8:2~6:4; adhesive paper industry wastewater 5~8mass%. First, all these raw materials are mixed uniformly in proportion, briquetted and dried, then the carbothermal reduction experiments are conducted in a multifunction sintering kiln with reducing temperature 1950~2150°C and reducing time 2h, the aluminum-silicon alloys containing 53~58mass% aluminum, 32~37mass% silicon are obtained with aluminum recovery rate 80~85% and silicon 70~75%.

11:50 AM

The Development and Application of Data Warehouse and Data Mining in Aluminum Electrolysis Control Systems: *Xiangtao Chen*¹; *Jie Li*¹; *Wengen Zhang*¹; *Zhong Zou*¹; *Fenqi Ding*¹; *Yexiang Liu*¹; *Yanqing Lai*¹; ¹Central South University

With the development of network and control systems, the amount of data acquired and stored in aluminum electrolysis control systems has been growing continuously. How to effectively mine useful information hidden in these data is an attractive research topic that will help to enhance the functions of the control systems. In this paper data warehouse and data mining concepts were introduced into aluminum electrolysis control systems and a data-mining tool called "aluminum electrolysis data miner" was developed. There are three core mining components in it: the gray association analysis, the cluster analysis based on connected components and the offset coefficient analysis. For different uses and from different profiles, these component models deeply analyze and mine the data stored in a control system, obtaining the knowledge that can reflect the status of every pot and every potline, in-time adjusting various operating and control parameters and providing decision support for operators.

12:15 PM

Navier-Stokes Equations in Presence of Laplace Forces in the Aluminum Reduction Cell: *Augustin Iosef Moraru*¹; *Aureliu Panaitescu*¹; ¹Politehnica University of Bucharest

Conventional mathematical models of aluminum reduction cells are based on general electromagnetic equations, two-dimensional Navier-Stokes equations and include common turbulence modeling (k-). These models are not able to describe the true mechanisms involved in the motion of two thin liquid layers, because they neglect the vertical transport impulse, which in fact is dominant over the horizontal one. This paper describes the development of a more complete, dynamic, two shallow-layer models which are based on the works of V. Boyarevich. This model takes into account the viscous drag and the surface drag, as well as the variation of the layer thickness.

12:40 PM END

Amiya Mukherjee Symposium on Processing and Mechanical Response of Engineering Materials: Modeling of Material Behavior

Sponsored by: The Minerals, Metals and Materials Society, TMS Materials Processing and Manufacturing Division, TMS Structural Materials Division, TMS/ASM: Mechanical Behavior of Materials Committee, TMS: Shaping and Forming Committee
Program Organizers: Judy Schneider, Mississippi State University; Rajiv S. Mishra, University of Missouri; Yuntian T. Zhu, Los Alamos National Laboratory; Khaled B. Morsi, San Diego State University; Viola L. Acoff, University of Alabama; Eric M. Taleff, University of Texas; Thomas R. Bieler, Michigan State University

Thursday AM
March 16, 2006

Room: 217C
Location: Henry B. Gonzalez Convention Ctr.

Session Chairs: Michael Josef Zehetbauer, University of Vienna; Peter Martin Anderson, Ohio State University

8:30 AM Invited

Uniform Terminology for Strain Induced Boundaries: *Hugh J. McQueen*¹; *Enrico Evangelista*²; *Marcello Cabibbo*²; ¹Concordia University; ²University Politecnica delle Marche

The terms for strain induced boundaries should reflect the creating mechanism, the function performed and the regions separated. Dislocation glide is the primary mechanism in creep and hot and cold working, being less influenced by dynamic recovery as temperature T falls and strain rate rises. Dependent on stress, boundaries contain dislocations geometrically necessary for the misorientations and dipoles (denser in cold work); cell walls are rather incidental whereas higher-angle block walls enclose cell clusters developing different slip. After hot forming, polygonized walls consist mainly of low-energy, geometrically-needed dislocations; such subgrain boundaries during steady state straining continually rearrange in a stress-defined substructure. Following Taylor-defined multiple-slip in polycrystals, grains divide into deformation bands slipping on different systems and rotating differently to create texture components. The separating transition boundaries being permanent increase in misorientation with strain, becoming indistinguishable from the grain boundaries that are disturbed by dislocations, extended under strain and serrated.

8:50 AM

Processing Path Design and the Integration of Texture and Micro-Texture Evolution: *Hamid Garmestani*¹; ¹Georgia Institute of Technology

A processing path model is proposed to quantitatively describe the texture and micro-texture evolution in an explicit mathematical formula. This model is used to guide the materials design by taking full advantage of the database of experimental data and simulation results from physical models for texture evolution. The streamline grid in material's hull developed from this model is used to investigate if any processing path may exist from an initial texture of raw material to a final texture with desired property. If the solutions exist, the family of processing paths presented by the streamline grid make it possible for further design optimization. This methodology provides a systematic approach to calculate the optimal processing path to the desired texture using statistical continuum mechanics based on one and two-point distribution functions in the calculation of the processing path evolution parameters and the corresponding micro-structure.

9:10 AM

Texture Development in BCC Metals during Upsetting: *Myoung-Gyu Lee*¹; *Levit I. Levit*²; *Charles E. Wickersham*²; *Peter Martin Anderson*¹; ¹Ohio State University; ²Cabot Corporation

A finite element analysis based on rate-dependent crystal plasticity is used to study texture development in BCC metals during upset deformation. Both {110}/<111> and {112}/<111> slip systems are modeled. Each integration point in the finite element mesh follows a polycrystalline constitutive relation for 200 grains that deform according to a Taylor isostrain assumption. Random, <111>, <110>, and <100> transversely-isotropic

initial textures are considered. For zero friction, random initial textures evolve to ~60% <111> and ~30-40% <100>. Transversely-isotropic <111> and <110> textures both produce <111>, but <100> textures remain <100>. Friction induces barreling and shear deformation, so that <111> and <100> textures becomes diffuse. These trends are compared to measured pole figures from upset BCC metal samples.

9:30 AM Invited

Constitutive Modelling of Large Strain Work Hardening of Metals under Different Conditions of Plastic Deformation: *Michael Josef Zehetbauer*¹; Jan Kohout²; Christian Holzleithner¹; ¹University of Vienna; ²University of Defence Brno

The paper introduces a composite model which has been originally developed by M. Zehetbauer for a quantitative description of large strain cold working. Later the model has been successfully modified for description of large strain hot working, too. Recently it has been shown that the model also accounts for cases of cold work under elevated hydrostatic pressure (the so-called "Severe Plastic Deformation - SPD") which achieve nanocrystalline structures. All model variants have been tested by strain-dependent measurements of the dislocation density as well as of the cell and/or subgrain size, and - concerning cold work conditions - of the concentration of deformation induced vacancies.

9:50 AM

On the Control of Microstructural Degrees of Freedom in Deformation Processes: *Veera Sundararaghavan*¹; Nicholas Zabaraz¹; ¹Cornell University

The high cost of manufacturing critical components can be greatly reduced with the development of mathematically and physically sound computational methodologies for multi-scale process design. We present our recent developments in expanding the design space in forming processes by including microstructural degrees of freedom as a design variable in addition to macro-constraints. We have developed a multi-length scale continuum sensitivity method for thermo-elasto-visco-plasticity combined with microstructure evolution in polycrystalline materials. In particular, sensitivities of fields dependent on microstructural degrees of freedom are exactly defined and an averaging principle (linking hypothesis) is developed to compute sensitivity fields at the macroscopic level. These computed sensitivities are used within a gradient-based optimization framework for the computational design of metal forming processes for polycrystalline materials. The effectiveness of the developed design techniques are demonstrated with examples involving control of distribution of elastic and plastic properties in the final product by tailoring the final microstructures.

10:10 AM

Mechanical Modeling of Bimodal Al-5083 Alloys: *K. T. Ramesh*¹; S. P. Joshi¹; H. Zhang¹; E. J. Lavernia²; E. S. C. Chin³; J. M. Schoenung²; ¹Johns Hopkins University; ²University of California, Davis; ³Army Research Laboratory

Cryomilled Al-5083, comprising a bimodal mixture of nano-crystalline (NC) and coarse-grained (CG) microstructure (of nominal grain sizes 200 nm and 1 μm respectively) has shown high strength while retaining ductility. The strengthening effect is due to the NC phase whereas the ductility is imparted by the CG phase. The rule-of-mixtures approach is insufficient to model the observed experimental mechanical behavior. In this paper, the Mori-Tanaka mean-field approach is adopted to predict the mechanical response of the alloy. The formulation allows elasto-plastic representation of both phases (Weng et al.) as observed in the material. The analysis indicates that the relative phase distribution appears to promote the strengthening behavior in this material. Acknowledgements: SPJ, KTR and HZ acknowledge the financial support provided by the Army Research Laboratory through Grant No. DAAL01-96-2-0047. JMS and EJL acknowledge the financial support provided by the Office of Naval Research under contract N00014-03-C-0164.

10:30 AM Break

10:40 AM Invited

On the Composition of bcc Cu Alloy Precipitates in bcc Fe: *Morris E. Fine*¹; Mark D. Asta¹; J. Zhe Liu¹; Axel Van De Walle¹; Gautam Ghosh¹; ¹Northwestern University

While ab initio calculations of the mixing energy at 0 K predict that bcc Cu precipitates in bcc Fe should be pure Cu, they contain actually a very substantial amount of Fe (almost 50%) according to atom probe studies. Possible sources of this difference include the following. At the aging temperature (approximately 800 K), at metastable equilibrium there may be a substantial amount of Fe in the bcc Cu precipitate. Also at 0 K bcc Cu is mechanically unstable, the elastic constant C' is negative but it increases with Fe content becoming positive near 50% Fe-50% Cu. Additionally, interfacial forces arising from coherency may act to suppress the mechanical instability. These possibilities will be discussed in light of the ab initio calculations. The effect of the negative C' on the yield stress will also be discussed.

11:00 AM

An Artificial Neural Network Material Model Implemented within Finite Element Analysis for Prediction of High Temperature Rheological Behavior of Nickel Aluminide: B. Scott Kessler¹; *Khaled B. Morsi*²; A. Sherif El-Gizawy³; ¹Kestek; ²San Diego State University; ³University of Missouri-Columbia

Accurate virtual modeling and process simulation prior to the start of actual production can many times save considerable time, effort, and money. Conventional constitutive material models have been developed and integrated with finite element analysis in an effort to achieve these ends. These models can only perform accurately if the constitutive model used properly reflects the materials behavior. More recently, artificial neural networks (ANN) have been suggested as a means to more properly describe rheological behavior. In the present work, a robust ANN with the ability to determine flow stresses of a nickel aluminide superalloy based on strain, strain rate, and temperature is developed and linked with finite element code. Comparisons of this novel method with conventional means are carried out to demonstrate the advantages of this approach.

11:20 AM

Influence of Grain Boundary Crystallography on the Flow Stress and Dynamic Failure Strength: *Mukul Kumar*¹; Roger Minich¹; Kerri Blobaum¹; James Stolken¹; ¹Lawrence Livermore National Laboratory

Recent results show that the Hall-Petch scaling of yield stress needs to take into account a parameter called grain boundary character distribution, which is related to the frequency of crystallographically "special" boundaries in the microstructure. This can be manipulated by a processing methodology called grain boundary engineering. The role of microstructures in the process of void nucleation and growth leading to failure during shock loading of materials is less understood. We shall report on the scaling observed in the case of dynamic failure or spall under shock deformation conditions in high purity copper. The spall strength is observed to increase as the length scales coarsen, which is counter to the Hall-Petch relationship. The role of nucleation site density and grain boundary character distribution in understanding this behavior as a function of impact pressure will be explored in the context of the scaling laws that emerge from this data.

11:40 AM

Molecular-Dynamics Based Cohesive Zone Model for Intergranular Fracture in Aluminum: *Vesselin Yamakov*¹; Dawn Phillips²; Erik Saether³; Edward H. Glaessen³; ¹National Institute of Aerospace; ²Lockheed Martin Space Operations; ³NASA Langley Research Center

The atomistic mechanisms of grain-boundary debonding during intergranular fracture in aluminum are modeled using molecular-dynamics simulation. Through a developed statistical procedure, a constitutive traction-displacement relationship that characterizes the load transfer across a growing nanoscopic intergranular crack is extracted from the atomistic simulations and is recast in a form that is suitable for inclusion within continuum finite element models. In this way, a finite-element cohesive zone model, which incorporates the atomistic aspects of the elasto-plastic processes at, and near the crack tip is created. Depending on the crystallography of the grain-boundary interface and the dynamics of crack propagation, the model can predict, both, ductile and brittle types of grain-boundary decohesion. The developed procedure represents a multiscale approach to model the influence of the plastic zone around a crack tip using finite-element continuum simulation parameterized by atomistic molecular-dynamics simulation.

12:00 PM

Simulation-Based Investigations of Intragranular Deformations in Single-Phase and Two-Phase Polycrystals: *Paul Dawson*¹; Jae-Hyung Cho¹; Tito Marin¹; ¹Cornell University

Numerical modeling of material systems provides a powerful complement to experiments for investigating the manner in which a system's constituent components individually respond to external loading and collectively act to bear a load. In polycrystalline systems, the elastic and plastic anisotropies of single crystals give rise to heterogeneous mechanical environments at the scale of grains. In responding to load, the crystals deform inhomogeneously with the stress and deformation varying spatially both within and among crystals. In this presentation, we describe three-dimensional, elastoplastic, finite element simulations of polycrystals in which individual crystals are resolved with many elements. Motivated by experimental trends, we examine the spatial distributions of strain and of slip system activity in single-phase and twophase polycrystals comprised of crystals with cubic and hexagonal lattice structures. Attention is given to the influences of such factors as the proximity to grain boundaries, the presence of a free surface, and the morphology of the grains on the distributions of strain and lattice misorientation.

12:20 PM

Modeling the Micro-Indentation of Metal Matrix Composites: *Mario Roberto Rosenberger*¹; Elena Forlerer²; Carlos Schvezov¹; ¹University of Misiones; ²National Commission of Atomic Energy

A dynamic finite element model is developed to quantify the effect of the depth and diameter of the reinforcement in the diameter of the indentation in test samples. The model includes a spherical indenter, which is pressed against a metal containing reinforcing particles. The results are validated comparing the predicted values of indentations, the given properties of the model material and the standard indentation given by the Brinell method, showing a very good agreement. The model is employed to predict indentations in simple configurations of composites consisting of a matrix containing one particle of the same diameter as the indenter. The diameters of the impression, and stress and strain fields for reinforced and matrix materials are compared. Impressions of reinforced materials smaller than those for non-reinforced materials were observed, the values depend on the position of the particle. The results are discussed in relation with the scatter of hardness values.

Bulk Metallic Glasses: Characterization and Mechanical Behaviors

Sponsored by: The Minerals, Metals and Materials Society, TMS Structural Materials Division, TMS/ASM: Mechanical Behavior of Materials Committee

Program Organizers: Peter K. Liaw, University of Tennessee; Raymond A. Buchanan, University of Tennessee

Thursday AM Room: 217B
March 16, 2006 Location: Henry B. Gonzalez Convention Ctr.

Session Chairs: Ralf Busch, Oregon State University; Yong Liu, Nanyang Technological University

8:30 AM **Invited**

Thermodynamics, Kinetics and Configurational Entropy in Bulk Metallic Glass Forming Liquids: *Ralf Busch*¹; ¹Universitaet des Saarlandes

The low critical cooling rate for glass formation in bulk metallic glass (BMG) forming liquids is of thermodynamic and kinetic origin. BMG forming liquids usually exhibit small entropies of fusions, which indicates short range order in the liquid as well as a high entropy of mixing in the crystalline phases. This small entropy difference between liquid and crystalline mixture leads to a small driving force for crystallization. BMG's exhibit small free volumes even at the melting point as well as small compressibilities, which indicates that they are very dense. This is also reflected in their high viscosity and strong liquid behavior, which slows down nucleation and growth kinetics. The strength parameter D increases

monotonically with the number of alloy components. Adam-Gibbs equation and Vogel-Fulcher-Tammann equation describe the kinetics very well. Pronounced shear thinning in the equilibrium melt indicates strong short range order and low configurational entropy in the melt.

8:55 AM

Transformations in Supercooled Pd_{40.5}Ni_{40.5}P₁₉: *Shantanu V. Madge*¹; Harald Rösner¹; Gerhard H. Wilde¹; ¹Forschungszentrum Karlsruhe GmbH

Previous work on amorphous Pd_{40.5}Ni_{40.5}P₁₉ suggests that the alloy phase-separates on annealing in the supercooled liquid region, manifest through the presence of apparent double glass transitions (Tgs) in subsequent differential scanning calorimetry (DSC) runs. In fact, this alloy system presented almost a model system for phase separating, yet thermally rather stable bulk metallic glasses. Here, Pd_{40.5}Ni_{40.5}P₁₉ glassy specimens have been investigated by transmission electron microscopy (TEM, including energy-filtered imaging), high-resolution TEM and DSC measurements. Energy-filtered TEM reveals that the specimens showing the supposed double Tgs are free from any compositional inhomogeneities. Results obtained using 3-D atom-probe will also be presented. Additionally, high-resolution TEM image analysis based on Fourier filtering and based on the calculation of the corresponding autocorrelation functions have been applied. The results are critically discussed with respect of possible phase separation reactions in the material. In addition, alternative origins of the apparent double Tgs will also be discussed.

9:15 AM

Effects of Partial Crystallization on the Mechanical Behaviours of Zr and Mg Based Amorphous Alloys in the Supercooled Liquid Region: S. Gravier¹; S. Puech²; A. Eshtewi¹; *Jean-Jacques Blandin*¹; J. L. Soubeyroux³; P. Donnadieu⁴; ¹INP Grenoble; ²INP Grenoble/CRETA/CNRS; ³CRETA/CNRS; ⁴INP Grenoble/LTPCM

High temperature deformation of zirconium and magnesium based BMG were studied in compression in the supercooled liquid region. The effects of temperature and strain rate were investigated, showing the usual transitions from Newtonian to non-Newtonian behaviours when temperature is decreased or strain rate is increased. Depending on the conditions of deformation, important hardening can be obtained during testing, attributed to crystallization effects. To study the interaction between crystallization and high temperature deformation, nanocomposites were elaborated thanks to appropriate heat treatments and the crystallisation mechanisms were investigated. Such nanocomposites were tested in the supercooled liquid region and the resulting changes in the viscoplastic rheologies were discussed in terms of predictions of mechanical models used for composite materials but also in relation with the variations in properties of the amorphous matrix.

9:35 AM

A Study on the Change of High Temperature Deformation Behavior for a Zr-Based Bulk Metallic Glass Due to Annealing in an Undercooled Liquid Region: *Min Soo Kim*¹; Kwang Seok Lee¹; Hyun-Joon Jun¹; Young Won Chang¹; ¹Pohang University of Science and Technology

A study has been made to investigate the influence of isothermal annealing with various times in an undercooled liquid region on structural changes and deformation behavior of a Zr_{41.2}Ti_{13.8}Cu_{12.5}Ni₁₀Be_{22.5} bulk metallic glass (BMG). Differential scanning calorimetry, X-ray diffraction and transmission electron microscope have been firstly performed to determine the structural state of the pre-annealed specimens with various annealing conditions. High temperature deformation behavior of these pre-annealed samples has been revealed by conducting a series of compression tests with various initial strain rates. Two different types of flow curves, a large plastic deformation after stress overshoot and a steady state plastic flow without stress overshoot, can be observed at various strain rates after different pre-annealing times. From the results, Newtonian and non-Newtonian viscous flows were characterized by the change of steady-state flow stress, and then the transition boundary could be identified as the specific values of critical initial strain rate.

9:55 AM

Dynamic Mechanical Properties of a W-Reinforced Zr-Based Bulk Metallic Glass Composite: *Morgana Martin*¹; Naresh N. Thadhani¹; Laszlo Kecskes²; Robert Dowding²; ¹Georgia Institute of Technology; ²U.S. Army Research Laboratory

We will report our current work on dynamic high-strain-rate mechanical properties of zirconium-based bulk metallic glass (Vitrelloy106) reinforced with tungsten particles. Dynamic mechanical properties measurements were conducted using reverse Taylor anvil-on-rod impact tests to generate strain rates of $10^3 - 10^5 \text{ s}^{-1}$. High-speed digital photography was used to obtain transient images of the deformation history. Velocity interferometry was used to determine the back surface velocity of the impacted rod-shaped sample. These tests provide qualitative and quantitative information about the transient deformation and failure response of the composites, which is used to better correlate the deformation path with the final recovered geometry. The deformation and failure mechanisms of recovered impact specimens are also characterized and correlated with their structure and tungsten phase distribution. In this paper, the dynamic mechanical property results and their correlations with constitutive equations will be presented. Funded by ARO Grant No. E-48148-MS-000-05123-1 (Dr. Mullins program monitor).

10:15 AM Break

10:25 AM

Microstructure and Shear Band Interactions in Amorphous Metal Matrix Composites Consolidated by ECAE: *Suveen N. Mathaudhu*¹; K. Ted Hartwig¹; Laszlo J. Kecskes²; Ibrahim Karaman¹; ¹Texas A&M University; ²Aberdeen Proving Grounds

Severe plastic deformation by warm equal channel angular extrusion (ECAE) in a 90° die is used to consolidate gas atomized amorphous metal powders (Hf-based: $\text{Hf}_{71.3}\text{Cu}_{16.2}\text{Ni}_{7.6}\text{Ti}_{2.2}\text{Al}_{12.6}$ -wt% and Zr-based: $\text{Zr}_{58.5}\text{Cu}_{15.6}\text{Ni}_{12.8}\text{Al}_{10.3}\text{Nb}_{2.8}$) with pure Cu, Ni and W crystalline powders at temperatures between Tg and Tx. A fully dense and uniformly consolidated product is achieved after one extrusion. Infiltration microstructures are compared for the three different crystalline phases tested. Subsurface shear band interactions between the amorphous matrix and crystalline phase particulate are reported with the bonded interface technique on samples deformed with a Vickers microhardness indentation under loads from 10-1000g. Mechanical properties and hardness for Hf- and Zr-based consolidated composites are compared with the properties of ECAE consolidated monolithic alloy.

10:45 AM

Relationship between Glass Forming Ability and Intermetallics in Fe-Based Multi-Component Alloy Systems: *Satyajeet Sharma*¹; Umesh Patil¹; Raj Vaidyanathan¹; C. Suryanarayana¹; ¹University of Central Florida

The technique of mechanical alloying has been employed to relate the number of intermetallics in the phase diagrams and glass forming ability in Fe-based multi-component alloy systems. A systematic study has been carried out on binary, ternary and quaternary systems based on the Fe-B system. Special attention was focused on the quaternary Fe42Zr10X28B20 (X = Al, Co, Ge, Mn, Ni, and Sn) alloy systems. The alloying elements were so chosen as to form intermetallics with Zr ranging from 1 (in Zr-Mn) to 10 (in Zr-Al) in number. The powders were milled in a SPEX 8000D milling machine with a ball-to-powder weight ratio of 10:1 and 20:1. The structural evolution was characterized using XRD and TEM techniques. Preliminary results demonstrate that it is possible to relate the number of intermetallics with the ease of amorphization.

11:05 AM

Thermophysical Properties Measurements of $\text{Zr}_{62}\text{Cu}_{20}\text{Al}_{10}\text{Ni}_8$ Using Containerless Processing: *Richard C. Bradshaw*¹; Mary E. Warren¹; Jan R. Rogers²; Tom J. Rathz³; Anup K. Gangopadhyay⁴; Ken F. Kelton⁴; Robert W. Hyers¹; ¹University of Massachusetts; ²NASA MSFC; ³University of Alabama, Huntsville; ⁴Washington University

Thermophysical property studies performed at high temperature can prove challenging because of reactivity problems brought on by the elevated temperatures. Contaminants from measuring devices and container walls can cause changes in properties. To prevent this, containerless processing techniques can be employed to isolate a sample during study. A common method used for this is levitation. Typical levitation methods used for containerless processing are, aerodynamically, electromagnetically and electrostatically based. All levitation methods reduce heterogeneous nucleation sites, which in turn provide access to metastable undercooled phases. In particular, electrostatic levitation is appealing because

sample motion and stirring are minimized; and by combining it with, optically based, non-contact measuring techniques, many thermophysical properties can be measured. Applying some of these techniques, surface tension, viscosity and density have been measured for the glass forming alloy $\text{Zr}_{62}\text{Cu}_{20}\text{Al}_{10}\text{Ni}_8$ and will be presented with a brief overview of the non-contact measuring techniques used.

11:25 AM

Thermodynamic and Experimental Investigation of Plastic Mg-Base Glass Matrix Composite: *X. D. Hui*¹; W. Dong¹; Z. G. Li¹; Z. K. Liu²; ¹University of Science and Technology Beijing; ²Pennsylvania State University

Mg-based bulk metallic glasses (BMGs) are regarded as one of the most attractive structural materials due to their low density and high strength. To date, Mg-based alloys with large glass-forming ability (GFA) have been developed in Mg-Ni-Y, Mg-Cu-Y, Mg-Cu-Al-Y, Mg-Cu-Ag-Y, Mg-Cu-Zn-Y and Mg-Cu-Y-Ag-Pd systems. However, monolithic Mg-based BMGs have been found to be brittle. To overcome the drawback of monolithic Mg-based BMGs alloys, thermodynamic modeling and experimental investigation are conducted on the Mg-base composite alloys with high GFA along with comprehensive mechanical properties. By using CALPHAD technique, we designed a series of Mg-base glass forming alloys, in which Mg-based solid solution phase is expected to precipitate in metallic glass matrix. The significant improvement in plastic strain, fracture strength, and specific strength will be reported in this presentation.

11:45 AM

Thermal Stability and Crystallization Behavior of $\text{Cu}_{60}\text{Hf}_{25}\text{Ti}_{15}$ Bulk Metallic Glass: *Hsin-Hsin Hsieh*¹; *Wu Kai*¹; Yu Lung Lin²; Ron Tang Huang³; ¹National Taiwan Ocean University; ²Chung Shan Institute of Science and Technology; ³National Tsing Hua University

Thermal stability and crystallization behavior of $\text{Cu}_{60}\text{Hf}_{25}\text{Ti}_{15}$ bulk metallic glass were studied by means of continuous heating and isothermal method. DSC analyses show that the crystallization process mainly proceeds in three stages. For continuous heating method, the activation energy of these three exothermic reactions are 321, 274, and 309 KJ/mol for the first, second, and third peak, respectively. For isothermal measurement, only one exothermic peak prior to crystallization can be detected. Avrami exponent values of Cu-base glassy alloy is 2.04 ± 0.19 , indicating the crystallization behavior of $\text{Cu}_{60}\text{Hf}_{25}\text{Ti}_{15}$ BMG is 3-dimensional diffusion-controlled growth of nuclei at a decreasing nucleation rate.

Characterization of Minerals, Metals and Materials: Advances in Methodologies

Sponsored by: The Minerals, Metals and Materials Society, TMS Extraction and Processing Division, TMS: Materials Characterization Committee

Program Organizers: Jiann-Yang James Hwang, Michigan Technological University; Arun M. Gokhale, Georgia Institute of Technology; Tzong T. Chen, Natural Resources Canada

Thursday AM
March 16, 2006

Room: 205
Location: Henry B. Gonzalez Convention Ctr.

Session Chairs: Benjamin L. Henrie, Los Alamos National Laboratory; Jeongguk Kim, Korea Railroad Research Institute

8:30 AM

A New Method for Fracture Plane Determination: *Robert E. Hackenberg*¹; Robert D. Field¹; Pallas A. Papin¹; David F. Teter¹; ¹Los Alamos National Laboratory

A new method for the determination of the crystallographic indices of planar fracture surfaces is described. The key innovation is the use of an in-situ micromanipulator in a focused ion beam to extract TEM foils from a bulk fracture surface. Selected area diffraction of these foils in the TEM allows the determination of the crystallographic line directions that are contained within the fracture plane. This allows the fracture plane indices

to be characterized. The validation of this method using cleavage fracture in pure Zinc, and its application to other materials will be described.

8:55 AM

Accuracy and Reproducibility of High-Temperature Differential Scanning Calorimetry: *Susan Jacob*¹; Mark E. Schlesinger¹; ¹University of Missouri-Rolla

High-temperature differential scanning calorimetry (HTDSC) is a relatively new research tool that offers considerable promise for thermochemical research. However, the reliability and reproducibility of HTDSC measurements is impacted by several experimental variables. The impact of these experimental variables on the results of HTDSC measurement of two well-known thermodynamic properties (the heat capacity of platinum, and the enthalpy of fusion of silver) has been assessed for one well-known model of HTDSC. The results provide a better idea of the conditions needed to obtain optimal experimental results from the instrument, and the degree of accuracy and reproducibility which can be obtained under these conditions.

9:20 AM

Cathodoluminescence Properties of Natural Sphalerite: *Musa Karakus*¹; Richard D. Hagni¹; ¹University of Missouri-Rolla

Optical cathodoluminescence (CL) microscopy and spectroscopy was used to study CL behavior of natural sphalerite samples associated with silver, tin, tungsten deposits, and carbonate hosted Zn-Pb-Cu deposits from world famous localities. This study involves determinations of the relationships between CL properties and trace element content of sphalerite. The CL spectrum of natural sphalerite is rather complex due to the presence of more than one luminescence center. Mn²⁺ activator is the most important activator ion in most sphalerites, and it produces an orange emission band centered at 585 nm. Translucent green sphalerite showed weak orange CL due to Mn²⁺ but their CL intensity was reduced by the presence of Co²⁺ and Fe²⁺. Those sphalerite whose Fe²⁺ content exceeded 1% did not show CL. Sphalerite from carbonate-hosted deposits exhibited interesting CL colors and spectra. The CL imaging and spectroscopy is found to be extremely useful technique for distinguishing different generation of sphalerite.

9:45 AM

Metallographic Preparation Techniques for Uranium and Its Alloys: *Ann Marie Kelly*¹; Dan J. Thoma¹; Robert D. Field¹; Paul S. Dunn¹; David F. Teter¹; ¹Los Alamos National Laboratory

Existing metallographic preparation techniques for uranium and uranium alloys are limited to elucidating specific microstructural characteristics, and some of the techniques are regarded as being environmentally unacceptable. This paper describes a newly developed technique, which is not only more environmentally friendly, but reveals most microstructural features simultaneously. Other attributes include a significant reduction in processing time and with only minor adjustment this technique may be applied to various uranium alloys. Examples of microstructures as revealed during various stages of preparation will be presented to highlight the new technique.

10:10 AM Break

10:20 AM

Using Rietveld Analysis with TOPAS for Modal Analysis of Geological Samples: *Holger Cordes*¹; ¹Bruker-AXS

X-ray diffraction has long been used for qualitative and quantitative mineral analysis but Rietveld data analysis is still an under utilized method for mineral exploration and processing applications. In this full-profile approach the structural parameters of each mineral phase, together with experimental parameters, are refined by least-squares methods to minimize the difference between observed and calculated diffraction patterns. The result is a standard-less, quantitative analysis of the mineral abundance in the sample that is more accurate and considerably faster compared to traditional methods. The TOPAS software package combines a user-friendly interface with a unique approach to resolve overlapping peaks. Automated analysis options are also available and significantly reduce analysis time for routine samples. Several examples on a wide range of naturally occurring rock types are shown that illustrate the capabilities

and limitations of the method. The examples include several options for the quantification of amorphous constituents like volcanic glasses.

10:45 AM

Robotic Automation of the Fire Assay Process for Rapid Quantitative Measurement of Platinum Group Elements in Mineral Concentrator Plants: *Jacques J. Eksteen*¹; Keith S. McIntosh²; Klaus Koch¹; Derek Auer²; ¹University of Stellenbosch; ²Anglo Platinum Ltd.

The fire assay process for the quantitative recovery of platinum group elements (PGE's) prior to subsequent analysis traditionally is a time-consuming process. Samples derive from various ore types and contain PGE's at the ppm or ppb levels, making concentration of the elements mandatory before assaying. Traditionally sample turn-around times are of the order of 24 hours. The whole sequence of sample preparation, fire assay and subsequent analysis of PGE's have been automated by Anglo Platinum. Some of the major challenges on the road to automation will be discussed and the novel solutions that were implemented. The engineered solution included robotic automation of the whole sequence, from sample preparation, up to the final element by element assay. The final system allowed for rapid (less than one hour) and accurate analysis of PGE's even in streams containing very low levels, such as flotation tailing streams and drill core samples.

11:10 AM

On-Line Radio Frequency Measurement of Bulk Mineralogy: *Daniel Bennett*¹; David Miljak¹; Joe Khachan²; ¹CSIRO; ²University of Sidney

There are few methods currently applied towards on-line bulk mineralogical analysis. Yet on line knowledge of process mineralogy could potentially provide large benefits, such as increased extraction efficiency or resource optimization. The work described in this paper involves the development of radio frequency methods for bulk mineralogical analysis. Some "zero field" magnetic resonances that occur in the radio frequency spectrum are mineral specific, and potentially allow quantitative estimation of mineralogy in an ore stream. Results will be presented on the specific detection of chalcopyrite. Initial quantitative measurements investigating matrix effects have indicated the feasibility of on-line mineralogical estimation using radiofrequency techniques.

11:35 AM

Pulsed Power Breaking-Up Technology for Resistant Gold-Containing Ores and Beneficiation Products: *Valentin Alekseevich Chanturiya*¹; *Igor Jeanovich Bunin*¹; ¹Research Institute of Comprehensive Exploitation of Mineral Resources

The aim of this paper is basically to show progress in the study of nanosecond processes involved in the disintegration and breaking-up of mineral complexes with fine noble metals. We studied the influence of nanosecond High-Power Electromagnetic Pulses (HPEMP) on the physicochemical and technological properties of refractory gold-containing ores and beneficiation products. Experimental data are presented to confirm the formation of breakdown channels and selective disintegration of mineral complexes as a result of pulse irradiation, which makes for efficient access of lixiviant solutions to precious metal grains and enhanced precious metal recovery into lixivium during leaching. Preliminary processing of gravity concentrate with a HPEMP resulted in significant increase of gold and silver extraction into lixivium during the cyanidation stage, with gold recovery increased by ~31% (from 51.2% in a blank test to 82.3% after irradiation). Gold recovery from stale gold-containing dressing tailings products increased after pulses-irradiation from 8-12% to 80-90%.

12:00 PM

Applied Mineralogical Studies of Nigerian Bulk Complex Sulphide Ore: *Peter A. Olubambi*¹; S. Ndlovu¹; J. H. Potgieter¹; J. O. Borode¹; ¹University of the Witwatersrand, Johannesburg

Representative samples of the hydrothermal vein deposits of the bulk complex sulphide ore deposit, 10 km south of Ishiagu, in Ebonyin State, South Eastern part of Nigeria were collected from two small scale mining companies. The samples were mixed and successively crushed in a jaw crusher and cone crusher, and ground in a rod mill. Characterization was carried out with SEM, EDX, XRD, XRF and ICP-OES. Mineralogical analysis revealed the presence of sphalerite, galena, siderite, pyrite, quartz and chalcopyrite. X-ray Diffractometry showed that sphalerite mineral in the ore occurs as sphalerite ferrous with varied percentage of Zn and Fe

within the various sizes while chalcopyrite occurs as a chalcopyrite group mineral with chemical formula $\text{Cu}_2\text{MnSnS}_4$. Results of the elemental analysis showed variations in elemental composition within the different sizes.

Characterization of Minerals, Metals and Materials: Mineralogical Studies

Sponsored by: The Minerals, Metals and Materials Society, TMS Extraction and Processing Division, TMS: Materials Characterization Committee

Program Organizers: Jiann-Yang James Hwang, Michigan Technological University; Arun M. Gokhale, Georgia Institute of Technology; Tzong T. Chen, Natural Resources Canada

Thursday AM
March 16, 2006

Room: 206A
Location: Henry B. Gonzalez Convention Ctr.

Session Chair: Jiann-Yang James Hwang, Michigan Technological University

8:30 AM

Temperature Measurements in Microwave Heating: *Xiang Sun*¹; Jiann-Yang James Hwang¹; Shangzhao Shi¹; Bowen Li¹; Xiaodi Huang¹; ¹Michigan Technological University

Microwave heating has been used in numerous industrial processes due to its great advantages by comparing with conventional heating method. However, microwave heated products can be affected by non-uniform temperature distribution due to the mechanisms of microwave heating. To overcome this problem, a critical step is to have a temperature-time profile. In order to characterize and diagnose microwave heating effects, an accurate temperature measurement is needed. This paper discusses the possibility of applying several temperature measurement techniques in microwave processing. Both contact and non-contact methods are introduced and compared.

8:55 AM

Mineralogical, Chemical and Ceramic Properties of Kaolinite-Illite Clays from the Tamnava Tertiary Basin – West Serbia: *Ana S. Radosavljevic-Mihajlovic*¹; Jovica N. Stojanovic¹; Vladan D. Kasic¹; ¹Institute for Technology of Nuclear and Other Mineral Raw Materials

Important quantities of ceramic clay, composed of kaolinite-illite with quartz have been determined in the Tamnava tertiary basin. XRPD, DTA/TG and electron microscope investigations were performed on representative samples. The main mineral association, determined by XRPD analysis, consists of kaolinite-illite, quartz, mica, feldspar, and Fe-oxide. The chemical composition generally shows high silica and alumina contents in all analysed samples, which is typical for strong kaolinized materials. The kaolinite-illite ratio is varying (generally 1:1) and influences in the change of their ceramic properties. These clays are classified as medium-plastic with enlarged range of sintering temperature, what makes them convenient for production of various kinds of ceramic tiles.

9:20 AM

Phase Transitions during Heating of Illite: *Xiaowen Liu*¹; Hengfeng Li¹; Jianrong Wang¹; Yuehua Hu¹; Danqing Yi¹; ¹Central South University

The DSC/TGA, IR and XRD analysis were used to characterize the heating phase transformation of illite, which come from Ouhai, Zhejiang, China. It was discovered that the dehydration and dehydroxylation of illite carried out stage by stage during heating. The adsorptive water and layer-inter water were dehydrated from room temperature to 773K; and dehydroxylated in the range of 773K~973K. In these stages of process, illite's layer structure kept almost unchanged. After 973K, illite began to change into disorder structure. At about 1373K, the layer structure of illite has been destroyed, and a morpous SiO_2 and crystallite mullite appeared. At about 1473K, the structure of illite was completely destroyed and mullite crystal phase has become perfect.

9:45 AM

The Direct Test of Swell Stress for Geosynthetic Clay Liners: *Junfeng Shen*¹; Shengrong Li¹; Shaohui He¹; Guangshan Zhang¹; Jingui Tong¹; Bokun Yan¹; ¹China University of Geosciences

Geosynthetic clay liner (GCL) is a kind of waterproofing material used widely in engineering. The waterproof mechanism is understood in terms of bentonite particles becoming a water-obstruct colloid layer after they sorb water and swell. The swell stress, however, has not been determined directly till now. In our experiment, the swell stresses of the GCL, which is made in CETCO company, America, under saturated water-sorbing conditions, are measured directly using a custom-made instrument. The results show that the instrument designed by the authors performed satisfactorily and the test results are reproducible. The drive force for water molecules are able to enter into montmorillonite particles and individual ontmorillonite crystals is understood in term of larger specific surface area, layer structure, layer charge, and broken bound in edge of crystal. Those measurement results will be significant for using GCL appropriately in engineering.

10:10 AM Break

10:20 AM

Mineralogical and Chemical Characterization of the W-Pb-Bi-Ag Ore from the Rudnik Mine, Serbia: *Slobodan A. Radosavljevic*¹; Jovica N. Stojanovic¹; Ana S. Radosavljevic-Mihajlovic¹; ¹Institute for Technology of Nuclear and Other Mineral Raw Materials

The polymetallic W-Pb-Bi-Ag ore from the "Nova jama" ore zone of the Rudnik ore field have been investigated. Contact-pneumatolytic (skam), pneumatolytic-hydrothermal, and hydrothermal mineralization phases are defined in this ore zone. The most significant mineralization phase that gave compact ore bodies is pneumatolytic-hydrothermal phase. A relatively pure Mo-free scheelite is the only tungsten-bearing mineral. Lead minerals are mostly presented by Pb-Bi sulphosalts and much less with galena. The image analysis coupled with Energy Dispersive Spectrometry (EDS) analysis on a Scanning Electron Microscope (SEM) was applied to the characterization of a W-Pb-Bi-Ag ore as an efficient tool for mineral quantification. Results of EDS (Energy Dispersive Spectrometry) analyses gave the empirical formulae: $\text{Pb}_{1.91}\text{Ag}_{0.05}\text{Cu}_{0.08}\text{Bi}_{1.93}\text{S}_5$ for cosalite, $\text{Pb}_{0.98}\text{Ag}_{0.03}\text{Cu}_{0.05}\text{Bi}_{1.99}\text{S}_4$ for galenobismutite and galena $\text{Pb}_{0.99}\text{Ag}_{0.03}\text{S}$.

10:45 AM

Research on the Dispersion and Aggregation between the Three Clay Minerals and Diaspore: *Xiaowen Liu*¹; Yuehua Hu¹; Danqing Yi¹; ¹Central South University

Slime coating and aggregation between the clay minerals and diaspore should be avoided in the diasporic bauxite flotation. The colloidal stability between the three plate dioctahedral phyllosilicate minerals and diaspore in water was quantitatively calculated by the DLVO theory. It shows that in acidic solution, the particles flocculate by particle (diaspore)-face (clay mineral) form; in neutral solution, they flocculate by particle (diaspore)-edge (clay mineral) form; and disperse in alkaline solution, approximately consistent with the results of measurement in precipitation analysis and the observation of SEM. The results obtained in this study should shed more lights on diasporic bauxite flotation and the dispersion and aggregation of nanoparticles.

11:10 AM

Barite Mineralization in Volcanic Rocks in Southern Flank of East-Magnitogorsk Palaeoisland Arc (South Urals): *Natalya Nikolaevna Ankusheva*¹; ¹Russian Academy of Science

East-Magnitogorsk palaeoisland arc was formed in devonian-carboniferous on the periphery of Urals palaeocean. Ore-bearing structures are early carboniferous palaeovolcanos. Barite veins are confined to diabase dikes and trachibasalt tuffs. Two barite types are allocated: white and pink. White barite forms crystalline-granular masses, fibrous, tabular, parallel-columnar aggregates, pink – radially-fibrous aggregates, columnar crystals. Roentgenofluorescencal analysis: white barite is enriched Sr (7500 gr/t) and impoverished Pb (120), in pink – more Pb (500–1000) and less Sr (2000). Roentgenostructural analysis: lattice parameters are lower in white barite, than in pink, it is connected to replacement Ba to Sr. There are inclusions of aurichalcite, biotite, rutile, microcline in white barite;

sulfides and hialophane in pink one. The temperatures of hydrothermal solutions were 155–180°C, high salinity (18.6 wt. %), testifying about magmatic origin. Two solutions groups – low- (155–165°C) and high-temperature (170–180°C) are allocated. These barite types concern to two generations – early (white), late (pink).

11:35 AM

Investigation on the Thermal Decomposition of Diaspore: *Xiaowen Liu¹; Jianrong Wang¹; Hengfeng Li¹; Yuehua Hu¹; Danqing Yi¹*; ¹Central South University

The kinetic curves are obtained by thermogravimetry(TGA) and differential scanning calorimetry (DSC). The mechanism of thermal decomposition of diaspore is discussed according to Coat-Redfer equation. The phase identification is carried out by X-ray diffraction(XRD) before and after thermal treatments. It is found that after thermal treatment at 500°C, the diaspore is transformed to corundum (a-Al₂O₃) and H₂O. The activation energies is 287KJ/mol. The crystal structure also changed greatly during thermal treatment. The value of a parameter, b parameter and the crystal lattice volume (V) of diaspore are increased greatly from 400°C to 500°C. When the heated temperature is below 400°C, the values change inobviously.

Computational Thermodynamics and Phase Transformations: Thermodynamic Models

Sponsored by: The Minerals, Metals and Materials Society, TMS Electronic, Magnetic, and Photonic Materials Division, TMS Materials Processing and Manufacturing Division, TMS Structural Materials Division, TMS: Chemistry and Physics of Materials Committee, TMS/ASM: Computational Materials Science and Engineering Committee
Program Organizers: Dane Morgan, University of Wisconsin; Corbett Battaile, Sandia National Laboratories

Thursday AM
March 16, 2006

Room: 210A
Location: Henry B. Gonzalez Convention Ctr.

Session Chair: Corbett C. Battaile, Sandia National Laboratories

8:30 AM

A Statistical-Thermodynamic Model for Ordering Phenomena in Thin Film Intermetallic Structures: *Olga Semenova¹; Regina Krachler¹; Herbert Ipser¹*; ¹University of Vienna

New advanced nano-crystalline materials are the key to technological progress and a focus of intensive research activity during the last decades. These materials found extensive application in industry in the production of microelectronic and optoelectronic devices and for modern computer technologies. To control the processes occurring in the structure under different treatment conditions during fabrication, a profound basic knowledge of order-disorder phenomena is of paramount importance. This paper presents a new and unified statistical-thermodynamic model for description of ordering phenomena in nano-crystalline intermetallics. The model is developed on the basis of the Ising approach and a Bragg-Williams mean-field approximation which are very powerful tools for studying ordering phenomena as well as order-disorder phase transitions in intermetallic phases. Based on a statistical thermodynamic model previously developed for binary B2 bulk intermetallic phases, the new model allows to estimate point defect concentrations and the degree of long range order in the structure.

8:50 AM

A Thermostatistical Model for Cell Formation: *Pedro Eduardo Jose Rivera diaz del Castillo¹; Mingxin Huang¹; Sybrand van der Zwaag¹*; ¹Delft University of Technology

A new thermostatics based approach to describe the conditions leading to the formation of cells is presented. The new theory is based on the minimisation of the free energy for different dislocation arrangements such as homogeneous and pattern distributions. The likelihood of the formation of subgrains is captured by the atom-to-atom computation of the entropy. The differences arising from crystallography and temperature are thus captured by the model. The effects of grain morphology and size on

the substructure type are analysed. It is shown that grains in the submicron scale cannot form cells in (meta)equilibrium; whereas deformation of grains in the nanometre scale has to occur with the aid of other mechanisms such as grain boundary sliding.

9:10 AM

Atom Bonds of Al-Zn Solid Solutions and Spinodal Decomposition: *Gao Yingjun¹*; ¹Guangxi University

The valence electron structures of Al-Zn solid solutions are analyzed according to Empirical Electronic Theory in Solid and Molecule(EET) with the average atom model. The results show that spinodal decomposition produces great change of the valence electron structure in Al-Zn solid solutions. The spinodal decomposition under room temperature enhance hardness and intensity of Al-Zn alloys are rationally explained according to the change of covalent bond in the solid solutions.

9:30 AM

Dilatometric Analysis of Phase Transformation Involving Multi-Phase in Steel: *Sang Hwan Lee¹; Ji Youn Kim¹; June Yeong Park¹; Kyung Jong Lee¹; Kyung Sub Lee¹; Dong Hyuk Shin¹; Kwang Geun Chin²*; ¹Hanyang University; ²POSCO Technical Research Laboratory

Dilatometric analysis is frequently used to figure out the overall phase transformation in steel. However, it is very difficult to separate the transformation for one phase from the others when transformation of two or more phases are superimposed. In this study, the rate of transformation(change of transformed volume fraction per unit time) was applied to step forward to get the individual transformation. Variation of the rate of transformation was first classified by simulating transformation kinetics determined by Avrami equations in the multi-phase system. The systematic analysis was carried out for the experimentally determined dilatation. The start, finish and peak of individual transformation were determined. They were compared with those determined by other methods.

9:50 AM Break

10:10 AM

Bond Analysis of Interface for Strengthening in Al-Mg-Si Alloy: *Gao Yingjun¹*; ¹Guangxi University

Through the calculation of the electronic bonding density of the main equilibrium phase β (Mg₂Si) and pure Si cell, the result show that the strongest bond in Si cell is more than three times of that in Mg₂Si cell, and the (electronic bonding density) in the Si cell is also more than three times of that in the Mg₂Si cell. These are the main reason that influences the growth of grain of Mg₂Si and the mechanical property of alloy such as hardness and intensity.

10:35 AM

Modeling of Reaustenitization of Hypoeutectoid Fe-C Steels with a Cellular Automaton Method: *B. J. Yang¹*; ¹Caterpillar Inc.

A model for simulation of reaustenitization of hypoeutectoid Fe-C steel has been developed by using cellular automaton approach(CA). The initial microstructure state for quenching can be predicted with such information as grain size and distribution of carbon concentration. The kinetics of austenitization is modeled by nucleation, grain growth and grain coarsening. The free energy and boundary energy are taken into account for grain coarsening, and carbon diffusion in ferrite and austenite and its interface dynamics are considered for the growth of austenite. The competition between the nucleation and early stage grain growth in the pearlite is investigated, and a simultaneous growth for ferrite to austenite and the grain coarsening is also revealed. A microstructure of hypoeutectic Fe-C steel of 1045 is digitized as an initial microstructure state using various heating rates. The effect of heating rates on the final grain size and homogeneity is studied.

10:55 AM

Thermodynamic Description of Liquid Steels and Metallurgical Slags by the "Generalized Central Atoms" Model: *Jean Lehmann¹; Frederic Bonnet¹; Manuel Bobadilla¹*; ¹Arcelor Research

This paper deals with the latest development in computational thermodynamics currently running at Arcelor Research to improve the representation of the properties of metallurgical slags and liquid steel. This development concerns the unification of two models developed and used by Arcelor Research to represent the properties of the metallurgical slags on

the one hand and of liquid metallic phases on the other hand is presented. These two models are respectively the cell model and the central atoms model as introduced primarily by Lupis and Elliot. The new prospects brought by this unification are explained. In particular, for the metallurgical slags, they arise from a more accurate description of the short-range ordering. Concerning the liquid steel, the model has been assessed on the system Fe-Al-Cr-Mn-Ni-Si-Ti-Ca-Mo-Cu-Nb-C-N-H-O-P-S and applications to nitrogen, sulphur and oxygen in various steel grades show that the central atoms model represents accurately multicomponent systems.

11:15 AM

Thermodynamic and Experimental Simulation of Urinary Stones Minerals Crystallization: *Olga Alexandrovna Golovanova*¹; Elena Vladimirovna Rosseyeva¹; Vladislav Jurjevich Yelnikov¹; Olga Victorovna Frank-Kamenetskaya¹; ¹St. Petersburg State University

The detail study of inorganic and organic components of Russian inhabitants urinary stones was carried out. Based on these data the thermodynamic model of urinary stones phases crystallization has been constructed. 3D solubility surfaces of a common crystallization of some phases have been calculated. During simulations the composition of the solid phases precipitating from urine-like solutions with different contents of calcium, magnesium, phosphate, oxalate, ammonium, chloride, sulphate, sodium and potassium ions at 37°C (pH24 h = 6.5 - 7.5) has been determined. Brushite with hydroxyapatite and newburyite at pH24 h = 6.5 have been appeared. Struvite, hydroxyapatite and amorphous calcium phosphates at pH24 h = 7.5 have been precipitated. Good correlation between experimental measured and theoretically predicted data has been revealed.

Deformation and Fracture from Nano to Macro: A Symposium Honoring W. W. Gerberich's 70th Birthday: Environmental and Material Alloying Effects

Sponsored by: The Minerals, Metals and Materials Society, TMS Materials Processing and Manufacturing Division, TMS Structural Materials Division, TMS/ASM: Mechanical Behavior of Materials Committee, TMS: Nanomechanical Materials Behavior Committee
Program Organizers: David F. Bahr, Washington State University; James Lucas, Michigan State University; Neville R. Moody, Sandia National Laboratories

Thursday AM Room: 214D
March 16, 2006 Location: Henry B. Gonzalez Convention Ctr.

Session Chairs: Neville R. Moody, Sandia National Laboratories; Hussein M. Zbib, Washington State University

8:30 AM Invited

Nanoindentation at Elevated Temperatures: Applied and Fundamental Studies of Materials Mechanics: *Christopher A. Schuh*¹; ¹Massachusetts Institute of Technology

Recent progress in the development of high-temperature nanoindentation techniques will be discussed. The practices required to obtain artifact-free data at temperatures as high as 410°C are established with reference to experiments on amorphous silica, and subtleties of hardness and modulus measurement at these temperatures will be discussed. The capability of in-situ contact-mode imaging at temperature is also described. Finally, the impact of these techniques for fundamental study of deformation mechanisms is discussed in the framework of the 'incipient plasticity' problem of the elastic-plastic transition.

8:50 AM

Mechanical Grain Growth: *James C. M. Li*¹; ¹University of Rochester
Grain growth usually takes place at high temperatures without external stress and the driving force is the energy of grain boundaries. However, recent experiments for nanocrystalline materials under an indenter, grain growth is observed at room temperature and even at liquid nitrogen temperatures. So obviously mechanical stress can induce grain growth. Motion of tilt boundaries by mechanical stress was first observed by Parker and Washburn in 1952 in a bent single crystal of Zn. This motion caused

one grain to grow into the other. So this is the first observation of grain growth under stress even though it is a bicrystal. In a polycrystal, a boundary can be decomposed by mechanical means after which the two grains merge into one. Some conditions and the critical stress needed to decompose a grain boundary will be shown including the effects of grain size and temperature.

9:05 AM

Stress Induced Grain Growth and Its Effect on the Mechanical Behavior of Nanocrystalline Aluminum Thin Films: Daniel S. Gianola¹; Kevin J. Hemker¹; ¹Johns Hopkins University

Recent studies of the mechanical behavior of nanocrystalline metals have focused on extensions of the Hall-Petch relation to smaller grain sizes and the identification of the deformation mechanism(s) that become operative when microcrystalline plasticity is abated. Here we report on the observation of high tensile strength and unusually high room temperature tensile ductility in submicron free-standing nanocrystalline aluminum thin films. In situ X-ray diffraction and post mortem transmission electron microscopy point to the importance of room temperature grain growth in transforming the underlying processes that govern the mechanical response of the films; nanoscale deformation mechanisms give way to microscale plasticity. Efforts to model this growth with traditional driving forces for grain boundary migration (e.g. reductions in grain boundary energy, surface energy, and elastic strain energy) have proven to be less than satisfactory, and the importance of grain boundary pinning and role of stress assisted grain boundary migration will be highlighted.

9:20 AM

Forced Chemical Mixing in Nanocrystalline and Amorphous Alloys Subjected to Sustained Plastic Deformation: *Pascal M. Bellon*¹; Samson Odunuga¹; Pavel Krasnochtchekov¹; Youhong Li¹; Robert S. Averback¹; ¹University of Illinois

Plastic deformation, at low temperatures, can force the interdiffusion of chemical species and stabilize supersaturated solutions in solid alloys. Despite the information available on that forced mixing, its characteristics are still not well understood, particularly for nanocrystalline and amorphous alloys, for which the mechanisms of plastic deformation remain unresolved. We present here a new method for analyzing forced chemical mixing that offers new insight into the mixing process. The method, which is similar to one used for characterizing turbulent flows, monitors the evolution of the separation distance between pairs of atoms, R, which is quantified by an effective diffusion coefficient. This diffusion coefficient is predicted to increase with R, and to saturate at a value R_c that is characteristic of the length scale of the defects responsible for plastic deformation. Our analytical predictions are tested by 3D molecular dynamic simulations of nanocrystalline and amorphous alloys cyclically deformed in compression.

9:35 AM

Effect of Copper Solution on Deformation Behavior of Nanocrystalline Gold: *Yinmin (Morris) Wang*¹; Alan F. Jankowski¹; Alex V. Hamza¹; ¹Lawrence Livermore National Laboratory

Nanocrystalline gold with copper solution additions in the range of 0-12 wt.% and grain sizes below ~10 nm were prepared using electrodeposition technique. These nanocrystalline foils have a typical thickness of above 10 nm, and thus allow us to carry out mechanical property assessment using traditional mechanical characterization techniques, such as tensile tests and instrumented nanoindentation experiments. The Young's modulus, hardness, tensile strength, and tensile ductility were determined as a function of grain size and solid solute content. Special attention was also paid to interpret the copper solid solute effect on strain rate sensitivity of these materials. New experimental evidence suggests that alloying could not only substantially improve the mechanical properties of nanocrystalline materials, but also fundamentally alternate their deformation behavior. This work was performed under the auspices of the U.S. Department of Energy by University of California, Lawrence Livermore National Laboratory under contract of No.W-7405-Eng-48. Y.M. Wang acknowledges the support of Graboske Fellowship at Lawrence Livermore National Laboratory.

9:50 AM

The Effects of Solute Impurities on the Onset of Plasticity in FCC Materials: *Gus Vasquez*¹; David F. Bahr¹; ¹Washington State University

The ability to quantify the stress required to nucleate dislocations in dislocation free regions in solid solutions of FCC metallic materials has been studied using nanoindentation. The effects of solute impurities in the copper-nickel system on the formation of dislocations in a previously dislocation free region have been demonstrated to be minimal. The shear stress required to nucleate dislocations in copper is approximately 1.6 GPa, while in nickel a 3.9 GPa shear stress is required. Changes in shear stress for nucleation track closely with changes in elastic modulus, showing the nucleation stress is approximately 1/30 to 1/20 of the shear modulus. The expected solid solution strengthening is identified within the same experimental method, demonstrating unambiguously the fact that solid solution impurities in this system will impact the propagation of dislocations during plastic deformation, but not alter the homogeneous nucleation of dislocations in these materials.

10:05 AM

Effect of Passivation on Stress Relaxation in Electroplated Copper Films: *Rui Huang*¹; Paul S. Ho¹; Dongwen Gan¹; ¹University of Texas, Austin

In copper interconnects, mass transport at Cu/passivation interface is the dominant path for electromigration, and the kinetics strongly depends on material and processing of the passivation layer. The present study investigated the effect of passivation on the kinetics of interfacial mass transport by measuring stress relaxation in electroplated Cu films, both unpassivated and passivated, with four different cap layers: SiN, SiC, SiCN, and a Co-based metal cap. Stress curves measured under a thermal cycling condition show different behavior in the unpassivated and passivated Cu films, but indifferent for films with different cap layers. On the other hand, stress relaxation measured under an isothermal annealing condition reveals clearly the effect of the cap layers, indicating that interface diffusion controls the kinetic process of isothermal stress relaxation. A kinetic model based on coupling of interface and grain boundary diffusion was used to deduce the interface diffusivities and the corresponding activation energies.

10:20 AM Break

10:40 AM Invited

Modeling Stress Controlled Crack Tip Hydrogen Embrittlement: *Richard P. Gangloff*¹; Matthew R. Begley¹; ¹University of Virginia

Gerberich provided a foundation for micromechanical modeling of H-enhanced subcritical crack growth. This paper reviews improved descriptions of crack tip stress and plasticity central to such predictions. Material models with explicit microstructure (dislocation free zone, strain gradient plasticity, and discrete dislocation) predict near tip stresses higher than those from J_2 plasticity, but only for restricted regimes of alloy hardening and stress intensity. The concentration of trapped H is enriched exponentially by such high local hydrostatic stresses to favor decohesion independent of a requirement for impurity segregation. Material-flow descriptions including length scale can be incorporated into finite element based H damage models to better predict the effects of key variables, and provide a basis for next generation multi-length physics based predictions. Examples elucidate the effects of temperature on internal H assisted cracking of low strength Cr-Mo steel and predissolved as well as environment-produced H concentration on cracking of ultra-high strength steel.

11:00 AM

Investigation of Hydrogen-Deformation Interactions Using Thermal Desorption Spectroscopy (TDS): *Dan Eliezer*¹; Ervin Tal-Gutmacher¹; Thomas Boellinghaus²; ¹Ben Gurion University of Negev; ²Federal Institute for Materials Research and Testing

TDS is a very sensitive and accurate technique for studying hydrogen diffusion and trapping processes in materials. It involves accurate measurement of the desorption rate of gas atoms, soluted or trapped in the material, while heating the sample at a known rate. This study was undertaken to investigate what happens when small amounts of hydrogen are trapped within microstructural defects and the mutual impact of hydrogen and deformation on the behavior of two different systems; hydride-

and non-hydride-forming materials, represented respectively by titanium based alloys and stainless steels. The relationships between hydrogen absorption/desorption and deformation, as well as various desorption and trapping parameters, are evaluated in detail. Utilizing TDS provides a comprehensive knowledge of hydrogen-trapping and hydrogen-deformation interactions, necessary to make any decision and/or judgment whether a trap site, or a particular trapped hydrogen content, is either useful or detrimental for safe service conditions of these structural materials.

11:15 AM

Transgranular Hydrogen Embrittlement of Modern Ultra-High Strength Steels: Richard P. Gangloff¹; *Yongwon Lee*¹; ¹University of Virginia

Hydrogen severely embrittles modern precipitation hardened martensitic steels in spite of outstanding strength and fracture toughness. AerMet®100 ($\sigma_{YS} = 1750$ MPa, $K_{IC} = 130$ MPa \sqrt{m}) is susceptible to transgranular cracking from predissolved H (1-8 wppm) or loading in NaCl solution at free corrosion (-470 mV_{SCE}), with a threshold for cracking (K_{TH}) of 15 MPa \sqrt{m} . K_{TH} rises toward K_{IC} with cathodic polarization to -625 mV_{SCE}, then falls to 8 MPa \sqrt{m} with polarization to -1100 mV_{SCE}. This behavior is understood based on crack pH and potential governing H uptake. K_{TH} decreases as environmental H concentration increases, paralleling the effect of predissolved H and predicted within a decohesion framework following Gerberich. Slow subcritical H cracking is resolved for potentials where apparent K_{TH} approaches K_{IC} , complicating characterization and consistent with reaction rate limitation dominating H diffusion control of growth rate. Work is in progress to mitigate H cracking by control of carbide and austenite precipitates.

11:30 AM

Cleavage Oriented Iron Single Crystal Toughness Temperature Curves: *Mike Hribernik*¹; G. Robert Odette¹; ¹University of California, Santa Barbara

Static, dynamic initiation and crack arrest toughness of cleavage oriented unalloyed Fe single crystals was measured over a wide range of temperatures. The two types of (100)[010] and (100)[011] composite diffusion bonded specimens used in these tests, compression bridge anvil beams and wedge loaded chevron short beams, gave comparable results. Initiation toughness was measured in 4-point bending at rates from < 1 to > 2x10⁴ MPavm/s. Arrest toughness increased slowly from ~ 3-4 MPavm at -196°C up to -50°C increasing more rapidly at higher temperatures. Corresponding initiation toughness curves temperatures were higher, with the shifts depending on the loading rate. Preliminary data suggests an effective activation energy of ~ 0.25±0.05 eV. Implications of the results to a universal master curve toughness temperature curve shape are discussed. Comparisons with limited literature toughness data on Fe-3%Si suggests a significant role of solid solution strengthening in single crystal mediating toughness temperature properties.

11:45 AM

Cleavage Annular Stress Required for Fracture Path Deflection in Cold Drawn Pearlitic Steels: *Jesús Toribio*¹; Javier Ayaso¹; ¹University of Salamanca

The fracture performance of axisymmetric notched samples taken from pearlitic steels with different levels of cold drawing is studied. To this end, a real manufacture chain was stopped in the course of the process, and samples of all intermediate stages were extracted. Thus the drawing intensity or straining level (represented by the yield strength) is treated as the fundamental variable to elucidate the consequences of manufacturing on the posterior fracture performance. A materials science approach is proposed, so that the strongly anisotropic fracture behaviour of heavily drawn steels (which exhibit a 90° step in the fracture surface) is rationalized on the basis of the markedly oriented pearlitic microstructure of such steels which influences the operative micromechanism of fracture in this case. A finite element analysis of the stress distribution at the fracture instant allows the computation of the cleavage annular stress required to produce the deflection of the fracture path.

Fatigue and Fracture of Traditional and Advanced Materials: A Symposium in Honor of Art McEvily's 80th Birthday: Fatigue and Fracture XI

Sponsored by: The Minerals, Metals and Materials Society, TMS Structural Materials Division, TMS/ASM: Mechanical Behavior of Materials Committee

Program Organizers: Leon L. Shaw, University of Connecticut; James M. Larsen, U.S. Air Force; Peter K. Liaw, University of Tennessee; Masahiro Endo, Fukuoka University

Thursday AM
March 16, 2006
Room: 216
Location: Henry B. Gonzalez Convention Ctr.

Session Chairs: Yoshiharu Mutoh, Nagaoka University of Technology; Leon L. Shaw, University of Connecticut

8:30 AM Invited

Striations and Crack-Arrest Markings on Fracture Surfaces: *Stan Lynch*¹; ¹Defence Science and Technology Organisation

The formation of fatigue striations are reviewed, starting with an historical outline of their first observations, followed by a summary of current understanding, and concluding with a discussion of aspects that are not well understood. Such aspects include: (i) details of the crack-advance process, such as the relative extents of dislocation emission, dislocation egress, and decohesion at crack tips, together with the extent of micro/nano-void formation ahead of crack tips, (ii) the role of microstructural changes ahead of cracks, (iii) the effects of environment (and cyclic frequency) on striation spacing and appearance, and (iv) the increasing discrepancy between striation spacings and macroscopic crack-growth rates with decreasing stress-intensity-factor range. The formation of crack-arrest markings on sustained-load fracture surfaces are also reviewed, and possible common factors between these markings and fatigue striations, such as microstructural changes and 'damage' ahead of cracks, are discussed.

8:55 AM

Quantitative Analysis of Microstructures and Fracture Surfaces of Common Turbine Engine Materials: *Kezhong Li*¹; William Porter¹; James Larsen²; ¹University of Dayton Research Institute; ²Air Force Research Laboratory/MLLMN

To understand the influence of microstructure on fatigue variability, the role of each microstructural feature on crack initiation, micro-crack propagation and macro-crack propagation must be determined. In nickel-base superalloys, features of interest include gamma grain size, primary and secondary gamma prime size and their respective volume fractions. For alpha+beta titanium alloys, features include prior-beta size, primary-alpha size and volume fraction, and secondary-alpha-lath width and volume fraction. Thus, in order to model fatigue performance using microstructure-based models, it is crucial to quantify these and similar features. A detailed investigation was conducted on a nickel-based superalloy, IN100, and an alpha+beta titanium alloy, Ti-6Al-2Sn-4Zr-6Mo, to determine quantitative values for the various microstructural features. Scanning electron microscopy, orientation imaging microscopy and various image-analysis-software tools were employed in the study. The methods used to characterize features of each material are described. Finally, an approach to quantitatively characterize features associated with fatigue-derived fracture surfaces is discussed.

9:20 AM

In Situ Measurement of Crystal Lattice Strain Evolution during Cyclic Loading: Jun-Sang Park¹; *Matthew Miller*¹; Seth Watts¹; Alexander Kazimirov¹; ¹Cornell University

Crystals in a polycrystalline material under uniaxial cyclic loading can experience a complicated, multiaxial set of deformation histories. Measuring the crystal aggregate response to a known macroscopic cyclic load can be a first step to understanding the conditions leading to microcrack initiation. This talk will describe a set of experiments using high energy synchrotron x-ray to measure the crystal aggregate lattice strains during cyclic loading. A sophisticated diffractometer/loadframe system, capable

of exerting high frequency cyclic load, was employed. The specimen was rotated relative to the x-ray beam to construct lattice strain pole figures. To capture the "real time" lattice strains of different {hkl}s, a rotating shutter was developed and used to synchronize a point in the load history with x-ray beam at every cycle. The results enable us to look at a live picture of the lattice strains and their evolutions in a cyclically loaded specimen.

9:45 AM

Temperature Dependency of Delayed Hydride Crack Velocity in Zr-2.5Nb Tubes: *Young Suk Kim*¹; ¹Korea Atomic Energy Research Institute

Delayed hydride crack (DHC) tests were conducted on Zr-2.5Nb tubes with different distributions of the b-Zr at temperatures ranging from 125 to 300°C. Compact tension specimens charged to 27 to 100 ppm hydrogen were used to determine the temperature dependences of their DHC velocity (DHCV) and their striation spacing. The CANDU Zr-2.5Nb tube with a higher yield strength and a semi-continuous b-Zr had a higher DHCV and a smaller striation spacing than the RBMK Zr-2.5Nb tube with a fully discontinuous b-Zr and a lower yield strength. It is found that the activation energy for the DHCV is the sum of the activation energies for hydrogen diffusion and the striation spacing representing the hydrogen concentration gradient at the crack tip. Quantitative contribution of hydrogen diffusion and the hydrogen concentration gradient to the DHCV is discussed. This study provides supportive evidence for the feasibility of Kim's DHC model.

10:10 AM Break

10:25 AM Invited

Stress Shielding Phenomena and Fatigue Crack Growth Resistance in F/P Steels with Various Pearlite Morphologies: *Yoshiharu Mutoh*¹; Akhmad A. Korda¹; Yukio Miyashita¹; Teruki Sadasue²; ¹Nagaoka University of Technology; ²JFE Steel

The stage IIb regime of fatigue crack growth is known as the Paris regime, in which microstructure of the material hardly influences fatigue crack growth resistance. It is also well known that stress shielding phenomena at the crack tip, such as crack closure, bridging, phase transformation, microcracking, etc. contribute to reducing the crack tip stress intensity factor and thus enhancing the crack growth resistance. In the present study, fatigue crack growth tests of three kinds of ferrite-pearlite steels with networked, distributed and banded pearlite morphologies were carried out under a constant delta K in the stage IIb regime. During the fatigue tests, detailed in-situ SEM observation of crack growth behavior was conducted. The results obtained suggest some possibilities of microstructural control for improving the fatigue crack growth resistance of steels.

10:50 AM

Superior High Cycle Fatigue Properties of a New High Strength 2026 Al Alloy: *Tongguang Zhai*¹; Jinxia Li¹; Matthew Garratt²; Gary Bray²; ¹University of Kentucky; ²Alcoa Technical Center

High cycle fatigue was performed on new generation Al alloys, AA 2026, using a self-aligning four-point bend rig, at 20 Hz, R=0.1, room temperature in air. The alloy, developed based on the traditional AA 2024 Al alloys, was hot extruded, and processed to a T3511 condition (solutionized, water quenched, stretched by 1-3% and naturally aged). It was found that the AA 2026 alloy exhibited a fatigue limit of 334 MPa, 90% its yield strength (372 MPa), compared to typically 140 MPa, 43% the tensile yield strength (326 MPa) for an AA2024 Al alloy in a same temper condition. The superior fatigue strength of the 2026 alloy was likely to be attributed to the fewer Fe-containing particles (preferred crack nucleation sites), large crack deflection and plywood-like or fibril grain structure in this alloy. Such grain structure gave rise to crack deflection at grain boundaries, which slowed down growth of fatigue cracks.

11:15 AM

Self-Generated Thermal Fingerprint of Fatigue Damage Process: *Bing Yang*¹; Peter K. Liaw²; J. Y. Huang³; R. C. Kuo³; J. G. Huang⁴; ¹Oak Ridge National Laboratory; ²University of Tennessee; ³Institute of Nuclear Energy Research; ⁴Taiwan Power Company

It has always been a great temptation in finding new methods to in-situ "watch" the material fatigue-damage processes so that in-time reparations

will be possible, and failures or losses can be minimized to the maximum extent. Realizing that temperature patterns may serve as fingerprints for stress-strain behaviors of materials, a state-of-art infrared (IR) thermography camera has been used to “watch” the temperature evolutions of reactor-pressure-vessel (RPV) steel “cycle by cycle” during 0.5 Hz low-cycle fatigue experiments in the current research. After using a combination of thermodynamics and heat-conduction theory, key issues in fatigue, such as in-situ stress-strain states, cyclic softening and hardening observations, and fatigue-life predictions, can be resolved by simply monitoring the specimen-temperature variation during fatigue. As a method requiring no special sample preparation or surface contact by sensors, thermography could open up wide applications for in-situ studying mechanical-damage processes of materials and components.

**General Abstracts: Light Metals Division:
Session III**

Sponsored by: The Minerals, Metals and Materials Society, TMS Light Metals Division, TMS: Aluminum Committee, TMS: Magnesium Committee, TMS: Reactive Metals Committee, TMS: Recycling Committee

Program Organizers: Jim McNeil, Novelis Inc; Neale R. Neelameggham, US Magnesium LLC

Thursday AM Room: 7D
March 16, 2006 Location: Henry B. Gonzalez Convention Ctr.

Session Chair: Dean M. Paxton, Pacific Northwest National Laboratory

8:30 AM

The Influence of Porosity on Compressive Behavior of Closed Cell Aluminum Foams: *Haijun Yu*¹; *Guangchun Yao*¹; *Bing Li*¹; *Hongjie Luo*¹; *Yihan Liu*¹; *Yong Wang*¹; ¹Northeastern University

A test is carried out for quasi-static compression of closed cell aluminum foams of different porosities, which is prepared by foaming in melt process. Its compressive stress-strain curves are determined, and its quasi-static compressive mechanic behaviour is studied. The result shows that the compressive process of closed cell aluminum foams is similar to that of brittle material; its stress-strain curves are indented. The compressive strength of closed cell aluminum foams decreases with the increase of the porosity.

8:55 AM

Factors Influence the Preparation of Foam Aluminum by Powder Metallurgy Method: *Guo Zhiqiang*¹; *Yao Guangchun*¹; *Liu Yihan*¹; ¹Northeastern University

Foam aluminum is new functional material that has been developed in recent years. In this paper several major factors that influence the process of preparation of foam aluminum by powder metallurgy method were studied: amount of foaming agent, pressure, foaming temperature, protection condition and the amount of additive and so on. Optimal conditions were concluded through the analysis of the foaming process of Al-Si-Ca alloy which has high viscosity thus can improve the stability of foam. The relationships and effects of the factors in the process of the preparation of foam aluminum were studied. It was found out that the pressure is the crucial factor in the foaming process.

9:20 AM

Analysis of Cause of Defect Forming in Aluminum Foam: *H. J. Luo*¹; *G. C. Yao*¹; ¹Northeastern University

Aluminum foam is one of new materials that are of great interest. Aluminum foam is fabricated by foaming in aluminum melt technique in this paper. The above technique is easier than the others in preparing aluminum foam and in which the bigger plate or block of aluminum foam can be made, but inner defect of foam body occurs easily, such as contracted hole, crack and big bubbles, etc. The cause of defect formation is analyzed and the method that avoided these defects is put forward in the paper.

9:45 AM

Study on Preparation of Aluminum Foam Sandwich and Combination Mechanism on Steel Plate/Foam Core Interface: *Zhang Min*¹; *Yao Guangchun*¹; *Yi-Han Liu*¹; ¹Northeastern University

Aluminum foam has shown a popular interest in recent years and is potentially used for many applications due to its light weight structure. As engineering structures, aluminum-foam sandwiches have super-light weight and high stiffness and strength. In this paper aluminum-foam sandwiches were manufactured by a Al-Si-Ca alloy powder and two steel plates rolling and foaming process. In this rolling and foaming process, steel-aluminum foam interface was bonded by alloyed process. Asymmetric foaming problem of aluminum foam core was investigated, alloyed combination process between steel plate and aluminum foam core before and after foaming was analyzed. And three combination mechanism was established. By diffusion a good metallic combination in skin-foam core interface was formed.

10:10 AM

Study on the Process of Increasing Viscosity for Producing Foam Aluminum by the Powder Metallurgy Method: *Wei Li*¹; ¹Shenyang Ligong University

Some of the factors which affect the foaming in a foamed aluminum casting process and microstructural evolution of metal foams have been investigated by applying the powder compact process in many literatures. But few studies on the effect of viscosity of the molten and on the mechanisms stabilizing the pore formation have been undertaken. In this paper, foamed aluminum was preparation by powder metallurgy, the viscosity of the liquid metal was adjusted by Ca-addition into the metal, resulting in improvement of stabilization of bubble and uniformity of pore microstructure. The mechanisms stabilizing of the pore formation have been investigated, and the effect of Ca addition on porosity and pore microstructure is studied. Moreover, it has been proved that the effect of viscosity on the stabilizing of the molten is more important than oxide layer by means of dynamic observation on foaming course.

10:35 AM

Application of Thread-Forming Fasteners in Net-Shaped Cast Holes in Lightweight Metal Alloys: *Dean M. Paxton*¹; *Greg J. Dudder*¹; *John Reynolds*²; *William Charron*³; *Todd Cleaver*⁴; ¹Battelle - Pacific Northwest National Laboratory; ²Research Engineering and Manufacturing, Inc.; ³Ford Motor Company; ⁴Tech Knowledge

The application of thread-forming fasteners (TFFs) in net-shaped cast holes of lightweight materials is being explored by the United States Automotive Materials Partnership (USAMP) through work at the Pacific Northwest National Laboratory (PNNL). Progress has been made applying TFFs in drilled hole applications for general assembly, and have reduced costs, reduced investment, and improved warranty while delivering comparable joint properties in an assembly. Successful application of TFFs in aluminum and magnesium alloy cast products with net-shaped holes will expand the use of lightweight materials due to the proven benefits already achieved in existing applications. This effort includes a parametric study of the relationship between joint strength and fastener reusability versus as-cast hole geometry in lightweight alloy test specimens. The strength of these thread-forming fastener joints with net-shape holes will be compared with two baseline joints, namely standard machine fasteners in tapped holes and thread-forming fasteners in drilled holes.

11:00 AM

Surface and Subsurface Damage in Al-Si Alloys Subjected to Lubricated Sliding Wear: *Mustafa Elmadagli*¹; *Ming Chen*¹; *Ahmet Alpas*¹; ¹University of Windsor

Wear and surface damage during lubricated wear of a eutectic Al-Si (12% Si) have been studied and compared with those of the two hypereutectic alloys, an A390 alloy (18.5%Si) and a spray formed alloy (25%Si). The roles of second phase particle fracture and matrix material deformation and transfer on the wear resistance of the alloys have been studied through single pass scratch tests under both dry and oil lubricated conditions. Multi-pass sliding wear tests were also performed using ball-on-disk configuration. Sample surfaces were etched with 10% NAOH solution in order to expose the hard phases. The fracture toughness of secondary phases in these alloys was estimated using micro-hardness tests and

nano-indentation tests. Wear mechanisms will be discussed based on the observations made using focused ion beam, SEM, and a non-contact optical profilometer.

General Abstracts: Structural Materials Division: Microstructure and Properties of Materials II

Sponsored by: The Minerals, Metals and Materials Society, TMS Structural Materials Division, TMS: Alloy Phases Committee, TMS: Biomaterials Committee, TMS: Chemistry and Physics of Materials Committee, TMS/ASM: Composite Materials Committee, TMS/ASM: Corrosion and Environmental Effects Committee, TMS: High Temperature Alloys Committee, TMS/ASM: Mechanical Behavior of Materials Committee, TMS/ASM: Nuclear Materials Committee, TMS: Product Metallurgy and Applications Committee, TMS: Refractory Metals Committee, TMS: Advanced Characterization, Testing, and Simulation Committee, TMS: Superconducting and Magnetic Materials Committee, TMS: Titanium Committee

Program Organizers: Rollie E. Dutton, U.S. Air Force; Ellen K. Cereta, Los Alamos National Laboratory; Dennis M. Dimiduk, U.S. Air Force

Thursday AM Room: 218
 March 16, 2006 Location: Henry B. Gonzalez Convention Ctr.

Session Chair: Patrick L. Martin, U.S. Air Force

8:30 AM

Effects of Chromium Concentration on Oxidation and Melting of Ni-Al-Pt-based Alloys: *Donna L. Ballard*¹; Brian Gleeson²; Sarath Menon³; Patrick Martin¹; ¹U.S. Air Force; ²Iowa State University; ³Universal Energy Systems, Inc

Chromium has long been seen as a beneficial elemental addition to Ni-based superalloys for oxidation resistance. This will be shown to be particularly true for model Pt-modified γ -Ni+ γ' -Ni₃Al alloys. However, recent results also indicate that increasing chromium concentration can also be deleterious to bulk alloy melting temperatures. Data will be presented showing the differences in melting temperature ranges for Pt-modified γ - γ' alloys with 0-10 at.% Cr addition. These effects will be described and related to their impact on attaining chemical homogeneity in cast buttons.

8:55 AM

Metal Ion Migration through Surface Oxides on NiTi Alloys: *Emma Jane Minay*¹; Gerdjan Busker²; ¹Imperial College; ²ClusterVision Ltd

The most widely used shape memory and superelastic alloy, NiTi, is finding increasing use in a diverse range of long and medium term medical implants including orthodontic components, orthopedic implants and stents. Ni ions are known to have allergic, toxic and carcinogenic effects and hence metal ion release from NiTi is of considerable concern. Experimentally, various single and multiphase oxide films can be formed on NiTi including rutile, anatase, brookite, NiO and nickel titanium oxides. It is generally felt that the production of a TiO₂-type surface film is desirable as this is known to have excellent biocompatibility, being the surface phase present on Ti and Ti-alloy biomaterials. In this paper solution and migration energies of various defects and ions in these oxide coatings have been determined with the aim of determining the most appropriate surface oxides to minimize Ni ion diffusion and ultimate release into the physiological environment.

9:20 AM

Relationship between Morphological Evolution of the γ/γ' Microstructure and Creep Behavior of Ni-Based Single Crystal Superalloys: *Pierre Caron*¹; ¹Onera/DMMP

In the high temperature regime ($T > 900^\circ\text{C}$), the creep behavior of the single crystal nickel based superalloys for turbine blade applications is strongly dependent on the morphological evolution of the strengthening γ' particles. In particular, the topological inversion of the γ/γ' rafted microstructure is generally associated with the increase of the creep rate which precedes the final tertiary creep stage. This phenomenon of topological inversion where the initially dispersed γ' phase becomes progres-

sively the matrix was analyzed in a series of single crystal superalloys deformed in creep at temperatures above 1050°C. The aim was to establish relationships between this phenomenon and the chemistry, the volume fraction of γ' phase and the creep behavior of these alloys.

9:45 AM

Metallurgical and Corrosion Behavior of Refractory Materials for Hydrogen Generation: Ajit K. Roy¹; *Ancila V. Kaiparambil*¹; Radhakrishnan Santhanakrishnan¹; ¹University of Nevada, Las Vegas

Hydrogen production using nuclear power is one of the alternate steps being considered by the United States Department of Energy to meet the growing energy crisis. Thermochemical cycle such as the sulfur-iodine process is among the leading technologies presently under consideration. Recently, some refractory materials have been identified as candidate structural materials for heat exchangers to be used in the hydrogen generation. Zr705 have been evaluated for its tensile properties at temperatures ranging between ambient and 400°C. The cracking susceptibility of this material has been determined in an environment relevant to the hydro-iodic acid decomposition process using constant-load and slow-strain-rate techniques. Cyclic potentiodynamic polarization technique has been used to evaluate the susceptibility of this material to localized corrosion in a similar environment. The metallographic and fractographic evaluations of all tested specimens have been performed by optical microscopy and scanning electron microscopy, respectively. This paper presents the comprehensive test results.

10:10 AM Break

10:25 AM

The Effects of Post Heat Treatment in Thermally Sprayed Superfine WC-Co Coatings: *Seongyong Park*¹; Changyung Park¹; Munchul Kim²; ¹Pohang University of Science and Technology; ²Research Institute of Industrial Science and Technology

WC-Co coatings with superfine carbide particles near the size of 100nm were fabricated by detonation gun spraying. Fabricated superfine WC-Co coatings showed improved hardness and wear resistance than those of conventional WC-Co coatings. The sprayed superfine coatings, however, revealed degraded properties compared with sintered superfine WC-Co bulk. The degradation of properties are explained as phase decomposition of WC to W₂C and amorphous phase due to exposure of carbide particles to high temperature detonation flame during spraying and rapid quenching after spraying. In order to improve the mechanical properties of the coatings by recovering of carbide phases, post heat treatment was conducted in vacuum environment at temperature range of 400–900°C. The improved properties of coatings were elucidated in terms of microstructural changes and the relationship between mechanical properties and phase of carbide was also discussed.

10:50 AM

Performance of Alloy 800H at Elevated Temperature for Heat-Exchanger Application: Ajit K. Roy¹; *Vinay Virupaksha*¹; ¹University of Nevada, Las Vegas

The structural materials for high-temperature heat exchangers to generate hydrogen using nuclear power must possess excellent resistance to environment-induced degradations and superior high-temperature metallurgical properties. A primary water splitting cycle known as sulfur-iodine (S-I) process consisting of chemical reactions leading to the production of hydrogen is presently under consideration. Nickel-base austenitic Alloy 800H has been identified as a structural material for heat exchanger to be used in the nuclear hydrogen generation. Since Alloy 800H will be subjected to very hostile environmental conditions, the susceptibility of this material to stress-corrosion-cracking, hydrogen-embrittlement and localized corrosion has been determined by state-of-the-art experimental techniques. The tensile properties of Alloy 800H have also been determined at temperatures ranging from ambient to 600°C. Scanning electron microscopy has been used to characterize the failure morphology of the tested specimens. Metallographic evaluations has been performed using optical microscopy. The overall data will be presented in this paper.

11:15 AM

The Effect of Heat Damage on the Mechanical Properties of 2014-T6, 2024-T3, 6061-T6, 7050-T6, and 7075-T6: Tomas Oppenheim¹; Kevin

Robinson¹; Nick Neylan¹; Rick Clark¹; *Omar Es-Said*¹; John Ogren¹;
¹Loyola Marymount University

In the past couple of months, the Navy in San Diego has been having technical problems with their F-18's. Hot Exhaust began bleeding into the center barrel compartment, weakening the surrounding metal. The Navy had to ground several planes as a result of this. The Navy wants to examine the change in mechanical properties and electrical properties of five Aluminum alloys (7050-T6, 6061-T6, 7075-T6, 2014-T6, 2024-T3) after varying the thermal exposure times (1 min, 10 min, 30 min, 1 hr, 3 hr, 10 hr, 1 day, 10 day, 20 day) and temperatures (350F, 400F, 500F, 600F, 700F, 800F, 900F). Correlations between the yield and ultimate strength and the hardness and conductivity will be made. The Navy would like to use a non-destructive test such as the hardness and conductivity test and correlate the data to the yield and ultimate strength. This will help them prevent future problems.

11:40 AM

Microstructure and Mechanical Properties of Investment Cast Ti-6Al-4V: *Lawrence S. Kramer*¹; Hao Dong¹; Kevin L. Klug¹; Ibrahim Uocok¹; Laurentiu Nastac¹; Mehmet N. Gungor¹; Wm. Troy Tack¹; ¹Concurrent Technologies Corporation

The microstructures and mechanical properties of investment cast Ti-6Al-4V have been studied as a function of casting thickness, weld-repair and heat treatment. Standard metallography and scanning electron microscopy fracture analysis techniques were utilized to characterize the material specimens. The microstructure study was focused on the size and distribution of prior- β grains, and on a/b phase morphology and distribution. Tensile and fatigue tests were performed on specimens extracted from cast components as well as on separately cast coupons and plates. Metallography and fractography were conducted on selected tensile and fatigue specimens. The results of these investigations are discussed as a function of section thickness, weld repair and heat treatment. This work was conducted by the National Center for Excellence in Metalworking Technology, operated by Concurrent Technologies Corporation under Contract No. N00014-00-C-0544 to the Office of Naval Research as part of the U.S. Navy Manufacturing Technology Program.

12:05 PM

Effects of Thermal Aging on 6061-T6 Aluminum Alloy: *Wail Salim Dahir*¹; Dalal S. Hassouna²; Bryan M. Gayer¹; Omar S. Es-Said³; Richard Clark⁴; John Ogrin³; ¹Los Angeles Unified School District; ²New Horizon School; ³Loyola Marymount University; ⁴College of the Canyons

The influence of varying the thermal aging parameters on the physical and mechanical properties of 6061-T6 aluminum alloy was studied. The variables altered were heat exposure to temperatures ranging from 120-230°C in 10 degree intervals over variable ranges of time from 5-30 minutes in 5 minute intervals. This envelope was chosen to encompass the range of conditions used in the curing of a proprietary powder coating on an aluminum alloy. The purpose of this work is to determine whether or not the curing process for the coating in any way degrades the properties of the aluminum alloy. The influence of varying these parameters on the tensile strength, electrical conductivity, and hardness of the alloy is discussed and correlated. The completion of low temperature testing revealed no significant changes, while higher temperature exposures revealed degradation in the properties of the samples. A correlation between hardness and yield and hardness and ultimate yield is presented.

Magnesium Technology 2006: Alloy Development II

Sponsored by: International Magnesium Association, TMS Light Metals Division, TMS: Magnesium Committee

Program Organizers: Alan A. Luo, General Motors Corporation; Neale R. Neelameggham, US Magnesium LLC; Randy S. Beals, DaimlerChrysler Corporation

Thursday AM
 March 16, 2006

Room: 6B
 Location: Henry B. Gonzalez Convention Ctr.

Session Chairs: Wayne Jones, University of Michigan; Per Bakke, Hydro Aluminium

8:30 AM

Behavior of Alkaline Earth Metal Oxides in Magnesium Alloys: *Shae K. Kim*¹; Jin-Kyu Lee¹; ¹Korea Institute of Industrial Technology

Magnesium alloys are gaining increased importance for many applications. Their range of applications could be further extended if their safety and elevated temperature properties were improved without damaging their original properties and increasing cost. The aim of this research is to manufacture CaO or SrO added magnesium alloys in terms of 1. increasing burning temperatures of alloys for ensuring safety during manufacturing and application, 2. reducing protection gas amount during melting and casting, 3. eliminating protection gas during forming processes of extrusion and rolling, etc., 4. maintaining or improving elevated temperature properties with lower amount of Ca or Sr than conventionally developed high-temperature magnesium alloys, 5. easy alloying of inexpensive CaO or SrO instead of expensive Ca or Sr with high oxidation tendency even during alloying. In this paper, effects of CaO or SrO on burning phenomena, oxidation resistance and optimum cover gas usage of magnesium alloys were evaluated.

8:55 AM

Computation of Local Constitutive Equations for Eutectic and Mg-Rich Dendritic Regions in High-Pressure Die-Cast AE44 Alloy: *Arun Sreeranganathan*¹; Arun M. Gokhale¹; ¹Georgia Institute of Technology

For modeling and simulations of the micro-mechanical and mechanical response of high-pressure die-cast Mg-alloy components, it is essential to have reliable quantitative data on the local constitutive behavior of various constituents (for example, eutectic region, Mg-rich dendrites, etc.) present in the microstructure. It is not possible to get such data from macro-scale mechanical tests. In this contribution, we present application of micro-indentation technique for computation of local stress-strain behavior of the eutectic constituent and Mg-rich dendrites in a high pressure die-cast AE44 alloy. The local constitutive equations of these constituents are computed through solution to an inverse problem using finite element (FE)-based numerical analyses. The computed constitutive equations are then utilized to simulate the overall global mechanical response of virtual alloys having different amounts of eutectic and dendritic constituents.

9:20 AM

Effect of Sr Additions on the Microstructure and Mechanical Properties of Mg-Al-Ca Alloys: *Akane Suzuki*¹; Nicholas D. Saddock¹; J. Wayne Jones¹; Tresa M. Pollock¹; ¹University of Michigan

The effect of Sr additions on the microstructure and mechanical properties was investigated in Mg-5Al-3(Ca, Sr) and Mg-4Al-4(Ca, Sr) quaternary alloys (wt%). The Mg-5Al-3(Ca, Sr) quaternary alloys consist of the dendritic α -Mg phase and intermetallic phases, C36-(Mg, Al)₂Ca and Mg₁₇Sr₂, along the grain boundaries. The Mg₁₇Sr₂ phase forms with the addition of more than 0.25wt% Sr. The mechanical properties of these alloys were tested in compression at room temperature and 448 K. At both temperatures, the flow stress exhibited a minimum at 0.5wt% Sr. The effect of Sr additions on the flow stress will be discussed from the viewpoints of intermetallic compounds at grain boundaries and the solid-solution strengthening of the α -Mg phase.

9:45 AM

Effects of Alloying Elements on Microstructures and Mechanical Properties of Mg-Mm-RE Alloy System: *Hyun Kyu Lim*¹; Ju Yeon Lee¹; Tae Eung Kim¹; Won Tae Kim²; Do Hyang Kim¹; ¹Yonsei University; ²Cheongju University

Although aluminum and zinc elements have been used as the most favorite alloying elements in magnesium alloys, their usage has been limited when the improvement of high temperature is required due to their lower eutectic temperatures. It has been reported that the addition of rare earth (RE) elements improves elongation as well as strength, thus improving high temperature formability. In the present study, the effects of rare earth elements, especially neodymium and yttrium, on Mg-Mm (Ce-based misch-metal) system have been investigated by observing the microstructures and mechanical properties. Moreover, we evaluated the properties of Mg-Mm-RE-X (X: Zn, Sn and In) alloy system. For example, the Mg-Re-Nd-Zn alloy sheet exhibited high yield strength and elongation at room temperature. Specimens have been fabricated by a hot-rolling method and tensile properties at ambient and elevated temperatures have been investigated. Phase identifications have been performed by X-ray diffraction and transmission electron microscope.

10:10 AM

Microstructure and Mechanical Properties of Mg-Zn-Si Wrought Alloys: *Kwang Seon Shin*¹; Ji Hoon Hwang¹; Young Gee Na¹; Dan Eliezer²; ¹Seoul National University; ²Ben-Gurion University of Negev

Mg-Zn alloys have a large age hardening response, stemming from the precipitation of a transition phase (β'). The objective of this study is to develop new wrought Mg alloys with improved strength based on the Mg-Zn alloy. The effects of Si addition on the microstructure and mechanical properties of the Mg-Zn alloys were investigated. The addition of Si introduces the intermetallic compound, Mg₂Si, which has high hardness and melting point, and thus improves the mechanical properties of the Mg-Zn alloys. However, it was found that the addition of more than 2 wt.% Si deteriorated the tensile properties of the Mg-Zn alloys, due to the occurrence of premature fracture along the interface between the polygonal Mg₂Si particles and the Mg matrix. It was also found that the double aging treatment after extrusion and solution heat treatment significantly increased both yield and tensile strengths of the ZS alloys, but at the expense of tensile ductility.

10:35 AM Break

10:55 AM

Effect of Ca, Sr, and Zn on Phase Stability in Mg-Al Based Alloys: *Yu Zhong*¹; Alan A. Luo²; Zi-Kui Liu¹; ¹Pennsylvania State University; ²General Motors Research and Development Center

Mg-Al based alloys are one group of the most popular magnesium-based alloys that are under development. The AM series with 2-6% Al and the AZ91 alloy offer good performance at room temperature. They have poor creep resistance at temperatures over 100°C, largely due to the g-Al₁₂Mg₁₇ phase. The additions of Ca and Sr into AM and AZ series alloys have been found to be beneficial not only to keep costs low but also to improve the mechanical properties, especially the creep resistance at elevated temperatures. In the present work, the effect of Ca, Sr, and Zn on phase stability of Mg-4.5wt.%Al alloy were investigated through thermodynamic modeling of the multicomponent system and by means of Scheil simulation and equilibrium calculations. Good agreement with available experimental observations was achieved. Proper Ca and Sr additions reduce the stability of g-Al₁₂Mg₁₇ in Mg-4.5wt.%Al alloys, while Zn addition does not.

11:20 AM

Microstructure and Thermal Response of Mg-Sn Alloys: Okechukwu Anopuo¹; Yuanding Huang¹; *Norbert Hort*¹; Carsten Blawert¹; Karl Ulrich Kainer¹; ¹GKSS Research Centre

The future demand for light weight constructions requires alloy development to achieve an appropriate combination of mechanical properties and corrosion behavior of modern magnesium alloys. Therefore a new class of magnesium alloys based on the Mg-Sn system has been developed. Besides the combination of alloying elements in the new Mg-Sn alloys the property profile is ruled by the development of microstructure during solidification and subsequent heat treatments. To obtain deeper

knowledge of the occurring phases Mg-Sn-Ca and Mg-Sn-Si alloys have been investigated in the F, T4 and T6 condition by means of electron microscopy, XRD and Vickers hardness to determine phases in accordance to the as cast and heat treated conditions. These experiments have been accompanied by the investigation of the corrosion behavior using salt spray tests and potentiodynamic measurements.

11:45 AM

Effects of Minor Addition and Cooling Rate on the Microstructure of Cast Magnesium - Silicon Alloys: *Patrick D. Quimby*¹; Shu-Zu Lu; ¹Michigan Technological University

Minor additions of antimony, calcium, sodium, and phosphorus were added to Mg-Al-Si alloys with the intention of refining/modifying the microstructure, thereby increasing its mechanical properties. The high cooling rate of the die-casting process was simulated using a graphite wedge mould. The effects of cooling rate and minor addition on the microstructure of both Mg-Si hypoeutectic (AS21) and hypereutectic Mg-3%Si-2%Al cast alloys were examined. It was found that antimony does not show any obvious refinement or modification effect, sodium shows some limited modification, while phosphorus and calcium show a significant refinement and modification effect on both primary and eutectic Mg₂Si phase. This may lead to the development of low cost, high temperature creep-resistant and wear resistant magnesium alloys for the automotive industry.

Magnesium Technology 2006: Welding and Joining

Sponsored by: International Magnesium Association, TMS Light Metals Division, TMS: Magnesium Committee

Program Organizers: Alan A. Luo, General Motors Corporation; Neale R. Neelameggham, US Magnesium LLC; Randy S. Beals, DaimlerChrysler Corporation

Thursday AM
March 16, 2006

Room: 6A
Location: Henry B. Gonzalez Convention Ctr.

Session Chairs: Naiyi Li, Ford Motor Company; Dan Eliezer, Ben Gurion University of Negev

8:30 AM

Effect of Grain Refinement on the Strength and Corrosion of Magnesium Alloy AZ31 Weld Metal: *Dan Eliezer*¹; Carl E. Cross²; Thomas Boeelinghaus²; ¹Ben Gurion University of Negev; ²Joining Div V5-BAM

Gas tungsten arc welds made on wrought magnesium AZ31 plate have been characterized for corrosion in saline solution (3.5% NaCl). Microstructural changes induced by the welding process resulted in different environmental behaviour of each zone (BM-base metal, HAZ-heat affected zone and FZ-fusion zone). The faster kinetics of corrosion in FZ and especially HAZ are attributed to (a) the coarse microstructure, consisting of large grains, and (b) very small amounts of β -phase in the grain boundaries. Also, hardness traverses have shown that these zones are weaker than the base metal. Based on the significant effect of grain size on strength in magnesium alloys, the weld metal grains have been systematically refined using controlled oscillation during welding, and by adding a grain refiner to the weld pool. Detailed microstructure analyses have been carried out and the relationships between corrosion behaviour, mechanical properties and microstructure (grain refinement and second-phases formation) are highlighted.

9:00 AM

Friction-Stir and Surface-Friction Welding of Twin-Roll Strip Cast Mg Alloy Sheets: Sung S. Park¹; C. D. Yim²; C. G. Lee²; Nack J. Kim¹; ¹Pohang University of Science and Technology; ²Korea Institute of Machinery and Materials

Mg alloys have the great potential for automotive applications mainly due to their low density and high specific strength. Recent development of twin-roll strip casting technology has shown that it can efficiently produce low cost, high performance wrought Mg alloy sheets. For the successful application of twin-roll strip cast Mg alloys, however, cost-effec-

tive and reliable ways of joining are needed. The present research is aimed at investigating the response of twin-roll strip cast Mg alloys to friction stir welding (FSW). In addition to FSW, surface friction welding (SFW), novel welding technique suited for thin sheets, has also been investigated. Two twin-roll strip cast alloys, AZ31 alloy and dispersion strengthened ZMA611 alloy, were subjected to FSW and SFW. Microstructure and mechanical properties of welded alloys will be discussed with respect to the effects of alloying elements and welding conditions. Comparison will also be made with commercial ingot cast AZ31 alloy.

9:30 AM

Micro-Alloying of Magnesium Wrought Alloys for Improved Electro-Magnetic Joining of Extruded Hollow Profiles: *Martin Bosse*¹; Friedrich-Wilhelm Bach¹; ¹University Hanover

Due to their low density, sufficient stability and high recycling potential, magnesium alloys offer an important potential as structural component in automotive and rail vehicle structures. In order to push the application of magnesium profiles in lightweight constructions, intensive research regarding an appropriate joining technology and the processing of alloys, which have to be adapted to this joining technology, is required. Therefore the essential aim of IW in the presented joint research project of the German Research Foundation (DFG) is to develop and characterize new alloys for joining extruded hollow profiles by electro-magnetic deformation. The electrical conductivity and formability of the base materials are of special importance for the electro-magnetic forming process. Therefore low-content wrought alloys are suited for the optimization by micro-alloying. Starting from known magnesium wrought alloys of the categories AZ, ZEK and ZME modified alloys are developed by addition of alloying elements such as calcium and zircon.

10:00 AM

The Laser Welding Characteristics of AZ31 Mg Alloy by Continuous Rolled for Automobile: *Mok-Young Lee*¹; Woong-Seong Chang¹; Byung-Hyun Yoon¹; Yeong-Gak Kweon¹; ¹Research Institute of Industrial Science and Technology

Magnesium alloys are becoming important material for light weight car body, due to their low specific density but high specific strength. However they have a poor weldability, caused high oxidization tendency and low vapor temperature. In this study, the welding performance of magnesium alloys was investigated for automobile application. The material was continuously rolled magnesium alloy sheet contains 3% Al and 1% Zn. Mg alloy sheets were welded using high power continuous wave Nd:YAG laser according to process parameters such as laser output power, travel speed, shielding conditions. The mechanical properties were evaluated for laser welded specimen and the microstructure was investigated also. For the results, the tensile properties of welded specimen were decreased obviously. The surface of welding bead was covered with oxidized magnesium dust but it was removed by simple cleaning work as wipe-out with paper tissue. Also under cut, that caused vaporization of base metal was occurred.

10:30 AM Break

11:00 AM

Intergranular Strains in the Dynamic Recrystallized Zone of a Friction-Stir Processed AZ-31B Magnesium Alloy: *Wanchuck Woo*¹; H. Choo¹; D. W. Brown²; Z. Feng³; P. K. Liaw¹; S. A. David³; C. R. Hubbard³; Mark M. A. Bourke²; ¹University of Tennessee; ²Los Alamos National Laboratory; ³Oak Ridge National Laboratory

Friction-stir processing (FSP) is a solid-state joining technique, which creates a strong bond through the frictional heating and severe plastic deformation. The heat and plastic deformation, however, can induce a significant amount of the residual stresses, which may approach the yield point of the base material and cause a drastic increase in the crack-growth rate. In the present study, the residual strains were measured using the spallation neutron source in a FSP AZ-31B magnesium alloy plate. The residual intergranular stresses were observed in the dynamic recrystallized zone, which has experienced the severe plastic deformation, using 2 x 2 x 2 mm 3 dimension of macroscopic-stress-released coupons taken out of the FSP plate. The results of the macroscopic stresses, intergranular strains, and other properties (e.g., chemical compositions, textures, tensile properties, and hardness) of FSP AZ-31B will be discussed.

11:30 AM

Interface Chemistry and Mechanical Behavior of Fe Base Metals/Magnesium Alloys Assemblies: *Myriam Sacerdote-Peronnet*¹; Jean-Claude Viala¹; ¹University of Lyon

Bimetallic joints resulting from the association of Mg alloys and ferrous substrates are interesting in the scope of manufacturing low-weight components for the automotive and aeronautic industries. To obtain assemblies with optimized properties, it is necessary to acquire a thorough understanding of their interface chemistry and mechanical properties. The interface reactivity of different Fe/Mg-M systems (M=Al, Si, Mn, Zn, Zr is an alloying element of magnesium) was studied by two complementary approaches: determination of the phase equilibria in the ternary systems at 730°C, characterization of the reaction zones formed at the interfaces. Synthetic Mg-M alloys and commercial magnesium alloys: GA6Z1, GM2, M2 and RZ5 were used. We determined the growth kinetics and mechanism at these interfaces. Mechanical characterizations were carried out ("push-out"). We will point out the relations existing between the mechanical behaviour of the assemblies and the composition of the corresponding reaction zones.

Phase Stability, Phase Transformation and Reactive Phase Formation in Electronic Materials V: Damage Structures: Ni Plating, Tin Whiskers and Thermal Cycling

Sponsored by: The Minerals, Metals and Materials Society, TMS Electronic, Magnetic, and Photonic Materials Division, TMS Structural Materials Division, TMS: Alloy Phases Committee
Program Organizers: Katsuaki Suganuma, Osaka University; Douglas J. Swenson, Michigan Technological; Srinivas Chada, Jabil Circuit, Inc.; Sinn Wen Chen, National Tsing-Hua University; Robert Kao, National Central University; Hyuck Mo Lee, Korea Advanced Institute of Science and Technology; Suzanne E. Mohny, Pennsylvania State University

Thursday AM
March 16, 2006

Room: 213B
Location: Henry B. Gonzalez Convention Ctr.

Session Chairs: Srinivas Chada, Jabil Circuit, Inc.; K. N. Subramanian, Michigan State of University

8:30 AM

High Energy Synchrotron X-Rays Study of Service-Related Damages in Lead-Free Solders: *K. N. Subramanian*¹; Deep Choudhri¹; Andre Lee¹; ¹Michigan State University

Due to its geometry, solder joint is modeled as a highly constrained, heterogeneous, layered composite. When exposed to external fields, highly inhomogeneous stresses arise in a very heterogeneous manner. The observed surface damage appears after a few hundred TMF cycles and intensified on further TMF cycling. However, effect of TMF on residual performances of joint is quite the opposite to the observed surface damage. Rapidly decreases in properties occur after few cycles, a stage with no visible surface damage, and then stabilize after several hundred cycles, a stage in which surface damage intensifies to form the catastrophic crack. Obviously, the surface damages cannot be used to predict the service reliability of solders. Using the high penetration depth of high-energy synchrotron X-rays, we examined the internal changes in tin-based electronic solder joints. X-ray results gave a more complete picture of internal changes in solder joints relating to applied fields.

8:55 AM

Impact of Thermal Cycling on Intermetallic Growth and Void/Crack Formation for SAC/ENIG PBGA Solder Joints: *Luhua Xu*¹; John H. L. Pang¹; Faxing Che¹; ¹Nanyang Technological University

Intermetallic growth and interfacial voids/crack formation between SAC/ENIG solder joint in 3161/O PBGA soldered assembly subject to thermal cycling are reported. The IMC thickness was measured on all solder joints and plotted vs location. Higher thickness was observed at the outermost solder after 1000 to 3000 thermal cycles. IMC growth under thermal cycling is faster than isothermal aging and subject to the loca-

tions. This indicates that thermal stress might accelerate element diffusion. The interfacial failure was commonly found at the component side of outmost solder joint. Voids/crack forms not only at the joint corners but also at the center of the interface. Coalescence of multiple voids causes the final breakdown. Young's Modulus of IMCs was characterized by Nanoindentation after different cycles. The modulus reduced from 180-200GPa to 130-150GPa after 3000 cycles. The impact of IMC thicknesses and Young's modulus was analyzed by Finite Element Modeling and shows different fatigue lifetime.

9:20 AM

The Kinetics of AuSn₄ Migration in Solders: *Chien Wei Chang*¹; C. E. Ho¹; C. Robert Kao¹; ¹National Central University

The fast migration of Au atoms in eutectic PbSn matrix was known as one of the main factors contributing to the Au embrittlement phenomenon in solder joint. In this study, we investigate whether such behavior also occurred in high-tin lead-free solders. Experimentally, Sn3.5Ag (wt.%) spheres with 500 microns diameter was soldered on BGA Au/Ni pads. It was found that those AuSn₄ also migrated back to the solder/pad interface during thermal aging, and formed discontinuous or continuous layer at solder/pad interface. The AuSn₄ layer became continuous when the Au in Au/Ni was thick. Finally, a simple sandwich structure of Au(1 micron)/Sn(100microns)/Ni was applied to study the kinetics of Au migration in tin-matrix.

9:45 AM

Kirkendall Voids at Cu/Solder Interface and Their Effects on Solder Joint Reliability: *Zequn Mei*¹; Sue Teng¹; ¹Cisco Systems Inc

Recent studies, especially by Chiu et al and Date et al in the 2004 ECTC conference, demonstrate extensive Kirkendall voids at the interface of solder joint to Cu substrate, and their significant effects on the impact and shock strength of the solder joints. In this study, we focus on two issues, the condition for the void formation, and effect of voids on solder joint reliability. Samples of electronic assemblies of different packages aged or thermal cycled were cross-sectioned by either FIB or sputtering etching. The results show that voids at Cu/solder interface formed extensively in some cases, but not so much in others. So far, we are not clear exactly what factors control the void formation; it seems that the Cu plating process and the small concentration of Ni in either solder or substrate influences the void density and distribution. Shock strength at 400G of BGA packages aged for 20 days at 125°C did not degrade; the failure occurred by either delamination at the fiber/resin interface underneath the non-solder mask defined Cu pads, or inside the solder where close to the solder mask defined Cu pads. We also curve-fitted the Chiu's result of voids growth vs time at different temperatures with the equation of $A = C t^{0.5} \exp(-Q/RT)$, to use it for prediction of the voided area at the product service condition.

10:10 AM Break**10:20 AM**

Optimal Phosphorous Content Selection for Ni-P UBM with Sn-Ag-Cu Solder: *Yung-Chi Lin*¹; Jenq-Gong Duh¹; ¹National Tsing Hua University

The nickel plating has been used as the under bump metallurgy (UBM) in the microelectronic industry. In this study, the electroplated Ni-P UBM with different phosphorous content (7, 10, and 13wt%) was used to evaluate interfacial reaction during multiple reflow between Ni-P UBM and Sn-3Ag-0.5Cu solder paste. (Cu,Ni)₆Sn₅ IMC formed in the SnAgCu solder/Ni-P UBM interface during the first cycles of reflow. With increasing cycles of reflow up to 3 times, (Ni,Cu)₃Sn₄ IMC formed, while (Cu,Ni)₆Sn₅ IMC spalled into the solder matrix. With further increasing cycles of reflow, the Ni-Sn-P layer formed between (Ni,Cu)₃Sn₄ IMC and Ni-P UBM for Ni-10wt%P and Ni-13wt%P UBM. However, almost no Ni-Sn-P layer was revealed for the Ni-7wt%P UBM even after 10th cycles of reflow. In consideration of surface morphology, wettability of Ni-P UBM, and interfacial reaction of SnAgCu/Ni-P, the optimal phosphorous content selection of Ni-P UBM was decided and also discussed.

10:45 AM

Root Cause of Black Pad Defect of the Electroless Nickel/Immersion Gold Plating on BGA Pads: *Kejun Zeng*¹; ¹Texas Instruments

Presence of high phosphorous (P) content in the failed pad surface was often cited as the evidence for black pad defect of the ENIG plating. It was proposed to decrease the P content in the nickel plating. On the contrary, some companies are proposing to use high P content to avoid the black pad defect. In the present work, solder reaction with ENIG plating and the resulted interfacial structure are studied. FIB polishing was used to reveal details of the microstructure of the ENIG plated pad with and without soldering. High speed pull test of solder joints was performed to expose the pad surface. Results of SEM/EDX analysis of the cross sections and fractured pad surfaces suggest that the black pad is the result of the galvanic corrosion of the electroless nickel plating by the gold plating bath. High P content is not the signature of black pad.

11:10 AM

Microstructural Feature of "Black Pad" Ni-P/Sn-Pb Interface: *Katsuaki Suganuma*¹; Keun-Soo Kim¹; Naoya Murata²; ¹Osaka University; ²JEOL

The microstructure of back pad Au/Ni-P and its soldered interface was analyzed primarily by TEM. Seriously oxidized crack-like structure, which is localized, was observed under Au thin layer. This region has amorphous porous structure containing Cu as well as Ni and O. The oxidized region does not form intermetallic compounds at the interface while the sound Ni-P surface react to form Ni-Sn intermetallic growing into the solder layer with a P-rich layer into the original Ni-P plating. The degradation mechanism will be discussed based on the observation.

11:35 AM

Tin Whisker Prevention by Treatment of Substrate Surface Structure: *Makoto Takeuchi*¹; Kouichi Kamiyama¹; Katsuaki Suganuma²; ¹Victor Company Japan, Ltd.; ²Osaka University

Tin coating on Cu substrate will cause tin whisker formation resulting in short circuit damage. Fine pitch connectors have serious problem of forming tin whisker under a pressure caused by mechanical connection. The authors have developed a new process for the prevention of whisker formation. The authors focused on the surface chemical treatment of substrates. The surface chemical state has a great influence on whisker formation. The various chemical conditions of substrates, especially Cu, are analysed and the most influential treatment will be proposed.

12:00 PM

JEITA Whisker Testing Methods for Connectors: *Hiroyuki Moriuchi*¹; ¹Fujikura Ltd

JEITA has proposed a new testing method for tin whisker formation especially for fine pitch connectors. This paper describes the details of this method and various factors on whisker formation will be discussed. Mechanical compression stress influences on whisker growth rate. Whisker is growth in room temperature rapidly. Tin thickness also influences whisker growth. Testing parameters will be also discussed in this paper.

Phase Transformations in Magnetic Materials: Processing and Characterization

Sponsored by: The Minerals, Metals and Materials Society, TMS Materials Processing and Manufacturing Division, TMS/ASM: Phase Transformations Committee

Program Organizers: Raju V. Ramanujan, Nanyang Technological University; William T. Reynolds, Virginia Tech; Matthew A. Willard, Naval Research Laboratory; David E. Laughlin, Carnegie Mellon University

Thursday AM Room: 213A
March 16, 2006 Location: Henry B. Gonzalez Convention Ctr.

Session Chairs: Ganapathiraman Ramanath, Rennselaer Polytechnic Institute; Matthew A. Willard, Naval Research Laboratory

8:30 AM Invited

Effects of Large Magnetic Fields on FeCo-Based Alloys: Phase Transformations and Induced Anisotropy: Paul R. Ohodnicki¹; Yuranan Hanlumyung¹; David E. Laughlin¹; *Michael E. McHenry*¹; ¹Carnegie Mellon University

FeCo-based nanocrystalline/amorphous nanocomposites are interesting due to large saturation inductions and high Curie temperatures. Structure sensitive properties can be tailored by inducing magnetic anisotropy through field annealing resulting in reduced high frequency core losses. In addition to directional ordering in the crystalline and amorphous phases, it may be possible to induce anisotropy by establishing some crystallographic texture in the nanocrystals through large field crystallization. It is therefore desirable to understand the effects of strong magnetic fields on relevant phase equilibria to design thermomagnetic processing schedules. Models of field induced anisotropy through directional pair ordering in crystalline FeCo alloys using Monte Carlo simulations will be discussed taking into account the tendency for chemical ordering. Effects of applied fields on the equilibrium bulk FeCo phase diagram will also be discussed including a predicted shift in the critical temperatures with increasing field for first (bcc to fcc) and higher order (order-disorder) phase transitions. The authors gratefully acknowledge financial support from the National Science Foundation through award number DMR-0406220.

9:05 AM Invited

Search for Very Large Magnetocaloric Effects in Materials with Field-Induced Crystallographic Phase Changes: *Robert D. Shull*¹; Virgil Provenzano¹; Alexander J. Shapiro¹; ¹National Institute of Standards and Technology

It has been found in the recent past, initially in Gd₅Ge₂Si₂, that large magnetocaloric effects can be obtained in materials which possess a crystallographic phase change induced by the application of a magnetic field. As a consequence of this discovery, many investigators have looked for the next breakthrough in magnetic refrigerants exclusively in such systems. Unfortunately, this investigation model may not be correct as these same systems usually also possess large magnetic hysteresis losses which must be subtracted from the magnetocaloric effects to determine the material's usefulness. Recently, it was shown¹ that when such a subtraction is performed, the resulting refrigeration "capacity" is not as good as expected. Here a new model is presented for circumventing this "show stopper" by changing the phase equilibria of the system upon the addition of small amounts of an additional constituent. ¹V. Provenzano, A.J. Shapiro, and R.D. Shull, Nature 429, 853 (2004).

9:40 AM

Rapid Solidification of Sm-Co Permanent Magnets: Vinod K. Ravindran¹; Shampa Aich¹; *Jeffrey E. Shield*¹; ¹University of Nebraska

Rapid solidification has been used effectively to produce Nd-Fe-B based permanent magnets. It has, however, been less widely investigated for the production of Sm-Co-based materials. Here, we report the microstructural evolution of rapidly solidified Sm-Co alloys from 6 to 16 atomic percent Sm. We have observed a wide variety of phase formation and microstructures, ranging from primary Co dendrite formation to eutectic structures to the hard magnetic SmCo₇ compound. Particularly, we ob-

served non-equilibrium formation of Co along with SmCo₇, whose presence caused a decrease in coercivity from ~10 kOe to 500 Oe. Alloying elements reduced the scale of the microstructure, effectively offsetting the detrimental effects of the Co phase formation and leading to a recovery of the coercivity. The eutectic structure with Co rods surrounded by SmCo₇, provides a natural path to nanoscale hard/soft magnetic nanocomposites, where control of scale and phase content is critical.

10:05 AM Break

10:25 AM

Ordering in Combined Reaction Processed FePd Bulk Intermetallics: Andreas Kulovits¹; Anirudha R. Deshpande¹; *Jorg Michael Wiezorek*¹; ¹University of Pittsburgh

It has been shown in numerous works that ordering heavily deformed Fe-50at%Pd via a combined reaction transformation mode leads to a fine grained equiaxed structure with enhanced magnetic properties as compared to the polytwinned micro - constituent that forms upon conventional ordering of undeformed gamma Fe-50at%Pd. In this study FePd alloys of different composition Fe-Xat%Pd, X=34, 50, 61, were severely plastically deformed in the gamma FePd state by an equal channel angular pressing or ECAP operation. The structural evolution of the phase - transformation of the combined reaction in Fe-50at%Pd was investigated by means of XRD, SEM and TEM and compared to the combined ordering and decomposition reactions for the off-stoichiometric compositions. The change in magnetic properties during the different phase - transformation modes was monitored via VSM. The magnetic domain structures in the different alloys were compared and correlated to the individual microstructures by means of AFM and MFM.

10:50 AM Invited

Advanced Transmission Electron Microscopy on Magnetic Phase Transformations: *Yasukazu Murakami*¹; Daisuke Shindo¹; ¹Tohoku University

This paper reports recent technical advances in electron holography and its applications to some issues on magnetic phase transformations in smart materials. Taking advantages of the direct observation of magnetic flux and the peripheral techniques aiming at in situ observations, the holography studies have revealed correlations between magnetic domains and crystallographic microstructures (twins, antiphase domains, precursor lattice modulation of the matrix, etc.) in ferromagnetic shape memory alloys. The observations demonstrate that this magnetic imaging can be a powerful tool for explorations of transformation mechanisms, e.g., pattern formation and its temperature dependence above the transformation point. Updated results will be also presented with respect to the simultaneous measurement of magnetism and conductivity, which will provide beneficial information about magnetic inhomogeneity as observed near phase transformation temperatures in several compounds.

11:25 AM Invited

Magnetoelastic Precursor Effects in Ferromagnetic Shape Memory Alloys: *Sai Prasanth Venkateswaran*¹; Marc J. DeGraef¹; ¹Carnegie Mellon University

Ferromagnetic shape memory alloys in the Ni-Mn-Ga and Co-Ni-Ga alloy systems exhibit pre-transformation modulations of two types: one modulation is structural, and gives rise to the conventional tweed contrast in electron microscopy two-beam observations. The other modulation has a magnetic origin, and is visible only in the out-of-focus Lorentz observation mode. In this contribution, we will review the contrast mechanisms that are responsible for this type of modulation contrast. A strong magnetoelastic coupling in these materials is responsible for the modulations, which occur upon approaching the martensitic transformation temperature. We will present detailed results of phase-reconstructed Lorentz observations, which enable us to study the modulations with high spatial resolution. The pre-transformation behavior in these materials will be contrasted with that in other non-magnetic systems.

12:00 PM

Micromagnetism in a Nanophase Alloy Studied by Small-Angle Neutron Scattering: *Werner Wagner*¹; Joachim Kohlbrecher¹; ¹Paul Scherrer Institute

Magnetic structures on the nanometer scale were studied by Small-Angle Neutron Scattering (SANS) in a two-phase alloy of the CuNiFe system. This system, upon annealing, undergoes a phase transition forming ferromagnetic Fe/Ni rich precipitates embedded in a paramagnetic Cu-rich matrix. Small Angle Neutron Scattering, with the dual interaction of neutrons with atoms, i.e. nuclear and magnetic, offers the unique opportunity to study both, compositional and magnetic correlations, accessing the size range of 5 to 200 nm. Further, in the case of non-isotropic magnetic alignment, the magnetic SANS turns anisotropic following the orientation distribution of the magnetic moments in the samples. In the present work a detailed analysis of the field dependent magnetic SANS signal from the alloy for different stages of aging has been carried out, aiming to show how the magnetic moments of the ferromagnetic precipitates, combined a preferred crystallographic orientation, react in the presence of the external field.

12:25 PM Concluding Comments by Raju V. Ramanujan

Simulation of Aluminum Shape Casting Processing: From Alloy Design to Mechanical Properties: Prediction of Mechanical Properties

Sponsored by: The Minerals, Metals and Materials Society, TMS Light Metals Division, TMS Materials Processing and Manufacturing Division, TMS Structural Materials Division, TMS: Aluminum Committee, TMS/ASM: Mechanical Behavior of Materials Committee, TMS: Process Modeling Analysis and Control Committee, TMS: Solidification Committee, TMS/ASM: Computational Materials Science and Engineering Committee

Program Organizers: Qigui Wang, General Motors Corporation; Matthew Krane, Purdue University; Peter Lee, Imperial College London

Thursday AM Room: 6D
March 16, 2006 Location: Henry B. Gonzalez Convention Ctr.

Session Chair: Paul N. Crepeau, General Motors Corporation

8:30 AM Invited

Multistage Fatigue Modeling of Cast A356 and A380 Aluminum Alloys: *Mark F. Horstemeyer*¹; Yibin Xue¹; David L. McDowell²; Christina Burton¹; ¹Center for Advanced Vehicular Systems; ²Georgia Institute of Technology

We present a multistage fatigue model with microstructure-property relations and descending order capturing deleterious effects inclusions: (1) Pores/Oxides > 200 microns, (2) > 100 microns free near-surface pores/oxides, (3) 60-90 pores/oxides microns w/large volume porosity fractions, (4) Pores/Oxides < 60 microns w/large volume porosity fractions, (5) Pores/Oxides w/low volume porosity fractions, signifying different casting features dominating fatigue life. Capturing cyclic responses, fatigue life compartmentalizes into four stages, fatigue crack growth incubation stage is modeled. Assuming a near-micron initial crack size, Microstructurally Small Cracks (MSC) initiate and grow to Physically Small Crack (PSC) to several dendrite cell sizes. Usually, 60-80% of life is spent in these three domains. Researchers combined these stages into crack initiation. We separate these mathematically different stages. Using the multistage fatigue model, two different cast aluminum alloys (A356 and A380) were studied in context of actual cast shapes.

8:55 AM Invited

Overview: Prediction of Fatigue Performance in Cast Aluminium Alloy Components: *Trevor Charles Lindley*¹; Peter D. Lee¹; Peifeng Li¹; Daan M. Maijer²; ¹Imperial College; ²University of British Columbia

The influence of cast processing conditions on the microstructure (SDAS) and defect population (pores, oxide films, intermetallic particles) has been studied in cast aluminium alloys. The size, distribution and complex three dimensional shape of the pores was characterized using 3-Di-

mensional X-ray tomography, giving more realistic dimensioning of pores compared to conventional 2-D metallography. For each cast condition, tensile and S-N fatigue properties were measured in the heat treated T6 condition. Using scanning electron microscopy, fractographic examination was performed in order to reveal the defect responsible for fatigue crack initiation. Models for situations where either crack initiation or small crack growth constituted the dominant phase of fatigue life were reviewed before formulating a methodology for the prediction of fatigue life of components. Residual stress effects resulting from machining or from the quench step in the T6 heat treatment were also included in life assessment.

9:20 AM Invited

Simulation of Tensile Test Bars: Does the Filling Method Matter?: *Mark R. Jolly*¹; ¹University of Birmingham

Tensile testing is used throughout the Aluminium shape casting industry as a method for proving quality of both materials and process. Simulation work at the University of Birmingham, combined with experimental work by NTec, has demonstrated that the very method of filling can significantly influence the distribution and location of porosity within cast tensile test pieces. Simulations are carried out for two Al-Si alloys covering eutectic and long freezing ranges. Test parameters such as pouring temperature and filling rate are also evaluated. Comparisons with previously published mould designs are made using simulation as the experimental tool. Validation of the simulations are made using the new mould designs and the new Crimson up-casting facility located at the University of Birmingham.

9:45 AM

Fatigue Life Prediction in Defect-Containing Aluminum Castings: *Qigui Wang*¹; Peggy Jones¹; ¹General Motors Corporation

Increasing use of aluminum shape castings in structural applications has drawn great concern in fatigue properties of cast aluminum alloys. Fatigue life of cast aluminum components is controlled by maximum defect size in the material. The larger the defect size the lower the fatigue life. In defect-containing aluminum castings, the fatigue life can be predicted using fracture mechanics models together with the estimated extreme defect size in the castings by Extreme-Value Statistics (EVS). The maximum defect size predicted by EVS agrees quite well with measurements of the initiation pore sizes from the fracture surface.

10:10 AM Break

10:25 AM

Characterization of Small Fatigue Cracks in an Aluminum Casting Alloy A356: *Jingen Zhou*¹; Guang Ran¹; Yongfang Wang¹; Qigui Wang²; ¹Xian Jiaotong University; ²General Motors Corporation

In this paper, a cast aluminum alloy A356 was used to study small fatigue crack behavior. The da/dN-delta k curves, fatigue thresholds and closure stresses of fatigue cracks with different sizes were measured. The effects of crack size and shape on crack growth behavior and their closure are discussed. It is showed that the anomalous growth behavior of physically small fatigue crack and mechanically small fatigue crack is due to lower and various closure level and the effect of notch field and excessive plastic zone, respectively. The models for characterizing thresholds of physically small fatigue cracks and predicting lifetime of mechanically small fatigue cracks in notch field are proposed by taking account of these factors based on experiments.

10:50 AM

Modeling of Creep and Bolt-Load Retention Behavior of a Die Casting A380 Aluminum Alloy: *Qigui Wang*¹; Cherng-Chi Chang¹; ¹General Motors Corporation

Aluminum casting alloys exhibit creep behavior when the materials are exposed to high temperature and load. The creep properties of aluminum castings strongly depend upon porosity level and microstructural constituents. In this paper, the stress- and temperature-dependent creep behavior of a die casting A380 aluminum alloy is simulated using a classical constitutive model. The bolt-load retention behavior of the material is analyzed in a head bolt joint in an aluminum engine under thermal cycle condition using finite element method. The analytical model for the bolt-load retention simulation comprehends not only the plasticity in all

Index

A

Abaffy, C	152
Abbott, T	274
Abdelshehid, M S	119
Abdul Wahab, A	253
Abe, T	280
Abedrabbo, S	33, 203
Abourialy, N	224
Abrantes, L M	184
Abreu, A L	67
Abu Leil, T	37
Abu-Farha, F	259
Acoff, V L	21, 61, 103, 152, 154, 170, 209, 224, 257, 299
Adams, B L	253
Adams, D P	29, 164
Adapa, R	118
Adel, G	116
Adeyeye, A O	236
Adharapurapu, R	292
Adrien, J	172
Adwait, T	170
Aga, B E	151
Aga, R	107
Agalotis, E M	245
Agarwal, A	136, 187, 241, 242, 286
Agena, A A	199
Aggarwal, G	117, 148
Agha, S O	77
Agnew, S R	32, 98, 114, 139, 172, 270, 276
Agrawal, B	110
Agren, J	42, 84
Agresti, F	150
Agüero, A	72
Aguirre, M	180
Ahlatci, H	190
Ahmad, G	54, 211
Ahn, B	153
Ahn, J	223, 282
Ahn, S	228, 277, 282
Aich, S	315
Aifantis, E C	164
Aifantis, K E	164
Aiquel, R	152
Aizawa, T	137
Ajayan, P M	90
Akase, Z	203
Akhtar, R J	108
Akiba, E	149, 296
Akimov, V	242
Akinc, M	120
Akkaram, S	234
Al-Ali, H H	263
Al-Kassab, T	138
Alapati, S V	59
Alaraj, S	141
Albrecht, J	270
Albright, S L	151
Albu, L	54
Aleksandrov, I	21, 94, 195, 196
Alexander, D	192, 194, 200, 249
Alexandre, J	68
Alexandrescu, R	54
Alfarsi, Y A	151
Alinger, M J	120
Allab, F	296
Allan, S M	54

Allard, L F	144
Allen, S M	180
Allen, T R	94, 131
Allendorf, M	30
Allioux, M	15
Allison, J E	80, 122, 166, 174, 184, 185
Alman, D E	30, 31, 175, 278
Almer, J	98, 158, 289
Alpas, A	309
Altan, T	277
Altay, A	188
Alterach, M A	136
Alvi, M	139
Amancherla, S	273
Amar, J	287
Amer, A	76
Amonette, J	136
An, K	72, 218
An, L	132, 178
Anderson, C G	116
Anderson, H	231
Anderson, I E	40, 56, 62, 82, 99, 146, 148, 170, 186
Anderson, P	112, 268, 299
Ando, K	116
Ando, T	84
Andrade, P M	68
Andre, J	108
Andreasen, A	294
Anento, N	131
Angeles-Hernández, M	76
Angeliu, T	88
Ankem, S	168
Ankusheva, N N	304
Anopuo, O	312
Antille, J	20
Antipov, E V	20
Anton, D	58, 59, 254
Antrekowitsch, H	183, 216, 283
Anyalebechi, P N	40, 83, 176, 232
Apel, M	186
Apelian, D	166
Apisarov, A	20
Aquino, R C	263
Arafah, D	33, 203
Arakelova, E R	177, 232
Arana, D	35
Arashima, H	150
Arbegast, W J	117
Ardoin, B	54
Ares, A	136, 140, 156
Argyropoulos, S A	228, 284
Ari-Gur, P	287
Arpe, R	256
Arroyave, R	27, 86, 134, 169, 171, 175, 227
Asadov, A	38
Asano, T	34
Asaro, R	196
Asatryan, G	177, 232
Ashkenazy, Y	237
Asmatulu, R	33
Asta, M	27, 77, 87, 111, 217, 264, 282, 300
Asthana, R	49, 190
Atanasiu, M	152
Atkinson, H	134
Atlee, J	183
Atreya, A	271
Atzmon, M	25, 106
Au, P	290
Auer, D	303
Augustyn, B	160
Aune, F	159
Aurrecoechea, J	218
Aust, E	80

Authier, M	59
Averback, R S	237, 306
Avishai, A	188
Awate, S	182, 183
Ayaso, J	307
Ayushin, B	152
Ayyar, A	114

B

Babakhanyan, S	168, 224
Babu, S S	205
Babushkina, L	214
Bach, F	275, 313
Backer, G	239
Backerud, L	109
Backes, B	163
Baclet, N	95
Badarinarayan, H	240
Bae, D	164
Bae, G T	171
Baer, D	136
Bahr, D F	28, 29, 70, 112, 163, 164, 218, 267, 306, 307
Bai, J	113, 209
Bailey, P	102
Bailey, W W	72
Bajaj, R	52, 94, 144, 201, 250, 292
Baker, F	295
Baker, I	75, 146, 219, 264
Baker, K C	211
Bakke, P	311
Bala, V	79
Balani, K	242
Balch, D K	140
Balk, T J	51
Ballard, D	223, 310
Balli, M	296
Ballout, Y	88
Balogh, L	193
Balsone, S	155
Bamberger, M S	124, 174
Banaszek, J	136
Bandaru, P	15, 251
Bandyopadhyay, A	157
Bandyopadhyay, D K	41
Banerjee, D	247
Banerjee, P	43
Banerjee, R	23, 25, 286
Banerjee, S	163
Bang, W	121, 277
Bannai, E	128
Banovic, S W	189, 244
Baquera, M T	161
Bar, H	287
Bar-Yosef, O	172
Barabash, O M	98, 199, 203
Barabash, R	98, 199, 218
Barandiarán, M	180
Barani, A A	153
Baranwal, R	88
Barbe, V	130
Barbee Jr., T W	22
Barber, R E	117, 167, 193
Barber, Z H	32
Barbosa III, N	30, 71
Barker, A J	145
Barnett, M	173
Barnett, S	16
Baron, J T	66
Barpanda, P	147, 287
Barrett, K	63
Barton, T	41
Bartsch, A	181
Baruchel, J	135
Basanta, D	17

Basaran, B	160, 293	Bieler, T R	21, 61, 103, 117, 152, 154, 155, 166, 170, 209, 222, 257, 288, 299	Branagan, D	61
Baskes, M	52, 53, 89, 104, 162	Biener, J	259	Brandes, M	191, 268
Bastl, Z	54	Billia, B	45, 135, 177	Braun, D	47
Bate, P	258	Billinghurst, D	60	Braun, P V	182
Batani, M	231	Bilodeau, J	109	Braun, R	246
Bathias, C	220	Biner, S	212	Bravo, M E	105
Batista, E S	19	Bing, L	174	Bray, G	270, 308
Batra, S	43	Bingert, J F	147, 252	Bray, S	192
Battaile, C	27, 69, 111, 162, 216, 264, 266, 282, 305	Biol, Y	189	Bright, R M	33
Battle, T P	34, 75, 76, 116, 132	Bischoff, B	40	Brindle, R	82
Baum, B	63	Biswas, A	146	Brinks, H	206
Baumann, M J	23	Biswas, K	186	Brinson, C	241
Bauri, R	190, 191	Biswas, S	188	Brodova, I G	195
Bautista, R G	17, 58, 99, 149, 205, 254, 294, 296	Blackburn, J	295	Brokmeier, H	276
Bavarian, F	17, 58	Blanchard, P	81	Bronfin, B	172
Baydogan, M	169, 215	Blandin, J	301	Brooks, C R	65
Beals, R S	37, 38, 80, 81, 122, 124, 171, 172, 227, 229, 274, 276, 311, 312	Blanpain, B	267	Brooks, G A	39, 41
Bearne, G	20, 60	Blasques, J M	60	Brown, D	224, 250, 293, 313
Beaudoin, A J	105	Blau, P	82	Brown, E N	224, 270
Becerra, A	228	Blawert, C	37, 312	Brown, G J	57
Beck Nielsen, I	30	Blobaum, K	300	Brown, J A	49
Beck, T	73	Blue, C A	84, 244, 281	Brown, L	72
Becker, C A	111	Blum, W	194	Brown, T L	144
Beckermann, C	87, 239, 240	Blust, J	218	Brown, W L	30
Becquart, C S	131	Bly, R	105	Browne, D J	136
Beeler, R M	152	Bobadilla, M	305	Browning, P	218
Begley, M R	139, 307	Bobrova, L	69, 216	Bruckner, J	216
Behera, S	287	Bocharov, O	83	Buchanan, D	269
Behi, M	153	Böcher, T	202	Buchanan, R A	24, 64, 65, 106, 157, 212, 219, 260, 301
Beleggia, M	130	Bochkareva, L	118	Budd, R	75, 111, 133
Belger, M A	140	Bodak, O	113, 241	Buehrig-Polaczek, A	174
Bell, S	39	Boelsinghaus, T	254	Buelow, N L	62
Bellemare, S	32	Boehrlert, C J	312	Bührig-Polaczek, A	80, 285
Bellhouse, E	153	Boellinghaus, T	23, 172, 247	Bulanova, M	120
Bellon, P M	265, 306	Boening, M	307	Bulkowski, B	184
Belova, I V	84, 127, 130, 181, 233	Boettcher, H	258	Bulla, A	285
Belt, C K	183, 238, 263, 282	Boettger, B	109	Bullard, S	30
Ben-Artzy, A	277	Boettinger, W J	174, 272	Bulmer, S	290
Bendavid, A	251	Boettinger, W J	42, 121	Bunin, I J	303
Bendersky, L A	48, 121	Bogdanov, Y	152	Buntenbach, S	151
Benicewicz, B C	182	Boger, R K	173	Burgos, G R	185
Benish, A	222	Bohlen, J	276	Burhan, N	201
Bennett, D	303	Bojarevics, V	208	Burkhard, M	210
Bennett, T	188	Bolognese, A M	24	Burns, J	115
Benson, D J	106	Bonarski, J	94	Burrell, R E	64
Benson, M	218	Bonczok, A	136	Burton, C	139, 316
Bentley, P	17	Bondarchuk, V	191	Busby, J T	88, 94
Bera, J	287	Bonetti, E	150	Busch, D W	67
Berczik, D	92	Bonfield, W	156	Busch, R	65, 301
Bergeon, N	45	Bonnet, F	305	Busker, G	310
Berger, R	285	Bonnetot, B	294	Buta, D	111
Berkmortel, R	172	Bonnetot, B	294	Butler, D T	210
Bernard, F	234	Booth-Morrison, C	137	Byler, D	89
Bernier, J	98, 148	Borelli, R	156	Byrne, J	32
Berry, J T	184, 284	Borgesen, P	79	Byrne, T	35
Bertram, M	222	Borivent, D	177	Byun, S	178
Besser, M F	212	Borode, J	303	Byun, T	144, 145
Besterci, M	203	Bose, S	157, 264		
Bettles, C	38, 80	Bosse, M	275, 313	C	
Bewlay, B	225, 273	Boteler, J M	212	C. van Duin, A	264, 282
Beyerlein, I J	104, 154, 196, 248, 249	Boucharat, N	292	Cabibbo, M	142, 299
Beygelzimer, Y	203	Boulianne, R	19	Cady, C M	173, 293
Bhamidipati, V	114	Bourke, M A	250	Cage, B	145
Bhandari, Y	148	Bourke, M M	313	Cahill, D G	43, 69
Bhanu Prasad, V	223	Bourne, N K	224	Cahn, J	48, 89
Bhat, S P	114	Bower, A	267	Cai, M	30, 293
Bhattacharya, A	218	Bowers, R	288	Cai, Y	54, 211
Bhattacharya, S	167, 287	Boyer, D C	66	Cai, Z	53, 139
Bhide, R J	117	Bozkurt, U	189	Cairney, J	286
Bice, D R	259	Bozzolo, G	77	Calvert, P	211
		Bozzolo, N	188	Camara, G	273
		Brackmann, T A	47	Campbell, C E	41, 42, 84, 85, 127, 177, 233, 279
		Bradshaw, R C	210, 212, 302	Campbell, J	239
		Brady, M	39, 82, 126, 127, 175, 231, 232, 278	Campbell, P G	18
		Brahme, A	55, 139		
		Brailovski, V	198		

TMS2006 Annual Meeting & Exhibition

Candan, E	190	Chawla, K K	49, 113, 245	Christ, H	74
Candia, A	136	Chawla, N	35, 36, 55, 78, 113, 114, 121, 157, 170, 220, 226, 245, 273, 289	Christodoulou, J A	147
Caneba, G T	110	Che, F	313	Chu, J	25, 113, 115, 128
Canfield, N L	40	Che, Y	151	Chu, Y	133
Cannon, R	29, 72, 89	Chellappa, R S	100, 254, 296	Chuang, C H	194
Cantelli, R	99	Chembarisova, R	21	Chuang, Y	281
Cao, D M	246	Chen, C	74, 226, 227, 234, 235, 252, 274	Chumbley, S L	186
Cao, G	81	Chen, E Y	259	Chumlyakov, Y	160, 293
Cao, H	81	Chen, G	249	Chung, C	36, 170
Cao, P	93, 290	Chen, G Z	34	Chung, H	222, 223
Cao, Q	152	Chen, H C	161, 196	Chung, H S	223
Cao, W	70, 125, 273, 278	Chen, I	179	Church, B	54
Cao, X	81, 135, 214	Chen, J	105, 281	Chuvil'deev, V N	197, 198, 276
Cao, Y	105	Chen, K	274	Chuzhoy, L	87
Cao, Z	118, 224	Chen, L	28, 32, 56, 70, 74, 114, 119, 120, 145, 162, 218, 235, 236, 266, 277	Ciftja, A	183
Capocchi, J D	195	Chen, L L	247, 278, 279	Çimen, S	285
Car, R	43, 181	Chen, M	274, 299, 309	Cimenoglu, H	169, 190, 215
Caram, R	136, 140	Chen, P	280	Cinθο, O M	195
Carletti, H G	284	Chen, Q	297	Ciulik, J R	210
Carlson, K D	239	Chen, S	122, 225, 226, 234, 272, 273, 278, 280, 299	Ciupina, V	54
Caron, P	310	Chen, S W	128, 178, 234, 280, 313	Ciupitu, J	110
Carreno-Bodensiek, C	285	Chen, T T	26, 27, 68, 110, 160, 215, 263, 302, 304	Claiss, P A	184
Carruthers, A	256	Chen, X	19, 133, 140, 289, 299	Clark, A	99
Carter, C	29, 112, 188	Chen, Y	149, 265, 290	Clark, J A	68, 271
Carter, J	276	Chen, Z	79, 121, 226	Clark, R	119, 168, 224, 272, 290, 310, 311
Carter, M	96, 146	Cheney, J L	260	Clarke, D	243
Carter, W	89	Cheng, C	268	Cleaver, T	309
Cassayre, L	20	Cheng, P	133	Clerin, P	207
Castro, M	208	Cheng, S	74	Coad, I	60
Castro-Cedeno, M H	223	Cheng, Y	268	Coates, B L	284
Catalina, A V	87	Chengshu, C	317	Cockcroft, S	185, 214
Cataneda, S	30	Cheong, Y	110	Cocke, D L	26, 54
Caton, M J	221, 270	Cherukuri, B	195	Cockeram, B V	46, 88, 95
Cavaliere, P	123	Cherzig, C	127	Coffey, G	127
Ceder, G	27, 69, 70	Chesonis, C	109	Cojocar, I	152
Cefalu, S A	125	Chiang, C	25, 115	Cole, A C	282
Celik, O	169	Chiang, H	171, 274	Cole, D M	219
Cerezo, A	137, 204	Chien, W	58, 255, 296	Cole, G S	80
Cerreta, E K	86, 105, 118, 168, 173, 223, 293, 310	Chin, E	218, 300	Coleman, M	150
Cerri, E	94, 123	Chin, K S	305	Collins, G S	42
Cha, P	26	Chinh, N	200	Collins, P	141, 142, 148
Chada, S	35, 78, 121, 128, 170, 178, 226, 234, 273, 280, 313	Chintamaneni, V K	74	Collins, W	31
Chaim, R	48, 89, 137, 188, 242, 243, 287	Chiou, G	121, 274	Colvin, J M	96, 146
Chan Gyung, P	269	Chirimbu, P	152	Comin, A	101
Chan, K S	24, 29, 46	Chisholm, M F	86	Comley, P	22
Chandra, D	17, 40, 58, 99, 100, 101, 149, 150, 205, 254, 255, 294, 296	Chithambaranadhan, D	183	Commet, B	109, 214
Chandran, K	218, 219, 221	Chiu, H	179	Compton, D	144
Chandrasekar, S	144, 193	Chiu, S	274	Compton, W	193
Chang, C	223, 234, 274, 314, 316	Chmelar, J	159	Contescu, C	295
Chang, K	171	Chmielarz, A	184	Cook, B	156
Chang, W	313	Cho, H	229, 282	Cooksey, M	39, 175, 209
Chang, Y	77, 81, 120, 124, 134, 169, 225, 226, 227, 272, 273, 278, 301	Cho, J	301	Cooper, A	35, 119
Chanturiya, V A	303	Cho, M	179	Copland, E H	169
Chapman, D	116	Cho, S	229	Cordes, H	303
Charbonnier, J	18	Cho, W	275	Cordill, M	29, 164
Charette, A	68, 140	Cho, W D	75	Correa-Duarte, M	112
Charit, I	202, 210	Choate, B	257	Corson, R P	254
Charpentier, L	84	Choe, H	35	Corwin, A D	29
Charron, W	309	Choi, C K	219	Costello, A C	167
Chatain, D	48, 90, 287	Choi, S	270	Cotten, H W	152
Chateau, J B	109	Choi, W	15, 121	Cotts, E J	79
Chathoth, S	128	Choi, Y S	155	Cotts, J A	256
Chatterjee, A	216	Chokshi, A H	258	Couper, M J	175, 215
Chattopadhyay, K	186	Choo, D	277	Courtenay, J	109
Chaubal, M V	150	Choo, H	25, 72, 107, 158, 210, 218, 220, 260, 261, 313	Courtney, T H	148
Chaudhuri, S	41	Chou, C	129, 235, 274	Cousineau, P G	256
Chaudhury, P K	195	Chou, C	145	Couteau, O	140
Chauhan, A P	233	Choudhary, S	313	Couturier, G	239
Chauhan, G I	110	Choudhri, D	313	Covino, B S	30
Chauhan, M	196, 249, 291	Chow, G	236	Cowen, C J	247
				Cox, B	82
				Crawford, G A	157
				Crepeau, P N	316
				Cretegn, L	225
				Cristea, P	43
				Cristol, B	207
				Croft, N	185, 284

Crosbie, P B 36
 Cross, C E 312
 Cross, M 185, 284
 Crum, J V 40
 Csicsovszki, G 77
 Cui, Y 46
 Cuitiño, A M 105
 Cullen, J 236
 Cumerford, B 215
 Curtarolo, S 169
 Curtis, C 295
 Cutler, C 133
 Cutler, E R 165
 Cutshall, E R 66
 Cytron, S J 161, 196

D

da Mota, G E 60
 D'Abreu, J C 41
 Daehn, G S 104
 Dagli, I 169
 Dahan, O 277
 Dahglian, C P 264
 Dahir, W S 311
 Dahle, A 160, 185, 240
 Dahotre, N B 136, 187, 241, 286
 Dai, B 59, 74, 252
 Dai, C 213
 Dai, K 62, 165, 166
 Dai, L 236
 Dai, Q 59
 Dai, Y 250
 Daida, P 26
 Daisa, D 110
 Dalgard, E C 227
 d'Almeida, J M 263, 264
 Dando, N R 19
 Dani, A 35
 Danielewski, M 44, 85, 127, 177
 Dao, M 32, 63, 243, 248
 Daoud, A 49
 Daraio, C 15
 Dariavach, N 285
 Darlak, P 91
 Darling, T 116
 Darragh, M 211
 Darras, B 288
 Das, G 290
 Das, K 157
 Das, S 128, 244, 288, 289
 Das, S K 26, 47, 138, 189,
 238, 244, 271, 288
 Dattelbaum, D M 224, 270
 Dauskardt, R 28, 74,
 115, 115, 187
 David, S 98, 199, 203, 313
 Davidson, D L 218
 Davis, B 39
 Davis, B R 34, 75, 76, 116
 Dawson, P 56, 301
 Dayananda, M A 41, 121,
 178, 234, 279
 de Boer, M P 29, 163
 de Castro, P T 166
 De Cooman, B 31
 de Deus, J F 263, 264
 De Gregoriis, G 60
 De Groot, J 67
 de Jonge, N 15
 De Jonghe, L 175
 De Marco, P 94, 123
 de Matos, P F 166
 de Melo, H G 161
 De Nora, V 20
 de Rango, P 18, 254, 296
 De Rojas, J 290

De Yoreo, J 105, 211
 DeAngelis, R 200
 Death, D L 133
 Deboer, D 207
 Deck, C P 251
 Decker, R F 58
 Deepatana, A 43, 44
 DeFouw, J D 289
 DeGraef, M J 17, 130, 236, 315
 Dehm, G 124
 DeHoff, R T 42
 DeHosson, J T 164, 213, 242
 Deibert, M C 231
 del Rio Perez, E 104
 Delaire, O 28, 237
 Delannoy, Y 84
 Delaplane, R 107
 Deliwala, J K 132
 Delucchi, T 46
 Demetrio, M D 98
 Demetriou, S 47
 Demopoulos, G P 44
 Deneen, J 29, 112
 Deng, X 113
 Dennis, K 62, 149
 Dennis, K W 146
 Deo, C S 52, 53, 181
 Deok Young, B 269
 Deppisch, C 79
 Deppisch, C L 36
 Deshpande, A R 198, 199,
 281, 315
 Deshpande, S A 166
 DeVries, J 81
 Dey, P 41
 Dhami, T L 50
 Dheeradhada, V S 178
 Dhulipala, P 200
 Dias, D P 68
 Dias, H P 60
 Diaz, G 184
 Dick, R E 139, 244
 Dickerson, M B 211
 Dickinson, J T 30, 293
 Dickinson, M E 260
 DiDomizio, R 201
 Dieckmann, R 113, 200
 Diercks, D R 75
 Dieumegard, D 15
 Dillon, A 295
 Dimiduk, D 17, 118, 148, 155,
 163, 168, 223, 253, 290, 310
 Dinda, G 292
 Ding, F 299
 Ding, J 32, 281
 Ding, R 116
 Ding, S 189
 Ding, W 229, 277
 Ding, Y 281
 Dinwiddie, R B 281
 Divi, S C 296
 Divinski, S 127, 182
 Dixon, J M 259
 Dixon, T W 66, 108,
 159, 213, 261
 Djurdjevic, M B 228
 Dmowski, W 107
 Dobatkin, S 22, 92,
 93, 193, 198
 Dobbins, T A 296
 Dobbs, C L 103
 Dobra, G C 152
 Dobrev, E 170
 Dobson, P 96
 Dogan, O 31, 240
 Domain, C 131, 265
 Donahue, R 160

Dong, H 76, 134, 135,
 155, 168, 200, 311
 Dong, W 302
 Donizak, J 298
 Donlon, W T 189
 Donnadieu, P 301
 Donohue, K D 139
 Doorn, S K 16
 Doppiu, S 101
 dos Santos Junior, E L 68
 Doty, H 272
 Doucet, J 59, 102, 103,
 150, 207, 255, 297
 Doud, A A 91, 191
 Dowding, R 301
 Doyle, F M 116, 187
 Dragomir-Cernatescu, I 53
 Drakic, M 255
 Drelich, J 211
 Drinkard, W F 255
 Driver, K 42
 Drnek, J 193
 Dron, J N 161
 Droubay, T C 293
 Druffel, T 70
 Dryepondt, S 31
 Du, D 242
 Du, Q 266
 Du Terrail-Couvat, Y 84
 Duan, X 189
 Duarte, C 268
 Duarte, M 190
 Dube, R K 223
 Dubois, J 168
 Dubravina, A 94
 Dudder, G J 309
 Dudek, M A 78
 Dufour, G 19
 Dugger, M T 71
 Duh, J 121, 122, 179,
 234, 274, 280, 314
 Duley, J 230
 Dulikravich, G S 108
 Dumitrache, F 54
 Dumont, D 270
 Dunand, D C 138, 140,
 205, 243, 259, 289
 Duncan, K L 86
 Dunin-Borkowski, R 147
 Dunlop, G 80, 274
 Dunn, P S 303
 Dunwoody, J 89
 Dupont, V 267
 Dupuis, C 109
 Dupuis, M 208, 261
 Durst, K 163
 Duscher, G 86
 Dutrizac, J E 26, 27
 Dutta, I 37, 78, 210
 Dutta, P K 57
 Dutton, R E 118, 168, 223, 310
 Duval, H 109
 Dvorak, J 291
 Dye, D 125, 134
 Dye, R C 206

E

Eagar, T W 171
 Ebara, R 164
 Ebenstein, D M 70
 Ebner, A B 206
 Ebrahimi, F 86, 163
 Eckert, J H 158
 Edwards, M 207
 Effgen, M P 47
 Efros, B M 144

Efros, N B	144
Egami, T	106, 107
Egorov-Yegorov, I N	108
Eifler, D	74
Eiken, J	174
Eksteen, J J	133, 303
El Gahoui, Y	108
El Houdaigui, F	195
El-Azab, A	136
El-Deiry, P A	30
El-Ghonimy, M	262
El-Gizawy, A	300
Elder, K	217, 266
Elias, C N	23, 24
Eliezer, D	307, 312
Ellerby, D T	104
Elliott, A	155
Elmadagli, M	309
Elsaesser, M	80
Embury, D	222
Emge, A	196
Emura, S	247
Endo, M	31, 32, 73, 114, 115, 164, 165, 219, 221, 269, 270, 308
Engelhard, M	136
Engh, T A	39, 109, 183
Enikeev, N A	196
Eom, C	188
EricksonKirk, M	268
Erkel, J v	184
Ernst, F	90, 137
Erol, M	285
Erukullu, M	245
Es-Said, O	119, 168, 224, 272, 290, 310, 311
Escudero, A	317
Eshthewi, A	301
Eskin, D	160, 214, 241
Esling, C	49
Esparza, C	317
Esquerre, V	207
Esquivel, E V	110
Essadiqi, E	39, 275, 276
Essuman, E	31, 83
Estrin, J	61
Estrin, Y	209, 248, 291
Etsell, T H	34
Evangelista, E	142, 299
Evans, D	142
Evans, J W	109, 116, 208
Eylon, D	92, 141, 191, 246, 247, 290

F

Fabritius, H	106
Fafard, M	261
Fahrmann, M	125, 126, 174, 230, 277
Fakra, S	58
Fan, C	107, 158, 261
Fan, G	25, 158, 220
Fan, J	44
Fan, L	33
Fan, X	36
Fan, Y	178
Fang, J S	128
Fang, L	164
Fang, S	20
Fardeau, S	208
Farias, E	256
Farkas, D	56, 162, 181, 188, 267
Farrell, J	47
Farrer, J K	188
Fasoyinu, F A	123

Faupel, F	146, 181
Fecht, H	249, 291
Fehlbier, M	80
Feiner, E L	68
Felicelli, S D	33
Feng, C	248
Feng, G	155
Feng, J	272
Feng, W	56, 266
Feng, X	45
Feng, Z	98, 199, 203, 313
Feret, F R	151
Fergus, J W	231, 278
Ferguson, J	141, 246
Ferkel, H	187
Fernandez, F	129
Fernández Fernández, J J	256
Ferreira, H	19
Ferreira, J d	242, 282
Ferron, C J	26
Ferry, M	65, 201, 213, 253
Feuchtwangner, J C	180
Fezzaa, K	289
Fichtner, M P	101
Field, A	244
Field, D P	244
Field, R D	161, 293, 302, 303
Fielden, D	165
Fielding, R A	262
Fields, R J	244
Filatov, A Y	20
Filipek, R	127
Filippov, V	202
Fine, M E	114, 115, 157, 300
Finlay, M	178
Fiorini, A	150
Firoozi, S	176
Firrao, D	215, 271
Fischer, C	69
Fischer, F D	85
Fitzgerald, T	36
Fjeld, A	109
Flanagan, T B	169
Flandorfer, H	280
Flater, P	200
Flinn, B D	260
Flores, K M	64, 157
Flores, P	151
Flueck, M	256
Fodor, A	195, 199
Foecke, T	70, 189, 219
Foiles, S M	111, 265
Follstaedt, D M	52, 193
Fonda, R W	97
Fong, K	43
Fonteno, J	251
Foon, R J	290
Foosnaes, T	66, 262, 66, 159
Forde, G	60
Forlerer, E	156, 301
Fossdal, A	206
Foster, R	35
Fournelle, R A	36
Fox, S P	141, 191, 246
Fragner, W	123
Franc, P M	47
Frank-Kamenetskaya, O	106, 161, 306
Frankel, P G	192
Franken, T	184
Frary, M E	16
Fraser, H	23, 56, 99, 141, 142, 148, 163, 230, 253, 286
Fray, D J	33, 34
Frazier, D O	132
Free, M L	34, 75, 76, 116, 117
Freels, M	65
Freeman, A J	86, 237, 238

Freeman, D	222
Fréty, N	234
Frias, C	184
Frick, C	71
Fridy, J	55
Friedman, L H	164
Fries, S G	78
Friesen, C	112
Frisch, J	61
Froehlich, M	246
Frohberg, G	128
Frolov, A	20, 214
Frommberger, M	146
Fruchart, D	18, 149, 254, 294, 296
Fryt, E M	178
Fthenakis, V M	183
Fu, C	131
Fu, G	105
Fu, H	261
Fu, S	170
Fu, X	65
Fuchs, G E	165
Fuerst, C	228
Fuerstenau, M	116
Fujii, H	100, 207
Fuller, E R	16
Fultz, B	28, 237
Furrer, D U	230
Furukawa, M	93
Fuwa, A	232

G

Gabb, T P	125, 126, 174, 230, 277
Gabbitas, B	290
Gaddis, C S	54
Gagne, J	19
Gagnon, M	59
Gaitanos, J	76
Galikova, A	54
Gall, K	71
Gallego, N	295
Galloway, T J	18, 20, 26, 47, 59, 60, 66, 67, 102, 103, 108, 109, 150, 151, 159, 207, 208, 213, 214, 255, 256, 261, 262, 297, 298
Galvan, D	242
Galvani, C	275, 276
Galy, D	90
Gambino, R	281
Gan, D	307
Gandhi, R L	151
Gandhi, T	99
Gandin, C A	135, 283
Ganesan, M	125, 134
Ganesan, V	287
Ganesh, V V	55, 220
Gangloff, L	15
Gangloff, R P	32, 98, 115, 165, 270, 307
Gangopadhyay, A	212, 302
Gannon, P	231
Gantois, M	230
Gao, B	214, 257
Gao, F	274
Gao, H	106
Gao, N	143, 258
Gao, P	53
Gao, W	37, 38
Gao, Y	100, 221, 260, 261
Garg, A	32
Garimella, N	127
Garmestani, H	290, 299
Garratt, M	308

Garrison, W M	118, 119	Golumbfskie, W	134	Gupta, A	79
Garvin, J	246	Gomes, J A	26, 54	Gupta, A K	50, 245
Garvin, J W	246	Gomes, V	19	Gupta, G	41, 94, 95
Garza, K	157	Gonzales, F	45	Gupta, M	141
Gasch, M J	104	González, B	220	Gupta, N	49, 90, 140, 141, 190, 245, 246, 289
Gash, A E	187	González, J	152	Gupta, V	32
Gaspar, D	136	González-López, S	76	Gupta, V K	98
Gaspar, J	27	Goolaup, S	236	Gurgov, H	287
Gasqueres, C	270	Gordon, P A	267	Guruswamy, S	222, 254
Gastaldi, J	135	Goren-Muginstein, G	124	Gusak, A M	170
Gaustad, G	238, 263	Gorner, H	109	Gusev, A	214
Gauthier, C	19	Gornostyrev, Y N	86, 237, 238	Gusman, M	104
Gayda, J	126	Gorny, A	124	Gustafsson, M	209
Gayer, B M	311	Gorsse, S	107	Gutfleisch, O	101
Gaytan, S M	110	Goshima, T	165	Guthrie, R I	213, 215
Gebert, J	63	Goswami, R	129, 130, 236	Gutierrez, I	193
Gee, J	270	Gottstein, G	48, 188	Gutierrez, M	72
Gegel, G A	190	Goulet, P	261	Gutierrez-Urrutia, I	193
Geiss, R	71	Goutiere, V	68	Guyer, E	187
Geltmacher, A B	55, 253	Goyal, R N	207	Guyer, J E	42, 266
Genc, A	286	Grabovetskaya, G P	291	Gwan, P	133
Gendre, M	108	Gracio, J	279		
Geng, K	70	Graczyk, D G	39	H	
Geng, S	231	Grady, T	26	Haataja, M	44, 266
Gennett, T	295	Graham, P D	54	Habel, U	92, 141, 191, 246, 247, 290
George, D B	35	Gramsch, S	100	Haberl, A	263
George, P	232	Grandfield, J F	215	Haberl, M H	272
George-Kennedy, D	35	Grant, G J	117	Habraken, A	195
Georgiadis, M C	206	Grant, P	96, 240, 284	Hackenberg, R E	161, 250, 302
Gerberich, W	29, 112, 164	Gravier, S	301	Hackett, M J	94
German, R M	148	Gray, G T	86, 119, 173, 224, 270, 293	Haeffner, D	98, 289
Gerosa, R	271	Greatz, J	59	Haensel, M	31, 83
Gertsberg, G	172	Green, J A	257	Haertling, C L	88
Ghidini, A	271	Green, J R	186	Hagelstein, K	238
Ghonem, H	247	Greenawalt, K R	47	Hagen, M E	159
Ghosh, A	22, 172, 173	Greenwood, G W	209	Hagiwara, M	247
Ghosh, G	27, 77, 300	Greer, A L	235	Hagmann, R	118
Ghosh, S	55, 73, 148, 245	Greer, J R	112	Hagni, A M	110
Ghosn, L J	104	Gregori, F	196	Hagni, R D	303
Gianola, D S	306	Gregory, J	183	Haiyan, D	48
Gibbons, T B	83	Greiveldinger, B	35	Halikia, I	76
Gibson, M	80	Greve, H	146	Hall, R	32
Gignoux, D	296	Griesche, A	128	Haluska, M	54
Gil Sevillano, J	249	Grigoryan, F	177, 232	Hamel, F G	213
Gilbert, K E	295	Groeber, M	148	Hamilton, C C	26
Gill, A	147	Groening, O	15	Hamilton, J C	243
Gill, D	191	Gross, K J	58	Hamilton, R W	91
Gill, J T	100	Grotheer, H	256	Hammel, P	43
Gill, K S	64	Grousto, T	102	Hammetter, C	107
Gillard, A	189	Groza, J R	62, 177	Hamza, A V	51, 259, 306
Giocondi, J	211	Gruber, J	188	Han, B Q	153, 155, 249
Giraud, P	95	Gruen, G	67, 109, 159, 214, 262	Han, E	37, 38
Girshick, S L	112	Grukke, E A	70	Han, G	282
Giurco, F	133	Gryaznov, M Y	276	Han, H	80, 122, 262
Givon, M	18	Gschneidner, K A	56	Han, J	172, 229
Glade, S C	201	Gu, S	297	Han, K	292
Glaessgen, E H	300	Guangchun, Y	84, 174, 233, 298, 309	Han, Q	44, 87, 122, 124, 135, 140, 185, 240, 271, 272, 284, 288
Glasbrenner, H	250	Guangjun, Z	129	Han, S J	71
Gleeson, B	120, 310	Gubicza, J	200	Han, T Y	187
Glicksman, M	16, 44, 85, 87	Guclu, M	168	Han, Y	154
Go, J	140	Guduru, R K	21	Hanan, J C	98
Goddard, W A	265	Gueijman, S	136	Hanbicki, A T	236
Godet, S	276	Guerrero, P A	110	Hanlon, A B	83
Godlewski, L A	174	Guillemot, G	135	Hanlon, T	32
Goeken, J	229	Guillot, J	109	Hanlumuang, Y	315
Goeres, G	213	Guin, J	287	Hannon, A C	158
Göken, M	143, 163	Gumaraes, G S	23	Hanrahan, R	46, 88
Gokhale, A	17, 26, 55, 68, 82, 110, 160, 192, 215, 253, 263, 302, 304, 311	Gun, B	65, 213	Hansen, J O	92
Golchert, B	67, 263, 271	Gunderov, D	149, 197, 198	Hansen, N	93
Golden, P	221	Gündüz, M	285	Hao, S	216
Goldenberg, B	23, 233	Gungor, M N	155, 200, 311	Haouaoui, M	93, 201
Goldstein, J	18	Guo, F	36, 79, 168, 216, 260	Hapugoda, S	38
Golovanova, O	106, 306	Guo, J	225		
Golovashchenko, S	189	Guo, Y	76, 77		
Golovin, I S	195	Guo, Z	99, 278		
Golubov, S	53	Guoqiu, H	317		

Haq, A J	251	Hersam, M C	157	Hoyt, J J	111, 112,
Hara, S	18	Herzig, C	182		163, 216, 217
Hardy, J S	40, 127, 231	Hess, P	115	Hribernik, M	307
Hardy, M	247	Hess, W P	293	Hryn, J	21, 39, 81, 82
Harlow, D G	114	Heuer, A H	287	Hsia, K	29, 106
Haroosh, S	124	Higgs, J	89	Hsiao, H	280
Harrell, J	282	Hijii, T	171	Hsiao, L	122, 234, 280
Harris, C L	34, 35, 119	Hildal, K	284	Hsiao, Y	227
Harris, R	176, 222	Hildebrand, M	54	Hsieh, H	302
Harris, S J	167, 245	Hilgraf, P	102	Hsieh, H Y	128
Harris, V G	129, 130	Hilpert, K	169	Hsu, E	184
Hartley, C S	16	Hiltmann, F	213	Hu, B	81
Hartmann, V	256	Hincliffe, C	96	Hu, D	142
Härtwig, J	135	Hines, J A	80	Hu, H	122, 123, 133, 239
Hartwig, K	62, 142, 167, 193, 199, 255, 257, 302	Hino, S	207	Hu, S	56, 162, 266, 277
Hashem, H	262	Hirsch, J R	139	Hu, W	64
Hashimoto, N	144	Hisker, F	127	Hu, X	32, 214, 222, 257
Hashimoto, S	291	Hitit, A	119	Hu, Y	304, 305
Haskins, A W	165	Hives, J	20	Hu, Z	261
Hasman, E	287	Hixson, R S	86	Hua, F	36, 227
Hassan, M	40, 123	Hjelm, R P	107	Huang, A	142
Hassan, S	141	Hlil, E	254, 296	Huang, A T	226, 235
Hassouna, D S	311	Ho, C	274, 314	Huang, C	122
Hasui, M	31	Ho, P S	307	Huang, F	286
Hatamaya, T	91	Hoagland, R	116	Huang, J	308
Hatanaka, K	31	Hoagland, R G	22, 63, 113	Huang, J C	194
Hatem, J J	271	Hochenhofer, M	283	Huang, J K	220
Hattori, N	269	Hodge, A M	22, 23, 63, 105, 156, 211, 259	Huang, J Y	22, 249
Hauback, B	206	Hodge, G	57	Huang, L	141, 219
Hawk, J A	31	Hodoshima, S	206	Huang, M	23, 305
Hayashi, S	120	Hoehbauer, T	116	Huang, R	302, 307
Hayes, J R	259	Hoelzer, D	46	Huang, W	87
Hayes, S	178	Hoepfel, H	192	Huang, X	93, 110, 176, 304
Haynes, A	72	Hoffman, M	251, 286	Huang, Y	29, 140, 312
Haynes, J A	72	Hofman, G L	128, 178	Huang, Z	77
He, M	170	Hogenboom, M	67	Hubbard, C	72, 113, 218, 313
He, S	304	Hohl, B	108	Hubbard, J B	190
Headrick, W L	68	Hojda, R	175	Hudak, S J	29
Healey, K	265	Holbery, J D	82	Hudanski, L	15
Healy, S	207	Holcomb, G R	30	Hufenbach, W	80
Heben, M	295	Holda, A	298	Hugenschuett, G	262
Heber, G	55	Holden, I	159	Hui, X	302
Hebert, R J	143	Holloway, P C	34	Huisman, J	183
Hector, L G	174	Holm, E A	17, 265	Hulbert, D M	62
Heidecker, M	132	Holzer, I	273	Hults, L	250
Heil, T	129	Holzleithner, C	300	Hults, W	161
Heil, T M	180	Homer, E R	253	Hundley, M F	157
Heilmaier, M	104, 258	Hong, C	134, 273	Hunt, W H	49, 90, 140, 190, 245, 289, 290
Heininger, E C	82	Hong, H	203	Huq, A	58
Heinke, F	159	Hong, S	51	Huser, T	259
Heinrich, J C	45	Hong, T	152	Hutchinson, C R	134
Heinze, J E	238	Hong, Y	226, 286	Hutson, A	269
Hellmig, R J	94, 248	Hono, K	129, 142, 143, 171, 281	Hwang, J	272, 312
Helm, D	92	Honsel, C	174	Hwang, J J	26, 68, 69, 110, 149, 160, 215, 263, 302, 304
Hemker, K J	104, 210, 306	Hooper-McCarty, J	219	Hwu, Y	187
Hemley, R	100	Hope-Weeks, L	54	Hyde, B	188
Hemmings, S	184	Höppel, H	143	Hyers, R	83, 210, 212, 302
Henderson, D W	37	Horbach, J	128	Hyland, M	66, 102, 213, 253
Henein, H	34, 119	Horita, Z	21, 50, 51, 92, 93, 142, 143, 192, 193, 194, 248, 291		
Henne, I	73	Hornak, P	153		
Hennequin, O	256	Horstemeyer, M F	103, 161, 316		
Hennessy, D	98	Hort, N	37, 80, 140, 229, 312		
Hennig, R G	42	Horton, J A	199, 203		
Hennig, W	118	Hosford, W F	138, 200		
Henrie, B L	147, 173, 252, 302	Hoshimoto, N	88		
Henriksen, B R	262	Hostetter, G J	200		
Henry, M F	125	Hou, P Y	175		
Hensen, K	74	Houghton, B J	263		
Hentsche, M	295	House, J W	200		
Heon Phil, H	285	Hovhannisyan, Z H	80		
Herd, P	133	Howard, S M	167		
Herling, D R	190, 289	Howell, S W	224		
Hermann, H	295	Hoyer, J	105		
Hermann, R	25				
Hermann, R P	25				
Hernandez-Santiago, F	265				
Herndon, W	252				

I

Iadicola, M A	189
Ibrahiem, M	262
Ice, G E	98
Ichikawa, T	100, 207
Idenyi, N E	77
Ienco, M G	271
Iffert, M	19, 298
Ikeda, K	205
Ikeda, S	81
Ikuhara, Y	48, 188
Iliescu, D	264
Ilyoukha, N	238
Im, J	255

Imam, M	17, 58, 99, 149, 150, 205, 207, 254, 272, 294, 296
Imamura, M	116
Inal, K A	276
Ingraffea, A R	55
Inoue, A	25, 64, 65, 107, 129
Inove, A	64
Inque, A	65
Intorne, S C	68
Ipser, H	169, 280, 305
Iqbal, Z	16
Irby, E	104
Irwin, G	26
Isac, M	213
Isaenkova, M	202
Isahakyan, A R	80
Isao, O	26
Ishida, K	179, 180, 225
Ishiga, Y	31
Ishihara, S	165
Ishikawa, J	26
Ishikawa, N	171
Islimgaliyev, R	21, 199
Isobe, S	100, 207
Ito, K	128
Itoh, H	150
Itoh, J	283
Ivanisenko, J	249
Ivanisenko, Y	291
Ivanov, K V	291
Ivanov, M B	279
Ivanov, V V	20
Ivasishin, O	191
Ivchenko, V A	144
Izumi, T	120

J

Jablonski, P D	31, 175, 278
Jabra, J	224
Jackson, J E	126, 148
Jackson, K A	45
Jackson, W	126
Jacob, I	150
Jacob, S	303
Jacobson, C	175, 231
Jacobson, N	30
Jacot, A	283
Jadhav, S	78
Jager, S	277
Jahanshahi, S	225
Jahazi, M	81
Jain, A	276
Jain, J	172
Jain, M	189
Jakobsen, B	98
James, M R	52, 53
Janecek, M	248
Jang, G	121, 234
Jang, S J	110
Jankowski, A F	306
Jansen, H J	184
Janssens, K G	265
Jarjoura, G	37
Jarmakani, H N	154
Jata, K V	218
Javaid, A	39, 276
Jayaram, V	188
Jayaraman, T V	254
Je, J	87
Jehan, M	18
Jehanno, P	258
Jena, P	100
Jensen, C	99, 205, 206
Jeong, J	183
Jereza, K	82
Jha, G	138, 189, 244, 288

Jha, S K	114, 221, 270
Jho, J	74
Ji, B	106
Ji, H	172
Ji, R	275
Ji Young, B	285
Jia, X	250
Jian, X	122, 272
Jiang, C	113, 120
Jiang, D	62, 229, 274
Jiang, F	292
Jiang, J	246
Jiang, L	125, 234, 276
Jiang, Q	141
Jiang, T	76, 77
Jiang, W	25, 132, 158, 203
Jiang, X	166
Jiang, Y	37
Jianping, P	298
Jiao, S	222
Jiao, Z	145
Jiles, D	149
Jimenez, J A	97, 204
Jin, S	15, 63, 64
Jin, Y M	180
Jin, Z	297
Jing, T	45, 184
Jinhong, L	61
Jinhui, X	298
Jinwu, K	284
Jo, H	229
Jog, J P	182
John, R	221, 269
Johnson, A	284
Johnson, C E	121
Johnson, D	30, 178
Johnson, G	192
Johnson, J	59
Johnson, K	59
Johnson, M L	87
Johnson, S M	104
Johnson, W L	24, 98
Johnston, A	133
Johnston, C	96
Jolly, M R	316
Joly, A G	293
Jonas, J J	276
Jones, A	46
Jones, H	87, 285
Jones, H N	248
Jones, J	81, 82, 114, 165, 166, 220, 221, 311
Jones, K	132, 295
Jones, P	166, 316
Jones, W	311
Jong Gu, B	269
Jonker, B T	236
Joo, Y	235, 274
Jorda, J	120
Jorgensen, S	17, 18, 58
Joshi, P	74, 286
Joshi, S	130, 300
Joshi, S P	218
Jou, H	277
Joubert, H	101
Jóvári, P	107
Juan, Y	242
Julia, P	95
Jun, H	301
Jung, B	62
Jung, H	275
Jung, I	172, 228, 277
Jung, J	235
Jungk, J	29
Jungk, J M	28, 71
Junior, A S	216
Juul Jensen, D	16, 55, 97, 98, 139, 147, 204, 252

K

Kabisch, J H	272
Kaburaki, H	260
Kabutomori, T	150
Kacprzak, D	209
Kad, B	63, 106, 124, 154, 196
Kadiri, H E	161
Kadolkar, P	84, 244, 245, 281
Kadri, S J	193
Kaduri, S	141
Kai, W	302
Kainer, K	37, 123, 140, 229, 276, 312
Kainuma, R	179, 180
Kaiparambil, A V	310
Kalay, E Y	186
Kalidindi, S	117
Kalu, P N	264
Kamakoti, P	40
Kamaraj, K	60
Kamavaram, V	176
Kameda, T	26
Kamikihara, D	158
Kamiyama, K	314
Kammer, D	16
Kamp, N	258
Kandarov, I	197
Kang, D	172, 228
Kang, J	178, 189, 229, 283
Kang, S	87, 93
Kang, S H	15, 53, 96, 145, 203, 251
Kang, S K	32, 35, 74, 78, 121, 170, 226, 273
Kao, C	121, 226, 227, 274, 280, 314
Kao, R	128, 178, 234, 280, 313
Kao, T	179
Kaplan, D	211
Kaplan, H I	38
Kaplan, W D	48, 89, 137, 188, 242, 287, 288
Kapoor, B	60
Kapoor, R	194
Kar, S	141, 230
Karabelchtchikova, O	233
Karaca, H E	160, 293
Karadge, M	192
Karakus, M	68, 303
Karaman, I	92, 93, 113, 154, 160, 199, 200, 201, 216, 292, 293, 302
Karen, V L	69
Karma, A S	217
Karnthaler, H	199
Kasama, T	147
Kaschner, G	105
Kaschner, G C	104, 105, 152
Kashyap, B P	258
Kasic, V D	304
Kasoju, S	167
Kassner, M	63, 142
Katgerman, L	160, 214, 241, 284
Kattner, U R	58
Kaufman, M	25, 75, 272
Kaufmann, H	81
Kautz, M	192
Kawamura, Y	276
Kawasaki, M	291
Kawazoe, R	31
Kayali, E	169
Kayali, S	215
Kayani, A	231
Kaybyshev, O A	258
Kaydanov, V I	148
Kazakov, S M	20

Lambros, J	105	Leisenberg, W	159	Lin, A Y	105
Lamus Molina, C	27	Lekakh, S N	186	Lin, B	36
Lan, H	224	Lennikova, I P	195	Lin, C	110, 128
Landry, D	54	Leo, P	94, 123	Lin, D	110
Laney, S	126	Leo, P H	180	Lin, J	187
Lang, K	269	Leonard, F	243	Lin, J C	226
Langdon, T	200	Leonard, K J	88	Lin, K	35, 78, 121, 122, 170, 226, 273
Langdon, T G	21, 50, 51, 92, 93, 142, 143, 192, 193, 194, 195, 248, 291	Leong, B	101	Lin, M	228
Langford, S C	293	LeRoux, H	35	Lin, R Y	136
Lanning, B R	29	LeSar, R A	23, 63, 105, 156, 211, 259	Lin, S	234, 274
Lanning, C	145	Lesoult, G	135, 240	Lin, X	73
Lanyon, M	39	Lesuer, D R	152, 153, 200	Lin, Y	121, 226, 302, 314
Lapovok, R	196	Letzig, D	276	Lin, Z	239
Lara-Curzio, E	31	Levashov, V	107	Lindley, T C	184, 316
Lárez, J	152	Lévesque, J	276	Lindsay, S J	18, 20, 60, 103, 151, 208, 256, 298
Larocque, J	256	Levi, G	124	Linga, H	159
Larouche, A	214	Levin, I	243	Linli, W	84, 233
Larsen, D A	263	Levine, L E	30	Lipko, S	242
Larsen, J	31, 73, 114, 115, 164, 165, 219, 221, 269, 270, 308	Levit, L I	299	Lipsitt, H A	92
Larson, D J	204, 264	Levitas, V I	266	Liu, B	18, 45, 184
Lasseigne, A N	148, 150, 207	Lewandowski, J J	64	Liu, C	122, 129, 173, 179, 227, 270, 275, 281
Latysh, V	195, 197, 199	Lewenstam, A	44	Liu, C T	219
Laughlin, D E	129, 180, 236, 281, 315	Lewis, A C	55, 113, 253	Liu, D	36, 170
Launey, M E	65	Lewis, S L	182	Liu, F	115, 213
Lauridsen, E M	97	Leyens, C	246	Liu, G	214
Lavernia, E	153, 155, 156, 191, 248, 249, 300	Li, A	106	Liu, H	97, 129, 204, 241
Laversenne, L	294	Li, B	36, 68, 69, 79, 149, 304, 309	Liu, J	138, 152, 189, 244, 288, 300
Laws, K	65, 213	Li, C	38, 145, 182	Liu, K	33
Lawson, A C	86, 161	Li, D	213, 290	Liu, P	275
Lázpita, P	180	Li, G	76, 77	Liu, Q	214, 299
Le Brun, P	109	Li, H	152, 172, 220, 229, 257, 261, 275, 304, 305	Liu, S	74, 87, 285
Le Hervet, M	208	Li, J	63, 73, 139, 166, 215, 217, 229, 260, 262, 268, 275, 297, 298, 299, 308	Liu, W	98, 244
Le Roy, G H	109	Li, J C	257, 306	Liu, X	304, 305
Lea, A	136	Li, K	270, 308	Liu, Y	21, 117, 118, 172, 213, 229, 262, 274, 275, 298, 299, 301, 309
Lebensohn, R A	55	Li, L	209	Liu, Z	27, 28, 37, 38, 56, 70, 86, 120, 125, 134, 140, 152, 169, 174, 175, 176, 218, 227, 230, 266, 275, 277, 302, 312
Lebouc, A	296	Li, M	64, 144, 173, 174, 185, 239	Livescu, V	173
Lech-Grega, M	160	Li, N	122, 123, 312	Livingston, D	248
Leclerc, A	59	Li, P	184, 238, 263, 316	Lloyd, D	189
Lee, A	36, 121, 170, 313	Li, Q	259	Llubani, S	75, 111, 133
Lee, B	65, 162, 282	Li, S	113, 231, 297, 304	Lo, J S	289
Lee, C	33, 196, 252, 280	Li, W	19, 309	Lo Russo, S	150
Lee, C G	312	Li, X	53, 71, 173, 182, 208, 286, 298	Loeche, D	73
Lee, C J	194	Li, X C	51	Lograsso, T A	99
Lee, D	87	Li, Y	24, 65, 120, 145, 162, 194, 212, 213, 306	Lohe, D	269
Lee, E	141, 163, 224	Li, Z	18, 44, 138, 189, 225, 228, 239, 244, 288, 302	Lohmann, M	182
Lee, E W	224	Liang, H	284	Lojkowski, W	22
Lee, H	144, 145, 154, 179, 280	Liang, J	285	Lok, Y	224
Lee, H M	128, 178, 234, 280, 313	Liang, S	226, 227	Loladze, L V	197
Lee, I	223	Liao, H	114	Løland, J	134
Lee, J	172, 173, 178, 179, 183, 210, 223, 229, 272, 274, 311, 312	Liao, X	21, 50, 51	Lombard, J H	60
Lee, J C	171	Liaw, P	24, 25, 31, 64, 65, 73, 106, 107, 114, 115, 157, 158, 164, 165, 166, 210, 212, 218, 219, 220, 221, 260, 261, 269, 270, 301, 308, 313	Long, Z	244, 288
Lee, J G	171, 213	Lieberman, S I	192, 253	Loomis, E N	155
Lee, J K	148	Lienert, T J	117	Loper, C	186
Lee, K	74, 178, 212, 280, 301, 305	Lienert, U	97, 98	Lopez, D A	110
Lee, M	137, 157, 299, 313	Light, G	29	Lopez, M I	110
Lee, P	44, 87, 91, 125, 134, 135, 184, 185, 239, 240, 283, 284, 316	Lijuan, Q	297	Lopez-Hirata, V M	265
Lee, S	79, 82, 160, 212, 226, 282, 305	Lijun, W	44	Lorenzo, M	165
Lee, T	227, 280	Lilleodden, E T	112, 267	Loretto, M	142, 191
Lee, W	289	Lim, C	23, 63, 105, 106, 156, 211, 259	Lossius, L P	159
Lee, Y	173, 235, 272, 307	Lim, H	172, 229, 312	Lothar, W	115, 192
Lee, Z	155	Lima, A C	263	Lou, X	173
Legagneux, P	15	Lima, S C	161	Louis, E	190
Lehman, L P	79	Limberg, W	80	Loukus, A	91, 140
Lehmann, J	305	Limoge, Y	181	Loureiro, S M	62
Lei, D	61			Louzguine, D	65, 129
Lei, Y	79, 286			Lowe, T	197, 198
				Lowe, T C	50, 92, 142, 192, 194, 248, 291

TMS2006 Annual Meeting & Exhibition

Lozhko, A N	102	Majetich, S	281	McCartney, D	44, 87, 135, 166,
Lu, A	170	Major, F J	166		167, 185, 240, 284
Lu, H	80, 84, 98, 152, 262, 299	Major, J F	159	McCartney, G	44
Lu, J	234, 286, 292	Majumdar, B S	37, 245	McClellan, K	89, 155
Lu, K	51, 93, 286	Malenfant, P	62	McClung, M	108
Lu, L	160, 248	Malkov, V	214	McCune, R C	80
Lu, S	87, 148, 312	Maloy, S A	52, 53, 181	McDermid, J	153
Lu, W	131, 251	Malshe, A	84	McDonald, K	39
Lu, X	257	Man, C	139, 166, 244	McDonald, S D	185
Lu, Y	218	Mangelinck-Noel, N	45, 135	McDowell, D L	164, 221, 316
Lubeck, C R	187	Manias, E	131, 132	McEvily, A J	32
Lucas, J	28, 35, 70, 71,	Maniruzzaman, M	283	McFadden, S A	136
	78, 112, 121, 163, 170,	Manjate, R S	282	McGrath, T	112
	218, 226, 267, 273, 306	Mann, V	18	McGreevy, T	46
Lucero, A	36	Mannava, S	147	McGrouther, D	253, 286
Luck, R	284	Mannava, S R	147	McHenry, M	180, 315
Ludian, T	115, 192	Manoharan, M	62	McHenry, M P	130
Ludwig, A	135, 285	Mansur, L K	52, 94, 144,	McIntosh, K S	303
Ludwig, W	97		201, 250, 292	McIntosh, P	207
Luft, J	73	Mantha, D	248	McKay, B	81
Lugo, G	256	Mao, S X	52, 113, 193	McKee, G S	252
Lukyanov, A	197, 198	Mao, Z	237, 264	McLean, M	125, 240
Lund, M S	112	Mara, N A	21, 61, 259	McMillen, R	193
Luo, A	37, 38, 80, 81, 122,	Marasli, N	285	McNally, B	255
	124, 171, 172, 189, 227,	Marcus, H L	33	McNaney, J	154
	229, 274, 276, 277, 311, 312	Marimuthu, S	41	McNeil, J	222, 272, 309
Luo, H	21, 248, 309	Marin, T	20, 301	McNelly, T R	143, 144,
Luo, J	254	Marines Garcia, I	220		152, 192
Luo, S	155, 169	Mark, J	90, 137	McQueen, H J	299
Luo, T	84, 233, 282, 298	Markmann, J	249	McWhinney, H	26
Lupulescu, A	85, 87	Marks, J	19	Meca, E	87
Lütjering, G	270	Marple, B	210	Mecozzi, M	217
Luton, M J	267	Márquez Godoy, M	27	Medlin, D L	49, 243
Lvov, Y	296	Marquis, E A	205, 243	Medvedeva, N I	86, 238
Lynch, F E	59	Marquis, F D	117, 166, 203, 222	Meek, T T	122, 272
Lynch, S	270, 308	Marrocco, T	167	Megahed, M	262
Lysenko, S	97, 129, 204	Marte, J S	201	Megahed, S	76
		Martin, G P	237, 264	Mehrer, H	177
		Martin, M	196, 301	Mei, Z	314
		Martin, O	60	Meier, G H	31, 126
		Martin, P	142, 247, 251, 310	Meier, M W	108
		Martin, T	35	Meindl, J D	96
		Martinez, F	110	Memongkol, N	232
		Martínez-Nicolas, P	76	Menard, V	44
		Marty, P	18	Mendelev, M	111, 112, 181
		Marya, M	174	Mendes, R R	19
		Masaki, K	219, 269	Mendez, P F	117
		Maslov, V	203	Mendis, B	210
		Massie, J	211	Mendoza, R	16, 216
		Mateescu, N	253	Menezes, G W	264
		Mathaudhu, S N	62, 302	Meng, D	97, 136
		Mathur, R B	50	Meng, W J	246
		Matl, B	183	Meng, X	286
		Matos, J	220	Menon, S	310
		Matson, D	83	Menzel, B	115
		Matsukawa, Y	53, 89	Merinov, B	265
		Matsumoto, Y	81	Mertens, A	153
		Matsumura, T	219, 269	Meskers, C E	39
		Matsunaga, T	91	Metson, J B	66, 102
		Matteis, P	271	Metwally, H	67, 271
		Matthews, D T	213	Meuris, M	261
		Matthews, R J	36	Mewes, T	43
		Maunder, S	133	Meyer, A	128
		Maupin, G	231	Meyers, M	23, 50, 52, 63, 105,
		Maxe, E	58		106, 154, 156, 196, 211, 259
		May, J	143	Meyyappan, M	99
		Mayer, G	260	Miao, J	221
		Mayer, H	245	Michael, N	97, 136
		Mayer, R	195	Michalik, M	83
		Maziasz, P J	83	Mididuddi, S	54
		Mazin, P M	20	Migchielsen, J	67
		Mazin, V M	20	Mikula, A	169, 225
		McBow, I	75, 111, 133	Milanova, D	166
		McBride, D	185, 284	Milhans, J	160
		McCabe, R J	105	Militzer, M	140, 217
		McCallum, B	62	Miljak, D	303
		McCallum, R	146, 149	Miller, M	36, 98, 147,
					148, 201, 308

M

Ma, D	81
Ma, E	50, 51, 107, 213
Ma, H	213
Ma, J	98
Ma, L	286
Ma, N	230, 273
Ma, R	80, 253, 262
Ma, S	37, 283
Ma, X	173, 250
Macht, M	128
Mackenzie, L W	275
Mackey, P	34
MacLaren, I	291
MacSleyne, J P	17
Maddalena, A	150
Maddela, S	38
Mader, E	88
Madge, S V	301
Madshus, S	66
Maeda, M	184, 283
Maehlen, J P	101
Magnan, J	19
Magyari-Kope, B	70
Mahajan, R	78
Mahanwar, P	264
Mahapatra, R N	62, 142
Maharsia, R R	91, 289
Maher, D	163, 286
Mahmodieh, K	119
Maier, H	93, 113, 160, 199,
	200, 201, 216, 293
Maijer, D	184, 185, 316
Maillet, L	66
Maire, E	172
Maitra, D	223
Maity, P C	167
Maiwald, D	159

Miller, M K	138, 146, 158, 201, 205
Miller, M M	130
Miller, W L	80
Mills, J	243
Mills, M	73, 163, 191, 266, 268
Millwater, H R	269
Milne, W	15
Mimaki, T	291
Min, Z	309
Minamiguchi, S	229
Minay, E	310
Mingler, B	199
Minich, R	300
Minisandram, R	125
Minor, A	29, 52, 112
Minoux, E	15
Miodownik, A P	278
Miodownik, M	17, 63, 265
Miotello, A	149
Miracle, D B	25, 107, 157, 158, 212, 245, 289
Miraglia, S	18, 254, 296
Mirkovic, D	123
Mirmiran, S	287
Mishin, Y	42, 49, 86, 89, 130, 181, 237
Mishra, A	196
Mishra, B	126, 148, 150, 207
Mishra, R	189, 245
Mishra, R K	189, 276
Mishra, R S	21, 61, 103, 152, 154, 209, 257, 299
Misra, A	22, 63, 105, 113, 116
Misra, D K	131, 132, 182, 183, 204
Misra, M	99, 295
Missalla, M	256
Miwa, K	123, 158
Miyake, M	184, 283
Miyamoto, H	291
Miyaoka, H	100
Miyashita, Y	308
Mizutani, Y	123, 158
Moelans, N	267
Moffatt, S	60
Mohamed, F A	196, 209, 249, 291
Mohamed, S	262
Mohanty, R R	85
Mohapatra, S	99
Mohney, S E	128, 178, 234, 280, 313
Mohri, T	78
Moinhos, C	195
Moinuddin, K	54
Mokadem, S	135
Molin, A	108
Molina, J	190
Molinero, V	265
Moll, O	187
Molodov, D A	49
Mona, M	121
Monasterio, P	202
Mondal, D P	289
Monlevade, E F	195
Monteiro, S N	68, 69, 216, 223, 263, 264
Montone, A	150
Moody, N	28, 29, 70, 112, 163, 164, 218, 267, 306
Mook, W	29, 112
Moon, C	121
Moon, K	121
Moon, M	121
Morais, L S	23
Moraru, A I	299
Mordike, B L	124

More, K	30, 72
Moreira, P M	166
Moreno, H	26, 54
Morfoise, J	108
Morgan, D	27, 69, 70, 111, 131, 162, 216, 264, 266, 282, 305
Mori, K	119, 198, 290
Mori, T	254
Morigasaki, N	18
Moriuchi, H	314
Moriyama, M	128
Morjan, I	54
Morrall, J E	41, 42, 84, 127, 177, 233, 279
Morris, C E	86
Morris, D	192
Morris, D G	193
Morris, J	107
Morris, J G	244
Morris, J R	112, 162
Morris, J W	280
Morris, Jr., J	227
Morrison, M L	25
Morse, D	105
Morsi, K	21, 61, 103, 152, 154, 209, 222, 257, 299, 300
Moscovitch, N	172
Mourer, D P	125
Mousa, A	39
Moxnes, B P	151
Mucciardi, F	41, 102
Mudaliar, A	132
Muddle, B C	134
Muelas, R	72
Mueller, K B	277
Mughrabi, H	73, 115, 192, 209
Mukai, T	171
Mukherjee, A	21, 51, 62
Mukherji, D	180
Mukhopadhyay, J	103
Mukhopadhyay, P	146
Mukhopadhyay, S M	74, 136, 187, 241, 286
Mullens, H M	252
Mullis, A M	186
Mullner, P	180
Mun, J	87
Mundy, C	111, 112
Munoz, J	63
Muñoz-Morris, M A	193
Munroe, P	251, 253, 286
Muppidi, T	162
Muraishi, S	136, 137
Murakami, H	280
Murakami, M	81, 128
Murakami, Y	281, 315
Murashkin, M	143, 199
Murata, N	314
Murch, G	233
Murch, G E	127, 130
Murr, L	110, 156, 157, 161, 196, 252
Murray, J L	174
Murray, M	80, 274
Murthy, G S	78
Murthy, V S	258
Murty, K L	21, 52, 78, 92, 94, 144, 201, 202, 210, 250, 292
Murty, V S	197
Murugesan, N	75
Murzaev, R T	181
Mutoh, Y	308
Muyco, J	105
Myers, D	30
Mylavarapu, P	289

N

Na, Y	312
Nacemi, A	96
Nag, S	23
Nagai, K	197
Nagar, N	172
Nagarajan, J	75
Nagarajan, N	255
Nagase, N	116
Nagasekhar, A V	194
Nagem, N F	19
Nageswaran, R	72
Nagireddy, R	254
Nagle, M	39, 41
Nagy, P B	215
Nah, J	226, 234, 273
Naik, R R	211
Naito, H	136, 137
Naixiang, F	298
Najafabadi, R	131
Najar, M	151
Nakamori, Y	205
Nakamura, T	203
Nakamura, Y	149
Nakayama, E	198
Nakazawa, K	84
Nalla, R K	156
Nam, H	70, 111
Nan, Z	165
Nancollas, G	105
Nanstad, R K	201
Napolitano, R E	117, 166, 222
Narasimhan, S	79, 176
Narayan, R J	259
Narayanan, R	279
Narciso, J	190
Nash, J C	104
Nash, P	222
Nastac, L	311
Nastar, M	130
Natesan, K	82, 118, 126
Nath, D	191
Nathani, H	182, 204
Navarra, P	41, 102
Navarro, P R	103
Nazarchuk, A T	192
Nazarov, A A	181, 196, 268
Ndlovu, S	303
Neale, K W	276
Needleman, A	267
Neelameggham, N R	37, 38, 80, 81, 122, 124, 171, 172, 222, 227, 229, 272, 274, 276, 309, 311, 312
Neife, S I	77
Neiva, A C	161
Nelson, R	88
Nemerenco, I	260
Neubauer, E	251
Newbery, P	153
Newcombe, P	123
Newhauser, W	251
Newman, C J	101
Newsome, G A	88
Nexhip, C	35
Neylan, N	310
Nguyen, J	154
Nguyen, T	20
Nguyen-Thi, H	135
Ni, C	251
Ni, W	268
Nicholson, D M	25, 107
Nicola, L	267
Nie, J	124, 134
Nie, S	39
Nieh, T	46

Nielsen, O	134, 186
Niewolak, L	31
Ningileri, S	288
Ningileri, S T	271
Nishibe, Y	179
Nishida, S	269
Nishikawa, H	274, 280
Nix, W D	70, 71, 112
Niyomwas, S	176, 232
Nkohla, M	133
Noebe, R D	137, 205, 237
Noel, H	120
Nogita, K	185
Noldin, J H	41
Nolen, B P	100
Nonell, J M	298
Norby, T	39
Noreus, D	254
Norfleet, D M	163
Normandin, M	59
Norval, D	34, 119
Norwood, J	151
Nosenko, V	203
Novy, Z	153, 193
Numakura, H	127, 128, 131
Nunes, A C	155
Nunna, R N	167
Nurislamova, G	143
Nurminen, E V	75
Nutt, S R	153, 155
Nyberg, E A	37

O

Oates, W A	77
Oba, F	28
Oba, H	28
Obbard, R	264
Oberschelp, C	80
Oberson, P G	168
Oboukhov, Y	43
O'Brien, C	85
O'Brien, J M	200
O'Brien, K L	59
Ocaña, N	184
Ocelik, V	213
Ochi, Y	219, 221, 269
O'Connell, M J	16
O'Connor, W K	35
Ode, M	280
Odette, G	120, 201, 202, 307
Odunuga, S	306
Oechsner, A	279
Oertel, C	292
Ogata, K	91
Ogata, S	260
Ogawa, H	31
Ogneva, A	106
Ogren, J	119, 224, 272, 290, 310
Ogrin, J	311
Oh, B	64
Oh, C	273
Oh, K	121
Oh, S	90
Oh, T	178
Oh, Y S	172, 213
O'Handley, R C	180
Ohgi, J	31
Ohlert, J	118
Ohmori, A	197
Ohno, M	123, 174, 227
Ohnuki, S	150
Ohnuma, I	179
Ohodnicki, P	198, 281, 315
Ohriner, E K	46, 88
Ohsaki, S	143

Oikawa, H	210
Oikawa, K	180
Oishi, K	144, 152, 192
Oja, M E	218, 221
Ojima, Y	116
Okabe, T	24
Okabe, T H	26, 110, 232
Okazaki, K	79
Okazaki, M	73
Okumura, K	176
Okuniewski, M A	52, 53
Okuno, O	24
Okuya, K	114
Oldenhof, G	60
Olevsky, E A	222
Olivier, J	296
Olminsky, J	30
Olmsted, D	111, 265
Olsen, D	59, 102, 103, 150, 207, 255, 297
Olson, D L	126, 148, 150, 207
Olson, G	230, 277
Olubambi, P A	303
Onishi, T	128
Onisi, K	150
Onodera, H	280
Onsel, M	189
Oostveen, J	15
Opalka, S M	58
Opila, E	30, 72
Oppenheim, T	310
Orban, S	168
Orchard, H T	235
Ordaz, G	18
Ordonez-Chu, A	272
Orgen, J	168
Orimo, S	205
Orlikowski, D	154
Orlova, T S	196
Orme, C	105, 211
Oryshchyn, D	240
Osetsky, Y	89, 131, 145
Osgerby, S	72
Oshinowo, L	207
Othon, M	201
Ott, R	282
Ott, R D	281
Ott, R T	212
Ouimet, L	80
Øvrelid, E J	183
Oye, H A	66, 159, 262
Ozolins, V	70, 162

P

Packard, C E	24
Padilla, H A	105
Pagliari, S N	40, 100, 150, 206
Pai, B	50, 289
Pai, C B	50
Paik, K	234
Pakiela, Z	22
Palade, P	150
Palenik, B P	54
Paley, M S	132
Palumbo, O	99
Pamuk, H	285
Pan, D	78
Pan, F	252
Pan, X	145, 188, 242
Panaitecu, A	299
Pancholi, A	96
Pandya, M	255
Pang, J	78, 226, 235, 313
Pang, J W	98
Pang, X	187
Pang, Y	48

Panov, A V	103
Pantleon, W	98
Panza-Giosa, R	222
Pao, P S	248
Paolone, A	99
Papadimitrakopoulos, F	33
Papin, P A	302
Pappula, L	167
Parada, F	75
Paret, J	177
Parga, J R	26
Parilla, P	295
Paris, P	73, 220
Park, B	260
Park, C	78, 310
Park, H	74
Park, J	98, 124, 126, 128, 305, 308
Park, S	148, 310
Park, S S	171, 172, 312
Park, W	228, 277
Park, Y	235, 274
Parker, W	42
Parra, M	89
Parra, R	75
Parthasarathy, T A	155
Partyka, E	237
Parvanyan, V	177, 232
Pasquini, L	150
Patel, M	35
Patel, P M	213
Patel, S J	57
Pathak, M P	137
Patil, S D	166
Patil, U	302
Patnaik, P	290
Patrick, S	246
Patten, T A	181
Patterson, B R	147, 244
Patterson, T	234
Paul, B	60
Paul, L	175
Paulino, L	67, 256
Paulonis, D F	92
Pawlek, R P	214
Paxton, D M	46, 127, 309
Payzant, A E	114
Peauger, F	15
Pecharsky, V K	56
Pecher, K	136
Pedersen, T B	18, 20, 60, 151, 208, 256, 298
Pederson, L R	40
Pehlke, R D	284
Pei, Y	242
Peker, A	65
Pekguleryuz, M	227, 228, 275, 276
Pelekhev, D	43
Péloquin, G	59
Pena, D J	130
Peng, L	79
Penn, B G	132
Peralta, P	89, 112, 155, 270
Perepezko, J	46, 143, 177, 185, 284
Peretti, M W	92, 141, 191, 246, 247, 290
Perez, E	234
Perez-Prado, M T	63
Perez-Trujillo, F J	30
Pericleous, K	208, 284
Perlovich, Y	202
Perron, A	257
Perron, S	257
Persson, K A	70
Pescia, D	236
Pesiri, D R	206

Peter, W H	65
Peterson, B	142
Peterson, E	26, 54
Peterson, R D	26, 47, 263
Petit, J	270
Petric, A	231
Petrosyan, G	177
Petrova, R	23, 233
Petrovic, J J	17, 18, 58, 99, 149, 205, 254, 294, 296
Petrucci, L J	263
Pettit, F S	31, 126, 175
Pfaendtner, J	125
Phillips, D	300
Phillips, E C	59
Pickens, J R	168
Picu, C	86
Pillai, M R	50
Pillai, P	295
Pillai, R	50
Pillai, S	50
Pinasco, M R	271
Pinocely, A	108
Pint, B	30, 31, 72, 83
Piper, T	184
Pippan, R	194
Pisch, A	120
Pizaña, C	161, 196
Plapp, M O	87
Plascencia, G	20
Platek, P	189
Pletcher, B	85
Plimpton, S J	265
Pochstein, C	146
Podschn, R	146
Poirier, D R	33, 239
Poirier, G	27
Pola, J	54
Polak, J	73, 221
Polasik, S	163
Polizos, G	132
Pollard, L J	133
Pollock, T M	57, 81, 82, 165, 210, 221, 311
Polyakov, L	195
Poncsak, S	257
Pond, B A	22
Pond, R C	250
Ponge, D	153
Pongsaksawad, W	266
Pontimiche, G	161
Poole, W	140, 172, 189
Poon, J	168, 260
Poortmans, S	195
Popa, I	254
Popov, M V	248
Porter, W	308
Porter, W D	284
Porter, W J	270
Portmann, O	236
Potesser, M	216, 283
Potgieter, J	303
Poths, J	100
Poulose, P K	272
Poulsen, H F	97, 98
Powell, A	40, 83, 176, 217, 224, 232, 241, 266
Powell, B R	80, 171
Powell, G L	206
Powell, S	102
Pownceby, M	39
Prasad, N	191
Prasad, R N	60
Prasad, S	29, 71, 190
Pratihar, S K	287
Pravdic, F	123
Preuss, M	192
Prietto, M	272

Principi, G	101, 150
Prins, S N	27, 86
Prior, F	183
Proffen, T	107
Prokofiev, E	198
Prokoshkin, S	198
Protasov, V	200
Protokovilov, I V	192
Proudhon, H	189
Proust, G	104
Provatas, N	44, 216, 266
Provenzano, V	315
Pudovkina, A	120
Puech, S	301
Pulikollu, R V	286
Purdy, G R	42
Purgert, R M	91
Purkayastha, A	281
Pushin, V	197, 198
Pustal, B	285
Puszynski, J A	96
Puthucode, A	25
Putrevu, A	118, 196, 223
Pyles, T	74

Q

Qi, L	297
Qiao, D	158
Qiao, Y	132, 187
Qiaofang, Y	297
Qiu, C	213
Qiu, D	262
Qiu, R	105, 211
Qiu, Z	152, 214, 257
Qu, H	187
Qu, S	110
Quach, D V	177
Quadakkers, W	31, 83, 175
Quandt, E	146
Quaresma, S F	242, 282
Quast, J P	23
Querin, J	103
Quimby, P D	312
Quinones, S	252

R

Raab, G	22, 61, 84, 144, 196, 197, 198
Raabe, D	106, 153
Rabba, S A	108
Rack, H J	24
Rack, P	115
Radmilovic, V	155
Radosavljevic, S A	304
Radosavljevic-Mihajlovic, A S	304
Radulescu, C	152
Rae, A	97
Rae, P J	224
Raetzke, K	181
Raghu, H	264
Rahman, M S	296
Raj, R	90, 137, 209, 246
Raj, S V	104
Raja, K S	99, 295
Rajan, T	50
Ram-Mohan, L R	41
Ramakrishnan, N	289
Ramalho, A M	69
Ramalingam, B	137
Raman, A	36, 79
Ramana, Y	66, 67, 108
Ramanath, G	281, 315
Ramanathan, T	241
Ramanujan, R V	129, 130, 146, 180, 236, 281, 315

Ramasubramanian, U	117
Ramesh, K	199, 218, 300
Ramesh, R	15
Ramirez, A	110
Ramirez, D A	110
Ramirez, J C	45
Ran, G	316
Rana, S	182
Ranganathan, S	48, 61, 89, 137, 188, 242, 243, 287
Rani, S	78
Rao, A	15
Rao, B	193
Rao, K P	37
Rao, V	226
Raphael, M P	130
Rappaz, M	45, 239, 240, 256
Rashkova, B	124
Rasty, J	215
Rath, B B	257
Rathod, C	210
Rathz, T J	210, 302
Ratke, L	88
Ratochka, I V	258, 279
Ratvik, A P	66
Ravat, B	95
Ravi, C	28, 70, 277
RaviKumar, B	167
Ravindra, N	203
Ravindra, R	33
Ravindran, V K	315
Ravishankar, N	188
Rawat, J	182, 204
Raynova, S	93
Rea, K E	166
Read, C	18, 99, 205
Read, D	71
Ready, J	252
Ready, W J	15, 53, 96, 145, 203, 251
Reddy, D	118
Reddy, R G	50, 176, 232, 248, 254, 257
Reddy, S	178
Redkin, A	20
Redondo, A	63
Reed, R C	131, 205
Reilly, J J	18, 59
Reinhart, G	135
Reip, C	118
Rémy, L	220
Ren, B	152
Ren, C	229
Ren, F	226, 273
Ren, Y	107, 220
Renavikar, M	36, 78
Reny, P	60
Restorff, J	99
Reuter, M A	39
Revuru, R	74
Reynolds, J	309
Reynolds, W T	129, 180, 236, 281, 315
Rhee, H	71
Rhorer, G	188
Ribárik, G	193
Ribeiro, A	24
Richard, C	60
Richard, D	261
Richard, M L	180
Richardson, Jr., J W	58
Richter, G	90
Richter, K	169
Ridgeway, K	176
Ridley, N	257, 258
Ried, P P	80
Riester, L	82
Riesterer, J L	188

Seok, H	26	Shuey, R	284	Sobyanin, V	83
Seol, S	87	Shuiping, Z	61	Sofronis, P	39, 82
Seong Yong, P	269	Shuler, S F	286	Sohn, Y	41, 84, 85, 122, 127, 177, 178, 233, 234, 279
Seraphin, S	33	Shull, R D	129, 145, 315	Sokabe, M	157
Sergiienko, R	203	Shurov, N	214	Sokalski, V M	198
Sergueeva, A V	21, 259	Shvinderman, L S	48, 188	Sokolov, M A	201
Serra, A	131	Si, W	233	Sokolowski, P K	62
Seshadri, V	111	Siafa, K	151	Solheim, A	151, 256
Setiawan, M	224	Sidhu, R S	36, 55, 78	Solomon, I M	126
Shabashov, V A	195	Siebert, K	277	Soloviev, V	195
Shackelford, J F	62	Siepmann, J I	112	Solovyev, V P	197
Shahrabi, K	153	Sieradzki, K	112	Somekawa, H	171
Shaimardanova, I	94	Siersma, K	239	Sommerhofer, H	262
Shan, D	38	Sietsma, J	217	Sommerhofer, P	262
Shan, Z	52, 193	Sigworth, G K	159	Sonderegger, B	273
Shandas, R	145	Sikand, R	50	Song, B	297
Shang, C	99	Silva, A F	19	Song, C	44
Shanguan, D	285	Silva, E V	68	Song, G	38
Shao, T	227	Silva, G	271	Song, H	200, 215, 216
Shapiro, A J	315	Silvestri, A	271	Song, J	171, 179
Sharma, K	118	Simakov, D A	20	Song, M	219
Sharma, S	302	Simard, G	59	Song, Y	38, 99, 100
Sharp, J	199, 255	Simensen, C	134, 186	Sophie, S	231
Sharratt, B M	74	Simielli, E A	244	Sorby, M	206
Shaw, L L	31, 62, 73, 114, 115, 164, 165, 166, 219, 221, 248, 269, 270, 308	Simmons, J P	16, 17, 55, 97, 125, 147, 204, 252	Sordelet, D	120, 157, 158, 212
Shaw, M J	29	Simone, A	268	Sorensson, M	182
Shechtman, D	48, 89, 137, 188, 242, 243, 287	Simonen, E P	52, 94, 144, 201, 250, 292	Sorlie, M	66, 108, 159, 213, 261
Shehata, M	276	Simpson, L	295	Sorokina, O V	102
Shekhar, S	48, 279	Sinclair, C W	172	Soto, K F	157
Shelyakov, A	149	Sinclair, I	258	Soubeyroux, J	301
Shelyapina, M	254, 296	Sinclair, K	108	Southwick, L M	102
Shen, C	217, 266	Sinelnikov, V	66	Spanos, G	97, 236, 252, 253
Shen, G	230	Singh, B N	53	Sparrow, G	222
Shen, J	304	Singh, G	90, 113, 137, 200	Speakman, S A	46
Shen, T	22, 99	Singh, H	17, 55	Spinat, A	277
Shen, Y	171	Singh, N	236	Spitzer, D P	59
Shepard, M	166, 221	Singh, N K	67	Sporer, N	290
Sherby, O	153, 200	Singh, P	127, 231	Spowart, J E	220, 252
Sherman, D H	205	Singh, R P	76	Sprague, A P	147
Shi, B	200	Singh, V	41	Spruiell, J E	114
Shi, S	68, 149, 304	Singheiser, L	31, 83, 175	Spruzina, W	183
Shi, X	37	Sinha, R K	287	Sreeranganathan, A	55, 311
Shi, Y	79	Sinha, V	73	Sridharan, S	260
Shi, Z	23, 152, 257	Sintay, S	55	Srikant, G	210
Shian, S	54	Sisson, R	41, 84, 127, 177, 233, 279, 283	Srinivasan, D	201
Shibata, E	203	Sitdikov, V	21	Srinivasan, R	195
Shibata, J	160	Sitnikov, L	214	Srinivasan, S	99, 294
Shieh, J	74, 252	Skillingberg, M H	26, 47	Srinivasan, S G	52
Shield, J E	146, 315	Sklenicka, V	291	Srivastava, A	130
Shiflet, G	168, 260	Skrotzki, W	292	Srivatsa, S	125
Shih, D	121	Skryabina, N	18, 149, 296	Srivilliputhur, S G	53, 89, 104, 113, 181
Shih, T	179, 274	Skury, A D	69, 216, 223, 263, 264	Srolovitz, D J	42, 43, 70, 86, 111, 112, 130, 181, 237, 242
Shim, J	52	Skyllas-Kazacos, M	19	St. John, D	38
Shima, M	281	Slaugenhaupt, M	151	St. John, D H	122
Shimizu, F	260	Slifka, A	71	Stach, E	52, 193
Shimmin, R G	182	Smid, I	117, 148, 251	Stadnyk, Y	254
Shin, D	93, 134, 169, 175, 196, 305	Smith, C D	105	Stafford, G R	121
Shin, D H	249	Smith, C E	29	Stagno, E	271
Shin, J	170	Smith, D	60, 115	Staley, J T	288
Shin, K	275, 312	Smith, G	57	Stan, M	43, 162, 169
Shin, K S	274	Smith, G D	57, 138	Stanciu, L A	177
Shinde, S	222	Smith, J	202	Stanescu, C T	152
Shindo, D	203, 315	Smith, R	88, 95, 231	Starink, M J	143, 258
Shinohara, G	283	Smolyakov, A	195, 197	Starke, T K	96
Shinozaki, K	91	Smugeresky, J E	56, 99, 148, 156, 191	Stasiak, M	279
Shirinkina, I G	195	Snead, L	88, 95	Steele, J	16
Shirota, T	26	Snow, R C	40, 206	Stefanakos, E K	294
Shoemaker, L E	57	Snyder, J	149	Stefanescu, D	87, 90, 134, 185
Shohadaee, A	153	Snyder, R L	53, 54	Stefanovic, P	266
Shojo, T	171	Sobczak, J	91	Steglich, D	227
Sholl, D	40, 59	Sobczak, N	91	Steinbach, I	174, 186, 272
Shollock, B A	240	Soboyejo, W	23, 63, 64, 105, 114, 116, 165, 220	Steinbach, S	88
Shtanov, V I	20			Steiner, G	51
Shtutca, M	202			Steinhoff, K	229
				Stejskal, O	153, 193

Stepanov, V	214	Swan-Wood, T	28, 237	Tewell, C R	206
Stephens, R L	43, 101, 132	Swenson, D	128, 178, 234, 280, 313	Teyseyre, S	94
Steriotis, T	206	Swift, D	155	Thadhani, N N	196, 301
Steuwer, A	192	Swiostek, J	276	Thangavelu, V	43
Stevens, A	183	Syed, A R	170	Thekdi, A	271
Stevenson, J	127, 231, 279	Sylvain, L	19	Thibault, M	19
Stevenson, K	137	Syn, C	153, 200	Thiebaut, C	95
Steward, R V	219	Synkov, A S	203	Thirumalai, N S	267
Støen, L	151	Synkov, S	203	Thoma, D J	250, 293, 303
Stoica, A D	158	Sysoev, A N	276	Thomas, B G	241
Stoica, G M	114, 218	Syvertsen, M	109	Thomas, G	18
Stojanovic, J N	304	Szczepanski, C	114	Thomas, V J	206
Stoldt, C	145	Szczygiel, P	194	Thompson, D	189
Stoleru, V G	96	Szpunar, J	93	Thompson, G B	244, 282
Stolken, J	300	Szymonski, M	29	Thompson, R J	104
Stoller, R	53, 89, 94, 145, 201			Thompson, S	218
Stolyarov, V	198			Thompson, W T	89
Stone, G A	117			Thonstad, J	20
Stone, M O	211			Thornton, K	216, 217
Støre, T	151			Thorpe, C	256
Stoudt, M R	30, 190			Thridandapani, R	132, 182, 183
Stoughton, T B	139			Thuanboon, S	254
Straumal, B	182			Thyse, E L	133
Street, S C	286			Tian, H	165
Strombeck, J	132			Tian, J	165, 166
Stubbins, J	52, 53, 145, 181			Tian, Z	298
Stubos, T	206			Tianyou, H	284
Stuczynski, T	160			Tibbetts, K	69
Sturm, D	104			Tick-Hon, Y	194
Su, J	74			Tierney, T	155
Subrahmanyam, V V	78			Tiley, J	55, 230
Subramanian, K	196			Timofeeva, V	238
Subramanian, K N	36, 170, 273, 313			Tin, S	125
Subramanian, P	201			Tiryakioglu, M	283, 284
Subramanian, S	79, 81			Titran, R H	46
Such, B	29			Tittsworth, R	296
Suda, S	17, 18, 294			Tiwari, A	54
Suda, T	150			Tiwari, S	245
Sundaresan, R	295			Tiwari, V	141
Sudarshan	91			Tkach, V	203
Sudbrack, C K	137, 204, 205, 237, 264			Tkatcheva, O	20
Sudbury, M P	35			Tobola, J	296
Suganuma, K	128, 178, 179, 234, 280, 313, 314			Tochiyama, O	283
Suh, D	35, 273			Tomasino, T	208
Suh, J	170, 226, 234			Tome, C N	104, 105, 154, 249
Sumner, M B	66			Tomescu, A	54
Sun, F	155			Tomlinson, R	101
Sun, N	244			Tong, J	304
Sun, N X	130			Topic, I	143
Sun, S	225			Torbet, C J	165
Sun, X	149, 304			Toribio, J	165, 220, 307
Sun, Y	18, 218, 240			Torizuka, S	197
Sundararaghavan, V	17, 267, 300			Torok, T I	77
Sunder, R	269			Torosyan, A	80
Sundlof, B	178			Torrens, A	196
Sung, H	277			Torres, P C	282
Suni, J	139, 244			Tortorelli, P	30, 72, 126, 232
Suppan, H	66			Totemeier, T C	165
Surani, F B	187			Tóth, L S	292
Surappa, M K	91, 190, 191			Toulouse, D	257
Suresh, S	32, 63, 163, 243, 248			Touzik, A	295
Suryanarayana, C	260, 302			Tran, T B	62
Suss, A G	103			Trang, S	39
Suter, R	98			Trannoy, N	216
Sutou, Y	180			Trassy, C	84
Sutter, S	199, 216			Treivus, E	161
Suwa, H	203			Trejo, R	31
Suwas, S	292			Trinkle, D R	42, 86, 130, 181, 237
Suwattananont, N	23, 233			Tripathy, D	236
Suzuki, A	81, 82, 89, 311			Trivedi, R	44
Suzuki, M	132			Trompetter, W	253
Svoboda, J	85			Trouw, F	157
Svoboda, M	291			Trubitsyna, I	198
Swadener, J G	22, 113, 116			Trujillo, C P	224
Swamy, K	34			Trumble, K P	144, 193
				Tryon, B	210
				Tryon, R	36, 114, 218, 221

T

Tabereaux, A T	103
Tack, T	200
Tack, W	155, 311
Tada, H	220
Tada, M	96
Tadigadapa, S	242
Takaku, Y	179
Takeda, K	116
Takeda, O	232
Takele, H	146
Takemoto, T	274, 280
Takeuchi, M	314
Tal-Gutelmacher, E	307
Taleff, E	21, 61, 103, 152, 154, 190, 209, 210, 257, 299
Talekar, A S	296
Talley, C E	259
Tamerler, C	211
Tamirisa, S	192, 253
Tamoria, T L	161, 196
Tamura, T	123, 158
Tan, H	212
Tan, K	106
Tan, L	94
Tan, P	34, 76, 133
Tanaka, I	28, 69
Tanase, M	281
Tandon, S C	60
Tang, F	218
Tang, H	56
Tang, J A	43, 44
Tang, M	89
Tang, R	19
Tang, W	62, 146
Tang, Z	120
Tanniru, M	183
Tao, L	61
Tao, N	286
Tarcy, G P	151, 208
Tatyanin, E	198
Tauson, V	242
Taylor, J E	48
Taylor, M	60, 209
Taylor, S T	62
Tchernychova, E	90
Tedenac, J	120, 170, 234
Teng, J	285
Teng, S	314
Teo, K	15
Ter Weer, P	255
TerBush, J R	82
Terpstra, R L	40
Terrones, L H	263
Terzoeff, P	225
Tessandori, J L	263
Teter, D F	161, 250, 302, 303
Tewari, A	245
Tewari, R	216

Tsai, C	227
Tsai, H	170
Tsai, S	234, 274, 280
Tseng, Y	280
Tsirlina, G A	20
Tsokol, A O	296
Tsuji, N	52
Tsukimoto, S	128
Tsumura, M	232
Tsurekawa, S	49, 258
Tu, K	117, 170, 226, 234, 235, 273
Tubeising, P K	293
Tucker, J D	131
Tuggle, J	230
Turano, S	252
Turbini, L J	35, 78, 121, 170, 226, 273
Turchi, P E	77, 120, 169, 225, 272
Turchin, A	214
Turcotte, S	213
Turenne, S	198
Turner, J	176, 232
Turner, P C	35
Turpin, T	230
Tuszynski, J A	259

U

Uan, J	38, 228
Ubertalli, G	271
Uberuaga, B P	43, 181
Uchic, M	16, 55, 97, 147, 148, 155, 163, 204, 252, 253
Uchida, M	128
Ucok, I	155, 168, 200, 311
Udaykumar, H	246
Ueshima, M	280
Ugues, D	215
Um, N	282
Umetsu, Y	26
Umrigar, C J	42
Umstead, W	47
Ungar, T	193, 200
Ustundag, E	98
Utigard, T	20
Utsunomiya, H	198, 229
Utyashev, F	84
Uz, M	46, 88

V

Vadlakonda, S	25
Vaia, R	131
Vaidyanathan, R	260, 293, 302
Vainik, R	109
Valeyev, O	26
Valiev, R	21, 51, 61, 142, 143, 197, 198, 199, 249, 291, 292
Valix, M	43, 44
Valtierra, S	317
Vamadevan, G	245
van Benthem, K	90
Van Dalen, M E	205, 243
Van De Putte, T	31
Van De Walle, A	27, 69, 77, 87, 175, 300
Van der Giessen, E	267, 268
Van der Ven, A	43, 111, 265
van der Zwaag, S	217, 305
van Duin, A C	265
van Heerden, D	113
Van Rompaey, T	41, 102
Van Vulpen, R	72
Vance, R P	29
Vander Jagt, D	263

Vanderspurt, T	58
VanEvery, K J	125
Varano, R	275
Varma, S	54
Varma, S K	118
Varyukhin, V	144, 197, 203
Vasquez, G	307
Vassilev, G P	170
Vassiliev, S Y	20
Vasudeva Rao, V	223
Vasudevan, V K	147, 215, 216
Vaterlaus, A	236
Vats, A	203
Veazey, C	98
Vecchio, K S	105, 211, 251, 252, 260, 292
Vedernikova, I	195
Vegge, T	294
Veit, A L	29
Velasco, E	67
Velea, T	184
Velikodny, Y A	20
Venk, S	273
Venkataraman, S	158
Venkatesh, T A	224
Venkateswaran, S	315
Vergara, D	165
Verlinden, B	195
Verma, R	124, 174, 229, 275, 276
Verreault, R	59
Verschuur, H	151
Verweij, H	82
Veselkov, V	152, 242
Viala, J	279, 313
Vidrich, G	187
Vieira, C F	68
Viera, C B	111
Vieyra, J	241
Vijay, R	295
Vikhnin, V	129
Vild, C	271
Villalobos, E	290
Villegas, J	165, 166
Vincent, E	131
Vinci, R P	30
Vineberg, D	176
Vinogradov, A	291
Virupaksha, V	310
Visco, S	175, 231
Viswanathan, G B	141, 148, 163, 230
Viswanathan, S	124
Vitek, J M	230
Viti, V	40, 123
Vittori Antisari, M	150
Vittoria, C	130
Vix, P	34, 76, 133
Vlcek, J	168
Vogel, S	89, 105, 170
Voice, W	142, 290
Volinsky, A A	29, 164
Volkert, C A	112
Volkova, G K	197
Volz, H M	161
Von Kaenel, R	20
Voorhees, P W	16, 216, 217
Vorhauer, A	194

W

Wachsman, E D	86
Wada, T	64
Wadasako, M	219
Wagenhofer, M	268
Wagner, B	252
Wagner, T	90

Wagner, W	250, 316
Wagoner, R H	173
Wahl, K J	70
Walgraeaf, D	164
Wall, J	158, 210
Walter, G	68
Walter, S G	260
Walther, F	74
Wan, J	62
Wan, S	223
Wan, Z	223
Wang, B	125
Wang, C	122, 136, 187, 218, 236, 280
Wang, G	25, 65, 172, 218, 219
Wang, H	23, 141, 176, 232, 261
Wang, J	75, 120, 149, 194, 206, 236, 248, 249, 304, 305
Wang, J C	58
Wang, K	16
Wang, M	211
Wang, P T	161
Wang, Q	134, 174, 184, 239, 272, 283, 316
Wang, S	33, 122, 143, 166, 258, 269
Wang, T	120, 277
Wang, W	183, 214
Wang, X	151, 158, 200
Wang, Y	16, 28, 38, 42, 51, 70, 80, 84, 86, 107, 108, 110, 113, 116, 125, 152, 154, 174, 178, 206, 217, 220, 230, 266, 273, 277, 306, 309, 316
Wang, Y M	22
Wang, Y U	250, 266
Wang, Z	15, 53, 137, 214, 222, 257, 298
Wangxing, L	297
Wanner, T	16
Wanquan, B	297
Ward, N	31
Warner, A E	119
Warner, J	107, 212
Warnken, N	272
Warren, J A	63, 266
Warren, M E	302
Warren, O L	52
Warrior, N	81
Waryoba, D R	264
Was, G S	94, 95, 144, 145, 250
Watanabe, T	48, 49, 89, 128, 137, 188, 242, 258, 287
Watts, S	308
Weathers, J	284
Weatherspoon, M R	54
Weaver, M L	286
Webb, E B	163
Weber, Y	287
Webler, B	199, 281
Webster, T	24
Wechsler, M	52, 251
Weertman, J	32, 164
Weertman, J R	50
Wegrzyn, J	59
Wei, C	235
Wei, D	125
Wei, L	117
Wei, M	166, 187
Wei, P	231
Wei, Q	199
Wei, W	249
Wei, X	156
Weihls, T P	113
Weil, K	39, 40, 82, 126, 127, 175, 231, 278
Weiland, H	139, 244

Zander, D	261
Zangiacomi, C E	256
Zaporojtchenko, V	146
Zarandi, F M	124
Zbib, A	164
Zbib, H M	306
Zehetbauer, M	50, 51, 92, 142, 192, 194, 199, 248, 291, 299, 300
Zelberg, B	242
Zeng, K	78, 314
Zeng, L	288
Zeng, Q	75, 139, 146, 244
Zeng, X	171, 277
Zeng, Z	118, 126
Zermout, Z	31
Zetterström, P	107
Zevgolis, E N	76
Zhai, C	37
Zhai, T	47, 115, 138, 139, 166, 189, 244, 288, 308
Zhai, X	152
Zhancheng, G	204
Zhang, B	185, 258
Zhang, C	36, 81
Zhang, D	93, 290
Zhang, F	225, 278
Zhang, G	97, 129, 204, 298, 304
Zhang, H	28, 107, 109, 112, 143, 152, 218, 261, 300
Zhang, J	56, 145, 173, 200, 212, 236, 277, 297
Zhang, K	50
Zhang, L	40, 178, 225, 238
Zhang, M	23, 257
Zhang, Q	262
Zhang, R	154
Zhang, S	140, 207, 295, 298
Zhang, T	72
Zhang, W	38, 107, 299
Zhang, X	21, 22, 113, 117, 211, 228, 265, 282
Zhang, Y	72, 77, 146, 249, 297
Zhang, Z	25, 33, 140, 214, 251, 275
Zhangfu, Y	204
Zhao, H	41, 45
Zhao, J	43, 69, 100, 104, 125, 174, 214, 230, 277, 296
Zhao, L	286
Zhao, M	113
Zhao, P	45, 236
Zhao, Q	208, 297
Zhao, X	49
Zhao, Y	21, 51, 91, 147, 248, 295
Zhao, Z	208, 281
Zheng, B	156, 191
Zheng, H	232
Zheng, L	16
Zheng, Q	213
Zheng, X	43, 69
Zheng, Y	251
Zhengyu, Z	317
Zhi, W	204
Zhijie, J	94
Zhilina, M	94
Zhilyaev, A	93
Zhilyaev, A P	144, 152, 192
Zhiqiang, G	309
Zhitomirsky, I	187, 255
Zhong, Y	100, 312
Zhonglin, Y	297
Zhou, B	217
Zhou, C	269
Zhou, H	173, 275
Zhou, J	23, 316
Zhou, K	268
Zhou, M	123
Zhou, N	266
Zhou, S	277
Zhou, W	29
Zhou, W M	59
Zhou, X	231
Zhou, Y	156, 191, 251, 283
Zhu, H	222
Zhu, J	70, 185, 214, 231, 281
Zhu, M	134, 273
Zhu, T	73, 268
Zhu, X	166
Zhu, Y	16, 21, 50, 51, 61, 92, 103, 142, 152, 154, 192, 193, 194, 197, 198, 199, 209, 248, 249, 257, 291, 299
Zidan, R	58, 205
Ziegler, D	208
Zimmerman, J A	163
Zindel, J W	174
Zinkle, S	46, 53, 88, 89, 94, 144, 145, 250
Ziomek-Moroz, M	30
Zoellmer, V	181
Zografidis, C	76
Zolotarsky, I	83
Zong, B	79
Zou, M	56
Zou, Z	299
Zrmik, J	153, 193
Zulumyan, N H	80
Zúñiga, A	155
Zuo, L	49, 107, 220
Zurek, J	31, 83

metal components but also the creep properties of aluminum threads in the engine block. The predicted head bolt load loss during engine thermal cycle is in good agreement with the experimental measurement. The simulation results also indicate that aluminum thread creep in the engine block is responsible for the load loss in the head bolt joint.

11:15 AM

Mechanical Properties Prediction Using MAGMAsoft for 319 Alloy Products with Copper Contents Variations: *Carlos Esparza¹; Alejandro Escudero¹; Salvador Valtierra¹; ¹NEMAK*

Determination of the relationship between the local solidification time and copper contents to predict UTS, Yield Stress and Hardness for Cylinder Heads casted on a gravity semi permanent mold process with variations of a typical 319 alloy.

11:40 AM

Brief Review of Multiaxial High Cycle Fatigue: *Ding Xiangqun¹; He Guoqiu¹; Chen Chengshu¹; Zhu Zhengyu¹; Liu Xiaoshan¹; ¹Tongji University*

In this paper the mechanism of multiaxial high cycle fatigue, especially under nonproportional loading is reviewed. The criteria used for life estimate in the multiaxial fatigue are discussed. Among the criteria reviewed, energy approach appears to be the most promising criterion for multiaxial fatigue life prediction. Accordingly, some suggestions are made for further work.

NOTES